Neurosonology in Critical Care

Monitoring the Neurological Impact of the Critical Pathology

Camilo N. Rodríguez
Claudio Baracchini
Jorge H. Mejía Mantilla
Marek Czosnyka
José I. Suárez
László Csiba
Corina Puppo
Eva Bartels
Editors

Springer

Neurosonology in Critical Care

Camilo N. Rodríguez • Claudio Baracchini
Jorge H. Mejía Mantilla • Marek Czosnyka
José I. Suárez • László Csiba • Corina Puppo
Eva Bartels
Editors

Neurosonology in Critical Care

Monitoring the Neurological Impact of the Critical Pathology

Springer

Editors
Camilo N. Rodríguez
Intensive Care Medicine
Hospital Nacional Prof. Dr. A. Posadas
University of Buenos Aires (UBA)
Buenos Aires
Argentina

Jorge H. Mejía Mantilla
Head Neurointensive Care Unit
Department of Critical Care and Anesthesiology
Hospital Universitario Fundación Valle del Lili
Cali
Colombia

José I. Suárez
Departments of Anesthesiology and Critical Care Medicine, Neurology and Neurosurgery
The Johns Hopkins University School of Medicine
Baltimore, MD
USA

Corina Puppo
Intensive Care Unit
Clinics Hospital, Universidad de la Republica School of Medicine
Montevideo
Uruguay

Claudio Baracchini
Stroke Unit & Neurosonology Lab
University of Padua School of Medicine
Padova
Italy

Marek Czosnyka
Department of Clinical Neurosciences
Cambridge Biomedical Campus
University of Cambridge
Cambridge
UK

László Csiba
Hungarian Neurological Society
Department of Neurology
Clinical Center Debrecen University
Debrecen
Hungary

Eva Bartels
Center for Neurological Vascular Diagnostics
Munich
Germany

ISBN 978-3-030-81418-2 ISBN 978-3-030-81419-9 (eBook)
https://doi.org/10.1007/978-3-030-81419-9

This Springer imprint is published by the registered company Springer Nature Switzerland AG
The registered company address is: Gewerbestrasse 11, 6330 Cham, Switzerland

Re: ESNCH endorsement of the NESSC Course

Dear Professor Rodriguez,

It is our pleasure to inform you, as the President and the Secretary General of the European Society of Neurosonology and Cerebral Hemodynamics (ESNCH), that the course "NEUROSONOLOGY IN CRITICAL CARE(NESCC): Monitoring the Neurological Impact of the Critical Pathology" meets the requirements for ESNCH endorsement.

Please include the ESNCH logo and link to the ESNCH website (http://www.esnch.org) on printed and electronic materials related to the Course.

With best wishes

Claudio Baracchini, MD, PhD, FESO
President of the ESNCH

Branko Malojcic, MD, PhD, FESO
ESNCH Secretary

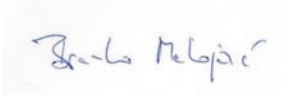

Zagreb, 19. 12. 2018.

Foreword

Transcranial Doppler, including TCD flow imaging modalities, allows us to access detailed information on the hemodynamics of the cerebral circulation. TCD was first introduced in neuro-critical care to monitor vasospasm in patients after subarachnoid hemorrhage. Since the 1980's, we have witnessed a remarkable widening of its range of applications. This book is a substantial documentation of this development, describing a true multidisciplinary approach to using TCD (and extracranial Doppler) as a tool to improve neuro-critical care for a broad range of trauma and diseases.

The book illustrates convincingly a paradigm change in how TCD is used in investigational studies as well as in clinical practice. Ultrasound Doppler used to be a relatively simple diagnostic handheld tool where the verdict was based on the measured velocities, the pulsatility, and eventual spectral broadening signaling disturbed flow. What led to a shift in paradigm is one of the most important advantages of TCD – the presence of the cranium (really!). In spite of its propensity to dampen the ultrasound and make signal acquisition a bit more difficult, the cranium provides an ideal platform for mounting monitoring TCD probes. And this monitoring can go on and on, and even be aided by robotic technology in an ambulatory setting without somebody there to keep that probe aimed right on its target.

So, early on, TCD invaded the territory of physiologists and pathophysiologists. This invasion of course met resistance, if not outright attempts to condemn TCD to the scrapheap of bad science: *"Therefore, the slopes that Aaslid et al. calculated have nothing to do with the rate of autoregulation of the cerebral vascular bed." (Editorial, Stroke Jan. 1989).* Hundreds of dynamic autoregulation studies later, the facts speak for themselves. And the cerebral autoregulation in the non-anesthetized human is indeed an almost incredibly fast mechanism—contrary to the much slower response as measured in anesthetized cats by physiologists in the pre-TCD era.

There is still a lot to be learned about the cerebral circulation. TCD is a convenient non-invasive tool on this journey. It provides a lot of complex data that must

be analyzed and understood. Particularly encouraging has been the way pioneering neuro-anesthesiologists have embraced the methodology. It speaks for the usefulness of this window on the cerebral circulation.

Rune Aaslid
Director of R&D at Hemodynamic ag
Bern, Switzerland
November 2020

Acknowledgments

A book such as this could only be developed through the commitment and humble dedication of a group of exceptional professionals, who, through their handwriting, their sacrifice, the academic love for sharing, and the time dedicated, have honored each of its pages. I would like to thank my colleagues and editors for their belief and their magnificent work. Thanks go to ESNCH for their support and confidence in this project. I would like to thank Springer for believing in us and for their professionalism in this work. I would also like to thank Prof. Rune Aaslid for his contribution and trust. Last but not least, my greatest thanks go to my wife, my son and my parents for their love and constant encouragement; without them, nothing would have been possible. And to my parents, the cornerstone of my essence and existence.

Camilo N. Rodríguez

Contents

Part III Neurosonology: Neurocritical Care Patient

Contributors

Rune Aaslid, PhD Hemodynamics Ag, Bern, Switzerland

Foad Abd-Allah, MD Kasr-Alainy School of Medicine, University of Cairo, Cairo, Egypt

Anselmo A. Abdo-Cuza, MD, PhD Medical Surgical Research Center, La Habana, Cuba

Leandro Aguirre, MD Favaloro Foundation University Hospital, Buenos Aires, Argentina

Claudio García Alfaro, MD University Hospital of Virgen del Rocío, Seville, Spain

Pablo F. Amaya, MD Hospital Universitario Fundación Valle del Lili, Cali, Colombia

Raffaele Aspide, MD IRCCS Istituto delle Scienze Neurologiche di Bologna, Anesthesia and Neurointensive Care Unit, Bologna, Italy

Elsa Azevedo, MD Neurologist, Department of Clinical Neurosciences and Mental Health, Faculty of Medicine of University of Porto, Porto, Portugal

Department of Neurology, Universitary Hospital São João, Porto, Portugal

Committee Member - ESNCH, Oslo, Norway

Milene Azzam, MD Department of Anesthesiology, Montreal Heart Institute, Université de Montréal, Montreal, QC, Canada

Dobri Baldaranov, MD Department of Neurology, Center for Vascular Neurology and Neurointensive Care, University of Regensburg, medbo Bezirksklinikum Regensburg, Regensburg, Germany

Pierluigi Banco, MD Anesthesiology and Intensive Care Medicine, CHU Grenoble Alpes Trauma Center, Grenoble, France

Claudio Baracchini, MD, FESO Director of Stroke center and Neurosonology Lab, University of Padua School of Medicine, President - ESNH, Padova, Italy

Eva Bartels, MD, PhD Neurologist, Center for Neurological Vascular Diagnostics, Munich, Germany

Educational Coordinator - ESNCH, Oslo, Norway

William Beaubien-Souligny, MD Department of Anesthesiology, Montreal Heart Institute, Université de Montréal, Montreal, QC, Canada

Department of Nephrology, Centre Hospitalier de l'Université de Montréal, Montreal, QC, Canada

Francis Bernard, MD Intensive Care Unit, Hôpital Sacré-Coeur de Montréal, Montreal, QC, Canada

Sara Bernardo-Castro, MD Neurosonology Laboratory, Centro Hospitalar e Universitário de Coimbra, Coimbra, Portugal

Faculdade de Medicina da Universidade de Coimbra, Coimbra, Portugal

Federico Bilotta, MD Department of Anesthesiology, Critical Care and Pain Medicine, Section of Neuroanaesthesia and Neurocritical Care, Sapienza University of Rome, Rome, Italy

Manuel Bolognese, MD Department of Neurology, Luzerner Kantonsspitals, Lucerne, Switzerland

Pierre Bouzat, MD CHU Grenoble Alpes, Grenoble Institut of Neurosciences, Grenoble, France

Sandra Boy, MD Department of Neurology, Asklepios Clinic Bad Tölz, Bad Tölz, Germany

Gretchen M. Brophy, PharmD, BCPS, FCCP, FCCM, FNCS Virginia Commonwealth University, Medical College of Virginia Campus, Richmond, VA, USA

José Manuel Velasco Bueno, RN Hospital Universitario Virgen de la Victoria, Málaga, Spain

Luis A. Bustamante, MD Trauma Intensive Care Unit, San Fernando/Valle Salud Clinic, Cali, Colombia

Digna Cabral, MD Department of Neurology, Miller School of Medicine, University of Miami, Miami, FL, USA

Simone Caccia, MD Department of Surgical Sciences, Division of Anesthesia and Intensive Care, University of Turin, Turin, Italy

Juliana Caldas, MD, PhD Department of Anesthesia, University of Sao Paulo, Butanta, Sao Paulo, Brazil

Critical Care Unit Hospital São Rafael Salvador, Salvador, Brazil

Leanne A. Calviello, BA, MSc Division of Neurosurgery, Department of Clinical Neurosciences, Cambridge Biomedical Campus, University of Cambridge, Cambridge, UK

Nelly Campo, MD Department of Neurology, Miller School of Medicine, University of Miami, Miami, FL, USA

Pol Camps-Renom, MD, PhD Department of Neurology, Hospital de la Santa Creu i Sant Pau, Universitat Autònoma de Barcelona, Barcelona, Spain

Biomedical Research Institute Sant Pau (IIB-Sant Pau), Barcelona, Spain

Danilo Cardim, MD, PhD Brain Physics Laboratory, Division of Neurosurgery, Department of Clinical Neurosciences, Addenbrooke's Hospital, University of Cambridge, Cambridge, UK

Institute for Exercise and Environmental Medicine, Texas Health Presbyterian Hospital Dallas, Dallas, TX, USA

Department of Neurology and Neurotherapeutics, University of Texas Southwestern Medical Center, Dallas, TX, USA

Anselmo Caricato, MD Department of Anesthesia and Intensive Care, NeuroIntensive Care, IRCCS Policlinico Universitario "A. Gemelli", Rome, Italy

Jorge Carrizosa, MD, MSc, NVS Intensive Care Medicine, Hospital Universitario Fundación Santa Fé, Bogotá, Colombia

Neurointensive Care section - AMCI, Bogotá, Colombia

Juan Fernando Gómez Castro, MD Pediatric Neurology Department, Hospital Universitario Valle del Lili, Cali, Colombia

Pedro Castro, MD, PhD Department of Clinical Neurosciences and Mental Health, Faculty of Medicine of University of Porto, Porto, Portugal

Department of Neurology and Stroke Unit, Centro Hospitalar Universitário de São João, E.P.E, Porto, Portugal

Giulia Catozzi, MD Department of Surgical Sciences, Division of Anesthesia and Intensive Care, University of Turin, Turin, Italy

Jorge Cerdá, MD, MSc, FACP, FASN Nephrology Division, Department of Medicine, Albany Medical College, Albany, NY, USA

Karthikka Chandrapatham, MD Department of Surgical Sciences and Integrated Diagnostics, Anaesthesia and Intensive Care, San Martino Policlinico Hospital, IRCCS for Oncology, University of Genoa, Genoa, Italy

Davide Chiumello, MD SC Anestesia e Rianimazione, Ospedale San Paolo – Polo Universitario, ASST Santi Paolo e Carlo, Milan, Italy

Dipartimento di Scienze della Salute, Università degli Studi di Milano, Milan, Italy

Centro Ricerca Coordinata di Insufficienza Respiratoria, Università degli Studi di Milano, Milan, Italy

Juan Diego Ciro, MD, MSc Anesthesiology – Intensive Care Medicine, ICU Department, Clínica Las Américas, Medellin, Colombia

Neurointensive Care Section – AMCI, Bogotá, Colombia

José Coelho, MD Neurosonology Laboratory, Centro Hospitalar e Universitário de Coimbra, Coimbra, Portugal

Alain Combes, MD, PhD Reanimation Service, Institute of Cardiology, Groupe Hospital Pitié–Salpêtrière, Public Assistance – Hospital of Paris, Paris, France

Sorbonne University, UPMC University Paris 06, Institute of Cardiometabolism and Nutrition, Paris, France

Etienne Couture, MD Department of Anesthesiology, Montreal Heart Institute, Université de Montréal, Montreal, QC, Canada

Ilaria Alice Crippa, MD Department of Intensive Care, University of Brussels, Erasme Hospital, Brussels, Belgium

László Csiba, MD, PhD, DSci, MHAS Neurologist, Department of Neurology, Clinical Center Debrecen University, Advisory Board - ESNCH. Hungarian Neurological Society, Debrecen, Hungary

Brett L. Cucchiara, MD Department of Neurology, University of Pennsylvania, Philadelphia, PA, USA

Thomas J. Cusack, MD, MSc Division of Neurosciences Critical Care, Departments of Neurology, Neurosurgery, and Critical Care Medicine, The Johns Hopkins Hospital, Baltimore, MD, USA

Marek Czosnyka, PhD Department of Clinical Neurosciences, Cambridge Biomedical Campus, University of Cambridge, Cambridge, UK

Rosa Elena de la Torre Gómez, MD National Medical Center of Western IMSS, Guadalajara, Mexico

André Y. Denault, MD Department of Anesthesiology and Intensive Care Unit, Montreal Heart Institute, Université de Montréal, Montreal, QC, Canada

Nicolás de Riva Solla, MD, PhD Neuroanesthesia Division, Anesthesiology Department, CLINIC Hospital, Barcelona, Spain

Bahattin B. Ergin, BSN, RVT Anesthesiology & Critical Care Medicine, The Johns Hopkins University School of Medicine, Baltimore, MD, USA

Michael Ertl, MD Department of Neurology, University Clinic Augsburg, Augsburg, Germany

Cyrus G. Escabillas, MD Jose R. Reyes Memorial Medical Center, Manila, Philippines

Laura Llull Estrany, MD Cerebral Vascular Pathology Unit, Hospital Clínic, Barcelona, Spain

David H. Evans, PhD, DSc Department of Cardiovascular Sciences, University of Leicester, Leicester, UK

Filippo Farina, MD Department of Neuroscience, University of Padua School of Medicine, Padova, Italy

Felix Schlachetzki, MD Department of Neurology, Center for Vascular Neurology and Neurointensive Care, University of Regensburg, medbo Bezirksklinikum Regensburg, Regensburg, Germany

Ryan Fillmore, MD Department of Neurology-Neurocritical Care, The University of California, Irvine, Orange, CA, USA

Tiffany Fong, MD, FACEP Division of Emergency Ultrasound, Department of Emergency Medicine, The Johns Hopkins University School of Medicine, Baltimore, MD, USA

Paolo Formenti, MD SC Anestesia e Rianimazione, Ospedale San Paolo – Polo Universitario, ASST Santi Paolo e Carlo, Milan, Italy

Marta García-Orellana, MD Neuroanesthesia Division, Anesthesiology Department, CLINIC Hospital, Barcelona, Spain

Thomas Geeraerts, MD Department of Anesthesiology and Intensive Care, University Hospital of Toulouse, Toulouse NeuroImaging Center (ToNIC), Inserm, Toulouse, France

Rick R. Gill, MD Department of Neurology, Loyola University, Chicago, IL, USA

Joffre Guzman, MD Neuroscience Institute, El Bosque University, INUB – Meditech Research Group, Bogotá, Colombia

Ryan Hakimi, DO, MSc, FNCS, NVS Neuro ICU, TCD Services, Prisma Health-Upstate, Greenville, SC, USA

Department of Medicine (Neurology), USC School of Medicine-Greenville, Greenville, SC, USA

American Society of Neuroimaging (ASN), Minneapolis, MN, USA

Antoine Halwagi, MD Department of Anesthesiology and Intensive Care Unit, Centre Hospitalier de l'Université de Montréal, Montreal, QC, Canada

C. Hoedemaekers, MD, PhD Department of Intensive Care, Radboud University Medical Center, Nijmegen, The Netherlands

Chiara Izzo, MD Department of Neurosciences and Mental Health, Neurosonology, Sapienza, University of Rome, Rome, Italy

Leilani Johnson, MSc Neurology, Wake Forest School of Medicine, Winston-Salem, NC, USA

Mohammed F. Kananeh, MD Department of Neurological Surgery, Vickie and Jack Farber Institute for Neuroscience, Thomas Jefferson University, Philadelphia, PA, USA

Vendel Kemény, MD, PhD Director of Early Phase Clinical Services at ICON plc, Budapest, Hungary

Szentendre Medical Center, Szentendre, Hungary

Mustafa Kilic, MD Department of Neurology, Center for Vascular Neurology and Neurointensive Care, University of Regensburg, medbo Bezirksklinikum Regensburg, Regensburg, Germany

Francisco Klein, MD Neuroscience Institute, Hospital Universitario Fundación Favaloro, Buenos Aires, Argentina

Monisha A. Kumar, MD, FNCS HUP Neuro ICU, Philadelphia, PA, USA

HUP Neuro ICU, Departments of Neurology, Neurosurgery and Anesthesiology and Critical Care, Hospital of the University of Pennsylvania, Philadelphia, PA, USA

University of Pennsylvania Health System, Philadelphia, PA, USA

Demetrios J. Kutsogiannis, MD Critical Care Medicine, Neurocritical Care (UCNS), Neurosciences ICU, The University of Alberta, Royal Alexandra Hospital ICU, University of Alberta Hospital, Edmonton, AB, Canada

Gabriel Heras La Calle, MD, PhD-Cand Head of Intensive Care Department, Hospital Comarcal Santa Ana de Motril, Motril, Granada, Spain

International Research Project for the Humanization of Intensive Care Units, HU-CI Project, Universidad Francisco de Vitoria, Madrid, Spain

Lehel Lakatos, MD Department of Neurology, Luzerner Kantonsspitals, Lucerne, Switzerland

Stéphane Langevin, MD Department of Anesthesiology and Intensive Care Unit, Institut universitaire de cardiologie et de pneumologie de Québec, Laval University, Québec, QC, Canada

Yoann Launey, MD, PhD Intensive Care Unit, Department of Anaesthesia, Critical Care and Perioperative Medicine, Centre Hospitalier Universitaire de Rennes, Rennes, France

Christos Lazaridis, MD, EDIC Neurocritical Care, Departments of Neurology and Neurosurgery, University of Chicago, Chicago, IL, USA

Loïc Le Guennec, MD, PhD Sorbonne University, Paris, France

Intensive Medicine Neurologic Reanimation, Hôpital Pitié-Salpêtrière, Paris, France

Peter Le Roux, MD, FACS, FNCS Division of Neurosurgery, Main Line Health, Wynnewood, PA, USA

Lankenau Institute of Medical Research, Wynnewood, PA, USA

Piergiorgio Lochner, MD, PhD Department of Neurology, Saarland University Medical Center, Homburg, Germany

Ezequiel Luna, MD Intensive Care Medicine, Sanatorio Güemes, Buenos Aires, Argentina

University of Buenos Aires (UBA), Buenos Aires, Argentina

Branko Malojcic, MD, PhD, FESO, FWSO Director of TIA Centre, Department of Neurology, University Hospital Center Zagreb, Zagreb School of Medicine, Zagreb, Croatia

Secretary - ESNCH, Oslo, Norway

Edward M. Manno, MD, MSc Department of Neurology, Northwestern University Feinberg School of Medicine, Chicago, IL, USA

Juliana Mendoza Mantilla, MD Neuroscience Institute, El Bosque University, INUB – Meditech Research Group, Bogotá, Colombia

Luciana Mascia, MD, PhD Dipartimento di Scienze Biomediche e Neuromotorie, University of Bologna, Bologna, Italy

Anna Teresa Mazzeo, MD Department of Adult and Pediatric Pathology, University of Messina, AOU Policlinico G. Martino, Messina, Italy

L. Luciano Ponce Mejia, MD Departments of Neurology, The Johns Hopkins University School of Medicine, Baltimore, MD, USA

Jorge H. Mejía Mantilla, MD, MSc, FNCS Head Neurointensive Care Unit, Department of Critical Care and Anesthesiology, Hospital Universitario Fundación Valle del Lili, Cali, Colombia

Milija Mijajlovic, MD, PhD, FEAN Clinical Case Reports Journal, EAN Neurosonology Scientific Panel, Neurology Clinic, Clinical Center of Serbia, Faculty of Medicine, University of Belgrade, Belgrade, Serbia

Member At-Large - ESNCH, Oslo, Norway, Oslo

Leandro Moraes, MD Intensive Care Center, Hospital de Clinicas, School of Medicine, University of the Republic, Montevideo, Uruguay

Martin Müller, MD Department of Neurology, Luzerner Kantonsspitals, Lucerne, Switzerland

Andrea Naldi, MD Department of Neuroscience Rita Levi Montalcini, University of Turin, Turin, Italy

Jose C. Navarro, MD Jose R. Reyes Memorial Medical Center, Department of Neurology, Institute of Neurosciences, St Luke's Medical Center, University of Santo Tomas, University of Santo Tomas Hospital, Manila, Philippines

László Oláh, MD, PhD, DSci Neurologist, Department of Neurology, Debrecen University, Committee Member - ESNCH, Debrecen, Hungary

Mareike Österreich, MD Department of Neurology, Luzerner Kantonsspitals, Lucerne, Switzerland

Alshimaa Shaban Othman, MD Kasr-Alainy School of Medicine, University of Cairo, Cairo, Egypt

Gyula Pánczél, MD, PhD Department of Neurology, Ferenc Flór County Hospital, Kistarcsa, Hungary

Ronney B. Panerai, PhD Department of Cardiovascular Sciences, University of Leicester, Leicester, UK

Fabienne Perren, MD, PhD University Hospital and Medical Faculty, Department of Clinical Neurosciences, LUNIC Laboratory, Neurocenter of Geneva, Geneva, Switzerland

Committee Member - ESNCH, Oslo, Norway

Oscar M. Pinillos, MD, MSc Intensive Care Medicine, Clinica de Occidente, Cali, Colombia

Neurointensive Care section - AMCI, Bogotá, Colombia

Deborah Pugin, MD Intensive Care Medicine and Neurology, FMH Chez Centre Qorpus. Clinique des Grangettes, Geneva, Switzerland

Corina Puppo, MD Intensive Care Unit, Clinics Hospital, Universidad de la Republica School of Medicine, Montevideo, Uruguay

Alexander Razumovsky, PhD, FAHA, NVS TCD Global Inc., York, PA, USA

Specialty Care, Inc., York, PA, USA

Lucía Rivera Lara, MD, MPH Department of Neurology, Anesthesiology and Critical Care Medicine, The Johns Hopkins School of Medicine, Baltimore, MD, USA

Chiara Robba, MD, PhD Department of Anaesthesia and Intensive Care, Ospedale Policlinico San Martino IRCCS, IRCCS for Oncology, University of Genoa, Genoa, Italy

Deputy Neurointensive Care section - ESICM, Brussels, Belgium

Pierre Robillard, MD Department of Radiology, Montreal Heart Institute, Université de Montréal, Montreal, QC, Canada

Camilo N. Rodríguez, MD Intensive Care Medicine, Hospital Nacional Prof. Dr. A. Posadas, University of Buenos Aires (UBA), Neurointensive Care Section -

ESICM, Neurointensive Care Section - AMCI, Neurointensive Care Committee - FEPIMCTI, Member of ESNCH, Buenos Aires, Argentina

José María Domínguez Roldán, MD Intensive Care Department, Hospital Universitario Virgen del Rocío, Seville, Spain

Andrés M. Rubiano, MD, PhD Neuroscience Institute, El Bosque University, INUB – Meditech Research Group, Bogotá, Colombia

Trauma Intensive Care Unit, San Fernando/Valle Salud Clinic, Cali, Colombia

Tatjana Rundek, MD Evelyn F. McKnight Brain Institute, Department of Neurology, Miller School of Medicine, University of Miami, Miami, FL, USA

Maher Saqqur, MD, MPH, FRCPC Division of Neurology, Department of Medicine and Department of Radiology, Mackenzie Health Sciences Centre, University of Alberta, Edmonton, AB, Canada

Neuroscience Institute, Hamad General Hospital Doha, Doha, Qatar

João Sargento-Freitas, MD Neurologist, Neurosonology Laboratory, Centro Hospitalar e Universitário de Coimbra, Coimbra, Portugal

Faculdade de Medicina da Universidade de Coimbra, Coimbra, Portugal

Committee Member - ESNCH, Oslo, Norway

Aarti Sarwal, MD, FNCS, FAAN Neurology, Wake Forest School of Medicine, Winston-Salem, NC, USA

Neurocritical Care Society (NCS), Chicago, IL, USA

Claudio E. Scherle Matamoros, MD Department of Neurology, Stroke Unit, Eugenio Espejo Hospital, Quito, Ecuador

Syed Omar Shah, MD, MBA Department of Neurological Surgery, Vickie and Jack Farber Institute for Neuroscience, Thomas Jefferson University, Philadelphia, PA, USA

Vijay K. Sharma, MD Division of Neurology, National University Health System, Singapore and Yong Lo Lin School of Medicine, National University of Singapore, Singapore, Singapore

Fernando Silva, MD Neurosonology Laboratory, Centro Hospitalar e Universitário de Coimbra, Coimbra, Portugal

Marialaura Simonetto, MD Department of Neurology, Miller School of Medicine, University of Miami, Miami, FL, USA

Antonio Siniscalchi, MD Department of Neurology and Stroke Unit, Annunziata Hospital, Cosenza, Italy

Sanjeev Sivakumar, MD Department of Neurology, University of South Carolina-Greenville School of Medicine, Greenville, SC, USA

Ricardo Soares-dos-Reis, MD, MSc Department of Clinical Neurosciences and Mental Health, Faculty of Medicine of University of Porto, Porto, Portugal

Department of Neurology, Centro Hospitalar Universitário de São João, E.P.E., Porto, Portugal

Farzeneh Sorond, MD, PhD Department of Neurology, Northwestern University Feinberg School of Medicine, Chicago, IL, USA

Ryan Splittgerber, PhD Department of Surgery, Vanderbilt University Medical Center, Office of Health Sciences Education, Vanderbilt University School of Medicine, Nashville, TN, USA

Eleonora Stival, MD Department of Anesthesia and Intensive Care, NeuroIntensive Care, IRCCS Policlinico Universitario "A. Gemelli", Rome, Italy

José I. Suárez, MD, FNCS, FANA, FAAN Division of Neurosciences Critical Care, Departments of Anesthesiology and Critical Care Medicine, Neurology, and Neurosurgery, The Johns Hopkins University School of Medicine, Baltimore, MD, USA

María Natalia Suárez, MD Health Faculty, South-Colombian University, Neiva, Colombia

Silvana Svampa, MD Intensive Care Medicine, CMIC Clinic, Neuquén, Argentina

Medical Foundation of Río Negro and Neuquén, Cipolletti, Río Negro, Argentina

SATI, Buenos Aires, Argentina

Fabio Silvio Taccone, MD, PhD Emergency Medicine, University Libre of Brussels, Brussels, Belgium

Department of Intensive Care, Laboratory of Experimental Research, Erasme Hospital, Brussels, Belgium

Francisco Tamagnone, MD Intensive Care Medicine, Critical Care Ultrasound, University of Buenos Aires (UBA), Buenos Aires, Argentina

Bernardino Rivadavia Hospital, Buenos Aires, Argentina

Jeanne Teitelbaum, MD Section of Neurocritical Care, Department of Neurology, Montreal Neurological Institute, McGill University, Montreal, QC, Canada

Michele Umbrello, MD SC Anestesia e Rianimazione, Ospedale San Paolo – Polo Universitario, ASST Santi Paolo e Carlo, Milan, Italy

Teelkien Van Veen, MD, PhD Department of Obstetrics and Gynecology, University of Groningen, Groningen, The Netherlands

Ricardo Varela, MD Neurosonology Laboratory, Centro Hospitalar e Universitário de Coimbra, Coimbra, Portugal

Panayiotis N. Varelas, MD, PhD, FNCS, FAAN Department of Neurology, Albany Medical Center, Albany, NY, USA

Sebastián Vásquez, MD Neurology Department, Rosario University, Bogotá, Colombia

Neuroscience Institute, El Bosque University, INUB – Meditech Research Group, Bogotá, Colombia

Carla Venegas, MD Critical Care Medicine, Mayo Clinic, Jacksonville, FL, USA

Edoardo Vicenzini, MD, PhD Department of Neurosciences and Mental Health, Neurosonology Sapienza, University of Rome, Rome, Italy

Member - ESNCH, Oslo, Norway

Leidy Gaviria Villarreal, MD Clinical Research Unit, Hospital Universitario Valle del Lili, Cali, Colombia

Markus Webert, MD Department of Neurology, Center for Vascular Neurology and Neurointensive Care, University of Regensburg, medbo Bezirksklinikum Regensburg, Regensburg, Germany

Dixon Yang, MD Department of Neurology, New York University Langone Health, New York, NY, USA

Bernardo Yelicich, Electronic Engineer Engineering (Ing), Universidad de la República – Montevideo Uruguay, Neuromonitoring Group of the Hospital de Clínicas, Montevideo, Uruguay

Frederick A. Zeiler, BSc, MD, PhD, CIP, FRCSC Section of Neurosurgery, Department of Surgery, Department of Human Anatomy and Cell Science, Rady Faculty of Health Sciences, University of Manitoba, Winnipeg, MB, Canada

Wendy Ziai, MD, MPH Division of Neurosciences Critical Care, Departments of Neurology, Neurosurgery, and Critical Care Medicine, The Johns Hopkins Hospital, Baltimore, MD, USA

Vasso Zisimopoulou, MD Air Force General Hospital, Athens, Greece

Part I
Neurocritical Care: Concepts to Review

Chapter 1
Neurocritical Patient in ICU: An Humanized View of Our Medical Care as a Gold Standard

Gabriel Heras La Calle and José Manuel Velasco Bueno

Key Points

1. You only have to walk through the door of a hospital to realize the discomfort of patients, families, and professionals.
2. To humanize is not "goodism": it is to promote professional excellence with the necessary human and technological means and attitudes. And this also requires economic investment.
3. When different personal, group, and organizational factors come together, personal wear and tear is very considerable, and the well-known burnout syndrome can appear. Recently, a 54% burnout rate has been published among intensivists in the United States.
4. So, how to humanize the medical care of the neurocritical patient? Well, that, dear reader, depends on you.

1.1 Introduction: What Do We Call the Humanization of Health Care?

Of all the professions, health care should be a paradigm of human treatment par excellence. Those of us who choose to serve others in the worst moments of their

G. Heras La Calle (✉)
Head of Intensive Care Department, Hospital Comarcal Santa Ana de Motril, Granada, Spain

International Research Project for the Humanization of Intensive Care Units, HU-CI Project, Universidad Francisco de Vitoria, Madrid, Spain
e-mail: gabi@proyectohuci.com

J. M. V. Bueno
Hospital Universitario Virgen de la Victoria, Málaga, Spain
e-mail: jm.velasco@proyectohuci.com

C. N. Rodríguez et al. (eds.), *Neurosonology in Critical Care*,
https://doi.org/10.1007/978-3-030-81419-9_1

lives, when illness is present, should be worthy of the admiration and respect from the rest of the society. But… Aren't we human beings who are posing the prospect of the humanization of our care?

Obviously we are, although for many reasons we have been able to put excellence in treatment to one side. One only has to walk through the door of a hospital to realize the discomfort of patients, families, and professionals.

Scientific development has contributed to a notable improvement in health outcomes, thanks to technological innovation, the strengthening of research, and the objectification of decision-making. Thus, in the last 50 years, survival rates and life expectancy have been improved.

But perhaps health care has focused on solving problems called diseases rather than on the expression of these diseases in people. Technological euphoria has been able to make us lose the true focus of our human condition, which is fallible, finite, and deadly.

On the other hand, we are part of a complex socio-health world in which relationships are established between people with different roles and interests: patients, families, and professionals. These relationships are affected by different factors: high care burden, job cuts, lack of means, and little margin of error, factors that can lead to depersonalized care and generate a poor experience for users of the system. The depersonalization of professionals, together with emotional fatigue and low personal fulfilment, constitutes the so-called burnout syndrome, a real epidemic that many scientific societies are beginning to echo and to which solutions must be found.

How can we not talk about humanizing health care?

For the experts in this ancestral subject, to humanize means "to refer to man in everything that is done to promote and protect health, to cure illnesses, to guarantee an environment that favors a healthy and harmonious life on a physical, emotional, social and spiritual level. To speak of humanization calls for the intrinsic dignity of every human being and the rights that derive from it. And this makes it a necessity of vital importance and transcendence" [1].

The affective-effective model inspired by the thought and values of Albert Jovell [2]: "It is the way to care for and cure the patient as a person, based on scientific evidence, incorporating the dimension of the patient's dignity and humanity, establishing care based on trust and empathy, and contributing to their well-being and the best possible health outcomes."

In recent years, different projects at the local and international level have made the humanization of health care a new discipline, as has happened with patients' safety, for example. This is an absolutely transversal issue that is of social interest and crosses the barriers of hospitals and health centers: patients, families, and professionals together with managers and health authorities are considering re-designing health systems and focusing them on the main actors [3]. Taking care of all the parties who live together in the health system on a daily basis is a necessity; we would say almost a matter of survival and the way to building excellent health. To do so, we believe that it is necessary to listen to and attend to the particular problems of each actor, to respond to their needs, and to understand that the balance depends on the well-being of all those involved, and that it is everyone's responsibility as well.

Therefore, and by way of summary, we could point out that:

1. Humanizing health care means transforming hospitals into friendlier and more human-centered places, regardless of their role.
2. To humanize is to seek excellent care, and also to understand and accept that we professionals are fallible, vulnerable, and have the right to express our emotions.
3. To humanize is to become aware of oneself: it is an important personal commitment to improve reality, our relationships, and the environment from each person: it is humanized from the inside out.
4. Humanizing means personalizing care by listening to what patients and families need, not what we think they need, and turning this into a clinical process where attitude is fundamental. Healthcare systems will be humanized when they are at the service of all people.
5. To humanize is not to "appear good": it is to promote professional excellence with the necessary human and technological means and attitudes. And this also requires economic investment.

And the key to this, on which to focus the meaning of humanizing health care, is to recover the meaning of people's true dignity.

1.2 How Is Critical Care Humanized?

In February 2014, the project HU-CI was born in Spain [4]: the international research project for humanizing intensive care. Through the creation of a multidisciplinary group of people, made up of patients, families, and health professionals (doctors, nurses, assistants, psychologists, etc.) and non-health professionals (architects, computer scientists, designers, and teachers), an international and collaborative research group was set up based on the following premises, with the aim of redesigning health care [5].

After listening to thousands of opinions collected through the project HU-CI blog and cocreated by all the main actors, the eight research lines of the project were defined [6] (Fig. 1.1). Through the network research, we intend to evaluate different areas and carry out the implementation of the corresponding improvement actions.

1.2.1 Open-Door ICU: Presence and Participation of Family Members in ICU

The policy of family visits to ICU patients has historically followed a restrictive model [7] due to different factors:

- False beliefs
- Customs

Fig. 1.1 The HU-CI project research lines

- Emotional exhaustion
- ICU structure problems
- Family interference in medical care
- Security
- Infection control
- Lack of communication skills

Currently, there is sufficient evidence in the literature to promote a change in this policy [8]. The experience in this regard of pediatric and neonatal ICUs, where parents and usual caregivers are considered fundamental in the comprehensive care of the patient, has much to contribute to adult therapies. Flexible schedules are beneficial for patients, families, and professionals.

The existing barriers to change in this sense are related to the physical structure of the units and the mental structure of the professionals. The solution must come

from dissemination and training based on the successful experiences of other units, new attitudes, and habits that allow a modification of the visiting policy and that are adapted to each unit. Likewise, it is essential to value the family as a "companion in care," thus eradicating the concept of "visit." Thus, family members can collaborate in basic care together with the staff: cleaning, rehabilitation, feeding, training, and supervised learning opportunities are encouraged for them. Giving the family the opportunity to contribute to the patient's recovery can have positive effects on the patient, themselves, and professionals by reducing emotional stress and facilitating closeness and communication between the parties involved.

Many critically ill patients are subjected to aggressive or interventional techniques. The presence of family members, also during certain procedures, is accompanied by changes in the attitude of professionals, in terms of privacy, dignity, and pain management, during such procedures. In addition, greater satisfaction of the families and a greater acceptance of the situation have been achieved by favoring the mourning process in the case of cardiopulmonary resuscitation. The presence and participation of the family members [9] in the daily rounds also contribute to the improvement of communication and favor the opportunity to ask questions and clarify information, increasing their satisfaction.

1.2.2 Communication

Communication is the key element in human relations, and improving it is one of the basic and priority pillars of HU-CI project.

With an effective communication (complete, clear, opportune, and concise) shared by the whole team, we avoid mistakes and we agree on treatments and care. The moments of transfer of information in the ICUs are frequent and very important since in them relevant information can be omitted or misinterpreted [10].

The use of tools such as working by daily objectives, checklists, briefings, random analysis of real-time security (RARTS), or the situation/background/assessment/recommendation (SBAR) technique facilitates multidisciplinary participation and makes these processes more effective and safe.

Team cohesion can be improved through support strategies and the acquisition of "non-technical" skills (human tools) that minimize the occurrence of conflicts related to communication problems. These conflicts affect the team and directly influence the well-being of the patient and the family, generate professional wear and tear, and have an impact on the results.

Many of the problems that are generated in hospitals stem from poor communication, and in critical care, from poor information to families and patients. Historically, professionals have not been taught at university in these skills, if it is known that proper communication with patients and families helps to foster a climate of trust and respect, and facilitates joint decision-making. Furthermore, on many occasions, the information demands of families and patients have little to do with the information provided by health professionals. The participation of the

nurse in the information is, in general, insufficient and not clearly defined, despite the fundamental role they play in the care of the critically ill patient and his/her family members.

The use of augmentative and/or alternative communication systems in those patients who cannot speak for different reasons and which replace oral language when it is not understandable or absent, is very useful as tools to facilitate communication, putting technology at the service of people.

1.2.3 Well-Being of the Patient

Although it is perhaps the most obvious line and one of the basic objectives of the critics' units, it is not always developed with excellence. The disease itself and the procedures necessary to achieve cure generate discomfort and pain in patients [11]. And on many occasions, the scales that ensure the well-being of the patient are not applied routinely.

Both physical and emotional factors generate suffering in critical patients: they suffer from pain, thirst, heat, and cold; difficulty in resting due to excessive noise or lighting; and are limited in their mobilization, often due to the use of unnecessary restraints and other sequelae generated in the ICU, such as polyneuropathy of the critical patient. Continuous assessment and pain control, dynamic sedation appropriate to the patient's condition [12], and prevention and management of acute delirium [13] are essential to improve patient's comfort.

In addition, patients and their families also experience feelings of loneliness, isolation, fear, loss of identity, intimacy, and dignity, feelings of dependency, uncertainty due to lack of information, and misunderstanding, among others [14]. The assessment and support of these needs must be considered a key element of quality care. Ensuring adequate training of professionals and promoting measures aimed at treating or mitigating these problems, ensuring the well-being of patients, is a major objective in the care of the critically ill [15].

1.2.4 Care of the Professional

Healthcare professionals, and more so in the critical care field, are exposed to human suffering on a daily basis. We achieve great miracles when patients who would have died survive thanks to our knowledge and its technical application. However, when various personal, group, and organizational factors come together, the personal wear and tear is very considerable, and the well-known burnout syndrome can appear. Recently, a 54% professional burnout rate has been published among intensivists in the United States.

The burnout syndrome is a disorder that encompasses different aspects: emotional exhaustion, depersonalization, and feelings of low professional self-esteem. This problem affects both personally and professionally and can lead to posttraumatic stress syndrome and other serious psychological disorders and even to suicide. The presence of these problems influences the quality of care, patient outcomes, and patient satisfaction, and is related to the lack of involvement of professionals in organizations [16].

Having a healthy organization where professionals feel cared for should become an essential requirement for any organization [17], which must set itself a series of objectives oriented toward the execution of preventive and therapeutic actions. Different scientific societies have tried to give diffusion and visibility to this problem, offering recommendations to reduce its appearance and to mitigate its consequences; establishing concrete strategies that allow to give an appropriate answer to the physical, emotional, and psychological needs of the professionals of intensive care, derived from their dedication and effort in the performance of their work.

1.2.5 Post-ICU Syndrome

A very high percentage of patients (more than 35%) go through the ICU with a series of possible complications that since 2010 are known as post-ICU syndrome:

- *Physical problems* (persistent pain, weakness acquired during hospitalization, malnutrition, pressure ulcers, sleep disturbances, and need for use of devices)
- *Neuropsychological disorders* (cognitive deficits, memory disorders, attention, and speed of mental process)
- *Emotional disorders* (anxiety, depression, or posttraumatic stress)

Their medium- and long-term consequences affect the quality of life of patients and families by increasing healthcare expenditure.

Minimizing the appearance of post-ICU syndrome requires preventive activities, as well as correct treatment and follow-up of known disorders. This requires sensitized and trained multidisciplinary teams that begin their work during admission to the unit and continue it once the unit has been abandoned.

Family members and relatives can be a fundamental part of the management of post-ICU syndrome, participating in the care of the patient and helping him/her to remain oriented [18]. In fact, it is known that primary caregivers bear a huge share of the overall health care costs of a country. Caregivers can also be affected by feelings of worry and confusion that can lead them to neglect their own health, and they can suffer from the post-ICU syndrome of the family member. The health care team must be aware of this in order to recognize and also provide support to the family members who need it: This is where the care of the patient-family pairing takes on fundamental importance.

1.2.6 Humanized Infrastructure

The architectural and structural design of the ICUs is one of the main arguments that hinder a humanized provision of care. In many parts of the world, there are still units with open spaces in which several patients are located, separated by screens or curtains, which do not respect the right to privacy. This makes the possibility of family accompaniment difficult; patients who are admitted feel exposed to others in moments of great weakness and vulnerability. On the other hand, these distributions do not contribute to the establishment of personalized relationships between the professionals and the patients they attend.

This strategic line proposes and promotes the creation of spaces where technical efficiency goes hand in hand with quality of care and the comfort of all users: patients, families, and professionals. There are recommendations focused on reducing stress and promoting comfort by focusing on architectural and structural improvements to ICUs [19], which often require significant economic resources, especially in those places built long ago and which require comprehensive reforms.

Other changes consider an appropriate location, as well as adaptation to users and workflows in adequate environmental conditions of light, temperature, noise, materials and finishes, furniture, and decoration. The incorporation of vinyl, artificial windows where natural light is not available, decorative elements, and others that facilitate the temporal and spatial orientation of patients requires minimal investment and can considerably increase the comfort and satisfaction of all involved. These modifications can have a positive influence on feelings and emotions by favoring human spaces adapted to the functionality of the units.

These concepts are equally applicable to waiting rooms, which must be redesigned to become "living rooms" and offer greater comfort and functionality to families, and equally to staff's work and rest spaces.

1.2.7 End-of-Life Care

Between 10% and 15% of the time, depending on the country, it is impossible to restore the patient's previous situation and achieve a cure. In these situations, we must be able to reconsider the objectives in order to direct them toward reducing suffering and providing the best possible care, especially at the end of life [20]. To allow a death free of discomfort and suffering for the patient and family members, according to their wishes and clinical, cultural, and ethical standards, is another of the objectives of the H-ICU project, starting from the idea that palliative and intensive care are not exclusive options, but should coexist during the whole process of care of the critically ill patient.

The limitation of life support, frequently in the critically ill patient, must be carried out following the guidelines and recommendations established by the scientific societies [21]. It should be applied as part of a global palliative care plan [22], in a

multidisciplinary manner, with the aim of covering the needs—physical, psychosocial, and spiritual—of the patients and their families. The existence of specific protocols and the periodic evaluation of the care offered should be considered basic requirements.

Decisions at the end of life are not exempt from discrepancies between health professionals and between health professionals and family members [23]. Professionals must have the necessary skills and tools for the resolution of these conflicts, incorporating open and constructive discussion in these situations, as coping strategies to reduce the emotional burden derived from them.

1.3 Conclusion: How to Give an Humanized Attention to a Neurocritical Patient?

In December 2017, the HU-CI project certification working group [24] prepared the Manual of Good Practices for the Humanization of Intensive Care Units (Fig. 1.2), which contains 159 tangible measures to make critical care units more friendly to all

Fig. 1.2 Manual of Good Practices for the Humanization of Intensive Care Units

their stakeholders. In May 2019, this document was revised and one more measure was added [25].

It is an exportable method that can be reproduced anywhere in the world, free to download, with the aim of betting on a revolution written with ¨H¨ [26] (the H-evolution of intensive care units) that will facilitate the reunion with those reasons why one day we decided to dedicate our lives to the service of others: People who help people.

Now then, how can we humanize the care of the neurocritical patient? [27]. Well, that, dear reader, depends on you.

Without a doubt, from our point of view, the fundamental tool will be listening to the protagonists: patients with neurological diseases and patient associations (multiple in the case of diseases with some kind of neurological deficit); the opinion and experience of the relatives, who in large part become the real caretakers of neurocritical patients once they leave the ICU, often victims of states of high dependency; and of course the professionals in the therapies, the real motors of the change that humanizes.

And to design together the health care we deserve wherever we are: The one we always wanted to have, not the one we have inherited from health systems that do not work. Rewriting this history is an exercise in responsibility, not only professional but also personal and social toward our children.

Sometimes utopia is not really different from reality, and of course, HU-CI project has shown that passion moves the world and that if you want to and work you can [28].

In many occasions, a thousand excuses and obstacles will be put to the change: this is also human. But on the other hand, you cannot put doors to the sea, and anyone who still does not understand this *blessed madness*, perhaps will understand it when he is a user of the system from another role. In the meantime, the question remains:

And you: What can you do to humanize the neurocritical patient units?

References

1. Bermejo JC. Humanizar la asistencia sanitaria. Bilbao: Desclée De Brouwer; 2014.
2. Jovell AJ. Medicina basada en la afectividad. Med Clin (Barc). 1999;113(5):173–5.
3. Davidson JE, Aslakson RA, Long AC, et al. Guidelines for family-centred care in the neonatal, pediatric and adult ICU. Crit Care Med. 2017;45(1):103–28.
4. Heras La Calle G, los miembros de Proyecto HU-CI. Humanizando los cuidados intensivos: presente y futuro centrado en las personas. Bogotá: Distribuna; 2017.
5. Velasco Bueno JM, La Calle GH. Humanizing intensive care: from theory to practice. Crit Care Nurs Clin North Am. 2020;32(2):135–47.
6. Heras G, Alonso A, Gómez V. A plan for improving the humanisation of intensive care units. Intensive Care Med. 2017;43:547–9.
7. Escudero D, Martín L, Viña L, Quindós B, Espina MJ, Forcelledo L, et al. Visitation policy, design and comfort in Spanish intensive care units. Rev Calid Asist. 2015;30(5):243–50.

8. Escudero D, Viña L, Calleja C. Por una UCI de puertas abiertas, más confortable y humana. Es tiempo de cambio. Med Intensiva. 2014;38(6):371–5.
9. Azoulay E, Chaize M, Kentish-Barnes N. Involvement of ICU families in decisions: fine-tuning the partnership. Ann Intensive Care. 2014;4:37.
10. Velasco Bueno JM, Alonso Ovies A, Heras La Calle G, Zaforteza Lallemand C, Equipo de investigación del Proyecto HUCI (Humanizando los Cuidados Intensivos). Principales demandas informativas de los familiares de pacientes ingresados en Unidades de Cuidados Intensivos. Med Intensiva. 2018;42(6):337–45.
11. Alonso-Ovies Á, Heras La Calle G. ICU: a branch of hell? Intensive Care Med. 2016;42:591–2.
12. Vincent JL, Shehabi Y, Walsh TS, Pandharipande PP, Ball JA, Spronk P, et al. Comfort and patient-centred care without excessive sedation: the eCASH concept. Intensive Care Med. 2016;42(6):962–71.
13. Pandharipande PP, et al. The intensive care delirium research agenda: a multinational, interprofessional perspective. Intensive Care Med. 2017;43(9):1329–39.
14. Chamorro C, Romera MA. Pain and fear in the ICU. Med Intensiva. 2015;39:442–4.
15. Morandi A, Piva S, Ely EW, Myatra SN, Salluh JIF, Amare D, et al. Worldwide Survey of the "Assessing Pain, Both Spontaneous Awakening and Breathing Trials, Choice of Drugs, Delirium Monitoring/Management, Early Exercise/Mobility, and Family Empowerment" (ABCDEF) Bundle. Crit Care Med. 2017;45(11):e1111–22.
16. Gálvez Herrer M, Gómez García JM, Martín Delgado MC, Ferrero Rodríguez M, Miembros del proyecto HU-CI. Humanización de la Sanidad y Salud Laboral: Implicaciones, estado de la cuestión y propuesta del Proyecto HU-CI. Med Segur Trab. 2017;63:103–19.
17. Gómez Tello V, Ruiz Moreno J, Weiss M, González Marín E, Merino de Cos P, Franco Garrobo N, et al. Estimación de las necesidades de profesionales médicos en los servicios de medicina intensiva. Med Intensiva. 2018;42(1):37–46.
18. Martín Delgado MC, García de Lorenzo y Mateos A. Surviving the Intensive Care Units looking through the family's eyes. Med Intensiva. 2017;41(8):451–3.
19. Harvey MA, Ninos NP, Adler DC, Goodnough-Hanneman SK, Kaye WE, Nikas DL. Results of the consensus conference on fostering more humane critical care: creating a healing environment. Society of Critical Care Medicine. AACN Clin Issues Crit Care Nurs. 1993;4(3):484–549.
20. Cook D, Rocker G. Dying with dignity in the intensive care unit. N Engl J Med. 2014;370(26):2506–14.
21. Monzón Marín JL, Saralegui Reta I, Abizanda I, Campos R, Cabré Pericas L, Iribarren Diarasarri S, Martín Delgado MC, Martínez Urionabarrenetxea K, Grupo de Bioética de la SEMICYUC. Recomendaciones de tratamiento al final de la vida del paciente crítico. Med Intensiva. 2008;32(3):121–33.
22. Aslakson RA, Curtis JR, Nelson JE. The changing role of palliative care in the ICU. Crit Care Med. 2014;42(11):2418–28.
23. Truog RD, Campbell ML, Curtis JR, Haas CE, Luce JM, Rubenfeld GD, Rushton CH, Kaufman DC, American Academy of Critical Care Medicine. Recommendations for end-of-life care in the intensive care unit: a consensus statement by the American College [corrected] of Critical Care Medicine. Crit Care Med. 2008;36(3):953–63.
24. Grupo de trabajo de certificación de Proyecto HU-CI. Manual de buenas prácticas de humanización en Unidades de Cuidados Intensivos. Madrid: Proyecto HU-CI; 2017.
25. Grupo de trabajo de certificación de Proyecto HU-CI. Manual de buenas prácticas de humanización en Unidades de Cuidados Intensivos. Madrid: Proyecto HU-CI; 2019.
26. Heras G, Zaforteza C. HUCI se escribe con H de Humano. Enferm Intensiva. 2014;25(4):123–4.
27. Heras La Calle G. Humanizar la sanidad es cosa de todos: ¿cómo humanizar la Neurología? Rev Cient Soc Esp Enferm Neurol. 2017;45:1–2.
28. Velasco Bueno JM, Heras La Calle G. Humanizando los cuidados intensivos. De un proyecto inspirador a nuevas realidades. Ética de los Cuidados. 2017;10(20).

Chapter 2
Neuro-ICU: Monitoring and Management of Intracranial Pressure. A Practical Review

Peter Le Roux

Key Points

1. Increased ICP, especially when refractory to treatment, is associated with increased mortality.
2. Total "ICP dose," "area under the ICP curve," temporal evolution of ICP, how ICP responds to treatment, or individualized ICP thresholds may be more important parameters associated with outcome than a simple numeric threshold.
3. Noninvasive technologies to monitor ICP are evolving but currently none are robust enough to allow continuous monitoring in routine practice. Consequently, invasive monitors such as parenchymal ICP monitors or an external ventricular drain are recommended.
4. Rather than treat the ICP number per se, it may be more important to regard this value as a marker of altered physiology and instead find the reason why ICP is elevated and treat that rather than the numeric value alone.
5. Interventions to manage increased ICP include optimizing normal patient physiology; sedation and analgesia; appropriate fluid therapy; blood pressure and hemoglobin management; ventilation; osmotherapy; cerebral spinal fluid (CSF) drainage; metabolic suppression; and surgery ideally performed according to a tiered approach and in a patient-specific targeted approach.

P. Le Roux (✉)
Division of Neurosurgery, Main Line Health, Wynnewood, PA, USA

Lankenau Institute of Medical Research, Wynnewood, PA, USA

C. N. Rodríguez et al. (eds.), *Neurosonology in Critical Care*,
https://doi.org/10.1007/978-3-030-81419-9_2

2.1 Introduction

The prevention and management of increased intracranial pressure (ICP) along with avoiding secondary insults, for example, hypotension and hypoxia, is fundamental to neurocritical care management of acute brain injury including traumatic brain injury (TBI), subarachnoid hemorrhage (SAH), and intracerebral hemorrhage (ICH) among other pathologies. This is important since untreated increased ICP, particularly when refractory to treatment, can reduce cerebral perfusion pressure (CPP) and so contribute to brain ischemia, hypoxia, alter metabolism, and hence, cause or aggravate brain damage [1–5]. In addition, increased ICP can cause herniation and is an important marker of disease severity. The Monro-Kellie doctrine (Eq. 2.1) provides a conceptual framework to understand ICP. Normal adult ICP is between 5 and 15 mmHg. It is lower in children (3–7 mmHg) and in adults will vary with age and body posture. The increase in ICP that results from an increase in intracranial volume follows an exponential curve, so that initial increases in volume are well compensated but further increases will lead to a sharp ICP increase. This compensatory reserve is known as cerebral compliance defined as the change in cerebral volume per unit change in pressure. Hence, the absolute ICP number is less important than the rate of rise and the pressure gradient between compartments. Patients can have a normal ICP and still herniate, and patients with slow, longstanding increases in ICP may be asymptomatic. This emphasizes the role of cerebral autoregulation (CA) and other parameters when considering how best to manage ICP [6].

$$\mathrm{IV} = \left(\mathrm{Brain_v} + \mathrm{CSF_v} + \mathrm{Blood_v} + \mathrm{Mass\ lesion_v}\right) \tag{2.1}$$

IV: intracranial volume, $\mathrm{Brain_v}$: brain volume, $\mathrm{CSF_v}$: cerebral spinal fluid volume, $\mathrm{Blood_v}$: blood volume, $\mathrm{Mass\ lesion_v}$: mass lesion volume.

There are a variety of causes for increased ICP (Table 2.1) [7]. Several clinical and imaging factors may help predict increased ICP and so guide treatment decisions (Table 2.2) [8, 9]. However, management of ICP is best accomplished with use of an ICP monitor [10–15]. ICP monitoring was introduced in the 1950s and today is the most frequently used neuromonitor. ICP has been most frequently studied in TBI, where despite much research and a variety of multidisciplinary consensus statements and guidelines [10–15], there remains much variation in the practice of ICP monitoring and management [16, 17], and debate about use [18]. In part, this is associated with inconsistency in reporting variables or heterogeneity in methodology [19]. Important clinical questions that are still being elucidated include:

1. Which patients should undergo ICP monitoring and for how long?
2. What defines intracranial hypertension?/What threshold should ICP be treated?
3. How should intracranial pressure be monitored?
4. How best to manage increased ICP?
5. Does control of ICP influence outcome?
6. Other monitors necessary to fully understand ICP?

Table 2.1 Causes of increased intracranial pressure

Intracranial
Trauma
• Mass lesion
• Depressed skull fracture
• Brain edema
• Hyperemia
• Hydrocephalus
• Extracranial causes
Nontraumatic intracranial hemorrhage
• Intracerebral
• Subarachnoid
Acute ischemic stroke
Hydrocephalus
• Communicating
• Obstructive
Brain tumor
Seizures
Cerebral vasospasm
Infection
Pseudotumor cerebri
Idiopathic intracranial hypertension
Extracranial (secondary)
Airway obstruction
Hypoventilation
• Hypoxia
• Hypercarbia
Hypertension
Head position or posture
Venous outflow obstruction
Hyperpyrexia
Agitation or pain
Increased intrathoracic or intra-abdominal pressure
Liver failure
Altered sodium balance
Hypoglycemia or hyperglycemia
High-altitude sickness
Drugs

Table 2.2 Predictors of intracranial hypertension

Major criteria
1. Compressed cisterns (Marshall diffuse injury III)
2. Midline shift >5 mm (Marshall diffuse injury IV)
3. Nonevacuated mass lesion (>25 cm^3)
Minor criteria
4. Glasgow Coma Scale ≤ 4
5. Pupillary asymmetry
6. Abnormal pupillary reactivity
7. Marshall diffuse injury II (basal cisterns are present with midline shift of 0–5 mm and/or high- or mixed-density lesion of ≥ 25 cm^3)

Criteria and clinical decision rule were developed by consensus and approved by 97% of participants in a working group of 43 neurosurgeons and intensivists. Increased ICP was considered in the presence of one major or ≥2 minor criteria obtained at baseline following the resuscitation of severe TBI patients [8]

In this chapter, these issues will be briefly reviewed and a pragmatic approach to ICP management provided [20]. The focus is on ICP in adults. There are important anatomic, physiologic, radiologic, and management differences in children, which are beyond the scope of this chapter [21–24].

2.2 Which Patients Should Undergo ICP Monitoring?

ICP monitoring is best studied in TBI, although its uses have been described in several other disorders, for example, SAH, ICH, meningitis, and liver encephalopathy, among others. Hence, the indications for ICP monitoring in neurocritical, in large part, are based on TBI guidelines. Evidence-based guidelines from both Europe and North America recommend use of ICP monitors to assess and manage intracranial hypertension [10–14]. However, the most recent edition (4th edition) [15] of The Brain Trauma Foundation's (BTF) Guidelines indicated there was insufficient evidence to support a level I or IIA recommendation in TBI. In general, an ICP monitor (ICPM) is indicated when clinical or imaging criteria suggest ICP is likely to be—or become—elevated (Table 2.2) [8, 9].

The 3rd edition of the BTF guidelines for TBI recommended ICP should be monitored:

1. In all salvageable TBI patients with a postresuscitation Glasgow Coma Scale (GCS) of 3–8 and an abnormal CT scan
2. In severe TBI patients with a normal CT scan, if two or more of the following admission features are present: age > 40 years, unilateral or bilateral motor posturing, or systolic blood pressure (BP) <90 mmHg [12]

In non-TBI patients (e.g., SAH or ICH), there is no defined consensus on indications for an ICPM. In these patients, TBI guidelines are applied and ICPMs recommended for: reduced GCS (≤8), cerebral edema or mass effect on imaging, and neurological worsening.

The BTF guidelines were based on studies from the 1980s. Since then, image quality has improved and neurocritical care has evolved. This has generated several questions, for example, is an ICPM necessary in a comatose patient with only mild traumatic SAH and open cisterns. This and other questions were addressed in the Milan consensus conference on ICPM [25]. Comatose patients with compressed or absent cisterns (in the absence of mass lesions) should undergo ICP monitoring, whereas those with diffuse brain injury but open cisterns should have repeat CT scanning and an ICPM be inserted in patients with evolving lesions or development of cisternal compression. Other clinical circumstances were addressed in Milan [25]. For example, an ICPM should be considered in select patients with multisystem injuries, severe respiratory issues, those who may require multiple anesthetic procedures or prolonged sedation that preclude neurological assessment, or have large bifrontal contusions even if they present with a GCS > 8. Second, an ICPM can be useful when the neurologic examination is not reliable, for example,

maxillofacial trauma or spinal cord injury. Third, an ICPM is useful in patients who undergo a decompressive craniectomy (DC) or undergo a craniotomy for a mass lesion particularly when there is hypoxia, hypotension, pupil abnormalities, midline shift >5 mm, or brain swelling.

Following surgery (i.e., a craniotomy for a mass lesion or a DCC), an ICPM is pathology dependent. Following evacuation of an acute extradural hematoma (AEDH), ICP increases are rare and, hence, an ICPM is not always needed [25]. By contrast, following removal of an acute subdural hematoma (ASDH), ICP increases associated with intraparenchymal contusions or hematomas or brain swelling are common and can double mortality [26]. In these patients, an ICPM is necessary. Similarly, after decompressive craniectomy, including primary DCC, increased ICP and reduced CPP are common. This increase in ICP is associated with poor outcome and, hence, an ICPM can help guide therapy after DCC [27]. Current DCC guidelines recommend ICPM placement after craniotomy for an ASDH including primary DCC [28].

2.3 How Should Intracranial Pressure Be Monitored?

Intracranial pressure can be monitored with invasive or noninvasive devices that should be supplemented with the clinical examination and CT imaging. There are a variety of signs and symptoms of increased ICP that depend in part on the severity of the increase. However, initial signs are unreliable and nonspecific in the critically ill patient or may be masked by medication, whereas definitive signs often are too late. On CT, compressed or absent basal cisterns suggest increased ICP; when absent, ICP values >30 mmHg are observed in 74% of cases [29, 30].

Noninvasive technologies to measure and monitor ICP are evolving but currently none are robust or accurate enough to allow accurate, continuous monitoring in routine practice. However, these technologies can be used in specific patients when invasive monitoring is contraindicated, for example, coagulopathy or is unavailable [31]. Among the many described noninvasive technologies, transcranial Doppler (including pulsatility index [PI]), optic nerve sheath diameter (ONSD), and automated pupillometry provide high sensitivity, diagnostic accuracy, and correlate well with ICP measurements including over time [32–34].

A variety of invasive techniques can be used: Today, intraparenchymal strain gauge or fiber optic monitors or a ventricular catheter (external ventricular drain [EVD]) are recommended [10, 11, 35]. Fluid-coupled or pneumatic devices placed in the subarachnoid, subdural, or epidural space are less accurate and not recommended [10, 11, 35, 36]. EVDs were long considered the “gold standard” but this is a matter of history (and perhaps cost) rather than merit. In Europe, surveys of neurotrauma centers enrolled in Collaborative European Neurotrauma Effectiveness Research in Traumatic Brain Injury (CENTER-TBI) indicate that one-third use only intraparenchymal monitors but <10% use only EVDs. In centers that use both, EVDs tend to be placed when the ventricles are enlarged or for cerebrospinal fluid

(CSF) diversion [16]. ICP measurements are equally accurate with EVDs or parenchymal monitors. However, EVD accuracy depends on setup and whether the device is being used to drain CSF. Indeed, when CSF is drained, correlation between the two methods can be lost and EVD measurements of ICP may be inaccurate [37, 38]. In addition, there remains a debate on whether CSF should be drained intermittently or continuously. When CSF is being drained, ICP is not measured, although newer devices allow both to occur. Other variables that may be more important than the numeric value of ICP also are not measured with an EVD.

One potential advantage of an EVD is CSF drainage, for example, ICP treatment. This may be relevant in patients with hydrocephalus, but in others CSF drainage influences compliance and in some circumstances may have a deleterious effect on other indices and even CBF. There are several disadvantages when using an EVD and meta-analytic studies demonstrate a greater risk of complications with EVDs [39, 40]. First, an EVD may be difficult to insert when there is brain swelling, small ventricles, or if anatomy is distorted by mass effect. In these patients, a parenchymal monitor that is easier to insert may be preferable. Second EVDs have a greater complication rate than parenchymal monitors. This includes misplacement or technical errors (12% vs. <3%), infection (5–20% vs. <1%), and hemorrhage (5% vs. 1%) [41–44]. However, the exact incidence of infection or hemorrhage depends on how infection (vs. contamination or CSF colonization) is diagnosed or whether routine head CT scans are obtained or not. On the other hand, parenchymal monitors share a common disadvantage, that is, recalibration is not possible after placement and not all devices are MRI compatible. The Spiegelberg catheter (which is pneumatic) is an exception from this rule since it recalibrates itself every hour.

Use of standardized protocols or care bundles (when adhered to) and simulator training can help to increase the safety of ICP monitoring [45, 46]. For example, EVD-associated infection can be reduced with closed drainage systems, a long-tunneled device, avoidance of flushing the system, and CSF sampling only if clinically indicated rather than routinely performed. Infection risk is less with a short duration of CSF drainage (<4 days), although there does not appear to be a role for routine EVD replacement or long-term antibiotic use to prevent infections [43, 47–49]. Today antibiotic impregnated EVDs are available and their use may help reduce infection [50–52]. Technical complications such as catheter dislodgement, breakage, or malfunction can also occur but are easily recognized and usually of little clinical consequence.

Does the type of ICPM (EVD or parenchymal) device make a difference? Several studies including a meta-analysis have compared the two devices and, in general, find a greater risk of complications with EVDs. Kasotakis et al. [53] examined 377 adult TBI patients who required an ICPM, 253 received a parenchymal monitor, and 124 EVD. While outcome was similar, the use of EVD was associated with threefold—more device-related complications, longer duration of monitoring, and longer ICU stays. In the American College of Surgeons Trauma Quality Improvement Program (ACS TQIP) database, 2562 patients who underwent ICP monitoring were analyzed; 1358 (53%) had an EVD and 1204 (47%) a parenchymal monitor [54]. In univariate analysis, 30-day mortality was significantly higher in the EVD patients

than in patients with a parenchymal monitor. This relationship was lost in multivariate analysis. More recently, Bales et al. [55] retrospectively examined 224 severe TBI patients included in the Citicoline Brain Injury Treatment trial (COBRIT); 45% received an EVD, the rest an intraparenchymal device. Propensity scores were used to reduce confounding by indication. Outcome, including in-hospital mortality and 6-month functional and neuropsychological outcomes, was better in the patients who received intraparenchymal devices. Hence, it is recommended that unless CSF drainage is needed (e.g., hydrocephalus) that a parenchymal ICPM be used.

2.4 When Should ICP Be Treated?

The mechanisms that underlie increased ICP are multifactorial and complex. In addition, what defines intracranial hypertension is uncertain [56] and several numeric thresholds at which to initiate ICP treatment have been used. These are best defined in TBI and then extrapolated to other pathologies. The 2007 BTF Guidelines recommend treatment when ICP is >20 mmHg [12]. The 4th edition of the BTF guidelines recommended a new ICP threshold (22 mmHg) [15]. The rational for this is based on one single-center retrospective observational study [57]. In this study, the association between mean ICP and outcome was examined, with a nadir threshold of 22 mmHg. However, the mean ICP is entirely different from a treatment threshold. Hence, this new threshold and the rationale for it have been questioned [58–60]. In addition, compliance with guidelines even in level I centers is low and there remains wide variation in the treatment for elevated ICP despite these guidelines [16, 61].

It seems reasonable to initiate therapy when ICP is >20–25 mmHg [10–15, 62]. These thresholds are lower in children [22, 23]. Consistent with this, physiologic studies demonstrate cerebral circulation disturbance (i.e., cerebral blood flow [CBF] decreases) at ICP values >20 mmHg [63]. It is important to recognize that a single numeric ICP threshold may be an oversimplification of complex physiology and not applicable in all patients. For example, herniation (prevention of which is a reason to treat ICP) can occur even when ICP is normal [64], and physiologic dysfunction, for example, cellular hypoxia or cell energy dysfunction, also may be present when ICP is normal [65, 66]. Similarly, metabolic failure often occurs before an ICP spike [67] and even ICP insults at lower levels (15–20 mmHg) aggravate outcome [68]. In addition, rather than treat the ICP number per se, it may be more important to regard this value as a marker of altered physiology and instead find the reason why ICP is elevated and treat that rather than the numeric value [69, 70].

Today the concept of a simple numeric treatment threshold is questioned. Instead, total "ICP dose", "area under the ICP curve", and temporal evolution of ICP, how ICP responds to treatment, or individualized ICP thresholds may be more important parameters associated with outcome [4, 5, 71–73]. Rather than apply a "one size fits all" threshold derived from population-based data, it appears that it may be preferable to individualize thresholds based on patient characteristics, pathology, other

physiologic parameters, and on a risk-benefit analysis of treating the specific ICP, that is, the threshold may vary from patient to patient and in the same patient depending on time and other variables [69, 70]. For example, when ICP is >20 mmHg, most insults in adults are deleterious after >35–40 min but when ICP is >25 mmHg, aggravate outcome within 10–15 min [68]. To best individualize targets requires multimodality monitoring (MMM) and interpretation of the ICP value based on clinical and imaging characteristics. Further research is required to validate this approach and at present it still is being elucidated whether treating patients to keep them below the given threshold or dose, based on either population-defined thresholds or individualized thresholds, improves outcome.

Guidelines for ICP management in non-TBI patients (SAH, ICH IVH, and cardiac arrest) have evolved but there remains no clear consensus on when to treat ICP in these patients [74, 75]. Intracranial hypertension (>20 mmHg) is common after SAH, including in good grade patients [5, 76] and, in particular, during the early phase after poor grade SAH. Episodes of elevated ICP > 5 min can aggravate outcome and control of ICP can improve circulation [77]. However, cerebral metabolic compromise may also be observed when ICP and CPP are normal [78–80]. In hypoxic ischemic brain injury (HIBI), for example, cardiac arrest, small clinical studies suggest compliance rather than ICP alone may be of greater importance [81]. Further study is required in non-TBI patients. Perhaps data from SYNAPSE, an ongoing observational study of ICP, will provide guidance [82].

2.5 How to Manage Increased ICP?

The mechanisms that underlie and consequences of increased ICP are multifactorial and complex, as is the interplay between injury and intervention. Therapy for increased ICP is in large part empiric and phenomological and based on population targets. However, in recent years, with a better understanding of pathophysiology, introduction of neurointensivists, and advances in neuromonitoring, there is a growing trend to use precision medicine where treatment and therapy targets are individualized to patient's need, rather than used on a "one size fits all" in ICP management [17, 83, 84].

The recent Seattle international Severe Traumatic Brain Injury Consensus [20] used a Delphi method-based consensus approach to address management of severe TBI patients who have ICPMs. The recent Seattle international Severe Traumatic Brain Injury Consensus [20] used an Intracranial pressure (ICP) delphi-method-based consensus approach to address management of severe TBI patients who have ICPMs. The resulting protocol was designed to assist ICP management in these patients (Fig. 2.1). In addition, several treatments that should not be used when only ICP is monitored are described (Table 2.3). With multimodality monitoring, however, some of these therapies may be feasible. Similarly, for severe TBI patients who do not have ICPMs, the Imaging and Clinical Examination Protocol (ICE) has been described to help guide care [85]. This protocol may be particularly useful in

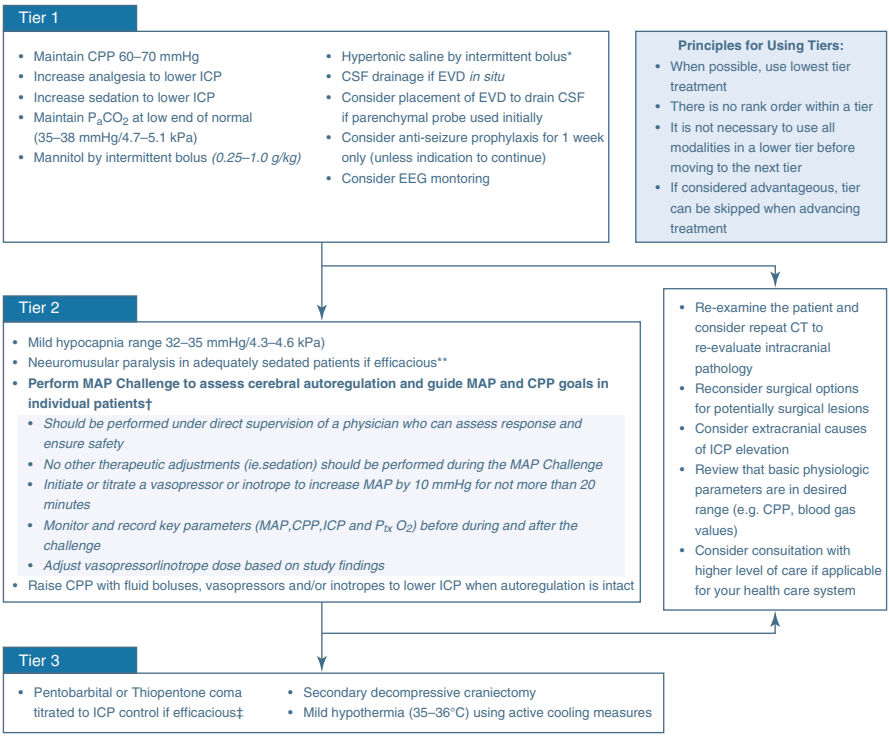

Fig. 2.1 Consensus-based algorithm for severe TBI management guided by ICP measurements Upper right box presents the principles for navigating through the treatments and tiers. Lower tier treatments are viewed as having a more favorable side effect profile than higher tiers and generally should be employed first. Inter-tier recommendations encourage patient reassessment for remediable causes of treatment resistance. CPP cerebral perfusion pressure, EEG electroencephalogram, EVD external ventricular drain, ICP intracranial pressure, kPa kiloPascals, MAP mean arterial pressure, $PaCO_2$ arterial partial pressure of carbon dioxide. (Courtesy: Hawryluk et al. [20])

Table 2.3 Treatment not recommended for use in severe traumatic brain injury management (when only ICP is monitored)

Mannitol by non-bolus continuous intravenous infusion
Scheduled infusion of hyperosmolar therapy (e.g., every 4–6 h)
Lumbar CSF drainage
Furosemide
Routine use of steroids
Routine use of therapeutic hypothermia to temperatures below 35 °C
due to systemic complications
High-dose propofol to attempt burst suppression
Routinely decreasing P_aCO_2 below 30 mmHg/4.0 kPa
Routinely raising CPP above 90 mmHg

Courtesy: Hawryluk et al. [20]
CPP cerebral perfusion pressure, *ICP* intracranial pressure, *kPa* kiloPascals, *$PaCO_2$* arterial partial pressure of carbon dioxide

low- and middle-income countries (LMICs) where limited resources may limit access to ICPMs [86, 87]. Neither protocol, however, can replace targeted, individualized care. The focus in this chapter will be on to manage patients who have an ICP monitor.

2.5.1 Initial Care and General Measures

If a mass lesion is identified on CT, it should be surgically evacuated. A tiered approach then is recommended [20]. Such an approach has been used successfully in BOOST-2, a phase II trial of multimodality monitoring in severe TBI [88]. Initial care requires ICU admission and is largely preventative and directed at optimizing normal physiology. This includes:

1. Appropriate head of bed elevation
2. Maintenance of the neck in a neutral position and avoidance of neck constriction (e.g., loosening endotracheal tube ties) to optimize venous return from the head
3. Endotracheal intubation and mechanical ventilation
4. Prevention of hypercapnia and hypoxia
5. Adequate treatment of pain, agitation, fever, and seizures
6. Appropriate fluid therapy to avoid hypotension (SBP <9–100 mmHg) and maintain hemoglobin (>7–8 g/dL)
7. Glucose control. Different physiologic targets are described in SEABICC [20] and recent trials that have used a similar tiered and targeted approach, for example, BOOST-2 or ProTECT [88, 89].

These physiologic targets may also differ in conditions such as SAH and ICH [90]. In addition, there are a paucity of studies on how individual components of this care (e.g., head of bed position) and whether bundles of care influence ICP [14]. Nevertheless, this goal-directed approach in critical care appears to be associated with enhanced outcome [91].

2.5.2 Tiers of Care

When ICP remains elevated (>20–22 mmHg), then a series of tiered therapies [1–3] can be used (Fig. 2.1). Items within a tier are not necessarily listed in order of completion and many interventions may occur simultaneously or be difficult to achieve (e.g., EVD insertion when there are slit ventricles). The tiers represent increased levels of intensity for the treatment of elevated ICP and lower tiers are considered to have less risk. Ideally, patients should be initiated in Tier I and then staged through Tier 3 if no response is observed within a prespecified time (e.g., in

BOOST-2 and 120 min in a tier). However, not all modalities in a tier need to be used before moving to the next and a tier can be skipped if it appears to be mechanistically advantageous to do so. Within each tier, there are several components of care (each briefly discussed below) including sedation, osmotherapy and fluid therapy, CSF diversion, ventilation, CPP augmentation, metabolic suppression including hypothermia, and decompressive craniectomy.

2.5.2.1 Sedation and Analgesia

In initial care, sedation is directed at pain control or agitation. In Tier 1, it is directed at ICP control. Robust evidence for a specific preferred opioid or sedative is lacking but systemic reviews suggest that bolus administration should be avoided [92].

2.5.2.2 Fluid Therapy and Hemoglobin Management

Negative fluid balance is associated with an adverse effect on outcome, independent of its relationship to ICP, MAP, or CPP [93]. However, aggressive administration of fluid to induce hypervolemia or augment CPP can be harmful in both TBI and SAH [94]. Hence, intravenous fluid is a fundamental component of brain injury care. In general, intravascular management should aim for euvolemia. Isotonic crystalloids are preferred, whereas colloids, glucose-containing hypotonic solutions, other hypotonic solutions, or albumin should be avoided [95–99]. Ideally, therapy should be individualized rather than standardized [100] and there is some evidence that hemodynamic goal, that is, what guides fluid administration, may be more important than the amount of fluid given [101]. Correcting volume status is complicated further by frequent abnormalities of sodium homeostasis that become important in osmotherapy. The role of anemia and transfusion is complex and beyond the scope of this chapter. However, low Hgb can lead to vasodilatation and, hence, aggravate ICP, whereas transfusion in some patients can correct brain hypoxia and so influence outcome [102–104].

2.5.2.3 CSF Drainage

CSF drainage through an EVD should be considered particularly when there is hydrocephalus. The optimal method of drainage (continuous vs. intermittent) has not been established. In addition, while CSF drainage may reduce ICP, it can have an adverse effect on compliance and CBF. In SAH, some studies demonstrate improved microcirculation with CSF drainage [77]. This, however, depends on the ICP. The role of external lumbar drainage (ELD) is limited but can be considered a therapeutic option if high ICP is due to communicating external hydrocephalus.

2.5.2.4 Osmotherapy

Typically, mannitol or hypertonic saline (HTS) is administered but, despite clinical use for >50 years, there are still questions about optimal use. While both are effective, there are insufficient data to suggest superiority of one agent over the other [104], and the optimal dose, mode of administration (e.g., bolus vs. continuous infusion), and concentration are still being elucidated. Some studies suggest HTS may be more effective [105–107], particularly for refractory intracranial hypertension [104], but to choose the appropriate hyperosmolar agent, patient characteristics, such as volume status, renal function, hemodynamic status, and sodium levels, among others, should be considered.

Mannitol treatment protocols vary from center to center, and the dose-response relationship is not understood and often the ICP decrease depends more on the administration protocol or the ICP level at the time the dose is given [108]. Initial use for increased ICP is a single bolus (not infusion) of a 20–25% solution of 0.5–1 g/kg, i.v., over 10–15 min and repeated every 2–6 h (although ideal dosing is not well described). ICP decreases may be greatest shortly after the dose is given because of its effect on viscosity and vessel caliber, that is, vasoconstriction. Unnecessarily large doses or prophylactic doses could lead to more mannitol being required later. In addition, when cerebral autoregulation (CA) or the blood brain barrier (BBB) is impaired, aggressive mannitol use can increase ICP since it will draw fluid into brain. Hence, it is important to measure serum osmolarity or osmolar gap (measured—calculated serum osmolarity) before infusing mannitol. Mannitol should not be given if serum osmolarity is >320 mOsm/kg H_2O or osmolar gap >10 or in patients with acute kidney injury (AKI) or renal failure. Side effects of mannitol include hypotension, hypovolemia, hypokalemia, hyperkalemia, and AKI.

Hypertonic saline (HTS) increases serum osmolarity directly rather than by inducing osmotic diuresis. Hence, it can reduce ICP and simultaneously maintain or even expand intravascular volume. Therefore, HTS may be preferable when mean arterial blood pressure (MABP) is reduced or patient volume status dictates caution with large infusions. There are several different concentrations that range from 3% to 23.4% NaCl solutions. Hypertonic saline should not be given if serum Na^{++} is >160 mmol/L. To administer HTS (>3%), central venous access is required and a 50% chloride/50% acetate mix is recommended to reduce the risk of hyperchloremia. There are a variety of protocols for HTS administration but therapy can be initiated with 3% saline at 75 cc/h (or greater if requiring fluid resuscitation). Serum sodium should be checked frequently and infusion continued to goal sodium of 150 mmol/L or a maximum of 160 mmol/L if ICP remains refractory. Once the goal sodium or ICP is achieved or ICP controlled, HTS can be continued as a 0.9% saline infusion or 2% if Na^{++} drifts downward.

2.5.2.5 Ventilation

Hyperventilation (HV) causes blood and CSF alkalosis; this causes vasoconstriction and, hence, reduces cerebral blood volume (CBV) and ICP. Sustained or prophylactic HV can be deleterious since it may cause cerebral ischemia. However, when herniation is present, transient HV may be lifesaving. In select patients, for example, those with hyperemia and increased ICP, optimized HV can be useful. Jugular bulb oximetry ($SjvO_2$) or monitors of CBF or brain oxygen ($P_{bt}O_2$) should be used to permit safer HV titration. For acute ICP management, HV should begin with a $PaCO_2$ goal of 34–36 mmHg and be advanced to $PaCO_2$ goal of 25–30 mmHg if there is no treatment response. In CENTER-TBI, the most commonly reported target for $PaCO_2$ was 36–40 mmHg (4.8–5.3 kPa) in cases of controlled ICP (<20 mmHg, 69% of centers) and $PaCO_2$ target of 30–35 mmHg (4–4.7 kPa) for increased ICP (62%; 17).

2.5.2.6 CPP Augmentation

Prevention of secondary injury, for example, hypotension and hypoxia, avoidance of systemic complications, and maintaining appropriate CPP, which is a surrogate for CBF among others, are fundamental goals in management of acute brain injury including TBI, SAH, and ICH. Cerebral perfusion pressure is defined as the difference between mean arterial pressure (MAP) and ICP (Eq. 2.2). To calculate CPP requires that arterial blood pressure and ICP be monitored. Ideally, the zero reference points should be the same, for example, the tragus as an external landmark. This is important when the head of the bed is elevated since measuring ICP at the level of the brain and BP at heart level can result in a CPP error of 15 mmHg. This error can be further exaggerated in tall patients. However, there is a variability in both clinical practice and research reports in how MAP is measured to determine CPP [109], prompting calls for adaptation of international standards for CPP measurements.

$$\text{CPP} = \text{MAP} - \text{ICP} \tag{2.2}$$

Single-center observational cohorts show that time indices for CPP ≥70 and <50 mmHg are associated with decreased and increased mortality, respectively [110]. However, the ideal CPP to maintain in patients with acute brain injury (ABI) remains debated. Early recommendations suggested a CPP >70 mmHg was preferable in severe TBI. However, while the incidence of cerebral ischemia is decreased using this threshold, an outcome benefit is not observed because of increased pulmonary complications associated with fluid and vasopressor use to maintain CPP (94). In addition, normal CPP also does not always mean normal brain metabolism

[65, 66, 79]. The 3rd edition of the TBI guidelines suggested maintaining a CPP between 50 and −70 mmHg and avoiding active CPP elevation above 70 mmHg with fluids and vasopressors. Using minute-by-minute data in 259 adult patients, Guiza et al. [111] recently observed that a "safe" zone between 60 and 70 mmHg could be identified for adults <65 years, provided CA was active and ICP was ≤25 mmHg. Deficient CA reduces the tolerability for low CPP and insults of CPP <50 mmHg were hardly tolerated, whereas ICP >25 mmHg was associated with poor outcome regardless of CPP. However, it should not be interpreted that CPP management is not important during increased ICP. It is likely that the ICP reflects the severity of the patient's condition, and hence, this drives the association with poor outcome. In a survey from 66 neurotrauma sites in CENTER-TBI [17], the most common CPP target was >60 mmHg (60% of sites) and/or an individualized target (38%). To support CPP, crystalloid fluid loading (91%) was generally preferred over albumin (23%), and vasopressors (%) over inotropes (44%).

Recent research suggests that rather than a population-based target (CPP 50–70), CPP should be individualized, that is, optimal patient-specific CPP (CCPopt). This value, CPPopt, can vary between patients and over time in the same patient and may range between 50 and 100 mmHg. When patients are managed at or close to the CPPopt, better outcomes are observed and levels both above and below the patient's optimal CPP level are associated with worse outcome [112, 113]. In particular, patients maintained within 5 mmHg of their optimal CPP do better, whereas patients with larger discrepancy (>10 mmHg) between real CPP and CPPopt more likely have adverse outcomes. Whether using this to guide treatment makes a difference is still to be elucidated at large because the quality of data is low [114].

2.5.2.7 Metabolic Suppression

The goal of metabolic therapy is to suppress cerebral metabolic rate of oxygen ($CMRO_2$). This in turn should decrease CBF, and because CBV is reduced, ICP should decrease. In addition, vulnerable brain tissue may be preserved since $CMRO_2$ is reduced in the face of decreased fuel delivery. CMRO2 may be reduced through pharmacological means or temperature modulation. This generally is a Tier 3 strategy. However, in some circumstances, it may be used earlier—for example, induced hypothermia for increased ICP in liver encephalopathy.

2.5.2.8 Pharmacologic Suppression

Agents such as barbiturates, benzodiazepines, or propofol may be administered to induce coma (burst suppression). There is insufficient data to guide choice of these agents. It should be remembered that barbiturates and propofol are myocardial depressants and peripheral vasodilators, and invasive hemodynamic monitoring and support often are needed when pharmacologic coma is induced. Barbiturates effectively treat increased ICP and are best indicated in patients who have adequate

cardiovascular function and intact CA. The most commonly used agent, pentobarbital, can be administered i.v. with a loading dose of 5 mg/kg, followed by an infusion of 1–3 mg/kg/h; a high-dose regimen may also be used with an i.v. bolus dose of 10 mg/kg over 30 min followed by 5 mg/kg/h infusion for 3 h, followed by 1 mg/kg/h titrated to either burst suppression on continuous electroencephalogram monitoring or an ICP reduction. Whether barbiturate use improves outcome is unclear since side effects such as immune suppression, hypotension (especially in volume depleted patients), and decreased mucociliary clearance can mitigate any benefit on ICP.

Another option for pharmacologic coma is propofol, which is given in an i.v. loading dose of 2 mg/kg, followed by a titrated infusion of up to 200 mg/kg/min. Propofol should be avoided in hypotensive or hypovolemic patients and prolonged infusions or high doses have been associated with the development of a "propofol infusion syndrome" of renal failure, hyperkalemia, myocardial failure, and metabolic acidosis, often resulting in death. The mechanism for this is not fully understood.

2.5.2.9 Temperature Modulation

Mild-to-moderate hypothermia (32–34 °C) can reduce ICP [115, 116]. Most single-center studies suggest that induced hypothermia is associated with better outcome. However, this outcome benefit is not observed in large randomized multicenter studies in adults or children with severe TBI and may even be harmful in patients with a lower injury severity [117, 118]. Furthermore, there is no role for prophylactic hypothermia [119]. There also is a limited role in malignant cerebral infarction [120]. In part, this lack of outcome benefit may have to do with shivering that can adversely affect brain metabolism [121] or the rate of posthypothermic rewarming, which if too rapid can exacerbate neuronal injury [122]. Hence, when hypothermia is used, rewarming should be considered if the patient's ICP is stable and <20 mmHg for at least 48 h, and implemented at a rate not faster than 0.1–0.25 °C/h.

2.5.2.10 Decompressive Craniectomy

Decompressive craniectomy (DC), either unilateral or bifrontal, and when correctly performed (i.e., of adequate size 12 × 15 cm), is the most effective way to reduce ICP, particularly when ICP is resistant to osmotic agents and medical management [123, 124]. In addition, DCC has favorable effects on CPP and other aspects of brain metabolism [123, 125–130]. Both intraabdominal and intrathoracic hypertension can increase ICP or aggravate increased ICP. In select patients, decompressive laparotomy (DL), even if intraabdominal pressure is normal, can reduce elevated ICP [131]. These procedures (DC and DL) often make care easier and eliminate the need for other therapies that may have deleterious effects.

In patients with stroke-related malignant hemispheric infarction, pooled analysis of several RCTs show that DC decreases mortality and improves functional outcome [132, 133]. In these patients, however, surgery is usually performed without knowledge of ICP since most of these patients do not receive an ICPM. Instead, the decision is based on the clinical and imaging findings. Questions remain about the effects of DC on long-term outcome in TBI, in part because of methodological differences and patient heterogeneity [134, 135]. In addition there is variability about the ICP cutoff for DC; in CENTER-TBI, 60% of sites use 25 mmHg, 18% 30 mmHg, and 17% 20 mmHg [136]. Consensus guidelines for DC (including primary—at the time of initial craniotomy and secondary DC for increased ICP) in TBI were recently published [28]. There does not appear to be a role for bifrontal DC in a patient with diffuse injury particularly if performed to prevent increased ICP. The optimal candidate for secondary DC is a patient whose ICP elevation is likely the primary contributor to poor outcome and the primary injury is deemed compatible with acceptable recovery and is receiving maximal medical management. Simple ICP thresholds alone may be insufficient to make this decision. However, should also consider clinical findings, CT-scan results and data from other monitors if available. The ICU-team should include a frank discussion with family members about recovery-expectations and clinical outcome [137, 138]. Technical aspects of the procedure, for example, size of bone flap, duraplasty, and postprocedure care (including continued ICP monitoring) can also affect outcome [28, 124].

In general, if TBI patients survive to discharge after DC, most have a good functional outcome since improvement occurs with time [139]. When to replace the bone flap or perform a cranioplasty, however, can further influence outcome [140]. Indeed, several studies show cranial reconstruction can improve CBF and aid in recovery [141, 142]. There has been limited study on this issue. A recent retrospective single-center analysis over a 10-year period suggests that cranioplasty performed between 15 and 30 days after initial DC may reduce infection and seizures, whereas waiting >90 days may decrease the risk of hydrocephalus but increase the seizure risk [143].

2.6 ICP Management and Outcome

Multiple, large cohort studies demonstrate that increased ICP is independently associated with mortality after TBI. The relationship with functional outcome is less clear. The risk of death is proportionally greater the higher the ICP, a longer duration of increased ICP and when increased ICP is refractory to treatment [1–5, 26, 29, 68, 71, 73, 144]. Although less studied, several clinical series demonstrate that elevated ICP and poor outcome are associated with SAH and ICH, although this outcome may depend more on disease severity [5, 145–148]. A variety of dynamic characteristics of the ICP signal that are associated with outcome have also been identified, for example, the duration of increased ICP episodes [149], the area under the ICP curve [71], the ICP variability [150], and the CPP/ICP ratio [151].

However, whether treating increased ICP makes a difference to outcome remains poorly defined. There are several reasons for this, including confounding by indication, methodological issues, and patient and management heterogeneity. In addition, it would be unethical to perform a trial where some patients with elevated ICP were treated and others were not, given the relationship between increased ICP and mortality. Hence, no RCT has addressed (or will address) the influence of ICP management. Attempts have been made to answer the question using analyses of trauma or TBI registries, quality assurance studies, guideline adherence, within- or across-institution protocol studies, and meta-analysis of clinical series. There are limitations to many of these studies; for example, they examine the use of an ICPM rather than the ICP treatment per se but in general the vast majority of studies demonstrate a significant outcome benefit to guideline adherence, and specifically, ICPM use and to ICP treatment [152–163]. For example, one of the largest studies comparing ICP-monitored patients to those without included 10,628 patients with severe TBI in the ACS TQIP [154]. Although ICPMs were only used in 17.6% of patients, its use was associated with a significant decrease in mortality. Studies that use propensity scores, which is a form of "retrospective randomization," show that the use of an ICPM is associated with an 8% reduction in risk-adjusted mortality [164]. There are rare case series or administrative databases that find a similar or no outcome benefit with ICPM use [165, 166].

Meta-analysis of studies published since 2007 that include 25,229 patients shows improved survival in patients who receive an ICP monitor [167]. Overall compliance with ICP and CPP goals remains variable and <50% adult patients eligible for ICP monitoring actually receive an ICP monitor [154, 156, 163, 168]. This allows comparativeness effectiveness research. For example, Cnossen et al. [169] examined care of 503 moderate or severe TBI in five level I trauma centers in the Netherlands. Treatment was associated with patient characteristics and varied widely among centers, even after case-mix correction. Outcome was more favorable in patients treated in aggressive centers than those treated in nonaggressive centers (defined on the frequency of ICP monitoring). The inference of these various studies is that adherence to guidelines on ICP- and CPP-directed therapies appears to be associated with decreased mortality, although it remains unclear if this association is causal. In addition, the studies do not confirm that ICP treatment (or what aspect of treatment) is beneficial per se but rather that the use of an ICPM helps.

The Benchmark Evidence from South American Trials: Treatment of Intracranial Pressure (BEST TRIP) trial was a recent RCT that attempted to answer how ICP monitor use may affect care in a resource-limited environment [170]. Patients (>13 years old) in general ICUs in Bolivia and Ecuador were randomized to management strategies for severe TBI, one of which was triggered by an ICP monitor. Outcome was similar in the two groups, which is to be expected since there is no control group. Care was more efficient in the ICPM group but the vast majority of patients did not develop increased ICP. Many have (mis) interpreted this trial to suggest that there is no need to treat ICP. This is far from the truth and, despite its title, BEST TRIPS is not a trial of ICP care per se and not even a trial of ICP monitoring. Indeed, a recent consensus meeting on the trial indicated that for those who

currently monitor ICP, there is no reason to change practice and that the trial lacks external validity and raises more research questions rather than answers any clinical questions [56]. In particular, it is important to define what constitutes intracranial hypertension and whether ICP as a numeric threshold is simply a marker for underlying pathophysiologic processes or an independent target. From a clinical standpoint, ICP monitoring should be used as part of a multimodal approach to the patient and viewed as an additional tool available to the clinician to manage patients with TBI.

2.7 Are Other Monitors Necessary to Fully Understand ICP and Its Management?

ICP and CPP treatment remain central and critical to care of acute brain injury (ABI). However, converging evidence from several different lines of research suggests that care based on only ICP and CPP thresholds may be an oversimplification of a complex problem [65–70, 73, 79, 88, 171–173]. The implication of this is that additional measures of ICP, for example, ICP waveform analysis, RAP, PRx, or CO_2 reactivity or use of other monitors, that is, MMM, can augment ICP care. In addition, autoregulation is known to play an important protective role in tolerating episodes of raised ICP (Klein) and when impaired is associated with poor outcome. However, cerebrovascular reactivity remains relatively independent of intracranial hypertension therapeutic intensity, suggesting that current therapies do not adequately modulate impaired autoregulation [174].

2.7.1 Other Measures of ICP

Based on the Monro-Kellie doctrine, the cranial compartment can accommodate between 50 and 150 mL of additional volume before ICP increases. This compensatory reserve or compliance is age dependent, and is not linear. In turn, it is influenced by CA. Knowing where a patient is on the curve at a given time provides important information about the risk of a rapid ICP increase (and so a change in CBF) or herniation.

Compliance and waveform analysis can be examined through the pressure volume index. However, this requires injection of fluid through an EVD. Instead, ICP waveform analysis provides important information about the state of compliance [175]. With every systole there is a certain pulsatile increase in the cerebral blood volume that leads to a corresponding ICP increase. This increase or dP/dV is proportional to the elastance (inverse of compliance of the cranial compartment at that point in time). In a noncompliant brain, the waveform changes and P2 (the rebound) of the wave becomes greater than P1 (the percussion or arterial wavelet). In recent

years, studies have examined the pressure-volume compensatory reserve index (RAP), which is defined as the correlation coefficient between the amplitude and mean pressure of the ICP. A RAP coefficient close to zero indicates little correlation between the ICP pulse amplitude and the mean ICP and reflects a good compensatory reserve. In contrast, a RAP coefficient that approximates one indicates that the pulse amplitude of the ICP varies directly with mean ICP, that is, the pressure volume curve has shifted to the right and that compensatory reserve has been exhausted [176]. ICP waveform analysis, therefore, has great promise as a tool to aid clinical evaluation and targeted ICP care. However, specialized software and high-frequency data collection systems are needed to effectively use these methods. In the ICU, there are qualitative estimates of compliance, for example, how does ICP respond or vary during stimulation and what is the therapeutic index, that is, what and how much treatment is need to control ICP?

2.7.1.1 Pressure Reactivity Index (PRx)

With recent data processing advances and computerized bedside monitoring, the relationship between ICP and MAP or pressure reactivity index (PRx) can be measured. PRx has the advantage that it can be measured continuously in any patient with a parenchymal ICPM, an arterial pressure line, and the appropriate analysis software. This provides a real-time analysis of CA. In the normal brain, increases in MAP result in cerebral vasoconstriction within 5–15 s, with an associated reduction in CBV and ICP, that is, an inverse correlation between MAP and ICP, indicated by a negative value for PRx. This represents a reactive vascular bed and intact CA. If cerebrovascular reactivity is impaired, CBV and ICP increase passively with blood pressure (BP), with opposite changes when BP is reduced. Hence, an increasingly positive PRx value (close to +1) indicates impaired cerebral pressure reactivity. This model works best when the cranium is intact since following DC changes in CBF and CBV will not necessarily lead to changes in ICP since the cranial compliance is altered [177]. PRx has been most studied in TBI where several studies demonstrate that impaired PRx is associated with poor outcome [112, 113, 178]. In nontraumatic pathologies, the mean flow index (Mx), derived from Transcranial Doppler (TCD), that measures the correlation between mean middle cerebral artery blood flow velocity and CPP (or MAP) may be a better measure.

Importantly PRx can be used to guide therapy and enhance prognostic decisions. First, choosing a CPP target can be speculative in individual patients but using PRx, patient-specific CPP, and ICP thresholds can be identified. These patient-specific thresholds show a more robust relationship with outcome than population-based targets [73, 112, 113, 178, 179]. Second, PRx can be used to estimate optimal CPP (CPPopt); the more time a patient is at their individual CPPopt, the more likely outcome will be favorable since it reduces the risks of excessively high or low CPP. However, there is potential to over interpret CPPopt targets when the values of pressure reactivity indices are close to zero. Finally, knowledge about PRx can help decide whether to use ICP- or CPP-based therapy with a CPP-targeted approach

being preferable when pressure reactivity is intact, while an ICP-oriented strategy is better in pressure passive patients (MAP/ICP regression line at least 0.13; Howells). However, further research is required to examine this concept that intuitively makes sense and that of personalization of ICP monitoring (i.e., waveform analysis, pulse amplitude, pressure reactivity, and longitudinal trajectories) to develop individualized targeted care.

2.7.1.2 Multimodality Monitoring

Cerebral microdialysis (CMD) studies show that cell energy dysfunction can occur before ICP or CPP changes and independently from ICP or CPP [66, 67, 79, 172, 180–182]. This implies that additional monitors are necessary to better understand what is happening in a patient and essential to targeted and mechanistic therapy, including that for increased ICP [69, 70]. Alternatively, predictive models based on machine learning (artificial intelligence) from continuous time series of ICP and other data may provide accurate predictions of physiologic crises and so allow earlier application of targeted interventions [183, 184]. There are a variety of monitors now available, for example, CBF, continuous EEG, brain oxygen, microdialysis, autoregulation, near-infrared spectroscopy, among others, that allow real-time bedside assessment. There is no one monitor that is "better" than the other and no single technique can be expected to provide complete information about the brain's health and, hence, a combination of monitors is needed. This approach, often called multimodality monitoring (MMM), has evolved in recent years along with the growth of bioinformatics. In reality, it is practiced all the time, that is, we combine data from the clinical exam, CT scan, and laboratory analysis. Several lines of evidence indicate that MMM can optimize care of brain-injured patients [184–187]. Indeed, in a recent phase II trial, goal-directed therapy guided by brain oxygen, ICP, and CPP monitoring appears to be superior to standard ICP- and CPP-guided therapy [88]. A phase III trial to examine this question is now underway. In short, ICP is best managed with more than just an ICP monitor.

2.8 Conclusion

The management of neurocritical care patients and specifically those with acute brain injury, for example, TBI, SAH, or ICH, to name a few, can be immensely complicated. Management of ICP is a cornerstone of this care. How best to manage ICP can be augmented with additional monitors and use of bioinformatics to better understand the mechanisms behind changes in ICP and to enhance targeted care with a physiologically integrative approach [183, 188]. To further help patient care, several guidelines about when and how to use different monitors and management

algorithms based on expert consensus are available for TBI and non-TBI pathologies [10–15, 20, 25, 28, 35, 74, 75]. In summary, it is important not to think of ICP (its numeric value) as the target but rather as an indicator of the existence of an underlying pathophysiological process that needs treatment, that is, the key question is not what to do if ICP is increased but why is it increased. Hence, in managing ICP, it is important not to get caught up in simply treating numbers but rather to integrate information from multiple sources to target individualized care.

Algorithm

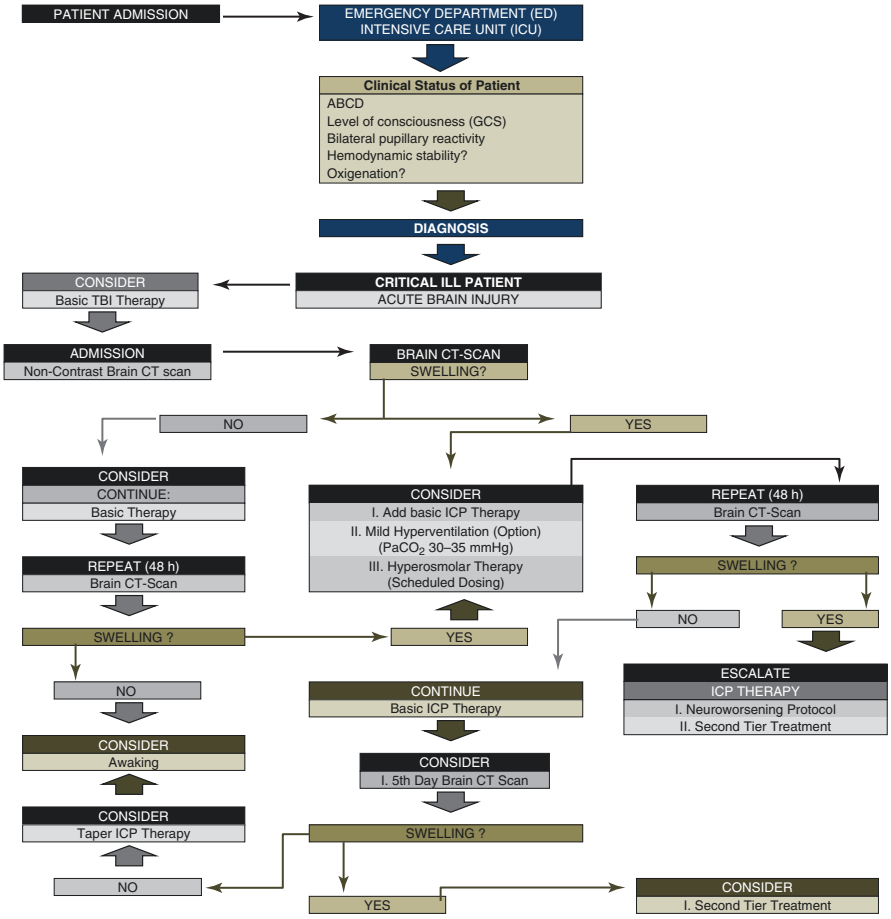

ABCD airway-breathing-circulation-disability, *CT* computed tomography, *ICP* intracranial pressure

References

1. Badri S, Chen J, Barber J, Temkin NR, Dikmen SS, Chesnut RM, et al. Mortality and long-term functional outcome associated with intracranial pressure after traumatic brain injury. Intensive Care Med. 2012;38:1800–9.
2. Balestreri M, Czosnyka M, Hutchinson P, Steiner LA, Hiler M, Smielewski P, et al. Impact of intracranial pressure and cerebral perfusion pressure on severe disability and mortality after head injury. Neurocrit Care. 2006;4:8–13.
3. Farahvar A, Gerber LM, Chiu YL, Härtl R, Froelich M, Carney N, et al. Response to intracranial hypertension treatment as a predictor of death in patients with severe traumatic brain injury. J Neurosurg. 2011;114:1471–8.
4. Treggiari MM, Schutz N, Yanez ND, Romand JA. Role of intracranial pressure values and patterns in predicting outcome in traumatic brain injury: a systematic review. Neurocrit Care. 2007;6(2):104–12.
5. Heuer G, Smith MJ, Elliott JP, Winn HR, Le Roux P. The relationship between intracranial pressure and other clinical variables in patients with aneurysmal subarachnoid hemorrhage. J Neurosurg. 2004;101(3):408–16.
6. Klein SP, Depreitere B. What determines outcome in patients that suffer raised intracranial pressure after traumatic brain injury? Acta Neurochir Suppl. 2018;126:51–4.
7. Oddo M, Le Roux P. What is the etiology, pathogenesis and pathophysiology of elevated intracranial pressure? In: Neligan P, Deutschman CS, editors. The evidenced based practice of critical care. Philadelphia: Elsevier Science; 2009. p. 399–405.
8. Alali AS, Temkin N, Barber J, Pridgeon J, Chaddock K, Dikmen S, et al. A clinical decision rule to predict intracranial hypertension in severe traumatic brain injury. J Neurosurg. 2018;131(2):612–9.
9. Pace J, Parry N, Vogt K, Hilsden R, Leeper RR, Markova Z, et al. A clinical prediction model for raised intracranial pressure in patients with traumatic brain injuries. J Trauma Acute Care Surg. 2018;85(2):380–6.
10. Le Roux P, Menon DK, Citerio G, et al. Consensus summary statement of the International Multidisciplinary Consensus Conference on Multimodality Monitoring in Neurocritical Care: a statement for healthcare professionals from the Neurocritical Care Society and the European Society of Intensive Care Medicine. Intensive Care Med. 2014;40:1189–09.
11. Chesnut R, Videtta W, Vespa P, et al. The participants in the International Multidisciplinary Consensus Conference on Multimodality Monitoring. Intracranial pressure monitoring: fundamental considerations and rationale for monitoring. Neurocrit Care. 2014;21:S64–84.
12. Brain Trauma Foundation; American Association of Neurological Surgeons; Congress of Neurological Surgeons. Guidelines for the management of severe traumatic brain injury. J Neurotrauma. 2007;24(Suppl 1):S1–106.
13. Maas AI, Dearden M, Teasdale GM, Braakman R, Cohadon F, Iannotti F, et al. EBIC-guidelines for management of severe head injury in adults. European Brain Injury Consortium. Acta Neurochir. 1997;139(4):286–94.
14. Cadena R, Shoykhet M, Ratcliff JJ. Emergency neurological life support: intracranial hypertension and herniation. Neurocrit Care. 2017;27(Suppl 1):82–8.
15. Carney N, Totten AM, O'Reilly C, et al. Guidelines for the management of severe traumatic brain injury, Fourth edition. Neurosurgery. 2017;80:6–15.
16. Cnossen MC, Huijben JA, van der Jagt M, Volovici V, van Essen T, Polinder S, et al. CENTER-TBI Investigators. Variation in monitoring and treatment policies for intracranial hypertension in traumatic brain injury: a survey in 66 neurotrauma centers participating in the CENTER-TBI study. Crit Care. 2017;21(1):233.
17. Huijben JA, Volovici V, Cnossen MC, Haitsma IK, Stocchetti N, Maas AIR, et al. CENTER-TBI investigators and participants Variation in general supportive and preventive intensive care management of traumatic brain injury: a survey in 66 neurotrauma centers participating

in the Collaborative European NeuroTrauma Effectiveness Research in Traumatic Brain Injury (CENTER-TBI) study. Crit Care. 2018;22(1):90.
18. Adams CA, Stein DM, Morrison JJ, Scalea TM. Does intracranial pressure management hurt more than it helps in traumatic brain injury? Trauma Surg Acute Care Open. 2018;3(1):e000142.
19. Samudra NP, Park SM, Gray SE, Sebai MA, Olson DM. Inconsistency in reporting variables related to intracranial pressure measurement in scientific literature. J Nurs Meas. 2018;26(3):415–24.
20. Hawryluk GWJ, Aguilera S, Buki A, Bulger E, Citerio G, Cooper DJ, et al. A management algorithm for patients with intracranial pressure monitoring: the Seattle International Severe Traumatic Brain Injury Consensus Conference (SIBICC). Intensive Care Med. 2019;45(12):1783–94.
21. Kochanek PM, Tasker RC, Bell MJ, Adelson PD, Carney N, Vavilala MS, et al. Management of pediatric severe traumatic brain injury: consensus and guidelines-based algorithm for first and second tier therapies. Pediatr Crit Care Med. 2019;20(3):269–79.
22. Lovett ME, O'Brien NF, Leonard JR. Children with severe traumatic brain injury, intracranial pressure, cerebral perfusion pressure, what does it mean? A review of the literature. Pediatr Neurol. 2019;94:3–20.
23. Figaji AA. Anatomical and physiological differences between children and adults relevant to traumatic brain injury and the implications for clinical assessment and care. Front Neurol. 2017;8:685.
24. Kayhanian S, Young AMH, Piper RJ, Donnelly J, Scoffings D, Garnett MR, et al. Radiological correlates of raised intracranial pressure in children: a review. Front Pediatr. 2018;6:32.
25. Stocchetti N, Picetti E, Berardino M, Buki A, Chesnut RM, Fountas K, et al. Clinical applications of intracranial pressure monitoring in traumatic brain injury: report of the Milan consensus conference. Acta Neurochir. 2014;156:1615–22.
26. Wilberger JE Jr, Harris M, Diamond DL. Acute subdural hematoma: morbidity, mortality, and operative timing. J Neurosurg. 1991;74:212–8.
27. Picetti E, Caspani ML, Iaccarino C, Pastorello G, Salsi P, Viaroli E, et al. Intracranial pressure monitoring after primary decompressive craniectomy in traumatic brain injury: a clinical study. Acta Neurochir. 2017;159:615–22.
28. Hutchinson PJ, Kolias AG, Tajsic T, Adeleye A, Aklilu AT, Apriawan T, et al. Consensus statement from the International Consensus Meeting on the Role of Decompressive Craniectomy in the Management of Traumatic Brain Injury: consensus statement. Acta Neurochir. 2019;161(7):1261–74.
29. Eisenberg HM, Gary HE Jr, Aldrich EF, Saydjari C, Turner B, Foulkes MA, et al. Initial CT findings in 753 patients with severe head injury. A report from the NIH Traumatic Coma Data Bank. J Neurosurg. 1990;73(5):688–98.
30. Toutant SM, Klauber MR, Marshall LF, Toole BM, Bowers SA, Seelig JM, et al. Absent or compressed basal cisterns on first CT scan: ominous predictors of outcome in severe head injury. J Neurosurg. 1985;61(4):691–4.
31. Thotakura AK, Marabathina NR, Danaboyina AR, Mareddy RR. Role of serial ultrasonic optic nerve sheath diameter monitoring in head injury. Neurochirurgie. 2017;63(6):444–8.
32. McNett M, Moran C, Janki C, Gianakis A. Correlations between hourly pupillometer readings and intracranial pressure values. J Neurosci Nurs. 2017;49(4):229–34.
33. Zhang X, Medow JE, Iskandar BJ, Wang F, Shokoueinejad M, Koueik J, et al. Invasive and noninvasive means of measuring intracranial pressure: a review. Physiol Meas. 2017;38(8):R143–82.
34. Robba C, Cardim D, Tajsic T, Pietersen J, Bulman M, Rasulo F, et al. Non-invasive intracranial pressure assessment in brain injured patients using ultrasound-based methods. Acta Neurochir Suppl. 2018;126:69–73.
35. Le Roux P, Menon DK, Citerio G, Vespa P, Bader MK, Brophy GM, et al. Consensus summary statement of the International Multidisciplinary Consensus Conference on

Multimodality Monitoring in Neurocritical Care: a statement for healthcare professionals from the Neurocritical Care Society and the European Society of Intensive Care Medicine. Neurocrit Care. 2014;21(Suppl 2):S1–26.
36. Bratton SL, Chestnut RM, Ghajar J, McConnell Hammond FF, Harris OA, Hartl R, et al. Guidelines for the management of severe traumatic brain injury. VII. Intracranial pressure monitoring technology. J Neurotrauma. 2007;24(Suppl 1):S45–54.
37. Oshorov AV, Popugaev KA, Savin IA, Potapov AA. Simultaneous measurement of intraventricular and parenchymal intracranial pressure in patients with severe trauma brain injury. Anesteziol Reanimatol. 2016;61(1):37–9.
38. Rogers M, Stutzman SE, Atem FD, Sengupta S, Welch B, Olson DM. Intracranial pressure values are highly variable after cerebral spinal fluid drainage. J Neurosci Nurs. 2017;49(2):85–9.
39. Volovici V, Huijben JA, Ercole A, Stocchetti N, Dirven CMF, van der Jagt M. Ventricular drainage catheters versus intracranial parenchymal catheters for intracranial pressure monitoring-based management of traumatic brain injury: a systematic review and meta-analysis. J Neurotrauma. 2019;36(7):988–95.
40. Tavakoli S, Peitz G, Ares W, Hafeez S, Grandhi R. Complications of invasive intracranial pressure monitoring devices in neurocritical care. Neurosurg Focus. 2017;43(5):E6.
41. Saladino A, White JB, Wijdicks E, Lanzino G. Malplacement of ventricular catheters by neurosurgeons: a single institution experience. Neurocrit Care. 2009;10(2):248–52.
42. Bekar A, Doğan S, Abaş F, Caner B, Korfali G, Kocaeli H, et al. Risk factors and complications of intracranial pressure monitoring with a fiberoptic device. J Clin Neurosci. 2009;16(2):236–40.
43. Lozier AP, Sciacca RR, Romagnoli MF, Connolly ES Jr. Ventriculostomy-related infections: a critical review of the literature. Neurosurgery. 2002;51(1):170–81; discussion 181–182
44. Binz D, Toussaint LG III, Riedman JA. Hemorrhagic complications of ventriculostomy placement: a meta-analysis. Neurocrit Care. 2009;10(2):253–6.
45. Dasgupta D, D'Antona L, Aimone Cat D, Toma AK, Curtis C, Watkins LD, et al. Simulation workshops as an adjunct to perioperative care bundles in the management of external ventricular drains: improving surgical technique and reducing infection. J Neurosurg. 2018:1–5. https://doi.org/10.3171/2018.5.JNS172881.
46. Champey J, Mourey C, Francony G, Pavese P, Gay E, Gergele L, et al. Strategies to reduce external ventricular drain-related infections: a multicenter retrospective study. J Neurosurg. 2018:1–6. https://doi.org/10.3171/2018.1.JNS172486.
47. Alleyne CH Jr, Hassan M, Zabramski JM. The efficacy and cost of prophylactic and perioprocedural antibiotics in patients with external ventricular drains. Neurosurgery. 2000;47(5):1124–7; discussion 1127–1129
48. Holloway KL, Barnes T, Choi S, Bullock R, Marshall LF, Eisenberg HM, et al. Ventriculostomy infections: the effect of monitoring duration and catheter exchange in 584 patients. J Neurosurg. 1996;85(3):419–24.
49. Dasic D, Hanna SJ, Bojanic S, Kerr R. External ventricular drain infection: the effect of a strict protocol on infection rates and a review of the literature. Br J Neurosurg. 2006;20(5):296–300.
50. Harrop JS, Sharan AD, Ratliff J, Prasad S, Jabbour P, Evans JJ, et al. Impact of a standardized protocol and antibiotic-impregnated catheters on ventriculostomy infection rates in cerebrovascular patients. Neurosurgery. 2010;67(1):187–91.
51. Babu MA, Patel R, Marsh WR, Wijdicks EF. Strategies to decrease the risk of ventricular catheter infections: a review of the evidence. Neurocrit Care. 2012;16(1):194–202.
52. Zabramski JM, Whiting D, Darouiche RO, Horner TG, Olson J, Robertson C, et al. Efficacy of antimicrobial-impregnated external ventricular drain catheters: a prospective, randomized, controlled trial. J Neurosurg. 2003;98(4):725–30.
53. Kasotakis G, Michailidou M, Bramos A, Chang Y, Velmahos G, Alam H, et al. Intraparenchymal vs extracranial ventricular drain intracranial pressure monitors in traumatic brain injury: less is more? J Am Coll Surg. 2012;214:950–7.

54. Aiolfi A, Khor D, Cho J, Benjamin E, Inaba K, Demetriades D. Intracranial pressure monitoring in severe blunt head trauma: does the type of monitoring device matter? J Neurosurg. 2018;128(3):828–33.
55. Bales JW, Bonow RH, Buckley RT, Barber J, Temkin N, Chesnut RM. Primary external ventricular drainage catheter versus intraparenchymal ICP monitoring: outcome analysis. Neurocrit Care. 2019;31(1):11–21.
56. Chesnut R, Bleck T, Citerio G, Classen J, Cooper DJ, Coplin WM, et al. A consensus-based guide to the interpretation of the BEST TRIP ICP trial. J Neurotrauma. 2015;32(22):1722–4.
57. Sorrentino E, Diedler J, Kasprowicz M, et al. Critical thresholds for cerebrovascular reactivity after traumatic brain injury. Neurocrit Care. 2012;16:258–66.
58. Meyfroidt G, Citerio G. Letter: Guidelines for the management of severe traumatic brain injury, Fourth edition. Neurosurgery. 2017;81(1):E1.
59. Volovici V, Haitsma IK, Dirven CMF, Steyerberg EW, Lingsma HF, Maas AIR. Letter: Guidelines for the management of severe traumatic brain injury, Fourth edition. Neurosurgery. 2017;81(2):E21.
60. Picetti E, Iaccarino C, Servadei F. Letter: Guidelines for the management of severe traumatic brain injury, Fourth edition. Neurosurgery. 2017;81(1):E2.
61. Alice P, Meghan L, Elizabeth B, Alberto A, Kenji I, Demetrios D. Intracranial pressure monitoring in severe traumatic brain injuries: a closer look at level 1 trauma centers in the United States. Injury. 2017;48(9):1944–50.
62. Marmarou A, Andersen RL, Ward JD, Choi SC, Young HF, Eisenberg HM, et al. Impact of ICP instability and hypotension on outcome in patients with severe head trauma. J Neurosurg. 1991;75(1S):S59–66.
63. Honda M, Ichibayashi R, Suzuki G, Yokomuro H, Seiki Y, Sase S, et al. Consideration of the intracranial pressure threshold value for the initiation of traumatic brain injury treatment: a xenon CT and perfusion CT study. Neurocrit Care. 2017;27(3):308–15.
64. Marshall LF, Barba D, Toole BM, Bowers SA. The oval pupil: clinical significance and relationship to intracranial hypertension. J Neurosurg. 1983;58(4):566–8.
65. Stiefel MF, Udoetuk JD, Spiotta AM, Gracias VH, Goldberg A, Maloney-Wilensky E, et al. Conventional neurocritical care and cerebral oxygenation after traumatic brain injury. J Neurosurg. 2006;105(4):568–75.
66. Vespa P, Bergsneider M, Hattori N, Wu HM, Huang SC, Martin NA, et al. Metabolic crisis without brain ischemia is common after traumatic brain injury: a combined microdialysis and positron emission tomography study. J Cereb Blood Flow Metab. 2005;25(6):763–74.
67. Belli A, Sen J, Petzold A, Russo S, Kitchen N, Smith M. Metabolic failure precedes intracranial pressure rises in traumatic brain injury: a microdialysis study. Acta Neurochir. 2008;150(5):461–9; discussion 470
68. Güiza F, Depreitere B, Piper I, et al. Visualizing the pressure and time burden of intracranial hypertension in adult and paediatric traumatic brain injury. Intensive Care Med. 2015;41:1067–76.
69. Chesnut RM. A conceptual approach to managing severe traumatic brain injury in a time of uncertainty. Ann N Y Acad Sci. 2015;1345(1):99–107.
70. Le Roux P. Intracranial pressure monitoring and management. In: Grant G, Laskowitz D, editors. Translational research in traumatic brain injury. CRC Press; 2015. p. 315–7.
71. Vik A, Nag T, Fredriksli OA, Skandsen T, Moen KG, Schirmer-Mikalsen K, et al. Relationship of "dose" of intracranial hypertension to outcome in severe traumatic brain injury. J Neurosurg. 2008;109(4):678–84.
72. Adams H, Donnelly J, Czosnyka M, Kolias AG, Helmy A, Menon DK, et al. Temporal profile of intracranial pressure and cerebrovascular reactivity in severe traumatic brain injury and association with fatal outcome: an observational study. PLoS Med. 2017;14(7):e1002353.
73. Lazaridis C, DeSantis SM, Smielewski P, Menon DK, Hutchinson P, Pickard JD, et al. Patient-specific thresholds of intracranial pressure in severe traumatic brain injury. J Neurosurg. 2014;120(4):893–900.

74. Helbok R, Olson DM, Le Roux PD, et al. The Participants in the International Multidisciplinary Consensus Conference on Multimodality Monitoring. Intracranial pressure and cerebral perfusion pressure monitoring in non-TBI patients: special considerations. Neurocrit Care. 2014;21(Suppl 2):S85–94.
75. Hemphill JC, Greenberg SM, Anderson CS, et al. Guidelines for the management of spontaneous intracerebral hemorrhage: a guideline for healthcare professionals from the American Heart Association/American Stroke Association. Stroke. 2015;46:2032–60.
76. Alotaibi NM, Wang JZ, Pasarikovski CR, Guha D, Al-Mufti F, Mamdani M, et al. Management of raised intracranial pressure in aneurysmal subarachnoid hemorrhage: time for a consensus? Neurosurg Focus. 2017;43(5):E13.
77. Wang AY, Hsieh PC, Chen CC, Chin SC, Wu YM, Chen CT, et al. Effect of intracranial pressure control on improvement of cerebral perfusion after acute subarachnoid hemorrhage: a comparative angiography study based on temporal changes of intracranial pressure and systemic pressure. World Neurosurg. 2018;120:e290–6.
78. Citerio G, Gaini SM, Tomei G, et al. Management of 350 aneurysmal subarachnoid hemorrhages in 22 Italian neurosurgical centers. Intensive Care Med. 2007;33:1580–6.
79. Chen HI, Stiefel MF, Oddo M, et al. Detection of cerebral compromise with multimodality monitoring in patients with subarachnoid hemorrhage. Neurosurgery. 2011;69:53–63.
80. Zoerle T, Lombardo A, Colombo A, et al. Intracranial pressure after subarachnoid hemorrhage. Crit Care Med. 2015;43:168–76.
81. Sekhon MS, Griesdale DE, Ainslie PN, Gooderham P, Foster D, Czosnyka M, et al. Intracranial pressure and compliance in hypoxic ischemic brain injury patients after cardiac arrest. Resuscitation. 2019;141:96–103.
82. Citerio G, Prisco L, Oddo M, Meyfroidt G, Helbok R, Stocchetti N, et al. International prospective observational study on intracranial pressure in intensive care (ICU): the SYNAPSE-ICU study protocol. BMJ Open. 2019;9(4):e026552.
83. Donnelly J, Czosnyka M, Adams H, Cardim D, Kolias AG, Zeiler FA, et al. Twenty-five years of intracranial pressure monitoring after severe traumatic brain injury: a retrospective, single-center analysis. Neurosurgery. 2019;85(1):E75–82.
84. Maas AIR, Menon DK, Adelson PD, Andelic N, Bell MJ, Belli A, et al. Traumatic brain injury: integrated approaches to improve prevention, clinical care, and research. Lancet Neurol. 2017;16(12):987–1048.
85. Chesnut RM, Temkin N, Dikmen S, Rondina C, Videtta W, Petroni G, et al. A method of managing severe traumatic brain injury in the absence of intracranial pressure monitoring: the imaging and clinical examination protocol. J Neurotrauma. 2018;35(1):54–63.
86. Bonow RH, Barber J, Temkin NR, Videtta W, Rondina C, Petroni G, et al. Global Neurotrauma Research Group. The outcome of severe traumatic brain injury in Latin America. World Neurosurg. 2018;111:e82–90.
87. Rubiano AM, Carney N, Chesnut R, Puyana JC. Global neurotrauma research challenges and opportunities. Nature. 2015;527(7578):S193–7.
88. Okonkwo DO, Shutter LA, Moore C, Temkin NR, Puccio AM, Madden CJ, et al. Brain oxygen optimization in severe traumatic brain injury phase-II: a phase II randomized trial. Crit Care Med. 2017;45(11):1907–14.
89. Wright DW, Yeatts SD, Silbergleit R, Palesch YY, Hertzberg VS, Frankel M, et al. NETT Investigators. Very early administration of progesterone for acute traumatic brain injury. N Engl J Med. 2014;371(26):2457–66.
90. McKhann GM, Mayer S, Le Roux P. Perioperative and ICU care of patients with aneurysmal subarachnoid hemorrhage. In: Le Roux P, Newell DW, Winn HR, editors. Management of cerebral aneurysms. Philadelphia: Elsevier Science; 2004. p. 431–54.
91. Merck L, Yeatts S, Silbergleit R, Palesch Y, LeRoux P, Manley G, et al. The effect of goal directed therapy on patient morbidity and mortality after traumatic brain injury: results from the ProTECTIII Clinical Trial. Crit Care Med. 2019;47(5):623–31.

92. Wiener J, McIntyre A, Janzen S, Mirkowski M, MacKenzie HM, Teasell R. Opioids and cerebral physiology in the acute management of traumatic brain injury: a systematic review. Brain Inj. 2019;33(5):559–66.
93. Clifton GL, Miller ER, Choi SC, Levin HS. Fluid thresholds and outcome from severe brain injury. Crit Care Med. 2002;30:739–45.
94. Robertson CS, Valadka AB, Hannay HJ, Contant CF, Gopinath SP, Cormio M. Prevention of secondary ischemic insults after severe head injury. Crit Care Med. 1999;27(10):2086–95.
95. Farrokh S, Cho SM, Suarez JI. Fluids and hyperosmolar agents in neurocritical care: an update. Curr Opin Crit Care. 2019;25(2):105–9.
96. Rossi S, Picetti E, Zoerle T, Carbonara M, Zanier ER, Stocchetti N. Fluid management in acute brain injury. Curr Neurol Neurosci Rep. 2018;18(11):74.
97. Oddo M, Poole D, Helbok R, Meyfroidt G, Stocchetti N, Bouzat P, et al. Fluid therapy in neurointensive care patients: ESICM consensus and clinical practice recommendations. Intensive Care Med. 2018;44(4):449–63.
98. SAFE Study Investigators; Australian and New Zealand Intensive Care Society Clinical Trials Group; Australian Red Cross Blood Service; George Institute for International Health, Myburgh J, Cooper DJ, Finfer S, Bellomo R, Norton R, Bishop N, Kai Lo S, Vallance S. Saline or albumin for fluid resuscitation in patients with traumatic brain injury. N Engl J Med. 2007;357(9):874–84.
99. Finfer S, Bellomo R, Boyce N, French J, Myburgh J, Norton R, SAFE Study Investigators. A comparison of albumin and saline for fluid resuscitation in the intensive care unit. N Engl J Med. 2004;350(22):2247–56.
100. Heifets BD, Tanaka P, Burbridge MA. Fluid management concepts for severe neurological illness: an overview. Curr Opin Anaesthesiol. 2018;31(5):526–31.
101. Corcoran T, Rhodes JE, Clarke S, Myles PS, Ho KM. Perioperative fluid management strategies in major surgery: a stratified meta-analysis. Anesth Analg. 2012;114(3):640–51.
102. Le Roux PD, Participants in the International Multi-disciplinary Consensus Conference on the Critical Care Management of Subarachnoid Hemorrhage. Anemia and transfusion after subarachnoid hemorrhage. Neurocrit Care. 2011;15(2):342–53.
103. Le Roux P. Treatment of anemia. In: Timmons S, editor. Controversies in the management of traumatic brain injury. Springer International Publishing; 2018. p. 117–43.
104. Oddo M, Levine JM, Kumar M, Iglesias K, Frangos S, Maloney-Wilensky E, Le Roux P. Anemia and brain oxygen after severe traumatic brain injury. Intensive Care Med. 2012;38(9):1497–504.
105. Gu J, Huang H, Huang Y, Sun H, Xu H. Hypertonic saline or mannitol for treating elevated intracranial pressure in traumatic brain injury: a meta-analysis of randomized controlled trials. Neurosurg Rev. 2019;42(2):499–509.
106. Alnemari AM, Krafcik BM, Mansour TR, Gaudin D. A comparison of pharmacologic therapeutic agents used for the reduction of intracranial pressure following traumatic brain injury. World Neurosurg. 2017;S1878-8750(17):31108–7.
107. Kamel H, Navi BB, Nakagawa K, Hemphill JC III, Ko NU. Hypertonic saline versus mannitol for the treatment of elevated intracranial pressure: a meta-analysis of randomized clinical trials. Crit Care Med. 2011;39:554–9.
108. Sorani MD, Manley GT. Dose-response relationship of mannitol and intracranial pressure: a metaanalysis. J Neurosurg. 2008;108(1):80–7.
109. Kosty J, Le Roux P, Levine J, Park S, Kumar M, Frangos S, et al. Comparison of clinical and research practices in measuring cerebral perfusion pressure (CPP): a literature review and multidisciplinary survey. Anesth Analg. 2013;117(3):694–8.
110. Griesdale DE, Örtenwall V, Norena M, Wong H, Sekhon MS, Kolmodin L, et al. Adherence to guidelines for management of cerebral perfusion pressure and outcome in patients who have severe traumatic brain injury. J Crit Care. 2015;30(1):111–5.

111. Güiza F, Meyfroidt G, Piper I, Citerio G, Chambers I, Enblad P, et al. Cerebral perfusion pressure insults and associations with outcome in adult traumatic brain injury. J Neurotrauma. 2017;34(16):2425–31.
112. Aries MJ, et al. Continuous determination of optimal cerebral perfusion pressure in traumatic brain injury. Crit Care Med. 2012;40(8):2456–63.
113. Donnelly J, Czosnyka M, Adams H, Robba C, Steiner LA, Cardim D, et al. Individualizing thresholds of cerebral perfusion pressure using estimated limits of autoregulation. Crit Care Med. 2017;45(9):1464–71.
114. Needham E, McFadyen C, Newcombe V, Synnot AJ, Czosnyka M, Menon D. Cerebral perfusion pressure targets individualized to pressure-reactivity index in moderate to severe traumatic brain injury: a systematic review. J Neurotrauma. 2017;34(5):963–70.
115. Shiozaki T, et al. Effect of mild hypothermia on uncontrollable intracranial hypertension after severe head injury. J Neurosurg. 1993;79(3):363–8.
116. Andrews PJ, Sinclair HL, Rodríguez A, Harris B, Rhodes J, Watson H, et al. Therapeutic hypothermia to reduce intracranial pressure after traumatic brain injury: the Eurotherm3235 RCT. Health Technol Assess. 2018;22(45):1–134.
117. Andrews PJD, Rodriguez A, Suter P, Battison CG, Rhodes JKJ, Puddu I, et al. Mortality risk stratification after traumatic brain injury and hazard of death with titrated hypothermia in the Eurotherm3235Trial. Crit Care Med. 2017;45(5):883–90.
118. Clifton GL, Valadka A, Zygun D, et al. Very early hypothermia induction in patients with severe brain injury (the National Acute Brain Injury Study: Hypothermia II): a randomized trial. Lancet Neurol. 2011;10:131.
119. Cooper DJ, Nichol AD, Bailey M, Bernard S, Cameron PA, Pili-Floury S, et al. POLAR Trial Investigators and the ANZICS Clinical Trials Group. Effect of early sustained prophylactic hypothermia on neurologic outcomes among patients with severe traumatic brain injury: the POLAR randomized clinical trial. JAMA. 2018;320(21):2211–20.
120. Schneider H, Krüger P, Algra A, Hofmeijer J, van der Worp HB, Jüttler E, et al. No benefits of hypothermia in patients treated with hemicraniectomy for large ischemic stroke. Int J Stroke. 2017;12(7):732–40.
121. Oddo M, Frangos S, Maloney-Wilensky E, Andrew Kofke W, Le Roux P, Levine JM. Effect of shivering on brain tissue oxygenation during induced normothermia in patients with severe brain injury. Neurocrit Care. 2010;12(1):10–6.
122. Povlishock JT, Wei EP. Posthypothermic rewarming considerations following traumatic brain injury. J Neurotrauma. 2009;26:333–40.
123. Timofeev I, Czosnyka M, Nortje J, Smielewski P, Kirkpatrick P, Gupta A, et al. Effect of decompressive craniectomy on intracranial pressure and cerebrospinal compensation following traumatic brain injury. J Neurosurg. 2008;108(1):66–73.
124. Jiang JY, Xu W, Li WP, Xu WH, Zhang J, Bao YH, et al. Efficacy of standard trauma craniectomy for refractory intracranial hypertension with severe traumatic brain injury: a multicenter, prospective, randomized controlled study. J Neurotrauma. 2005;22:623–8.
125. Weiner GM, Lacey MR, Mackenzie L, Shah DP, Frangos SG, Grady MS, et al. Decompressive craniectomy for elevated intracranial pressure and its effect on the cumulative ischemic burden and therapeutic intensity levels after severe traumatic brain injury. Neurosurgery. 2010;66(6):1111–8.
126. Allen CJ, Baldor DJ, Hanna MM, Namias N, Bullock MR, Jagid JR, et al. Early craniectomy improves intracranial and cerebral perfusion pressure after severe traumatic brain injury. Am Surg. 2018;84(3):443–50.
127. Ho CL, Wang CM, Lee KK, Ng I, Ang BT. Cerebral oxygenation, vascular reactivity, and neurochemistry following decompressive craniectomy for severe traumatic brain injury. J Neurosurg. 2008;108:943–9.
128. Olivecrona M, Rodling-Wahlström M, Naredi S, Koskinen LO. Effective ICP reduction by decompressive craniectomy in patients with severe traumatic brain injury treated by an ICP targeted therapy. J Neurotrauma. 2007;24:927–35.

129. Lazaridis C, Czosnyka M. Cerebral blood flow, brain tissue oxygen, and metabolic effects of decompressive craniectomy. Neurocrit Care. 2012;16:478–84.
130. Reithmeier T, Löhr M, Pakos P, Ketter G, Ernestus RI. Relevance of ICP and ptiO2 for indication and timing of decompressive craniectomy in patients with malignant brain edema. Acta Neurochir. 2005;147:947–51.
131. Joseph DK, Dutton RP, Aarabi B, Scalea TM. Decompressive laparotomy to treat intractable intracranial hypertension after traumatic brain injury. J Trauma. 2004;57(4):687–93.
132. Vahedi K, Hofmeijer J, Juettler E, Vicaut E, George B, Algra A, et al. DECIMAL, DESTINY, and HAMLET Investigators. Early decompressive surgery in malignant infarction of the middle cerebral artery: a pooled analysis of three randomised controlled trials. Lancet Neurol. 2007;6(3):215–22.
133. Jüttler E, Unterberg A, Woitzik J, Bösel J, Amiri H, Sakowitz OW, et al. DESTINY II Investigators. Hemicraniectomy in older patients with extensive middle-cerebral-artery stroke. N Engl J Med. 2014;370(12):1091–100.
134. Cooper DJ, Rosenfeld JV, Murray L, et al. Decompressive craniectomy in diffuse traumatic brain injury. N Engl J Med. 2011;364(16):1493–502.
135. Hutchinson PJ, Kolias AG, Timofeev IS, Corteen EA, Czosnyka M, Timothy J, et al. RESCUEicp Trial Collaborators. Trial of decompressive craniectomy for traumatic intracranial hypertension. N Engl J Med. 2016;375(12):1119–30.
136. Van Essen TA, den Boogert HF, Cnossen MC, de Ruiter GCW, Haitsma I, Polinder S, et al. CENTER-TBI Investigators and Participants. Variation in neurosurgical management of traumatic brain injury: a survey in 68 centers participating in the CENTER-TBI study. Acta Neurochir. 2019;161(3):435–49.
137. Gupta D, Singla R, Mazzeo AT, Schnieder EB, Tandon V, Kale SS, et al. Detection of metabolic pattern following decompressive craniectomy in severe traumatic brain injury: a microdialysis study. Brain Inj. 2017;31(12):1660–6.
138. Kaushal A, Bindra A, Kumar A, Goyal K, Kumar N, Rath GP, et al. Long term outcome in survivors of decompressive craniectomy following severe traumatic brain injury. Asian J Neurosurg. 2019;14(1):52–7.
139. Moskowitz E, Melendez CI, Dunn J, Khan AD, Gonzalez R, Liebscher S, et al. Long-term effects of decompressive craniectomy on functional outcomes after traumatic brain injury: a multicenter study. Am Surg. 2018;84(8):1314–8.
140. Nasi D, Dobran M, Di Rienzo A, di Somma L, Gladi M, Moriconi E, et al. Decompressive craniectomy for traumatic brain injury: the role of cranioplasty and hydrocephalus on outcome. World Neurosurg. 2018;116:e543–9.
141. Wen L, Lou HY, Xu J, Wang H, Huang X, Gong JB, et al. The impact of cranioplasty on cerebral blood perfusion in patients treated with decompressive craniectomy for severe traumatic brain injury. Brain Inj. 2015;29:1654–69.
142. Malcom JG, Rindler RS, Chu JK, Chokshi F, Grossberg JA, Pradilla G, et al. Early cranioplasty is associated with greater neurological improvement: a systematic review and meta-analysis. Neurosurgery. 2018;82(3):278–88.
143. Morton RP, Abecassis IJ, Hanson JF, Barber JK, Chen M, Kelly CM, et al. Timing of cranioplasty: a 10.75-year single-center analysis of 754 patients. J Neurosurg. 2018;128(6):1648–52.
144. Miller JD, Butterworth JF, Gudeman SK, Faulkner JE, Choi SC, Selhorst JB, et al. Further experience in the management of severe head injury. J Neurosurg. 1981;54(3):289–99.
145. Ziai WC, Melnychuk E, Thompson CB, Awad I, Lane K, Hanley DF. Occurrence and impact of intracranial pressure elevation during treatment of severe intraventricular hemorrhage. Crit Care Med. 2012;40:1601–8.
146. Cossu G, Messerer M, Stocchetti N, Levivier M, Daniel RT, Oddo M. Intracranial pressure and outcome in critically ill patients with aneurysmal subarachnoid hemorrhage: a systematic review. Minerva Anestesiol. 2016;82(6):684–96.

147. Sykora M, Steinmacher S, Steiner T, Poli S, Diedler J. Association of intracranial pressure with outcome in comatose patients with intracerebral hemorrhage. J Neurol Sci. 2014;342(1–2):141–5.
148. Ko SB, Choi HA, Parikh G, Helbok R, Schmidt JM, Lee K, et al. Multimodality monitoring for cerebral perfusion pressure optimization in comatose patients with intracerebral hemorrhage. Stroke. 2011;42:3087–92.
149. Signorini DF, Andrews PJ, Jones PA, et al. Adding insult to injury: the prognostic value of early secondary insults for survival after traumatic brain injury. J Neurol Neurosurg Psychiatry. 1999;66:26–31.
150. Kirkness CJ, Burr RL, Mitchell PH. Intracranial pressure variability and long-term outcome following traumatic brain injury. Acta Neurochir Suppl. 2008;102:105–8.
151. Kahraman S, Hu P, Stein DM, et al. Dynamic three-dimensional scoring of cerebral perfusion pressure and intracranial pressure provides a brain trauma index that predicts outcome in patients with severe traumatic brain injury. J Trauma. 2011;70:547–53.
152. Fakry SM, Trask AL, Waller MA, Watts DD. Management of brain-injured patients by an evidence-based medicine protocol improves outcomes and decreases hospital charges. J Trauma. 2004;56(56):492–9; discussion 499–500
153. Gerber LM, Chiu YL, Carney N, Härtl R, Ghajar J. Marked reduction in mortality in patients with severe traumatic brain injury. J Neurosurg. 2013;119(6):1583–90.
154. Alali AS, et al. Intracranial pressure monitoring in severe traumatic brain injury: results from the American College of Surgeons Trauma Quality Improvement Program. J Neurotrauma. 2013;30(20):1737–46.
155. Stein SC, et al. Relationship of aggressive monitoring and treatment to improved outcomes in severe traumatic brain injury. J Neurosurg. 2010;112:1105–12.
156. Talving P, Karamanos E, Teixeira PG, Skiada D, Lam L, Belzberg H, et al. Intracranial pressure monitoring in severe head injury: compliance with Brain Trauma Foundation guidelines and effect on outcomes: a prospective study. J Neurosurg. 2013;119(5):1248–54.
157. Farahvar A, et al. Increased mortality in patients with severe traumatic brain injury treated without intracranial pressure monitoring. J Neurosurg. 2012;117(4):729–34.
158. Arabi YM, et al. Mortality reduction after implementing a clinical practice guidelines-based management protocol for severe traumatic brain injury. J Crit Care. 2010;25(2):190–5.
159. Haddad S, et al. Relationship between intracranial pressure monitoring and outcomes in severe traumatic brain injury patients. Anaesth Intensive Care. 2011;39(6):1043–50.
160. Bulger EM, et al. Management of severe head injury: institutional variations in care and effect on outcome. Crit Care Med. 2002;30(8):1870–6.
161. Barmparas G, et al. Decreased intracranial pressure monitor use at level II trauma centers is associated within creased mortality. Am Surg. 2012;78(10):1166–71.
162. Whitmore RG, Thawani JP, Grady MS, Levine JM, Sanborn MR, Stein SC. Is aggressive treatment of traumatic brain injury cost-effective? J Neurosurg. 2012;116(5):1106–13.
163. Shafi S, Barnes SA, Millar D, Sobrino J, Kudyakov R, Berryman C, et al. Suboptimal compliance with evidence-based guidelines in patients with traumatic brain injuries. J Neurosurg. 2014;120:773–7.
164. Dawes AJ, Sacks GD, Cryer HG, Gruen JP, Preston C, Gorospe D, et al. Intracranial pressure monitoring and inpatient mortality in severe traumatic brain injury: a propensity score-matched analysis. J Trauma Acute Care Surg. 2015;78:492–501.
165. Cremer OL, van Dijk GW, van Wensen E, Brekelmans GJ, Moons KG, Leenen LP, et al. Effect of intracranial pressure monitoring and targeted intensive care on functional outcome after severe head injury. Crit Care Med. 2005;33:2207–13.
166. Shafi S, Diaz-Arrastia R, Madden C, Gentilello L. Intracranial pressure monitoring in brain-injured patients is associated with worsening of survival. J Trauma. 2008;64:335–40.
167. Shen L, Wang Z, Su Z, Qiu S, Xu J, Zhou Y, et al. Effects of intracranial pressure monitoring on mortality in patients with severe traumatic brain injury: a meta-analysis. PLoS One. 2016;11(12):e0168901.

168. Lee JC, Rittenhouse K, Bupp K, Gross B, Rogers A, Rogers FB, et al. An analysis of Brain Trauma Foundation traumatic brain injury guideline compliance and patient outcome. Injury. 2015;46(5):854–8.
169. Cnossen MC, Polinder S, Andriessen TM, van der Naalt J, Haitsma I, Horn J, et al. Causes and consequences of treatment variation in moderate and severe traumatic brain injury: a multicenter study. Crit Care Med. 2017;45(4):660–9.
170. Chestnut RM, Temkin N, Carney N, et al. A trial of intracranial-pressure monitoring in traumatic brain injury. N Engl J Med. 2012;367(26):2471–81.
171. Menon DK, Maas AI. Traumatic brain injury in 2014. Progress, failures and new approaches for TBI research. Nat Rev Neurol. 2015;11(2):71–2.
172. Veenith TV, Carter EL, Geeraerts T, Grossac J, Newcombe VF, Outtrim J, et al. Pathophysiologic mechanisms of cerebral ischemia and diffusion hypoxia in traumatic brain injury. JAMA Neurol. 2016;73(5):542–50.
173. Howells T, Elf K, Jones PA, Ronne-Engström E, Piper I, Nilsson P, et al. Pressure reactivity as a guide in the treatment of cerebral perfusion pressure in patients with brain trauma. J Neurosurg. 2005;102(2):311–7.
174. Zeiler FA, Ercole A, Beqiri E, Cabeleira M, Aries M, Zoerle T, et al. CENTER-TBI High Resolution ICU (HR ICU) Sub-Study Participants and Investigators. Cerebrovascular reactivity is not associated with therapeutic intensity in adult traumatic brain injury: a CENTER-TBI analysis. Acta Neurochir. 2019;161(9):1955–64.
175. Eide PK, Bentsen G, Sorteberg AG, Marthinsen PB, Stubhaug A, Sorteberg W. A randomized and blinded single-center trial comparing the effect of intracranial pressure and intracranial pressure wave amplitude-guided intensive care management on early clinical state and 12-month outcome in patients with aneurysmal subarachnoid hemorrhage. Neurosurgery. 2011;69(5):1105–15.
176. Balestreri M, Czosnyka M, Steiner LA, Schmidt E, Smielewski P, Matta B, et al. Intracranial hypertension: what additional information can be derived from ICP waveform after head injury? Acta Neurochir. 2004;146(2):131–41.
177. Liu X, Donnelly J, Czosnyka M, Aries MJH, Brady K, Cardim D, et al. Cerebrovascular pressure reactivity monitoring using wavelet analysis in traumatic brain injury patients: a retrospective study. PLoS Med. 2017;14(7):e1002348.
178. Zeiler FA, Donnelly J, Calviello L, Smielewski P, Menon DK, Czosnyka M. Pressure autoregulation measurement techniques in adult traumatic brain injury, part II: a scoping review of continuous methods. J Neurotrauma. 2017;34(23):3224–37.
179. Svedung Wettervik T, Howells T, Enblad P, Lewén A. Temporal neurophysiological dynamics in traumatic brain injury: role of pressure reactivity and optimal cerebral perfusion pressure for predicting outcome. J Neurotrauma. 2019;36(11):1818–27.
180. Menon DK, Coles JP, Gupta AK, Fryer TD, Smielewski P, Chatfield DA, et al. Diffusion limited oxygen delivery following head injury. Crit Care Med. 2004;32:1384–90.
181. Vespa PM, O'Phelan K, McArthur D, Miller C, Eliseo M, Hirt D, et al. Pericontusional brain tissue exhibits persistent elevation of lactate/pyruvate ratio independent of cerebral perfusion pressure. Crit Care Med. 2007;35(4):1153–60.
182. Adamides AA, Rosenfeldt FL, Winter CD, et al. Brain tissue lactate elevations predict episodes of intracranial hypertension in patients with traumatic brain injury. J Am Coll Surg. 2009;209:531–9.
183. Al-Mufti F, Dodson V, Lee J, Wajswol E, Gandhi C, Scurlock C, et al. Artificial intelligence in neurocritical care. J Neurol Sci. 2019;404:1–4.
184. Lazaridis C, Rusin CG, Robertson CS. Secondary brain injury: predicting and preventing insults. Neuropharmacology. 2019;145(Pt B):145–52.
185. Bouzat P, Sala N, Payen JF, Oddo M. Beyond intracranial pressure: optimization of cerebral blood flow, oxygen, and substrate delivery after traumatic brain injury. Ann Intensive Care. 2013;3(1):23.

186. Lazaridis C, Robertson CS. The role of multimodal invasive monitoring in acute traumatic brain injury. Neurosurg Clin N Am. 2016;27(4):509–17.
187. Dellazizzo L, Demers SP, Charbonney E, Williams V, Serri K, Albert M, et al. Minimal PaO2 threshold after traumatic brain injury and clinical utility of a novel brain oxygenation ratio. J Neurosurg. 2018;1:1–9.
188. Godoy DA, Lubillo S, Rabinstein AA. Pathophysiology and management of intracranial hypertension and tissular brain hypoxia after severe traumatic brain injury: an integrative approach. Neurosurg Clin N Am. 2018;29(2):195–212.

Chapter 3
Intracerebral Hemorrhage (ICH) Approach: Bedside Practical Review

Thomas J. Cusack and Wendy Ziai

Key Points

1. Recognize intracerebral hemorrhage (ICH) and stabilize the patient's airway and circulation. Recognize intracranial hemorrhage as soon as possible utilizing computed tomography (CT) and computed tomography angiography (CTA). Unstable patients (those with rapidly declining Glasgow Coma Scale or anyone with a Glasgow Coma Scale less than 8) should undergo emergent intubation to secure their airway and be sedated after a thorough neurologic exam has been obtained. The ICH score and Functional Outcome in Patients with Primary Intracerebral Hemorrhage (FUNC) scores should be assessed.
2. Systolic blood pressure should be rapidly controlled to a range of 140–180 mmHg in small hemorrhages without intracranial hypertension using beta blockers or calcium channel blockers. Target the goals of normothermia, normoglycemia, and normonatremia.
3. Elevate the head of the bed to 30° and treat elevated intracranial pressure if present with appropriate surgical and medical measures. Patients should be assessed for the need for surgical intervention for control of elevated intracranial pressure; using an external ventricular drain or, in appropriately selected patients, decompressive craniotomy. Also, consideration of evacuation may be appropriate in a select subset of ICH patients. Not all patients benefit from surgical intervention.
4. Correct any coagulopathy if present. Reverse anticoagulation in patients with ICH who are on anticoagulant or antiplatelet drugs.
5. Once stabilized, patients should be reassessed with CT imaging and have ongoing management of blood pressure, cerebral edema, intracranial pressure, and seizures as they arise.

T. J. Cusack · W. Ziai (✉)
Division of Neurosciences Critical Care, Departments of Neurology, Neurosurgery, and Critical Care Medicine, The Johns Hopkins Hospital, Baltimore, MD, USA
e-mail: tcusack1@jhmi.edu; weziai@jhmi.edu

C. N. Rodríguez et al. (eds.), *Neurosonology in Critical Care*,
https://doi.org/10.1007/978-3-030-81419-9_3

3.1 Introduction

The delivery of neurocritical care is not so much the performance of one large life-saving act but rather the careful execution and minding of hundreds of smaller things that taken together can add up to saving a life that might otherwise be lost and hopefully improving a life that otherwise would be greatly limited. This is particularly true in the care of intracerebral hemorrhage (ICH), a challenging entity faced around the world by neurosurgeons, neurologists, and emergency care providers of all stripes. The past 40 years have seen marked improvement in the mortality of ICH from around 47% to 29% for those cases that make it to the hospital [1], but while a great deal of research has demonstrated the safety of a number of approaches that will be discussed in this chapter, very little research has been definitively shown to improve outcomes or mortality. Only 10–20% of patients who survive hospitalization currently regain functional independence [2]. It is not possible to point to any one intervention or approach that has improved outcomes, so obtaining the best possible outcomes for your patient will involve minding both the specific issues surrounding management of ICH as well as the general principles of good quality critical care. In this sense the problem space for ICH is limited by the solutions available to the caregiver at the time. In this chapter, we will review the approach to ICH from the practical perspective of the bedside practitioner, distilling the approach the authors take at the bedside, and showing the evidence from which that approach is derived. At the end of the chapter an algorithm for care is presented, but please understand that the care of ICH is far from standardized as the range of patients and pathology that falls under this category is exceedingly broad.

3.2 Intracerebral Hemorrhage (ICH)

Intracerebral hemorrhage is a type of intracranial bleed that occurs specifically within the tissue of the brain or ventricles. In the field, the sudden onset of neurologic deficits should immediately raise concern for a stroke. Rapid recognition of neurologic deficits by bystanders or trained emergency medical responders is essential and rapid transport to a hospital capable of rapid imaging with a CT scan of the head and brain is the essential first step in appropriate diagnosis and treatment. Brain CT and careful history and neurologic exam can serve to help delineate an ischemic stroke from an intracranial bleed. Intracranial bleeds can occur within the parenchyma of the brain or in the meninges and associated potential spaces including the epidural space, subdural space, and subarachnoid space. Bleeds in these areas are covered in detail in other chapters. Intracerebral hemorrhage is a subtype of intracranial bleed that is intraparenchymal with or without extension into the ventricles and can occur anywhere in the brain. It is broadly categorized as either “deep” or “lobar.” “Deep ICH” describes ICH within the basal ganglia and internal

capsule (35–70% of cases), brain stem (5–10% of cases), or cerebellum (5–10% of cases). "Lobar ICH" describes the other 15–30% of cases where it is seen in cortical and subcortical areas [3].

3.3 ICH: Presenting Symptoms

The presenting symptoms of ICH are as varied as the regions of the brain that can be affected. Headache and vomiting are seen in approximately one half of patients with ICH [4]. While there can be sudden onset during marked physical exertion or emotional moments, most occur during routine activity. Unlike ischemic embolism or subarachnoid hemorrhage, the neurologic symptoms of ICH are often not abrupt or maximal at the time of onset but rather the symptoms usually worsen over a period of minutes to hours. Symptoms can be absent in small hemorrhages, which clinically are indistinguishable from a gradually progressing stroke until imaging can be obtained. ICH is rarely a clinical diagnosis alone, but exam and history can help. If a headache is present, it can be due to elevated intracranial pressure or blood in the cerebral spinal fluid irritating the meninges. Most headaches occur with lobar or cerebellar hemorrhages. Patients may also have stiff neck or meningismus if there is intraventricular blood.

If the putamen is involved, the white matter tracts will be affected with hemisensory loss, hemiplegia, possible homonymous hemianopsia, and possible gaze palsy. A cerebellar hemorrhage will often have extension into the fourth ventricle and often originate in the dentate nucleus. There is often a sudden loss of balance with consequent inability to ambulate, notably without any hemiparesis, as well as vomiting, headache (sometimes with referred pain to the back of head or shoulders), and neck stiffness, and in patients with extension into the pontine tegmentum gaze, palsy and facial weakness can be observed. A hemorrhage in the thalamus can cause hemiparesis, hemisensory loss, and aphasia if the bleed is in the dominant hemisphere and hemineglect if it is in the nondominant hemisphere. Most lobar hemorrhages occur in the parietal and occipital lobes. Lobar hemorrhages have a higher incidence of seizures as seizure is a cortical symptom. Occipital hemorrhages often present with dense contralateral homonymous hemianopsia. Frontal hemorrhages often cause a contralateral paresis of the leg with relative sparing of the upper extremity. The most neurologically severe location for an ICH is the pons, which often causes a deep coma and total paralysis with pinpoint pupils and absent horizontal eye movements. Facial palsy, deafness, dysarthria, and ocular bobbing may be observed if the patient is awake. Seizures will occur in the first 72 h after ICH in 4–29% of patients [5], again most commonly in those with lobar hemorrhages. In larger bleeds, decreased level of consciousness is commonly seen. Stupor or coma is an ominous sign in ICH.

3.4 ICH: Who Gets and Why

Intracerebral hemorrhage is a particularly challenging entity because it can happen virtually anywhere in the brain with severity ranging from nearly clinically undetectable to the almost invariably fatal. ICH is prevalent throughout the world, with ICH and subarachnoid hemorrhage (SAH) together accounting for roughly 10–20% of the world's strokes, while ischemic stroke accounts for the remaining 80–90% [6]. There were 5.3 million ICH cases worldwide in 2010 with 3 million deaths of which 84% were borne by low- and middle-income countries (80% of the cases and 63% of the deaths occurred in Sub-Saharan Africa, Central Asia, and Southeast Asia) [7]. Between 1990 and 2010, the global incidence of hemorrhagic strokes (ICH and SAH combined) increased by 47%. In high-income countries, the age-adjusted incidence rate of hemorrhagic stroke reduced by 8% during those two decades but rose by 22% in the low- and middle-income countries [7]. The incidence of primary ICH in low- and middle-income countries from 2000 to 2008 was 22 per 100,000 person-years, while in high-income countries it was 10 per 1000,000 person-years [6]. The incidence of primary ICH by population closely tracks the incidence of hypertension in those populations, with a systematic review of 36 population-based epidemiological studies showing the incidence rate of ICH per 100,000 person years to be 51.8 in Asians, 24.2 in Whites, 22.9 in Blacks, and 19.6 in Hispanics [2]. Patients who make it to the hospital still face 30-day fatality risk of up to 45% in some studies [8]. Those who survive have markedly limited function in activities of daily living, with only 10–20% regaining functional independence [9, 10]. The challenge facing the world in coming decades will be not only treating the ICH in countries with less developed public health infrastructure but also preventing it in the first place, which brings us to our discussion of risk factors.

3.5 Risk Factors for ICH

3.5.1 Blood Hypertension

Spontaneous ICH is the product of a complex interplay of risk factors, the most important of which is hypertension [11, 12]. A meta-analysis of 14 case-control studies demonstrated an increased relative risk for ICH in hypertensive subjects of 3.68 (95% CI, 2.52–5.38) over normotensive people [11]. Patients with baseline blood pressure over 160/90 were shown in another meta-analysis to have a ninefold increased risk of ICH [12]. Even among those with normal blood pressure, increasing blood pressure is related linearly to increasing risk of lobar and nonlobar hemorrhagic stroke [13]. Chronic hypertension is generally associated with ICH in the basal ganglia, thalamus, brainstem, and cerebellum. Cocaine intoxication and malignant hypertension should also be considered at the time of presentation.

3.5.2 Other Risk Factors

Smoking carries a 1.5-fold relative risk for ICH [14, 15]. ICH is also more likely in those with high alcohol intake, low cholesterol levels [16, 17], or diabetics with a relative risk of 1.6 [18]. Cerebral amyloid angiopathy (CAA) alone accounts for roughly 50% of all lobar hemorrhages [19]. The ICH seen with CAA is often lobar and rarely cerebellar. Patients taking aspirin [20], warfarin [21], and direct anticoagulants (DOACs) (dabigatran etexilate, rivaroxaban, and apixaban) have an increased risk of ICH, although this risk is often far exceeded by the benefit provided by the prevention of ischemic strokes [22]. Although no prospective studies have evaluated the impact of specific modifiable risk factor management (e.g., antihypertensive management and smoking cessation on the risk of intraparenchymal hemorrhage), such lifestyle modifications are likely to reduce the risk of ICH significantly. The job of prevention is largely in the hands of primary care providers but, after an ICH mitigating, future risk ideally would involve lifestyle modification and medical treatment for any of the above risk factors.

3.6 ICH: Pathophysiology

ICH occurs after a parenchymal blood vessel in the brain ruptures. Common etiologies include amyloid angiopathy, tumors, ischemic stroke with subsequent hemorrhagic conversion, thrombosis of dural venous sinuses and cortical veins, vasculitis, and vascular malformations such as cavernous angiomas, arteriovenous fistulas, arteriovenous malformations, venous angiomas, and aneurysms. Most "primary" cases of spontaneous ICH are thought to be caused by the rupture of Charcot Bouchard aneurysms in the cerebellum, basal ganglia, pons, and thalamus, where small penetrating vessels are abundant. Charcot Bouchard aneurysms are presumed to be the result of chronic hypertension-related lipohyalinosis of small arterioles which causes defects in the muscular layer making them prone to rupture [23]. The "primary" etiology is a diagnosis of exclusion based on a thorough investigation for "secondary" structural causes of ICH. "Secondary" causes of ICH can include arteriovenous malformation (AVM), cerebral venous sinus thrombosis, hemorrhagic transformation of ischemic stroke, Moyamoya disease, tumor, and aneurysms. If a patient is younger, and has a lobar ICH or intraventricular blood, this suggests higher risk of secondary ICH [24].

Advanced age, deep location (basal ganglia, thalami, or posterior fossa), or history of hypertension are often taken to suggest primary ICH, although cerebral angiography studies show that these are not always reliable indicators, and patients with these features may have coexisting vascular abnormalities [25, 26].

3.7 ICH: Initial Management

The initial triage of a neurological patient should always focus on quickly identifying life-threatening issues and stabilizing the patient before moving on to identify the cause of neurologic deficit with a focus on what is common and what is treatable. The first step in management should focus on the stabilization of the airway, breathing, and circulation. The airway should be secured if the patient does not appear to be able to protect their airway. The need for an accurate neurologic exam, while of great importance, must be balanced against the risk of airway compromise.

3.7.1 Airway: Intubation

Rapid sequence endotracheal intubation (RSI) may be necessary in the emergent setting for the rapidly deteriorating patient. Patients undergoing RSI may benefit from pretreatment with lidocaine 1.5 mg/kg if they appear to have ICP issues as this may blunt the rise in intracranial pressure that can be associated with intubation [27]. Induction with etomidate (0.2 mg/kg) may preserve cerebral perfusion pressure. Paralysis can be obtained with succinylcholine (1.5 mg/kg), rocuronium (1 mg/kg), or vecuronium (0.15 mg/kg). Propofol 5–80°μg/kg/min may be a good initial choice as a continuous drip but does carry the risk of propofol infusion syndrome [28]. Elevated creatine kinase, amylase, lipase, or serum triglycerides can indicate a need to discontinue propofol and initiate another sedative such as midazolam or dexmedetomidine.

3.7.2 Clinical Scoring and Examination

Once stable from a cardiopulmonary perspective, clinical severity should be scored and documented using the NIH Stroke Scale (NIHSS) and Glasgow Coma Scale (GCS) [29–31]. Hourly or more frequent neurologic exams should be scheduled thereafter.

3.7.3 ICH: Imaging

The American Heart Association considers neuroimaging with CT (the gold standard) or MRI mandatory, with the use of contrast-enhanced CT angiography (CTA) when available to assess for vascular pathology and likelihood of further clot expansion [26]. Vascular abnormalities should be suspected in women, those under the age of 65, those with lobar ICH, intraventricular hemorrhage (IVH), and patients without a history of hypertension, smoking, or coagulopathy [32]. Catheter

angiography can confirm definitively if there is an underlying vascular lesion, but this is often only available at larger centers [33]. If cerebral venous sinus thrombosis is suspected based on hematoma location, unusual appearance of cerebral sinuses, or increased relative edema volume then CT venography or magnetic resonance venography (MRV) should be performed [34].

The volume of ICH is an important factor in outcomes, with volumes over 30 mL tending to have increased mortality and morbidity [10]. One recent meta-analysis suggested that for each 1 mL increase in hemorrhage volume at hospital admission, the odds of early neurological deterioration increases by 37% [35]. The volume of ICH can be accurately assessed using a range of automated computational techniques if the required software is available, but a quick estimate can be garnered by applying the ABC/2 method to the initial noncontrast CT image. All measurements should be obtained on axial slices, with A being the largest diameter of hematoma seen in any slice and B the diameter taken perpendicular to that on the same slice. C is the slice thickness multiplied by the number of slices. These three values multiplied together and then divided by two give an estimate of the volume of the hematoma assuming a spherical shape. While not as accurate as image analysis software available commercially, it is an effective method for quickly assessing hematoma volume [36].

3.7.4 ICH: Grading Scales

Intracranial hemorrhage (ICH) grading scales are routinely used to assess baseline severity, to facilitate communication between providers, and to frame expectations of family members. They should not be used in isolation, however, as reliance on grading scales risks producing a self-fulfilling prophecy in which patients expected to do poorly will have poor outcomes due to limitations of acute interventions [37, 38]. The ICH score [39] has seen broad clinical adoption as a number of studies have validated its use. The ICH score includes five independent risk factors for 30-day mortality which are assigned weights to derive a score from 0 to 6 (Table 3.1). The timing of the GCS is important, with studies showing that the GCS assessed once the patient has clinically stabilized has the most utility as compared to an initial assessment [40]. Another useful prognostication tool, the FUNC score was developed to estimate the likelihood of functional independence at 90 days and can help frame expectations for families and caregivers (Table 3.1) [41].

3.7.5 Fluid Management

Volume status should be assessed along with routine monitoring of electrolytes. To avoid exacerbating any brain edema, it is recommended that hyponatremia be avoided. Hyponatremia has been shown to occur in roughly 15% of ICH patients

Table 3.1 The components of the ICH and FUNC scores presented along with their respective point weights and the mortality and independence implications for each total score, respectively

ICH score		FUNC score	
Component	Points	Component	Points
GCS		ICH volume	
3–4	2	<30	4
5–12	1	30–60	2
13–15	0	>60	0
Age		Age	
≥80	1	< 70	2
<80	0	70–79	1
ICH volume		≥80	0
≥30 ml	0	ICH location	
<30 ml	1	Lobar	2
IV hemorrhage		Deep	1
Yes	1	Infratentorial	0
No	0	GCS	
Infra-tentorial origin		≥9	2
Yes	1	≤8	0
No	0	Pre-ICH cognitive impairment	
Total ICH score	30-days mortality (%)	Yes	0
0	10	No	1
1	13	Total FUNC score	Independent at 90 days (%)
2	26	0–4	0
3	72	5–7	29
4	97	8	48
5–6	100	9–10	75
		11	95

IV intraventricular, *FUNC score* functional outcome in patients with primary intracerebral hemorrhage score, *ICH score* intracerebral hemorrhage score, *ICH* intracerebral hemorrhage

and to worsen outcomes in two retrospective case series, with the syndrome of inappropriate antidiuretic hormone being the most common etiology [42, 43]. Normovolemia should be maintained with isotonic fluids to avoid exacerbating brain edema [44]. In patients with elevated ICP from significant perihematomal edema or marked mass effect, hyperosmolar therapy with hypertonic saline (either 2% or 3% solution) may be considered. The goal is to target a hypernatremic state (150–155 mEq/L) and a serum hyperosmolarity (300–320 mOsm/L). Serum sodium should never be allowed to decline more than 12 mEq/L in a 24-h period as this can cause rebound cerebral edema and further exacerbate ICP.

3.7.6 Follow-Up Imaging

After initial hemorrhage, the hematoma can expand further in up to one-third of patients and generally occurs within 24 h, although delayed expansion is described [45]. Expansion is significantly associated with clinical deterioration and worsened outcomes, especially when resulting in midline shift or cerebral herniation [10, 46]. The “spot sign” is a hyperdense spot initially defined on CTA source images, which when seen is predictive of hematoma growth (Fig. 3.1) [47]. If a subsequent non-contrast head CT demonstrates extravasation of contrast into the hematoma, this, along with the spot sign, is significantly associated with ICH growth and poor

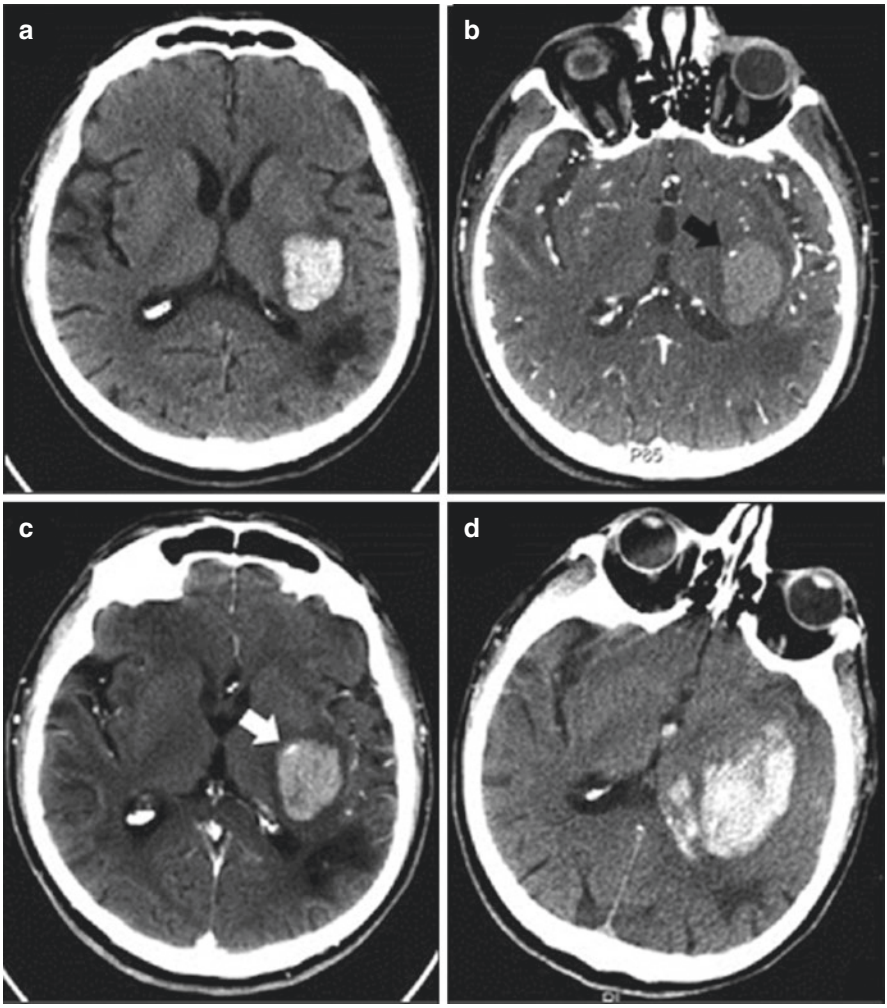

Fig. 3.1 (**a**) Patient with a spot sign visible in a putaminal ICH. (**a**) Demonstrates left posterior putaminal ICH with mild surrounding edema. In (**b**), an arrow indicated the small focus of contrast enhancement seen on CTA consistent with the spot sign. (**c**) Shows the postcontrast CT wherein the white arrow shows the spot sign has enlarged. (**d**) Shows an unenhanced CT taken 1 day later showing the development of IVH and expansion of the ICH (Wada et al. [48])

outcome [47]. Although it is possible to assess for both an "early" (30 s postcontrast injection) and "late" (2–5 min postcontrast injection) spot sign on CTA or postcontrast CT, the current utility of this information is not well defined in the absence of therapies specifically targeted to prevent ICH expansion. In the PREDICT study, patients with the spot sign have significantly higher mortality at 3 months (43.4%) as compared to patients who were spot sign negative (19.6%) [42].

3.7.7 Blood Pressure Management

A number of trials have tried to arrest the further expansion of ICH by managing hypertension. INTERACT1 was a feasibility study that demonstrated the safety and feasibility of intensive blood pressure reduction in acute cerebral hemorrhage. This led to INTERACT2, an international, multicenter, prospective, randomized, open-label, blinded end-point trial of patients with hypertension and ICH occurring in the prior 6 h which randomly assigned patients to receive either intensive treatment of systolic blood pressure (SBP) to less than 140 mmHg or guideline recommended targeting of SBP to less than 180 mmHg [49]. This intensive treatment of blood pressure failed to result in significant reduction in hematoma volume or improvement in outcomes on the primary outcome. Another large intensive blood pressure lowering trial was ATACH2 [50]. This randomized, multicenter, open-label trial looked at patients with ICH volume <60 mL and GCS score of 5 or more, randomizing them to either an intensive SBP target of 110–139 mmHg or a standard target of 140–179 mmHg using intravenous nicardipine. The primary outcome was death or disability at 3 months, which was equivalent between the two groups. The aggressive treatment of blood pressure in ATACH2 did not improve outcomes. Therefore, while a goal SBP of 140 mmHg seems to be a safe target, it does not represent an evidence-based target proven to improve outcomes or reduce mortality, and SBP < 140 mmHg may cause adverse effects in some patients. Following the evidence, a target range of SBP 140–180 mmHg is what is employed at our institution. Any blood pressure over 180 mmHg or MAP over 130 mmHg is treated with a titrated antihypertensive drip, usually nicardipine (5–15 mg/h infusion). Oral antihypertensive agents are used to help achieve longer term blood pressure control, but are not immediate enough in their antihypertensive effects to be used in the acute setting.

3.7.8 When to Use and Not to Use Hemostatic Therapy?

Patients with abnormalities of platelets, coagulation factors, or who are taking anticoagulants have an increased likelihood of ICH expansion due to their decreased propensity to form stable clot. Ultra-early hemostatic therapy with replacement of the deficient factors or transfusion with functional platelets is indicated. Patients on oral anticoagulants account for up to 20% of patients with ICH [51]. Patients on vitamin K antagonists (VKAs) should have their drug withheld and should receive vitamin K but as this takes up to 24 h to work they benefit from prothrombin complex concentrate (PCC), since this corrects the INR more quickly (5.7 h vs. 11.8 h, respectively) and has a better safety profile than fresh-frozen plasma (FFP) [52, 53]. If PCC is unavailable, FFP can be administered. Direct oral anticoagulants including direct thrombin inhibitors (DTIs) and factor Xa inhibitors (FXa-Is) are increasingly used due to their apparent advantages over warfarin and increased indications for anticoagulation. Currently, only dabigatran has a reversal agent (idarucizumab,

a humanized monoclonal antibody fragment against dabigatran) and, for the others, there is no high-quality evidence for drug removal from the circulation, prohemostatic therapies like desmopressin (DDAVP) or antifibrinolytic agents, or the administration of prothrombin complex concentrates [54]. Andexanet alfa is a factor Xa inhibitor antidote intended for patients presenting with major bleeds who are taking FXa-Is. Most hospital protocols include the administration of PCC for the reversal of FXa-Is, while there is currently no randomized prospective data to base this decision on, there are case series and some animal experiments [55–58]. Please see the algorithm at the end of this chapter for specific doses.

The management of patients on antiplatelet agents is currently a matter of debate. In the recent past, several reports described worse clinical outcomes and increased hematoma expansion in these patients [59, 60]. Recent studies show that rates of hematoma expansion and outcome are independent of antiplatelet use [61, 62]. A number of recent observational studies suggested that platelet transfusion could be of benefit in ICH, so a randomized phase 3 trial (the PATCH trial) was recently completed in Europe looking at whether platelet transfusion in ICH patients improved outcomes [63, 64]. Patients who received platelets were actually more likely to have poor outcomes at 3 months than those who did not (OR 2.5, 95% CI 1.18–3.56, $p = 0.0114$). Further, 42% of patients who got platelets have serious adverse events compared to 29% in the control group. Platelet transfusion is not currently indicated in ICH patients pending further clinical trials and can only be considered as a risk reduction measure in patients planned for urgent neurosurgical intervention [65, 66].

3.7.9 ICP Monitoring

The recommendations for ICP monitoring in ICH is largely borrowed from the traumatic brain injury literature, where ICP monitor placement is recommended in patients with a GCS of 8 or less, with a goal of maintaining ICP <20 and CPP at 50–70 mmHg [67]. The use of ICP monitoring would seem to make intuitive sense in patients with an ICH, but ICP monitoring exposes patients to nonnegligible risk for hemorrhage and infection and the present literature is limited in the setting of ICH [68]. In a cohort study of 243 ICH patients, 57 (23%) underwent ICP monitoring and of those 70% had at least one episode of elevated intracranial pressure but this did not negatively impact mRS scores (OR 0.8, 95% CI 0.3–2.3) [69].

In analysis of 100 patients from two prospective multicenter trials of patients with intraventricular hemorrhage (IVH), who underwent placement of external ventricular drain (EVD) for injection of intraventricular alteplase or saline, most (91.5%) of the transduced ICP readings were within normal range, demonstrating the effectiveness of cerebral spinal fluid (CSF) drainage for controlling ICP [70]. ICP readings >30 mmHg in this analysis were an independent predictor of 30-day mortality after adjustment for other outcome predictors. External ventriculostomy should be performed only in a select group of ICH patients with evidence of herniation, significant hydrocephalus, and GCS < 8.

3.7.10 Surgical Considerations

Presently, the evidence does not show open surgical evacuation Intracerebral hemorrhage (ICH) does to hold significant advantage over medical therapy. The Surgical Treatment of Intracerebral Hemorrhage (STICH) trial compared early surgical evacuation of ICH to medical therapy [71]. The trial did not show a survival advantage in patients with early surgery. STICH II investigated the subgroup of patients from STICH I who appeared to have improved outcomes: those with superficial hematomas with no IVH present and with GCS between 8 and 15. STICH II randomized patients to receive either craniotomy within 12 h or best medical care with the goal of improved functional outcome. Despite the demonstration of noninferiority in STICH II, the surgical technique did not demonstrate statistically significant clinical improvement using existing surgical techniques employing open craniotomy with resection of the hemorrhagic tissue. At present, the evidence shows craniotomy to remove clots may only be effective in a select subset of patients and generally has clinical equipoise with medical management.

A number of studies have compared standard craniotomy versus conservative treatment. A recent meta-analysis of ten randomized controlled trials (2059 participants) showed that craniotomy reduced the odds of death or disability at final follow-up (OR 0.74) [72]. In clinical practice, craniotomy is offered to patients who are having rapid neurological decline, but none of the included trials specifically considered these patients, so this continues to be at the discretion of the consulting neurosurgeon. Newer minimally invasive techniques are currently being tested, which aim to decrease the damage to cortex and cortical tracts while at the same time offering increased access to the region of ICH. These will not be considered here, as it remains to be seen whether the successful volumetric reduction in clot is matched with improvement in patient outcomes, but as techniques with increasingly low morbidity emerge it is hoped that appropriately selected patients will increasingly benefit from such treatment.

3.7.11 ICH: Surgical Option for Cerebellar Hemorrhage Patients

Patients with cerebellar hemorrhage causing brainstem compression and rapid neurologic deterioration should undergo surgical removal of the hemorrhage if aggressive management is pursued [9]. Treatment of cerebellar ICH patients with ventricular drainage alone is not recommended. Evacuation of a supratentorial hematoma or decompressive hemicraniectomy can be considered lifesaving for deteriorating patients, but early hematoma evacuation is not clearly beneficial for otherwise stable patients. The effectiveness of minimally invasive techniques for clot evacuation has not been proven with a randomized controlled trial, and surgical evacuation has been associated with excellent clinical outcomes. Moreover, posterior fossa hemorrhage is often quickly followed by decompensation in 25–75% of

patients [73]. Retrospective series have suggested that suboccipital decompression significantly lowers mortality [73, 74]. Patients with cerebellar hemorrhage >3 cm^3, those with brainstem compression or symptomatic hydrocephalus have better outcomes with surgical decompression. Treatment with ventricular drainage alone is ineffective [74].

3.7.12 ICH: Patients with Intraventricular Extension

Intraventricular extension of ICH (IVH) is seen in almost half of the patients with ICH [75]. The presence of IVH doubles the likelihood or poor outcomes in spontaneous ICH [76]. Meta-analysis has shown that ICH with IVH increases the risk of mortality from 20% to 51% [77]. Removing the blood from the ventricles via catheter alone is difficult as blood tends to occlude the catheter and the speed of drainage is slow [78]. The use of adjunctive thrombolytic agents makes catheter-assisted drainage a viable treatment option and has been demonstrated to be safe and effective in the large, randomized, double-blind, placebo controlled CLEAR-III trial [79]. The CLEAR-III protocol involves administering 12 doses of alteplase 1 mg or 0.9% saline through an extraventricular drain every 8 h. At present, this protocol is the only one demonstrated via a large, multicenter, randomized, controlled trial to be safe. Intraventricular alteplase is not currently recommended for the routine management of IVH, although ongoing studies are evaluating conditions under which this treatment may have long-term functional benefit which may be related to more complete reduction in ventricular clot burden.

3.7.13 ICH: Venous Thromboembolism Prophylaxis

The priority of stopping the bleeding in ICH and avoiding triggering further bleeding must be balanced against the need to prevent deep venous thromboembolism (DVT). The incidence of symptomatic DVT in patients with ICH has been reported in retrospective case series to be on the order of 1–2% [80, 81], with symptomatic pulmonary embolism in 0.5–1% of ICH patients [82]. The CLOTS3 trial showed an absolute risk reduction of 3.6% (95% confidence interval 1.4–5.8) of DVT in patients with the use of IPC [83]. It is, therefore, recommended that patients receive DVT prophylaxis with pneumatic compression devices (with or without compression stockings) immediately upon hospital admission and continuing until discharge [84]. The evidence for the use of DVT prophylaxis with subcutaneous unfractionated (UFH) or low molecular weight (LMWH) heparin in ICH relies on two small prospective randomized trials, which were limited by their small size on low frequency of hemorrhagic or thromboembolic events [85, 86]. A comprehensive meta-analysis of these and two other observational studies showed the use of UFH or LMWH to be effective in reducing pulmonary embolism (PE) (RR 0.37, 95% CI 0.17–0.80) but no effect on the incidence of DVT, expansion of hematoma, or death

[87]. Current guidelines recommend the use of subcutaneous UFH or LMWH only in those ICH patients who have had stable hematomas for 48 h and who have no coagulopathy [84].

3.7.14 ICH: Seizure Management

Most patients with ICH do not experience seizures, but in the first 7 days up to 16% experience clinical seizures and up to 31% have electrographic seizures [87–89]. Current guidelines support continuous EEG monitoring in patients with clinical seizures or patients with mental status out of proportion to their ICH [9]. Seizures are the product of cortical irritation, and are most likely in patients with cortical extension of their ICH [90, 91]. Of note, while a large single-center study has shown that prophylaxis decreases the risk of seizures in ICH, prospective studies report that seizures do not seem to effect mortality or neurologic outcome [92–94]. In fact, the available data seem to suggest that antiepileptic prophylaxis is associated with worse outcomes and increased mortality in particular with phenytoin [95, 96]. In response, levetiracetam use for seizure prophylaxis has been on the rise despite limited knowledge about its potential effects on outcomes [97]. Present guidelines do not support the use of antiseizure medications for prophylaxis in ICH but do recommend treating patients who have seizures accompanied by a change in mental status.

3.8 ICH: Medical Complications

ICH is associated with a number of medical complications that must be managed along with the primary insult. In the 607 patients Cerebral Hematoma and NXY-059 Treatment trial, 88% of patients have at least one adverse event [98]. These included, in order of frequency, pneumonia, pulmonary embolism, respiratory failure, aspiration pneumonia, sepsis, and urinary tract infection. Given that medical complications of stroke cause up to 50% of mortality in this context, aggressive management of these complications is imperative. Dysphagia is a risk factor for aspiration and consequent aspiration pneumonia or chemical pneumonitis, but formal bedside swallow screening for all stroke patients has been shown in a prospective multicenter study to reduce the absolute risk of pneumonia from roughly 5% to 2% [99]. A Cochrane meta-analysis of 33 studies looking at nutrition and swallowing in stroke showed that avoiding malnutrition is possible with placement of an orogastric or nasogastric feeding tube and that PEG placement reduces treatment failures and gastrointestinal bleeding while increasing food delivery [100]. Up to 21% of patients with ICH require mechanical ventilation for inability to protect their airway

[101]. Ventilated patients are at risk for in-hospital mortality as high as 48%, and should be surveilled for ventilator-associated pneumonia and acute respiratory distress syndrome [102]. To minimize risk of aspiration pneumonia, the head of the bed should be kept at 30°, frequent oral care should be instituted, and the duration of intubation should be minimized inasmuch as it is possible.

3.8.1 Glycemic Management

Hyperglycemia is an independent risk factor for death and poor outcomes in patients with ICH, regardless of whether there is underlying diabetes mellitus [103]. Intensive control of glucose to 80–110 mg/dL has been shown to both increase incidence of hypoglycemia and intracranial hypertension in one study [104] and to decrease it in another [105]. At present, there is no large, randomized, controlled trial demonstrating the effectiveness of strict normoglycemia in ICH and it is not recommended [106]. ICH patients should have frequent monitoring of glucose to avoid extreme hypo- and hyperglycemia, but normoglycemia should not be an aggressively pursued goal.

3.8.2 Avoiding Hyperthermia and Hypothermia

Fever is common after ICH, and has an established relationship with worse outcomes and growth of hematoma [107]. While a causal relationship has not been established between the complex inflammatory, neurohormonal, and metabolic cascades involved in temperature management and their derangement in the context of ICH, it seems intuitive that targeting normothermia could improve outcomes. However, maintenance of normothermia has not been shown to have an impact on improving outcomes [108]. There have been no trials of targeted hypothermia in ICH, so cooling is currently only for investigational use and per the current guidelines and management of fever "may be reasonable" [5]. The authors in their own practice treat fever >38.5 °C and try to maintain normothermia in ICH patients.

3.8.3 Disposition

Upon stabilization, patients with ICH should be dispositioned to dedicated neurological intensive care or stroke units, especially in the initial 24 h of care [109]. Patients requiring ventriculostomy drainage or mechanical ventilation will necessarily require ICU care, ideally in a dedicated neurological unit.

3.9 Conclusion

By adhering to present evidence and guidelines for clinical practice, practitioners caring for ICH can decrease mortality, minimize harm, and increase the likelihood of functional outcome.

Algorithm

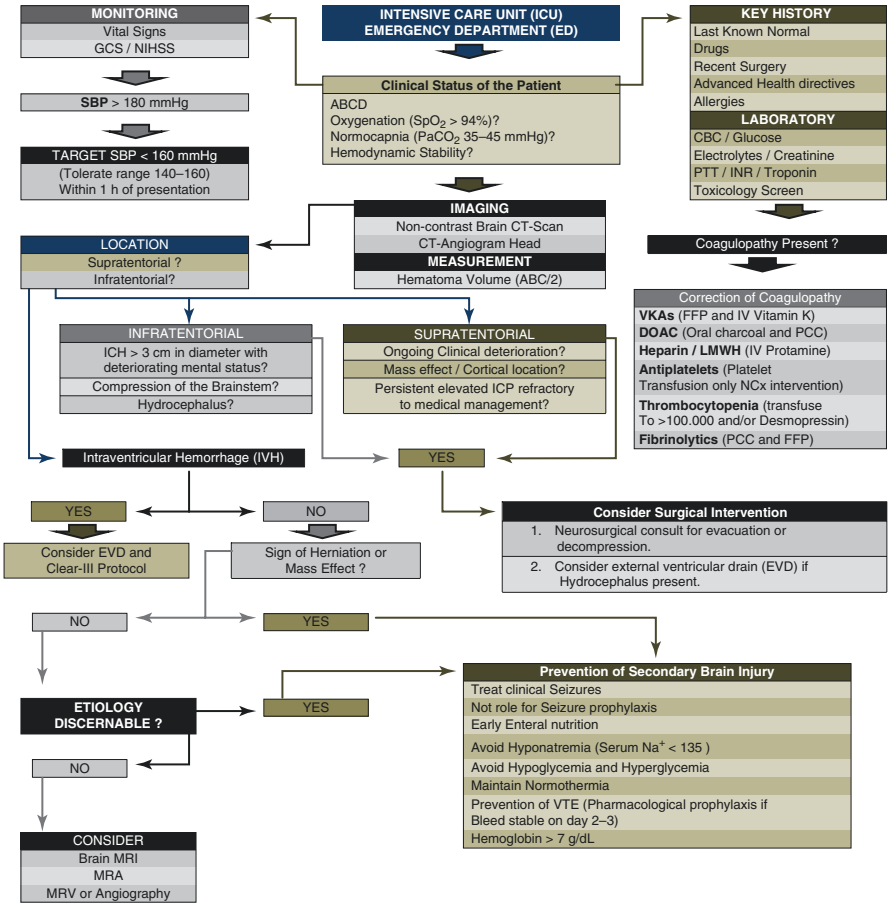

ABCD airway-breathing-circulation-disability, *PCC* prothrombin complex concentrate, *VKAs* vitamin K antagonist, *MRA* magnetic resonance angiography, *MRV* magnetic resonance venography, *NCx* neurosurgery, *FFP* fresh frozen plasma, *SBP* systolic blood pressure

Appendix: Direct Oral Anticoagulant Reversal

After five half-lives, anticoagulation can be considered fully resolved.
Apixaban: 8–15 h; 5 half-lives: 24–75 h after last dose (day 1.5–3)
Betrixaban: 19–27 h; 5 half-lives: 95–135 h after last dose (day 4–5.5)
Dabigatran: 12–17 h; 5 half-lives: 60–85 h after last dose (day 2.5–3.5)
Edoxaban: 6–11 h; 5 half-lives: 30–55 h after last dose (day 1.3–2)
Rivaroxaban: 5–9 h; 5 half-lives: 30–45 h after last dose (day 1–2)

Activated charcoal to absorb drug if taken in prior:
Apixaban: up to 6 h
Edoxaban: up to 2 h
Rivaroxaban: up to 8 h

Reversal Strategies

Dabigatran: Idarucizumab (Praxbind) 5 g IV; if unavailable, FEIBA 50–80 μ/kg; if unavailable, use a three- or four-factor PCC at 25–50 μ/kg. If using three-factor PCC, consider supplementation with FFP for factor VII. Tranexamic acid (TXA) may be considered. Hemodialysis has been shown to remove active dabigatran from circulation.

Apixaban, betrixaban, edoxaban, and rivaroxaban: If emergent surgery is required, andexanet alfa may be given. Low dose (for those who received rivaroxaban <10 mg, apixaban <5 mg, or >8 h since last dose of factor Xa inhibitor) is a bolus 400 mg at rate of 30 mg/min followed by infusion of 480 mg at rate of 4 mg/min. High dose (for those who are on rivaroxaban >10 mg, apixaban >5 mg, or dose unknown or <8 h since last dose of factor Xa inhibitor) is bolus of 800 mg at 30 mg/min followed by infusion of 960 mg at a rate of 8 mg/min. If andexanet alfa not available, four-factor PCC.

References

1. Rincon F, Mayer SA. The epidemiology of intracerebral hemorrhage in the United States from 1979 to 2008. Neurocrit Care. 2013;19(1):95–102.
2. van Asch CJ, Luitse MJ, Rinkel GJ, van der Tweel I, Algra A, Klijn CJ. Incidence, case fatality, and functional outcome of intracerebral haemorrhage over time, according to age, sex, and ethnic origin: a systematic review and meta-analysis. Lancet Neurol. 2010;9(2):167–76.

3. Grysiewicz RA, Thomas K, Pandey DK. Epidemiology of ischemic and hemorrhagic stroke: incidence, prevalence, mortality, and risk factors. Neurol Clin. 2008;26(4):871–95.
4. Gorelick PB, Hier DB, Caplan LR, Langenberg P. Headache in acute cerebrovascular disease. Neurology. 1986;36(11):1445–50.
5. Hemphill JC III, Greenberg SM, Anderson CS, Becker K, Bendok BR, Cushman M, et al. Guidelines for the management of spontaneous intracerebral hemorrhage a guideline for healthcare professionals from the American Heart Association/American Stroke Association. Stroke. 2015;46(7):2032–60.
6. Feigin VL, Lawes CM, Bennett DA, Barker-Collo SL, Parag V. Worldwide stroke incidence and early case fatality reported in 56 population-based studies: a systematic review. Lancet Neurol. 2009;8(4):355–69.
7. Krishnamurthi RV, Moran AE, Forouzanfar MH, Bennett DA, Mensah GA, Lawes CM, et al. The global burden of hemorrhagic stroke: a summary of findings from the GBD 2010 study. Glob Heart. 2014;9(1):101–6.
8. Zahuranec DB, Lisabeth LD, Sánchez BN, Smith MA, Brown DL, Garcia NM, et al. Intracerebral hemorrhage mortality is not changing despite declining incidence. Neurology. 2014;82(24):2180–6.
9. Bamford J, Sandercock P, Dennis M, Burn J, Warlow C. A prospective study of acute cerebrovascular disease in the community: the Oxfordshire Community Stroke Project--1981-86. 2. Incidence, case fatality rates and overall outcome at one year of cerebral infarction, primary intracerebral and subarachnoid haemorrhage. J Neurol Neurosurg Psychiatry. 1990;53(1):16.
10. Broderick JP, Brott TG, Duldner JE, Tomsick T, Huster G. Volume of intracerebral hemorrhage – a powerful and easy-to-use predictor of 30-day mortality. Stroke. 1993;24(7):987–93.
11. Ariesen MJ, Claus SP, Rinkel GJE, Algra A. Risk factors for intracerebral hemorrhage in the general population. A systematic review. Stroke. 2003;34(8):2060–5.
12. O'Donnell MJ, Xavier D, Liu L, Zhang H, Chin SL, Rao-Melacini P, et al. Risk factors for ischaemic and intracerebral haemorrhagic stroke in 22 countries (the INTERSTROKE study): a case-control study. Lancet. 2010;376(9735):112–23.
13. Zia E, Hedblad B, Pessah-Rasmussen H, Berglund G, Janzon L, Engström G. Blood pressure in relation to the incidence of cerebral infarction and intracerebral hemorrhage. Hypertensive hemorrhage: debated nomenclature is still relevant. Stroke. 2007;38(10):2681–5.
14. Zhang Y, Tuomilehto J, Jousilahti P, Wang Y, Antikainen R, Hu G. Lifestyle factors on the risks of ischemic and hemorrhagic stroke. Arch Intern Med. 2011;171(20):1811–8.
15. Andersen KK, Olsen TS, Dehlendorff C, Kammersgaard LP. Hemorrhagic and ischemic strokes compared stroke severity, mortality, and risk factors. Stroke. 2009;40(6):2068–72.
16. Suh I, Jee SH, Kim HC, Nam CM, Kim IS, Appel LJ. Low serum cholesterol and haemorrhagic stroke in men: Korea Medical Insurance Corporation Study. Lancet. 2001;357(9260):922–5.
17. Suzuki K, Izumi M, Sakamoto T, Hayashi M. Blood pressure and total cholesterol level are critical risks especially for hemorrhagic stroke in Akita, Japan. Cerebrovas Dis. 2011;31(1):100–6.
18. Sarwar N, Gao P, Seshasai SRK, Gobin R, Kaptoge S, Di Angelantonio E, et al. Diabetes mellitus, fasting blood glucose concentration, and risk of vascular disease: a collaborative meta-analysis of 102 prospective studies. Lancet. 2010;375(9733):2215–22.
19. Knudsen KA, Rosand J, Karluk D, Greenberg SM. Clinical diagnosis of cerebral amyloid angiopathy: validation of the Boston criteria. Neurology. 2001;56(4):537–9.
20. He J, Whelton PK, Vu B, Klag MJ. Aspirin and risk of hemorrhagic stroke – a meta-analysis of randomized controlled trials. JAMA. 1998;280(22):1930–5.
21. Flaherty ML, Kissela B, Woo D, Kleindorfer D, Alwell K, Sekar P, et al. The increasing incidence of anticoagulant-associated intracerebral hemorrhage. Neurology. 2007;68(2):116–21.
22. Chatterjee S, Sardar P, Biondi-Zoccai G, Kumbhani DJ. New oral anticoagulants and the risk of intracranial hemorrhage: traditional and Bayesian meta-analysis and mixed treatment comparison of randomized trials of new oral anticoagulants in atrial fibrillation. JAMA Neurol. 2013;70(12):1486–90.

23. Dye JA, Rees G, Yang I, Vespa PM, Martin NA, Vinters HV. Neuropathologic analysis of hematomas evacuated from patients with spontaneous intracerebral hemorrhage. Neuropathology. 2014;34(3):253–60.
24. Delgado Almandoz JE, Schaefer PW, Forero NP, Falla JR, Gonzalez RG, Romero JM. Diagnostic accuracy and yield of multidetector CT angiography in the evaluation of spontaneous intraparenchymal cerebral hemorrhage. AJNR Am J Neuroradiol. 2009;30(6):1213–21.
25. Halpin SFS, Britton JA, Byrne JV, Clifton A, Hart G, Moore A. Prospective evaluation of cerebral-angiography and computed-tomography in cerebral hematoma. J Neurol Neurosurg Psychiatry. 1994;57(10):1180–6.
26. Zhu XL, Chan MSY, Poon WS. Spontaneous intracranial hemorrhage: which patients need diagnostic cerebral angiography? A prospective study of 206 cases and review of the literature. Stroke. 1997;28(7):1406–9.
27. Robinson N, Clancy M. In patients with head injury undergoing rapid sequence intubation, does pretreatment with intravenous lignocaine/lidocaine lead to an improved neurological outcome? A review of the literature. Emerg Med J. 2001;18(6):453–7.
28. Kam PCA, Cardone D. Propofol infusion syndrome. Anaesthesia. 2007;62(7):690–701.
29. Jauch EC, Pineda JA, Claude Hemphill J. Emergency neurological life support: intracerebral hemorrhage. Neurocrit Care. 2015;23(2):83–93.
30. Goldstein LB, Bertels C, Davis JN. Interrater reliability of the NIH stroke scale. Arch Neurol. 1989;46(6):660–2.
31. Wang C-W, Liu Y-J, Lee Y-H, Hueng D-Y, Fan H-C, Yang F-C, et al. Hematoma shape, hematoma size, Glasgow coma scale score and ICH score: which predicts the 30-day mortality better for intracerebral hematoma? PLoS One. 2014;9(7):e102326.
32. Bekelis K, Desai A, Zhao W, Gibson D, Gologorsky D, Eskey C, et al. Computed tomography angiography: improving diagnostic yield and cost effectiveness in the initial evaluation of spontaneous nonsubarachnoid intracerebral hemorrhage. J Neurosurg. 2012;117(4):761–6.
33. Delgado Almandoz JE, Jagadeesan BD, Moran CJ, Cross DT 3rd, Zipfel GJ, Lee JM, et al. Independent validation of the secondary intracerebral hemorrhage score with catheter angiography and findings of emergent hematoma evacuation. Neurosurgery. 2012;70(1):131–40; discussion 40.
34. Stam J. Thrombosis of the cerebral veins and sinuses. N Engl J Med. 2005;352(17):1791–8.
35. Specogna AV, Turin TC, Patten SB, Hill MD. Factors associated with early deterioration after spontaneous intracerebral hemorrhage: a systematic review and meta-analysis. PLoS One. 2014;9(5):e96743.
36. Webb AJS, Ullman NL, Morgan TC, Muschelli J, Kornbluth J, Awad IA, et al. Accuracy of the ABC/2 score for intracerebral hemorrhage. Systematic review and analysis of MISTIE, CLEAR-IVH, and CLEAR III. Stroke. 2015;46(9):2470–6.
37. Hemphill JC, White DB. Clinical nihilism in neuro-emergencies. Emerg Med Clin North Am. 2009;27(1):27–37, vii–viii.
38. Becker KJ, Baxter AB, Cohen WA, Bybee HM, Tirschwell DL, Newell DW, et al. Withdrawal of support in intracerebral hemorrhage may lead to self-fulfilling prophecies. Neurology. 2001;56(6):766–72.
39. Hemphill JC, Bonovich DC, Besmertis L, Manley GT, Johnston SC. The ICH score. A simple, reliable grading scale for intracerebral hemorrhage. Stroke. 2001;32(4):891–7.
40. Maas MB, Francis BA, Sangha RS, Lizza BD, Liotta EM, Naidech AM. Refining prognosis for intracerebral hemorrhage by early reassessment. Cerebrovasc Dis. 2017;43(3–4):110–6.
41. Rost NS, Smith EE, Chang Y, Snider RW, Chanderraj R, Schwab K, et al. Prediction of functional outcome in patients with primary intracerebral hemorrhage. The FUNC score. Stroke. 2008;39(8):2304–9.
42. Kuramatsu JB, Bobinger T, Volbers B, Staykov D, Lucking H, Kloska SP, et al. Hyponatremia is an independent predictor of in-hospital mortality in spontaneous intracerebral hemorrhage. Stroke. 2014;45(5):1285–91.

43. Gray JR, Morbitzer KA, Liu-DeRyke X, Parker D, Zimmerman LH, Rhoney DH. Hyponatremia in patients with spontaneous intracerebral hemorrhage. J Clin Med. 2014;3(4):1322–32.
44. van der Jagt M. Fluid management of the neurological patient: a concise review. Crit Care. 2016;20:126.
45. Dowlatshahi D, Demchuk AM, Flaherty ML, Ali M, Lyden PL, Smith EE. Defining hematoma expansion in intracerebral hemorrhage: relationship with patient outcomes. Neurology. 2011;76(14):1238–44.
46. Brott T, Broderick J, Kothari R, Barsan W, Tomsick T, Sauerbeck L, et al. Early hemorrhage growth in patients with intracerebral hemorrhage. Stroke. 1997;28(1):1–5.
47. Hallevi H, Abraham AT, Barreto AD, Grotta JC, Savitz SI. The spot sign in intracerebral hemorrhage: the importance of looking for contrast extravasation. Cerebrovasc Dis. 2010;29(3):217–20.
48. Wada R, Aviv RI, Fox AJ, Sahlas DJ, Gladstone DJ, Tomlinson G, et al. CT angiography "spot sign" predicts hematoma expansion in acute intracerebral hemorrhage. Stroke. 2007;38(4):1257–62.
49. Anderson CS, Heeley E, Huang Y, Wang J, Stapf C, Delcourt C, et al. Rapid blood-pressure lowering in patients with acute intracerebral hemorrhage. N Engl J Med. 2013;368(25):2355–65.
50. Qureshi AI, Palesch YY, Barsan WG, Hanley DF, Hsu CY, Martin RL, et al. Intensive blood-pressure lowering in patients with acute cerebral hemorrhage. N Engl J Med. 2016;375(11):1033–43.
51. Huhtakangas J, Tetri S, Juvela S, Saloheimo P, Bode MK, Hillbom M. Effect of increased warfarin use on warfarin-related cerebral hemorrhage: a longitudinal population-based study. Stroke. 2011;42(9):2431–5.
52. Hickey M, Gatien M, Taljaard M, Aujnarain A, Giulivi A, Perry JJ. Outcomes of urgent warfarin reversal with frozen plasma versus prothrombin complex concentrate in the emergency department. Circulation. 2013;128(4):360–4.
53. Sarode R, Milling TJ, Refaai MA, Mangione A, Schneider A, Durn BL, et al. Efficacy and safety of a 4-factor prothrombin complex concentrate in patients on vitamin K antagonists presenting with major bleeding. A randomized, plasma-controlled, phase IIIb study. Circulation. 2013;128(11):1234–43.
54. Mayer SA, Brun NC, Begtrup K, Broderick J, Davis S, Diringer MN, et al. Efficacy and safety of recombinant activated factor VII for acute intracerebral hemorrhage. N Engl J Med. 2008;358(20):2127–37.
55. Marlu R, Hodaj E, Paris A, Albaladejo P, Cracowski JL, Pernod G. Effect of non-specific reversal agents on anticoagulant activity of dabigatran and rivaroxaban: a randomised crossover ex vivo study in healthy volunteers. Thromb Haemost. 2012;108(2):217–24.
56. Maurice-Szamburski A, Graillon T, Bruder N. Favorable outcome after a subdural hematoma treated with feiba in a 77-year-old patient treated by rivaroxaban. J Neurosurg Anesthesiol. 2014;26(2):183.
57. Lambourne MD, Eltringham-Smith LJ, Gataiance S, Arnold DM, Crowther MA, Sheffield WP. Prothrombin complex concentrates reduce blood loss in murine coagulopathy induced by warfarin, but not in that induced by dabigatran etexilate. J Thromb Haemost. 2012;10(9):1830–40.
58. Pragst I, Zeitler SH, Doerr B, Kaspereit FJ, Herzog E, Dickneite G, et al. Reversal of dabigatran anticoagulation by prothrombin complex concentrate (Beriplex P/N) in a rabbit model. J Thromb Haemost. 2012;10(9):1841–8.
59. Saloheimo P, Ahonen M, Juvela S, Pyhtinen J, Savolainen ER, Hillbom M. Regular aspirin-use preceding the onset of primary intracerebral hemorrhage is an independent predictor for death. Stroke. 2006;37(1):129–33.
60. Toyoda K, Okada Y, Minematsu K, Kamouchi M, Fujimoto S, Ibayashi S, et al. Antiplatelet therapy contributes to acute deterioration of intracerebral hemorrhage. Neurology. 2005;65(7):1000–4.

61. Sansing LH, Messe SR, Cucchiara BL, Cohen SN, Lyden PD, Kasner SE. Prior antiplatelet use does not affect hemorrhage growth or outcome after ICH. Neurology. 2009;72(16):1397–402.
62. Moussouttas M, Malhotra R, Fernandez L, Maltenfort M, Holowecki M, Delgado J, et al. Role of antiplatelet agents in hematoma expansion during the acute period of intracerebral hemorrhage. Neurocrit Care. 2010;12(1):24–9.
63. Naidech AM, Liebling SM, Rosenberg NF, Lindholm PF, Bernstein RA, Batjer HH, et al. Early platelet transfusion improves platelet activity and may improve outcomes after intracerebral hemorrhage. Neurocrit Care. 2012;16(1):82–7.
64. Baharoglu MI, Cordonnier C, Salman RA-S, de Gans K, Koopman MM, Brand A, et al. Platelet transfusion versus standard care after acute stroke due to spontaneous cerebral haemorrhage associated with antiplatelet therapy (PATCH): a randomised, open-label, phase 3 trial. Lancet. 2016;387(10038):2605–13.
65. Frontera JA, Lewin JJ 3rd, Rabinstein AA, Aisiku IP, Alexandrov AW, Cook AM, et al. Guideline for reversal of antithrombotics in intracranial hemorrhage: a statement for healthcare professionals from the Neurocritical Care Society and Society of Critical Care Medicine. Neurocrit Care. 2016;24(1):6–46.
66. Li X, Sun Z, Zhao W, Zhang J, Chen J, Li Y, et al. Effect of acetylsalicylic acid usage and platelet transfusion on postoperative hemorrhage and activities of daily living in patients with acute intracerebral hemorrhage. J Neurosurg. 2013;118(1):94–103.
67. Bratton SL, Chestnut RM, Ghajar J, McConnell Hammond FF, Harris OA, Hartl R, et al. VI. Indications for intracranial pressure monitoring. J Neurotrauma. 2007;24(supplement 1):S-37–44.
68. Fried HI, Nathan BR, Rowe AS, Zabramski JM, Andaluz N, Bhimraj A, et al. The insertion and management of external ventricular drains: an evidence-based consensus statement. Neurocrit Care. 2016;24(1):61–81.
69. Kamel H, Hemphill JC. Characteristics and sequelae of intracranial hypertension after intracerebral hemorrhage. Neurocrit Care. 2012;17(2):172–6.
70. Ziai WC, Melnychuk E, Thompson CB, Awad I, Lane K, Hanley DF. Occurrence and impact of intracranial pressure elevation during treatment of severe intraventricular hemorrhage. Crit Care Med. 2012;40(5):1601–8.
71. Mendelow AD, Gregson BA, Fernandes HM, Murray GD, Teasdale GM, Hope DT, et al. Early surgery versus initial conservative treatment in patients with spontaneous supratentorial intracerebral haematomas in the International Surgical Trial in Intracerebral Haemorrhage (STICH): a randomised trial. Lancet. 2005;365(9457):387–97.
72. Prasad K, Mendelow AD, Gregson B. Surgery for primary supratentorial intracerebral haemorrhage. Cochrane Database Syst Rev. 2008;(4):CD000200.
73. Luney MS, English SW, Longworth A, Simpson J, Gudibande S, Matta B, et al. Acute posterior cranial fossa hemorrhage—is surgical decompression better than expectant medical management? Neurocrit Care. 2016;25(3):365–70.
74. van Loon J, Van Calenbergh F, Goffin J, Plets C. Controversies in the management of spontaneous cerebellar haemorrhage. A consecutive series of 49 cases and review of the literature. Acta Neurochir. 1993;122(3–4):187–93.
75. Bhattathiri PS, Gregson B, Prasad KSM, Mendelow AD. Intraventricular hemorrhage and hydrocephalus after spontaneous intracerebral hemorrhage: results from the STICH trial. In: Hoff JT, Keep RF, Xi G, Hua Y, editors. Brain Edema XIII. Vienna: Springer Vienna; 2006. p. 65–8.
76. Hallevi H, Albright KC, Aronowski J, Barreto AD, Martin-Schild S, Khaja AM, et al. Intraventricular hemorrhage: anatomic relationships and clinical implications. Neurology. 2008;70(11):848–52.
77. Gaberel T, Magheru C, Emery E. Management of non-traumatic intraventricular hemorrhage. Neurosurg Rev. 2012;35(4):485–95.

78. Huttner HB, Köhrmann M, Berger C, Georgiadis D, Schwab S. Influence of intraventricular hemorrhage and occlusive hydrocephalus on the long-term outcome of treated patients with basal ganglia hemorrhage: a case-control study. J Neurosurg. 2006;105(3):412–7.
79. Hanley DF, Lane K, McBee N, Ziai W, Tuhrim S, Lees KR, et al. Thrombolytic removal of intraventricular haemorrhage in treatment of severe stroke: results of the randomised, multicentre, multiregion, placebo-controlled CLEAR III trial. Lancet. 2017;389(10069):603–11.
80. Skaf E, Stein PD, Beemath A, Sanchez J, Bustamante MA, Olson RE. Venous thromboembolism in patients with ischemic and hemorrhagic stroke. Am J Cardiol. 2005;96(12):1731–3.
81. Kim KS, Brophy GM. Symptomatic venous thromboembolism: incidence and risk factors in patients with spontaneous or traumatic intracranial hemorrhage. Neurocrit Care. 2009;11(1):28–33.
82. Maramattom BV, Weigand S, Reinalda M, Wijdicks EFM, Manno EM. Pulmonary complications after intracerebral hemorrhage. Neurocrit Care. 2006;5(2):115–9.
83. Dennis M, Sandercock P, Reid J, Graham C, Forbes J, Murray G. Effectiveness of intermittent pneumatic compression in reduction of risk of deep vein thrombosis in patients who have had a stroke (CLOTS 3): a multicentre randomised controlled trial. Lancet. 2013;382(9891):516–24.
84. Nyquist P, Bautista C, Jichici D, Burns J, Chhangani S, DeFilippis M, et al. Prophylaxis of venous thrombosis in neurocritical care patients: an evidence-based guideline: a statement for healthcare professionals from the Neurocritical Care Society. Neurocrit Care. 2016;24(1):47–60.
85. Boeer A, Voth E, Henze T, Prange HW. Early heparin therapy in patients with spontaneous intracerebral haemorrhage. J Neurol Neurosurg Psychiatry. 1991;54(5):466–7.
86. Orken DN, Kenangil G, Ozkurt H, Guner C, Gundogdu L, Basak M, et al. Prevention of deep venous thrombosis and pulmonary embolism in patients with acute intracerebral hemorrhage. Neurologist. 2009;15(6):329–31.
87. De Herdt V, Dumont F, Henon H, Derambure P, Vonck K, Leys D, et al. Early seizures in intracerebral hemorrhage: incidence, associated factors, and outcome. Neurology. 2011;77(20):1794–800.
88. Bladin CF, Alexandrov AV, Bellavance A, Bornstein N, Chambers B, Cote R, et al. Seizures after stroke: a prospective multicenter study. Arch Neurol. 2000;57(11):1617–22.
89. Szaflarski JP, Rackley AY, Kleindorfer DO, Khoury J, Woo D, Miller R, et al. Incidence of seizures in the acute phase of stroke: a population-based study. Epilepsia. 2008;49(6):974–81.
90. Beghi E, D'Alessandro R, Beretta S, Consoli D, Crespi V, Delaj L, et al. Incidence and predictors of acute symptomatic seizures after stroke. Neurology. 2011;77(20):1785–93.
91. Biffi A, Rattani A, Anderson CD, Ayres AM, Gurol EM, Greenberg SM, et al. Delayed seizures after intracerebral haemorrhage. Brain. 2016;139(Pt 10):2694–705.
92. Passero S, Rocchi R, Rossi S, Ulivelli M, Vatti G. Seizures after spontaneous supratentorial intracerebral hemorrhage. Epilepsia. 2002;43(10):1175–80.
93. Mullen MT, Kasner SE, Messé SR. Seizures do not increase in-hospital mortality after intracerebral hemorrhage in the nationwide inpatient sample. Neurocrit Care. 2013;19(1):19–24.
94. Zandieh A, Messe SR, Cucchiara B, Mullen MT, Kasner SE. Prophylactic use of antiepileptic drugs in patients with spontaneous intracerebral hemorrhage. J Stroke Cerebrovasc Dis. 2016;25(9):2159–66.
95. Battey TW, Falcone GJ, Ayres AM, Schwab K, Viswanathan A, McNamara KA, et al. Confounding by indication in retrospective studies of intracerebral hemorrhage: antiepileptic treatment and mortality. Neurocrit Care. 2012;17(3):361–6.
96. Messe SR, Sansing LH, Cucchiara BL, Herman ST, Lyden PD, Kasner SE. Prophylactic antiepileptic drug use is associated with poor outcome following ICH. Neurocrit Care. 2009;11(1):38–44.
97. Naidech AM, Beaumont J, Jahromi B, Prabhakaran S, Kho A, Holl JL. Evolving use of seizure medications after intracerebral hemorrhage: a multicenter study. Neurology. 2017;88(1):52–6.

98. Lyden PD, Shuaib A, Lees KR, Davalos A, Davis SM, Diener HC, et al. Safety and tolerability of NXY-059 for acute intracerebral hemorrhage: the CHANT trial. Stroke. 2007;38(8):2262–9.
99. Hinchey JA, Shephard T, Furie K, Smith D, Wang D, Tonn S. Formal dysphagia screening protocols prevent pneumonia. Stroke. 2005;36(9):1972–6.
100. Geeganage C, Beavan J, Ellender S, Bath PM. Interventions for dysphagia and nutritional support in acute and subacute stroke. Cochrane Database Syst Rev. 2012;10:CD000323.
101. Yaghi S, Moore P, Ray B, Keyrouz SG. Predictors of tracheostomy in patients with spontaneous intracerebral hemorrhage. Clin Neurol Neurosurg. 2013;115(6):695–8.
102. Elmer J, Hou P, Wilcox SR, Chang Y, Schreiber H, Okechukwu I, et al. Acute respiratory distress syndrome after spontaneous intracerebral hemorrhage. Crit Care Med. 2013;41(8):1992–2001.
103. Kimura K, Iguchi Y, Inoue T, Shibazaki K, Matsumoto N, Kobayashi K, et al. Hyperglycemia independently increases the risk of early death in acute spontaneous intracerebral hemorrhage. J Neurol Sci. 2007;255(1–2):90–4.
104. Meier R, Bechir M, Ludwig S, Sommerfeld J, Keel M, Steiger P, et al. Differential temporal profile of lowered blood glucose levels (3.5 to 6.5 mmol/l versus 5 to 8 mmol/l) in patients with severe traumatic brain injury. Crit Care. 2008;12(4):R98.
105. Van den Berghe G, Wilmer A, Hermans G, Meersseman W, Wouters PJ, Milants I, et al. Intensive insulin therapy in the medical ICU. N Engl J Med. 2006;354(5):449–61.
106. Godoy DA, Di Napoli M, Rabinstein AA. Treating hyperglycemia in neurocritical patients: benefits and perils. Neurocrit Care. 2010;13(3):425–38.
107. Rincon F, Lyden P, Mayer SA. Relationship between temperature, hematoma growth, and functional outcome after intracerebral hemorrhage. Neurocrit Care. 2013;18(1):45–53.
108. Broessner G, Beer R, Lackner P, Helbok R, Fischer M, Pfausler B, et al. Prophylactic, endovascularly based, long-term normothermia in ICU patients with severe cerebrovascular disease. Bicenter prospective, randomized trial. Stroke. 2009;40(12):e657–e65.
109. Diringer MN, Edwards DF. Admission to a neurologic/neurosurgical intensive care unit is associated with reduced mortality rate after intracerebral hemorrhage. Crit Care Med. 2001;29(3):635–40.

Chapter 4
Organ Maintenance After Death by Neurological Criteria (DNC) in Neuro-ICU: The Importance of Donation

Vasso Zisimopoulou and Panayiotis N. Varelas

Key Points

1. Many patients with severe brain injury, despite all efforts to save them, die by neurological death criteria. Many of these brain-dead patients become organ and tissue donors.
2. The management of these patients before they are declared brain dead may differ from the management after they are pronounced and may be organ specific.
3. Hemodynamic instability is a common problem in these organ donors and has to be managed with fluid replacement, vasopressors, or inotropes and, if not responding, hormonal replacement therapy.
4. Aggressive respiratory management with maneuvers aiming at increased alveolar recruitment should be instituted in every organ donor.
5. Cardiopulmonary resuscitation in the brain-dead organ donor is controversial and should be discussed with the family of the patient.

4.1 Introduction

The advent of modern ventilators and the development of intensive care units have created a uniquely modern, largely hospital-based phenomenon, the death by neurological criteria (DNC) or brain death (BD). Without mechanical ventilation, the cessation of brain function leads inevitably to apnea and cardiac arrest, but with it,

V. Zisimopoulou
Air Force General Hospital, Athens, Greece

P. N. Varelas (✉)
Department of Neurology, Albany Medical Center, Albany, NY, USA

C. N. Rodríguez et al. (eds.), *Neurosonology in Critical Care*,
https://doi.org/10.1007/978-3-030-81419-9_4

patients continue to have heartbeat and circulation for a period of time that usually spans few days to a week.

Since the seminal paper by Mollaret and Goulon almost 60 years ago [1], the concept of BD was gradually adopted by clinical, ethical, and legal authorities as an alternative to cardiorespiratory death in every country. The determination of BD, however, is not uniform and has led to variability across borders [2] or even within countries such as the USA [3]. The first systematic attempt to address this problem and establish standard practice parameters for the determination of BD was not made until the American Academy of Neurology's 1995 guidelines were issued [4], with an update published in mid-2010 [5]. Therefore, following these clear and succinct guidelines, the vast majority of health practitioners worldwide recognize that declaration of BD is a complex process that requires familiarity and includes six stages:

1. Detection of an irreversible coma.
2. Prerequisites that have to be met before a patient is evaluated for BD.
3. Thorough clinical examination by a physician who has expertise on assessing brain function.
4. Apnea testing to exclude any spontaneous respirations.
5. Ancillary testing in specific situations, where parts of 3 and 4 are not certain or cannot completely be assessed.
6. Precise documentation of all the above and the time of death of the individual.

Because details about the BD declaration process and the role of transcranial Doppler have been discussed in another chapter of this book, our aim here is different. But before we delve into details, let us clarify here the three periods that these very seriously ill patients pass through during their stay in the intensive care unit (ICU):

1. The patient is admitted to the ICU with a severe brain injury, but brain function is detected and is not BD. All the efforts by the treating team are aiming at preserving life, despite the fact that in many situations futility is obvious and it is a matter of time until all brain activity ceases.
2. There is no detectable brain activity, the BD process is initiated and is completed later on, with the patient declared BD.
3. If the patient is an organ donor, all efforts aim at optimizing organ function to allow safe transplantation to a living recipient.

Although it is obvious that the ICU team manages the patient during periods 1 and 2, it is not clear who manages the dead patient during period 3. In the USA, this is usually accomplished by a coordination of care between the local intensivists who were managing the patient before and during the declaration and the Organ Procurement Organization (OPO) team, which takes over after the patient is confirmed an organ donor. These health professionals (usually nurses and a physician medical director) have been already notified as soon as the, still alive, patient meets

clinical triggers (usually deep coma, on a ventilator, without sedation, or paralytics masking the presence or absence of clinical function). After the patient is declared BD, this same team discusses with the family, confirms consent for donation, starts histocompatibility matching, decides which organs are potentially transplantable, and orders additional procedures, tests, or biopsies. However, who really manages the dead patient in the ICU during the third period is variable, with the intensivists or the OPO team providing care until the patient reaches the operating room. There are emerging data, however, that an intensivist-led management of brain-dead donors increases the number of organs recovered for transplantation, more specifically lungs and kidneys [6].

Independently of whoever is the leader, the goal should be common and the cooperation between the various teams imperative. This is our aim in this chapter: to provide information on how to manage the BD patient in the ICU, maximize organ recovery, and optimize posttransplant organ function.

4.2 ICU Management of the Brain-Dead Organ Donor

The majority of transplanted organs come from donors who meet Death by Neurological Criteria (DNC). Once these criteria are met, the neurointensivist's goal shift from optimizing cerebral perfusion to maximizing organ preservation by compensating the physiologic deterioration leading to and following brain death. The care of the potential organ donor aims at stabilizing hemodynamic changes and endocrine abnormalities resulting from a complex interplay of neurohumoral, hormonal, proinflammatory phenomena, and other not yet fully understood mechanisms [7, 8]. The Society of Critical Care Medicine, the American College of Chest Physicians, and the Association of Organ Procurement Organizations have published guidelines for donor management [7], which should be used as a framework in these situations.

4.2.1 Hemodynamic Management

Monitoring is essential for balancing interventions needed for optimal organ preservation. Routine monitoring with parameters such as temperature, blood pressure, heart rate and rhythm, pulse oxygen saturation, and urine output should be combined with serial or continuous measurements of central venous pressure (CVP), pulmonary artery occlusion pressure (PAOP), stroke volume, cardiac output (CO), cardiac index, and mixed venous oxygen saturation. The latter are measured by placement of central venous and pulmonary artery catheters, but noninvasive methods have gained grounds, although with fewer data in this situation.

Intense monitoring, based on serial assessments of the aforementioned parameters, is crucial to achieve normovolemia and control extremes of blood pressure. General guidelines for adequate IV fluid resuscitation are as follows:

1. Mean arterial pressure (MAP) > 60 mmHg.
2. Urine output >1 ml/kg/hr.
3. Left ventricle ejection fraction >45%.
4. Lower vasopressor dose (e.g., dopamine ≤10 μg/kg/min).

These goals are essential since the rostrocaudal brain herniation, which eventually leads to brain death, is associated with a massive sympathetic discharge also known as autonomic storm. Autonomic storm includes physiologic changes such as catecholamine-induced increased heart rate, increased myocardial oxygen consumption, and hypertension. B-adrenergic agents such as esmolol have been traditionally used to treat this phase in an effort to preserve cardiac function. This phase is later followed by an abrupt hypotensive period attributed to vasodilation or cardiac dysfunction as the cardiorespiratory medullary centers collapse, usually in the context of hypovolemia [9].

Hypovolemia according to guidelines is initially treated with replacement of intravascular volume with crystalloids or colloids. The optimal choice of fluid therapy has not yet been finalized since studies addressing the issue are missing. Lactated Ringer solution and 0.9% saline are traditionally used, but in case of hypernatremia that needs to be treated, hypotonic fluids such as dextrose 5% or saline 0.45% are also utilized. Colloids such as albumin 5% and hydroxyethyl starch (HES) in bolus solutions are commonly available in ICUs to treat acute hypotension. Nevertheless, HES should be used with caution and is not recommended for infusions especially above 500–1000 mL since it has been associated with acute kidney injury, coagulopathy, delayed graft function, and graft failure. Packed RBCs can also serve as colloidal solutions in cases of bleeding or hematologic conditions with hemoglobin levels <7 g/dL but the optimal hemoglobin level for organ preservation is not known.

Vasodilation with hypotension has been traditionally treated with pressors or inotropes in parallel with fluid administration or when fluid correction fails to quickly achieve hemodynamic stability. Dopamine is the preferred vasoactive agent in these situation. In addition to having renal vasodilatory properties, and inotropic and vasoconstrictive effects as the dose increases, it also has immunomodulatory properties that may counterbalance the proinflammatory cascade of cytokines by induction of enzymes like heme oxygenase-1. Nevertheless, there are no studies to strongly support dopamine over other vasopressor agents such as vasopressin, but most intensivists prefer to use the latter as first or second agent. Generally, there is a desirable dopamine goal of ≤10 μg/kg/min and vasopressin can be added if this dose is exceeded. Norepinephrine, phenylephrine, dobutamine, and epinephrine are more commonly considered and used for severe shock. Use of norepinephrine and phenylephrine should be done with caution in brain-dead patients and only as tertiary agents when dopamine dose is above 10 μg/kg/min or there is no adequate

response to vasopressin, as they exhibit more potent α-receptor agonist activity leading to increased pulmonary capillary permeability causing increased extravascular lung water and coronary and mesenteric vasoconstriction [7].

Transthoracic echocardiography (TTE) is used to access myocardial function but it should be delayed after the early course of brain death and after the patient is weaned off catecholamines or repeated following aggressive donor management. Myocardial dysfunction may be due to underlying cardiac disease, cardiac injury from chest trauma, or stress cardiomyopathy. Guidelines suggest that if hemodynamic goals are not met and/or left ventricular ejection fraction remains less than 45%, then hormonal replacement therapy (HRT) may be undertaken [7].

4.2.2 Hormonal Replacement Therapy

Up to 80% of brain-dead patients develop signs of central diabetes insipidus (DI) due to ischemic—or other—injury of the hypothalamic-pituitary axis. Hypothyroidism and hypocortisolism also occur but in lower rates.

High, dilute urine output (>3–4 L/d or 2.5–3.0 mL/kg/hr) associated with hypovolemia, serum hyperosmolality, and rising hypernatremia ($Na^+ > 145$ mmol/L) may indicate the presence of DI due to arginine vasopressin (AVP or antidiuretic hormone) deficiency in the absence of other causes (e.g., hyperglycemia and mannitol administration). Treatment with AVP as a replacement therapy should be considered when hypotension persists despite high rate fluid resuscitation since it improves vasodilatory shock and reduces the need for catecholamines. A typical dosing regimen is an initial bolus infusion of 1 unit, followed by a continuous infusion of 0.01 to 0.1 units/minute (typical doses are 0.01 to 0.04 units/minute), titrating to a systemic vascular resistance of 800 to 1200 dynes-sec/cm^5. Desmopressin (DDAVP, a vasopressin analogue) is a more reasonable option in the presence of DI without hypotension due to greater affinity for V2 receptors (in the distal nephron) than V1 (on vascular smooth muscles) compared to AVP. Initial dose of 1–4 μg is given intravenously and then the dose is adjusted to achieve a urine volume <4 mL/kg/hour (typical required dose of 1–2 μg intravenously every 6–12 hours). Desmopressin can be used concurrently with AVP in patients with severe hypernatremia and hypotension. When DI occurs, electrolytes should be closely monitored (at least every 4 hours) and replenished to avoid hypokalemia, hypophosphatemia, and hypomagnesemia.

Corticosteroid therapy is used to reduce brain death-induced inflammation and more specifically to optimize donor lung quality, as it is associated with reduced extravascular lung water accumulation. The typical dose of methylprednisolone is 15 mg/kg as an intravenous infusion or 250 mg as an intravenous bolus followed by an infusion of 100 mg/hour, but it should be administered after blood has been collected for tissue typing.

Routine administration of thyroid hormone therapy has been controversial since the potential benefit has not been clearly shown in all studies. Guidelines suggest use of thyroid replacement therapy alone or in combination with AVP, corticosteroids, and insulin in hemodynamically unstable donors or with decreased left ventricular ejection fraction (<45%). Suggested dose is T4 as a 20 μg bolus IV, followed by an infusion at 10 μg/hr., or administration of T3 as a 4.0 μg bolus IV, followed by an infusion at 3 μg/hr.

Hyperglycemia is common in deceased organ donors and it should be treated even though target glucose levels are in debate. Most ICUs aim for glucose level less than 180 mg/dL while routine use of dextrose IV fluids is generally avoided, unless the water deficit from DI aquaresis cannot be easily corrected with 0.45% saline and AVP or DDAVP.

4.2.3 Respiratory Management

Brain-dead patients may have significant lung dysfunction from trauma (pulmonary contusions), pulmonary edema (either cardiogenic or neurogenic), infection (pneumonia), or V/Q mismatch (pulmonary embolism or atelectasis). The goal of the managing team is to optimize the function of lungs, by inducing diuresis, and achieve euvolemia, treat the infection, recruit more alveoli, and decrease the oxygen and positive end expiratory pressure (PEEP) requirements. The goal should be to reach a PaO_2/FiO_2 ratio $\geq$ 300 mm Hg on high oxygen and low PEEP (i.e., PaO_2 > 300 mm Hg with 100% FiO_2 and 5 cm PEEP). Survivability of recipients, however, has not been different in recipients with lower compared to higher than 300 ratio in large studies with over 10,000 patients [10].

There is abundance of lung donor management protocols. A combination of therapeutic bronchoscopy, chest physiotherapy, and lung recruitment maneuvers usually improve oxygenation even in donors who initially fail to meet these goals. Lung protective protocol, similar to acute respiratory distress syndrome (ARDS) ventilation settings, using tidal volumes of 6–8 mL/kg, 8–10 cm PEEP, a closed circuit for suctioning, and continuous positive airway pressure equal to previous PEEP for apnea test led to increased lung recovery rates compared to conventional ventilator protocol with 10–12 ml/kg tidal volume [11]. Increased alveolar recruitment may also explain the increased lung recovery found with airway pressure release ventilation (APRV) compared with traditional assist control ventilation in a small retrospective study [12].

4.3 Cardiopulmonary Resuscitation (CPR)

Brain-dead patients can sustain a cardiac arrest (CAA). In a large study from New York, 12% of patients sustained a CAA between the two brain death examinations or after the second examination [13]. Physicians should be prepared since

these patients are critically ill, with several comorbidities, including previous CAA that contributed to BD declaration.

There are many philosophical and ethical issues regarding any attempt to resuscitate a brain-dead patient, who has been declared officially and legally dead. Who will lead the efforts, the ICU team or the OPO? What is the purpose of doing cardiopulmonary resuscitation (CPR) in a dead patient? For how long these efforts should continue? If a second CAA happens in a different but alive patient, how the triage of resources should be done? There are also several periods during the process of BD declaration and after and for each a clear response plan regarding resuscitation or not (the Code Status) should be implemented:

1. Period between the two brain death exams. Although the patient may seem BD during the first exam, but is not officially declared BD. The Code Status remains the same.
2. Period after patient is declared BD and before discussion with family. Should the patient be resuscitated if a CAA occurs to allow the family to have the option of organ donation? What if the patient is already a registered donor and his/her wishes are already clear?
3. Period during discussion with family. As above. However, a decision to resuscitate can be made quickly and in real time.
4. Period after the patient became a donor and before the operating room for organ procurement. Does the Code Status automatically change from pre-brain death to do resuscitate in every case because the patient became a donor? Is a separate consent from the family required or is it implied when consent for donation is signed?

4.4 Conclusion

There are no data about national, state, or hospital policies on these issues. The meager literature available is revealing. Ethicists, however, have developed the notion of organ preserving cardiopulmonary resuscitation (OP-CPR), which is defined as the use of CPR in cases of cardiac arrest to preserve organs for transplantation, rather than to revive the patient [14]. They conclude that although successful resuscitation may benefit the society by saving recipients lives, CPR in the brain-dead patient can cause physical damage and may provoke psychological harm to families and healthcare professionals. What is certain is that without clear and predefined plans on how to react in a not so rare situation, confusion among ICU health providers will ensue. Therefore, we recommend this issue to be addressed in the hospital or National policies of Organ Donation and families to be questioned on their preferences during the process of consent for donation.

Algorithm

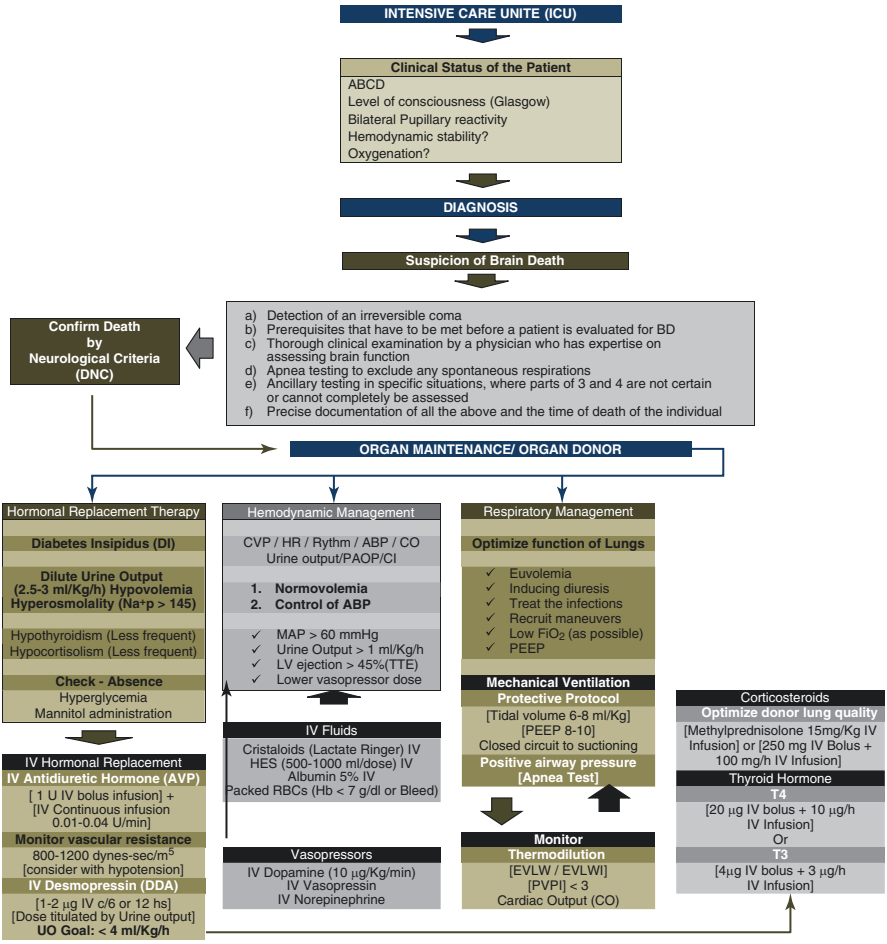

Na + p plasmatic sodium, *IV* Intravenous, *EVLW* extravascular lung water, *EVLWI* extravascular lung water index, *PVPI* permeability vascular, *MAP* mean artery pressure, *ABP* arterial blood pressure, *TTE* transthoracic echocardio, *BD* brain death, *LV* left ventricule, *CVP* central venous pressure, *HR* heart rate, *CO* cardiac output, *CI* cardiac index, *PAOP* pulmonary artery occlusion pressure, *HES* hydroxyetilstarch, *RBC* red blood cells

References

1. Mollaret P, Goulon M. The depassed coma (preliminary memoir). Rev Neurol. 1959;101:3–15.
2. Wahlster S, Wijdicks EF, Patel PV, et al. Brain death declaration: practices and perceptions worldwide. Neurology. 2015;84:1870–9.

3. Greer DM, Wang HH, Robinson JD, Varelas PN, Henderson GV, Wijdicks EF. Variability of brain death policies in the United States. JAMA Neurol. 2015;73:213–8.
4. Practice parameters for determining brain death in adults (summary statement). The Quality Standards Subcommittee of the American Academy of Neurology. Neurology. 1995;45:1012–4.
5. Wijdicks EF, Varelas PN, Gronseth GS, Greer DM, American Academy of N. Evidence-based guideline update: determining brain death in adults: report of the Quality Standards Subcommittee of the American Academy of Neurology. Neurology. 2010;74:1911–8.
6. Singbartl K, Murugan R, Kaynar AM, et al. Intensivist-led management of brain-dead donors is associated with an increase in organ recovery for transplantation. Am J Transplant Off J Am Soc Transplant Am Soc Transplant Surg. 2011;11:1517–21.
7. Kotloff RM, Blosser S, Fulda GJ, et al. Management of the Potential Organ Donor in the ICU: Society of Critical Care Medicine/American College of Chest Physicians/Association of Organ Procurement Organizations Consensus Statement. Crit Care Med. 2015;43:1291–325.
8. Watts RP, Thom O, Fraser JF. Inflammatory signalling associated with brain dead organ donation: from brain injury to brain stem death and posttransplant ischaemia reperfusion injury. J Transpl. 2013;2013:521369.
9. Wood KE, Becker BN, McCartney JG, D'Alessandro AM, Coursin DB. Care of the potential organ donor. N Engl J Med. 2004;351:2730–9.
10. Reyes KG, Mason DP, Thuita L, et al. Guidelines for donor lung selection: time for revision? Ann Thorac Surg. 2010;89:1756–64. discussion 64–5.
11. Mascia L, Pasero D, Slutsky AS, et al. Effect of a lung protective strategy for organ donors on eligibility and availability of lungs for transplantation: a randomized controlled trial. JAMA. 2010;304:2620–7.
12. Hanna K, Seder CW, Weinberger JB, Sills PA, Hagan M, Janczyk RJ. Airway pressure release ventilation and successful lung donation. Arch Surg. 2011;146:325–8.
13. Lustbader D, O'Hara D, Wijdicks EF, et al. Second brain death examination may negatively affect organ donation. Neurology. 2011;76:119–24.
14. Dalle Ave AL, Gardiner D, Shaw DM. Cardio-pulmonary resuscitation of brain-dead organ donors: a literature review and suggestions for practice. Transpl Int. 2016;29:12–9.

Chapter 5
Neuropharmacology in the ICU: Monitoring the Therapeutic Response and Neurological Hemodynamic Impact of Our Therapeutic Decisions in Real Time

Ryan Fillmore and Gretchen M. Brophy

Key Points

1. Vasoactive drugs impact both systemic and cerebral hemodynamic parameters.
2. Impaired cerebral autoregulation (CA) may cause an unwanted effect of a drug on central nervous system (CNS) vasculature.
3. Avoid abrupt hemodynamic changes that may lead to unwanted increases in intracranial pressure.
4. Optimization of mean arterial pressure (MAP) and cerebral perfusion pressure (CPP) needs to be considered when selecting certain drugs due to their potential side effects.
5. Comorbid disease states, organ dysfunction, and temperature must be considered when administering medications that may alter cerebrovascular hemodynamics.
6. The use of noninvasive techniques, such as transcranial Doppler (TCD/TCCS), can serve as a tool for determining the therapeutic response of pharmacological treatments in neurocritical care patients.

R. Fillmore
Department of Neurology-Neurocritical Care, The University of California, Irvine, Orange, CA, USA

G. M. Brophy (✉)
Virginia Commonwealth University, Medical College of Virginia Campus, Richmond, VA, USA
e-mail: gbrophy@vcu.edu

C. N. Rodríguez et al. (eds.), *Neurosonology in Critical Care*,
https://doi.org/10.1007/978-3-030-81419-9_5

5.1 Introduction

It is essential to understand the systemic and central effects of different medications when managing patients with acute, life-threatening neurological injuries. Patients with a severe acute brain injury, secondary to ischemic/hemorrhagic strokes, anoxic injury after cardiac arrest, status epilepticus, or traumatic brain injury, may have impaired cerebral autoregulation. Therefore, changes in systemic blood pressure can have a profound effect on central nervous system (CNS) hemodynamics [1]. The use of vasoactive drugs in this population may have variable and possibly unwanted results due to this impaired cerebral autoregulation. The impact of these agents on the cerebrovasculature may ultimately result in decreased cerebral tissue oxygenation and poor outcomes. In addition, acute/chronic comorbidities (e.g., chronic hypertension, renal insufficiency, or hepatic failure), hyperthermia/hypothermia, alterations in acid/base status, and even volume status can alter the pharmacokinetics of these drugs [2]. In patients with aneurysmal SAH, tailoring therapy can be challenging as cerebral vasospasm along with other pathophysiologic mechanisms are thought to contribute to morbidity and mortality in these patients [3–6]. There is a paucity of data describing the effects of medications on the cerebrovasculature when using multimodality monitoring devices, such as transcranial Doppler (TCD/TCCS). Therefore, this chapter will review the available evidence in this regard.

5.2 Systemic and Cerebral Vasculature: Drug Effects

Select medications are given to directly influence system hemodynamic characteristics (e.g., vasodilation and vasoconstriction) through varying mechanisms. However, there can be secondary effects of these medications on cerebrovascular hemodynamics, such as increased or decreased ICP, which must be taken into account when optimizing cerebral perfusion pressure and oxygenation in patients within the neurocritical care setting [7, 8].

5.2.1 Vasoactive Agents

5.2.1.1 **Vasodilators** (Table 5.1)

Calcium Channel Blockers

Dihydropyridine calcium channel blockers (CCB) act on L-type slow-conducting calcium channels in vascular smooth muscle causing vasodilation. Potential adverse effects of these agents are reflex tachycardia and systemic hypotension.

Table 5.1 Vasodilator drugs

Drug/Drug Class:	MOA	Systemic Vascular Effects	Cerebrovascular Effects/TCD findings	Clinical Pearls
Calcium Channel Blockers	Act on L-type slow-conducting Ca^{2+} channels in smooth muscle	↓ ABP	No significant effect on ICP	Avoid rapid titration: systemic hypotension, reflex tachycardia (esp. IV nicardipine)
Magnesium	Calcium ion antagonist in smooth muscle	Possible ↓ ABP	Possible ↑CBF. No significant effect on ICP	Continuous infusions can lead to high concentrations and cardiac/systemic adverse effects
Statins	HMG-COA reductase inhibitors, induction of NO pathway.	No significant effect	Possible ↑CBF and therefore ↑ICP	Caution in hepatic dysfunction
Nitroprusside	Metabolized to NO→cGMP→vasodilation in smooth muscle of arterioles and venules	↓ ABP	↑ICP with large dosage adjustments or toxicity	Small titrations recommended, monitor for thiocyanate toxicity, Expensive
Clazosentan	Endothelin-1 antagonist	↓ ABP	↑cerebral vasospasm, no significant effect on ICP	Not FDA approved, pulmonary complications, anemia
Hydralazine	Not fully understood. Causes smooth muscle relaxation and peripheral vasodilation	↓ ABP	Possible ↑CBF and therefore ↑ICP/velocity	Reflex tachycardia, headache, flushing, hypotension
Sildenafil citrate	Phosphodiesterase-5-Inhibitor→decrease cGMP→vasodilation	↓ ABP	Observed Vasodilatory effect in normal and spastic vessels	Headache Main use: pulmonary hypertension and erectile dysfunction
Papavarine	Inhibits cyclic cAMP, cGMP, and calcium ion channels in smooth muscle	↓ ABP	↑ICP/velocity	Intra-arterial administration for the treatment of vasospasm

MOA mechanism of action, *ABP* arterial blood pressure, *TCD* transcranial Doppler, *CPP* cerebral perfusion pressure, *CBF* cerebral blood flow, *ICP* intracranial pressure; ↑ Decrease, ↓ Increase

Nimodipine

It is the only CCB indicated for reducing the incidence and severity of ischemic deficits following aneurysmal SAH [4]. Unfortunately, nimodipine is not available as an intravenous (IV) formulation in the United States, which increases the unwanted systemic hypotensive effects with immediate-release capsule oral administration. It can be very problematic and sometimes warrants the administration of a vasoconstrictor to counter these effects to decrease the risk of lowering cerebral perfusion and oxygenation. Other countermeasures include lower dosages given every 2 hours orally or via feeding tube by extracting the gel from the capsule. There is a new liquid formulation of nimodine available, but it is very expensive and is not available at all institutions. The most recent randomized, controlled trial, Nimodipine Microparticles to Enhance Recovery While Reducing Toxicity After Subarachnoid Hemorrhage (NEWTON), evaluated nimodipine gel administered intraventricularly and slowly released over 21 days [8]. Although animal studies of this formulation showed promise, the NEWTON trial did not show clinical benefit in aSAH patients.

Nicardipine

It is ideal for system blood pressure control in patients who require continuous IV administration and has been shown to reduce the incidence of symptomatic vasospasm in patients with aSAH. However, it was not shown to improve overall

outcome after 3 months [9]. Exercise caution with nicardipine due to potential systemic hypotension if titrated too rapidly, prolonged effects as treatment duration increases, and volume overload due to low concentrations required for peripheral administration [4]. There have been some reports of headache as an adverse effect with IV nicardipine administration, especially in studies for the treatment of symptomatic vasospasm after aSAH [10]. More recently, IV nicardipine was shown to paradoxically increase intracerebral arterial contractility based on an elevated pulsatile index (PI) calculated from TCD measurements in a small group of patients with aSAH [11]. However, it is still unclear if IV nicardipine ultimately increases ICP. Other formulations have been studied for use in aSAH, such as nicardipine prolonged-release implants (NPRIs), and intraarterial administration (IA). The NPRIs were shown in one study to decrease the incidence of delayed ischemic neurologic deficit (DIND) in patients with thick subarachnoid clots (Fisher grade 3) if implanted adjacent to arteries located within the clots [12, 13]. IA nicardipine administration was shown in one prospective study to reverse vasospasm without any sustained effect on ICP or on systemic hemodynamics in patients who required interventional treatment for vasospasm [14].

The newest CCB available for IV administration is clevidipine**.** This is a short-acting CCB administered as a continuous infusion for rapid control of hypertension. One study has evaluated the cerebrovascular effects of clevidipine and it was not found to significantly increase cerebral blood flow velocity (CBFV) or CO_2 responsiveness [15]. The key to reducing adverse effects from CCB agents is to avoid abrupt changes in dosage and maintaining euvolemia throughout the duration of treatment.

Other Vasodilators

Magnesium

Calcium has been shown to play a role in vasoconstriction via its action on smooth muscle within the arterial walls. Intravenous magnesium antagonizes calcium, which can increase cerebral blood flow via decreasing cerebral vasoconstriction. Several studies have evaluated the use of continuous IV magnesium infusions in patents with aSAH, but the most recent prospective study (MASH-II trial) showed no benefit in reducing ischemic deficits. Currently, no data exist to support continuous intravenous infusions of magnesium for improving clinical outcomes in patients with aSAH [16].

3-Hydroxy-3-Methyl-Glutaryl-CoA (HMG-CoA) Reductase Inhibitors (Statins)

HMG-CoA reductase enzyme inhibitors, often called statins, are thought to induce the nitric oxide (NO) pathway (via inhibition of Rho protein) resulting in increased NO production and dilation of cerebral blood vessels improving cerebral blood flow

(CBF). Some studies report that both simvastatin and pravastatin can reduce the incidence of angiographically proven vasospasm and delayed ischemic neurological deficit (DIND) in patients treated with statins for management of aSAH [17, 18]. One randomized prospective study showed simvastatin reduced the highest mean velocities within the middle cerebral artery (using TCDs), postulating that it inhibited biochemical inflammatory markers that are thought to cause vasospasm [18]. The most recent study evaluating statins for prevention of ischemic deficits following aSAH (STASH trial) was unable to show benefit with these agents [19]. However, if a patient is on a statin prior to admission, the statin should not be stopped as this has been associated with rebound vasoconstriction and worse outcomes [20, 21].

Nitroprusside

Nitric oxide activates guanylate cyclase in vascular smooth muscle and increases the intracellular production of cyclic guanosine monophosphate (cGMP) causing vascular smooth muscle relaxation and vasodilation. Nitroprusside, a potent vasodilator, breaks down in the systemic circulation to release NO causing vasodilation of arterioles (and venules). Caution should be used with prolonged high-dose infusions, especially in patients with renal dysfunction, due to potential cyanide/thiocyanate toxicity. This toxicity manifests as systemic hypotension, massive vasodilation, increased cerebral blood flow (shunted from systemic autoregulation), and increased ICP [22, 23]. Large dosage adjustments should also be avoided as this can result in decreased systemic blood pressure and increased ICP.

Endothelin-1 Antagonists

The interaction between endothelin-1 (ET-1) and NO is essential for maintaining adequate cerebral blood flow (via cerebral vasodilatation) in patients with aSAH [3]. Clazosentan, an ET-1 antagonist**,** has been found to reduce cerebral vasospasm in a dose-dependent fashion in patients undergoing endovascular coiling, but it did not change the overall clinical outcome (CONSCIOUS-III TRIAL). Additionally, adverse effects observed were pulmonary complications, hypotension, and anemia with the use of clazosentan [24].

Hydralazine

It directly acts on peripheral vasculature causing relaxation of smooth muscle and vasodilation. In rodent animal models, dihydralazine caused increased CBF if autoregulation was intact. The extent and duration of systemic vasodilatory effects are highly variable and caution should be used due to potential reflex tachycardia, headache, flushing, and systemic hypotension [25].

Phosphodiesterase Inhibitors

Cyclic guanosine monophosphate (cGMP) is an important nucleotide involved in endovascular smooth muscle contraction. The phosphodiesterase isoenzyme type V (PDE-V) hydrolyzes cGMP, which lowers its intracellular concentration subsequently causing vasoconstriction. Sildenafil citrate (PDE-V inhibitor), commonly used for erectile dysfunction and pulmonary hypertension, has been shown in animal models to have a vasodilatory effect in normal and spastic cerebral vessels [3, 26]. These cerebrovascular changes may result in headache, which is reported to occur in up to 46% of patients [27].

Papaverine

It is a benzylisoquinoline alkaloid derived from opium, and acts as a nonselective vasodilator via its inhibition of cyclic adenosine monophosphate (cAMP), cGMP, and calcium ion channels in smooth muscle. Intraarterial administration has been shown in some studies to reduce cerebral vasospasm angiographically (TCD proven) and clinically [28]. Papaverine can increase ICP, and its use has fallen out of favor with the availability of safer and more effective vasodilatory agents [29].

5.2.1.2 **Vasoconstrictors** (Table 5.2)

Generally, an increase in systemic vasoconstriction can cause an increase in cerebral blood volume (CBV) and CBF, which may increase ICP. Remember, however, that in patients with impaired cerebral autoregulation, the secondary effect of vasoconstrictive drugs can change [30, 31].

Table 5.2 Vasoconstrictors

Drug:	MOA	Systemic Vascular Effects	Cerebrovascular Effects/TCD Findings	Clinical Pearls
Norepinephrine	α-adrenergic and β-1 adrenergic agonist	↑ ABP	No significant impact on CBF or ICP	Can cause tachyarrythmias
Epinephrine	α-1, β-1, and β-2 agonist	↑ ABP	No significant impact on CBF or ICP	Can cause tachyarrythmias
Dopamine	α-adrenergic, β-1, and dopamine receptor agonist	↑ ABP	↑ CBF and ICP: may see ↑ velocities	Likely to cause tachyarrythmias at high doses
Phenylephrine	α-adrenergic agonist	↑ ABP	↑ CPP, ↑ CBF, possible ↑ ICP/velocities	Caution: reflex bradycardia
Vasopressin	V1-endothelium receptor	↑ ABP	↑ CPP, ↑CBF, possible ↑ ICP/velocities	Adjunctive therapy for refractory hypotension

MOA mechanism of action, *ABP* arterial blood pressure, *TCD* transcranial Doppler, *CPP* cerebral perfusion pressure, *CBF* cerebral blood flow, *ICP* intracranial pressure, ↑ Increase, ↓ Decrease

Norepinephrine

It is an alpha adrenergic and beta-1 adrenergic agonist that can cause systemic hypertension and increased cardiac output, respectively [30]. No significant impact on CBF or ICP has been observed [32].

Epinephrine

Acts on alpha, beta-1, and beta-2 adrenergic receptors, but has no significant impact on CBF or ICP [32].

Dopamine (DA)

It is an alpha adrenergic, beta-1 adrenergic, and dopamine receptor agonist that has been shown to directly increase CBF and ICP [32].

Phenylephrine

It is an alpha-adrenergic receptor agonist that causes vasoconstriction of peripheral blood vessels. It has been shown to cause an increase in CPP (cerebral perfusion pressure), which then increases CBF [33]. Caution should be used due to the potential for reflex bradycardia [30].

Vasopressin

Acts on the V1 endothelium receptor, and is often used in refractory hypotension due to sepsis as adjunctive therapy. It has also been shown to be effective in maintaining CPP in TBI swine models without a significant increase in ICP [34].

Neuromonitoring

Can be extremely helpful when using vasoconstrictive agents in patients with neurological injury and impaired autoregulation in order to optimize therapeutic strategies.

5.2.2 *Anesthetics/Sedative Agents* (Table 5.3)

We know from prior studies that IV sedatives generally cause a dose-dependent decrease in CBF as well decrease the cerebral metabolic rate for oxygen ($CMRO_2$), ultimately causing a reduction in ICP [35–37]. However, the reduction in CBF can be variable between drugs, and there may be compensatory cerebral vasodilation which can increase ICP in the setting of preserved autoregulation [37]. In addition to the coupled reduction of both $CBF/CMRO_2$, sedatives can also cause peripheral vasodilation, therefore leading to a reduction in the systemic mean arterial blood pressure (MAP). In patients with impaired cerebral autoregulation, lowering the MAP can cause a decrease in CPP and brain tissue ischemia/hypoxia [35, 38]. Keep this in mind when selecting agents for sedation and/or pain control by avoiding hypotension, therefore maintaining MAP and CPP in patients with impaired cerebral autoregulation [38].

5.2.2.1 Benzodiazepines

Benzodiazepines (e.g., diazepam, lorazepam, midazolam, and clonazepam) are $GABA_A$ receptor agonists. The amount of reduction in CBF as a result of benzodiazepines administration can be variable. Common adverse reactions are

Table 5.3 Anesthetics/sedatives

Drug/Drug Class	MOA	Systemic Effects	CNS effects/TCD findings	Clinical Pearls
Benzodiazepines	$GABA_A$ receptor agonists	↓ ABP	Indirectly ↑ ICP (hypercarbia)/possible ↑ velocities	Respiratory depression. IV LZP and DZP contain propylene glycol
Barbiturates	$GABA_A$ agonists	↓ ABP	Directly ↓ ICP/possible ↓ velocities	Phenobarbital has longest half-life. IV contains propylene glycol
Anticonvulsants[a]	Depends on drug class	Can cause ↓ ABP	May cause ↑ or ↓ICP (Topiramate observed to ↑ICP, causes metabolic acidosis).	IV phenytoin contains propylene glycol
Opioids	Mu receptor agonists	↓ ABP	Can ↑ ICP/velocities, and cause hypercarbia (respiratory depression)	Caution in renal and hepatic failure
Propofol	Not completely understood; probable $GABA_A$ agonist activity	↓ ABP	Possible ↓ ICP/↓velocities	Systemic hypotension, Propofol-related infusion syndrome (PRIS)
Dexmedetomidine	α-2 agonist	Bradycardia and ↓ ABP	No significant effect on ICP	Does not cause significant respiratory depression
Clonidine	α-2 agonist	Bradycardia and ↓ ABP	No significant effect on ICP	
Ketamine	Non-competitive NMDA antagonist	↑ ABP, preservation of MAP	No significant effect on ICP	Dissociative symptoms; hallucinations,

[a] **Cause sedation, however primary indication is for seizure control**

MOA mechanism of action, *ABP* arterial blood pressure, *TCD* transcranial Doppler, *CPP* cerebral perfusion pressure, *CBF* cerebral blood flow, *ICP* intracranial pressure, *LZP* lorazepam, *DZP* diazepam, ↑ Decrease, ↓ Increase

respiratory depression and systemic hypotension when dosed aggressively or administered as continuous infusions. The ICP can be indirectly elevated from benzodiazepine administration due to hypercarbia (acidity causing cerebral vasodilation) in patients with respiratory depression. Midazolam is typically used to control elevated ICP in patients with hemodynamic instability over propofol, as it does not have as much of an effect on reducing systemic blood pressure. However, due to the potential for tachyphylaxis, higher doses of midazolam infusion may be required to adequately control ICP [39]. Midazolam has high lipid content and can accumulate in tissues causing prolonged sedation but has a relatively short half-life (1 hour) [40]. Additionally, diazepam and lorazepam containing propylene glycol, which can reduce blood pressure with rapid administration and monitoring for signs of propylene glycol toxicity (e.g., high anion gap metabolic acidosis, osmolar gap, and a sepsis-like picture), are recommended with prolonged therapy [41, 42].

5.2.2.2 Barbiturates

Barbiturates (i.e., pentobarbital, phenobarbital, and thiopental) are also $GABA_A$ agonists and can also cause respiratory depression and hypotension. Studies have shown a direct effect of reduction in ICP in patients with severe head injury and refractory elevated ICPs; however, hypotension was also observed in some of the patients [43, 44]. Intravenous formulations of phenobarbital and pentobarbital also contain propylene glycol, and therefore, one should monitor for toxicity and may require vasopressor support during continuous infusion therapy [45]. Barbiturates are typically used as adjunctive therapy to reduce ICP, and in a select group of patients for the treatment of refractory status epilepticus [1, 45].

5.2.2.3 Opioids

Opioids are Mu receptor agonists, and are commonly used for analgesia. In one study of patients with severe closed-head injuries, both morphine and fentanyl were shown to significantly increase ICP without any significant change in CBF based on TCD measurements, regardless of whether or not cerebral autoregulation was preserved. A decrease in systemic MAP and hypotension was also observed [46]. Another common side effect of opioids is respiratory depression, producing a rise in $PaCO_2$ (hypercarbia), and increased ICP [38, 45, 47]. The effect on ICP was noted to be transient after boluses of fentanyl, sufentanil, and alfentanil in head trauma patients [47]. In patients who are hemodynamically unstable, morphine would not be recommended as it causes histamine release and subsequent vasodilation/hypotension [46]. Fentanyl, however, has a fast onset of action and is easily titratable and is commonly used as analgosedation in patients with neurological injury [45]. Fentanyl is less expensive than remifentanil, a shorter acting agent that is metabolized by plasma esterases and most commonly used in the operating room versus

intensive care unit. Remifentanil may also reduce CBF, similar to intravenous anesthetics [7, 48]. Also keep in mind that opioids' concentrations and effects are influenced by hepatic and renal dysfunction (refer to section below on drug clearance and metabolism).

5.2.2.4 Anticonvulsant Medications

Apart from the previously mentioned benzodiazepines and barbiturates, there is not much literature on the relationship between antiseizure drugs and cerebral vasculature. A common side effect of anticonvulsant agents is sedation and systemic hypotension [42].

Levetiracetam (proposed MOA: binds SV2A synaptic vesicle glycoprotein) and lacosamide (proposed MOA: inhibits sodium channels) did not have a significant effect on systemic vasculature. However, phenytoin (which blocks voltage-gated sodium channels) was shown to cause systemic hypotension [49]. Recall that changes in systemic blood pressure can effect ICP via cerebral autoregulation. Medications that effect the systemic pH can also have an effect on cerebral vasculature. Topiramate (proposed MOA: acts on multiple cellular targets including inhibiting *carbonic anhydrase*) was shown to increase cerebral blood flow velocities on TCDs in the MCA and PCA in one study as it causes a metabolic acidosis leading to cerebral vasodilation [50]. Drugs with similar mechanisms of action, such as zonisamide, should also be monitored for these effects.

5.2.2.5 Other Sedatives/Anesthetics

The MOA of propofol is not completely understood, but it appears to be an agonist at the GABA receptor, making it useful for sedation and seizure control. One of the major adverse effects of propofol is systemic hypotension, especially with bolus dosing or large titrations. It may also increase ICP as a result of this systemic hypotensive effect due to compensatory cerebral vasodilation, but decreased ICP and CBF can be observed in patients with impaired cerebral autoregulation [1]. In one study comparing propofol, pentobarbital, and isoflurane, all three were shown to increase both CBF and CBV; however, the greatest effect was seen with isoflurane. Remember that acute changes in ICP are determined primarily by CBV [3, 7]. Dexmedetomidine and clonidine (presynaptic alpha$_2$ receptor agonists) cause bradycardia and hypotension but did not significantly effect ICP in swine animal models [51]. Therefore, bolus dosing and large dosage titrations commonly cause these effects and should be avoided [51]. Ketamine (a noncompetitive NMDA receptor antagonist) is ideal for nonintubated patients as it does not affect respiratory drive [1]. Contrary to other sedatives, ketamine has been shown to cause systemic hypertension, and preservation of the MAP. Earlier studies of ketamine suggested that it caused an increased ICP [52]. However, based on more current data, ketamine was not found to increase ICP when compared with opioids [53]. Ketamine was shown to increase CBF, decrease ICP by 92.7%, and decrease the occurrence of DCI in a

cohort study of patients with aneurysmal subarachnoid hemorrhage being treated with sedation (in addition to ketamine) [54].

5.2.3 Hemodynamic Agents

The use of agents that increase the systemic circulating volume (e.g., normal saline and lactated ringers) can increase ICP acutely. The use of diuretics may have the opposite effect. Large fluctuations in volume status can effect cerebral vasculature; however, central mechanisms usually preserve CPP and, ultimately, the ICP may not change [55–57]. In patients with impaired cerebral autoregulation, changes in volume status have variable affects on ICP which can impact TCD measurements. Therefore, it is important to monitor intake and output (I/Os) and use noninvasive methods (e.g., ultrasound) to evaluate if a patient's volume status is adequate.

5.3 Drug Clearance and Metabolism*:* Disease Effects

Different disease states can change a drug's metabolism, which may augment or depress its effect. This is particularly true in patients with hepatic or renal dysfunction as many medications are metabolized in these organs [58]. Ultimately, medications that are not cleared as quickly due to hepatic or renal failure could cause more enhanced side effects, such as hypotension and respiratory depression, which can alter cerebral hemodynamics and possibly increased ICP [59]. Patients with fulminant liver failure tend to have higher ICPs at baseline, which must be taken into consideration when using medications that are hepatically cleared that could increase the ICP [60]. Disease states that change intravascular volume, such as chronic renal failure/volume overload, heart failure, or sepsis, can alter a medication's metabolism as well. Drug metabolism is also affected by temperature, and decreases in metabolism are observed with each degree the core temperature drops below 37 °C, especially when utilizing targeted temperature management and therapeutic hypothermia [1, 57, 61].

5.4 Conclusion

The use of noninvasive techniques, such as transcranial Doppler (TCD/TCCS), can serve as a tool for determining the therapeutic response of pharmacological treatments in neurocritical care patients. However, one must keep in mind the complexities of different disease pathologies, volume status, acute changes in pH, and the relationship between systemic vasculature and cerebral hemodynamics by using a multivariable approach to management. It is recommended to avoid abrupt large dosage adjustments to prevent large fluctuations in systemic blood pressure, intracranial pressure, and cerebral blood flow.

Algorithm

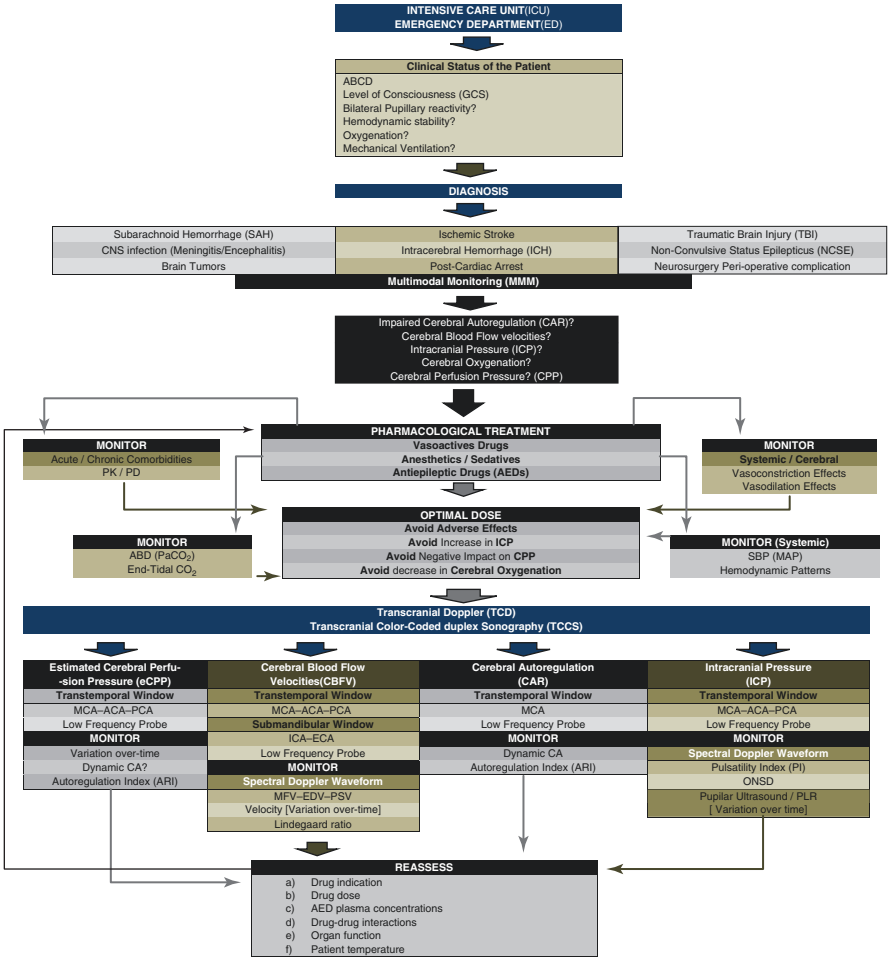

ABCD airway – breath – circulation- disturbances, *ABD* acid-base disturbance, *MFV* mean flow velocity, *EDV* end-diastolic velocity, PSV peak flow velocity, *ONSD* optic nerve sheath diameter, *PLR* pupilar light reflex, *SBP* systolic blood pressure, *MAP* mean arterial pressure, *CA* cerebral autoregulation

References

1. Oddo M, Crippa IA, Mehta S, et al. Optimizing sedation in patients with acute brain injury. Crit Care. 2016;20:128.
2. Fei Y-X, Zhang T-H, Zhao J, He R, Ya-Nan D, Yu C-L, et al. In vitro and in vivo evaluation of hypothermia on pharmacokinetics and pharmacodynamics of nimodipine in rabbits. J Int Med Res. 2018;46(1):335–47.

3. Siasios I, Kapsalaki EZ, Fountas KN. Cerebral vasospasm pharmacological treatment: an update. Neurol Res Int. 2013;2013:571328.
4. Webb A, Kolenda J, Martin K, Wright W, Samuels O. The effect of intraventricular Administration of Nicardipine on mean cerebral blood flow velocity measured by transcranial Doppler in the treatment of vasospasm following aneurysmal subarachnoid hemorrhage. Neurocrit Care. 2010;12(2):159–64.
5. Geraghty JR, Testai FD. Delayed cerebral ischemia after subarachnoid hemorrhage: beyond vasospasm and towards a multifactorial pathophysiology. Curr Atheroscler Rep. 2017;19(12):50.
6. Leonardo de Oliveira Monoel A, Loch Macdonald R. Neuroinflammation as a target for intervention in Subarachnoid Hemorrhage. Front Neurol. 2018;9:292.
7. Mikkelsen MLG, Ambrus R, Miles JE, Poulsen HH, Moltke FB, Eriksen T. Effect of propofol and remifentanil on cerebral perfusion and oxygenation in pigs: a systematic review. Acta Vet Scand. 2016;58
8. Hänggi D, Etminan N, Macdonald RL, et al. NEWTON: Nimodipine microparticles to enhance recovery while reducing toxicity after subarachnoid hemorrhage. Neurocrit Care. 2015;23(2):274–84.
9. Haley EC Jr, et al. A randomized controlled trial of high-dose intravenous nicardipine in aneurysmal subarachnoid hemorrhage. A report of the cooperative aneurysm study. J Neurosurg. 1993;78(4):537–47.
10. Shibuya M, Suzuki Y, Enomoto H, Okada T, Ogura K, Sugita K. Effects of prophylactic intrathecal administrations of nicardipine on vasospasm in patients with severe aneurysmal subarachnoid haemorrhage. Acta Neurochir. 1994;131(1–2):19–25.
11. Lahiri S, Nezhad M, Schlick KH, et al. Paradoxical cerebrovascular hemodynamic changes with nicardipine. J Neurosurg. 2017;128(4):1015–9.
12. Kasuya H, Onda H, Sasahara A, Takeshita M, Hori T. Efficacy and safety of nicardipine prolonged-release implants for preventing vasospasm in humans. Stroke. 2002;33(4):1011–5.
13. Kasuya H, Onda H, Takeshita M, Okada Y, Hori T. Application of Nicardipine prolonged-release implants: analysis of 97 consecutive patients with acute subarachnoid hemorrhage. Neurosurgery. 2005;56(5):895–902.
14. Badjatia N, Topcuoglu MA, Pryor JC, et al. Preliminary experience with intra-arterial Nicardipine as a treatment for cerebral vasospasm. Am J Neuroradiol. 2004;25(5):819–26.
15. Lemkuil BP, Gierl BT, Patel PM, et al. The effect of Clevidipine on cerebral blood flow velocity and carbon dioxide reactivity in human volunteers. J Neurosurg Anesthesiol. 2016;28(4):337–40.
16. Leijenaar JF, Dorhout Mees SM, Algra A, Bergh WM, Rinkel GJE. Effect of magnesium treatment and glucose levels on delayed cerebral ischemia in patients with subarachnoid hemorrhage: a substudy of the Magnesium in Aneurysmal Subarachnoid Haemorrhage trial (MASH-II). Int J Stroke. 2015;10:108–12.
17. Tseng M-Y, Czosnyka M, Richards H, Pickard JD, Kirkpatrick PJ. Effects of acute treatment with pravastatin on cerebral vasospasm, autoregulation, and delayed ischemic deficits after aneurysmal subarachnoid hemorrhage: a phase II randomized placebo-controlled trial. Stroke. 2005;36(8):1627–32.
18. Lynch JR, Wang H, McGirt MJ, et al. Simvastatin reduces vasospasm after aneurysmal subarachnoid hemorrhage: results of a pilot randomized clinical trial. Stroke. 2005;36(9):2024–6.
19. Kirkpatrick PJ, Turner CL, Smith C, Hutchinson PJ, Murray GD. Simvastatin in aneurysmal subarachnoid haemorrhage (STASH): a multicentre randomised phase 3 trial. Lancet Neurol. 2014;13(7):666–75.
20. Hernández-Perera O, Pérez-Sala D, Navarro-Antolín J, et al. Effects of the 3-hydroxy-3-methylglutaryl-CoA reductase inhibitors, atorvastatin and simvastatin, on the expression of endothelin-1 and endothelial nitric oxide synthase in vascular endothelial cells. J Clin Invest. 1998;101(12):2711–9.
21. Mascitelli L, Francesca Pezzetta SV, et al. Statin treatment withdrawal in ischemic stroke: a controlled randomized study. Neurology. 2018;69(9):904–10.

22. Morris AA, Page RL, Baumgartner LJ, et al. Thiocyanate accumulation in critically ill patients receiving nitroprusside infusions. J Intensive Care Med. 2017;32(9):547–53.
23. Agrawal A, Patir R, Kato Y, Chopra S, Sano H, Kanno T. Role of intraventricular sodium nitroprusside in vasospasm secondary to aneurysmal subarachnoid Haemorrhage: a 5-year prospective study with review of the literature. Min Minim Invasive Neurosurg. 2009;52(01):5–8.
24. Macdonald RL, Higashida RT, Keller E, et al. Randomized trial of clazosentan in patients with aneurysmal subarachnoid hemorrhage undergoing endovascular coiling. Stroke. 2012;43(6):1463–9.
25. Harms H, Wiegand F, Megow D, Prass K, Einhäupl KM, Dirnagl U. Acute treatment of hypertension increases infarct sizes in spontaneously hypertensive rats. Clin Neurosci Neuropathol. 2000;11(2):355–9.
26. Atalay B, Caner H, Cekinmez M, Ozen O, Celasun B, Altinors N. Systemic administration of phosphodiesterase V inhibitor, sildenafil citrate, for attenuation of cerebral vasospasm after experimental subarachnoid hemorrhage. Neurosurgery. 2006;59(5):1102–8.
27. Sildenafil Citrate. Lexicomp Inc. https://online.lexi.com/lco/action/doc/retrieve/docid/fc_dfc/5548922. Published 2014. Accessed May 29, 2018.
28. Kaku Y, Yonekawa Y, Tsukahara T, Kazekawa K. Superselective intra-arterial infusion of papaverine for the treatment of cerebral vasospasm after subarachnoid hemorrhage. J Neurosurg. 1992;77(6):842–7.
29. Dabus G, Nogueira RG. Current options for the Management of Aneurysmal Subarachnoid Hemorrhage-Induced Cerebral Vasospasm: a comprehensive review of the literature. Interv Neurol. 2013;2(1):30–51.
30. Roy B, McCullough LD, Dhar R, Grady J, Wang Y-B, Brown RJ. Comparison of initial vasopressors used for delayed cerebral ischemia after aneurysmal subarachnoid hemorrhage. Cerebrovasc Dis. 2017;43(5–6):266–71.
31. Ract C, Vigué B. Comparison of the cerebral effects of dopamine and norepinephrine in severely head-injured patients. Intensive Care Med. 2001;27(1):101–6.
32. Myburgh JA, Upton RN, Grant C, Martinez A. A comparison of the effects of norepinephrine, epinephrine, and dopamine on cerebral blood flow and oxygen utilisation. Acta Neurochir Suppl. 1998;71:19–21.
33. Cherian L, Chacko G, Goodman JC, Robertson CS. Cerebral hemodynamic effects of phenylephrine and L- arginine after cortical impact injury. Crit Care Med. 1999;27:2512–7.
34. Bruins B, Kilbaugh TJ, Margulies SS, Friess SH. The anesthetic effects on vasopressor modulation of cerebral blood flow in an immature swine model. Anesth Analg. 2013;116(4):838–44.
35. [Effect of Disoprivan (propofol) on the circulation and oxygen consumption of the brain and CO2 reactivity of brain vessels in the human]. PubMed – NCBI. Anesthesist. 1987;36(2):60–5.
36. Adembri C, Venturi L, Pellegrini-Giampietro DE. Neuroprotective effects of propofol in acute cerebral injury. CNS Drug Rev. 2007;13(3):333–51.
37. Van Hemelrijck J, Fitch W, Mattheussen M, Van Aken H, Plets C, Lauwers T. Effect of Propofol on cerebral circulation and autoregulation in the baboon. Anesth Analg. 1990;71(1):49–54.
38. Girard F, Moumdjian R, Boudreault D, Chouinard P, Bouthilier A, Ruel M. The effect of sedation on intracranial pressure in patients with an intracranial space-occupying lesion: remifentanil versus Propofol. Anesth Analg. 2009;109(1):194–8.
39. Roberts DJ, Hall RI, Kramer AH, Robertson HL, Gallagher CN, Zygun DA. Sedation for critically ill adults with severe traumatic brain injury: a systematic review of randomized controlled trials*. Crit Care Med. 2011;39(12):2743–51.
40. Bauer TM, Ritz R, Haberthür C, et al. Prolonged sedation due to accumulation of conjugated metabolites of midazolam. Lancet. 1995;346(8968):145–7.
41. Riker RR, Fraser GL. Adverse events associated with sedatives, analgesics, and other drugs that provide patient comfort in the intensive care unit. Pharmacother J Hum Pharmacol Drug Ther. 2005;25(5P2):8S–18S.
42. Pillai U, Hothi JC, Bhat ZY. Severe propylene glycol toxicity secondary to use of antiepileptics. Am J Ther. 2014;21(4):e106–9.

43. Ward JD, Becker DP, Miller JD, et al. Failure of prophylactic barbiturate coma in the treatment of severe head injury. J Neurosurg. 1985;62(3):383–8.
44. Eisenberg HM, Frankowski RF, Contant CF, Marshall LF, Walker MD. High-dose barbiturate control of elevated intracranial pressure in patients with severe head injury. J Neurosurg. 1988;69(1):15–23.
45. Mirski MA, Hemstreet MK. Critical care sedation for neuroscience patients. J Neurol Sci. 2007;261(1–2):16–34.
46. de Nadal M, Munar F, Poca MA, Sahuquillo J, Garnacho A, Rosselló J. Cerebral hemodynamic effects of morphine and fentanyl in patients with severe head injury absence of correlation to cerebral autoregulation. Anesthesiol J Am Soc Anesthesiol. 2000;92(1):11.
47. Sperry RJ, Bailey PL, Reichman MV, Peterson JC, Petersen PB, Pace NL. Fentanyl and sufentanil increase intracranial pressure in head trauma patients. Anesthesiology. 1992;77(3):416–20.
48. Fodale V, Schifilliti D, Praticò C, Santamaria LB. Remifentanil and the brain. Acta Anaesthesiol Scand. 2008;52(3):319–26.
49. Höhne J, Schebesch KM, Ott C, Brawanski A, Lange M. The risk of hypotension and seizures in patients receiving prophylactic anti-epileptic drugs for supratentorial craniotomy. J Neurosurg Sci. 2016;62(4):418–22.
50. Karadas O, Gul HL, Ozturk B, Eroglu E, Demirkaya S. The effects of topiramate therapy on cerebral metabolism in migraine with aura patients. Turk Neurosurg. 2014;24(5):704–9.
51. Mikkelsen MLG, Ambrus R, Rasmussen R, et al. The effect of dexmedetomidine on cerebral perfusion and oxygenation in healthy piglets with normal and lowered blood pressure anaesthetized with propofol-remifentanil total intravenous anaesthesia. Acta Vet Scand. 2017;59:27.
52. White PF, Way WL, Trevor Anthony J. Ketamine—its pharmacology and therapeutic uses. Anesthesiol J Am Soc Anesthesiol. 1982;56(2):119–36.
53. Wang X, Ding X, Tong Y, et al. Ketamine does not increase intracranial pressure compared with opioids: meta-analysis of randomized controlled trials. J Anesth. 2014;28(6):821–7.
54. Von der Brelie C, Seifert M, Rot S, et al. Sedation of patients with acute aneurysmal subarachnoid hemorrhage with ketamine is safe and might influence the occurrence of cerebral infarctions associated with delayed cerebral ischemia. World Neurosurg. 2017;97:374–82.
55. Dagal A, Lam AM. Cerebral autoregulation and anesthesia. Curr Opin Anaesthesiol. 2009;22(5):547–52.
56. Dagal A, Lam AM. Cerebral blood flow and the injured brain: how should we monitor and manipulate it? Curr Opin Anaesthesiol. 2011;24(2):131–7.
57. Butterworth JF, Mackey DC, Wasnick JD. Morgan & Mikhail's clinical anesthesiology. 5th ed. NY, USA: McGraw Hill Books; 2013.
58. Wendon JA, Harrison PM, Keays R, Williams R. Cerebral blood flow and metabolism in fulminant liver failure. Hepatology. 1994;19(6):1407–13.
59. Aggarwal S, Brooks DM, Kang Y, Linden PK, Patzer JF. Noninvasive monitoring of cerebral perfusion pressure in patients with acute liver failure using transcranial Doppler ultrasonography. Liver Transpl. 2008;14(7):1048–57.
60. Larsen FS, Hansen BA, Ejlersen E, et al. Cerebral blood flow, oxygen metabolism and transcranial Doppler sonography during high-volume plasmapheresis in fulminant hepatic failure. J Gastroenterol. 1996;8(3):261–6.
61. Haktanir A, Demir S, Acar M, et al. Doppler sonographic evaluation of cerebral blood flow in Anemia resulting from chronic renal failure. J Ultrasound Med. 2005;24(7):947–52.

Part II
Neurosonology: Basic Principles

Chapter 6
Transcranial Doppler Ultrasound: Physical Principles

David H. Evans

Key Points

1. Ultrasound is a valuable noninvasive technique for studying the brain. It is, however, subject to a number of physical limitations which need to be appreciated in order to ensure the correct interpretation of its results.
2. Because the skull causes rapid attenuation of ultrasound, it is necessary to use relatively low transmitted ultrasound frequencies in transcranial applications which limits spatial resolution in comparison to that achievable in soft tissue imaging. The complex structure of the skull distorts ultrasound beams, further degrading spatial resolution.
3. Doppler ultrasound is a powerful method for measuring blood flow velocities and changes in velocity; however, because the sizes of cerebral vessel cannot be measured accurately, it is not possible to convert velocity into flow. Furthermore, because vessel sizes may change with time, it cannot reliably be assumed that velocity changes are proportional to flow changes.
4. Doppler ultrasound is a powerful technique for detecting cerebral emboli.
5. While ultrasound is usually considered to be completely safe, users need to be aware that it does have a potential to cause tissue damage, and strive to keep exposure as low as compatible with obtaining good clinical results. It should be remembered that transcranial Doppler employs relatively high intensities in order to penetrate the skull bone, and may be used for lengthy periods of time in monitoring applications.

D. H. Evans (✉)
Department of Cardiovascular Sciences, University of Leicester, Leicester, UK
e-mail: dhe@le.ac.uk

C. N. Rodríguez et al. (eds.), *Neurosonology in Critical Care*,
https://doi.org/10.1007/978-3-030-81419-9_6

6.1 Introduction

Ultrasound is an important technique for studying neurovascular physiology and pathology. As with any measurement or imaging technique, it has strengths and weaknesses, and there are a number of potential pitfalls for those interpreting its results. This chapter describes the basic physics and instrumentation behind both imaging and Doppler ultrasound techniques, with a special emphasis on their application to the cerebral circulation.

Medical ultrasound is used to image the body in much the same way as radar is used to detect the range and speed of an aircraft, except that instead of using radio waves, pulses of high-frequency sound are used. A transducer transmits a very short pulse of ultrasound (often lasting much less than one-millionth of a second) into the body, and then receives any reflected ultrasound. Once a sufficient time has elapsed for all the reflections to return from the tissue of interest, another pulse is emitted and the process repeated. The position of any structure producing a reflection can be calculated from the direction in which the pulse has been transmitted and received, and from the delay between the transmission of the pulse and the reception of the reflection. Further information about the characteristics of the structure can be determined from the size of the echo, and information about the movement of the structure (particularly important for echoes from blood) can be extracted from slight changes in the ultrasound phase between successive pulses (the so-called Doppler effect). Ultrasound is an ideal technique for imaging soft tissue but cannot penetrate gas, and is distorted and rapidly attenuated by bone.

6.2 Ultrasound and Its Propagation Through Tissue

Ultrasound is generally taken to mean any sound that has a frequency above the limit of human hearing (about 20 kHz or 20,000 cycles per second). In medical diagnostic applications, however, the frequencies used are approximately 100 to 1000 times greater than this, that is, in the range of 2 MHz to 20 MHz. The reason for this is that spatial resolution is limited by the wavelength, which is inversely related to the frequency. Ultrasonic waves in soft tissue, like audible sound waves, are compressional wave produced by the push-pull action of the sources on the propagating media. These waves are known as ‘longitudinal’ waves, since the oscillatory motion of the particles in the tissue is parallel to the direction of propagation. Other modes of vibration such as ‘shear’ or ‘transverse’ waves can occur in bone, but are not usually of great importance.

6.2.1 Speed of Ultrasound in Tissue

The speed of sound in tissue is important for a number of reasons. It must be known in order to convert the time delay between the transmission of a pulse and the subsequent reception of echoes into physical distances, it determines the maximum rate at which pulses can be transmitted (it is usually necessary to wait until all the relevant echoes from one pulse return to the transducer before another is transmitted), it determines the wavelength of the ultrasound (and hence resolution), it determines the amount of refraction that takes place at tissue interfaces, and it is needed to convert Doppler shift frequencies into tissue velocities. The speed of sound in tissue depends on the elastic properties and density of the tissue, and in general the less compressible the tissue the higher the speed of sound, so that, for example, ultrasound propagates much more rapidly through bone than through soft tissue. Table 6.1 gives approximate values for the speed of sound in some relevant tissues. The important thing to note from this table is that, with the exception of air and bone, all the values are very similar, at around 1540 ms^{-1} (metres per second). The value for air is much lower, but since ultrasound does not propagate through air this is of little significance; the value for bone is much higher, which is of some relevance when performing transcranial examinations. Taking the value of 1540 ms^{-1} as representative, it is easy to calculate that it takes pulses of ultrasound approximately 6.5 μs to travel 1 cm, and therefore, to convert the delay between the transmission of a pulse and the reception of an echo into a depth (remembering that it will take 13 μs for a round trip of 1 cm). Ultrasound scanners do this automatically, but it should be noted that a scanner has no way of telling what tissues the pulse has travelled through, and must use the same conversion factor for all acoustic paths. Because the speed of sound is much higher in bone than soft tissue, the apparent thickness of bone will be less than half its actual thickness. This may not matter

Table 6.1 Speed of sound and acoustic impedance of some common materials

Material	Speed (metres per second)	Acoustic impedance (rayls)
Air	330	0.0004×10^6
Aqueous humour	1500	1.50×10^6
Blood	1570	1.61×10^6
Bone	3500	7.80×10^6
Brain	1540	1.58×10^6
Fat	1450	1.38×10^6
Lens of eye	1620	1.84×10^6
Muscle	1580	1.70×10^6
Soft tissue average	1540	1.63×10^6
Vitreous humour	1520	1.52×10^6

when making transcranial measurements on the brain through a relatively small aperture because it may simply mean the entire image is shifted, but where there are significant variations in the thickness of bone underlying the transducer it can introduce undesirable distortions into the image of the brain. Knowing the speed of ultrasound enables us to calculate the wavelength (given by sound speed divided by frequency) which gives us an idea of the best spatial resolution available from the technique, and which in soft tissue will be approximately 0.77 mm at 2 MHz and 0.1 mm at 15 MHz.

6.2.2 *Attenuation of Ultrasound by Tissue*

As ultrasound propagates through tissue, it is attenuated; that is to say the energy in the beam is reduced. This happens through two main mechanisms: absorption and scattering. Absorption is the conversion of the mechanical energy in the beam into heat (which will cause a temperature rise in the tissue – see section on ultrasound safety), while scattering is the process by which energy is redirected out of the beam. In most soft tissue, the most important mechanism is absorption, but in blood scattering dominates. Attenuation varies from tissue to tissue, and is strongly frequency dependent. It is usually measured in decibels (dB), and may be written as (Eq. 6.1):

$$\text{Attenuation}\left(\text{dB}\right) = -10\log_{10}\left(I_x / I_0\right) \tag{6.1}$$

where I_0 is the initial intensity and I_x is the final intensity. Thus, if the final intensity is one-tenth of the initial intensity, the attenuation is said to be −10 dB; likewise reductions in intensity to be one-hundredth and one-thousandth of the initial intensity would be written as −20 dB and -30 dB respectively. Typical values of the attenuation of 1 MHz ultrasound in some biological materials are given in Table 6.2. With the exception of water, the attenuation coefficients for higher frequencies may be obtained approximately by multiplying the attenuation at 1 MHz by the frequency in MHz. For example, the attenuation in soft tissue at 2 MHz would be

Table 6.2 Attenuation coefficients for some biological materials at 1 MHz. The values at a higher frequency may be obtained approximately by multiplying by the frequency in MHz (note however that for water the value should be multiplied by the square of frequency)

Material	Attenuation coefficient at 1 MHz (dB cm^{-1})
Blood	0.2
Bone	10
Brain (adult)	0.8
Brain (infant)	0.3
Fat	0.6
Muscle	1.5
Water	0.002
Soft tissue average	0.7

1.4 dB cm^{-1}, and at 10 MHz would be 7 dB cm^{-1}. The strong frequency dependency of attenuation is the factor that limits the highest frequency that can be used in any particular situation (ideally we would always use the highest frequency possible because the shorter the wavelength, the better the spatial resolution). The higher the attenuation coefficient, the higher the frequency, and the deeper the target, the smaller will be the returning echoes. We are able to obtain very high-resolution images of arteries like the extra-cranial carotid arteries because they are relatively superficial and the overlying tissue has a relatively low attenuation coefficient; the same is not true for deep vessels. The rapid attenuation of ultrasound by bone means that if we wish to insonate through the skull, we have to use relatively low ultrasound frequencies (note, however, that the poor resolution we obtain when imaging the brain is a result of both using a low frequency and the distortion of the ultrasound beam by the skull bone).

6.2.3 Ultrasound Behaviour at Acoustic Boundaries

Ultrasonic imaging is reliant on variations in the acoustic properties of tissues to generate the echoes that reveal the range and direction of target structures. The behaviour of sound when it encounters a change in acoustic properties depends on the relative dimensions of the ultrasound wavelength and the target in its path. If the target is small compared with the wavelength (such as the case with a red blood cell or the inhomogeneities in the parenchyma of an organ), then the wave is said to be scattered. If the target is large (such as the case at the interface between two organs), then the wave is said to be reflected or refracted. Both types of behaviour are important in ultrasonic scanning. In the case of scattering, the incident energy is retransmitted in all directions (though not necessarily equally), while in the case of reflection and refraction, the energy remains confined to a well-defined, reflected and transmitted beam.

Figure 6.1a, b illustrate the behaviour of ultrasound at a plain boundary for perpendicular and non-perpendicular incidence respectively. In the first case, a proportion of the ultrasound is reflected directly back to the source (the angle of incidence and reflection are both equal to zero), and a proportion continues along the original path. In the second case, the angle of incidence and reflection are also equal, but not to zero, and therefore, the reflected wave does not return to the transducer (this is why it is much easier to image large surfaces that are perpendicular to the ultrasound beam). In the second case, there is also a transmitted wave, but its direction depends both on the angle of incidence and the relative speeds of ultrasound on either side of the boundary. The relationship between the angle of the incident wave θ_i and the transmitted wave θ_t is given by Eq. 6.2:

$$\frac{\sin\theta_i}{\sin\theta_t} = \frac{c_1}{c_2} \tag{6.2}$$

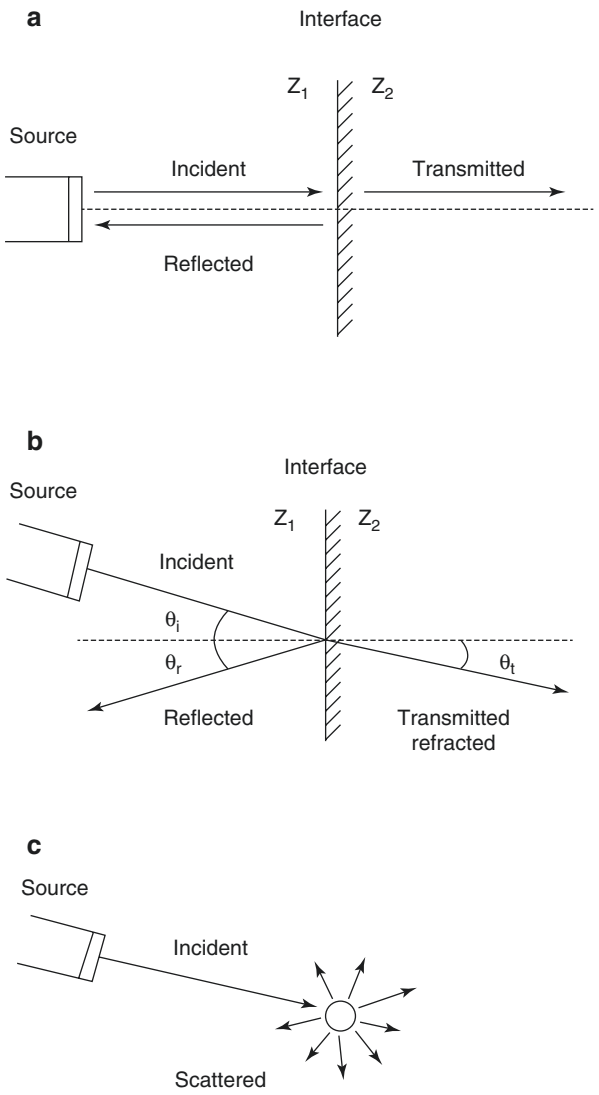

Fig. 6.1 (**a**) Reflection of ultrasound at a plane boundary (perpendicular incidence). (**b**) Reflection and refraction of ultrasound at a plane boundary (non-perpendicular incidence). (**c**) Scattering of ultrasound by a target with dimensions smaller or comparable to the ultrasound wavelength

where c_1 is the sound speed before the boundary and c_2 the speed after the boundary. If the speeds of sound on either side of the boundary are similar, the direction of propagation changes very little, but if they are dissimilar then the direction may change significantly (i.e. it is said to be refracted). Refraction effects are particularly important at interfaces between soft tissue and bone (recall the speed of sound in bone is 2 to 3 times higher than in soft tissue), and can lead to considerable distortion as an ultrasound beam propagates through the skull. The proportion of energy reflected at a boundary depends on the difference in the acoustic impedance on the two sides of the boundary and for normal incidence may be written (Eq. 6.3):

$$\alpha_r = \frac{I_r}{I_i} = \left(\frac{Z_2 - Z_1}{Z_2 + Z_1} \right) \tag{6.3}$$

where I_i and I_r are the incident and reflected intensities, and Z_1 and Z_2 are the acoustic impedance of the tissue before the boundary and after the boundary, respectively. If Z_1 and Z_2 are similar, then most of the energy is transmitted and little reflected; if Z_1 and Z_2 are very dissimilar, then the converse is true. Values of acoustic impedance for some relevant tissues are given in Table 6.1. It can be seen that the values for most soft tissues are very similar, but that air has a very low value and bone has a relatively high value. The result of this is that the percentage of energy reflected at soft tissue interfaces is of the order of 1%, but that, at soft tissue/bone interfaces, approximately 50% of the energy is reflected. The impedance of air is so low that effectively no transmission at all takes place at a soft tissue/air interface. The low acoustic impedance of air is the main reason why it is impossible to image through air and why it is essential to exclude air from the interface between the transducer and the skin.

Figure 6.1c illustrates the phenomenon of scattering. Scattering is important because it is the process that allows us to image the parenchyma of organs and to image blood flow. The scattering pattern and the amount of scattering that occur at a target depend on the size of the target, and the distribution of compressibility and density in the target volume. For targets that are very much smaller than the ultrasound wavelength, the wave is scattered more or less uniformly in all directions, while for larger targets, the scattering pattern is more complex but still takes place over a wide range of angles. For very small targets, such as red blood cells, the scattering is called Rayleigh scattering and is proportional to the fourth power of frequency; for larger targets, the scattered power still increases with frequency but less rapidly so. The power returned to the ultrasound transducer by scattering is much less than that returned by specular reflectors, but is also much less angle dependent. Therefore, echoes from the internal structure of organs and from blood are much weaker than those from distinct boundaries, but do not change significantly as the angle of insonation changes.

6.3 Pulse-Echo Principles (B-Mode Techniques)

The basic principle behind B-scanning has been described in the introduction. A B-mode display is essentially a cross-sectional image of the tissue in the scan plane, built up using an echo ranging technique. A transducer transmits a short ultrasound pulse into the tissue in a predetermined direction, then switches to receive mode and gathers echoes due to reflection or scattering in the tissue from that same direction. Since the direction of transmission and reception and the time delay between pulse transmission and echo reception are known, the position of any structure producing an echo can be determined. The size of each of the echoes provides information

about the amount of ultrasound reflected or scattered by the structure (although it is necessary to compensate for the attenuation of the pulse by intervening tissue). Once all the echoes have been received from depths of interest, then another pulse is transmitted along a slightly different path, and the whole process repeated until the required plane, perpendicular to the transducer face, has been interrogated. The rate at which pulses can be transmitted (the pulse repetition frequency or PRF) is limited by the speed of ultrasound in the tissue and the maximum depth of interest; so, for example, if it is required to image to a depth of 10 cm, it will be necessary to wait 13 μs × 10, that is, 130 μs, before another pulse is transmitted. Clearly considerable processing by the ultrasound scanner is necessary to produce acceptable images from the simple echo information described above, and the interested reader is referred to Hoskins et al. [1] for further information.

6.4 Transducers

At one time the method used for scanning the ultrasound beam through tissue involved physical movements within the transducer. All transducers for B-scan imaging are now array transducers where the beam is steered electronically. There are two basic types of arrays: linear arrays and phased arrays, both of which contain a large number of very small piezoelectric elements capable of transmitting and receiving ultrasound.

In linear arrays, each beam is generated using only a limited number of adjacent array elements at any one time. Each successive beam is generated by selecting another group of elements, so if the first beam is generated using elements 1–8, for example, then the second beam might be generated using elements 2–9 and so on. Thus, the beam steps along the array. Linear array transducers produce rectangular- or parallelogram-shaped fields where all the scan lines are parallel to each other, and are the transducers of choice for imaging the extra-cranial carotid arteries.

In phased arrays, each beam is generated using most or even all of the elements at the same time. Each successive beam is generated by steering the direction of transmission and reception by appropriate phasing of the signals applied to the transducer elements. Phased arrays produce sector-shaped fields where the scan lines are not parallel to each other and are the transducers of choice for intracranial imaging because their small footprint, which allows them to be used with the limited acoustic windows available in the skull.

Modern ultrasound systems not only move the beam electronically, but dynamically vary their aperture (the number of elements used) and apodisation (relative weighting of the contribution of different elements), and also use electronic focussing on both transmit (multiple-zone focussing) and receive (dynamic focussing) to achieve excellent lateral resolution in the scan plane. Some modern transducers also use more than one row of elements to improve the focussing in the elevation plane (i.e. the out of plain dimension or the slice thickness).

6.5 Artefacts

It is important that users of ultrasound instruments are aware of the many image artefacts that can arise. Two of the most important types are described briefly below.

6.5.1 Speed of Sound and Beam Deviation Artefacts

To generate ultrasound images, it is necessary to assume that the beam has followed a straight path through the tissue, and that the speed of sound in the tissue is constant and known. Anything that invalidates these assumptions will lead to misregistration of targets. Beam direction may be changed either by refraction effects (i.e. where the beam meets a boundary between two tissues with different ultrasound velocities, at nonnormal incidence), or by very strong specular reflectors that are not at right angles to the beam. Deviations from the assumed velocity of sound will make targets appear closer or farther away than they should. If the tissue with the higher or lower velocity is a parallel-sided layer, then all the structures behind the layer will be moved so as to appear closer or further from the transducer, which may not matter. On the other hand, if the layer is not parallel sided or is incomplete, then some parts of the structure behind the layer will be moved more than others, so that a straight boundary might appear ragged. Strong specular reflectors, not at right angles to the beam, may act as acoustic mirrors completely redirecting the beam direction away from that assumed by the machine.

6.5.2 Shadowing and Flaring Artefacts

Attenuation of ultrasound in bodily tissues is very significant so that echoes returning from deep structures are always very much smaller than those returning from similar superficial structures. In order to overcome this, ultrasound instruments employ what is known as time gain compensation (TGC) to the returning echoes, so that echoes from deeper structures are amplified more than those from superficial structures. In order to do this, the instrument needs to assume an average rate of attenuation in the tissue so it can calculate the appropriate gain to apply to echoes from each depth. Shadowing and flaring artefacts occur when the attenuation is either underestimated or overestimated respectively. One common example of shadowing occurs behind an atheromatous plaque in the carotid artery, where the plaque attenuates the ultrasound much more rapidly than soft tissue, and so the TGC does not adequately compensate for the reduction in the size of the echoes returning from behind the plaque. The converse effect can be seen when there is a cyst in the tissue. The fluid in a cyst does not attenuate ultrasound as rapidly as soft tissue, but the TGC continues to increase gain with depth as though there is soft tissue present. The

result of this is that the echoes from behind the cyst are amplified more than is appropriate, and the region behind the cyst appears to be very highly reflecting. Although these are artefacts, they do in fact convey diagnostic information, in that they reveal the presence of tissue with an unexpectedly high or low attenuation values.

6.6 Doppler Principles

If an observer is stationary relative to a source of waves, then the frequency the observer measures is the same as the frequency transmitted. If, however, the observer is moving towards or away from the source of waves, then a greater or lesser number of wave fronts will pass the observer in a given time interval, and so the observer will measure a higher or lower frequency than that which was transmitted. This effect is known as the Doppler effect after the Austrian physicist, Christian Doppler, who first described the phenomenon in 1842. In medical ultrasound, the targets do not emit spontaneously, and therefore, to make use of this effect, it is necessary to transmit ultrasound into the body, and to observe the change of frequency as the wave is reflected or scattered from the target. Under these conditions, it can be shown [2] that the 'Doppler frequency', f_d, i.e. the difference between the transmitted frequency f_t and the received frequency f_r, is given by Eq. 6.4:

$$f_d = f_t - f_r = 2 f_t v \cos\theta / c \tag{6.4}$$

where v is the velocity of the target, c the velocity of sound in tissue and θ the angle between the ultrasound beam and the direction of motion of the target. The velocity of sound and the transmitted frequency are known in any situation, and therefore, the velocity of a target can be found from Eq. 6.5:

$$v = \mathrm{K} f_d \cos\theta \tag{6.5}$$

where K is a known constant ($c/2f_t$). This equation may be used to monitor changes in velocity, and if the angle θ can be determined, then absolute velocity may be calculated. In practice, where blood flow is concerned, there will be many targets in the Doppler sample volume with a range of velocities, and so the Doppler shift signal will contain a spectrum of frequencies. Figure 6.2 shows the spectral display (usually called a sonogram) of the Doppler signal recorded from an internal carotid artery. The horizontal axis represents time, the vertical axis the Doppler shift frequency and the grey level of each pixel the power of the Doppler signal at the corresponding frequency and time.

Under 'ideal' conditions, the spectrum of Doppler frequencies at any moment in time would correspond to the distribution of velocities in the sample volume, but there are a number of factors which distort the spectrum and limit the accuracy with which the velocity distribution can be determined (note also that the shape of the sample volume itself will mean that the flow within a vessel is unlikely to be

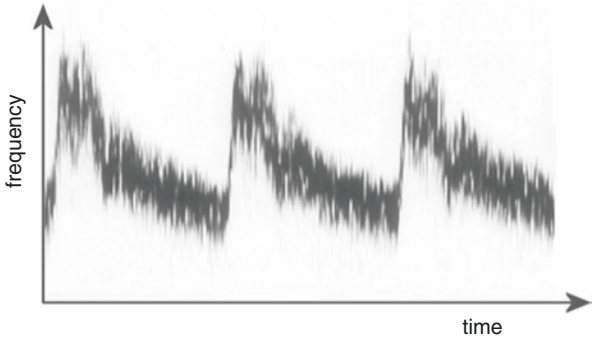

Fig. 6.2 Sonogram of the Doppler signal from a normal internal carotid artery. The horizontal axis represents time, the vertical axis Doppler shift frequency (or velocity), and the grey scale the power of the Doppler shift frequency at the corresponding time and frequency. Three complete cardiac cycles are shown

sampled uniformly, and therefore, the distribution of velocities in the sample volume may not exactly correspond to the distribution of velocities in the vessel). The reader is referred to Evans and McDicken [2] for an in-depth discussion of these effects, but the effect of 'wall-thump' filters is briefly described here because of its importance. As already mentioned, the signals reflected by structures such as blood vessel walls are orders of magnitude greater than those scattered by blood, and therefore, it is necessary to reject such signals if we wish to study the motion of the blood. This is possible because in general such solid structures move with much lower velocities than those of blood flow, and therefore, these signals can be rejected using a high-pass (wall-thump) filter. While this can be quite effective, the filter will also reject the signals from slowly moving blood. This means that blood flow close to a vessel wall cannot be studied, and that the mean blood flow velocity in a vessel tends to be slightly overestimated, although is not usually a major problem as long as the operator is aware of the effect.

6.6.1 Pulsed Wave Doppler

Early Doppler ultrasound devices were continuous-wave devices (that is to say they both transmitted and received ultrasound continuously), but such devices had little or no range resolution. Because in general it is important to be able to select signals from a particular depth, nearly all ultrasound Doppler instruments now use pulsed transmission. Pulses of ultrasound are transmitted at regular intervals, and after a fixed (but controllable) delay, a receive gate attached to the transducer opens for a brief period of time and allows signals from a pre-determined range of depths to be collected for Doppler processing. The delay between pulse transmission and the opening of the receive gate determines the depth from which signal samples are collected, and the time for which the receive gate is open in combination with the transmitted pulse length determines the sample volume length.

Pulsed wave (PW) ultrasound systems actually operate by measuring the rate of change of phase of the returning ultrasound pulses rather than the Doppler shift frequency per se and because of this are subject to the effects of aliasing. Aliasing is the phenomenon that occurs when a moving object is not sampled sufficiently rapidly to be able to reconstruct its true movement. If a Doppler signal is to be correctly interpreted, then the rate at which it is sampled (i.e. the pulse repetition frequency) must be at least twice the maximum frequency component of the Doppler signal (with certain caveats). Failure to respect this limit can lead to artefacts such as rapid forward flow being interpreted as reverse flow. The obvious way to avoid this problem is to increase the PRF, but as we have already seen this is limited by the fact that if we wish to avoid range ambiguity we must collect all the returning echoes of interest before transmitting a subsequent pulse. It can be shown [2] that there is a maximum range-velocity product limit given by Eq. 6.6:

$$z_{\max} v_{\max} = c^2 / 8 f_t \cos\theta \tag{6.6}$$

where $z_{\max}$ is the maximum range a PW system can gather echoes from unambiguously and $v_{\max}$ is the maximum velocity that can be unambiguously measured. Therefore, it is possible to measure high velocities in superficial structures correctly and low velocities in deep structures correctly, but not high velocities in deep structures. This limit is particularly troublesome in cardiac work where there may be very high velocities through stenosed heart valves, but it is possible to encounter aliasing in more superficial structures such as stenosed carotid arteries. Equation 6.6 reveals that one of the ways to avoid aliasing is to use a lower transmitted ultrasound frequency, and this is one of the reasons why Doppler studies are often performed at slightly lower frequencies than imaging studies.

6.6.2 Duplex Scanning

Duplex scanners are scanners that combine B-mode imaging with PW Doppler measurements. The B-scan image is used to guide the Doppler beam and to place a Doppler sample volume in a region of interest. Since blood vessels may be imaged, the Doppler angle, θ, can also be measured (by assuming that the blood flow is parallel to the vessel wall) and, therefore, the Doppler shift frequency can be calibrated in terms of blood flow velocity.

6.6.3 Colour Flow Imaging (CFI)

Colour flow imaging systems are similar to pulse-echo B-mode systems, except that both the amplitude and the 'Doppler shift' on the returning echoes are measured. Where no Doppler shift is detected, the usual grey-scale information is written to

the display device, but where a Doppler shift is detected, it is colour coded to show the measured relative velocity between the transducer and the detected target. Usually flow towards the transducer will be coded in one colour (often red), and flow away from the transducer in another (often blue).

CFI is an extremely good technique for imaging anatomy and related blood flow, but it has a number of limitations that the operator must bear in mind. First and foremost, it must be remembered that the Doppler angle, θ, will affect the measured Doppler shift, and therefore, flow with the same speed in different parts of the image may be represented by different shades of colour, or even completely different colours, depending on the component of their velocity relative to the transducer. Also CFI, just as ordinary PW Doppler, is susceptible to aliasing, and it is important to differentiate between regions of reverse flow in a vessel and regions of aliasing, both of which lead to a change in the displayed flow direction. Frame rates in CFI are significantly lower than in standard B-mode imaging because in order to detect and quantify a Doppler shift, it is necessary to interrogate a sample volume several times (typically between 8 and 16), and this is the reason why the so-called 'colour box' where colour flow information is displayed is often significantly smaller than the total area of the scan. Finally, colour flow estimates of velocity are based on a relatively small number of samples when compared with PW Doppler, and so their velocity resolution is much lower. Colour flow imaging is an excellent way to gain an impression of the overall haemodynamics in a region of the body, but if quantitative measurements are to be made, CFI should be used to identify a region of interest and PW Doppler used to make the measurements.

6.6.4 Power Doppler Imaging (PDI)

An alternative to coding and displaying the Doppler shift frequency measured from each sample volume is to measure and display the total Doppler power, which is determined mainly by the volume of moving blood rather than its velocity. Thus, changes in angle, and even aliasing, do not alter the colour coding – indeed because of a mechanism known as intrinsic spectral broadening, it is even possible to image flow perpendicular to the transducer face, which is not possible with ordinary CFI. The result of this is that images of tortuous vessel can often be more complete and easier to understand. Power Doppler is more sensitive than colour Doppler for imaging of flow but provides no information about the direction of flow.

6.7 Transcranial Doppler Ultrasound (TCD)

Transcranial Doppler ultrasound is the application of Doppler ultrasound techniques through the intact skull. Where imaging techniques are involved, such techniques are usually called transcranial coded sonography (TCCS). In general, the skull bone

is too thick to penetrate adequately with ultrasound, but there are a number of 'acoustic windows' where there is a natural foramina, or the bone is sufficiently thin for a significant percentage of ultrasound energy to penetrate. The most commonly used window is the temporal bone window, which allows insonation of the middle, anterior and posterior cerebral arteries. The foramen magnum window (or suboccipital approach) allows insonation of the basilar and vertebral arteries, and the orbital approach allows insonation of the ophthalmic arteries and the internal carotid siphon. TCD techniques have many similarities to ordinary pulsed Doppler techniques but also differ in a number of ways. In order to penetrate the skull, it is necessary to use very low transmitted frequencies (recall that attenuation increases with frequency), and most simple TCD examinations are performed with 2 MHz ultrasound or thereabouts. Low frequencies generate much lower levels of scattering from blood, (an advantage when monitoring for emboli since small signals from small emboli are less likely to be masked by the blood flow signal, but a disadvantage if it is the blood flow itself that is to be studied). Low frequencies also give poor spatial resolution, but the major contribution to poor spatial resolution in transcranial studies is the distortion of the ultrasound beam by the skull.

6.7.1 Velocity Measurement

The method used to estimate blood flow velocity in TCD applications is different from that used elsewhere in the body. The standard method is to average the instantaneous intensity weighted mean velocity over the cardiac cycle, but in TCD it is the instantaneous maximum velocity that is usually averaged. The reason for this is that it is easier to extract a good maximum frequency envelope than a good mean envelope when the signal-to-noise ratio is poor. Fortunately, because of the type of flow found in cerebral vessels, the mean of the maximum over the cardiac cycle is more or less proportional to the true mean, and the constant of proportionality is approximately 2 [3]. In other words, the true mean velocity is half the figure usually quoted as 'mean velocity'. It is vital when reporting TCD velocity measurements that investigators explain exactly which velocity they have calculated. Another particular issue with TCD velocity measurements is that they are usually made blind, and the Doppler angle, θ, assumed. Although this may be valid for some patients, in others it can introduce significant errors which must be recognised if absolute velocity values are of interest.

6.7.2 Flow Changes

In most arteries in the body, it is reasonable to assume that, in the short term at least, changes in blood flow velocity are proportional to changes in flow. This is not necessarily a valid assumption in TCD as there is evidence that even the major arteries

exhibit considerable vasoactivity. Certainly arterial spasm leads to dramatic increases in blood flow velocity that are not representative of changes in flow, and other stimuli are thought to affect cerebral arterial diameter. It is vital that this fact is borne in mind when interpreting velocity changes in TCD. Unfortunately, cerebral vessels are too small to have their diameters accurately measured by ultrasound, but attempts have been made to monitor changes in diameter by measuring changes in the total amount of power backscattered by the moving blood within the sample volume. This technique can only be partially successful because it relies on uniform insonation of the blood vessel, which cannot be achieved due to the distortion of the ultrasound beam by the skull bone.

6.7.3 Cerebrovascular Resistance

Cerebrovascular resistance (CVR) can be calculated by dividing mean blood pressure by mean blood flow. TCD, however, measures velocity (i.e. flow divided by vessel cross section). Therefore, dividing mean blood pressure by mean blood flow velocity leads to a value of CVR multiplied by vessel cross section (at the point of ultrasound insonation). This quantity has been called ‘resistance-area product’ or RAP [4], both to distinguish it from true CVR, and to emphasise that it is also dependent on any changes in the cross section of the vessel where the measurement is being made.

6.7.4 TCD – Embolus Detection

Embolus detection has become a major application of TCD. The basis of embolus detection is very simple. As an embolus passes through the Doppler sample volume, if its scattering cross section is sufficiently large, it will give rise to an additional Doppler component that can be heard or seen on the Doppler display. Whether or not an embolus can be detected depends on its size and composition, the ultrasound frequency, the size of the sample volume, the embolus trajectory and its interaction with the ultrasound beam. In general, even relatively small gas bubbles will be detected, but some larger solid emboli may not. Several techniques have been proposed for distinguishing between different types of emboli, and while some progress has been made towards this goal, there are still significant challenges. Microembolic signals are discussed in a later chapter in this book, and for an in-depth discussion of the physics of embolus detection, the reader is referred to [5].

6.8 Transcranial Colour-Coded Duplex Sonography (TCCS)

Transcranial colour-coded sonography is simply CFI or PDI performed through the cranial bones. As for simple TCD, it can only be done through the 'bone windows', must be done at relatively low frequencies to achieve adequate penetration and is subject to the effects of beam distortion (and, therefore, image distortion) by the skull.

Transcranial color-coded duplex ultrasonography (TCCS) provides the imaging of large intracranial arteries through the intact skull by colour coding of blood flow velocity. The circle of Willis can be identified by their anatomic location with respect to the brain stem structures and by the flow direction. TCCS is an important imaging method due to its excellent time resolution. This technique is useful for detecting vasospasm. Application of echo-contrast agent can increase the accuracy of investigation [6].

6.9 Ultrasound Safety

No chapter on the physical and technical principles of neurovascular ultrasound would be complete without the mention of ultrasound safety. Diagnostic ultrasound is generally assumed to be perfectly safe, and even if there are potential hazards, these are greatly outweighed by the benefits to the patient. It is, however, important to remember that this may not always necessarily be the case. There are two broad classes of mechanism by which ultrasound is capable of damaging tissue, the 'thermal effects' and the 'non-thermal effects', which may be further broken down into cavitation, streaming and other direct effects.

Thermal effects, that is, heating of the tissue, are related to the conversion of ultrasound energy into heat energy, and hence to the temporal average intensity of the ultrasound beam and the rate at which it is absorbed by the tissue. Non-thermal effects are related to the peak negative pressure of the ultrasound wave as it propagates through the tissue. It should be noted that these two mechanisms are virtually independent of each other, as the relationship between average intensity and peak negative pressure depends on the pulsing regime selected. One potential area for caution in neurovascular ultrasound is TCD. There are three reasons for this. Firstly, in order to overcome the rapid attenuation of ultrasound by the skull, it is necessary to use relatively high ultrasound intensities; secondly, bone is a rapid absorber of ultrasound and thirdly, TCD monitoring may last for considerable periods of time where the same region of tissue is being insonated continuously. All these effects can lead to significant heating of the skull bone, and potentially to secondary heating of brain tissue by conduction from the bone.

There are two indices that are of value in evaluating the potential hazard of ultrasonic examinations, the thermal index (TI) and the mechanical index (MI). The TI

is an estimate of the rise in tissue temperature in °C under worse case conditions. The MI is an attempt to indicate the probability of mechanical damage by non-thermal processes. When these indices have a value of 1 or more, the possibility of hazard should be considered. There are in fact three different thermal indices, the soft tissue index (TIS) and bone index (TIB), and most relevant to TCD, the cranial index (TIC), which is the *TI* that should be used when there is bone at the surface (this is because, in this situation, the greatest temperature rise occurs in the bone and adjacent tissue). Operators of TCD instruments should strive to maintain as low a value of TIC as is compatible with obtaining a good signal, and have clear justification for using unusually high values.

One final area of caution with TCD is in relation to the use of contrast agents, as they may potentially lower the threshold for cavitational activity. Clearly, it is important with respect to any potential for hazard related to the ultrasound that the operator must do all they can to reduce unnecessary exposure, and to ensure that the benefits to the patient outweigh potential hazards. It is also important that ultrasound practitioners keep up to date with the current literature on safety. The European Federation of Societies for Ultrasound in Medicine and Biology (EFSUMB) issue safety statements regularly and can be found on their website at www.efsumb.org. Much more in-depth discussions of ultrasound safety can be found in [7, 8].

6.10 Conclusion

Ultrasound is a powerful diagnostic technique. It is important that any user of the technique is familiar with the physical and technical principles behind the method, as these provide an insight into its strengths and weaknesses, and sources of possible artefacts.

References

1. Hoskins PR, Martin K, Thrush A, editors. Diagnostic ultrasound: physics and equipment. 3rd ed. FL, USA: CRC Press; 2019.
2. Evans DH, McDicken WN. Doppler ultrasound: physics, instrumentation and signal processing. 2nd ed. Chichester: Wiley; 2000.
3. Evans DH. On the measurement of the mean velocity of blood flow over the cardiac cycle using Doppler ultrasound. Ultrasound Med Biol. 1985;11(5):735–41.
4. Evans DH, Levene MI, Shortland DB, Archer LNJ. Resistance index, blood flow velocity, and resistance-area product in the cerebral arteries of very low birthweight infants during the first week of life. Ultrasound Med Biol. 1988;14(2):103–10.
5. Evans DH. Ultrasonic detection of cerebral emboli. In Yuhas DE and Schneider SC, editors. Proc. 2003 IEEE ultrasonics symposium, IEEE, Piscataway, 2003. p. 316–26.

6. Bartels E. Transcranial color-coded duplex ultrasonography in routine cerebrovascular diagnostics. Pers Med. 2012;1(1–12):325–30.
7. Ter Haar G, editor. The safe use of ultrasound in medical diagnosis. 3rd ed. London: British Institute of Radiology; 2012.
8. Csiba L, Baracchini C, editors. Manual of neurosonology. Cambridge, Uk: Cambridge University Press; 2016. p. 1–322.

Chapter 7
Transcranial Doppler (TCD) and Trancranial Color-Coded Duplex Sonography (TCCS): Applied Neuroanatomy

Camilo N. Rodríguez and Ryan Splittgerber

Key Points

1. It is important to know the anatomy of the parenchymal brain and cerebral vascular landmarks (circle of Willis) for an adequate US approach and interpretation of the findings in the critical patient bedside.
2. Within the circle of Willis the most frequent anatomical variation is hypoplasia or absence of the posterior communicating artery (PComA).
3. It is paramount to choose the most appropriate bone window according to the clinical condition of the patient, his decubitus, and the specific objective to be studied.
4. The transtemporal acoustic window is the most used because it allows access to the most important axial exploration planes: mesencephalic, diencephalic, and ventricular.
5. The submandibular acoustic window is an alternative and very useful access, especially in the critically ill patient and his frequent supine decubitus, when studying the vertebrobasilar system.
6. The anatomical identification of the deep venous cerebral system and the dural venous sinuses is not easy. It requires training and dedication to the bedside of the patient.

C. N. Rodríguez (✉)
Intensive Care Medicine, Hospital Nacional Prof. Dr. A. Posadas, University of Buenos Aires (UBA), Neurointensive Care Section - ESICM, Neurointensive Care Section - AMCI, Neurointensive Care Committee - FEPIMCTI, Member of ESNCH, Buenos Aires, Argentina
e-mail: camilo.rodriguez@nesccco.com

R. Splittgerber
Department of Surgery, Vanderbilt University Medical Center, Office of Health Sciences Education, Vanderbilt University School of Medicine, Nashville, TN, USA
e-mail: ryan.splittgerber@vanderbilt.edu

C. N. Rodríguez et al. (eds.), *Neurosonology in Critical Care*,
https://doi.org/10.1007/978-3-030-81419-9_7

7.1 Introduction

Transcranial Doppler (TCD) and/or transcranial color-coded duplex sonography (TCCS) are frequently used as noninvasive and rapid access neurological monitoring tools in the intensive care unit [1, 2].

The anatomical correlation of the brain parenchyma and its vascular components will be better scanned when approaching the patient with the TCCS technique where the 2D image (parenchyma and brain structures) is combined with the color-coded Doppler of the patients' vessels corresponding to the circle of Willis.

7.2 Brain Parenchyma: Anatomy and Ultrasound

There are two main techniques for transcranial Doppler: the conventional TCD ("blind") and the transcranial color-coded duplex sonography (TCCS). The main advantage of TCCS versus TCD (¨blind technique¨) is that the intracranial vessels can be identified in relation to some anatomical landmarks. Within this fact lies the importance of recognizing the anatomical structures and their access windows [3].

We will approach the intracerebral anatomy from the insonation windows, which are most commonly used in clinical practice.

7.2.1 Anatomy of Acoustic Windows

7.2.1.1 Transtemporal Acoustic Window (Fig. 7.1)

The transtemporal window is the most frequently used as it allows access to the most important axial exploration planes: mesencephalic, diencephalic, and ventricular [3, 4].

Mesencephalic Plane

This plane is obtained by projection of the transducer at a 90° angle to the temporal bone via the transtemporal bone window.

A. *Brain parenchyma structures identified by TCCS* (Fig. 7.2).

- *TCCS*: B-mode.
- *Depth*: 14–16 cm.

  a. *Cerebral peduncles* [Mesencephalon] (hypoechoic >> "Butterfly") [5, 13]
  b. *Basal cisterns* (space around the mesencephalon).
  c. *Contralateral skull bone* (hyperechoic).

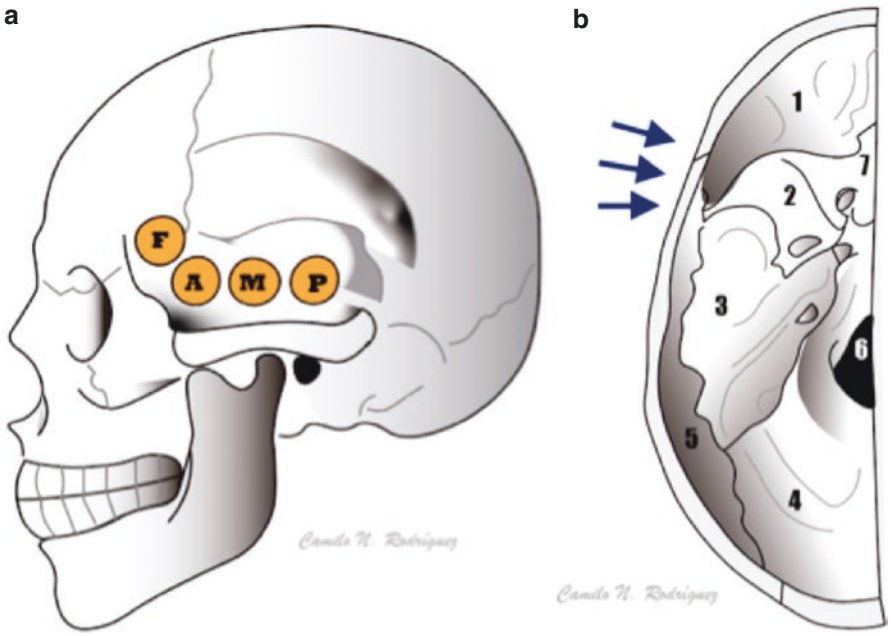

Fig. 7.1 (**a**) Scheme: anatomy of transtemporal acoustic window and different approaches; (F) frontal, (A) anterior, (M) medial, and (P) posterior above zygomatic process of temporal bone. (**b**) Scheme: anatomy of the floor of the cranial cavity: (1) anterior fossa, (2) sphenoid bone, (3) middle fossa, (4) posterior fossa, (5) parietal bone, (6) foramen magnum, and (7) sphenoid bone. (blue arrows): direction of insonation beam from transducer through temporal bone. (Author: Camilo N. Rodríguez)

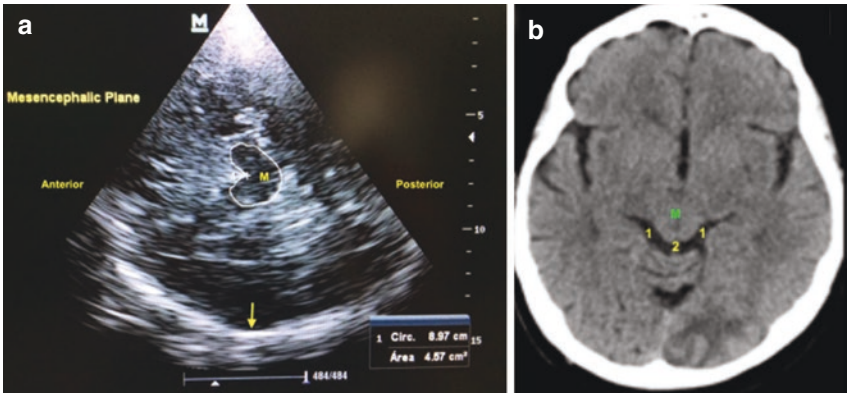

Fig. 7.2 (**a**) Mesencephalic plane by TCCS: (M) mesencephalon; (arrow) contralateral skull. (**b**) Brain anatomy by CT scan: (M): mesencephalon; (1) ambient cistern and (2) quadrigeminal cistern. (Author: Camilo N. Rodríguez)

These are (Fig. 7.2a) the neuroanatomical landmarks used to localize the circle of Willis with Doppler technique [3, 4, 6].

B. Vascular structures identified by TCCS.

- TCCS: Doppler mode.

1. *Circle of Willis* [7–9] (Fig. 7.3).

1.1 Internal carotid artery (ICA).
1.2 Middle cerebral artery (MCA).
1.3 Anterior cerebral artery (ACA).
1.4 Posterior cerebral artery (PCA).

7.2.1.2 Diencephalic Plane (Thalamic Plane)

This plane is obtained by a slight displacement of the transducer toward the cephalic 10° from the mesencephalic plane through the transtemporal window.

A. Brain parenchyma structures identified by TCCS (Fig. 7.4).

- TCCS: B-mode.
- Depth: 14–16 cm.

1. *Third Ventricle*.
[Two hyperechoic horizontal parallel lines]

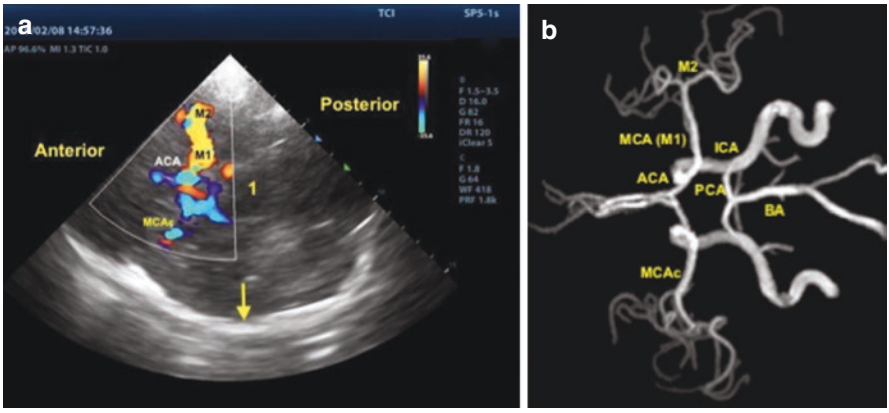

Fig. 7.3 (**a**) Circle of Willis by TCCS through transtemporal acoustic window: (1) mesencephalon, (M1) ipsilateral M1 segment of middle cerebral artery (red), (M2) M2 segment of middle cerebral artery, (ACA) anterior cerebral artery, (MCAc) contralateral middle cerebral artery (blue), (arrow) contralateral skull. (**b**) Angio-MRI of circle of Willis: MCA (M1): M1 segment of middle cerebral artery, (M2) M2 segment of MCA, (ICA) internal carotid artery, (PCA) posterior cerebral artery, (BA) Basilar artery, (ACA) anterior cerebral artery, and (MCAc) contralateral middle cerebral artery. (Author: Camilo N Rodríguez)

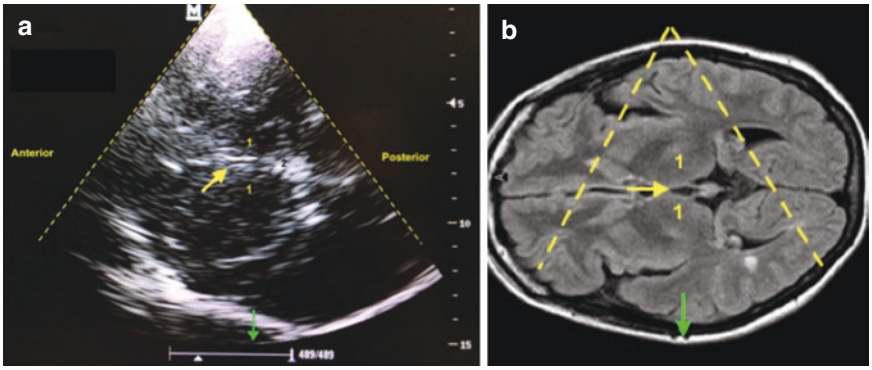

Fig. 7.4 (**a**) Diencephalic plane by TCCS through of transtemporal acoustic window: (1) thalamus, (2) pineal gland, (yellow arrow) third ventricle and (green arrow) contralateral skull; (**b**) brain MRI: (1) thalamus, (yellow arrow) third ventricle, (dotted line) ultrasound beam through transtemporal window and (green arrow) contralateral skull. (Author: Camilo N. Rodríguez)

2. *Thalamus*.
   [Two hypoechoic structures next to third ventricle]
3. *Pineal Gland*.
   [Posterior hyperechoic structure] [3, 4]
4. *Contralateral Skull Bone*.
   [Posterior hyperechoic structure]

B. Vascular structures identified by TCCS.

- TCCS: Doppler mode.

1. *Middle cerebral artery* (M2 segment).
2. *Middle cerebral artery* (M3 segment).

7.2.1.3 Ventricular Plane (Cella Media)

This plane is obtained by a slight displacement of the transducer toward the cephalic 10° from the diencephalic plane through the transtemporal window.

A. Brain parenchymal structures identified by TCCS.

- *TCCS*: B-mode.

1. *Anterior horns of lateral ventricles* (Fig. 7.5).
   [Two anterior hypoechoic structures]

B. Vascular structures identified by TCCS.

- TCCS: Doppler mode.

1. Middle cerebral artery (M3 segment).

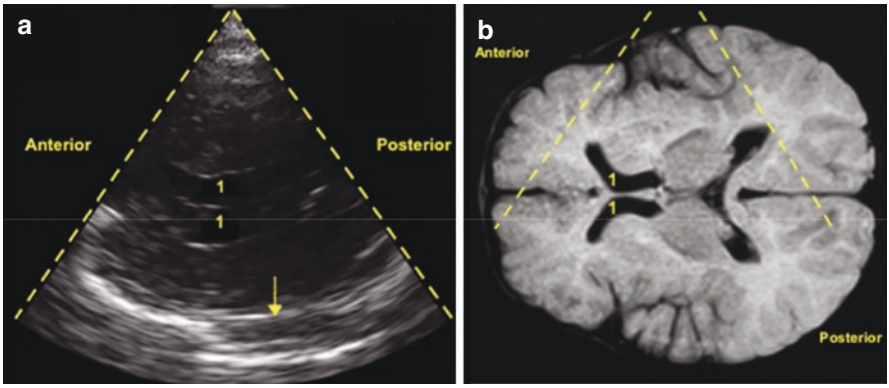

Fig. 7.5 (**a**) Ventricular plane by TCCS through transtemporal acoustic window: (1) anterior horns of lateral ventricles, (arrow) contralateral skull. (**b**) Brain MRI: (1) anterior horns of lateral ventricles and ultrasound beam (dotted line). (Author: Camilo N Rodríguez)

7.2.1.4 Upper Pons Plane

This plane is obtained by a caudal projection of the transducer toward the base of the skull from the mesencephalic plane [10].

A. Skull and brain parenchyma structures identified by TCCS.

- TCCS: B-mode.

1. *Sphenoid bone* (anterior).
2. *Cerebellum* (posterior).

B. Vascular structures identified by TCCS.

- TCCS: Doppler mode.

1. *Internal carotid artery* (carotid siphon).
2. *Ophthalmic artery*.

7.2.1.5 Lower Pons Plane

This plane is obtained by a caudal projection of the transducer toward the base of the skull from the superior pontine plane [10].

A. Skull structures identified by TCCS.

- TCCS: B-mode.

1. *Sphenoid bone* (anterior).

B. Vascular structures identified by TCCS.

- TCCS: Doppler mode.

1. *Internal carotid artery* (C6 segment).

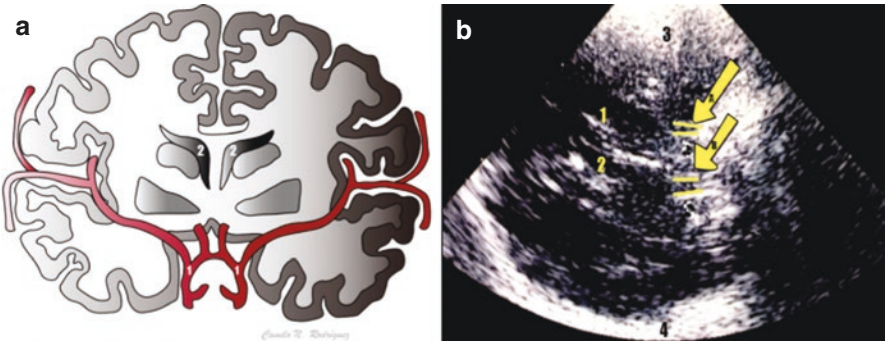

Fig. 7.6 (**a**) Scheme (coronal cut): anatomy of C1 segment of ICA and MCA; (1) C1 segment of internal carotid artery (ICA) and (2) anterior horns of lateral ventricle. (**b**) TCCS B-mode: anterior coronal plane by transtemporal window; (1, 2) anterior horns of lateral ventricle, (3) transtemporal acoustic beam, (4) contralateral skull bone, and (A, B) (yellow arrows) carotid groove of the sphenoid bone (C1 segment of ICA). (Author: Camilo N. Rodríguez)

7.2.1.6 Coronal Plane (Anterior) (Fig. 7.6)

From the transtemporal window, at the level of the mesencephalic plane, a 90° rotation of the probe is performed by the operator [10].

A. Brain parenchymal structures identified by TCCS.

- TCCS: B-mode.

  1. *Anterior horns of lateral ventricles***.**
  2. *Midline* (hyperechoic).

B. Vascular structures identified by TCCS.

- TCCS: Doppler mode.

  1. *Carotid sulcus* (Carotid groove of the sphenoid bone: horizontal hyperechoic lines on each side of midline).
  2. *M1 segment* (MCA).

7.2.2 Transforaminal Window

This window allows to localize the insonation of the basilar artery and the intracranial portion of the vertebral arteries (V4 segments) by projecting the ultrasound beam between the atlas (C1) and the base of the skull [11].

A. Skull structure identified by TCCS (Fig. 7.7).

- TCCS: B-mode.

  1. *Foramen magnum* (*occipital foramen*) [3, 7–9, 12] (Hypoechoic).

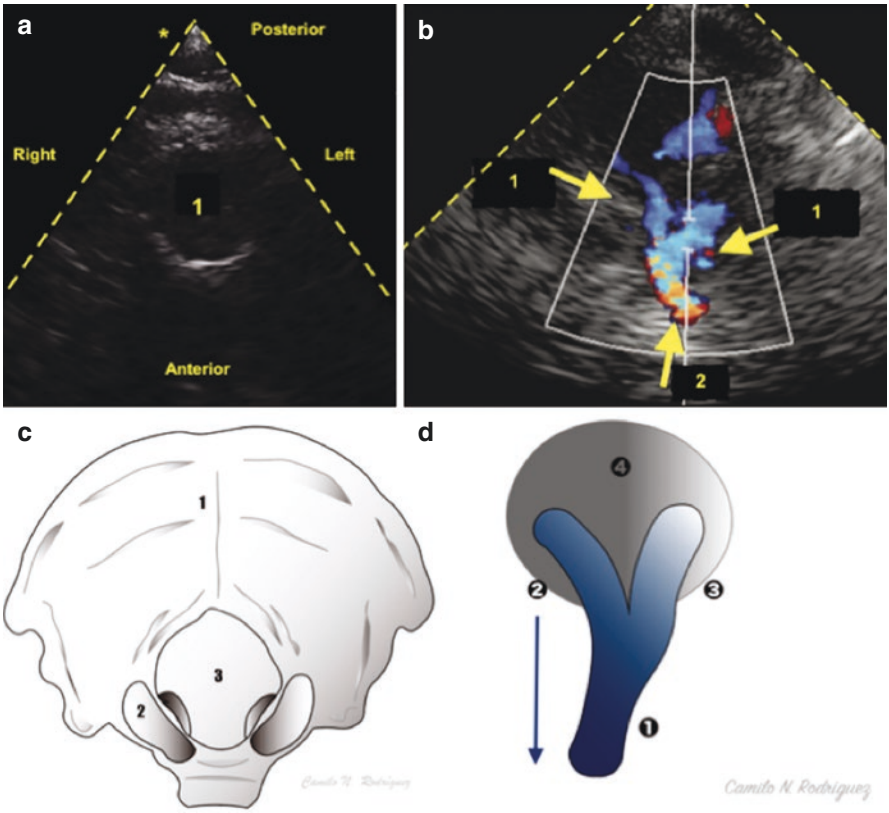

Fig. 7.7 (**a**) Transforaminal acoustic window by TCCS (B-Mode): (1) foramen magnum. (**b**) Transforaminal acoustic window by TCCS (duplex): (1) vertebral artery (blue), (2) basilar artery (blue). (**c**) Scheme: anatomy of occipital bone;(1) occipital bone, (2) occipital condyle, and (3) foramen magnum. (**d**) Scheme of insonation through transforaminal window by TCCS: (1) basilar artery, (2) and (3) vertebral arteries, and (4) foramen magnum. (arrow) It highlights that the flow away from transducer. (Blue color). (Author: Camilo N. Rodríguez)

B. Vascular structures identified by TCCS (Fig. 7.7).

- TCCS: Doppler mode.

1. *Vertebral arteries (VA)* (Intracranial portion – V4).
2. *Basilar artery (BA)*.

7.2.3 Neuroorbital Acoustic Window (Fig. 7.8)

By placing the probe on the eyeball (upper eyelid), either on an axial or sagittal axis, the ultrasound beam projection is very useful to explore neurovascular-orbital structures [10, 11].

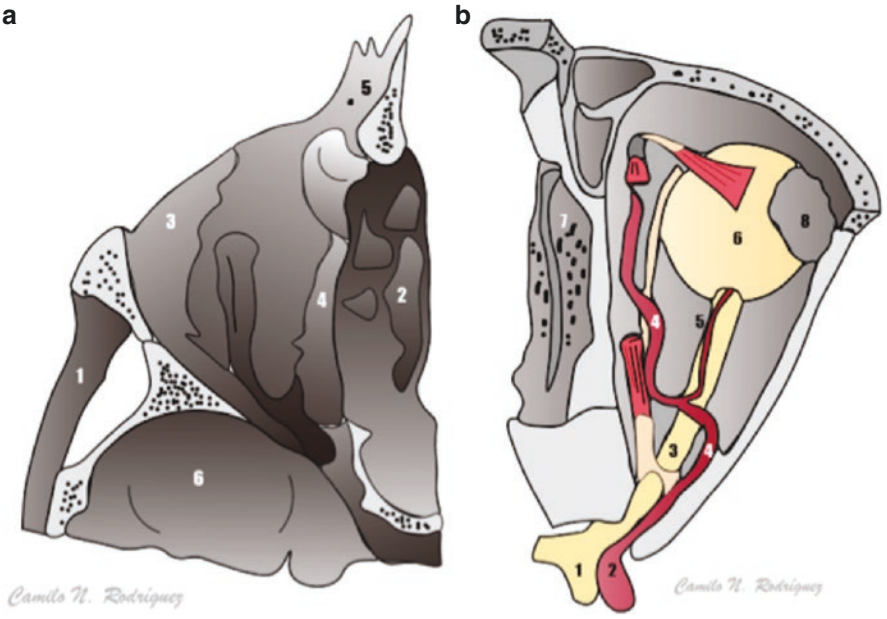

Fig. 7.8 (**a**) Scheme: axial cut through the orbit; (1) zygoma, (2) ethmoidal sinus, (3) zygomatic bone, (4) orbital sheet of ethmoidal bone, (5) frontal process of maxillary bone, and (6) middle fossa. (**b**) Scheme: superior view of right orbit; (1) optic chiasm, (2) internal carotid artery, (3) optic nerve, (4) ophthalmic artery, (5) central retinal artery, (6) eyeball, (7) cribriform sheet of ethmoid bone, and (8) lacrimal gland. (Author: Camilo N. Rodríguez)

A. Structures of the orbit identified by TCCS.

- TCCS: B-mode.
- *Anterior*.

  1. *Eyeball* (hypoechogenic).
  2. *Pupil*.

- *Posterior*.

  1. *Papilla* (Normal diameter: 1–1.5 mm).
  2. *Optic nerve*.
  3. *Optic nerve sheath diameter* (ONSD) (NV: 4–5 mm).

B. Vascular structures of the orbit identified by TCCS.

- TCCS: Doppler mode.

  1. *Central retinal artery* (CRA).
  2. *Ophthalmic artery* (OA).

7.2.4 Submandibular Acoustic Window (Figs. 7.9 and 7.10)

The submandibular acoustic insonation window is used to study neck vessels (internal carotid artery (ICA)). It is also an alternative access to the vessels of the posterior cerebral circulation (vertebral arteries (VA) and basilar artery (BA)) during transcranial color-coded duplex sonography (TCCS) in the ICU patient [14].

A. Cerebrovascular structures.

1. *Carotid system* (Fig. 7.10).
   (a) Common carotid artery (CCC).
   (b) Internal carotid artery.
   (c) External carotid artery.
2. *Vertebral arteries*.
3. *Basilar artery*.

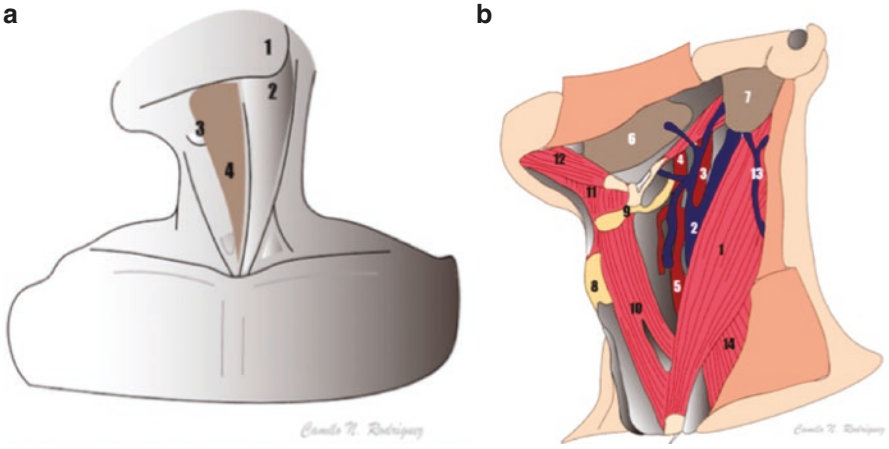

Fig. 7.9 (**a**) Scheme: superficial anatomy of neck: (1) angle of the mandible,(2) sternocleidomastoid muscle, (3) thyroid cartilage, and (4) anterior (carotid) triangle of neck. (**b**) Scheme: anatomy of anterior (carotid) triangle of neck: (1) sternocleidomastoid muscle, (2) internal jugular vein, (3) internal carotid artery, (4) external carotid artery, (5) common carotid artery, (6) submandibular gland, (7) parotid gland, (8) thyroid cartilage, (9) hyoid bone, (10) sternohyoid muscle, (11) mylohyoid muscle, (12) anterior belly of the digastric muscle, (13) external jugular vein, and (14) clavicular portion of sternocleidomastoid muscle. (Author: Camilo N. Rodríguez)

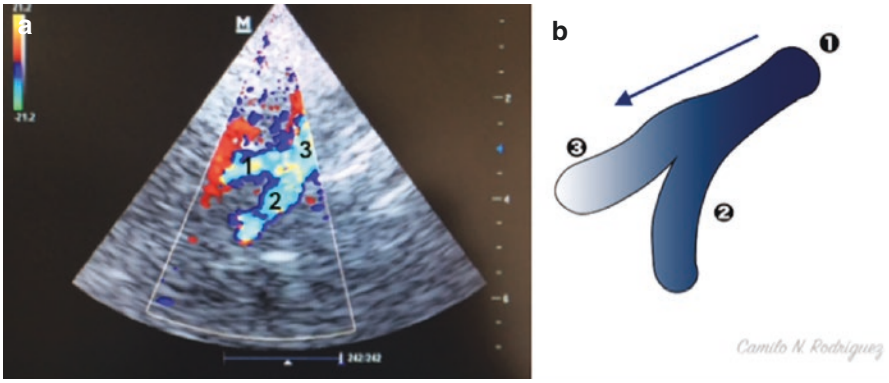

Fig. 7.10 (**a**) Submandibular acoustic window by TCCS: (1) external carotid artery (blue), (2) internal carotid artery (blue), and (3) common carotid artery (blue) (primitive). (**b**) Scheme of carotid system insonation by TCCS: (3) external carotid artery (blue), (2) internal carotid artery (blue), and (1) common carotid artery (blue). Arrow: indicates flow away from transducer. (Author: Camilo N. Rodríguez)

7.3 Arteries of the Brain: Anatomy and Ultrasound

The goal of transcranial Doppler (TCD) combined with the transcranial color-coded duplex sonography (TCCS) is an integral approach to measure the velocities of the cerebral blood flow (CBF) in the circle of Willis.

A deep understanding of cerebral vascular anatomy and its common anatomical variations is an absolute prerequisite to interpret TCD/TCCS.

7.3.1 Cerebral Circulation: Circle of Willis (Fig. 7.11)

The circle of Willis is an anastomotic vascular structure located at the base of the brain (around the interpeduncular cistern) constituted by two large arterial systems: The anterior circulation system is supplied by both internal carotid arteries and the posterior circulation system, which consists of the vertebrobasilar arterial system.

This vascular structure is often asymmetric with absent and/or hypoplastic vessels (51%) on its conformation and anatomical presentation. Between 20% and 49% of the population have anatomical variations in the circle of Willis [15, 18].

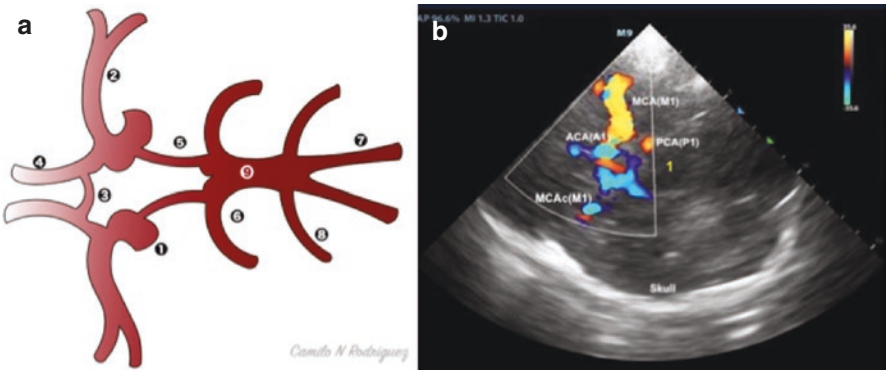

Fig. 7.11 (**a**) Scheme of anatomy of the circle of Willis: (1) internal carotid artery; (2) middle cerebral artery M1–M2 segments; (3) anterior communicating artery; (4) anterior cerebral artery; (5) posterior communicating artery; (6) posterior cerebral artery; (7) vertebral artery; (8) posterior inferior cerebellar artery; (9) basilar artery. (**b**) Circle of Willis by TCCS through transtemporal acoustic window: (1) mesencephalon, (MCA-M1) ipsilateral M1 segment of middle cerebral artery, (PCA-P1) P1 segment of posterior cerebral artery, (ACA-A1) A1 segment of anterior cerebral artery, and (MCAc-M1) contralateral M1 segment of MCA. (Author: Camilo N. Rodríguez)

7.3.1.1 Structure of Circle of Willis

A. *Anterior circulation system (carotid system)***.**

A.1 Internal carotid artery.
A.2 Middle cerebral artery.
A.3 Anterior cerebral artery.
A.4 Anterior communicating artery (AComA).
A.5 Posterior communicating artery (PComA)

B. *Posterior circulation system (vertebrobasilar system).*

B.1 Vertebral arteries.
B.2 Basilar artery.
B.3 Posterior cerebral artery (PCA).

7.3.1.2 Anterior Circulation

Carotid System

The carotid arteries originate bilaterally at the base of the neck from the subclavian artery. Both common carotid arteries may differ in length and origin. Right CCA is branched from the brachiocephalic trunk, and the left CCA branches directly from the aortic arch. The CCA, in the carotid triangle of neck, will then divide into the ICA and the ECA [15].

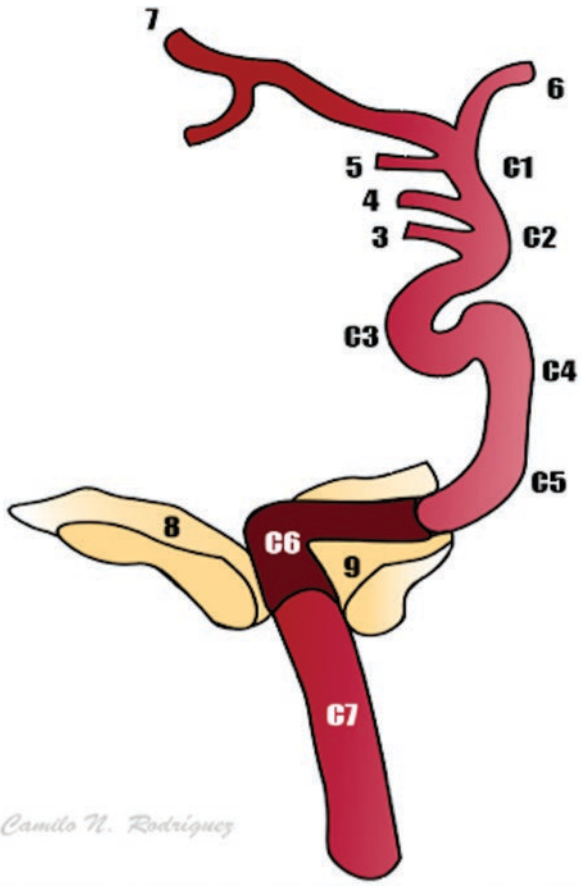

Fig. 7.12 Scheme of anatomy of internal carotid artery: (C7) cervical portion, (C6) petrosal portion, (C3-C4-C5) cavernous portion where C3 (carotid syphon), (C1-C2) cerebral portion, (3) ophthalmic artery, (4) posterior communicating artery, (5) anterior choroidal artery, (6) anterior cerebral artery, (7) middle cerebral artery, 8) temporal bone, and (9) petrous portion of the temporal bone. (Author: Camilo N. Rodríguez)

Internal Carotid Artery (Fig. 7.12)

This artery supplies most of the cerebral hemispheres, the eye, and other accessory organs.

- *Diameter*: 4.5 mm.
- *Length*: 250 mm.

The *ICA* is divided into *four portions* (caudal to cephalic) and seven subsegmentations [16] (Fig. 7.12):

(a) *Cervical portion* (C7 Segment).
(b) *Petrosal portion* (C6 Segment).
(c) *Cavernous portion*.

- C3 segment (carotid syphon).
  - Can be monitored by TCD and TCCS through transorbital and transtemporal acoustic windows [24].

TCD: Depth 55–70 mm (transorbital window).
TCCS: Transtemporal window (axial approach: superior pontine plane and anterior coronal plane approach)

- C4 segment.
- C5 segment.

(d) *Cerebral portion***.**

- C1 segment.
  Before terminal bifurcation can be measured:
  TCCS: Anterior coronal plane through transtemporal window.
  Duplex: Ipsilateral C1 segment: red color
- C1 segment: Terminal branches.

1. *Anterior cerebral artery*.
2. *Middle cerebral artery*.

- C2 segment (caudal to cephalic).

1. Ophthalmic artery (OA).
   *TCD***:** Depth 40–50 mm (transorbital window).
   TCCS: Transtemporal acoustic window (superior pontine plane) and transorbital acoustic window
2. Posterior communicating artery.
3. Anterior choroidal artery (AChA).

Other Anatomical Classification

The *ICA* is divided into *four segments* (caudal to cephalic): [17].

1. *C1 segment (cervical).*
2. *C2 segment (petrosal).*
3. *C3 segment (cavernous).*
4. *C4 segment (supraclinoid).*

- Ophthalmic artery.
- Posterior communicating artery.
- Anterior choroidal artery.

Anterior Cerebral Artery

It is the smallest branch of the two terminals of the internal carotid artery. It branches at the inner end of the Sylvian fissure [19, 24].

The *anterior cerebral artery* is subdivided into five segments:

(a) *Precommunicating segment*.
A1 Segment

- *Average diameter*: 1.6–2.5 mm.

- *Average length*: 12.7–20 mm.
- *Insonation*: Through transtemporal bone window.
- *TCD >> Depth*: 60–75 mm.
- *TCCS*: Blue color (ipsilateral)/red color (contralateral).
- *Note*: Chosen routinely by TCD/TCCS.

(b) *Postcommunicating segment*.
A2 Segment

- *Insonation*: Through frontal bone window.
- *TCCS*: Duplex: red color (flow forward to the transducer).

(c) *Postcommunicating segments*.
A3 to A5 segments

- *Insonation*: Difficult.

Anterior Communicating Antery

The anterior communicating artery arises from the anterior cerebral artery and serves as an anastomotic bridge between the left and right anterior circulation [19].

- Length: 3–4 mm.
- Diameter: 2 mm.
- *Note*: Great physiological utility in the occlusion of the internal carotid artery.

Middle Cerebral Artery (Fig. 7.13)

It is the largest terminal branch of the ICA and is the initial artery to insonate at the beginning of any TCD/TCCS study.

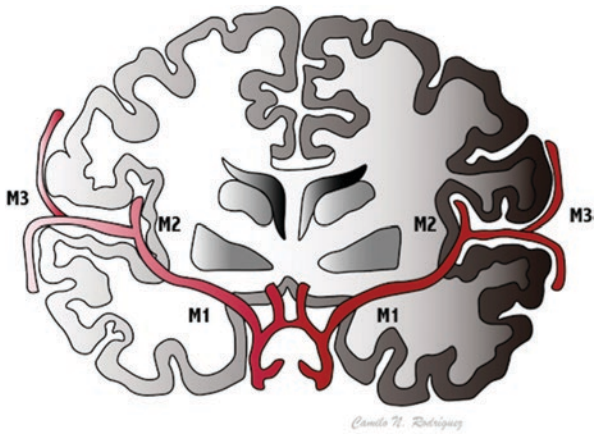

Fig. 7.13 Scheme: anatomy of middle cerebral artery segmentation; MCA-M1 (horizontal), MCA-M2 (insular), and MCA-M3 (cortical–distal). (Author: Camilo N. Rodríguez)

On its journey from the internal carotid artery, the MCA is fragmented into four segments from its origin to the convexity, where three of those segments (M1, M2, and M3 segments) become more accessible [18, 23, 24, 26]:

A. *Origin of MCA*: Terminal branch of the internal carotid artery (ICA).
B. *Vessel route*: Sylvian fissure to convexity.

1. *Horizontal Segment (M1)* (Figs. 7.3 and 7.13).
   Note: The most proximal segment chosen routinely for the TCD/TCCS study.
   Length: 19 ± 3.8 mm.
   Insonation: Transtemporal window (mesencephalic plane).
   TCCS: Red color (ipsilateral) / blue color (contralateral).
   TCD (depth): 35–60 mm
2. *Insular Segment (M2)* (Figs. 7.3 and 7.13).
   Note: In general, there are two M2 segments.
   Bifurcation: (63%) Upper branch and lower branch.
   Sometimes three segments can be found (trifurcation (32%)).
   Insonation: Transtemporal window (mesencephalic plane).
   TCCS: Red color (ipsilateral: flow forward to the transducer)
3. *Opercular or distal segment (cortical) (M3)*.
   Note: Difficult to access by TCD/TCCS.
   TCCS: Through transtemporal window in cella media plane (ventricular plane).

7.3.1.3 Posterior Circulation

Vertebrobasilar System

Vertebral Arteries (Fig. 7.14)

The VA originate from the subclavian artery, ascend toward the foramen magnum by passing through the transverse foramen of the cervical vertebrae of C6 to C2. At the pontine-medullary junction, the vertebral artery joins with its contralateral to form the basilar artery [15, 23].

- *Diameter*: 2.5–3 mm.
- *Length*: 250 mm.

A. The VA are subdivided into four segments.

   (a) *Segment (V1)*.
   From its origin to transverse process foramen of C5 or C6
   (b) *Segment (V2)*.
   From transverse foramen of C6 to transverse process foramen of C2
   (c) *Segment (V3)*.

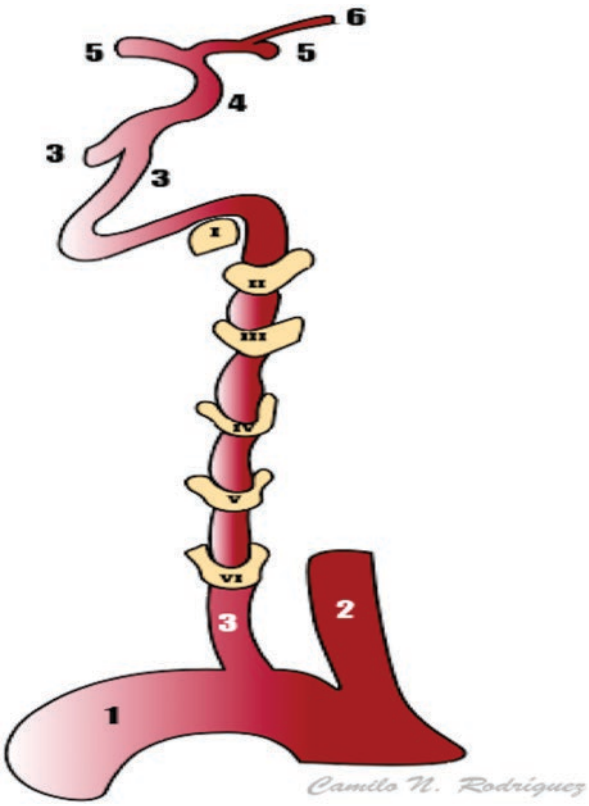

Fig. 7.14 Scheme: anatomy of vertebral artery (VA); (1) subclavian artery, (2) internal carotid artery, (3) vertebral arteries, (4) basilar artery, (5) posterior cerebral arteries, and (6) posterior communicating artery and (I-VI) cervical vertebrae. (Transverse processes). (Author: Camilo N. Rodríguez)

From its exit from the transverse foramen of C2 to the foramen magnum (occipital foramen)

(d) *Segment (V4)*.

From its entry into the skull, through the foramen magnum, to its anastomosis with the contralateral homonymous vessel and formation of the basilar artery

- *TCCS*: Blue color (flow away from transducer).
- *TCD*: Suboccipital window (transforaminal).

Depth: 45–75 mm.

Basilar Artery (Fig. 7.15)

BA is formed by the anastomosis of the two vertebral arteries at the medulla-pontine junction and ascends adjacent to the abducens nerve and oculomotor nerve through the basilar sulcus on the ventral aspect of the pons. It terminally forms the right and left posterior cerebral arteries (PCA) [23].

- *Length*: 20–40 mm.

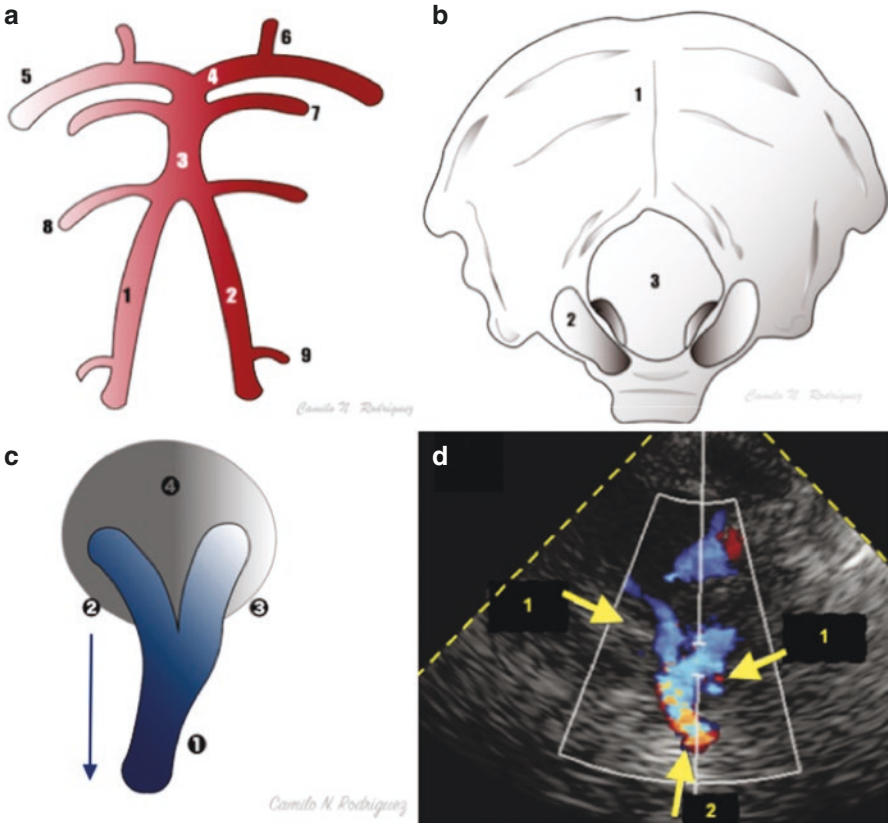

Fig. 7.15 (**a**) Scheme: anatomy of vertebrobasilar system; (1) and (2) vertebral arteries, (3) basilar artery, (4) posterior cerebral artery – P1 segment, (5) posterior cerebral artery – P2 segment, (6) posterior communicating artery, (7) superior cerebellar artery, (8) anteroinferior cerebellar artery (AICA), and (9) posterior inferior cerebellar artery (PICA). (**b**) Scheme of occipital bone: (1) occipital bone, (2) occipital condyle, and (3) foramen magnum. (**c**) Scheme of the anatomy of the vertebrobasilar system by TCCS through transforaminal acoustic window: (1) basilar artery; (2) right vertebral artery – V4 segment; (3) left vertebral artery – V4 segment; (4) foramen magnum, (arrow) It highlights that the flow moves away from the transducer (blue color). (**d**) Vertebrobasilar system insonation by TCCS through transforaminal acoustic window: (1) V4 segment of vertebral artery (blue), (2) basilar artery (blue). Arterial flow moves away from the transducer. (Author: Camilo N. Rodríguez)

- *Diameter*: 2.5–3.5 mm.
- *TCD*.
  - *Bone window*: Transforaminal.
  - *Depth*: 70–120 mm.
- *TCCS*.
  - *Window*: Transforaminal/submandibular.
  - *Duplex*: Blue color.

Posterior Communicating Artery

After its origin in the internal carotid artery (C1–C2 segments), it extends posteriorly (above the common ocular nerve) to anastomose with the posterior cerebral artery (terminal branch of the basilar artery) [15, 20, 23].

- *Length*: 12,5 ± 3,2 mm.
- *Diameter*: 1,5 ± 0,6 mm.
- *TCD*.
  - Insonation: Transtemporal window.
  - Depth: 55–65 mm.
    Flow: The flow velocity is difficult to measure as it is located perpendicularly to the probe
- *TCCS* (difficult).
  - *Window*: Transtemporal window.
  - *Plane*: Mesencephalic.
  - *Duplex*: Blue Color.

Posterior Cerebral Arteries

The PCA are the terminal branches of the basilar artery, receiving the posterior communicating artery from the internal carotid artery. It surrounds the cerebral peduncle defining two clinically relevant segments: a precommunicating segment (P1) and another postcommunicating segment (P2) [15].

The PCA branches are divided into four anatomical segments [17, 21–24]:

A. *Precommunicating Segment (P1 segment)* (Fig. 7.15).

- *Origin*: From the basilar artery to the anastomosis with the posterior communicating artery, found within the interpeduncular cistern.
- *Length*: 3–20 mm.
- *Diameter*: 1.9–2.1 mm.
- *TCD***.**

1. *Window*: Transtemporal.
   Depth: 65–80 mm
2. *Window*: Transforaminal.
   Depth: 95–100 mm.
   Flow: Forward to the Transducer

- *TCCS*.
  - Window: Transtemporal window.
  - Duplex: Red color (flow forward to the transducer).

B. *Anterior Postcommunicating Segment (P2A)* (Fig. 7.15).

- *Origin*: From the posterior communicating artery (lateral to the cerebral peduncle) to the origin of the P2P subsegment in the ambiens cistern.

- *Length*: 18–30 mm.
- *Diameter*: 1–3 mm.
- *TCD***.**
  - *Window*: Transtemporal.
  - *Depth*: 65–80 mm.
  - *Window*: Transforaminal.
  - *Depth*: 95–100 mm.
  - *Flow*: Away from transducer.
- *TCCS*:
  - *Window*: Transtemporal window.
  - *Duplex*: Blue color (flow away from transducer).

C. *Posterior Postcommunicating Segment (P2P)*.

- *Origin*: From the P2A subsegment (lateral to the brainstem) to the origin of P3 segment, it runs through the ambiens cistern.
- *Length*: 9–25 mm.
- *Diameter*: 0.8–2 mm.
- *TCD***.**
  - *Window*: Transtemporal.
  - *Depth*: 65–80 mm.
  - *Window*: Transforaminal.
  - *Depth*: 95–100 mm.
  - *Flow*: Away from transducer.
- *TCCS*.
  - Transtemporal window.
  - *Duplex*: Blue color (flow away from transducer).

D. *Quadrigeminal Segment (P3 Segment)*.

- *Origin*: From the ambiens cistern through the quadrigeminal cistern; it runs through the quadrigeminal cistern.
- *Length*: 19,8 mm.
- *Diameter*: 1,1 mm.
- *TCD*: Difficult insonation.
- *TCCS* [25].
  - Window: Transtemporal (mesencephalic-diencephalic planes).
  - *Duplex*: Blue color.

E. *P4 Segment*.

- *Origin*: Runs from the parieto-occipital fissure to the distal calcarine fissure.

Posterior-Inferior Cerebral Artery (PICA) (Fig. 7.15)

The PICA is the most variable and tortuous cerebral artery. Its origin can be variable both extracranially and intracranially as a branch of the vertebral artery (VA). It may even be absent. In 84% of the population, PICA has a single trunk; in the 83%, it arises superior to the foramen magnum.

PICA supplies the cerebellar vermis, cerebellar hemispheres, and structures of the medulla oblongata, and has a close relationship with cranial nerves: III, V, VI, VIII, IX, and XII [17, 23].

- *Diameter*: 1.7–1.8 mm.
- *TCCS*.
  - Window: Transforaminal.
  - Duplex: Red color (flow forward to the transducer).
- *TCD*.
  - Depth: 50–70 mm.
  - Window: Transforaminal.

7.4 Cerebral Circulation: Anatomical Distribution of Cerebral Blood Flow (CBF)

By studying the anatomy of the circle of Willis with magnetic resonance imaging (MRI), it is possible to demonstrate the anatomical distribution (%) of the CBF in the population where the circle was complete [26].

1. *Internal carotid system* (Right).
   1.1 ICA >> (36% ± 4).
   1.2 MCA >> (21% ± 3).
   1.3 ACA >> (12% ± 4).
2. *Internal carotid system* (Left).
   1.1 ICA >> (36% ± 4).
   1.2 MCA >> (21% ± 3).
   1.3 ACA >> (11 ± %4).
3. *Vertebrobasilar system* (right and left).
   1.1 VA >> (15% ± 5).
   1.2 PCA >> (8% ± 1).
   1.3 BA >> (20% ± 4).

The CBF in the anterior and posterior communicating vessels is especially evident during situations of CBF obstruction in one of the two feeding systems of the arterial circle (circle of Willis) [37, 38].

7.5 Cerebral Circulation: Anatomical Variations

The circle of Willis probably has two theoretical functions in human brain. Despite the communicating arteries being too small or hypoplastic in a majority of the population, these branches probably serve two particular functions: (1) as a passive pressure dissipating system, where they transfer pressure, without considerable blood flow, from the high pressure end to the low pressure end, and (2) circulation compensatory function, especially on impairment function (stenosis/occlusion) of ICA.

The circle of Willis was discovered with its complete anatomy with autopsy studies, CT studies, and MRI, where it is visible 14–55% of its entire part [27–29].

7.5.1 Anatomical Variations in the Circle of Willis

7.5.1.1 Anterior Circulation

Most Common Variations [28]

Anterior Communicating Artery
(a) Hypoplastic or absent (7–13%).
(b) Doubled (9–30%).
(c) Unique artery (56%).

Anterior Cerebral Artery
(a) (A1) Segment: hypoplastic or absent (2–12%)

Posterior Communicating Artery
The most variable artery within the circle of Willis [11, 28–30].

(a) Bilaterally hypoplastic (7%).
(b) Unilateral absent or hypoplastic (27%).
(c) Bilateral present (54%).
(d) Hypoplastic or unilateral absence of posterior communicating artery (PComA), absence of P1 segment, or hypoplastic PCA (1%).

7.5.1.2 Posterior Circulation

Most Common Variants [28]

Posterior Cerebral Artery
(a) Blood supply comes from the BA (82%).
(b) Blood supply comes from the ICA (11%).
(c) Hypoplastic or unilateral absence of P1 segment (1%).
(d) Hypoplastic or unilateral absence of P1 segment and PComA (1%).

Vertebral Artery
(a) Dominant left vertebral artery (45%).
(b) Dominant right vertebral artery (21%).
(c) Shared dominance (34%).

7.6 Veins and Venous Sinuses of the Brain: Anatomy and Ultrasound

Three venous systems that drain blood from the brain:

1. *Deep cerebral veins*.
2. *Dural venous sinuses*.

We will focus on the identification of the deep cerebral veins and the dural venous sinuses by TCD/TCCS.

Ultrasound of deep intracranial venous does not belong, even, to the routine examination techniques applied in daily practice in the ICU. However, the deeper and more serious the pathological effects on the intracerebral venous circulation, the easier it is to detect them by TCCS/TCD [11, 31].

The relevant anatomy of intracerebral are the venous structures with a high probability of access by ultrasound (Table 7.1).

Table 7.1 Normal venous blood flow values

Vein / Sinus	Flow Velocities (cm/s) [a]	Detection Rate (%)
Basal vein (of *Rosenthal*)	7–20/5–15	80–100%
Deep middle cerebral vein	4–15/3–11	50–95%
Great vein (of *Galen*)	6–32/4–25	80–95%
Straight sinus	6–39/4–27	23–82%
Transverse sinus	6–56/5–38	20–84%
Sphenoparietal sinus	27±17	84%
Superior petrosal sinus	27±17	84%

[a]Systolic/Diastolic velocities. Adapted from manual of Neurosonology; Csiba L, Baracchini C. 2016. Cambridge. [11, 32–39]

Ultrasound of the deep intracerebral venous system and sinuses of the dura is a complementary tool (diagnostic modality for a rapid screening at the bedside of the critical patient) in which there is no consensus in the sequence of examination approach [36].

7.6.1 Deep Cerebral Veins (Fig. 7.16)

- Normal Flow: Low flow velocity (Table 7.1).
- Identification: B-mode + Doppler.

7.6.1.1 Deep Middle Cerebral Vein (DMCV)

Identification: The deep middle cerebral vein is adjacent to the middle cerebral artery (MCA) with drainage in the basal vein.

TCCS

Acoustic bone window: Transtemporal.

Insonation plane: Mesencephalon.

Duplex: Flow away from transducer into the dural venous sinuses (blue color).

TCD

Acoustic bone window: Transtemporal.

Flow: Increase in the flow velocity (thrombosis?) [35, 37].

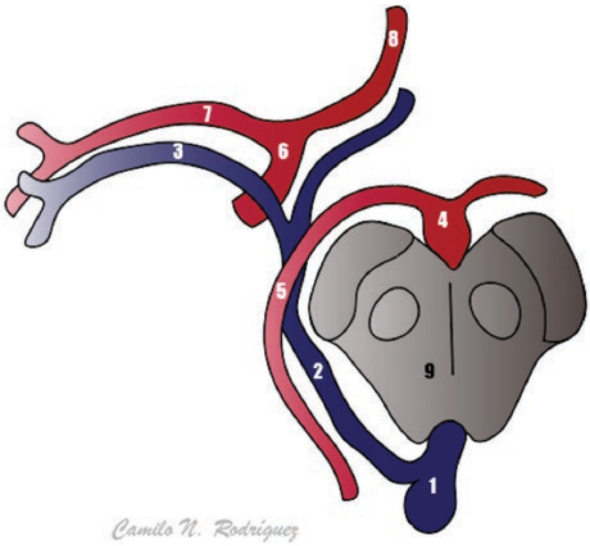

Fig. 7.16 Scheme: cerebral veins detectable by TCCS and arterial relationship; (1) vein of Galen, (2) basal vein (Rosenthal), (3) deep middle cerebral vein, (4) basilar artery, (5) posterior cerebral artery, (6) internal carotid artery, (7) middle cerebral artery, (8) anterior cerebral artery, and (9) mesencephalon (midbrain). (Author: Camilo N. Rodríguez)

7.6.1.2 Basal Vein (of Rosenthal)

Identification: The basal vein is very close (slightly cranial) to the P2A segment of the posterior cerebral artery.

TCCS
Acoustic bone window: Transtemporal.
Insonation plane: It starts in the mesencephalic plane and then the probe is positioned with a slight angulation to the diencephalic plane (thalamic), following the direction of the posterior cerebral artery.
Duplex: Flow away from the probe to venous sinus of dura mater (blue color).
Note: Decrease the depth [11, 33].

TCD
Acoustic bone window: Transtemporal.
Flow: Increase in the flow velocity (thrombosis?) [35, 37].

7.6.1.3 Great Cerebral Vein (of Galen)

Identification: It is immediately behind the pineal gland (hyperechoic structure) behind the two lines (hyperechoic) corresponding to the third ventricle (diencephalic plane).

TCCS
Acoustic bone window: Transtemporal.
Insonation plane: Diencephalic (thalamic).
Duplex: Flow away from transducer to venous sinus of dura mater drainage (blue color).
Note: Decrease the depth [11, 33, 37].

7.6.2 Dural Venous Sinuses (Fig. 7.17)

7.6.2.1 Sphenoparietal Sinus

Identification: Identify the edges of the lower wing of the sphenoid and the pyramid that makes up the sphenoid bone. The sphenoparietal sinus is located at the hyperechoic edge of the sphenoid wing.

TCCS
Acoustic Bone window: Transtemporal.
Insonation plane: Superior pons plane and inferior pontine plane.
Duplex: Blue color (flow away from transducer).

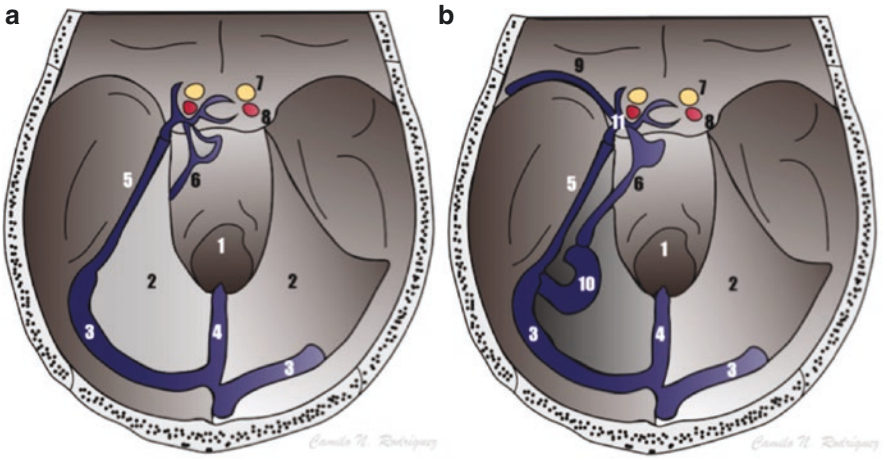

Fig. 7.17 (**a**) Scheme: sinuses detectable by TCCS (floor of the cranial cavity); (1) foramen magnum, (2) cerebellar tentorium, (3) transverse sinus, (4) straight sinus, (5) superior petrosal sinus, (6) inferior petrosal sinus, (7) optic nerve, (8) internal carotid artery. (**b**) Scheme: sinuses detectable by TCCS (floor of the cranial cavity, left cerebellar tentorium removed); (1) foramen magnum, (2) cerebellar tentorium, (3) transverse sinus, (4) straight sinus, (5) superior petrosal sinus, (6) inferior petrosal sinus, (7) optic nerve, (8) internal carotid artery, (9) sphenoparietal sinus, (10) sigmoid sinus, and (11) cavernous sinus. (Author: Camilo N. Rodríguez)

7.6.2.2 Superior Petrosal Sinus

Identification: Identify the edges of the lower wing of the sphenoid and the pyramid that makes up the sphenoid bone. The sphenoparietal sinus is located at the hyperechoic edge of the sphenoid wing.

TCCS

Acoustic window: Transtemporal.

Insonation plane: Superior pons plane and inferior pontine plane.

Duplex: Blue color (flow away from transducer).

7.6.2.3 Inferior Petrosal Sinus

Identification: It runs close to the basilar artery. Close to this artery, the vertebral venous plexus and the inferior petrosal sinus can be identified.

TCCS

Acoustic Window: Transforaminal.

Duplex: Red color (flow forward to the transducer close to the Basilar artery).

7.6.2.4 Cavernous Sinus

Identification: Difficult insonation.

TCCS
Acoustic bone window: Transtemporal.

7.6.2.5 Transverse Sinus

Identification: From the plane of insonation of the straight sinus, it is necessary to perform a downward (and posterior) probe rotation for the location of the contralateral transverse sinus.

TCCS
Acoustic bone window: Transtemporal.

Duplex: Blue color (contralateral transverse sinus)/red color (ipsilateral transverse sinus). Both transverse sinuses drain to sigmoid sinuses [11, 32, 37].

7.6.2.6 Straight Sinus

Identification: From the diencephalic plane, it is necessary to rotate the transducer upwards to align the plane of insonation with the beginning of the tentorium of the cerebellum (hyperechoic). The straight sinus is directed, on this anatomical structure, until its drainage in the confluent sinus.

TCCS
Acoustic Bone window: Transtemporal.

Duplex: Blue color (flow away from the transducer to confluent sinus) [32].

TCD
Acoustic Bone window: Transforaminal.

Flow: Increase in the flow velocity (thrombosis) [34, 37].

Operator training requires more time and patience. The insonation and identification of the intracerebral venous system is more difficult, given the low flow of the system under normal conditions.

There is evidence of an alternative frontal acoustic window (paramedian projection and lateral projection) at the access of the deep venous system and/or anterior cerebral artery (A2 segment). It presents a lower efficiency than the transtemporal window, a difficulty that can be resolved with the administration of contrast [38].

7.7 Conclusion

To introduce transcranial Doppler (TCD) or transcranial color-coded duplex Sonography (TCCS) into critical care practice, the operator should be fully trained into acquiring the following:

- Adequate knowledge of cerebrovascular and brain parenchyma anatomy.

- A correct understanding of the anatomical US landmarks and hemodynamics measures for an accurate interpretation of the results.

This knowledge will allow the operator to choose the most appropriate acoustic window in correlation with the current clinical condition of the patient, patient's decubitus, insonation technique, and the anatomical objective to be studied.

Algorithm

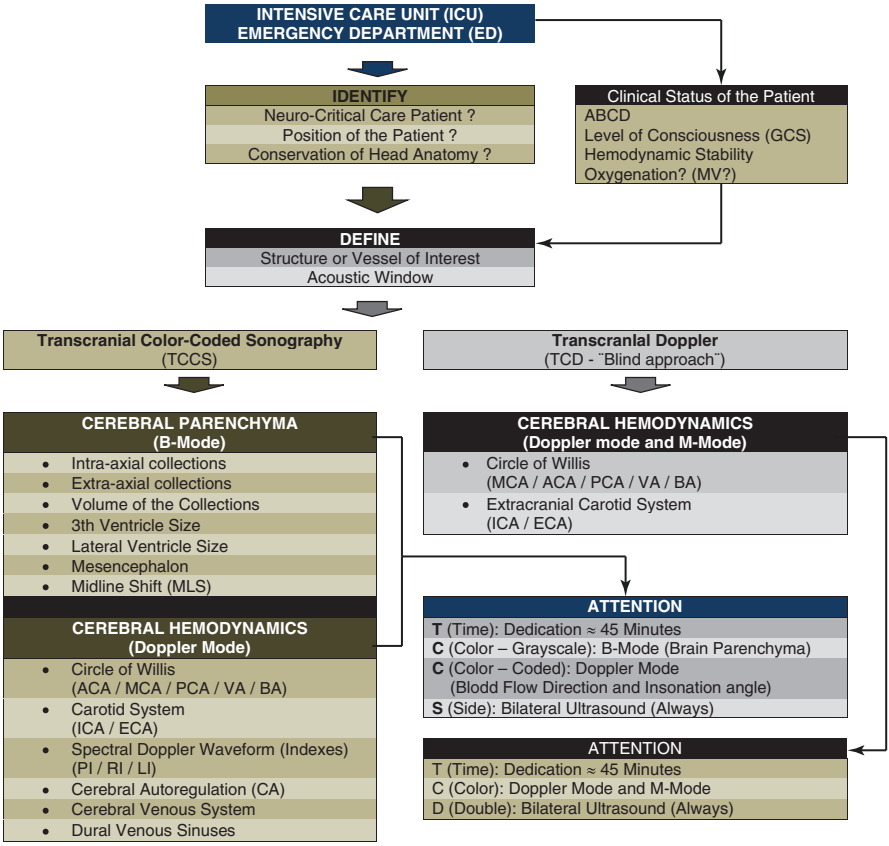

ABCD airway-breathing-circulation-disability, *MV* mechanical ventilation, *ACA* anterior cerebral artery, *MCA* middle cerebral artery, *PCA* posterior cerebral artery, *VA* vertebral artery, *BA* Basilar artery, *PI* Pulsatility index, *RI* resistance index, *LI* Lindegaard index, *ICA* internal carotid artery, *ECA* external carotid artery

References

1. Kalanuria A, et al. Use of transcranial Doppler (TCD) ultrasound in the Neurocritical care unit. Neurosurg Clin N Am. 2013;24:441–56.
2. Blanco P, Blaivas M. Applications of transcranial color-coded sonography in the emergency department. J Ultrasound Med. 2017;36:1251–66.
3. Blanco P, Blaivas M. Applications of transcranial color-coded sonography in the emergency department. J Ultrasound Med. 2017;36:1251–66.
4. Zipper SG, Stolz E. Clinical application of transcranial color-coded duplex sonography—a review. Eur J Neurol. 2002;9:1–8.
5. Llompart-Pou JA, Abadal JM, Rodríguez-Yago M, Ferreruela M. Transcranial color coded duplex sonography in the intensive care unit. Crit Ultrasound J. 2011;3:47–9.
6. Blanco P. Transcranial color-coded duplex sonography: another option besides the blind method. J Ultrasound Med. 2016;35:668–73.
7. Testut L, Latarjet A. Descriptive anatomy, vol. 2. 9th ed. Barcelona, Spain: Salvat; 1984.
8. Williams PL, Warwick R. Gray's anatomy, vol. I. 36th ed. Barcelona, Spain: Salvat; 1985. p. 762–3.
9. Carpenter MB. Fundamentals of neuroanatomy. 4th ed. Williams & Wilkins; 1994.
10. Csiba L, Baracchini C. Manual of Neurosonology; chapter 9. 1st ed. Cambridge University Press; 2016.
11. Babikian VL, Wechsler LR, Toole JF. Transcranial Doppler ultrasonography. 2da edición, Butterworth Heinemann; 1999.
12. Chung KW, Chung HM, Halliday NL. Gross anatomy. 8th ed. Board Review Series, Philadelphia, PA, USA: Wolters Kluwer; 2014.
13. D'Andrea A, et al. Transcranial Doppler ultrasound: physical principles and principal applications in Neurocritical care unit. J Cardiovasc Echogr. 2016;26(2):28–41.
14. Geeraerts T, Thome W, Tanaka S, Leblanc PE, Duranteau J, Vigué B. An alternative ultrasonographic approach to assess basilar artery flow. Neurosurgery. 2011;68(2 Suppl Operative):276–81.
15. Williams PL, Warwick R. Gray's anatomy, vol. I. 36th ed. Salvat; 1985. p. 756–62.
16. Eggers J, Pade O, Rogge A, Schreiber SJ, Valdueza JM. Transcranial color-coded sonography successfully visualizes all intracranial parts of the internal carotid artery using the combined transtemporal axial and coronal approach. AJNR Am J Neuroradiol. 2009;30:1589–93.
17. Spetzler RF, Kalani MY, Nakaji P. Neurovascular surgery. 2nd ed. Thieme; 2015.
18. Poveda Fernández J. Basical brain anatomy for the interventional cardiologist; Costarr Cardiol. 2009;11(2).
19. Zhu G, Yuan Q, Yang J, Yeo JH. Experimental study of hemodynamics in the circle of Willis. BioMed Eng OnLine. 2015;14(Suppl 1):S10.
20. Pedroza A, Dujovny M, Artero JC, Umansky F, Berman SK, Diaz FG, et al. Microanatomy of the posterior communicating artery. Neurosurgery. 1987;20(2):228–35.
21. Ahmed O, et al. Accuracy of CT angiography in detection of blood supply dominance of posterior cerebral artery in patients with posterior communicating artery aneurysm. Neuroradiol J. 2015;28(6):598–603.
22. Zeal AA, Rhoton AL Jr. Microsurgical anatomy of the posterior cerebral artery. J Neurosurg. 1978;48:534–59.
23. Párraga RG, Ribas GC, Andrade SE, de Oliveira E. Microsurgical anatomy of the posterior cerebral artery in three-dimensional images. World Neurosurg. 2011;75:233–57.
24. Frid PE, Schreiber SJ, Pade O, Doepp F, Valdueza J. The posterior cerebral artery and its Main cortical branches identified with noninvasive transcranial color-coded duplex sonography. Ultrasound Int Open. 2015;1(2):E53–7.
25. Rogge A, et al. Transcranial color-coded duplex sonography of the middle cerebral artery, more than just the M1 segment. J Ultrasound Med. 2015;34:267–73.

26. Zarrinkoob L, et al. Blood flow distribution in cerebral arteries. J Cereb Blood Flow Metab. 2015;35:648–54.
27. Riggs HE, Rupp C. Variation in form of circle of Willis. Arch Neurol. 1963;8:24–30.
28. Hartkamp MJ, et al. Circle of Willis collateral flow investigated by magnetic resonance angiography. Stroke. 1999;30:2671–8.
29. Vrselja Z, Brkic H, Mrdenovic S, Radic R, Curic G. Function of circle of Willis. J Cereb Blood Flow Metab. 2014;34:578–84.
30. Alpers BJ, Berry RG, Paddison RM. Anatomical studies of the circle of Willis in normal brain. AMA Arch Neurol Psychiatry. 1959;81:409–18.
31. Williams PL, Warwick R. Gray's anatomy, vol. I. 36th ed. Salvat; 1985. p. 818–25.
32. Zedde M, Malferrari G, De Berti G, Maggi M. Ipsilateral evaluation of the transverse sinus: transcranial color-coded sonography approach in comparison with magnetic resonance venography. Pers Med. 2012;1:390–4.
33. Baumgartner RW, Nirkko AC, Muri RM, Gonner F. Transoccipital power-based color-coded dúplex sonography of cerebral sinuses and veins. Stroke. 1997;28:1319–23.
34. Valdueza JM, Schultz M, Harms L, Einhaupl KM. Venous transcranial Doppler ultrasound monitoring in acute dural sinus thrombosis. Stroke. 1995;26:1196–9.
35. Schreiber SJ, Stolz E, Valdueza JM. Transcranial ultrasonography of cerebral veins and sinuses. Eur J Ultrasound. 2002;16:59–72.
36. Stolz E, Kaps M, Kern A, Babacan SS, Dorndorf W. Transcranial color-coded duplex sonography of intracranial veins and sinuses in adults. Reference data from 130 volunteers. Stroke. 1999;30(5):1070–5.
37. Stolz E, Kaps M, Kern A, Dorndorf W. Frontal bone windows for transcranial color-coded dúplex sonography. Stroke. 1999;30:814–20.
38. Lownie SP, Larrazabal R, Kole MK. Circle of Willis collateral during temporary internal carotid artery occlusion I: observations from digital subtraction angiography. Can J Neurol Sci. 2016;43:533–7.
39. Wang BH, Leung A, Lownie SP. Circle of Willis collateral during temporary internal carotid artery occlusion II: observations from computed tomography angiography. Can J Neurol Sci. 2016;43:538–42.

Chapter 8
Transcranial Doppler (TCD/TCCS) and Cerebral Blood Flow: Applications in the Neurological Intensive Care Unit

Edward M. Manno and Farzeneh Sorond

Key Points

1. Cerebral blood flow originally directly measured more recently is measured through external detection systems. Transcranial Doppler ultrasound can serve as a surrogate for measurements under select circumstances.
2. Cerebral autoregulation is a pressure phenomenon that maintains relatively constant cerebral blood flow over a wide range of cerebral perfusion pressures. CO_2 vasoreactivity measures the response of cerebral blood flow to alterations in PCO_2.
3. Transcranial Doppler ultrasound represents a noninvasive method to measure direction of flow and velocities of the basal cerebral arteries. Cerebral autoregulation can be tested under static and dynamic conditions.
4. Transcranial Doppler ultrasound is used in a variety of pathologies in the neurological intensive care unit. Its main use is for the detection of cerebral vasospasm after subarachnoid hemorrhage.
5. Transcranial Doppler ultrasound has attained greater acceptance as a confirmatory test in the diagnosis of brain death.

8.1 Introduction

In 1982, Rune Aaslid reported the capability of insonating through the skull using a low-frequency pulsed Doppler ultrasound wave [1]. Thus, with the development of transcranial Doppler ultrasound (TCD), the cerebrovascular tree could be mapped.

E. M. Manno (✉) · F. Sorond
Department of Neurology, Northwestern University Feinberg School of Medicine, Chicago, IL, USA
e-mail: edward.manno@nm.org; Farzaneh.Sorond@nm.org

C. N. Rodríguez et al. (eds.), *Neurosonology in Critical Care*,
https://doi.org/10.1007/978-3-030-81419-9_8

Subsequent techniques were developed that allowed for the identification of vessel narrowing or occlusion, the assessment of cerebral blood flow and autoregulation, and the discovery of high-intensity transient signals (HITS). TCD became increasingly important in its use for discovering patients at risk for cerebral infarction from a variety of neurological conditions. The technology became increasingly widespread due to its portability, low cost, and ease of use. Due to the overall utility of the technology, TCD became a critical diagnostic tool in the neurological intensive care unit. This chapter will review basic cerebrovascular physiology and describe TCD technology and its application in the neurological intensive care unit for a variety of pathological conditions.

8.2 Cerebral Blood Flow Measures

In the 1940s, Kety and Schmidt using the Fick principle described a direct method of quantifying cerebral blood flow (CBF) [2]. Using nitrous oxide, an inert, diffusible, non-metabolizable tracer, they were able to calculate CBF based on a differential equation incorporating arterial and venous concentrations of nitrous, the time to reach equilibrium, and the partition coefficient of the brain [3]. All methods of CBF are subsequently compared to the Kety–Schmidt measures which are considered the gold standard.

The development of external detection systems permitted the use of radioactive tracers to measure global and regional areas of CBF. Perfusion and the time to washout of radioactivity are used to determine regional flow. A variety of substances have been used with increasingly sophisticated methods to detect regional flow. Some commonly employed methods now include single-photon emission computed tomography SPECT and positron emission tomography [4].

Both computed tomography (CT) and magnetic resonance imaging (MRI) have developed the bolus-tracking methods to determine and quantify regional blood flow. MRI uses gadolinium to detect a decrease in the T2 signal caused by the magnetic susceptibility of this agent [5]. CT is able to similarly detect the rate of appearance and disappearance of a contrast bolus to detect regional flow. CT and MRI perfusion is now commonly used in emergency departments to detect acute large vessel occlusions and to determine if additional brain tissue is at risk for infarction.

All of the above-listed methods, however, are relatively invasive and require transport of the patient to radiology.

8.3 Transcranial Doppler (TCD/TCCS)

TCD/TCCS represents a noninvasive method to evaluate flow velocities through the basal cerebral arteries. By evaluating the flow velocity spectrum of the cerebral arteries, TCD/TCCS can provide information on the direction of flow, patency of

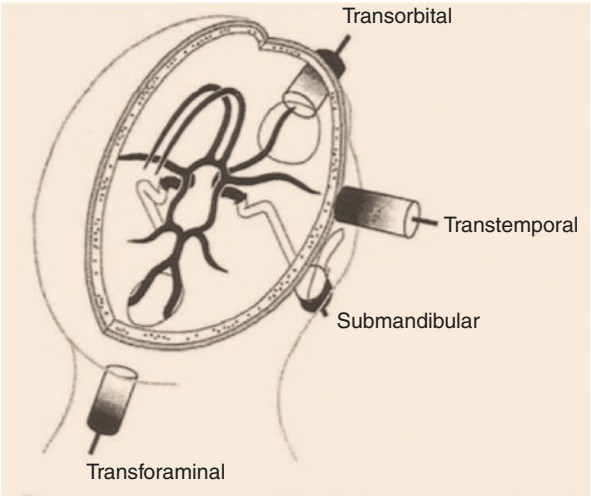

Fig. 8.1 Multiple approaches to obtain flow velocities of the basal cerebral arteries. Approaches listed include transtemporal, transforaminal, transorbital, and submandibular. These "windows allow for insonation of these vessels. (Aaslid [5])

vessels, focal stenosis, and cerebrovascular reactivity [5]. TCD/TCCS utilizes a 2 MHz ultrasound probe to emit a pulsed Doppler wave which is both range gated and directionally sensitive. Range gating allows for the depth to be adjusted by altering the time the pulsed wave is received. The Doppler principle allows the determination of direction of flow. The ultrasonic beam encompasses the insonated artery, thus reflecting a wave of erythrocyte velocities that have the highest velocities detected at the center of the artery [6]. Systolic peak velocities can be measured, and mean flow velocities calculated form the waveform. The shape of the waveform will determine a pulsatility index (PI) with a low PI representing a dampened waveform. High PIs are generally believed to be a marker for increased downstream resistance [7].

Using a low-frequency transmitted wave, TCD can insonate through the temporal bone. Examination is performed through the use of transtemporal, ophthalmic, and posterior approaches or "windows" (Fig. 8.1). Through these approaches, a map of the cerebrovascular tree can be generated (Fig. 8.2). Normal ranges for TCD flow velocities of the cerebral arteries are well documented [6].

8.4 TCD/TCCS: Assessment of Cerebral Blood Flow

TCD has been used to assess both volume flow and relative changes in CBF after dynamic changes in blood pressure. Absolute blood flow can be estimated for TCD flow velocities only when the diameter of the vessel lumen is known [8]. Calculations of CBF using TCD flow velocities under "static" or non-changing conditions have determined values similar to expected values of CBF but direct comparisons with other measures of CBF are lacking [9]. Similarly, due to the nature of the disease processes in the intensive care unit, the two variables of lumen diameter and arterial

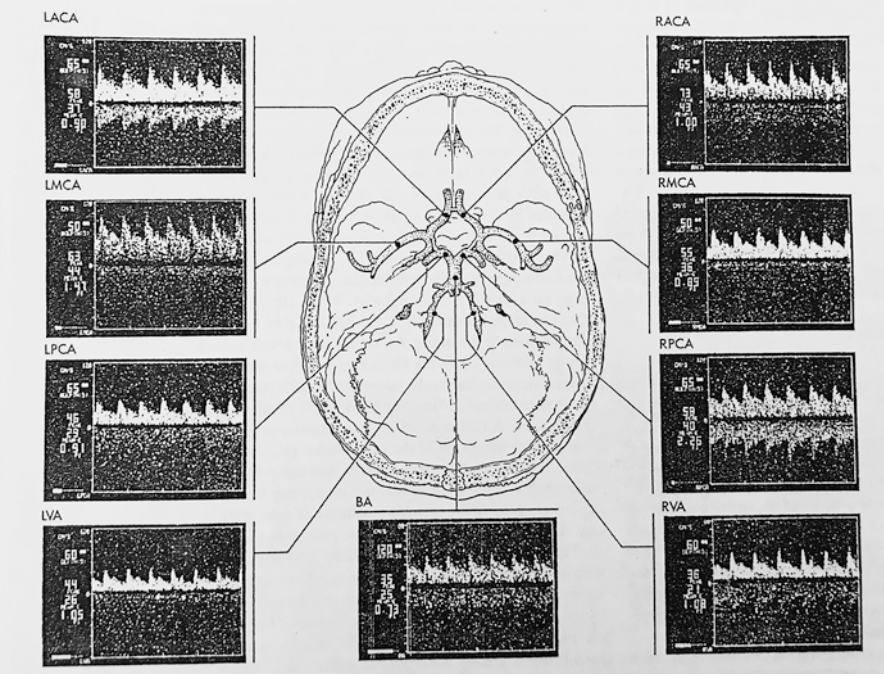

Fig. 8.2 Transcranial waveforms and directions of the basal cerebral arteries obtained through the multiple approaches. (LACA = left anterior cerebral artery; LMCA = left middle cerebral artery; LPCA = left posterior cerebral artery; LVA = left vertebral artery; BA = basilar artery; RACA = right anterior cerebral artery; RMCA = right middle cerebral artery; RPCA = right posterior cerebral artery; RVA = right vertebral artery.) (Saver and Feldmann [6])

perfusion territories are rarely constant. Thus, calculation of absolute CBF in the neurological intensive care unit is fraught with difficulties. Transcranial color-coded duplex sonography can provide a better estimate of luminal diameter but is rarely used under dynamic testing [10].

A more practical use of TCD/TCCS in the neurological intensive care unit is measuring relative changes in flow velocities [11–16]. Several studies have investigated the relationship between changes in TCD flow velocities and CBF. A linear relationship has been reported between flow velocities and the mean transit time of technetium [14], and percentage changes in flow velocities and percentage changes in CBF [15]. Flow velocity and CBF changes to hyperventilation in normal volunteers revealed changes that reflected a slope 0.8 with a y-intercept close to zero, again suggesting that relative changes in flow velocities approximated changes in CBF [16].

8.4.1 *Cerebral Autoregulation (CA)*

Cerebral autoregulation (CA) is defined as the ability of the cerebrovascular system to maintain relative constant CBF despite changes in cerebral perfusion pressure [17]. Thus, cerebral autoregulation is defined as a pressure phenomenon. The majority of autoregulatory control occurs at the level of the cerebral arterioles. Arterioles will constrict and dilate in response to increases and decreases in cerebral perfusion pressure, respectively, to maintain constant CBF between a cerebral perfusion pressure (CPP) of 50–150 mmHg [18]. CBF outside of these ranges becomes dependent upon the perfusion pressure. A significant proportion of vascular resistance, however, is also mediated at the level of the small arteries. Alterations in sympathetic tone of these pial arteries can shift the autoregulatory curve upward or downward [19] (Fig. 8.3).

The theoretical mechanisms by which CBF is maintained over a wide range of perfusion pressures are quite extensive and beyond the scope of this review. Briefly, however, hypothesized mechanisms can be grouped into myogenic, metabolic, and neurogenic categories. The myogenic theory postulates that smooth muscle cells of the arteries and arterioles constrict or dilate in response to changes in transmural pressure generated across the vessel wall [20]. This may be mediated through alterations in the position of the actin-myosin filaments in these smooth muscles [21].

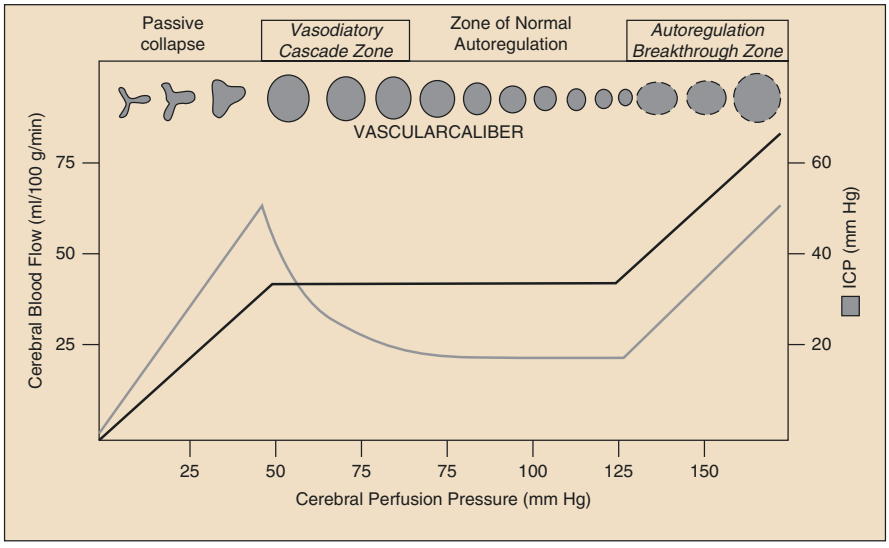

Fig. 8.3 Dark line representing the autoregulatory curve. Note CBF matches CPP at the extremes of the curve. The lighter line represents cerebral blood volume and the above vessels refer to the state of patency at varying cerebral perfusion pressures. (Rose and Mayer [18])

The metabolic theory postulates that local changes in cerebral blood flow release a variety of substances that both affect vessel diameter and couple flow with metabolism [22]. The neurogenic theory suggests that small intrinsic nerves may be responsible for changes in CBF [23].

8.4.2 CO_2 Vasoreactivity

Unlike cerebral autoregulation which is a pressure phenomenon, CO_2 vasoreactivity is a metabolic phenomenon. There is a direct increase in CBF with increasing $PaCO_2$ [24, 25]. The response curve of CBF to Pa CO_2 is sigmoidal with the CBF response flattening below 15–20 mmHg and above 100 mmHg (Fig. 8.3). $PaCO_2$ will freely diffuse across the blood–brain barrier; however, changes in CBF are mediated through changes in cerebral spinal fluid (CSF) hydrogen ion concentration. These changes, however, are short-lived as the choroid plexus of the brain will equilibrate and buffer these changes over a few hours [26] returning CBF to its baseline level. Cerebrovascular reserve is a terminology that is used to define the amount of flow during maximal arteriolar dilation. It is described as a percentage of maximal dilation [27].

8.5 TCD/TCCS: Assessment of Cerebral Autoregulation and CO_2 Vasoreactivity

The assessment of cerebral autoregulation and CO_2 vasoreactivity requires continuous monitoring of TCD/TCCS flow velocities during manipulations of blood pressure and CO_2, respectively. Technically, this is achieved through the use of a head holder that locks down the probes during insonation of bilateral flow velocities in the vessels of interest.

Cerebral autoregulation can be evaluated under dynamic or static conditions. Dynamic testing involves an induced drop in blood pressure or spontaneous blood pressure oscillations during continuous TCD monitoring. Induced changes are often performed during rapid deflation of thigh blood pressure cuffs. The abrupt drop in blood pressure leads to a mirrored drop in TCD flow velocities. In patients with poor autoregulation, TCD flow velocities will parallel a slow return in blood pressure. In patients with intact autoregulation, TCD/TCCS flow velocities will return to baseline immediately and will precede improvements in blood pressure. A similar type of response called a transient hyperemic response to carotid compression can also be employed [28]. In practice, however, these tests are rarely utilized in the intensive care unit.

Static autoregulation is measured using pharmacologic manipulation of blood pressure during continuous TCD monitoring. It is calculated as a percentage change in cerebrovascular reserve (CVR) / a percent change in CPP x 100. CVR is defined

as CPP /mean TCD velocities Using this method, autoregulation is expressed as a percentage with 100% signifying intact autoregulation [29, 30].

CO_2 vasoreactivity can similarly be addressed while measuring continuous TCD flow velocities during manipulation of PCO_2. This can be achieved through breath holding or changes in inspired pCO_2. Acetazolamide can similarly be used, but concerns have been raised using this pharmacology since acetazolamide may directly affect middle cerebral artery (MCA) diameter during testing and may complicate the calculation of changes in CBF [31].

8.6 TCD/TCCS: Use in the Neurological Critical Care Unit

8.6.1 TCD/TCCS: Use in Subarachnoid Hemorrhage

TCD can be used in the neuro ICU for a variety of neurological processes. It is most commonly used to detect the development of cerebral vasospasm after subarachnoid hemorrhage. Cerebral vasospasm is a self-limited vasculopathy that develops 4–14 days after subarachnoid hemorrhage. Pathologically, the basal cerebral arteries develop a T-cell infiltrate, collagen remodeling, and smooth muscle proliferation [32]. This can potentially lead to vessel narrowing and cerebral ischemia. Vasospasm appears to be a reaction to the amount and location of subarachnoid blood as first described by Fisher [33] and later verified by Kistler [34].

Prior to the development of TCD, vasospasm could only be detected through the use of cerebral angiography. Aaslid was able to demonstrate, however, a good correlation between MCA flow velocities and actual vessel luminal diameter as measured by angiography. Mean MCA flow velocities greater than 120 cm/s represented mild narrowing, while flow velocities greater than 200 cm/sec represented severe narrowing [1].

While TCD flow velocities can correlate with vessel narrowing, using TCD to predict which patients will develop subsequent cerebral ischemia has been more problematic. Initial studies suggested that absolute or rapid increases in flow velocities were indicative of impending neurological deficits [35, 36]. However, subsequent studies could not reproduce these findings [37].

The reasons for this discrepancy in findings may be technical. TCD flow velocities need to be corrected for a variety of physiological parameters [38] but in practice rarely are. In an attempt to differentiate increased blood flow from vessel narrowing, Lindegaard developed a ratio of flow velocities from the extracranial carotid artery to the MCA. Elevated flow velocities in the MCA not matched in the extracranial internal carotid artery (ICA) would suggest vessel narrowing, while similar changes would suggest hyperemia [39]. Similar ratios have been developed for the posterior circulation [40]. Disturbances in cerebral autoregulation after subarachnoid hemorrhage can lead to a misinterpretation of TCD flow velocities. Manipulations of blood volume and blood pressure commonly employed for

treatment of cerebral vasospasm can directly affect TCD flow velocities in patients with disturbed autoregulation [30]. Measurements of cerebral vascular reserve in patients with vessel narrowing may prove to be predictive of which patients are at risk for developing ischemic deficits [41].

Finally, the premise that vessel narrowing is the source of cerebral ischemia after subarachnoid hemorrhage may be inaccurate. Recent speculations have suggested that the hemoglobin released into the subarachnoid space binds spinal fluid nitrous oxide which is needed for vasomotor coupling of metabolism to CBF [42]. Rabinstein reported that most cerebral infarcts after subarachnoid hemorrhage occurred in vascular territories unaffected by vessel narrowing [43]. Similarly, the results of the Conscious-2 trial a randomized study of an endothelin receptor antagonist reported significant improvement in vessel narrowing after subarachnoid hemorrhage with no effect on ischemic deficits or outcome [44].

8.6.2 TCD/TCCS: Use After Traumatic Brain Injury (TBI)

TCD/TCCS has been used to facilitate management in the intensive care unit [45]. TCD use after TBI can be utilized to estimate intracranial pressure (ICP), determine the status of cerebral autoregulation, and determine if cerebral vasospasm.

Changes in TCD waveforms have been documented with increases in ICP. Loss of distal compliance leads to an increased pulsatility index. Continued increases lead to loss of diastolic flow velocities. At extreme levels, systolic spikes and loss of TCD waveforms are noted [46]. Pulsatility indexes have been correlated with ICP in a variety of cerebral conditions; however, attempts to define ICP based on TCD/TCCS waveform analysis have fallen short [47].

While TCD/TCCS waveforms as yet cannot be used to replace ICP, monitoring increases in pulsatility indexes can be used to potentially identify expanding lesions, focal or global increases in ICP, and decreases in CPP. Continuous TCD monitoring has noted an increase in pulsatility indexes in head trauma patients at their CPP dropped below 70 mmHg, thus potentially providing a warning for inadequate perfusion [48]. Flow velocities below 35 cm/sec suggesting decreased CBF after head trauma have been associated with poor outcomes [48, 49]. Similarly, loss of cerebral autoregulation is common after head trauma and has been associated with worse outcomes. Identifying these disturbances early in the post-traumatic course may allow for individualized therapies [50, 51].

Traumatic subarachnoid hemorrhage is common, and cerebral vasospasm can develop in similar patterns as detected after aneurysmal subarachnoid hemorrhage. Cerebral vasospasm after head trauma has been identified as a predictor of poor outcome [52], and medical maneuvers designed to increase CBF can potentially be employed. Interestingly, posterior circulation vasospasm is more common after traumatic subarachnoid hemorrhage [53].

8.6.3 TCD/TCCS: Confirmation of Brain Death

TCD can be utilized as a confirmatory test to assess for the absence of CBF in patients that have met criteria for brain death. The portability of TCD allows for the assessment of hemodynamically unstable patients that may not tolerate transfer outside of the intensive care unit. TCD use as a confirmation test has been reported to shorten the time of diagnosis.

Several patterns of waveforms have been described to indicate the absence of effective perfusion. These include small systolic spikes, oscillating flow, and loss of signal which had previously been isolated [54]. If vessels have not been previously insonated, the absence of signal cannot be utilized since in about 10% of patients' vessels cannot be insonated through the temporal bone. Sensitivity increases with the number of vessels which can be isolated. A lower false-positive rate has been reported when using a transorbital approach [55].

A recent meta-analysis confirmed the diagnostic accuracy or TCD confirmation of brain death, and most countries accept TCD as an ancillary test to confirm brain death [56]. Consensus guidelines for the determination of circulatory arrest have been proposed by the World Federation of Neurology [57]. Despite this, Canada, Australia, and New Zealand prefer other methods for confirmation [58].

8.6.4 TCD/TCCS: Use in Intracerebral Hemorrhage

TCD use after intracerebral hemorrhage traditionally had limited value. Poorer outcomes have been noted in patients with disturbed cerebral autoregulation and CO_2 vasoreactivity [59]. Differences in the middle cerebral artery pulsatility indexes may suggest side-to-side differentials in ICP.

Newer sonographic techniques have been used in the ICU to evaluate intracerebral hemorrhages. Transcranial color-coded sonography has identified spontaneous hemorrhages [60]. Transcranial duplex sonography has identified midline shift after intracerebral hemorrhage and has been utilized to predict outcome after hemorrhage [61, 62].

8.6.5 TCD/TCCS: Other Uses in the Intensive Care Unit

A variety of information can be gathered during routine TCD evaluation. Evidence for midline shift or a different location of a vessel previously insonated can suggest the development of a mass lesion. High-intensity transient signals (HITS) suggest recurrent emboli which can be detected during transient ischemic attack evaluation

or post-carotid endarterectomy [63]. Reversal or patency of vessels can be evaluated using TCD after bypass operations. Changes in vascular resistance can signify a local mass lesion or decreased perfusion. All may point to the need for additional imaging. More recently, increased continuous MCA flow velocities were noted during episodes of non-convulsive status epilepticus [64].

8.7 Conclusion

TCD/TCCS has gained increasing acceptance and use due to its many advantages of ease of use and access, cost, portability, and reliability. By measuring flow velocities, both cerebral and CO_2 vasoreactivity can be assessed providing valuable information to the neurological status of the patient. TCD, while unable to predict with confidence which patients will develop ischemic complications after subarachnoid hemorrhage, is quite useful in identifying that cerebral vasospasm is developing. Subsequently, this can focus neurological assessments and treatments. It is a useful tool in several circumstances for confirming brain death in the hemodynamically unstable patient. Newer sonographic techniques have been developed that will offer promising new insights into both the pathogenesis and prognosis of a number of acute neurological conditions.

References

1. Aaslid R, Markwalder T-M, Nornes H. Noninvasive transcranial Doppler ultrasound recording of flow velocity in basal cerebral arteries. J Neurosurg. 1982;57:769–74.
2. Fick A. Ueber die Messung des Blutquantums in den Herzventrikeln. Sitz ber Physik-Med Ges Wurzburg. 1870;2:16–28.
3. Kety SS, Schmidt CF. The determination of cerebral blood flow in man by the use of nitrous oxide in low concentrations. Am J Phys. 1945;143:53–66.
4. Manno EM, Koroshetz WJ. Cerebral blood flow. Chapter 5. In: Babikian VL, Wechsler LR, editors. Transcranial Doppler ultrasonography. 2nd ed. Boston: Butterworth Heinmann; 1999. p. 67–87.
5. Aaslid R. Development of the principles of transcranial Doppler ultrasound. In: Aaslid R, Newell DE, editors. Transcranial Doppler. New York: Raven Press; 1992. p. 1–8.
6. Saver JL, Feldmann E. Basic transcranial Doppler examinations. In: Babikian VL, Wechsler LR, editors. Transcranial Doppler ultrasonography. Mosby-Year Book: St Louis; 1993. p. 11–28.
7. Manno EM. Transcranial Doppler ultrasonography in the neurocritical care unit. In: Diringer MN, editor. Critical care clinics, vol. 13. Philadelphia: W.B. Saunders; 1997. p. 79–104.
8. Sorteberg W. Cerebral artery blood velocity and cerebral blood flow. In: Newell DW, Aaslid R, editors. Transcranial Doppler. New York: Raven; 1992. p. 57–66.
9. Sorteberg W, Lindegaard KF, Rootwell K, et al. Blood velocity and regional blood flow in defined cerebral artery systems. Acta Neurochir. 1989;97:47–52.
10. Schoning M, Walter J, Scheel P. Estimation of cerebral blood flow through color duplex sonography of the carotid and vertebral arteries in healthy adults. Stroke. 1994;25:17–22.

11. Kirkham FJ, Padayachee TS, Parsons S, et al. Transcranial measurement of blood velocities in the basal cerebral arteries using pulsed Doppler ultrasound: velocity as an index of flow. Ultrasound Med Biol. 1986;12:15–21.
12. Dahl A, Russell D, Nyberg-Hansen R, et al. Simultaneous assessment of vasoreactivity using transcranial Doppler ultrasound and cerebral blood flow in healthy subjects. J Cereb Blood Flow Metab. 1994;14:974–81.
13. Sorteberg W, Lindegaard KF, Rootwell K, et al. Effect of acetazolamide on cerebral artery blood velocity and regional cerebral blood flow in normal subjects. Acta Neurochir. 1989;97:47–52.
14. Naylor AR, Merrick MV, Slattery JM, et al. Parametric imaging of cerebrovascular reserve. Eur J Nucl Med. 1991;18:259–64.
15. Kofke WA, Brauer P, Policare R, et al. Middle cerebral artery blood flow velocity and stable xenon-enhanced computed blood flow during test balloon occlusion of the internal carotid artery. Stroke. 1995;26:1603–6.
16. Hartmann A, Ries F, Tsuda Y, et al. Correlation of regional cerebral blood flow and blood flow velocity in normal volunteers and patients with cerebro-vascular disease. Neurochirgia (Stuttg). 1991;34:6–13.
17. Manno EM, Rabinstein AA. Central nervous system. Chapter 43. In: Gabriella A, Layton AJ, Yu M, editors. Civetta, Taylor, and Kirby's critical care. 4th ed. Philadelphia: Wolters Kluver Lippincott Williams and Wilkins; 2009. p. 649–65.
18. Rose JC, Mayer SA. Optimizing blood pressure in neurological emergencies. Neurocrit Care. 2004;1:287–99.
19. Edvisson L. Neurogenic mechanisms in the cerebrovascular bed. Autonomic nerves, amine receptors, and their effects on cerebral blood flow. Acta Physiol Scand Suppl. 1975;427:1.
20. Kontos HA, Wei EP, Navari RM, et al. Responses of cerebral arteries and arterioles to acute hypotension and hypertension. Am J Physiol Heart Circ Physiol. 1978;234:H371.
21. Folkow B. Description of the myogenic hypothesis. Circ Res. 1964;15:279–87.
22. Chillon JM, Baumbach JL. Autoregulation: arterial and intracranial pressure. In: Edvisson L, Krause DN, editors. Cerebral blood flow and metabolism. 2nd ed. Philadelphia: Lippincott Williams and Wilkens; 2002. p. 395–412.
23. Lou HC, Edvission L, MacKenzie ET. The concept of coupling blood flow to brain function: revision required? Ann Neurol. 1987;22:289.
24. Ginsberg MD. Cerebral circulation: its regulation, pharmacology, and pathophysiology. In: Asbury AK, McKhann GM, McDonald WI, editors. Diseases of the nervous system clinical neurobiology. Philadelphia: Saunders; 1992. p. 989–1001.
25. Harper AM, Glass HI. Effect of alterations in the arterial carbon dioxide tension on the blood flow through the cerebral cortex at normal and low arterial pressures. J Neurol Neurosurg Psychiatry. 1965;28:449–52.
26. Ropper AH. Treatment of intracranial hypertension. In: Ropper AH, editor. Neurological and neurosurgical intensive care. 3rd ed. New York: Raven Press; 1993. p. 29–52.
27. Ringelstein EB, Otis SM. Physiological testing of vasomotor reserve. Chapter 8. In: Newell DW, Aaslid R, editors. Transcranial Doppler. New York: Raven; 1992. p. 83–100.
28. Aaslid R. Cerebral Hemodynamics chapter 5. In: Newell DW, Aaslid R, editors. Transcranial Doppler. New York: Raven; 1992. p. 49–55.
29. Tiecks FP, Lam AM, Aaslid R, Newell DW. Comparison of static and dynamic autoregulation measurements. Stroke. 1995;26:1014–9.
30. Manno EM, Gress DR, Schwamm LH, et al. Effects of induced hypertension on transcranial Doppler ultrasound velocities in patients after subarachnoid hemorrhage. Stroke. 1998;29:422–8.
31. Ringelstein EB, van Eyck S, Mertens I. Evaluation of cerebral vasomotor reactivity by various vasodilating stimuli: comparison of CO2 with acetazolamide. J Cereb Blood Flow Metab. 1992;12:162–8.
32. Tresser SJ, Selmon WR, Ratcheson RA. Pathophysiological alterations following aneurysm rupture. Concepts Neurosurg. 1994;6:23–45.

33. Fisher CM, Kistler JP, Davis JM. Relation of cerebral vasospasm to subarachnoid hemorrhage visualized on computed tomographic scanning. Neurosurgery. 1980;6:1–9.
34. Kistler JP, Crowell RM, Davis KR, et al. The relation of cerebral vasospasm to the extent and location of subarachnoid blood visualized by CT scan: a prospective study. Neurology. 1983;33:424–36.
35. Seckhar LN, Wechsler LR, Yonas H, et al. Value of transcranial Doppler examination in the diagnosis of cerebral vasospasm after subarachnoid hemorrhage. Neurosurgery. 1988;22:813–21.
36. Sloan MA, Rigamonti D, Rothman M, et al. Sensitivity and specificity of transcranial Doppler ultrasound in the diagnosis of vasospasm following subarachnoid hemorrhage. Neurology. 1989;39:1514–8.
37. Laumer R, Steinmeier R, Gonner F, et al. Cerebral hemodynamics in subarachnoid hemorrhage evaluated by transcranial Doppler ultrasonography. Part 1: reliability of flow velocities in clinical management. Neurosurgery. 1993;33:1–9.
38. Brass LM, Pavlakis SG, DeVivo D, et al. Transcranial Doppler measurements of the middle cerebral artery: effect of hematocrit. Stroke. 1988;19:1466–9.
39. Lindegaard KF, Nornes H, Bakke SJ, et al. Cerebral vasospasm after subarachnoid hemorrhage investigated by means of transcranial Doppler ultrasound. Acta Neurochir Suppl (Wien). 1988;42:81–4.
40. Soustiel JF, Shik V, Schreiber R, et al. Basilar vasospasm diagnosis: investigation of a modified "Lindegaard index" based on imaging studies and blood velocity measurements of the basilar artery. Stroke. 2002;33:72–7.
41. Hassler W, Chioffi F. CO2 reactivity of cerebral vasospasm after aneursysmal subarachnoid hemorrhage. Acta Neurochir. 1989;98:167–75.
42. Siuta M, Zuckerman SL, Mocco J. Nitric oxide in cerebral vasospasm. Theories measurement and treatment. Neurology Research International; 2013;2013:11. Article ID 972417.
43. Rabinstein AA, Weigand S, Atkinson JL, Wijdicks EF. Patterns of cerebral infarction in aneurysmal subarachnoid hemorrhage. Stroke. 2005;36:992–7.
44. MacDonald RL, Higashida RT, Keller E, et al. Clazosentan, an endothelian receptor antagonist in patients with subarachnoid hemorrhage undergoing surgical clipping: a randomized double blinded placebo controlled phase 3 trial (conscious −2). Lancet Neurol. 2011;10:618–25.
45. White H, Venkatesh B. Applications of transcranial Doppler in the ICU: a review. Intensive Care Med. 2006;32:981–94.
46. Hassler W, Steinmetz H, Gawloswski J. Transcranial Doppler ultrasongraphy in raised intracranial pressure and in circulatory arrest. J Neurosurg. 1988;68:745–51.
47. Klingelhofer J, Conrad B, Benecke R, et al. Evaluation of intracranial pressure from transcranial Doppler studies in cerebral disease. J Neurol. 1988;235:159–62.
48. Chan K-H, Miller JD, Dearden NM. Intracranial blood flow velocity after head injury: relationship to severity of injury, time, neurological status, and outcome. J Neurol Neurosurg Psychiatry. 1992;55:787–91.
49. Van Santbrink H, Schouten JW, Steyerberg EW, et al. Serial transcranial Doppler measurements in traumatic brain injury with special focus on the early posttraumatic period. Acta Neurochir. 2002;144:1141–9.
50. Vavilala MS, Lee LA, Boddu K, et al. Cerebral autoregulation in pediatric traumatic brain injury. Pediatr Crit Care Med. 2004;5:257–63.
51. Schmidt EA, Czosnyka M, Steiner LA, et al. Asymmetry of pressure autoregulation after traumatic brain injury. J Neurosurg. 2003;99:991–8.
52. Compton JS, Teddy PJ. Cerebral arterial vasospasm following severe head injury: a transcranial Doppler study. Br J Neurosurg. 1987;1:435–9.
53. Martin NA, Doberstein C, Zane C, et al. Posttraumatic cerebral arterial spasm: transcranial Doppler ultrasound, cerebral blood flow, and angiographic findings. J Neurosurg. 1992;77:575–83.
54. Azevedo E, Teixeira J, Neves JC, Vaz R. Transcranial Doppler and brain death. Transplant Proc. 2000;32:2579–81.

55. Dominguez-Roldan JM, Jimenez-Gonzalez PI, Garcia-Alfaro C, et al. Diagnosis of brain death by transcranial Doppler sonography: solutions for cases of difficult sonic windows. Transplant Proc. 2004;36:2896–7.
56. Chang JJ, Tsivgoulis G, Katsanos AH, et al. Diagnostic accuracy of transcranial Doppler for brain death confirmation: systemic review and meta-analysis. AJNR. 2016;37:408–14.
57. Ducrocq X, Hassler W, Moritake K, et al. Consensus opinion on diagnosis of cerebral circulatory arrest using Doppler-sonography: task force group on cerebral death of the neurosonology research group of the World Federation of Neurology. J Neurol Sci. 1998;159:145–50.
58. Young GB, Shemie SD, Doig J, Teitelbaum JT. Brief review: the role of ancillary tests in the neurological determination of death. Can J Anesth. 2006;53:620–7.
59. Klingelhofer J, Sander D. Doppler CO2 test as an indicator of cerebral vasoreactivity and prognosis in severe intracerebral hemorrhage. Stroke. 1992;23:962–6.
60. Kukulska-Pawluczul B, Ksiazkiewicz B, Nowaczewska M. Imaging of spontaneous intracerebralhemorrhages by means of transcranial colr-coded sonography. Europ J Radiol. 2012;81:1253–8.
61. Kiphuth IC, Huttmer HB, Breuer L, et al. Songraphic monitoring of midline shift predicts outcome after intracerebral hemorrhage. Cerebrovascular Dis. 2012;34:297–304.
62. Camps-Renom P, Granell JME, Prats-Sanchez L, et al. Transcranial duplex sonography predicts outcome following intracerebral hemorrhage. AJNR. 2017;38:1543–9.
63. Spencer MP, Thomas GI, Nicholls SC, Sauvage LR. Detection of middle cerebral emboli during carotid endarterectomy using transcranial doppler ultrasound. Stroke. 1990;21:415–23.
64. Merceron S, Geeraerts T, Montlahuc C, et al. Assessment of cerebral blood flow in nonconvulsive status epilepticus in comatose patients: a pathophysiological transcranial Doppler study. Seizure. 2014;23:284–9.

Part III
Neurosonology: Neurocritical Care Patient

Chapter 9
Transcranial Doppler (TCD/TCCS) and Cerebral Blood Flow Velocities: Parameters of Normality

Jorge H. Mejía Mantilla, Pablo F. Amaya, and Leidy Gaviria Villarreal

Key Points

1. The interpretation of the values obtained by TCD/TCCS examination is dependent on the clinical context and the systemic circulatory status, with reference to the normal values expected for a patient.
2. The identification of the insonated vessel depends on the window, the direction of the probe points, the depth of insonation and the direction of flow in the vessel; therefore, after appropriate training an examiner can accurately identify the vessels.
3. Studies discovered that cerebral blood flow velocity is not the same in women as in men. It found that females usually have higher velocity than contemporary males without differences in pulsatility or resistance indexes.
4. Cerebral blood flow is auto-regulated, and its distribution throughout the brain depends partially on the metabolic activity of the tissue. Therefore, in actively working brains, we can expect to find higher CBF, hence higher cerebral blood flow velocities (CBFV) in the side with higher metabolic activity.
5. Cerebral blood flow velocities (CBFVs) are higher in younger persons. The decline in velocities is found in most series after the fifth decade, and thereafter there is a steady decrease in mean velocity in most series.

J. H. Mejía Mantilla (✉)
Head Neurointensive Care Unit, Department of Critical Care and Anesthesiology, Hospital Universitario Fundación Valle del Lili, Cali, Colombia
e-mail: Jorge.mejia@fvl.org.co

P. F. Amaya
Hospital Universitario Fundación Valle del Lili, Cali, Colombia
e-mail: pablo.ricardo@fvl.org.co

L. G. Villarreal
Clinical Research Unit, Hospital Universitario Valle del Lili, Cali, Colombia
e-mail: leidy.gaviria@fvl.org.co

C. N. Rodríguez et al. (eds.), *Neurosonology in Critical Care*,
https://doi.org/10.1007/978-3-030-81419-9_9

6. Reference values for a local population should be constructed by insonating healthy subjects at rest in a calm and comfortable setting. The operator should be an expert in the TCD technique, and it is preferable to limit the number of operators in order to avoid potential bias of inter-observer variability.

9.1 Introduction

Transcranial Doppler (TCD) is a low-cost bedside, noninvasive method to evaluate a patient's cerebral haemodynamics in real time [1]. TCD variations have a good correlation with invasive methods for the measurement of cerebral blood flow (CBF), as intravenous $Xenon^{133}$ [2], indicating that TCD accurately evaluates changes in CBF.

TCD allows the measurement of blood flow velocity in intracranial arteries and the indexes derived: pulsatility, resistance and hemispheric index. It allows to evaluate the anterior and posterior circulation throughout the cranial windows: transorbital and transtemporal for supra-tentorial circulation, and suboccipital for infra-tentorial circulation. Cervical Doppler allows to evaluate internal carotid artery in its extracranial portion, to estimate the hemispheric Lindegaard ratio, which is useful to discriminate between situations of hyper-flux and vasospasm [3].

The reproducibility of TCD has been studied by Maeda et al. both for inter-observer and intra-observer variabilities; they found a good agreement for repeated measurements provided arterial pressure and $PaCO_2$ are kept constant in the subject [4]. They found a Coefficient of Variation (CV) of 7.5% and a correlation coefficient (r) of 0.95 for Middle Cerebral Artery (MCA) mean blood flow velocity, and a CV of 13.5% and r of 0.83 for Basilar Artery (BA) mean blood flow velocity for intra-observer reproducibility. The values for inter-observer variability show a slightly wider variability: CV of 10.5% and r of 0.9 for MCA and CV of 17.5% and r of 0.78 for BA assessment. Even though these values are statistically significant, the clinical impact of such differences is considered acceptable for a bedside measurement method of CBF velocity, especially for MCA. According to their analysis, the main source of variation of results is the position of the probe in the sonographic window of the patient, since small variation in the insonation angle can lead to important discrepancy in reported blood flow velocity [5]. They note that the insonation window is smaller for MCA than the window for BA exam; this might explain the wider variation in the assessment of posterior circulation.

The interpretation of the values obtained by TCD/TCCS examination is dependent on the clinical context and the systemic circulatory status, with reference to the normal values expected for a patient; those normal values have been published by several authors since the beginning of the technique. We will discuss in this chapter the published reference values for different populations, the normal values we found in our city, and the recommendations for local reference value findings.

9.2 TCD/TCCS and CBFV: Normal Values in Early Studies

The identification of the insonated vessel depends on the window, the direction the probe points, the depth of insonation and the direction of flow in the vessel; therefore, after appropriate training an examiner can accurately identify the vessels [6]. It is important to know the reference values for depth of insonation, direction of flow and normal velocity for a correct interpretation of the examination, so early authors undertook the task of building reference values' tables that are commented in this text.

Since the beginning of the technique in 1980s, the use of TCD ultrasonographers committed to the task with 1 to 2 MHz dedicated probes has produced similar results in various countries. It was later evident that the reference values varied according to age and sex of the subjects (Arnolds 1986). The first works reported the shift of ultrasound in its original units: Kilohertz, but this was not useful to the clinician [7]. Soon afterward, the corresponding velocity of flow was reported in cm/s, a much more useful information at the bedside. One of the first reports of normal values for peak (systolic), end-diastolic and mean velocities is by Hennerici et al. from Düsseldorf [8] (Table 9.1), one of the first reporting an age drift. Other investigators reported the reference values for daily variation [4, 9], spontaneous or induced variations of $EtCO_2$ [9, 10], right and left side velocities [11] and wakefulness–sleep cycle [12]; we will not address those topics here.

Table 9.1 Normal values as reported by Hennerici in normal subjects from Germany

Arteries (depth in mm)	Systolic peak velocity (cm/sec)	Averaged mean velocity (cm/sec)	Diastolic peak velocity (cm/sec)	Age (years)
MCA (50 mm)	94.5 ± 13.6 91.0 ± 16.9 78.1 ± 15.0	58.4 ± 8.4 57.7 ± 11.5 44.7 ± 11.1	45.6 ± 6.6 44.3 ± 9.5 31.9 ± 9.1	<40 40–60 >60
ACA (70 mm)	76.4 ± 16.9 86.4 ± 20.1 73.3 ± 20.3	47.3 ± 13.6 53.1 ± 10.5 45.3 ± 13.5	36.0 ± 9.0 41.1 ± 7.4 34.2 ± 8.8	<40 40–60 >60
PCA (60 mm)	53.2 ± 11.3 60.1 ± 20.6 51.0 ± 11.9	34.2 ± 7.8 36.6 ± 9.8 29.9 ± 9.3	25.9 ± 6.5 28.7 ± 7.5 22.0 ± 6.9	<40 40–60 >60
VA/BA (75 mm)	56.3 ± 7.8 59.5 ± 17.0 50.9 ± 18.7	34.9 ± 7.8 36.4 ± 11.7 30.5 ± 12.4	27.0 ± 5.3 29.2 ± 8.4 21.2 ± 9.2	<40 40–60 >60

MCA middle cerebral artery, *ACA* anterior cerebral artery, *PCA* posterior cerebral artery, *VA* vertebral artery, *BA* basilar artery

9.3 TCD Hemodynamic Parameters: Variations by Sex

The earliest studies did not agree in their results about this point; Macchi et al. in a sample of 120 volunteers from 19 to 89 years old found no difference between males and females [13] in artery calibre, systolic and mean blood flow velocity, despite differences in cranial size and body weight.

By contrast, other studies discovered that cerebral blood flow velocity is not the same in women than in men; Vriens in 120 subjects aged 20 to 70 years found that females usually have higher velocity than contemporary males [10] without differences in pulsatility or resistance indexes [14]. Other groups report the same finding [13, 15–17]; this difference disappears with hyperventilation, resulting in a decrease of CBF velocity to similar values in both sexes. We summarized those reports in Tables 9.2, 9.3, and 9.4.

Table 9.2 Mean flow velocity (MFV) in TCD by sex. Data extracted from the original publications

Study	Country	Year	*N*	Sex	MFV Velocity (cm/seg)					
					MCA	ACA	PCA	ICA	VA	BA
P. Grolimund	Switzerland	1986	535	Female	59.9 ± 31	51.1 ± 33	40.2 ± 22	39.2 ± 19		
				Male	55.7 ± 28	48 ± 7	35.2 ± 19	34.3 ± 25		
Macchi C	Italy	1994	120	Female	61.9 ± 23	49.9 ± 23	42.8 ± 26			
				Male	63.0 ± 23	50.0 ± 26	44.0 ± 22			
Tegeler CH	USA	2013	364	Female	61.6 ± 23	51.9 ± 19	30.6 ± 12	37.2 ± 20	36.2 ± 19	43.7 ± 21
				Male	56.4 ± 24	47.1 ± 20	27.5 ± 10	35.4 ± 16	29.3 ± 16	35.8 ± 18
Dixon Yang	USA	2015	369	Female	32.8 ± 1	30.6 ± 1	27.9 ± 1		19.8 ± 1	22.0 ± 1
				Male	33.9 ± 1	30.9 ± 1	28.7 ± 1		20.3 ± 1	23.3 ± 1

MCA middle cerebral artery, *ACA* anterior cerebral artery, *PCA* posterior cerebral artery, *ICA* Internal Carotid Artery, *VA* vertebral artery, *BA* basilar artery

Table 9.3 Resistance index (RI) in TCD by sex. Data extracted from the original publications

Study	Country	Year	*n*	Sex	Resistance Index (RI)				
					MCA	ACA	PCA	VA	BA
Dixon Yang	USA	2015	369	Female	0.78 ± 0.01	0.80 ± 0.01	0.78 ± 0.01	0.70 ± 0.01	0.72 ± 0.01
				Male	0.74 ± 0.01	0.76 ± 0.01	0.76 ± 0.01	0.69 ± 0.01	0.72 ± 0.01

MCA middle cerebral artery, *ACA* anterior cerebral artery, *PCA* posterior cerebral artery, *VA* vertebral artery, *BA* basilar artery

Table 9.4 Pulsatility in TCD by sex. Data extracted from the original publications

Study	Country	Year	*n*	Sex	Pulsatility Index					
					MCA	ACA	PCA	ICA	VA	BA
Tegeler CH	USA	2013	364	Female	0,80 ± 0.26	0,80 ± 0.3	0,76 ± 0.24	0,87 ± 0.34	0,79 ± 0.26	0,79 ± 0.26
				Male	0,84 ± 0.26	0,85 ± 0.3	0,79 ± 0.34	0,87 ± 0.4	0,81 ± 0.36	0,84 ± 0.54
Dixon Yang	USA	2015	369	Female	1.64	1.75	1.65		1.33	1.41
				Male	1.51	1.59	1.55		1.33	1.45

MCA middle cerebral artery, *ACA* anterior cerebral artery, *PCA* posterior cerebral artery, *ICA* internal carotid artery, *VA* vertebral artery, *BA* basilar artery

It has been suggested that the gender difference was due to the lower haematocrit in women; furthermore, the hormonal status, especially oestrogen levels, appeared to contribute to the reactivity and in the vascular tone in the cerebral microcirculation of women [7, 18].

9.4 TCD Hemodynamic Parameters: Variations by Age

The seminal work by Aaslid in 50 subjects aged 20 to 65 years reported similar velocities in CBF [1]; several other studies have addressed this issue, with highly concordant results in every population reviewed: CBF velocity is higher in younger persons [7, 8, 10, 14, 19]. The Brazilian group found that the variations in velocity are more consistent in MCA, probably because the characteristics of this artery have little variability with age and are easier to insonate than the other intracranial vessels [20]. The decline in velocity is found in most series after the fifth decade [21], and thereafter there is a steady decrease in mean velocity in most series. The results of the available studies are summarized in Table 9.5.

9.5 TCD Hemodynamic Parameters: Variations by Laterally

Cerebral blood flow is auto-regulated, and its distribution throughout the brain depends partially on the metabolic activity of the tissue [22]; therefore, in actively working brains, we can expect to find higher CBF, hence, higher CBF velocity in the side with higher metabolic activity. Most studies for the determination of reference values are performed in resting subjects. Nevertheless, asymmetry between left and right sides has been described by Schmidt [11] as well as Farhoudi [23] in a recent study in Iranian population and by us in subgroups of subjects. This inconstant finding is probably due to mental activity during the insonation and not a permanent anatomical or physiological characteristic of cerebral circulation.

9.6 TCD Hemodynamic Parameters: Geographic and Ethnic Trends

We did not find any pattern in the distribution of reference values, as reported in several studies in Table 9.5 for velocity and Tables 9.6 and 9.7 for resistance and pulsatility indexes, respectively.

We searched for differences in cerebral haemodynamics related to living in altitude, but most studies have been performed in cities below 1000 m above sea level; one report from Iran was made at 1400 m above sea level. They report higher velocities in one of its tables, but the values are not consistent with another table in the

Table 9.5 Mean flow velocity in TCD by age

Author	Country	Date	*n*	Age	MFV velocity cm/s				
					MCA	ACA	PCA	VA	BA
Rune Aaslid	Switzerland	1982	50	20–65	62 ± 24	51 ± 24	44 ± 22		
P. Grolimund	Switzerland	1986	535	22–86	57.3 ± 30	49.2 ± 30	37.2 ± 19		
M. Hennerici	Germany	1987	50	<40	58.4 ± 17	47.3 ± 27	34.4 ± 16		
				40–60	57.7 ± 23	53.1 ± 19	36.6 ± 19		
				>60	44.7 ± 22	45.3 ± 27	29.9 ± 27		
E.B. Ringelstein	USA	1990	106	10–29	70 ± 32	61 ± 30	55 ± 18	45 ± 20	46 ± 22
				30–49	57 ± 23	48 ± 15	42 ± 18	35 ± 17	38 ± 18
				50–59	51 ± 20	46 ± 19	39 ± 20	37 ± 20	32 ± 14
				60–70	41 ± 14	38 ± 14	36 ± 16	35 ± 14	32 ± 14
RGA Ackerstaff	The Netherlands	1990	125	14–70	60.9 ± 28				
P.J. Martin	UK	1993	115	20–39	74 ± 3	60 ± 3	53 ± 2	44 ± 3	50 ± 3
				40–59	47 ± 3	61 ± 4	49 ± 2	40 ± 2	44 ± 5
				>60	58 ± 3	51 ± 3	42 ± 3	33 ± 3	35 ± 4
J. Krejza	Poland	1998	182	20–40	81 ± 40	56 ± 14	52 ± 34		
				41–60	73 ± 38	53 ± 16	51 ± 26		
				>60	59 ± 22	44 ± 22	40 ± 18		
M.F Barbosa	Brazil	2006	88	16–68	62 ± 20	48 ± 20	37 ± 16	32 ± 16	43 ± 9
S. Demirkaya	Turkey	2008	63	21–30	57.4 ± 23	43.6 ± 18	33.1 ± 11		
				31–40	57.9 ± 22	41.2 ± 19	37.7 ± 24		
				41–50	65.9 ± 29	43.0 ± 19	35.9 ± 19		
				51–60	51.3 ± 26	39.3 ± 19	32.2 ± 17		
				>60	46.9 ± 11	37.7 ± 13	31.6 ± 17		
M. Farhoundi	Iran	2010	80	25–55	62 ± 20	52 ± 20	43 ± 14	36 ± 18	48 ± 16
Tegeler CH	USA	2013	364	<30	66.6 ± 29	53.6 ± 20	30.9 ± 11	36.1 ± 22	42.1 ± 26
				30–39	64.6 ± 17	54.4 ± 17	31.8 ± 10	35.1 ± 16	41.0 ± 19
				40–49	60.0 ± 23	51.0 ± 18	30.0 ± 15	35.6 ± 18	40.7 ± 19
				50–59	56.6 ± 19	48.5 ± 18	28.8 ± 10	32.9 ± 17	38.0 ± 19
				60–69	51.2 ± 20	43.8 ± 18	26.4 ± 11	30.6 ± 16	35.5 ± 17
				70–80	49.6 ± 21	42.4 ± 23	25.3 ± 11	30.8 ± 23	35.6 ± 21
Dixon Yang	USA	2015	369	70–74	33.8 ± 1	32.2 ± 2	29.8 ± 2	20.7 ± 1	24.6 ± 2
				75–79	33.9 ± 2	29.4 ± 2	28.3 ± 1	19.4 ± 1	22.7 ± 1
				80–84	32.9 ± 3	30.1 ± 2	26.9 ± 2	20.9 ± 2	22.8 ± 2
				>85	32.2 ± 4	31.0 ± 3	27.6 ± 1	19.0 ± 2	21.0 ± 2

Data extracted from the original publication. Early works reported the shift of frequency instead of velocity, we performed the conversion to velocity according to Doppler equation. Data shown is limited to mean velocity, see original report for systolic or diastolic velocities

MCA middle cerebral artery, *ACA* anterior cerebral artery, *PCA* posterior cerebral artery, *ICA* Internal Carotid Artery, *VA* vertebral artery, *BA* basilar artery

Table 9.6 Resistance index in TCD by age

Author	Country	Date	*n*	Age	Resistance Index				
					MCA	ACA	PCA	VA	BA
RGA Ackerstaff	The Netherlands	1990	125	14–70	0.53 ± 0.12				
P.J. Martin	UK	1993	115	20–39	0.55 ± 0.01	0.53 ± 0.02	0.54 ± 0.02	0.54 ± 0.02	0.51 ± 0.05
				40–59	0.54 ± 0.01	0.53 ± 0.01	0.53 ± 0.02	0.53 ± 0.01	0.53 ± 0.02
				>60	0.62 ± 0.02	0.59 ± 0.02	0.60 ± 0.02	0.59 ± 0.02	0.60 ± 0.04
J. Krejza	Poland	1998	182	20–40	0.54 ± 0.02	0.53 ± 0.02	0.52 ± 0.03		
				41–60	0.55 ± 0.02	0.56 ± 0.02	0.53 ± 0.02		
				>60	0.60 ± 0.03	0.62 ± 0.03	0.60 ± 0.04		
M.F Barbosa	Brazil	2006	88	16–68	0.51 ± 0.05	0.52 ± 0.07	0.53 ± 0.08	0.51 ± 0.08	0.74 ± 0.02
Dixon Yang	USA	2015	369	70–74	0.75 ± 0.02	0.77 ± 0.02	0.76 ± 0.02	0.69 ± 0.02	0.72 ± 0.02
				75–79	0.76 ± 0.02	0.79 ± 0.02	0.76 ± 0.02	0.70 ± 0.02	0.71 ± 0.02
				80–84	0.76 ± 0.02	0.78 ± 0.02	0.77 ± 0.02	0.71 ± 0.02	0.73 ± 0.02
				>85	0.78 ± 0.02	0.80 ± 0.02	0.78 ± 0.02	0.69 ± 0.02	0.72 ± 0.02

Table 9.7 Pulsatility index in TCD by age

Study	Country	Year	*N*	Age	Pulsatility Index				
					MCA	ACA	PCS	VA	BA
RGA Ackerstaff	The Netherlands	1990	125	14–70	0.8 ± 0.34				
P.J. Martin	UK	1993	115	20–39	0.84 ± 0.02	0.82 ± 0.04	0.84 ± 0.04	0.82 ± 0.03	0.81 ± 0.05
				40–59	0.81 ± 0.02	0.76 ± 0.03	0.78 ± 0.03	0.78 ± 0.04	0.77 ± 0.04
				>60	0.97 ± 0.04	0.92 ± 0.05	0.97 ± 0.06	0.94 ± 0.05	0.95 ± 0.09
J. Krejza	Poland	1998	182	20–40	0.83 ± 0.07	0.80 ± 0.07	0.76 ± 0.06		
				41–60	0.82 ± 0.06	0.85 ± 0.08	0.79 ± 0.06		
				>60	0.96 ± 0.09	1.02 ± 0.09	0.94 ± 0.08		
M.F Barbosa	Brazil	2006	88	16–68	0.75 ± 0.13	0.78 ± 0.17	0.76 ± 0.18	0.73 ± 0.20	0.74 ± 0.19
M. Farhoundi	Iran	2010	80	25–55	0.76 ± 0.24	0.83 ± 0.34	0.76 ± 0.32	0.73 ± 0.26	0.82 ± 0.40
Tegeler CH	USA	2013	364	<30	0.85 ± 0.26	0.85 ± 0.28	0.77 ± 0.22	0.79 ± 0.26	0.82 ± 0.30
				30–39	0.80 ± 0.30	0.78 ± 0.24	0.71 ± 0.20	0.77 ± 0.25	0.76 ± 0.28
				40–49	0.76 ± 0.20	0.77 ± 0.22	0.74 ± 0.22	0.76 ± 0.30	0.77 ± 0.26
				50–59	0.80 ± 0.20	0.79 ± 0.20	0.77 ± 0.22	0.78 ± 0.24	0.79 ± 0.22
				60–69	0.85 ± 0.20	0.86 ± 0.20	0.83 ± 0.26	0.84 ± 0.22	0.85 ± 0.18
				70–80	0.95 ± 0.34	1.06 ± 0.66	0.99 ± 0.52	1.01 ± 0.48	1.03 ± 0.42
Dixon Yang	USA	2015	369	70–74	1.55 ± 0.08	1.61 ± 0.10	1.60 ± 0.08	1.29 ± 0.06	1.42
				75–79	1.56 ± 0.06	1.71 ± 0.08	1.58 ± 0.08	1.32 ± 0.06	1.40
				80–84	1.61 ± 0.08	1.71 ± 0.08	1.63 ± 0.08	1.37 ± 0.06	1.46
				>85	1.66 ± 0.08	1.73 ± 0.10	1.64 ± 0.06	1.33 ± 0.08	1.42

same paper [23]. We found a report from Sao Paulo [20], a multiethnic metropolis in Brazil, located at 760 m above sea level, and our own results are from 1000 m above sea level; we found no differences in transcranial Doppler results.

9.7 TCD Normal Values: Latin American Population Sample

We performed an evaluation of normal subjects in order to build our local reference values for Cali, Colombia, a multiethnic city at 995 meters above sea level [24]. Our published results on 51 healthy volunteers showed variation of velocities in intracranial arteries pending on age, sex, laterality and body mass index, but the magnitude of these variations and the strength of the associations are limited by the power of the study. We found slightly higher CBF velocity in subjects with body mass index under 25 than the CBF velocity in subjects over 30, but the comparison did not reach statistical significance. Therefore, we complemented our sample to improve the statistical power of our analysis, and the results are summarized in Table 9.8.

9.8 TCD Hemodynamic Parameters: Altitude

Analysis of the hemodynamic parameters (CBFVs and hemodynamic indexes/ratios) of cerebral basal arteries makes it possible to assess the changes that occur in each clinical situation and arrive at a specific diagnosis. Keep in mind, these hemodynamic parameters are influenced by anatomical and physiological variables as well as by the altitude.

Table 9.8 Normal values for the entire sample in Cali, Colombia

Artery	Pulsatility Index	MFV Velocity (cm/s)	Depth (mm)
Left side			
MCA	0.81 (0.63–1.14)	61.5 (35–93)	52 (48–59)
ICA	0.89 (0.62–1.26)	53 (33–75)	64 (59–71)
ACA	0.93 (0.65–1.78)	46 (27–64)	69 (62–78)
PCA	0.9 (0.61–1.28)	44 (27–64)	63 (57–72)
Right side			
MCA	0.83 (0.58–1.12)	62 (33–87)	53 (48–58)
ICA	0.86 (0.64–1.14)	53.5 (36–77)	64 (59–71)
ACA	0.93 (0.64–1.52)	45 (28–63)	70 (62–79)
PCA	0.865 (0.63–1.49)	41.5 (26–63)	64 (58–70)
Sub-occipital			
Basilar	0.78 (0.75–0.82)	45.0 (41.7–48.4)	87.5 (85.5–89.5
Vertebral	0.76 (0.72–0.80)	36.1 (33.0–39.2)	66.4 (64.7–68.1)

MCA middle cerebral artery, *ICA* Internal Carotid Artery, *ACA* anterior cerebral artery, *PCA* posterior cerebral artery

Table 9.9 Comparison of hemodynamic parameter values obtained with the results of other studies [27]

Study	Parameter	MCA(A1)	ACA(A1)	eICA	PCA (P1)	Basilar	Vertebral(V4)
Ecuador (2850 m) S.Matamoros et al. (2019) $n = 45$	MFV (cm/s)	49.3	39.9	34.6	34.6	36.7	26.0
	PI	0.8	0.8	0.8	0.8	0.8	0.7
Colombia (995 m) Franco et al. (2015) $n = 51$	MFV (cm/s)	59.8	47.4	31.5	37.4	45.1	35.8
	PI	0.74	1.01	0.8	0.77	0.78	0.76
Sao Paulo (760 m) Fregonesi B. et al. (2006) $n = 88$	MFV (cm/s)	62	48	–	37	43	32
	PI	0.51	0.52	–	0.53	0.51	0.51
Bern (Switzerland) (540 m) Aaslid et al. (1982) $n = 50$	MFV (cm/s)	62	51	37	44	–	–
	PI	–	–	–	–	–	–
Girona (Spain) (76 m) Segura et al. (1999) $n = 118$	MFV (cm/s)	54	43	–	34	37	29.1
	PI	0.98	1.01	–	1.01	1.03	1.01

ACA anterior cerebral artery, *MCA* middle cerebral artery, *eICA* extracranial internal carotid artery, *PCA* posterior cerebral artery, *PI* pulsatility index, *V4* intracranial vertebral artery, *MFV* mean flow velocity

In populations living at altitude, increased haemoglobin concentration is observed as a result of physiologically elevated red blood cell production, with a concomitant increase in blood viscosity [25]. This rheological change of the blood, together with arterial lumen area and vessel length, is the main determiners of CBF resistance, meaning that CBFV is inversely correlated with haematocrit level [26].

Table 9.9 compares the results of several studies conducted in normal subjects in populations at different altitudes.

Matamoros et al. (2019) [27] recruited 47 healthy Ecuadorian volunteers (altitude 2850 m); two patients were excluded because they did not have a viable cranial window for TCD study. Thus, we recorded mean flow velocity (MFV), peak systolic velocity, end-diastolic velocity and pulsatility indices (PI) in 45 patients (62.2% women; mean age, 35.9 years); recorded patient's age, sex and haematocrit; and analysed cerebrovascular hemodynamic parameters by sex and age groups.

Analysing the relationship between MFVs and sex, Table 9.10 showed results very similar figures to those obtained in other series. We recorded higher MFV values for women, a difference that appears to be dependent on the lower haematocrit levels found. Age is the most important factor modifying CBFVs in TCD. In the study, Table 9.11 showed analysed CBFVs in two age groups (over and under 40 years) and found a difference of 16.4% for the MCAs and 14.9% for the ACAs

Table 9.10 Mean flow velocity (MFV) and pulsatility index (PI) values by sex [27]

Artery	MFV (cm/s), SD		PI, SD	
	Men	Female	Men	Female
MCA(M1)	48.7 ± 15.5	49.6 ± 14.4	0.8 ± 0.1	0.7 ± 0.1
ACA(A1)	40.4 ± 12.9	39.7 ± 12.6	0.8 ± 0.2	0.8 ± 0.2
eICA	31.5 ± 5	36.4 ± 6.7	0.9 ± 0.2	0.8 ± 0.1
PCA(P1)	34 ± 12.3	34.9 ± 12.2	0.8 ± 0.1	0.8 ± 0.1
PCA(P2)	33.8 ± 9.9	35 ± 8.2	0.8 ± 0.2	0.9 ± 0.3
Basilar	32.5 ± 8.9	39.2 ± 10	0.8 ± 0.2	0.8 ± 0.2
V4	25.6 ± 6	26.3 ± 6.9	0.7 ± 0.2	0.7 ± 0.2

ACA anterior cerebral artery, *ICA* internal carotid artery, *MCA* middle cerebral artery, *PCA* posterior cerebral artery, *SD* standard deviation, *MFV* mean flow velocity

Table 9.11 Mean flow velocity (MFV) and pulsatility index (PI) by age [27]

Artery	MFV (cm/s), SD		PI, SD	
	<40 years	>40 years	<40 years	>40 years
MCA(M1)	52.7 ± 14.4	44.1 ± 13.8	0.8 ± 0.1	0.7 ± 0.1
ACA(A1)	42.4 ± 13	36.1 ± 11	0.8 ± 0.2	0.8 ± 0.1
eICA	35.3 ± 6.3	33.5 ± 6.8	0.8 ± 0.1	0.8 ± 0.2
PCA(P1)	35.7 ± 13.7	32.9 ± 9.5	0.8 ± 0.1	0.8 ± 0.1
PCA(P2)	35.7 ± 9.1	32.9 ± 8.4	0.8 ± 0.2	0.9 ± 0.3
Basilar	37.4 ± 11.3	35.7 ± 8.1	0.8 ± 0.1	0.8 ± 0.2
V4	25.7 ± 6.2	26.5 ± 7.1	0.7 ± 0.2	0.7 ± 0.2

ACA anterior cerebral artery, *ICA* internal carotid artery, *MCA* middle cerebral artery, *PCA* posterior cerebral artery, *SD* standard deviation, *MFV* mean flow velocity

between the two groups. In the posterior circulation, the inter-hemispheric differences were fewer and not statistically significant.

The hemodynamic parameters recorded using TCD differ from those published in other series with subjects with no history of disease. The lower CBFV values recorded appear to be influenced by altitude and haematocrit [28]. Hence, the consideration of these results could have an impact on the assessment and therapeutic decisions in patients with acute neurological injury.

9.9 TCD Hemodynamic Parameters: Recommendations for Local Assessment of Normal Values

Reference values for a local population should be constructed by insonating healthy subjects at rest in a calm and comfortable setting. The operator should be an expert in the TCD technique, and it is preferable to limit the number of operators in order to avoid potential bias of inter-observer variability, although if the operators have similar level of expertise the variability should be non-significant [4].

The sample should include subjects of both sexes in similar proportions and a distribution of ages similar to the potential patient's ages for the laboratory, for adult laboratory ages from 18 to 90 years old. In order to obtain statistical power for each subgroup, there must be at least 10 subjects for each decade for each gender (A. Garcia, personal communication). Considering 10 to 15% of non-insonable window, it would be better to include 12 cases per decade [24].

The criteria for definition of normal or the criteria to include non-normal individuals should be explicit, considered as part of the reference population of interest for the authors.

9.10 Conclusion

Transcranial Doppler ultrasound is an established technology useful to evaluate cerebral circulation at the bedside. Its portability, absence of irradiation and non-invasiveness make this approach especially useful in critically ill patients; furthermore, TCD/TCCS can be repeated as many times as needed with no harm to the patient and at low cost, making TCD the most versatile way to evaluate cerebral circulation at the ICU.

The interpretation of TCD/TCCS is operator dependent and can be influenced by the reference values considered normal for a given population; it is important for each TCD/TCCS laboratory to develop its own table of normal values for the local population.

References

1. Aaslid R, Markwalder TM, Nornes H. Noninvasive transcranial Doppler ultrasound recording of flow velocity in basal cerebral arteries. J Neurosurg. 1982;57(6):769–74.
2. Bishop CC, Powell S, Rutt D, Browse NL. Transcranial Doppler measurement of middle cerebral artery blood flow velocity: a validation study. Stroke. 1986;17(5):913–5.
3. Lindegaard KF, Nornes H, Bakke SJ, Sorteberg W, Nakstad P. Cerebral vasospasm after subarachnoid haemorrhage investigated by means of transcranial Doppler ultrasound. Acta Neurochir Suppl (Wien). 1988;42:81–4.
4. Maeda H, Etani H, Handa N, Tagaya M, Oku N, Kim BH, et al. A validation study on the reproducibility of transcranial Doppler velocimetry. Ultrasound Med Biol. 1990;16(1):9–14.
5. Puppo Vallini BC. Doppler transcraneano en el paciente neurocrítico. Paciente crit (Uruguay). 2001:52–68.
6. Baumgartner I, Behrendt P, Rohner P, Baumgartner RW. A validation study on the intraobserver and interobserver reproducibility of renal artery duplex ultrasound. Ultrasound Med Biol. 1999;25(2):225–31.
7. Arnolds BJ, von Reutern GM. Transcranial Doppler sonography. Examination technique and normal reference values. Ultrasound Med Biol. 1986;12(2):115–23.
8. Hennerici M, Rautenberg W, Sitzer G, Schwartz A. Transcranial Doppler ultrasound for the assessment of intracranial arterial flow velocity--part 1. Examination technique and normal values. Surg Neurol. 1987;27(5):439–48.

9. Sorteberg W, Langmoen IA, Lindegaard KF, Nornes H. Side-to-side differences and day-to-day variations of transcranial Doppler parameters in normal subjects. J Ultrasound Med. 1990;9(7):403–9.
10. Vriens EM, Kraaier V, Musbach M, Wieneke GH, van Huffelen AC. Transcranial pulsed Doppler measurements of blood velocity in the middle cerebral artery: reference values at rest and during hyperventilation in healthy volunteers in relation to age and sex. Ultrasound Med Biol. 1989;15(1):1–8.
11. Schmidt EA, Piechnik SK, Smielewski P, Raabe A, Matta BF, Czosnyka M. Symmetry of cerebral hemodynamic indices derived from bilateral transcranial Doppler. J Neuroimaging. 2003;13(3):248–54.
12. Droste DW, Ludemann P, Anders F, Kemeny V, Thomas M, Krauss JK, et al. Middle cerebral artery blood flow velocity, end-tidal pCO2 and blood pressure in patients with obstructive sleep apnea and in healthy subjects during continuous positive airway pressure breathing. Neurol Res. 1999;21(8):737–41.
13. Macchi C, Catini C. The measurement of the calibers and blood-flow velocities of the arteries of the circle of Willis: a statistical investigation of 120 living subjects using transcranial color-Doppler ultrasonography. Ital J Anat Embryol. 1994;99(1):9–16.
14. Krejza J, Mariak Z, Walecki J, Szydlik P, Lewko J, Ustymowicz A. Transcranial color Doppler sonography of basal cerebral arteries in 182 healthy subjects: age and sex variability and normal reference values for blood flow parameters. AJR Am J Roentgenol. 1999;172(1):213–8.
15. Tegeler CH, Crutchfield K, Katsnelson M, Kim J, Tang R, Passmore Griffin L, et al. Transcranial Doppler velocities in a large, healthy population. J Neuroimaging. 2013;23(3):466–72.
16. Grolimund P, Seiler RW. Age dependence of the flow velocity in the basal cerebral arteries--a transcranial Doppler ultrasound study. Ultrasound Med Biol. 1988;14(3):191–8.
17. Yang D, Cabral D, Gaspard EN, Lipton RB, Rundek T, Derby CA. Cerebral hemodynamics in the elderly: a transcranial Doppler study in the Einstein aging study Cohort. J Ultrasound Med. 2016;35(9):1907–14.
18. Brouwers PJ, Vriens EM, Musbach M, Wieneke GH, van Huffelen AC. Transcranial pulsed Doppler measurements of blood flow velocity in the middle cerebral artery: reference values at rest and during hyperventilation in healthy children and adolescents in relation to age and sex. Ultrasound Med Biol. 1990;16(1):1–8.
19. Ringelstein EB, Kahlscheuer B, Niggemeyer E, Otis SM. Transcranial Doppler sonography: anatomical landmarks and normal velocity values. Ultrasound Med Biol. 1990;16(8):745–61.
20. Barbosa MF, Abdala N, Carrete H Jr, Nogueira RG, Nalli DR, Fonseca JR, et al. Reference values for measures of blood flow velocities and impedance indexes in healthy individuals through conventional transcranial Doppler. Arq Neuropsiquiatr. 2006;64(3B):829–38.
21. Demirkaya S, Uluc K, Bek S, Vural O. Normal blood flow velocities of basal cerebral arteries decrease with advancing age: a transcranial Doppler sonography study. Tohoku J Exp Med. 2008;214(2):145–9.
22. Donnelly J, Budohoski KP, Smielewski P, Czosnyka M. Regulation of the cerebral circulation: bedside assessment and clinical implications. Crit Care. 2016;20(1):129.
23. Farhoudi M, Kermani S, Sadeghi-Bazargani H. Relatively higher norms of blood flow velocity of major intracranial arteries in North-West Iran. BMC Res Notes. 2010;3:174.
24. Franco M, Ariza-Araújo Y, Mejía-Mantilla JH. Estimación de valores hemodinámicos mediante el uso del doppler transcraneal en un grupo de voluntarios habitantes de Cali (Colombia), una ciudad a 995 m sobre el nivel del mar. Imagen Diagnóstica. 2015;6(2):49–56.
25. Moller K, Paulson OB, Hornbein TF, Colier WN, Paulson AS, Roach RC, et al. Unchanged cerebral blood flow and oxidative metabolism after acclimatization to high altitude. J Cereb Blood Flow Metab. 2002;22:118–26.
26. Brass LM, Pavlakis SG, DeVivo D, Piomelli S, Mohr JP. Transcranial Doppler measurements of the middle cerebral artery effect of hematocrit. Stroke. 1988;19:1466–9.

27. Scherle Matamoros CE, Rivero RD. Transcranial Doppler ultrasound measurements of cerebral hemodynamic parameters in healthy volunteers at 2850 meters altitude. Radiology. 2019;61(5):405–11.
28. Isikay CT, Uzuner N, Gücüyener D, Ozdemir G. The effects of hematocrit and age on transcranial Doppler measurements in patients with recent ischemic stroke. Neurol India. 2005;53:51–4.

Chapter 10
Transcranial Doppler (TCD/TCCS) Approaches: Acoustic Windows

Jorge Carrizosa

Key Points

1. Proper insonation technique is essential to achieve better visualization of structures and trustable flow velocities in transcranial Doppler evaluation.
2. A standardized routine of insonation should be applied to decrease intra- and interobserver variability.
3. Transcranial color-coded duplex sonography is an easy, reproducible, and non-invasive method to evaluate critical care patients at the bedside.
4. To know the acoustic windows and their related target structures will allow a complete evaluation of the brain hemodynamics in most cases.
5. The sonographer/physician must know considerations about age, gender, ethnicity, and other conditions related to hard-to-insonate windows.

10.1 Introduction

Neurological evaluation is not easy in neurocritical care patients to understand brain dynamics and to anticipate complications as deep sedation is common. Multimodal neuromonitoring has emerged as a strategy to evaluate the central nervous system in critical care patients. Hemodynamic instability, risk of complications during transfer to the imaging department, and need for frequent evaluation of brain hemodynamics represent usual conditions of the neurocritical ill patient. Non-invasive monitoring strategies are essential and necessary to avoid complications during transfer to other wards and to enable frequent evaluation. Transcranial Doppler

J. Carrizosa (✉)
Intensive Care Medicine, Hospital Universitario Fundación Santa Fé, Bogotá, Colombia

Neurointensive Care section - AMCI, Bogotá, Colombia
e-mail: magnusdronjak@hotmail.com

C. N. Rodríguez et al. (eds.), *Neurosonology in Critical Care*,
https://doi.org/10.1007/978-3-030-81419-9_10

sonography was described first by Aaslid in 1982 as a technique for examination of intracranial cerebral arteries [1].

In the last years, with the advent of focused ultrasound protocols [2], routine evaluation of the critical care patient is becoming a mandatory skill, including assessment of the central nervous system. Nowadays, there are two methods to assess brain with ultrasound: transcranial Doppler limited to evaluation of brain flow velocities and transcranial color-coded duplex sonography, which permits assessment of central nervous system in brightness mode (B-mode). To master skills performing an ultrasound to obtain the best images possible is necessary to avoid misdiagnosis.

The purpose of this chapter is to guide the technique of the insonation of the brain through different acoustic windows, structured assessment, the target of evaluation, and evaluation routine on both sides—additionally, a description of some recommendations to optimize structure visualization and optimize image views.

10.2 TCD/TCCS: Acoustic Windows

Inner skull structures are not easy to evaluate randomly with ultrasound as the bone is a strong reflector. To know anatomy to identify thinner areas of the skull is mandatory in routine evaluation during ultrasound evaluation. In order to achieve visualization of relevant anatomical structures, a 2.0–3.5 MHz phased array transducer is necessary (Fig. 10.1).

Additionally, transcranial Doppler ultrasound preset in ultrasound machines with similar software facilitates quick identification of different structures (Fig. 10.1b).

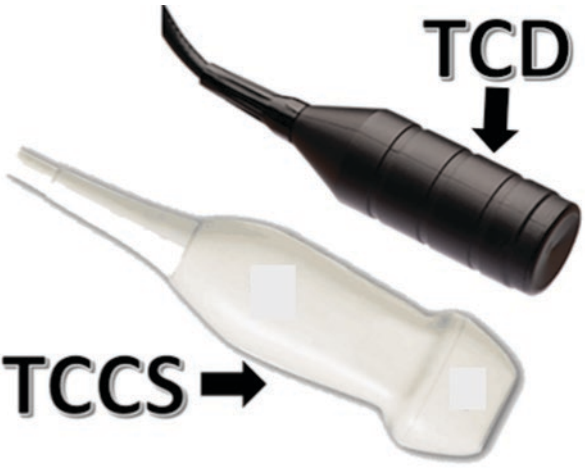

Fig. 10.1 Ultrasound probes indicated for transcranial Doppler ultrasound in comparison. TCD transcranial Doppler; TCCD transcranial color-coded sonography

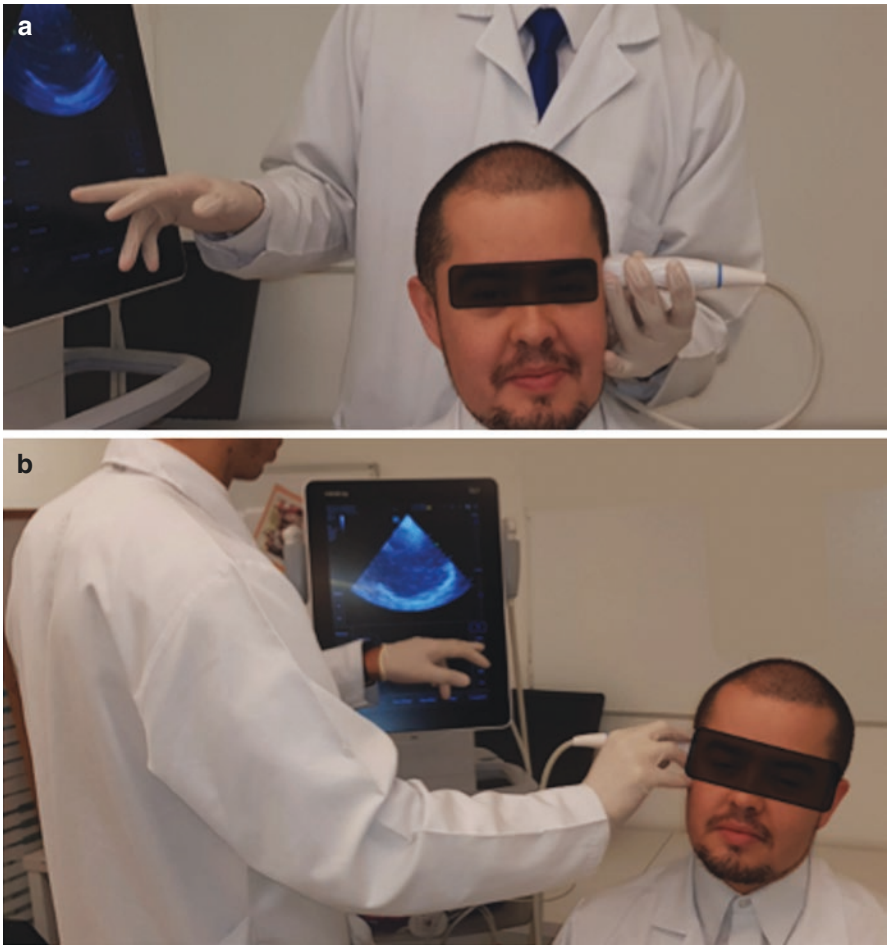

Fig. 10.2 (**a**) Sonographer/physician position behind the patient, ensuring comfort to perform complete transcranial Doppler evaluation. (Author: Jorge Carrizosa). (**b**) Physician showing dexterity in transcranial Doppler examination with both hands. (Author: Jorge Carrizosa)

Comfort is fundamental for the sonographer/physician, who should be located behind the patient when it is possible (Fig. 10.2a). However, head access in that way could be difficult in critical care patients due to other monitoring devices, wires, and extracorporeal support machines. Some modifications to the usual position should be done in many cases. Acquiring skills to insonate the brain with both hands is essential to achieve adequate insonation (Fig. 10.2b).

10.2.1 Transtemporal Acoustic Window (Table 10.1)

10.2.1.1 Technique

Place the 2.0–3.5 MHz phased array transducer in B-mode image at the temporal bone cephalad to the zygomatic arch and anterior to the ear with probe indicator alienated with the plane of the eye of the patient -*axial*- (Fig. 10.3). In this position, the very first target of visualization is the midbrain, visualized as a hypoechoic butterfly-shaped surrounded by the hyperechoic cisterns (Fig. 10.4a, b). The initial depth of insonation of 15 centimeters is recommended, recognizing the contralateral side of the skull as a hyperechoic image [3]. Then, slight tilt movements in cephalocaudal direction scanning downward and upward identify different planes with particular anatomical structures, as shown in Fig. 10.5.

After scanning of transtemporal planes in B-mode image, color-coded Doppler is activated with midbrain visualization in the center of the image in order to identify the circle of Willis. The probability of recognizing the circle of Willis as midbrain is displayed is high, even in non-expert practitioners [4].

Table 10.1 Target of visualization: transtemporal window

Targets of visualization
B-mode: midbrain, third ventricle, thalami, basal ganglia, frontal horns, pineal gland, and insula
Color Doppler and pulsed wave Doppler modes: circle of Willis (middle cerebral artery [MCA], anterior cerebral artery [ACA], posterior cerebral artery [PCA], top of the basilar cerebral artery), terminal segment of the internal carotid artery [ICA])

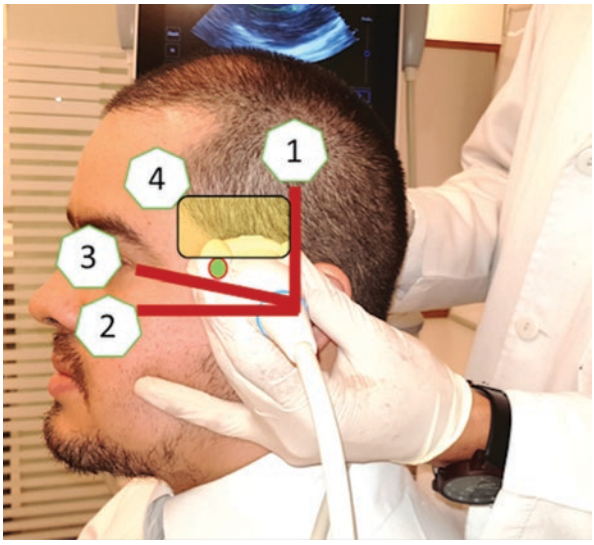

Fig. 10.3 Transtemporal window showing position of the transducer: 1-vertical axis anterior to the ear; 2-horizontal axis cephalad to the zygomatic arch; 3-probe indicator (green dot), alienated with the plane of the eye of the patient. Yellow window indicates the area for exploration of the anterior temporal window. (Author: Jorge Carrizosa)

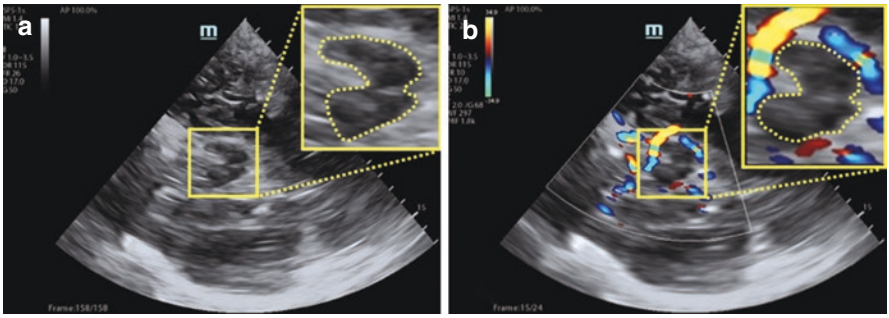

Fig. 10.4 Transtemporal window examination. (**a**) B-mode image highlighting in the zoomed yellow square the hypoechoic area of the midbrain. (**b**) Color-coded image of the same plane of insonation showing midbrain and surrounding vascular structures of the circle of Willis. (Author: Jorge Carrizosa)

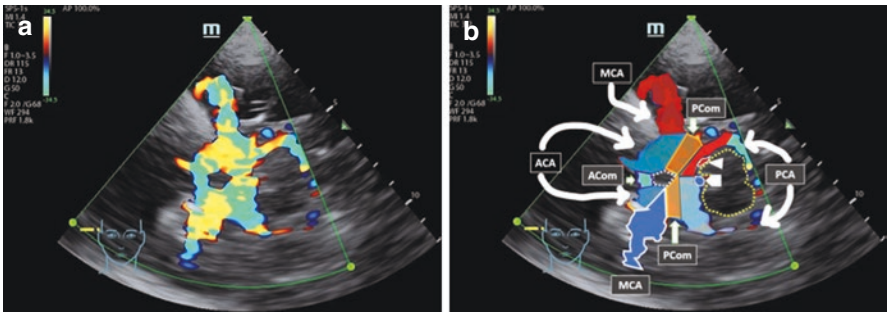

Fig. 10.5 (**a**) Complete circle of Willis is shown with gain increased for educational clarity. (**b**) Same picture in image A with demarcation of the different arteries in the circle of Willis with different colors. Black boxes are indicating every artery name. Triangle: superior cerebellar artery; pentagon: top of the basilar artery. (Author: Jorge Carrizosa)

The direction of blood flow should be useful to a better understanding of brain vascular anatomy in the color-coded Doppler display as vessels with flow toward the transducer are coded red while those with flow away from the transducer are coded blue. In this insonation plane, the ipsilateral middle cerebral artery (MCA) (red) is M1–M2 segments, M3 (blue) segment; the ipsilateral anterior cerebral artery (blue) is A1–A2 segments; and the ipsilateral posterior cerebral artery (red) is P1 and P2 (blue) segments as displayed.

In the complete circle of Willis patients, anterior communicating artery and posterior communicating artery could be identified. Contralateral A1 and M1 segments are also common in patients with an adequate transtemporal window (Fig. 10.5a, b). Once identified the circle of Willis in color-coded Doppler display, the practitioner can proceed to pulsed-wave Doppler mode to appraise cerebral arterial and venous spectral waves and measure velocities of blood flow at every point of interest.

Color-coded Doppler scanning in the same planes as B-mode image explained before is also recommended. By slightly tilting the transducer in a caudal direction, the terminal segment of the internal carotid artery can be noticed. Coronal plane insonation could also be done by rotating the transducer by 90° at the P1 segment (posterior coronal plane), allowing the visualization of the top of the basilar artery [4].

10.2.2 Transforaminal Acoustic Window (Table 10.2)

10.2.2.1 Technique

Place the 2.0–3.5 MHz phased array transducer in B-mode image suboccipital at the midline and pointed toward the nasion (Fig. 10.6), identifying the bone border of the foramen magnum and the clivus. Activate the color Doppler mode box and identify both intracranial segments of vertebral arteries lateral to the foramen magnum. Sigmoid sinus is usually visualized at this point. Then, tilt the transducer upward following the vertebral arteries to find their junction with the basilar artery at 75–80 millimeters approximately (Fig. 10.7). The path of the basilar artery can be tracked

Table 10.2 Target of visualization: transforaminal Window

Targets of visualization
B-mode: foramen magnum
Color Doppler and pulsed wave Doppler modes: vertebral arteries, basilar artery, posterior inferior cerebral arteries, sigmoid sinus

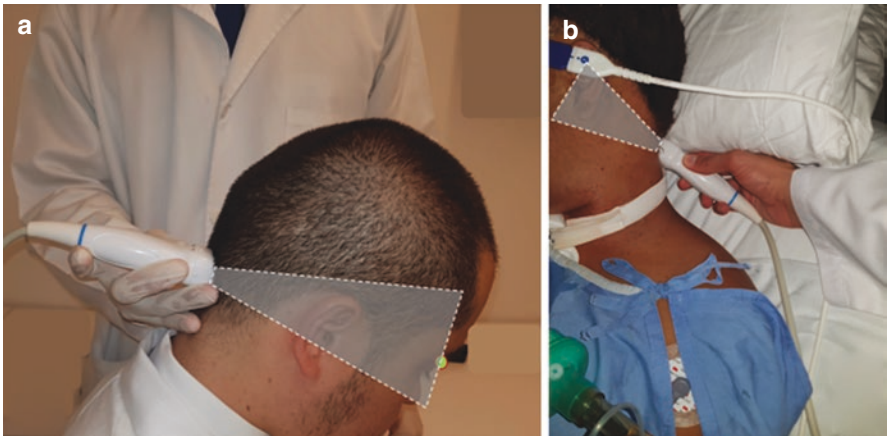

Fig. 10.6 (**a**) Insonation of transforaminal window showing correct angle of insonation with ultrasound beam toward the nasion (green dot). (**b**) Transforaminal window insonation in a critical care patient. Note how a folded pillow helps to place the transducer in proper position. (Author: Jorge Carrizosa)

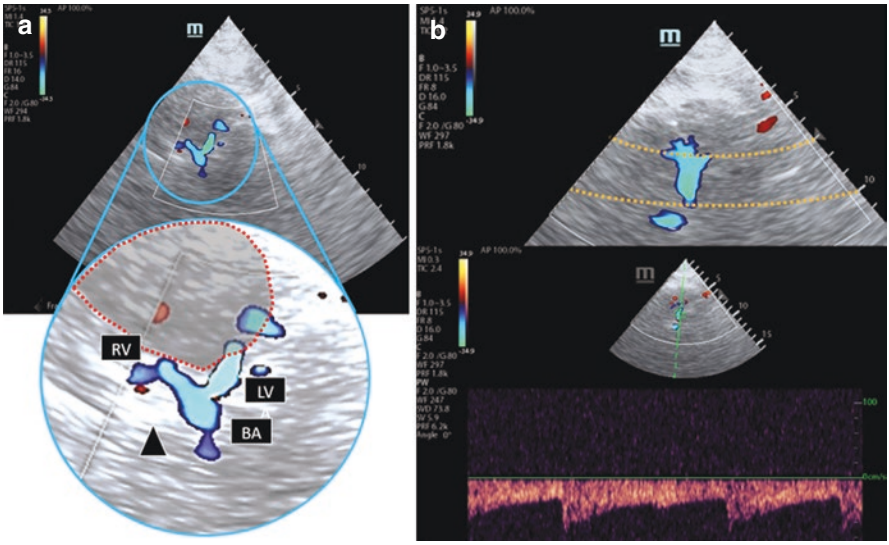

Fig. 10.7 (**a**) Transforaminal insonation at vertebral arteries plane. The blue circle is magnified to better understanding of the insonated structures. See how both vertebral arteries find each other to follow as the basilar artery. Red dots with shades area demarcate the foramen magnum (hypoechoic), the black triangle indicates the location of the clivus (hyperechoic). (**b**) Complete insonation of the basilar artery in depth range between 70 and 100 millimeters (area between orange dotted lines), and spectral Doppler showing basilar flow velocity. (Author: Jorge Carrizosa)

Table 10.3 Targets of visualization: transorbital Window

Targets of visualization
B-mode: retrobulbar space
Color Doppler and pulsed wave Doppler modes: ophthalmic artery, carotid siphon, central retinal artery, central retinal vein, posterior ciliary artery

and measured in different segments at 80–90–100 millimeters [5]. Vertebral arteries and basilar arteries are coded blue as their flow direction goes away from the transducer. The posterior inferior cerebellar artery can also be visualized through this window emerging from the distal segment of the vertebral artery with red color-coding as its flow goes toward the transducer.

10.2.3 Transorbital Acoustic Window (Table 10.3)

10.2.3.1 Technique

Adjust power output and decrease 10% before placing the 2.0–3.5 MHz phased array transducer in B-mode image on the closed upper eyelid. Remember the as low as reasonably achievable (ALARA) principle ("as low as reasonably achievable"), in order to decrease thermal and mechanical effects [6]. Lightest pressure possible

must be applied to minimize the risk of injuries to eyeball and retina. Set depth to 10 centimeters: eyeball and retrobulbar structures (intraconal and extraconal) are seen. Activate the color mode box right behind the eyeball and place the color box between 3 and 6 centimeters in order to identify the ophthalmic artery (red color-coded with peripheral vessel morphology in spectral Doppler mode). Tilt the transducer downward and medial to identify the ipsilateral carotid siphon. This structure is usually found between 55 and 75 millimeters. Flow direction varies according to the insonated segment of the carotid siphon (Figs. 10.8 and 10.9).

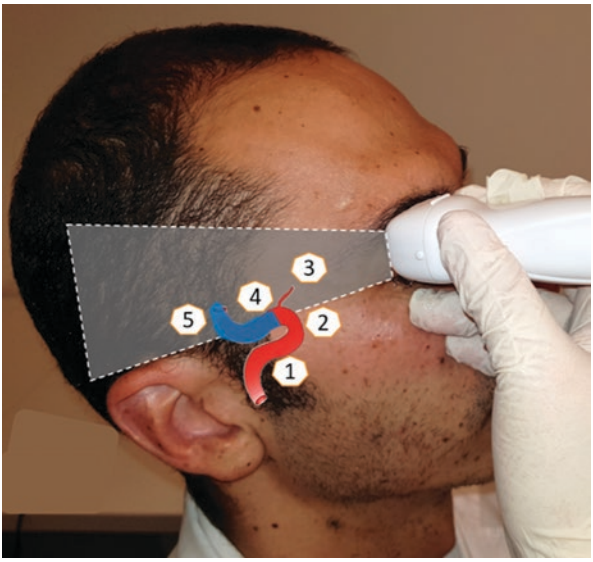

Fig. 10.8 Insonation of the transorbital window. A chart of the internal carotid artery has been drawn on the picture for educational purposes. The ultrasound beam is represented with the shaded gray box. Note that tilting exploration with the transducer must be done to finally insonate the different segments of the carotid syphon and the ophthalmic artery (OA) (number 1 to 5). 1: C4 segment; 2: C3 segment; 3: ophthalmic artery; 4: C2 segment; 5: C1 segment. (Author: Jorge Carrizosa)

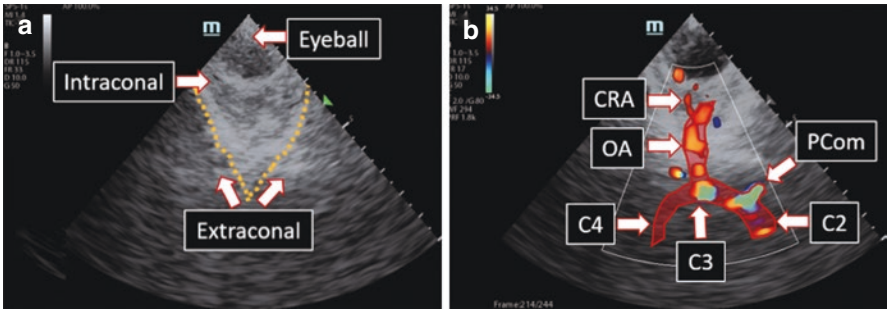

Fig. 10.9 Transorbital window examination. (**a**) B-mode image identifying the hyperechoic line in the retrobulbar space, separating intraconal and extraconal structures (orange dashed line). (**b**) Color-coded Doppler at the same level illustrated above with a chart of the path of the carotid syphon for clarity (red shaded area). Three different segments of the carotid syphon can be identified as C4-C3-C2. CRA central retinal artery, OA ophthalmic artery, PCom posterior communicating artery. (Author: Jorge Carrizosa)

Examination of specific structures requires a switch to a linear-array transducer emitting 7.5–12 MHz in order to achieve better resolution. Ophthalmic or neuro-orbital preset is available in many ultrasound machines, and it is strongly recommended to keep safety aspects. Place the linear-array transducer on the closed upper eyelid. B-mode image will allow examining optical nerve, optic nerve sheath, papilla [7]. Color Doppler mode box placed right behind the papilla will allow to insonate ophthalmic artery, central retinal artery, central retinal vein, and posterior ciliary artery.

10.2.4 Submandibular Acoustic Window (Table 10.4)

10.2.4.1 Technique

Place the 2.0–3.5 MHz phased array transducer in B-mode image at the submandibular level. The objective of this approach is to insonate and measure blood flow velocity of the distal internal carotid artery right before the entrance of the artery to the skull (40 to 60 millimeters) (Figs.10.10 and 10.11). Data from these measurements are required to calculate the MCA/internal carotid artery (ICA) mean flow velocity ratio or Lindegaard ratio. Lindegaard ratio is useful in the differentiation process between vasospasm and hyperemia [8]. A review of carotid protocol and examination of neck vascular structures is detailed in another chapter in this book.

10.2.5 Frontal Bone Window (Table 10.5)

10.2.5.1 Technique

Place the 2.0–3.5 MHz phased array transducer in B-mode image above the lateral aspect of the eyebrow (Fig. 10.12). The Sylvian fissure and the mesencephalon are the reference structures. Frontal horns of the lateral ventricles, orbital roof, and hypophyseal groove can also be identified (Fig. 10.13) [9].

Activate the color Doppler mode box and adjust pulse repetition frequency to medium range (20 cm/s). The anterior cerebral artery is identified with flow direction toward the probe in A2 segment and away from the probe in A1 segment [10] (Fig. 10.14). Other structures of the Circle of Willis could be determined according to the depth of insonation. However, blood flow velocity measurement is not

Table 10.4 Targets of visualization: submandibular window

Targets of visualization
B-mode: jugular vein, common carotid artery, external carotid artery, internal carotid artery
Color Doppler and pulsed wave Doppler modes: the terminal segment of the extracranial internal carotid artery

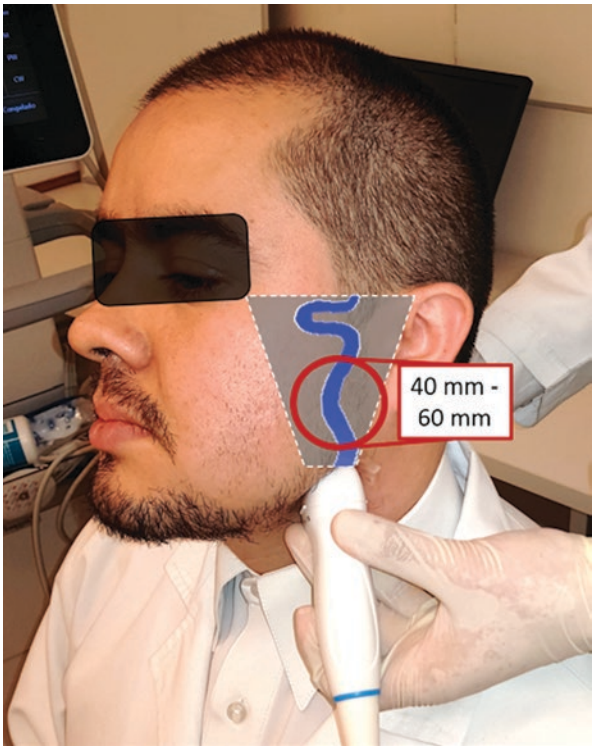

Fig. 10.10 Submandibular window insonation. An internal carotid artery chart has been drawn for clarity. Note the color flow direction away the probe as the transducer position is pointing in cranial direction. Red circle is indicating the target depth of insonation between 40 and 60 millimeters. (Author: Jorge Carrizosa)

recommended routinely at this level in order to avoid misinterpretation of the brain blood flow dynamics. Proper selection of a suitable window for every specific vessel in a protocolized way is recommended.

Placing the transducer slightly lateral of the midline of the forehead and positioned vertically allows identifying the choroid plexus of the third ventricle (hyperechogenic), the corpus callosum (hypoechogenic), and the orbital roof (hyperechogenic). Activate the color Doppler mode box and adjust pulse repetition frequency to a low range. A3 segment of the anterior cerebral artery is identified with flow direction away from the probe as it surrounds the corpus callosum (Fig. 10.15). Change the depth of insonation to identify the internal cerebral vein at 9 to 10 centimeters, slightly above the choroid plexus of the third ventricle (Fig. 10.16) [11].

10.3 Ethnicity, Age, and Gender: TCD/TCCS Special Considerations

There are some considerations regarding ethnicity described as initial reports that estimate an inadequate acoustical temporal bone window of about 9% in Caucasian people [12]. However, higher rates of an inadequate acoustical temporal bone

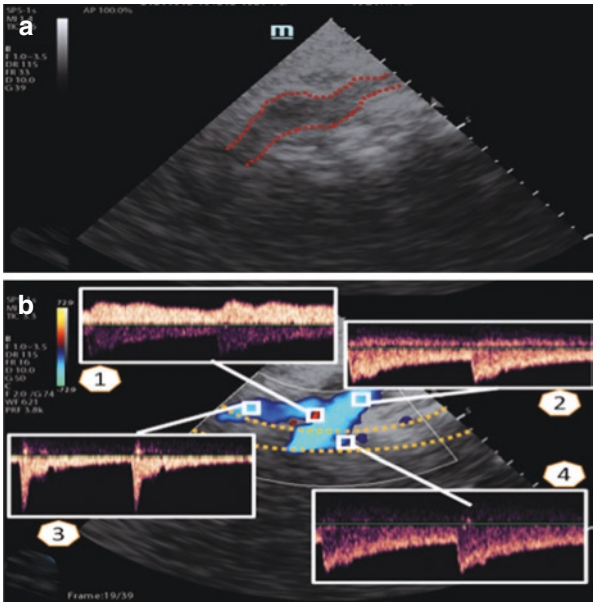

Fig. 10.11 Submandibular window in B-mode and color-coded Doppler ultrasound. (**a**) B-mode image at submandibular level indicating the hypoechoic area (red dotted line) corresponding with the carotid artery. (**b**) Color-coded Doppler and pulsed-Doppler ultrasound at the same level above. As the direction of the transducer is pointing in cranial direction, carotid artery flow direction is away the probe. Small red area at the carotid bifurcation level corresponds to the jugular vein (flow direction toward the transducer). Different spectral-Doppler waves are shown in order to identify the vascular structures. 1: jugular vein; 2: common carotid artery; 3: external carotid artery; 4: internal carotid artery. Orange dashed lines were sketched between 40 and 60 millimeters to prove the correct depth of insonation to proper measurement of the internal carotid artery. (Author: Jorge Carrizosa)

Table 10.5 Targets of visualization: frontal bone window

Targets of visualization
B-mode: third ventricle and choroid plexus of the third ventricle, Sylvian fissure, corpus callosum, orbital roof
Color Doppler and pulsed wave Doppler modes: anterior cerebral artery *[ACA],* internal cerebral vein

window have been reported in Hispanic and Asian people [13, 14]. Also, age and gender are related to a high proportion of suboptimal windows in older women, especially those older than 80 years old, in whom an optimal temporal window has been seen in less than 50%. It is well known that the rate of successful insonation of brain circulation through transcranial Doppler decreases with age [15–17]. This probability of unsuccessful insonation is related to the thickness of temporal bone advancing with age [13].

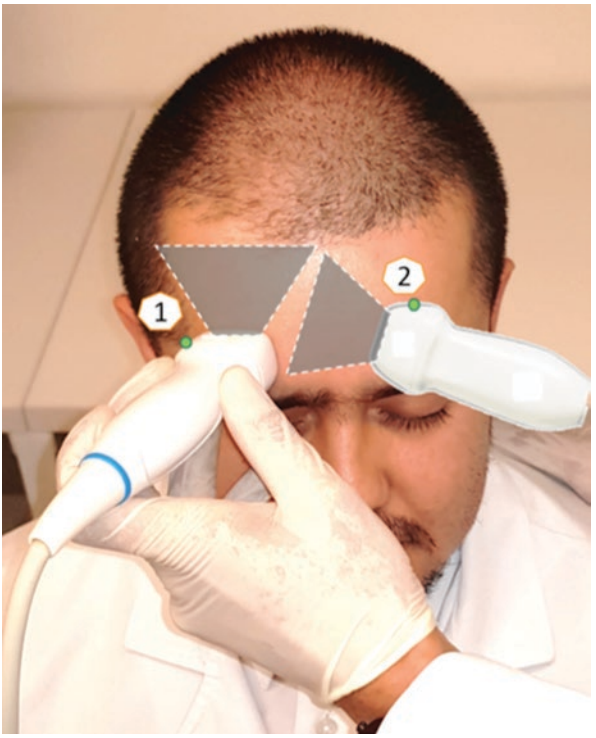

Fig. 10.12 Frontal bone window insonation. 1: transducer position above the eyebrow (supraorbital zone) with probe indicator (green dot) pointing to the right side in horizontal position. 2: transducer position in paramedial zone with probe indicator (green dot) pointing in cephalic direction in vertical position. (Author: Jorge Carrizosa)

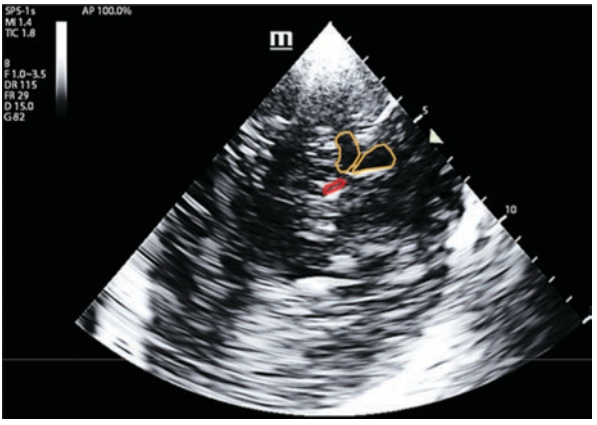

Fig. 10.13 B-mode image in frontal window insonation at supraorbital zone. Typical anatomy is showed: third ventricle in the red box; frontal horns of lateral ventricles in orange lines. (Author: Jorge Carrizosa)

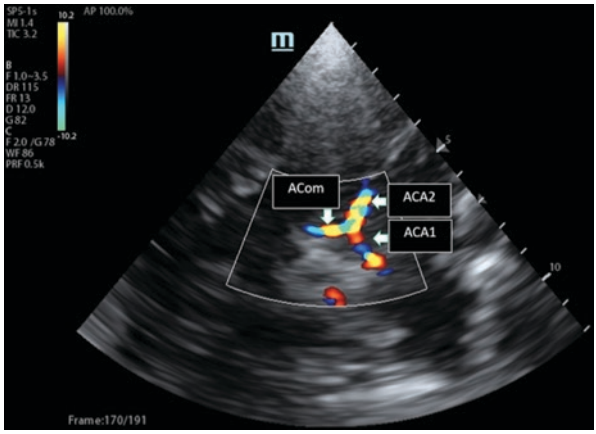

Fig. 10.14 Color-coded Doppler image at frontal window insonation through supraorbital zone. Path of the ipsilateral anterior cerebral artery is shown. AComA (ACom) anterior communicating artery; ACA1 anterior cerebral artery segment A1; ACA2 anterior cerebral artery segment A2. (Author: Jorge Carrizosa)

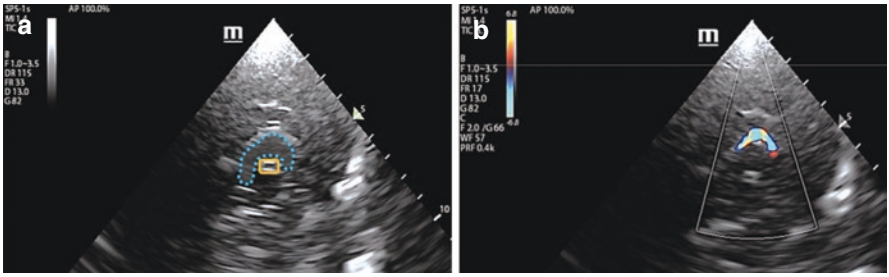

Fig. 10.15 Frontal window insonation at the paramedian frontal zone. (**a**) B-mode image delimiting the corpus callosum (light blue dashed line) and the choroid plexus of the third ventricle (yellow rectangle). (**b**) Color Doppler image at the same level in the image above. Path of the anterior cerebral artery segment A3 (pericallosal artery) is seen in the color scale surrounding the corpus callosum. (Author: Jorge Carrizosa)

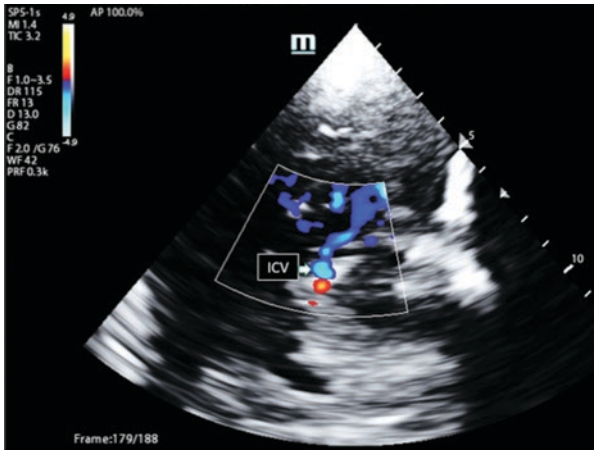

Fig. 10.16 Color-coded Doppler image at the paramedial frontal bone window with depth adjustment showing the internal cerebral vein (ICV) with flow direction away from the probe. (Author: Jorge Carrizosa)

10.4 TCD/TCCS: Special Clinical Situations in ICU

10.4.1 Decompressive Craniectomy

Nowadays, patients with decompressive craniectomy are not infrequent in neurocritical care units. The procedure is performed on patients with refractory intracranial hypertension, malignant brain edema in middle cerebral artery infarction, or to manage expansive focal injury in traumatic brain injury. One of the most relevant publications to date is the decompressive craniectomy in diffuse traumatic brain injury (DECRA) trial [18]. Fronto-temporoparietal decompressive craniectomy, bifrontal decompressive craniectomy, and occipital decompressive craniectomy, among others, have been described.

As part of the skull has been removed surgically, images are easier to get, but the sonographer/physician must take care of the pressure applied to the tissues. Lightest pressure possible should be enough to achieve the insonation of interesting structures. By applying excessive pressure, increased intracranial pressure, direct injuries to the brain parenchyma, and wrong measurements can occur. Changes in blood flow velocities have been described before and after a decompressive craniectomy. The most common difference after decompressive craniectomy is an asymmetrical increase in cerebral blood flow velocities with a higher increase in the decompressed side than the opposite side. A decrease in the pulsatility index has also been reported [19–21]. Monitoring the decompressed patient with transcranial Doppler ultrasound is remarkably important as different hemodynamic patterns have been described after the procedure.

10.4.2 Patient's Position

Access to some windows in critical care patients could be challenging. Due to the inability to flex the neck, risk of secondary injury removing the cervical collar, or prone position as a complement of mechanical ventilation strategy for severe acute respiratory distress syndrome, a complete evaluation of brain circulation is sometimes limited. No diagnostic approach should generate a risk of injury to the patient.

As a primary goal in transcranial Doppler evaluation is to identify and measure blood flow velocities in the middle cerebral artery, transtemporal window usually remains accessible even in conditions mentioned before [22, 23]. Identifying proper time to perform the evaluation is recommended in synchronous work with the nurse

team as the schedule for patient's position change must be taken advantage of for the insonation. In very extreme conditions in which it is impossible to insonate every window, the sonographer/physician should try to take information from the transtemporal window, transorbital window, submandibular window, transforaminal window, and the transfrontal window in that priority order.

10.5 TCD/TCCS: Contrast-Enhanced

The quality of the acoustic window has been related to the thickness of the temporal squama. Insufficient temporal bone window using transcranial color-coded sonography has been described between 10% and 38% [12, 14–16, 24]. To date, there are two agents currently approved for use in neuro sonography: Levovist® and SonoVue®. For patients with inadequate acoustical temporal bone window, absent or insufficient to perform an accurate diagnosis, use of echo contrast agents may be useful to achieve better images where available. Echo contrast agents are comprised of stabilized microbubbles with a diameter lesser than 8 μm. The physical effect is through enhancement of the scattering phenomenon related to the size of the microbubbles [25, 26]. This contrast-enhanced strategy has been described for different conditions in addition to an insufficient window like brain death determination, stroke, dural arteriovenous fistulae, and intracranial collaterals examinations [17, 25, 27].

10.6 Conclusion

Transcranial Doppler ultrasound has become the stethoscope for the brain to evaluate the critical care patient's brain parenchyma and cerebral hemodynamics. To achieve a proper evaluation of the patient's central nervous system with ultrasound, accessible windows, and their target structures to be identified must be part of the knowledge of the sonographer/physician. Standardization of the routine of evaluation is recommended. In some specific groups of patients, a hard-to-find acoustic window could represent a challenge for the sonographer/physician. Echo contrast agents can be intravenously applied to achieve adequate insonation of targeted brain vascular structures.

Algorithm

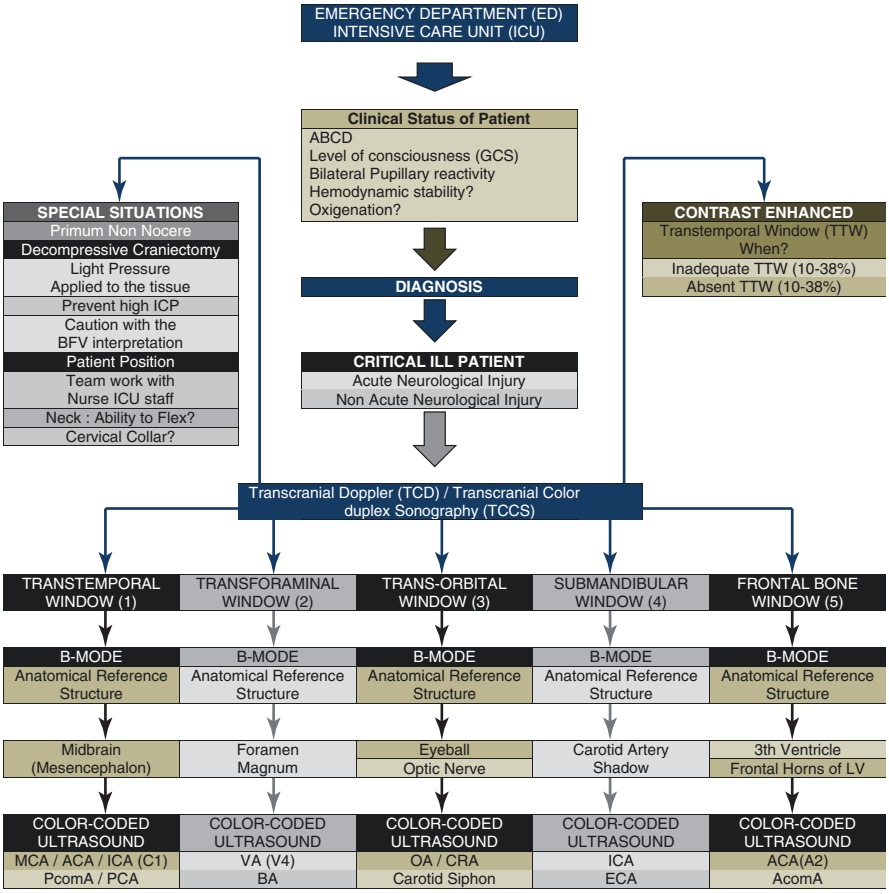

ABCD Airway-Breathing-Circulation-Disability, *MCA* Middle cerebral artery, *ICA* Internal carotid artery, *C1* C1 segment of ICA, *PcomA* Posterior communicating artery, *PCA* Posterior cerebral artery, *BA* Basilar artery, *VA* Vertebral artery, *V4* V4 segment of VA, *OA* Ophthalmic artery, *CRA* Central retinal artery, *ECA* External carotid artery, *ACA* Anterior cerebral artery, *A2* A2 segment of ACA,*ICP* Intracranial pressure, *GCS* Glasgow coma scale., *1-2-3-4-5* Sequence of Insonation Protocol, *TTW* Transtemporal window, *ICP* intracranial pressure, *LV* Lateral ventricle

References

1. Aaslid R, Markwalder T-M, Nornes H. Noninvasive transcranial Doppler ultrasound recording of flow velocity in basal cerebral arteries. J Neurosurg. 1982;57(6):769.
2. Lau VI, Arntfield RT. Point-of-care transcranial Doppler by intensivists. Crit Ultrasound J. 2017;9(1):21.

3. Valdueza Barrios JM, Schreiber S, Röhl J-E, Connolly F, Klingebiel R. Neurosonology and neuroimaging of stroke: a comprehensive reference; 2017.
4. Bartels E. TCCS protocol. In: Baracchini C, Csiba L, editors. Manual of Neurosonology. Cambridge: Cambridge University Press; 2016. p. 118–29.
5. Valdueza JM. TCCS advanced arterial protocol. In: Baracchini C, Csiba L, editors. Manual of Neurosonology. Cambridge: Cambridge University Press; 2016. p. 130–9.
6. Abramowicz J. ALARA: the clinical view. Ultrasound Med Biol. 2015;41(4, Supplement):S102.
7. Siebler M. Neuro-orbital ultrasound. In: Baracchini C, Csiba L, editors. Manual of Neurosonology. Cambridge: Cambridge University Press; 2016. p. 300–5.
8. Robba C, Taccone FS. How I use transcranial Doppler. Crit Care. 2019;23(1):420.
9. Stolz E, Kaps M, Kern A, Dorndorf W. Frontal bone windows for transcranial color-coded duplex sonography. Stroke. 1999;30(4):814–20.
10. Sentenac P, Charbit J, Maury C, Bory P, Dagod G, Greco F, et al. The frontal bone window for transcranial Doppler ultrasonography in critically ill patients: validation of a new approach in the ICU. Neurocrit Care. 2019;33:115.
11. Yoshimura S, Koga M, Toyoda K, Mukai T, Hyun B-H, Naganuma M, et al. Frontal bone window improves the ability of transcranial color-coded sonography to visualize the anterior cerebral artery of Asian patients with stroke. Am J Neuroradiol. 2009;30(6):1268–9.
12. Marinoni M, Ginanneschi A, Forleo P, Amaducci L. Technical limits in transcranial Doppler recording: Inadquate acoustic windows. Ultrasound Med Biol. 1997;23(8):1275–7.
13. Brunser AM, Silva C, Cárcamo D, Muñoz P, Hoppe A, Olavarría VV, et al. Transcranial Doppler in a Hispanic-Mestizo population with neurological diseases: a study of sonographic window and its determinants. Brain Behav. 2012;2(3):231–6.
14. Kwon J-H, Kim JS, Kang D-W, Bae K-S, Kwon SU. The thickness and texture of temporal bone in brain CT predict acoustic window failure of transcranial Doppler. J Neuroimaging. 2006;16(4):347–52.
15. Itoh T, Matsumoto M, Handa N, Maeda H, Hougaku H, Hashimoto H, et al. Rate of successful recording of blood flow signals in the middle cerebral artery using transcranial Doppler sonography. Stroke. 1993;24(8):1192–5.
16. Lin Y-P, Fu M-H, Tan T-Y. Factors associated with no or insufficient temporal bone window using transcranial color-coded sonography. Journal of Medical Ultrasound. 2015;23(3):129–32.
17. Wijnhoud AD, Franckena M, van der Lugt A, Koudstaal PJ, Dippel eDWJ. Inadequate acoustical temporal bone window in patients with a transient ischemic attack or minor stroke: role of skull thickness and bone density. Ultrasound Med Biol. 2008;34(6):923–9.
18. Cooper DJ, Rosenfeld JV, Murray L, Arabi YM, Davies AR, D'Urso P, et al. Decompressive Craniectomy in diffuse traumatic brain injury. N Engl J Med. 2011;364(16):1493–502.
19. Bor-Seng-Shu E, de-Lima-Oliveira M, Nogueira RC, Almeida KJ, Paschoal EHA, Paschoal FM Jr. Decompressive Craniectomy for traumatic brain injury: postoperative TCD cerebral hemodynamic evaluation. Front Neurol. 2019;10:354.
20. Bor-Seng-Shu E, Paiva WS, Figueiredo EG, Fujimoto Y, de Andrade AF, Fonoff ET, et al. Posttraumatic refractory intracranial hypertension and brain herniation syndrome: cerebral hemodynamic assessment before decompressive craniectomy. Biomed Res Int. 2013;2013:750809.
21. Chang T, Li L, Yang Y, Li M, Qu Y, Gao L. Transcranial Doppler ultrasonography for the management of severe traumatic brain injury after decompressive Craniectomy. World Neurosurg. 2019;126:e116–e24.
22. Rasulo FA, Bertuetti R, Robba C, Lusenti F, Cantoni A, Bernini M, et al. The accuracy of transcranial Doppler in excluding intracranial hypertension following acute brain injury: a multicenter prospective pilot study. Crit Care. 2017;21(1):44.
23. Rincon F. Bedside transcranial sonography: a promising tool for the neurointensivist*. Read online: critical care medicine | Society of Critical Care Medicine. Crit Care Med. 2012;40(6):1969–70.

24. Kollar J, Schulte-Altedorneburg G, Sikula J, Fulesdi B, Ringelstein EB, Mehta V, et al. Image quality of the temporal bone window examined by transcranial Doppler sonography and correlation with postmortem computed tomography measurements. Cerebrovasc Dis. 2004;17(1):61–5.
25. Droste DW. Clinical utility of contrast-enhanced ultrasound in neurosonology. Eur Neurol. 2008;59(suppl 1):2–8.
26. Grant EG. Sonographic contrast agents in vascular imaging. Seminars in Ultrasound, CT and MRI. 2001;22(1):25–41.
27. Welschehold S, Geisel F, Beyer C, Reuland A, Kerz T. Contrast-enhanced transcranial Doppler ultrasonography in the diagnosis of brain death. J Neurol Neurosurg Psychiatry. 2013;84(8):939–40.

Chapter 11
Neurocritical Patient in ICU: Transcranial Doppler (TCD/TCCS) as the Brain Stethoscope

Chiara Robba and Danilo Cardim

Key Points

1. *Cerebral blood flow velocity*
   The spectral waveform derived from TCD is characterized by three components: peak systolic flow velocity (PSV), mean flow velocity (MFV), and end-diastolic velocity (EDV) values.
2. *Pulsatility index*
   Pulsatility index (PI) can provide information about the downstream cerebral vascular resistance and describe quantitative and qualitative changes in the morphology of the TCD waveform resulting from cerebral perfusion pressure changes.
3. *Cerebral compliance*
   Cerebral compliance (C) is the ability of the brain to adapt to changes in volume inside the cranium in response to a change in pressure to avoid intracranial hypertension.
4. *Cerebrovascular time constant*
   The cerebrovascular time constant (TAU) is a non-invasive TCD-based index indicating theoretically the time to establish a change in cerebral blood volume after a sudden change in arterial blood pressure during one cardiac cycle.

C. Robba (✉)
Department of Anaesthesia and Intensive Care, Ospedale Policlinico San Martino IRCCS, IRCCS for Oncology, University of Genoa, Genoa, Italy

Deputy Neurointensive Care section - ESICM, Brussels, Belgium
e-mail: kiarobba@gmail.com

D. Cardim
Brain Physics Laboratory, Division of Neurosurgery, Department of Clinical Neurosciences, Addenbrooke's Hospital, University of Cambridge, Cambridge, UK

Institute for Exercise and Environmental Medicine, Texas Health Presbyterian Hospital Dallas, Dallas, TX, USA

Department of Neurology and Neurotherapeutics, University of Texas Southwestern Medical Center, Dallas, TX, USA

C. N. Rodríguez et al. (eds.), *Neurosonology in Critical Care*,
https://doi.org/10.1007/978-3-030-81419-9_11

5. *Critical closing pressure*
   Critical Closing Pressure (CrCP) is described as the sum of intracranial pressure (ICP) and vascular wall tension (WT). The latter represents the active vasomotor tone that alongside ICP determines the CrCP. Clinically, CrCP represents a lower threshold of arterial blood pressure, below which the brain microvasculature collapses and cerebral blood flow (CBF) ceases.
6. *Cerebral autoregulation*
   Cerebral blood flow autoregulation refers to the intrinsic ability of the brain to maintain a stable CBF despite fluctuations in cerebral perfusion pressure.
7. *Non-invasive assessment of intracranial pressure*
   ICP evaluation is crucial in many neurological diseases, and it is commonly measured through intraventricular or intraparenchymal catheters, but their invasive nature and related complications preclude their use in many conditions. TCD waveform analysis has been widely investigated as a technique for non-invasive ICP (nICP) estimation.

11.1 Introduction

Transcranial Doppler ultrasonography (TCD)/TCCS has the potential to be used as an alternative diagnostic tool for the assessment of cerebral hemodynamics rather than costly and potentially risky investigations such as invasive ICP monitoring.

In the neurointensive care setting, the monitoring of TCD-derived indices may provide an early detection of the onset of cerebrovascular derangements. The knowledge of cerebrovascular dynamics can facilitate clinical management of cerebral pathologies, including traumatic brain injury (TBI), aneurysmal subarachnoid hemorrhage (aSAH), intra- and extracranial arterial stenosis and occlusion, brain death, cerebral infections, and hydrocephalus [1].

The aim of this chapter is to provide an overview of the basic and advanced TCD-derived methods (Table 11.1) and clinical applications of TCD in critically ill

Table 11.1 Basic and advanced signals derived from transcranial Doppler ultrasonography

Basic signals	Flow velocity
	Pulsatility index
Advanced signals	Autoregulation
	CrCP
	WT
	C_a, C_i
	Tau
	nCPP
	nICP

Abbreviations: *CrCP* critical closing pressure, *WT* wall tension of the cerebral vasculature, C_a compliance of the cerebral arterial bed, C_i compliance of the intracranial space, *Tau* cerebrovascular time constant, *nCPP* non-invasive cerebral perfusion pressure, *nICP* non-invasive intracranial pressure

Table 11.2 Clinical applications of transcranial Doppler ultrasonography

Clinical Applications	Role of TCD	Main references
TBI	Non-invasive ICP and CPP estimation	[7, 10]
	Autoregulation	[45, 46]
	Compliance and cerebrovascular dynamics	[49]
	Prediction of neurological deterioration in the emergency room	[50, 51]
SAH (Aneurysms and AVM)	Vasospasm	[55, 56, 66]
	Autoregulation	[58, 60]
Stroke	Diagnosis and treatment of ischemic stroke	[62–65]
Brain death	Diagnosis of brain death	[66]
Sickle cell disease	Risk from a spectrum of brain injuries that include subclinical infarction, acute stroke and hemorrhage	[67]
Cerebral venous thrombosis		[6]
Right to left cardiac shunt	Evaluation of paradoxical embolism through right to left cardiopulmonary shunts (e.g., patent foramen ovale)	[68]
Peri-procedural/operative	Autoregulation Non-invasive ICP and CPP	[69–71]
Liver failure and hepatic encephalopathy	Non-invasive ICP estimation and prognosis for acute liver failure	
Preeclampsia	Assessment of autoregulation and FV as prognostic for preeclampsia	[82]
Sepsis	Assessing cerebral perfusion changes in septic patients as risk of Sepsis-associated encephalopathy	[83]

Abbreviations: *AVM* arteriovenous malformation, *CPP* cerebral perfusion pressure, *FV* cerebral blood flow velocity, *ICP* intracranial pressure, *SAH* subarachnoid hemorrhage, *TBI* traumatic brain injury, *TCD* transcranial Doppler ultrasonography

patients in the neurointensive care setting (Table 11.2), and to describe the utility of TCD in the diagnosis and monitoring of cerebrovascular diseases as a "stethoscope for the brain."

11.2 Basic Methods

11.2.1 Flow Velocities

The spectral waveform derived from TCD/TCCS is characterized by three components:

1. Peak systolic flow velocity (PSV),
2. Mean flow velocity (MFV), and
3. End-diastolic velocity (EDV) values (Fig. 11.1).

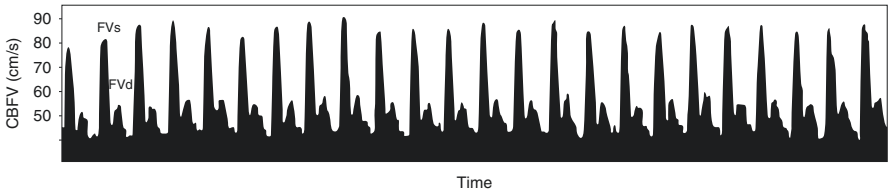

Fig. 11.1 Representation of the TCD cerebral blood flow velocity (CBFV) waveform, presenting a peak systolic and an end diastolic. (FVs = PSV); (FVd = EDV)

PSV is predominantly dependent on the cardiac output, that is, systemic hemodynamics, rather than depicting cerebral hemodynamics.

The use of EDV as a relevant parameter is currently thriving in clinical practice, especially in intensive care. Some authors have reported a reduction of CPP by rising ICP or by falling arterial blood pressure (ABP) in head-injured patients, which resulted in a greater fall in diastolic flow velocity than other flow parameters [2].

TCD/TCCS cerebral blood flow velocities are commonly measured modalities in clinical and experimental environments. Through analysis of TCD waveform, many authors attempted to investigate the relationship between the cerebral blood flow (CBF) and cerebrospinal fluid (CSF) dynamics, proposing several mathematical and hydrodynamic models derived mostly from flow velocity (FV), ABP, and intracranial pressure (ICP) signals as inputs [3, 4].

11.2.2 Pulsatility Index (PI)

Gosling's pulsatility index (PI) can provide information about the downstream cerebral vascular resistance and describe quantitative and qualitative changes in the morphology of the TCD/TCCS waveform resulting from cerebral perfusion pressure changes [5].

PI is calculated as the relationship between the difference of systolic flow velocity and diastolic flow velocity divided by mean flow velocity, and in normal conditions, it usually ranges from 0.5 to 1.19 [6]. Proximal stenosis or occlusion may lower PI below 0.5 due to downstream arteriolar vasodilation, whereas distal occlusion or constriction may increase PI above 1.19 [7]. A PI less than 0.5 may also indicate an arteriovenous malformation as the resistance in proximal vessels is reduced due to continuous distal venous flow [8]. More recently, a larger study including more than 350 healthy individuals has reported normative values for TCD assessment of arteries in the circle of Willis [9]. Normal PI values have been reported as 0.82 ± 0.16 and 0.81 ± 0.13 for distal and proximal middle cerebral artery (MCA),

respectively. Being a ratio, PI is not affected by the angle of insonation and therefore may be a sensitive parameter for early detection of intracranial hemodynamic changes [9] (Eq. 11.1).

$$\mathrm{PI} = \left(\mathrm{PSV} - \mathrm{EDV}\right) / \mathrm{MFV} \tag{11.1}$$

Mathematically, PI can be calculated as inversely proportional to CPP, directly proportional to pulse amplitude of ABP, and nonlinearly proportional to the compliance of the arterial bed (C_a), heart rate (HR), and cerebrovascular resistance (CVR) [5].

PI has been used for the assessment of distal CVR [10] as many experimental and clinical studies have supported the concept that PI is a reflection of the distal CVR, attributing greater PI to higher CVR [8]. However, an experimental study demonstrated that hypercapnia causes a decrease in both CVR and PI, whereas a reduction in CPP with intact autoregulation induces a decrease in CVR but an increase in PI [11].

PI has been also widely investigated as non-invasive estimator of ICP, as it has been demonstrated that ICP and PI are positively correlated during increases of ICP (Fig. 11.2). However, the role of PI as non-invasive estimator of ICP can be controversial [12].

11.3 Advanced Methods

Several secondary advanced model-based methods for cerebral hemodynamics assessment have been introduced.

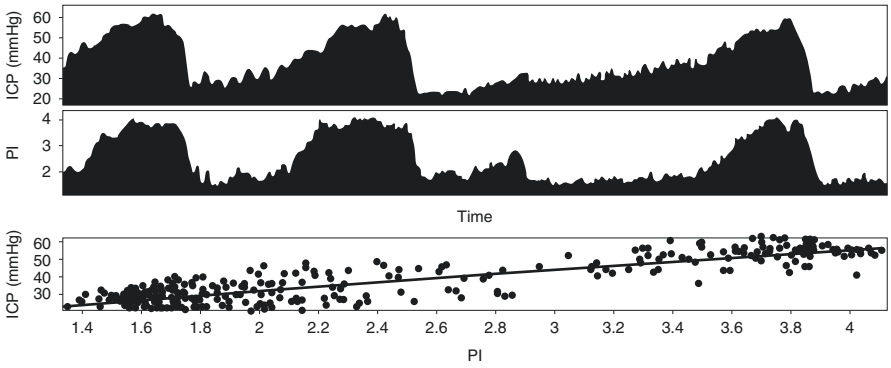

Fig. 11.2 Plot showing the positive relationship between pulsatility index (PI) and intracranial pressure (ICP) in traumatic brain injury

11.3.1 Compliance of Arterial and CSF Compartments

Cerebral compliance (C) is the ability of the brain to adapt to changes in volume inside the cranium in response to a change in pressure to avoid intracranial hypertension. This parameter includes the cerebrovascular arterial compliance (C_a), which describes the change of arterial blood volume in response to change in arterial pressure, and the compliance of the cerebrospinal space (C_i), which refers to changes of volume of the intracranial space in regards to changes in ICP [13].

TCD/TCCS allows a non-invasive estimation of cerebral arterial blood volume (CaBV) [14] and enables the assessment of the relative changes in C_a and C_i. These two parameters reflect the relationship between pulsatile changes in ABP and CaBV (C_a) and ICP and CaBV (C_i). This model is based on the mechanism of brain pulsatility that describes the physiological interactions of the intracranial compartments undergoing volumetric changes during the cardiac cycle.

This method was widely described in patients with TBI during "plateau waves" of ICP [13, 15] monitored using TCD. The origin of plateau waves includes intrinsic cerebral vasodilatation, with a rise in cerebral blood volume and a rise in ICP. Therefore, according to the "vasodilatory cascade" hypothesis, these changes are associated with rapid increase in C_a caused by vasodilatation of cerebral resistive vessels during a wave and a reduction of C_i due to the decrease in cerebrospinal compensatory reserve caused by the increase in cerebral blood volume [16, 17]. More recently, Kim et al. confirmed this relative inverse change in C_a and C_i in head injury patients, illustrating that both compartmental compliances can be continuously monitored over a cardiac cycle [18].

The pulsatile component of ICP (Fig. 11.3) and a clinical management guided by cerebral compliance has been associated with outcome prediction in several contexts, including SAH, TBI, and normal pressure hydrocephalus [19].

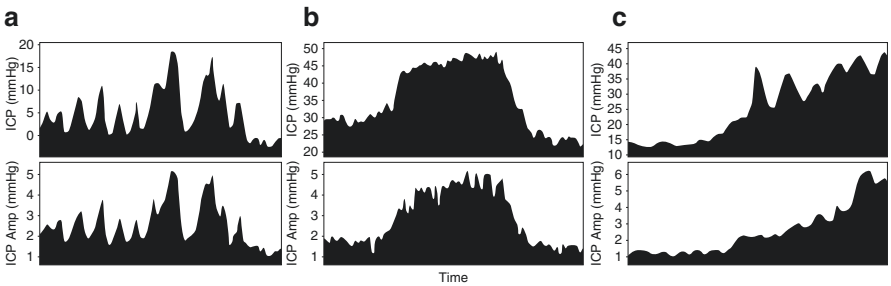

Fig. 11.3 Amplitude of intracranial pressure (ICP Amp) in different clinical conditions: (**a**) B waves of ICP; (**b**) increase in ICP during plateau wave; (**c**) increase in ICP during cerebral spinal fluid infusion test in patient with normal pressure hydrocephalus. In all cases, an increase in intracranial pressure is followed by an increase in ICP amplitude

11.3.2 TAU (Cerebrovascular Time Constant)

The cerebrovascular time constant (TAU) is a non-invasive TCD-based index indicating theoretically the time to establish a change in cerebral blood volume after a sudden change in arterial blood pressure during one cardiac cycle [20] (Eq. 11.2).

TAU is an analog to time constant and is calculated as a product of cerebral arterial compliance (C_a) and cerebrovascular resistance (CVR), expressed in time units (seconds).

$$\text{Tau} = C_a \times \text{CVR}(\text{s}) \tag{11.2}$$

The dependence of TAU on hemodynamic and cerebrovascular parameters was studied on 46 New Zealand rabbits undergoing hemodynamic manipulations. TAU resulted to be inversely correlated with the changes in ABP (during arterial hypo- and hypertension) and CPP (during intracranial hypertension). Specifically, during a decrease in CPP, C_a increased while CVR decreased. During hypercapnia, the decrease in CVR was more pronounced than the increase in C_a, resulting in a total decrease in Tau [20].

In normal subjects, where C_a and CVR were estimated using mathematical transformations of ABP and TCD, Tau was studied following cerebral blood flow velocity waveform changes in end-tidal CO_2 ($EtCO_2$). The time constant resulted to be shortened with increasing $EtCO_2$, while hypocapnia lengthened the time constant [21].

TAU was also studied in healthy volunteers and in patients with severe stenosis of the internal carotid artery (ICA), and it was found to be significantly shorter in severe internal carotid artery stenosis [21] than in controls and that it correlated with the degree of stenosis. Moreover, TAU was found to be significantly decreased during vasospasm in SAH patients [22], and in particular, it was found to be shortened on the side of the aneurysmal SAH before the vasospasm was identified by the clinical or conventional TCD signs of vasospasm.

In a recent study [23], TAU was assessed in patients with traumatic brain injury (TBI) with and without intracranial hematomas (epidural, subdural, and multiple hematomas). Tau was shorter in both groups in comparison with normal data, but in patients with intracranial hematomas, the time constant was even shorter, indicating a failure of autoregulation of cerebral capillary blood flow after severe TBI occurs.

11.3.3 Critical Closing Pressure and Wall Tension

Critical Closing Pressure (CrCP) was first introduced by Burton's model, and it is described as the sum of ICP and vascular wall tension (WT) [24]. Wall tension (WT) represents the active vasomotor tone that alongside intracranial pressure determines the critical closing pressure. Clinically, CrCP represents a lower

threshold of ABP, below which the brain microvasculature collapses and CBF ceases [24].

CrCP can be assessed non-invasively using TCD/TCCS, by comparing the pulsatile waveforms of blood flow velocity and ABP, and given the association with the vasomotor tone of small blood vessels (wall tension), CrCP can provide important information regarding cerebral hemodynamics and changes in cerebral perfusion pressure in several neurological conditions [25, 26]. The estimation of CrCP through TCD has also been shown to be clinically useful for estimating changes in ICP non-invasively or for cerebrovascular tone assessment to direct therapies in patients at risk to develop vasospasm after subarachnoid hemorrhage or hyperemia [27].

With TCD/TCCS, CrCP can be assessed non-invasively by comparing the pulsatile waveforms of CBFV and ABP [27–29] assuming a linear relationship between these two parameters during one cardiac cycle. Alternatively, the fundamental harmonics of the pulse waveforms of ABP and CBFV can also be used [25, 30]. However, a limitation of all these methods consists in the possibility to obtain negative values of CrCP, which cannot be clinically and physiologically explained [31, 32]. Varsos et al. proposed a new method for estimating CrCP derived based on the model of cerebrovascular impedance [26], eliminating the issue of rendering negative values (Eq. 11.3).

$$\mathrm{CrCP} = \mathrm{ABP} - \frac{\mathrm{ABP}}{\sqrt{\left(\mathrm{CVR} \cdot C_{\mathrm{a}} \cdot \mathrm{HR} \cdot 2\pi\right)^2 + 1}} \left(\mathrm{mmHg}\right)\# \tag{11.3}$$

where $\mathrm{CVR} = \dfrac{\mathrm{ABP}}{\mathrm{FV}}$

$$C_{\mathrm{a}} = \frac{C_{\mathrm{a}}\mathrm{BV1}}{\mathrm{a1}}$$

Here, CVR (mmHg/(cm/s)) represents cerebral vascular resistance, C_{a} (cm/mmHg) denotes compliance of the cerebral arterial bed (arteries and arterioles), and HR is the heart rate given in beat/s. a1 represents the pulse amplitude of the first harmonic of the ABP waveform, and C_{a}BV1 is the pulse amplitude of the first harmonic of the cerebral arterial blood volume waveform (C_{a}BV). The pulse amplitude of the first harmonics is determined with fast Fourier transformation.

Derived from CrCP and ABP, other indices, such as the diastolic closing margin (DCM) of the brain microvasculature, can be obtained. Previous works have demonstrated that diastolic ABP ($\mathrm{ABP_d}$) below CrCP is associated with the loss of measurable CBFV during diastole [33], causing an acceleration of brain ischemia when CPP decreases further. The difference in pressures between $\mathrm{ABP_d}$ and CrCP (DCM) represents the force that allows cerebral blood flow circulation during diastole. When DCM is exhausted ($\leq$0 mmHg), vessels will collapse resulting in cessation of cerebral blood flow [33, 34] (Eq. 11.4).

$$\mathrm{DCM} = \mathrm{ABP_d} - \mathrm{CrCP}\left(\mathrm{mmHg}\right) \tag{11.4}$$

11.3.4 Autoregulation

Cerebral blood flow autoregulation refers to the intrinsic ability of the brain to maintain a stable cerebral blood flow (CBF) despite fluctuations in cerebral perfusion pressure [35]. In many neurological diseases (including TBI, stroke), an impairment of this autoregulatory response has been demonstrated [36, 37] and seems that the degree of impairment is related to poor outcome.

Traditionally, assessment of cerebral autoregulation has been performed under steady-state conditions, at constant baselines ABP and CBF, and then another steady-state measurement was performed following manipulation of ABP. Many authors adopted TCD as a static model for autoregulation assessment in patients using the static autoregulatory index or static rate of regulation, defined as the net change in cerebral blood flow following the manipulation of cerebral perfusion pressure under steady state [38, 39].

Although for decades this classic static approach has been widely applied in clinical practice, it does not take into account different factors including the different upper and lower limits of autoregulation or different slopes of the "autoregulatory zone" among different individuals [40]. Thus, the investigation of dynamic cerebral autoregulation using TCD is an area of significant research given the high temporal resolution, which allows to measure the timing and the magnitude of the changes of CBF to the CPP/ABP challenge. This "dynamic" approach uses the induced or spontaneous rapid changes in ABP as an autoregulatory stimulus and compares ABP and CBFV during the whole autoregulatory process (dynamic pressure autoregulation) [41].

In brain monitoring, TCD/TCCS can be useful to calculate an index of autoregulation called mean flow index (Mx) which is the correlation coefficient index between MFV and CPP [42]. Zero or negative correlation indicates preserved autoregulation, whereas a positive correlation between CPP and CBFV indicates impaired autoregulation. Mx index has shown to be strongly associated with poor outcome at 6 months in patients with impaired autoregulation after severe head injury [57]. More recently, Budohoski et al. [43] demonstrated in a cohort of 300 head-injured patients that a new autoregulation index, the Sx index (correlation between PSV and CPP), shows a stronger association with the patient outcome than Mx.

Despite the wide and generally accepted value of TCD in the assessment of cerebral autoregulation, this technique has some limitations. Measurements of CBFV are frequently only taken from the MCA, and thus autoregulatory changes in the posterior circulation may not be detected [44]. Moreover, TCD-based studies use CBFV as a surrogate measure of CBF. However, CBFV is only proportional to CBF when vessel cross-sectional area remains constant, as previously mentioned.

11.3.5 Non-invasive ICP and CPP

ICP evaluation and management is crucial in many neurological diseases, and it is commonly measured through intraventricular or intraparenchymal catheters which are accurate, but their invasive nature and related complications preclude their use in many conditions such as coagulopathy [45, 46]. TCD/TCCS waveform analysis has been widely investigated as a technique for nICP estimation.

TCD-derived nICP methods are based on the relationship between ICP and indices derived from cerebral blood flow velocity. The correlation between PI and ICP has been extensively studied. However, reports on its usefulness for predicting ICP and CPP are discordant [47, 48]. Bellner et al. [25] found a significant correlation ($R = 0.94$, $P < 0.0001$) between invasively measured ICP and PI, with good sensitivity and specificity to detect ICP > 20 mmHg. Other authors found less positive results; Zweifel et al. [26] in a cohort of 290 patients found a weak correlation between PI and ICP (0.31; $P < 0.001$), with a 95% prediction interval of ICP values wider than ±15 mmHg. In a recent study, Cardim et al. [12] demonstrated a non-significant correlation between nICP derived from PI and ICP measured invasively.

The role of PI in the assessment of ICP is not clear, and the variability of these results can be explained by the fact that increase in PI is not specific to increase in ICP. PI can increase following a decrease in CPP and ABP, or during decrease in partial pressure of CO_2 or increase in pulsatility of ABP waveform [5].

Many authors have proposed mathematical models that simulate the cerebrovascular dynamics using simultaneous CBFV and ABP measurements. In a Black-Box model for estimation of ICP, the intracranial compartment is considered a black-box system, with ICP being a system response (output signal ICP) to the incoming signal ABP (input signal). Cardim et al. [12] evaluated the black-box method in a cohort of 40 TBI patients, obtaining a moderate correlation with measured ICP ($R = 0.39$, $P < 0.05$). Other mathematical models have also been proposed, such as the cerebrovascular dynamics model for non-invasive estimation of ICP according to Heldt [49].

Many authors have also studied and proposed methods based on the primarily intended calculation of non-invasive cerebral perfusion pressure (nCPP), and secondarily calculating non-invasive ICP based on the assumption that (Eq. 11.5)

$$\text{nICP} = \text{ABP} - \text{nCPP}. \tag{11.5}$$

Aaslid et al. [50] first developed a mathematical model for non-invasive estimation of CPP based on transcranial Doppler waveform analysis based on spectral pulsatility index and the first harmonic component of the arterial blood pressure, but this method demonstrated low accuracy.

Czosnyka et al. [51] proposed a similar but modified formula, based on the waveform analysis of CBFV, which uses the EDV for the estimation of nCPP. In 96 patients suffering from head injury, the correlation between nCPP and measured CPP was $R = 0.73$ ($P < 0.001$), with estimation error less than 15 mmHg and in 84% of the examinations.

Varsos et al. used a method based on CrCP [52]. According to this method, nCPP seems to be correlated with measured CPP ($R = 0.85$, $P < 0.001$), with a mean ± SD difference of 4.02 ± 6.01 mmHg, and 83.3% of the cases with an estimation error below 10 mmHg [52].

Considering the distinct categories for nICP estimation, there has been a considerable variability in the reported accuracy of these methods, and various methods demonstrated wide confidence intervals for prediction and remain to be fully validated [53]. Nevertheless, it is known that even the standard invasive techniques might not comply with the specified limits for error [54–56]. Thus, it is debatable whether these accuracy requirements are realistic for all sorts of ICP monitoring.

In view of this, an important concept that should be stressed is ICP not solely "as a number," once dynamical features of this parameter, such as its waveform and relative changes in time, are fundamental for a proper assessment of the clinical state of the patient [57]. Therefore, despite the intrinsic limitations and inaccuracy to predict ICP mean absolute values, TCD-based nICP methods may have a potential clinical utility since this technique allows a non-invasive assessment of cerebral circulation dynamics as ICP changes over the time domain.

These features also allow tracking nICP changes in real time in a variety of clinical settings (emergency rooms, ambulatories, operating theaters). This is one of the advantages of transcranial Doppler ultrasonography and may become particularly useful as a primary assessment tool in centers where ICP monitoring is not routinely applied or unavailable. It may also suit patients in whom invasive ICP monitoring may not be clearly indicated (mild closed head injury, for example) or contraindicated (coagulopathy, for instance).

11.4 Applications of TCD/TCCS Monitoring in Clinical Practice

11.4.1 Traumatic Brain Injury

Traumatic brain injury (TBI) is a relevant cause of morbidity and mortality, and several important disturbances of cerebral hemodynamics occur after TBI, including hyperemia, cerebral ischemia, and vasospasm.

Monitoring and targeted management of ICP and CPP are necessary for patients with severe traumatic brain injury. Intracranial hypertension and low CPP are associated with poor outcome, and the literature is clear about the importance of a strict neuromonitoring in order to avoid secondary brain insults [58].

TCD has been widely applied in TBI patients, in particular, for the assessment of ICP and CPP in human and animal studies [12]; moreover, some authors showed that impaired autoregulation, determined by TCD methods (Mx or Sx index), is strongly associated with poor outcome at 6 months [42, 43]. TCD demonstrated to be useful in TBI patients as it is able to avoid the use of invasive techniques for the measurement of CBF and provide similar prognostic information [43].

TCD can be also useful in TBI patients for the assessment of cerebral dynamics and cerebral swelling through the calculation of cerebral compliance. Hyperemia may occur a few hours after TBI, lasting 2 to 4 days, and also be assessed using TCD patterns suggestive of high vascular resistance, consistent with elevated intracranial pressure [59], or following an ischemic event.

EDV and PI have been shown to have a role in the decision between "fast track" and standard ICP monitoring at admission in patients with TBI [60]. In the emergency room, TCD might complement brain computed tomography scan and clinical examination to screen patients at risk of further neurological deterioration after TBI. In a recent study [61], transcranial Doppler parameters showed a strong negative predictive value (NPV) in TBI patients who did not undergo secondary neurologic deterioration, and patients with abnormal TCD patterns had greater disability 4 weeks after TBI.

11.4.2 Aneurysmal Subarachnoid Hemorrhage

Aneurysmal subarachnoid hemorrhage (aSAH) has an incidence of 6–10 per 100,000 people per year [62], with a 6-month mortality rate ranging from 32 to 67%, and 30% of survivors harbor permanent neurological impairment [63].

In 20 to 40% of patients, new ischemic neurological deficits that were not present on hospital admission become apparent in the days and weeks following the ictus and are mainly associated with vasospasm consequent to aSAH. Vasospasm usually occurs 3 to 14 days following aneurysmal subarachnoid hemorrhage (aSAH), and it is known to be one of the causes leading to delayed cerebral ischemia (DCI) and poor outcomes [64].

Angiography is considered the gold standard for the detection of vasospasm; however, TCD has been extensively used for monitoring patients with aSAH, and it has been demonstrated to be able to assess vasospasm and monitor and guide the clinical treatment (triple-H therapy, angioplasty, etc.) [65].

TCD for the detection of vasospasm, usually performed on the MCA, has been studied by several authors. TCD is able to detect vasospasm as the constriction of the cerebral vessels leads to an increase of cerebral blood flow velocities [65].

According to a recent meta-analysis [66] including 2870 patients, TCD was found to be highly predictive of evidence of vasospasm in patients with aSAH with sensitivity of 90% (95% confidence interval (CI) 77%–96%), specificity of 71% (95% CI 51%–84%), positive predictive value (PPV) of 57% (95% CI 38%–71%), and NPV of 92% (95% CI 83%–96%) at pooled estimates for TCD diagnosis of vasospasm.

Vora et al. [66] in a retrospective study of 101 patients found that MCA means flow velocity higher than 120 cm/s had a specificity of 72% and sensitivity of 88% for ≥33% of angiographic vasospasm with a NPV of 94% for MFV < 120 cm/s. Moreover, MFV > 200 cm/s was 98% specific and 27% sensitive with a PPV of 87% for angiographic vasospasm of ≥33%.

To differentiate an increase of the CBFV related to systemic hyperdynamic flow and vasospasm, the Lindegaard ratio (LR) [67] is normally used, which is defined as MFV on the MCA divided for the extracranial ICA MFV. LR < 3 indicates hyperdynamic flow (hyperemia) and >3 indicates vasospasm. Mild vasospasm is defined as MFV > 120 and <149 cm/s (LR = 3–6); moderate vasospasm is defined as MFV > 150 and <199 (LR = 3–6) and severe vasospasm as MFV > 200 cm/s with LR > 6.

TCD has been extensively used for the detection of cerebral vasospasm showing good sensitivity and specificity, but TCD can also have a role in the detection of cerebral autoregulation after aSAH. Late detection of impaired cerebral autoregulation in these patients [68] is associated with increased risk to develop DCI independently of the incidence of vasospasm [69], and it is associated with poorer outcome [70].

11.4.3 Stroke

In patients affected by internal carotid artery (ICA) stenosis, impaired autoregulation assessed by significant increases in Mx and decreases in dynamic autoregulation index observed in the pathological stenoocclusive arteries have shown to correlate with the degree of stenosis and is considered a tool to identify patients at risk of stroke and for need of surgical decompression [71]. For instance, in a cohort of 48 patients with angiographic occlusion, TCD showed an overall sensitivity of 83% and specificity of 94%, especially in the anterior circulation [72].

TCD can also be a reliable prognostic indicator in MCA occlusive stroke [73], and its role in the assessment of cerebral autoregulation after stroke has been extensively studied. Some authors have consistently shown an impairment in ipsilateral cerebral autoregulation and an association with the need for decompressive surgery, neurological decline, and poor outcome [44].

TCD may also have a role in the prediction of outcome in patients with stroke, according to the site and severity of occlusion observed. In a study of 335 patients with acute stroke who received thrombolytic treatment, distal MCA occlusions assessed through TCD were associated with the greatest chance of early recanalization (44%), compared with 30% in the proximal MCA, 30% in the basilar artery, and <10% in the terminal ICA [74].

Despite the important role of TCD in patients with ischemic stroke, CTA and MRI are still considered first-line imaging techniques due to the operator dependency and poor ability of TCD to access the posterior cerebral circulation [6].

11.4.4 Other Clinical Scenarios

TCD presents a wide range of clinical applications in the context of anesthesiology, neurology, neurosurgery, and neurointensive care settings (Table 11.2).

Besides the common previously described applications in neurointensive care settings (TBI, SAH, stroke), it has been successfully applied in the diagnosis of brainstem death [75] in central nervous system infections and in many ischemic cerebrovascular diseases (sickle cell disease, right to left cardiac shunt, venous thrombosis) in adult and pediatric populations [6, 76, 77].

Moreover, TCD is gaining interest even in the intraoperative settings. It has been successfully applied in order to assess nCPP and nICP in surgical procedures at risk of intracranial hypertension [78, 79], such as laparoscopic procedures with pneumoperitoneum and Trendelenburg position [80]. It has been also successfully used for neuromonitoring during carotid endarterectomy or during cardiopulmonary bypass [81].

Growing and recent evidences support the use of TCD even in metabolic coma (such as during liver transplant or hepatic encephalopathy) or in pregnant patients to assess autoregulation and cerebrovascular changes as prognostic factor for pre-eclampsia and cerebrovascular events during pregnancy [82].

Finally, TCD has been recently applied in septic patients to assess nCPP and PI. Some authors found higher values of PI and cerebral vascular constriction in septic patients compared to control group, suggesting a possible role of TCD in the assessment of the mechanisms underlying the pathogenesis of sepsis-related encephalopathy [83].

11.5 Conclusion

The non-invasiveness, repeatability, portability, and high temporal resolution of TCD have promoted the wide use of this technique, especially for bedside monitoring of CBF in the neurocritical care settings.

Invasive techniques still appear to remain the gold standard across most of the clinical applications; moreover, operator dependency and the need for an appropriate temporal window are significant limitations to TCD clinical utility.

However, despite some limitations including operator dependency and 10–20% of patients having inadequate transtemporal acoustic windows, TCD remains a valuable tool for the assessment of cerebral hemodynamics in critically ill patients. Its wide utility as a diagnostic tool makes it a useful “stethoscope for the brain.”

Algorithm

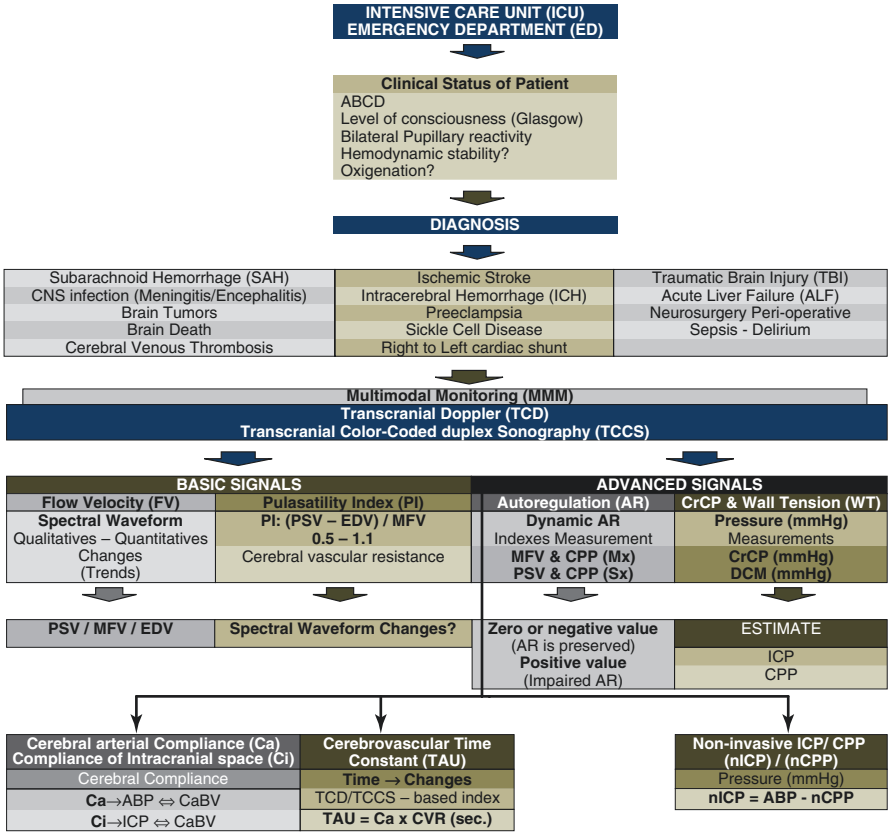

ABCD Airway-breathing-circulation-disability, *CPP* Cerebral Perfusion Pressure, *ICP* Intracranial Pressure/*MFV* Mean flow velocity, *EDV* diastolic flow Velocity, *PSV* Peak systolic flow velocity, *Ca* Cerebral arterial compliance, *Ci* Compliance of intracranial space, *CVR* Cerebrovascular resistance

References

1. White H, Venkatesh B. Applications of transcranial Doppler in the ICU: a review. Intensive Care Med. 2006;32:981–94.
2. Trabold F, Meyer PG, Blanot S, Carli PA, Orliaguet GA. The prognostic value of transcranial Doppler studies in children with moderate and severe head injury. Intensive Care Med. 2004;30(1):108–12.
3. Hoffmann O, Zierski JT. Analysis of the ICP pulse-pressure relationship as a function of arterial blood pressure: clinical validation of a mathematical model. Acta Neurochir. 1982;66:1–21.

4. Bekker A, Wolk S, Turndorf H, Kristol D, Ritter A. Computer simulation of cerebrovascular circulation: assessment of intrac rani al hemodynamics during induction of anesthesia. J Clin Monit. 1996;12(6):433–44.
5. De Riva N, Budohoski KP, Smielewski P, Kasprowicz M, Zweifel C, Steiner LA, et al. Transcranial doppler pulsatility index: what it is and what it isn't. Neurocrit Care. 2012;17(1):58–66.
6. Naqvi J, Yap KH, Ahmad G, Ghosh J. Review article transcranial Doppler ultrasound: a review of the physical principles and major applications in critical care. 2013;2013(March).
7. Nicoletto HA, Burkman MH. Transcranial Doppler series part III: interpretation. Am J Electroneurodiagnostic Technol [Internet]. 2009 Sep [cited 2017 Aug 25];49(3):244–59.
8. Nicoletto HA, Burkman MH. Transcranial Doppler series part IV: case studies. Am J Electroneurodiagnostic Technol [Internet]. 2009 Dec [cited 2017 Aug 25];49(4):342–60.
9. Tegeler CH, Crutchfield K, Katsnelson M, Kim J, Tang R, Passmore Griffin L, et al. Transcranial doppler velocities in a large, healthy population. J Neuroimaging. 2013;23(3):466–72.
10. Giller CA, Hodges K, Batjer HH. Transcranial Doppler pulsatility in vasodilation and stenosis. J Neurosurg. 1990;72:901–6.
11. Czosnyka M, Richards HK, Whitehouse HE, Pickard JD. Relationship between transcranial Doppler-determined pulsatility index and cerebrovascular resistance: an experimental study. J Neurosurg. 1996;84(1):79–84.
12. Cardim D, Robba C, Bohdanowicz M, Donnelly J, Cabella B, Liu X, et al. Non-invasive monitoring of intracranial pressure using transcranial Doppler ultrasonography: is it possible? Neurocrit Care [Internet]. 2016 [cited 2016 Mar 7].
13. Czosnyka M, Smielewski P, Piechnik S, Schmidt EA, Al-Rawi PG, Kirkpatrick PJ, et al. Hemodynamic characterization of intracranial pressure plateau waves in head-injured patients. J Neurosurg. 1999;91(1):11–9.
14. Avezaat C, Van Eijndhoven J. Cerebrospinal fluid pulse pressure and craniospinal dynamics: a theoretical, clinical and experimental study. Resuscitation. 1984:111–26.
15. Cardim D, Schmidt B, Robba C, Donnelly J, Puppo C, Czosnyka M, et al. Transcranial Doppler monitoring of intracranial pressure plateau waves. Neurocrit Care [Internet]. Springer US; 2016 Dec 20 [cited 2017 May 15];1–9.
16. Oktar SO, Yücel C, Karaosmanoglu D, Akkan K, Ozdemir H, Tokgoz N, et al. Blood-flow volume quantification in internal carotid and vertebral arteries: comparison of 3 different ultrasound techniques with phase-contrast MR imaging. Am J Neuroradiol. 2006;27(2):363–9.
17. Rosner MJ, Becker DP. Origin and evolution of plateau waves. Experimental observations and a theoretical model. J Neurosurg. 1984;60(2):312–24.
18. Kim DJ, Kasprowicz M, Carrera E, Castellani G, Zweifel C, Lavinio A, et al. The monitoring of relative changes in compartmental compliances of brain. Physiol Meas [Internet]. 2009;30(7):647–59.
19. Eide PK, Sorteberg A, Bentsen G, Marthinsen PB, Stubhaug A, Sorteberg W. Pressure-derived versus pressure wave amplitude-derived indices of cerebrovascular pressure reactivity in relation to early clinical state and 12-month outcome following aneurysmal subarachnoid hemorrhage. J Neurosurg. 2012;116(5):961–71.
20. Czosnyka M, Richards HK, Reinhard M, Steiner LA, Budohoski K, Smielewski P, et al. Cerebrovascular time constant: dependence on cerebral perfusion pressure and end-tidal carbon dioxide concentration. Neurol Res. 2012;34(1):17–24.
21. Kasprowicz M, Diedler J, Reinhard M, Carrera E, Smielewski P, Budohoski KP, et al. Time constant of the cerebral arterial bed. Acta Neurochir Suppl [Internet]. 2012 Jan [cited 2016 Mar 24];114:17–21.
22. Kasprowicz M, Czosnyka M, Soehle M, Smielewski P, Kirkpatrick PJ, Pickard JD, et al. Vasospasm shortens cerebral arterial time constant. Neurocrit Care. 2012;16(2):213–8.
23. Trofimov A, Kalentiev G, Gribkov A, Voennov O, Grigoryeva V. Cerebrovascular time constant in patients with head injury. Acta Neurochir Suppl. 2016;121:295–7.

24. Nichol J, Girling F, Jerrard W, Claxton EB, Burton AC. Fundamental instability of the small blood vessels and critical closing pressures in vascular beds. Am J Physiol [Internet]. 1951 Feb [cited 2015 Aug 4];164(2):330–44.
25. Michel E, Hillebrand S, von Twickel J, Zernikow B, Jorch G. Frequency dependence of cerebrovascular impedance in preterm neonates: a different view on critical closing pressure. J Cereb Blood Flow Metab. 1997;17(10):1127–31.
26. Varsos GV, Richards H, Kasprowicz M, Budohoski KP, Brady KM, Reinhard M, et al. Critical closing pressure determined with a model of cerebrovascular impedance. J Cereb Blood Flow Metab [Internet]. 2013;33(2):235–43.
27. Panerai RB. The critical closing pressure of the cerebral circulation. Med Eng Phys. 2003;25(8):621–32.
28. Czosnyka M, Smielewski P, Piechnik S, Al-Rawi PG, Kirkpatrick PJ, Matta BF, et al. Critical closing pressure in cerebrovascular circulation. J Neurol Neurosurg Psychiatry [Internet]. 1999;66(5):606–11.
29. Aaslid R, Lash SR, Bardy GH, Gild WH, Newell DW. Dynamic pressure–flow velocity relationships in the human cerebral circulation. Stroke. 2003;34(7):1645.
30. Aaslid R, Lash SR, Bardy GH, Gild WH, Newell DW. Dynamic pressure-flow velocity relationships in the human cerebral circulation. Stroke. 2003;34(7):1645–9.
31. Puppo C, Camacho J, Yelicich B, Moraes L, Biestro A, Gomez H. Bedside study of cerebral critical closing pressure in patients with severe traumatic brain injury: a transcranial Doppler study. Acta Neurochir Suppl. 2012;114:283–8.
32. Soehle M, Czosnyka M, Pickard JD, Kirkpatrick PJ. Critical closing pressure in subarachnoid hemorrhage: effect of cerebral vasospasm and limitations of a transcranial Doppler-derived estimation. Stroke. 2004;35(6):1393–8.
33. Varsos GV, Richards HK, Kasprowicz M, Reinhard M, Smielewski P, Brady KM, et al. Cessation of diastolic cerebral blood flow velocity: the role of critical closing pressure. Neurocrit Care. 2014;20(1):40–8.
34. Donnelly J, Czosnyka M, Harland S, Varsos GV, Cardim D, Robba C, et al. Cerebral haemodynamics during experimental intracranial hypertension. J Cereb Blood Flow Metab [Internet]. 2017;37(2):694–705.
35. Czosnyka M, Smielewski P, Piechnik S, Pickard JD. Clinical significance of cerebral autoregulation. Acta Neurochir Suppl. 2002;81:117–9.
36. Bouma GJ, Muizelaar JP, Bandoh K, Marmarou A. Blood pressure and intracranial pressure-volume dynamics in severe head injury: relationship with cerebral blood flow. J Neurosurg. 1992;77(1):15–9.
37. Zweifel C, Lavinio A, Steiner LA, Radolovich D, Smielewski P, Timofeev I, et al. Continuous monitoring of cerebrovascular pressure reactivity in patients with head injury. Neurosurg Focus. 2008;25(4):E2.
38. Panerai RB. Transcranial Doppler for evaluation of cerebral autoregulation. Clin Auton Res. 2009;19(4):197–211.
39. Tiecks FP, Lam AM, Aaslid R, Newell DW. Comparison of static and dynamic cerebral autoregulation measurements. Stroke. 1995;26(6):1014–9.
40. Donnelly J, Aries MJ, Czosnyka M. Further understanding of cerebral autoregulation at the bedside: possible implications for future therapy. Expert Rev Neurother. 2015;15(2):169–85.
41. Zhang R, Zuckerman JH, Giller CA, Levine BD. Transfer function analysis of dynamic cerebral autoregulation in humans. Am J Phys. 1998;274:233–41.
42. Czosnyka M, Smielewski P, Kirkpatrick P, Menon DK, Pickard JD. Monitoring of cerebral autoregulation in head-injured patients. Stroke. 1996;27:1829–34.
43. Budohoski KP, Reinhard M, Aries MJH, Czosnyka Z, Smielewski P, Pickard JD, et al. Monitoring cerebral autoregulation after head injury. Which component of transcranial Doppler flow velocity is optimal? Neurocrit Care. 2012;17(2):211–8.
44. Aries MJH, Elting JW, De Keyser J, Kremer BPH, Vroomen PCAJ. Cerebral autoregulation in stroke: a review of transcranial doppler studies. Stroke. 2010;41:2697–704.

45. Bratton SL, Chestnut RM, Ghajar J, McConnell Hammond FF, Harris OA, Hartl R, et al. Guidelines for the management of severe traumatic brain injury. IX. Cerebral perfusion thresholds. J Neurotrauma. 2007;24 Suppl 1:S59–64.
46. Holloway KL, Barnes T, Choi S, Bullock R, Marshall LF, Eisenberg HM, et al. Ventriculostomy infections: the effect of monitoring duration and catheter exchange in 584 patients. J Neurosurg. 1996;85(3):419–24.
47. Bellner J, Romner B, Reinstrup P, Kristiansson KA, Ryding E, Brandt L. Transcranial Doppler sonography pulsatility index (PI) reflects intracranial pressure (ICP). Surg Neurol. 2004;62:45–51.
48. Zweifel C, Czosnyka M, Carrera E, de Riva N, Pickard JD, Smielewski P. Reliability of the blood flow velocity pulsatility index for assessment of intracranial and cerebral perfusion pressures in head-injured patients. Neurosurgery [Internet]. 2012 Oct [cited 2015 Jul 21];71(4):853–61.
49. Kashif FM, Verghese GC, Novak V, Czosnyka M, Heldt T. Model-based noninvasive estimation of intracranial pressure from cerebral blood flow velocity and arterial pressure. Sci Transl Med. 2012;4(129):129ra44.
50. Aaslid R, Lundar T, Lindegaard KF, et al. No title. In: Miller JD, Teasdale GM, Rowan JO, editors. Intracrani. Berlin: Springer- Verlag; 1986. p. 226–32.
51. Czosnyka M, Matta BF, Smielewski P, Kirkpatrick PJ, Pickard JD. Cerebral perfusion pressure in head-injured patients: a noninvasive assessment using transcranial Doppler ultrasonography. J Neurosurg. 1998;88:802–8.
52. Varsos G V, Kolias AG, Smielewski P, Brady KM, Varsos VG, Hutchinson PJ, et al. A noninvasive estimation of cerebral perfusion pressure using critical closing pressure. J Neurosurg. 2015;11.
53. Cardim D, Schmidt B, Robba C, Donnelly J, Puppo C, Czosnyka M, et al. Transcranial Doppler monitoring of intracranial pressure plateau waves. Neurocrit Care [Internet]. Springer US; 2016 Dec 20 [cited 2017 Feb 15];1–9.
54. Koskinen LOD, Olivecrona M. Clinical experience with the intraparenchymal intracranial pressure monitoring Codman microsensor system. Neurosurgery. 2005;56(4):693–7.
55. Eide PK, Park E-H, Madsen JR. Arterial blood pressure vs intracranial pressure in normal pressure hydrocephalus. Acta Neurol Scand [Internet]. 2010 [cited 2012 Mar 11];122(4):262–9.
56. Zacchetti L, Magnoni S, Di Corte F, Zanier ER, Stocchetti N. Accuracy of intracranial pressure monitoring: systematic review and meta-analysis. Crit Care [Internet]. 2015;19(1):420.
57. Czosnyka M, Smielewski P, Timofeev I, Lavinio A, Guazzo E, Hutchinson P, et al. Intracranial pressure: more than a number. Neurosurg Focus. 2007;22(5):E10.
58. Lane PL, Skoretz TG, Doig G, Girotti MJ. Intracranial pressure monitoring and outcomes after traumatic brain injury. Can J Surg. 2000;43(6):442–8.
59. Muttaqin Z, Uozumi T, Kuwabara S, Arita K, Kurisu K, Ohba S, et al. Hyperaemia prior to acute cerebral swelling in severe head injuries: the role of transcranial Doppler monitoring. Acta Neurochir. 1993;123(1–2):76–81.
60. Bouzat P, Oddo M, Payen J-F. Transcranial Doppler after traumatic brain injury: is there a role? Curr Opin Crit Care. 2014;20(2):153–60.
61. Bouzat P, Almeras L, Manhes P, Sanders L, Levrat A, David J-S, et al. Transcranial Doppler to predict neurologic outcome after mild to moderate traumatic brain injury. Anesthesiology. 2016;PublishedA(May).
62. Rincon F, Rossenwasser RH, Dumont A. The epidemiology of admissions of nontraumatic subarachnoid hemorrhage in the United States. Neurosurgery. 2013;73(2):217–22.
63. Hop JW, Rinkel GJE, Algra A, van Gijn J. Case-fatality rates and functional outcome after subarachnoid hemorrhage: a systematic review. Stroke. 1997;28(3):660–4.
64. Diringer MN, Bleck TP, Hemphill JC, Menon D, Shutter L, Vespa P, et al. Critical care management of patients following aneurysmal subarachnoid hemorrhage: recommendations from the neurocritical care society's multidisciplinary consensus conference. Neurocrit Care. 2011;15:211–40.

65. Kumar G, Shahripour RB, Harrigan MR. Vasospasm on transcranial Doppler is predictive of delayed cerebral ischemia in aneurysmal subarachnoid hemorrhage: a systematic review and meta-analysis. J Neurosurg. 2015:1–8.
66. Vora Y, Suarez-Almazor M, Steinke D, Martin M, Findlay J. Role of transcranial Doppler monitoring in the diagnosis of cerebral vasospasm after subarachnoid hemorrhage. Neurosurgery. 1999;44(6):1237-47-8.
67. Lindegaard KF, Nornes H, Bakke SJ, Sorteberg W, Nakstad P. Cerebral vasospasm after subarachnoid haemorrhage investigated by means of transcranial Doppler ultrasound. Acta Neurochir Suppl (Wien). 1988;42:81–4.
68. Budohoski KP, Czosnyka M, Kirkpatrick PJ, Smielewski P, Steiner LA, Pickard JD. Clinical relevance of cerebral autoregulation following subarachnoid haemorrhage. Nat Rev Neurol Nature Publishing Group. 2013;9(3):152–63.
69. Budohoski KP, Czosnyka M, Smielewski P, Kasprowicz M, Helmy A, Bulters D, et al. Impairment of cerebral autoregulation predicts delayed cerebral ischemia after subarachnoid hemorrhage: a prospective observational study. Stroke. 2012;43(12):3230–7.
70. Budohoski KP, Czosnyka M, Kirkpatrick PJ, Reinhard M, Varsos GV, Kasprowicz M, et al. Bilateral failure of cerebral autoregulation is related to unfavorable outcome after subarachnoid hemorrhage. Neurocrit Care. 2014;22(1):65–73.
71. Reinhard M, Roth M, Müller T, Czosnyka M, Timmer J, Hetzel A. Cerebral autoregulation in carotid artery occlusive disease assessed from spontaneous blood pressure fluctuations by the correlation coefficient index. Stroke. 2003;34(9):2138–44.
72. Demchuk a M, Christou I, Wein TH, Felberg R a, Malkoff M, Grotta JC, et al. Accuracy and criteria for localizing arterial occlusion with transcranial Doppler. J Neuroimaging. 2000;10(1):1–12.
73. Alexandrov AV, Burgin WS, Demchuk AM, El-Mitwalli A, Grotta JC. Speed of intracranial clot lysis with intravenous tissue plasminogen activator therapy: sonographic classification and short-term improvement. Circulation. 2001;103(24):2897–902.
74. Moppett IK, Mahajan RP. Transcranial Doppler ultrasonography in anaesthesia and intensive care. Br J Anaesth Br J Anaesth. 2004;93(93):710–24.
75. Ducrocq X, Braun M, Debouverie M, Junges C, Hummer M, Vespignani H. Brain death and transcranial Doppler: experience in 130 cases of brain dead patients. J Neurol Sci. 1998;160(1):41–6.
76. Adams RJ. TCD in sickle cell disease: an important and useful test. Pediatr Radiol. 2005;35:229–34.
77. Cabanes L, Mas JL, Cohen A, Amarenco P, Cabanes PA, Oubary P, et al. Atrial septal aneurysm and patent foramen ovale as risk factors for cryptogenic stroke in patients less than 55 years of age: a study using transesophageal echocardiography. Stroke. 1993;24(12):1865–73.
78. Robba C, Bragazzi NL, Bertuccio A, Cardim D, Donnelly J, Sekhon M, et al. Effects of prone position and positive end-expiratory pressure on noninvasive estimators of ICP: a pilot study. J Neurosurg Anesthesiol [Internet]. 2016 Mar 18 [cited 2016 May 19].
79. Robba C, Cardim D, Donnelly J, Bertuccio A, Bacigaluppi S, Bragazzi N, et al. Effects of pneumoperitoneum and Trendelenburg position on intracranial pressure assessed using different non-invasive methods. Br J Anaesth [Internet]. 2016;117(6):783–91. Available from: http://bja.oxfordjournals.org/lookup/doi/10.1093/bja/aew356.
80. Joshi B, Ono M, Brown C, Brady K, Easley RB, Yenokyan G, et al. Predicting the limits of cerebral autoregulation during cardiopulmonary bypass. Anesth Analg. 2012;114(3):503–10.
81. Aggarwal S, Brooks DM, Kang Y, Linden PK, Patzer JF. Noninvasive monitoring of cerebral perfusion pressure in patients with acute liver failure using transcranial doppler ultrasonography. Liver Transpl. 2008;14:1048–57.
82. Williams K, Galerneau F. Maternal transcranial Doppler in pre-eclampsia and eclampsia. Ultrasound Obstet Gynecol. 2003;21:507–13.
83. Pierrakos C, Antoine A, Velissaris D, Michaux I, Bulpa P, Evrard P, et al. Transcranial doppler assessment of cerebral perfusion in critically ill septic patients: a pilot study. Ann Intensive Care. 2013;3:28.

Chapter 12
Neurosonology in the ICU: Transcranial Doppler (TCD) Protocol

Corina Puppo

Key Points

1. TCD is a non-invasive ultrasound technique at the patient's bedside, measuring cerebral blood flow velocities (CBFV) of basal cerebral arteries.
2. It measures flow velocities and estimates changes in cerebral blood flow but does not measure cerebral blood flow in absolute values.
3. It uses areas or natural orifices of the skull as acoustic windows to insonate intracerebral hemodynamic changes.
4. The most used acoustic window to evaluate global cerebral hemodynamics is the transtemporal window through the middle cerebral artery (MCA) insonation.
5. TCD, through an envelope wave, determines the three flow velocities and the derived hemodynamic indexes: PSV, EDV, MFV, PI, RI, and LR.
6. In normal conditions, the intracranial blood flow circulates only in one direction, accelerating during systole and decelerating during diastole, without ever stopping or reversing its direction.
7. The cerebral arteries' blood flow is less pulsatile than in the rest of the arteries of the body, given the important collateral circulation of the system (circle of Willis) that maintains a low resistance pattern.
8. It is essential to repeat the TCD examinations in order to measure the hemodynamic changes in real time and to assess the trends of the parameters evaluated and/or the response to an established therapeutic trial.

C. Puppo (✉)
Intensive Care Unit, Clinics Hospital, Universidad de la Republica School of Medicine, Montevideo, Uruguay
e-mail: coripuppo@gmail.com

C. N. Rodríguez et al. (eds.), *Neurosonology in Critical Care*,
https://doi.org/10.1007/978-3-030-81419-9_12

12.1 Introduction

Transcranial Doppler (TCD) is a non-invasive ultrasound method that measures cerebral blood flow velocities (CBFVs) in the basal cerebral arteries (circle of Willis), without transferring the patient out of the ICU.

It measures the circulatory velocity of the blood. It does not measure cerebral blood flow (C BF). However, under certain conditions, changes in CBFV are proportional to changes in CBF.

In intensive care unit (ICU), it can be used (a) uniquely, (b) repeatedly, observing the trend of changes in CBFVs and pulsatility, (c) continuously alone, or (d) combined with other variables, for example, arterial blood pressure and intracranial pressure (ICP), constituting multimodal neuromonitoring.

12.2 TCD: Spectral Wave

The screen of the TCD equipment shows the circulation velocity in time. The circulatory velocity of a complete arterial pulse cycle is called sonogram.

At each instant the blood particle velocities can be seen. Since the ultrasound is reflected by multiple moving blood particles in a certain segment of the artery (the depth and size of this segment are chosen by the operator), a "spectrum" of velocities is generated [1]. This spectrum is different if the flow is laminar or turbulent (Fig. 12.1). In arterial segments without stenosis or bifurcations, the flow is laminar.

By taking only the maximum velocities at each point in this spectrum, the TCD equipment outlines an "envelope" wave. The envelope wave, therefore, shows the values of the particles moving at the highest velocity within the arterial vessel. The values of the envelope wave thus generated are those analyzed and displayed by the ultrasound equipment. In the graph of the envelope wave of each arterial pulse, three variables are defined: peak systolic velocity (PSV), mean flow velocity (MFV), and end-diastolic velocity (EDV) (Fig. 12.2).

Spectrum and envelope wave characteristics: Under normal conditions, cerebral blood flow moves in a single direction within the vessel, slows down in the diastole, and accelerates when a new blood pulse arrives. It does not stop or reverse its direction. The final diastolic rate is the lowest of each pulse, greater than zero.

By convention, the flow toward the transducer is given a positive value and the flow away from it is given a negative value. In the arterial bifurcations, a bidirectional flow is seen.

A relatively constant diameter of the studied vessel is assumed, and thus the changes of CBFV are directly proportional to the changes of CBF. For this, the transducer must remain fixed without changes in its angulation.

TCD measures CBFV and estimates changes in CBF but does not measure CBF in absolute values.

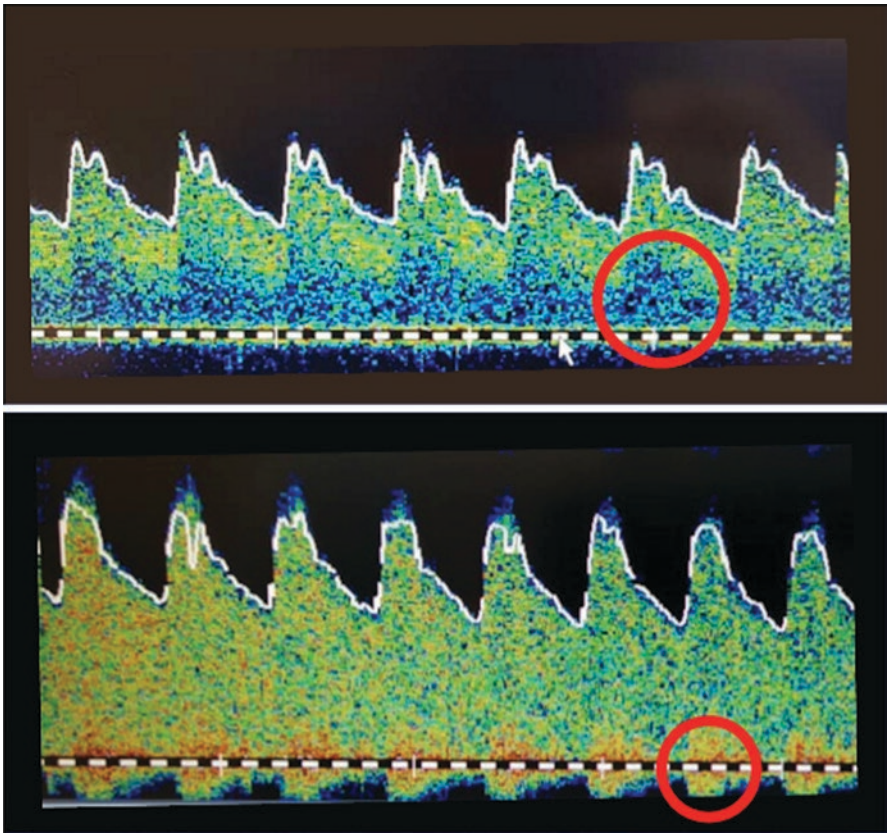

Fig. 12.1 Difference between laminar flow spectrum (upper) and turbulent flow spectrum (lower). In the first one most of the circulating particles are of high velocity and therefore form a thick line near the maximum velocity in each instant; the different colors translate more or less particles concentration. A lower triangle remains where there is a spectral window, indicated by a red circle. In turbulent flow, which can be seen in bifurcations, or in severe stenoses, the angles of intonation are formed between the direction of the particles rotating in turbulent form and the direction of the ultrasound emitted by the transducer are large, so they look as low velocities. The vascular murmur is marked with a circle, evidencing the turbulence, which has a special sound, like that of a ¨seagull's song¨, superimposed on the normal sound

12.3 TCD: Identification of Vessels

Transcranial Doppler identifies the different arteries according to

1. Characteristics of the Doppler signal.
2. Topography of the Doppler signal (acoustic window, direction of the ultrasound beam, and depth).
3. Hemodynamic response to maneuvers.

1. *Characteristics of the Doppler Signal:*

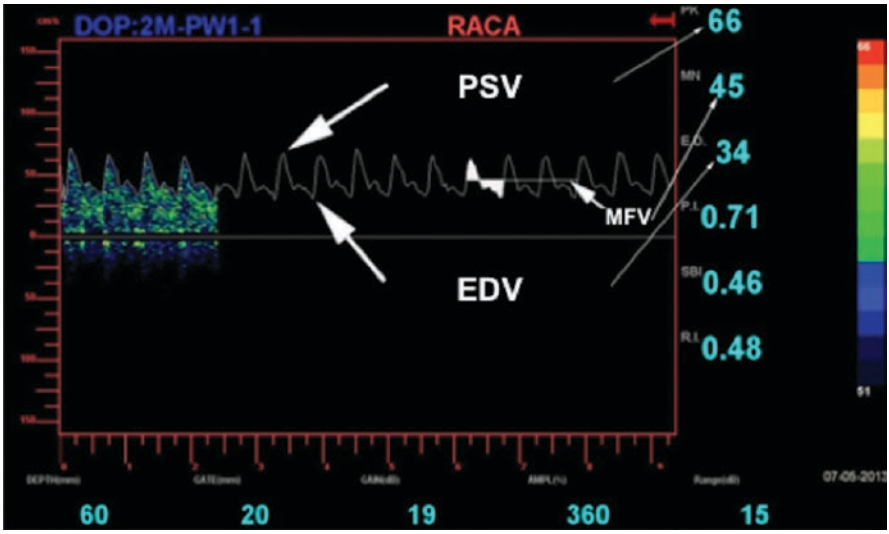

Fig. 12.2 On the left you can see a Doppler spectrum velocities (sonogram) in the first four cycles. In the following cycles the spectrum has been erased and only the envelope wave is seen. The arrows show the point where the PSV, the EDV and the MFV. You can also see the graphical calculation of the average velocity which in this case coincides with the value calculated by the equipment since the envelope wave correctly follows the maximum values of the Doppler spectrum. The average velocity calculated graphically is the one that marks a horizontal line that divides the envelope wave in two parts of similar area as seen in the figure

By convention, if the flow is directed toward the transducer, it is shown as positive spectrum wave; if it is directed in the opposite direction, it is shown as negative spectrum wave. If a bifurcation is insonated, it is displayed as a bidirectional spectrum wave.

2. *Topography:*

   Different acoustic windows allow to insonate different arteries of the circle of Willis. From each acoustic window, the direction of the ultrasound beam from transducer allows the identification of the different basal cerebral arteries, as well as the depth at which each of them is located.

3. *M-Mode*: *Power Motion Mode Doppler*

   Transcranial Doppler emits pulsed ultrasound. This means that it obtains information only from a small volume of the intracranial space whose depth is permanently defined throughout the examination. This small volume is called the "sample volume." The operator must, therefore, know which vessel he is going to look for, through which window, and at what depth he is going to look for it.

   The operator must also know the insonation angle that he must give to the transducer. This generated the concept that the technique is operator dependent. The introduction of the M-mode (PMD) facilitates the examination, even for inexperienced operators, since it makes it possible to simultaneously see the

intensity and direction of the flow along 6 cm or more of the intracranial space that the ultrasound beams cross.

When using the PMD, the screen of TCD machine is divided into two sectors:

1. In the main sector (generally upper), you can see the sonogram of the vessel under examination (at a predetermined depth), that is, the full characteristics (spectrum, envelope wave, PSV, EDV, MFV, PI) of the flow velocity at the chosen point of the artery under study.
2. In the M-mode sector screen (generally lower), the different flows that appear along the path (3–6 cm or more, configurable by the examiner) of the ultrasound beam in that direction are shown simultaneously (Fig. 12.3). This sector graphs the flows along the beam path, showing in the different depths, if there is any flow or not, and in case there is, in red or blue color if it is directed toward or moves away from the transducer, respectively.

   Over time these segments are seen as red or blue horizontal bands crossing the screen. The display allows to choose any point of interest in this sector, so that the main screen shows the sonogram of the flow at the chosen point and the characteristics of both the spectrum and its envelope waves (PSV, EDV, MFV, PI, etc.).

Normal values of CBFVs vary according to (a) insonated vessel and (b) physiological variables. CBFV in the cerebral arteries varies with age, where they are greatest in childhood and decrease with age. Normal values of CBFV in healthy adults for three age groups are shown in Table 12.1.

To have a global idea of the values in mind, the following scheme is useful: average velocity in cm/s (±10): ACM 60, ACA 50, ACP 40, and posterior circulation sector 35.

Other important physiological variables that influence the CBFV in the cerebral arteries are blood viscosity (one of whose main determinants is hematocrit), temperature, PaCO2, and heart rate.

The trends of values are more important than a single CBFV value.

12.4 TCD: Clinical Utility

TCD is known as the "Stethoscope of the brain." The use of the TCD is directed to the detection and follow-up of cerebral hemodynamics alterations in the patients with neurological injury: acute ischemic stroke (AIS), subarachnoid hemorrhages (SAH), intracerebral hematoma, traumatic brain injury (TBI), and other pathologies such as central nervous system (CNS) infections, cerebral vasculitis, etc. It is especially useful in neurocritically ill patients whose state of consciousness is altered (secondary to different injuries and/or sedation/analgesia/neuromuscular block requirements), and complete neurological examination is not possible. Unlike the TCCS, it does not show anatomical images (B-mode) but only the blood flow velocities in the basal cerebral arteries.

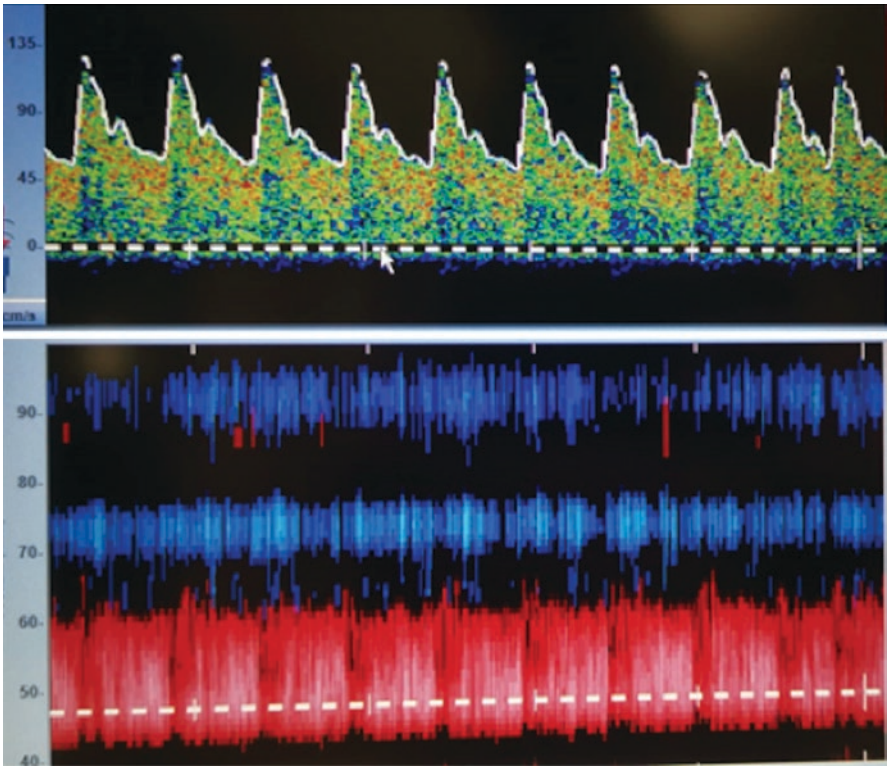

Fig. 12.3 The M mode or "Power Mode". The two panels that appear on the computer screen when using this mode are shown. The insonation is through transtemporal acoustic window. In the upper panel you can see the Doppler spectrum, where equipment has delineated the spectral Doppler envelope. In this case it is a laminar blood flow. The lower panel shows the M-mode, which displays all the flows in the path of the ultrasonic beam, their depths in relation to the surface of the transducer and their directions (towards the transducer in red and away from it in blue). The scale on the left shows at what depth, in mm, these flows are seen. Between 40 and 60 mm there is a flow that approaches the transducer, which corresponds to the middle cerebral artery (MCA). In this red band there is a dotted line, which shows the depth at which the artery is being observed, in this case about 48 mm; at this depth corresponds the spectrum seen in the upper panel. Any point can be chosen, so that the volume of the sample will inspect and show on the upper display the spectrum and the corresponding envelope with its PSV, MFV, EDV and PI. Between 70 and 75 mm a flow is seen that moves away, corresponding to the anterior cerebral artery (ACA). The carotid bifurcation is not clearly seen in this image, but at about 62 mm a blue band can be seen at times, so it can be thought that this is the bifurcation and that by slightly angulating the transducer it could be clearly found

The alterations of cerebral hemodynamics, monitored by TCD, are generally secondary to

1. Increase of ICP.
2. Vasospasm.
3. Hyperemia.

Table 12.1 Normal values of CBFVs in adults [32]

Artery (Depth / mm)	PSV (cm/s)	EDV (cm/s)	MFV (cm/s)	Age (yr.)
MCA (50 mm)	95 ± 14	46 ± 7	58 ± 8	<40
	91 ± 17	44 ± 10	58 ± 12	40–60
	78 ± 15	32 ± 9	45 ± 11	>60
ACA (70 mm)	76 ± 17	36 ± 9	47 ± 14	<40
	86 ± 20	41 ± 7	53 ± 11	40–60
	73 ± 20	34 ± 9	45 ± 14	>60
PCA (60 mm)	53 ± 11	26 ± 7	34 ± 8	<40
	60 ± 21	29 ± 8	37 ± 10	40–60
	51 ± 12	22 ± 7	30 ± 9	>60
VA / BA (75 mm)	56 ± 8	27 ± 5	35 ± 8	<40
	60 ± 17	29 ± 8	36 ± 12	40–60
	51 ± 19	21 ± 9	31 ± 12	>60

MCA Middle cerebral artery, *ACA* Anterior cerebral artery, *PCA* Posterior cerebral artery, *VA* Vertebral artery, *BA* Basilar artery

4. Alterations in cerebrovascular reactivity.
5. Coexistence of two or more of the previously mentioned points.

When the interest is to assess whether there are global alterations of the cerebral hemodynamics, we must insonate the anterior circulation; middle cerebral artery (MCA), anterior cerebral artery (ACA), and the posterior circulation; and basilar artery (BA) and vertebral arteries (VA). When the interest of the study is to detect a segmental alteration (vasospasm), the assessment must be global initially and then detailed, along each vessel.

12.5 TCD: Frequent Uses in Intensive Care Unit

1. Detect and estimate changes of intracranial pressure (ICP) [2–11].
2. Diagnose cerebral circulatory arrest [12–18], collaborating in the diagnosis of brain death.
3. Diagnosis and monitoring of cerebral artery vasospasm in the clinical evolution of SAH [19, 20], TBI [21, 22], and CNS infections [23–27].
4. In AIS: Monitor arterial recanalization when thrombolytics are performed [28]. To increase the action of these drugs (sonothrombolysis) [29, 30]. To evaluate the presence of microembolism signals and the presence of right–left shunt in cryptogenic AIS.
5. To evaluate the state of cerebral autoregulation (CA) [31], by means of integrated neuromonitoring through mean flow reactive index (Mx).
6. Cerebral vasomotor reactivity to CO_2. Time constant of cerebral circulation and critical closing pressure.

12.6 TCD: Technique

12.6.1 Position of the Patient and Examiner

Frequently, the neurocritical patient is in dorsal decubitus, with the head elevated about 30°, aligned with the trunk. It is not necessary to modify the patient's position. The examiner can be placed at the patient's bedside, but given the large number of catheters and devices that are frequently found around critical patients, it is usually placed at the side of the bed.

The different vessels are insonated through the different acoustic windows (Fig. 12.4). Acoustic windows are areas of the skull that are more permeable to ultrasound beams, because they are thinner or because they are natural orifices. The transducer should be placed by exerting moderate pressure (except when using transorbital window), with abundant gel to ensure proper coupling between the transducer and the skin. It must be known in which direction the ultrasound beam will be emitted, and at what depth each artery will be searched. In this way, the depth will be fixed in advance.

The exploration will begin more superficially and will be deepened by a few millimeters, optimizing the angle of insonation at each point to find the spectrum whose blood flow velocity is maximum, which is the one that will coincide with the minimum angle of insonation (angle between the ultrasonic beam and the direction of blood flow at the point of insonation).

12.6.2 Transtemporal Acoustic Window

TCD assessment begins through the transtemporal acoustic window to insonate middle cerebral artery (MCA). The transtemporal acoustic window extends above the zygomatic arch, in front of the swallow, and behind the lateral corner of the homolateral eye. It has a projection that can be anterior, medial, and posterior. Each patient is different, so the best approach should always be sought in each case.

12.6.2.1 Anterior Circulation

Middle Cerebral Artery (MCA)

1. *Acoustic Window:* Transtemporal
2. *Depth*: (M1 Segment)
   The depth should be between 45 and 60–65 mm and followed along its entire length.
3. *Acoustic Window*: Transtemporal
4. *Depth*: (M2 Segment)

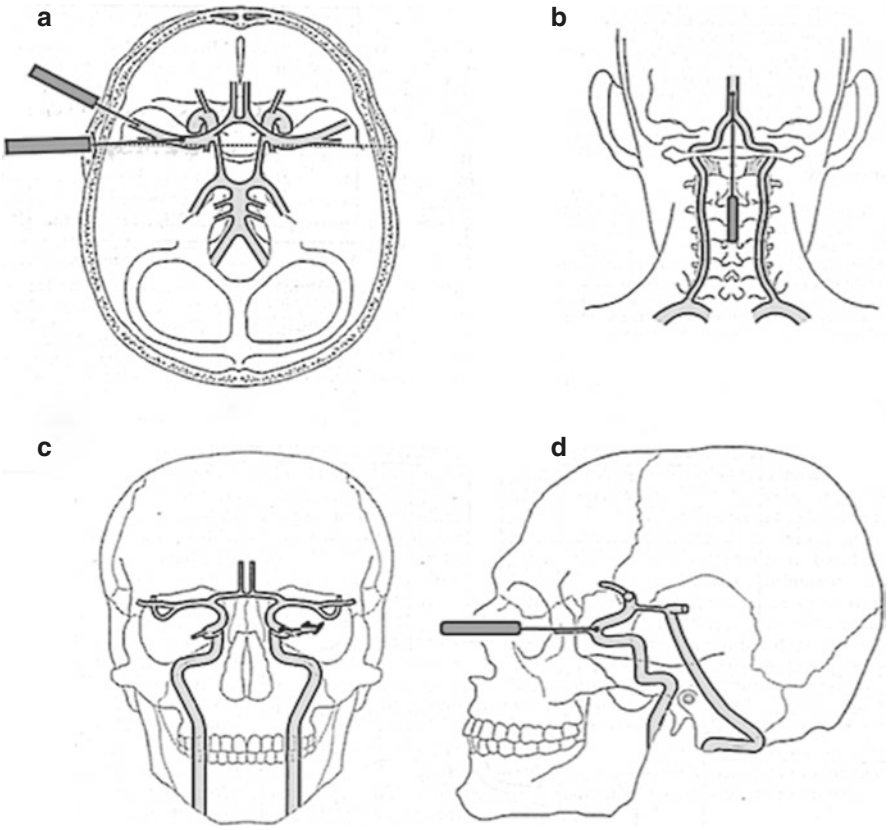

Fig. 12.4 The circle of Willis and their relationships to the different acoustic windows. In (**a**) it is shown the whole circle of Willis, its main branches and the vessels that form it, the transducer in transtemporal acoustic window and the different intonation angles that must be given to it (in this plane) to find the lowest angle of insonation with the MCA and. In (**b**) the transoccipital acoustic window and its relationship with the blood flow in the posterior circulation can be observed. In (**c**) the anterior sector is seen in a coronal view and, in (**d**) the transorbital acoustic window and its relationship with the vessels of the carotid siphon and OA is observed in a sagittal section

In certain cases, it is important to insonate more superficially, from 45 mm to 30 mm (e.g., distal vasospasm).

In all cases, the transducer will be slightly rotated to apical (about 10°), caudal (about 10°), occipital, and frontal direction [7], independent of the sector of the transtemporal window that the operator is located to record Doppler signals.

As the flow of the MCA is toward the transducer, it will be seen as a positive sonogram.

At 65 mm depth of insonation is the carotid bifurcation, where the MCA and the anterior cerebral artery (ACA) originate. The carotid bifurcation is insonated as a bidirectional blood flow, with a simultaneous positive and negative sonogram.

At greater depth of insonation, the flow in the ACA (A1 segment) is seen as a sonogram with negative blood flow velocities that originates at 65 mm depth (in the carotid bifurcation) and extends about 5–10 mm inward and forward, with values always negative.

12.6.2.2 Posterior Circulation

Posterior Cerebral Artery (PCA)

1. *Acoustic Window*: Transtemporal
2. *Depth*:
   The transducer should be rotated slightly to occipital direction, between 70 and 90 mm depths. The blood flow is directed toward the transducer, where it will be seen as a positive sonogram.

To differentiate whether a positive spectrum found in the transtemporal window is MCA or PCA, we must consider the following:

1. *Direction of the probe*: PCA is found with transducer rotated to occipital direction.
2. *Depth*: MCA is usually less than 65 mm, and PCA is deeper.
3. *Carotid compression maneuvers*: Homolateral compression will generate decrease in sonogram blood flow velocity if it is MCA and increase if it is PCA, in which the blood flow in this artery originates in the posterior sector. This depends on the patient having a functioning posterior communicating artery. If the circle of Willis does not compensate, carotid compression will not generate changes if it is PCA.

12.6.3 Submandibular Acoustic Window

12.6.3.1 Internal Carotid Artery (ICA—Extracranial Portion)

1. *Transducer*: 2 MHz
2. *Depth*: 40–50 mm
   The blood flow is away from the transducer (negative spectrum wave).
   The velocity in this artery is approximately 30 cm/s.

As a complement to the insonation of MCA, mainly when the velocities are high, this velocity is compared with extracranial internal carotid artery (ICA) velocity, to study the Lindegaard ratio (vasospasm vs. hyperemia). The transducer is placed below the angle of the mandible, parallel to, and behind the upright branch.

12.6.4 Transoccipital Acoustic Window

12.6.4.1 Posterior Circulation

1. *Vessels*: Basilar artery (BA) and vertebral artery (VA)
2. *Acoustic Window*: Foramen magnum
   The transducer is positioned under the external occipital protuberance and is directed toward the nasion.
3. *Depth*: 80–100 mm (BA)
   Follow the vertebral arteries to their central confluence with the BA.
4. *Depth*: 60 mm (VA)
   Therefore, with an initial depth of 60 mm, angulate the transducer to the right and left of the midline until the signals from the vertebral arteries are found. If no Doppler signal is found, the transducer can be moved slightly sideways to optimize the window through retromastoid position. The identification of right and left vertebral arteries will be based on the direction of the ultrasonic beam and landmarks between the observed vessels.

The patient can be positioned in a dorsal decubitus with a pillow under the occiput and the head flexed to the side opposite the operator, or (without absolute contraindications for cervical flexion) the patient can be lateralized very carefully to access the acoustic window.

12.6.5 Transorbital Acoustic Window

1. *Vessels*: Ophthalmic artery (OA) and carotid siphon
2. *Depth*: 40–60 mm (OA)
   The OA flow is directed toward the transducer (positive spectral Doppler).
   Unlike basal cerebral arteries, OA is an extracranial artery with high resistance flow pattern. Homolateral carotid compression results in a decrease of the Doppler signal. This artery can act as collateral in case of significant carotid disease. In this clinical context, a negative flow is visualized since the direction of blood flow away from the transducer.
3. *Depth:* 60–80 mm (Carotid siphon)
   The flow can be directed toward the transductor or away from it, according to the portion of the carotid siphon that is insonated.

The ultrasound intensity should be lowered to 10% to minimize eye exposure (prevent cavitation effects). The transducer, using abundant gel, is placed on the closed upper eyelid, a few millimeters inward from the middle of the eyelid. No pressure should be exerted on the eye, and the exposure should be for a short time.

Figure 12.5 shows a scheme of basal cerebral arteries studied by TCD and the depths at which they are found each.

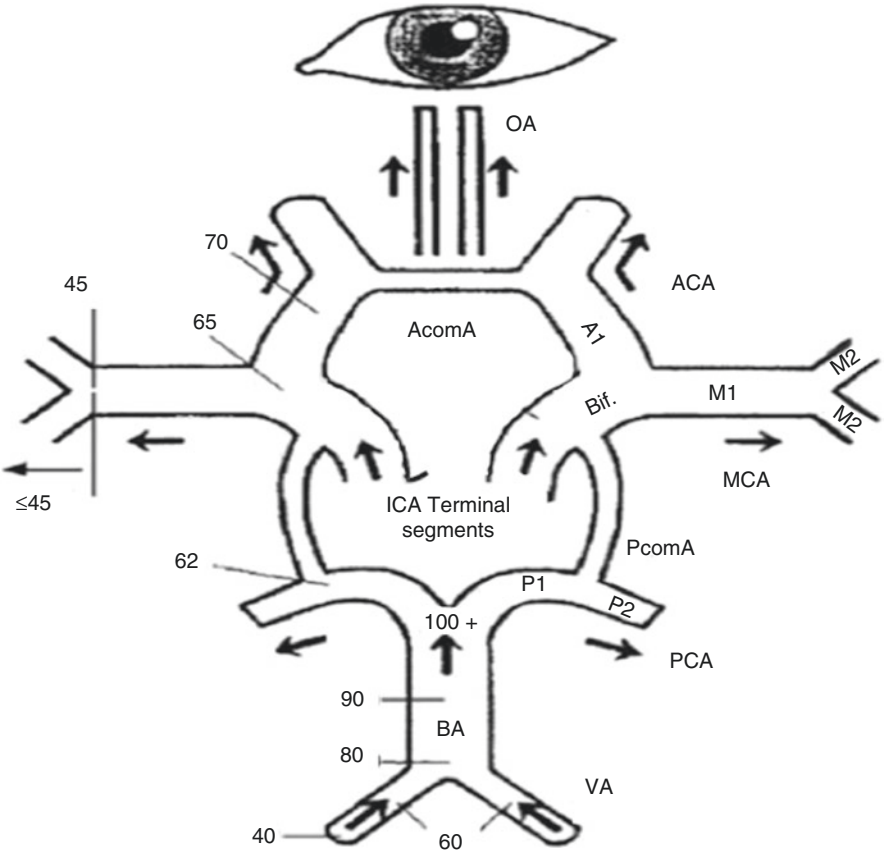

Fig. 12.5 Scheme of the basal cerebral arteries being studied with TCD, their approximate depths (mm), and CBF direction. Anterior circulation; ICA (terminal segment); Bif carotid bifurcation, MCA middle cerebral artery. (M1: M1 segment and M2 segment). ACA anterior cerebral artery. AComA anterior communicating artery, OA ophthalmic artery. In the posterior circulation; VA vertebral arteries, BA basilar artery. Connecting the anterior and posterior sector we see the PComA posterior communicating artery. Communicating arteries do not have flow in normal conditions, they do when they function as collaterals

12.6.6 Blood Flow Velocities and Hemodynamic Indexes

12.6.6.1 Interpretation of Doppler Spectrum Wave (Sonogram)

The PSV corresponds to the highest measuring of the Doppler spectrum wave (sonogram). It is related to the left ventricular contractility. The EDV corresponds to the lowest point of the sonogram, before starting a new cardiac cycle. It makes it possible to infer the blood flow velocity output, related to cerebrovascular resistances (CVR). In comparison with the circulatory flow velocities of the extracranial vessels, this CBFV output in the basal cerebral arteries is high. It evidenced a

characteristic of the cerebral circulation: it is a system of low resistance. The MFV is calculated mathematically as the average on time of the CBFVs during each Doppler spectrum wave. It can also be calculated graphically in the Doppler sonogram.

12.6.6.2 Pulsatility Index

There are two hemodynamic indices: the pulsatility index (PI) or Gosling's index and the resistance index (RI) or Pourcelot's index.

The PI is the most widely used. It is calculated by the following formula (Eq. 12.1):

$$PI^{*} = \left(PSV + EDV\right) / MFV \tag{12.1}$$

*Normal value: 0.6–1.2

The higher the differential velocity (high PSV and low EDV), the higher the PI value [7]. In general, it reflects a higher (high PI) or lower (low PI) resistance to the cerebral blood flow, and it can be modified by (1) conditions specific to the intracerebral arteries (small resistance vessels), (2) change of cerebral parenchyma compliance, and/or (3) changes in cerebral perfusion pressure. PI > 1.2 (integrating clinical evolution of the patient with PI absolute and trends values) in patients with acute neurological injury and risk of developing intracranial hypertension, should always alert the clinician. Repeated and bilateral neurological monitoring with TCD is crucial.

The other hemodynamic index that can be measured by TCD is RI (less used). The RI is calculated with the following formula (Eq. 12.2):

$$RI = \left(PSV + EDV\right) / PSV \tag{12.2}$$

12.7 The Different Patterns of Cerebral Blood Flow

12.7.1 High-Velocity Pattern

It is seen mainly in vasospasm or hyperemia.

12.7.2 Low-Velocity Pattern

This pattern refers to cerebral hypoperfusion.

12.7.3 High Resistance Pattern

In general, it coexists with low CBFV. A PI > 1.2 should lead to suspicion of intracranial hypertension in critically ill patients with acute neurological injury (Fig. 12.6).

12.7.4 Cerebral Circulatory Arrest Pattern

Reverberant flow and systolic spikes are seen diffusely in the patient progressing to brain death.

All these patterns will be described in depth in the corresponding chapters.

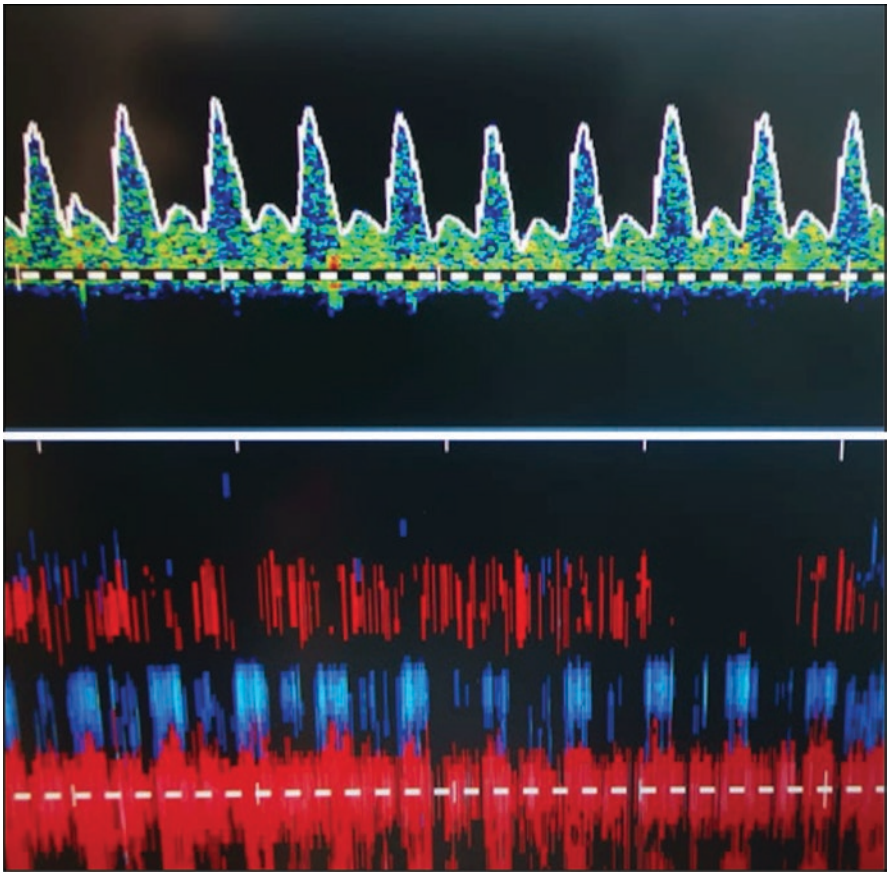

Fig. 12.6 Sonogram: High resistance pattern (MCA)

12.8 TCD: Other Clinical Uses

Among the advantages that TCD has over other monitoring methods, it is the possibility of performing prolonged neurological monitoring, constituting a very useful tool in multimodal neuromonitoring (MMM).

12.8.1 Through the MMM You Can Study the Following

12.8.1.1 Cerebral Vascular Reactivity

Capacity of the cerebral arteriolar bed to respond to different stimuli with changes in CVR. Depending on the stimulus, cerebrovascular reactivity can be classified as follows:

1. Reactivity to CO_2.
2. Metabolic reactivity.
3. Reactivity to drugs.
4. Cerebral autoregulation.

12.9 TCD: Limitations

The most important limitations of TCD are (a) operator dependent and (b) 10–15% of patients do not have a good acoustic window.

12.10 Conclusion

Transcranial Doppler is a useful monitoring tool for assessing cerebral hemodynamics in the critically ill patient. It allows suspecting or ruling out serious alterations that need urgent management, at the patient's bedside, in a non-invasive way. Unlike imaging studies, which give an anatomical evaluation that provides little information about functionality, TCD can be done as many times as desired (repeated or continuous way), with excellent temporal resolution.

It is complementary to the anatomical evaluation. The TCD protocol in ICU is different from that performed in the neurological laboratory. The study can be done to evaluate hemodynamics globally and/or segmental changes (vasospasm, stenoocclusion, etc.). In this case, it should be remembered that there may be intracranial pressure gradients and, therefore, the arteries of the anterior and posterior circulations (bilaterally) should be assessed through the four acoustic windows in order to evaluate CBFV, hemodynamic indexes, and right/left CBF asymmetry.

Algorithm

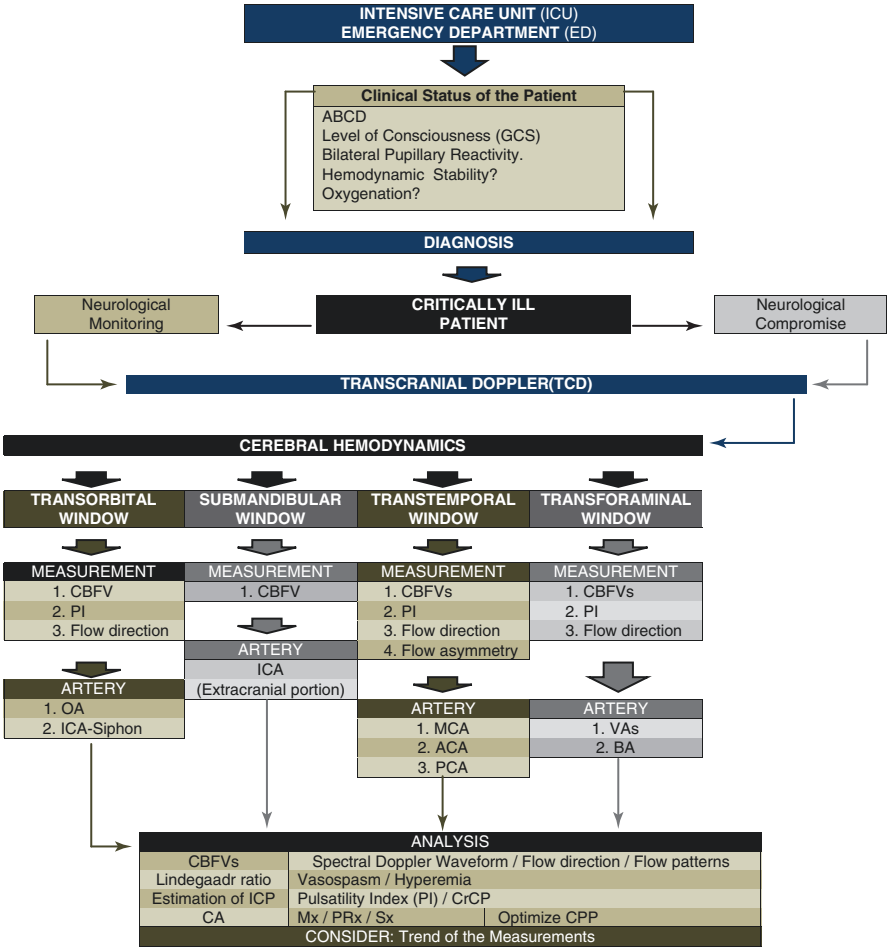

ABCD Airway-breathing-circulation-disability, *GCS* Glasgow coma scale, *ACA* Anterior Cerebral Artery, *PCA* Posterior Cerebral Artery, *BA* Basilar Artery, *VA* Vertebral Artery, *OA* Ophthalmic artery, *ICPn* Noninvasive intracranial pressure, *CBFVs* Cerebral blood flow velocities, *Mx* Mean flow index, *Sx* systolic flow index, *PRx* Pressure reactivity index, *CA* Cerebral autoregulation, *CrCP* Critical closing pressure, *CPP* Cerebral perfusión pressure

References

1. Hakimi R, Alexandrov AV, Garami Z. Neuro-ultrasonography. Neurol Clin. 2020;38(1):215–29.
2. Nornes H, Aaslid R, Lindegaard KF. Intracranial pulse pressure dynamics in patients with intracranial hypertension. Acta Neurochir. 1977;38:177–86.

3. Hassler W, Steinmetz H, Gawlowski J. Transcranial Doppler ultrasonography in raised intracranial pressure and in intracranial circulatory arrest. J Neurosurg. 1988;68:745–51.
4. Melon E. Indications for monitoring intracranial pressure. Ann Fr Anesth Reanim. 1997;16:415–9.
5. Sidi A, Messinger G, Mahla ME. Transcranial Doppler monitoring compared with invasive monitoring of intracranial pressure during acute intracranial hypertension. J Clin Monit Comput. 1999;15:185–95.
6. Schmidt B, Czosnyka M, Klingelhöfer J. Clinical applications of a non-invasive ICP monitoring method. Eur J Ultrasound. 2002;16:37–45.
7. Reinhard M, Petrick M, Steinfurth G, Ziyeh S, Hetzel A. Acute increase in intracranial pressure revealed by transcranial Doppler sonography. J Clin Ultrasound. 2003;31:324–7.
8. Edouard AR, Vanhille E, Le Moigno S, Benhamou D, Mazoit JX. Non-invasive assessment of cerebral perfusion pressure in brain injured patients with moderate intracranial hypertension. Br J Anaesth. 2005;94:216–21.
9. Splavski B, Radanović B, Muzević D, Has B, Janculjak D, Kristek J, et al. Assessment of intracranial pressure after severe traumatic brain injury by transcranial Doppler ultrasonography. Brain Inj. 2006;20:1265–70.
10. Sharma VK, Chan BP. Comment on 'Assessment of intra-cranial pressure after severe traumatic brain injury by transcranial Doppler ultrasonography' by Splavski et al. Brain Inj. 2007;21:1093–4.
11. Aggarwal S, Brooks DM, Kang Y, Linden PK, Patzer JF 2nd. Noninvasive monitoring of cerebral perfusion pressure in patients with acute liver failure using transcranial doppler ultrasonography. Liver Transpl. 2008;14:1048–57.
12. Powers AD, Graeber MC, Smith RR. Transcranial Doppler ultrasonography in the determination of brain death. Neurosurgery. 1989;24:884–9.
13. Hassler W, Steinmetz H, Pirschel J. Transcranial Doppler study of intracranial circulatory arrest. J Neurosurg. 1989;71:95–201.
14. Werner C, Kochs E, Rau M, Schulte EJ. Transcranial Doppler sonography as a supplement in the detection of cerebral circulatory arrest. J Neurosurg Anesthesiol. 1990;2:159–65.
15. Ducrocq X, Hassler W, Moritake K, Newell DW, von Reutern GM, Shiogai T, et al. Consensus opinion on diagnosis of cerebral circulatory arrest using Doppler-sonography: Task Force Group on cerebral death of the Neurosonology Research Group of the World Federation of Neurology. J Neurol Sci. 1998;159:145–50.
16. Sloan MA, Alexandrov AV, Tegeler CH, Spencer MP, Caplan LR, Feldmann E, et al. Transcranial Doppler ultrasonography: report of the Therapeutics and Technology Assessment Subcommittee of the American Academy of Neurology. Neurology. 2004;62:1468–81.
17. Monteiro LM, Bollen CW, van Huffelen AC, Ackerstaff RG, Jansen NJ, van Vught AJ. Transcranial Doppler ultrasonography to confirm brain death: a meta-analysis. Intensive Care Med. 2006;32:1937–44.
18. Calleja S, Tembl JI, Segura T. Recommendations of the use of transcranial Doppler to determine the existence of cerebral circulatory arrest as diagnostic support of brain death. Neurologia. 2007;22:441–7.
19. Vora YY, Suarez-Almazor M, Steinke DE, Martin ML, Findlay JM. Role of transcranial Doppler monitoring in the diagnosis of cerebral vasospasm after subarachnoid hemorrhage. Neurosurgery. 1999;44:1237–47.
20. Soustiel JF, Shik V, Shreiber R, Tavor Y, Goldsher D. Basilar vasospasm diagnosis: investigation of a modified "Lindegaard Index" based on imaging studies and blood velocity measurements of the basilar artery. Stroke. 2002;33:72–7.
21. Martin NA, Doberstein C, Zane C, Caron MJ, Thomas K, Becker DP. Posttraumatic cerebral arterial spam: transcranial Doppler ultrasound, cerebral blood flow, and angiographic findings. J Neurosurg. 1992;77:575–583martin.

22. Lee JH, Martin NA, Alsina G, McArthur DL, Zaucha K, Hovda DA, et al. Hemodynamically significant cerebral vasospasm and outcome after head injury: a prospective study. J Neurosurg. 1997;87:221–33.
23. Müller M, Merkelbach S, Huss GP, Schimrigk K. Clinical relevance and frequency of transient stenoses of the middle and anterior cerebral arteries in bacterial meningitis. Stroke. 1995;26:1399–403.
24. Gupta R, Mahapatra AK, Bhatia R. Serial transcranial Doppler study in meningitis. Acta Neurochir. 1995;137:74–7.
25. Müller M, Merkelbach S, Hermes M, Schimrigk K. Transcranial Doppler sonography at the early stage of acute central nervous system infections in adults. Ultrasound Med Biol. 1996;22:173–8.
26. Müller M, Merkelbach S, Hermes M, König J, Schimrigk K. Relationship between short-term outcome and occurrence of cerebral artery stenosis in survivors of bacterial meningitis. J Neurol. 1998;245:87–92.
27. Kiliç T, Elmaci I, Ozek MM, Pamir MN. Utility of transcranial Doppler ultrasonography in the diagnosis and follow-up of tuberculous meningitis-related vasculopathy. Childs Nerv Syst. 2002;18:142–6.
28. Saqqur M, Tsivgoulis G, Molina CA, Demchuk AM, Shuaib A, Alexandrov AV, CLOTBUST Investigators. Residual flow at the site of intracranial occlusion on transcranial Doppler predicts response to intravenous thrombolysis: a multi-center study. Cerebrovasc Dis. 2009;27:5–12.
29. Alexandrov AV. Ultrasound enhancement of fibrinolysis. Stroke. 2009;40:S107–10.
30. Alexandrov AV, Köhrmann M, Soinne L, Tsivgoulis G, Barreto AD, Demchuk AM, et al. CLOTBUST-ER Trial Investigators. Safety and efficacy of sonothrombolysis for acute ischaemic stroke: a multicentre, double-blind, phase 3, randomised controlled trial. Lancet Neurol. 2019;18(4):338–47.
31. Martínez-Sánchez P, Tsívgoulis G, Lao A, Sharma V, Alexandrov A. Ultrasound in acute ischemic stroke. Neurologia. 2009;24:59–68.
32. Hennerici M, Rautenberg W, Sitzer G, Schwartz A. Transcranial Doppler ultrasound for the assessment of intracranial arterial flow velocity-Part 1. Examination technique and normal values. Surg Neurol. 1987;27:439–48.

Chapter 13
Transcranial Doppler (TCD/TCCS) Monitoring in the Intensive Care Unit: Usefulness of Two-Dimensional Ultrasound (2D) to Guide Neuromonitoring

André Y. Denault, Antoine Halwagi, Francis Bernard, Stéphane Langevin, Etienne Couture, Milene Azzam, William Beaubien-Souligny, and Pierre Robillard

Key Points

1. There are several applications of transcranial Doppler (TCD/TCCS) in the intensive care unit (ICU).

A. Y. Denault (✉)
Department of Anesthesiology and Intensive Care Unit, Montreal Heart Institute, Université de Montréal, Montréal, QC, Canada
e-mail: andre.denault@umontreal.ca

A. Halwagi
Department of Anesthesiology and Intensive Care Unit, Centre Hospitalier de l'Université de Montréal, Montreal, QC, Canada
e-mail: a.halwagi@umontreal.ca

F. Bernard
Intensive Care Unit, Hôpital Sacré-Coeur de Montréal, Montreal, QC, Canada

S. Langevin
Department of Anesthesiology and Intensive Care Unit, Institut universitaire de cardiologie et de pneumologie de Québec, Laval University, Quebec, QC, Canada

E. Couture · M. Azzam
Department of Anesthesiology, Montreal Heart Institute, Université de Montréal, Montreal, QC, Canada

W. Beaubien-Souligny
Department of Anesthesiology, Montreal Heart Institute, Université de Montréal, Montreal, QC, Canada

Department of Nephrology, Centre Hospitalier de l'Université de Montréal, Montreal, QC, Canada

P. Robillard
Department of Radiology, Montreal Heart Institute, Université de Montréal, Montreal, QC, Canada

C. N. Rodríguez et al. (eds.), *Neurosonology in Critical Care*,
https://doi.org/10.1007/978-3-030-81419-9_13

2. Two-dimensional (2D) ultrasound and TCCS can facilitate placement of a continuous TCD monitoring system.
3. 2D ultrasound and Doppler (TCCS) can also be used in order to optimize TCD acquisition and improve its interpretation by differentiating between an intracranial and an extracranial source of an abnormal TCD signal.
4. 2D ultrasound and Doppler (TCCS) can be used to image intra- and extracranial structures which can be the source of neurological disorders.

13.1 Introduction

Transcranial Doppler (TCD) ultrasound (US) is a simple, non-invasive, relatively inexpensive bedside tool that can provide real-time dynamic information regarding cerebral blood flow velocity (CBFV) in the proximal cerebral blood vessels. Since its first clinical application in 1982 [1], the use of TCD has expanded rapidly over the past two decades. The portability and non-invasive nature of TCD allow both assessments during emergencies and continuous or serial monitoring in the intensive care unit (ICU). The clinical applications of TCD in the ICU are summarized in Table 13.1. TCD is commonly used in neuro-critical care units,

Table 13.1 Applications of transcranial Doppler (TCD/TCCS) in the operating room and the intensive care unit

1. *Neuro-critical care*
(a) Cerebral vasospasm screening and monitoring to assess progression and treatment effect (angioplasty or medical treatment) after aneurysmal subarachnoid hemorrhage
(b) Non-invasive intracranial pressure (ICP) screening and monitoring, combined with optic nerve sheath diameter, in the absence of invasive ICP monitoring (fulminant hepatic failure, etc.)
(c) Assessment of the degree of hyperemia after arteriovenous malformation resection, carotid endarterectomy, carotid surgical or endovascular angioplasty and in patients with malignant hypertension
(d) Assessment of cerebral circulatory arrest in suspected brain death
2. *Stroke Unit*
(a) Diagnosis of proximal arterial occlusion in acute ischemic stroke
(b) Assessment of arterial patency after thrombolytic treatment
(c) Diagnosis of hyperemia after conversion of acute ischemic to hemorrhagic stroke
3. *Various*
(a) Assessment of cerebral autoregulation and cerebrovascular carbon dioxide reactivity
(b) Diagnosis of intracranial artery stenosis
(c) Guiding chronic red cell transfusion therapy in patients with sickle cell disease who are at risk of developing stroke
(d) Intraoperative monitoring during carotid endarterectomy and procedures at risk of causing systemic emboli and hypoperfusion
(e) Detection of cardiac or pulmonary right to left shunt (e.g. patent foramen ovale)

Adapted with permission of Taylor and Francis Group, LLC, a division of Informa plc. from Denault et al. [21]
Abbreviations: *TCD* transcranial Doppler

acute stroke units, operating rooms, ICUs, and emergency departments. It can even be useful in an outpatient setting to assess the hemodynamic changes associated with stenosis of major cerebral arteries or to determine the risk of stroke in patients with sickle cell disease. For the experienced vascular neurologist, neurointensivist, and neuro-anesthesiologist, the small portable TCD device serves as a "stethoscope for the brain" [2]. The addition of two-dimensional (2D) US to a standardized TCD assessment allows optimization of TCD acquisition and improves its interpretation by differentiating an intracranial from an extracranial source of an abnormal TCD signal. Finally, 2D US and Doppler can be used to image intracranial as well as extracranial structures, which can be the source of neurological disorders.

13.2 Acoustic Windows

In order to interrogate the brain, it is essential to obtain an acoustic window through the skull. Normally, US waves undergo gradual loss of intensity as they move through different body structures. The degree of attenuation is directly proportional to the attenuation coefficient of the medium and to the emitted US frequency. Since bone has a relatively high attenuation coefficient, it is difficult to measure CBFV using a conventional 5–10 MHz Doppler probe. The use of a lower frequency (1–2 MHz) probe is required. TCD examinations are commonly performed through four acoustic windows where the bone is relatively thin or absent. However, in the ICU, for monitoring purposes, we typically concentrate on the temporal window. The middle cerebral artery, anterior cerebral artery, posterior cerebral artery, and terminal internal carotid artery can be examined (Fig. 13.1) through the transtemporal window.

13.3 2D-Guided TCD Monitoring

In order to examine the brain through the temporal window, the depth has to be adjusted to at least twice the distance from the midline cerebral falx which is typically at 8 cm. The skull is formed by two layers of compact bone separated by a porous layer called diploë that allows US wave propagation by creating an acoustic interface [3]. However, in up to 38% of patients, Doppler signals cannot be acquired because of an inadequate or narrow temporal acoustic window [4]. Blind placement of a TCD probe in these patients can be time-consuming and may ultimately result in an inadequate signal. The use of 2D cranial ultrasonography can potentially facilitate localization of the temporal acoustic window prior to TCD probe placement. The most commonly used planes are the mesencephalic plane, the diencephalic plane, and the diencephalic-ventricular plane which includes the lateral ventricles

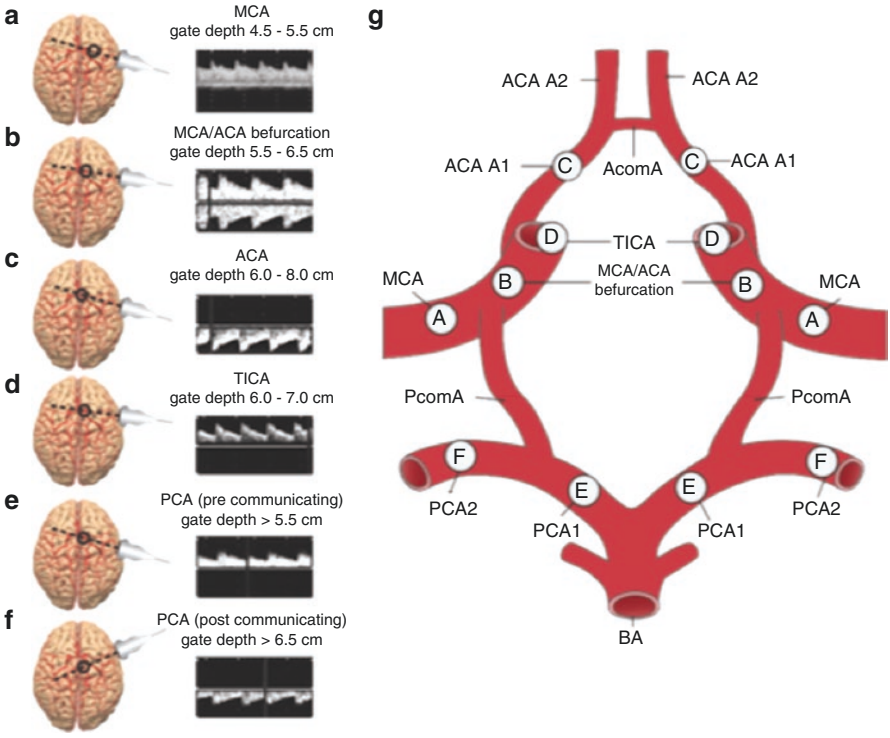

Fig. 13.1 Transcranial Doppler signals. Probe position in the temporal window and normal transcranial Doppler (TCD) signals are shown for the (**a**) middle cerebral artery (MCA), (**b**) bifurcation of the MCA and anterior cerebral artery (ACA), (**c**) ACA, (**d**) terminal internal carotid artery (TICA), (**e**) pre-communicating posterior cerebral artery (PCA) and (**f**) post-communicating PCA (PcomA). (**g**) Corresponding position in the circle of Willis. (Abbreviations: AcomA anterior communicating artery, BA basilar artery). (Reproduced and adapted by permission of Taylor and Francis Group, LLC, a division of Informa plc. from Denault et al. [21])

(Fig. 13.2) [5]. The probe is placed over the area just above the zygomatic arch along the orbitomeatal line which extends from the lateral canthus of the eye to the midpoint of the external auditory meatus. The acoustic window can be located in the anterior part of the temporal bone, close to the vertical portion of the zygomatic bone, or, more frequently, posterior and close to the tragus of the ear.

Any transthoracic or hand-held low-frequency transducer probe (1–2 MHz) can be used. In patients with prior craniectomy (Fig. 13.3b), visualization of cerebral anatomy and TCD signals are easily obtained (Fig. 13.3b–d). The gain and depth (14 to 16 cm) are adjusted to localize the bony structures (Fig. 13.4). The contralateral cranial bone is first located in the far field. In the mid-field, the petrous ridge can be identified posteriorly and sphenoid wing anteriorly. The carotid siphon and foramen lacerum can be localized anteriorly. The cerebral peduncle, third ventricle, and the cerebral falx can be localized in the middle field with the mesencephalic

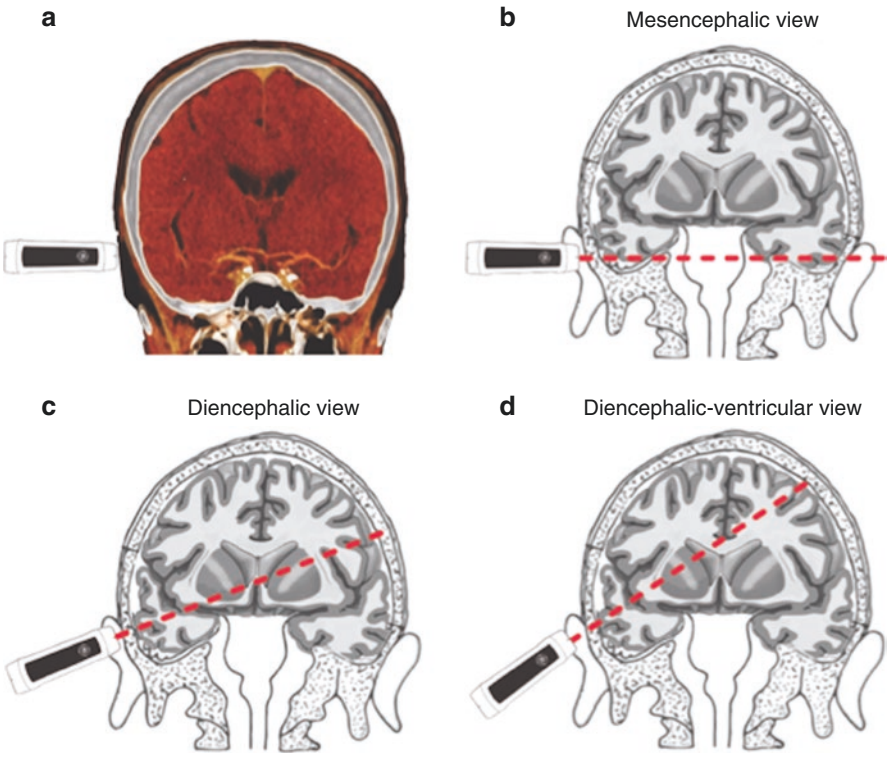

Fig. 13.2 Axial trans-temporal brain computed tomography (**a**) and ultrasound at 3 different levels. (**b**) Upper brainstem or mesencephalic view at the level of the zygomatic arch, (**c**) diencephalic view at the level of the third ventricle obtained by tilting the probe 10° upward and (**d**) diencephalic-ventricular view obtained by tilting the probe another 10° upward. In this view, the lateral ventricle can be seen. (Reproduced and adapted by permission of Taylor and Francis Group, LLC, a division of Informa plc. from Denault et al. [21])

brainstem appearing as a ¨butterfly shape¨ surrounded by the echogenic basal cisterns in the axial plane, parallel to the orbitomeatal line [6].

Doppler imaging (scale between 20 and 100 cm/s) allows identification of the major vascular structures. Depth and direction of flow are the main characteristics of the Doppler signal that help to differentiate the various vessels [7]. Identification of the vascular structures usually takes less than one minute. TCD monitoring probes are then positioned, adjusted, and stabilized with the other cerebral monitoring modalities. The above TCD monitoring technique has been used at our institution as part of a multimodal neurologic monitoring strategy since 2015. We recently reported that 95 patients out of 100 had at least a unilateral adequate temporal acoustic window available for TCD monitoring during cardiac surgery. An adequate bilateral window was found in 70 patients. In five patients, neither right nor left temporal acoustic window was present and TCD could not be used [8]. The use of

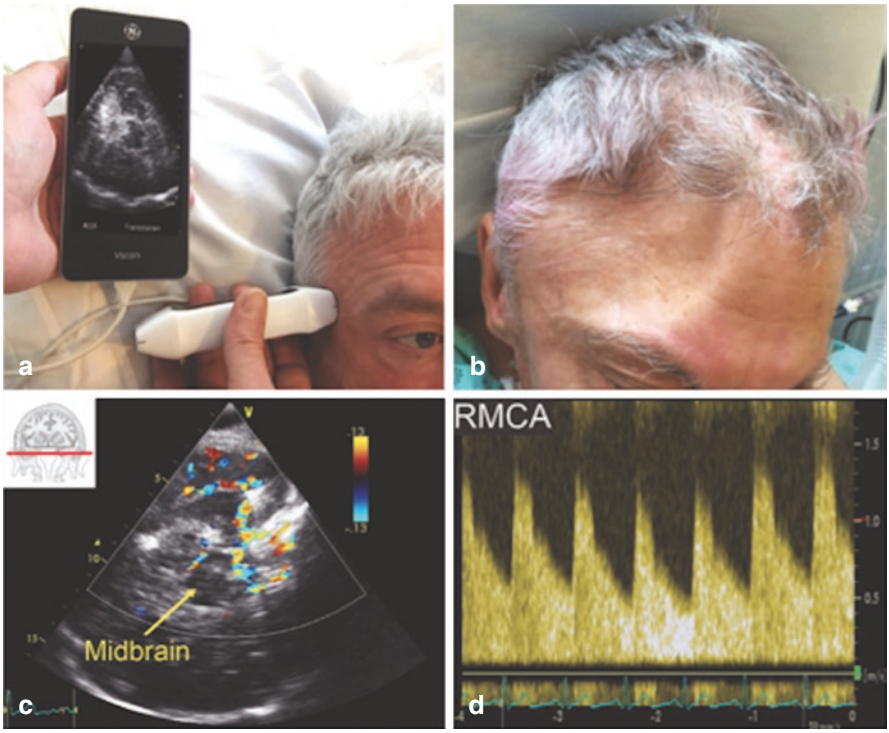

Fig. 13.3 (**a**) Normal position of hand-held ultrasound on the temporal region. (**b**) Patient after right-sided craniectomy for cerebral edema is shown. (**c**) 2D cerebral ultrasound image with color Doppler (Nyquist 13 cm/s) that shows part of the circle of Willis. Note the butterfly aspect of the midbrain. (**d**) Transcranial Doppler investigation of the right middle cerebral artery (RMCA) velocity. (Reproduced by permission of Taylor and Francis Group, LLC, a division of Informa plc. from Denault et al. [21])

2D cranial US can rapidly facilitate TCD monitoring in most patients despite the high reported failure rates in TCD monitoring [4]. Table 13.2 summarizes the approach used for obtaining continuous TCD monitoring from the temporal acoustic window. Transcranial Color-Coded Duplex Sonography (TCCS) can also help identify the cerebral vascular anatomy and allow proper angle correction when assessing flow velocities [9].

13.4 Applications of TCD Monitoring in the ICU

We use TCD monitoring as part of multimodal monitoring mostly in the cardiac operating room but also in the cardiothoracic, general, and neuro ICU. The following signals will be displayed:

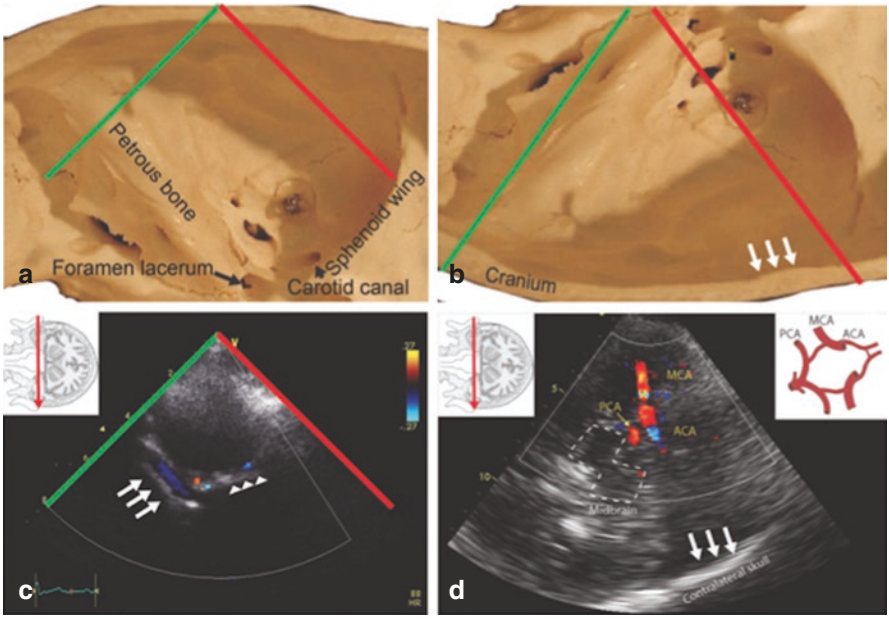

Fig. 13.4 Temporal windows. (**a**, **b**) Using 2D imaging, anatomic reference points shown with these cut portions of the skull are the petrous bone, foramen lacerum, sphenoid wing and the opposite cranial wall (arrows). (**c**) Color Doppler (Nyquist 27 cm/s) showing blood flow in the petrous bone (arrows). The sphenoid wing is shown (triangles). (**d**) The display depth is initially adjusted in order to see the contralateral skull at the mesencephalic level. (Abbreviations: ACA anterior cerebral artery, MCA middle cerebral artery, PCA posterior cerebral artery). (Reproduced by permission of Taylor and Francis Group, LLC, a division of Informa plc. from Denault et al. [21])

1. The peak systolic flow velocity (PSV)
2. The end-diastolic flow velocity (EDV)
3. The mean flow velocity (MFV)
4. The pulsatility index (PI)
5. The resistance index (RI)

US machines with automatic or manual spectral waveform tracing calculate MFV as the area under the traced curve.

- *Mean flow velocity (MFV)* = (PSV + (2 x EDV))/3 or (PSV – EDV)/3 + EDV
- *Pulsatility Index (PI)* = (PSV – EDV)/MFV (normal 0.8–1.2)
- *Resistance Index (RI)* = (PSV – EDV)/PSV (normal 0.6 ± 0.1)

Velocity signals will be significantly altered in the presence of increased intracranial pressure (ICP). However, there are several other roles of cranial and

Table 13.2 General procedural steps in echo-guided transcranial Doppler monitoring through temporal window

1. *Probe selection*: select a low frequency probe (1–2 MHz) and the transcranial profile
2. *Patient*: Supine position
3. *Position the ultrasound machine* so that the ultrasound images and the chosen site for vascular investigation will be in the same visual field
4. *Position of the operator*: head of the bed while stabilizing the hand using a pillow
5. *Preparation*: adjust gain, depth (14–16 cm for contralateral skull bone and 5–6 cm for MCA), color scale, M-mode and pulsed-wave Doppler. Use a 10–15 mm sample volume initially, then adjust
6. *Identify with 2D US* the petrous ridge posteriorly, carotid canal (C2-C3 segments), foramen lacerum, cerebral falx, sphenoid wing anteriorly, cerebral peduncle and the contralateral cranial bone (Fig. 13.1). Use color Doppler (scale 25 cm/s) to identify the vessels in the following order: bidirectional « butterfly » TICA signal (C7 segment) in the foramen lacerum, MCA, ACA, ACoA, then move back to TICA and find the PCoA then the PCA, proximal (P1 segment) and distal (P2 segment) portion around the cerebral peduncle
7. *Position the TCD*: Position in the acoustic bone window into the same probe position
8. *Report velocities* and refer to normal values adjusted by age

Adapted with permission of Taylor and Francis Group, LLC, a division of Informa plc. from Denault et al. [21]

Abbreviations: *2D* two-dimensional, *ACA* anterior cerebral artery, *ACoA* anterior communicating artery, *C* carotid segments (C2,petrous segment; C3, lacerum segment; C7, communicating or terminal (t) segment), *MCA* middle cerebral artery, *PCA* posterior cerebral artery, *PCoA* posterior communicating artery, *TICA* terminal internal carotid artery, *US* ultrasound

extracranial 2D US. In the presence of signs of increased ICP, 2D US of the brain can be used to diagnose dilated ventricles in patients with previous craniotomy (Fig. 13.5), midline shift (Fig. 13.6), and regional increase in ICP (Fig. 13.7), and facilitate the monitoring of vasospasm versus hyperemia through direct visualization of the circle of Willis (Fig. 13.8). In addition, examination of the optic nerve sheath diameter (ONSD) is another method of evaluating increased ICP. For adults, normal values taken at 3 mm of the optic disk are 5.4 ± 0.6 mm, and abnormal values range between 6 and 7 mm [5]. As mentioned by Harrer et al., overlaps between normal and pathological values are possible given the nature of the dynamic process [5]. The diagnosis of papilledema can be easily performed; however, the ONSD will change more rapidly than the appearance or disappearance of papilledema [5]. In patients with increased ICP, both ONSD and CBF velocities obtained by TCD will be abnormal. However, ONSD seems to be more sensitive and specific than CBF velocities obtained by TCD in detecting elevated ICP [10–15].

Furthermore, a recent study by Chelly et al. demonstrated that ONSD on the first day after cardiac arrest was significantly associated with in-hospital mortality (OR 6.3; 95%CI [1.05–40] per 1 mm of ONSD above 5.5 mm; $p = 0.03$) and correlated with brain edema measured using computed tomography [16].

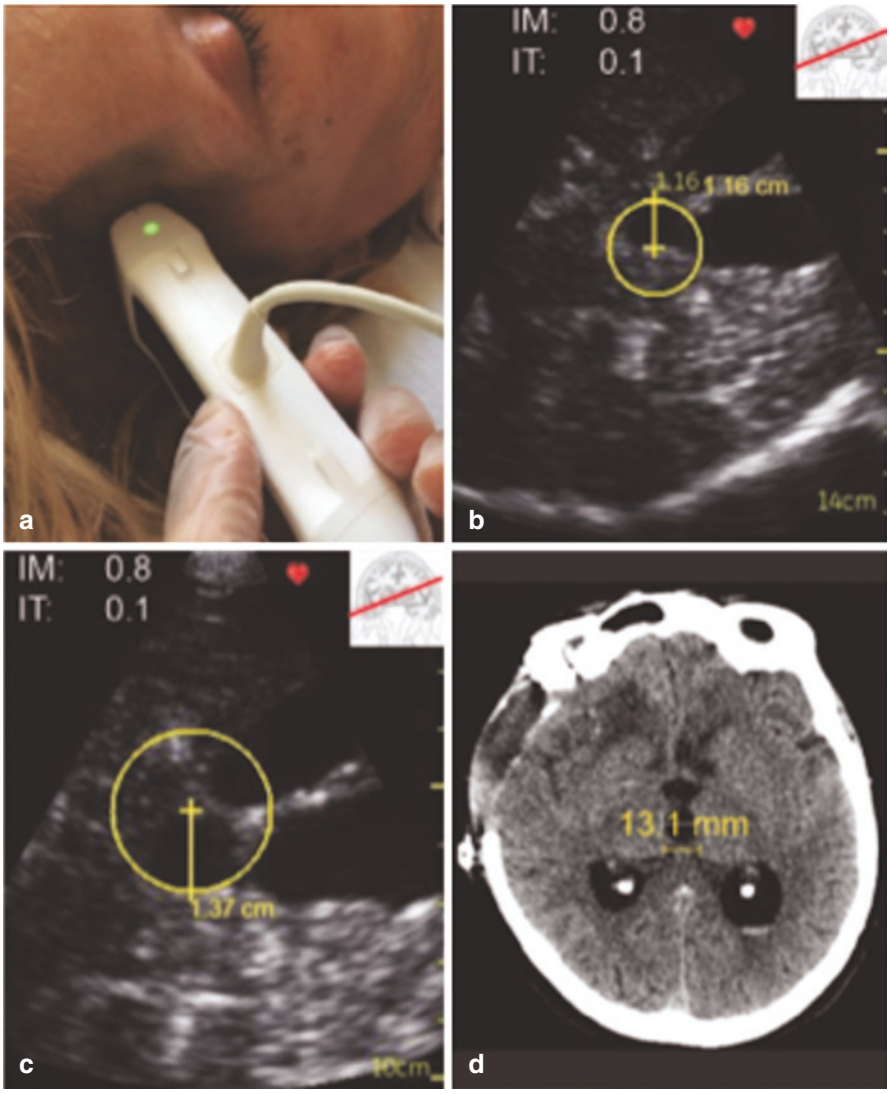

Fig. 13.5 (**a**) Transcranial sonography (TCS) using a hand-held pocket ultrasound device (GE Vingmed Ultrasound AS, Horten, Norway) on a patient with craniectomy. (**b**) Prior to external ventricular drain (EVD) clamping, TCS showed a measurement of the 3rd ventricle at approximately 1.16 cm. (**c**) On the third day, TCS showed a dilated 3rd ventricle measuring 1.37 cm. (**d**) Computed tomography scan showed a dilated 3rd ventricle measuring 13.1 mm. (**e**) One day after reopening the EVD, the size of the 3rd ventricle decreased to 0.99 cm as measured by TCS. (**f**) The following day, it went down to 0.69 cm. (Abbreviations: IM mechanical index, IT thermal index). (With permission of Najjar et al. [22])

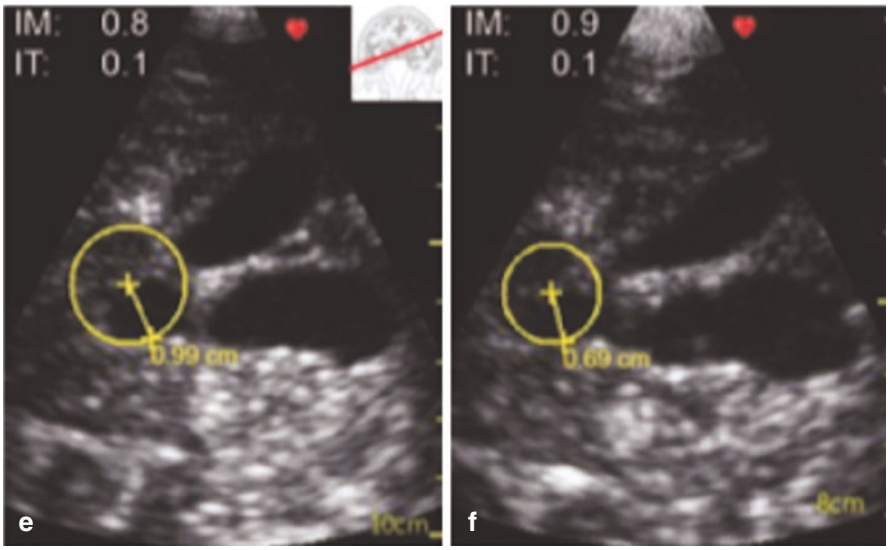

Fig. 13.5 (continued)

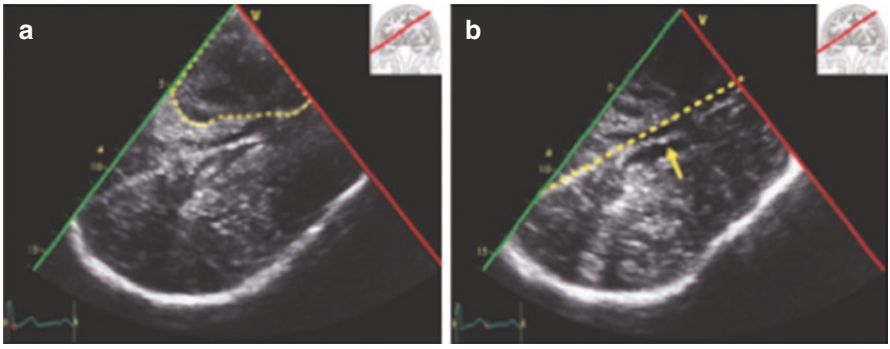

Fig. 13.6 Cerebral hematoma. (**a**) Transcranial 2D diencephalic-ventricular image of an intraparenchymal hematoma (dotted line) with a (**b**) persistent left midline shift (arrow). (**c**) Initial computed tomography upon presentation with midline shift (arrow) and (**d**) magnetic resonance imaging following craniectomy taken at different axial planes are presented for comparison. (Reproduced by permission of Taylor and Francis Group, LLC, a division of Informa plc. from Denault et al. [21])

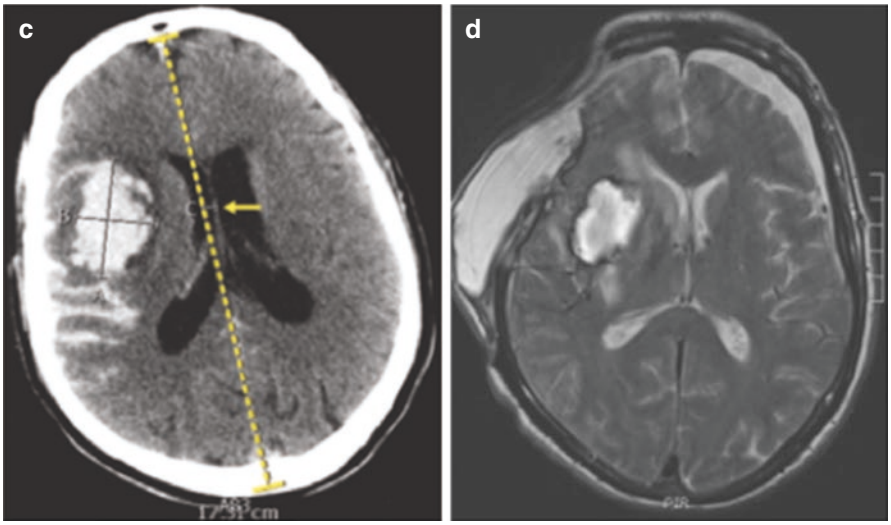

Fig. 13.6 (continued)

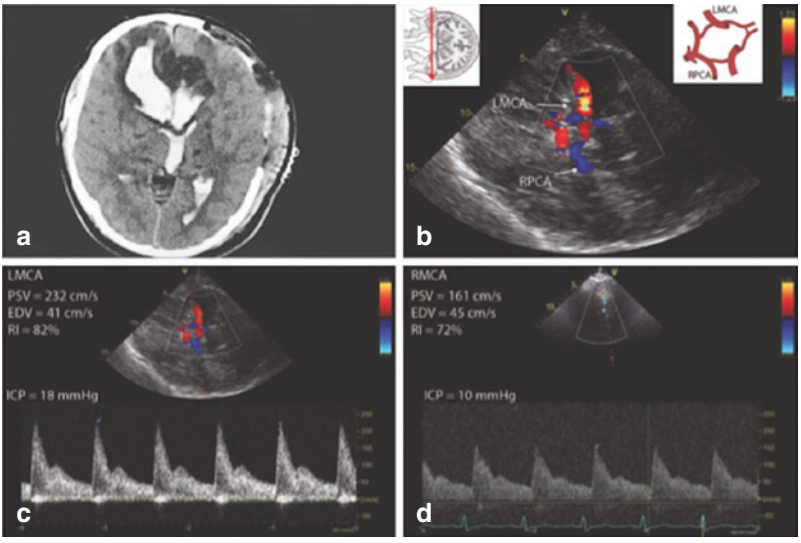

Fig. 13.7 A 47-year-old man with (**a**) grade V subarachnoid hemorrhage, bilateral intra-cranial pressure (ICP) monitoring and left-sided craniectomy shown on computed tomography. (**b**) Mesencephalic brain ultrasound view with color Doppler showing parts of the circle of Willis. Note the increased velocity of the left middle cerebral artery (LMCA), greater than the 123 cm/s Nyquist limit (normal peak velocity 90–110 cm/s). (**c**, **d**) Transcranial Doppler velocities of both the LMCA and right middle cerebral artery (RMCA). The latter was obtained through a normal right temporal window. The peak systolic velocity (PSV), end-diastolic velocity (EDV), resistance index (RI) and ICP were higher in the LMCA compared to the RMCA. (Abbreviations: RPCA right posterior cerebral artery). (Reproduced and adapted by permission of Taylor and Francis Group, LLC, a division of Informa plc. from Denault et al. [21])

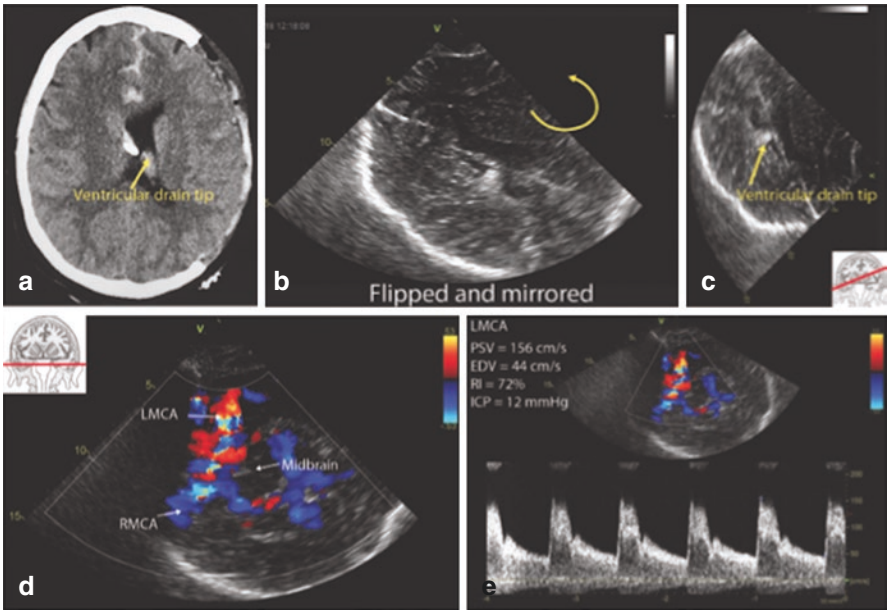

Fig. 13.8 A 54-year-old woman with a (**a**) grade IV subarachnoid hemorrhage and left craniectomy shown on computed tomography. Corresponding diencephalic view obtained using two-dimensional echocardiography. With rotation (**b**), the diencephalic view allows close monitoring of ventricular dimensions which were more significant on the left side. Note on both images the tip of the ventricular drainage system. (**c**, **d**) Color Doppler allows visual screening of flow velocities of arteries of the circle of Willis. Direct examination using pulsed-wave Doppler of the left middle cerebral artery (LMCA) allows more precise quantification. (**e**) Direct examination using pulsed-wave Doppler of the left middle cerebral artery (LMCA) allows more precise quantification. (Abbreviations: EDV end-diastolic velocity, ICP intracranial pressure, PSV peak systolic velocity, RI resistant index, RMCA right middle cerebral artery). (Reproduced and adapted by permission of Taylor and Francis Group, LLC, a division of Informa plc. from Denault et al. [21])

13.5 Pitfalls in Cranial 2D Ultrasound and TCD Monitoring

The use of cranial 2D US, ONSD, and TCD/TCCS must be carefully interpreted in conjunction with extracranial conditions that can be associated with neurological abnormalities. For instance, intravenous milrinone can induce left ventricular outflow tract obstruction in patients with subarachnoid hemorrhage treated for vasospasm (Fig. 13.9). This condition can be associated with significant high-velocity signals in the cerebral arteries which are unrelated to the degree of vasospasm. We have observed elevated PI and increased ONSD in various conditions such as left heart failure, associated with Cheyne–Stokes respiration and possibly intermittent hypercapnia, right heart failure (Fig. 13.10), congenital heart disease with pulmonary hypertension, pneumonia complicating chronic pulmonary hypertension

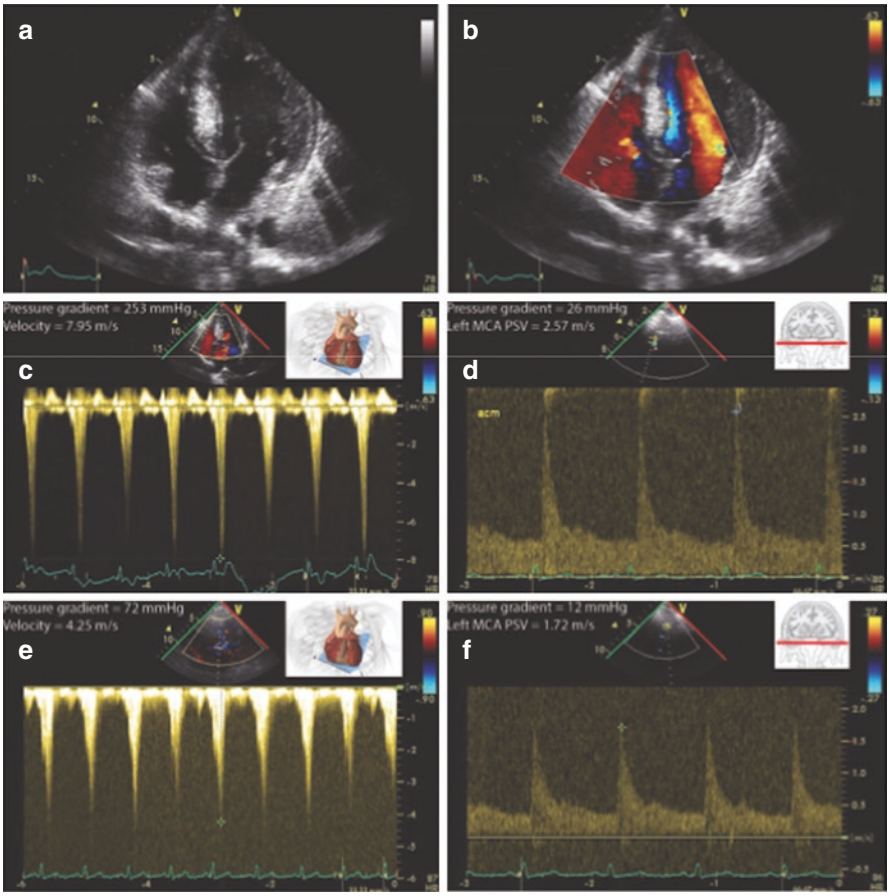

Fig. 13.9 Transcranial Doppler (TCD) and left ventricular outflow tract (LVOT) obstruction. A 31-year-old man with subarachnoid hemorrhage receiving intravenous milrinone develops LVOT obstruction. (**a**, **b**) Apical four-chamber view showing a hyperdynamic heart and flow acceleration in the LVOT using color Doppler. (**c**) Note the significant pressure gradient (PG) of 253 mmHg and LVOT velocities of 7.95 m/s using the apical five-chamber view. (**d**) The associated TCD velocity of the left middle cerebral artery (MCA) was 2.57 m/s (normal peak velocity 0.9–1.1 m/s). Following a bolus of 500 ml of crystalloid, (**e**) the LVOT PG drops to 72 mmHg and (**f**) the left MCA velocity decreases to 1.72 m/s. Examples like this one demonstrates that extra-cranial pathology can have a profound impact on the left MCA pulsatility index measured by TCD. (Abbreviations: PSV peak systolic velocity). (Reproduced and adapted by permission of Taylor and Francis Group, LLC, a division of Informa plc. from Denault et al. [21])

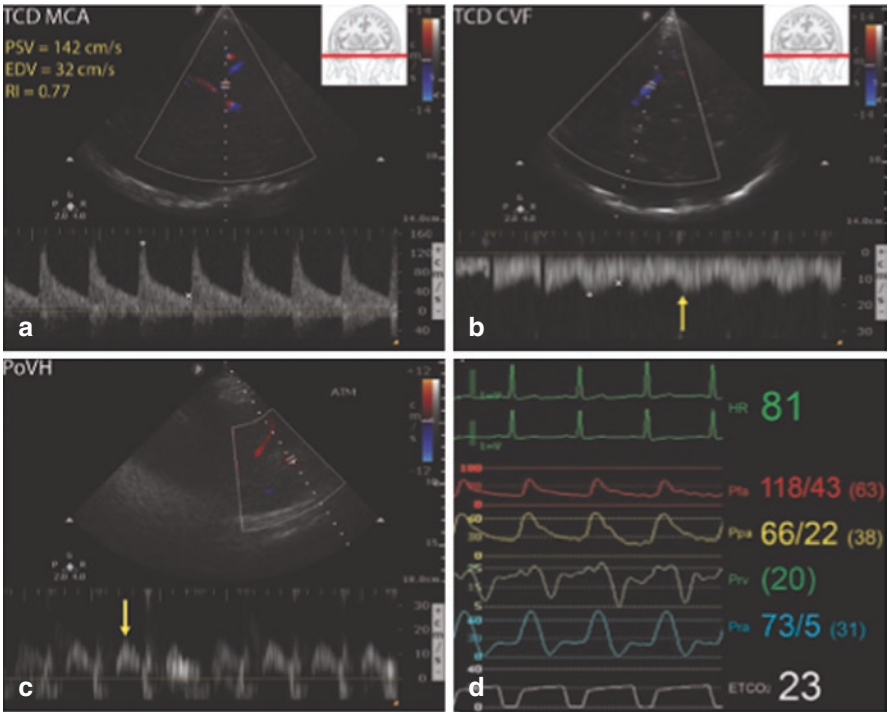

Fig. 13.10 A 71-year-old comatose woman with severe right ventricular failure associated with (**a**) increased resistance index (RI = 0.77) on transcranial Doppler (TCD) of the middle cerebral artery (MCA), (**b**) pulsatile TCD cerebral venous flow (CVF) of the petrosal sinus (arrow), (**c**) pulsatile portal venous flow (PoVF) (arrow) and (**d**) elevated pulmonary artery pressure (Ppa) associated with abnormal right ventricular pressure (Prv) and right atrial pressure (Pra) waveform suggesting right ventricular dysfunction with significant tricuspid regurgitation resulting in cerebral and portal venous congestion. The patient died post-operatively of multisystem organ failure. (Abbreviations: EDV end-diastolic velocity, $ETCO_2$ end-tidal carbon dioxide, HR heart rate, Pfa femoral artery pressure, PSV peak systolic velocity). (Reproduced and adapted by permission of Taylor and Francis Group, LLC, a division of Informa plc. from Denault et al. [21])

(Fig. 13.11), and severe aortic regurgitation. All these examples indicate that PI can significantly be affected by cardiac conditions and possibly also vascular conditions such as arterial stiffness [17, 18].

TCD/TCCS can be used in the ICU for continuous monitoring of high-intensity transient signals (HITS), which represent microemboli (gaseous or solid). HITS can also be present in hypoxemic patients with a patent foramen ovale. This condition

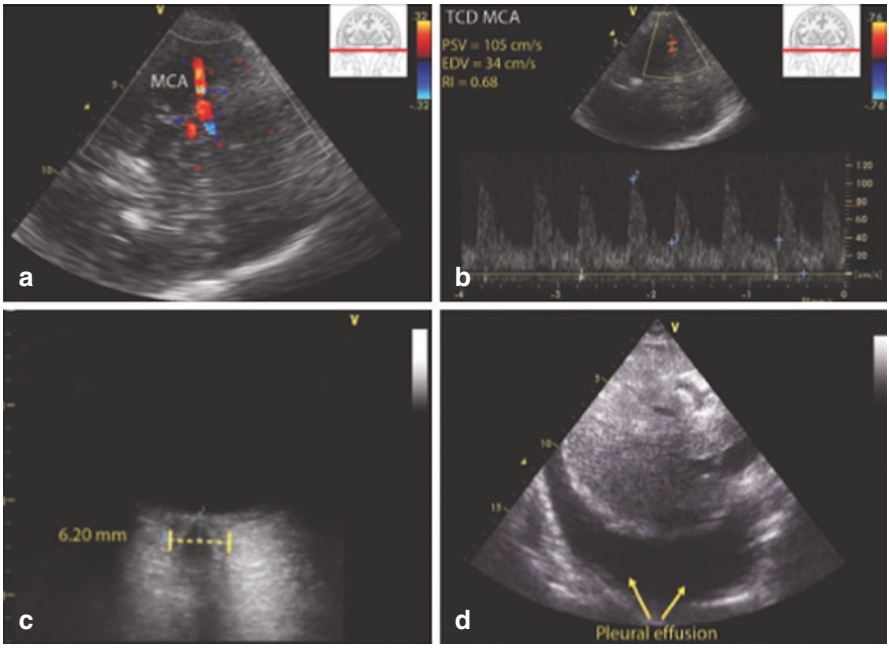

Fig. 13.11 A 75-year-old man admitted to the intensive care unit for pneumonia and hypercapnic encephalopathy with right ventricular dysfunction from pulmonary hypertension. (**a**) Transcranial Doppler (TCD) of the right middle cerebral artery (MCA) showed a (**b**) resistance index (RI) of 0.68. (**c**) The optic nerve sheath diameter was 6.2 mm and (**d**) using a left subcostal view, a pleural effusion was diagnosed. (Abbreviations: EDV end-diastolic velocity, PSV peak systolic velocity, RI resistance index). (Reproduced and adapted by permission of Taylor and Francis Group, LLC, a division of Informa plc. from Denault et al. [21])

can be present in up to 20% of the normal population [19, 20]. Intraoperatively, HITS can be associated with right ventricular dysfunction as microemboli can also migrate in the right coronary artery. In this situation, reduction in electroencephalographic activity and near-infrared spectroscopy signals can be observed.

13.6 Conclusion

In conclusion, TCD analysis and interpretation should always be performed with 2D ultrasound of the brain, optic nerve, and also careful examination of the extracranial organs that could be altered from cardiac dysfunction.

Algorithm

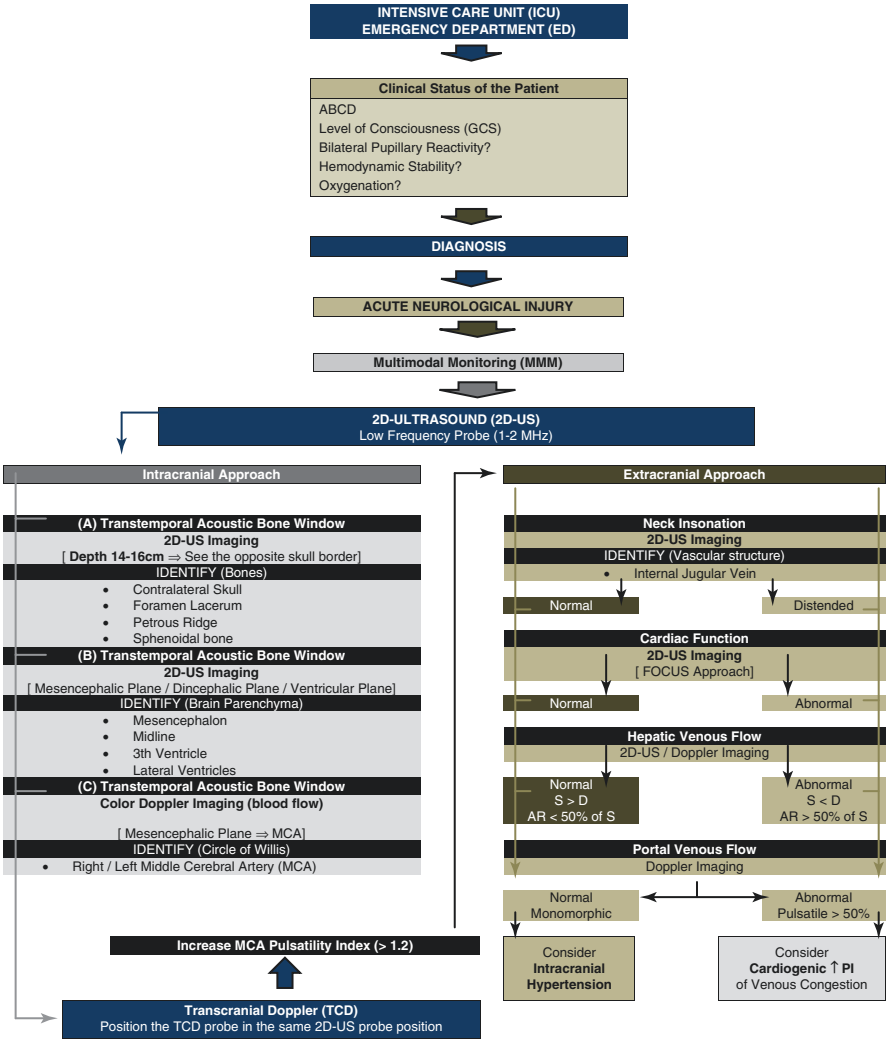

Our approach to using TCD in the presence of elevated PI is summarized in the algorithm. Neglecting the extracranial information in interpreting TCD may lead to inappropriate interventions that would reduce the benefit of this type of monitoring.

PI Pulsatility Index, *AR* atrial reversal hepatic venous flow velocity, *D* diastolic hepatic venous flow velocity, *S* systolic hepatic venous flow velocity, ↑ Increase, *MCA* middle cerebral artery

References

1. Aaslid R, Markwalder TM, Nornes H. Noninvasive transcranial Doppler ultrasound recording of flow velocity in basal cerebral arteries. J Neurosurg. 1982;57(6):769–74.
2. Tsivgoulis G, Alexandrov AV, Sloan MA. Advances in transcranial Doppler ultrasonography. Curr Neurol Neurosci Rep. 2009;9(1):46–54.
3. Rigamonti A, Ackery A, Baker AJ. Transcranial Doppler monitoring in subarachnoid hemorrhage: a critical tool in critical care. Can J Anesth. 2008;55(2):112–23.
4. Del Brutto OH, Mera RM, de la Luz AM, Espinosa V, Castillo PR, Zambrano M, et al. Temporal bone thickness and texture are major determinants of the high rate of insonation failures of transcranial Doppler in Amerindians (the Atahualpa Project). J Clin Ultrasound. 2016;44(1):55–60.
5. Harrer JU, Eyding J, Ritter M, Schminke U, Schulte-Altedorneburg G, Kohrmann M, et al. The potential of neurosonography in neurological emergency and intensive care medicine: monitoring of increased intracranial pressure, brain death diagnostics, and cerebral autoregulation- part 2. Ultraschall Med. 2012;33(4):320–31; quiz 32–6.
6. D'Andrea A, Conte M, Cavallaro M, Scarafile R, Riegler L, Cocchia R, et al. Transcranial Doppler ultrasonography: from methodology to major clinical applications. World J Cardiol. 2016;8(7):383–400.
7. Caricato A, Pitoni S, Montini L, Bocci MG, Annetta P, Antonelli M. Echography in brain imaging in intensive care unit: State of the art. World J Radiol. 2014;6(9):636–42.
8. Couture EJ, Desjardins G, Denault AY. Transcranial Doppler monitoring guided by cranial two-dimensional ultrasonography. Can J Anesth. 2017;64(8):885–7.
9. Krejza J, Kochanowicz J, Mariak Z, Lewko J, Melhem ER. Middle cerebral artery spasm after subarachnoid hemorrhage: detection with transcranial color-coded duplex US. Radiology. 2005;236(2):621–9.
10. Girisgin AS, Kalkan E, Kocak S, Cander B, Gul M, Semiz M. The role of optic nerve ultrasonography in the diagnosis of elevated intracranial pressure. Emerg Med J. 2007;24(4):251–4.
11. Geeraerts T, Launey Y, Martin L, Pottecher J, Vigue B, Duranteau J, et al. Ultrasonography of the optic nerve sheath may be useful for detecting raised intracranial pressure after severe brain injury. Intensive Care Med. 2007;33(10):1704–11.
12. Kimberly HH, Shah S, Marill K, Noble V. Correlation of optic nerve sheath diameter with direct measurement of intracranial pressure. Acad Emerg Med. 2008;15(2):201–4.
13. Rajajee V, Vanaman M, Fletcher JJ, Jacobs TL. Optic nerve ultrasound for the detection of raised intracranial pressure. Neurocrit Care. 2011;15(3):506–15.
14. Dubourg J, Javouhey E, Geeraerts T, Messerer M, Kassai B. Ultrasonography of optic nerve sheath diameter for detection of raised intracranial pressure: a systematic review and meta-analysis. Intensive Care Med. 2011;37(7):1059–68.
15. Choi SH, Min KT, Park EK, Kim MS, Jung JH, Kim H. Ultrasonography of the optic nerve sheath to assess intracranial pressure changes after ventriculo-peritoneal shunt surgery in children with hydrocephalus: a prospective observational study. Anaesthesia. 2015;70(11):1268–73.
16. Chelly J, Deye N, Guichard JP, Vodovar D, Vong L, Jochmans S, et al. The optic nerve sheath diameter as a useful tool for early prediction of outcome after cardiac arrest: a prospective pilot study. Resuscitation. 2016;103:7–13.
17. Kwater A, Gasowski J, Gryglewska B, Wizner B, Grodzicki T. Is blood flow in the middle cerebral artery determined by systemic arterial stiffness? Blood Press. 2009;18(3):130–4.
18. Xu TY, Staessen JA, Wei FF, Xu J, Li FH, Fan WX, et al. Blood flow pattern in the middle cerebral artery in relation to indices of arterial stiffness in the systemic circulation. Am J Hypertens. 2012;25(3):319–24.

19. Sukernik MR, Mets B, Bennett-Guerrero E. Patent foramen ovale and its significance in the perioperative period. Anesth Analg. 2001;93(5):1137–46.
20. Sukernik MR, Bennett-Guerrero E. The incidental finding of a patent foramen ovale during cardiac surgery: should it always be repaired? A core review. Anesth Analg. 2007;105(3):602–10.
21. Denault A, Vegas A, Lamarche Y, Tardif J, Couture P. Basic transesophageal and critical care ultrasound. 2018.
22. Najjar A, Denault AY, Bojanowski MW. Bedside transcranial sonography monitoring in a patient with hydrocephalus post subarachnoid hemorrhage. Crit Ultrasound Jl. 2017;9(1):17.

Chapter 14
Neurosonology in ICU: Transcranial Color-Coded Duplex Sonography (TCCS) Protocol

Camilo N. Rodríguez and Deborah Pugin

Key Points

1. The transcranial color-coded duplex sonography (TCCS) is a technique that enables a direct visualization of the basal cerebral arteries. The visualization is possible through Doppler sonography and the blood flow velocities of the arteries which are color-coded. On the opposite, TCD allows only to record the arterial blood flow velocities without direct visualization. The identification of the arteries is based on the depth of recording and flow direction.
2. A good knowledge of the anatomy of the intracranial and extracranial arteries is requested to evaluate them in an efficient way with TCCS.
3. The Circle of Willis is incomplete in 40–65% of the cases.
4. In total, 10–20% of patients do not have an accessible transtemporal acoustic window to insonate.
5. The insonation angle during the transcranial color-coded duplex sonography (TCCS) study is very important. It is mandatory to keep it as low as possible (<60°), for an optimal interpretation of the flow velocity in the cerebral arteries.
6. Transcranial color-coded duplex sonography (TCCS) is very useful to approach the brain perfusion, but many elements should be taken into consideration to analyze the results (anemia, fever, systemic blood pressure, angle of insonation, etc.) of cerebral hemodynamics in many clinical contexts of critical patients. But remember that we must contemplate that there are certain general limitations at the time of the

C. N. Rodríguez (✉)
Intensive Care Medicine, Hospital Nacional Prof. Dr. A. Posadas, University of Buenos Aires (UBA), Neurointensive Care Section - ESICM, Neurointensive Care Section - AMCI, Neurointensive Care Committee - FEPIMCTI, Member of ESNCH,
Buenos Aires, Argentina
e-mail: camilo.rodriguez@nesccco.com

D. Pugin
Intensive Care Medicine and Neurology, FMH Chez Centre Qorpus. Clinique des Grangettes, Geneva, Switzerland

C. N. Rodríguez et al. (eds.), *Neurosonology in Critical Care*,
https://doi.org/10.1007/978-3-030-81419-9_14

examination (acoustic windows, clinical interpretation of pulsatility index (PI), etc.) and certain specific aspects that we should consider when we approach the patient in a critical pathology determined with or without acute neurological injury.

14.1 Introduction

The insonation of intracranial blood vessels through the skull was first reported by Aaslid and colleagues in 1982 with transcranial Doppler (TCD). Transcranial Doppler (TCD) is based on the use of low-frequency ultrasound probe through various anatomical windows (area of thin skull), allowing an exploration of the Doppler signal of the basal cerebral arteries [1].

The TCD records the blood flow velocities of these arteries, and they are identified by the position of the probe, the depth of recording, and the flow direction. Sometimes, the exact identification of the arteries may be challenging, especially in anatomical variations.

The major limitations of the TCD are the lack of

1. Visualization of the insonated arteries.
2. Evaluation of the angle between the beam of insonation and the vessel, and the potential misidentification of the artery.

Unlike the Transcranial Doppler (TCD), TCCS allows a direct visualization of the basal cerebral arteries through the temporal window of the skull, a thorough identification, and a potential correction of the angle is therefore possible.

TCCS is a non-invasive ultrasound that combines images of parenchymal structures (B-Mode) allowing the visualization of different brain structures through the temporal window and the Doppler evaluation of basal cerebral arteries. The main cerebral arteries of the Circle of Willis may be insonated. The blood flow velocities may be recorded and are color-coded according to the direction of the flow (Doppler). This helps to better identify the different basal cerebral arteries, and the direct visualization of the arteries may show arterial stenosis or kinking.

The scope of TCCS allows an evaluation of the parenchyma, midline shift, visualization of intra- or extracranial hematoma, monitoring of vasospasm, monitoring of indirect signs of increased intracranial pressure, and diagnosis of cerebral circulatory arrest.

To analyze correctly the flow velocities and B-Mode (2D) images, special attention should be paid to possible anatomical variations [2–5].

14.2 TCCS: Anatomical Aspects

The objective of the study by transcranial Doppler (TCD) is the evaluation of blood flow velocities in basal cerebral arteries, and transcranial color-coded duplex sonography (TCCS) includes also the evaluation of cerebral blood flow velocities in the

cerebral intracranial and extracranial arteries and the evaluation of extravascular structures.

A basic knowledge of anatomy is mandatory to realize an effective study of these parameters.

The intracranial and extracranial vascular and the parenchymal structures can be accessed through the transcranial color-coded duplex sonography (TCCS).

Remember, 10–20% of patients do not have an accessible transtemporal acoustic window to insonate.

14.3 Basal Cerebral Arteries: Circle of Willis

The Circle of Willis is a vascular structure located in the brain base connecting two arterial systems: the anterior system constituted by both Internal Carotid Arteries and the posterior system, originating from the vertebro-basilar circulation [6]. From the Circle of Willis, intracranial arteries can be individualized: Middle Cerebral Artery (MCA), Anterior Cerebral Artery (ACA), Posterior communicating Artery (PcomA), and Posterior Cerebral Artery (PCA) (Figs. 14.1 and 14.2).

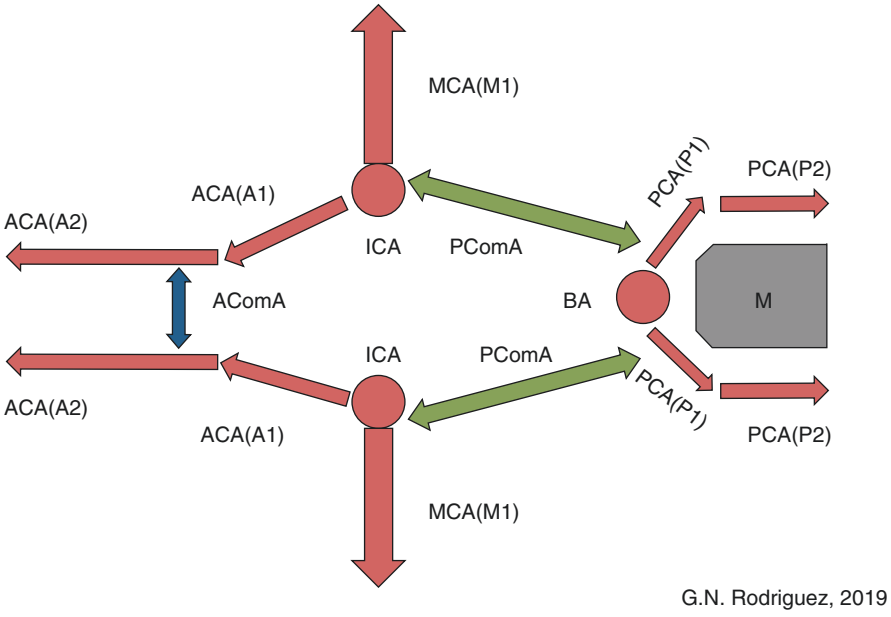

Fig. 14.1 Scheme: Circle of Willis and most common blood flow direction; ACA anterior cerebral artery, MCA middle cerebral artery, PCA posterior cerebral artery, ICA internal carotid artery, AComA anterior communicating Artery, PComA posterior communicating artery, M mesencephalon, (Arrows): points out the most common direction of flow

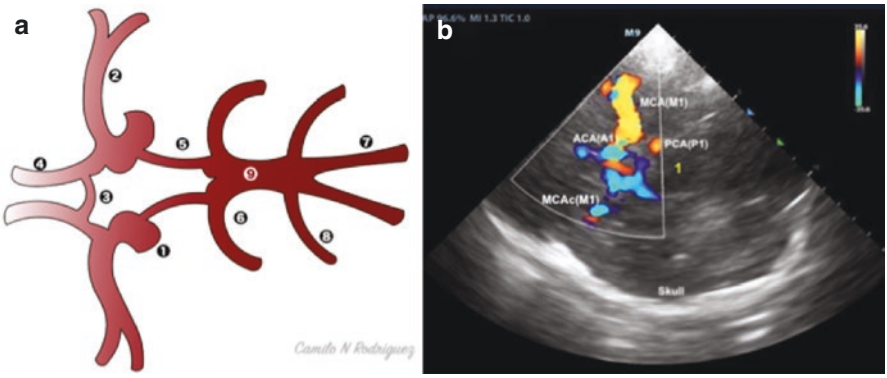

Fig. 14.2 (**a**) Schema: Circle of Willis; (1) internal carotid artery (ICA), (2) middle cerebral artery (MCA) M1-segment and M2 segment, (3) anterior communicating artery (AcomA), (4) anterior communicating artery (ACA) A1-segment, (5) posterior communicating artery (PcomA), (6) posterior cerebral artery (PCA) P1-segment and P2-segment, (7) vertebral arteries (VA) V4-segments, (8) postero-inferior cerebellar artery (PICA), and (9) basilar artery (BA). (**b**) TCCS: Circle of Willis by mesencephalic plane through transtemporal acoustic window; ACA: anterior cerebral artery (A1 segment), MCA middle cerebral artery (M1 segment), PCA posterior cerebral artery (P1 segment), MCAc contralateral middle cerebral artery and (1) mesencephalon

14.3.1 Anterior Circulation

14.3.1.1 Carotid System

- *Internal Carotid Artery (ICA)*

  (a) Carotid siphon
  (b) Ophthalmic artery
  (c) Middle Cerebral Artery (MCA)

  c.1 M1 Segment
  c.2 M2 Segment
  c.3 M3 Segment

  (d) Anterior Cerebral Artery (ACA)

  d.1 A1 Segment
  d.2 A2 Segment

  (e) Posterior communicating artery (PcomA)

14.3.2 Posterior Circulation

14.3.2.1 Vertebro-Basilar System

- *Vertebral Artery (VA)*

  (a) V1 segment
  (b) V2 segment
  (c) V3 segment
  (d) V4 segment
  Most common insonated through transforaminal window.

- *Basilar Artery (BA)*

  (a) Posterior Cerebral Artery (PCA)

  a.1 P1 segment
  a.2 P2 segment

- *Postero-inferior Cerebellar Artery (PICA)*

  Note that the Circle of Willis is incomplete in 40–65% of population [7–9].

14.4 TCCS: Brain Parenchyma and Non-vascular Structures

The milestones displayed regularly with identification rates of >75% are as follows [10, 11]:
Transcranial Ultrasonography: B-Mode (Gray Scale)

1. Sphenoid bone/Petrosal bone
2. Medial Cerebral Fossa
3. Cerebellum
4. Mesencephalon
5. Thalamus
6. Pineal gland
7. Frontal horns of lateral ventricles
8. Choroidal plexus
9. Third ventricle
10. Cerebral midline
11. Intra-axial/extra-axial collections

There are intracerebral anatomical structures such as medulla oblongata, fourth ventricle, cerebellar structures, insula, frontal, parietal, and occipital lobes that can be visualized with greater difficulty except in craniectomized patients [10].

There is a good correlation between the computed tomography (CT) and the transcranial color-coded duplex sonography (TCCS) when studying and interpreting the anatomical structures of the brain parenchyma in non-craniectomized

patients: third ventricle (and its displacement), midline shift, perimesencephalic cistern, and Sylvian fissure [12, 13]. This correlation is better between CT and TCCS in craniectomized patients, where lateral ventricles, hyper- or hypodense lesions, and the location of the intraventricular catheter can be seen [14].

14.5 TCCS: Examiner Considerations

The ultrasonography examination in the intensive care unit or the emergency department presents unique characteristics as the patients are less mobile, often intubated, sometimes hemodynamically instable. TCCS needs to be completed quickly. Furthermore, different parameters may influence the blood flow velocities such as fever, anemia, brady or tachycardia, and hypo- or hypercapnia, and must be recorded at the same time to allow an integrative analysis of the measures.

1. *Mobility of the Patient and Clinical Context?*
   Patients with suspected cervical lesions or intubated and patients with intracranial hypertension cannot be mobilized freely, and the TCCS exam could be limited. Usually, the temporal window is accessible, even if the patient's head needs to be maintained in a neutral position. It is up to the treating physicians to evaluate the clinical situation and define the best strategy.
2. *Time to Conduct the Study*
   In a trained professional, TCCS requires usually between 20 and 45 minutes for a complete and comprehensive evaluation of the different elements (parenchyma, blood flow velocities of the different arteries of interest) [22–24].

14.6 TCCS: Acoustic Windows

There are five insonation acoustic windows for TCCS approach:

1. Transtemporal
2. Transforaminal (suboccipital)
3. Transorbital
4. Submandibular
5. Frontal

In general, the patient is examined in supine position (with the exception of the evaluation through the suboccipital window) with the head preferably aligned with the body and with the head at 30° (whenever possible). The operator is located behind the patient's head (sitting or standing) or on patient's side.

The study of TCCS in the intensive care unit requires time and dedication on the part of the operator to obtain reliable information, often dedicating 30 to 45 minutes per examination depending on the critical pathology of the patient [22–24].

Consider that TCCS and the "blind" TCD techniques are complementary exams that require time and dedication if a reliable and complete interpretation of them is required. In the TCD, the insonation angle of the vessels and the ultrasound beam is unknown. There is no visual orientation, so the flow and its speed can be underestimated, but a small angle of insonation is presumed (0°–30°) [2]. The angle of insonation during the development of the TCCS study is very important when interpreting the results. It is necessary to be able to maintain an angle of insonation <60° for an optimal interpretation of the flow velocity in cerebral arterial vessels [25–27].

14.7 TCCS: Examination Protocol

The transcranial color-coded duplex sonography (TCCS) requires the use of a low-frequency transducer (1.75–3.5 MHz), as cardiac transducers. This probe is adequate for penetration of the temporal skull and enables the visualization of the cerebral parenchyma (B-mode) and the evaluation of cerebral arteries through the Doppler signal [15, 16].

To evaluate the optic nerve sheath diameter, the vascular probe should be used (5–12 MHz).

As the optic nerve is subject to the same pressure changes as the intracranial compartment [17, 18], the optic nerve sheath diameter has an anterior enlargement in case of increased intracranial pressure. Several studies have found a correlation between optic nerve sheath diameter and increased intracranial pressure (ICP) [19–21].

The upper limit of normal value of optic nerve sheath diameter is 5 mm if recorded as described below. With this cut-off for intracranial hypertension, the specificity is 93% and negative predictive value 100% [21].

14.7.1 Transtemporal Acoustic Window Examination (Axial Planes)

The transtemporal window is most frequently used for insonation in an axial plane of the arterial vessels. At the 1998 annual meeting of the European Transcranial Color-Coded Duplex Study Group (TCCS study group), the following exploration planes were recommended:

1. Mesencephalic plane (Figs. 14.3 and 14.4)
2. Diencephalic plane (Fig. 14.5)
3. Ventricular plane (Cella media) (Fig. 14.6)
4. Upper pontine plane (Fig. 14.8b)
5. Lower pontine plane (Fig. 14.8a)

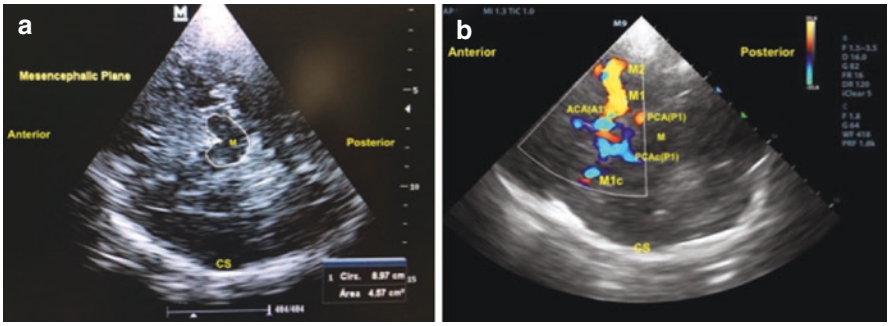

Fig. 14.3 (**a**) Mesencephalic plane by TCCS through transtemporal acoustic window. M: mesencephalon, CS: contralateral skull. (**b**) Circle of Willis. M1 M1 segment of middle cerebral artery (MCA), M2 M2 segment of MCA, M1c contralateral M1 segment of MCA, ACA A1 segment, PCA P1 segment, PCAc contralateral P1 segment, M mesencephalon, and CS:contralateral skull

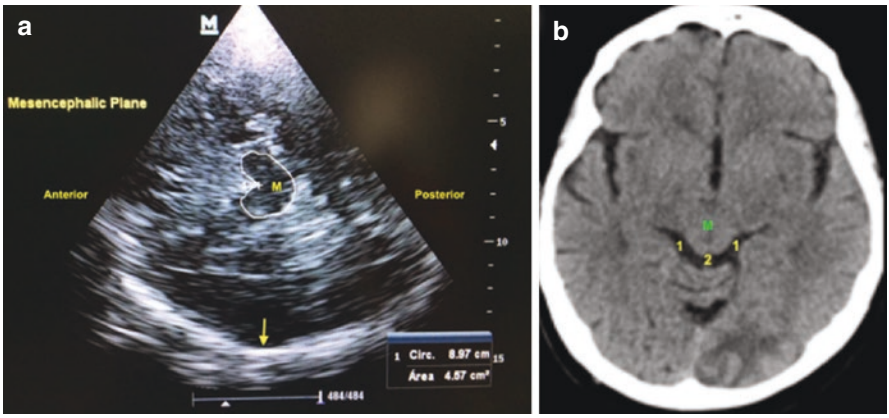

Fig. 14.4 (**a**) Mesencephalic plane by TCCS through transtemporal acoustic window; M: mesencephalon (¨Butterfly¨), (Arrow) contralateral skull. (**b**) Brain TC-scan; M: mesencephalon, (1) ambiens cistern and (2) quadrigeminal cistern

This is the main window of insonation when we start a study with the transcranial color-coded duplex sonography (TCCS) and the gray-scale brain ultrasound (B-Mode). It allows a direct visualization of the anatomical references and therefore a correct identification of the structures (carotid arterial system and main parenchymal structures).

14.7.1.1 Considerations

Recommended Depth: 140–160 mm

Which allows a direct visualization of the contralateral skull.

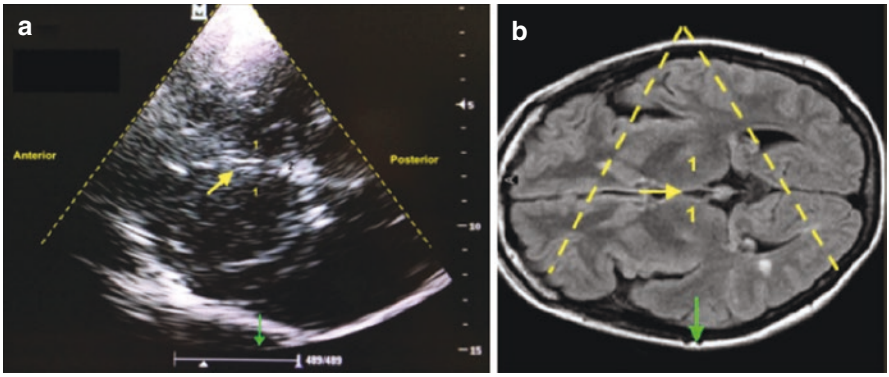

Fig. 14.5 (**a**) Diencephalic plane by TCCS through transtemporal acoustic window: (1) Thalamus. (2) Pineal gland, (yellow arrow) 3rd ventricle and (green arrow) contralateral skull. (**b**) Brain MRI: (1) Thalamus, (yellow arrow) 3rd ventricle, (dotted line) ultrasound beam through transtemporal window and (green arrow) contralateral skull

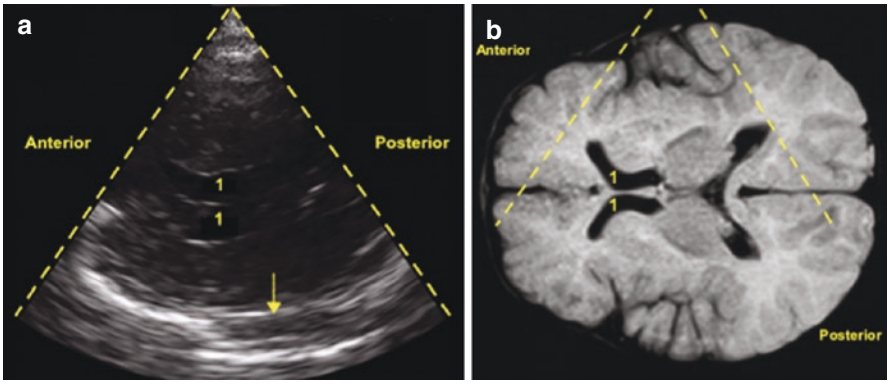

Fig. 14.6 (**a**) Ventricular plane by TCCS through transtemporal acoustic window: (1) anterior horns of lateral ventricles, (arrow) contralateral skull. (**b**) Brain MRI: (1) anterior horns of lateral ventricles and ultrasound beam (dotted line)

Doppler: (Convention)

- Blue color: Flow away from transducer.
- Red color: Flow forward to the transducer.

We suggest the following protocol order so as not to leave any detail unstudied:

(a) *Transducer*: (Probe)

- Cardiac low-frequency probe (1.75–3.5 MHz)

(b) *Patient Positioning*:

- Supine position with the head at a 30° angle, aligned with the body
- (Not always possible in critically ill patients)

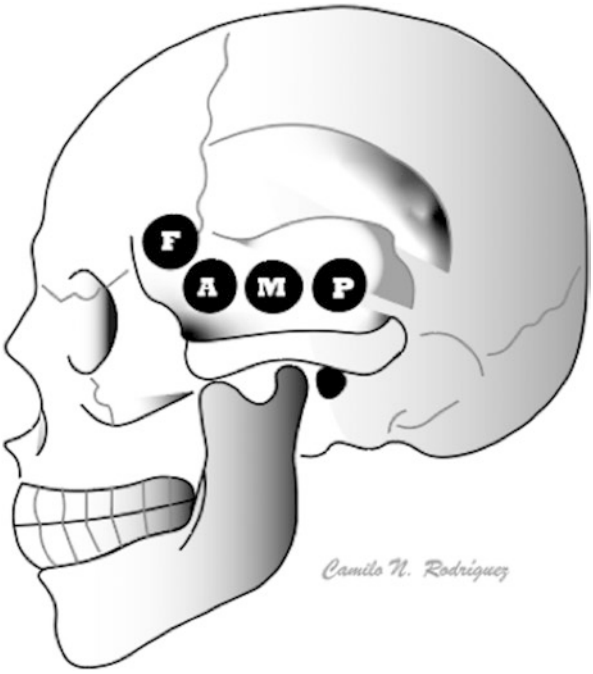

Fig. 14.7 Scheme: Transtemporal acoustic window. F frontal, A anterior, M mean, and P posterior position

(c) *Depth*:

- 14–16 cm
- (Allows the direct visualization of the contralateral skull)

(d) *Insonation Window: Transtemporal Acoustic Window:*

- With the probe mark looking forward
- Position the probe in front of the tragus in the temporal bone above the zygomatic arch (Fig. 14.7)

(e) *B-Mode:*

- Localize the contralateral skull
- Localize the cerebral peduncles (mesencephalon: Butterfly-shaped cerebral peduncles) (Figs. 14.3 and 14.4)

(f) *Color Doppler: Location of Circle of Willis:* (Fig. 14.2)

- Start the color-coded Doppler (red color–blue color)
- Identify the different arteries of the circle of Willis around mesencephalic brainstem

(g) *Color Doppler: Location of the Ipsilateral Middle Cerebral Artery (MCA):*

- Start the color-coded Doppler (red color–blue color)

- Identify the M1 segment of MCA (horizontal segment) (Fig. 14.2)

(h) *Arterial Blood Flow Velocities (PW Doppler): Doppler Spectrum Analysis:*

- Place the pulsed Doppler (PW) on the M1 segment of MCA (proximal)
- The PW Doppler allows to obtain the spectral Doppler wave and the flow velocities (MFV /PSV/EDV) of each insonated vessel

(i) *Identify Other Intracerebral Arteries of the Circle of Willis*: [28]
Anterior Circulation:

- *Identification*: (color Doppler) A1 segment of ipsilateral ACA
- (They can be very useful for the evaluation of collateral circulation in case of an occlusive disease) [29]
- *Identification*: (color Doppler) Contralateral M1 segment of MCA
- (sometimes is possible)
- *Identification*: (color Doppler) AcomA and PcomA

(j) *Identify Other Intracerebral Arteries of the Circle of Willis*:
Posterior Circulation:

- It is usually not identified in the same plane of the MCA; it is therefore required to tilt the transducer caudally.
- *Identification*: (Color Doppler) P1 and P2 segments of PCA
- [Ipsilateral vessels: P1 segment (red color) and P2 (blue color)].
- Sometimes a blue non-pulsatile signal could be identified, next to the P2 segment. It is the Basal vein of Rosenthal [30].

(k) *Tilt the Transducer 10º Cephalic from the Mesencephalic Plane: Diencephalic Plane (Thalamic Plane)*:

- *B-Mode*: Midline
- Visualization of the third ventricle (linear hyperechoic structure)
- *B-Mode*: Thalamus: Next to the third ventricle (bilateral hypoechoic structures)
- *B-Mode*: Pineal gland: A posterior calcified structure (hyperechoic structure)
- *Color Doppler*: M2 and M3 segments of ipsilateral MCA. A2 segment of ACA

(l) *Tilt the Transducer 10° cephalic from thalamic plane: Ventricular plane (Cella Media plane):* [31]

- *B-Mode*: Frontal horns of the lateral ventricles (Hypoechoic bilateral structures)
- *Color Doppler*: M3 segment of ipsilateral MCA

(m) *B-Mode and color Doppler: Lowering the insonation angle by 10° from the mesencephalic plane: Pontine plane:* (Fig. 14.8b)

- *B-Mode*: (Anteriorly) Sphenoid bone

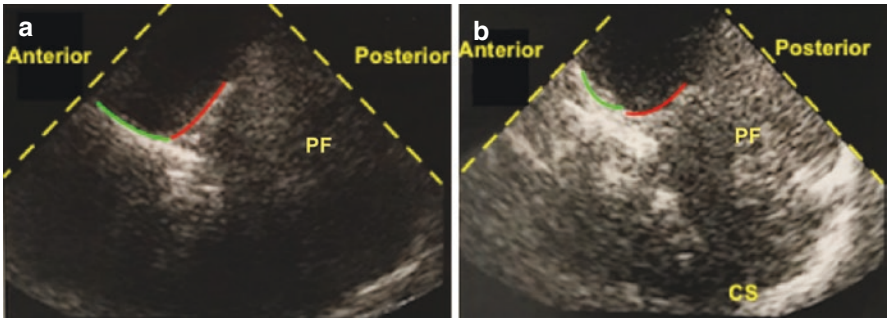

Fig. 14.8 (**a**) Lower pontine plane through transtemporal window by TCCS approach: (red line) petrosal bone and (green line) sphenoid bone. (**b**) Upper pontine plane through transtemporal window by TCCS approach: (CS) contralateral skull, (PF) posterior fossa, (red line) petrosal bone, and (green line) sphenoid bone

- *B-Mode*: (Posteriorly) Petrosal bone
- *Sphenoid* + *Petrosal* bones: Forms middle temporal fossa
- Cerebellum: Hypoechoic structure
- *Color Doppler*: ICA-Siphon and ophthalmic artery (OA)

(n) *B-Mode and color Doppler: Lowering the insonation angle by 10° from the upper pontine plane: Lower Pontine plane:* (Fig. 14.8a)

- *B-Mode*: (Anteriorly) Sphenoid bone
- *B-Mode*: (Posteriorly) Petrosal bone
- *Color Doppler*: C1 segment–ICA

14.7.2 Transtemporal Acoustic Window Examination (Coronal Planes)

The transtemporal window is most frequently used for insonation. The coronal planes may be a complementary ultrasound view to insonate vessels with difficult access.

2.1 *Anterior Coronal Plane*
2.2 *Posterior Coronal Plane*

We suggest the following protocol order so as not to leave any detail unstudied:

(a) *Transducer*: (Probe)

- Cardiac low-frequency probe (1.75–3.5 MHz)

(b) *Patient Positioning*:

- Supine position with the head at a 30° angle, aligned with the body

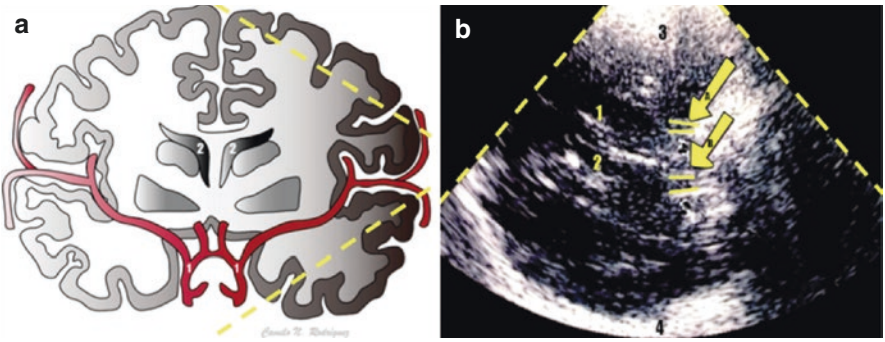

Fig. 14.9 (**a**) Scheme: Anatomical coronal section; (1) C1 segment of ICA, (2) Frontal horns of lateral ventricles and (Yellow Dotted line) coronal ultrasound beam. (**b**) Anterior coronal plane through transtemporal window by TCCS approach: (1)(2) frontal horns of lateral ventricles, (3) brain parenchyma proximal to the probe, (4) contralateral skull. (A) Yellow arrows: carotid Groove of the sphenoid bone (C1 segment of Internal carotid artery (ICA))

- (Not always possible in critically ill patients)

(c) *Depth*:

- 14–16 cm
- (Allows the direct visualization of the contralateral skull)

(d) *Rotate the Transducer 90° from the Mesencephalic Plane: Anterior Coronal Plane*: (Fig. 14.9)

- *B-Mode*: Frontal horns of the lateral ventricles (Hypoechoic structures)
- *B-Mode*: Carotid groove of the sphenoid bone
- *Color Doppler*: Terminal internal carotid artery (C1 segment of ICA)
- *Color Doppler*: Carotid siphon: Can be visualized more completely with the combination of two planes: a transtemporal axial and coronal approach

(e) *Rotate the transducer by 90° from the transtemporal axial plane, once visualized P1–P2 (PCA): Posterior coronal plane*

- Color Doppler: Top of the basilar artery (BA) [32]

14.7.3 Transoccipital (Transnuchal/Transforaminal) Acoustic Window Examination

This acoustic window is the same to insonate the vertebro-basilar arterial system by TCD or TCCS (Figs. 14.10 and 14.11).

We suggest the following protocol order so as not to leave any detail unstudied of vertebro-basilar system.

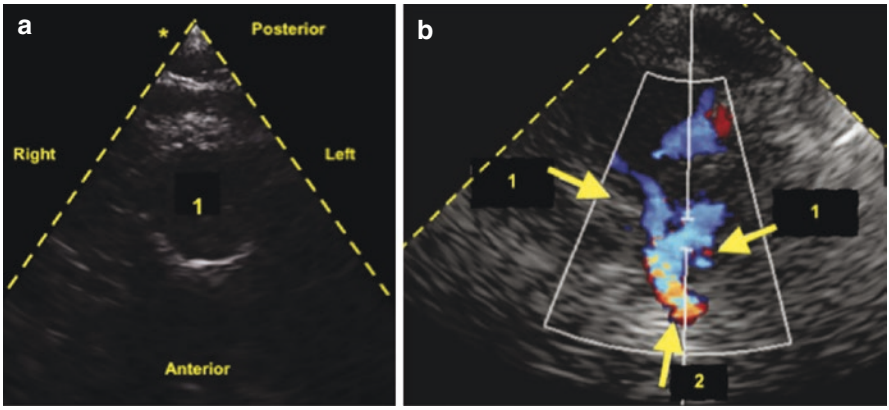

Fig. 14.10 (**a**) Transforaminal (Transnuchal) acoustic window by TCCS (B-Mode). (1) foramen magnum. (**b**) Transforaminal acoustic window by TCCS (duplex): (1) vertebral artery (blue color), (2) basilar artery (blue color)

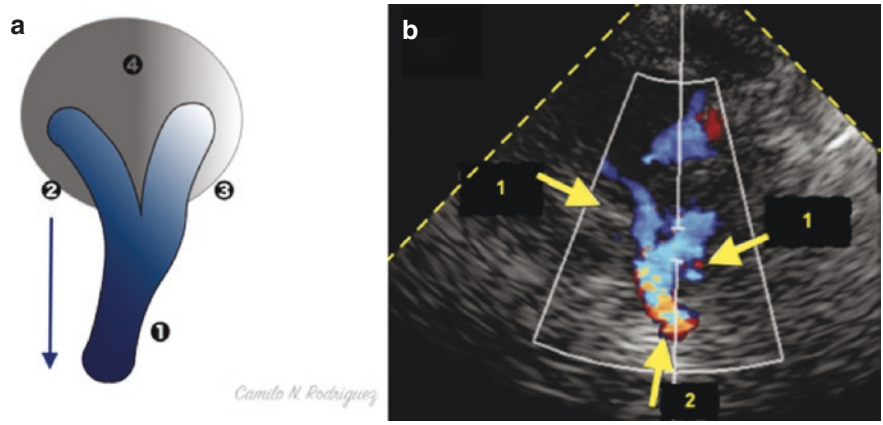

Fig. 14.11 (**a**) Scheme of the anatomy of the vertebro-basilar system by TCCS through transforaminal acoustic window: (1) basilar artery; (2) right vertebral artery – V4 segment; (3) left vertebral artery – V4 segment; (4) foramen magnum, (Arrow) It highlights that the flow moves away from the transducer (Blue color). (**b**) Vertebro-basilar system insonation by TCCS through transforaminal acoustic window: (1) V4 segment of vertebral artery (blue), (2) basilar artery (blue). Arterial flow moves away from the transduce

(a) *Transducer*:

- Cardiac (array) low-frequency probe (1.75–3.5 MHz)

(b) *Patient positioning*:

- Lateral position on the bed with the head slightly tilted forward
- (Sometimes impossible in the ICU)

(c) *Depth*: 7–8 cm
Visualize the Foramen magnum in the center of the image (Hypoechoic structure)

(d) *Insonation window: Transforaminal acoustic window:*

- Probe marker looking cephalad.
- The transducer is positioned suboccipitally in the midline and pointed toward the nasion.

(e) *B-Mode:*

- Locate the echoreflective osseous border of the hypoechoic foramen magnum (Fig. 14.10a).

(f) *Color Doppler: Location of vertebro-basilar vessels:* (Figs. 14.10 and 14.11)

- Possible to visualize the ¨Y¨ configuration of the converging vessels
- Vertebral Arteries (VA): V4 segments (blue color)
- Basilar Artery (BA) (blue color) [33–35]
- Sometimes: Possible to visualize Postero-inferior Cerebellar Artery (PICA). Origin in V4 segment of VA with the blood flow toward the probe (red Color)

(g) *Arterial Blood flow Velocities (PW Doppler): Doppler spectrum analysis:*

- Place the pulsed Doppler (PW) on the V4 segment of VA and BA.
- The PW Doppler allows to obtain the spectral Doppler wave and the flow velocities (MFV / PSV / EDV) of each insonated vessel.

Occasionally, during the examination through the transforaminal window and the study of the vertebro-basilar arterial system, the operator can image one of the two V4 segments of the vertebral arteries with their flow directed toward the transducer (red color), because sometimes these segments present some tortuosity. From time to time, due to kinking of the vertebral arteries, a red color-coded signal can be identified, as the flow in the loop is moving toward the probe.

14.7.4 Submandibular Acoustic Window Examination

This window allows to insonate the extracranial carotid system: Common Carotid Artery (CCA), External Carotid Artery (ECA), and Internal Carotid Artery (ICA). In intubated patients (ICU), it also allows to visualize the vertebro-basilar system, because sometimes transoccipital approach (requires neck flexion) is not always available [36] (Fig. 14.12).

We suggest the following order for the insonation and the arterial carotid system (CCA-ICA-ECA) (Fig. 14.12):

(a) *Transducer*:

- Cardiac (array) low-frequency transducer (1.75–3.5 MHz)

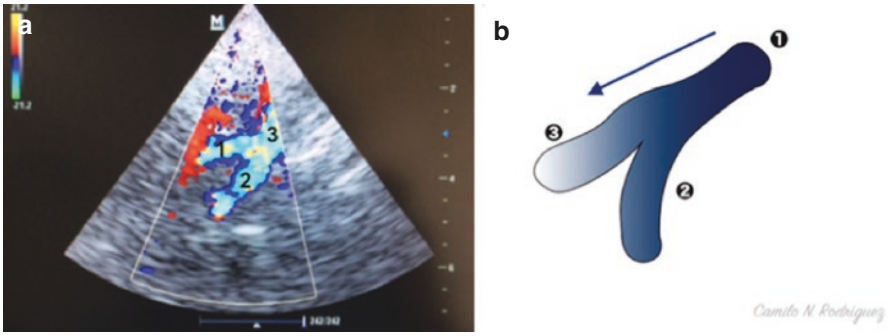

Fig. 14.12 (**a**) Submandibular acoustic window by TCCS: (1) external carotid artery (blue color), (2) internal carotid artery (blue color), and (3) common carotid artery (blue color) (primitive). (**b**) Scheme of carotid system insonation by TCCS: (3) external carotid artery (blue color), (2) internal carotid artery (blue color) and (1) primitive carotid artery (blue color). (Arrow): It highlights the flow away from transducer

- Linear (High frequency): Axial and longitudinal insonation to assess the arterial carotid system with most detail. Useful in the carotid ultrasound approach

(b) *Patient and examiner positioning*:

- *Patient*: Supine position with the head aligned with the body and slightly (if possible) tilted toward the opposite side (Head of the bed at 30°)
- (It is difficult in prone position)
- *Examiner*: In comfortable position at the patient's side or behind the head

(c) *Insonation window: Anatomical location:* (Fig. 14.13)

- *Location*: Anterior triangle of the neck [6]
- *The transducer position*: Cephalic and posterior angle insonation
- *The probe marker*: To cephalic

(d) *B-Mode*:

- *Mapping*: Cross-sectional insonation plane, beginning caudally in the neck. Follow the vessel as high as possible to the angle of mandible
- (Most common during Carotid approach than TCCS approach)

(e) *Color Doppler: Location of Carotid system vessels:*

- *Identification*: Common Carotid Artery (CCA) (Blue color)
- *Identification*: Internal Carotid Artery (ICA) (Blue color)
- *Identification*: External Carotid Artery (ECA) (Blue color)
- *Remember*: The carotid blood flow away from the probe (Fig. 14.12)

(f) *Arterial blood flow velocities (PW Doppler): Doppler spectrum analysis*:

- *Internal Carotid Artery* (ICA): Low resistance spectral waveform velocity profile. High diastolic component (Figs. 14.14 and 14.15)

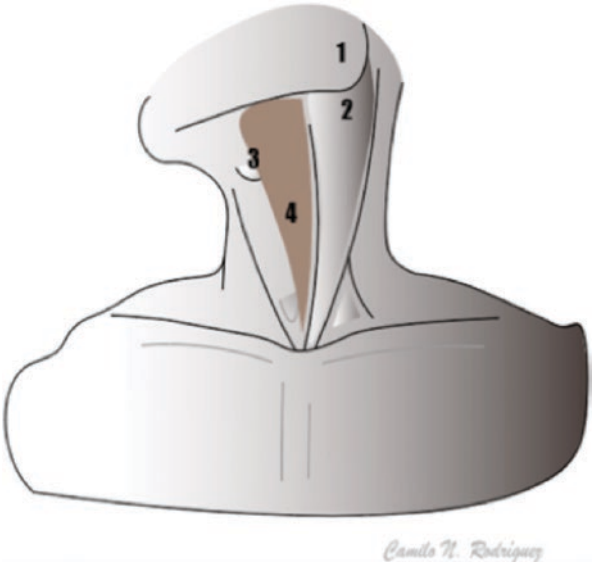

Fig. 14.13 Scheme: Superficial anatomy of neck: (1) angle of the mandible, (2) sternocleidomastoid muscle, (3) thyroid cartilage, and (4) anterior (carotid) triangle of neck

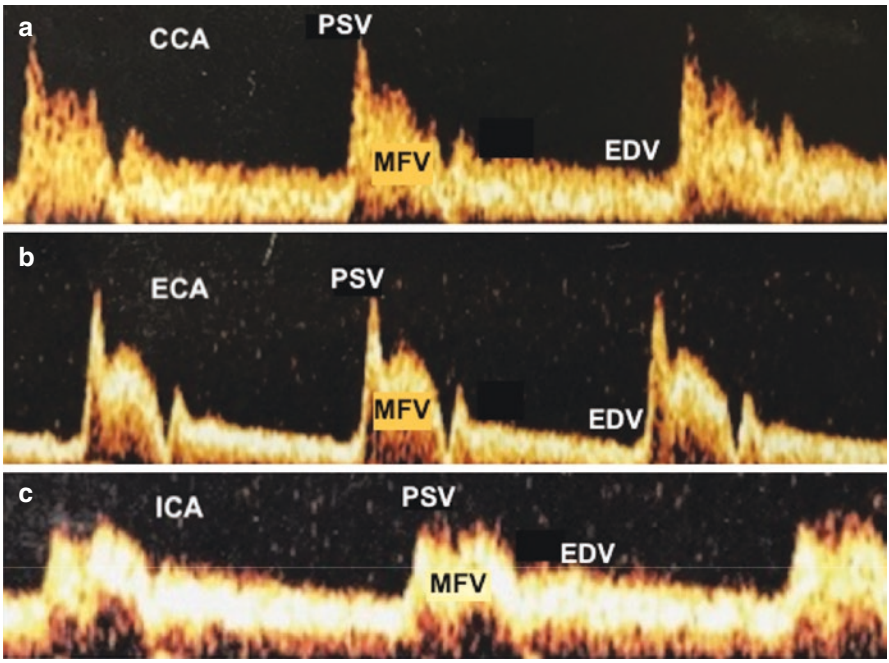

Fig. 14.14 Spectral Doppler waveform of carotid vessels: (**a**) common carotid artery (CCA); (**b**) external carotid artery (ECA); (**c**) internal carotid artery (ICA); (PSV) peak systolic velocity, (MFV) mean velocity, (EDV) end-diastolic velocity

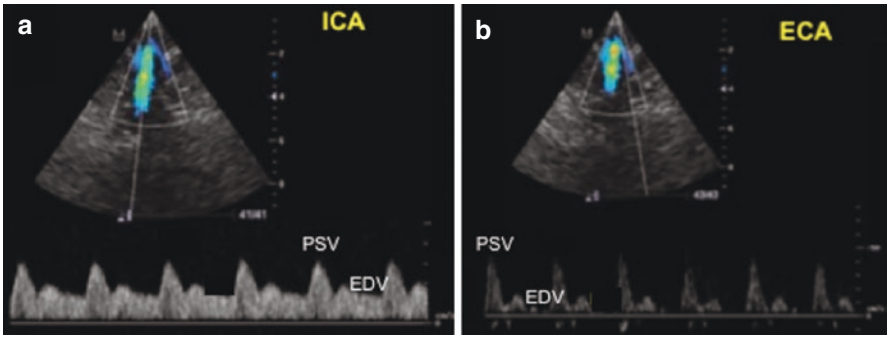

Fig. 14.15 Doppler spectral waveform by TCCS approach through submandibular acoustic window: (**a**) internal carotid artery (ICA), peak systolic velocity, (PSV) and end-diastolic velocity (EDV) (low resistance); (**b**) external carotid artery (ECA), peak systolic velocity (PSV), and end-diastolic velocity(EDV) (high resistance)

Table 14.1 Ultrasound criteria to differentiate between ICA and ECA [38] (Fig. 14.12)

ICA	ECA
No ramification	Ramification
Low pulsatility	High pulsatility
No changes in the pulsed Doppler waveform morphology (¨Tapping¨)[a]	Changes in the pulsed Doppler waveform morphology (¨Tapping¨)[a]
(Blue color)	(Blue color)
Pulsed Doppler (low resistance) *High* diastolic component *Low systolic component*	*Pulsed Doppler* (high resistance) Low diastolic component High systolic component

[a]Maneuver that facilitates the identification of the ICA: internal carotid artery and ECA: external carotid artery

- *External Carotid Artery* (ECA): High resistance spectral waveform velocity profile. Low diastolic component (Figs. 14.14 and 14.15)
- *Common Carotid Artery* (CCA): Mixed spectral waveform velocity profile (Fig. 14.14)

It is essential to record the ICA velocities as the mean flow velocity is requested to calculate the Lindegaard ratio; this must be an essential part of a complete and comparative examination. Remember that when calculating the Lindegaard index, you should take the MFV (also called TAMAX) of the Internal Carotid Artery (ICA), in order to obtain a more reliable hemodynamic value (Table 14.1) [37, 52].

We suggest the following order for the insonation of the vertebro-basilar arterial system through this window:

(a) *Transducer*:

- Cardiac (array) low-frequency transducer (1.75–3.5 MHz)

- Linear (High frequency): Axial and longitudinal insonations to assess the arterial carotid system with most detail. Useful in the carotid ultrasound approach

(b) *Depth:* 8–12 cm
Locate the echoreflective osseous border of the hypoechoic foramen magnum

(c) *Patient and examiner positioning*:

- *Patient*: Supine position with the head aligned with the body and slightly (if possible) tilted toward the opposite side (Head of the bed at 30°)
- *Examiner*: In comfortable position at the patient's side or behind the head

(d) *Insonation window: Anatomical location:* (Fig. 14.13)

- *Location*: Anterior triangle of the neck [6]
- *The transducer position*: Cephalic and posterior angle insonations
- *The probe marker*: To cephalic

(e) *B-Mode*:

- *Locate*: Foramen Magnum

(f) *Color Doppler: Location of vertebro-basilar system:*

- Possible to visualize the ¨Y¨ configuration of the converging vessels
- Vertebral Arteries (VA): V4 segments (blue color)
- Basilar Artery (BA) (blue color)

(g) *Arterial blood flow velocities (PW Doppler): Doppler spectrum analysis*:

- Place the pulsed Doppler (PW) on the V4 segment of VA and BA.
- The PW Doppler allows to obtain the spectral Doppler wave and the flow velocities (MFV/PSV/EDV) of each insonated vessel.

14.7.5 Transorbital Acoustic Window Examination

We suggest the following order for insonation of the Optic Nerve (ON) as a part of TCCS approach:

(a) *Transducer*:

- High-frequency linear transducer (5–12 MHz)
- Low-frequency sector transducer (1.6–3.5 MHz)

(b) *Patient positioning:*

- *Patient*: Supine position with the head aligned with the body
  (Head of the bed at 30°)
- *Examiner*: In comfortable position at the patient's side or behind the head

(c) *Depth*: 4 cm

It is necessary to record all patients with the same settings to have similar measures of the optic nerve sheath diameter.

(d) *Machine: Set the safety:*

- *Consider*: ALARA
- *Safety setting*: Mechanical Index: <0.23
- *Safety setting*: Thermal Index: <0.2

(e) *Patient: Safety procedure:*

- Occlude the eyelids, before placing the ultrasound gel, preferably with a disposable and transparent film (Tegaderm®) to avoid any corneal and/or conjunctival irritation [39].

(f) *B-Mode: Insonate axial and sagittal planes:*

- *Transducer*: Place on the eyeball (on the upper closed eyelid) that you want to insonate. The thenar eminence, at the time of the study, should be in contact with the ipsilateral superciliary region of the patient as a point of support for the examining hand and thus minimize the pressure on the eyeball.
- *Identification*: Eyeball (Hypoechoic structure).
- *Identification*: Papilla.
- *Identification*: Optic nerve.

(g) *B-Mode: Optic nerve (ON):*

- *Location*: Posterior pole of the eyeball (Hypoechoic structure)
- *Study documentation*: Optic Nerve Sheath Diameter (ONSD). Measure bilaterally 3 mm behind the papilla through longitudinal and sagittal view [41]
- *ONSD(cut-off)*: <5 mm

(h) *Color Doppler: Location of intra-orbital vessels:*

- Ophthalmic Artery (OA): (red color)
- Central Retinal Artery: (red color)

(i) *Arterial blood flow velocities (PW Doppler): Doppler spectrum analysis*:

- Place the pulsed Doppler (PW) on the Ophthalmic Artery (OA).
- The PW Doppler allows to obtain the spectral Doppler wave and the flow velocities (MFV/PSV/EDV) of each insonated vessel.

(j) *Interpretation*:

See chapter of neuro-orbital ultrasound.

A greater number of quality scientific papers is needed to achieve stronger evidence for an individualized and accurate applicability with respect to the best cut-off value of ONSD for each population.

14.7.6 Frontal Bone Window Examination

Sometimes, the transtemporal acoustic window (TAW) often fails to measure blood flow velocities in approximately 10–30% of patients. Besides, the TAW is most often inadequate approach to insonate the anterior cerebral artery (ACA), especially A2 segment where the insonate angle is unfavorable. In this scenario, frontal bone window may have the ability to assess ACA velocities in patients admitted to ICU [69–71] (Fig. 14.16).

We suggest the following order for insonation of the Optic Nerve (ON) as a part of TCCS approach:

(a) *Transducer*:

- Low-frequency sector transducer (1.6–3.5 MHz)

(b) *Patient positioning:*

- *Patient*: Supine position with the head aligned with the body and slightly (Head of the bed at 30°)
- *Examiner*: In comfortable position at the patient's side

(c) *Depth*: 13–16 cm

(d) *B-Mode: Insonate brain parenchyma: Paramedian zone*

- Positioned transducer vertically at the paramedian zone
- (Probe mark at the top)
- *Brain Parenchyma Structures*:
- Contralateral skull bone

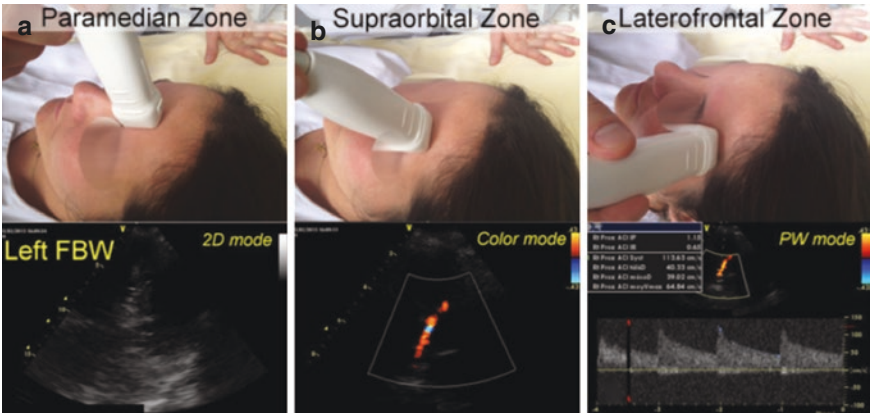

Fig. 14.16 Frontal lobe window approach by TCCS: (**a**) (B-Mode: brain parenchyma) The transducer is positioned vertically at the paramedian frontal zone with probe mark at the top; (**b**) (Color Doppler: A2 segment of the ACA) Rotated the probe 90° outward and shifted horizontally with probe mark laterally to the supraorbital zone at the top of the orbital arcade; (**c**) Pulsed wave Doppler: blood flow velocity using pulsed Doppler. From the supraorbital zone slides laterally to access to the laterofrontal zone. (Modified from Sentenac et al. [69])

- Corpus callosum
- Choroid plexus of the third ventricle
- Cerebellar tentorium

(e) *Color Doppler: Rotated the probe 90° to insonate supra-orbital zone and latero-frontal zone*

- Positioned probe mark laterally
- *Identification*: A1 and A2 segments of ACA (red color)
- *Identification*: Circle of Willis (especially in latero-frontal zone)

(f) *Arterial blood flow velocities (PW Doppler): Doppler spectrum analysis*:

- Place the pulsed wave Doppler (PW) on the anterior cerebral artery (ACA).
- The PW Doppler allows to obtain the spectral Doppler wave and the flow velocities (MFV / PSV / EDV) of each insonated vessel.
- Place the pulsed wave Doppler (PW): Circle of Willis.

14.8 TCCS Protocol: Clinical Applications

The clinical applications of transcranial color-coded duplex sonography (TCCS) include evaluation of the arterial blood flow velocities and their modifications, and evaluation of the parenchymal structures and any abnormalities like hematoma, bleeding, or midline shift [42] (Table 14.2). In the following table, only pathologies relevant to ICU specialists are listed; there are of course other pathologies which can be evaluated with TCCS but non-relevant to our practice.

Table 14.2 Clinical applications of TCCS

Trauma brain injury (TBI)	Non-invasive estimation of ICP CPP estimation through index of pulsatility (IP) Cerebral autoregulation (CA) Cerebrovascular reactivity Vasospasm Middle line shift (MLS)
Subarachnoid hemorrhage (SAH)	Non-invasive estimation of ICP Estimation of CPP Cerebral autoregulation (CAR) Cerebrovascular reactivity Vasospasm Middle line shift (MLS)
Ischemic stroke	Diagnosis. Estimation of CPP Non-invasive estimation of ICP Monitoring of treatment Monitoring of micro-embolism Middle line shift (MLS) Stenosis / occlusion diagnosis

Table 14.2 (continued)

Brain death (BDD)	Brain death diagnosis (BDD)
Intracerebral hemorrhage (ICH)	Non-invasive estimation of ICP Size measurement Middle line shift (MLS)
Preeclampsia	Cerebral autoregulation and flow velocities as a prognosis Non-invasive estimation of ICP
Sickle cell disease	Detection and monitoring
Liver failure	Non-invasive estimation of ICP
A-V malformation	Diagnosis and monitoring
Hydrocephalus	Middle line shift (MLS) Non-invasive estimation of ICP Estimation of the size of ventricles Cerebral autoregulation Cerebrovascular reactivity
Cerebral tumors	Non-invasive estimation of ICP Vasospasm Detection of Intracerebral hematoma. Estimation the size and location of the tumor Middle line shift (MLS)
Right-left cardiac shunt	Evaluation of PFO with microbubbles
Infection of CNS	Non-invasive estimation of ICP Middle line shift (MLS) Detection of Intra-extra-axial collection Detection changes of the cerebral hemodynamic (blood flow velocity)
Carotid surgery	Post-surgical evaluation after endarterectomy or stent placement. (risk of cerebral hypoperfusion or embolism)
ARDS	Non-invasive estimation of ICP Changes in the cerebral perfusion pressure (CPP) and blood flow velocities Cerebral autoregulation
VV-ECMO / VA-ECMO	Non-invasive estimation of ICP Middle line shift (MLS) Cerebral autoregulation Changes in the cerebral perfusion pressure (CPP) and blood flow velocities Detection of Intra-extra-axial collection. Detection of cerebral circulatory arrest
Renal replacement therapy (RRT)	Non-invasive estimation of ICP Cerebral autoregulation Changes in the cerebral perfusion Pressure (CPP) and blood flow velocities Middle line shift (MLS)

Table 14.2 (continued)

NCSE	Non-invasive estimation of ICP Cerebral autoregulation Changes in the cerebral perfusion pressure (CPP) and blood flow velocities Detection of intra-extra-axial space-occupying lesions
Perioperative cardiovascular and aortic counterpulsation balloon	Non-invasive estimation of ICP Cerebral autoregulation Changes in the cerebral perfusion pressure (CPP) and blood flow velocities Detection of Intra-extra-axial collection
Cerebral venous thrombosis (CVT)	Non-invasive estimation of ICP Middle line shift (MLS) Assessment of the cerebral deep venous system and dural sinuses Detection of intra-axial space-occupying lesion
Sepsis	Changes in the cerebral perfusion pressure (CPP) as a risk factor to develop sepsis-associated encephalopathy Non-invasive estimation of ICP

BDD brain death diagnosis, *NCSE* non-convulsive epileptic status, *VV* venous-venous/*VA* veno-arterial, *ARDS* acute respiratory distress syndrome, *CPP* cerebral perfusion pressure, *TCCS* transcranial color-coded duplex sonography [43–51]

14.9 TCCS Protocol: Hemodynamic Parameters

With the use of transcranial color-coded duplex sonography (TCCS), we can obtain information, in real time, about hemodynamic behavior and anatomical distribution of the basal cerebral arteries:

1. Visualize: Access the anatomical landmarks to identify the different basal cerebral arteries to insonate
   (B-Mode and color Doppler).
2. Flow Direction: Identify intracranial anatomical distribution of the basal cerebral arteries and flow direction of each one (Color-coded Doppler).
3. Flow Patterns: Identify the blood flow velocities and spectral Doppler waveform of each insonated basal cerebral artery (PW Doppler) (Table 14.3).

After identifying the vessel to insonate (Color Doppler), the pulsed wave Doppler (PW Doppler) is placed to obtain the signal corresponding to the Doppler spectrum. The hemodynamic parameters derived from the pulsed Doppler are as follows:

(a) Peak Systolic Velocity (PSV)
(b) End-Diastolic Velocity (EDV)
(c) Mean Flow Velocity (MFV)
(d) Pulsatility Index (PI)
(e) Resistance Index (RI)

Table 14.3 Normal velocity values in the basal cerebral arteries [14, 16, 40, 53–60]

Artery	PSV (cm/s)	EDV (cm/s)	MFV (cm/s)
Middle cerebral artery (MCA)	90 ± 16	45 ± 10	62 ± 12
Anterior cerebral artery (ACA)	78 ± 18	35 ± 6	50 ± 15
Posterior cerebral artery (PCA)	53 ± 11	26 ± 7	37 ± 10
Vertebral artery (VA)	40 ± 12	20 ± 5	29 ± 15
Basilar artery (BA)	52 ± 9	31 ± 9	39 ± 9

Table 14.4 Flow direction and waveform

Artery	Flow direction	Spectral waveform
Middle cerebral artery (M1 – M2)	Toward to the probe (red color)	Low resistance
Anterior cerebral artery (A1)	Away from the probe (blue color)	Low resistance
Posterior cerebral artery (P1)	Toward to the probe (red color)	Low resistance
Posterior cerebral artery (P2)	Away from the probe (blue color)	Low resistance
Vertebral artery (VA)	Away from the probe (blue color)	Low resistance
Basilar artery (BA)	Away from the probe (blue color)	Low resistance
Ophthalmic artery (OA)	Toward to the probe (red color)	High resistance

Table 14.5 Normal values of the hemodynamic indexes [54]

Artery	Pulsatility index (PI)
Middle cerebral artery (MCA)	0.9 ± 0.24
Anterior cerebral artery (ACA)	0.83 ± 0.17
Posterior cerebral artery (PCA)	0.88 ± 0.2
Vertebral artery (VA)	0.86 ± 0.08
Basilar artery (BA)	0.86 ± 0.09

As previously stated, if the blood flows toward the probe, it is color-coded red and is positive. On the opposite, if the flow moves away from the probe, it is color-coded blue and is negative (Table 14.4). The shape of the flow curve gives an indication of the system's resistance. If the diastolic velocities are low, the resistances are high, while if the diastolic velocities are high, the resistances are low.

Using the velocities recorded for each vessel, a Pulsatility Index (PI) and Resistance Index (RI) can be calculated (Table 14.5). Only the PI is used in the TCCS analysis and is an indirect indication of the increased intracranial pressure. It is worth noting that the flow rates of intracerebral arterial vessels decrease with the age of the patient. On the contrary, pulsatility increases with the age of the patient [61].

Remember that to obtain a more accurate measurement of the flow velocity, the correction of the insonation angle with the positioning of the pulsed wave spectral Doppler cursor as parallel as possible to the flow is mandatory (< 60°) [62].

14.10 TCCS Protocol: Limitations

The TCCS is not a perfect technique. Many aspects (technical and interpretative) must be considered in order to obtain a reliable examination. Therefore, we should keep in mind operator dependency and a 10–20% of patients having inadequate transtemporal acoustic window.

14.10.1 Limitations

14.10.1.1 Acoustic Windows

The effectiveness of the transcranial color-coded duplex sonography (TCCS) depends on the good penetrance of the ultrasound through the temporal bone and/or through the suboccipital window:

Transtemporal Acoustic Window

There is a 10–30% of patients, in middle age, in which the study cannot be carried out due to the lack of an adequate acoustic window. These values are decreasing as the quality of the TCCS improves. Sometimes, the A2 segment of ACA is not possible insonated. Then, we should elect another acoustic window (Frontal bone window).

Suboccipital Acoustic Window

Sometimes, the anatomical morphology of the vertebro-basilar arterial system is tortuous where the insonation is difficult.

In the cervical syndromes, especially in the spinal cord injury, a neck flexion to access the suboccipital acoustic window to insonate the vertebro-basilar system is not possible. Then, the submandibular acoustic window can be selected.

14.10.1.2 Middle-Line Shift Measurement

This technique allows to measure the midline shift changes at bedside. It is important to keep in mind that a little tilt of the probe may alter the results [63–66]. This ultrasound measure is difficult in case of subdural or epidural hematomas and in clinical situations where the temporal window is temporarily (post-operative) blocked or absent [48, 67].

On the other hand, the hydrocephalus should not alter the measurement [68, 72].

14.10.1.3 Limitations in Specific Clinical Situations

Intra-/Extra-Axial Space-Occupying Lesions: Diagnosis and Monitoring

The TCCS is useful in the diagnosis and monitoring of intra- or extra-axial collections, which can be seen on the B-Mode. In case of subdural and epidural hematoma, a midline shift could be observed. This bedside exam may limit the use of brain CT scan and their repetition. The suspicion of the location of the intra-axial space-occupying lesions is important in determining the usefulness of brain ultrasound. Frontal and parietal collections may be the most difficult to detect.

14.11 Conclusion

The increase of ICU specialists with ultrasound abilities and availability of ultrasound machines in the ICU creates the best condition for a wider use of transcranial color-coded duplex sonography (TCCS). As discussed in this chapter, this technique provides many relevant clinical information at bedside that directly impact the therapeutic strategies in the acute neurological patients. TCCS allows intensivists to provide an immediate evaluation next at patient's bedside (24 hours a day, 7 days a week) in both acute neurological injury (TBI, SAH, etc.) and non-neurological critical pathology (Sepsis, Acute liver failure, ARDS, RRT, etc.). Therefore, it is expected and necessary that the use of the TCCS becomes a very valuable complement in the routine clinical investigations of the intensive care units.

Algorithm

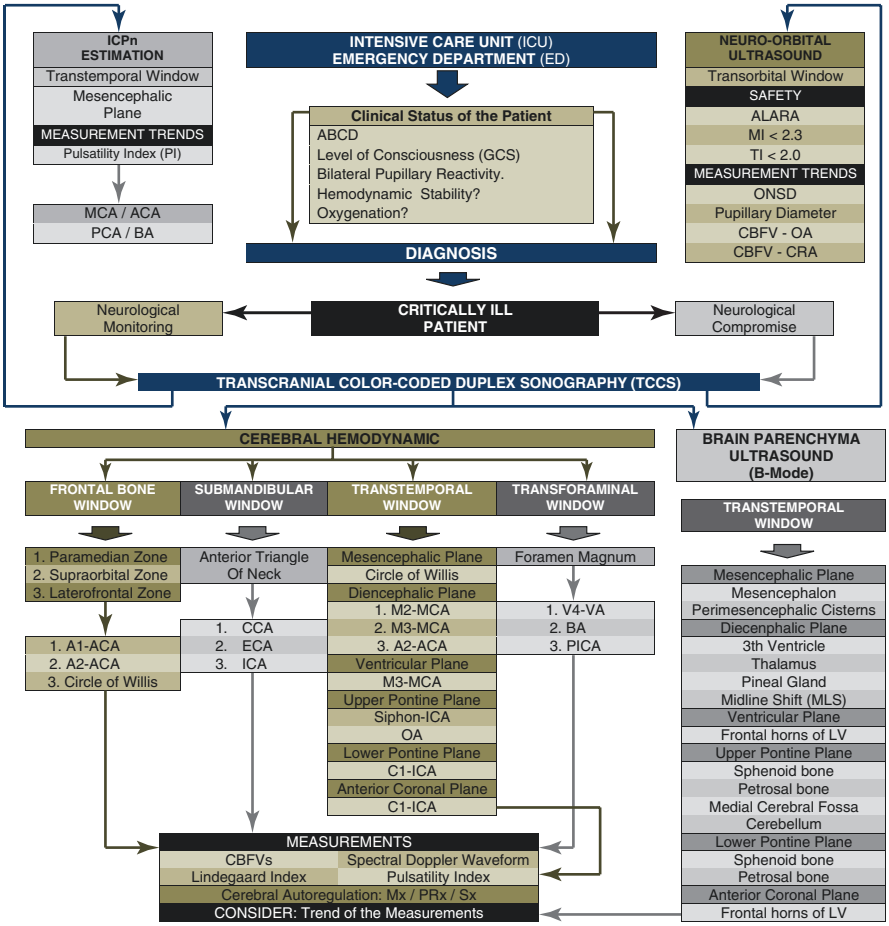

ABCD Airway-breathing-circulation-disability, *GCS* Glasgow coma scale, *FVs* Peak systolic velocity, *FVm* Mean velocity, *MCA* Middle cerebral artery, *ACA* Anterior Cerebral Artery, *PCA* Posterior Cerebral Artery, *BA* Basilar Artery, *VA* Vertebral Artery, *OA* Ophthalmic artery, *ONSD* optic nerve sheath diameter, *CRA* Central retinal artery, *ICPn* Non-invasive intracranial pressure, *CBFV* Cerebral blood flow velocity, *LV* Lateral ventricle, *PICA* Postero-inferior cerebellar artery, *TI* Thermal index, *MI* Mechanical index, *Mx* Mean flow index, *Sx* systolic flow index, *PRx* Pressure reactivity index.

References

1. Arnolds BJ, Von Reutern GM. Transcranial Doppler sonography examination technique and normal reference values. Ultrasound Med Biol. 1986;12:115–23.
2. Aaslid R, Markwalder TM, Nornes H. Noninvasive transcranial Doppler ultrasound recording of fow velocity in basal cerebral arteries. J Neurosurg. 1982;57:769–72.

3. Sloan MA, Alexandrov AV, Tegeler CH, Spence MP, Caplan LR, Feldmann E, et al. Assessment: transcranial Doppler ultrasnongraphy: report of the therapeutics and technology assessment Subcommittee of the American Academy of Neurology. Neurology. 2004;62:1468–81.
4. Bogdahn U, Becker G, Winkler J, Greiner K, Perez J, Meurers B. Transcranial colour-coded sonography in adults. Stroke. 1990;21(12):1680–8.
5. Olatunji RB, et al. Role of Transcraneal colour-coded Duplex sonography in stroke management-review article. West Afr J Ultrasound. 2015;16(1):33–42.
6. Williams, Warwick. Gray's Anatomy, vol. I; 1986. p. 755–762;813–827).Salvat.
7. Hartkamp MJ, et al. Circle of Willis collateral flow investigated by magnetic resonance angiography. Stroke. 1999;30:2671–8.
8. Zhu G, Yuan Q, Yang J, Hock YJ. Experimental study of hemodynamics in the circle of Willis. Biomed Eng. 2015;14(Suppl 1):S10.
9. Hoksbergen AWJ, Legemate DA, Ubbink DT, Jacobs MJHM. Collateral variants in circle of Willis in atherosclerotic population assessed by means of transcranial color-coded duplex sonography. Stroke. 2000;31:1656–60.
10. Kern R, Perren F, Kreisel S, et al. Multiplanar transcranial ultrasound imaging: standards, landmarks and correlation with magnetic resonance imaging. Ultrasound Med Biol. 2005;31:311–5.
11. Walter U. Transcranial sonography of the cerebral parenchyma:update on clinically relevant applications. Pers Med. 2012;1:334–43.
12. Oliveira R, de Oliveira LM, Silva Paiva W, de Sá Malbouisson LM, Teixeira MJ, Bor-Seng-Shu E. Comparison between brain computed tomography scan and transcranial sonography to evaluate third ventricle width, Peri-mesencephalic cistern, and sylvian fissure in traumatic brain-injured patients. Front Neurol. 2017;8:44.
13. Seidel G, Gerriets T, Kaps M, Missler U. Dislocation of the third ventricle due to space-occupying stroke evaluated by transcranial duplex sonography. J Neuroimaging. 1996;6(4):227–30.
14. Caricato A, Mignani V, Bocci MG, Pennisi MA, Sandroni C, Tersali A, et al. Usefulness of transcranial echography in patients with decompressive craniectomy: a comparison with computed tomography scan. Crit Care Med. 2012;40(6):1745–52.
15. Zipper SG, Stolz E. Clinical application of transcranial color-coded dúplex sonography – a review. Eur J Neurol. 2002;9:1–8.
16. AIUM practice guideline for the performance of a transcranial Doppler ultrasound examination for adults and children. American College of Radiology (ACR); Society for Pediatric Radiology (SPR); Society of Radiologists in Ultrasound (SRU). J Ultrasound Med. 2012;31(9):1489–500.
17. Liu D, Kahn M. Measurement and relationship of subarachnoid pressure of the optic nerve to intracranial pressures in fresh cadavers. Am J Ophthalmol. 1993;116(5):548–56.
18. Hayreh SS. Pathogenesis of oedema of the optic disc. Doc Ophthalmol. 1968;24(2):289–411.
19. Newman WD, Hollman AS, Dutton GN, Carachi R. Measurement of optic nerve sheath diameter by ultrasound: a means of detecting acute raised intracranial pressure in hydrocephalus. Br J Ophthalmol. 2002;86(10):1109–13.
20. Helmke K, Burdelski M, Hansen HC. Detection and monitoring of intracranial pressure dysregulation in liver failure by ultrasound. Transplantation. 2000;70(2):392–5.
21. Geeraerts T, Launey Y, Martin L, Pottecher J, Vigué B, Duranteau J, et al. Ultrasonography of the optic nerve sheath may be useful for detecting raised intracranial pressure after severe brain injury. Intensive Care Med. 2007;33(10):1704–11.
22. Bartels E. Transcranial color-coded duplex ultrasonography in routine cerebrovascular diagnostics. Pers Med. 2012;1:325–30.
23. Bartels E, Fuchs H-H, Flugel KA. Color Doppler imaging of basal cerebral arteries. Examination technique and normal reference values. Angiology. 1995;10:844–77.
24. Geeraerts T, Thome W, Tanaka S, Leblanc PE, Duranteau J, Vigué B. An alternative ultrasonographic approach to assess basilar artery flow. Neurosurgery. 2011;68(2 Suppl Operative):276–81.
25. Kim MJ, et al. Technical essentials of hepatic Doppler sonography. Curr Probl Diagn Radiol. 2009;38:53–60.

26. Giller CA. Is angle correction correct? J Neuroimaging. 1994;4:51–2.
27. Krejza J, Mariak Z, Babikian VL. Importance of angle correction in the measurement of blood flow velocity with transcranial Doppler sonography. AJNR Am J Neuroradiol. 2001;22(9):1743–7.
28. Bartels E. Color – coded Duplex ultrasonography of the cerebral vessels: atlas and manual. Stuttgart: Schattauer; 1999.
29. Nedelmann M, Stolz E, Gerriets T, et al. Consensus recommendations for transcranial color-coded dúplex sonography for the assessment of intracranial arteries in clinical trials in acute stroke. Stroke. 2009;40:3238–44.
30. Stolz E. Ultrasound examination techniques of extra – and intracranial veins. Pers Med. 2012;1:366–70.
31. Bartels E. The axial imaging plane-the main domain of the transcranial color-coded duplex ultrasonography? Eur J Ultrasound. 2002;16:47–57.
32. Becker G, Lindner A, Bogdahn U. Imaging of the vertebro-basilar system by transcranial colour-coded real-time sonography. J Ultrasound Med. 1993;12:395–401.
33. Stolz E, Nückel M, Mendes I, Gerriets T, Kaps M. Vertebrobasilar transcranial colour-coded duplex ultrasonography: improvement with echo enhancement. Am J Neuroradiol. 2002;23:1051–4.
34. Becker G, Lindner A, Bogdahn U. Imaging of the vertebrobasilar system by transcranial colour-coded real-time sonography. J Ultrasound Med. 1993;12:395–401.
35. Schöning M, Walter J. Evaluation of the Vertebrobasilar-posterior system by transcranial color duplex sonography in adults. Stroke. 1992;23:1280–6.
36. Geeraerts T, Thome W, Tanaka S, Leblanc PE, Duranteau J, Vigué B. An alternative ultrasonographic approach to assess basilar artery flow. Neurosurgery. 2011;68(2 Suppl Operative):276–81.
37. Alexandrov AV, Sloan MA, Wong LK, Douville C, Razumovsky AY, Koroshetz WJ, et al. American Society of Neuroimaging Practice Guidelines Committee Practice standards for transcranial Doppler ultrasound: part I—test performance. J Neuroimaging. 2007;17(1):11–8.
38. Csiba L, Baracchini C. Manual of neurosonology. Chapter 2A. Cambridge; 2016.
39. Christopher H. Optic nerve sheath diameter ultrasound and the diagnosis of increased intracranial pressure. Crit Care Nurs Clin N Am. 2016;28:95–9.
40. Ertl M, Barinka F, Torka E, et al. Ocular color-coded sonography – a promising tool for neurologists and intensive cara physicians. Ultraschall Med. 2014;35:422–31.
41. Bäuerle J. Nedelmann M.B-mode sonography of the optic nerve in neurological disorders with altered intracranial pressure. Pers Med. 2012;1:404–7.
42. Abadal JM, Llompart-Pou JA, Homar J, Pérez-Bárcena J, Ibáñez J. Applications of transcranial color-coded duplex sonography in monitoring neurocritical patients. Med Intensiva. 2007;31(9):510.
43. Kavi T, Esch M, Rinsky B, Rosengart A, Lahiri S. Transcranial Doppler changes in patients treated with extracorporeal membrane oxygenation. J Stroke Cerebrovasc Dis. 2016;25(12):2882–5.
44. Pierrakos C, Antoine A, Velissaris D, Michaux I, Bulpa P, Evrard P, et al. Transcranial Doppler assessment of cerebral per- fusion in critically ill septic patients: a pilot study. Ann Intensive Care. 2013;3:28.
45. Joshi B, Ono M, Brown C, Brady K, Easley RB, Yenokyan G, et al. Predicting the limits of cerebral autoregulation during car- diopulmonary bypass. Anesth Analg. 2012;114(3):503–10.
46. Rasulo FA, De Peri E, Lavinio A. Transcranial Doppler ultrasonography in intensive care. Eur J Anaesthesiol. 2008;25(S42):167–73.
47. Rasulo FA, Bertuetti R, Robba C, Lusenti F, Cantoni A, Bernini M, et al. The accuracy of transcranial Doppler in excluding intracranial hypertension following acute brain injury: a multicenter prospective pilot study. Crit Care. 2017;21(1):44.
48. Moppett IK. Transcranial Doppler ultrasonography in anaesthesia and intensive care. Br J Anaesth. 2004;93(5):710–24.

49. Motuel J, Biette I, Srairi M, Mrozek S, Kurrek MM, Chaynes P, et al. Assessment of brain midline shift using sonography in neurosurgical ICU patients. Crit Care. 2014;18(6):676.
50. Naqvi J, Yap KH, Ahmad G, Ghosh J. Transcranial Doppler ultra- sound: a review of the physical principles and major applications in critical care. Int J Vasc Med. 2013;2013:629378.
51. Saqqur M, Zygun D, Demchuk A. Role of transcranial Doppler in neurocritical care. Crit Care Med. 2007;35(5):S216–23.
52. Blanco P, Abdo-Cuza A. Transcranial Doppler ultrasound in the ICU: it is not all sunshine and rainbows. Crit Ultrasound J. 2018;10:2.
53. Schöning M, Buchholz R, Walter J. Comparative study of transcranial color duplex sonography and transcranial Doppler sonography in adults. J Neurosurg. 1993;78:776–84.
54. Rigamonti A, Ackery A, Baker AJ. Transcranial Doppler monitoring in subarachnoid hemorrhage: a critical tool in critical care. Can J Anaesth. 2008;55:112–23.
55. Schöning M, Walter J. Evaluation of the vertebrobasilar-posterior system by transcranial color duplex sonography in adults. Stroke. 1992;23:1280–6.
56. D'Andrea A. Transcranial Doppler ultrasonography: from methodology to major clinical applications. World J Cardiol. 2016;8(7):383–400.
57. Schöning M, Niemann G, Hartig B. Transcranial color duplex sonography of basal cerebral arteries: reference data of flow velocities from childhood to adulthood. Neuropediatrics. 1996;27:249–55.
58. Blanco P, Blaivas M. Applications of transcranial color-coded sonography in the emergency department. J Ultrasound Med. 2017;36:1251–66.
59. Aaslid R, Markwalder TM, Nornes H. Noninvasive transcranial Doppler ultrasound recording of flow velocity in basal cerebral arteries. Neurosurgery. 1982;57:769–74.
60. Babikian VL, Wechsler LR, Toole JF. Transcranial Doppler ultrasonography. 2nd ed. Butterworth Heinemannn; 1999.
61. Grolimund P, Seiler RW. Age dependence of the flow velocity in the basal cerebral arteries:a transcranial Doppler ultrasound study. Ultrasound Med Biol. 1988;14:191–8.
62. Bartels E, Flügel KA. Quantitative measurements of blood flow velocity in basal cerebral arteries with transcranial color Doppler imaging. J Neuroimag. 1994;4:77–81.
63. Wu TY, Sharma G, Strbian D, et al. Natural history of perihematomal edema and impact on outcome after intracerebral hemorrhage. Stroke. 2017;48(4):873–9.
64. Kiphuth IC, Huttner HB, Struffert T, et al. Sonographic moni- toring of ventricle enlargement in posthemorrhagic hydrocephalus. Neurology. 2011;76:858–62.
65. Llompart Pou JA, Abadal Centellas JM, Palmer Sans M, et al. Moni- toring midline shift by transcranial color-coded sonography in traumatic brain injury. A comparison with cranial computerized tomography. Intensive Care Med. 2004;30:1672–5.
66. Tang SC, Huang SJ, Jeng JS, et al. Third ventricule evidence shift due to spontaneous supratentorial intracerebral hemorrhage evaluated by transcranial color-coded sonography. J Ultrasound Med. 2006;25:203–9.
67. White H, Venkatesh B. Applications of transcranial Doppler in the ICU: a review. Intensive Care Med. 2006;32(7):981–94.
68. Lau VI, Arntfield RT. Point-of-care transcranial Doppler by intensivists. Crit Ultrasound J. 2017;9:21.
69. Sentenac P, et al. The frontal bone window for transcranial Doppler ultrasonography in critically ill patients: validation of a new approach in the ICU. Neurocrit Care. 2020;33(1):115–23.
70. Yoshimura S. Frontal bone window improves the ability of transcranial color-coded sonography to visualize the anterior cerebral artery of Asian patients with stroke. AJNR Am J Neuroradiol. 2009;30:1268–9.
71. Stolz E, Kaps M, Kern A, Dorndorf W. Frontal bone windows for transcranial color-coded duplex sonography. Stroke. 1999;30:814–20.
72. Lau VI, Jaidka A, Wiskar K, Packer N, Tang JE, Koenig S, et al. Better with ultrasound: transcranial Doppler. Chest. 2020;157(1):142–50.

Chapter 15
Transcranial Color-Coded Duplex Sonography (TCCS): Importance of Angle Correction

Piergiorgio Lochner, Antonio Siniscalchi, and Andrea Naldi

Key Points

1. Angle correction can be performed by TCCS, allowing a more real measurement of cerebral vessels' flow velocity compared to not angle-corrected ones.
2. TCCS angle-corrected velocity is proportional but not equal to the true velocity.
3. Angle correction should be performed when the Doppler sample volume identifies a sufficient straight vessel segment (at least 15 mm in length) in order to ensure a correct assessment.
4. Angle correction should be performed when the angle between the ultrasonic beam and the vessel is small, in other way be likely to produce significant errors.
5. The angle-corrected velocity with TCCS is significantly higher as compared to the uncorrected velocity of the same system or to conventional TCD.

15.1 Introduction

Based on the Doppler equation (Eq. 15.1)

$$\Delta F = \left(2v \bullet F \bullet \cos\alpha\right) / c \tag{15.1}$$

P. Lochner (✉)
Department of Neurology, Saarland University Medical Center, Homburg, Germany
e-mail: piergiorgio.lochner@uks.eu

A. Siniscalchi
Department of Neurology and Stroke Unit, Annunziata Hospital, Cosenza, Italy

A. Naldi
Department of Neuroscience Rita Levi Montalcini, University of Turin, Turin, Italy

C. N. Rodríguez et al. (eds.), *Neurosonology in Critical Care*,
https://doi.org/10.1007/978-3-030-81419-9_15

where ΔF is the Doppler shift, F is the frequency of incident wave, and c is the propagation speed. Flow velocity (v) of a target vessel depends on the cosine of the angle (α) between the ultrasonic beam and blood flow (Fig. 15.1).

Thus, in ideal circumstances, if the ultrasound (US) beam is parallel to flow direction (angle $\alpha = 0$), the cos $\alpha = 1$ and flow velocity will correspond to reality. On contrary, when the US beam is perpendicular to flow direction (angle $\alpha = 90°$), the cos $\alpha = 0$, resulting in a weak receiving signal and false flow velocity. Therefore, one of the most important limiting factors for the estimation of correct blood flow velocity is represented by the angle of insonation. The impact of the angle insonation on flow velocities is relatively low in a range of 0–30°, and it is still considered acceptable until 60°. On contrary, angle >60° generates large variation in the cosine used for the correction, resulting in significant errors of measurements [1] (Fig. 15.2).

Moreover, we should keep in mind that the arteries of circle of Willis can have a different angle of insonation of ultrasound and angle of vessel. In 10%, the insonation angle of anterior cerebral artery (ACA) is more than 40° and in 33% the angle of posterior cerebral artery (PCA) is between 31° and 40° [2].

Two techniques are currently available for the assessment of intracranial vessel flow velocity: transcranial Doppler (TCD) (Fig. 15.3) and transcranial color-coded duplex sonography (TCCS).

In conventional TCD, the identification of cerebral arteries is based on the position of transducer, flow direction, and insonation depth. Introduced since the 80s, this technique was also defined as "blind sonography," because it does not allow a direct visualization of brain vessels. Even if the insonation angle is uncertain, it is assumed to be 0 degree, or anyway small enough (range 0–30°) to not determine significant errors of measurements [3, 4]. On this basis, normative values of intracranial arteries blood velocity have been proposed and widely used (Table 15.1).

On the other hand, the more recent TCCS allows the combination of B-mode and color Doppler imaging, permitting the real-time visualization of parenchymal

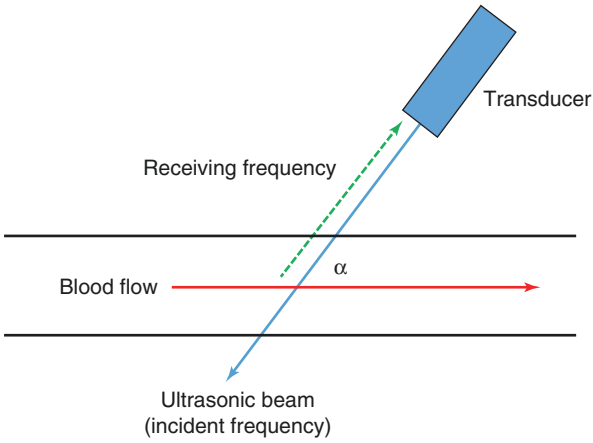

Fig. 15.1 The alpha angle (α) of the Doppler equation is determined by the intersection between the incident frequency emitted by the ultrasound transducer and the direction of blood flow

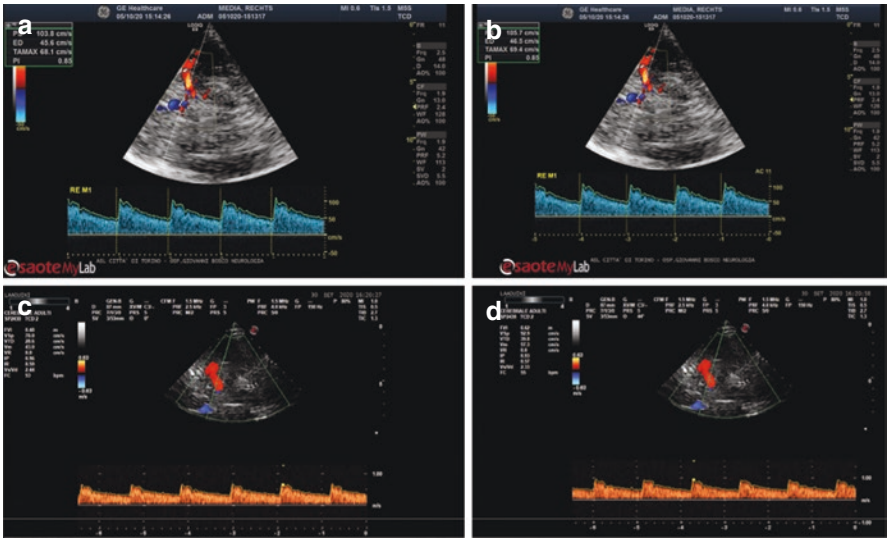

Fig. 15.2 TCCS findings obtained by transtemporal insonation with axial scanning plane of middle cerebral artery. (**a**) Example without and (**b**) with angle correction of 11°. The absence of significant velocity variations is remarkable. Conversely, if the angle correction is increased: (**c**) Flow velocity without angle correction: peak systolic velocity = 70 cm/s, end diastolic velocity = 28.6 cm/s, mean velocity = 43 cm/s. (**d**) the same insonation frame like C with angle correction (46°): peak systolic velocity = 92.9 cm/s, end diastolic velocity = 39.8 cm/s, mean velocity = 57.3 cm/s. Flow measurements are higher than not corrected ones. Note the regular flow pattern, reflecting laminar flow of blood cells

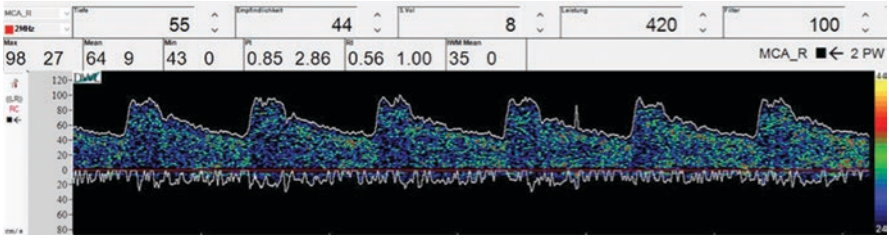

Fig. 15.3 Example of transcranial Doppler (TCD) using pulsed Doppler system operating at 2 MHz emitting frequency showing the velocity parameters of middle cerebral artery

structures and intracranial vessels, as well as their anatomical course. The two modalities consent to an easier identification and allocation of blood flow in specific intracranial vessel segments and the possibility for image-based angle correction. However, angle-corrected flow velocity may be affected by the geometry of intracranial vessels that may reduce the accuracy of flow measurements, particularly in case of vessel tortuosity or irregularities. In fact, at the level of a tortuous artery, the direction of blood flow may be turbulent or helical rather than laminar, indeed not corresponding to the arterial axis included in the sample volume in analysis [1].

Table 15.1 Reports of flow values in intracranial cerebral arteries of healthy adults using TCD and TCCS

	TCCS without angle correction	TCCS with angle correction	Doppler	Doppler	
Author	Eicke [3]			Hennerici [13]	
PY	1994			1987	
Number	15			50	
Age	Range 23-37			40-60	
RMCA	57.3/93.1[a]	66.4/107.7	60.4/95.7	MCA 50 mm)	91.0 ± 16.9[b] 44.3–9.5
LMCA	50.6/82.7	60.2/97.4	53.6/86.0	ACA (70) mm)	86.4–20.1 4 1–7.4
RACA	48.2/80.0	55.8/92.8	48.4/77.1	PCA (60 mm)	60.1–20.6I 28.7–7. 511
LACA	43.2/70.2	56.6/91.4	49.1/76.6	VA/BA (75 tom)	59.5_17.0 29.2–8.4
RPCA	35.2/55.6	38.42/60.7	33.8/53.7		
LPCA	34.4/54.2	40.5/63.9	33.8/52.6		

Abbreviations: *MCA* middle cerebral artery, *ACA* anterior cerebral artery, *lo-A* posterior cerebral artery, *VA* vertebral artery, *BA* basilar artery, nn s .,*R* right, *L* left

[a]temporal averaged// peak systolic velocities in cerebral basal arteries (cm/sec)

[b]Normal Age-Adjusted Calculated Mean - SD Values of TC-Doppler Flow Velocity within the Basal Cerebral Arteries as Recorded from Selected Reference Points (systolic and diastolic peak velocity cm/sec

Thus, a sufficient length of the insonated vessel (1–2 cm) is required in order to ensure a correct assessment of flow velocity, because it more likely may reproduce the laminar pattern. However, TCCS allows the evaluation of cerebral vessels on several planes (axial and coronal), reducing—at least in part—the issue of non-uniform vessel course.

Due to these considerations, angle-corrected velocity may be more easily applied to certain cerebral vessels such as middle cerebral arteries (MCA) or segments of other intracranial vessels if they appear well visible in their length.

Comparative studies between the two methods have shown that the insonation angle of intracranial vessel was often greater than expected [3–5]. As a result, flow velocities of cerebral arteries were different when measured with TCD or TCCS, being significantly higher by using TCCS angle correction. Similar results have been obtained comparing TCCS uncorrected and angle-corrected velocities. These findings suggest that different normative values should be used, based on the applied technique, and that TCCS should be preferred when a sufficiently long segment of the target vessel can be visualized, because it reduces the inaccuracy in flow measurements [6]. In addition, the AC measurements are repeatable with no differences in intrarater or interrater reproducibility as compared to uncorrected ones [7]. Table 15.1 shows comparison of the two methods, with their relative values.

15.2 Clinical Applications

15.2.1 Intracranial Stenosis

Intracranial stenosis is caused from 3 up to 10% of all ischemic strokes, depending on races. They mostly affect the first segment of MCA, but potentially all vessels may be involved, representing an independent risk factor for stroke. Through TCCS technique, Baumgartner et al. assessed and defined ≥50% and <50% of basal cerebral narrowing of intracranial stenosis, compared with the gold standard digital subtraction angiography. Based on the above prerequisite, TCCS-AC criteria were able to detect all 31 of ≥50% intracranial stenosis with 1 false-positive, and 35 of 38 <50% stenosis with 3 false-positives. The positive predictive value was 100% for ≥50% intracranial stenosis, and the negative predictive value was 91% to 100% [8].

Due to the fact that AC velocity is greater than not-AC ones, the importance of AC becomes clear in order to correctly identify potential acceleration of flow due to intracranial stenosis [9]. Globally, it has been shown that AC allows defining diagnostic criteria with a higher sensitivity to detect intracranial stenosis [6]. An adequate AC may precisely define a hemodynamic stenosis and can result in therapeutic changes for secondary prevention of symptomatic intracranial stenosis with an intensive medical therapy (Fig. 15.4).

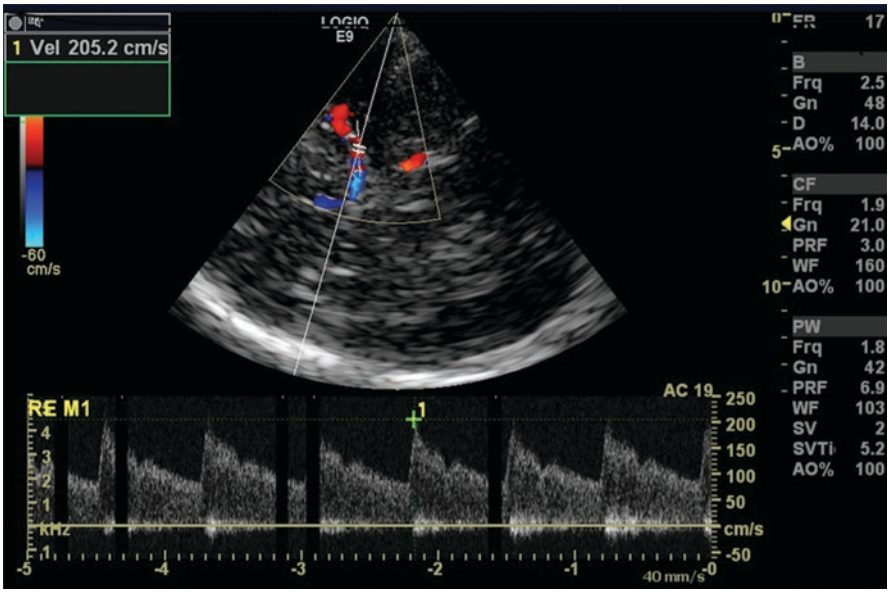

Fig. 15.4 TCCS findings obtained by transtemporal insonation with axial scanning plane in a patient with intracranial stenosis of the middle cerebral artery (about 50%). Spectral analysis shows an increased angle-corrected velocity and high-intensity low frequency signals

15.2.2 Cerebral Vasospasm

Cerebral vasospasm is a severe complication of subarachnoid hemorrhage and often presents from 7 to 21 days after the symptoms onset. The condition is related to a diffuse constriction of cerebral arteries, causing a remarkable increase of flow velocity usually involving multiple vessels, most often well detectable on the MCA. Based on the recorded velocity, a grading of severity of vasospasm using TCD is available [10], emphasizing the impact of a clear estimation of flow velocity, for both the detection of vasospasm and monitoring its evolution.

A meta-analysis by Mastantuono et al. evaluated the accuracy of TCD and TCCS for the diagnosis of cerebral vasospasm of the MCA. Both the techniques were able to detect it, but neither were useful to exclude it [11]. However, a moderate but not significant superiority of TCCS was detected, requiring further investigation.

In this context, AC measurements of flow velocity at MCA level are likely to be fundamental, also because early increases in velocity may be a predictor for delayed cerebral ischemia, resulting crucial for changing in the therapeutic approach.

15.2.3 Cerebral Veins

Intracranial venous system hemodynamic can be assessed with both TCD and TCCS. However, because of the great anatomical variability of cerebral veins and sinuses, the direct visualization of the vessel provided by TCCS may help for a correct identification of the target structure. Some of the systematic reports of flow values in intracranial veins of healthy adults using TCD and TCCS are provided in Table 15.2. There are no visible changes in the flow velocity of the venous circulation with the angle correction, with the exception of a significant change of flow velocity in straight sinus and transverse sinus.

15.3 Conclusion

TCCS may be of aid in overcoming the difficulties related to the wide anatomic variations of cerebral vessels and reducing the inaccuracy in flow velocity measurements by ensuring angle-corrected imaging-guided values. Advantages and limitations of angle-corrected measurements should be considered in order to allow the definition of diagnostic criteria for different vascular clinical conditions.

Table 15.2 Reports of flow values in intracranial veins of healthy adults using TCD and TCCS with and without angle correction

	TCD	TCCD	
Author	Valdueza [15]	Baumgartner without angle correction [12][a]	Stolz with angle correction [14][b]
PY	1996	1997	1999
Number	60	120	75
Age	42 ± 15	60 ± 18	46 ± 17
DMCV	11.1 ± 2.7	10, 7	8.5 ± 2.9 8.7 ± 1.9
BV	10.1 ± 2.3	13, 9	12.4 ± 4.0 8.9 ± 3.0
SRS	n.r.	26,17	13.1 ± 5.1 9.4 ± 4.0
TS	n.r.	32,21	14.9 ± 6.7 10.4 ± 5.3

BV basal vein of RosenthaI, *DMCV* deep middle cerebral vein, *n.r* not reported, *number* number of the studied subjects, *PY* publication year, age presented as mean ± Standard deviation in years (if available). *SRS* straight sinus, *TS* transverse sinus.
Mean flow velocity values presented as mean ± Standard deviation in cm/s.)
[a]Peak systolic and end-diastolic flow velocity values (not angle corrected) presented as mean± standard deviation in cm/s (if available)
[b]Peak systolic and end-diastolic flow velocity values (angle corrected) presented as mean± standard deviation in cm/s (if available)

References

1. Giller CA. Is angle correction correct? J Neuroimaging. 1994;4(1):51–2.
2. Fujioka KA, Gates DT, Spencer MP. A comparison of transcranialcolor Doppler imaging and standard static pulsed wave Doppler inthe assessment of intracranial hemodynamics. J Vasc Tech. 1994;18:29–35.
3. Eicke BM, Tegeler CH, Dalley G, Myers LG. Angle correction in transcranial Doppler sonography. J Neuroimaging. 1994;4(1):29–33.
4. Bartels E, Flügel KA. Quantitative measurements of blood flow velocity in basal cerebral arteries with transcranial duplex color-flow imaging. A comparative study with conventional transcranial Doppler sonography. J Neuroimaging. 1994;4(2):77–81.
5. Barrientos-Guerra JD, Flores-Silva F, Cantú-Brito C, Chiquete E. Evaluation of cerebral hemodynamics with color-coded duplex sonography: normative values with correction of insonation angles. J Stroke Cerebrovasc Dis. 2020;29(3):104595.
6. Nedelmann M, Stolz E, Gerriets T, Baumgartner RW, Malferrari G, Seidel G, et al. TCCS Consensus Group. Consensus recommendations for transcranial color-coded duplex sonography for the assessment of intracranial arteries in clinical trials on acute stroke. Stroke. 2009;40(10):3238–44.
7. Baumgartner RW, Mathis J, Sturzenegger M, Mattle HP. A validation study on the intraobserver reproducibility of transcranial color-coded duplex sonography velocity measurements. Ultrasound Med Biol. 1994;20:233–7.
8. Baumgartner RW, Mattle HP, Schroth G. Assessment of >/=50% and <50% intracranial stenoses by transcranial color-coded duplex sonography. Stroke. 1999;30(1):87–92.

9. Krejza J, Mariak Z, Babikian VL. Importance of angle correction in the measurement of blood flow velocity with transcranial Doppler sonography. AJNR Am J Neuroradiol. 2001;22(9):1743–7.
10. Samagh N, Bhagat H, Jangra K. Monitoring cerebral vasospasm: how much can we rely on transcranial Doppler. J Anaesthesiol Clin Pharmacol. 2019;35(1):12–8.
11. Mastantuono JM, Combescure C, Elia N, Tramèr MR, Lysakowski C. Transcranial Doppler in the diagnosis of cerebral vasospasm: an updated meta-analysis. Crit Care Med. 2018;46(10):1665–72.
12. Baumgartner RW, Gönner F, Arnold M, Müri RM. Transtemporal power- and frequency-based color-coded duplex sonography of cerebral veins and sinuses. AJNR Am J Neuroradiol. 1997;18(9):1771–81.
13. Hennerici M, Rautenberg W, Sitzer G, Schwartz A. Transcranial Doppler ultrasound for the assessment of intracranial arterial flow velocity--part 1. Examination technique and normal values. Surg Neurol. 1987;27(5):439–48.
14. Stolz E, Kaps M, Dorndorf W. Assessment of intracranial venous hemodynamics in normal individuals and patients with cerebral venous thrombosis. Stroke. 1999;30(1):70–5.
15. Valdueza JM, Schmierer K, Mehraein S, Einhäupl KM. Assessment of normal flow velocity in basal cerebral veins. A transcranial doppler ultrasound study. Stroke. 1996;27(7):1221–5.

Chapter 16
Neurocritical Care Monitoring in ICU: Measurement of the Cerebral Autoregulation by Transcranial Doppler (TCD)

Leanne A. Calviello and Marek Czosnyka

Key Points

1. Transcranial Doppler ultrasonography (TCD) is a simple tool that can be used to image the middle cerebral artery (MCA) after traumatic brain injury (TBI).
2. TCD measures cerebral blood flow velocity (CBFV) through the MCA and can alert clinicians to both structural and dynamic irregularities of cerebral vessels resultant from pathology. This information is vital to assessments of cerebral autoregulation, a balance between blood pressure and blood flow, that can be compromised by TBI.
3. TCD devices can be utilized in conjunction with pre-existing bedside monitors and can be connected to computerized data collection systems, such as ICM+ (Cambridge Enterprise, Ltd.).
4. Analysis of TCD-based data facilitates patient outcome prediction, with some parameters such as the autoregulation index (ARI) and the mean flow velocity index (Mx) acting as established surrogate indicators of either favorable or unfavorable clinical outcome.
5. Although TCD is both inexpensive and portable, the technique suffers from a lack of inter-operator validity and a reliance on intermittent monitoring sessions.

L. A. Calviello
Division of Neurosurgery, Department of Clinical Neurosciences, Cambridge Biomedical Campus, University of Cambridge, Cambridge, UK

M. Czosnyka (✉)
Department of Clinical Neurosciences, Cambridge Biomedical Campus, University of Cambridge, Cambridge, UK
e-mail: mc141@medschl.cam.ac.uk

C. N. Rodríguez et al. (eds.), *Neurosonology in Critical Care*,
https://doi.org/10.1007/978-3-030-81419-9_16

16.1 Introduction

Cerebral autoregulation (CA) is a delicate balance between cerebral arterial blood pressure and blood flow [1]. It is a protective mechanism for the brain that enables it to withstand dynamic changes; however, traumatic brain injury (TBI) often disrupts this process and leaves the brain in a state of "dysautoregulation" that can prove fatal if left untreated. TBI is commonly attributed to events such as blunt force, falls, or motor vehicle accidents that result in a decrease or loss in consciousness, memory deficit, or neurological and/or mental state alterations such as weakness or disorientation [2]. Moderate to severe TBI cases are generally easier to diagnose with imaging techniques such as magnetic resonance imaging (MRI) and computed tomography than are mild TBI cases, but standard scoring criteria for both cannot be determined as absolute predictors of the damage sustained by the cerebral autoregulatory reserve following the initial insult [3]. Where does this leave clinicians, if it is impossible to quantify a patient's cerebral autoregulation by the results of a radiological examination? Most importantly, what does this mean for the patient?

To provide the greatest and the most reliable amount of clinical information, neurocritical care professionals have increasingly been focusing their attention on non-invasive, bedside multi-modal brain monitoring in conjunction with traditional imaging techniques. One of, if not the most, popular methods of non-invasively assessing cerebral autoregulation comes in the form of transcranial Doppler ultrasonography (TCD). TCD evaluates irregularities or obstructions in cerebral blood flow after TBI; it is applied to the middle cerebral artery (MCA), which is considered the primary conduit for the cerebral circulatory system and is assumed to have a constant diameter [1]. Ultrasonic penetration of the MCA returns a pulse wave spectrum that can be immediately visually classified as either normal or abnormal (i.e., vasospastic [4]) and can be further analyzed to provide more in-depth prognostic information about the state of cerebral autoregulation.

16.2 TCD: As a Technique

TCD is the most validated technique for non-invasively measuring the blood flowing through cerebral arteries [1, 5–12]. The "traditional" TCD instrument used in neurocritical care centers features a headframe, supporting bilateral 2 MHz probes that are fixed onto the temporal window (located above the zygomatic arch) in order to insonate the MCA [13]. Once in place, an ultrasonic beam is transmitted that penetrates the skull, commonly at a depth of 50–60 mm, to return the Doppler spectra from the artery on accompanying software [14] (Fig. 16.1). This waveform demonstrates the systolic, mean, and diastolic values of the cerebral blood flow velocity

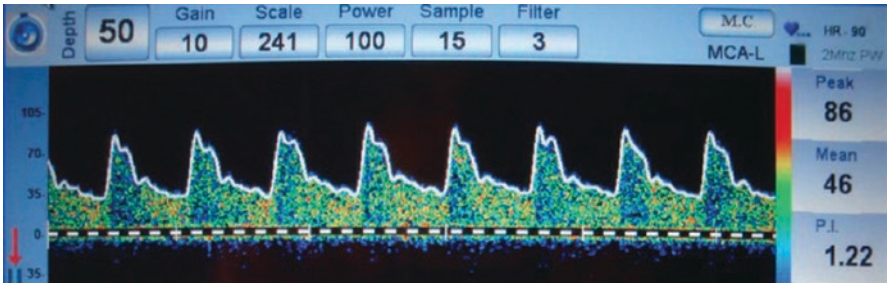

Fig. 16.1 Transcranial Doppler waveform showing the middle cerebral artery (MCA), identified by the characteristic tracing in the upward direction. (Courtesy: Marda and Prabhakar [15])

(CBFV), which can be further examined individually in detailed studies of outcome prediction [12]. CBFV in healthy subjects has been previously determined to perfuse at a rate of 62 ± 12 cm/s and was found to be nearly symmetrical between the left and the right branches of the MCA [14].

TCD/TCCS can be highly instrumental in the prediction of secondary insults and/or complications of TBI. For example, TCD-based CBFV can be indicative of vasospasm (the narrowing of a vessel accompanied by MCA mean flow velocity (MFV) > 120 cm/s) following subarachnoid hemorrhage [4]. Routine monitoring sessions are undertaken daily for an average duration of about 30 minutes. TCD devices can be connected to bedside monitors that provide invasively quantified clinical information, such as arterial blood pressure (ABP), intracranial pressure (ICP), and cerebral perfusion pressure (CPP, the calculated difference between ABP and ICP).

16.3 TCD: As a Clinical Informant

In addition to CBFV, TCD yields several descriptive parameters that paint a broader picture of prognosis. TCD-based CBFV can be compared against readily available clinical information from bedside monitors (i.e., ABP, ICP, CPP, etc.) to provide distinctive correlational assessments of surrogate markers of CA, such as the pressure reactivity index (PRx) or the mean flow velocity index (Mx) within ICM+[1]. The dynamic autoregulation index (ARI) demonstrates the interactions between non-invasive TCD and standard invasively quantified measurements to produce a graded score of cerebral autoregulation. Analyses of these parameters are increasingly becoming a part of clinical practice and represent the patient's autoregulatory reserve at any observed time point.

16.3.1 Autoregulation Index (ARI)

The concept of creating a holistic TCD-based autoregulatory index was first developed by Aaslid et al. [16] to assess the dynamic changes in cerebral autoregulation that occur following step changes in CPP. By manipulating ABP in decrements of 20 mmHg via thigh-cuff deflation, the rapid physiological response (or lack thereof) of the cerebral blood supply to these fluctuations in ABP is examined as a predictor of autoregulatory capacity. This experimental setup was revisited by Tiecks et al. [17], who collected CBFV and ABP values following the thigh-cuff release to calculate a graded reference index (ARI—the index of autoregulation) that would describe the cerebrovascular resistance as a function of ABP. ARI effectively answers the question of whether cerebral blood flow moderates itself appropriately when ABP varies.

The validity of ARI to mirror dynamic changes in cerebral autoregulation was further examined by Panerai et al. [18] via Monte Carlo simulations that mimed random input and output signals of both CBFV and ABP over a 5-minute interval. As transfer function analysis is crucial to the calculation of ARI, the strength of the index is tied to its spectral components [18, 19]. ARI's utility to gauge patient outcome is limited if the recorded signals have a low signal-to-noise ratio. For each harmonic, the amount of output power that can be linearly explained by the input power is expressed by the squared coherence function. A coherence of 1 for pure, univariate systems is indicative of high signal-to-noise ratio, whereas a coherence at or near 0 represents the latter [18, 19]. The phase shift between the Fourier components of both the input and the output signals reflects the "interdependence" of CBFV and ABP, with a positive phase shift (optimally 90°) revealing the presence of an intact, non-passive autoregulatory reserve [19–21]. When applied to the Glasgow Outcome Score (GOS), a higher ARI is compatible with GOS 1 or 2 (favorable outcome), whereas a lower ARI implies the converse, GOS 3–5 (unfavorable outcome) [19]. However, ARI is less sensitive when discriminating scores along the lower end of its 0–9 scale and is largely dependent on how accurately the template model [17, 22] matches the individual physiological events captured by TCD and ABP monitors.

16.3.2 Mean Flow Velocity Index (Mx)

The mean flow velocity index (Mx) is derived from the linear correlation coefficient between MFV and CPP [23, 24]; this marker of cerebral autoregulation is fundamentally dependent on non-invasive TCD monitoring data as opposed to invasive parameters (i.e., ABP and ICP). A central tenet to the success of Mx as a surrogate for the autoregulatory reserve is the assumption that the diameter of the MCA remains constant, which has yet to be either proven or disproven [24]. As the first 48 hours of admission are crucial to the recovery of autoregulation after TBI [1],

TCD and subsequently Mx can assess this rather easily; values of Mx less than or equal to 0 are representative of an intact autoregulatory reserve in which CBFV actively responds to changes in CPP, whereas positive Mx trends state the opposite [23], which provides an example of a patient with disturbed autoregulation, as assessed with Mx.

However, the time-domain calculation of Mx itself does not rely entirely on non-invasive data collection to express autoregulatory reserve; once again, CPP is the difference between ABP and ICP, making Mx somewhat dependent on ICP fluctuations as a result. Lang et al. [11] attempted to attain Mx with two separate input signals: CPP and ABP, the latter rendering the parameter to be quantifiable with non-invasive measures. Although possible to use, Mx determined from ABP is not as sensitive as Mx determined from CPP [19]. Continuing the search for an entirely non-invasive Mx function, Budohoski et al. [12] cited correlations between the systolic (Sx), diastolic (Dx), and mean (Mx) components of the CBFV waveform when using the input signals of either ABP or CPP. Separate analyses yielded the same result: Mx calculated with CPP is the superior predictor of functional patient outcome [1, 12].

16.4 TCD: Benefits and Limitations

TCD/TCCS is an important tool to have in neurocritical care units. It is inexpensive, portable, and relatively simple to use once trained in how to do so. TCD examinations are as accurate as MRI when assessing vascular pathology [9] and do not require patients to be moved to imaging suites. Additionally, TCD devices can be paired with clinical monitoring software such as ICM+ (Cambridge Enterprise, Ltd.) to return pertinent information about a TBI patient's state of cerebral autoregulation that cannot be gleaned from bedside monitors. Without TCD and dedicated analytical platforms such as ICM+, mortality and functional outcome could not be determined on the basis of one or two functions (ARI is a more robust predictor of mortality than Mx is more sensitive to functional outcome [19, 23, 25]). The benefit of both ARI and Mx is that they assign scalar value to cerebral autoregulation to the "weighted spatial averages as seen from the aspect of the MCA" [26] when employing the TCD monitoring technique.

Although there is a shortage of "autoregulation markers" [5], the above surrogates (ARI, Mx) can technically be monitored continuously, as their respective values can be repeatedly calculated over any specified time period during the patient's neuro-intensive care stay. Therefore, ARI and Mx can be reported in the same fashion as ABP and ICP. Despite this important point, TCD and thus its derived parameters are only intermittently affixed to the patients (<1 hour) due to the relative "clumsiness" and potential disruptiveness of the instrument to routine nursing interventions (i.e., turning the patient, preparing the patient for an X-ray or scan, etc.). TCD is primarily viewed as a research tool and is treated as an accessory to the patient; for example, it is nearly impossible to retain a stable probe position if a

patient is being re-positioned or examined, as nurses are not obligated to be vigilant over the TCD recording session itself. TCD's time dependence only permits clinicians to receive "snapshots" of cerebral hemodynamic activity [1]. Another drawback of TCD is its reliance on operator validity [10]; even experienced technicians may not agree on the probe placement, depth of the MCA, etc. If the diameter of the MCA were ever to be proven variant, the core of TCD monitoring technology and thus its credibility would be undermined.

16.5 Conclusion

TCD monitoring is entirely non-invasive and allows unique insight into cerebral hemodynamics, particularly through the MCA. The activity within the MCA is central to the brain's ability to balance pressure and flow load demands that can be altered by TBI. Although limited by time and technicalities related to its operation, TCD remains a popular tool in neurocritical care centers due to its ability to provide surrogate markers of cerebral autoregulation.

References

1. Calviello LA, Donnelly J, Zeiler FA, Thelin EP, Smielewski P, Czosnyka M. Cerebral autoregulation monitoring in acute traumatic brain injury: what's the evidence? Minerva Anestesiol. 2017;83(8):844–57.
2. Menon DK, Schwab K, Wright DW, Maas AI. Position statement: definition of traumatic brain injury. Arch Phys Med Rehabil. 2010;91(11):1637–40.
3. Zeiler FA, Donnelly J, Nourallah B, Thelin EP, Calviello L, Smieleweski P, et al. Intra- and extra-cranial injury burden as drivers of impaired cerebrovascular reactivity in traumatic brain injury. J Neurotrauma. 2018;35(14):1569–77.
4. Budohoski KP, Czosnyka M, Kirkpatrick PJ, Smielewski P, Steiner LA, Pickard JD. Clinical relevance of cerebral autoregulation following subarachnoid haemorrhage. Nat Rev Neurol. 2013;9(3):152–63.
5. Czosnyka M, Miller C. Monitoring of cerebral autoregulation. Neurocrit Care. 2014;21:95–102.
6. Sorrentino E, Budohoski KP, Kasprowicz M, Smielewski P, Matta B, Pickard JD, et al. Critical thresholds for transcranial doppler indices of cerebral autoregulation in traumatic brain injury. Neurocrit Care. 2011;14(2):188–93.
7. Cecil S, Chen PM, Callaway SE, Rowland SM, Adler DE, Chen JW. Traumatic brain injury advanced multimodal neuromonitoring from theory to clinical practice. Crit Care Nurse. 2011;31(2):25–36.
8. Donnelly J, Aries MJ, Czosnyka M. Further understanding of cerebral autoregulation at the bedside: possible implications for future therapy. Expert Rev Neurother. 2015;15(2):169–85.
9. Panerai RB, Jara JL, Saeed NP, Horsfield MA, Robinson T. Dynamic cerebral autoregulation following acute ischemic stroke: comparison of transcranial Doppler and magnetic resonance imaging techniques. J Cereb Blood Flow Metab. 2015;36:2194–202.
10. Minciotti P, Ceravolo MG, Provinciali L. Inter-examiner variability of transcranial Doppler procedure and reports: a multicenter survey. Italian Transcranial Doppler Group. Ital J Neurol Sci [Internet]. 1997;18(1):21–30.

11. Lang EW, Lagopoulos J, Griffith J, Yip K, Mudaliar Y, Mehdorn HM, et al. Noninvasive cerebrovascular autoregulation assessment in traumatic brain injury: validation and utility. J Neurotrauma. 2003;20(1):69–75.
12. Budohoski KP, Reinhard M, Aries MJH, Czosnyka Z, Smielewski P, Pickard JD, et al. Monitoring cerebral autoregulation after head injury. Which component of transcranial Doppler flow velocity is optimal? Neurocrit Care. 2012;17(2):211–8.
13. De Riva N, Budohoski KP, Smielewski P, Kasprowicz M, Zweifel C, Steiner LA, et al. Transcranial doppler pulsatility index: what it is and what it isn't. Neurocrit Care. 2012;17(1):58–66.
14. Aaslid R, Markwalder T-M, Nornes H. Noninvasive transcranial Doppler ultrasound recording of flow velocity in basal cerebral arteries. J Neurosurg. 1982;57(6):769–74.
15. Marda M, Prabhakar H. Transcranial Doppler. J Neuroanaesth Crit Care. 2015;2(3):215–20.
16. Aaslid R, Lindegaard KF, Sorteberg W, Nornes H. Cerebral autoregulation dynamics in humans. Stroke. 1989;20(1):45–52.
17. Tiecks FP, Lam AM, Aaslid R, Newell DW. Comparison of static and dynamic cerebral autoregulation measurements. Stroke. 1995;26(6):1014–9.
18. Panerai RB, Haunton VJ, Hanby MF, Salinet ASM, Robinson TG. Statistical criteria for estimation of the cerebral autoregulation index (ARI) at rest. Physiol Meas. 2016;37(5):661–72.
19. Liu X, Czosnyka M, Donnelly J, Budohoski KP, Varsos GV, Nasr N, et al. Comparison of frequency and time domain methods of assessment of cerebral autoregulation in traumatic brain injury. J Cereb Blood Flow Metab. 2015;35(2):248–56.
20. Latka M, Turalska M, Glaubic-Latka M, Kolodziej W, Latka D, West BJ. Phase dynamics in cerebral autoregulation. Am J Physiol Heart Circ Physiol. 2005;289:2227–9.
21. Diehl RR, Linden D, Lucke D, Berlit P. Phase relationship between cerebral blood flow velocity and blood pressure: a clinical test of autoregulation. Stroke. 1995;26(10):1801–4.
22. Elting JW, Maurits NM, Aries MJH. Variability of the autoregulation index decreases after removing the effect of the very low frequency band. Med Eng Phys. 2014;41(1):11–7.
23. Czosnyka M, Smielewski P, Kirkpatrick P, Laing RJ, Menon D, Pickard JD. Continuous assessment of the cerebral vasomotor reactivity in head injury. Neurosurgery. 1997;41(1):11–7.
24. Hlatky R, Furuya Y, Valadka AB, Gonzalez J, Chacko A, Mizutani Y, et al. Dynamic autoregulatory response after severe head injury. J Neurosurg. 2002;97(5):1054–61.
25. Schmidt B, Reinhard M, Lezaic V, McLeod DD, Weinhold M, Mattes H, et al. Autoregulation monitoring and outcome prediction in neurocritical care patients: does one index fit all? J Clin Monit Comput. 2016;30(3):367–75.
26. Czosnyka M, Smielewski P, Lavinio A, Pickard JD, Panerai R. An assessment of dynamic autoregulation from spontaneous fluctuations of cerebral blood flow velocity: a comparison of two models, index of autoregulation and mean flow index. Anesth Analg. 2008;106(1):234–9.

Chapter 17
Neuro-ICU: Cerebral Hemodynamics and Transcranial Doppler (TCD/TCCS) Waveform Interpretation in the Most Common Neurocritical Pathologies

L. Luciano Ponce Mejia, Bahattin B. Ergin, and Lucía Rivera Lara

Key Points

1. Adequate brain function requires sufficient, uninterrupted blood flow. Thus, fast-acting mechanisms are needed to restore blood flow when it drops acutely. Cerebrovascular reactivity is the ability of vascular smooth muscle to change basal tone in response to variations in physiologic parameters, such as arterial blood pressure (ABP), and metabolic factors, such as cerebral carbon dioxide and oxygen levels.
2. The flow velocity decreases as it reaches small vessel branches. Local diminished vessel diameter (i.e., vasoconstriction) results in a dramatic acceleration in blood flow velocity and a decrease in the pressure. This phenomenon is governed by Bernoulli's principle, described by Daniel Bernoulli in 1738.
3. Only around 50% of the population has a classic configuration of the circle of Willis [1]. Stenotic segments are found in more than 25% of people [2]. When the degree of proximal vessel stenosis in the ICA is severe, the blood flow is largely dependent on the collateral vessels. Such collateral circulation tends to be more effective within the circle of Willis because ECA-ICA anastomotic vessels are very small and narrow and therefore generate significant resistance.

L. L. P. Mejia
Departments of Neurology, The Johns Hopkins University School of Medicine, Baltimore, MD, USA

B. B. Ergin
Anesthesiology & Critical Care Medicine, The Johns Hopkins University School of Medicine, Baltimore, MD, USA
e-mail: bergin1@jhmi.edu

L. Rivera Lara (✉)
Department of Neurology, Anesthesiology and Critical Care Medicine, The Johns Hopkins School of Medicine, Baltimore, MD, USA
e-mail: lriver14@jhmi.edu

C. N. Rodríguez et al. (eds.), *Neurosonology in Critical Care*,
https://doi.org/10.1007/978-3-030-81419-9_17

4. The spectral waveform of blood flow velocity can be used to evaluate resistance to the flow. High-resistance vascular beds are characterized by a waveform with a sharp upstroke accompanied by a relatively abrupt waning in velocity immediately after peak systole with low end-diastolic velocity. Low-resistance waveforms are characterized by a steadier upstroke, a more gradual decline, and a higher end-diastolic velocity. The cerebral vascular bed is a low-resistance bed. Changes in the resistance, as detected by spectral waveform analysis, can be secondary to local stenosis or to the effects of proximal or distal disease within the insonated vascular bed.
5. The Lindegaard ratio (LR) tends to increase in relation to the degree of vasospasm. Normal reference range is from 1.1 to 2.3 and in the absence of vasospasm is <3.

17.1 Introduction

Transcranial Doppler (TCD) has gained popularity among physicians because it is a quick, inexpensive, and noninvasive way to evaluate blood flow in the basal cerebral arteries. The applications of TCD in the neurologically or neurosurgically critically ill patient include vasospasm screening in those with aneurysmal subarachnoid hemorrhage (aSAH) or traumatic brain injury (TBI), detection of embolism after transient ischemic attack or cerebrovascular accident, and evaluation of total cerebral circulatory arrest in those with brain death. TCD has also been used for estimating cerebral autoregulation and cerebrovascular reactivity and for detecting abnormally high intracranial pressure (ICP).

Interpreting the findings of TCD requires an understanding of cerebral hemodynamic principles. Cerebral hemodynamics is influenced by a complicated interaction among various factors in critically ill patients, namely, (1) mean arterial blood pressure (MAP), (2) ICP, (3) blood viscosity, (4) degree of proximal vessel stenosis, (5) vessel caliber, (6) degree of collateral circulation, and (7) integrity of cerebral autoregulation. In this chapter, we will review the physiology of cerebral hemodynamics and focus on TCD waveform interpretation.

17.2 Cerebral Blood Flow (CBF) and Cerebral Perfusion Pressure (CPP)

The CPP is equivalent to MAP minus the ICP. The drive to generate blood flow through the cerebral arteries, branches, and capillaries is produced in the left ventricle and maintained by the elastic properties of the aorta and extracranial arteries (common carotid artery [CCA] and internal carotid artery [ICA]), resulting in a pulsatile forward pressure. Although the venous blood pressure cannot be

discounted, its hemodynamics are far more complex. Often the intracranial venous pressure does not equal the central venous pressure, especially under pathological conditions when an increase in the ICP leads to collapse of the vein wall and a resulting change in flow resistance. Some authors have proposed to use instead of the venous sinus blood pressure (vSBP) because the venous sinuses do not collapse when the ICP rises above that of the vSBP [3]. Nevertheless, the veins that drain into the cerebral sinuses (bridging veins) do collapse when ICP increases, isolating the cerebral venous sinus pressure, an indication that vSBP matches ICP.

17.2.1 Cerebrovascular Resistance (CVR)

CVR is maintained mainly by small arteries, resistance vessels, capillaries, and venules. It has been defined as in Eq. 17.1. This special pressure–flow relationship is known as Starling resistance, which was first described in 1912 [4]. The flow in collapsible systems that allows us to define vSBP as equal to ICP has also been described in detail [5–7]. Microinvasive methods show a significant descent in pressure from distributing arteries (about 90 mmHg) to the arterioles (<30 mmHg) [8].

$$\mathrm{CVR} = \mathrm{CPP} / \mathrm{CBF} \tag{17.1}$$

In 1838, using tubes of fine bore in a series of experiments, Jean Leonard Marie Poiseuille (1797–1869) established that flow is inversely proportional to the length of the tube and directly proportional to the pressure gradient and to the fourth power of the tube diameter, the now famed Law of Poiseuille (Eq. 17.2):

$$\mathbf{D}P = 8.\mathrm{m.L.Q} / \mathrm{p.R}^4 \tag{17.2}$$

where ΔP is the pressure difference between the two ends, L is the length of tube (vessel), μ is the dynamic viscosity (hematocrit), Q is the volumetric flow rate (flow velocity), and R is the radius of the vessel. Notably, the radius of the cerebral vessels decreases distally and changes according to physiologic and pathophysiologic states. Consequently, the quantitative use of the Law of Poiseuille is limited. Also, the blood viscosity is non-Newtonian because it is proportional to the velocity of flow. One useful lesson deduced from the Law of Poiseuille is that a modest change in vessel diameter induces a dramatic increase in flow resistance.

17.2.2 Cerebral Autoregulation

Adequate brain function requires sufficient, uninterrupted blood flow. Thus, fast-acting mechanisms are needed to restore blood flow when it drops acutely. Cerebrovascular reactivity is the ability of vascular smooth muscle to change basal

tone in response to variations in physiologic parameters, such as arterial blood pressure, and metabolic factors, such as cerebral carbon dioxide and oxygen levels [9]. Cerebral autoregulation is one aspect of cerebrovascular reactivity that involves vascular tone changes in response to fluctuations in arterial blood pressure [10]. The first studies of cerebral autoregulation showed that in a normal physiologic state, CBF remains constant when MAP fluctuates within 50–150 mmHg margin [11]. Modern multimodal monitoring techniques of cerebral autoregulation and cerebrovascular reactivity have shown that the cerebral autoregulation plateau may be much narrower. In a study of adults with acute subarachnoid hemorrhage, the cerebral autoregulatory plateau was found to be 80–120 mmHg [12]. Adjustments of CVR are responsible for maintaining a constant CBF. Thus, CBF is not disturbed by modest degrees of stenosis or spasm of proximal vessels. The resistance vessels dilate yielding a lower CVR, which in turn restores CBF [13]. Conversely, a sudden increase in CPP (i.e., MAP) that threatens the integrity of the fragile cerebral capillaries results in rapid vasoconstriction of the proximal resistance vessels to avoid high transmural pressures. Evidently, more complex and slow metabolic adaptations occur in response to abrupt changes in CPP in addition to the fast-myogenic response [14–18].

17.2.3 Determination of Cerebrovascular Reactivity Via TCD

In a study of dogs, a 20–25 mmHg change in systemic blood pressure produced only a 2.5% change in diameter of the coronary arteries, thanks to their relative stiffness [19]. Cerebral arteries have similar properties. A mean change in blood pressure of 30 ± 16 mmHg and a change in end-tidal CO_2 ($EtCO_2$) of 14 ± 6 mmHg resulted in a mean diameter change in the large cerebral arteries (carotid, middle cerebral artery [MCA], vertebral artery) of less than 4%, but the smaller arteries (anterior cerebral artery, M2 segment of MCA) showed diameter changes as large as 29% to $ETCO_2$ changes and 21% to blood pressure changes [20, 21]. Hence, as the diameter of the large vessels is relatively stable to changes in blood pressure and CO_2, one can assume that the CBF is proportional to the CBF velocity (CBFV). Such changes in CBFV can be measured using TCD technology. Under this premise, CBFV approximates CBF [22]. Cerebrovascular reactivity can be calculated clinically, with the most common methods being (1) dose-controlled CO_2 inhalation, (2) acetazolamide injection, and (3) breath-holding index [23–25].

17.2.4 Carbon Dioxide Reactivity

Changes in the partial pressure of CO_2 (PCO_2) cause changes in CVR because CO_2 affects the degree of vasodilation of the smaller vessels responsible for regulating CVR. However, the effect of PCO_2 on basal cerebral artery diameter is insignificant.

By measuring $EtCO_2$ in normal subjects, Markwalder et al. [26] established that flow velocity in the MCA changes 3.4 ± 0.5% per each mmHg change in $EtCO_2$. According to the Poiseuille equation, a change in flow resistance of 3–4% is attained by approximately 1% change in vessel caliber in the resistance vessels. Cerebrovascular reactivity in the neurocritical intensive care unit will be reviewed extensively in a different chapter.

17.3 Physiology of Blood Vessel Stenosis

The flow velocity decreases as it reaches small vessel branches. Local diminished vessel diameter (i.e., vasoconstriction) results in a dramatic acceleration in blood flow and a decrease in the pressure. This phenomenon is governed by Bernoulli's principle, described by Daniel Bernoulli in 1738. It states that pressure and velocity in a moving fluid have an inverse proportional relationship [27]. Energy is involved in accelerating the fluid. Energy is transformed from static energy, namely, pressure, into kinetic energy during acceleration. Such transformation of energy is derived from Bernoulli's equation (Eq. 17.3):

$$P_2 - P_1 = \mathrm{DP½}r\left(V_2^2 - V_1^2\right) \tag{17.3}$$

where ΔP is the pressure difference between the two points with velocities V_1 and V_2, respectively, and ρ is the density of blood.

The energy is lost, or rather transformed, in turbulence distal to the stenosis. Note that Bernoulli's principle takes into consideration the density (viscosity) of the blood. A higher viscosity (hematocrit) results in a higher ΔP. In the brain, there are basically three pathological conditions that can affect blood flow acceleration: (1) large- and mid-size stenosis due to atherosclerotic disease of the extra- and intracranial arteries, (2) vasospasm (i.e., subarachnoid hemorrhage), and (3) narrowed congenital communicating vessels in the circle of Willis (anterior and posterior communicating arteries).

17.3.1 Evaluation of Intracranial Stenosis by TCD

Using Doppler ultrasound technology to evaluate atherosclerotic disease resulting in stenosis of the CCA bifurcation predates TCD [28]. The development of TCD technology with a transorbital approach of the carotid siphon made possible the evaluation of intracranial stenotic disease with an overall accuracy of 88%, a 95% specificity, and a 73% sensitivity when compared to angiography [29]. The transtemporal and suboccipital approaches were later described with a correlation coefficient of 0.89 ($p = 0.0001$) [30, 31]. A proposed model of unilateral carotid artery

stenosis suggests that for a severe unilateral stenosis of the right carotid artery, the partial pressure of oxygen in the brain area at risk can be restored only if the corresponding cerebral resistance is significantly decreased and if the circle of Willis is complete [32]. Another report showed no preoperative difference in number of intracerebral arteries with reverse flow between symptomatic and asymptomatic patients with severe unilateral carotid stenosis. In contrast, pulsatility index, cerebrovascular reactivity, and flow acceleration on the side of stenosis were significantly lower in symptomatic patients. After surgery, all TCD parameters improved significantly in both symptomatic and asymptomatic patients [33]. The Doppler findings showed increased flow velocity at the site of stenosis, a decrease in velocity with a dampened waveform distally, and at least a 20–30 mmHg pressure loss. This phenomenon has a parabolic relationship. Stenotic atherosclerotic lesions have obvious hemodynamic effects. The inverse correlation of low velocity obtained by TCD as a function of lumen dimension has been reported in patients with intracranial artery disease when the measurements of diameter were corrected by angiography [34]. Such inverse correlation findings appear to deviate less in atherosclerotic disease than in vasospasm.

17.3.2 Collateral Flow

Only around 50% of the population has a classic configuration of the circle of Willis [1]. Stenotic segments are found in more than 25% of people [2]. When the degree of proximal vessel stenosis in the ICA is severe, the blood flow is largely dependent on the collateral vessels. Such collateral circulation tends to be more effective within the circle of Willis, because ECA-ICA anastomotic vessels are very small and narrow and therefore generate significant resistance. Variability in the pressure of the various collateral connecting vessels (stumps) in the circle of Willis has been reported to be high, ranging from as low as 10 mmHg to almost equating the systemic blood pressure [35]. The resistance to flow in a given collateral connection is determined by vessel diameter, length, and viscosity. The effect of the circle of Willis configuration on cerebrovascular hemodynamics and the distribution of flow appears to be highly variable from individual to individual [36, 37]. Consequently, studying its influence is very difficult [38–40]. One of the most common noninvasive TCD techniques used to assess collateral flow within circle segments uses carotid compression [41]. Because blood volume is directly proportional to flow velocity, common carotid compression measures its effect on blood flow velocity in the ipsilateral posterior cerebral artery and contralateral anterior cerebral artery. Thus, this test shows that the communicating arteries are open and to what degree. The presence of chronic atherosclerotic lesion and its effect on flow velocity in the circle of Willis has also been studied. Researchers have shown increased, reversed, and crossover flow in the different compensating vessels ipsilateral and contralateral to the atherosclerotic lesion, sometimes greater than 1.5

times the velocity in the ipsilateral MCA when the extracranial ICA occlusion reached about 90% [30, 34].

17.3.3 Elastic Reservoir ("Windkessel Effect")

It is important to remember that the properties described so far (resistance, turbulence, etc.) and their effects on flow apply only to a model with a static pressure–flow relationship. However, the pulsatile nature of the pressure in extra- and intracranial vessels results in a dynamic pressure–flow relationship because these vessels are elastic. The most important dynamic relationship is known as the "Windkessel" effect. The Windkessel model described by Otto Frank [42, 43] defines the hemodynamics of the arterial system in terms of resistance and compliance. It describes the aortic pressure decline during diastole but not entirely so during systole. Impedance was proposed as a third component of the Windkessel model. The heart ejects blood intermittently; however, the flow is more continuous as the blood pressure pulsates because the elasticity of the arterial system acts as a reservoir of the energy supplied during systole, thus making the system more efficient. This model can then predict the classic shape of the flow waveform seen in a pulsatile system [42, 43]. Windkessel is roughly translated from German to English as "air chamber," drawing the analogy with the air chamber used in fire engines in the eighteenth century [44]. CBF waveforms obtained by TCD are consistent with low-resistance flow, which changes in pathological states. The Windkessel model is a lumped model and therefore not appropriate for the evaluation of wave travel, but it is a fair approximation of ventricular afterload.

Compliance (C) is the ability of a vessel to distend and increase volume with increasing transmural pressure or the tendency to resist recoil toward its original dimensions on application of a distending or compressing force. It is defined as (Eq. 17.4)

$$C = \Delta V / \Delta P \tag{17.4}$$

The following are scenarios in which the effect of compliance markedly affects the flow velocity waveform. (1) Proximal stenosis resulting in a dampened velocity waveform [34, 45]. The *Windkessel* effect produces a more smoothed waveform because of the increased inflow resistance. (2) Size and amount of arteriovenous malformation feeders. Because arteriovenous malformations have high volume stiffness and very low flow resistance, they result in a dampened waveform. (3) Hypocapnia results in increased flow velocity pulsatility [26]. Low PCO_2 leads to vasoconstriction that increases resistance, revealing the Windkessel effect. (4) Pathological ICP elevation also results in a very pulsatile waveform [46]. Two factors have been proposed to explain this phenomenon. First, the pulsatility of the CPP increases with increasing ICP, and second, the total volume compliance increases so that more blood is required in systole to fill the "Windkessel."

The interaction between the profile of the waveform and the total parallel resistance of stenotic and/or collateral vessel is rather intricate [34, 45]. The waveform changes when the pulsatile wave travels through an arterial narrowing with significant flow resistance. This reduces the sensitivity of the pulsatility index (PI) (Eq. 17.5). Its sensitivity is again augmented when PI is normalized by dividing the observed PI by a reference PI (PI_{ref}). The pulsatility transmission index can be calculated as PI/PI_{ref}.

$$PI = \left[PSV - EDV\right] / MFV \tag{17.5}$$

17.4 TCD: Waveform Interpretation

The feasibility of using TCD technology to measure CBFV in the basal arteries of the brain's anterior circulation was first demonstrated in the early 1980s in 50 healthy subjects [41, 47]. It was then proposed that TCD could be used to monitor vasospasm in aSAH and cerebrovascular disease, when using a Doppler operating at a lower range (1–2 MHz). Instruments operating at higher ranges (typically 5–10 MHz) were used to evaluate extracranial vessels, and they do not penetrate the skull. Before this, ultrasound technology had been used to examine CBF, but only intraoperatively during craniotomies.

TCD technology has been used in the clinical evaluation of cerebral autoregulatory reserve, and different indices have been proposed to study cerebral hemodynamics. The indices include those that are "static," which require artificially increasing or decreasing blood pressure using intravenous vasopressors or vasodilators in steady-state conditions (static cerebral autoregulation), and those that are "dynamic," which measure the cerebrovascular hemodynamic response to interventions such as changes in arterial CO_2/pH, rapid pneumatic thigh cuff deflation, or transient carotid occlusion (e.g., autoregulatory index, transient hyperemic response ratio). The third category has been created to describe more advanced methods, wherein CBFV calculated from TCD is used to derive a third variable (e.g., noninvasive ICP, critical closing pressure).

Current practices in the neurocritical care unit do not routinely include maneuvers to challenge the injured brain to measure its autoregulatory response, mainly because that type of testing may require the patient to be cooperative (e.g., squatting) or because the safety remains debatable (e.g., carotid compression). It has been proposed that cerebral autoregulation be estimated by measuring it from spontaneous variations of MAP [48]. Transform function analysis is a mathematical representation in frequency domain of a system between input and output data and has emerged as a technology suiting this purpose. The effect of oscillations in

MAP over CBFV can be studied by recording a series of times as input and output of the system. This has been done in a range of frequencies, and it is attained by employing a Fast Fourier Transformation (FFT) [49]. Typically, oscillation frequencies are separated into three bands: low (<0.07 Hz), intermediate (0.07–0.3 Hz), and high (>0.3 Hz), although the limits vary among authors [47]. The behavior of the system interprets cerebral autoregulation as a high-pass filter based on three parameters: coherence, gain, and phase shift [48]. At high frequencies, (1) the oscillations of CBFV follow those of ABP, so coherence (which is simply a correlation coefficient within defined frequency range) is high; (2) these parameters oscillate almost synchronously, so the phase lag between them is near zero degrees (low phase shift); and (3) the ABP oscillations are transmitted undampened to the output (CBFV), so gain (amplitude) is usually >1. The opposite occurs toward the low-frequency band, with low coherence and gain and higher phase shift values. That is the way cerebral autoregulation is believed to exert its effect in the lower band of frequencies. This type of response is expected from a physiologic point of view, as vascular tone takes a few seconds to adjust to changes in ABP. To apply transform function analysis, researchers have proposed using CBFV and ABP time series monitoring for at least 10 minutes. Module of coherence varies between 0 and 1, from good to impaired cerebral autoregulation. Phase shift varies between 0 and 90 degrees, from nonexistent to effective cerebral autoregulation. Lower gain means adequate cerebral autoregulation and higher gain means poor cerebral autoregulation.

Currently available software uses proprietary algorithms to obtain different indices. Such numbers can be altered from physiologic changes (e.g., vessel caliber) but also by FFT size (number of points used), FFT length (time), FFT transformation overlap (%), transmitted ultrasound frequency (MHz), high-pass filter settings (Hz), and recording time (minutes). Standard settings have not been universally agreed upon. Nonetheless, cerebral autoregulation studies with TCD always rely on the assumption that MCA diameter does not change during the monitoring time. Another consideration to keep in mind is that CBF is measured in units of ml/min/100 g, whereas TCD technology provides CBF velocity (CBFV) in units of cm/s. There is a positive correlation between the absolute increase in CBF obtained by regional CBF with single-photon emission computed tomography and the increase in CBF velocity by TCD after acetazolamide administration (modest correlation $r = 0.63$, $p < 0.01$) [50, 51]. These results suggest that TCD combined with acetazolamide test may be used in clinical situations to assess cerebral vasoreactivity.

The major advantages of TCD are that it is noninvasive, has remarkable temporal resolution (~5 ms), and is highly reproducible (~5% variability). Some have called TCD “a stethoscope for the brain.” Disadvantages include the lack of temporal window in up to 10% of patients and the fact that continuous monitoring of TCD is very sensitive to movement.

17.4.1 TCD Waveforms

The spectral waveform of blood flow velocity can be used to evaluate resistance to the flow. High-resistance vascular beds are characterized by a waveform with a sharp upstroke accompanied by a relatively abrupt waning in velocity immediately after peak systole with low end-diastolic velocity. Low-resistance waveforms are characterized by a steadier upstroke, a more gradual decline, and a higher end-diastolic velocity. The cerebral vascular bed is a low-resistance bed. Changes in the resistance, as detected by spectral waveform analysis, can be secondary to local stenosis or to the effects of proximal or distal disease within the insonated vascular bed [52].

The TCD waveform of flow is represented by blood flow velocity over time during the cardiac cycle. The sonographer must recognize a waveform pattern visually by its appearance on the screen as well as by the sound of the flow signal. Sonographers must annotate the machine settings, including (1) transducer and sample volume (gate) positioning, (2) flow direction, (3) angle of insonation, (4) scale settings, and (5) sweep speed. Then, the different components of the cardiac cycle are identified, namely, (1) beginning of systole, (2) peak velocity during systole, (3) dicrotic notch (signifying the closure of the aortic valve), (4) end-diastolic velocity, and (5) shape and magnitude of flow deceleration during the cardiac cycle.

The crucial aspects to waveform presentation are the identification of the following components: (1) early systolic upstroke (slow, sharp, or delayed); (2) late systolic and diastolic deceleration (uninterrupted, stepwise, or smoothed); (3) waveform shape (flat, sharpened, or dampened); (4) systolic—diastolic velocity difference (flow pulsatility); and (5) other components of the Doppler spectra (embolism, bruit, narrowing, etc.). Normal waveforms exhibit sharp systolic flow acceleration and stepwise deceleration with positive end-diastolic flow. Additionally, end-diastolic flow velocity falls between 20% and 50% of the peak systolic velocity values (low resistance). Finally, at the level of the ICA bifurcation, a bidirectional signal with simultaneous sharp systolic upstrokes and similar stepwise deceleration in both flow directions denotes low-resistance flow patterns.

The flow velocity in a blood vessel is roughly parabolic in shape, with the fastest velocity in the center of the vessel. Consequently, the Doppler spectrum represents a distribution of velocities that requires mathematical calculations to derive useful velocity values. Normally, a power spectrum distribution is produced from segments of about 2–5 seconds using an FFT, and maximum or mean velocity is calculated from the maximum or intensity-weighted mean, respectively [53] (Fig. 17.1).

Modern TCD ultrasonographic instruments that are currently available use computer-based statistical pattern recognition systems developed for the analysis of the spectral waveforms. The various indices obtained from such wave analysis are as follows:

$$\text{Systolic Acceleration Rate}\left(\text{SAR}\right) = \frac{\text{Height}}{\text{Rise time}}$$

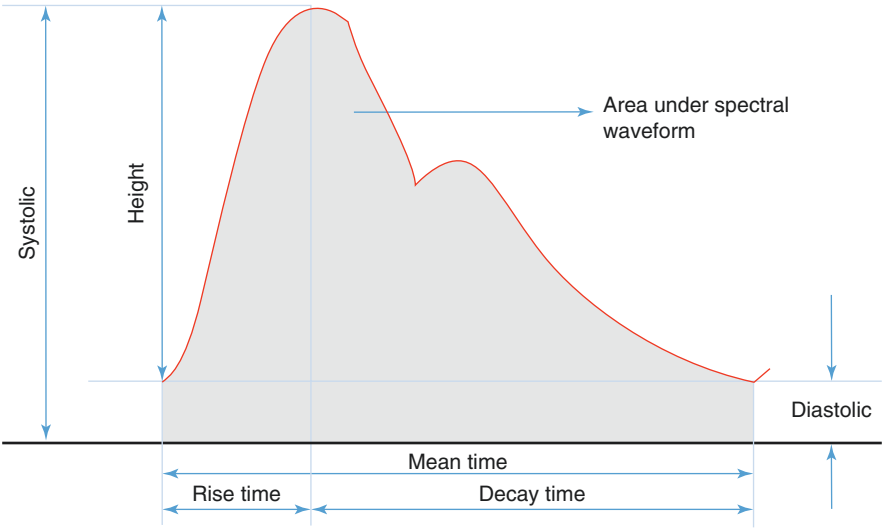

Fig. 17.1 An example of the feature extraction from the spectral waveform of the middle cerebral artery

$$\text{Pulsatility Index of Gosling and King}\left(\text{PI}\right) = \frac{\text{Peak systolic velocity} - \text{End} - \text{Diastolic velocity}}{\text{Mean time}}$$

$$\text{Resistivity Index of Pourcellot}\left(\text{RI}\right) = \frac{\text{Peak systolic velocity} - \text{End} - \text{Diastolic velocity}}{\text{Peak systolic velocity}}$$

$$\text{Systolic / Diastolic Ratio}\left(\text{SDR}\right) = \frac{\text{Peak systolic velocity}}{\text{End} - \text{Diastolic velocity}}$$

$$\text{Rise / Decay Time Ratio}\left(\text{RDTR}\right) = \frac{\text{Rise time}}{\text{Decay time}}$$

$$\text{Rise / Mean Time Ratio}\left(\text{RMTR}\right) = \frac{\text{Rise time}}{\text{mean time}}$$

$$\text{Blood Volume Rate} = \frac{\text{Area under spectral waveform}}{\text{Mean time}}$$

$$\text{The Lindergaard Ratio}\left(\text{LR}\right) = \frac{\text{MCA velocity}}{\text{ICA velocity}}$$

If the gain settings are correct, the envelope outlines the waveform shape after the peak systolic rise, the flow deceleration, and the proportion of the end-diastolic flow component. These computer-based pattern recognition approaches have been developed to analyze TCD signals by detecting the boundary edge (envelope or follower) of spectral waveform using the Sobel edge detection algorithm [54].

Gosling's pulsatility index (PI) and the Pourcelot resistivity index (RI) give an estimation of cerebral perfusion pressure, pulsatility of arterial blood pressure, downstream resistance in cerebral circulation, and compliance of cerebral vessels. The PI reference range is between 0.5 and 1.19 [55]. In the presence of proximal stenosis or occlusion, the PI may be <0.5 due to arteriolar vasodilation distally; conversely, a distal occlusion or constriction increases the PI to >1.19 secondary to increased resistance distally [56]. A PI >1.17 correlates with the presence of silent brain damage on magnetic resonance imaging (MRI) (e.g., microvascular disease) in patients with chronic systemic hypertension [57]. Conversely, despite an elevated PI in young people free of chronic systemic hypertension (PI = 1.2), a high pulsatility waveform in the MCA indicates normal patency of its proximal segment.

PI is regarded by many as an often misleading or imprecise reflection of the true resistance, as it has limitations. Critical closing pressure is the internal pressure at which the blood vessel collapses and closes completely. Cerebral perfusion pressure (CCP) is the principal determinant of PI. Consequently, some experts argue that PI has no distinctive physiologic meaning by itself [58]. Michel and Zernikow [58] concluded that the use of PI as a measure of resistance in autoregulated circuits should be abandoned because the autoregulation models that use PI do not uniformly match experimentally induced changes in vascular resistance.

A Pourcelot RI > 0.8 suggests increased distal resistance [59] or abnormally decreased cerebral perfusion pressure. Elevated RI in different intracranial pathologies that result in increased ICP is comparable to that of an abnormal PI. Nonetheless, the RI is less sensitive to ICP variations than is PI [60].

The Lindegaard ratio (LR) tends to increase in relation to the degree of vasospasm. Normal reference range is from 1.1 to 2.3 and in the absence of vasospasm is <3 [61].

In patients with irregular heart rhythm (extrasystole, atrial fibrillation, etc.), the end-diastolic velocities may fall below 30% of peak systole. This decrease also affects estimation of flow resistance (increased values of PI calculated with envelope tracings) from the averaged values of 2–5 cycles. A single cycle may be selected for manual measurements. Prolonged pauses between cardiac cycles may lead to lower end-diastolic velocities that excessively underestimate the velocity and overestimate the PI. In those cases, a manual measurement of the highest velocity cycle is recommended instead, a practical but inaccurate solution.

Various efforts to examine the use of TCD ultrasound for the assessment of intracranial arterial flow velocity have been published [29, 30, 34, 62–64]. The common techniques used are simply to measure the values of the peak systolic, peak diastolic, and mean flow velocity from FFT Doppler spectra at selected depths. Nonetheless, the standard deviation of normal values is wide. Physiologic variability in parameters such as blood pressure, cardiac output, peripheral resistance, and

arterial compliance lead to high intra-individual variation in peak systolic flow in the MCA (91.0 ± 16.9 cm/s), peak diastolic flow (44.3 ± 9.5 cm/s), and average mean velocity (57.7 ± 11.5 cm/s) [63] and can result in diagnostic errors. It is difficult with this approach to objectively classify in quantitative terms those spectral features that are associated with varying degrees of stenosis in the intracranial arteries. The use of a more quantitative and objective approach to analyzing Doppler spectral waveforms and classifying the varying degree of stenosis in the intracranial arteries is thus highly desirable.

17.5 Transcranial Flow Velocity Monitoring in Neurocritical Care

In this section, we are limiting our discussion to those conditions in which TCD has been applied: (1) daily monitoring of CBFV during aSAH-induced vasospasm, (2) imminent brain death, and (3) MCA blood flow during increased ICP. In the following chapters, each of these applications will be described in detail. In this section, we focus on the physiology of the waveform interpretation.

17.5.1 Aneurysmal Subarachnoid Hemorrhage

Delayed cerebral ischemia after aSAH is a major cause of morbidity and mortality. Frequently, the presenting sign is a neurologic deficit, which may be detected too late to reverse. TCD ultrasonography is used to guide clinical decision-making in regard to additional diagnostic evaluation and therapeutic interventions. When performed in isolation, the contribution of TCD to improving patient outcome has not been established. Nevertheless, TCD has become a regularly used tool in neurocritical care and perioperative settings. A specific condition called hyperemia will produce a unique pattern of high-velocity–low-resistance waveforms in one or several arteries, whereas the remainder of the vessels will have normal velocities and PIs. This phenomenon can be seen in hyperdynamic states after aSAH and must not be confused with vasospasm [61]. When the CBFV is elevated but the LR is lower than 3, the elevation is considered to be caused by hyperemia. An LR > 6 indicates severe vasospasm [61, 65–67], and LR > 3 denotes mild to moderate vasospasm. A modified LR (mLR; basilar artery mean CBFV divided by left or right extracranial vertebral artery mean CBFV) has also been proposed for evaluation of posterior circulation vasospasm. mLR = 2–2.49 indicates possible vasospasm; mLR = 2.5–2.99 suggests moderate vasospasm; and mLR >3 signifies severe vasospasm. A CBFV variation of more than 14% with TCD side-to-side is considered abnormal; most individuals (95%) will not have day-to-day variation of mean CBFV of more than 10 cm/s [68, 69].

In patients with severe vasospasm, the use of a large sample volume (gate) may produce a simultaneous display of waveforms detected at different arterial segments

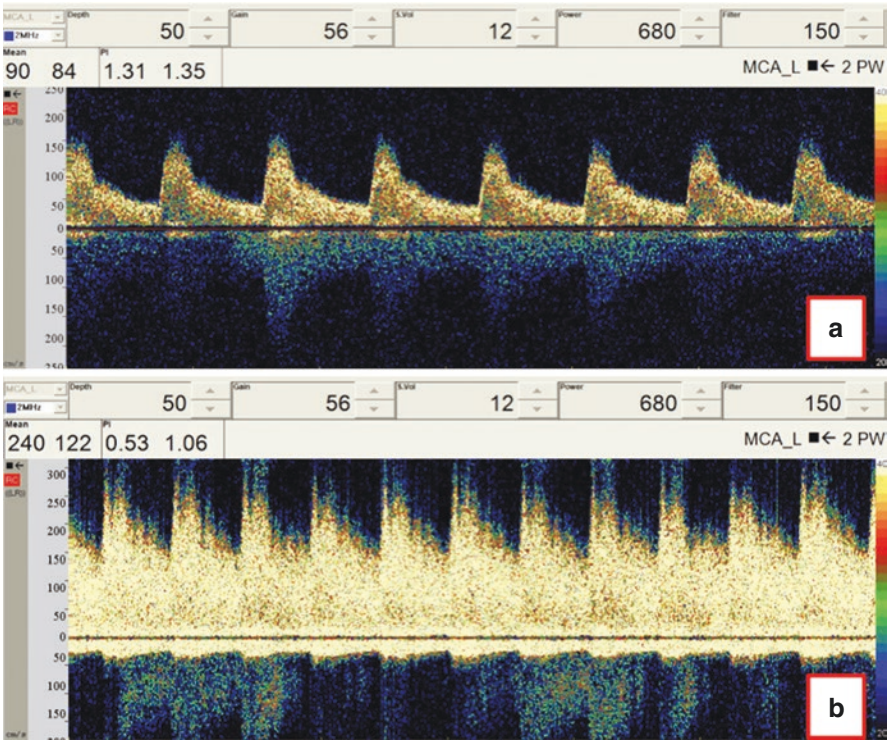

Fig. 17.2 Vasospasm. **Panel A**. Transcranial Doppler waveform from the left middle cerebral artery in a patient on day 3 after aneurysmal subarachnoid hemorrhage shows a mean velocity of 90 cm/s. **Panel B**. Transcranial Doppler waveform from the left middle cerebral artery in the same patient from Panel A on day 11 shows a mean velocity of 240 cm/s (diastolic notch is still present)

(i.e., terminal ICA, proximal M1, or adjacent segments with different patency). The highest velocities in waveform are often considered to be the site of maximum vasospasm (Fig. 17.2). However, a mirror artifact and/or hyperemia must be excluded by using the LR. The signal-to-noise ratio appears to be optimized (i.e., no noise in the background).

17.5.2 Increased ICP

A flow signal above baseline that shows sharp systolic upstrokes followed by sharp deceleration represents an increased flow resistance. Elevated PI and RI have been observed in patients with increased ICP (Fig. 17.3). The Doppler signal shows a sharpened waveform secondary to a fast flow deceleration. Also, a waveform above baseline that exhibits a significant diastolic flow likely suggests that some flow is

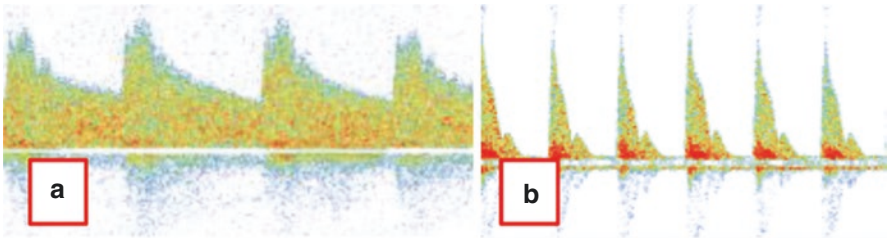

Fig. 17.3 Increased intracranial pressure. **Panel A**. Transcranial Doppler waveform from a low-resistance vessel exhibiting continuous forward flow throughout both systole and diastole. **Panel B**. Transcranial Doppler waveform from a vessel with high resistance caused by elevated intracranial pressure shows a sharp systolic upstroke, a narrow peak in systole, and less flow in diastole

directed to a vascular bed with a lower resistance. This can happen in patients with TBI because different brain areas may sustain various degrees of disturbed autoregulation or unequal distribution of ICP and mass effect.

No irrefutable, close relationship between ICP and mean MCA flow velocity or the shape of the flow waveform has been demonstrated. Nevertheless, some general statements can be made regarding the MCA flow signal alterations after ICP elevation. For instance, in TBI, flow velocity increases immediately after the injury onset and lasts for several days or even weeks. However, ICP is not markedly elevated during this period. When ICP increases sharply, a hyperperfusion profile (i.e., high velocities, decrease of pulsatility) appears initially but rapidly evolves to an increasingly pulsatile, high-resistance flow profile, and finally to a reversed flow of the blood volume. PI is intrinsically related to ICP. A PI variation of 2.4% is reflected by a 1 mmHg change in ICP in the same direction [70]. Indeed, several studies have proposed a strong correlation between PI and ICP, independent of the type of intracranial pathology [59, 60, 71].

Unfortunately, correlation-based approaches are not able to measure absolute ICP accurately enough for TCD ultrasonography to be used in clinical treatment planning. Yet, one study found that the noninvasive ICP measurement technique based on two-depth TCD ultrasound had a better diagnostic reliability in neurological patients than the optic nerve sheath diameter ultrasonography when expressed by the sensitivity and specificity for detecting elevated ICP >14.7 mmHg. Another study showed that changes of ICP in time domain during plateau waves are replicated by noninvasive ICP methods with strong correlations. In addition, the methods offered high performance for detecting intracranial hypertension [72].

17.5.3 Impending Brain Death: Progression to Brain Death

An oscillating or reverberating flow spectrum represents two waveforms (above and below the baseline) with an extremely high resistance to flow. Flow signals above baseline appear as sharp spikes, and a rushed flow deceleration to zero corresponds

with the time of the aortic valve closure and absence of positive end-diastolic flow. The same blood volume bounces back its direction during the entire diastole, generating the sign of flow reverberation or oscillation. An exceptionally high resistance to flow impedes brain perfusion. This waveform typically is observed in patients who have developed substantial cerebral edema with progression to cerebral circulatory arrest. When reverberating flow is found in all intracranial basal arteries, it accurately predicts the absence of brain perfusion in nuclear CBF studies. Hemodynamically, this waveform indicates that all blood that registered through the sample volume toward the brain in systole was pushed out of the distal vasculature in diastole as a result of no flow traveling to brain parenchyma (Fig. 17.4).

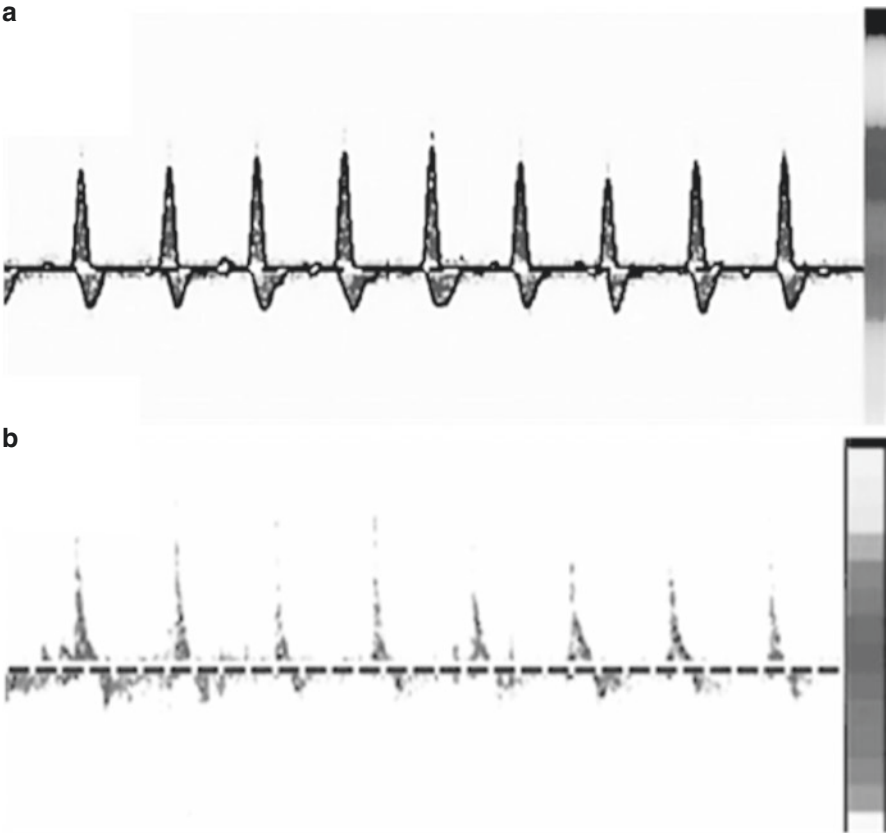

Fig. 17.4 Impending brain death. **Panel A**. Transcranial Doppler waveform of oscillating flow. A sharp forward flow is present in systole with reversal of flow in diastole. **Panel B**. Transcranial Doppler waveform of a systolic spike. There is brief forward flow during systole and no flow during diastole. Both waveforms are consistent with brain death

17.6 Conclusion

TCD is an imperfect technique. As such, several technical and interpretative aspects must be considered to obtain a dependable TCD exam. Nevertheless, TCD ultrasound is capable of following dynamic cerebrovascular processes noninvasively. Daily or continuous monitoring of flow velocities and profiles can help clinicians to recognize trends or pattern changes that alert them to deterioration and the need for a therapeutic response in the care of neurocritically ill patients.

References

1. Alpers BJ, Berry RG, Paddison RM. Anatomical studies of the circle of Willis in normal brain. AMA Arch Neurol Psychiatry. 1959;81(4):409–18.
2. Lehrer HZ. Relative calibre of the cervical internal carotid artery. Normal variation with the circle of Willis. Brain. 1968;91(2):339–48.
3. Sorteberg W, Lindegaard KF, Rootwelt K, Dahl A, Russell D, Nyberg-Hansen R, et al. Blood velocity and regional blood flow in defined cerebral artery systems. Acta Neurochir. 1989;97(1–2):47–52.
4. Knowlton FP, Starling EH. The influence of variations in temperature and blood-pressure on the performance of the isolated mammalian heart. J Physiol. 1912;44(3):206–19.
5. Griffiths DJ. Steady fluid flow through veins and collapsible tubes. Med Biol Eng. 1971;9(6):597–602.
6. Skalak R, Keller SR, Secomb TW. Mechanics of blood flow. J Biomech Eng. 1981;103(2):102–15.
7. Brower RW, Noordergraaf A. Pressure-flow characteristics of collapsible tubes: a reconciliation of seemingly contradictory results. Ann Biomed Eng. 1973;1(3):333–55.
8. Stromberg DD, Fox JR. Pressures in the pial arterial microcirculation of the cat during changes in systemic arterial blood pressure. Circ Res. 1972;31(2):229–39.
9. Czosnyka M, Smielewski P, Kirkpatrick P, Laing RJ, Menon D, Pickard JD. Continuous assessment of the cerebral vasomotor reactivity in head injury. Neurosurgery. 1997;41(1):11–7. discussion 7–9
10. Rivera-Lara L, Zorrilla-Vaca A, Geocadin RG, Healy RJ, Ziai W, Mirski MA. Cerebral autoregulation-oriented therapy at the bedside: a comprehensive review. Anesthesiology. 2017;126(6):1187–99.
11. Lassen NA. Cerebral blood flow and oxygen consumption in man. Physiol Rev. 1959;39(2):183–238.
12. Budohoski KP, Czosnyka M, Smielewski P, Varsos GV, Kasprowicz M, Brady KM, et al. Cerebral autoregulation after subarachnoid hemorrhage: comparison of three methods. J Cereb Blood Flow Metab. 2013;33(3):449–56.
13. Fog M. Autoregulation of cerebral blood flow and its abolition by local hypoxia and-or trauma. Scand J Clin Lab Invest Suppl. 1968;102:V:B.
14. Strandgaard S, Paulson OB. Cerebral autoregulation. Stroke. 1984;15(3):413–6.
15. Halpern W, Osol G. Influence of transmural pressure of myogenic responses of isolated cerebral arteries of the rat. Ann Biomed Eng. 1985;13(3–4):287–93.
16. Symon L, Held K, Dorsch NW. A study of regional autoregulation in the cerebral circulation to increased perfusion pressure in normocapnia and hypercapnia. Stroke. 1973;4(2):139–47.
17. Winn HR, Rubio R, Berne RM. Brain adenosine production in the rat during 60 seconds of ischemia. Circ Res. 1979;45(4):486–92.

18. Winn HR, Bryner C, Curnish RR, Rubio R, Berne RM. Changes in brain metabolites during the first 60 seconds of ischemia: adenosine production during hypotension. Trans Am Neurol Assoc. 1978;103:59–61.
19. Reneman RS, Arts T. Dynamic capacitance of epicardial coronary arteries in vivo. J Biomech Eng. 1985;107(1):29–33.
20. Giller CA, Bowman G, Dyer H, Mootz L, Krippner W. Cerebral arterial diameters during changes in blood pressure and carbon dioxide during craniotomy. Neurosurgery. 1993;32(5):737–41. discussion 41–2
21. Linfante I, Delgado-Mederos R, Andreone V, Gounis M, Hendricks L, Wakhloo AK. Angiographic and hemodynamic effect of high concentration of intra-arterial nicardipine in cerebral vasospasm. Neurosurgery. 2008;63(6):1080–6. discussion 6–7
22. Lindegaard KF, Lundar T, Wiberg J, Sjoberg D, Aaslid R, Nornes H. Variations in middle cerebral artery blood flow investigated with noninvasive transcranial blood velocity measurements. Stroke. 1987;18(6):1025–30.
23. Ringelstein EB, Van Eyck S, Mertens I. Evaluation of cerebral vasomotor reactivity by various vasodilating stimuli: comparison of CO2 to acetazolamide. J Cerebral Blood Flow Metab. 1992;12(1):162–8.
24. Schreiber SJ, Gottschalk S, Weih M, Villringer A, Valdueza JM. Assessment of blood flow velocity and diameter of the middle cerebral artery during the acetazolamide provocation test by use of transcranial Doppler sonography and MR imaging. AJNR Am J Neuroradiol. 2000;21(7):1207–11.
25. Markus HS, Harrison MJ. Estimation of cerebrovascular reactivity using transcranial Doppler, including the use of breath-holding as the vasodilatory stimulus. Stroke. 1992;23(5):668–73.
26. Markwalder TM, Grolimund P, Seiler RW, Roth F, Aaslid R. Dependency of blood flow velocity in the middle cerebral artery on end-tidal carbon dioxide partial pressure--a transcranial ultrasound Doppler study. J Cereb Blood Flow Metab. 1984;4(3):368–72.
27. Bernoulli D. Hydrodynamica, sive de viribus et motibus fluidorum commentarii: opus academicum ab auctore, dum Petropoli ageret, congestum 1738.
28. Spencer MP, Reid JM. Quantitation of carotid stenosis with continuous-wave (C-W) Doppler ultrasound. Stroke. 1979;10(3):326–30.
29. Spencer MP, Whisler D. Transorbital Doppler diagnosis of intracranial arterial stenosis. Stroke. 1986;17(5):916–21.
30. Lindegaard KF, Bakke SJ, Aaslid R, Nornes H. Doppler diagnosis of intracranial artery occlusive disorders. J Neurol Neurosurg Psychiatry. 1986;49(5):510–8.
31. Schneider PA, Rossman ME, Bernstein EF, Torem S, Ringelstein EB, Otis SM. Effect of internal carotid artery occlusion on intracranial hemodynamics. Transcranial Doppler evaluation and clinical correlation. Stroke. 1988;19(5):589–93.
32. Koppl T, Schneider M, Pohl U, Wohlmuth B. The influence of an unilateral carotid artery stenosis on brain oxygenation. Med Eng Phys. 2014;36(7):905–14.
33. Telman G, Kouperberg E, Nitecki S, Karram T, Schwarz HA, Sprecher E, et al. Cerebral hemodynamics in symptomatic and asymptomatic patients with severe unilateral carotid stenosis before and after carotid endarterectomy. Eur J Vasc Endovasc Surg. 2006;32(4):375–8.
34. Lindegaard KF, Bakke SJ, Grolimund P, Aaslid R, Huber P, Nornes H. Assessment of intracranial hemodynamics in carotid artery disease by transcranial Doppler ultrasound. J Neurosurg. 1985;63(6):890–8.
35. Calligaro KD, Dougherty MJ. Correlation of carotid artery stump pressure and neurologic changes during 474 carotid endarterectomies performed in awake patients. J Vasc Surg. 2005;42(4):684–9.
36. Nornes H. The role of the circle of Willis in graded occlusion of the internal carotid artery in man. Acta Neurochir. 1973;28(3):165–77.
37. Nornes H. Hemodynamic aspects in the management of carotid-cavernous fistula. J Neurosurg. 1972;37(6):687–94.

38. Nornes H. Internal carotid artery blood flow during cerebral angiography. Neuroradiology. 1977;12(4):219–25.
39. Nornes H, Grip A, Wikeby P. Intraoperative evaluation of cerebral hemodynamics using directional Doppler technique. Part 1: arteriovenous malformations. J Neurosurg. 1979;50(2):145–51.
40. Nornes H, Grip A, Wikeby P. Intraoperative evaluation of cerebral hemodynamics using directional Doppler technique. Part 2: saccular aneurysms. J Neurosurg. 1979;50(5):570–7.
41. Aaslid R, Markwalder TM, Nornes H. Noninvasive transcranial Doppler ultrasound recording of flow velocity in basal cerebral arteries. J Neurosurg. 1982;57(6):769–74.
42. Sagawa K, Lie RK, Schaefer J. Translation of Otto Frank's paper "Die Grundform des Arteriellen Pulses" Zeitschrift fur Biologie 37: 483-526 (1899). J Mol Cell Cardiol. 1990;22(3):253–4.
43. Westerhof N, Lankhaar JW, Westerhof BE. The arterial Windkessel. Med Biol Eng Comput. 2009;47(2):131–41.
44. Frank O. The basic shape of the arterial pulse. First treatise: mathematical analysis. 1899. J Mol Cell Cardiol. 1990;22(3):255–77.
45. Gosling RG, Dunbar G, King DH, Newman DL, Side CD, Woodcock JP, et al. The quantitative analysis of occlusive peripheral arterial disease by a non-intrusive ultrasonic technique. Angiology. 1971;22(1):52–5.
46. Greenfield JC Jr, Tindall GT. Effect of acute increase in intracranial pressure on blood flow in thw internal carotid artery of man. J Clin Invest. 1965;44:1343–51.
47. Panerai RB. Assessment of cerebral pressure autoregulation in humans--a review of measurement methods. Physiol Meas. 1998;19(3):305–38.
48. Zhang R, Zuckerman JH, Giller CA, Levine BD. Transfer function analysis of dynamic cerebral autoregulation in humans. Am J Phys. 1998;274(1 Pt 2):H233–41.
49. Panerai RB, Coughtrey H, Rennie JM, Evans DH. A model of the instantaneous pressure-velocity relationships of the neonatal cerebral circulation. Physiol Meas. 1993;14(4):411–8.
50. Dahl A, Lindegaard KF, Russell D, Nyberg-Hansen R, Rootwelt K, Sorteberg W, et al. A comparison of transcranial Doppler and cerebral blood flow studies to assess cerebral vasoreactivity. Stroke. 1992;23(1):15–9.
51. Dahl A, Russell D, Nyberg-Hansen R, Rootwelt K, Bakke SJ. Cerebral vasoreactivity in unilateral carotid artery disease. A comparison of blood flow velocity and regional cerebral blood flow measurements. Stroke. 1994;25(3):621–6.
52. Ringelstein EB, Kahlscheuer B, Niggemeyer E, Otis SM. Transcranial Doppler sonography: anatomical landmarks and normal velocity values. Ultrasound Med Biol. 1990;16(8):745–61.
53. Lohmann H, Ringelstein EB, Knecht S. Functional transcranial Doppler sonography. Front Neurol Neurosci. 2006;21:251–60.
54. Miao J, Benkeser PJ, Nichols FT. A computer-based statistical pattern recognition for Doppler spectral waveforms of intracranial blood flow. Comput Biol Med. 1996;26(1):53–63.
55. Gosling RG, King DH. Arterial assessment by Doppler-shift ultrasound. Proc R Soc Med. 1974;67(6 Pt 1):447–9.
56. Nicoletto HA, Burkman MH. Transcranial Doppler series part III: interpretation. Am J Electroneurodiagnostic Technol. 2009;49(3):244–59.
57. Kidwell CS, el-Saden S, Livshits Z, Martin NA, Glenn TC, Saver JL. Transcranial Doppler pulsatility indices as a measure of diffuse small-vessel disease. J Neuroimag. 2001;11(3):229–35.
58. Michel E, Zernikow B. Gosling's Doppler pulsatility index revisited. Ultrasound Med Biol. 1998;24(4):597–9.
59. Zweifel C, Czosnyka M, Carrera E, de Riva N, Pickard JD, Smielewski P. Reliability of the blood flow velocity pulsatility index for assessment of intracranial and cerebral perfusion pressures in head-injured patients. Neurosurgery. 2012;71(4):853–61.
60. Ursino M, Giulioni M, Lodi CA. Relationships among cerebral perfusion pressure, autoregulation, and transcranial Doppler waveform: a modeling study. J Neurosurg. 1998;89(2):255–66.

61. Lindegaard KF, Nornes H, Bakke SJ, Sorteberg W, Nakstad P. Cerebral vasospasm after subarachnoid haemorrhage investigated by means of transcranial Doppler ultrasound. Acta Neurochir Suppl. 1988;42:81–4.
62. Schwartz A, Hennerici M. Noninvasive transcranial Doppler ultrasound in intracranial angiomas. Neurology. 1986;36(5):626–35.
63. Hennerici M, Rautenberg W, Sitzer G, Schwartz A. Transcranial Doppler ultrasound for the assessment of intracranial arterial flow velocity–Part 1. Examination technique and normal values. Surg Neurol. 1987;27(5):439–48.
64. Hennerici M, Rautenberg W, Schwartz A. Transcranial Doppler ultrasound for the assessment of intracranial arterial flow velocity–Part 2. Evaluation of intracranial arterial disease. Surg Neurol. 1987;27(6):523–32.
65. Arnolds BJ, von Reutern GM. Transcranial Doppler sonography. Examination technique and normal reference values. Ultrasound Med Biol. 1986;12(2):115–23.
66. Martin PJ, Evans DH, Naylor AR. Transcranial color-coded sonography of the basal cerebral circulation. Reference data from 115 volunteers. Stroke. 1994;25(2):390–6.
67. Rasulo FA, De Peri E, Lavinio A. Transcranial Doppler ultrasonography in intensive care. Eur J Anaesthesiol Suppl. 2008;42:167–73.
68. Moppett IK, Mahajan RP. Transcranial Doppler ultrasonography in anaesthesia and intensive care. Br J Anaesth. 2004;93(5):710–24.
69. Maeda H, Matsumoto M, Handa N, Hougaku H, Ogawa S, Itoh T, et al. Reactivity of cerebral blood flow to carbon dioxide in various types of ischemic cerebrovascular disease: evaluation by the transcranial Doppler method. Stroke. 1993;24(5):670–5.
70. Homburg AM, Jakobsen M, Enevoldsen E. Transcranial Doppler recordings in raised intracranial pressure. Acta Neurol Scand. 1993;87(6):488–93.
71. Bellner J, Romner B, Reinstrup P, Kristiansson KA, Ryding E, Brandt L. Transcranial Doppler sonography pulsatility index (PI) reflects intracranial pressure (ICP). Surg Neurol. 2004;62(1):45–51; discussion.
72. Cardim D, Schmidt B, Robba C, Donnelly J, Puppo C, Czosnyka M, et al. Transcranial Doppler monitoring of intracranial pressure plateau waves. Neurocrit Care. 2017;26(3):330–8.

Chapter 18
Non-invasive Multimodal Neuromonitoring in the ICU: The Role of Transcranial Doppler (TCD/TCCS)

Demetrios J. Kutsogiannis

Key Points

1. Multimodality neuromonitoring (MMM) is both static and dynamic, evaluating cerebral structure, vasculature, and electrochemical function.
2. The various technologies included in MMM provide complementary information with various degrees of inter-modality correlation.
3. The use of MMM permits earlier therapeutic interventions that may prevent cerebral tissue hypoxia, metabolic stress, and irreversible cerebral damage.
4. The best method of monitoring, optimal physiological cutoffs, and threshold for treatments must be individualized for every acutely brain-injured patient.
5. Multimodality neuromonitoring technologies offer predictive value in prognosticating neurological outcomes.

18.1 Introduction

The term multimodal monitoring (MMM) encompasses the various clinical and technological modalities available to the contemporary physician caring for critically ill neurological patients. Injured patients include those with trauma, infections, and hemorrhagic or ischemic stroke. For many years, scoring systems (Glasgow Coma Score, FOUR Score) utilizing the neurological examination were used as the only stochastic method of following changes in neurological function. However, it is well recognized that the neurological examination is limited in comatose patients and those under sedation and analgesia, and neurological changes may

D. J. Kutsogiannis (✉)
Critical Care Medicine, Neurocritical Care (UCNS), Neurosciences ICU, The University of Alberta, Royal Alexandra Hospital ICU, University of Alberta Hospital, Edmonton, AB, Canada
e-mail: djk3@ualberta.ca

C. N. Rodríguez et al. (eds.), *Neurosonology in Critical Care*,
https://doi.org/10.1007/978-3-030-81419-9_18

not manifest or may lag important changes in cerebral vascular perfusion, electrophysiology, and metabolism. Two major acute brain injury diagnoses have been the most informative in motivating the development of MMM techniques and research. The first being that of delayed neurological deterioration after subarachnoid hemorrhage (SAH), specifically delayed cerebral ischemia (DCI). The second being the identification of mechanisms for secondary brain injury after traumatic brain injury (TBI) and the importance of abnormal cerebral autoregulation in worsening outcomes in TBI. Research utilizing transcranial Doppler and Transcranial Color-Coded duplex Sonography (TCCS) and other forms of MMM have DCI after SAH is not specifically related to catheter angiographically defined areas of proximal vasospasm. Multidimensional and complex processes such as arteriolar constriction and thrombosis, hypoxemic and non-hypoxemic mitochondrial metabolic failure, and cortical spreading depolarization-related hypoperfusion are important etiological factors [1, 2]. In TBI, intracranial hypertension is an important secondary insult after TBI, and its identification, prevention, and treatment are important in optimizing clinical outcomes [3]. The ability of the brain to regulate its blood flow despite the level of cerebral perfusion pressure (CPP) is important in the prevention of secondary brain injury through its effect on intracranial hypertension, hypoxia, ischemia, and hyperemia. The loss of this cerebral autoregulation is detrimental to patient outcomes. However, utilizing MMM techniques for the measurement of dynamic cerebrovascular autoregulation assists in determining patient-specific optimal targets for CPP in order to mitigate the detrimental effects of poor intracranial compliance. Such methods require the ability to calculate real-time moving correlation coefficients between intracranial pressure (ICP), or cerebral blood flow by TCD/TCCS, and arterial blood pressure [4, 5].

18.2 TCD/TCCS: Role and Importance in the Non-invasive Multimodal Neuromonitoring in the ICU

In the Consensus Summary Statement of the International Multidisciplinary Consensus Conference on Multimodality Monitoring in Neurocritical Care [6], the quality of the evidence was reviewed and recommendations were developed using the GRADE system. Recommendations are classified as strong or weak based on a consensus balance among benefits, risks, burden, and costs according to the quality of the evidence [7–9]. These recommendations are as follows.

1. *High*: Further research is very unlikely to change our confidence in the estimate of effect.
2. *Moderate*: Further research is likely to have an important impact on our confidence in the estimate of effect and may change the estimate.
3. *Low*: Further research is very likely to have an important impact on our confidence in the estimate of effect and is likely to change the estimate.
4. *Very low*: Any estimate of effect is very uncertain.

18.3 TCD/TCCS: Frequent Pathologies. What Do We Monitor?

18.3.1 Subarachnoid Hemorrhage (SAH)

18.3.1.1 Cerebral Autoregulation (CA)

Dysfunctional cerebral autoregulation is a component of risk for delayed cerebral ischemia (DCI) in SAH. Otite assessed the relationship between cerebral autoregulation measured using dynamic transfer analysis (phase and gain) of the spontaneous blood pressure and blood flow velocities on days 2 to 4 after SAH. Multivariate analysis indicated that a higher transfer function gain and a lower transfer function phase were independently associated with angiographically confirmed vasospasm, and computed tomography (CT) confirmed delayed cerebral ischemia (DCI) [10]. Disturbed autoregulation within the first 5 days after SAH, as measured by Sx (TCD-derived autoregulatory index) and Tox (Near-infrared spectroscopy, NIRS-derived autoregulatory index) significantly increases the risk of DCI [11]. In another study, neither cerebral autoregulation impairment as measured by TCD (Sx) nor large artery vasospasm alone was associated with DCI. However, the combination of large artery vasospasm with increasing loss of cerebral autoregulation within the first 7 days from a SAH was significantly associated with DCI [12].

18.3.1.2 Intraparenchymal Cerebral Oxygen Monitoring

A study of 46 patients representing 5424 hours of $PbtO_2$ monitoring the number of episodes of compromised $PtbO_2$ (15–25 mmHg) and the number of episodes of cerebral hypoxia ($PtbO_2 < 15$ mmHg) was independently associated with mortality [13]. An important limitation of $PbtO_2$ placement in SAH is that placement of the probe must be congruent with the most probable site of cerebral vasospasm or infarction. In one study, congruence was achieved in >88% of the insertions for internal carotid artery and middle cerebral artery aneurysms but as low as 23% of the insertions for vertebrobasilar arteries [14].

18.3.1.3 Cerebral Blood Flow

Using bedside xenon-enhanced computed tomography (XeCT), patients with poor-grade SAH and initial low CBF at day 0–3 post SAH who received hypertension, hypervolemia, and hemodilution (HHH) therapy had a significant increase in their CBF at day 4–7 as compared to those not receiving HHH [15]. In a study performed in 17 patients within 12 hr. after SAH using XeCT, CBF was significantly reduced in all patients with SAH (mean 34 ml/100 g × min) as compared to controls (mean 67 ml/100 g × min) with significantly worse CBF in patients with more severe SAH

(Hunt Hess 4–5) versus Hunt Hess 1–3. This was attributable to acute peripheral vasospasm of the microvasculature which is not detectable by conventional angiography or TCD/TCCS [16]. The coupling between cerebral blood flow (CBF) and neuronal activity as measured by electroencephalogram (EEG) occurs within seconds [17]. As CBF falls below 30 ml/100 g/min, faster frequencies are lost, and a progressive slowing of EEG activity occurs, and at CBF <10 ml/100 g/min all EEG frequencies are suppressed [18]. EEG may complement neuroimaging as a continuous monitor of ongoing ischemia. Historically, middle cerebral artery (MCA) mean flow velocities of <120 cm/sec and >200 cm/sec reliably predict the absence or presence of clinically significant angiographic vasospasm with a high negative predictive and positive predictive value, respectively [19]. More recently, a meta-analysis has assisted in reconciling the complementary MMM information obtained from cerebral catheter angiography and TCD in predicting DCI in SAH. Synthesizing the results from 15 studies, Kumar compiled the sensitivity, specificity, positive predictive value, and negative predictive value of cerebral catheter angiography for prediction of DCI as 57%, 68%, 32%, and 90%. For TCD, the respective measures were better than those using cerebral catheter angiography, being 90%, 71%, 57%, and 92%, respectively [20].

18.3.1.4 Electrophysiology

Seizure Detection

In a systematic review of 18 studies which used continuous EEG (cEEG) to monitor 481 patients with SAH, the incidence of non-convulsive seizures (NCSz) was 7–18% and that of non-convulsive status epilepticus was 3–13%. The presence of non-convulsive status epilepticus (NCSE) was associated with increasing age and mortality [21]. In SAH patients undergoing continuous EEG (cEEG) monitoring in the intensive care unit (ICU), up to 19% have non-convulsive seizures (NCSz) and 13% have NCSE. Using the GRADE system, the Neurointensive Care Section of the European Society of Intensive Care Medicine (ESICM) recommends EEG monitoring to rule out NCSz in all SAH patients with unexplained and persistent altered consciousness [22].

Ischemia Detection

The Neurointensive Care Section of the ESICM suggests EEG to detect DCI in comatose patients in whom neurological physical examination is unreliable [22]. Automated quantitative EEG (QEEG) algorithms using predetermined thresholds for the decrease in alpha band power and increase in theta band power have also been demonstrated to precede the angiographic detection of vasospasm or DCI by 2.3 days [23]. In a systematic review of cEEG in SAH, Kondziella concluded that a QEEG pattern of a decreased alpha/delta ratio, decrease in relative alpha variability, and total power had a weak association with the development of DCI. However, all the included studies were subject to a high risk of methodological bias [21].

A poor prognosis, defined as modified Rankin score of 4–6 (dead or moderately to severely disabled), was independently associated with cEEG evidence of the absence of sleep architecture, the presence of periodic or generalized periodic lateralized epileptiform discharges, the absence of EEG reactivity, and the presence of NCSE [24, 25].

18.3.1.5 Cerebral Metabolism

Cerebral microdialysis (CMD) abnormalities are defined as increases in lactate/glucose (L/G) and lactate/pyruvate (L/P) levels of greater than 20% followed by a 20% increase in glycerol concentration defined ischemia of the cerebral territory of the microdialysis probe. Delayed cerebral ischemia was identified in 17 of 18 patients with this degree of elevation, 14 of whom had cerebral CT evidence of infarction [26]. Using CMD in comatose SAH patients, Oddo characterized elevated CMD lactate (>4 mmol/L) as either hypoxic, defined as PbtO2 < 20 mmHg, or as hyperglycolytic, defined as having a CMD pyruvate of >119 μmol/L. A pattern of hypoxic lactate elevations was associated with a high mortality versus a pattern of increased cerebral hyperglycolytic lactate which was associated with good long-term recovery [27]. Cerebral microdialysis probes should be placed in the vascular territories with the highest infarct risk in relation to the aneurysm location. These territories being the anterior cerebral arteries for anterior communicating artery aneurysms and the ipsilateral middle cerebral artery territory for internal carotid artery, middle cerebral artery, and posterior communicating artery aneurysms [28]. The Consensus Statement from the 2014 International Microdialysis Forum recommends the use of CMD in mechanically ventilated poor-grade SAH patients and those with secondary neurological deterioration. As a primary monitoring device, the probe location recommended is in the frontal lobe in the watershed anterior cerebral–middle cerebral artery territory. In SAH patients with secondary deterioration, the recommended probe location should be in brain regions at risk for ischemia guided by TCD/TCCS or CT perfusion scanning [29].

18.3.2 Intracerebral Hemorrhage (ICH)

18.3.2.1 Intraparenchymal Cerebral Oxygen Monitoring

There is little experience with the use of intraparenchymal oxygen monitoring in ICH. Hemphill described the use of the LICOX® catheter in swine and seven patients with ICH. Tissue hypoxia, defined as the area under the curve with tissue $PbtO_2$ < 15 mmHg, was common with increasing FiO2, mean arterial pressure, and CPP predicting increasing $PbtO_2$ [30]. Invasively monitoring perihematomal brain tissue oxygenation has also demonstrated a significant increase in the risk of brain tissue hypoxia (PbtO2 < 15 mmHg) in those patients with a CPP < 80 mmHg [31].

Targeting CPP in these patients to their optimal CPP (CPPopt) guided by their pressure reactivity index (PRx) has the potential to improve clinical outcomes in ICH. However, larger studies utilizing this MMM interventional approach are required to more firmly determine this [32].

18.3.2.2 Intracerebral Volume, Midline Shift, and Pulsatility Index Measurements by TCCS

ICH is a dynamic process with the advantage provided by TCCS being its availability to provide rapid repeated assessments at the bedside. In a cohort of patients suffering from spontaneous ICH, TCCS measurements of hematoma volume (HV) and midline shift demonstrated a strong correlation with brain CT measurements. The optimal threshold to predict mortality at 1 month was an HV of 47.62 mL measured by CT (85.7% sensitivity, 85.7% specificity) and an HV of 30.36 mL measured by TCCS (85.7% sensitivity, 82.2% specificity). TCCS tended to overestimate the volume of smaller ICHs and to underestimate the volumes of larger ICHs. In previous univariate analysis, an increased pulsatility index (PI) from the ipsilateral MCA was associated with higher mortality. In separate multivariable analysis, both CT and TCCS measurements of HV size were the only independent predictors of 1-month mortality with an equal magnitude of effect [33]. For real-time bedside monitoring, the use of serial TCD/TCCS monitoring has been proven to be reliable in determining the extent of early hematoma expansion. Prior studies have demonstrated that the initial size of the ICH, percentage of hematoma growth, Glasgow Coma Score, hypertension, the presence of intraventricular hemorrhage (IVH), and age are predictive of mortality and poor functional outcome [34, 35]. Serial TCD examinations every 30 minutes for 6 hours have demonstrated good volume estimation compared to cerebral CT, and this early hematoma expansion appears to be exclusive to spot sign positive patients [36–38]. This information may be used at the bedside to predict early hematoma expansion and clinical worsening so as to allocate these patients to higher levels of neurocritical care monitoring.

18.3.2.3 Electrophysiology

Electrographic seizures found on cEEG and periodic epileptiform discharges are common in ICH, occurring in up to one-third of patients [39, 40]. The Consensus Statement from the Neurointensivist Section of the ESICM recommends EEG to rule out NCSz in all ICH patients with altered levels of consciousness [22].

18.3.3 Traumatic Brain Injury (TBI)

18.3.3.1 Intracranial Pressure and Cerebral Perfusion Pressure

When intracranial pressure increases, cerebral vascular autoregulation is gradually lost, and cerebral arterioles and veins are compressed reducing blood return and increasing vascular resistance. The consequence is a reduced MFV and a reduced or reversed (negative) end-diastolic velocity. Collectively, this increases the numerator and lowers the denominator of the equation for the pulsatility index, PI = (Peak-systolic velocity – End-diastolic velocity)/ Mean flow velocity (MFV). The MCA PI has been demonstrated to have a strong positive correlation with ICP measurements in various etiologies of cerebral brain injury with one study indicating an estimated ICP = 10.93 × PI – 1.28 [41]. Other investigators have determined that a resistive index and PI cutoff value of 0.705 and 1.335, respectively, predicted ICP > 15 mmHg with a sensitivity of 0.885 and a specificity of 0.970 [42]. Likewise, in a cohort of 365 TBI patients with mild TBI, an abnormal TCD examination defined as a PI >1.25 and an end-diastolic flow velocity <25 had an 80% sensitivity and a 79% specificity in predicting neurological worsening [43]. These findings may enable clinicians to risk stratify patients into higher risk groups requiring an increased level of monitoring. At present, the current edition of the Guidelines for the Management of Severe Traumatic Brain injury does not offer any guidance for the use of TCD/TCCS in the management of severe TBI. The guidelines do, however, recommend, treating ICP > 22 mm Hg and maintaining a CPP between 60 and 70 mm Hg with the ideal CCP target depending on the autoregulatory status of the patient [3].

18.3.3.2 Cerebral Autoregulation

Static and dynamic autoregulation measure the amount and rapidity with which cerebrovascular resistance changes when CPP varies. Failure of autoregulation is associated with poor outcomes in TBI and other neurological injuries. Measurements from TCD (Mx), ICP (PRx) brain tissue oxygenation $PbtO_2$ (ORx), and near-infrared spectroscopy (THx) have been utilized dynamically and correlated with CPP in order to determine the range within which CPP is optimal (CPPopt). Patients with TBI whose CPP is targeted in the CPPopt range have been demonstrated to have improved outcomes. The most validated approach uses a correlation coefficient method between ICP and CPP to determine a pressure reactivity index (PRx) for which a recent systematic review has offered a weak recommendation using the GRADE system [4]. In retrospective studies, optimizing cerebral autoregulation (CPPopt) to maximize cerebrovascular reactivity reduces neurological disability and mortality [44, 45]. Current MCA TCD-based methods of determining cerebral autoregulation appear to have a good correlation with the more commonly used pressure reactivity index (PRx) [46]. However, more research is required to define the role of TCD/TCCS-based measures of cerebral autoregulation in the management of TBI.

18.3.3.3 Intraparenchymal Cerebral Oxygen Monitoring

Although the fourth edition of the Guidelines for the Management of Severe Traumatic Brain Injury does not provide guidance for the use of $PbtO_2$ to monitor patients with TBI, the International Multidisciplinary Consensus Conference on Multimodality Monitoring in Neurocritical Care strongly recommends monitoring brain oxygen in patients with or at risk of cerebral ischemia or hypoxia using $PbtO_2$. This recommendation was made with a low quality of evidence [6]. However, subsequent to these recommendations, the phase II randomized trial (BOOST II) comparing monitoring TBI patients with ICP plus $PbtO_2$ versus ICP alone has demonstrated that monitoring with both ICP and $PbtO_2$ reduced the proportion of time with brain tissue hypoxia after severe TBI by more than 50% to only 16% of the time, and with a trend to lower mortality and more favorable neurological outcomes [47].

18.3.3.4 Cerebral Blood Flow

A recent systematic review has collectively identified SAH, IVH, a low admission glasgow coma scale (GCS), and age less than 30 years as independent predictors of developing TBI-induced vasospasm [48]. Separate TCD indexes describing cerebral hypoperfusion or vasospasm both predicted poor outcomes in severe TBI [49]. The use of TCD/TCCS has also emerged as an important technique to monitor patients with blunt cerebrovascular trauma or dissection. Transcranial ultrasound microemboli detection has demonstrated a strong association between the number of microemboli per hour and daily persistence of microemboli with the development of stroke in patients with blunt cerebrovascular injuries [50].

18.3.3.5 Electrophysiology

The current recommendations from the neurointensive care section of the ESICM for the use of EEG in TBI include (1) a strong recommendation for its use in all TBI patients with unexplained and persistent altered consciousness and (2) a suggestion for the use of EEG to exclude NCSz in patients with TBI and GCS < 8, especially in those with large cortical contusions/hematoma, depressed skull fracture, or penetrating injury [22]. As well the prospect for the future use of cortical depth electrodes to monitor for spreading depolarizations as a surrogate for metabolic failure and excitotoxic injury has recently łed to a consensus statement outlining standards for their recording, analysis, and interpretation [2].

18.3.3.6 Cerebral Metabolism

The recommended location for microdialysis placement in TBI patients is the non-dominant frontal lobe in patients with diffuse TBI and within radiographically normal brain ipsilateral to a focal lesion in focal TBI. The measurement of glucose, lactate, and lactate–pyruvate (LP) ratio is recommended [29]. Periods of low brain glucose (<0.8 mmol/L) are associated with poor outcomes. An elevated LP ratio in the presence of low pyruvate and low $PbtO_2$ indicates ischemia, whereas an increase in the LP ratio with a high pyruvate and normal $PbtO_2$ indicates mitochondrial dysfunction. A rise in LP ratio concomitant with a fall in CPP and a loss of cerebrovascular reactivity (PRx) corresponds to ischemia as the likely etiology. Cerebral perfusion pressure augmentation, increasing $PaCO_2$, increasing inspired oxygen, or treating anemia should be considered [5, 29]. Nonischemic metabolic crises appear to be responsible for most of the incidents of LP elevation and are thought to be related to mitochondrial dysfunction and reduced oxidative metabolism [51]. The Consensus Statement from the 2014 International Microdialysis Forum described cerebral microdialysis to be a reliable and safe technique for the clinical management of TBI or SAH patients [29]. It includes reference values for commonly measured substrates and ranks them based on quantity and usefulness of clinical data, with glucose and lactate/pyruvate ratio (LPR) being at the top, followed by glutamate and then glycerol. Moreover, when using cerebral microdialysis, one must be aware of the location of the catheter (peri-contusional versus normal brain) as results vary widely [52].

18.3.4 Acute Ischemic Stroke (AIS)

18.3.4.1 Cerebral Blood Flow

Flow velocity reduction or occlusion of the MCA in acute ischemic stroke is better discerned using transcranial color-coded duplex sonography than with standard TCD methods and the absence of flow reduction/occlusion on TCCS predicted early clinical improvement [53]. Greater than 30% of patients with successful angiographic recanalization post mechanical thrombectomy for large vessel occlusion stroke were demonstrated to have abnormally low MCA flow velocities by postintervention TCD. This was defined as thrombosis in brain ischemic grade 0–4. Such a mismatch between angiographic post-thrombectomy recanalization and poor TCD flow velocities predicted poor 90-day outcomes [54]. Although TCCS is not primarily used to direct the decision for angiographic recanalization, consensus recommendations on how to examine intracranial arteries by TCCS in acute ischemic stroke and its use in monitoring recanalization have been published [55].

More recently, CT perfusion, diffusion-weighted magnetic resonance imaging (MRI), or MR diffusion/perfusion studies have been recommended in selected patients with large vessel acute ischemic stroke within 6 to 24 hours of last known normal

function to aid in patient selection for mechanical thrombectomy based on the DAWN and DEFUSE 3 trial [56–58]. These imaging methods define an initial infarct volume (ischemic core) and volume of potentially reversible ischemia (penumbra) for the selection of patients for which thrombolytics and thrombectomy are useful. The requirement for these measurements currently limits the use of TCD/TCCS in this setting.

18.3.4.2 Electrophysiology

Quantitative EEG (QEEG) specifically using the delta/alpha power ratio (DAR) has demonstrated good accuracy in classifying patients with acute ischemic stroke [59]. The DAR, relative alpha power, and national institute of health stroke scale (NIHSS) score were independent predictors of worsening 30-day NIHSS score in ischemic cortical stroke patients.

18.3.5 Meningitis and Encephalitis

18.3.5.1 Cerebral Blood Flow

Although there has been a limited description of significant cerebral blood flow abnormalities in cases of encephalitis, significant cerebrovascular abnormalities have been more notable in meningitis [60]. By varying mean arterial pressure (MAP) and measuring MCA MFV and jugular oxygen saturation, autoregulation was found to be impaired but temporarily recovered with hyperventilation in a series of patients with acute bacterial meningitis. Outcomes were good for those patients who recovered cerebral autoregulation; however, those who did not, either died or had a protracted hospital course [61, 62]. Three phases of tuberculous meningitis have been described with progressively worsening outcomes. The first phase includes patients with focal reversible neurological deficits and a GCS of 15 who have increased MCA flow velocities (MFV) and normal or slightly decreased PI. The second phase characterizes patients with focal neurological deficits, a GCS 12–14, and decreased MCA MFV and PI. The third phase characterizes patients with GCS less than 12, severely reduced or absent MCA MFV, and severely reduced PI. Phase II and III patients have cerebral CT evidence of inflammatory meningitis and infarction with clinical findings of permanent neurological dysfunction or death [63]. Disturbed cerebral hemodynamics including MCA stenosis and an increased PI has been shown using TCCS in a small series of patients with non-HIV cryptococcal meningitis. Good concordance between the TCCS findings and those seen on MR angiography was not evident; however, the small number of study patients limits its conclusions [64]. The same investigators have demonstrated in a small series of patients with tuberculous or cryptococcal meningitis that the presence of unilateral or bilateral MCA stenosis seen on TCCS was associated with 5.3 odds of a poor outcome (Barthel Index <12) at 6 months [65].

18.4 Conclusion

All current and evolving MMM technologies provide complementary information for caring for patients in the neurointensive care unit with acute cerebral injuries of various etiologies. Given the resources required to have these technologies available within neurointensive care units and to maintain the necessary skills required to interpret information from these technologies, appropriately designed cohort studies and clinical trials should inform a high level of evidence for their use in clinical practice. Other current limitations with the use of MMM are that of real-time data integration, presentation, and analysis. Several sophisticated methods of data analysis such as hierarchical cluster analysis are utilizing physiological data from critically ill patients to formulate patterns predictive of various outcomes. It is hoped that implementing these intelligent systems in the future will aid in effecting treatment decisions within the neurocritical care unit [66].

References

1. Macdonald RL. Delayed neurological deterioration after subarachnoid haemorrhage. Nat Rev Neurol. 2014;10(1):44–58.
2. Dreier JP, Fabricius M, Ayata C, Sakowitz OW, Shuttleworth CW, Dohmen C, et al. Recording, analysis, and interpretation of spreading depolarizations in neurointensive care: review and recommendations of the COSBID research group. J Cereb Blood Flow Metab. 2017;37(5):1595–625.
3. O'Reilly C, Totten AM, Carney N, Tasker RC, Wilberger J, Wright DW, et al. Guidelines for the management of severe traumatic brain injury, Fourth Edition. Neurosurgery. 2016;80(1):6–15.
4. Czosnyka M, Miller C. Monitoring of cerebral autoregulation. Neurocrit Care. 2014;21(2):95–102.
5. Lazaridis C, Andrews CM. Brain tissue oxygenation, lactate-pyruvate ratio, and cerebrovascular pressure reactivity monitoring in severe traumatic brain injury: systematic review and viewpoint. Neurocrit Care. 2014;2:345.
6. Le Roux P, Menon DK, Citerio G, Vespa P, Bader MK, Brophy G, et al. The international multidisciplinary consensus conference on multimodality monitoring in Neurocritical care: evidentiary tables: a statement for healthcare professionals from the Neurocritical care society and the European Society of Intensive Care Medicine. Neurocrit Care. 2014;21(Suppl 2):S297–361.
7. Holger SJ, Guyatt G, Oxman A. Handbook for grading the quality of evidence and the strength of recommendations using the GRADE approach. GRADE Handbook Updated. GRADE working group, October 2013. (gradeworkinggroup.org).
8. Rochwerg B, Alhazzani W, Jaeschke R. Clinical meaning of the GRADE rules. Intensive Care Med. 2014;40(6):877–9.
9. Jaeschke R, Guyatt GH, Dellinger P, Schünemann H, Levy MM, Kunz R, et al. Use of GRADE grid to reach decisions on clinical practice guidelines when consensus is elusive. BMJ. 2008;337:a744.
10. Otite F, Mink S, Tan CO, Puri A, Zamani AA, Mehregan A, et al. Impaired cerebral autoregulation is associated with vasospasm and delayed cerebral ischemia in subarachnoid hemorrhage. Stroke. 2014;45(3):677–82.

11. Budohoski KP, Czosnyka M, Smielewski P, Kasprowicz M, Helmy A, Bulters D, et al. Impairment of cerebral autoregulation predicts delayed cerebral ischemia after subarachnoid hemorrhage: a prospective observational study. Stroke. 2012;43(12):3230–7.
12. Calviere L, Nasr N, Arnaud C, Czosnyka M, Viguier A, Tissot B, et al. Prediction of delayed cerebral ischemia after subarachnoid hemorrhage using cerebral blood flow velocities and cerebral autoregulation assessment. Neurocrit Care. 2015;23(2):253–8.
13. Ramakrishna R, Stiefel M, Udoteuk J, Spiotta A, Levine JM, Kofke WA, et al. Brain oxygen tension and outcome in patients with aneurysmal subarachnoid hemorrhage. J Neurosurg. 2008;109(6):1075.
14. Ulrich CT, Fung C, Vatter H, Setzer M, Gueresir E, Seifert V, et al. Occurrence of vasospasm and infarction in relation to a focal monitoring sensor in patients after SAH: placing a bet when placing a probe? PLoS One. 2013;8(5):e62754.
15. Engquist H, Rostami E, Enblad P. Temporal dynamics of cerebral blood flow during the acute course of severe subarachnoid hemorrhage studied by bedside xenon-enhanced CT. Neurocrit Care. 2019;30(2):280–90.
16. Schubert GA, Seiz M, Hegewald AA, Manville J, Thomé C. Acute Hypoperfusion immediately after subarachnoid hemorrhage: a xenon contrast-enhanced CT study. J Neurotrauma. 2009;26(12):2225–31.
17. Sundt TM Jr, Sharbrough FW, Piepgras DG, Kearns TP, Messick JM Jr, O'Fallon WM. Correlation of cerebral blood flow and electroencephalographic changes during carotid endarterectomy: with results of surgery and hemodynamics of cerebral ischemia. Mayo Clin Proc. 1981;56(9):533–43.
18. Jordan KG. Emergency EEG and continuous EEG monitoring in acute ischemic stroke. J Clin Neurophysiol. 2004;21(5):341–52.
19. Vora YY, Suarez-Almazor M, Steinke DE, Martin ML, Findlay JM. Role of transcranial Doppler monitoring in the diagnosis of cerebral vasospasm after subarachnoid hemorrhage. Neurosurgery. 1999;44(6):1237–47. discussion 47–8
20. Kumar G, Dumitrascu OM, Chiang C-C, O'Carroll CB, Alexandrov AV. Prediction of delayed cerebral ischemia with cerebral angiography: a Meta-analysis. Neurocrit Care. 2019;30(1):62–71.
21. Kondziella D, Friberg CK, Wellwood I, Reiffurth C, Fabricius M, Dreier JP. Continuous EEG monitoring in aneurysmal subarachnoid hemorrhage: a systematic review. Neurocrit Care. 2015;3:450.
22. Claassen J, Taccone FS, Horn P, Holtkamp M, Stocchetti N, Oddo M. Recommendations on the use of EEG monitoring in critically ill patients: consensus statement from the neurointensive care section of the ESICM. Intensive Care Med. 2013;39(8):1337–51.
23. Gollwitzer S, Groemer T, Rampp S, Hagge M, Olmes D, Huttner HB, et al. Early prediction of delayed cerebral ischemia in subarachnoid hemorrhage based on quantitative EEG: a prospective study in adults. Clin Neurophysiol. 2015;126(8):1514–23.
24. Claassen J, Hirsch LJ, Frontera JA, Fernandez A, Schmidt M, Kapinos G, et al. Prognostic significance of continuous EEG monitoring in patients with poor-grade subarachnoid hemorrhage. Neurocrit Care. 2006;4(2):103–12.
25. Bosco E, Marton E, Feletti A, Scarpa B, Longatti P, Zanatta P, et al. Dynamic monitors of brain function: a new target in neurointensive care unit. Crit Care. 2011;15(4):R170.
26. Skjøth-Rasmussen J, Schulz M, Kristensen SR, Bjerre P. Delayed neurological deficits detected by an ischemic pattern in the extracellular cerebral metabolites in patients with aneurysmal subarachnoid hemorrhage. J Neurosurg. 2004;100(1):8.
27. Oddo M, Levine JM, Frangos S, Maloney-Wilensky E, Carrera E, Daniel RT, et al. Brain lactate metabolism in humans with subarachnoid hemorrhage. Stroke. 2012;43(5):1418–21.
28. Tholance Y, Barcelos GK, Perret-Liaudet A, Omar E, Carrillon R, Grousson S, et al. Placing intracerebral probes to optimise detection of delayed cerebral ischemia and allow for the prediction of patient outcome in aneurysmal subarachnoid haemorrhage. J Cereb Blood Flow Metab. 2017;37(8):2820–32.
29. Hutchinson PJ, Jalloh I, Helmy A, Carpenter KLH, Rostami E, Bellander B-M, et al. Consensus statement from the 2014 international microdialysis forum. Intensive Care Med. 2015(9):1517.

30. Hemphill JC, Morabito D, Farrant M, Manley GT. Brain tissue oxygen monitoring in intracerebral hemorrhage. Neurocrit Care. 2005;3(3):260–70.
31. Ko SB, Choi HA, Parikh G, Helbok R, Schmidt JM, Lee K, et al. Multimodality monitoring for cerebral perfusion pressure optimization in comatose patients with intracerebral hemorrhage. Stroke. 2011;42(11):3087–92.
32. Diedler J, Santos E, Poli S, Sykora M. Optimal cerebral perfusion pressure in patients with intracerebral hemorrhage: an observational case series. Crit Care. 2014;18(2):R51.
33. Camps-Renom P, Méndez J, Granell E, Casoni F, Prats-Sánchez L, Martínez-Domeño A, et al. Transcranial duplex sonography predicts outcome following an intracerebral hemorrhage. Am J Neuroradiol. 2017;38(8):1543–9.
34. Davis SM, Broderick J, Hennerici M, Brun NC, Diringer MN, Mayer SA, et al. Hematoma growth is a determinant of mortality and poor outcome after intracerebral hemorrhage. Neurology. 2006;66(8):1175–81.
35. Leira R, Dávalos A, Silva Y, Gil-Peralta A, Tejada J, Garcia M, et al. Early neurologic deterioration in intracerebral hemorrhage. Predictors and associated factors. Neurology. 2004;63(3):461–7.
36. Pérez ES, Delgado-Mederos R, Rubiera M, Delgado P, Ribó M, Maisterra O, et al. Transcranial duplex sonography for monitoring Hyperacute intracerebral hemorrhage. Stroke. 2009;40(3):987–90.
37. Ovesen C, Christensen AF, Krieger DW, Rosenbaum S, Havsteen I, Christensen H. Time course of early postadmission hematoma expansion in spontaneous intracerebral hemorrhage. Stroke. 2014;45(4):994–9.
38. Al-Shahi Salman R, Frantzias J, Lee RJ, Lyden PD, Battey TWK, Ayres AM, et al. Absolute risk and predictors of the growth of acute spontaneous intracerebral haemorrhage: a systematic review and meta-analysis of individual patient data. Lancet Neurol. 2018;17(10):885–94.
39. Claassen J, Jetté N, Chum F, Green R, Schmidt M, Choi H, et al. Electrographic seizures and periodic discharges after intracerebral hemorrhage. Neurology. 2007;69(13):1356–65.
40. Vespa PM, O'Phelan K, Shah M, Mirabelli J, Starkman S, Kidwell C, et al. Acute seizures after intracerebral hemorrhage. A factor in progressive midline shift and outcome. Neurology. 2003;60(9):1441–6.
41. Bellner J, Romner B, Reinstrup P, Kristiansson K-A, Ryding E, Brandt L. Transcranial Doppler sonography pulsatility index (PI) reflects intracranial pressure (ICP). Surg Neurol. 2004;62(1):45–51.
42. Wang Y, Duan YY, Zhou HY, Yuan LJ, Zhang L, Wang W, et al. Middle cerebral arterial flow changes on transcranial color and spectral Doppler sonography in patients with increased intracranial pressure. J Ultrasound Med. 2014;33(12):2131–6.
43. Bouzat P, Almeras L, Manhes P, Sanders L, Levrat A, David J-S, et al. Transcranial Doppler to predict neurologic outcome after mild to moderate traumatic brain injury. Anesthesiology. 2016;125(2):346–54.
44. Steiner LA, Czosnyka M, Piechnik SK, Smielewski P, Chatfield D, Menon DK, et al. Continuous monitoring of cerebrovascular pressure reactivity allows determination of optimal cerebral perfusion pressure in patients with traumatic brain injury. Crit Care Med. 2002;30(4):733–8.
45. Aries MJ, Czosnyka M, Budohoski KP, Steiner LA, Lavinio A, Kolias AG, et al. Continuous determination of optimal cerebral perfusion pressure in traumatic brain injury. Crit Care Med. 2012;40(8):2456–63.
46. Zeiler FA, Donnelly J, Calviello L, Smielewski P, Menon DK, Czosnyka M. Pressure autoregulation measurement techniques in adult traumatic brain injury, part II: a scoping review of continuous methods. J Neurotrauma. 2017;34(23):3224–37.
47. Okonkwo DO, Shutter LA, Moore C, Temkin NR, Puccio AM, Madden CJ, et al. Brain oxygen optimization in severe traumatic brain injury phase-II: a phase II randomized trial. Crit Care Med. 2017;45(11):1907–14.
48. Al-Mufti F, Amuluru K, Changa A, Lander M, Patel N, Wajswol E, et al. Traumatic brain injury and intracranial hemorrhage–induced cerebral vasospasm: a systematic review. Neurosurg Focus. 2017;43(5):E14.

49. Ziegler D, Cravens G, Poche G, Gandhi R, Tellez M. Use of transcranial Doppler in patients with severe traumatic brain injuries. J Neurotrauma. 2017;34(1):121–7.
50. Bonow RH, Witt CE, Mosher BP, Mossa-Basha M, Vavilala MS, Rivara FP, et al. Transcranial Doppler microemboli monitoring for stroke risk stratification in blunt cerebrovascular injury. Crit Care Med. 2017;45(10):e1011–e7.
51. Vespa P, Bergsneider M, Hattori N, Wu HM, Huang SC, Martin NA, et al. Metabolic crisis without brain ischemia is common after traumatic brain injury: a combined microdialysis and positron emission tomography study. J Cereb Blood Flow Metab. 2005;25(6):763–74.
52. Engstrom M, Polito A, Reinstrup P, Romner B, Ryding E, Ungerstedt U, et al. Intracerebral microdialysis in severe brain trauma: the importance of catheter location. J Neurosurg. 2005;102(3):460–9.
53. Goertler M, Kross R, Baeumer M, Jost S, Grote R, Weber S, et al. Diagnostic impact and prognostic relevance of early contrast-enhanced transcranial color-coded duplex sonography in acute stroke. Stroke. 1998;29(5):955–62.
54. Kneihsl M, Niederkorn K, Deutschmann H, Enzinger C, Poltrum B, Horner S, et al. Abnormal blood flow on transcranial duplex sonography predicts poor outcome after stroke Thrombectomy. Stroke. 2018;49(11):2780–2.
55. Nedelmann M, Stolz E, Gerriets T, Baumgartner Ralf W, Malferrari G, Seidel G, et al. Consensus recommendations for transcranial color-coded duplex sonography for the assessment of intracranial arteries in clinical trials on acute stroke. Stroke. 2009;40(10):3238–44.
56. Powers WJ, Rabinstein AA, Ackerson T, Adeoye OM, Bambakidis NC, Becker K, et al. 2018 guidelines for the early management of patients with acute Ischemic stroke: a guideline for healthcare professionals from the American Heart Association/American Stroke Association. Stroke. 2018;49(3):e46–e110.
57. Nogueira RG, Jadhav AP, Haussen DC, Bonafe A, Budzik RF, Bhuva P, et al. Thrombectomy 6 to 24 hours after stroke with a mismatch between deficit and infarct. N Engl J Med. 2018;378(1):11–21.
58. Albers GW, Marks MP, Kemp S, Christensen S, Tsai JP, Ortega-Gutierrez S, et al. Thrombectomy for stroke at 6 to 16 hours with selection by perfusion imaging. N Engl J Med. 2018;378(8):708–18.
59. Finnigan S, Wong A, Read S. Defining abnormal slow EEG activity in acute ischaemic stroke: Delta/alpha ratio as an optimal QEEG index. Clin Neurophysiol. 2016;127(2):1452–9.
60. Kargiotis O, Safouris A, Magoufis G, Stamboulis E, Tsivgoulis G. Transcranial color-coded duplex in acute encephalitis: current status and future prospects. J Neuroimaging. 2016;26(4):377–82.
61. Moller K, Larsen FS, Qvist J, Wandall JH, Knudsen GM, Gjorup IE, et al. Dependency of cerebral blood flow on mean arterial pressure in patients with acute bacterial meningitis. Crit Care Med. 2000;28(4):1027–32.
62. Moller K, Skinhoj P, Knudsen GM, Larsen FS. Effect of short-term hyperventilation on cerebral blood flow autoregulation in patients with acute bacterial meningitis. Stroke. 2000;31(5):1116–22.
63. Kiliç T, Elmaci I, Özek MM, Pamir NM. Utility of transcranial Doppler ultrasonography in the diagnosis and follow-up of tuberculous meningitis-related vasculopathy. Childs Nerv Syst. 2002;18(3):142–6.
64. Chang W-N, Lu C-H, Chang H-W, Lui C-C, Tsai N-W, Huang C-R, et al. Time course of cerebral hemodynamics in cryptococcal meningitis in HIV-negative adults. Eur J Neurol. 2007;14(7):770–6.
65. Lu C-H, Chang W-N, Chang H-W, Chung K-J, Tsai N-W, Lui C-C, et al. Clinical relevance of intracranial arterial Stenoses in tuberculous and Cryptococcal meningitis. Infection. 2007;35(5):359–63.
66. Cohen MJ, Grossman AD, Morabito D, Knudson MM, Butte AJ, Manley GT. Identification of complex metabolic states in critically injured patients using bioinformatic cluster analysis. Crit Care. 2010;14(1):R10.

Chapter 19
Acute Neurologic Injury in ICU: Vasomotor Reactivity Testing by Transcranial Doppler (TCD/TCCS)

Pedro Castro and Elsa Azevedo

Key Points

1. Breath-hold test, carbogen inhalation and acetazolamide are the most commonly used stimulus.
2. Worse vasoreactivity has been linked to prognosis in critical care patients.
3. Decreased cerebral vasoreactivity increases the risk of cerebral ischemic lesions.

19.1 Introduction

Cerebral vasoreactivity or vasomotor reactivity (VMR) is an index of cerebral blood flow (CBF) or velocity (CBFV) in response after administration of a vasomodulatory stimulus, whether it is a drug (e.g. acetazolamide intravenous), gases (e.g. carbogen), or a manoeuvre that causes changes in $PaCO_2$ (e.g. apnoea or hyperventilation) [1]. Important note is that such a definition leaves reactivity to change in cerebral perfusion pressure (PP) in a chapter related to autoregulation. Vasodilation is most commonly studied. The aim of VMR or vasomotor evaluation is to measure the capacity and amplitude of variation of resistance vessel calibre, which for some

P. Castro (✉)
Department of Clinical Neurosciences and Mental Health, Faculty of Medicine of University of Porto, Porto, Portugal

Department of Neurology and Stroke Unit, Centro Hospitalar Universitário de São João, E.P.E, Porto, Portugal
e-mail: pedromacc@gmail.com

E. Azevedo
Neurologist, Department of Clinical Neurosciences and Mental Health, Faculty of Medicine of University of Porto, Porto, Portugal

Department of Neurology, Universitary Hospital São João, Porto, Portugal

Committee Member - ESNCH, Oslo, Norway

C. N. Rodríguez et al. (eds.), *Neurosonology in Critical Care*,
https://doi.org/10.1007/978-3-030-81419-9_19

authors can be understood as "cerebrovascular reserve" [2–4]. Generally, both middle cerebral arteries (MCA) are monitored because they represent a larger brain area and have reference values in the literature [2]. The VMR to CO_2 test is mostly used in research, while the simpler apnoea test [5] may be more practical in the clinical setting. Literature is confusing about VMR testing since the term vasomotor is sometimes used to refer to cerebral autoregulation, which is a different physiological property of cerebral vessels than concerns blood pressure influences and is measured with different techniques.

19.2 Cerebral Blood Haemodynamic Measurements

VMR testing requires measurement of CBF or equivalent. The first can be assessed by measuring regional CBF by single-photon emission computed tomography or positron emission tomography. CBFV is measured by transcranial Doppler (TCD). The imaging methods have the advantage of spatial discrimination when compared to TCD but lack time resolution and involve cumbersome, expensive protocols and irradiation. New methods are being tested with arterial spin labelling magnetic resonance imaging, which can be difficult to put in practice in ICU patients [2]. TCD has the advantage of being more practical, with bedside testing and monitoring of the patient through the time course of its condition.

19.3 Cerebral Blood Flow (CBF): Physiology Principles

Blood flow does not follow the simple laws of Newtonian fluids and is best studied by rheological principles [6]. However, in a more simplistic perspective, we can describe the blood flow by Ohm's law according to the formula $\dot{Q} = \Delta P / R$, where $\dot{Q}$ represents the flow in ml.min-1, ΔP is the blood pressure gradient, and R is the vascular resistance. In the case of the brain [7], ΔP is the cerebral PP, the difference between the mean BP (MAP) and the transmural pressure opposing the flow. In the systemic circulation, the only contributory and relevant factor for this is the venous pressure (2–5 mm Hg) [6]. Considering the normal values of peripheral MAP (≈80 mm Hg), we can approximate the formula such that $\dot{Q} \cong MAP / R$ for the general peripheral circulation.

The determinants of R are explained by the Hagen–Poiseuille law (Eq. 19.1), where L is the length of the vessel and η is the blood viscosity of the cross-sectional radius of the vessel [8]. From this, we can see the central importance of resistance vessels, in which small variations in their diameter exponentially modify the blood flow in the organ they nourish.

$$R = \left(8 \times L\eta\right) / \left(\Pi \times r \wedge 4\right) \tag{19.1}$$

Despite what has already been said, some precautions are necessary for the CBF study because intracranial circulation has a special character, in which the perfused organ is inside a rigid skull bathed in cerebrospinal fluid (CSF). Thus, CSF pressure, that is, intracranial pressure (ICP), which is usually between 0 and 15 mm Hg, may dominate and replace venous pressure in ΔP. In non-invasive conditions, we do not have access to the value of ICP and it is ignored. However, in certain ICU patients ICP may reach values higher than 30–40 mm Hg and significantly alter the parameters to be taken into account in the formula. In conclusion, both MAP and ICP should be kept constant during CO_2 challenge since these are factors that altered per se CBF.

19.4 Vasoreactivity Determining: Methods

There are three main methods for determining VMR:

1. Breath-Hold Test [5]: After a period of rest and a normal inspiration, the individual is instructed to remain in apnoea for about 30 seconds (minimum of 24 seconds) with consequent increase of $PaCO_2$. A breath-hold index (BHI) is calculated by using mean CBFV (MFV) values by formula BHI = (MFVmax – MFVbaseline)/MFVbaseline/apnoea time (in seconds) × 100, where MFVmax corresponds to the average MFV in the last 4 seconds of apnoea and MFVbaseline to the average values of MFV in the minute preceding apnoea, which requires a cooperative conscious patients but no capnography. Some authors couple this manoeuvre with hyperventilation to access global VMR capacity as described below [1]. Disadvantage is that change in CBFV cannot be compared with change of $PaCO_2$.
2. CO_2 VMR Test [9]: Here, MFV changes are monitored continuously with those of the $EtCO_2$ by capnography [Figs. 19.1, 19.2, and 19.3]. In non-intubated patients, we can use a mask with non-recirculating circuit coupled to a reservoir

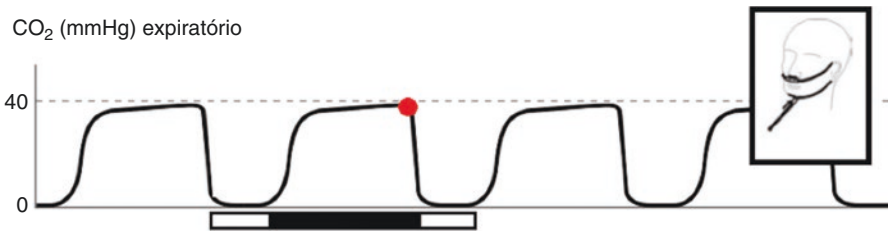

Fig. 19.1 Capnography nasal line for non-invasive end-tidal CO_2 measurement**.** Normal subject. After the inspiratory phase (white bar), during which there is no flow in the cannula, the device detects a sudden increase in carbon dioxide (CO_2) during expiration, leading to a plateau stage believed to be in equilibrium with alveolar CO_2 partial pressure. Therefore, the end-tidal CO_2 level approaches the real value of arterial $PaCO_2$. In intubated patients, capnography produces similar waveform from sample line in the orotracheal apparatus

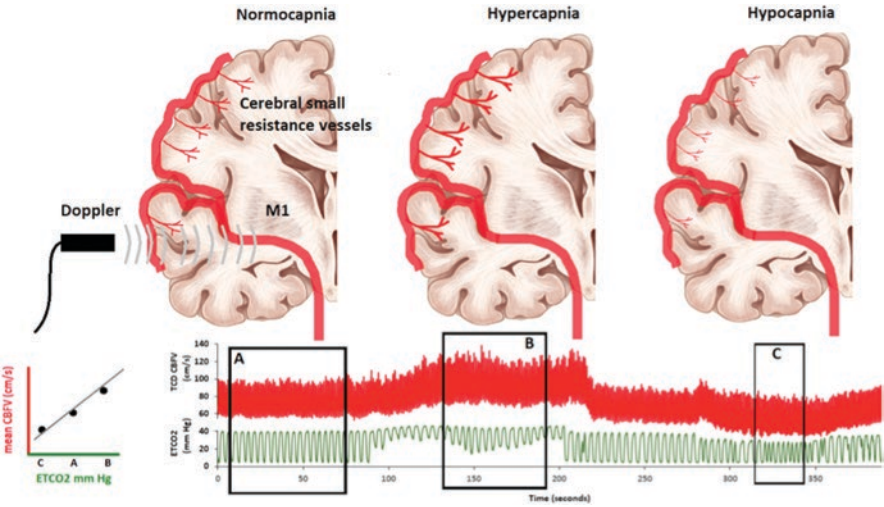

Fig. 19.2 Representative changes in cerebral blow flow velocity and cerebral vasculature calibre during CO_2 vasoreactivity testing. During CO_2 vasoreactivity testing, after a resting period, the patient is first summited to hypercapnia, e.g. achieved by carbogen inhalation (CO_2 at 5%) or through manipulation of ventilator parameters and after recovery of physiological parameters, it follows a hypocapnia challenge (hyperventilation less than 7–10 mm Hg from baseline). In the upper part of the figure, we see that cerebral resistance vessels (mainly small arterioles) vasodilate in response to hypercapnia and vasoconstrict to hypocapnia. It should be noticed that despite transcranial Doppler insonates the M1 segment of middle cerebral artery, the changes in cerebral blood flow velocity (CBFV) depicted in lower part of the figure, are caused by the calibre changes in the small distal parenchymal microvessels and not M1, which remains with constant diameter throughout the challenge. The lower part of the figure represents an actual record from a patient. When compared to normocapnia, hypercapnia induces CBFV increase and a subtle hypocapnia causes a visible CBFV decrease. End-tidal CO_2 ($EtCO_2$) concomitant changes were derived by a nasal capnograhy. By plotting the averaged mean CBFV and EtCO2 at each of the three stages we can calculate the vasoreactivity by deriving the inclination of that line (bottom left)

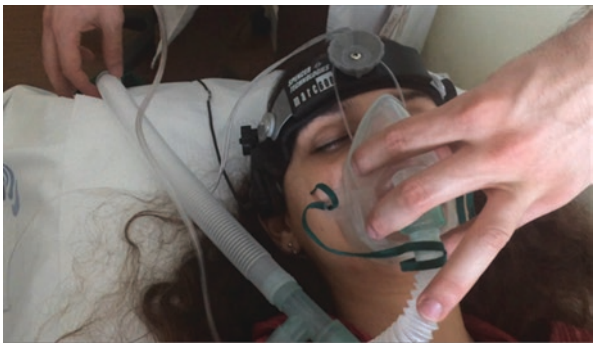

Fig. 19.3 Apparatus for measuring CO_2 reactivity in a non-intubated patient. Transcranial Doppler probes and bilaterally hold in place by a proper steady probe-holder. Nasal cannula is also in place. A T-tube with a safety expansion bag is adapted for a supply gas (carbogen) for inhalation during hypercapnia

or a non-return valve. Hypercapnia is achieved by inhaling a 2–8% CO_2 (carbogen) mixture, causing an increase in $EtCO_2$ of at least 7–10 mm Hg. In addition, we can test response to hypocapnia through hyperventilation to reduce $EtCO_2$ by about 7–10 mm Hg. In order to obtain the overall VMR (% or $cm.s^{-1}$ per mm Hg of CO_2), we calculated the slope of the linear regression line between the mean values of $EtCO_2$ in the abscissa axis and the respective mean values of mean flow velocity (MFV) in the phases of hyperventilation, resting and carbogen. We can also calculate VMR values separately for the phases of hypercapnia and hypocapnia [9]. Another parameter that can be calculated, although less frequently, is the total vasodilator capacity given by the following formula (Eq. 19.2):

$$\left(\mathrm{MFV}_{\mathrm{hypercapnia}} - \mathrm{MFV}_{\mathrm{hypocapnia}}\right) / \mathrm{MFV}_{\mathrm{resting}} \times 100\% \tag{19.2}$$

In intubated patients, $EtCO_2$ can be measured directly from the capnography linked to ventilatory apparatus. To achieve higher and lower CO_2 levels of around 10 mm Hg from baseline, we can manipulate the ventilator parameters.

3. Pharmacological Challenge [13]: Vasodilator substances such as L-arginine (500 mg/kg for 30 minutes) or acetazolamide (15 mg/kg for 5 minutes, maximum effect in 10–12 minutes) are perfused, which promote cerebral vasodilation by increasing the production of NO [10] or of cerebral tissue pH [11], respectively. Diamox® (acetazolamide), a potent, reversible inhibitor of carbonic anhydrase, is widely more frequently used. It is most probable that these effects are stimulated by metabolic acidosis but this is debatable in literature [1].

19.5 Vasoreactivity (VMR): Interpretation of the Results

- The following criteria can be used to evaluate the breath-holding index results [3, 5, 12]:
  - >0.6 is normal.
  - 0.21 to 0.60 is impaired.
  - ≤0.20 is significantly impaired VMR.
- The following criteria are used to evaluate the CO_2 challenge results as vasomotor reserve [4, 13, 14]:
  - Normal vasomotor reserve 86% ± 16%.
  - Mild to moderately reduced 69% to 39%.
  - Severely reduced 38% to 16%.
  - Exhausted <=15%.
- The following criteria are used to evaluate the CO_2 challenge as expressed by % MFV per mm Hg (linear regression method) [15]:
  - VMR to CO_2 5.26 ± 1.61 [%/mmHg].

  - Relative reduction of VMR: side difference more than 3%/mmHg or 2%/mmHg < VMR < 5%/mmHg.
  - Restricted VMR: VMR < 2%/mmHg.
  - Exhausted VMR: VMR < 1%/mmHg.
- The following criteria are used to evaluate acetazolamide test [13]:
  - VMR to acetazolamide: normal is ~40 ± 15% increase in MFV.
  - Pathological <10% increase in MFV.

19.6 Technical Tips

- There are standard normality values derived from larger cohorts, and the values reported in this chapter are only for reference purposes.
- Use a TCD probe holder to minimize the errors in CBFV measurement.
- Use MCA M1 (45–60 mm in depth) segment bilaterally since these are the values most frequently encountered in the literature.
- The times for hypercapnia or hypocapnia, as well as resting phases between them are only references. It is possible that they can be shortened or increased depending on the individual differences in reaching steady-state values of $EtCO_2$ or CBFV. For this purpose, it is important to visually control capnography, and CBFV time trends monitor to ensure that these plateau levels are reached.
- Before proceeding with the VMR tests, a complete extracranial and intracranial examination is advisable to exclude the presence of haemodynamic stenosis that may influence the test results.

19.7 Vasoreactivity: Clinical Importance

The grade of cerebral vasoreactivity has been linked to prognosis in critical care patients.

In a small cohort of patients with subarachnoid haemorrhage, impaired VMR to CO_2 challenge was more frequent in patients with a poor clinical grade on admission and at the time of examination [16]. A persistently decreased VMR to CO_2 also predicted those that developed delayed cerebral ischemia. In patients with carotid occlusion, patients with exhausted, reduced and normal VMR to CO_2 showed 50%, 28% and 18% suffering from ischemic stroke [17]. In intensive care unit patients, was found clinical correlation between VMR and ICP variations [18], where progressive decrease in VMR (worse cerebral hemodynamic state) was associated with worse clinical outcomes in long term [18].

19.8 Conclusion

Cerebral vasoreactivity or vasomotor reactivity is an index of cerebral blood flow or velocity in response after administration of a vasomodulatory stimulus. It is a simple and non-invasive test that can inform you about the vasodilatory vasomotor reserve of the cerebral microvascular bed. A transcranial Doppler with probe holder and a capnographic line is all the necessary equipment. A persistently decreased vasoreactivity predicted those that developed delayed cerebral ischemia in subarachnoid haemorrhage patients and those with increased risk of stroke in carotid occlusion.

References

1. Gur A, Csányi A, Bornstein N. Vasomotor reactivity. In: Csibá L, Baracchini C, editors. Manual of neurosonology. Cambridge: Cambridge University Press; 2016.
2. Malojcic B, Giannakopoulus P, Sorond FA, Azevedo E, Diomedi M, Oblak JP, et al. Ultrasound and dynamic functional imaging in vascular cognitive impairment and Alzheimer's disease. BMC Med. 2017;15:27.
3. Silvestrini M, Vernieri F, Troisi E, Passarelli F, Matteis M, Pasqualetti P, et al. Cerebrovascular reactivity in carotid artery occlusion: possible implications for surgical management of selected groups of patients. Acta Neurol Scand. 1999;99:187–91.
4. Ringelstein EB, Sievers C, Ecker S, Schneider PA, Otis SM. Noninvasive assessment of CO2-induced cerebral vasomotor response in normal individuals and patients with internal carotid artery occlusions. Stroke. 1988;19:963–9.
5. Markus HS, Harrison MJ. Estimation of cerebrovascular reactivity using transcranial Doppler, including the use of breath-holding as the vasodilatory stimulus. Stroke. 1992;23:668–73.
6. Segal SS. Regulation of blood flow in the microcirculation. Microcirculation. 2005;12:33–45.
7. Panerai RB. Complexity of the human cerebral circulation. Philos Transact A Math Phys Eng Sci. 2009;367:1319–36.
8. Segal SS. Special circulations. In: Boulpaep WFBEL, editor. Medical physiology. Philadelphia, PA, USA: W. B. Saunders Company; 2008.
9. Madureira J, Castro P, Azevedo E. Demographic and systemic hemodynamic influences in mechanisms of cerebrovascular regulation in healthy adults. J Stroke Cerebrovasc Dis. 2017;26:500–8.
10. Zimmermann C, Wimmer M, Haberl RL. L-arginine-mediated Vasoreactivity in patients with a risk of stroke. Cerebrovasc Dis. 2004;17:128–33.
11. Vorstrup S, Henriksen L, Paulson OB. Effect of acetazolamide on cerebral blood flow and cerebral metabolic rate for oxygen. J Clin Invest. 1984;74:1634–9.
12. Muller M, Voges M, Piepgras U, Schimrigk K. Assessment of cerebral vasomotor reactivity by transcranial Doppler ultrasound and breath-holding. A comparison with acetazolamide as vasodilatory stimulus. Stroke. 2005;26:96–100.
13. Ringelstein EB, Van Eyck S, Mertens I. Evaluation of cerebral vasomotor reactivity by various vasodilating stimuli: comparison of CO2 to acetazolamide. J Cereb Blood Flow Metab. 1992;12:162–8.
14. Park CW, Sturzenneger M, Douville CM, Aaslid R, Newell DW. Autoregulatory response and CO2 reactivity of the basilar artery. Stroke. 2003;34:34–9.

15. Diehl RR, Henkes H, Nahser HC, Kuhne D, Berlit P. Blood flow velocity and vasomotor reactivity in patients with arteriovenous malformations. A transcranial Doppler study. Stroke. 1994;25:1574–80.
16. Carrera E, Kurtz P, Badjatia N, Fernandez L, Claassen J, Lee K, et al. Cerebrovascular carbon dioxide reactivity and delayed cerebral ischemia after subarachnoid hemorrhage. Arch Neurol. 2010;67:434–9.
17. Widder B, Kleiser B, Krapf H. Course of cerebrovascular reactivity in patients with carotid artery occlusions. Stroke. 1994;25:1963–7.
18. Klinglelhofer J, Sander D. Doppler CO2 test as an indicator of cerebral vasoreactivity and prognosis in severe intracranial hemorrhages. Stroke. 1992;23:962–6.

Chapter 20
Critical Closing Pressure in Acute Brain Injury: Usefulness of Transcranial Doppler as Neuromonitoring

Corina Puppo, Leandro Moraes, and Bernardo Yelicich

Key Points

1. CrCP is a blood pressure value, expressed in mmHg, greater than or equal to ICP. It is the ABP at which small vessels collapse and circulation stops.
2. Negative values do not have a physiological explanation, being probably a methodologic limitation.
3. The difference between ICP and CrCP represents the tone of cerebral arteriolar vessels and has been called wall tension.
4. The difference between ABP and CrCP represents the effective cerebral perfusion pressure or closing margin.
5. Vasospasm in the patient with SAH temporarily and spatially decreases CrCP.

20.1 Introduction

Before defining the critical closing pressure of cerebral circulation (CrCP) and in order to better understand its concept, we must refer to another concept closely related to CrCP: cerebral perfusion pressure (CPP). The perfusion pressure of an organ is the pressure that propels blood through its vascular circuit, calculated as the

C. Puppo (✉)
Intensive Care Unit, Clinics Hospital, Universidad de la Republica School of Medicine, Montevideo, Uruguay
e-mail: coripuppo@gmail.com

L. Moraes
Intensive Care Center, Hospital de Clinicas, School of Medicine, University of the Republic, Montevideo, Uruguay

B. Yelicich
Engineering (Ing), Universidad de la República – Montevideo Uruguay, Neuromonitoring Group of the Hospital de Clínicas, Montevideo, Uruguay

C. N. Rodríguez et al. (eds.), *Neurosonology in Critical Care*,
https://doi.org/10.1007/978-3-030-81419-9_20

difference between the pressure in the arterial vessel arriving at the specific organ and the pressure in the veins which drain it. In the case of the brain it should be the arterial blood pressure minus the cerebral venous pressure (CVP) (Eq. 20.1):

$$\text{CPP} = \text{ABP} - \text{CVP} \tag{20.1}$$

The veins that leave the brain and lead the blood to the dura sinuses are called bridge veins. The pressure in these veins is the outlet pressure of the cerebral vascular circuit. These veins have thin, predominantly adventitious walls; the pressure around them is transferred to them. On certain occasions, when there is an increase in intracranial pressure (ICP), these veins are compressed. Cerebral bridge veins' pressure is not measurable in clinical practice. The formula used for cerebral perfusion pressure is the difference between the arterial blood pressure that reaches the brain and intracranial pressure. If ICP is normal, both pressures are similar, so the formula is useful in both situations, during normal and high ICP:

$$\text{CPP} = \text{ABP} - \text{ICP} \tag{20.2}$$

From this formula, broadly used, it can be erroneously inferred that, if CPP approaches zero, either because ABP decreases or ICP increases, cerebral circulation traverses the brain with decreasing driving force, and when it reaches zero, circulation stops.

That is, if ABP = PIC, CPP = 0 (Eq. 20.2).

However, circulation stops before these pressures are equal. This is because the small resistance vessels have a tone which exerts an inward force, facilitating the closure of the vessels, before ABP and ICP are equal. This force is not included in CPP formula.

Burton coined the term "critical closing pressure" for systemic circulation in 1951. He described, through a theoretical model, that brain vessels can collapse when their pressure drops to a critical value, for which he coined the name "critical closing pressure" (CrCP) [1].

Based on Burton's model, critical closing pressure of the cerebral circulation is defined as the arterial blood pressure (ABP) at which small cerebral arteries close and cerebral blood flow (CBF) ceases [2–4]. That is, the force generated by the heart is insufficient to propel circulation through the cerebral vascular bed. It is greater than ICP.

20.2 CrCP Therefore Represents a Critical Lower Threshold of Cerebral Circulation

20.2.1 What Is the Importance of CrCP Concept?

When measuring CPP with the conventional formula presented above, there may be an acceptable CPP value of 70 mmHg, with an ABP of 90 mmHg and an ICP of 20 mmHg, for example, pressures that do not worry the intensivist. But if the tone

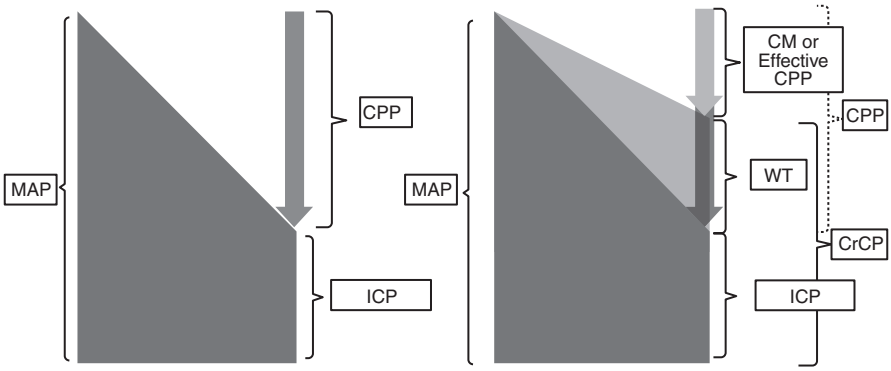

Fig. 20.1 Scheme of the different pressures to which the text refers. On the left it is shown how the cerebral perfusion pressure is conventionally measured (CPP). CPP is the difference between the inlet pressure to the circuit (ABP) and the output pressure (ICP). On the right, vascular wall tension (WT) added to ICP constitutes the critical closing pressure. Observe how "classical" CPP calculation (left panel) can overestimate the effective CPP value (CM in the right panel). [Abbreviations: MAP: mean arterial pressure; ICP: intracranial pressure; CPP: cerebral perfusion pressure; CM: closing margin; WT: wall tension; CrCP: critical closing pressure]

of the cerebral arterioles is high, it may happen that the cerebral circulation of this patient is at risk of stopping, which is not evidenced by CPP with its classical measurement. Therefore, some researchers have proposed the terms "effective CPP" [5, 6] or "collapsing" or "closing margin" (CM) [7, 8], to get a closer idea of the real hemodynamic situation and the risk of arteriolar collapse. This closing margin is calculated as the difference between the patient's ABP and CrCP (Eq. 20.3):

$$\mathrm{CM} = \mathrm{ABP} - \mathrm{CrCP} \tag{20.3}$$

The difference between ICP and CrCP corresponds to the tone of cerebral arteriolar vessels and has been called "wall tension"(WT) (Fig. 20.1).

20.3 Methods to Study Cerebral Critical Closing Pressure

The advent of TCD has been extremely useful to non-invasively measure different parameters of cerebral hemodynamics, based on the possibility of visualizing cerebral blood flow velocity (CBFV) at patient's bedside, in real time, with excellent temporal resolution. One of the calculated parameters based on CBFV has been CrCP.

When using TCD, CBFV is measured in conductance brain basal large vessels. When continuous monitoring is performed, the middle cerebral artery is the vessel studied in more than 90% of the cases. This artery delivers approximately one-third of the total CBF. This allows CBFV and ABP changes to be simultaneously followed. Since in most clinical situations ABP does not decrease to extreme values leading to circulatory arrest, CrCP cannot be measured directly in clinical grounds.

Aaslid studied CrCP during transient cardiac arrest—generated at the evaluation of patients with implantable defibrillators—thus being able to directly visualize the pressure at which cerebral blood flow stopped.

Methods initially used assumed that the relationship between ABP and cerebral blood flow was linear in the dynamic situation of each arterial pulse, that is, if ABP continued to decline, CBFV would continue to decrease at the same rate, proportionally to ABP descent. The relationship between rapid changes in CBF (studied through CBFV recorded continuously with TCD) and the rapid changes in ABP began to be studied graphically. The decrease in cerebral blood flow was virtually continued (linearly extrapolated), projecting it to its zero value, recording the ABP corresponding to zero flow as the CrCP. These methods can be displayed graphically for better understanding.

20.4 Parameters to Monitor

The methods which estimate CrCP use two parameters to measure CrCP: ABP and CBF. Continuous recordings of both variables have to be obtained in order to calculate the ABP value at which flow stops. Changes in CBF, as explained above, are estimated by a surrogate method: CBFV measured with TCD. This allows continuous monitoring of CBF changes occurring over time in one or both middle cerebral arteries. Although TCD does not measure CBF in absolute values, CBFV changes are proportional to CBF changes.

There are two types of methods to estimate CrCP:

1. What we will call "graphic" methods, based on comparing how the simultaneous waves of ABP and CBFV behave graphically and calculate CrCP based on this comparison.
2. Multiparameter or impedance methods, which add other high-frequency parameters of cerebral circulation, can be derived from CBFV and ABP, such as arterial compliance and cerebrovascular resistance, heart rate, and angular frequency.

Impedance concept is similar to resistance, but it varies with the cyclic variation of the waves. Therefore, the multiparametric models use the value π ("pi") and the heart rate. These impedance methods have been initially described using ICP in their formula, but eventually they were also calculated without this parameter if ICP value was considered to be normal.

Details for its measurement or estimation can be seen in the appendix.

20.5 Clinical Importance of Critical Closing Pressure

We will review here the most important experimental and clinical publications on this subject.

20.5.1 Critical Closure Pressure During Vasospasm in Patients with Subarachnoid Hemorrhage

Two papers were published by Czosnyka and coworkers [9, 10] (2004 and 2014).

(a) The first one prospectively evaluated 32 patients with SAH. Patients were followed with daily TCD studies, diagnosing vasospasm when mean blood flow velocity (MFV) was greater than 120 cm/s, and Lindegaard ratio was greater than 3. CrCP was studied with two graphic-based methods [appendix]. Vasospasm was identified in 18 patients. Three patients were excluded because vasospasm was bilateral. In the 15 patients that were eventually included in the study, two comparisons were performed: (1) the level of baseline, pre-vasospasm CrCP was compared with the intra-vasospasm level and (2) CrCP ipsilateral to vasospasm was compared with contralateral (no vasospasm side) CrCP (Fig. 20.2).

(b) In the second study, also carried out by members of the same group 10 years later, CBFV and ABP records of 52 patients with SAH in whom cerebral vasospasm of the cerebral arteries had been diagnosed with TCD were retrospectively studied. The diagnosis of vasospasm was made with the measurement of CBFV and Lindegaard ratio with TCD, using the same criteria as in the previous (2004) study. They used the impedance model described by Varsos (using CPP in the formula in patients who had ICP monitoring, and ABP in those without ICP). Since CrCP expresses the sum of intracranial pressure (ICP) and vascular wall tension, the researchers used the estimation of CrCP to indirectly evaluate the changes in vascular tone that occur in small vessels distal to vasospasm. From the pathophysiological point of view, when vasospasm develops, the caliber of the spastic cerebral conductance arteries decreases, thereby increasing the resistance to flow in that proximal sector.

This leads to a perfusion pressure decrease at the zone distal to vasospasm. If autoregulation is maintained, the small arteriolar vessels of the hypoperfused area, responsible for the so-called cerebrovascular resistance, will dilate, decreasing resistance so that perfusion is maintained. This response decreases these vessels' wall tension.

The development of cerebral arteries vasospasm caused significant decreases in CrCP, without any significant change observed in ICP. Vasospasm, as in the previous study, induced asymmetry; CrCP ipsilateral to vasospasm of cerebral arteries was significantly lower than contralateral. Patients with poor clinical outcomes (at discharge and at 3 months) had a significantly lower CrCP after the onset of cerebral vasospasm. In other words, they also verified that CrCP is reduced in the presence of cerebral vasospasm in both temporal and spatial evaluations. Since ICP remained unchanged during vasospasm of the cerebral arteries, all the change in CrCP was attributed to a decrease in cerebrovascular resistance (CrCP = ICP + WT). This agrees with the interpretation that CrCP evaluates the change in wall tension of small resistance vessels distal to vasospasm. They dilate during vasospasm as an autoregulatory response to a decrease in regional perfusion pressure of the area irrigated by spastic arteries.

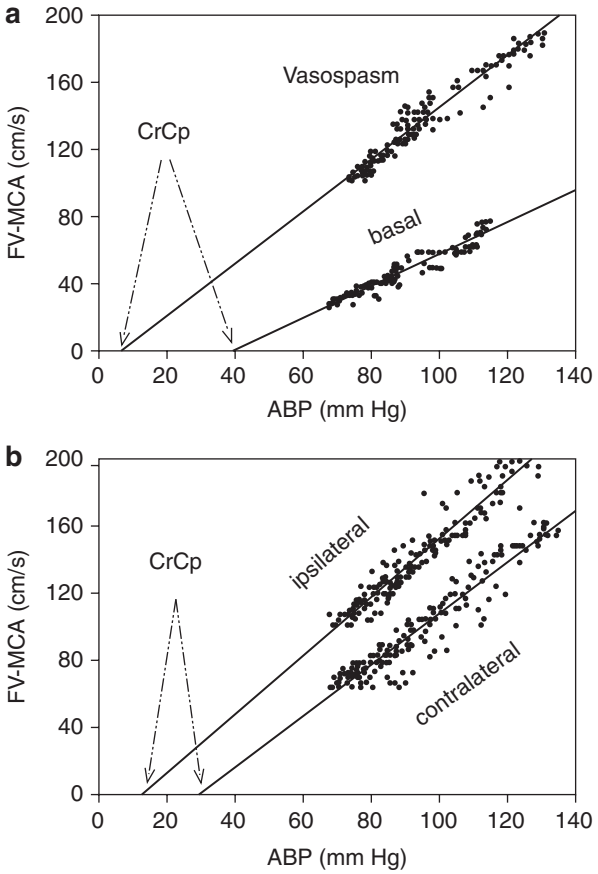

Fig. 20.2 Critical closing pressure values in two different patients [modified from [7]] Critical closing pressure (CrCP) in a patient who developed vasospasm in the middle cerebral artery (FV_{MCA}) is shown in panel "a". CrCP value during vasospasm was lower than 10 mmHg, while the baseline value, prior to the onset of vasospasm, was 40 mmHg. In panel "b" the difference in CrCP between the vasospasm side and the contralateral (no vasospasm), is shown, with values close to 15 and 30 mmHg respectively. In this way, a temporary and regional evaluation of the changes of the CrCP was obtained. A CrCP decrease was demonstrated in cerebral vasospasm. The hypothesis of the researchers was the opposite, since they had assumed that the increase in resistance caused by middle cerebral artery vasospasm would increase CrCP. The importance of distal vasodilation of small arteriolar vessels, as the origin of this decrease in CrCP is underlined. Since TCD insonates the spastic segment, the increased FV at this level is the result of a decrease in the diameter of the artery; on the other hand, the decrease in cerebrovascular resistance is due to arteriolar reactive vasodilation. [ABP: arterial blood pressure]

20.5.2 Critical Closing Pressure and Intracranial Hypertension

With controlled increase in ICP in patients with normotensive hydrocephalus, we will refer to two research papers on ICP-controlled increase in patients with normotensive hydrocephalus.

(a) Monitoring data obtained in a clinical study in patients with suspected normotensive hydrocephalus were retrospectively used to study CrCP and its changes during a controlled rise in ICP [11]. The lumbar infusion test evaluates how cerebral hemodynamics reacts to an increase in volume; in patients with normotensive hydrocephalus, it helps to predict the need for placement of a peritoneal ventricular shunt or to change a dysfunctional shunt. Thirty-seven patients were studied. ICP was recorded by means of a lumbar catheter, continuous noninvasive ABP with Finapres and CBFV with TCD, during a slow lumbar infusion of normal saline. CrCP was calculated using three methods: A method described by Aaslid using the first harmonics of ABP and CBFV pulsatile waveforms and two methods based on Varsos cerebrovascular impedance model, using CPP or ABP [appendix]. They found good agreement among the three CrCP calculation methods, with correlation coefficients greater than 0.8. During the controlled increase in ICP, CrCP values increased significantly with all three methods. The strongest correlation between ICP and CrCP was found for the impedance method that used CPP in its formula. This study evaluates and compares the three methods. With the Aaslid method [appendix], negative results of CrCP frequently appear; they were not observed with the impedance multiparameter methods. These researchers conclude that invasive CrCP (Varsos method including CPP instead of ABP) is more sensitive to variations in ICP and can be used as an indicator of the reserve of the cerebrovascular system during infusion tests. The authors do not discuss the origin of the increase in the CrCP in this work. As CrCP is the sum of two components, ICP and parietal tension, the interpretation of this CrCP increase has to be searched in the behavior of these two parameters. ICP increased (it was the objective of the test). Wall tension may have decreased or increased, since the change in the vasoconstriction or vasodilation state of the resistance arterioles depends on the CPP that reaches the arteriolar sector and the state of autoregulation. In the event of an increase in ICP without compensation, CPP would go down, but a reflex increase in ABP may turn up to maintain (or even raise) CPP. In case of a not compensated decrease in CPP, this should cause an autoregulatory response with vasodilation of small resistance vessels, with a decrease in wall tension. If CPP were maintained, there would be no changes in wall tension, and if it increased, the normal autoregulatory response would generate an increase in resistance. We can conclude that compensatory vasodilation, if it existed, was of a lesser degree than the rise of ICP.

(b) Another work by Varsos et al. [12] studied the possible correlations between cerebral hemodynamic indices based on CrCP and the compensatory dynamics of cerebrospinal fluid, also evaluated during lumbar infusion tests. They evaluated data from 34 patients with normotensive hydrocephalus undergoing infusion tests, with simultaneous monitoring of CBFV by TCD. CrCP was calculated from the monitored signals: ICP, ABP, and CBFV, while the vascular wall tension was estimated as WT = CrCP - ICP. The closing margin was calculated as the difference between ABP and CrCP. ICP increased during the infusion from 7 ± 5 to 25 ± 11 mmHg (mean ± SD), which caused an increase of CrCP of 23%, with WT decreasing by 11% due to vasodilation. CM showed a tendency to decrease, although not significantly, due to a 9% increase in ABP. In general, CrCP increases and WT decreases during infusion tests, while the initial CM may act as an indicator that characterizes the compensatory reserve of the cerebrospinal sector.

20.5.3 Spontaneous Increase in ICP in Patients with Neurotrauma

This second study aimed to describe the behavior of CrCP and WT during spontaneous increases in ICP, with the characteristics of plateau waves. The objective of this work was to quantify the ischemic risk during these waves. These researchers used Varsos's multiparametric method, which is based on the cerebrovascular impedance module. Arteriolar WT was estimated as CrCP–ICP. Clinical data included records of ABP, ICP, and CBFV of 38 plateau wave events, recorded in 20 patients with TBI. CrCP increased significantly from 52 ± 9 mmHg at the beginning of the study to 63 ± 11 mmHg at the top of the plateau waves (mean ± SD; $p < 0.001$). WT decreased significantly during plateau waves by 34.3% ($p < 0.001$), which is in favor of their vasodilator origin. No non-physiological negative values of CrCP were observed that have been described with the traditional methods for its calculation; therefore, the method used resulted in a more plausible estimate of the CrCP than the "graphic" methods. The researchers conclude that increased CrCP during plateau waves increases the likelihood of cerebral vascular collapse and zero flow when the difference: ABP–CrCP ("the collapsing margin") becomes zero or negative.

20.5.4 Critical Closing Pressure in Septic Patients

20.5.4.1 Experimental Endotoxemia

A prospective study in critical care studied CrCP in 40 volunteers and 10 septic patients [13]. An experimental endotoxemia was generated in volunteers by the administration of bacterial lipopolysaccharides (LPS). The registered changes were

compared with those of 10 septic patients with or without septic shock. CrCP was estimated using the cerebrovascular impedance model, recording CBFV and invasive ABP (no ICP). Volunteers who received LPS were randomized to receive an infusion of one of the following vasopressor drugs: norepinephrine (NE), phenylephrine (PhE), or vasopressin (VP). The corresponding vasopressor drug was started 1 hour before the administration of LPS, and the infusion was administered for 5 hours. In the third group, placebo was administered. In septic patients, the decision to use vasopressors and fluids, as well as which fluid to use, was freely taken by the treating medical team. The objective was to achieve normovolemia and an average blood pressure > 65 mmHg, using NE.

The LPS bolus was followed by a decrease in CrCP, without differences between groups.

In septic patients, CrCP was 35.7 mmHg, lower than that presented by volunteers after receiving LPS. After the administration of LPS, CBFV decreased, most likely as a result of the decrease in Circle of Willis outflow to the middle and anterior cerebral arteries, not compensated for by distal vasodilation. This decrease in flow shows that autoregulation is not functioning at the pressures studied. However, the decrease in CrCP maintains for a longer time an adequate effective cerebral perfusion pressure constituting a protective mechanism against ischemia. The authors conclude that human experimental endotoxemia results in a decrease in CrCP due to the decrease in resistance of the cerebral arterial bed (arteriolar dilation), which is not prevented by vasopressors. The alterations presented in septic patients are similar to those of volunteers who are administered LPS.

20.5.5 Critical Closing Pressure in Survivors of Cardiac Arrest

A study estimated CrCP during post-cardiac arrest syndrome (post-CA) and determined whether it differs between survivors and non-survivors [14]. It also compared post-CA patients with normal controls. This prospective observational study was conducted in the ICU of a tertiary university hospital in Nijmegen, the Netherlands. Eleven patients in coma resuscitated from CA, treated with mild therapeutic hypothermia, and 10 normal controls were studied. CBFV was recorded in the middle cerebral artery at several time points after admission to the ICU. CrCP was determined by Varsos model using ABP instead of CPP. CBFV at ICU admission was similar in patients who survived and in those who died, but throughout the observation period it increased in patients who evolved to death compared to survivors. Immediate post-CA CBFV was significantly lower in survivors compared to normal controls, with a gradual restoration to normal values. CrCP decreased significantly from 61 mmHg to 42 mmHg in the first 48 hours and remained stable. CrCP was significantly higher in survivors compared to non-survivors. CrCP immediately post-CA was also significantly higher compared to the control group. The researchers concluded that CrCP rises post-CA with high cerebrovascular resistance and low CBFV. This means that the effective CPP or closing margin is lower, suggesting that cerebral perfusion pressure should be maintained at a sufficiently high level in

patients in post-CA, to avoid further ischemic brain damage. On the other hand, the lack of normalization of the cerebrovascular profile can be a predictor of poor results.

20.6 Conclusion

Intracranial hypertension, during controlled (infusion tests) or spontaneous (plateau waves) ICP increases, causes an increase in CrCP, and simultaneously a lower closing margin with higher risk of ischemia if we are guided by CPP calculated as ABP–ICP. CrCP decreases in sepsis, which helps to maintain longer adequate effective cerebral perfusion pressure constituting a protective mechanism against ischemia.

Appendix

Methods

Methods used to measure CrCP can be divided into two groups. All are based on data acquired with ABP and TCD, at a frequency that allows to reproduce arterial pulse and CBFV waves, for example, at 50 Hz (50 measurements in 1 second).

Group 1: Graphic Methods

The first group is based on "graphic" concepts. The data used are non-invasive. It assumes that the relationship between flow and pressure is linear; therefore, when pressure falls below the minimum value recorded in the patient, the flow pressure relationship would be unchanged.

Changes in cerebral blood flow (through changes in CBFV) and arterial blood pressure are graphically evaluated; the line of best fit between recorded values is found and its equation is calculated. This line is extrapolated to cross the pressure axis at a point (CrCP) where flow would be theoretically zero. There are three different models using this approach.

Method Using the Values of Several Pulse Waves ("Systo-Diastolic Method")

Several simultaneous ABP and CBFV waves are selected, and only the maximum (systolic) and minimum (diastolic) values of each one are plotted, ABP in the x-axis and CBFV in the y-axis. Thus, a cloud of systolic points and another of diastolic

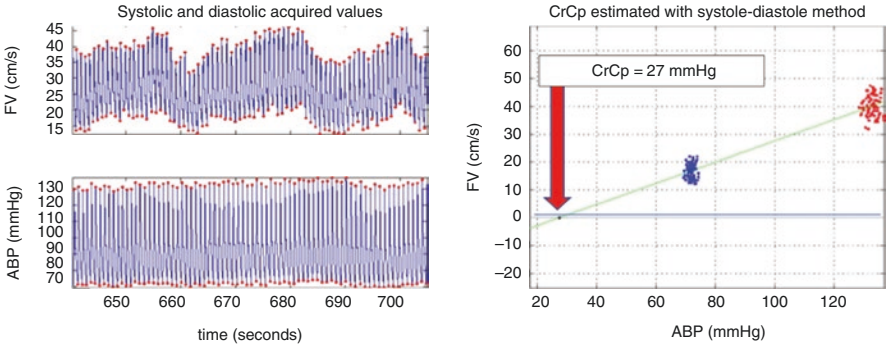

Fig. 20.3 Systole and diastole method. All waves of a certain time period are studied. In this case about 100 seconds. Two values are obtained from each BFV pulse wave: maximum systolic and final diastolic. The same process is repeated with the maximum and minimum values of each ABP wave (left panel). These values are shown on a scatterplot (right panel) displaying BFV in the abscissa (cm/s) and ABP in the ordinates (mmHg). Two point clouds are thus obtained: one with the systolic values of the selected BFV and ABP pulsatile waves (red line around the blue wave) and another with their diastolic values (blue wave). A line of best fit is inserted between these points. The ABP point corresponding to the BFV zero value is the CrCP. In this example, the value of CrCP is 27 mm Hg

points are obtained. These clouds are joined with the corresponding best fit line, and this line is extrapolated to zero flow. The cut-off point of this line on the ABP axis (zero flow) corresponds to CrCP (Fig. 20.3).

"Beat-by-Beat Method"

Instead of using several beats, one value per pulse is calculated. The descending values of a CBFV wave (in most models all points—ascending and descending—are used) are plotted against the simultaneous descending values of ABP (each point in the ABP pulse curve has its corresponding point in the descending part of the CBFV pulse curve). CBFV does not reach zero in diastole, but the line with the best fit is extrapolated to the zero-flow point. The point in the abscissa (ABP) where this line reaches zero corresponds to the CrCP value (Figs. 20.4 and 20.5).

Method Described by Aaslid

This method is similar to the previous ones, but instead of taking the recorded ABP and CBFV values, the values of the first harmonic of both variables are taken. It has the advantage of eliminating the upper harmonics that distort the arterial wave. It uses Fourier analysis to determine the amplitude of the first harmonic in the ABP and in the CBFV register. With this approach, it is possible to perform the regression analysis with almost perfect linear data. Using the value of the first harmonic

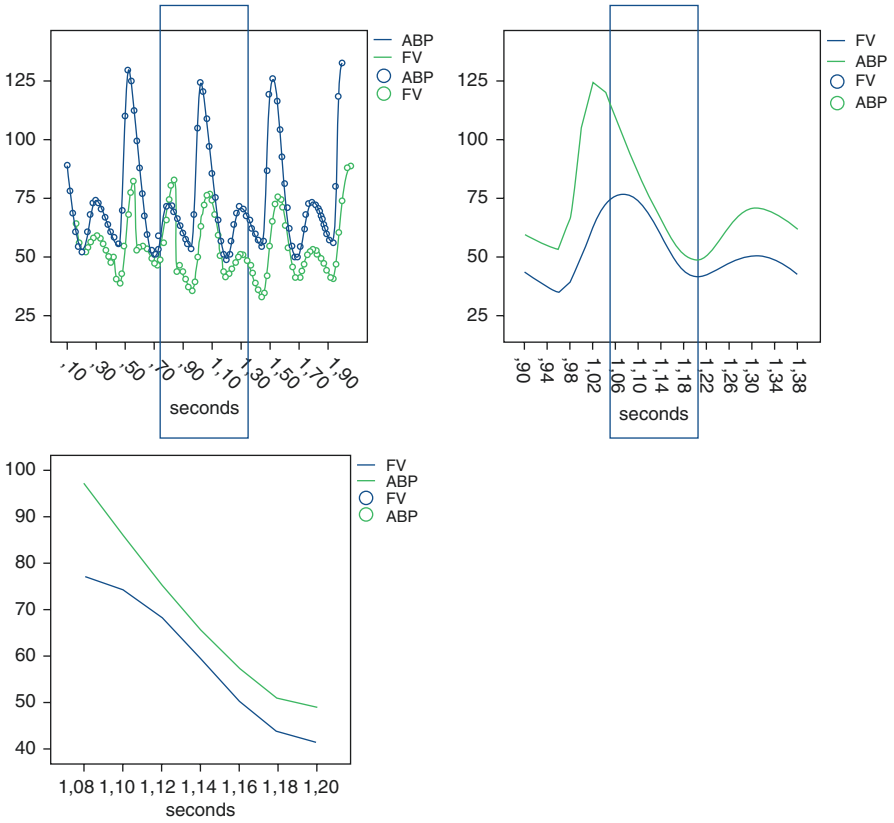

Fig. 20.4 "Beat to beat" measurement method of the critical closing pressure of the cerebral circulation. CrCP is studied for each pulse. The record of several simultaneous waves of arterial blood pressure (ABP) and BFV is displayed on the left panel. A blue rectangle shows an ABP wave and the simultaneous PV wave. The values of the descending zones of each beat are displayed in blue in the central panel. The simultaneous studied data is shown in the right panel

eliminates, the distortions generated by the fact that the measurements are recorded at different sites and with artifact values due to the Windkessel effect. The Windkessel effect is the cushioning effect that ensures that the blood flow that is generated intermittently in the heart reaches the arteries, arterioles, and capillaries continuously. The ideal way of measuring these parameters (but for now impossible in clinical practice) would be to take both measures at the brain level. Actually, ABP is measured far away from cerebral arteries, such as the radial artery. In this location, the wave is distorted with respect to what would be recorded directly in the cerebral vessels. This is due to the transmission of the pulse and the existence of reflections or reverberations of the waves. The high-frequency components of the wave are more distorted than the fundamental component (first harmonic). Therefore, eliminating the error caused by higher frequency harmonics before processing the data

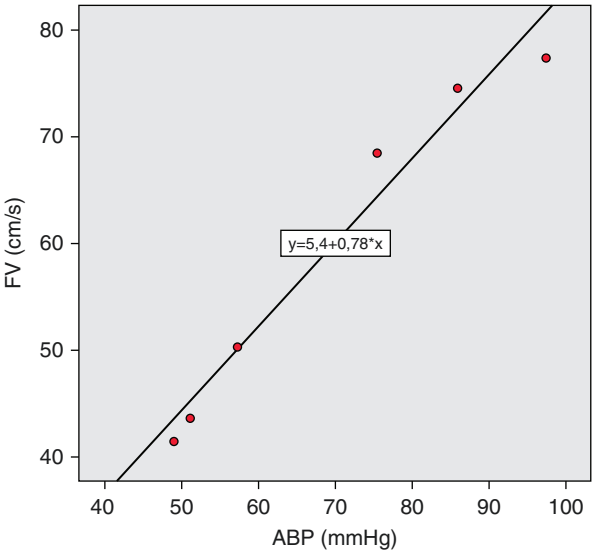

Fig. 20.5 Linear correlation between data shown in (Fig. 20.3), right panel. Each point in this graphic corresponds to a ABP and CBFV (FV) simultaneous value. The best fit line is calculated and its linear extrapolation to zero flow crosses ABP axis at a value which is the CrCP of this pulse wave. In this case the value is higher than 40 mm Hg

results in a more accurate estimate of the CrCP. For this reason, the waves are analyzed with a Fourier transform, which finds the amplitude of the first harmonic of both the ABP and the BFV, and its relative intensity. With this model, the formula that calculates the intersection of the descent of the flow with the axis of the abscissa, corresponding to zero flow, is the following:

$$\mathrm{CrCP_f} = \left(\mathrm{ABP_0} - \mathrm{CBFV_0}\right) \times \left(\mathrm{ABP_1} / \mathrm{CBFV_1}\right)$$

where $\mathrm{CrCP_f}$ is the critical "filtered" closing pressure (calculated with the variables devoid of the mentioned distortion); $\mathrm{ABP_0}$ and $\mathrm{CBFV_0}$ refer to the average values of ABP and CBFV of each beat; and $\mathrm{ABP_1}$ and $\mathrm{CBFV_1}$ refer to the amplitude of the first harmonic of ABP and CBFV (after the higher frequency components have been removed).

The above-analyzed methods, or "graphic methods," are based on the shape of the recorded waves. They have the main drawback that negative, non-physiological CrCP values may result. If we rethink the concept of critical closure pressure, such as the blood pressure at which the circulation stops, we cannot find a plausible physiological or pathophysiological explanation. Anyhow, these approaches can be used to see the trends of CrCP over time, evaluating the effects of drugs, pathological situations, etc., on the state of vasodilation or vasoconstriction of the arteriolar bed, and not as an absolute value. These values away from the physiological values are probably due to the fact that in the "graphic" models it is assumed that there is a linear relationship between the variables, a circumstance that is probably more complex.

Group 2: Multiparameter or Impedance Methods [14]

To overcome the negative value problem, researchers at the University of Cambridge have generated a more complex model, multiparameter model, or "impedance" model [14].

It is called multiparameter because, in addition to the values recorded directly from the ABP and the CBFV, it uses other parameters derived from the cerebral circulation for CrCP calculation. Several of them originate in turn from ABP and CBFV, such as arterial complacency and cerebrovascular resistance. The formula also uses heart rate, which can be inferred from any of the registers, from ABP or CBFV. Impedance is a similar concept to cerebrovascular resistance, but variable throughout the cycle (remember that the circulation is pulsatile). The formula used is

$$\mathrm{CrCP} = \mathrm{ABP} - \frac{\mathrm{CPP}}{\sqrt{\left(\mathrm{CVR} \times \mathrm{Ca} \times \mathrm{HR} \times 2\pi\right)^2 + 1}}$$

As we can see, CPC value is included in this formula (CPP = ABP – ICP). However, in patients in whom there is no suspicion of an increase in ICP, this same formula has been used with ABP instead of ICP.

References

1. Nichol J, Girling F, Jerrard W, Claxton EB, Burton AC. Fundamental instability of the small blood vessels and critical closing pressures in vascular beds. Am J Phys. 1951;164:330–44.
2. Czosnyka M, et al. Critical closing pressure in cerebrovascular circulation. J Neurol Neurosurg Psychiatry. 1999;66:606–11.
3. Panerai RB, et al. The critical closing pressure of the cerebral circulation. Med Eng Phys. 2003;25:621–32.
4. Aaslid R, Lash SR, Bardy GH, Gild WH, Newell DW. Dynamic pressure—flow velocity relationships in the human cerebral circulation. Stroke. 2003;34:1645–9.
5. Thees C, et al. Relationship between intracranial pressure and critical closing pressure in patients with neurotrauma. Anesthesiology. 2002;96:595–9.
6. Jägersberg M, Schaller C, Boström J, Schatlo B, Kotowski M, Thees C. Simultaneous bedside assessment of global cerebral blood flow and effective cerebral perfusion pressure in patients with intracranial hypertension. Neurocrit Care. 2010;12:225–33.
7. Varsos GV, et al. Critical closing pressure during intracranial pressure plateau waves. Neurocrit Care. 2013;18:341–8.
8. Varsos GV, et al. Cessation of diastolic cerebral blood flow velocity: the role of critical closing pressure. Neurocrit Care. 2014;20:40–8.
9. Soehle M, Czosnyka M, Pickard JD, Kirkpatrick PJ. Critical closing pressure in subarachnoid hemorrhage: effect of cerebral vasospasm and limitations of a transcranial Doppler-derived estimation. Stroke. 2004;35:1393–8.
10. Varsos GV, et al. Cerebral vasospasm affects arterial critical closing pressure. J Cereb Blood Flow Metab. 2015;35:285–91.
11. Kaczmarska K, et al. Critical closing pressure during controlled increase in intracranial pressure-comparison of three methods. IEEE Trans Biomed Eng. 2018;65:619–24.

12. Varsos GV, et al. Cerebral critical closing pressure during infusion tests. Acta Neurochir Suppl. 2016;122:215–20.
13. Van den Brule JMD, et al. Vasopressors do not influence cerebral critical closing pressure during systemic inflammation evoked by experimental Endotoxemia and Sepsis in humans. Shock. 2018;49:529–35.
14. Van den Brule JM, Vinke E, van Loon LM, van der Hoeven JG, Hoedemaekers CW. Middle cerebral artery flow, the critical closing pressure, and the optimal mean arterial pressure in comatose cardiac arrest survivors-an observational study. Resuscitation. 2017;110:85–9.

Chapter 21
Transcranial Doppler Ultrasound Pulsatility Index: Utility and Clinical Interpretation

Oscar M. Pinillos, Camilo N. Rodríguez, and Ryan Hakimi

Key Points

1. Physical examination of a critically ill patient with acute primary or secondary neurological injury is often insufficient for medical decision making. Transcranial Doppler/transcranial color coded sonography (TCD/TCCS) is a useful physiologic tool allowing one to individualize the management of each patient to optimize cerebral hemodynamics.
2. Pulsatility index (PI) is calculated by subtracting the peak systolic velocity (PSV) from the end diastolic flow velocity (EDV) and dividing the difference by the mean flow velocity (MVF); [PI = (PSV − EDV)/MVF].
3. Pulsatility Index is dependent on multiple variables including cerebrovascular resistance (CVR).
4. Despite the correlative value of PI obtained from TCD/TCCS, the external ventricular drain remains the gold standard in the measurement of intracranial pressure (ICP).

O. M. Pinillos
Intensive Care Medicine, Clinica de Occidente, Cali, Colombia

Neurointensive Care section - AMCI, Bogotá, Colombia

C. N. Rodríguez (✉)
Intensive Care Medicine, Hospital Nacional Prof. Dr. A. Posadas, University of Buenos Aires (UBA), Neurointensive Care Section - ESICM, Neurointensive Care Section - AMCI, Neurointensive Care Committee - FEPIMCTI, Member of ESNCH, Buenos Aires, Argentina
e-mail: camilo.rodriguez@nesccco.com

R. Hakimi
Department of Medicine (Neurology), USC School of Medicine-Greenville, Greenville, SC, USA

Neuro ICU, TCD Services, Prisma Health-Upstate, Greenville, SC, USA

American Society of Neuroimaging (ASN), Minneapolis, MN, USA

C. N. Rodríguez et al. (eds.), *Neurosonology in Critical Care*,
https://doi.org/10.1007/978-3-030-81419-9_21

5. The absolute numerical value of the PI is less valuable than the PI trend in a given patient when assessing ICP.
6. The PI numerically reflects changes in the morphology of the TCD/TCCS waveform, which is dependent on cerebral perfusion pressure and changes in CVR.

21.1 Introduction

Obtaining a comprehensive medical history and performing a thorough neurological examination is always the first step in assessing patients with acute neurological injury. However, critically ill neurological patients often require sedation or analgesia limiting their clinical examination.

During the course of a neurocritical care patient's ICU stay, there are frequent fluctuations in a given patient's ICP and cerebral hemodynamics (PSV, MFV, EDV, etc.) which represent the evolution of the acute neurological injury. These factors are important in assessing and mitigating the extent of secondary brain injury and its severity and duration and clinically correlate with the patient's ultimate outcome.

Transcranial Doppler ultrasonography (TCD) and transcranial color-coded Duplex sonography (TCCS) are non-invasive, bedside, portable tools for the assessment of cerebral hemodynamics (Table 21.1) and detection of focal stenosis, arterial occlusion, monitoring the treatment effect of intravenous tissue plasminogen activator and assessment of vasomotor reactivity. These instruments display spectral waveforms that represent the depth, direction, and intensity of the blood flow through the intracranial vasculature. Although these instruments do not measure blood flow directly, the parameters they do calculate do correlate with cerebral blood flow (CBF) [1].

In the past, TCD machines were only able to display a spectral waveform. The operator was left to deduce which vessel was being insonated by attempting to obtain the same waveform or an inverted version of the same waveform using a variety of different approaches, termed windows, at different depths. With the addition of power motion–mode Doppler (PMD), sonographers are able to obtain the spectral waveform as well as knowing the depth of the insonated vessel, the direction of flow relative to the probe and the intensity of the signal.

TCD and TCCS are bedside, non-invasive monitoring tool which provide "real time" clinical information about changes in cerebral perfusion based on cerebral hemodynamics derived from the spectral Doppler waveform. The Pulsatility index

Table 21.1 Transcranial Doppler ultrasonography parameters [1]

PSV (peak systolic velocity)
EDV (end diastolic velocity)
MFV (mean flow velocity) = 1/3 PSV + 2/3 EDV
Pulsatility index = (PSV − EDV)/MFV
Resistivity index = (PSV − EDV)/PSV
Lindegaard ratio = (MFV of middle cerebral artery)/MFV of ipsilateral extracranial internal carotid artery

Courtesy Hakimi et al. [1]

(PI) [Gosling's Index] is the most commonly used measure of the pulsatility of TCD/TCCS waveforms.

21.2 TCD/TCCS: Interpretation of Pulsatility Index (PI)

Conventional TCD is a "blind" technique wherein the location of the intracranial vessels is ascertained based on depth, direction, and waveform morphology. In contrast, TCCS offers a non-invasive means of evaluating cerebral blood flow (CBF) hemodynamics (flow velocities and indices) in the intracranial arterial and venous vasculature with color and spectral Doppler as well as structural imaging of the brain [2, 3].

Optimization of CBF and oxygen delivery are the key goals of neurologic management of patients with traumatic brain injury. Historically, this has been monitored by measuring ICP and monitoring cerebral perfusion pressure (CPP). However, this model is inadequate because some patients have poor neurologic outcomes despite appropriate management of these two parameters. Among non-invasive modalities, TCD is the most accurate tool for measuring brain perfusion at the bedside [33].

The brain's cerebral perfusion is maintained in both systole and diastole, as shown by the systolic and diastolic component of the TCD waveform. In contrast, the hand is perfused only in systole, as shown by a radial arterial line waveform. This difference is caused by the marked difference in resistance, with the brain being a low-resistance system and the hand being a high-resistance system, as well as the higher energy requirements of the brain compared with the hand. Therefore, the adequacy of CBF can be assessed by evaluating the diastolic component of the TCD waveform and ensuring that its amplitude is approximately half of the peak systolic amplitude. If it is less, the clinician can:

(a) Increase the patient's blood pressure using IV fluids, vasopressors, or by giving a blood transfusion
(b) Decrease the $PaCO_2$ by increasing the respiratory rate on the ventilator (with intubated patients) or increasing the patient's sedation
(c) Reducing the patient's ICP by cerebrospinal fluid diversion, increasing sedation, or treating the patient's fever, among other means (Fig. 21.1)

TCD can non-invasively monitor cerebral perfusion by the diastolic component of the spectral waveform (EDV). Left panel shows high-resistance waveforms with EDV (CBF) is not static. The cardiac cycle, through systolic blood pressure increase, causes regular variations in blood flow into the brain that are synchronous with the heart. The brain is contained in a rigid vault. Therefore, these pulsations in flow and pressure are transferred into brain tissue, intracranial blood volume, and cerebrospinal fluid (CSF) [4].

In the brain, these variations are due to the variation in arterial blood pressure (ABP) over the cardiac cycle (beat by beat), known as cardiac pulsatility. However,

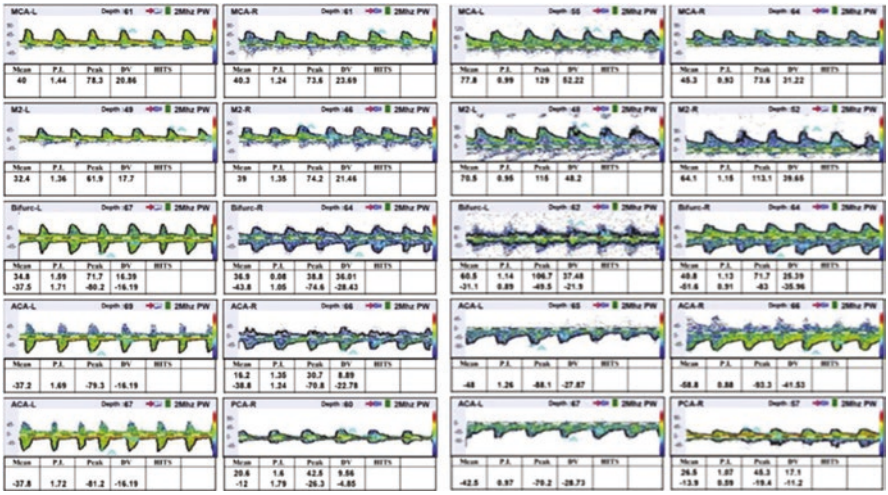

Fig. 21.1 TCD can non-invasively monitor cerebral perfusion by assessing the diastolic component of the spectral waveform (EDV). Left panel shows high resistance waveforms with EDV less than 50% of the PSV. The patient then had an external ventricular drain placed (right panel) and the pulsatility indices normalized resulting in an increase in the diastolic component of the waveform such that the EDV is greater than 50% of the PSV. (Courtesy Hakimi et al. [1])

there are other pulsatile variations, such as respiratory and vasomotor induced oscillations, which affect pressure and flow over time but have less of an effect than cardiac cycle-induced variations.

Variations in cardiac output (through preload, contractility, and afterload) have two distinct effects on intracranial hemodynamics (brain pulsatility):

1. *Variations in brain arterial blood pressure*
   [Pressure pulsation]
2. *Variations in brain blood flow*.
   [Flow Pulsation]

When we approach the interpretation and measurement of brain pulsatility via PI, we should consider: (Figs. 21.2, 21.3, and 21.4) [4].

1. The intracranial pressure (ICP) monitoring is used to measure pressure pulsatility and requires placement of a pressure sensor within the brain. Pressure-based measure of brain pulsatility.
   [Measure of Pressure Pulsatility]
2. TCD/TCCS measures the velocity of CBF and displays it as a spectral waveform, where the net flow can be determined by the area under the curve.
   [Measure of Flow Pulsatility]

It is important to consider that PI obtained with TCD/TCCS is derived from blood flow velocity pulsatility (arterial/venous flow), which correlates with the pressure pulsatility (ICP) obtained with invasive intracranial pressure monitoring, but is not necessarily a linear correlation.

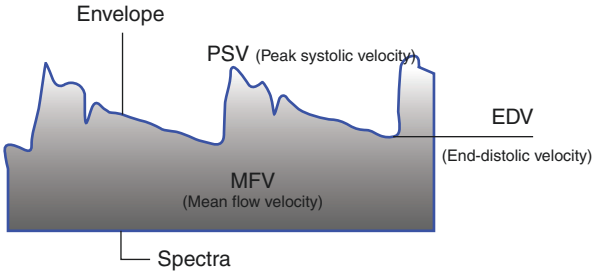

Fig. 21.2 ICP and TCD/TCCS normal waveforms: TCD/TCCS spectral Doppler waveform with its pulsatile component (PSV, EDV, and MFV) to calculate the transcranial Pulsatility Index (PI) which represents the flow pulsatility. (Blue line): Envelope wave

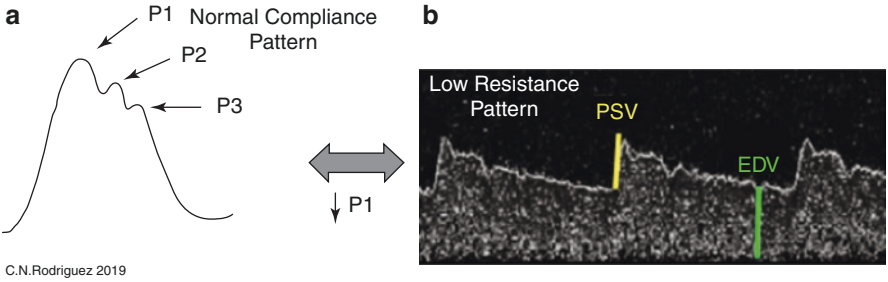

Fig. 21.3 Relationship between ICP waveform and spectral Doppler waveform. (**a**) Pressure pulsatility: ICP waveform obtained via invasive monitoring with normal compliance pattern (P1 > P2). (**b**) Flow pulsatility: spectral Doppler waveform with a low resistance pattern (High EDV and low PSV). When these two sets of waveforms are obtained, one would expect a low or normal PI (pulsatility index)

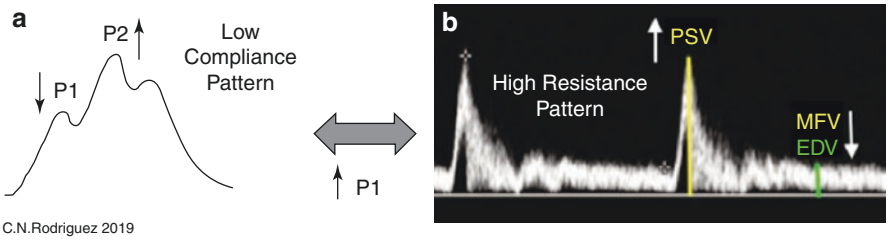

Fig. 21.4 Relationship between ICP waveform and Spectral Doppler waveform. (**a**) Pressure pulsatility: ICP waveform from invasive monitoring with low compliance pattern (P2 > P1). (**b**) Flow pulsatility: Spectral Doppler waveform with a high resistance pattern (low EDV, low MFV and high PSV). When these two sets of waveforms are obtained, one would expect a high PI (pulsatility index)

TCD/TCCS are valuable tools when integrated with other clinical information in the proper clinical context (Figs. 21.3 and 21.4).

21.2.1 Brain Compliance

Compliance is the relationship between intracranial volumes and pressure. It is the property of the brain to maintain a stable ICP, despite variations in intracranial volumes (Eq. (21.1))

$$\mathrm{C}\left(\text{compliance}\right) = \Delta V / \Delta P \tag{21.1}$$

- Δ V: Variations in volume
- Δ P: Variations in pressure

This compliance is comprised of four main components:

1. Brain tissue compliance
2. Arterial compliance
3. Venous compliance
4. CSF compliance

Intracranial compliance is assumed to decrease primarily with increased ICP. Decreased compliance with elevated ICP (initially, before compliance is exhausted and brain impedance overcomes pulsatile blood flow) leads to increased pressure pulsatility.

Transfer of pulsations through either the venous system or CSF is another way in which intracranial pulsatility can also be affected manifesting as a change in either pressure (brain compression) or flow pulsatility (hypoperfusion). Such is the case with venous congestion from sino-venoocclusive disease, extracranial cervical venous stenosis or thrombosis, elevated right atrial pressure, or blockage of CSF outflow pathways (obstructive hydrocephalus) [5].

Pressure pulsatility serves as a sensitive indicator of intracranial compliance. The increase in intracranial pulsatility in obstructive hydrocephalus is most commonly due to raised ICP from ventriculomegaly leading to brain compression (increase brain impedance). However, intracranial compliance also depends on changes in pulse pressure, which depends on changes in cerebral blood volume (CBV) which in turn depends on the presence or absence of preserved cerebral autoregulation.

We can consider two clinical scenarios:

1. *A high compliance system*:
   A large increase in volume will only result in small increase in pressure.
2. *A low compliance system*:
   A small increase in volume can lead to a significant pressure rise.

21.2.2 TCD/TCCS: Cerebral Hemodynamics

TCD/TCCS provides two clinically important measures:

1. Mean blood flow velocity (MFV): a measure of the integrity of cerebral perfusion
2. Pulsatility index (PI): an estimate of cerebrovascular resistance and intracranial compliance [6]

Prevention and treatment of secondary injury are the goals of bedside multimodal monitoring. TCD/TCCS measures systolic, mean, and diastolic CBF velocities and calculates the pulsatility index (PI) from basal intracranial arteries (circle of Willis) allowing for the interpretation of the cerebral hemodynamic behavior in real time. However, the clinical interpretation of the waveform morphology with careful attention to the changes in PSV and EDV is most important as it allows for precision medicine (Fig. 21.4).

Pulsatility index describes quantitative and qualitative changes in the morphology of the TCD/TCCS waveform resulting from cerebral perfusion pressure and cerebrovascular impedance changes [9, 10].

The normal value of pulsatility index, in the most of the arterial territories, is <1.2.(0.6–1.2). However, in the Ophthalmic artery, the PI is higher as it is an "externalized" intracranial vessel demonstrating a high-resistance spectral pattern [8, 11] (Table 21.2).

Some features to remember when interpreting PI:

(a) Consider that the PI is not affected by the angle of insonation [16].
(b) Consider that PI should be interpreted by taking into account variations by sex, age, and ethnicity [15, 17, 18].
(c) PI is dependent on both pulsatility and mean flow velocity (cerebral perfusion). Therefore, an increase in PI may not be strictly related to an increase in pulsatility (decrease intracranial compliance). Rather, it may be related to a decrease in MFV (decreased CBF) [4].

Table 21.2 TCD/TCCS PI values [12–15]

Artery	Pulsatility index (PI)
Anterior cerebral artery (ACA)	0.71–1.04
Middle cerebral artery (MCA)	0.76–1.08
Posterior cerebral artery (PCA)	0.70–1.02
Basilar artery (BA)	0.60–1.03
Vertebral artery (VA)	0.60–1.07
Ophthalmic artery (OA)	>1.2

21.3 Pulsatility Index (PI): Cerebrovascular Resistance (CVR)

The regulation of CBF depends on the interplay between three interconnected components: [19] (Fig. 21.5).

1. *Arterial Blood Pressure (ABP)*
   Systemic blood pressure supplied and the presence or absence cerebral autoregulation
2. *Intracranial Pressure (ICP)*
   Volume of brain tissue, cerebral blood volume, and cerebral spinal fluid volume
3. *Cerebrovascular Resistance (CVR)*
   Diameter of arteriole and/or capillary vessels

In acute neurologic injury, the PI has been shown to be directly related to the distal CVR. Thus, greater PI usually means higher CVR. However, this positive correlation is not seen in two clinical scenarios; namely hypercapnia which causes a decrease in both CVR and PI, and during reductions in CPP with intact cerebral autoregulation (such as systemic hemorrhagic shock) which results in a decrease in CVR, but an increase in PI (Figs. 21.6 and 21.7) [20–22].

21.4 Pulsatility Index (PI): Intracranial Pressure (ICP)

Elevated ICP is the final common pathway of any space-occupying lesion. ICP essentially consists of three components, driven by different patho-physiological mechanisms [23]:

1. *Inflow and volume of arterial blood/venous blood outflow*
   [Blood volume]
2. *CSF circulation*
   [CSF volume]

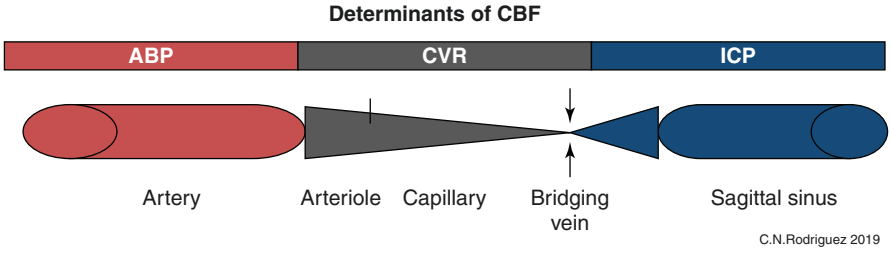

Fig. 21.5 Determinants of CBF: (ABP) arterial blood pressure (arteries); (CVR) cerebrovascular resistance (arterioles, capillaries, bridging veins), and (ICP) intracranial pressure

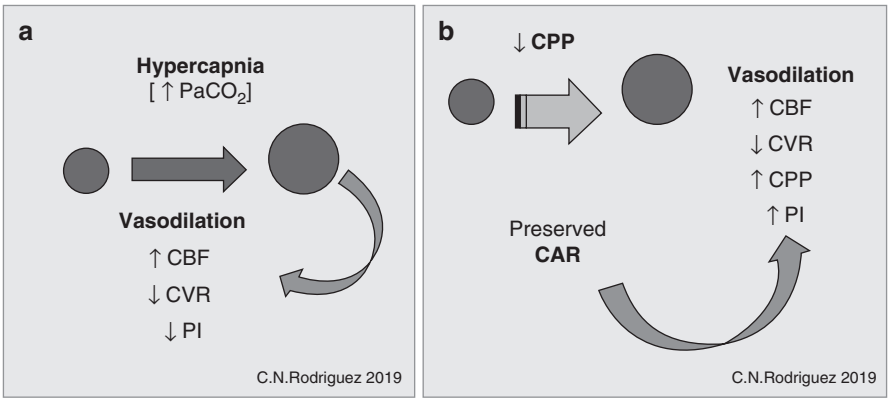

Fig. 21.6 (**a**) Effect of hypercapnia: vasodilation on CBF, CVR and PI. (**b**) Effect of decrease CPP on CBF, CVR, CPP and PI

Heart (Pump)	Considerations
Contractility	Starling's Law Effects SV → Effects CO
Pre-load	Ventricular filling Effects SV → Effects CO
Post-load	Ventricular emptying ←→Ventricular filling Effects SV → Effects CO
Heart Rate Cardiac Rhythm	Effect diastolic phase of the cardiac cycle Ventricular filling Effects SV → Affects CO
ABP (Content)	Considerations
Heart Contractility	Effects CO
Preload	Effects SV → Effects CO
Afterload	Ventricular emptying ↑SVR effects SV → Effects CO ↓SVR (inflammation) → Vasoplegia → Low ABP
Heart rate Cardiac Rhythm	Effects diastolic phase of the cardiac cycle Ventricular Filling Affects SV → Effects CO

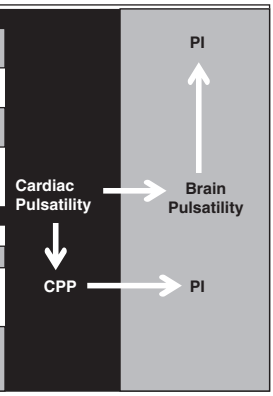

Fig. 21.7 Transcranial Pulsatility Index: Influenced by Cardiovascular factors. ABP arterial blood pressure, SV stroke volume, SVR systemic vascular resistance, CO cardiac output, PI pulsatility index, ↓ low/decrease, ↑ high/increase

3. *Brain parenchyma*
   [Parenchymal volume]

An increase in one component must cause a proportional decrease in the others (Monro-Kellie Doctrine).

When there is an ICP increase, the following changes occur in this order:

1. CSF moves from the intracranial compartment to the spinal canal
2. An increase venous outflow from the cerebral veins
3. Decrease in cerebral arterial inflow (in extreme cases)

One should consider:

1. These compensation mechanisms are temporarily effective.

2. ICP is compartmentalized and not evenly distributed throughout the skull. Therefore, the ICP in the posterior fossa may be quite different than the right middle cranial fossa.

The Guidelines for the Management of Severe Trauma Brain Injury (TBI) [24] recommend ICP monitoring:

1. All salvageable patients with a severe TBI (GCS 3-8 after resuscitation) and an abnormal head computed tomography (CT) scan. A brain CT-scan is deemed abnormal when there is a presence of:

   1.1 Hematomas
   1.2 Contusions
   1.3 Swelling
   1.4 Herniation
   1.5 Compressed basal cisterns

2. In patients with severe TBI with a normal head CT, ICP monitoring is warranted if two or more of the following features are noted on admission:

   2.1 Age over 40 years
   2.2 Unilateral or bilateral motor posturing
   2.3 Systolic blood pressure (BP) <90 mm Hg

3. Other clinical situations supporting the need for ICP monitoring are often based on local practice. The indications for an ICP monitor remain debated in several circumstances [25].

   3.1 Intracranial hemorrhage
   3.2 Coma
   3.3 Cerebral edema
   3.4 Hydrocephalus
   3.5 Hepatic encephalopathy
   3.6 Acute ischemic stroke

Elevated ICP is an important cause of secondary brain injury, and its severity and duration have been correlated with poor outcomes. Intracranial hypertension (a surrogate for poor intracranial compliance) is the most common and harmful complication in the progression of acute neurological injury [26–28]. Therefore, it is important to monitor ICP and to assess the effect of various medical and surgical therapies.

Brain oxygen delivery and CPP optimization has assumed a central role in the real-time treatments of neurocritical care patients (Eq. (21.2)).

$$\mathrm{CPP} = \mathrm{MAP} - \mathrm{ICP} \tag{21.2}$$

- CPP: Cerebral perfusion pressure
- MAP: Mean arterial pressure
- ICP: Intracranial pressure

Cerebral autoregulation (CA) is maintained through variable vascular resistance, wherein the radius of small and large arteries change to maintain constant CBF, over a wide range of CPP values and metabolic changes. Variation in minute ventilation alters the $PaCO_2$ which has a powerful hemodynamic effect in response to metabolic supply and demand (coupling).

Therefore, real-time simultaneous monitoring of ICP and MAP allows one to make the best therapeutic decisions to individualize the patient's CPP. Moreno et al. (2000) describe the relationship between decrease CPP and increase in PI, suggesting a reduction of 1 unit in CPP results in an increase in 0.02 units in the PI [29].

Invasive ICP measurement modalities are considered the Gold Standard and are widely used in neurocritical care populations [30]. However, this procedure has a risk of life-threatening complications and has many contraindications related to device placement and misplacement: principally infections, bleeding, and technical failure [31–34].

Non-invasive ICP estimation would be helpful in clinical situations where the risk-benefit balance of invasive ICP monitoring is unclear or invasive ICP monitoring modalities are not immediately available or are contraindicated [35, 36].

Ideally, a non-invasive ICP monitor should be readily available at the bedside in the ICU, inexpensive, accurate, and simple to use. Using Gosling's pulsatility index, TCD/TCCS, is a validated tool for estimating ICP in certain scenarios [37–40].

When trended, TCD/TCCS can be used to give a rough estimate for ICP (correlated PI to ICP in clinical practice) [29], but not as a surrogate for accurate invasive ICP monitors. When ICP increases, the intracranial blood flow velocities change (PSV increases and EDV decreases), while cerebral vessels narrow from external pressure resulting in an increased resistance to CBF [35, 38, 41, 42].

The clinical correlation and interpretation of the PI depends of several factors: [7, 9, 41, 43, 44].

1. Pulse amplitude of arterial blood pressure
2. Heart rate (HR)
3. CPP
4. $PaCO_2$
5. CV
6. Compliance of the arterial bed (C_a)

Non-invasive ICP, based on TCD/TCCS, had been estimated by different hemodynamic parameters proposal, such as Gosling's pulsatility index (PI), Critical Closing Pressure (CrCP), Optic Nerve Sheath Diameter (ONSD), pupillary light reflex (PLR), straight sinus systolic flow velocity (SSFV) [45], etc. However, none of these methods seem to be accurate enough to be used as a replacement for invasive ICP measurement and, at present, TCD/TCCS is reserved for assessing changes (ICP trends) of non-invasive ICP, rather than absolute ICP.

Other than PI, the mean flow index (Mx) (which is the correlation coefficient between MFV and CPP) and systolic flow index (Sx) (which is the correlation coefficient between PSV and CPP) are useful parameters for assessing increased ICP [46, 47].

21.5 Transcranial Pulsatility Index (PI): Clinical Factors to Consider

The performance and clinical interpretation of the pulsatility index depends on the various physiological and pathophysiological conditions as well as the clinical context of each critical patient (Table 21.3).

We recommend taking into account all cerebrovascular and systemic factors when analyzing a given patient's PI. Consider the following: (Fig. 21.13).

21.5.1 Cardiovascular Factors

The cardiovascular status of the critical patient, with or without acute neurological injury, depends on beat to beat changes in the following hemodynamic parameters:

1.1 CPP (pulsatility pressure)
1.2 CBF (pulsatility flow)

Therefore, the cardiac pulsatility induces real-time changes on the brain pulsatility, resulting in changes in PI (Fig. 21.7) [4, 7, 9].

21.5.2 Cerebrovascular Factors

Except in extreme circumstances, during the primary or secondary injury, the brain will adjust intracranial hemodynamic parameters (Table 21.3) through intracranial compliance changes (Monro-Kellie Doctrine) [48].

Table 21.3 Conditions that can modify TCD/TCCS Gosling's pulsatility index (PI)

Decrease PI	Increase PI
Hypercapnia (high $PaCO_2$)	Hypocapnia (low $PaCO_2$)
Hyperemia	Raised ICP
Vasospasm	Hypothermia
Arteriovenous malformation	Blood hyperviscosity
Anemia	Decrease CPP
Fever	Cerebral circulatory arrest
High cardiac output	Aortic regurgitation
Rewarming following hypothermia	Intracranial artery occlusion
Arterial hypertension	Advanced age
Intracranial artery stenosis	Hypovolemia
VA-ECMO (miss-interpretation)	Bradycardia
	Elevated right atrial pressure

V-A ECMO veno-arterial ECMO

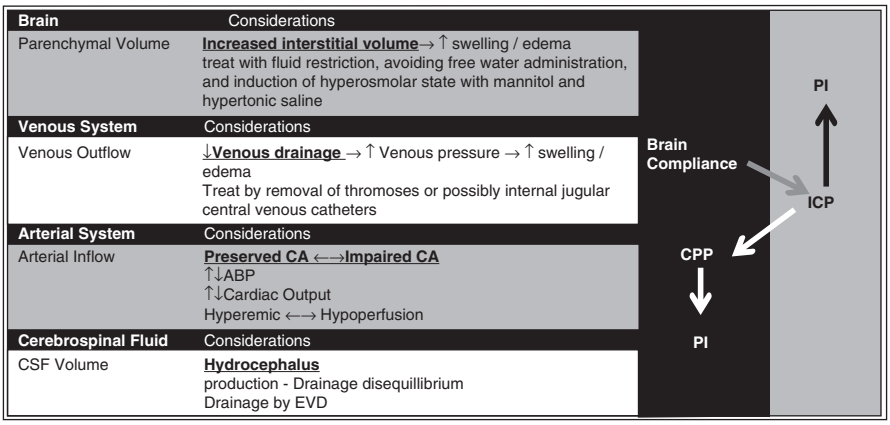

Fig. 21.8 Pulsatility index: influenced by cerebrovascular factors. CSF cerebrospinal fluid, EVD external ventricular drain, CPP cerebral perfusion pressure, ICP intracranial pressure, ABP arterial blood pressure, CA cerebral autoregulation, PI pulsatility index, ↓ low/decrease, ↑ high/increase, ↓↑ maybe increase or decrease

The brain pulsatility is the consequence of the interaction between these hemodynamic parameters and intracranial impedance, which will vary during the clinical course of the brain injury (Fig. 21.8).

21.5.3 Cardiopulmonary Factors

Maintenance of normal ICP through treatments aimed at affecting the intracranial components which contribute to ICP is critical in patients with acute brain injury (parenchymal volume, CSF volume, and blood volume) [48]. This includes ensuring appropriate venous outflow, CSF diversion, modification of the parenchymal volume by treatment of edema, and augmentation of the MAP, among others. These factors must be taken into consideration when interpreting a given patient's PI (Fig. 21.9) [5, 49, 50].

21.5.4 Metabolism Factors

Brain oxygenation and metabolism is the confluence of cardiovascular (O_2 delivery) and pulmonary systems (gas exchange – ventilation). In the clinical interpretation of the PI, we should consider the following variables: [51, 52] (Fig. 21.10).

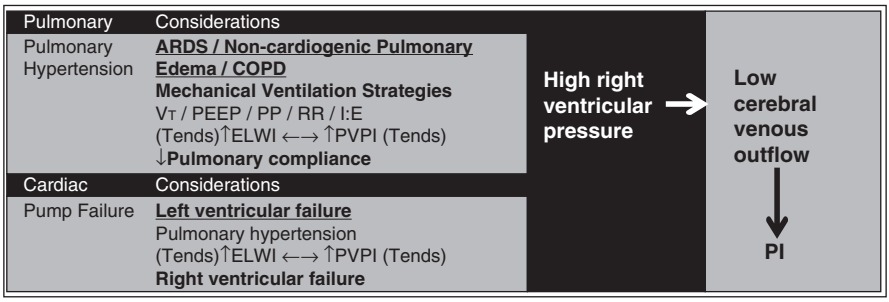

Fig. 21.9 Transcranial pulsatility index: influenced by cardiopulmonary factors. ARDS acute respiratory distress syndrome, COPD chronic obstructive pulmonary disease, V_T tidal volume, PP prone position, RR respiratory rate, I:E inspiration: expiration relationship, EVLWI extra-vascular lung water index, PVPI pulmonary vascular permeability index, PI pulsatility index, ↓ low/decrease, ↑ high/increase

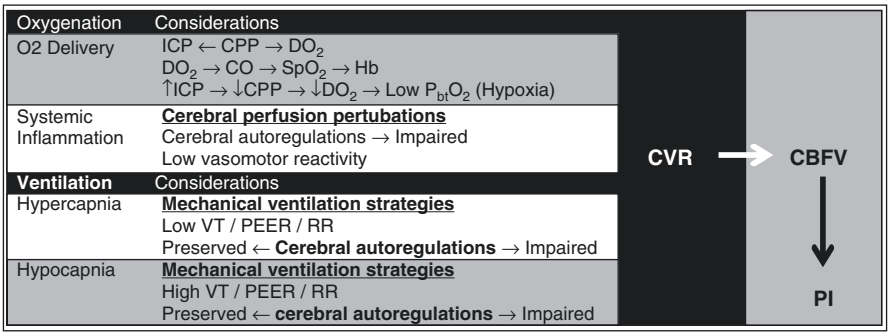

Fig. 21.10 Metabolic factors which influence PI. ICP intracranial pressure, CPP cerebral perfusion pressure, CO cardiac output, DO_2 delivery of oxygen, SpO_2 peripheral capillary oxygen saturation, Hb hemoglobin, $P_{bt}O_2$ brain tissue oxygen tensión, V_T tidal volume, RR respiratory rate, CVR cerebrovascular resistance, CBFV cerebral blood flow velocity, PI pulsatility index, ↓ low/decrease, ↑ high/increase

21.5.5 Vascular Factors

The focal or segmental stenoses of intracranial vessels, whether due to intracranial atherosclerosis, cerebral artery vasospasm, or vasculitis, influence ICP and cerebral perfusion. TCD/TCCS is a useful non-invasive tool in monitoring cerebral perfusion over time via MFV and PI. Although there is a lack of data in this arena, monitoring of trends in MFV and PI as vascular factors are manipulated, such as induced hypertension, allows one to customize each patient's treatments and hemodynamic parameters [53–57] (Fig. 21.11).

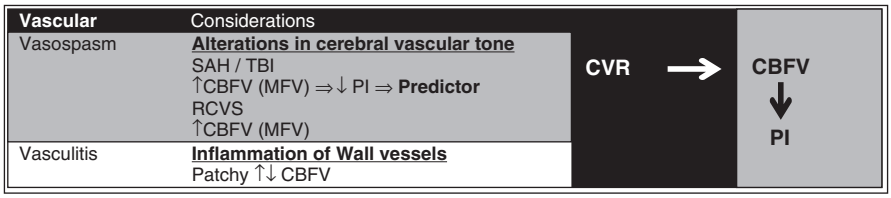

Fig. 21.11 The effect of vascular factors on PI. SAH subarachnoid hemorrhage, TBI traumatic brain injury, RCVS reversible cerebral vasoconstriction syndrome, CBFV cerebral blood flow velocity, MFV mean flow velocity, CVR cerebrovascular resistance, PI pulsatility index, ↓ low/decrease, ↑ high/increase, ↓↑ maybe increase or decrease

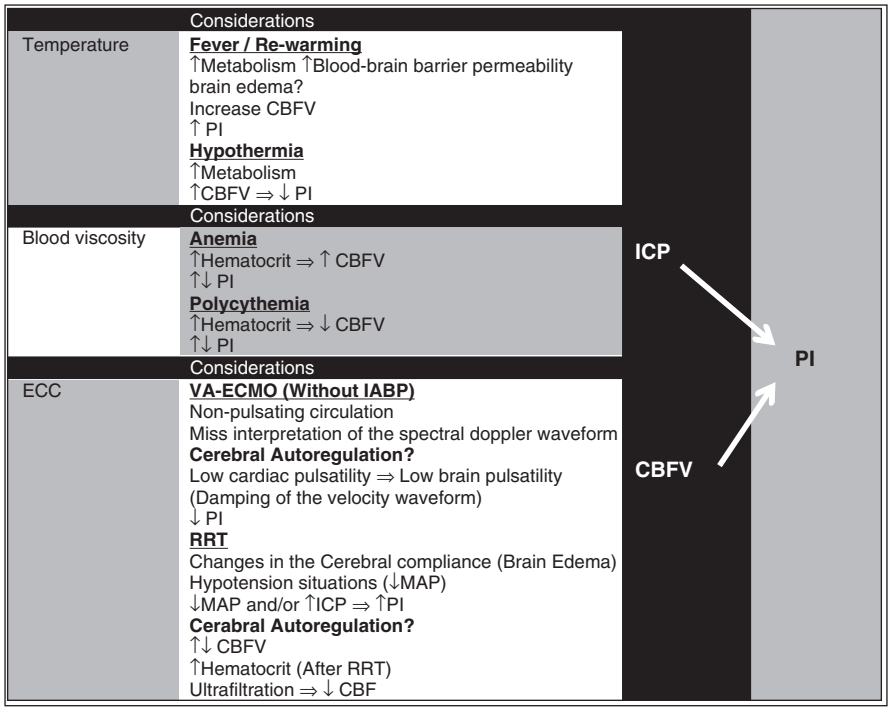

Fig. 21.12 Other systemic factors affecting PI. CBFV cerebral blood flow velocity, PI pulsatility index, IABP intra-aortic blood pump, RRT renal replacement therapy, MAP mean arterial pressure, ICP intracranial pressure, CBF cerebral blood flow, ECC extracorporeal circulation, ↓ low/decrease, ↑ high/increase, ↓↑ maybe increase or decrease

21.5.6 Other Factors

Other systemic factors that influence cerebrovascular hemodynamics can affect PI. These include fever, CNS infections, hypothermia, among others and are listed in the table below [58–60] (Figs. 21.12 and 21.13).

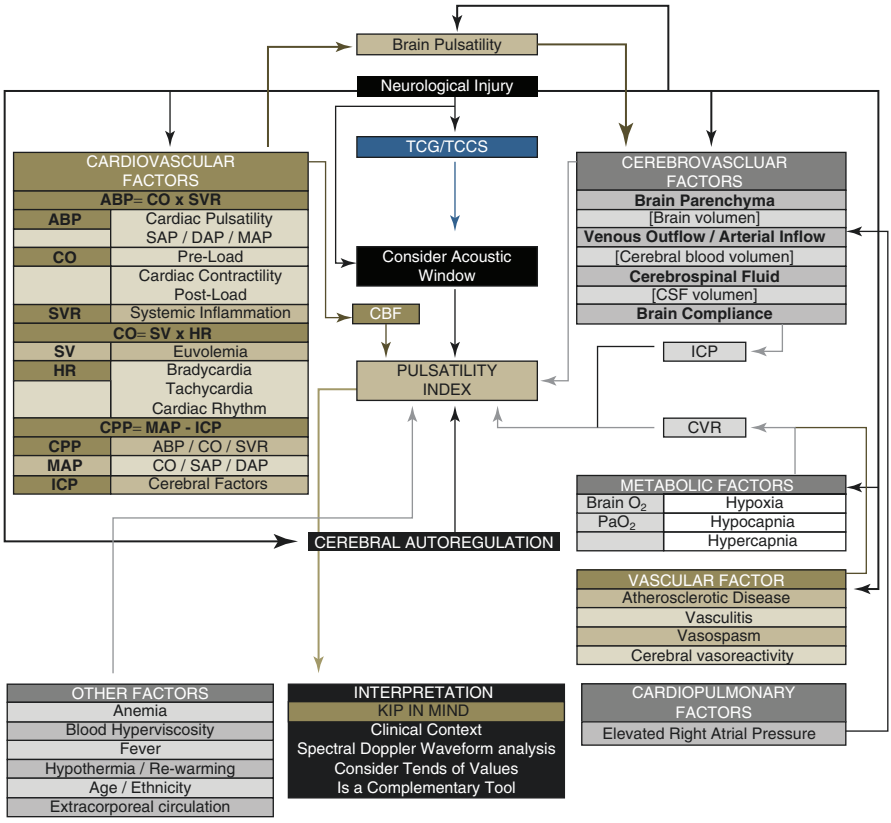

Fig. 21.13 Schema of clinical considerations in the pulsatility index interpretation. Transcranial pulsatility index can be variable and affected by physiological as well as pathologic conditions. ABP arterial blood pressure, CO cardiac output, SV stroke volume, CPP cerebral perfusión pressure, SVR systemic vascular resistance, HR heart rate, MAP mean arterial pressure, ICP intracranial pressure, CVR cerebrovascular resistance, SAP systolic arterial pressure, DAP diastolic arterial pressure, CSF cerebrospinal fluid, CBF cerebral blood flow

21.6 Conclusion

Although invasive monitoring is the gold standard, non-invasive monitoring should be considered in certain clinical scenarios. TCD/TCCS, through Gosling's pulsatility index, is a validated tool for estimating changes in ICP. TCD/TCCS can be used to give a rough estimate for ICP (correlated PI to ICP in clinical practice), but not as a surrogate for accurate invasive ICP monitors. The clinical correlation and interpretation of the Gosling's pulsatility index depends on several factors.

During TCD/TCCS monitoring, it is important to consider the spectral Doppler waveform. Cerebral perfusion is driven primarily by the diastolic component of the TCD/TCCS waveform. Therefore, we recommend that the PI should be interpreted

in conjunction with the spectral Doppler waveform morphology noting qualitative and quantitative changes.

Absolute ICP measurements based on TCD/TCCS have been estimated by various methods. However, none of these methods seem to be accurate enough to be used as a replacement for invasive ICP measurement and, at present, TCD/TCCS is reserved for assessing changes (ICP trends) of non-invasive ICP, rather than absolute ICP.

Algorithm

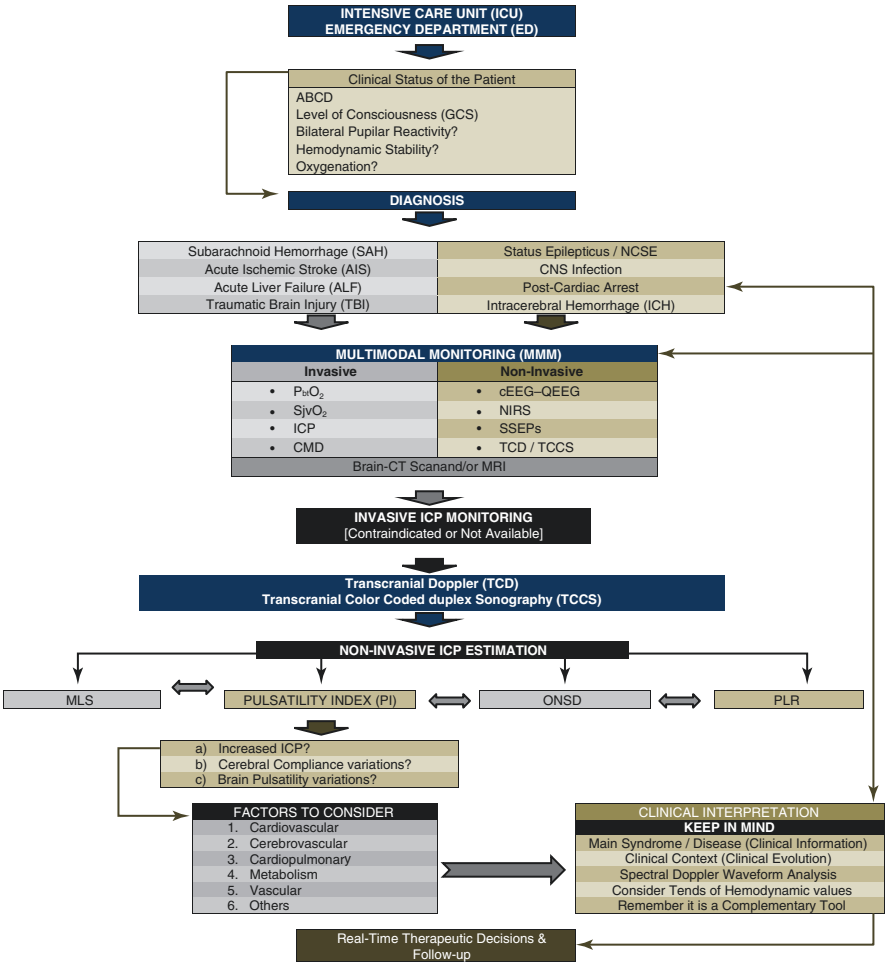

SE status epilepticus, *NCSE* non-convulsive status epilepticus, *CNS* central nervous system, *PRL* pupillary light reflex, *MLS* middle-line shift, *SSEPs* somatosensory evoked potentials, *ABCD* airway, breathing, circulation, disability, $SjvO_2$ jugular bulb venous oxygen saturation, $PbtO_2$ brain tissue oxygen tensión, *MRI* magnetic resonance imaging, ←→ inter-related, *CMD* cerebral microdialysis

References

1. Hakimi R, et al. Neuro-ultrasonography. Neurol Clin. 2020;38:215–29.
2. Aaslid R, et al. Noninvasive transcranial Doppler ultrasound recording of ow velocity in basal cerebral arteries. J Neurosurg. 1982;57(6):769–74.
3. Bartels E. Transcranial color-coded duplex ultrasonography in routine cerebrovascular diagnostics. Pers Med. 2012;1:325–30.
4. Wagshul, et al. The pulsating brain: a review of experimental and clinical studies of intracranial pulsatility. Fluids Barriers CNS. 2011;8:5.
5. Lahiri S, et al. Cerebral Pulsatility index is elevated in patients with elevated right atrial pressure. J Nerurosurg. 2017;28(1):95–8.
6. Gosling RG, et al. Arterial assessment by Doppler-shift ultrasound. Proc R Soc Med. 1974;67(6 Pt 1):447–9.
7. De Riva N, et al. Transcranial Doppler pulsatility index: what it is and what it isn't. Neurocrit Care. 2012;17:58–66.
8. Naqvi J, et al. Transcranial Doppler ultrasound: a review of the physical principles and major applications in critical care. Int J Vasc Med. 2013;2013:13.
9. Robba C, et al. Transcranial Doppler: a stethoscope for the brain-neurocritical cara use. J Neuro Res. 2018;96(4):720–30.
10. Cardim D, et al. Non-invasive monitoring of intracranial pressure using transcranial Doppler ultrasonography: is it possible? Neurocrit Care. 2016;25(3):473–91.
11. Schreiber SJ, et al. Transcranial duplex ultrasound of the ophthalmic artery. Ultrasound Med Biol. 2006;32(3):309–13.
12. Rojanapongpun P, et al. Ophthalmic artery flow velocity in glaucomatosus and normal subjects. Br J Ophthalmol. 1993;77:25–9.
13. Schöning M, et al. Comparative study of transcranial color duplex sonography in adults. J Neurosurg. 1993;78:776–84.
14. Rigamonti A, et al. Transcranial doppler monitoring in subarachnoid hemorrhage: a critical tool in critical care. Can J Anaesth. 2008;55:112–23.
15. Martin PJ, et al. Transcranial Color-Coded sonography of the basal cerebral circulation: reference data from 115 volunteers. Stroke. 1994;25(2):390–6.
16. Moppet IK. Transcranial Doppler ultrasonography in anaesthesia and intensive care. Br J Anaesth. 2004;93(5):710–24.
17. Tegeler CH, et al. Transcranial Doppler velocities in a large, healthy population. J Neuroimaging. 2013;23(3):466–72.
18. Yang D, et al. Cerebral Hemosynamics in the elderly: Tranncranial Doppler study in the Einstein Aging study cohort. J Ultrasound Med. 2016;35(9):1907–14.
19. Donelly J, et al. Regulation of the cerebral circulation: bedside assessment and clinical implications. Crit Care. 2016;20:129.
20. Giller CA, et al. Transcranial Doppler pulsatility in vasodilation and stenosis. J Neurosurg. 1990;72(6):901–6.
21. Lau VI, Arntfield RT. Point-of-care transcranial Doppler by intensivists. Crit Ultrasound J. 2017;9:21.
22. Hsu HY, et al. Correlations among critical closing pressure, pulsatility index and cerebrovascular resistance. Ultrasound Med Biol. 2004;30(10):1329–35.
23. Czosnyka M, et al. Monitoring and interpretation of intracranial pressure. J Neurol Neurosurg Psychiatry. 2004;75:813–21.
24. Guidelines for the management of severe traumatic brain injury: indications for intracranial pressure monitoring. 4th ed. Brain Trauma Foundation; 2016.
25. Nag DS, et al. Intracranial pressure monitoring: gold standard and recent innovations. World J Clin Cases. 2019;7(13):1535–53.
26. Marmarou A, et al. Contribution of raised ICP and hypotension to CPP reduction in severe brain injury: correlation to outcome. Acta Neurochir Suppl. 2005;95:277–80.

27. Aiolfi A, et al. Brain trauma foundation guidelines for intracranial pressure monitoring: compliance and effect on outcome. World J Surg. 2017;41(6):1543–9.
28. Balestreri M, et al. Impact of intracranial pressure and cerebral perfusion pressure on severe disability and mortality after head injury. Neurocrit Care. 2006;4:8–13.
29. Moreno J, et al. Evaluating the outcome of severe head injury with transcranial Doppler ultrasonography. Neurosurg Focus. 2000;8(1):1–7.
30. Forsyth RJ, Raper J, Todhunter E. Routine intracranial pressure monitoring in acute coma. Cochrane Database Syst Rev. 2015;11:CD002043.
31. Tavakoli S, et al. Complications of invasive intracranial pressure monitoring devices in neurocritical care. Neurosurg Focus. 2017;43(5):E6.
32. Dimitriou J, et al. Comparison of complications in patients receiving different types of intracranial pressure monitoring: a retrospective study in a single center in Switzerland. World Neurosurg. 2016;89:641–6.
33. Bauer DF, et al. Meta-analysis of hemorrhagic complications from ventriculostomy placement by neurosurgeons. Neurosurgery. 2011;69:255–60.
34. Binz DD, et al. Hemorrhagic complications of ventriculostomy placement: a meta-analysis. Neurocrit Care. 2009;10:253–6.
35. Bellner J, et al. Transcranial Doppler sonography pulsatility index (PI) reflects intracranial pressure (ICP). Surg Neurol. 2004;62(1):45–51.
36. Carney, et al. Guidelines for the management of severe traumatic brain injury, fourth edition. Neurosurgery. 2017;80(1):6–15.
37. Wakerley BR, et al. Usefulness of transcranial Doppler-derived cerebral hemodynamic parameters in the noninvasive assessment of intracranial pressure. J Neuroimaging. 2015;25:111–6.
38. Splavski B, et al. Assessment of intracranial pressure after severe traumatic brain injury by transcranial Doppler ultrasonography. Brain Inj. 2006;20:1265–70.
39. Homburg AM, et al. Transcranial Doppler recordings in raised intracranial pressure. Acta Neurol Scand. 1993;87:488–93.
40. Ragauskas A, et al. Innovative non-invasive method for absolute intracranial pressure measurement without calibration. Acta Neurochir Suppl. 2005;95:357–61.
41. Gura M, et al. Correlation of pulsatility index with intracranial pressure in traumatic brain injury. Turk Neurosurg. 2011;21(2):210–5.
42. Kingelhofer J, et al. Evaluation of intracranial pressure from transcranial Doppler studies in cerebral disease. J Neurol. 1988;235:159–62.
43. Czosnyka M, et al. Relationship between transcranial doppler-determined pulsatility index and cerebrovascular resistance: an experimental study. J Neurosurg. 1996;84:79–84.
44. Calviello LA, et al. Relationship between brain Pulsatility and cerebral perfusion pressure: replicated validation using different drivers of CPP change. Neurocrit Care. 2017;27:392–400.
45. Robba C, et al. Ultrasound non-invasive measurement of intracranial pressure in neurointensive care: a prospective observational study. PLoS Med. 2017;14(7):e1002356.
46. Budohoski KP, et al. Monitoring cerebral autoregulation after head injury. Which component of transcranial Doppler flow velocity is optimal? Neurocrit Care. 2012;17(2):211–8.
47. Viski S, Olah L. Use of transcranial Doppler in intensive care unit. J Crit Care Med. 2017;3(3):99–104.
48. Mokri B. The Monro-Kellie hypothesis: applications in CSF volume depletion. Neurology. 2001;56(12):1746–8.
49. Verein M, et al. Dynamics of extravascular Pulmonary water and intracranial pressure in patient with ischemic stroke. Sage J. 2010;14(4):226–30.
50. Corradi F, et al. Combined lung and brain ultrasonography for an individualized "brain-protective ventilation strategy" in neurocritical care patients with challenging ventilation needs. Crit Ultrasound J. 2018;10:24.
51. de Azevedo DS, et al. Cerebral hemodynamics in sepsis assessed by transcranial Doppler: a systematic review and meta-analysis. J Clin Monit Comput. 2017;31(6):1123–32.

52. Pierrakos C, et al. Cerebral perfusion alterations and cognitive decline in critically ill sepsis survivors. Acta Clin Belg. 2017;72(1):39–44.
53. Razumovsky AY, et al. Cerebral vasculitis: diagnosis and follow-up with transcranial doppler ultrasonography. J Neuroimaging. 2001;11(3):333–5.
54. Egido JA, et al. Takayasu's arteritis: transcranial Doppler findings and follow-up. J Neurosurg Sci. 1996;40(2):121–4.
55. Terasawa Y, et al. Transcaranial color-coded sonography findings of patients with Reversible Cerebral Vasoconstriction Syndrome. J Clin Neurosci. 2019;61:290–1.
56. Morgenlander JC, et al. Transcranial doppler sonography to monitor cerebral vasculitis. J Rheumatol. 1996;23(3):561–3.
57. Rajajee V, et al. Low Pulsatility index on transcranial Doppler predicts symptomatic large-vessel vasospasm after aneurysmal subarachnoid hemorrhage. Neurosurgery. 2012;70(5):1195–206.
58. Stretti F, et al. Body temperature affects cerebral hemodynamics in acutely brain injured patients: an observational transcranial color-coded duplex sonography study. Crit Care. 2014;18:552.
59. Hata R, et al. Effects of hemodialysis on cerebral circulation evaluated by transcranial Doppler ultrasonography. Stroke. 1994;25:408–12.
60. Fiermonte G, et al. Polycythaemia Vera and cerebral blof flow: a preliminary study with transcranial doppler. J Intern Med. 1993;234(6):595–602.

Chapter 22
Transcranial Doppler in Subarachnoid Hemorrhage: Usefulness in the Diagnosis and Monitoring of Cerebral Vasospasm

Fabienne Perren

Key Points

1. TCD/TCCS should be performed by experienced sonographers.
2. TCD/TCCS is a very useful noninvasive bedside tool allowing detection and monitoring of vasospasm.
3. TCD/TCCS can be used to detect the onset of asymptomatic vasospasm and follow vasospasm progression.
4. TCD/TCCS can be used to facilitate treatment and to prevent the onset of DCI.
5. TCD/TCCS can be used to early select candidates for angioplasty.
6. TCD/TCCS can detect the resolution of vasospasm.

22.1 Introduction

After aneurysmal subarachnoid hemorrhage (SAH), a major complication and a cause of poor outcome is the occurrence of vasospasm of the cerebral vessels (CVs). Indeed, CVs, which lead to a progressive arterial narrowing, can result in cerebral ischemia/infarction and delayed cerebral ischemia (DCI) significantly increasing disability and death [1–5].

Despite early treatment of ruptured cerebral aneurysms, postoperative vasospasm with 2–20% of DCI remains a major complication [6, 7].

Cerebral vasospasm is seen in approximately 70% of SAH patients on digital subtraction angiography (DSA) that although invasive, is still considered as the gold standard for the diagnosis of CVS [8]. CT angiography (CTA) that tends to be more

F. Perren (✉)
University Hospital and Medical Faculty, Department of Clinical Neurosciences, LUNIC Laboratory, Neurocenter of Geneva, Geneva, Switzerland

Committee Member - ESNCH, Olso, Norway
e-mail: fabienneperren@yahoo.com

C. N. Rodríguez et al. (eds.), *Neurosonology in Critical Care*,
https://doi.org/10.1007/978-3-030-81419-9_22

widely used requires radiation exposure and contrast injection and thus cannot be used to monitor clinical changes. Moreover, it does not allow cerebral blood flow measurement [9, 10].

Transcranial Doppler (TCD) first developed in Switzerland by Aaslid et al. in the early 1980s to warn the development of CVs after SAH – and a decade later, using color-coded duplex sonography (TCCS) – has been proved to be a safe, noninvasive, bedside, dynamic monitoring technique widely used in neurosurgery to detect and follow CVs [11–13]. TCD has been approved by the American Heart Association/American Stroke Association (AHA/ASA), American Academy of Neurology (AAN), and Neurocritical Care Society for daily noninvasive monitoring of mean flow velocity (MFV) of the basal cerebral arteries to detect the onset of CVs after SAH [14, 15]. Furthermore, TCD/TCCS can be applied as frequently as needed pre- and postoperatively and can guide the therapy of aneurysmal SAH [16]. Although the scope of this chapter is limited to present transcranial ultrasound methods (TCD, TCCS) for diagnosis and monitoring vasospasm assessment after SAH, the methods would be similar in cerebral vasospasm as a complication of head trauma [17].

22.2 Aneurysmal Subarachnoid Hemorrhage (aSAH)

Subarachnoid hemorrhage (SAH) may commonly occur after head trauma. SAH without preceding trauma occurs mainly in the setting of intracranial aneurysm rupture. Other causes have been identified including arteriovenous malformation and vasculitis but it may also occur in the absence of vascular abnormality [18]. It refers to extravasation of blood into the subarachnoid space situated between the pia and arachnoid (Fig. 22.1). Symptoms include generally acute severe headache "thunderclap headache," neck pain/stiffness, vomiting, decrease of consciousness, and sometimes seizures. Main complications of aneurysmal SAH include hydrocephalus, re-bleeding, vasospasm, DCI, and seizures.

Although clinically recognized since Hippocrates and cerebral aneurysmal rupture described by Bramwell in 1886, SAH symptoms were only fully described by Symonds in 1924, who also introduced the use of lumbar puncture and xantochromia for its diagnosis [19–21]. A few years later, neurosurgical treatment of SAH was first introduced by Dott who also pioneered the use of angiograms [22]. In 1938, Dandy used the first clips but it is only over 30 years later that in Switzerland, Krayenbühl, Yaşargil, et al. introduced microsurgical aneurysm therapy [23, 24].

The first medical treatment, the so-called "triple H therapy" for delayed cerebral ischemia due to vasospasm after SAH, was introduced in the 1980s, then followed by transluminal balloon angioplasty and finally by endovascular coil treatment by Guglielmi in 1991 [25–27].

The incidence of SAH has geographical variations. With 19–23 per 100'000, it has been reported to be especially high in Japan and Finland [28, 29]. Mean age at aneurysmal rupture is 55 years and there is a slightly higher incidence of aneurysmal SAH in women [30, 31].

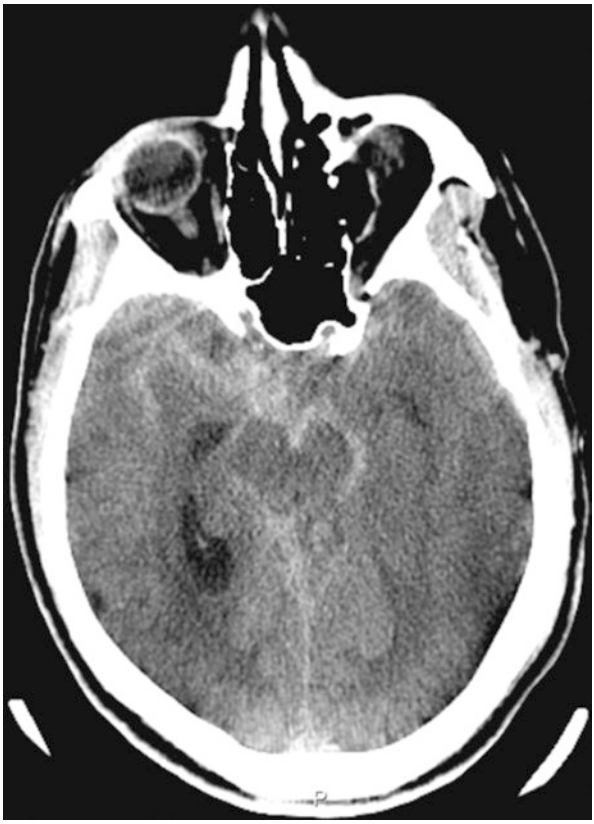

Fig. 22.1 Cerebral CT scan showing extensive SAH: There is subarachnoid hemorrhage located around the brainstem, in the supracellar cistern, and in the right lateral fissure. (Courtesy: Hov et al. [61])

Several risk factors have been associated with an increased risk of aneurysm rupture including black race and Hispanics, hypertension, active smoking, alcohol abuse, use of sympathomimetic drugs, and larger (>7 mm) intracranial aneurysms [32–34].

Cerebral aneurysms are related to hemodynamic stress due to pulsatile flow and turbulences on the arterial walls at bends and bifurcations. Intracranial arteries lack an external lamina and have a very thin adventitia. This predisposes to the formation of saccular or berry aneurysms. However, acquired factors like atherosclerosis, hypertension, smoking, advancing age, and hemodynamic stress are thought to be associated with aneurysmal formation [35, 36]. Moreover, a number of diseases leading to arterial wall weakness such as fibromuscular dysplasia, polycystic kidney disease, aortic coarctation, cerebral AVM, aplastic or hypoplastic contralateral vessel, SLE, Neurofibromatosis type I, moya-moya disease, pseudoxanthoma elasticum, Marfan, Ehler-Danlos, and hereditary hemorrhagic telangiectasia syndromes are associated with higher incidence of berry aneurysms [35, 37]. It has been described that structural integrity damage of the arterial wall by shear stress causes an inflammatory response with the recruitment of T-, mast-cells, macrophages, and inflammatory mediators (IL-1β,-6,TNFα, MMP-1,-2,-9, complement system, and

angiotensin II). Finally, it results in arterial wall fibrosis and abnormal collagen synthesis leading to arterial wall thinning, formation of aneurysm, and risk of rupture [38].

22.3 Cerebral Vasospasm After aSAH

Subarachnoid hemorrhage, whether of aneurysmal origin or not, has been graded according to the following grading scales:

1. The Hunt and Hess scale, created in 1968, is based on signs and symptoms.
2. The Modified Fisher Scale, which describes the severity of SAH according to CT.
3. The WFNS scale, developed in 1988 for patients suffering from SAH, is using the Glasgow coma scale (GCS) combined with the presence or absence of focal deficits to determine severity of injury and to predict patient outcomes [39–41] (Tables 22.1, 22.2, and 22.3).

Table 22.1 Hunt and Hess grading scale

Grade 0	Unruptured aneurysm
Grade I	Asymptomatic or mild headache and slight nuchal rigidity
Grade Ia	Fixed neurologic deficit without acute meningeal/brain reaction
Grade II	Cranial nerve palsy, moderate to severe headache, nuchal rigidity
Grade III	Mild focal deficit, lethargy, or confusion
Grade IV	Stupor, moderate to severe hemiparesis, early decerebrate rigidity
Grade V	Deep coma, decerebrate rigidity, moribund appearance

Table 22.2 Modified Fisher grading scale (CT scan findings)

Grade 0	No SAH and No IVH
Grade 1	Focal or diffuse, thin SAH (<5 mm thick); No IVH
Grade 2	Focal or diffuse, thin SAH; bilateral IVH
Grade 3	Focal or diffuse, thick SAH (>5 mm thick); No IVH
Grade 4	Focal or diffuse, thick SAH; bilateral IVH present

Table 22.3 WFNS grading scale

Grade 1	GCS of 15	Motor deficit absent
Grade 2	GCS of 13–14	Motor deficit absent
Grade 3	GCS of 13–14	Motor deficit present
Grade 4	GCS of 7–13	Motor deficit absent/present
Grade 5	GCS of 3–6	Motor deficit absent/present

The Hunt & Hess and the WFNS grading systems have been shown to correlate well with patient outcome, and in a recent study, the importance of neurological deficits in addition to level of consciousness has been shown for cut-off values – suggesting unfavorable outcome for Hunt & Hess and WFNS – of 4–5 and 3–5, respectively [2, 42]. The Fisher classification has been used successfully to predict one major complication of SAH that is symptomatic cerebral vasospasm [43]. Both Fisher Scale and Hunt & Hess Grade are related to the severity of aneurysmal SAH and correlate with the incidence of cerebral vasospasm (CVS) [39, 40].

Cerebral vasospasm (CVS) is a progressive but reversible cerebral arterial narrowing and a major complication of aSAH that may significantly increase disability and mortality rates [44]. CVS may be clinically silent but it is a well-known complication that can occur at any time within the 3–4 weeks – generally within 3–7 days – after aneurysmal SAH [45]. It is seen on angiography in as many as 70% of patients and involves large and medium-sized cerebral arteries [44, 46]. The overall incidence of cerebral angiographic vasospasm after aneurysm rupture has been estimated between 50% and 90% [45]. In the literature, its occurrence has been estimated as follows: moderate or more severe vasospasm in at least one cerebral artery will develop in two-thirds of patients with ruptured aneurysms, half of these patients will become symptomatic as a result of ischemia, and a cerebral infarct will develop in about half of these symptomatic patients [46].

22.4 Diagnosis of Cerebral Vasospasm and Role of Transcranial Ultrasound

Several imaging modalities are used to diagnose CVS after aSAH. Among the current techniques, DSA and CT angiography are invasive, and they require contrast-dye injection, have radiation exposure, and do not allow dynamic monitoring of vasospasm [31]. This implies that they are not used to detect subclinical vasospasm prior onset of symptoms. They are frequently restricted to confirm vasospasm in patients who are already symptomatic. A less invasive but not dynamic imaging technique is magnetic resonance angiography (MRA) using time of flight (TOF) sequences. However, this technology is less available and less used in this setting.

Currently, the primary screening imaging technique for asymptomatic vasospasm is transcranial Doppler ultrasound [47, 48]. Besides its noninvasiveness, it has many advantages such as its ability to measure in real-time cerebral hemodynamic changes, its bedside availability that makes it ideal for monitoring, and its low cost.

Transcranial Doppler ultrasound has a high sensitivity, specificity, and positive and negative predictive value and can, unlike other imaging techniques, early detect and predict the development of symptomatic vasospasm with delayed cerebral ischemia [8, 49, 50]. Therefore, it has been approved and recommended by the American Heart Association/American Stroke Association-AHA/ASA (Class IIA/Level B evidence) and by the American Academy of Neurology as a safe and effective modality for noninvasive daily monitoring of the development of vasospasm after aSAH [47].

22.5 Transcranial Ultrasound Assessment of Cerebral Vasospasm

Cerebral vasospasm typically affects the basal cerebral arteries of the circle of Willis (MCA, ACA, PCA, ACoA, ACoP) which run through the basal cisterns where blood accumulates after intracranial aneurysm rupture. Depending on the location of the aneurysm rupture, CVS may occur in the proximal or more distal segments of the basal cerebral arteries in which latter case it can be missed. CVS may affect one or several intracranial arteries and is characterized by a segmental acceleration of the CBFV fluctuating over time and responding to therapy. This is why a baseline measurement of the velocities should always be performed.

Since Aaslid et al. developed TCD and demonstrated its ability to noninvasively detect flow-velocity acceleration due to narrowing in the cerebral arterial segments affected by CVS, transcranial ultrasound imaging has been used to monitor it after aSAH [11, 12]. However, frequent factors (Table 22.4) may influence cerebral blood flow velocities (CBFV) and should, therefore, be considered.

↓ increase, ↓ decrease

While there is no clear consensus for threshold velocity values of all the intracranial vessels, above which CVS should be considered, we propose to use cut-off mean flow velocities (MFV): (Table 22.5) and to combine these to additional criteria [51–53]. Indeed, in case of hyperemia, CBFV will also increase and therefore in order to diagnose CVS, correction using following indices have been introduced:

Table 22.4 Examples of factors influencing cerebral blood flow velocities measured by transcranial ultrasound

Factors	CBFV
Increasing age (>60 years)	↓
Increased intracranial pressure (ICP)	↓
Decreased hematocrit	↑
Cerebral hyperperfusion	↑
Hypercapnia/hypoventilation	↑
Hypocapnia/hyperventilation	↓
Hypertension	↑

Table 22.5 Vasospasm: cut-off mean flow velocities

	Moderate CVS	Severe CVS
Anterior circulation: MCA (ACA, ICA)	≥120 cm/s (≥3 KHz)	≥160 cm/s (≥4 KHz)
Posterior circulation: BA, VA, PCA	≥80 cm/s (≥2 KHz)	≥120 cm/s (≥3 KHz)

MCA **middle cerebral artery,** *ACA* **anterior cerebral artery,** *ICA* **internal carotid artery,** *BA* **basilar artery,** *VA* **vertebral artery,** *PCA* **posterior cerebral artery,** *CVS* **cerebral vasospasm**

1. The Lindegaard ratio: ratio between MCA and ICA mean flow velocities: (Eq. (22.1))

$$\mathrm{LR} = \mathrm{MFV}_{\mathrm{MCA}}\left(\mathrm{cm/s}\right) / \mathrm{MFV}_{\mathrm{ICA}} * \left(\mathrm{cm/s}\right) \tag{22.1}$$

$$\left(*\text{Mean submandibular ICA}\right)$$

$$\mathrm{LR}\left\langle 2 : \text{hyperemia}; \mathrm{LR}^{\ddagger} 3 : \mathrm{CVS}; \mathrm{LR}\right\rangle 6 \text{severe CVS}$$

2. The Soustiel ratio: ratio between BA and VA mean flow velocities: (Eq. (22.2))

$$\mathrm{SR} = \mathrm{MFV}_{\mathrm{BA}}\left(\mathrm{cm/s}\right) / \mathrm{MFV}_{\mathrm{VA}} * \left(\mathrm{cm/s}\right) \tag{22.2}$$

$$\left(*\text{Mean of both VA3 segments}\right)$$

$$\mathrm{SR} > 2 : \mathrm{CVS}; \mathrm{SR} > 3 : \text{severe CVS}$$

3. The Sloan ratio: ratio between ACA and ICA mean flow velocities: (Eq. (22.3))

$$\text{Sloan R} = \mathrm{MFV}_{\mathrm{ACA}}\left(\mathrm{cm/s}\right) / \mathrm{MFV}_{\mathrm{ICA}} * \left(\mathrm{cm/s}\right) \tag{22.3}$$

$$\left(*\text{Mean submandibular ICA}\right)$$

$$\text{Sloan R} > 4 : \mathrm{CVS}$$

As maximal acceleration of CBFV often occurs after neurological deficits, a close monitoring with transcranial ultrasound, allowing a comprehensive hemodynamic view, is mandatory. Indeed, according to our experience and as shown in a few studies, CVS risk prone to clinical symptoms may be identified by the time course of the CBFV in the MCA:

4. MFV increase >50 cm/s per day.
5. MFV increase ≥50% per day within the 1st week after SAH onset.

Moreover, it has been also described that an asymmetry between mean MCA CBFV with a ratio ipsi- vs contralateral side >1.5 may help to identify CVS "at risk" of delayed cerebral ischemia (DCI) [50]. And a few studies have shown that early impairment of cerebral autoregulation is associated with delayed cerebral ischemia and unfavorable outcome after SAH [54–59].

Finally, a vasospasm probability index for the MCA, taking into account Fisher and Hunt and Hess grades, Lindegaard ratio, and spasm index (TCD velocities/Xe-CT hemispheric CBF), has been also proposed to improve the detection of CVS at risk of DCI [60].

22.5.1 TCD/TCCS: Examination Protocol

Since the introduction of noninvasive low-frequency (~2 MHz) transcranial Doppler (TCD) measuring "blindly" cerebral blood flow velocities, technical advances in ultrasound imaging resolution and color-coding of blood flow (transcranial color-coded duplex Sonography (TCCS) have allowed to additionally visualize brain parenchyma (B-mode) (Fig. 22.2) and the main basal cerebral arteries (color-coded mode) (Fig. 22.3). Both techniques can be used to detect and monitor CVS after aSAH. Several "acoustic bone windows," where ultrasound waves can be transmitted through thinner skull bone regions or foramina, are used for the insonation of the cerebral arteries: the temporal (TW), orbital (OW), suboccipital/transforaminal (OTW), and submandibular (MW) bone windows (Fig. 22.4a, b) [50]. In case of insufficient ultrasound penetration, TCCS has the advantage over TCD to allow cerebral vessel examination after the injection of an echocontrast agent. TCD, depending on the length of the examination, consists of a 2 MHz ultrasound probe that can be fixed in a headset (making bilateral monitoring possible) or applied manually in the region of acoustic windows.

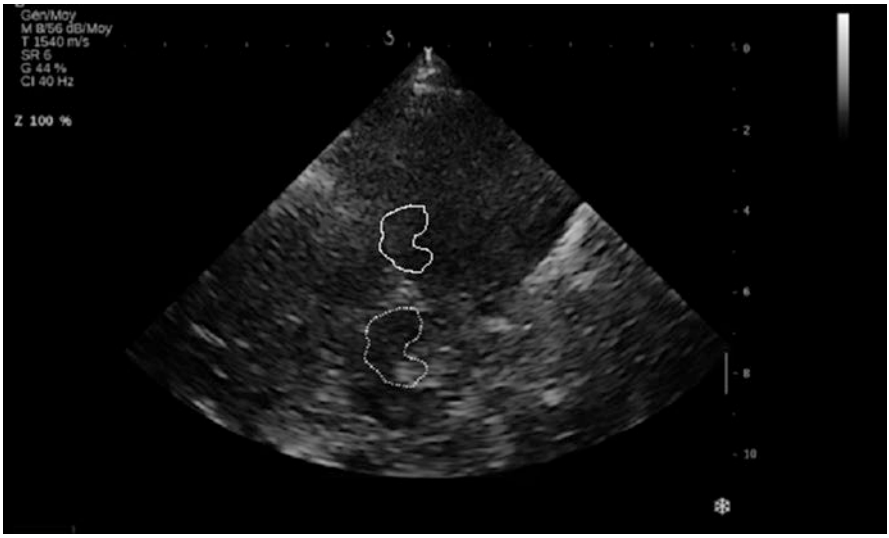

Fig. 22.2 Standard transtemporal axial examination plane using TCCS (B-mode) showing the mesencephalon (dotted line)

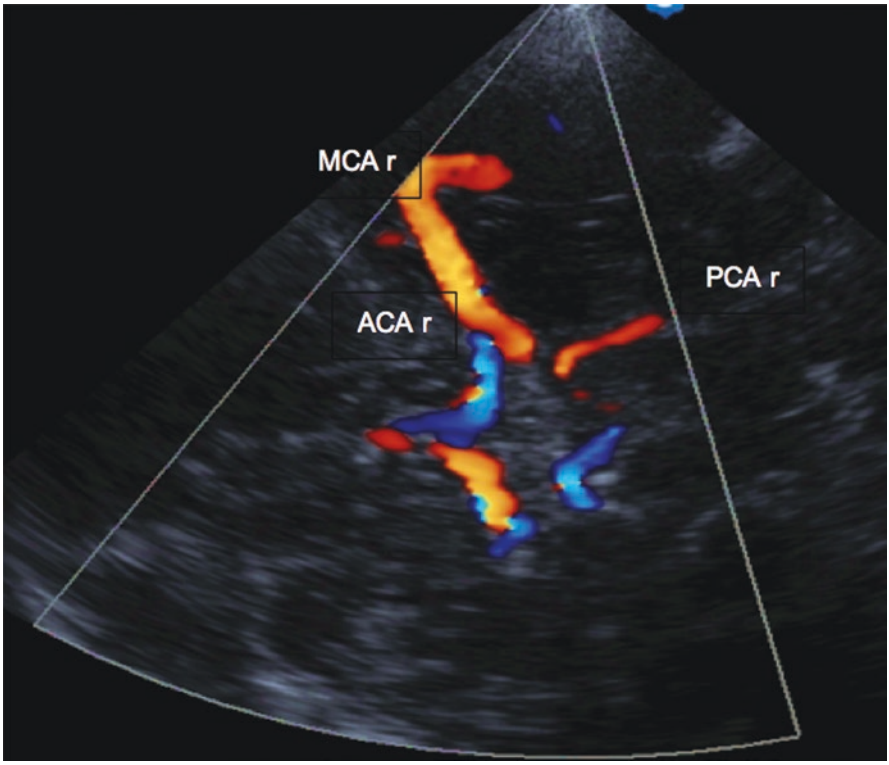

Fig. 22.3 TCCS through the right temporal acoustic bone window showing color-coded duplex imaging of the ipsilateral: middle cerebral artery (MCAr), anterior cerebral artery (ACAr) and posterior cerebral artery (PCAr)

22.5.1.1 Transtemporal Window

It allows blood flow velocity, flow direction measurement, and visualization (TCCS) (Fig. 22.3) of the distal internal carotid artery (TICA), carotid siphon, the middle cerebral (MCA, M1-2), anterior cerebral (ACA, A1-2), posterior cerebral arteries (PCA, P1-2), and communicating arteries (ACoA, ACoP).

22.5.1.2 Orbital Window

It allows blood flow velocity, flow direction measurement, and visualization (TCCS): the ophthalmic (OA) and internal carotid (ICA) siphon.

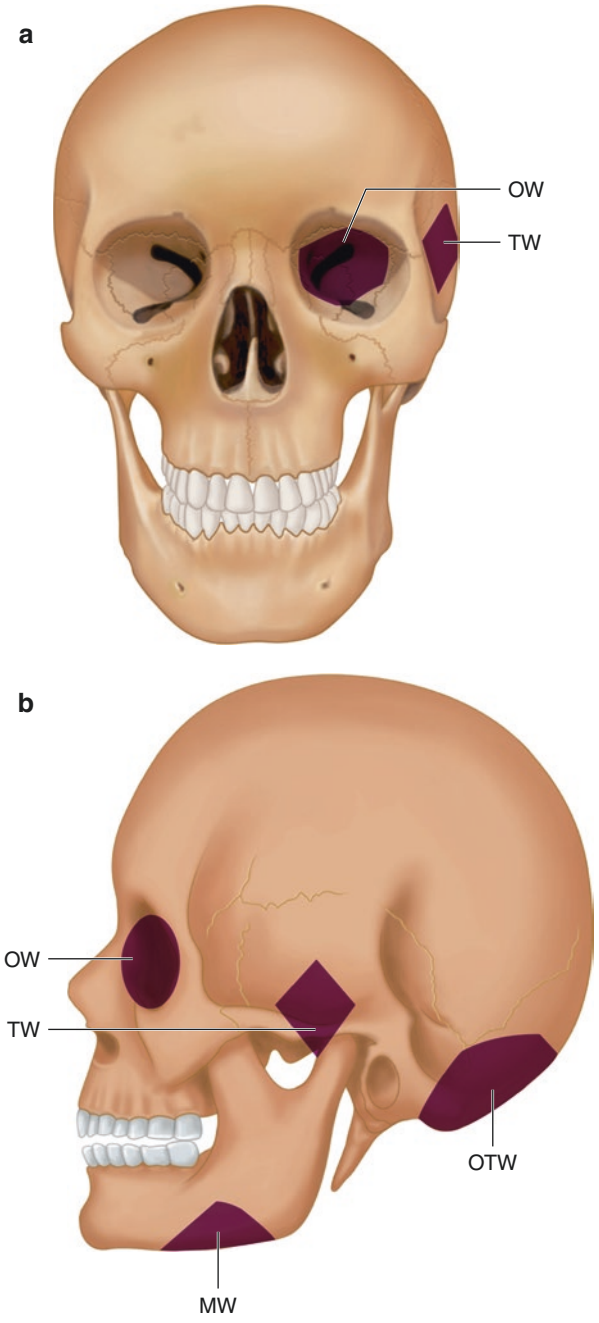

Fig. 22.4 (**a**) Human skull, front view, showing (in black): orbital (OW) and temporal (TW) acoustic bone windows. (**b**) Human skull, lateral view, showing (in black): orbital (OW), temporal (TW), sub-mandibular (MW), and sub-occipital/transforaminal (OTW) acoustic bone windows

22.5.1.3 Suboccipital/Transforaminal Window

It allows blood flow velocity, flow direction measurement, and visualization (TCCS) (Fig. 22.5): the distal vertebral arteries (VA, V4), basilar artery (BA).

22.5.1.4 Submandibular Window

The submandibular part of the ICA as it enters the skull.

In order to ensure better quality and reproducibility of ultrasound examination by a certified sonographer, a standardized scanning protocol, including patient and transducer positioning and orientation, depth selection, vessel and flow direction identification, blood flow velocity measurement, is mandatory. Transcranial ultrasound monitoring should always include a baseline examination in patients suffering from acute aSAH. Furthermore, in order to detect and to follow CVS, insonation

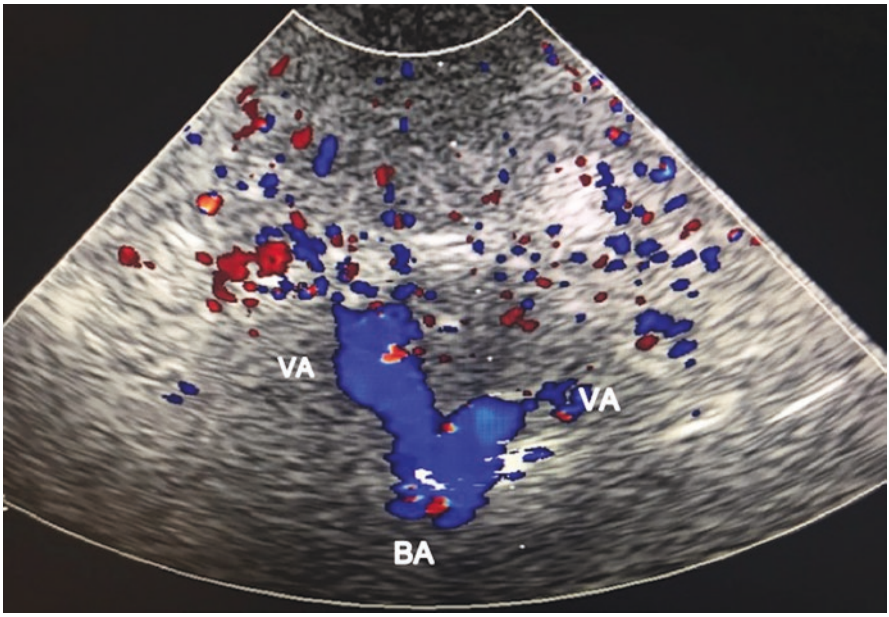

Fig. 22.5 TCCS through the sub-occipital/transforaminal acoustic bone window showing color-coded duplex imaging of the "Y-shaped" vertebral (VA) and basilar arteries (BA)

of the basal cerebral arteries should be daily performed during a period of time of at least 15–20 days after aSAH. However, the duration of the monitoring period should be adapted individually, according to the occurrence and to the course and severity of CVS.

As transcranial ultrasound (TCD, TCCS) blood flow velocities are up to a certain degree of narrowing, inversely related to arterial diameter, cut-off values of the mean flow have been established to diagnose and to measure the degree of CVS in the basal cerebral arteries. It should be known that CBFV gained with TCCS may be lower than those gained with TCD.

Transcranial ultrasound examinations, either TCD or TCCS, should be performed – using a 2 MHz pulsed Doppler or a 1–5 MHz sectorial transducer – with the patients in a supine position. In order to allow a comparison with TCD, if both exams are performed, angle correction should not be performed in TCCS exams. Spectral or color Doppler is used to locate the basal arteries through the dedicated acoustic bone windows. Doppler settings and color gain have to be adjusted for each vessel and CBFV should be measured along the vessel at very close intervals (2 mm to max. 5 mm) in both – right and left – sides of the cerebral vasculature. To calculate the Lindegaard and Sloan ratios, mean CBFV of the distal ICAs is measured via a submandibular approach without angle correction. Regarding the Soustiel index, mean CBFV of both VA3 segments without angle correction should be used.

22.5.2 Transtemporal Ultrasound Examination (TCD/TCCS): (Figs. 22.3 and 22.6)

The patient is lying in a supine position with the head turned laterally

- The *MCA*, which flow is normally directed toward the transducer, should be performed as much distal/superficial, beyond the bi-/trifurcation (M2 segment), as possible down to the ACA (A1 segment) bifurcation.
- The *ACA*, which flow is normally directed away from the transducer, should be examined from its proximal part (from the bifurcation, A1 segment) to distal, as far as possible (A2 segment).
- The *PCA* is found anteriorly to the mesencephalon (Fig. 22.2). It has two segments (P1 and P2) that are defined, by sonographers, according the direction of the flow: P1 toward the transducer and P2: away from the transducer. Therefore, one has to be aware that they do not correspond to the anatomical definition (P1: precommunicating, P2: postcommunicating segments).

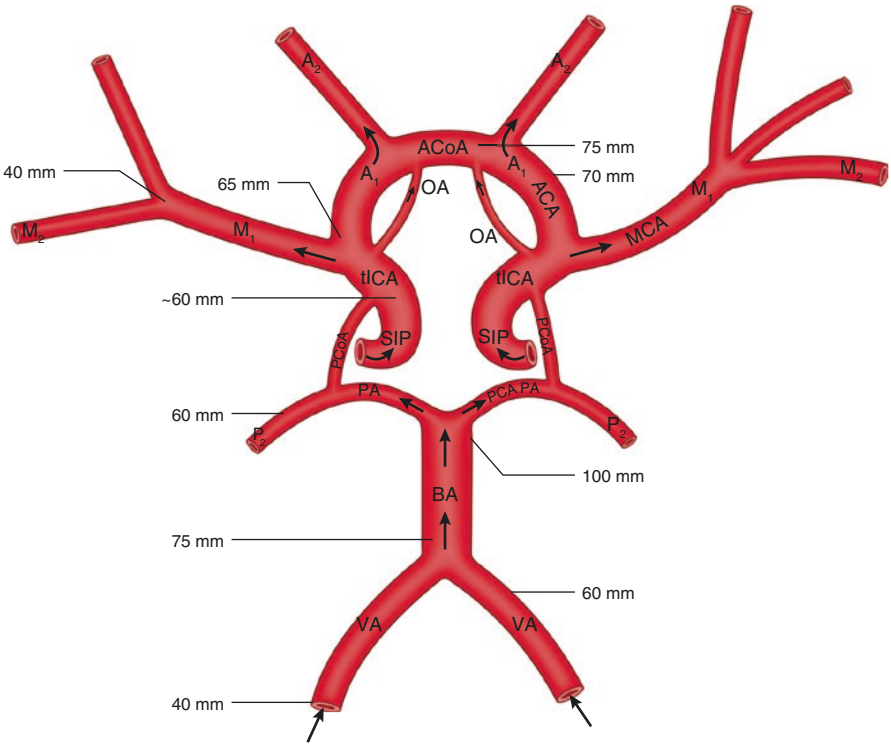

Fig. 22.6 Schematic drawing of the Circle of Willis showing flow directions and insonation depths of several segments of the basal arteries. SIP carotid siphon, tICA terminal ICA, OA ophthalmic artery, ACA anterior cerebral artery, ACoA anterior communicating artery, MCA middle cerebral artery, PCA posterior cerebral artery, PcoA posterior communicating artery, BA basilar artery, VA vertebral pathway

22.5.3 Sub-Occipital/Transforaminal Ultrasound Examination (TCD/TCCS): (Figs. 22.5 and 22.6).

The patient is lying in a lateral position, the neck is flexed forward in order that the chin is touching the chest

- The *VAs* and the *BA* are easily found as they form a Y-shape on TCCS examination (Fig. 22.5). They should be examined (probe placed over the upper neck at the skull base and angled toward the nose) at 2–5 mm intervals up to the most distal end of the BA. Their flow is directed away from the probe.

22.6 Monitoring of Cerebral Vasospasm

An examination guide of the main cerebral arterial segments showing flow direction and depth of insonation is presented below (Fig. 22.6). Regarding cerebral blood flow velocities, under normal conditions, it is important to remind the "hierarchy" of the MFV: MCA > ACA > Carotid Siphon > PCA > BA > VA. It is also useful to remember that anatomic variations are common (a fully developed symmetric Circle of Willis is present in only 20% of the patients); therefore, the fact that an arterial segment is not found does not automatically mean that there is an occlusion.

A comprehensive examination of all the segments of the major basal arteries with a report of the MFV, flow direction (including any unusual waveform), pulsatility indices, ratios of CVS (Lindegaard, Soustiel, Sloan) is mandatory. It is important to search in every arterial segment the highest CBFV. In case of missing arterial segments, a double check should be performed.

Ultrasound monitoring of cerebral vasospasm after SAH should start with a comprehensive baseline examination, including the extracranial vessels, in order to follow any sign of increased CBFV. A very simple transcranial ultrasound protocol that may be used as a guideline in the monitoring of CVS is presented below.

22.7 Conclusion

Cerebral vasospasm may occur after subarachnoidal hemorrhage due to ruptured intracranial aneurysm. CVS is a feared complication that if not diagnosed and untreated can lead to delayed neurological deficit and sustained disability. Therefore, beside careful neurological examination, DSA, CT-, and MR-angiography, a noninvasive repeatable bedside diagnostic tool, such as Transcranial Ultrasound (TCD,TCCS), is important. Comprehensive ultrasound examination and monitoring of the blood flow velocities and vasospasm cut-off indices in the basal cerebral arteries should be performed by experienced sonographers using a strict protocol.

Algorithm

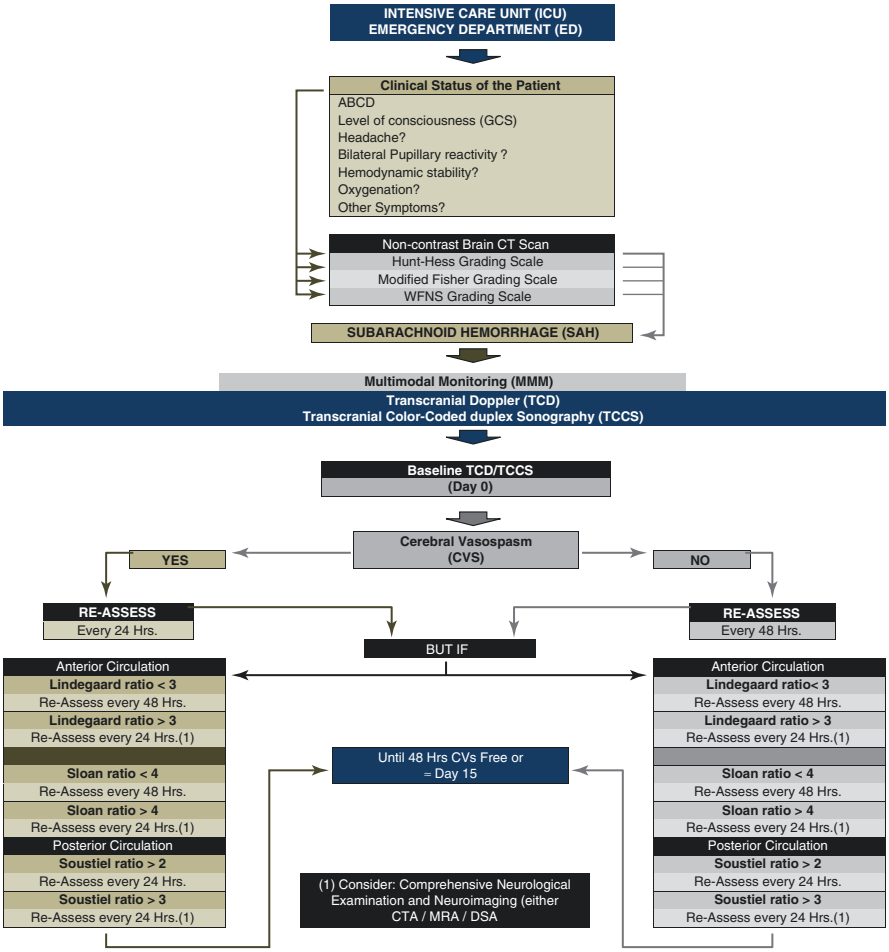

ABCD Airway-breathing-circulation-disability, *CTA* CT Angiography, *MRA* MRI Angiography, *DSA* digital subtraction angiography

References

1. Moftakhar P, et al. Extent of collateralization predicting symptomatic cerebral vasospasm among pediatric patients: correlations among angiography, transcranial doppler ultrasonography, and clinical findings. J Neurosurg Pediatr. 2015;15:282–90.
2. Neulen A, Prokesch E, Stein M, Konig J, Giese A. Image-guided transcranial Doppler sonography for monitoring of vasospasm after subarachnoid hemorrhage. Clin Neurol Neurosurg. 2016;145:14–8.

3. Kassell NF, Sasaki T, Colohan AR, Nazar G. Cerebral vasospasm following aneurysmal subarachnoid hemorrhage. Stroke. 1985;16:562–72.
4. Macdonald RL, Hunsche E, Schüler R, Wlodarczyk J, Mayer SA. Quality of life and healthcare resource use associated with angiographic vasospasm after aneurysmal subarachnoid hemorrhage. Stroke. 2012;43:1082–8.
5. Aaslid R. Transcranial Doppler assessment of cerebral vasospasm. Review. Eur J Ultrasound. 2002;16:3–10.
6. Alien GS, et al. Cerebral arterial spasm - a controlled trial of nimodipine in patients with subarachnoid hemorrhage. N Engl J Med. 1983;308:619–24.
7. Harders AG, Gilsbach JM. Time course of blood velocity changes related to vasospasm in the circle of Willis measured by transcranial Doppler ultrasound. J Neurosurg. 1987;66:718–28.
8. Kumar G, Shahripour RB, Harrigan R. Vasospasm on transcranial Doppler is predictive of delayed cerebral ischemia in aneurysmal subarachnoid hemorrhage: a systematic review and meta-analysis. J Neurosurg. 2016;124:1257–64.
9. Li DD, Chang JY, Zhou CX, Cui JB. Clinical diagnosis of cerebral vasospasm after subarachnoid hemorrhage by using transcranial Doppler sonography. Eur Rev Med Pharmacol Sci. 2018;22:2029–35.
10. Moppett IK, Mahajan RP. Transcranial Doppler ultrasonography in anaesthesia and intensive care. Br J Anaesth. 2004;93:710–24.
11. Aaslid R, Markwalder T-M, Nornes H. Noninvasive transcranial Doppler ultrasound recording of flow velocity in basal cerebral arteries. J Neurosurg. 1982;57:769–74.
12. Aaslid R, Nornes H. Musical murmurs in human cerebral arteries after subarachnoid hemorrhage. J Neurosurg. 1984;60:32–6.
13. Kantelhardt SR, Greke C, Keric N, Vollmer F, Thiemann I, Giese A. Image guidance for transcranial Doppler ultrasonography. Neurosurgery. 2011;68:257–66.
14. Lysakowski C, Walder B, Costanza MC, Tramèr MR. Transcranial Doppler versus angiography in patients with vasospasm due to a ruptured cerebral aneurysm: a systematic review. Stroke. 2001;32:2292–8.
15. Diringer MN, Bleck TP, Hemphill JC III, Menon D, Shutter L, Vespa P, et al. Critical care management of patients following aneurysmal subarachnoid hemorrhage: recommendations from the Neurocritical Care Society's Multidisciplinary Consensus Conference. Neurocrit Care. 2011;15:211–40.
16. Perren F, et al. Transcranial ultrasound is useful in guiding treatment of cerebral vasospasm in aneurysmal subarachnoid haemorrhage. J Neurol. 2010;257:S84.
17. Weber M, Grolimund P, Seiler RW. Evaluation of posttraumatic cerebral blood flow velocities by transcranial Doppler ultrasonography. Neurosurgery. 1990;27:106–12.
18. Spitzer C, Mull M, Rohde V, Kosinski CM. Non-traumatic cortical subarachnoid haemorrhage: diagnostic work-up and aetiological background. Neuroradiology. 2005;47:525.
19. Bramwell B. Spontaneous meningeal haemorrhage. Edinb Med J. 1886;32:101.
20. Symonds CP. Spontaneous subarachnoid hemorrhage. Q J Med. 1924;18(69):93–122.
21. Symonds CP. Spontaneous subarachnoid haemorrhage. Proc R Soc Med. 1924;17:39–52.
22. Todd NV, Howie JE, Miller JD. Norman Dott's contribution to aneurysm surgery. J Neurol Neurosurg Psychiatry. 1990;53(6):455–8.
23. Dandy WE. Intracranial aneurysm of the internal carotid artery: cured by operation. Ann Surg. 1938;107(5):654–9.
24. Krayenbühl HA, Yaşargil MG, Flamm ES, Tew JM. Microsurgical treatment of intracranial saccular aneurysms. J Neurosurg. 1972;37(6):678–86.
25. Kassell NF, Peerless SJ, Durward QJ, Beck DW, Drake CG, Adams HP. Treatment of ischemic deficits from vasospasm with intravascular volume expansion and induced arterial hypertension. Neurosurgery. 1982;11(3):337–43.
26. Zubkov IN, Nikiforov BM, Shustin VA. 1st attempt at dilating spastic cerebral arteries in the acute stage of rupture of arterial aneurysms. Zh Vopr Neirokhir Im N N Burdenko. 1983;5(5):17–23.

27. Guglielmi G, Viñuela F, Dion J, Duckwiler G. Electrothrombosis of saccular aneurysms via endovascular approach. Part 2: preliminary clinical experience. J Neurosurg. 1992;75(1):8–14.
28. Ingall T, Aslund K, Mahönen M, Bonita R. A multinational comparison of subarachnoid hemorrhage epidemiology in the WHO MONICA stroke study. Stroke. 2000;31:1054.
29. de Rooij NK, Linn FH, van der Plas JA, Algra A, Rinkel GJ. Incidence of subarachnoid haemorrhage: a systematic review with emphasis on region, age, gender and time trends. J Neurol Neurosurg Psychiatry. 2007;78(12):1365.
30. Brown RD Jr, Broderick JP. Unruptured intracranial aneurysms: epidemiology, natural history, management options, and familial screening. Lancet Neurol. 2014;13:393–404.
31. Kataoka K, Taneda M, Asai T, Kinoshita A, Ito M, Kuroda R. Structural fragility and inflammatory response of ruptured cerebral aneurysms: a comparative study between ruptured and unruptured cerebral aneurysms. Stroke. 1999;30:1396–401.
32. Bor AS, Koffijberg H, Wermer MJ, Rinkel GJ. Optimal screening strategy for familial intracranial aneurysms: a costeffectiveness analysis. Neurology. 2010;74:1671–9.
33. Lall RR, Eddleman CS, Bendok BR, Batjer HH. Unruptured intracranial aneurysms and the assessment of rupture risk based on anatomical and morphological factors: sifting through the sands of data. Neurosurg Focus. 2009;26(5):E2.
34. Gondar R, et al. Unruptured intracranial aneurysm follow-up and treatment after morphological change is safe: observational study and systematic review. J Neurol Neurosurg Psychiatry. 2016;87(12):1277–82.
35. Goljan EF. Rapid review pathology. 2nd ed. St. Louis: Mosby; 2006. p. 158.
36. Alway D, Cole WJ, et al. Stroke essentials for primary care: a practical guide, vol. 153. New York: Humana Press; 2009. p. 86–8.
37. Caranci F, Briganti F, Cirillo L, Leonardi M, Muto M. Epidemiology and genetics of intracranial aneurysms. Eur J Radiol. 2012;82(10):1598–605.
38. Chalouhi N, Loh BL, Hasan D. Review of cerebral aneurysm formation, growth, and rupture. Stroke. 2013;44(12):3613–22.
39. Hunt WE, Hess RM. Surgical risk as related to time of intervention in the re-pair of intracranial aneurysms. J Neurosurg. 1968;28:14–20.
40. Fisher CM, Kistler JP, Davis JM. Relation of cerebral vasospasm to subarachnoid hemorrhage visualized by computed tomographic scanning. Neurosurgery. 1980;6:1–9.
41. Drake CG, et al. Report of world Federation of Neurological Surgeons committee on a universal subarachnoid hemorrhage grading scale. J Neurosurg. 1988;68:985–6.
42. Aggarwal A, et al. Comparative evaluation of H&H and WFNS grading scales with modified H&H (sans systemic disease): a study on 1000 patients with subarachnoid hemorrhage. Neurosurg Rev. 2018;41(1):241–7.
43. Fisher C, Kistler J, Davis J. Relation of cerebral vasospasm to subarachnoid hemorrhage visualized by computerized tomographic scanning. Neurosurgery. 1980;6(1):1–9.
44. Hunt W, Hess R. Surgical risk as related to time of intervention in the repair of intracranial aneurysms. J Neurosurg. 1968;28(1):14–20.
45. Dorsch NWC, King MT. A review of cerebral vasospasm in aneurysmal subarachnoid haemorrhage: I. incidence and effects. J Clin Neurosci. 1994;1:19–26.
46. Findlay JM, Nisar J, Darsaut T. Cerebral vasospasm: a review. Can J Neurol Sci. 2016;43(1):15–32.
47. Connolly ES Jr, For the American Heart Association Stroke Council, Council on Cardiovascular Radiology and Intervention, Council on Cardiovascular Nursing, Council on Cardiovascular Surgery and Anesthesia, Council on Clinical Cardiology, et al. Guidelines for the management of aneurysmal subarachnoid hemorrhage: a guideline for healthcare professionals from the American Heart Association/American Stroke Association. Stroke. 2012;43(6):1711–37.
48. Westermaier T, et al. Value of transcranial Doppler, perfusion-CT and neurological evaluation to forecast secondary ischemia after aneurysmal SAH. Neurocrit Care. 2014;20(3):406–12.
49. Frontera JA, et al. Prediction of symptomatic vasospasm after subarachnoid hemorrhage: the modified fisher scale. Neurosurgery. 2006;59(1):21–7.

50. Nakae R, Yokota H, Yoshida D, Teramoto A. Transcranial Doppler ultrasonography for diagnosis of cerebral vasospasm after aneurysmal subarachnoid hemorrhage: mean blood flow velocity ratio of the ipsilateral and contralateral middle cerebral arteries. Neurosurgery. 2011;69(4):876–83.
51. Lindegaard KF, Nornes H, Bakke SJ, Sorteberg W, Nakstad P. Cerebral vasospasm diagnosis by means of angiography and blood velocity measurements. Acta Neurochir. 1989;100:12–24.
52. Soustiel JF, Shik V, Shreiber R, Tavor Y, Goldsher D. Basilar vasospasm diagnosis: investigation of a modified "Lindegaard Index" based on imaging studies and blood velocity measurements of the basilar artery. Stroke. 2002;33:72–7.
53. Kirsch JD, Mathur M, Johnson MH, Gunabushanam G, Scoutt LM. Advances in transcranial Doppler US: imaging ahead. Radiographics. 2013;33:E1–E14.
54. Budohoski KP, et al. Impairment of cerebral autoregulation predicts delayed cerebral ischemia after subarachnoid hemorrhage: a prospective observational study. Stroke. 2012;12:3230–7.
55. Pickard JD, Matheson M, Patterson J, Wyper D. Prediction of late ischemic complications after cerebral aneurysm surgery by the intraoperative measurement of cerebral blood flow. J Neurosurg. 1980;53:305–8.
56. Lam JM, Smielewski P, Czosnyka M, Pickard JD, Kirkpatrick PJ. Predicting delayed ischemic deficits after aneurysmal subarachnoid hemorrhage using a transient hyperemic response test of cerebral autoregulation. Neurosurgery. 2000;47:819–25.
57. Rätsep T, Asser T. Cerebral hemodynamic impairment after aneurysmal subarachnoid hemorrhage as evaluated using transcranial Doppler ultrasonography: relationship to delayed cerebral ischemia and clinical outcome. J Neurosurg. 2001;95:393–401.
58. Jaeger M, Schuhmann MU, Soehle M, Nagel C, Meixensberger J. Continuous monitoring of cerebrovascular autoregulation after subarachnoid hemorrhage by brain tissue oxygen pressure reactivity and its relation to delayed cerebral infarction. Stroke. 2007;38:981–6.
59. Rynkowski C, et al. Early transcranial Doppler evaluation of cerebral autoregulation independently predicts functional outcome after aneurysmal subarachnoid hemorrhage. Neurocrit Care. 2019;31:253–62.
60. Gonzalez NR, Boscardin WJ, Glenn T, Vinuela F, Martin NA. Vasospasm probability index: a combination of transcranial Doppler velocities, cerebral blood flow, and clinical risk factors to predict cerebral vasospasm after aneurysmal subarachnoid hemorrhage. J Neurosurg. 2007;107:1101–12.
61. Hov MR, Ryen A, Finsnes K, Storflor J, Lindner T, Gleditsch J, Lund CG. Pre-hospital ct diagnosis of subarachnoid hemorrhage. Scand J Trauma Resusc Emerg Med. 2017;25(1):1–4.

Chapter 23
Subarachnoid Hemorrhage (SAH) in the Neuro-ICU: Usefulness of Transcranial Doppler (TCD/TCCS) for Delayed Cerebral Ischemia (DCI) Monitoring

Frederick A. Zeiler and Jeanne Teitelbaum

Key Points

1. Transcranial Doppler (TCD) employs non-invasive ultrasound technology for the assessment of cerebral blood flow velocity (CBFV).
2. CBFV measurement via TCD can occur in both the anterior and posterior cerebral circulation.
3. TCD can be employed to monitor for the development of cerebral vasospasm through the measuring middle cerebral artery (MCA) CBFV and assessing the Lindegaard ratio.
4. Through signal processing techniques, either offline or in real-time, TCD can provide continuous measures of cerebral autoregulatory capacity.
5. Non-invasive intra-cranial pressure (ICP) measurement techniques using TCD are currently being developed.
6. Newer robotic TCD technology will allow for longer duration continuous CBFV recording.

F. A. Zeiler
Section of Neurosurgery, Department of Surgery, Department of Human Anatomy and Cell Science, Rady Faculty of Health Sciences, University of Manitoba, Winnipeg, MB, Canada
e-mail: frederick.zeiler@umanitoba.ca

J. Teitelbaum (✉)
Section of Neurocritical Care, Department of Neurology, Montreal Neurological Institute, McGill University, Montreal, QC, Canada
e-mail: Jeanne.teitelbaum@mcgill.ca

C. N. Rodríguez et al. (eds.), *Neurosonology in Critical Care*,
https://doi.org/10.1007/978-3-030-81419-9_23

23.1 Introduction

Aneurysmal subarachnoid hemorrhage (SAH) carries significant upfront risk of mortality, ranging up to 20–30% mortality prior to reaching specialist hospital care [1]. For those fortunate enough to reach specialized care after onset of SAH, the risk of complications during the acute and subacute phases of illness remains high [1, 2]. Such complications include, but are not limited to: aneurysm re-rupture prior to microsurgical or endovascular therapy, seizures, neurogenic pulmonary edema, subendocardial ischemia, electrolyte disturbances, hydrocephalus, and the development of DCI [3]. The mentioned complication profile of SAH argues in favor of specialized care within experienced dedicated neuro-ICUs (NICUs) [4].

DCI, also referred to as symptomatic cerebral vasospasm, is one of the major contributors to mortality in the short-term post-SAH and long-term morbidity [3, 4]. The underlying premise behind DCI hinges on the concept of increased cerebrovascular tone, reduction in cerebral blood flow (CBF), and subsequent ischemia and/or infarction. However, exact pathophysiologic mechanisms leading to the development of increase cerebrovascular tone are unclear [5]. Current theories focus on the role of hemoglobin and its byproducts within the subarachnoid space leading to an inflammatory cascade that results in increased vascular tone and subsequent reduction in cerebral blood flow [5, 6].

The reduction in CBF post-SAH can occur both regionally and globally [7]. Furthermore, a reduction in cerebral vessel caliber can occur in the absence of clinical symptomatology, referred to as radiographic vasospasm. Our current understanding from epidemiologic studies in SAH patients indicates a risk of approximately 20% for developing symptomatic DCI secondary to cerebral vasospasm [3, 4, 6]. The risk of developing radiographic cerebral vasospasm (i.e., non-symptomatic spasm) has been quoted to occur in up to 60% of SAH patients [3, 4, 6]. Increased risk of radiographic vasospasm and DCI appears to be linked to: females, young age, smokers, hypertensive patients, high modified Fisher computed tomography (CT) grade, and severe Hunt and Hess (H + H) or World Federation of Neurological Surgeons (WFNS) clinical grade SAH. Despite these associations, it still proves difficult to predict those who will develop DCI [8].

The differing rates of DCI and radiographic vasospasm post-SAH highlight the discrepancy between radiographic abnormalities and the development of symptomatic disease. In an ideal world, we would be able to accurately predict those who will develop DCI, devoting our attention to the prevention of cerebral vasospasm in these cases and mitigating the risk of ischemia and its downstream consequences. However, our current understanding limits us to the early detection of cerebral vasospasm, employing various intermittent and continuous monitoring techniques. These techniques include: transcranial Doppler (TCD), continuous electroencephalogram (cEEG), transcutaneous near infrared spectroscopy (NIRS), invasive assessment of parenchymal CBF and metabolism, and intermittent neuro-imaging such as computed tomographic angiography/perfusion and Xenon enhanced CT [4, 5].

With the push to employ non-invasive technology within the NICU, given risk reduction to the patient and wider accessibility to non-surgeon treating physicians, TCD has been readily employed within the SAH population as a means of monitoring for the development of symptomatic and asymptomatic cerebral vasospasm. It has even received support for its application in SAH patients from the Neurocritical Care Society [9]. This chapter will focus on the application of TCD monitoring for cerebral vasospasm in SAH, highlighting: technique, indices of vasospasm, autoregulation monitoring, intra-cranial pressure (ICP) monitoring, and newer/emerging TCD technologies.

23.2 TCD Assessment of Cerebral Vascular Territories

TCD employs the use of ultrasound technology for the assessment CBFV within a vascular territory of interest. This typically involves the use of a Doppler transducer with an emission frequency of 2.0–3.5 MHz to assess, or "insonate," a vessel of interest [10–12]. Various areas of the skull, referred to as "windows," have been described for optimal assessment of various cerebral blood vessels, all at different depths of ultrasound insonation. These areas are where the skull is the thinnest or deficient, allowing for a clear and direct path for insonation of the cerebral vessel. Table 23.1 describes the main windows for TCD, the vessel territory assessed, depth

Table 23.1 TCD acoustic windows

Window name	Cranial location	Vessels assessed (insonation depth)	Limitations
Transorbital	Over closed eyelid, direct toward carotid canal	Carotid siphon (depth 55–50 mm) Ophthalmic artery (depth 40–50 mm)	Beam power must be kept <10% to avoid subluxation of lens Difficult to obtain for long durations
Transtemporal	Some literature discusses an anterior, middle, and posterior sub-window Located above root of zygoma over squamous temporal bone	ICA bifurcation (depth ~65 mm) MCA (depth 35–55 mm) ACA (depth 60–70 mm – with flow away from the probe)[a] PCA (1–2 cm posterior to ICA bifurcation, depth 60–70 mm)	Most commonly utilized window for TCD assessment Not all patients have symmetric windows Not all patients have adequate window Long duration recording difficult for ACA and PCA

(continued)

Table 23.1 (continued)

Window name	Cranial location	Vessels assessed (insonation depth)	Limitations
Suboccipital	Flexed neck, probe directed through foramen magnum toward clivus and posterior clinoid processes	Distal vertebral arteries (depth 80–115 mm just lateral of midline)[a] Basilar artery (depth 60–100 mm at midline)[a]	Difficult to obtain longer duration recordings Uncomfortable for patient to remain in this position for extended periods
Submandibular	At angle of jaw	Distal cervical ICA (depth 40–60 mm)	Limited to extracranial ICA only Requires operator to hold probe in direction of vessel for duration of recording (i.e., rigid probe holders not readily available)

ACA anterior cerebral artery, *cm* centimeters, *mm* millimeters, *MCA* middle cerebral artery, *PCA* posterior cerebral artery
Note: "a" denotes that these vascular territories will have flow directed away from the probe during insonation, where all other vessels mentioned above typically have flow toward the probe
Purkayastha et al. [12]

of insonation, and some of the region-specific limitations. It should be noted that not all patients have perfect cerebral vasculature, and not all patients have good windows for insonation at every vascular territory. Figure 23.1 displays the position of the window and ultrasound probe placement for the common windows of interest in TCD assessment.

The overarching premise is that the Doppler probe assesses the Doppler frequency shift in ultrasound signal that occurs in response to cerebral blood flow. This Doppler frequency shift is then utilized to calculate CBFV and other TCD indices. In order to obtain the purest measure via TCD, ideally one would have the ultrasound probe in perfect line with the direction of CBF (i.e., 0-degree angle of insonation). For sake of practicality, an insonation angle of 30 degrees or less is considered acceptable for accurate measurements [10].

Though each window and territory of interest has different positioning, the general technique for TCD is as follows: first, identify the vascular territory of interest and the desired window for insonation. Second, apply ultrasound gel to the skin overlaying the window. Third, using a 2.0–3.5 MHz Doppler probe, attempt to insonate the vessel of interest through the window. Fourth, using the pulse waveform CBFV window on the ultrasound machine, assess the shape of the CBFV waveform, it should have the classic pulsatile shape as seen in Fig. 23.2a. Fifth,

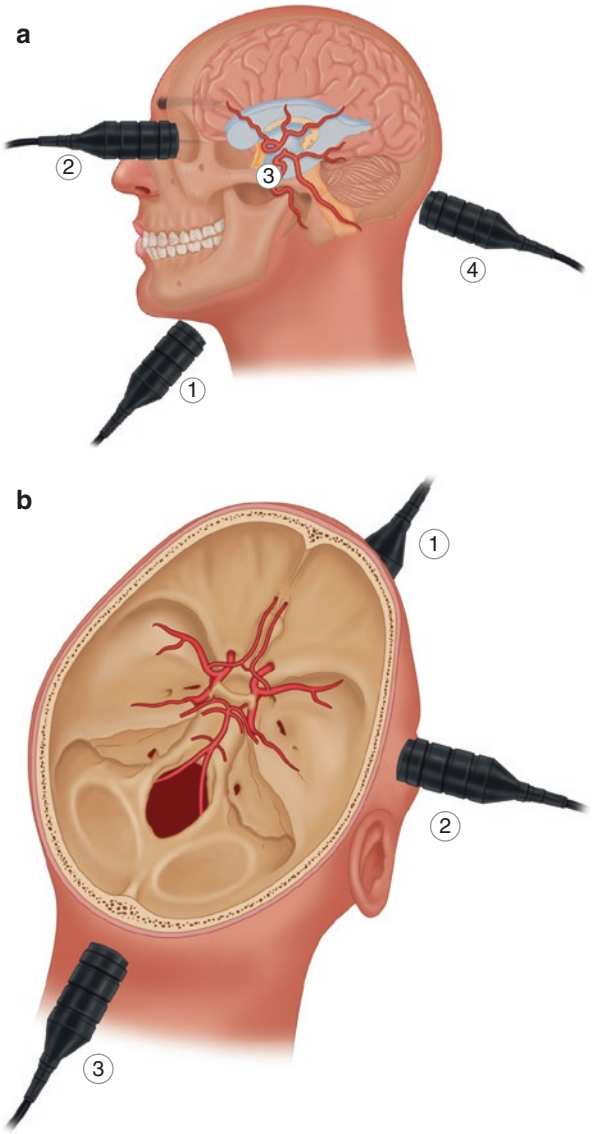

Fig. 23.1 TCD windows TCD transcranial Doppler. (Panel **a**): Sagittal view depicting various TCD windows. #1 = submandibular window, #2 = transorbital, #3 = transtemporal, #4 = suboccipital. (Panel **b**): Axial view depictive circle of Willis and various TCD windows. #1 = transorbital, #2 = transtemporal, #3 = subocciptial. (Illustrations by Jon Stepaniuk)

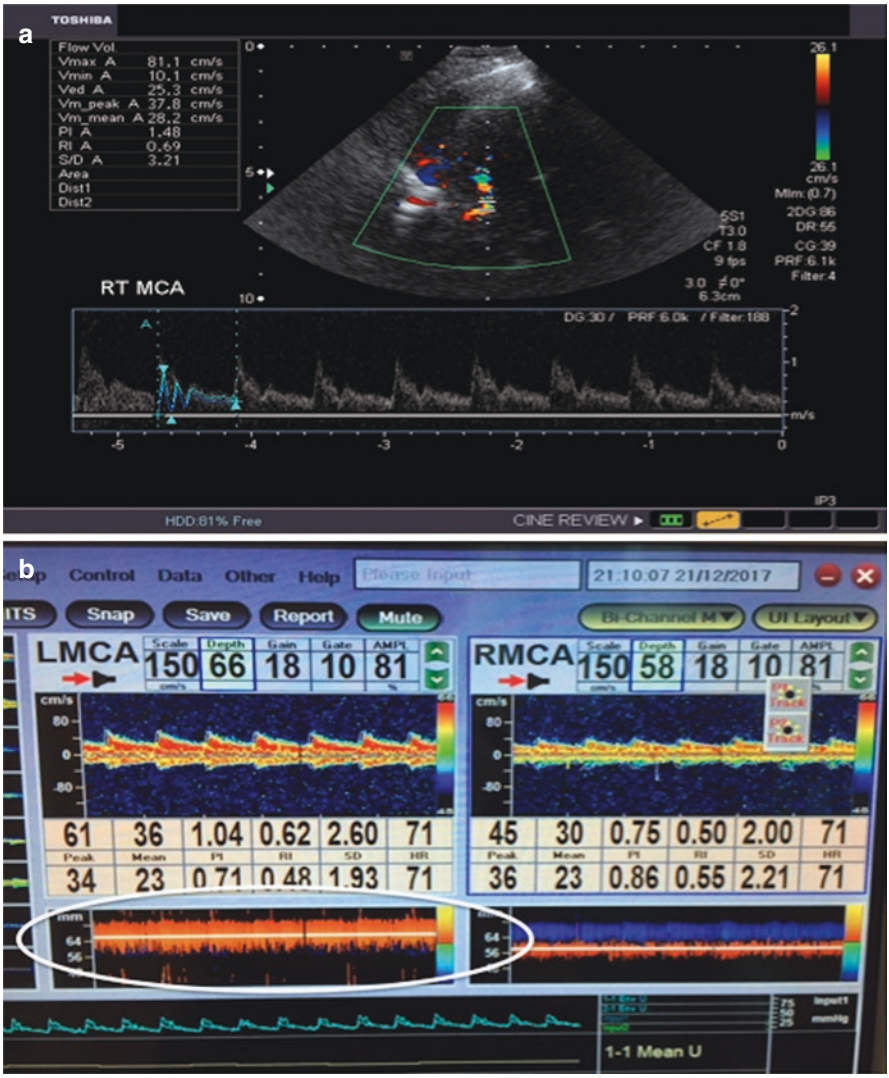

Fig. 23.2 CBFV waveform and M-Mode via TCD of the MCA. CBFV cerebral blood flow velocity, MCA middle cerebral artery, TCD transcranial Doppler. Panel (**a**): Unilateral insonation of the right MCA. Panel (**b**): Bilateral simultaneous insonation of the MCA, with the white circle highlighting the M-mode display

once an adequate CBFV waveform is obtained, use the M-mode (Power Motion Doppler mode) window to assess the signal flow intensity over various depths in the direction of insonation. This allows for the selection of the appropriate depth of insonation, depending on the vascular territory of interest [13]. The M-mode display can be seen in Fig. 23.2b. Finally, once adequate CBFV waveform and depth of

insonation are obtained, one should obtain at least 30 s of stable recording prior to obtaining measurements for clinical purposes.

In order to obtain longer duration recordings, various companies have developed frames or headbands, allowing for hands-free insonation. These are typically designed for TCD of the middle cerebral artery (MCA) only. These devices still suffer from shifting and signal loss from patient movement and are thus not perfect, requiring intermittent attention at the bedside for long recordings. Newer technology has been developed to potentially solve this issue and will be briefly covered in the "Future Directions" section of this chapter.

23.3 TCD for Assessment of Cerebral Vasospasm

23.3.1 Premise

Increase in cerebral vascular tone leads to the reduction in vessel caliber. This reduction in luminal diameter leads to an increase in CBFV. Thus, in the setting of cerebral vasospasm post-SAH, TCD can be utilized to follow the trend in CBFV over time. As vessel spasm worsens, CBFV subsequently increases. Though the values that indicate cerebral vasospasm are unclear, an increase by 30 cm/s or more in CBFV in a particular territory likely indicates vasospasm.

23.3.2 Literature in SAH

Given that the MCA is the most accessible artery for TCD and that it feeds a major hemispheric territory, the majority of the literature on TCD for SAH focuses on insonation of the MCA via a trans-temporal window. Within the MCA territory, values indicative of cerebral vasospasm are as follows. CBFV below 100 cm/s is unlikely to be associated with spasm, whereas those between 120 and 200 cm/s indicate potential vasospasm. Finally, CBFV above 200 cm/s are thought to clearly indicate the presence of vasospasm [9]. One other metric of MCA TCD in SAH is called the Lindegaard ratio. This is the ratio between the mean flow velocity of MCA (MFV_{MCA}) and extra-cranial internal cerebral artery (ICA) MFV_{ICA} (obtained through the insonation of the ICA in the neck). This ratio is also trended over time as a method of monitoring for cerebral vasospasm. A ratio less than 3 indicates, in the absence of increased MCA CBFV, no vasospasm. A ratio less than 3 with increased MCA CBFV potentially signals hyperemia. A ratio between 3 and 6 indicates mild to moderate vasospasm. Finally, a ratio greater than 6 indicates severe cerebral vasospasm [1, 9, 14].

$$\text{Lindegaard Ratio}\left(\text{LR}\right) = \text{MFV}_{\text{MCA}} \,/\, \text{MFV}_{\text{ICA}}$$

Numerous studies have been published linking the above MCA CBFV values and Lindegaard ratio values to the risk of developing DCI. A recent systematic review and meta-analysis have also been published in this context [14]. This review found 17 unique manuscripts documenting objective TCD measures of CBFV and the development of symptomatic cerebral vasospasm, or DCI, post-SAH. TCD evidence of vasospasm was defined as MFV_{MCA} of 120 cm/s or greater and a Lindegaard ratio of 3 or greater. Overall, TCD-based assessment of the MCA in SAH patients carried a 90% sensitivity (95% CI: 77–96) and 71% specificity (95% CI: 51–84) to predict symptomatic cerebral vasospasm/DCI. However, this did not address the association between TCD-based vasospasm and presence of angiographic confirmed spasm. Despite this oversight, the Neurocritical Care Society supports these metrics, if one desires to employ TCD in for monitoring cerebral vasospasm in SAH [9].

An algorithmic approach to standard TCD CBFV monitoring of the MCA in aneurysmal SAH patients can be found at the end of this chapter, prior to the reference section (section 8.0). This provides a schematic for the approach to various TCD-based CBFV recording values and Lindegaard ratio values, highlighting what these values indicate and the potential risk for underlying cerebral vasospasm in the SAH patient.

23.3.3 Limitations

There are clear limitations of this technique for monitoring DCI in SAH patients. First, the reference ranges for MCA CBFV and the Lindegaard ratio are vague and not entirely precise. Literature supports the potential for the presence of radiographic spasm in the absence of TCD abnormalities, thus highlighting its limitations. Second, the majority of the existing literature evaluates monitoring of the MCA territory in SAH patients, and the reference ranges and quantitative ratio measures described for the MCA are not readily described for other vascular territories. Both the anterior cerebral arteries (ACA) and posterior circulation are difficult to insonate, not always being feasible for every patient. This does not minimize the importance of being able to monitor them. Finally, the technique for TCD is labor intensive and tedious, even with newer probe holding devices. Signal is easily lost and sometimes difficult to re-obtain. Accurate measures require trained staff. This all limits the duration of recording that is obtainable with current commonly employed technology, leading to intermittent assessments of regional cerebral vascular accessible through available patient TCD windows. Thus, longer duration continuous recordings (i.e., over 30 min) are the exception, not the expectation.

23.4 TCD for Semi-Intermittent Assessment of Cerebral Autoregulation in SAH

23.4.1 Technical Requirements

Various techniques for cerebral autoregulation testing have been developed and are described across the spectrum of neuro-pathologic conditions [11, 15–17]. A few utilize TCD as a means of cranial monitoring. Most techniques employing TCD refer to purely intermittent methods, either via thigh-cuff deflation technique, transient hyperemic response, or orthostatic response testing [11, 15, 18]. All of these intermittent techniques obtain spot measures of autoregulatory capacity either through assessing direct changes in MCA CBFV or through the application of more complex first order differential equation modeling. These will not be cover in more detail here, given they are intermittent and require direct manipulation of the patient's physiology.

Continuously updating measures of cerebral autoregulation are possible using TCD, though we refer to them as "semi-intermittent" given the labor intensity of TCD signal acquisition. These require either offline or real-time complex CBFV signal processing. With the advent of commercially available signal acquisition/processing software, this signal manipulation is available for real-time application within the NICU [19, 20]. The most widely described program for such application in neurocritically ill patients is the software called intensive care monitoring plus (ICM+) (Cambridge Enterprise Ltd., Cambridge, UK, http://www.neurosurg.cam.ac.uk/icmplus). This software, like others, records physiologic signals from various multi-modal monitoring devices employed within the NICU (including TCD), linking the high frequency digital signals (typically sampled at 100–200 Hz) in time-series, for further complex analysis techniques.

To assess cerebral autoregulatory capacity, we require assessing the relationship between a surrogate measure of pulsatile cerebral blood volume (CBV) or CBF (i.e., CBFV) and a driving pressure, either mean arterial pressure (MAP) or cerebral perfusion pressure (CPP). This is done through assessing the response in slow waves (i.e., frequency range 0.05–0.005 Hz) of TCD CBFV to slow wave fluctuations in MAP or CPP [21, 22].

In order to obtain this information, high frequency (i.e., 100–200 Hz) digital signals from TCD MCA CBFV and MAP (from arterial line) or CPP (from ICP and MAP monitoring) are recorded. A non-overlapping moving average filter is applied to these high frequency signals, to decimate the signal to 0.1 Hz, allowing for assessment of slow wave responses. This frequency range has been linked to cerebral autoregulatory capacity [21]. Then, using time-domain analysis techniques, we derive continuously updating moving Pearson correlation coefficients between mean CBFV (also denoted MFV) and either MAP or CPP, using 30 consecutive 10 s windows of data (i.e., 5 min of data), typically updated every minute. The most commonly described TCD index of cerebral autoregulation is called mean flow index (Mx – correlation between MFV and CPP), with its MAP version denoted

Table 23.2 TCD-based autoregulation/cerebrovascular reactivity indices and calculation methods

Index	Signals correlated	Signal averaging (sec)	Pearson correlation coefficient calculation window (min)	Index calculation update frequency (sec)
Mx	MFV and CPP	10	5	60
Mx-a	MFV and MAP	10	5	60
Sx	PSV and CPP	10	5	60
Sx-a	PSV and MAP	10	5	60
Dx	EDV and CPP	10	5	60
Dx-a	EDV and MAP	10	5	60

CBF cerebral blood flow, *CPP* cerebral perfusion pressure, *Dx* diastolic flow index, *Dx-a* diastolic flow index based on MAP, *EDV* End-diastolic flow velocity, *MFV* mean flow velocity, *PSV* Peak systolic flow velocity, *MAP* mean arterial pressure, *min* minute, *sec* seconds, *Mx* mean flow index, *Mx-a* mean flow index derived from MAP, *Sx* systolic flow index, *Sx-a* systolic flow index based on MAP, *TCD* transcranial Doppler. Note: FVs = calculated using maximum FV over 1.5 s period, updated every 1 s; EDV = calculated using the minimum FV over 1.5 s period, updated every 1 s

Mx-a (correlation between MFV and MAP) [16, 22]. For all of the described continuous indices of cerebral autoregulation, positive values typically denote "impaired" autoregulation, while negative values are believed to denote "intact" autoregulation. Table 23.2 displays the various TCD-derived indices of cerebral autoregulation and method of derivation.

Note that in the absence of either an external ventricular drain or parenchymal ICP monitor, CPP cannot be utilized in the derivation of these indices. However, the MAP versions can be derived through either continuous blood pressure obtained invasively through an arterial line or non-invasively through finger-tip-based blood pressure cuff technology (Finapres Medical Systems, Netherlands, http://www.finapres.com). This non-invasive version of MAP monitoring allows for a completely non-invasive means of cerebral autoregulation assessment through applying TCD assessment of CBFV.

23.4.2 Literature in SAH

Though the current literature body on TCD-based cerebral autoregulation monitoring in SAH patients is limited, the results to date are promising [17, 23, 24]. One small study found a link between progressive worsening in TCD base Mx index and the incidence of large vessel vasospasm ($p = 0.007$) [25]. Another study of 98 patients found increased odds of developing DCI post-SAH when early (i.e., within first 5 days) impaired autoregulation was found, when using TCD-based systolic flow index based on MAP (Sx-a) (OR 7.46; 95% CI: 3.03–18.40, $p < 0.000001$). This was confirmed in multi-variate analysis (OR 12.66; 95%CI: 2.87–54.07, $p = 0.001$), including age, sex, WFNS grade, modified Fisher CT score, present of

hydrocephalus, development of sepsis, metabolic derangements, and standard TCD-based assessment for cerebral vasospasm (i.e., MCA CBFV >120 cm/s and Lindegaard ratio >3.0) [26]. Furthermore, the presence of bilateral impairment of cerebral autoregulation, as measured by TCD-based Sx-a, was found to be linked to worse outcome post-SAH, with those developing DCI having a larger inter-hemispheric difference in Sx-a measurements ($p = 0.035$, 95%CI: 0.003–0.08) [27]. These results require validation in larger populations, but are promising for continuous cerebral autoregulation monitoring with TCD in SAH and its link to DCI.

23.4.3 Limitations

Despite the interesting application of complex signal processing and the promising initial literature supporting its association with cerebral vasospasm post-SAH, there are significant limitations. First, it requires specialized software to record high frequency digital signals, later used for processing. It also requires integration of this software with ICU monitoring devices, allowing for capture of digital physiologic signals. Second, though recent software development has improved accessibility, deriving these continuously updating indices requires some specialized knowledge and training. Finally, the literature is currently limited and requires much further validation before widespread application of this type of monitoring for clinical decision making in SAH patients.

23.5 Non-invasive Estimation of ICP

Though not indicative of cerebral vasospasm or DCI in SAH, elevations in ICP are of interest to the treating physician, particularly in those SAH patients whom have developed ischemic insults secondary to cerebral vasospasm. Current gold standard ICP monitoring employs either the use of a ventricular catheter or parenchymal pressure monitoring for the measurement of ICP. Both of these options are invasive and require technical expertise for insertion, precluding their use by many physicians involved in the care of the SAH patients.

Recent literature suggests that through the application of TCD, one can potentially obtain a non-invasive estimation of ICP [28, 29]. This can be achieved through three main methods: (A) use of TCD-based pulsatility index, (B) CPP estimation method, and (C) mathematical modeling. Detailed exploration of these methods is beyond the scope of this chapter, and we thus refer the reader to the referenced articles for further information [28, 29]. Though promising, the future is still unclear regarding this method of ICP estimation, but warrants mention in reference to TCD in SAH.

23.6 Future Directions

By exploring the above application of TCD in monitoring for cerebral vasospasm, DCI, and their consequences in SAH, it can be seen that there exists a role for TCD in this patient population. The main limitations of the above-mentioned monitoring relate to the technical demands of TCD insonation and intermittent nature of recording. Recent advances in technology have led to the commercial availability of robotic TCD devices, allowing for bilateral simultaneous insonation of the MCA. These devices employ TCD sensor technology with an automatic algorithm to aid with the set-up and acquisition of initial CBFV signal, followed by sensing technology to correct for any shift in the head frame or signal loss during recording. This automatic technology carries the potential to increase the speed and ease of signal acquisition, followed by allowing for much long continuous recordings of MCA CBFV. In addition, these devices are currently under evaluation and being integrated with signal acquisition software, allowing for longer continuous assessment of cerebral autoregulatory capacity. Figure 23.3 displays an example of the newer robotic TCD device (Delica EMS 9D System, Shenzen Delica Medical Equipment Co. Ltd., China).

As these devices and technological advances like it become more available, the role for TCD in SAH will surely expand and become more accessible to units where expertise and staff availability for the application of TCD and prolonged recording are limited. Furthermore, integration of TCD monitoring with other multi-modal monitoring devices employed within the NICU (such as NIRS, cerebral microdialysis, CBF monitoring, and advanced neuro-imaging), and we will be able to gain better understanding in the pathophysiologic process.

23.7 Conclusion

TCD monitoring in SAH for cerebral vasospasm and DCI is feasible and provides potential for quick, non-invasive bedside monitoring. This currently requires assessing trends in TCD monitoring over time via region-specific transcutaneous cranial windows. The technique caries limitations given its labor intensity, which may be overcome with emerging technological advances in TCD monitoring.

Fig. 23.3 New robotic TCD system TCD = transcranial Doppler. Panel (**a**): Head band holder for bilateral robotic controlled TCD probes. Solid black arrow denotes the encased robotic control system. Dashed arrow indicates black TCD probe, which is automatically moved by robotic device in response to automated signal detection algorithm. Panel (**b**): Robotic TCD touch-screen monitor. Panel (**c**): Bilateral TCD recording in real time. Panel (**d**): Robotic TCD probed controlling system displaying various probes positions insonated automatically via robotic system, with color-coded intensities

Algorithm

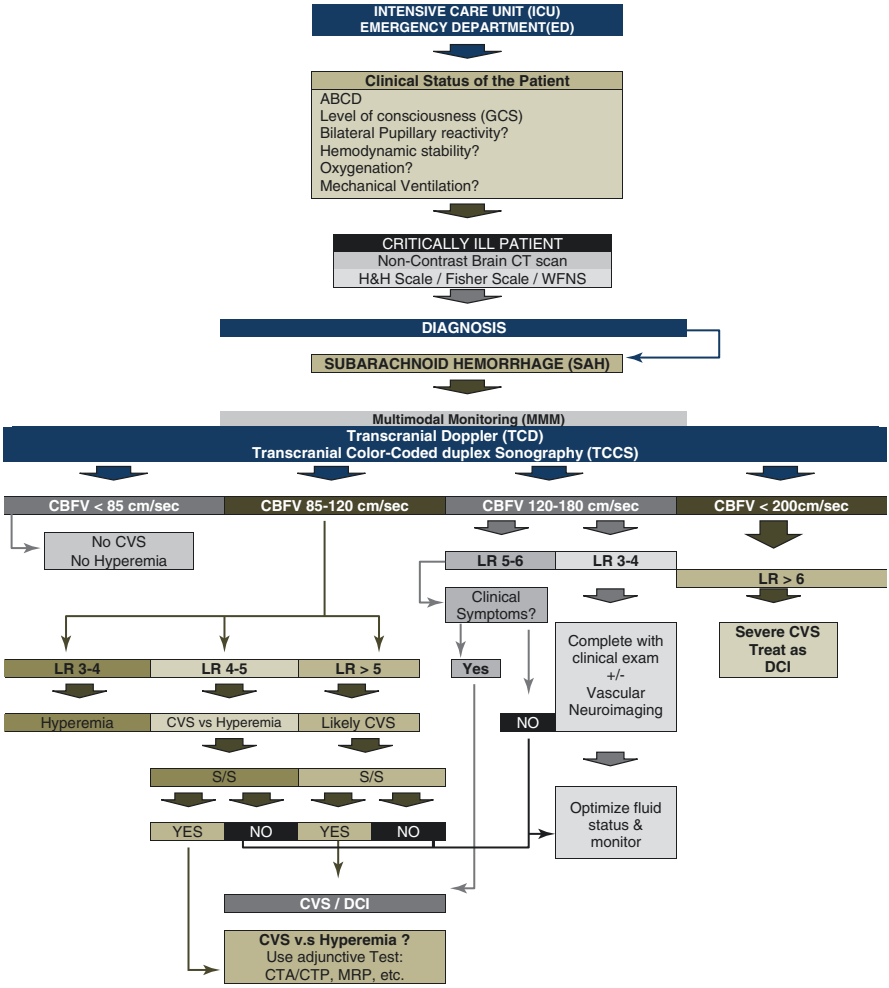

ABCD Airway-Breathing-Circulation-Disability, *LR* Lindegaard Ratio, *DCI* Delayed cerebral ischemica, *CBFV* Cerebral Blood Flow Velocity, *S/S* Signs – Symptoms, *VS* Vasospasm, *WFNS* Word Federation of neurosurgeons scale, *H&H* Hunt & Hess scale, *CVS* Cerebral vasospasm

References

1. Solenski NJ, Haley EC Jr, Kassell NF, Kongable G, Germanson T, Truskowski L, et al. Medical complications of aneurysmal subarachnoid hemorrhage: a report of the multicenter, cooperative aneurysm study. Participants of the Multicenter Cooperative Aneurysm Study. Crit Care Med. 1995;23(6):1007–17.

2. Hop JW, Rinkel GJ, Algra A, van Gijn J. Case-fatality rates and functional outcome after subarachnoid hemorrhage: a systematic review. Stroke. 1997;28(3):660–4.
3. Kassell NF, Sasaki T, Colohan AR, Nazar G. Cerebral vasospasm following aneurysmal subarachnoid hemorrhage. Stroke. 1985;16(4):562–72.
4. Diringer MN, Bleck TP, Claude Hemphill J 3rd, Menon D, Shutter L, Vespa P, et al. Neurocritical Care Society. Critical care management of patients following aneurysmal subarachnoid hemorrhage: recommendations from the Neurocritical Care Society's Multidisciplinary Consensus Conference. Neurocrit Care. 2011;15(2):211–40.
5. Francoeur CL, Mayer SA. Management of delayed cerebral ischemia after subarachnoid hemorrhage. Crit Care. 2016;20(1):277.
6. Budohoski KP, Guilfoyle M, Helmy A, Huuskonen T, Czosnyka M, Kirollos R, Menon DK, et al. The pathophysiology and treatment of delayed cerebral ischaemia following subarachnoid haemorrhage. J Neurol Neurosurg Psychiatry. 2014;85(12):1343–53.
7. Dorsch N. A clinical review of cerebral vasospasm and delayed ischaemia following aneurysm rupture. Acta Neurochir Suppl. 2011;110(Pt 1):5–6.
8. de Rooij NK, Rinkel GJ, Dankbaar JW, Frijns CJ. Delayed cerebral ischemia after subarachnoid hemorrhage: a systematic review of clinical, laboratory, and radiological predictors. Stroke. 2013;44(1):43–54.
9. Washington CW, Zipfel GJ, Participants in the International Multi-disciplinary Consensus Conference on the Critical care management of subarachnoid hemorrhage. Detection and monitoring of vasospasm and delayed cerebral ischemia: a review and assessment of the literature. Neurocrit Care. 2011;15(2):312–7.
10. D'Andrea A, Conte M, Cavallaro M, Scarafile R, Riegler L, Cocchia R, et al. Transcranial Doppler ultrasonography: from methodology to major clinical applications. World J Cardiol. 2016;8(7):383–400.
11. Kalanuria A, Nyquist PA, Armonda RA, Razumovsky A. Use of transcranial Doppler (TCD) ultrasound in the neurocritical care unit. Neurosurg Clin N Am. 2013;24(3):441–56.
12. Purkayastha S, Sorond F. Transcranial Doppler ultrasound: technique and application. Semin Neurol. 2012;32(4):411–20.
13. Alexandrov AV, Demchuk AM, Burgin WS. Insonation method and diagnostic flow signatures for transcranial power motion (M-mode) Doppler. J Neuroimaging. 2002;12(3):236–44.
14. Kumar G, Shahripour RB, Harrigan MR. Vasospasm on transcranial Doppler is predictive of delayed cerebral ischemia in aneurysmal subarachnoid hemorrhage: a systematic review and meta-analysis. J Neurosurg. 2016;124(5):1257–64.
15. Zeiler FA, Donnelly J, Calviello L, Menon DK, Smielewski P, Czosnyka M. Pressure autoregulation measurement techniques in adult traumatic brain injury, part I: a scoping review of intermittent/semi-intermittent methods. J Neurotrauma. 2017;34(23):3207–23.
16. Zeiler FA, Donnelly J, Calviello L, Smielewski P, Menon DK, Czosnyka M. Pressure autoregulation measurement techniques in adult traumatic brain injury, part II: a scoping review of continuous methods. J Neurotrauma. 2017;34(23):3224–37.
17. Rivera-Lara L, Zorrilla-Vaca A, Geocadin R, Ziai W, Healy R, Thompson R, et al. Predictors of outcome with cerebral autoregulation monitoring: a systematic review and meta-analysis. Crit Care Med. 2017;45(4):695–704.
18. Budohoski KP, Czosnyka M, Smielewski P, Varsos GV, Kasprowicz M, Brady KM, et al. Cerebral autoregulation after subarachnoid hemorrhage: comparison of three methods. J Cereb Blood Flow Metab. 2013;33(3):449–56.
19. Smielewski P, Czosnyka M, Steiner L, Belestri M, Piechnik S, Pickard JD. ICM+: software for on-line analysis of bedside monitoring data after severe head trauma. Acta Neurochir Suppl. 2005;95:43–9.
20. Guendling K, Smielewski P, Czosnyka M, Lewis P, Nortje J, Timofeev I, Hutchinson PJ, Pickard JD. Use of ICM+ software for on-line analysis of intracranial and arterial pressures in head-injured patients. Acta Neurochir Suppl. 2006;96:108–13.

21. Fraser CD 3rd, Brady KM, Rhee CJ, Easley RB, Kibler K, Smielewski P, Czosnyka M, Kaczka DW, Andropoulos DB, Rusin C. The frequency response of cerebral autoregulation. J Appl Physiol (1985). 2013;115(1):52–6.
22. Sorrentino E, Budohoski KP, Kasprowicz M, Smielewski P, Matta B, Pickard JD, Czosnyka M. Critical thresholds for transcranial Doppler indices of cerebral autoregulation in traumatic brain injury. Neurocrit Care. 2011;14(2):188–93.
23. Budohoski KP, Czosnyka M, Kirkpatrick PJ. The role of monitoring cerebral autoregulation after subarachnoid hemorrhage. Neurosurgery. 2015;62(Suppl 1):180–4.
24. Budohoski KP, Czosnyka M, Kirkpatrick PJ, Smielewski P, Steiner LA, Pickard JD. Clinical relevance of cerebral autoregulation following subarachnoid haemorrhage. Nat Rev Neurol. 2013;9(3):152–63.
25. Calviere L, Nasr N, Arnaud C, Czosnyka M, Viguier A, Tissot B, Sol JC, Larrue V. Prediction of delayed cerebral ischemia after subarachnoid hemorrhage using cerebral blood flow velocities and cerebral autoregulation assessment. Neurocrit Care. 2015;23(2):253–8.
26. Budohoski KP, Czosnyka M, Smielewski P, Kasprowicz M, Helmy A, Bulters D, Pickard JD, Kirkpatrick PJ. Impairment of cerebral autoregulation predicts delayed cerebral ischemia after subarachnoid hemorrhage: a prospective observational study. Stroke. 2012;43(12):3230–7.
27. Budohoski KP, Czosnyka M, Kirkpatrick PJ, Reinhard M, Varsos GV, Kasprowicz M, Ząbek M, Pickard JD, Smielewski P. Bilateral failure of cerebral autoregulation is related to unfavorable outcome after subarachnoid hemorrhage. Neurocrit Care. 2015;22(1):65–73.
28. Khan MN, Shallwani H, Khan MU, Shamim MS. Noninvasive monitoring intracranial pressure – a review of available modalities. Surg Neurol Int. 2017;8:51.
29. Cardim D, Robba C, Bohdanowicz M, Donnelly J, Cabella B, Liu X, Cabeleira M, Smielewski P, Schmidt B, Czosnyka M. Non-invasive monitoring of intracranial pressure using transcranial Doppler ultrasonography: is it possible? Neurocrit Care. 2016;25(3):473–91.

Chapter 24
Aneurysmal Subarachnoid Hemorrhage and Endovascular Treatment: Usefulness of Transcranial Doppler (TCD/TCCS) for Cerebral Hemodynamic Monitoring

Laura Llull Estrany

Key Points

1. Subarachnoid hemorrhage (SAH) is a devastating disease with high morbidity and mortality. Delayed cerebral ischemia due to vasospasm is one of the main hemodynamic complications. Up to 30% of patients may develop delayed cerebral ischemia related to vasospasm. Early detection can guide clinical decisions at patient's bedside.
2. Transcranial Doppler (TCD/TCCS) is an accessible and reproducible tool, applicable for the monitoring of cerebral blood flow velocities (CBFVs) and hemodynamic indexes derived from them.
3. The use of Echo-contrast may increase the sensitivity of the detection of unruptured intracranial aneurysms and their recanalization after endovascular treatment.
4. New technologies of TCD can improve its sensitivity. It allows intraoperative and continuous monitoring in patients at high risk of developing vasospasm.

24.1 Introduction

Transcranial Doppler (TCD/TCCS) is a non-invasive method with numerous clinical applications in critically ill patients with acute brain injury (ABI). In addition to diagnostic and monitoring of vasospasm in patients with SAH, the use of TCD has recently been extended to the detection and characterization of intracranial aneurysms.

TCD is performed by a low-frequency transducer ($\leq$2 MHz) through acoustic window in the skull (bone window or natural hole), allowing visualization of basal cerebral arteries and measuring CBFVs in different clinical scenarios [1] (Fig. 24.1).

L. Llull Estrany (✉)
Cerebral Vascular Pathology Unit, Hospital Clínic, Barcelona, Spain
e-mail: llull.laura@gmail.com

C. N. Rodríguez et al. (eds.), *Neurosonology in Critical Care*,
https://doi.org/10.1007/978-3-030-81419-9_24

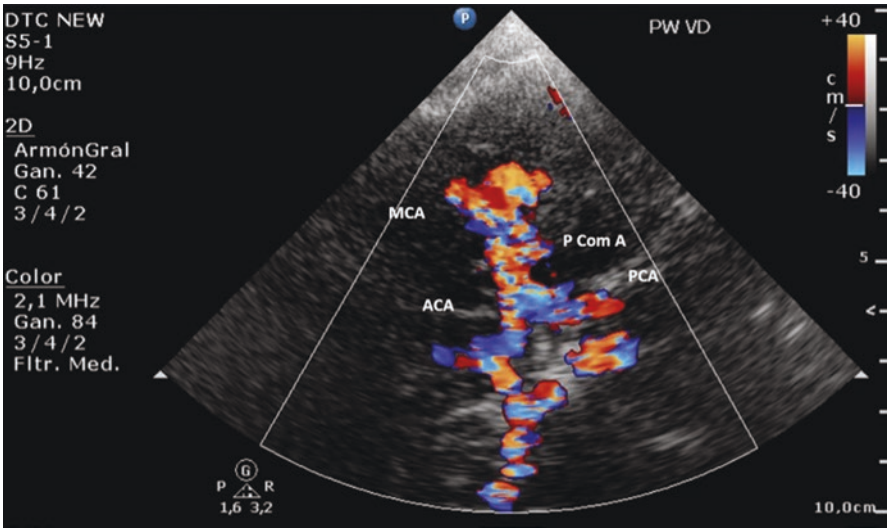

Fig. 24.1 Image obtained by TCCS: transtemporal acoustic window showing the circle of Willis in a patient with SAH. MCA middle cerebral artery, ACA anterior cerebral artery, PCA posterior cerebral artery, PcomA posterior communicating artery

24.2 Subarachnoid Hemorrhage (SAH): Epidemiology and Pathophysiology

Subarachnoid hemorrhage (SAH) is a disease with high morbidity and mortality with high social impact [2]. SAH is the third most common cerebrovascular disorder (after intracranial hemorrhage and acute ischemic stroke). Approximately 80% of spontaneous, non-traumatic SAH result from aneurysm rupture [2, 3]. Worldwide, incidence is approximately 9.1/100,000 adults. In the USA, the incidence of SA is higher in woman (2:1), African Americans, Hispanics, and above 55-year-olds.

After SAH triggers the activation of numerous deleterious mechanisms: (1) increased intracranial pressure; (2) decreased cerebral blood flow (CBF); (3) impairment of cerebral auto-regulation (CA); and (4) exposure to inflammation and cerebral metabolism changes. All of these clinical circumstances can lead to the appearance of early secondary brain injury, occurring most commonly in the first 72 h after bleeding [3, 4].

SAH patients are at high risk for multiple complications in the weeks following their initial bleed. Delayed cerebral ischemia (usually present after the first 72 h from symptom onset) is the second most common cause of morbidity and mortality after the early brain injury of the initial SAH and is most commonly due to arterial vasospasm. Both early and delayed cerebral ischemia have been established as important predictors of poor prognosis [2], and it is accepted that their pathogenesis is multifactorial. The exact underlying pathophysiological mechanisms remain unknown.

24.2.1 Vasospasm

Vasospasm, the leading cause of delayed cerebral ischemia, is one of the major complications of SAH. Vasospasm is defined as a CBF reduction induced by vasoconstriction of intracranial arteries not attributable to: atherosclerosis, spasm induced by catheter manipulation, or vessel hypoplasia. It occurs in up to 70% of patients between 3 and 14 days after initial bleeding (has been reported up to 21 days). Vasospasm becomes symptomatic in 20–40% of patients and is considered responsible for 20% of morbidity and mortality in SAH [5].

The main risk factors for the appearance of vasospasm include initial clinical severity, the amount of bleeding, and the presence of intraventricular hemorrhage (IVH) [6]. Therefore, vasospasm has a multifactorial origin.

Digital subtraction angiography (DSA) is considered the gold standard technique for vasospasm detection (CT angiography may be a valid option). However, DSA is an invasive technique and therefore not applicable if serial monitoring is required. On the other hand, TCD/TCCS is a non-invasive, repeatable, and low-cost method that allows the diagnosis and daily monitoring of vasospasm of critically ill patients in the ICU.

TCD/TCCS is a useful and reliable method for the detection of hemodynamic changes. Therefore, it is considered a suitable tool for daily monitoring of vasospasm and early diagnosis of neurological worsening related to vasospasm.

In many institutions, TCD (as a blind technique) has been used as a tool for cerebral vasospasm monitoring due to its reproducibility and ability to detect variations in cerebral hemodynamics. However, TCD is an operator-dependent technique and that the measurement can be influenced by the angle of insonation, giving rise to under- or overestimates of CBFVs values.

The hemodynamic parameters most commonly measured are: (1) CBFVs (Peak systolic velocity (PSV), end-diastolic velocity (EDV), and mean flow velocity (MFV)), (2) direction of CBFVs, (3) spectral Doppler waveform analysis (flow patterns), (4) sound (turbulence or attenuation cerebral blood flow), and (5) hemodynamic indexes/ratios: pulsatility index (PI), resistance index (RI), and Lindegaard ratio (LR).

In recent years, most centers have incorporated transcranial color-coded duplex sonography (TCCS) methodology. The main advantage of TCCS is the visualization of intracranial vessels (B-mode), which allows for a targeted evaluation of each arterial segment and its corresponding CBFVs [7, 8]. The direct visualization of the cerebral basal arteries (circle of Willis) through color-Doppler mode allows the detection of segments in main arteries of anterior and posterior circulation, facilitating the detection of hemodynamic alterations secondary to vasospasm [9].

The MFV in cerebral basal arteries is directly proportional to CBF and inversely proportional to the section area of the insonated vessel, where any clinical situation that causes a variation of vessel diameter will affect the MFV. Hence, vasospasm is one of the most common causes of increased MFV after SAH. CBFVs that define the severity of vasospasm are clearly established for the MCA, but not for the ACA, PCA, and BA [10].

Progressive or persistent elevation in CBFV may be due to hyperemia or vasospasm, where LR (relationship of MFV between MCA and extra cranial portion of

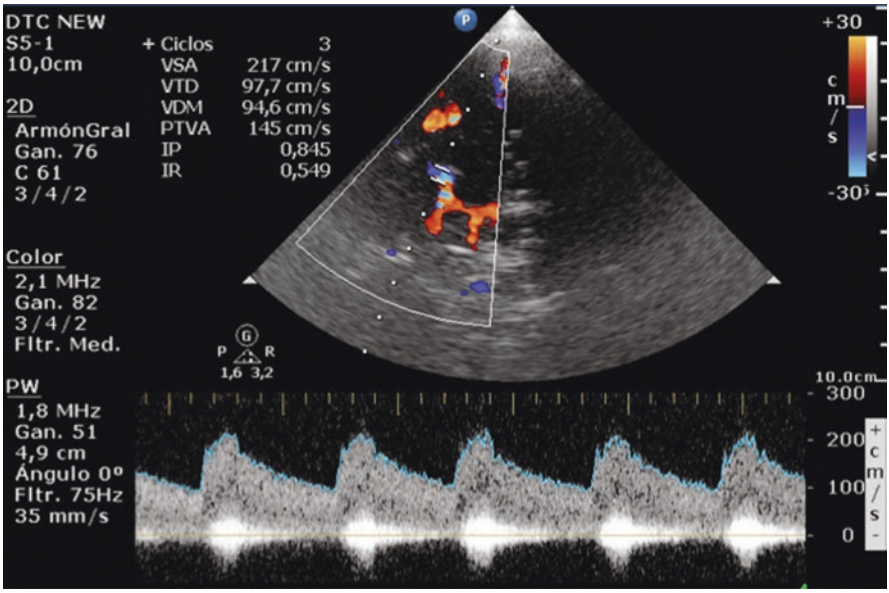

Fig. 24.2 TCCS insonation performed on a patient with aneurysmal SAH (MCA) in which moderate vasospasm and artifact corresponding to the presence of the coils used are observed

ICA) allows for the differentiation between them, while helping to classify the vasospasm severity (Fig. 24.2).

There have been reports in the literature of another ratio obtained by TCD/TCCS that correlates better with vasospasm than MFV measurement in patients with SAH.

This ratio has been calculated from the relationship between MFV in the ipsilateral MCA (defined ipsilateral MCA where highest CBFV) and MFV of the contralateral MCA (ipsilateral MFV_{MCA}/contralateral MFV_{MCA}). The value of this ratio to predict DCI was more auspicious than MFV measurement. The cut-off value that best discriminated the risk of DCI was 1.5 [11].

24.2.2 Vasospasm Diagnostic Criteria

Adapted from Marshal et al. [12].

24.2.2.1 Diagnostic Criteria of Vasospasm (VSP) by TCD/TCCS in MCA

Major (severe vasospasm):

- Change in MFV with respect to baseline greater than 50 cm/s
- Mean flow velocity (MFV) >200 cm/s
- Lindegaard ratio >6

Minor (moderate vasospasm):

- Mean flow velocity (MFV) >120 cm/s
- Lindegaard ratio >3

It is necessary to consider the appearance of a decrease in the CBFV in the poststenotic segment and the appearance of CBF turbulence when the degree of stenosis, secondary to vasospasm, is higher than 50% of diameter of the insonated vessel [10].

Due to the segmental nature of vasospasm and the need for daily monitoring by TCD/TCCS, it is important to identify the arterial segment affected. Therefore, it is convenient to record the MFV measurement corresponding to the depth of each segment of each cerebral basal artery insonated for a real-time control at the patient's bedside in the ICU.

In patients with SAH admitted to the ICU, daily monitoring using TCCS methodology can be useful to define the need for neuroimaging (CT, MRI, CTA, DSA) to evaluate brain parenchyma impact and/or decide intra-arterial therapy (angioplasty or drug administration) [13].

The prevalence of early angiographic vasospasm, defined as the appearance of angiographic vasospasm in the first 48 h after SAH, is estimated at around 10%. In some studies, the presence of vasospasm on admission has been identified as an independent prognostic factor in this patients [14, 15]. Patients with intracerebral hematoma, intraventricular hemorrhage, large aneurysm size (>12 mm), and MCA aneurysms appear to have a greater risk of early vasospasm [16].

24.3 TCD/TCCS: Cerebral Vasoreactivity

Dilatation of the cerebral arterioles results in a reduction in cerebrovascular resistance (CVR) allowing CBF to increase in the proximal segments of the cerebral basal arteries. While arteriolar vasoconstriction increases CVR and therefore causes CBF reduction. Cerebral vasoreactivity is the vasoconstriction and vasodilatation capacity of intracranial vessels after stimulus (e.g. vasoactive drugs) and is a measure of the integrity of CA. Vasoreactivity can be assessed measuring by CBFV changes. Those hemodynamic changes can be measured by TCD/TCCS [17, 18].

Cerebral vasoreactivity can be assessed by TCD/TCCS after acetazolamide administration in patients with ruptured intracranial aneurysms [19, 20]. In these trials, vasoreactivity was normal in both brain hemispheres, and the location of the aneurysm did not influence the final results. Likewise, the development of vasospasm in the acute stage of SAH did not cause an alteration in cerebral vasoreactivity.

Since the influence of cerebral vasoreactivity on vasospasm development has been proposed, researchers evaluated the existence of differences in hemodynamic response of cerebral basal arteries after acetazolamide administration in a group of 37 patients with unruptured cerebral aneurysm [21] and detected no differences

between affected and non-affected brain hemisphere or between subjects with aneurysm compared to healthy subjects.

These results suggest that patients with unruptured aneurysm have no alterations in cerebral vasoreactivity after aneurysm treatment (e.g., clipping, coiling).

24.4 TCD/TCCS: Intraoperative Monitoring

Several intraoperative monitoring modalities, including indocyanine angiography, electrophysiological studies, and micro-Doppler ultrasonography, are used to verify correct positioning of the surgical clip to secure cerebral aneurysm. Siasios et al. in 2012 [22] studied a series of 19 patients in whom micro-Doppler had been performed during surgery. In all of these patients, the high diagnostic capacity of this technique was demonstrated.

Given the technical difficulties of microsurgery for ruptured intracranial aneurysms and the accessibility and reliability of intraoperative ultrasonography, its use as a complementary tool during aneurysm clipping could be considered with the intention to minimize the risk of intraoperative complications or improper clip placement.

24.5 Detection of Intracranial Aneurysms and Recanalization of Treated Aneurysms

Recanalization of the aneurysmal neck is a complication that can appear after treatment, so long-term follow-up and detection of this recanalization is relevant.

Power Doppler mode is an accessible and non-invasive technique for anterior circulation aneurysms detection, but less sensitive than other diagnostic methods (e.g. DSA, CTA, MR angiography). The sensitivity of power Doppler is low for small aneurysms (<5 mm). Also, the terminal segment of the ICA is the most difficult to interpret [23] (Fig. 24.3).

The use of non-invasive imaging techniques such as TCD/TCCS, capable of detecting the residual neck in a secured aneurysm, would significantly reduce diagnostic costs, as well as potential complications, radiation exposure, and the use of radiological contrast.

Turner et al. in 2005 [24] evaluated the ability of TCCS with and without an echo-contrast to detect aneurysmal neck recanalization in patients with secured intracranial aneurysms by coiling. The authors reported that their results compared with those of the arteriography. The sensitivity of TCCS was approximately 80% for the detection of occluded aneurysms and, in the case of recanalized aneurysms, TCCS sensitivity increased as the degree of recanalization of the neck increases.

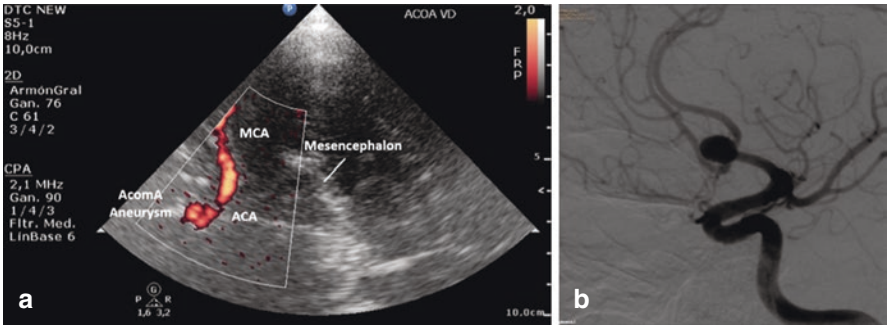

Fig. 24.3 (**a**) TCCS: Power Doppler mode image of an anterior communicating artery aneurysm (AcomA). (**b**) Diagnostic arteriography of the same patient in which the AcomA aneurysm of 7 mm maximum diameter is visualized

The administration of the echo-contrast contributed to the diagnosis of other recanalized aneurysms that had not been detected without it. Hence, TCCS and echo-contrast could be useful to monitoring the recanalization of aneurysmal neck reducing the use of invasive monitoring methods such as cerebral arteriography.

The use of flow-diverter stents for the treatment of unruptured aneurysms and ruptured aneurysms, where surgical clipping or coiling is not possible, has been increasing. Several studies have reported on the probability of long-term stenosis after deployment of flow-diverter stents. Therefore, TCD/TCCS should be considered as a useful monitoring tool to detect stenosis of flow-diverter stents [25, 26].

24.6 Cerebral Aneurysms and Cerebral Blood Flow: Other Techniques

Non-invasive monitoring of the brain microcirculation by means of a laser-Doppler flowmeter system allows for the availability of sensitive and real time information of the brain microcirculation during the surgery. In a small number of patients, it was evaluated how the detection of local pathological changes in the microcirculation would act as a predictor of post-operative prognosis, validating these intraoperative findings with other monitoring techniques such as somatosensory evoked potentials (SSEPs) [27].

Recent advances in robotics have contributed to the development of transcranial Doppler probes incorporating automated algorithms for flow rate detection and optimization of the signal recorded in the MCA (Delica EMS 9D robotic TCD system®). Today, this technique is beginning to be applied in the management and monitoring of patients with traumatic brain injury (TBI). Indeed, a new field of study in SAH is opening. This type of probe allows for the automatic recording CBFVs of both MCA continuously for 4 h and correlates these values with other systemic hemodynamic parameters [28, 29]. This technology has not been applied

at present in SAH patients. A possible limitation of this technique includes the detection of vasospasm from arteries other than the middle cerebral artery, which should be evaluated further (more details see Chap. 66).

24.7 Conclusion

Subarachnoid hemorrhage (SAH) is a devastating disease with high morbidity and mortality. The most frequent neurological complication, after the acute effects of initial SAH, is delayed cerebral ischemia due to vasospasm, which can appear in up to 70% of patients, with an incidence peak between days 4 and 14, and can last until day 21 after bleeding. Up to 30% of cases can be associated with focal neurological deficits.

Transcranial Doppler (TCD/TCCS) is a non-invasive, reproducible technique performed at the bedside, which allows for the monitoring of CBFVs. TCD/TCCS also allows for the daily detection and monitoring of vasospasm, even in patients admitted to ICU.

In addition to the absolute values of MFV (MCA, ACA, PCA, and BA) defined as vasospasm, it is important to keep in mind that an increase of MFV greater than 50 cm/s from the previous day must be considered as a vasospasm criterion.

In unruptured aneurysms, no alterations in cerebral vasoreactivity have been detected in cerebral basal arteries.

The power Doppler mode allows for the detection of intracranial aneurysms (diameter >5 mm). The use of echo-contrast increases diagnostic sensitivity both for the identification of unruptured aneurysms and for the detection of neck recanalization in secured aneurysms.

New techniques are being developed that incorporate Doppler as a diagnostic tool and could be applied in normal clinical practice, such as laser-Doppler for intraoperative monitoring and/or robotic-TCD for the detection and monitoring vasospasm in patients with SAH.

References

1. D'Andrea A, Conte M, Cavallaro M, Scarafile R, Riegler L, Cocchia R, et al. Transcranial Doppler ultrasonography: from methodology to major clinical applications. World J Cardiol. 2016;8(7):383–400.
2. Macdonald RL, Schweizer TA. Spontaneous subarachnoid hemorrhage. Lancet. 2017;389(10069):655–66.
3. Fujii M, Yan J, Rolland WB, Soejima Y, Caner B, Zhang JH. Early brain injury, an evolving frontier in subarachnoid hemorrhage research. Transl Stroke Res. 2013;4(4):432–46.
4. Lucke-Wold BP, et al. Aneurysmal subarachnoid hemorrhage and neuroinflammation: a comprehensive review. Int J Mol Sci. 2016;17(4):497.

5. Vivancos J, et al. Guia de actuacion clinica en la hemorragia subaracnoidea. Sistematica diagnostica y tratamiento. Neurologia. 2012;S0213-4853(12):00249–6.
6. Singh H, et al. Subarachnoid hemorrhage. In: Frontera JA, editor. Decision making in neurocritical care. Primera ed. New York: Thime Medical Publishers, Inc.; 2009. p. 1–20.
7. Platz J, Güresir E, Wagner M, Seifert V, Konczalla J. Increased risk of delayed cerebral ischemia in subarachnoid hemorrhage patients with additional intracerebral hematoma. J Neurosurg. 2017;126(2):504–10.
8. Ehlert A, et al. Molsidomine for the prevention of vasospasm-related delayed ischemic neurological deficits and delayed brain infarction and the improvement of clinical outcome after subarachnoid hemorrhage: a single-center clinical observational study. J Neurosurg. 2016;124(1):51–8.
9. Wang JL, Li XN, Zhang YH, Li X, Yang YL. Evaluation function of transcranial two-dimensional and color Doppler ultrasonography (TCCS) for patients with different degrees of cerebral vasospasm before and after the nimodipine treatment. Eur Rev Med Pharmacol Sci. 2017;21:2757–63.
10. Rasulo FA, De Peri E, Lavinio A. Transcranial Doppler ultrasonography in intensive care. Eur J Anaesthesiol Suppl. 2008;42:167–73.
11. Nakae R, Yokota H, Yoshida D, Teramoto A. Transcranial Doppler ultrasonography for diagnosis of cerebral vasospasm after aneurysmal subarachnoid hemorrhage: mean blood flow velocity ratio of the ipsilateral and contralateral middle cerebral arteries. Neurosurgery. 2011;69(4):876–83.
12. Marshall SA, Nyquist P, Ziai WC. The role of transcranial Doppler ultrasonography in the diagnosis and management of vasospasm after aneurysmal subarachnoid hemorrhage. Neurosurg Clin N Am. 2010;21:291–303.
13. D'Andrea A, et al. Transcranial Doppler ultrasound: physical principles and principal applications in neurocritical care unit. J Cardiovasc Echogr. 2016;26(2):28–41.
14. Baldwin ME, et al. Early vasospasm on admission angiography in patients with aneurysmal subarachnoid hemorrhage is a predictor for in-hospital complications and poor outcome. Stroke. 2004;35:2506–11.
15. Qureshi AI, Sung GY, Suri MA, Straw RN, Guterman LR, Hopkins LN. Prognostic value and determinants of ultraearly angiographic vasospasm after aneurysmal subarachnoid hemorrhage. Neurosurgery. 1999;44:967–73.
16. Phan K, et al. Ultra-early angiographic vasospasm after aneurysmal subarachnoid hemorrhage: a systematic review and meta-analysis. World Neurosurg. 2017;102:632–8.
17. Gur AY, Bornstein NM. TCD and the Diamox test for testing vasomotor reactivity: clinical significance. Neurol Neurochir Pol. 2001;35(3):51–6.
18. Aaslid R, Markwalder TM, Nornes H. Noninvasive transcranial Doppler ultrasound recording of flow velocity in basal cerebral arteries. J Neurosurg. 1982;57(6):769–74.
19. Szabo S, Sheth RN, Novak L, Rozsa L, Ficzere A. Cerebrovascular reserve capacity many years after vasospasm due to aneurysmal subarachnoid hemorrhage. A transcranial Doppler study with acetazolamide test. Stroke. 1997;28(12):2479–82.
20. Jarus-Dziedzic K, Głowacki M, Warzecha A, Jurkiewicz J, Czernicki Z, Fersten E. Cerebrovascular reactivity evaluated by transcranial Doppler sonography in patients after aneurysmal subarachnoid hemorrhage treated with microsurgical clipping or endovascular coiling technique. Neurol Res. 2011;33(1):18–23.
21. Bøthun ML, Haaland ØA, Logallo N, Svendsen F, Thomassen L, Helland CA. Cerebrovascular reactivity after treatment of unruptured intracranial aneurysms–a transcranial Doppler sonography and acetazolamide study. J Neurol Sci. 2016;363:97–103.
22. Siasios I, Kapsalaki EZ, Fountas KN. The role of intraoperative micro-Doppler ultrasound in verifying proper clip placement in intracranial aneurysm surgery. Neuroradiology. 2012;54(10):1109–18.
23. White PM, Wardlaw JM, Teasdale E, Sloss S, Cannon J, Easton V. Power transcranial Doppler ultrasound in the detection of intracranial aneurysms. Stroke. 2001;32:1291–7.

24. Turner CL, et al. Intracranial aneurysms treated with endovascular coils: detection of recurrences using unenhanced and contrast-enhanced transcranial color-coded duplex sonography. Stroke. 2005;36(12):2654–9.
25. Briganti F, Leone G, Cirillo L, de Divitiis O, Solari D, Cappabianca P. Postprocedural, midterm, and long-term results of cerebral aneurysms treated with flow-diverter devices: 7-year experience at a single center. Neurosurg Focus. 2017;42(6):E3.
26. McDougall CM, et al. Ultrasound for the evaluation of stenosis after flow diversion. J Neurointerv Surg. 2018;10(3):297–300.
27. Schmitz E, et al. Intraoperative vascular neuromonitoring in patients with subarachnoid hemorrhage: a pilot study using combined laser-doppler spectrophotometry. World Neurosurg. 2017;107:542–8.
28. Zeiler FA, Smielewski P. Application of robotic transcranial Doppler for extended duration recording in moderate/severe traumatic brain injury: first experiences. Crit Ultrasound J. 2018;10(1):16.
29. Zeiler FA, Czosnyka M, Smielewski P. Optimal cerebral perfusion pressure via transcranial Doppler in TBI: application of robotic technology. Acta Neurochir. 2018;160:2149–57.

Chapter 25
Carotid Dissection in ICU: Usefulness of Bedside Ultrasound Examination and Pupillary Early Approach

Claudio Baracchini and Filippo Farina

Key Points

1. A carotid artery dissection (CAD) is often an obscure and unrecognized cause of stroke.
2. A polytraumatic patient admitted to the ICU with a CAD carries a 70% risk of stroke.
3. Ultrasound is the most widely available and rapidly accessible tool for CAD screening.
4. Daily monitoring is mandatory as multivessel dissection develops in up to 25% of cases in the first week of hospitalization.
5. Bedside ultrasound examination of the pupil might reveal a subtle pupillary dysfunction determined by a hidden distal CAD.

25.1 Introduction

Carotid artery dissection (CAD) is a major cause of ischemic stroke in young and middle-aged adults accounting for up to 25% of cases, with a mean age of occurrence of 44 years [1, 2].

In population-based studies, the annual incidence of internal carotid artery (ICA) dissection (ICAD) is estimated to be about 1.7 new cases/100.000; common carotid artery (CCA) dissections are very rare (<1% of all CADs) [3]. The true incidence of CAD is probably underestimated, because cases of CAD with little or no clinical signs – mainly non-ischemic CADs – are likely to remain undiagnosed [4].

C. Baracchini (✉)
Director of Stroke center and Neurosonology Lab, University of Padua School of Medicine, President - ESNH, Padova, Italy
e-mail: claudiobaracchini@gmail.com

F. Farina
Department of Neuroscience, University of Padua School of Medicine, Padova, Italy

C. N. Rodríguez et al. (eds.), *Neurosonology in Critical Care*,
https://doi.org/10.1007/978-3-030-81419-9_25

Noteworthy, multivessel dissections have been reported in 15–25% of cases [5–7]. However, many of these CADs may go undetected because they are asymptomatic or oligosymptomatic and they frequently recanalize spontaneously.

CADs involve more frequently the extracranial vessel segments probably due to a higher mobility of the vessel at these sites compared to the intracranial segments and therefore more exposed to traumas. In fact some CADs are traumatic, often due to motor vehicle accidents. However, in most instances, CADs are spontaneous [2] and in such cases a multifactorial disease has been suggested with an intrinsic non-atheromatous alteration of the vessel wall as the main predisposing factor. A higher incidence of arterial elongation, namely, kinking or coiling, has been reported in patients with CAD [8, 9], but this finding has not been confirmed by other investigators [10].

The clinical features of internal carotid dissection (ICAD) are very well known by physicians (TIA/ischemic stroke in young adults). Nonetheless a potentially dangerous dissection with a high risk for an embolic intracranial artery occlusion may present with a seemingly harmless headache or neck pain in the first few days and escape correct interpretation [11]. Notably, an ICAD carries more than 70% risk of stroke [4]; consequently a correct clinical suspicion is of paramount importance for an early diagnosis and stroke prevention.

25.2 Anatomy of the Carotid Arteries

The common carotid arteries provide the main blood supply to the brain, the face, and the neck. On the left, the CCA arises directly from the aortic arch, whereas on the right it originates from the brachiocephalic trunk, although numerous anatomic variations have been described [12, 13]. The CCA ascends through the neck without branching up to the level of the thyroid cartilage, approximately at C4–C5, where it widens at the carotid bifurcation and separates into the internal carotid artery (ICA) and external carotid artery (ECA). The former, characterized by a dilated proximal segment called the carotid bulb or sinus, supplies the brain, while the latter supplies the neck and the face. Useful features to distinguish ICA from ECA are: (1) location: ICA usually lies in a dorsolateral position in relation to ECA; (2) caliper: ICA is larger than ECA; (3) branching: ICA usually does not branch until it reaches the skull, while ECA has many branches: superior thyroid, lingual, facial, maxillary, superficial temporal, occipital arteries. The extracranial ICA location, course, and caliper are known to vary from one patient to another and even from one side to the other of the same subject [14].

The intracranial course of ICA is subdivided into six segments [15] according to the structures crossed by the vessel along its route. The ICA enters the skull through the carotid foramen, where it runs medially in the carotid petrosal canal (C6

segment), leaving the skull through the foramen lacerum in a vertical direction (C5 segment). Then the vessel bends over itself while crossing the cavernous sinus (C4–C3 segment) to form the carotid syphon and branches into the ophthalmic artery. After entering the subarachnoid space (C2 segment) and branching into the posterior communicating and the choroidal arteries, the ICA rises to its terminal part (C1) where it finally bifurcates into the middle cerebral artery (MCA) and the anterior cerebral artery (ACA).

25.3 Anatomy of the Pupil

The pupil is a small hole in the center of the iris regulating the amount of light reaching the retina. The pupillary diameter is controlled by two muscles, the sphincter pupillae, which is primarily under the control of the parasympathetic nervous system, and the dilator pupillae, which is primarily under the control of the sympathetic nervous system [16]. Contraction of the sphincter, accompanied by relaxation of the dilator, produces pupil constriction (miosis), while contraction of the dilator, accompanied by relaxation of the sphincter, produces pupil dilation (mydriasis).

The pupillary light reflex (PLR) is the constriction of the pupil due to an increase in illumination rate of the retina. It is a four-neuron pathway made-up by an afferent pathway [from retinal cells through the optic nerve to the mesencephalic pretectal nucleus and then to the ipsilateral/contralateral Edinger-Westphal nucleus (EWn)] and an efferent pathway (from EWn neurons through the oculomotor nerve to the ciliary ganglion and then to the sphincter muscle of the iris). A direct PLR is observed in the stimulated eye, while the consensual PLR occurs in the contralateral eye. The presence of a direct PLR represents the integrity of the anterior visual pathways, while a consensual PLR reflects the integrity of the mesencephalic nuclei and oculomotor nerves. The assessment of pupillary reflexes is a clinically useful tool to detect any pathological process that might impair these pathways.

The ciliospinal reflex (CR) is the dilation of the pupil in reaction to a painful stimulus applied at the base of the neck or face. Afferent inputs are carried by the trigeminal nerve or cervical pain fibers (lateral spinothalamic tract). The afferent input, when arising from the neck and upper trunk, may activate the second-order sympathetic neurons at the ciliospinal center of Budge bypassing the first order sympathetic neurons or brainstem [17, 18].

The sympathetic neurons of the ciliospinal center are found at C8-T1 in the spinal cord. The axons of these neurons via the dorsal roots enter the sympathetic trunk and then run rostrally to the superior cervical ganglion. Ascending fibers from the superior cervical ganglion follow the carotid course into the orbit, ending in the ciliary nerves and innervating the dilator pupillae. The presence of a CR reflects the integrity of the ascending sympathetic pathway.

25.4 CAD: Diagnosis

Thanks to the technological advancement, color-coded duplex sonography has become the most widely available and rapidly accessible tool in everyday practice for CAD screening [19], revealing the surprising frequency of CAD as a cause of stroke.

The cornerstone of spontaneous CAD pathophysiology and diagnosis is the presence of an intramural hematoma of unknown etiology, possibly caused by a tear in the tunica intima, a primary rupture of vasa vasorum in the medio-adventitial borderzone [20], or an underlying arteriopathy impairing vasomotion [6, 21]. The mural hematoma occurs within the media layer expanding distally and circumferentially. It is usually subintimal and causes arterial stenosis or occlusion, leading to cerebral ischemia due to embolization or less frequently due to hemodynamic failure; sometimes, the subintimal hematoma can also rupture back through the intima, forming a perfused false lumen which is separated from a true lumen by a dissecting membrane. More rarely, the mural hematoma is subadventitial, causing only pain and local symptoms due to the compression of adjacent structures [22]. Ultrasound sensitivity in detecting CAD is quite high (80–95%). It frequently shows luminal and vessel wall alterations that suggest dissections, yet pathognomonic findings are few and rarely detected [19, 23]. Furthermore, an ultrasound study might be normal in case of a subtle intramural hematoma, a low grade narrowing of the vessel lumen, and when the vessel segment is not accessible by ultrasound. Therefore, ultrasound alone is rarely definitively diagnostic. For this reason, the diagnostic work-up should include an axial cervical MRI using the T1 fat suppression technique that best detects intramural hematomas [24–26] as a hyperintense crescent-shaped signal of various intensities depending on the stage and an eccentric flow void of the patent lumen, a pathognomonic finding in dissections (Fig. 25.1).

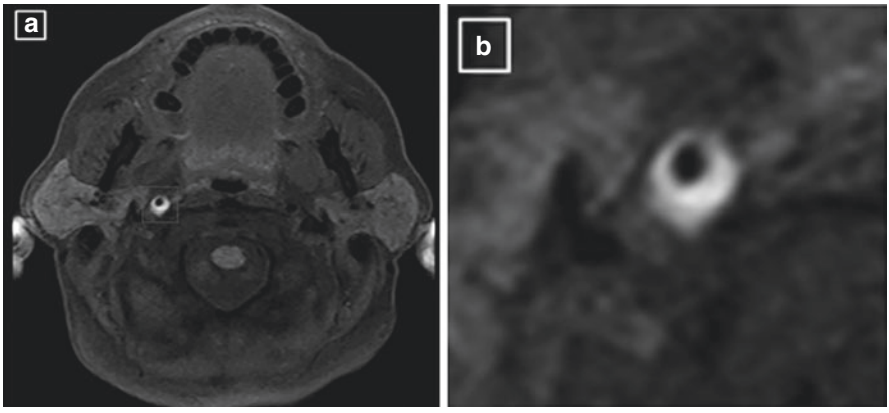

Fig. 25.1 Cervical MRI (axial plane and T1 fat suppression technique): (**a**) Carotid artery dissection. (**b**) Enlarged view of the semilunar signal hyperintensity representing intramural hematoma

With regards to other neuroimaging techniques, invasive catheter angiography has been replaced by MRI as the gold standard for extracranial dissections, while CTA and MRA are chosen to localize the dissection site and demonstrate its extension and possible complications such as pseudoaneurysms. In occlusive dissections, only MRI is able to show the cause, as both catheter angiography and MRA/CTA show aspecific findings. In dissected vessels of smaller diameter and/or tortuous course, specific MRI findings are less frequent due to small dimensions of the mural hematoma and artifacts such as flow related enhancement. Thus, in these instances (e.g., intracranial dissections), catheter angiography is considered the most reliable diagnostic method.

When compared to MRI, ultrasound has some advantages: (1) In addition to local morphological signs, it documents vessel wall hemodynamics which may be suggestive of dissection. (2) It evaluates hemodynamic consequences in the intracranial circulation. (3) It can be easily repeated, and this property of ultrasound is crucial as dissections are dynamic processes with extension of mural hematoma in the longitudinal and/or transversal plane, possibly turning from a normal finding to an occlusion of the vessel within a short time. This characteristic of the disease makes the sensitivity of any diagnostic method clearly time-dependent and represents the main determinant of discrepant findings in different studies, especially when compared to other imaging modalities performed later on. Therefore, it is strongly recommended in the case of initially normal results to repeat the exam the day after since it might disclose completely different findings. (4) The realm of ultrasound is monitoring the recanalization process once the diagnosis is established and treatment started, in order to guide the decision on the duration of antithrombotic therapy [27].

25.5 Scanning Tips for the Carotid Arteries

Ultrasound evaluation of patients with a clinical suspicion of carotid dissection should include a complete study of the anterior circulation: (i) a morphological and hemodynamic assessment of both CCAs and of the extracranial portion of the ICAs; (ii) a hemodynamic evaluation of the intracranial portion of the ICAs, of the MCAs and ACAs; and (iii) documentation of collateral circulation.

High-frequency (5–10 MHz) linear transducers allow a detailed evaluation of the carotid wall in proximal cervical segments. However, the distal parts of both internal carotids are not accessible with this approach; consequently for studying these segments, low-frequency (1.8–3.6 MHz) sector probes are used. But a limit of these probes is their significantly lower spatial resolution at B-mode and Color Doppler imaging, and therefore, they have a lower chance of detecting directly the intramural hematoma. The intracranial vessels should be investigated via the transtemporal, submandibular, and transorbital approaches with a phased array transducer ($\geq$2 MHz).

25.6 Pupil: Ultrasound Examination

Insonation of the eye should be performed in dimmed light with the patient in supine position and eyes closed. According to current recommendations on orbital insonation [28], the mechanical index (MI) must be adjusted below 0.26 and the total insonation time must be kept as short as possible. The examination can be performed either with a linear (11 MHz) or with a surgical probe (15 MHz). Due to the superficial localization of the structures to be assessed, ultrasound settings should be adjusted to proper near field examination. The probe is placed on the inferior rim of the orbit, then it is tilted downwards approximately 45° in order to insonate the iris plane. The pupil is viewed as an anechoic round structure in the middle of a hyperechogenic ring (i.e., the iris). In order to achieve a more stable image, the patient is asked to look upwards. Having obtained a clear B-mode image, pupillary function is tested. To elicit the PLR, a simple diagnostic penlight should be turned on approximately 2 cm in front of the patient's closed eyes [29] (Fig. 25.2).

To test the CR, a painful stimulation (pinching) should be applied at the base of the neck on the trapezius muscle ipsilaterally to the tested eye. The stimulus should be vigorous in order to achieve a reliable CR [30] (Fig. 25.3). The pupillary reactions should be documented either in M-mode or by continuous video recording. In particular, pupillary diameters (PD) and pupillary constriction/dilation times (PCT/PDT) should be measured at the point of maximum miosis/mydriasis. PD and PCT/PDT can be easily measured offline.

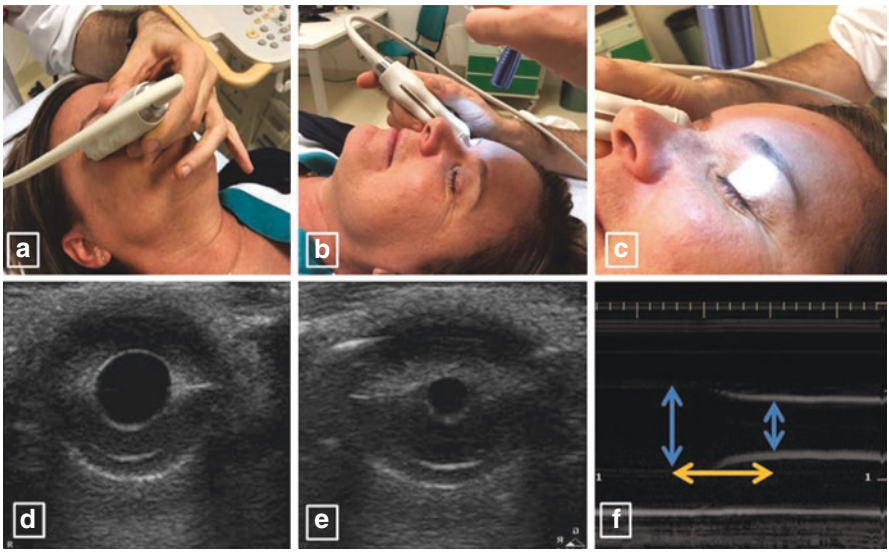

Fig. 25.2 Ultrasound assessment of pupillary light reflex (PLR). (**a**) Initial probe positing; (**b**) elicitation of direct PLR; (**c**) elicitation of consensual PLR; (**d**) B-mode visualization of pupil at rest; (**e**) B-mode visualization of pupil in miosis after stimulus; (**f**) M-mode measurement of pupillary diameter (in blue) and pupillary constriction time (in yellow)

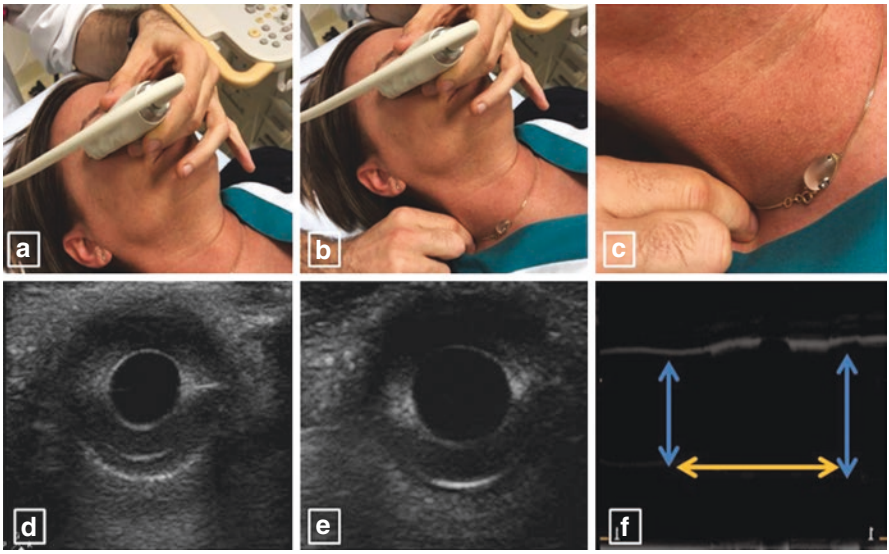

Fig. 25.3 Ultrasound assessment of ciliospinal reflex (CR). (**a**) Initial probe positing; (**b**) elicitation of CR; (**c**) site of stimulation; (**d**) B-mode visualization of pupil at rest; (**e**) B-mode visualization of pupil in mydriasis after stimulus; (**f**) M-mode measurement of pupillary diameter (in blue) and pupillary dilation time (in yellow)

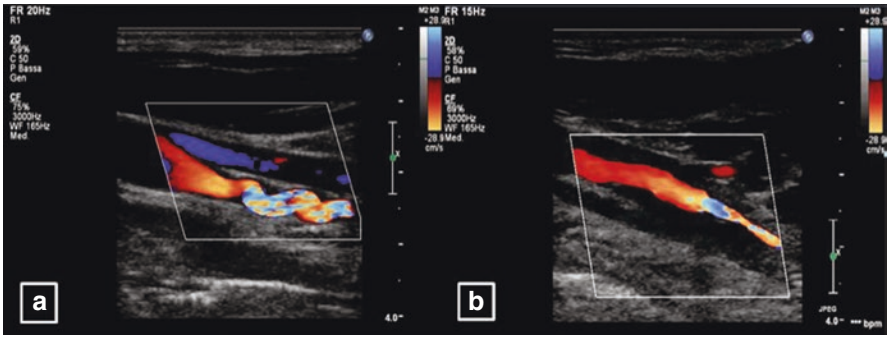

Fig. 25.4 Internal carotid artery dissection: (**a**) serpiginous stenosis, surrounded by a hypoechogenic thickening of the vessel wall representing the intramural hematoma. (**b**) Distal tapering stenosis

25.7 Internal Carotid Artery Dissection (ICAD): Ultrasound Findings

In patients with ICAD, there are two main types of ultrasound findings, morphological and hemodynamic; moreover, they can be direct or indirect (Fig. 25.4).

Direct morphological findings are represented by hypoechogenic thickening of the vessel wall, lumen narrowing, echolucent intramural hematoma, double lumen, intimal flap, dissecting membrane, and pseudoaneurysm [31–33]. Notably, pathognomonic signs are found in only one quarter of patients; specifically, the detection rates of an intramural hematoma, a double lumen, and an intimal flap are about 15–25%, ≤2%, and 2%, respectively [19, 23].

Indirect morphological findings are characterized by a normal carotid bifurcation or only mild atherosclerotic wall changes [4, 32, 34], distal tapering stenosis, increase of outer vessel diameter or circumference, and early thrombus detection [35]. Noteworthy, the most common finding of ICAD, found in 90% of patients, is a hypoechogenic wall thickening determining a stenosis or occlusion at a site not typically involved in atherosclerotic disease [31, 36]. Compared to atherosclerotic luminal narrowing, ICAD stenosis usually begins a few centimeters distal to the bifurcation and extends over a longer distance [23, 32]. Consequently, beware that in a patient with a clinical suspicion of ICAD, an examination of the carotid system must include the distal part of the ICA, especially with a sector probe. In patients with fibromuscular dysplasia, a known risk factor for CAD [37], irregular wall thickening, multisegmental stenosis, or an aberrant course of the ICA are frequently found [38, 39]. Morphological criteria alone are diagnostic in only about 50% (20–63%), mainly due to inadequate direct imaging for retromandibular location.

Regarding direct hemodynamic criteria, these are mainly represented by a significant increase of blood flow velocities due to a distal stenosis, that is, high-cervical, retromastoidal stenosis. Beware when comparing flow velocities with the contralateral vessel, since up to 25% of patients have dissections affecting multiple vessels at the same time [6]. The combination of morphological and hemodynamic criteria is diagnostic in 74–78–95% of ICAD patients and increases with repeated examinations [19, 32, 33, 40].

Indirect hemodynamic criteria are present in patients with intracranial ICAD and they are characterized by pre-stenotic high resistance flow profiles, post-stenotic dampened flow profiles, and intracranial collateral circulation [19].

Taking into consideration any abnormal finding, sensitivity of combined ultrasound techniques is high ranging from 80% to 96% [4, 19, 32–34, 36, 41–43]. Sensitivity, specificity, and positive and negative predictive values for color-coded duplex (CCD) sonography diagnosis of patients with ICAD causing carotid territory ischemia were 96%, 94%, 92%, and 97%, respectively [42]. However, different ultrasound techniques yield different sensitivities: 82% for CCD, 91% for Power Doppler (PD), and 98% for B-flow [44]. Intimal flaps, fissures of membranes, and residual flow within the true and false lumen were better detected by B-flow than by CCD and PD [45]. Compared to CCD and PD, B-flow has a better spatial resolution and no angle dependency of the probe during the examination; as B-flow is not based on the Doppler principle, velocity measurements are not possible. Sensitivity is also different according to symptoms: 96% in patients having suffered ischemic events and 71% in patients without ischemic events (painful Horner's syndrome, cranial nerve palsies: IX–XII or more rarely III, IV, VI) [4, 46]. Accordingly, patients with ischemic events have more often high-grade stenoses or occlusions (83%) than those without ischemic symptoms (40%) [4].

Ultrasound has also limitations, as false-negative findings are reported in 2.8–16% of cases: subadventitial dissections without lumen compromise, low-grade stenosis with mild mural hematoma, and vessel segment not directly accessible by ultrasound, [19, 47]. These limitations are more often encountered in patients without cerebral ischemic signs [4]. Since a normal ultrasound exam does not exclude ICAD, the gold standard for diagnosis is an axial cervical MRI using the T1 fat suppression technique, as it detects the pathognomonic intramural hematoma in more than 90% of cases. Yet, MRI and ultrasound are considered complementary because only ultrasound can show the hemodynamic consequences.

The best method for following patients with CAD is ultrasound as it determines the time of recanalization and therefore the necessary duration of antithrombotic treatment. Recanalization, which results from the resorption of the wall hematoma and from the resolution of the intraluminal thrombus, occurs in about 76% of ICAD; specifically, a complete recanalization has been reported in 55% of patients (58.7% in case of initial ICA stenosis, 40% in subjects with initial ICA occlusion). Most lumen changes occur within the first 6 months after dissection and they are only rarely seen (<1%) after 1 year [27]. High-grade (>80%) stenosis and occlusion recanalized less frequently [48]. In very selected cases of ICAD associated with critical hemodynamic insufficiency or thromboembolic events that occur despite medical therapy, the patient undergoes endovascular stent placement; in these instances, ultrasound is useful in checking treatment efficacy.

Ultrasound monitoring is also valuable for detecting CAD recurrence: two reports have shown a surprisingly high recurrence rate ranging from 19% to 26% in the acute phase of the disease [27, 39]. Conversely, late recurrence is an uncommon event, occurring only in 2.7% of patients [27].

25.8 Common Carotid Artery Dissection (CCAD): Ultrasound Findings

Common carotid artery dissection (CCAD) is a rare disease representing less than 1% of all CADs. This is possibly due to a different ultrastructure of the vessel wall: the ICA is a muscular artery, whereas the CCA is an elastic artery. The main difference between the two arteries is in the tunica media: in muscular arteries, the tunica media consists mainly of smooth muscle tissue, whereas in elastic arteries, it consists of mostly elastic fibers. Muscular arteries have two elastic layers in the tunica media (the external elastic lamina and internal elastic lamina), which might make them more susceptible to dissection [49].

CCAD can be traumatic, iatrogenic, spontaneous, or associated with aortic dissection. Specifically, CCAD is the most common mechanism of ischemic stroke of type A thoracic aortic dissection (AAD), seen in 85% of cases in one series, more commonly on the right side [50].

The most frequently reported ultrasound findings (Fig. 25.5) include a double lumen, mural thrombus, intraluminal hyperechoic/isoechoic lesion, and intimal flap; more rare findings are carotid occlusion and pseudoaneurysm [3]. When urgent

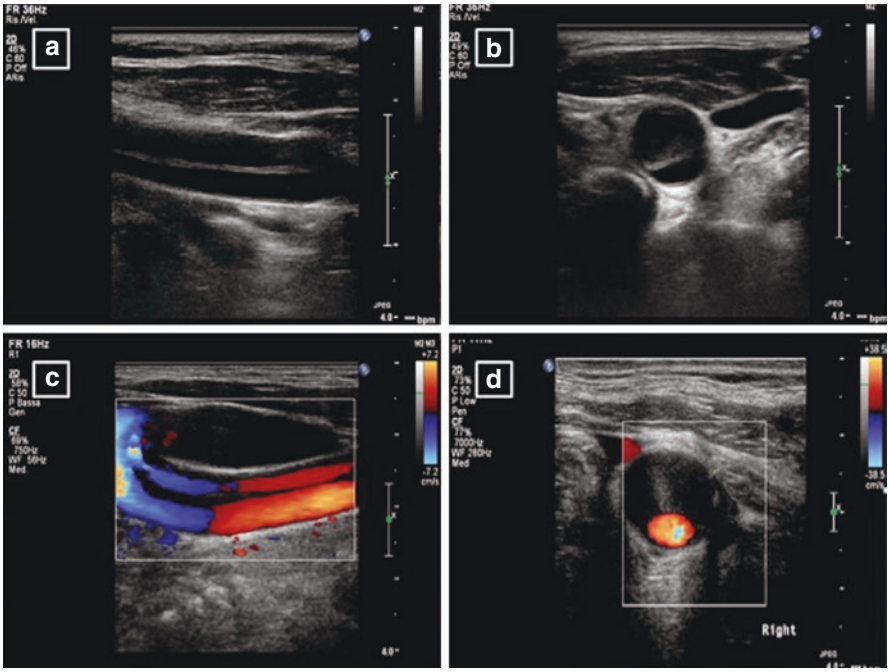

Fig. 25.5 Common carotid artery dissection. (**a**, **c**) Longitudinal view showing a double lumen and a dissecting membrane. (**b**, **d**) Axial view showing a dissecting membrane and intramural hematoma

ultrasound is performed for suspected CCAD, axial views of the vessel should be acquired. In cases of CCA occlusion, blood will usually flow from the ECA to the ICA, even though occasionally flow reversal may be seen with the ICA flowing retrograde and into the ECA. This dynamic information regarding flow within the ICA and ECA distal to the CCA occlusion provides complementary information for cerebral angiography and revascularization planning. Given its possible association with aortic dissection, early recognition of CCAD might affect the decision regarding thrombolysis in acute ischemic stroke patients. Since thrombolysis is potentially harmful in patients with CCAD secondary to AAD, a chest CT scan is mandatory to exclude an aortic dissection extending to the cerebroafferent vessels [51].

25.9 Ultrasound of Intracranial Arterial Dissection

Intracranial ICADs seem to occur most frequently in the supraclinoid segment [52]. Overall they are rare and affect younger patients with a mean age less than 30 years. Clinically, they present with severe headache, ischemic symptoms, or subarachnoid hemorrhage. An extensive diagnostic workup which includes conventional angiography is usually necessary not to miss a correct diagnosis. The visualization of the

mural hematoma in intracranial arteries is very difficult with any non-invasive method. Ultrasound examination usually shows stenosis or occlusion of the involved vessel, but there are no data regarding sensitivity or specificity of ultrasound findings.

25.10 Pupillary Ultrasound: Findings in Carotid Dissection

In patients with CAD, pupillary response to light is comparable on both sides, while mydriatic dilation after CR elicitation is completely absent ipsilaterally in the acute phase (Fig. 25.6). This finding is especially important when CAD involves the distal segments and/or is subadventitial, and the pupillary dysfunction is not easily apparent to the clinician's eye.

25.11 Conclusion

In summary, ultrasound is a fundamental diagnostic tool for patients with a clinical suspicion of CAD since it is widely available, non-invasive and it has a high sensitivity, especially in patients with signs of cerebral ischemia. Moreover, bedside ultrasound examination of the pupil might reveal a subtle pupillary dysfunction determined by a hidden distal/subadventitial CAD, especially in the acute phase. This might be extremely useful when assessing a polytraumatic patient admitted to the ICU.

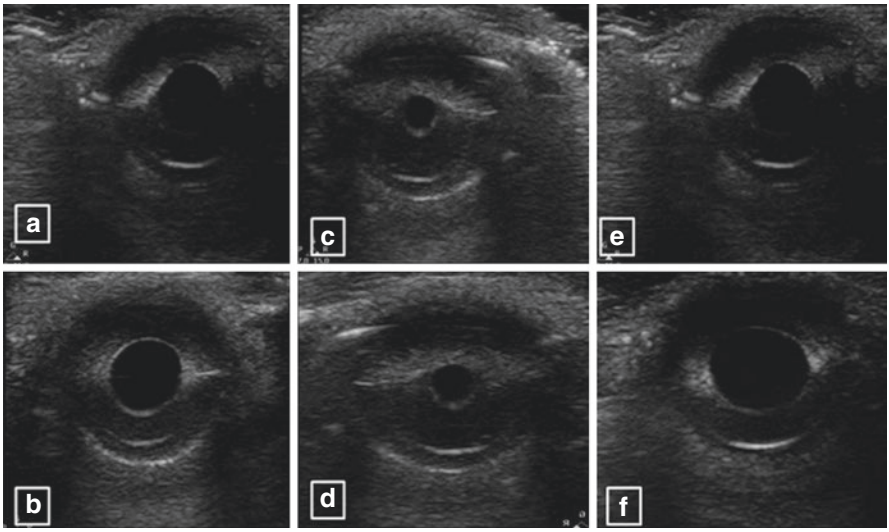

Fig. 25.6 Right internal carotid artery dissection. (**a**, **b**) Pupillary diameter at rest in both eyes; (**c**, **d**) normal pupillary reflex to light in right and left eye; (**e**) no pupillary reaction to ciliospinal stimulus (pinching of the trapezius muscle) on the right side; (**f**) normal mydriatic reaction on the nonaffected side

CAD diagnosis should be confirmed by MRI because of its exquisite sensitivity in detecting intramural hematoma also in patients with local symptoms only. Complementarily to MRI, ultrasound discloses hemodynamic consequences in the intracranial circulation which might indicate the need for an endovascular treatment.

Ultrasound is the method of choice for monitoring recanalization once treatment is started, detecting CAD recurrence and establishing the duration of antithrombotic therapy.

Algorithm

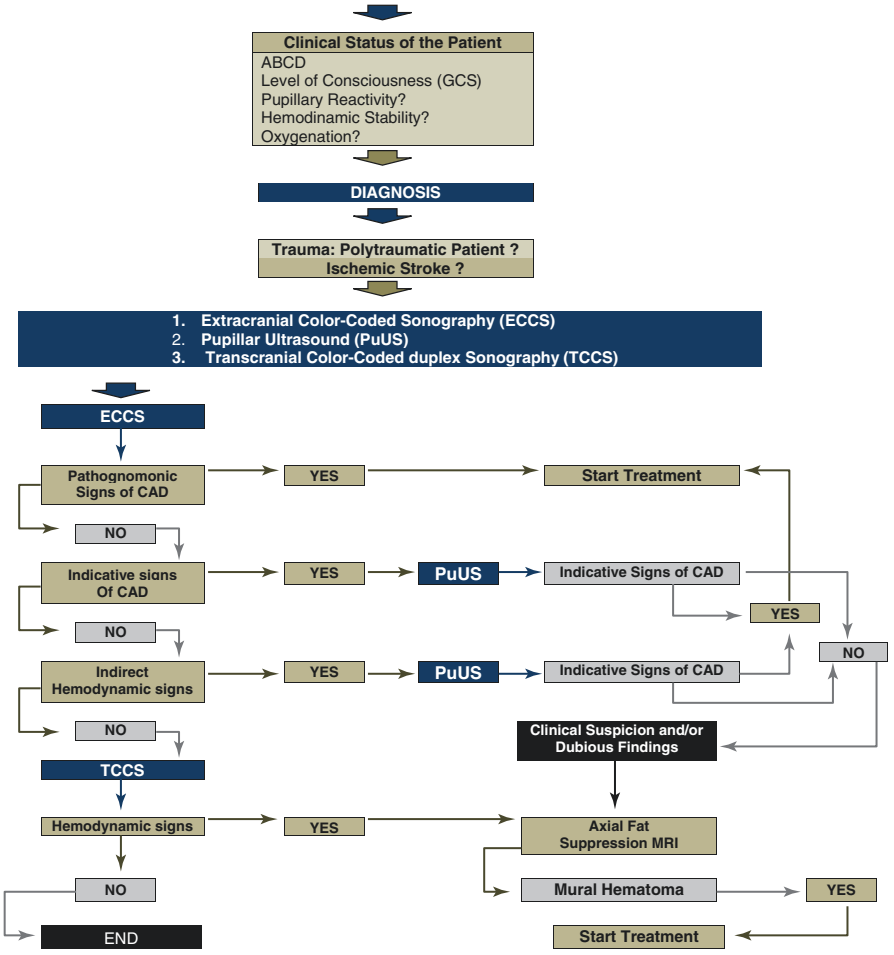

ABCD Airway-Breathing-Circulation-Disability, *GCS* Glasgow coma scale, *CAD* Carotid Dissection, *MRI* Magnetic resonance image

References

1. Schievink WI. Spontaneous dissection of the carotid and vertebral arteries. N Engl J Med. 2001;344:898–906.
2. Debette S. Pathophysiology and risk factors of cervical artery dissection: what have we learnt from large hospital-based cohorts? Curr Opin Neurol. 2014;27:20–8.
3. Zach V, Zhovtis S, Kirchoff-Torres KF, Weinberger JM. Common carotid artery dissection: a case report and review of the literature. J Stroke Cerebrovasc Dis. 2012;21(1):52–60.
4. Baumgartner RW, Arnold M, Baumgartner I, et al. Carotid dissection with and without ischemic events: local symptoms and cerebral artery findings. Neurology. 2001;57:827–32.
5. Hassan AE, Zacharatos H, Mohammad YM, et al. Comparison of single versus multiple spontaneous extra-and/or intracranial arterial dissection. J Stroke Cerebrovasc Dis. 2013;22:42–8.
6. Baracchini C, Tonello S, Vitaliani R, Giometto B, Meneghetti G, Ballotta E. Vasomotion in multiple spontaneous cervical artery dissections. Stroke. 2008;39:1148–51.
7. Béjot Y, Aboa-Eboulé C, Debette S, CADISP Group, et al. Characteristics and outcomes of patients with multiple cervical artery dissection. Stroke. 2014;45(1):37–41.
8. Barbour PJ, Castaldo JE, Rae-Grant AD, et al. Internal carotid artery redundancy is significantly associated with dissection. Stroke. 1994;25:1201–6.
9. Baracchini C, Farina F, Tonello S, et al. Endothelial dysfunction in carotid elongation. J Neuroimaging. 2013;23(1):18–20.
10. Dittrich R, Nassenstein I, Harms S, et al. Arterial elongation ("redundancy") is not a feature of spontaneous cervical artery dissection. J Neurol. 2011;258:250–4.
11. Menon RK, Norris JW. Cervical arterial dissection – current concept. Ann N Y Acad Sci. 2008;1142:200–17.
12. Vučurević G, Marinković S, Puškaš L, Kovačević I, Tanasković S, et al. Anatomy and radiology of the variations of aortic arch branches in 1,266 patients. Folia Morphol (Warsz). 2013;72(2):113–22.
13. Natsis K, Tsitouridis I, Didagelos M, Fillipidis A, Vlasis K, et al. Anatomical variations in the branches of the human aortic arch in 633 angiographies: clinical significance and literature review. Surg Radiol Anat. 2009;31:319–23.
14. Sacco S, Totaro R, Baldassarre M, Carolei A. Morphological variations of the internal carotid artery: prevalence, characteristics and association with cerebrovascular disease. Int J Angiol. 2007;16(2):59–61.
15. Osborn AG. Diagnostic cerebral angiography. 2nd ed. Philadelphia: Lippincott Williams & Wilkins; 1999.
16. McDougal DH, Gamlin PD. Autonomic control of the eye. Compr Physiol. 2015;5:439–73.
17. Mullaguri N, Katyal N, Sarwal A, Beary JM, George P, Karthikeyan N, et al. Pitfall in pupillometry: exaggerated ciliospinal reflex in a patient in barbiturate coma mimicking a nonreactive pupil. Cureus. 2017;9(12):e2004.
18. Tripathy K, Simakurthy S, Jan A. Ciliospinal reflex. StatPearls Publishing; 2020.
19. Nebelsieck J, Sengelhoff C, Nassenstein I, et al. Sensitivity of neurovascular ultrasound for the detection of spontaneous cervical artery dissection. J Clin Neurosci. 2009;16:79–82.
20. Völker W, Dittrich R, Grewe S, et al. The outer arterial wall layers are primarily affected in spontaneous cervical artery dissection. Neurology. 2011;76:1463–71.
21. Baumgartner RW, Lienhardt B, Mosso M, Gandjour J, Michael N, Georgiadis D. Spontaneous and endothelial-independent vasodilation are impaired in patients with spontaneous carotid dissection: a case-control study. Stroke. 2007;38:405–6.
22. Benninger DH, Georgiadis D, Kremer C, Studer A, Nedeltchev K, Baumgartner RW. Mechanism of ischemic infarct in spontaneous carotid dissection. Stroke. 2004;35:482–5.
23. Benninger D, Caso V, Baumgartner RW. Ultrasound assessment of cervical artery dissection. In: Baumgartner RW, Bogousslavsky J, Caso V, Paciaroni M, editors. Handbook of cerebral artery dissection. Frontiers of neurology and neuroscience, vol. 20. Basel: Karger; 2005. p. 87–101.

24. Ozdoba C, Sturzenegger M, Schroth G. Internal carotid artery dissection: MR imaging features and clinical-radiologic correlation. Radiology. 1996;199:191–8.
25. Guillon B, Levy C, Bousser MG. Internal carotid artery dissection: an update. J Neurol Sci. 1998;153:146–58.
26. Kirsch E, Kaim A, Engelter S, et al. MR angiography in internal carotid artery dissection: improvement of diagnosis by selective demonstration of the intramural hematoma. Neuroradiology. 1998;40:704–9.
27. Baracchini C, Tonello S, Meneghetti G, Ballotta E. Neurosonographic monitoring of 105 spontaneous cervical artery dissections: a prospective study. Neurology. 2010;75:1864–70.
28. Barnett SB. World Federation for Ultrasound in Medicine and Biology (WFUMB) Symposium on safety of ultrasound in medicine: conclusions and recommendations on thermal and non-thermal mechanisms for biological effects of ultrasound. Ultrasound Med Biol. 1998;24:1–55.
29. Sargsyan AE, Hamilton DR, Melton SL, Amponsah D, Marshall NE, Dulchavsky SA. Ultrasonic evaluation of pupillary light reflex. Crit Ultrasound J. 2009;1:53–7.
30. Farina F, Brunner C, Schreiber SJ, Palmieri A, Struhal W, Baracchini C, Vosko MR. Ultrasound examination of the pupil suggestive for carotid dissection. Neurology. 2017;89:973–4.
31. de Bray JM, Lhoste P, Dubas F, Emile J, Saumet JL. Ultrasonic features of extracranial carotid dissections: 47 cases studied by angiography. J Ultrasound Med. 1994;13:659–64.
32. Sturzenegger M, Mattle HP, Rivoir A, Baumgartner RW. Ultrasound findings in carotid artery dissection: analysis of 43 patients. Neurology. 1995;45:691–8.
33. Arning C. Ultrasonographic criteria for diagnosing a dissection of the internal carotid artery. Ultraschall Med. 2005;26:24–8.
34. Steinke W, Rautenberg W, Schwartz A, Hennerici M. Non-invasive monitoring of internal carotid artery dissection. Stroke. 1994;25:998–1005.
35. Pannone A, Bertoletti GB, Nesi F, Varakin I, Maritati G, Rabitti G. Carotid artery dissection. Correlation of different diagnostic techniques. Minerva Cardioangiol. 2000;48:19–27.
36. Benninger DH, Baumgartner RW. Ultrasound diagnosis of cervical artery dissection. Front Neurol Neurosci. 2006;21:70–84.
37. de Bray JM, Marc G, Pautot V, et al. Fibromuscular dysplasia may herald symptomatic recurrence of cervical artery dissection. Cerebrovasc Dis. 2007;23:448–52.
38. Dittrich R, Nassenstein I, Ringelstein EB, Kuhlenbaumer G, Nabavi DG. A distinctive case of fibromuscular dysplasia. Neurol Res. 2007;29:551–2.
39. Dittrich R, Nassenstein I, Bachmann R, et al. Polyarterial clustered recurrence of cervical artery dissection seems to be the rule. Neurology. 2007;69:180–6.
40. Gobin-Metteil MP, Oppenheim C, Domigo V, et al. Critères diagnostiques en échographie-Doppler des dissections artérielles cervicales à la phase aigue. J Radiol. 2006;87:367–73.
41. Treiman GS, Treiman RL, Foran RF, et al. Spontaneous dissection of the internal carotid artery: a nineteen-year clinical experience. J Vasc Surg. 1996;24:597–607.
42. Benninger DH, Georgiadis D, Gandjour J, Baumgartner RW. Accuracy of color duplex ultrasound diagnosis of spontaneous carotid dissection causing ischemia. Stroke. 2006;37:377–81.
43. Alecu C, Fortrat JO, Ducrocq X, Vespignani H, de Bray JM. Duplex scanning diagnosis of internal carotid artery dissections. A case control study. Cerebrovasc Dis. 2007;23:441–7.
44. Clevert DA, Rupp N, Reiser M, Jung EM. Improved diagnosis of vascular dissection by ultrasound B-flow: a comparison with color-coded Doppler and power Doppler sonography. Eur Radiol. 2005;15:342–7.
45. Clevert DA, Jung EM, Johnson T. Cervical artery dissection: improved diagnosis with B-flow ultrasound. Clin Hemorheol Microcirc. 2007;36:141–53.
46. Arnold M, Baumgartner RW, Stapf C, et al. Ultrasound diagnosis of spontaneous carotid dissection with isolated Horner syndrome. Stroke. 2008;39:82–6.
47. Dittrich R, Dziewas R, Ritter MA, et al. Negative ultrasound findings in patients with cervical artery dissection. J Neurol. 2006;253:424–33.
48. Nedeltchev K, Bickel S, Arnold M, et al. R2-recanalization of spontaneous carotid artery dissection. Stroke. 2009;40:499–504.

49. Dittrich R, Draeger B, Nassenstein I, et al. Dissection of the common and external carotid artery. Cerebrovasc Dis. 2006;21:208–10.
50. Cambria RP, Brewster DC, Gertler J, et al. Vascular complications associated with spontaneous aortic dissection. J Vasc Surg. 1988;7:199–209.
51. Uchino K, Estrera A, Calleja S, Alexandrov AV, Garami Z. Aortic dissection presenting as an acute ischemic stroke for thrombolysis. J Neuroimaging. 2005;15(3):281–3.
52. Chaves C, Estol C, Esnaola MM, et al. Spontaneous intracranial internal carotid artery dissection: report of 10 patients. Arch Neurol. 2002;59:977–81.

Chapter 26
Carotid Disease: Usefulness of the Ultrasound

Gyula Pánczél, Vendel Kemény, László Oláh, and László Csiba

Key Points

1. Carotid ultrasound is the first noninvasive imaging modality for diagnosis and follow-up of different carotid diseases.
2. Duplex ultrasound (DUS) is the optimal method for investigation.
3. The DUS should assess the degree of stenosis, plaque characteristics, intima-media-thickness and hemodynamic parameters.
4. Peak systolic velocities of 125–230 cm/s are typical for 50–69% stenosis (NASCET) and ≥230 cm/s for ≥70% internal carotid artery stenosis. But in some cases, peak systolic velocity ratio, end-diastolic velocity and velocity ratios may depict better the degree of stenosis.
5. Using spectral Doppler criteria can be also useful for increasing the sensitivity or specificity.

G. Pánczél
Department of Neurology, Ferenc Flór County Hospital, Kistarcsa, Hungary
e-mail: panczel.gyula@florhosp.hu

V. Kemény
Director of Early Phase Clinical Services at ICON plc, Budapest, Hungary

Szentendre Medical Center, Szentendre, Hungary

L. Oláh
Neurologist, Department of Neurology, Debrecen University, Committee Member - ESNCH, Debrecen, Hungary
e-mail: olah@med.unideb.hu

L. Csiba (✉)
Neurologist, Department of Neurology, Clinical Center Debrecen University, Debrecen, Hungary. Advisory Board - ESNCH, Hungarian Neurological Society, Debrecen, Hungary
e-mail: csiba@med.unideb.hu

C. N. Rodríguez et al. (eds.), *Neurosonology in Critical Care*,
https://doi.org/10.1007/978-3-030-81419-9_26

26.1 Introduction

Stroke is an important cause of disability and mortality and has an estimated incidence of 795,000/year [1]. The stenotic diseases of carotids represent 15–20% of ischemic stroke. Successful medical or surgical therapy prevents the development of cerebrovascular symptoms due to carotid stenosis. Although screening is not recommended for unselected population, some surveys found high percent of individuals with asymptomatic carotid stenosis without statins and/or antiplatelet therapy. On the other hand, almost all guidelines recommend carotid screening for people with numerous vascular risk factors.

Carotid stenosis occurs most commonly at the carotid bifurcation. Carotid ultrasound (CUS) is a noninvasive, cost-effective, bedside, cheap imaging modality for detecting, grading and monitoring ICA stenosis due to its high sensitivity and specificity, relatively low cost, lack of radiation hazard. Three modalities should be carried out: (a) B-mode (intima-media thickness and plaque morphology) [2], (b) color Doppler (visualization of flow abnormalities) [3], and (c) velocity measurements (one of the most important parameter used for grading the severity of carotid stenosis); therefore, the correct positioning, sampling and insonation are important for accurate assessment [4–6].

26.2 Optimal Settings

The duplex scan makes blood flow audible with the help of the Doppler effect (spectral and color Doppler), and on the other hand, it visualizes the vessels and the surrounding tissues in real time (B-mode). 5–10 MHz range is usually used during the duplex scan of the large vessels of the neck [4, 7].

26.2.1 Probe Types

- *Linear array*: The piezoelectric crystals are located next to each other, forming one line.
- *Sector probes*: (“phased array,” mechanically rotating and mechanically oscillating US-probes)

26.2.2 Frequencies

Higher frequencies (e.g., 7.5 MHz) are used for the examination of more superficial structures (e.g., carotid arteries), while deeper vessels (e.g., vertebral arteries) and calcified plaques are examined using 5–5.5 MHz. Higher frequency US has less energy but better axial image resolution than lower frequency US beams. The frequency setting of Doppler mode is usually 4–5 MHz during duplex scans and these frequencies should be used for color coding as well.

26.2.3 Focus

The depth where the image resolution is the highest. Linear probes can produce better lateral resolution than sector types.

26.2.4 Depth

It should be set so that the examined structures are located in the optimal focus distance of the ultrasonic probe. A maximum depth of 4–5 cm should be used in patients with an "average" neck.

26.2.5 Pulse Repetition Frequency (PRF)

It provides information about how often the device sends each "US-pulse." It should be set for B-mode image, Doppler-examination and color-coding. It affects the maximum depth that can be examined and the maximum flow velocity that can be measured.

26.2.6 Frame Rate

Image refresh rate (in B-mode and color-mode). Typically its value is between 4 and 30 Hz.

26.2.7 Preprocessing (Parameters that Should Be Set Before the Examination)

- *Dynamic range*:
  - 30 dB: hard image; 60 dB: soft image.
- *Edge enhancement*:
  - Level 1–4, it influences contours.
- *Scan correlation (SCC):*
  - Level 1–4, it reduces noise by (temporal) averaging image points.
- *Fast/detailed (line density):*
  - Greater line density – better, but slower image.
- *Time gain compensation (TGC):*
  - The waves that are reflected from deeper structures are weaker (more are absorbed); therefore, these require more gain. TGC is suitable for this gain (that depends on the time of reflection).
- *Zoom*:
  - It is used for vessel segments that are difficult to visualize and to examine plaques and IMT measurements.

26.2.8 Freeze

"Freezing" the image on the display for measurements or documentation. If the US probe is not in use, the image should always be freezed to prevent unnecessary warming and untimely deterioration of the probe.

26.2.9 Cine Loop

It stores the most recent sequence preceding the freeze in the system's memory, allowing the replay of the last few seconds.

26.2.10 Smoothing (Interpolation), Interlacing, Correlation

Procedures to make the image smoother.

26.2.11 Postprocessing

Technical procedures for the optimal display of the screen and the documentation. These filter out the unnecessary parts of the available grayscale and display the necessary ones.

26.2.12 Resolution

- *Axial resolution*: The minimum distance that can be differentiated between two points that are parallel to the ultrasound beam (frequency-dependent).
- *Lateral resolution*: The minimum distance that can be differentiated between two points that are perpendicular to the ultrasound beam (frequency-dependent).

26.2.13 Doppler-Technique

- *Doppler shift*:
  - The frequency of the emitted US changes (shifts) if it is reflected from a moving surface (a reflector moving towards the source will increase the registered frequency and a reflector moving away from the source will decrease it). Since the Doppler shift that is caused by the blood flow is within the hearing range, therefore the sounds that are produced by the flow are audible.

26.2.14 PW-Doppler (Pulsed-Wave Doppler)

The Doppler probe emits US pulses and the same piezoelectric crystal receives the reflected US. This way, knowing the velocity of the US within the tissue, the depth of interest and the sample volume can be determined. The number of emitted pulses in a specific time is characterized by the so-called PRF (pulse repetition frequency).

- *Aliasing/Nyquist limit*:
  - The frequency of a wave can be measured if at least two samplings are performed in each period (Nyquist-limit). In case of high velocities (e.g., high-degree stenosis), the sampling cannot be performed fast enough (PRF can only be increased until a certain limit and the deeper the examined vessel is located, the lower this limit is); therefore, the velocity range above the limit (the top of the spectrum) shifts below the zero line (into the negative range) and also, color aliasing occurs.

- *Spectrum*:
  - The time function of frequency shift (velocity shift in case of angle correction); it illustrates the change of Doppler shift in time. Since blood flow consists of reflectors with different velocities (RBCs), a spectrum is received instead of a linear curve.
- *Angle correction/steering*:
  - A velocity value is only received from the frequency of the Doppler shift, if the angle between the US beam and the direction of the blood (reflector) is considered (cos).
- *Doppler-gain*:
  - Its setting is considered optimal if there are no mirror artifacts, the whole spectrum is visible, and it can be easily differentiated from the background.

26.2.15 Color Duplex

- *Steering/angle correction*:
  - As color mode is based on the Doppler effect, angle correction is very important in this case as well.
- *PRF*:
  - It should be set at the beginning of the examination according to the expected velocity and then it can be gradually changed depending on whether we wish to visualize the vessel or the flow (see there).
- *Window size*:
  - The size of the color window should be adjusted so that it contains the vessel segment of interest. A smaller window allows faster and more precise visualization.
- *Color gain*:
  - If the gain is not enough, no color signal is seen in spite of existing flow and if the gain is too strong, confusing artifacts occur in the color window.

26.3 Indications

- Screening of patients with vascular risk factors (primary prevention)
- Established peripheral artery and coronary disease
- TIA, hemi-or brainstem symptoms suggesting stroke

- Follow-up of stroke patients (secondary prevention)
- Bruits during auscultation of the supra-aortic vessels
- Unilateral visual disturbance (amaurosis fugax, ischemic ophthalmopathy, visual field defect)
- Syncope
- More than 20 mmHg difference between blood pressures measured on the two arms
- To look for plaques before carotid massage
- Preceding major surgeries (e.g., coronary bypass surgery)
- Regular follow-up after vascular intervention (endarterectomy, stenting)
- Neck tumor
- Sudden neck pain (if dissection suspected)
- Follow-up after transplantation [4].

26.4 Carotid Ultrasound: How to Start the Investigation?

The patient is in the semi-sitting or supine position, and the examiner is next to or behind the patient. The examination starts with B mode scan of the vessels. First, the proximal segment of the common carotid artery is visualized: the probe is positioned dorsal to the sternocleidomastoid muscle, above the clavicle. The common carotid artery is followed until its bifurcation and then the internal carotid artery is visualized by positioning the probe and continuing cranially. It should be followed until its most distal segment (it is usually possible until the lower edge of the mandible) and then the external carotid artery should be examined after returning to the bifurcation [4].

26.4.1 Differentiating the Internal and External Carotids

26.4.1.1 Positioning the Probe

The longitudinal section of the common carotid artery is visualized until its bifurcation and then the cranial side of the probe is rotated forward toward the mandibular angle to visualize the internal carotid. Caution: the initial portions of the external and internal carotids might be located inversely.

26.4.1.2 Morphological Differences

The bulb of the internal carotid is dilated similar to an onion and has no side branches in its cervical segment. The external carotid is usually more gracile and branches (especially the superior thyroid artery) are usually visible.

26.4.1.3 Flow Differences

The spectrum of the internal carotid is less pulsatile (the end diastolic velocity is higher than in the external carotid) which is caused by the lower resistance of the cerebral vessels (Fig. 26.1). The spectrum of the external carotid is more pulsatile and features "spikes" and its end diastolic velocity is lower (the arteries that supply the muscles and the skin are more resistant), frequently triphasic (Fig. 26.2).

26.4.1.4 Compression

Repeated tapping/compression of the superficial temporal artery creates retrograde pulse waves that appear as oscillations in the spectral analysis of the external carotid (Fig. 26.2).

During the examination of the carotid system, the course, dilation and mural abnormalities of the vessels are described in the report (see the end of the chapter).

It is followed by the color duplex scan. The vessels are examined using the color window and their course, caliber and mural abnormalities are reported. The morphological examinations are followed by Doppler spectral analysis to describe hemodynamic conditions. Pathological abnormalities must be also recorded. Finally, if needed, contrast-enhanced ultrasound should be performed [8].

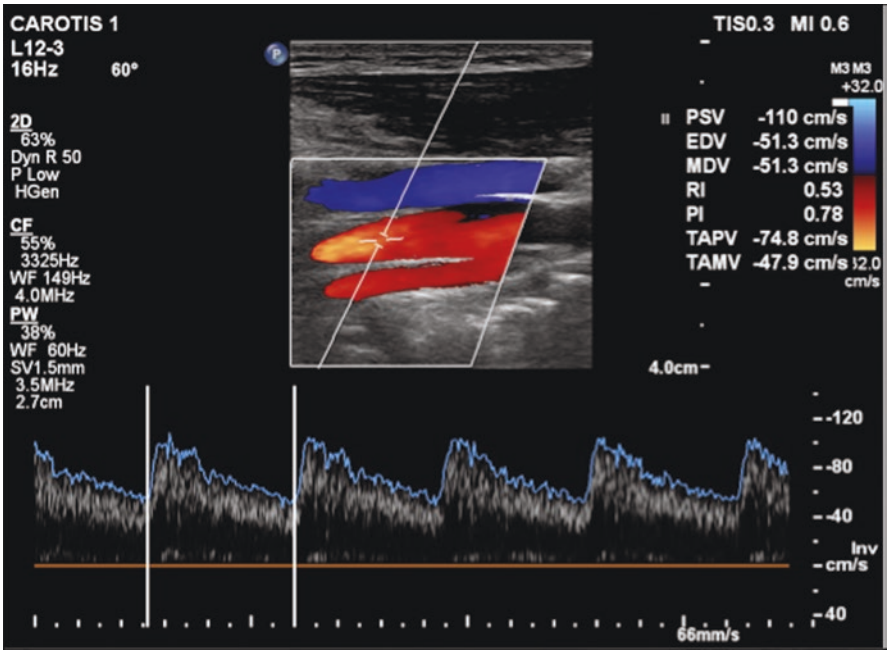

Fig. 26.1 The normal internal carotid artery. The spectrum is biphasic (less pulsatile), the peak systolic velocity 110 cm/s

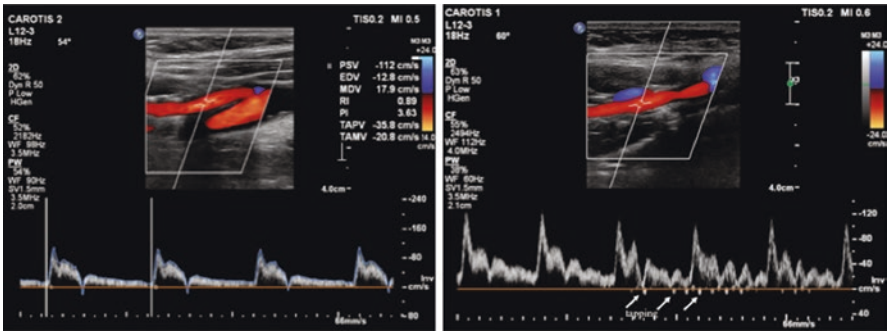

Fig. 26.2 The spectrum of the external carotid is more pulsatile (left picture), the end diastolic velocity is lower, frequently triphasic. Repeated tapping/compression (arrows) of the superficial temporal artery creates retrograde pulse waves that appear as oscillations in the spectral analysis of the external carotid (right picture)

26.5 B-Mode Examination

Longitudinal and then cross-sectional scans of the vessels of interest are performed in caudocranial direction, first in B-mode and then in color mode. Any occurring abnormalities are documented:

I. Elongation
II. Kinking (acute angulation of the artery, it might be mild in case of larger angles or lead to distortion that could result in flow obstruction).
III. Coiling (a complete loop of the artery, it usually does not cause flow disturbances).
IV. Bifurcation level. In case of a high bifurcation (that is near the lower mandibular ramus), the internal carotid artery is often difficult to visualize if it can be visualized at all.

Mean diameters of ICA (4.7+/−0.8 mm) and CCA (6.1+/−0.8 mm) in women are significantly smaller than in men: 5.1+/−0.9 mm and 6.5 +/−1.0 mm, respectively [4].

26.5.1 Dilation

The caliber of the vessel and any occurring abnormalities are observed.

- *Dilated*:
  - Diffuse dilation: anatomical variation; circumscribed dilation: aneurysm (fusiform); but the carotid bulb is often dilated, and it is not an aneurysm in itself.

- *Narrowed*:
  - Diffuse narrowing in the whole vessel: hypoplasia; a decrease in caliber can often be observed distally from an occlusion due to a fall in transmural pressure; segmental narrowing: fibromuscular dysplasia (rare in the cervical area).

26.5.2 Intima-Media Thickness (IMT)

A zoomed, longitudinal scan of the CCA is performed and the measurement is carried out 1–3 cm below the bifurcation (if a plaque is located at this level, then right below the plaque), on the wall that is farer from the probe (dorsomedial wall). A thin white stripe, the blood-intima interface (A) is located between the arterial lumen (in black) and the vessel wall. Below the white stripe, a black and then another white stripe (usually the thickest layer) are seen. The border between the latter two is the media-adventitia interface (B). IMT equals to the distance between A and B and its normal value is 0.4–0.8 (Fig. 26.3). Aging, hypertension, hyperlipidemia, diabetes, smoking, and extreme alcohol consumption increase the IMT and numerous observations prove the correlation between the pathological thickness of IMT and risk of vascular events. Similarly, an IMT decrease after long lasting pharmacotherapy (e.g., statin) is associated with decreased vascular risk. The standards of IMT measurement were published by the Mannheim Consensus Meeting [9].

26.5.3 Plaque Analysis

During B-mode examination, every circumscribed plaque is detected in the vessel segments that are in the field of view. Plaques are characterized based on the following features:

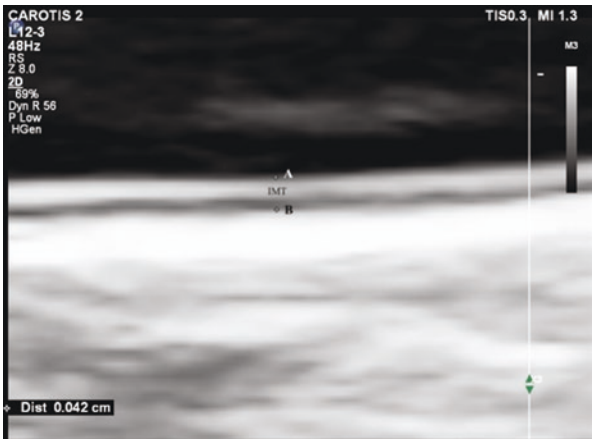

Fig. 26.3 IMT. A thin white stripe, the blood-intima interface (A) is located between the arterial lumen (black) and the vessel wall. Below the white stripe, a black and then another white stripe (usually the thickest layer) are seen. The border between the latter two is the media-adventitia interface (B). IMT equals to the distance between (A, B)

26.5.3.1 Location

Which vessel portion, which wall (according to their relation to the probe, near, far or lateral walls are distinguished).

26.5.3.2 Shape and Configuration

In cross-sectional scans, plaques can appear circumscribed, sickle-like and attached to the lateral wall, concentric or semicircular (eccentric); connecting plaques can form plaque systems.

26.5.3.3 Maximal Thickness

The thickness of the plaques that seem the thickest is measured during cross-sectional scan of the artery.

26.5.3.4 Surface

Smooth (usually soft plaques), moderately irregular (usually fibrous or calcified plaques), severely irregular (usually calcified plaques), ulcerated (focal, sudden excavation of the surface with a usual depth of >2 mm). Its significance: irregular, especially ulcerated surfaces significantly increase the risk of stroke.

26.5.3.5 Echogenicity

It indicates which range of the grayscale the plaque belongs to. Echolucent (soft) plaque: dark, its density is similar to blood; such are lipid-rich, hemorrhagic plaques and newly formed thrombi. Isodense (moderately dense): its density is similar to the sternocleidomastoid muscle (such are fibrous plaques and chronic thrombi. Hyperdense, hyperechoic plaque: its density is similar to the cervical vertebra, it is white (such are collagen-rich, fibrous and calcified plaques, the latter also produce an acoustic shadow). Importance: echolucent plaques indicate a significantly increased risk of stroke. Measurement: the density of blood is set between 0 and 5, and the density of the adventitia is set to 230. Echolucent plaques with a density below 32 indicate increased risk of stroke [10–12].

26.5.3.6 Homogeneity – Heterogeneity

It indicates how similar or different are the parts of a plaque (Figs. 26.4, 26.5, 26.6, and 26.7).

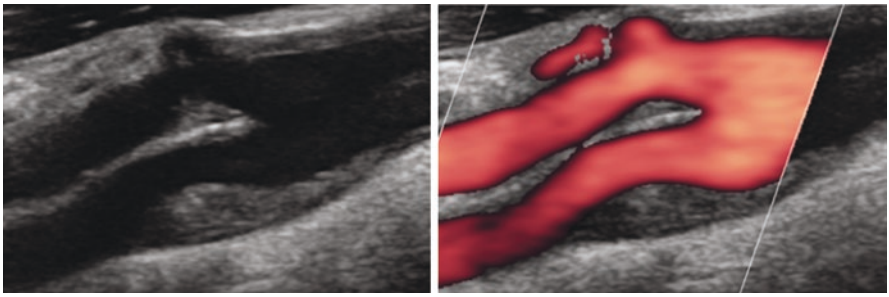

Fig. 26.4 Non-ulcerated homogenous plaque (left side: B-mode). The power-mode picture confirms the smooth surface of the plaque (right side). (From the courtesy of L. Németh)

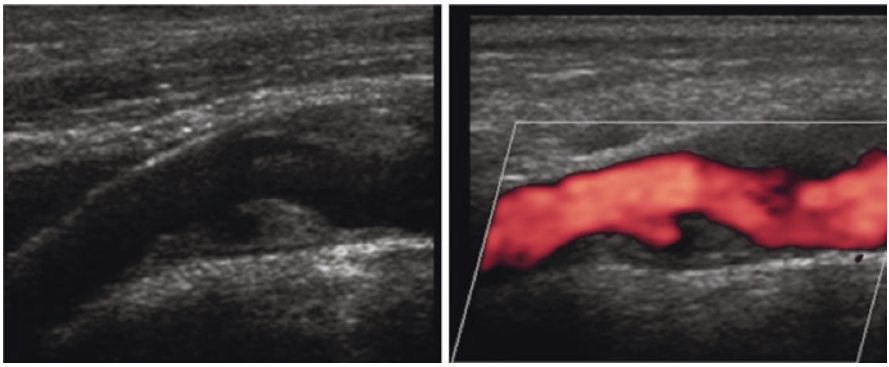

Fig. 26.5 Ulcerated plaque. The power-mode picture depicts the presence of flow in the ulcerated part of the plaque. (From the courtesy of L. Németh)

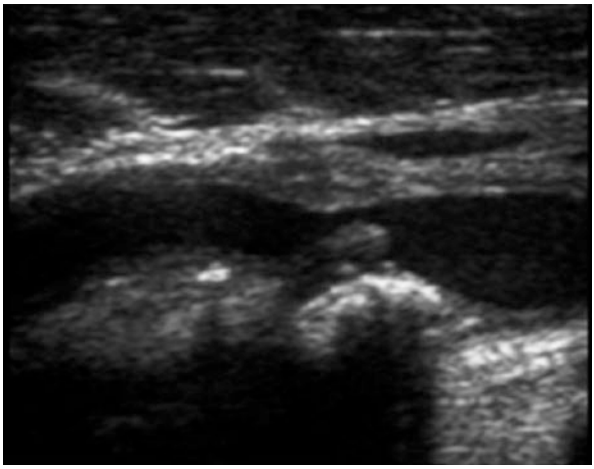

Fig. 26.6 B-mode picture of a hyperdense, hyperechoic plaque with acoustic shadowing. (From the courtesy of L. Németh)

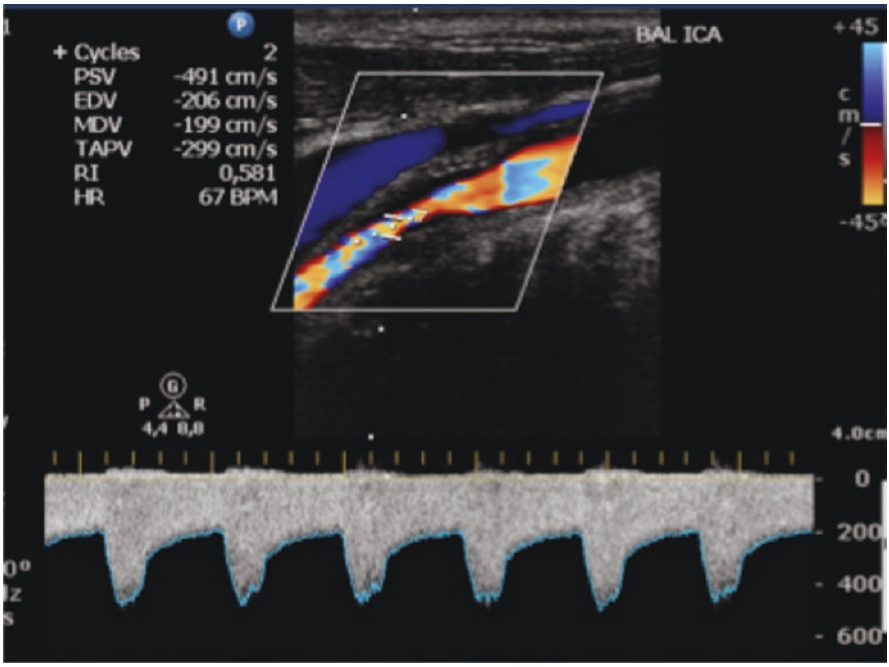

Fig. 26.7 Color Duplex image of a severe ICA stenosis. The peak systolic velocity (491 cm/s) confirms the severe stenosis. (From the courtesy of L. Németh)

The so-called "floating thrombus" is rare but important finding and needs urgent vascular intervention [13] (e.g., carotis endarterectomy).

26.5.4 B-Flow Imaging

An imaging technique for the detection of blood flow by using sonography (B-flow) has been developed one and half decade ago. B-flow applies digitally encoded methods to boost blood echoes and to suppress nonmoving tissue signals. B-flow imaging results in real-time visualization of blood flow by directly visualizing blood reflectors and presenting this information in gray-scale. B-flow imaging has better spatial and temporal resolution than Doppler imaging because of the better definition of the vessel lumen. The imaging of the flow is possible without the limitations of Doppler technology such as aliasing and wall filter limitations. Compared with power Doppler imaging, B-flow provides higher spatial resolution and higher frame rate hemodynamic imaging without information on velocity and direction. However, resolution of vessel wall tissue was inferior to that of the conventional B-mode and power Doppler imaging methods [4, 12].

26.6 Color Doppler Imaging (CDI), Power Doppler Imaging (PDI)

26.6.1 Color Doppler Imaging (CDI)

The system uses different colors to indicate different blood velocity flow; therefore, information can be obtained about the velocity and direction of the flow. Its disadvantage: it depends on angle correction, aliasing occurs at high velocities, and the color signal does not always fill the lumen completely.

26.6.2 Power Doppler Imaging (PDI)

Every flow is displayed using the same color and the displayed intensity is proportional to the energy of the US beam that reflects back from the flowing particles. Its advantage: independent of angle correction, no aliasing, low-velocity flows can also be visualized well, but flows with different directions are displayed with the same color, therefore arteries cannot be differentiated from veins.

Using these methods makes the display (detection) of the vessels easier and it also provides visual information about the flow conditions. The optimal display of the lumen is performed using lower PRF, but flow studies require an initially higher and then gradually decreased PRF setting [4, 12].

26.7 Technique of Examination

Color duplex scan is the next step after B-mode examination. If this mode is activated, a color window appears which is positioned so that it contains the vessel segment of interest (angle correction should be kept in mind). Different flows are displayed using different shades of cold and warm colors depending of the direction and the velocity of the flow and it is at the examiner's discretion which direction is displayed with which color. Observing the vessels through the color window may reveal the following pathological abnormalities:

(a) *Plaque detection*:

- Echolucent plaques that are not displayed on traditional black and white B-mode images (due their almost blood-like density) show up as colorless areas. A typical feature of plaques with excavated surfaces is a color change, indicating the turn in the direction of the flow in its surface groove [4, 10–12].

(b) *Stenosis*:

- The prestenotic color signal often appears normal, but in case of high-degree stenoses, it might suggest a more pulsatile flow. The flow in the narrowest

part of the stenosis creates the so-called "jet phenomenon"; this is where the largest flow velocity can be detected with consequential aliasing effect (caution: a color change in this case does not mean that the flow turns back, it merely indicates high flow velocity). Due to the poststenotic turbulence, the color signal appears as a mosaic of different colors and it becomes ragged ("confetti phenomenon") (Fig. 26.7).

26.7.1 Stenosis Measurement

CDI is essential to accurately measure the degree of a stenosis. The three most common methods are the following [14–17].

26.7.1.1 Diameter Stenosis

A longitudinal scan is used to visualize the segment of interest. The residual lumen (the width of the color signal at the site of the maximal stenosis) is compared either to the original lumen of the vessel (ECST method) or to the preserved lumen distal to the stenosis (NASCET method, it results in a lower degree stenosis than the ECST method) (Fig. 26.8).

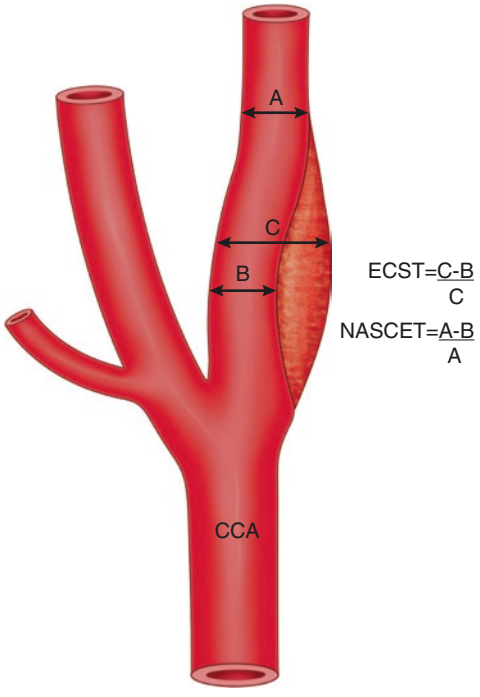

Fig. 26.8 The NASCET and ECST stenosis

26.7.1.2 Area Stenosis

Cross-sectional study. The residual area (color signal) at the site of the maximal stenosis is compared to the original area of the lumen (it is not as commonly used, it results in a higher number than the previous method due to the squared effect).

26.7.1.3 Residual Luminal Diameter

The width of the color signal at the site of the maximal stenosis.

26.7.2 Occlusion

Color signal cannot be detected in an occluded lumen even when very low PRF is used. Occasional color change might be seen in the occluded stump; it indicates that the flow turns around.

26.7.3 Subtotal Stenosis: (>95% Stenosis)

Perfusion pressure falls significantly, and the flow is depressed with a low velocity and intensity. Therefore, color signal is often undetectable in the stenosis, but it appears in the poststenotic segment and fills the lumen (distal color filling).

26.7.4 Long Segment Stenosis

A thin, irregular, low intensity color signal is seen in the vessel lumen that corresponds to the residual lumen (string sign). PDI is the best method of detection. This image is often seen in dissections as well.

Kinking coiling: Color coding changes together with the direction of the course of the vessel.

26.8 Doppler Spectrum

After turning on Doppler mode, the so-called sample volume (SV) appears on the screen and this is moved into the lumen of the vessel of interest. Its size should be adjusted as large as possible as long as it fits within the lumen without reaching the vessel walls.

Angle correction: the angle-indicator line that appears with the SV should be positioned into the longitudinal axis of the flow as it is a prerequisite of accurate velocity measurements. If the angle of measurement is over 60 degrees, even the slightest angle setting error will lead to a significant change in velocity so this angle should be kept below 60 degrees. If necessary, correction should be performed by tilting the probe.

The whole visualizable length of the vessel should be examined in a caudocranial direction while the SV is kept in the lumen and the angle is corrected. Duplex mode should be chosen for this examination if it is possible as it allows real time B-mode imaging and continuous Doppler spectral analysis. At least one typical spectrum should be recorded in the documentation if the examination of an internal carotid artery is normal.

26.9 Hemodynamic Parameters for Stenosis Estimation

(Society of Radiologists in Ultrasound) [6]

[PSV = Peak systolic velocity; EDV = End-diastolic velocity; ICA = internal carotid artery; CCA = common carotid artery]

I. *Normal*

- ICA PSV is <125 cm/sec and no plaque or intimal thickening is visible sonographically.
- Additional criteria include ICA/CCA PSV ratio <2.0 and ICA EDV <40 cm/sec.

II. *<50% ICA Stenosis*

- ICA PSV is <125 cm/sec and plaque or intimal thickening is visible sonographically.
- Additional criteria include ICA/CCA PSV ratio <2.0 and ICA EDV <40 cm/sec.

III. *50–69% ICA Stenosis*

- ICA PSV is 125–230 cm/sec and plaque is visible sonographically.
- Additional criteria include ICA/CCA PSV ratio of 2.0–4.0 and ICA EDV of 40–100 cm/sec.

IV. *≥70% ICA Stenosis but Less Than Near Occlusion*

- ICA PSV is >230 cm/sec and visible plaque and luminal narrowing are seen at gray-scale and color Doppler ultrasound (the higher the Doppler parameters lie above the threshold of 230 cm/sec, the greater the likelihood of severe disease) (Fig. 26.8).
- Additional criteria include ICA/CCA PSV ratio >4 and ICA EDV >100 cm/sec.

V. *Near Occlusion of the ICA*

- Velocity parameters may not apply, since velocities may be high, low or undetectable.
- Diagnosis is established primarily by demonstrating a markedly narrowed lumen at color or power Doppler ultrasound.

VI. *Total Occlusion of the ICA*

- No detectable patent lumen at gray-scale ultrasound and no flow with spectral, power and color Doppler ultrasound.
- There may be compensatory increased velocity in the contralateral carotid.

26.10 Contrast Enhanced Ultrasound (CEU)

After B-mode, color Doppler and spectral analysis, you can start CEU investigation if needed. The contrast materials consist of gas-containing microbubbles. SonoVue® (Bracco Spa) is the most frequently used US contrast agent (with pulse inversion or amplitude modulation technique). Low-Mechanical Index (MI, from 0.06 to 0.2) is an important feature. Shortly before administration of microbubbles, the probe should be placed over the most stenotic part of the carotid artery. The arterial lumen enhancement starts approximately after 10–20 s and lasts for up to 3–4 min [18].

CEU delineates the plaque surface well, visualizes the wall irregularities and offers improved imaging of flow in the stenotic part of the lumen, even in elongated plaques and high-grade stenosis. This method is a valuable method for the detection of intraplaque neovascularization.

The plaque enhancement can be classified into three grades: mild if microbubbles could be seen only at the outer part of the plaque; moderate when microbubbles are both at the plaque shoulder and within the plaque but not at the plaque's apex; and severe if microbubbles could be seen throughout the plaque. A special software can provide quantitative time–intensity curves. Previous studies founded a higher neovascularization within hypoechoic or mixed type plaques as compared to calcified ones.

CEUS is very useful in carotid dissection (15–20% of strokes in young adults) and giant cell arteritis by assessing the vascularization of the carotid wall. Quantification of arterial wall enhancement on CEUS is possible using the Gray-Scale Median (GSM) technique [4, 18].

Summary: CEUS improves the flow visualization without artifacts. It delineates all parts of a stenotic plaque, diagnoses ulcers and hypoechoic parts, differentiates total occlusion from severe stenosis and detects restenosis after vascular intervention. It offers the possibility to detect and grade intraplaque neovascularization, vascular wall inflammation in patients with arteritis.

26.11 The Most Important Pathological Findings of Carotids

26.11.1 Common Carotid Artery

If occluded, the lumen is filled with a thrombus, its caliber is decreased, no color signal or spectrum can be obtained. If the internal and external arteries are not occluded, then the internal carotid is filled from the external (which is filled by collaterals): the flow is very low, collateral type with flattened spectrum.

26.11.2 Internal Carotid Artery

26.11.2.1 Stenosis

The prestenotic flow is often normal. The higher the degree of the stenosis is, the more likely it is that proximally, the flow is lower and more pulsatile. In the intrastenotic portion, the flow is increased and the velocities are associated with the degree of the stenosis. The latter can be determined based on the ratio of the peak systolic and end diastolic velocities and the velocities of the internal/common carotid arteries. The poststenotic flow velocity is significantly decreased with prominent turbulence and loss of the systolic spectral window (the spectrum becomes broader and the area below the envelope becomes full), the spectrum becomes sharper and notched, and retrograde flow can be detected in the lateral parts of the poststenotic, slightly dilated lumen. Systolic acceleration decreases (the systolic upslope becomes less steep and the curve becomes flattened – delta sign). The higher the stenotic degree, the more distally from the stenosis the spectrum begins to regenerate. The flow velocity in the internal carotid artery is often higher if the contralateral common or internal carotid is occluded [4]. This phenomenon can be observed if there is collateral flow from the intact internal carotid toward the contralateral middle cerebral artery (that is above the occlusion) through the anterior communicating artery. On the normal side, the flow is hyperkinetic and the diastolic velocity is more increased than the systolic; therefore, pulsatility is increased (in these cases, the vascular resistance of the supplied areas of the two internal carotids is coupled in parallel; therefore, the resistance decreases). If there is a stenosis contralaterally to the occlusion, then the above-mentioned phenomenon causes a flow velocity that indicates a falsely high-degree stenosis. In this case, the degree of the morphological stenosis, that is, visualized during color mode, should be given priority to [4, 7, 12, 14, 16].

26.11.2.2 Dissection

In case of a subintimal dissection, the vessel wall, which was expanded into the lumen by the flow, can be usually visualized well: a gradually narrowing lumen ("flame sign") or a long segment stenosis (string sign). No spectral sign can be obtained in case of an occlusion. If distally the flow returns to the original lumen, flow can be detected in the false lumen with typical features of a long segment stenosis. Color method can help in the detection of this disease [4, 12].

26.11.2.3 Occlusion

Flow velocity suddenly falls at the orifice of the occluded vessel and only a few spikes are seen that do not indicate any volume and after a few millimeters, these also disappear. The flow in the common carotid artery is more pulsatile and flattened, no flow can be detected in the internal carotid, and the flow of the external carotid is hyperkinetic or normal.

26.11.2.4 Subtotal Occlusion: (95–99% Stenosis)

As the perfusion pressure falls, the flow is low (unlike in the case of less severe stenoses), the velocity is decreased, and systolic acceleration is also reduced; therefore, the spectrum is flattened (delta sign).

26.11.2.5 Multiple (Tandem) Stenosis

Perfusion pressure is decreased to a larger degree than in the case of single stenoses; thus, the intrastenotic flow velocities are lower than in single stenoses and the flow indicates a lower stenotic degree than there actually is. In cases like this, morphological stenosis measured in color mode becomes more important.

26.11.2.6 Long Segment Stenosis

The situation is similar to the case of multiple stenoses but the fall in perfusion pressure is more pronounced and usually no velocity increase (that is typical of stenoses) is detected. The flow is markedly low in the whole stenotic segment, the spectrum is flattened, and the flow is often turbulent due to the irregular surface. The poststenotic segment is usually located in a too proximal location to allow visualization.

26.11.3 External Carotid Artery (ECA)

26.11.3.1 Occlusion

No flow can be detected in the orifice of the external carotid artery but collateral flow usually appears distally (due to the extensive collateral network). There is normal flow in the internal and common carotid arteries.

26.12 Diagnostic Value of Reversed Flow in Ophthalmic Artery (OA)

The assessment of flow direction in the ophthalmic artery can raise the suspicion of ipsilateral severe ICA stenosis or occlusion. In healthy persons, the flow direction is intra-extracranial in the ophthalmic artery. But in case of hemodynamically significant stenosis or ICA occlusion, the flow direction will be reversed to extra-intracranial (higher pressure at the origin). Besides, by pressing the branches of extracranial carotid artery, you can identify the source of collateral circulation [19]. This simple and quick investigation could be performed bedside, using a cheap and pocket size pencil probe.

26.12.1 Interpretation and Report

(Modified suggestions of AIUM [20].)

Each laboratory must have criteria that are used by all members of the technical and physician staff.

- Diagnostic criteria must be derived from the literature or from internal validation based on correlation with other imaging modalities or surgical and/or pathologic correlation.
- The report must indicate internal carotid artery stenosis categories that are clinically useful (70% to near occlusion) or a numeric grade (e.g., 60% ± 10%) to provide adequate information for clinical decision making.
- Numerous factors may falsely increase or decrease velocities (e.g., systemic disease, cardiovascular disease, contralateral severe disease or occlusion, near occlusive stenoses).
- Simple velocity criteria may not be valid for a younger-than-usual population.
- Secondary criteria such as ratios may be helpful in these circumstances.
- The report should describe abnormal waveforms, if present.
- The report must indicate vertebral artery flow direction.
- The report may characterize plaques, depending on the laboratory interpretation criteria.

- The report should describe significant nonvascular abnormalities.
- The criteria for common carotid and vertebral artery stenosis differ from internal carotid artery criteria.
- A velocity threshold that indicates an external carotid stenosis is not established.
- A simple description indicating a stenosis, if present, may be reported.
- Identification of stenosis can be based on gray-scale and/or color flow narrowing, elevated velocity through the stenosis and typical poststenotic waveforms.
- The velocity criteria for stenosis after interventions may require different criteria than native vessels. Stents require different velocity criteria than native vessels [20].

26.13 Negative Report

Standardized examination and reporting is recommended to ensure that the examination contains every necessary information. The report should include the course of the vessels, their wall structure, flow characteristics of the internal carotid and vertebral arteries, and comparison of the two sides. Every report should include an opinion. A graphic report that includes a preprinted schematic figure with velocities and any abnormalities can be drawn onto could be useful for comparison during follow-up.

Example: The course of the carotid arteries is normal on both sides. The wall of the vessels and the measured IMT are normal. Antegrade, equal flow can be detected in both common (left: right:) and internal (left: right:) carotid arteries with normal spectrum and normal velocity.

Opinion: No wall abnormalities or flow disturbances can be detected in the examined vessels. Signature, date.

26.14 Conclusion

Carotid ultrasound is a cost-effective bedside diagnostic tool for assessing carotid artery diseases without radiation hazard and risk of claustrophobia.

Doppler US is an important method for following mild to moderate stenoses and for follow-up after stent or endarterectomy. PSV and/or EDV may provide more accurate assessment of stenosis. Contrast-enhanced ultrasound further improves the accuracy. In case of contralateral stenosis, tandem lesions, nearly occlusive ICA stenosis the gray-scale and color Doppler findings can be helpful. The carotid ultrasound provides information regarding plaque characteristics (stability, homogeneity, vascularization, etc.) The quantitative IMT measurement and follow-up (a marker of arteriosclerosis) is also possible using the modern equipment. Pitfalls: The accuracy of carotid ultrasound depends on the operator's skill and image quality.

In stenoses within the low (<50%) and moderate (50–70%) range, intrastenotic velocity increases only modestly relative to the luminal loss that requires additional morphologic estimation of stenosis using B-mode.

Algorithm

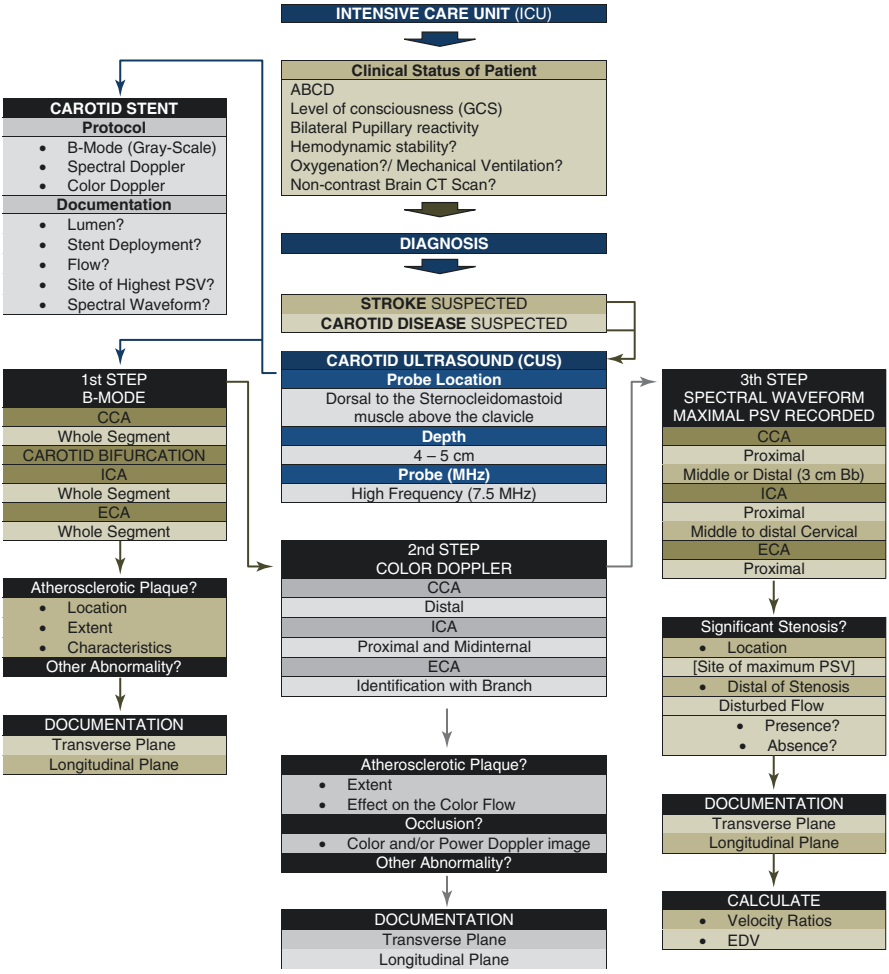

ABCD Airway-Breathing-Circulation-Disability, *CCA* Common carotid artery, *ICA* Internal carotid artery, *ECA* External carotid artery, *Bb* Below bifurcation, *PSV* Peak systolic velocity, *EDV* End-Diastolic velocity

References

1. Benjamin EJ, Virani SS, Callaway CW, et al. Heart disease and stroke statistics – 2018 update: a report from the American Heart Association. Circulation. 2018;137:e67–e4921.
2. Clevert DA, Johnson T, Jung EM, et al. Color Doppler, power Doppler and B-flow ultrasound in the assessment of ICA stenosis: comparison with 64-MD-CT angiography. Eur Radiol. 2007;17(8):2149–59.
3. Bartels E. Color-coded duplex ultrasonography of the cerebral vessels. Atlas and manual. Schattauer: Stuttgart; 1999.
4. Csiba L, Baracchini C, editors. Manual of neurosonology. Cambridge University Press; 2016. p. 1–214.
5. Grant EG, Benson CB, Moneta GL, et al. Carotid artery stenosis: gray-scale and Doppler US diagnosis-Society of Radiologists in Ultrasound Consensus Conference. Radiology. 2003;229(2):340–6.
6. Grant EG, Benson CB, Moneta GL, et al. Society of Radiologists in Ultrasound. Carotid artery stenosis: grayscale and Doppler ultrasound diagnosis–Society of Radiologists in Ultrasound consensus conference. Ultrasound Q. 2003;19:190–8.
7. Scoutt LM, Gunabushanam G. Carotid ultrasound. Radiol Clin N Am. 2019;57(3):501–18.
8. Rafailidis V, Charitanti A, Tegos T, et al. Contrast-enhanced ultrasound of the carotid system: a review of the current literature. J Ultrasound. 2017;20(2):97–109.
9. Touboul PJ, Hennerici MG, Meairs S. Mannheim carotid intima-media thickness and plaque consensus (2004–2006–2011). An update on behalf of the advisory board of the 3rd, 4th and 5th watching the risk symposia, at the 13th, 15th and 20th European Stroke Conferences, Mannheim, Germany, 2004, Brussels, Belgium, 2006, and Hamburg, Germany, 2011. Cerebrovasc Dis. 2012;34(4):290–6.
10. Saba L, Anzidei M, Marincola BC, et al. Imaging of the carotid artery vulnerable plaque. Cardiovasc Intervent Radiol. 2014;c37:572–85.
11. Reiter M, Horvat R, Puchner S, et al. Plaque imaging of the internal carotid artery – correlation of B-flow imaging with histopathology. AJNR Am J Neuroradiol. 2007;28(1):122–6.
12. Valdueza JM, Schreiber SJ, Roehl JE, Klingebiel R. Neurosonology and neuroimaging of stroke. Stuttgart: Georg Thieme Verlag; 2008.
13. Fridman S, Lownie SP, Mandzia J. Diagnosis and management of carotid free-floating thrombus: a systematic literature review. Int J Stroke. 2019;14(3):247–56.
14. Ota H, Takase K, Rikimaru H, et al. Quantitative vascular measurements in arterial occlusive disease. Radiographics. 2005;25(5):1141–58.
15. Rafati M, Havaee E, Moladoust H, et al. Appraisal of different ultrasonography indices in patients with carotid artery atherosclerosis. EXCLI J. 2017;16:727–41.
16. von Reutern GM, Goertler MW, Bornstein NM, et al. Grading carotid stenosis using ultrasonic methods. Stroke. 2012;43(3):916–21.
17. Hathout GM, Fink JR, El-saden SM, et al. Sonographic NASCET index: a new doppler parameter for assessment of internal carotid artery stenosis. AJNR Am J Neuroradiol. 2005;26(1):68–75.
18. Varetto G, Gibello L, Castagno C, et al. Use of contrast-enhanced ultrasound in carotid atherosclerotic disease: limits and perspectives. Biomed Res Int. 2015;2015:293163.
19. Csiba L. Ultrasonic methods used in the diagnosis of changes in the carotid artery system. Orv Hetil. 1990;131(27):1455–60.
20. AIUM practice parameter for the performance of an ultrasound examination of the extracranial cerebrovascular system. J Ultrasound Med. 2016;35(9):1–11.

Chapter 27
Acute Neurologic Injury in the ICU: Role of Transcranial Doppler in Disorders of the Vertebrobasilar Circulation

Rick R. Gill, Brett L. Cucchiara, and Monisha A. Kumar

Key Points

1. TCD of the vertebrobasilar system helps guide clinical management in aneurysmal subarachnoid hemorrhage. Sensitivity and specificity are better for the basilar artery than for the vertebral arteries; they are both enhanced when using thresholds >85 cm/s or a BA/VA ratio greater than 3.0.
2. A novel approach combining mean flow velocity (MFV) and stenotic to prestenotic ratio (SPR) improves the sensitivity of transcranial Doppler (TCD) in the detection of intracranial stenosis.
3. Microembolus signal detection (MES) in the vertebrobasilar circulation is correlated with both the presence of intracranial vertebrobasilar atherosclerosis and the degree of stenosis making it a useful tool in determining stroke etiology.
4. Intracardiac right to left shunt (RLS) has been implicated in cryptogenic stroke and closure has emerged as a viable therapeutic option. Detection of a RLS using gaseous contrast TCD of the vertebrobasilar circulation through a suboccipital window is both highly sensitive and specific when transtemporal windows are insufficient.

R. R. Gill
Department of Neurology, Loyola University, Chicago, IL, USA
e-mail: rrgill@lumc.edu

B. L. Cucchiara
Department of Neurology, University of Pennsylvania, Philadelphia, PA, USA
e-mail: cucchiar@pennmedicine.upenn.edu

M. A. Kumar (✉)
HUP Neuro ICU, Philadelphia, PA, USA

HUP Neuro ICU, Departments of Neurology, Neurosurgery and Anesthesiology and Critical Care, Hospital of the University of Pennsylvania, Philadelphia, PA, USA

University of Pennsylvania Health System, Philadelphia, PA, USA
e-mail: monisha.kumar@pennmedicine.uppen.edu

C. N. Rodríguez et al. (eds.), *Neurosonology in Critical Care*,
https://doi.org/10.1007/978-3-030-81419-9_27

5. TCD may assist in identifying disturbances in cerebral autoregulation, cerebral hypoperfusion, vasomotor reactivity, and stroke risk in patients with traumatic brain injury.
6. Examination of basilar artery flow characteristics is part of a complete TCD assessment for brain death.

27.1 Introduction

Transcranial Doppler (TCD) of the anterior circulation is a well-established non-invasive diagnostic imaging modality that has broad application in the intensive care unit (ICU). TCD may enable the clinical diagnosis of acute ischemic stroke, arterial vasospasm, and brain death and is a convenient way to monitor dynamic vascular changes in response to interventions at the bedside. TCD may evaluate brain tissue health by measuring cerebral autoregulation, cerebral vasoreactivity, and neurovascular coupling or functional hyperemia, which are all important physiologic assessments in the ICU, especially in patients with traumatic brain injury (TBI). TCD may have particular utility in hospitals with reduced access to neurovascular imaging such as CTA or MRA or advanced neuromonitoring. However, the role of TCD of the posterior circulation in the ICU is less well defined.

Assessment of the vertebrobasilar circulation is intuitively part of a complete assessment of the cerebral circulation. However, due to variations in vertebral artery (VA) anatomy, visualization can be technically difficult, and thus, its utility is limited [1, 2]. TCD/TCCS is a reasonably accurate screening technique for size, patency, and direction of blood flow in the vertebral arteries when compared with angiography and can reasonably assess blood flow velocity and detect microemboli [3]. Similarly, TCD can be used to diagnose subclavian steal and pre-steal phenomena. As technology has evolved and new clinical applications have been rigorously evaluated, the utility of vertebrobasilar ultrasound to assess for stenosis, dissection, occlusion, vasospasm, and even brain death has also increased. TCD-based assessments augment physiological data gleaned from other multimodal neuro monitors and thus may provide important insights for patients with severe neurological injury, such as those with TBI. This chapter serves to review the application of TCD of the posterior circulation to critically ill patients in the neuro ICU.

27.2 Anatomy: Vertebrobasilar System

The two vertebral arteries consist of three extracranial segments (V1–3) and one intracranial segment (V4) before terminating in a single basilar artery (BA) at the level of the pons. Asymmetry is common, with hypoplasia seen more often on the

right. The V1 segment extends from the subclavian artery (SCA) which is a branch from the arch of the aorta; this segment can be tortuous and typically originates from the cranio-dorsal SCA. In a small minority of cases, the left VA may arise from the aortic arch directly or very rarely from the common carotid artery. The V2 segment typically enters the transverse foramen of the cervical vertebral column at C6, although in variants it may enter at C5 or C7. The V3 segment exits the transverse foramen at C1 and traverses the posterior arch of C1 before entering the foramen magnum and the V4 (intradural) segments extend from the dura to their confluence as the basilar artery (Fig. 27.1) [4].

Collateral blood flow can confound ultrasound evaluation of a vascular territory. In the vertebrobasilar circulation, the pre-Willisian collaterals include the deep cervical artery which can contribute antegrade filling of the VA in patients with proximal stenosis. Within the Circle of Willis, the posterior communicating arteries (PCA) connect the left and right side of the posterior circulation, as well as the ipsilateral anterior and posterior circulation when a fetal PCA is present. Cortical anastomoses between distal branches of the PCA provide a post-Willisian communication [4].

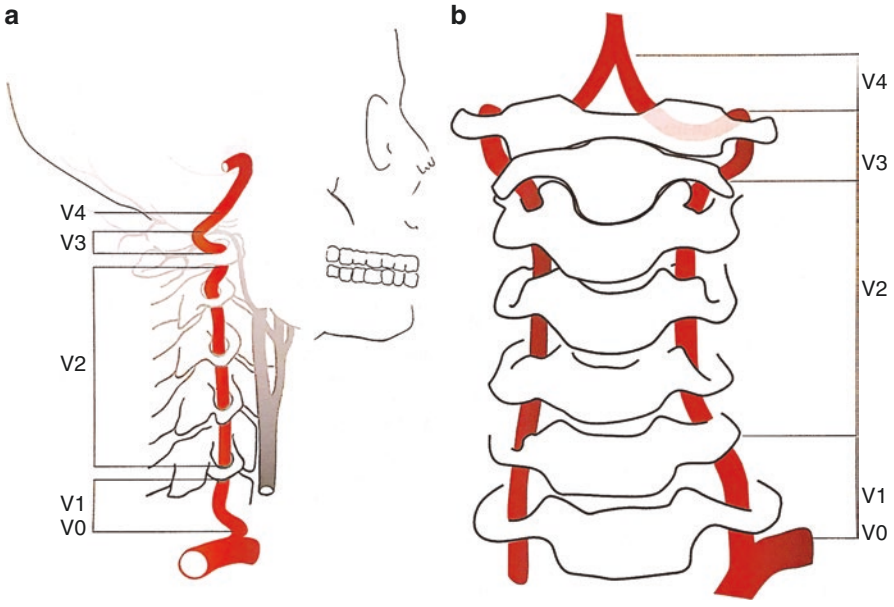

Fig. 27.1 The vertebrobasilar circulation: (**a**) Lateral anatomical view and (**b**) Frontal anatomical view; V0-V4: segments of the vertebral artery: V0: the origin, V1: from the origin of VA to its entry into transverse foramen of C6 vertebra, V2: from the entry into transverse foramen of C6 vertebra until the exit from the C2 vertebra, V3: Atlas loop and V4: intracranial part. (Courtesy: Baltgaile [68])

27.3 Vertebrobasilar Circulation: Ultrasound Examination

The VA is divided into four segments with segments 1–3 representing the extracranial components. The extracranial VA is best visualized by vascular ultrasound using a linear probe (5–7.5 MHz) with the patient supine and the neck extended. Once the common carotid artery is visualized in longitudinal section on B-mode, the probe is slid posteriorly and the acoustic shadows of the cervical vertebral transverse processes are identified and the VA (V2 segment) can be insonated in between these acoustic shadows in approximately 95% of patients [5]. Normal peak systolic velocity (PSV), measured using pulsed wave Doppler, for the V2 segment is 20–60 cm/s, with velocities >100 cm/s consistent with a significant stenosis. Knowledge of normal anatomical variants and asymmetry of the VA diameter, often larger on the left, can be useful in interpreting variations in peak systolic velocity (PSV). The most proximal V1 segment is visible with ultrasound in 65–85% of patients, with the right being more easily visualized than the left which tends to be deeper and originating from the aortic arch in a minority of cases [6]. The origin of the VA is susceptible to a variety of pathology including atherosclerotic disease making visualization and assessment of VA diameter and volume flow by tracking proximally from the V2 segment clinically useful. Alternatively, imaging of the supraclavicular subclavian artery can lead to visualization of the VA origin. The V3 segment of the VA may also be visualized as it exits the transverse process of C1. Color Doppler should be applied, and in a routine carotid assessment, it is often only the V2 segment that is visualized and assessed for direction of flow, which is always cephalad in normal subjects.

Insonation of the final intracranial segment of the VA (V4) as well as the BA is achieved transcranially. Unlike extracranial insonation where a high-frequency probe can be used, for TCD a 2 MHz probe better penetrates through the skull [7]. The suboccipital window can be found inferior and medial to the mastoid process with the probe oriented medially toward the bridge of the nose or the contralateral eye; turning the head to the contralateral side with or without the neck flexed may aid visualization [7, 8]. This window utilizes the foramen magnum's opening into the skull, and through this window at a depth of 50–75 mm, flow signals of the ipsilateral VA can be obtained. Insonation of the BA is achieved by tracking the VA cephalad and medially through the suboccipital window and increasing the depth to 75–110 mm [7]. Alternatively, placing the probe below the occipital protuberance and fanning the probe cephalad with a projection toward the bridge of the nose can also aid in visualizing the BA. Like the VA, the flow within the BA is always cephalad and away from the probe in normal healthy subjects. The greater variability of these vessels can often make insonation challenging in comparison to the anterior circulation [2, 7].

27.4 TCD: Aneurysmal Subarachnoid Hemorrhage

One of the most common applications of TCD in the Neuro ICU is the detection of cerebral vasospasm, or arterial narrowing, after aneurysmal subarachnoid hemorrhage (SAH). TCD can be used to follow the onset, time course, and resolution of arterial narrowing, and it can be combined with other blood flow measurement techniques to provide useful information to clinicians managing patients with subarachnoid hemorrhage. Chapters 23 and 24 discuss the approach to delayed cerebral ischemia (DCI) and cerebral vasospasm and thus will not be discussed in detail here.

27.4.1 Delayed Cerebral Ischemia

The main indication of TCD after SAH is to monitor for the development of DCI, a syndrome that manifests as neurological deterioration typically occurring days after aneurysm rupture and potentially associated with cerebral infarction [9]. Although the pathophysiology of DCI remains unclear, an association between arterial narrowing and the development of DCI is frequently considered. It should be noted that the incidence of arterial narrowing nears 70%, but only a fraction of those patients are clinically symptomatic [10]. Therefore, since the incidence of TCD-diagnosed arterial narrowing is much higher than that of clinically significant narrowing, therapy is not usually escalated on the basis of TCD findings alone.

27.4.2 Vasospasm

Detection of vasospasm using TCD in the vertebrobasilar system after subarachnoid hemorrhage is routinely performed, but remains less sensitive compared to the anterior circulation. Elevated flow velocities may not always imply arterial narrowing, as increased blood flow and cerebral hyperemia may confound the diagnosis of cerebral vasospasm. The incidence of basilar artery vasospasm is approximately 40% [11, 12]. Sensitivity and specificity of cerebral vasospasm are better for the basilar artery than for the vertebral arteries [12]. BA mean velocities higher than 60 cm/s are associated with 60% specificity and 100% sensitivity for vasospasm; however, increasing the MFV threshold reduces the sensitivity significantly [11]. The specificity of TCD for arterial narrowing is improved when using flow velocity cutoffs of ≥80 cm/s in the vertebral artery and ≥95 cm/s in the basilar artery [11]. Increasing the MFV thresholds improves to discriminate between hyperemia and vasospasm and improves specificity but results in a loss of sensitivity.

A ratio of BA to extracranial VA flow velocities may help discriminate between BA vasospasm and vertebrobasilar hyperemia. This is similar to the function of the Lindegaard ratio in the anterior circulation. This enhances the utility of TCD in

detecting BA vasospasm, although well-defined thresholds do not exist [11, 13]. When the BA velocity is greater than 85 cm/s, a BA/VA ratio greater than 2.5 is associated with 86% sensitivity and 97% specificity for a 25% reduction in BA diameter; a ratio greater than 3.0 is associated with 92% sensitivity and 97% specificity for a 50% reduction in BA diameter [13]. Despite the lack of well-defined thresholds, BA vasospasm may be an independent prognostic factor associated with unfavorable outcome at 90 days [14].

27.5 TCD: Vertebrobasilar Dissection

Vertebral and basilar artery dissection are associated with posterior circulation territory stroke and transient ischemic attack (TIA) as well as subarachnoid hemorrhage (SAH). Stroke occurs in 63% of cases of vertebral artery dissection (VAD), more commonly related to extracranial than intracranial VAD (66% vs 32%), and is most common in those aged 18–45 years carrying an overall annual incidence of 1–1.5 per 100.000 [15]. Some degree of ischemic symptoms (TIA or stroke) involving the brainstem, thalamus, cerebral or cerebellar hemispheres, or rarely the cervical spinal cord occur in upwards of 90% of patients [16]. Subarachnoid hemorrhage occurs in 10% of cases of VAD and it is seen exclusively in intracranial dissection. Basilar dissection is rare, but it carries a high morbidity and mortality from associated SAH. Similarly, intracranial vertebral dissection carries a high morbidity and mortality, and there is a male predominance [17, 18]. Additional diagnostic clues include a young age at onset, severe occipital or neck pain, preceding stroke, and a progressive onset of ischemic symptoms.

While there are no pathognomonic ultrasound findings for VAD in the V2–V4 segments (and the V1 segment has a high failure rate of examination with both Doppler and duplex sonographic techniques), a patient with high grade stenosis or occlusion and a history and examination consistent with vertebral dissection or posterior circulation stroke should prompt further evaluation with CTA, MRA, or DSA [19]. Typical analysis of the vertebral circulation includes extracranial and transcranial pulsed-wave Doppler sonography for the V3–4 segments and duplex sonography for the evaluation of the prelesional intertransverse V2 segment at cervical spine levels 5 and 6. During ultrasound analysis, systolic (PSV) and end-diastolic (EDV) blood flow velocities as well as time mean flow velocity (MFV) should be recorded for each vessel typically using pulsed Doppler gate with correction for insonation angle and the resistive index (RI) and pulsatility index (PI) calculated [18] (Eqs 27.1 and 27.1):

$$\mathrm{RI} = \left(\mathrm{PSV} - \mathrm{EDV}\right) / \mathrm{PSV} \tag{27.1}$$

$$\mathrm{PI} = \left(\mathrm{PSV} - \mathrm{EDV}\right) / \mathrm{MFV} \tag{27.2}$$

Despite a lack of uniform diagnostic criteria, studies have established the sensitivity of neurovascular ultrasound in the detection of VA dissection at 70–92% [20]. Data remains limited for the evaluation of primary isolated BA dissection. Microembolic signals, diminished pulsatility index in the posterior cerebral arteries and increased CBFV in the BA can all be clues to the presence of a basilar dissection [21, 22].

Direct signs of vessel abnormality include increased MFV (>120 cm/s) or a >50% increase in velocity compared with an unaffected segment of the vessel. Severely reduced or absent MFV, increased PI, and increased contralateral MFV may be an indirect sign of VA dissection; however, variability in VA diameter is common in the population confounding this examination observation. Occlusion of the vessel detected by a focal absence of flow particularly in the intertransverse segments should raise concern for vertebral dissection. An intraluminal abnormality such as an echo-lucent hematoma or double lumen sign may also suggest dissection in the right clinical context [23]. In this respect, color-coded Doppler can be useful in visualizing segmental dilation or an eccentric channel in the proximal or distal parts of the artery with an increased velocity in the residual channel [18]. Segmentally, the proximal VA (V1–V2) can have distinct findings of increased arterial diameter and decreased PI. The atlas loop is a vulnerable, mobile segment of the VA to which additional attention should be paid, and signs of absent flow signals, low bidirectional flow signals or low post-stenotic flow signals should prompt further investigation with angiography [19]. Ultrasound has also been shown to be useful in determining the length of dissection in addition to being a practical means of follow-up in cases of angiographic confirmed dissection [18]. The sensitivity of sonographic evaluation of the posterior circulation for dissection is preserved only when all potential abnormalities are considered, and sensitivity decreases when definite abnormal findings of absent or severely reduced flow velocities, absent diastolic flow, bidirectional flow or stenotic signals are used as strict criteria [19].

Pitfalls in the detection of dissection with ultrasound include the detection of pseudoaneurysms of the VA as well as small hematomas or hematomas not within the visible vertebral arterial segment, such as those obscured by the transverse processes of the cervical spine. Finally, a normal ultrasound evaluation in a patient presenting with a history or exam findings concerning for posterior circulation dissection requires further workup, as a negative ultrasound study does not reliably exclude arterial dissection.

27.6 TCD: Intracranial Stenosis

Intracranial atherosclerotic disease (IAD) is responsible for an estimated 8–10% of ischemic strokes globally and remains an independent risk factor for the high recurrence rate of stroke seen in these patients [24–27]. Recurrent stroke risk can be as high as 15% per year in the territory of the stenotic artery with subgroups with severe disease (70–99% stenosis) or those with vertebrobasilar disease at a

particularly high risk [24, 25]. Black, Hispanic, Indian, and Asian populations have the highest prevalence of ICA stenosis with risk of IAD-related stroke as high as 30–50% in Asian populations [28].

The gold standard evaluation of the intracranial vasculature remains catheter angiography, but it is an invasive procedure which comes with risks. Clinicians often turn to non-invasive alternatives such as magnetic resonance angiography (MRA), computed tomographic angiography (CTA) and TCD, which are safer, more practical, and cost effective. Angiographically verified severe stenosis of 70–99% portends an increased risk of stroke recurrence compared to moderate stenosis (50–69%). Robust collateral circulation mitigates this increased risk to some degree [29]. This high risk was also profoundly reduced with aggressive medical management, putting an emphasis on early non-invasive identification with the goal of primary and secondary stroke prevention.

The validity of ultrasound in the evaluation of the extracranial carotid arteries as both a screening and diagnostic tool is well established. The utility of TCD to evaluate for intracranial stenosis (Table 27.1) is less well described, particularly in the vertebral-basilar circulation. Factors limiting the reliability of TCD include the hemodynamic effects of coexisting stenotic lesions proximal to the region being assessed (e.g., extracranial disease) or the effect of collateral circulation on TCD velocities.

The Stroke Outcomes and Neuroimaging of Intracranial Atherosclerosis (SONIA) study was a companion study to the Warfarin-Aspirin Symptomatic Intracranial Disease (WASID) trial aimed to define the ability of TCD and MRA to diagnose and quantify the severity of intracranial atherosclerosis of 50–99% compared to cerebral angiography [28]. SONIA was a prospective multicenter study utilizing standardized, reproducible ultrasound protocols and diagnostic criteria to identify large vessel intracranial stenoses of 50–99%. The study demonstrated the ability of TCD to reliably exclude the presence of moderate and severe intracranial stenosis, utilizing a mean flow velocity (MFV) cutoff of 80 cm/s in both the VA and BA. By adjusting the cutoff MFV to 130 cm/s, TCD maintains a strong NPV to exclude severe intracranial stenosis in the VA and BA [29].

The vertebrobasilar circulation shows considerable variability in its size and course limiting the sensitivity and specificity of TCD in detecting vertebrobasilar stenotic lesions. A novel approach combining velocity cutoffs in conjunction with the stenotic/pre-stenotic ratio for ≥70% stenosis demonstrated improved sensitivity with good agreement with digital subtraction angiography [29, 30]. In the VA/BA,

Table 27.1 Mean TCD velocities in the assessment of intracranial atherosclerosis [30]

	Mean velocity	
Blood vessel	≥50% Stenosis	≥80% Stenosis
Vertebral	80 cm/s	110 cm/s
Basilar	80 cm/s	130 cm/s
MCA	100 cm/s	240 cm/s
ICA	90 cm/s	120 cm/s

a MFV > 110 cm/s or a stenotic/pre-stenotic ratio (SPR) of ≥3 had a sensitivity of 60% and specificity of 95% [30]. This approach shows good agreement with invasive angiography and may be a reasonable cost-effective alternative in resource limited settings. TCD may also supplement other forms of non-invasive imaging, with concordant findings potentially eliminating the need for conventional angiography.

27.7 TCD: Microembolus Detection

Transcranial Doppler is the only modality capable of detecting circulating cerebral microemboli, both gaseous and solid (e.g., fibrinogen, cholesterol, platelets). Diseases commonly associated with intracranial microemboli include carotid stenosis, arterial dissection, atrial fibrillation, patent foramen ovale, and mechanical cardiac valves as well as during vascular surgical procedures to address the aforementioned conditions [7, 31]. These intracranial microthrombi can be detected on TCD as microembolic signals (MES). The clinical significance of MES in the posterior circulation remains unclear; for example, the presence of intracranial arterial emboli on TCD in a case suspicious for dissection can aid in establishing a diagnosis and prompt further evaluation, but in itself MES are not diagnostic. Detection of intracranial emboli makes the likelihood of an ischemic event much higher [31]. High-intensity transient signals (HITS) are characteristic and are the result of backscatter of ultrasound waves from gaseous or solid microemboli on TCD [7]. Brief (<0.01–0.03 second) unidirectional high intensity increases within the Doppler frequency spectrum (>3 dB) producing a characteristic "chirp," "click," or "whistle" sound during TCD insonation occurring randomly characterize HITS. Technical difficulties of vessel insonation can be overcome by power M-mode Doppler (PMD) which uses multiple sample gates placed with 2 mm spacing increasing the ease of insonation through transcranial windows [31].

While the vast majority of MES are clinically silent, patients with microemboli appear to have an increased macroembolic risk. TCD assessment for microemboli can help tailor therapeutic interventions in this population such as antithrombotic therapy or endovascular intervention [32, 33].

A Korean trial studied the utility of MES in patients with acute neurological symptoms referable to posterior circulation ischemia [34]. The study protocol used a 2-MHz transducer mounted to the head using a fixed frame and required insonation of the basilar artery for 30 consecutive minutes through a suboccipital window. HITS were required at two insonation depths to confirm MES [34]. MES were detected in 13% of patients and were strongly associated with intracranial, but not extracranial, vertebrobasilar artery stenosis [34]. MES occurred more frequently in patients with severe degree of V-BA stenosis and were more common in patients with lesions on diffusion weighted MRI. An optimal timing of MES testing, relative to stroke onset, has not been established for the posterior circulation. Quantification and subsequent grading of MES in the posterior circulation has not been utilized as

it has in the assessment of MES in right to left cardiac shunts with the International Consensus Criteria (ICC) or Spencer's Logarithmic Scale.

In stroke patients with posterior circulation symptoms, the presence of MES in the vertebrobasilar circulation suggests the possibility of large artery vertebrobasilar disease, which may be atherosclerotic or due to dissection. The severity of stenosis appears to correlate with the likelihood of detecting MES. Autopsy studies also suggest that extracranial atherosclerotic disease of the posterior circulation less often embolizes to cause stroke than intracranial stenosis [34]. TCD for MES detection in the vertebrobasilar circulation can be a useful tool in guiding the management of patients with acute ischemia in the posterior circulation.

27.8 Intracardiac Right to Left Shunt

Intracardiac right to left shunt (RLS) has been implicated in stroke (particularly in patients <60 years old and all patients with cryptogenic stroke), migraine and cluster headache, obstructive apnea, and hypoxemia and is most commonly caused by a patent foramen ovale (PFO) [35]. A PFO is present in 20–25% of the general population as a remnant of the fetal circulation, and transcatheter closure has evolved into a viable treatment for PFO in recent years. This necessitates accurate diagnosis of PFO with transesophageal echocardiogram (TEE) remaining the gold standard diagnostic approach. However, the invasive nature of TEE and the requirement for sedative anesthesia make it less than ideal when screening populations with disease states which implicate PFO as a potential etiological factor. In this light, the gaseous contrast TCD ("bubble study") has emerged as a practical and cost-effective alternative.

During a contrast TCD study, a solution with microbubbles is injected peripherally during continuous TCD examination, ideally with power mode for increased sensitivity. A Valsalva maneuver is performed 4–6 seconds after injection of the gaseous contrast medium, causing an increase in right atrial pressure and an increase in flow through a potential PFO. A significant reduction in TCD mean flow velocity of the insonated vessel indicates an adequate Valsalva maneuver. TCD monitoring is continued for a further 16–20 seconds and the number of MES counted and graded using the International Consensus Criteria (ICC) or Spencer's Logarithmic Scale [36]. A meta-analysis of 27 studies and 1968 patients compared gaseous contrast TCD with TEE and found the weighted mean sensitivity to be 97% and specificity to be 93% [37]. The vast majority of existing studies utilize the MCA as the vessel insonated in their evaluation.

In situations where TCD of the MCA cannot be performed due to an insufficient transtemporal window, insonation of the BA through a transoccipital window is a viable and reliable alternative. In a study by Del Sette and colleagues (2007) comparing the right MCA to the vertebrobasilar circulation, the vertebrobasilar circulation achieved a sensitivity of 83.7% and a specificity of 100% [35]. This improved to 100% sensitivity and specificity for only medium and large shunts. A similar study by Guo et al. (2016) showed no significant difference between the VA and

MCA, both achieving excellent sensitivity and specificity [38]. TCD of the vertebrobasilar circulation is thus a practical, cost-effective, and highly accurate means of diagnosing a clinically significant PFO.

27.9 Subclavian Steal Syndrome

Proximal high-grade steno-occlusive disease of the pre-vertebral subclavian artery (SA), most commonly due to atherosclerotic vascular disease, can lead to a phenomenon known as subclavian steal syndrome. In subclavian steal syndrome (SSS), exertion of the arm that is supplied by the stenotic SA results in a drop in SA pressure distal to the lesion. This results in redirecting flow from the contralateral VA via the BA in a retrograde direction down the ipsilateral VA and away from the posterior cerebral circulation. Occasionally, this flow pattern may even be seen at rest. Most often SA stenosis is clinically silent and may be found incidentally with an observed blood pressure difference in the upper extremities (the left SA is affected in a 4:1 ratio compared to the right). Clinical consequences of subclavian steal include arm ischemia, which is most common, and vertebrobasilar ischemia which occurs more often in patients with concurrent cerebrovascular lesions. Symptoms may include dizziness and vertigo, ataxia, drop attacks, and deficits associated with the cranial nerves; however, symptoms often persist after correction of SA stenosis or improvement in retrograde VA flow, suggesting in many cases the steal is not the cause of presenting symptoms [39].

Duplex ultrasonography can diagnose SA stenosis with a peak systolic velocity >240 cm/s being predictive of a >70% stenosis [40]. It can also assess the extracranial VA for flow reversal, which has been shown to be intermittent in 30% and permanent in 65% of patients with >80% SA stenosis. TCD can further evaluate the direction of flow in the BA and this may be more predictive of symptoms as patients who have antegrade flow in the BA are less likely to be symptomatic. Less than 25% of patients with retrograde flow in the VA were found to have a corresponding reversal of flow in the BA [41]. If the symptomatic vertebral artery waveform appears normal or shows only absent diastolic flow proceed with provocative maneuvers such as raising the arm, squeezing a ball, or inflating and deflating a blood pressure cuff on the affected side. In patients with confirmed symptoms attributable to SA stenosis and demonstrable retrograde vertebral and basilar flow, therapeutic options such as stenting or surgery can be considered.

27.10 TCD: Multimodal Monitoring

Multimodality monitoring has become an important tool in the management of critical ill patients in the Neuro ICU. Information gathered from intracranial pressure (ICP) monitors, jugular bulb oximetry, brain tissue oximetry, cerebral microdialysis, near infrared spectroscopy, and electroencephalography often guides clinical

management. TCD may be considered a component of multimodality monitoring in the Neuro ICU, either supplementing information gleaned from these other monitors or serving as a surrogate for invasive neuromonitoring. TCD may provide non-invasive estimations of cerebral perfusion pressure (CPP) and ICP and can describe cerebral hemodynamics including cerebrovascular reactivity and cerebral pressure autoregulation [42]. These measurements are largely derived from anterior circulation TCD assessments and are beyond the scope of this chapter. Cerebral autoregulation and vasomotor reactivity are important parameters in severe brain injury and are described briefly.

Cerebral pressure autoregulation represents the relationship between CBF and CPP. Autoregulation is a physiologic mechanism that serves to reduce the variation in CBF when CPP varies between 50 and 150 mmHg. The cerebral vessels take time to react to spontaneous physiological perturbations (changes in CPP, $PaCO_2$, PaO_2) or induced ones (breath holding, Valsalva maneuver). Fast responses reflect mechano-elastic properties of the cerebrovascular bed, such as cerebrovascular resistance and compliance [42]. Slow responses reflect cerebral autoregulation. TCD allows non-invasive measurement of both the static and dynamic autoregulatory response. Static autoregulation is calculated by augmenting blood pressure, typically with pressors, while recording MCA flow velocities and MAP. The estimated CVR is CVRe = MAP/FV [42]. The static rate of autoregulation (SRoR) is the ratio of percent change in CVRe to MAP, or CPP if ICP is available [42]. An SRoR of 100% suggests perfect autoregulation, while an SRoR of 0% connotes complete failure of autoregulation [42]. Dynamic autoregulation is tested by measuring the time to recovery of flow velocities after a rapid but transient decrease in mean blood pressure. This may be accomplished by the leg cuff test wherein a modified blood pressure cuff is placed around one or both thighs and inflated to 50 mmHg above the systolic pressure for 3 minutes. Deflation produces an abrupt drop in blood pressure. The time it takes for blood pressure and mean flow velocities to normalize is measured and fitted to a series of curves in a validated algorithm [43]; this determines the rate of dynamic cerebral autoregulation or autoregulation index (ARI). The threshold between good and disturbed autoregulation is an ARI of 5 [44].

Vasomotor reactivity (VMR) represents the cerebrovascular response to fluctuations in arterial CO_2 concentration with rapid adjustment of cerebrovascular resistance. Hypercapnia or elevated arterial $PaCO_2$ can be provoked in a number of ways to evaluate the cerebral blood flow velocity response, the simplest being voluntary breath holding, breathing CO_2 or pharmacologically with the administration of acetazolamide in patients who cannot voluntarily breath-hold. Control of ventilation in intubated patients can also be utilized in the ICU. Hypercapnia leads to cerebral arteriolar vasodilation, via changes in extracellular pH, and subsequent increase in MFV on TCD examination of the upstream larger cerebral arteries which can be insonated with TCD [7]. Hypocapnia can conversely be triggered with induced hyperventilation and has a vasoconstrictive cerebrovascular response. Vasomotor reactivity may become impaired in arterial stenotic diseases and cerebral ischemia and can be quantified as the percentage change in MFV. The breath holding index

(BHI) is the change associated with a timed breath hold and several studies have shown a similar degree of reactivity in the anterior circulation (MCA) and the BA following the same change in $PaCO_2$ [45, 46]. Cerebrovascular reactivity can help guide the management of patients who may require revascularization procedures and has been shown to predict a higher rate of annual distal cerebral ischemic events in patients with ICA stenosis and impaired VMR [47].

The application of vasomotor reactivity exclusively to the posterior circulation is sparse. Park and colleagues evaluated a small cohort of patients with occlusive vascular disease in the anterior circulation and assessed the BA for VMR as it may serve as a critical collateral supply to the impaired anterior circulation in these patients. Patients with anterior circulation stenotic disease showed increased baseline MFV in the BA and impaired VMR [48]. This may represent a novel adjunctive assessment, which may guide clinicians in the management of patients with intracranial and extracranial stenotic disease of the anterior circulation.

27.11 TCD: Traumatic Brain Injury

Traumatic brain injury (TBI) has been classified as a serious public health concern by the Centers for Disease Control and Prevention. The mainstay of treatment in TBI is pre-empting or mitigating secondary injury, as secondary ischemic brain injuries are the major prognostic factors after severe TBI. Despite the fact that TBI is a very heterogeneous disease, TCD shows considerably promise to guide management and predict outcomes in both mild and severe forms of injury. Similarly, TCD appears useful in both pediatric and adult populations [49, 50].

In mild injury, TCD is largely used to identify patients without intact cerebral autoregulation. Cerebral autoregulation denoted by the autoregulation index (ARI) is defined as ARI = % ΔeCVR/% ΔMAPe, as noted above [41]. In sports related concussion, TCD may demonstrate persistent impairment of autoregulation for up to 5 days post-injury, despite a normal clinical exam as defined by the Glasgow Coma Score (GCS) [51]. Disturbances of autoregulation may be more associated with hemorrhagic lesions than other traumatic lesions [52]. TCD with tilt table testing may identify impairments of cerebral autoregulation in nearly 50% of pediatric patients with complicated mild TBI [52]. The vast majority of disturbances are unilateral (70%) although over 30% of those patients with disturbed autoregulation exhibit bilateral involvement [53]. In patients with complicated mild TBI (GCS 13–15), disturbances of autoregulation often persist until after hospital discharge [51, 53].

TCD may be used to identify severe TBI patients with cerebral hypoperfusion, a significant predictor of long-term functional outcome. Hypoperfusion is typically defined by a mean velocity (MFV_{MCA}) of <35 cm/s, end-diastolic velocity (EDV_{MCA}) <20 cm/s, and/or pulsatility index (PI) >1.4 [52–54] In severe TBI, patients may have cerebral hypoperfusion despite mean arterial pressures in target range [55]. In one of the largest TCD studies of 255 severe TBI patients, TCD identified

hypoperfusion in 28% of patients, of whom nearly all died [53]. Studies suggest that TCD, albeit anterior circulation thresholds, may be used to guide early brain resuscitation and to define optimal cerebral perfusion pressure targets [55].

Cerebral vasoreactivity (C_{VR}), a measure of hemodynamic reserve, may also be assessed by TCD after TBI. As previously mentioned, C_{VR} is assessed by evaluating the response to changes in the arterial content of carbon dioxide. Studies show that C_{VR} may be impaired as early as 4 days and remain impaired for months after mild or concussive injury despite symptom resolution [51]. Importantly, CVR impairment after TBI is associated with gray matter atrophy [55–57], headache [51–53] and cognitive deficits [58].

TCD may also be used to assess stroke risk in patients with TBI. Among patients with blunt cerebrovascular injury, TCD with MES may be used to predict risk of stroke [59]. Patients with known carotid artery dissection and MES by TCD are at higher risk for embolism in a dose dependent manner. However, TCD with MES appears to be ineffective at monitoring stroke risk from extracranial vertebral injuries [59]. TCD may also be used to assess the risk of arterial narrowing after TBI. The incidence of arterial narrowing in the MCAs after TBI is near 30%; over 50% of patients with evidence of MCA vasospasm experience death or disability [54]. BA vasospasm may be particularly important in the cause of secondary brain injury in TBI [52].

27.12 TCD: Brain Death Determination

Brain death, or the final clinical expression of complete and irreversible neurologic coma, was first described in 1959 and has gone through several iterations of definition, which vary from country to country, and even among hospitals within a nation. The American Academy of Neurology (AAN) defines brain death as a complete lack of evidence of responsiveness (coma) with a complete lack of brain stem reflexes on clinical assessment and an absent respiratory drive as demonstrated with an apnea test [60].

However, in some situations, the exam finding may be inconclusive or ambiguous, or performing a clinical exam may be limited by factors such as facial trauma or pre-existing conditions such as post-operative pupil dysfunction. In these cases, ancillary testing such as cerebral angiography, electroencephalogram (EEG) and transcranial Doppler (TCD) can be used. The AAN endorses TCD with Type A, Class II level evidence supporting the modality for the assessment of cerebral circulatory arrest (CCA) in support of a clinical diagnosis of brain death. A pooled analysis of 22 studies found the sensitivity of TCD in assessing for CCA to be 90% and specificity of 98%; these figures being consistent with published guidelines of the American Academy of Neurology [61–63]. TCD as a confirmatory test of cerebral circulatory arrest is a viable adjunctive test in the determination of brain death, although in some retrospective analyses lower sensitivities have been reported and, in that respect, serial testing has been shown to increase sensitivity [64].

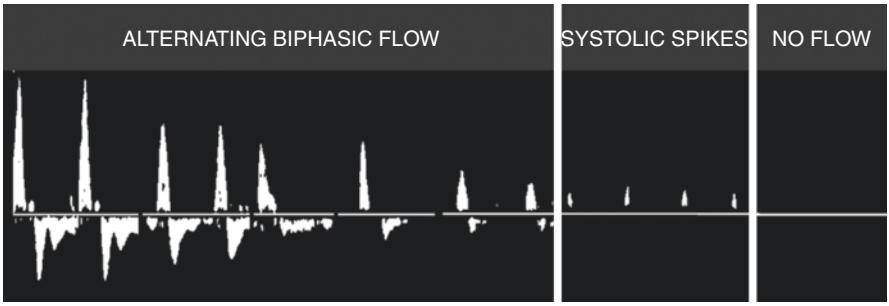

Fig. 27.2 Typical waveform observed in the basilar artery confirming cerebral circulatory arrest. (Courtesy: Schreiber [69])

There are limiting factors however, and for TCD to be useful, a reliable signal must be found. As part of a complete evaluation, the vertebrobasilar circulation is assessed through a suboccipital transcranial window and at the time of TCD the patient's arterial blood pressure should be noted. Early findings in elevated intracranial pressure include a mild decrease in the diastolic flow velocity and an increase in the difference between peak-systolic and end-diastolic velocities. The characteristic findings of an oscillating flow pattern with a negative diastolic component represent an increase in intracranial pressure above diastolic pressure during the process of brain death and short systolic spikes are often seen as cerebral perfusion pressure approaches zero. Figure 27.2 outlines these findings which are considered to be very specific for cerebral circulatory arrest (CCA) [61, 65]. A complete absence of flow may not in itself be reliable due to an inadequate window, and in this respect, it should be noted that TCD is generally less reliable in patients with prior craniotomies [66]. TCD remains a viable ancillary investigation along with clinical examination in the determination of brain death but is not viable as the sole determinant.

Kuo and colleagues assessed the time-dependent validity in the diagnosis of brain death using TCD. Specific diagnostic patterns described above increased in prevalence in the first 24 hours of confirmed brain death reaching a plateau at 36 hours [67]. Additionally, the group found consistency of the BA and the middle cerebral artery (MCA) in the diagnosis of brain death. However, it should be noted the BA had a greater sensitivity, higher positive predictive value, and fewer false negatives, lending further credence to the value of TCD of the vertebrobasilar circulation as a part of a complete sonographic evaluation in the determination of brain death [67].

27.13 Conclusion

TCD is an important non-invasive tool to monitor cerebral hemodynamics, which is an integral part of assessing patients in the Neuro ICU. Although treatment thresholds and outcome evaluations have been largely defined by anterior circulation

criteria, evidence suggests that basilar artery assessments may provide important additional and complementary information to complete the assessment. Not only do patients with ischemic and hemorrhagic stroke subtypes benefit from TCD assessment, but also patients with TBI, from mild to severe forms of injury and across the age spectrum.

Algorithm 27.1 TCD/TCCS: Use of Posterior Circulation in Diagnosis of Acute Brain injury

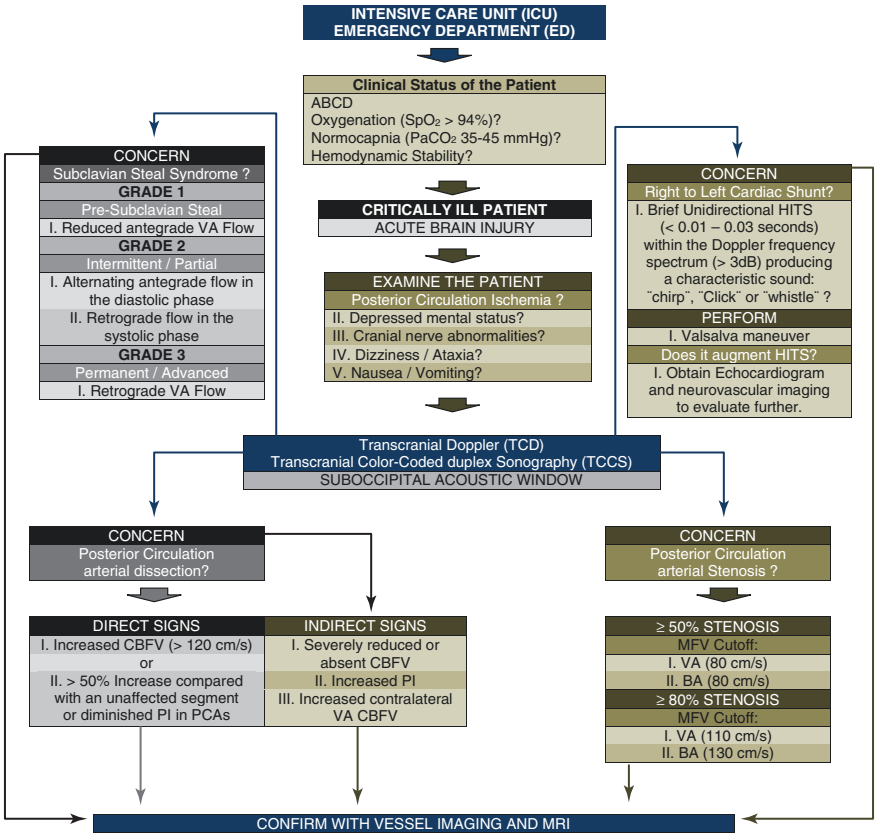

ABCD Airway-breathing-circulation-disability, *CBFV* Blood flow velocity, *MFV* Mean flow velocity, *VA* Vertebral artery, *BA* Basilar artery, *PI* Pulsatility index, *PCA* Posterior cerebral artery

Algorithm 27.2 Monitoring disease states with posterior circulation TCD/TCCS

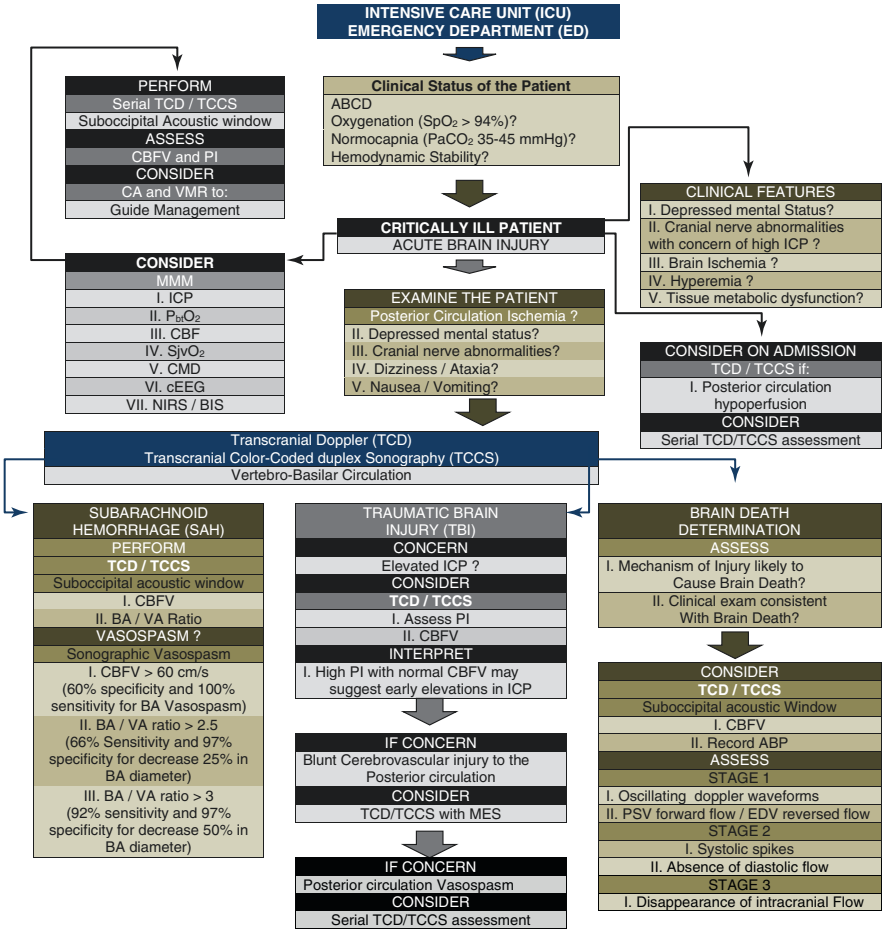

ABCD Airway-breathing-circulation-disability, *CBFV* cerebral Blood flow velocity, *PI* Pulsatility index, *PSV* Peak systolic velocity, *EDV* End-diastolic velocity, *MES* microemboli signal, *BA* Basilar artery, *VA* vertebral artery, *ABP* arterial blood pressure, *ICP* intracranial pressure, *CPP* cerebral perfusion pressure, *CMD* cerebral micro-dialysis, *CA* cerebral autoregulation, *VMR* vasomotor reactivity, *CBF* cerebral blood flow

References

1. Bluth EI, Merritt CR, Sullivan MA, Bernhardt S, Darnell B. Usefulness of duplex ultrasound in evaluating vertebral arteries. J Ultrasound Med. 1989;8(5):229–35.

2. Buckenham TM, Wright IA. Ultrasound of the extracranial vertebral artery. Br J Radiol. 2004;77(913):15–20.
3. Davis PC, Nilsen B, Braun IF, Hoffman JC. A prospective comparison of duplex sonography vs angiography of the vertebral arteries. Am J Neuroradiol. 1986;7(6):1059–64.
4. Uflacker R. Atlas of vascular anatomy. An angiographic approach. Philadelphia, PA: Lippincott Williams; 1997.
5. Nicolau C, Gilabert R, Chamorro A, Vázquez F, Bargalló N, Brú C. Doppler sonography of the intertransverse segment of the vertebral artery. J Ultrasound Med. 2000;19(1):47–53.
6. Trattnig S, Hübsch P, Schuster H, Pölzleitner D. Color-coded Doppler imaging of normal vertebral arteries. Stroke. 1990;21(8):1222–5.
7. Purkayastha S, Sorond F. Transcranial Doppler ultrasound: technique and application. In: Seminars in neurology, vol. 32, No. 4. NIH Public Access; 2012. p. 411.
8. Bathala L, Mehndiratta MM, Sharma VK. Transcranial Doppler: technique and common findings (Part 1). Ann Indian Acad Neurol. 2013;16(2):174.
9. Vergouwen MDI, Vermeulen M, van Gijn J, Rinkel GJE, Wijdicks EF, Muizelaar JP, et al. Definition of delayed cerebral ischemia after aneurysmal subarachnoid hemorrhage as an outcome event in clinical trials and observational studies: proposal of a multidisciplinary research group. Stroke. 2010;41:2391–5.
10. Kassell NF, Torner JC, Jane JA, et al. The international co-operative study on the timing of aneurysm surgery. Part 1: overall management results. J Neurosurg. 1990;73(18).
11. Sloan MA, Burch CM, Wozniak MA, Rothman MI, Rigamonti D, Permutt T, et al. Transcranial Doppler detection of vertebrobasilar vasospasm following subarachnoid hemorrhage. Stroke. 1994;25(11):2187–97.
12. Soustiel JF, Shik V, Shreiber R, Tavor Y, Goldsher D. Basilar vasospasm diagnosis: investigation of a modified "Lindegaard Index" based on imaging studies and blood velocity measurements of the basilar artery. Stroke. 2002;33(1):72–8.
13. Sviri GE, Ghodke B, Britz GW, Douville CM, Haynor DR, Mesiwala AH, et al. Transcranial Doppler grading criteria for basilar artery vasospasm. Neurosurgery. 2006;59(2):360–6.
14. Sviri GE, Newell DW, Lewis DH, Douville C, Ghodke B, Chowdhary M, et al. Impact of basilar artery vasospasm on outcome in patients with severe cerebral vasospasm after aneurysmal subarachnoid hemorrhage. Stroke. 2006;37(11):2738–43.
15. Gottesman RF, Sharma P, Robinson KA, Arnan M, Tsui M, Ladha K, et al. Clinical characteristics of symptomatic vertebral artery dissection. A systematic review. Neurol. 2012;18(5):245.
16. Schievink WI. Spontaneous dissection of the carotid and vertebral arteries. N Engl J Med. 2001;344(12):898–906.
17. Kim BM, Suh SH, Park SI, Shin YS, Chung EC, Lee MH, et al. Management and clinical outcome of acute basilar artery dissection. Am J Neuroradiol. 2008;29(10):1937–41.
18. De Bray JM, Penisson-Besnier I, Dubas F, Emile J. Extracranial and intracranial vertebrobasilar dissections: diagnosis and prognosis. J Neurol Neurosurg Psychiatry. 1997;63(1):46–51.
19. Sturzenegger M, Mattle HP, Rivoir A, Rihs F, Schmid C. Ultrasound findings in spontaneous extracranial vertebral artery dissection. Stroke. 1993;24(12):1910–21.
20. Nebelsieck J, Sengelhoff C, Nassenstein I, Maintz D, Kuhlenbäumer G, Nabavi DG, et al. Sensitivity of neurovascular ultrasound for the detection of spontaneous cervical artery dissection. J Clin Neurosci. 2009;16(1):79–82.
21. Vassileva E, Getsov P, Vavrek E, Daskalov M. Detection of basilar artery dissection by ultrasound. J Stroke Cerebrovasc Dis. 2015;24(5):e127–8.
22. Ruecker M, Furtner M, Knoflach M, Werner P, Gotwald T, Chemelli A, et al. Basilar artery dissection: series of 12 consecutive cases and review of the literature. Cerebrovasc Dis. 2010;30(3):267–76.
23. Dittrich R, Dziewas R, Ritter MA, Kloska SP, Bachmann R, Nassenstein I, et al. Negative ultrasound findings in patients with cervical artery dissection. J Neurol. 2006;253(4):424–33.

24. Kasner SE, Chimowitz MI, Lynn MJ, Howlett-Smith H, Stern BJ, Hertzberg VS, et al. Predictors of ischemic stroke in the territory of a symptomatic intracranial arterial stenosis. Circulation. 2006;113(4):555–63.
25. Chimowitz MI, Lynn MJ, Derdeyn CP, Turan TN, Fiorella D, Lane BF, et al. Stenting versus aggressive medical therapy for intracranial arterial stenosis. N Engl J Med. 2011;365(11):993–1003.
26. White H, Boden-Albala B, Wang C, Elkind MS, Rundek T, Wright CB, et al. Ischemic stroke subtype incidence among whites, blacks, and Hispanics: the Northern Manhattan Study. Circulation. 2005;111(10):1327–31.
27. Wong KS, Huang YN, Gao S, Lam WW, Chan YL, Kay R. Intracranial stenosis in Chinese patients with acute stroke. Neurology. 1998;50(3):812–3.
28. Chimowitz MI, Lynn MJ, Howlett-Smith H, Stern BJ, Hertzberg VS, Frankel MR, et al. Comparison of warfarin and aspirin for symptomatic intracranial arterial stenosis. N Engl J Med. 2005;352(13):1305–16.
29. Feldmann E, Wilterdink JL, Kosinski A, Lynn M, Chimowitz MI, Sarafin J, et al. The stroke outcomes and neuroimaging of intracranial atherosclerosis (SONIA) trial. Neurology. 2007;68(24):2099–106.
30. Zhao L, Barlinn K, Sharma VK, Tsivgoulis G, Cava LF, Vasdekis SN, et al. Velocity criteria for intracranial stenosis revisited: an international multicenter study of transcranial Doppler and digital subtraction angiography. Stroke. 2011;42(12):3429–34.
31. Vuković-Cvetković V. Microembolus detection by transcranial Doppler sonography: review of the literature. Stroke Res Treat. 2012;2012
32. Srinivasan J, Newell DW, Sturzenegger M, Mayberg MR, Winn HR. Transcranial Doppler in the evaluation of internal carotid artery dissection. Stroke. 1996;27(7):1226–30.
33. Droste DW, Junker K, Stögbauer F, Lowens S, Besselmann M, Braun B, et al. Clinically silent circulating microemboli in 20 patients with carotid or vertebral artery dissection. Cerebrovasc Dis. 2001;12(3):181–5.
34. Hwang J, Kim SJ, Hong JM, Bang OY, Chung CS, Lee KH, et al. Microembolic signals in acute posterior circulation cerebral ischemia: sources and consequences. Stroke. 2012;43(3):747–52.
35. Del Sette M, Dinia L, Rizzi D, Sugo A, Albano B, Gandolfo C. Diagnosis of right-to-left shunt with transcranial Doppler and vertebrobasilar recording. Stroke. 2007;38(8):2254–6.
36. Sharma AK, Bathala L, Batra A, Mehndiratta MM, Sharma VK. Transcranial Doppler: techniques and advanced applications: part 2. Ann Indian Acad Neurol. 2016;19(1):102.
37. Mojadidi MK, Roberts SC, Winoker JS, Romero J, Goodman-Meza D, Gevorgyan R, et al. Accuracy of transcranial Doppler for the diagnosis of intracardiac right-to-left shunt: a bivariate meta-analysis of prospective studies. JACC Cardiovasc Imaging. 2014;7(3):236–50.
38. Guo YZ, Gao YS, Guo ZN, Niu PP, Yang Y, Xing YQ. Comparison of vertebral artery and middle cerebral artery monitoring for right-to-left shunt detection by contrast-enhanced transcranial Doppler. Sci Rep. 2016;6:24932.
39. Osiro S, Zurada A, Gielecki J, Shoja MM, Tubbs RS, Loukas M. A review of subclavian steal syndrome with clinical correlation. Med Sci Monit. 2012;18(5):RA57.
40. Mousa AY, Morkous R, Broce M, Yacoub M, Sticco A, Viradia R, et al. Validation of subclavian duplex velocity criteria to grade severity of subclavian artery stenosis. J Vasc Surg. 2017;65(6):1779–85.
41. Harper C, Cardullo PA, Weyman AK, Patterson RB. Transcranial Doppler ultrasonography of the basilar artery in patients with retrograde vertebral artery flow. J Vasc Surg. 2008;48(4):859–64.
42. Matta B, Czosnyka M. Chapter 7: Transcranial Doppler Ultrasonography in Anesthesia and Neurosurgery. In: Cottrell JE, Patel P, editors. Neuroanesthesia. 6th ed. Philadelphia, PA: Elsevier; 2017.
43. Aaslid R, Lindegaard KF, Sorteberg W, et al. Cerebral autoregulation in humans. Stroke. 1989;20:45.

44. Aaslid R, Newell DW, Stooss R, et al. Assessment of cerebral autoregulationmdynamics from simultaneous arterial and venous transcranial Doppler recordings in humans. Stroke. 1991;22:1148.
45. Jiménez-Caballero PE, Segura T. Normal values of cerebral vasomotor reactivity using the breath-holding test. Rev Neurol. 2006;43(10):598–602.
46. Park CW, Sturzenegger M, Douville CM, Aaslid R, Newell DW. Autoregulatory response and CO2 reactivity of the basilar artery. Stroke. 2003;34(1):34–9.
47. Kimiagar I, Bass A, Rabey JM, Bornstein NM, Gur AY. Long-term follow-up of patients with asymptomatic occlusion of the internal carotid artery with good and impaired cerebral vasomotor reactivity. Eur J Neurol. 2010;17(10):1285–90.
48. Park TH, Park SH, Yoon YC, Kwon OS. Vasomotor reactivity of the basilar artery in patients with occlusive vascular diseases in the anterior circulation. J Korean Neurol Assoc. 2006;24(3):204–9.
49. Ract C, Le Moigno S, Bruder N, Vigue B. Transcranial Doppler ultrasound goal-directed therapy for the early management of severe traumatic brain injury. Intensive Care Med. 2007;33:645–51.
50. Sloan MA, Alexandrov AV, Tegeler CH. Assessment: Transcranial Doppler ultrasonography: report of the therapeutics and technology assessment subcommittee of the American Academy of Neurology. Neurology. 2004;62:1468.
51. Purkayastha S, Sorond FA, Lyng S, Frantz J, Murphy MN, Hynan LS, et al. Impaired cerebral vasoreactivity despite symptom resolution in sports-related concussion. J Neurotrauma. 2019;
52. Lele AV, Watanitanon A, Lakireddy V, Clark-Bell C, Moore A, Zimmerman JJ, et al. Prevalence, evolution, and extent of impaired cerebral autoregulation in children hospitalized with complex mild traumatic brain injury. Pediatr Crit Care Med. 2018;
53. Vavilala MS, Farr CK, Watanitanon A, Clark-Bell BC, Chandee T, Moore A. Early changes in cerebral autoregulation among youth hospitalized after sports-related traumatic brain injury. Brain Inj. 2018;32(2):269–75.
54. Ziegler D, Cravens G, Poche G, Gandhi R, Tellez M. Use of transcranial Doppler in patients with severe traumatic brain injuries. J Neurotrauma. 2017;34:121–7.
55. Ract C, Le Moigno S, Bruder N, Vigué B. Transcranial Doppler ultrasound goal-directed therapy for the early management of severe traumatic brain injury. Intensive Care Med. 2007;33:645–51.
56. Bailey DM, Jones DW, Sinnott A, Brugniaux JV, New KJ, Hodson D, et al. Impaired cerebral haemodynamic function associated with chronic traumatic brain injury in professional boxers. Clin Sci. 2013;124:177–89.
57. da Costa L, van Niftrik CB, Crane D, Fierstra J, Bethune A. Temporal profile of cerebrovascular reactivity impairment, gray matter volumes, and persistent symptoms after mild traumatic head injury. Front Neurol. 2016;7:70.
58. Albalawi T, Hamner JW, Lapointe M, Meehan WP III, Tan CO. The relationship between cerebral vasoreactivity and post-concussive symptom severity. J Neurotrauma. 2017;34:2700–5.
59. Bonow RH, Witt CE, Mosher BP, Mossa-Basha M, Vavilala MS, Rivara FP, et al. Transcranial Doppler microemboli monitoring for stroke risk stratification in blunt cerebrovascular injury. CCM. 2017;45(10):e1011–7.
60. Wijdicks EF, Varelas PN, Gronseth GS, Greer DM. Evidence-based guideline update: determining brain death in adults: report of the Quality Standards Subcommittee of the American Academy of Neurology. Neurology. 2010;74(23):1911–8.
61. Hadani M, Bruk B, Ram Z, Knoller N, Spiegelmann R, Segal E. Application of transcranial doppler ultrasonography for the diagnosis of brain death. Intensive Care Med. 1999;25(8):822–8.
62. Sloan MA. Therapeutics and Technology Assessment Subcommittee of the American Academy of Neurology: Assessment: transcranial Doppler ultrasonography: report of the Therapeutics and Technology Assessment Subcommittee of the American Academy of Neurology. Neurology. 2004;62:1468–81.

63. Chang JJ, Tsivgoulis G, Katsanos AH, Malkoff MD, Alexandrov AV. Diagnostic accuracy of transcranial Doppler for brain death confirmation: systematic review and meta-analysis. Am J Neuroradiol. 2016;37(3):408–14.
64. Alexandrov AV, Tsivgoulis G, Rubiera M, Vadikolias K, Stamboulis E, Molina CA, et al. End-diastolic velocity increase predicts recanalization and neurological improvement in patients with ischemic stroke with proximal arterial occlusions receiving reperfusion therapies. Stroke. 2010;41(5):948–52.
65. Ducrocq X, Braun M, Debouverie M, Junges C, Hummer M, Vespignani H. Brain death and transcranial Doppler: experience in 130 cases of brain dead patients. J Neurol Sci. 1998;160(1):41–6.
66. Blanco P, Abdo-Cuza A. Transcranial Doppler ultrasound in neurocritical care. J Ultrasound. 2018:1–6.
67. Kuo JR, Chen CF, Chio CC, Chang CH, Wang CC, Yang CM, et al. Time dependent validity in the diagnosis of brain death using transcranial Doppler sonography. J Neurol Neurosurg Psychiatry. 2006;77(5):646–9.
68. Baltgaile G. Cerebral circulatory arrest. In: Csiba L, Baracchini C, editors. Manual of neurosonology. Cambridge: Cambridge University Press; 2016. p. 23–33.
69. Schreiber S. Cerebral circulatory arrest. In: Csiba L, Baracchini C, editors. Manual of neurosonology. Cambridge: Cambridge University Press; 2016. p. 262–8.

Chapter 28
Intracerebral Venous System: Monitoring by Transcranial Color-Coded Duplex Sonography (TCCS)

Dixon Yang, Marialaura Simonetto, Nelly Campo, Digna Cabral, and Tatjana Rundek

Key Points

1. Cerebral venous drainage is divided into the deep and superficial venous drainage, with most reliably insonated vessels in the deep venous system.
2. Venous transcranial color-coded duplex sonography (vTCCS) imaging has good reliability.
3. vTCCS has potential utility as a quick, bedside, complementary diagnostic and monitoring tool.
4. Hemodynamic characteristics on vTCCS in cerebral venous sinus thrombosis may complement the first diagnostic line by CT or MR imaging.
5. vTCCS has clinical utility in AVM but also may be useful in ischemic stroke, subarachnoid hemorrhage, and intracranial hypertension.
6. Further studies are needed to determine clinical value of vTCCS.

D. Yang
Department of Neurology, New York University Langone Health, New York, NY, USA
e-mail: Dixon.Yang@nyulangone.org

M. Simonetto · N. Campo · D. Cabral
Department of Neurology, Miller School of Medicine, University of Miami, Miami, FL, USA
e-mail: NCampo@med.miami.edu

T. Rundek (✉)
Evelyn F. McKnight Brain Institute, Department of Neurology, Miller School of Medicine, University of Miami, Miami, FL, USA
e-mail: trundek@med.miami.edu

C. N. Rodríguez et al. (eds.), *Neurosonology in Critical Care*,
https://doi.org/10.1007/978-3-030-81419-9_28

28.1 Introduction

Transcranial Doppler (TCD) and transcranial color-coded duplex sonography (TCCS) have been widely used in examination and monitoring of extra- and intracranial arterial hemodynamics [1]. Less attention has been paid to the cerebral venous counterpart due to early technical limitations and low clinical prevalence of known cerebral venous disease. In adults, we were not able to formally study the cerebral venous system using sonography until 1991 because of its technical limitations [2]. Although recent technical advances in neurosonology, venous transcranial color-coded duplex sonography (vTCCS) does not currently belong to routine clinical examination modalities. However, vTCCS has potential utility as a quick, bedside, supplementary diagnostic and monitoring tool notably for cerebral vein and sinus thrombosis (CVST) and arteriovenous malformations (AVM), and it has a possible clinical value in ischemic stroke, subarachnoid hemorrhage (SAH), and raised intracranial pressure (ICP) [3]. This chapter intends to review application and clinical usefulness of vTCCS based on available evidence.

28.2 Cerebral Venous System: Anatomy

Relevant and reliably insonated cerebral venous anatomy to sonography consists of the deep cerebral venous drainage, contributories of the cavernous sinus, posterior fossa sinuses, inferior petrosal sinus, and vertebral plexus [4]. Beginning anteriorly, blood drained from frontal brain regions into anterior cerebral veins forms the deep middle cerebral vein (DMCV), which is often located adjacent to the middle cerebral artery. The DMCV drains into the basal vein (BV), which runs a course distally to the follow in the P2 segment of the posterior cerebral artery around the midbrain. Bilateral BVs (also known as the veins of Rosenthal) join midline to form the unpaired great cerebral vein (GCV) or the vein of Galen behind the pineal gland. Along with the inferior sagittal sinus (ISS), the GCV drains mostly into the unpaired straight sinus (SRS) located at the apex of the cerebellum tentorium [5].

The SRS flows to the confluens sinuum (COS), where it meets superficial cerebral venous drainage that is functionally separated from deep cerebral venous vasculature by a venous watershed. Notably of the superficial system, the superior sagittal sinus (SSS) drains into the COS and then bifurcates into the transverse sinuses (TS), which dives underneath the occipital bone to eventually forms the sigmoid sinus and drains into the internal jugular vein. It should be noted that the low flow velocities, unfavorable insonation windows, and frequent anatomic variations of the SSS, COS, and TS make them less detectable vessels on vTUS [6, 7] (Fig. 28.1).

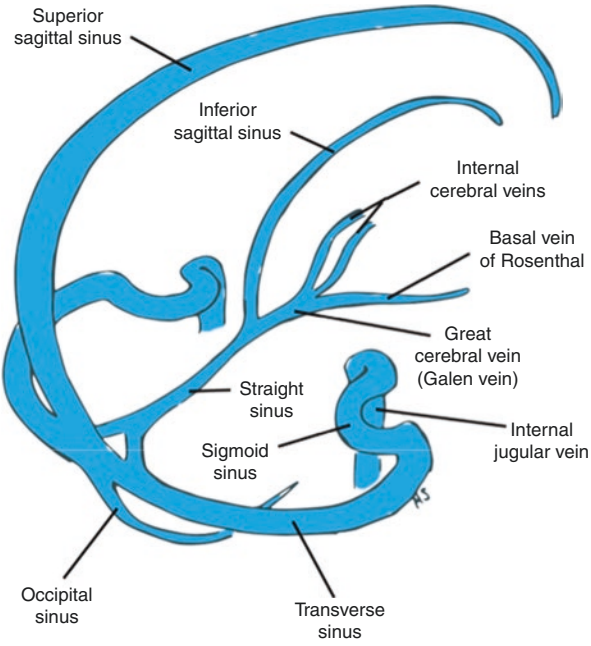

Fig. 28.1 Intracerebral venous system anatomy

28.3 vTCCS: Ultrasound Investigation Technique

Intracranial venous examination with ultrasound (TCCS) generally begins with insonation through the temporal window to identify the mesencephalon as a landmark. From there, the deep middle cerebral vein is found adjacent to the middle cerebral artery, with venous flow toward the center of the brain, away from the probe. Downward angulation can visualize the sphenoid bone and superior petrosal sinus with flow away from the probe, draining into the cavernous sinus that usually cannot be insonated. Upward angulation from the mesencephalon can visualize the basal vein of Rosenthal (Fig. 28.2), which is slightly cranial from the P2 segment of the posterior cerebral artery.

Brightness mode (B-mode) increases depth so that contralateral structures can be insonated. The great cerebral vein (Fig. 28.3) can be found behind the echogenic pineal gland and third ventricle. The straight sinus (Fig. 28.4) can be located after upward rotation of the transducer to visualize the echogenic cerebellar tentorium. It drains away from the transducer toward the confluens sinuum. The contralateral transverse sinus (Fig. 28.5) can be seen with downward angulation. Transforaminal examination will reveal the vertebral venous plexus and the inferior petrosal sinus near the basilar artery, with venous flows directed toward the transducer.

There are no consensus guidelines regarding vTCCS examination, but there are several validated TCCS and TCD protocols that use this general approach [8]. TCCS is often preferred because it can display vascular anatomy in relation to brain parenchyma and not only flow velocities and flow direction as in non-imaging TCD. Further signal improvement can be achieved by intravenous administration of echo-contrast, which is not commonly used in most TCCS or TCD protocols. Established normative data are presented in Table 28.1.

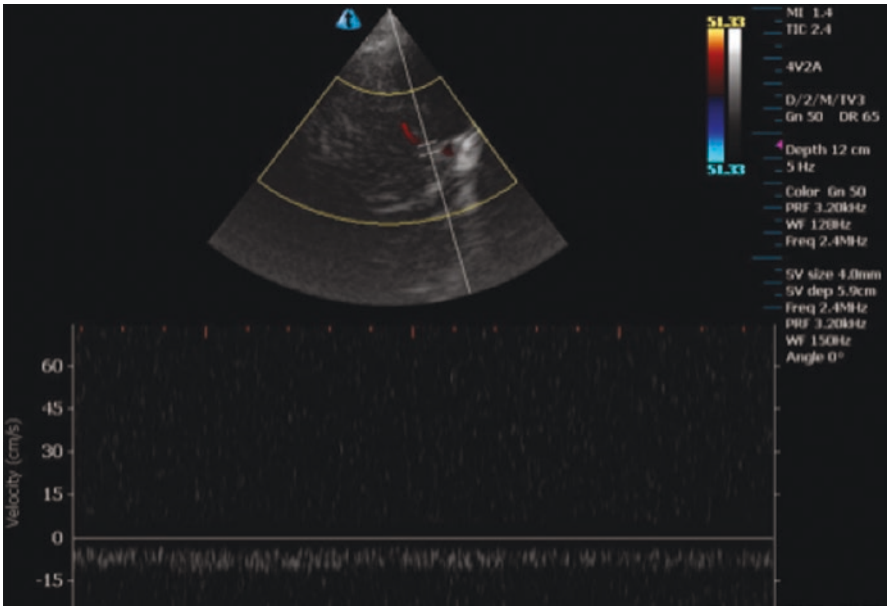

Fig. 28.2 Basal vein of Rosenthal

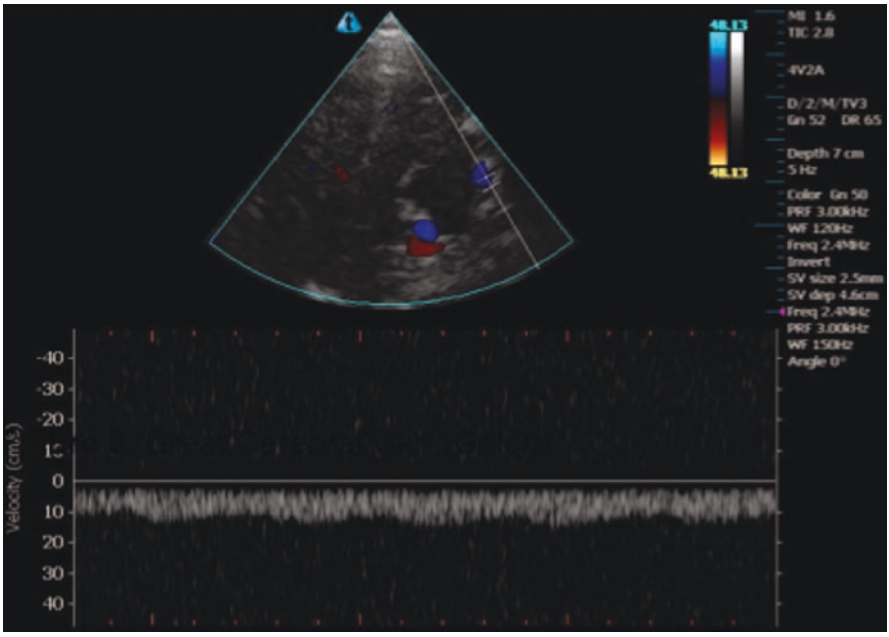

Fig. 28.3 Great Cerebral vein (Galen)

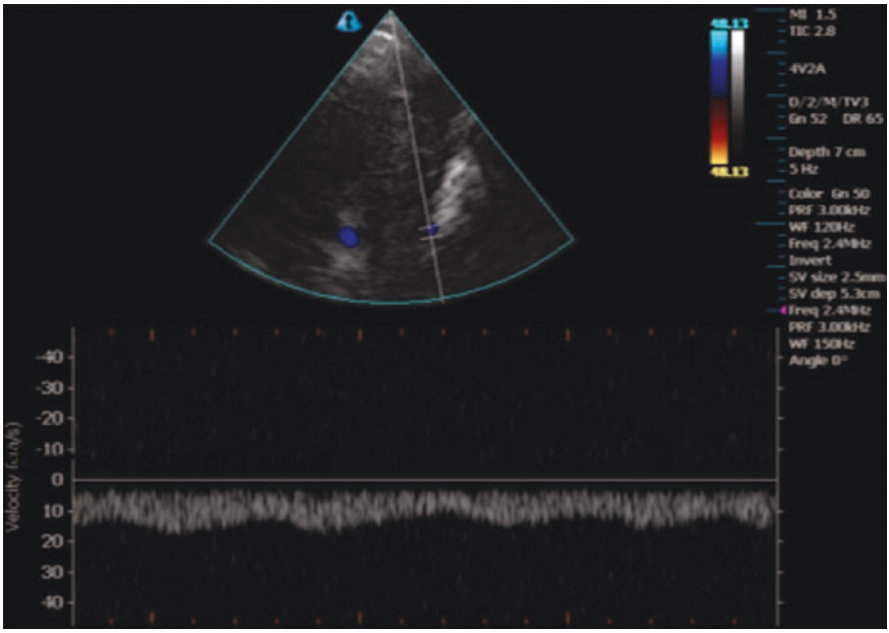

Fig. 28.4 Straight sinus

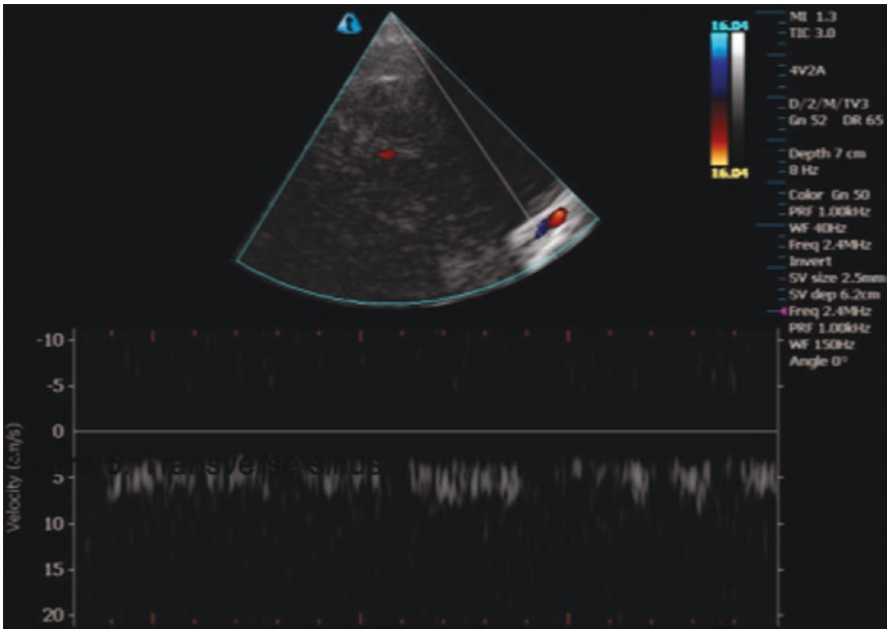

Fig. 28.5 Transverse sinus

Table 28.1 Venous flow velocities of healthy adults using TCCS without angle-correction

Vessel	Peak systolic flow (cm/s)	End diastolic flow (cm/s)	Visualization (%)
DMCV	8.5 ± 2.9 8.7 ± 2.9 8.6 ± 1.9	5.7 ± 1.9 5.8 ± 1.9 5.9 ± 1.4	76-91
BV	12.4 ± 4.0 12.2 ± 3.8 11.9 ± 2.9	8.9 ± 3.0 8.6 ± 3.7 7.2 ± 1.8	89-95
SRS	13.1 ± 5.1 12.2 ± 3.8 11.6 ± 2.3	9.4 ± 4.0 8.6 ± 3.7 7.2 ± 1.8	71-83
GCV	10.6 ± 3.7 11.9 ± 3.6 10.2 ± 1.8	7.5 ± 2.8 7.7 ± 2.8 7.4 ± 1.5	89-98
TS	4.9 ± 6.7 14.0 ± 5.9 16.4 ± 4.4	10.4 ± 5.3 9.7 ± 4.8 11.8 ± 3.7	67-69
SSS/CON	10.6 ± 3.6 9.8 ± 3.6 12.2 ± 4.1	6.7 ± 2.6 6.1 ± 2.5 8.7 ± 3.3	52-58

Data within each cell is listed in order from Stolz [8–10]
Percent visualization of veins is presented in range across the three studies

28.4 CVST: Venous Ultrasound Findings

Urgent neuroimaging using magnetic resonance imaging (MRI) with venography or computed tomography (CT) with venography are the first choice diagnostic tools for acute CVST, with digital subtraction angiography as the gold standard [11]. Normal sonographic findings in vTCCS cannot positively rule out CVST even if contrast enhancers are used; however, vTCCS may serve as a complementary tool to MRI or CT [3]. In 1994, increased venous flow signal in bilateral DMCVs was first reported in SSS thrombosis, which normalized after anticoagulant therapy [12]. Smaller reports have supported changed venous hemodynamics in SSS thrombosis though in different vessels [13, 14]. Given the absence of valves in the cerebral venous drainage, intracranial veins may serve as collaterals and their flow may even reverse [5]. Four sonographic flow characteristics of CVST have been described, broadly classified as one direct criterion and three indirect criteria.

The direct criterion involves missing venous flow signals that would theoretically suggest cut-off flow from thrombosis. However, vTCCS cannot reliably distinguish between frequently encountered anatomical variations and occlusive clot. Even with echo-contrast TCCS, occluded flow was either aplastic TS or complete TS occlusion after MRI confirmation, while residual sonographic signals were either hypoplastic vessel or non-occluded TS thrombosis. Examination with vTCCS in one study missed one case of complete TS occlusion due to false-positive signal from a dural fistula [15]. Clinically, this direct criterion's sensitivity and specificity are too low for practical use.

The three indirect criteria are based on the observations of collateral flow from thrombosis. These include path pathologic side-to-side flow differences, increased flow velocities, and reversed venous flow direction. Side-to-side differences have been observed in paired segments of the DMCV and BV even after normalization of absolute flow rates in TS thrombosis. These differences persisted for an extended period of time, and up to 266 days in one patient after diagnosis. Additionally, a compensatory increased flow in contralateral TS can be frequently observed in TS thrombosis [16].

Secondly, vTCCS may detect increased flow velocities of collateral flow in CVST. Intracranial venous drainage velocity increases have been noted in several vessels in SSS thrombosis. However, in the case of the cavernous sinus, increased flow velocities of the inflow and outflow tracts of the cavernous sinus may often be a normal variant and therefore must be interpreted with caution [3]. Lastly, retrograde flow of the BV in patients with SRS occlusion and proximal TS in distal TS thrombosis has been reported [16–18].

After CVST treatment, normalization of venous sonographic hemodynamic parameters within 90 days were significantly associated with better disability outcomes. This correlation persisted after analyzing only patients with initial pathologic venous sonography [16]. In other case report evidences, initial severity of venous velocity changes was associated with severity of disease, but not directly with outcomes [13].

28.5 vTCCS: Arterial-Venous Malformation Monitoring

Intracranial AVMs are generally thought to be low resistance direct connections in which feeding arteries exhibit increased flow [19]. While information on the utility of vTCCS on intracranial vascular malformations is limited, some smaller studies and case reports have identified altered venous signals that may indicate a hemodynamically significant shunt [20–22]. After repair, dramatic changes in arterial hemodynamics determined by ultrasound have been often supported, but they are less well documented in the venous system [23]. A reduced pulsatility and mean velocity in the venous return were observed after embolization, suggesting possible real-time use of vTCCS intraoperatively [24]. At least in the arterial system, ultrasound may provide an adjunctive modality in treatment of AVM; however, venous system has not been as extensively studied [25].

28.5.1 Practice Parameters and Performance

Assessment of AVM, pre- and post-treatment, in adults and children and assessment of dural venous sinus patency in children are among 16 suggested indications for use of TCD [26] endorsed by the US professional organizations including the American College of Radiology (ACR), the American Institute of Ultrasound in Medicine (AIUM), the Society for Pediatric Radiology (SPR), and the Society of

Radiologists in Ultrasound (SRU). These practice parameters provide an educational tool designed to assist practitioners in providing appropriate care for patients and can be used as a framework for TCD performance standards in diagnosis and treatment of patients with these venous disorders.

28.6 vTCCS: Potential Utility in Other Neurologic Conditions

28.6.1 Malignant Ischemic Stroke

Space-occupying edema in ischemic stroke may affect intracranial venous flow due to the compressibility of venous vasculature. In a small study of 21 patients with malignant ischemic stroke, several hemodynamic changes were described within 5 days of stroke with midline shift in the contiguous venous drainage of the BVs, GCV, and straight sinus (SS) using vTCCS. In fatal cases, significantly decreased ipsilateral BV velocities were reported in 5 days, except day 2 post-stroke when compared to normative data. This second day was thought to be a temporary hyperemic response. Interestingly, BV flow velocities displayed an inverse relationship with magnitude of midline shift. These velocities gradually downtrended with day 5 velocities significantly lower than days 1–3. In survivors, only day 5 showed significantly decreased ipsilateral BV velocities compared to healthy controls. Contralateral BV flow velocities to the stroke were only significantly decreased on day 5 with fatal cases, not in those who survived. In the GCV, flow velocities steeply increased after midline shift exceeded 1.5 cm in fatal cases. Surviving patients exhibited only slight GCV flow changes. Lastly, the SS showed a U-shaped flow curve with peaked increased flow at 1.5 cm midline shift. Together, these hemodynamic changes suggest a possible clinical value of bedside monitoring for prognostic implications of vTCCS, similar to sonographic monitoring of the MCA, although further studies are needed [27, 28].

28.6.2 Subarachnoid Hemorrhage (SAH)

An early prospective study with 66 patients after SAH showed that both elevated MCA velocities and high BV flow had better mortality and disability outcomes than patients with low BV flow. These hemodynamic changes were noticed on the first day after hemorrhage. The authors suggest that patients with higher BV flow had a hyperemic state rather than vasospasm. Additionally, the study reports a better correlation between BV flow velocities and total cerebral blood flow than arterial hemodynamics and total cerebral blood flow, indicating possible value in indirect monitoring of the global blood flow [29].

TCCS has been proven to be reliable in assessing cerebral artery vasospasm after SAH typically using blood flow velocity ratios between the MCA and ICA

(Lindegaard index) [30]. In the intensive care unit, sonography of extracranial vessels may be difficult; therefore, a recent study analyzed the relation of mean time-averaged blood flow velocity and peak systolic velocity of the MCA and BV, called an arteriovenous index (AVI). The study suggests an AVI cut-off of >10 for mean velocity and >12 for systolic velocity as most accurate for vasospasm after SAH (up to 87%). Combined analysis with absolute MCA blood flow velocity and the AVI resulted in a slight increase in specificity and positive predictive value, suggesting analysis of sonographic hemodynamics using both MCA and BV can yield reliable assessments of vasospasm after SAH [31].

28.6.3 Elevated Intracranial Pressure (ICP)

A pilot study examining ICP and intracranial venous hemodynamics using ultrasound examined the BV and SS of intensive care unit patients mostly without space-occupying focal lesions. Within a certain range (15–40 mmHg), ICP was linearly correlated with maximal venous blood flow velocities. An increase above BV basal values of up to 5 cm/s was observed in ICP of 16–25 mmHg and up to 14 cm/s in 25–40 mmHg. Stasis in smaller veins, however, may be an early compensatory mechanism in increased ICP, which subsequently leads to venous redistribution to larger vessels and detectable hemodynamic changes. Therefore, vTCCS may represent an early, noninvasive clinical assessment of early ICP dysregulation [32].

More recently, a study in critically ill patients with brain injury requiring invasive ICP monitoring found that SS systolic flow velocity by vTCCS correlated strongly with ICP. Combining SS systolic flow and optic nerve sheath diameter yielded even stronger correlation with ICP, suggesting noninvasive sonographic technique may identify critically ill patients with intracranial hypertension [33].

28.7 Conclusion

Venous transcranial color-coded sonography (vTCCS) has a great potential to serve as a quick and complementary bedside diagnostic and monitoring imaging modality. The cerebral venous drainage system accessible for vTCCS includes deep cerebral veins, contributors of the cavernous sinus, posterior fossa sinus, inferior petrosal sinus, and vertebral plexus. While no consensus guidelines have been established for vTCCS, several validated TCCS protocols have been published with a good reliability. The normative vTCCS values have been established for the deep middle cerebral vein, basal vein, straight sinus, great cerebral vein, transverse sinus, and superior sagittal sinus. One direct and three indirect criteria for vTCCS findings have been proposed. The direct criterion involving missing venous flow signals that suggests venous thrombosis has, however, low sensitivity and specificity. Indirect criteria that involve evaluations of collateral flow (pathological side-to-side flow differences, increased flow velocities, and reversed venous flow direction) may be

more reliable. Given the advantages of TCCS as being a noninvasive, portable, and low-cost technology and with improved reliability, TCCS may be an adjunct modality for the assessments of patients with cerebral venous sinus thrombosis, arteriovenous malformation, malignant ischemic stroke, subarachnoid hemorrhage, and intracranial pressure dysregulation. The TCCS applications in these conditions have been studied only in small series and case reports; therefore, larger investigations are needed to further determine their clinical value and impact on patient outcomes.

Algorithm

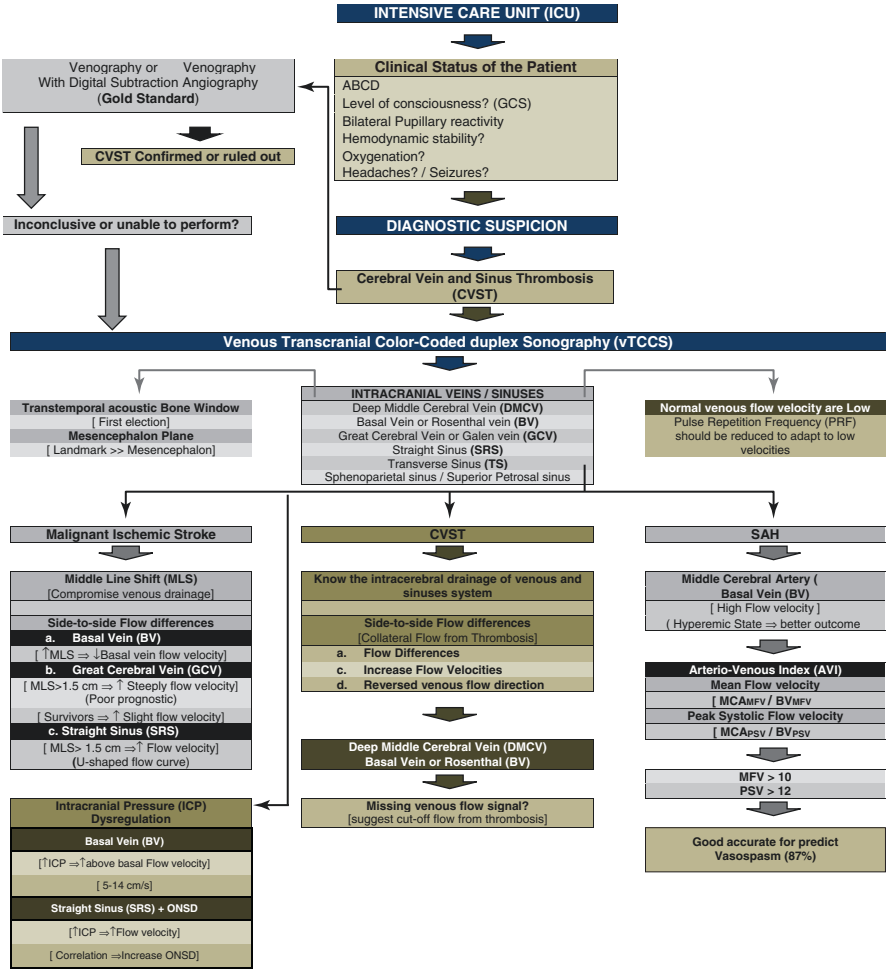

ABCD Airway-breathing-circulation-disability, *CVST* Cerebral Vein and Sinus Thrombosis, *SAH* Subarachnoid Hemorrhage, *MFV* Mean flow velocity, *PSV* Peak flow velocity, *ONSD* Optic Nerve Sheath Diameter, ↑ Increase, MRI Magnetic resonance imaging, *CT* computed tomography.

References

1. Aaslid R, Markwalder TM, Nornes H. Noninvasive transcranial Doppler ultrasound recording of flow velocity in basal cerebral arteries. J Neurosurg. 1982;57:769–74.
2. Aaslid R, Newell DW, Stooss R, Sorteberg W, Lindegaard KF. Assessment of cerebral autoregulation dynamics from simultaneous arterial and venous transcranial Doppler recordings in humans. Stroke. 1991;22:1148–54.
3. Schreiber SJ, Stolz E, Valdueza JM. Transcranial ultrasonography of cerebral veins and sinuses. Eur J Ultrasound. 2002;15:59–72.
4. Stolz E. Intracranial venous ultrasound. In: Csiba L, Baracchini C, editors. Manual of neurosonology. Cambridge Univ Press; 2016. p. 269–77.
5. Ono M, Rhoton AL Jr, Peace D, Rodriguez RJ. Microsurgical anatomy of the deep venous system of the brain. Neurosurgery. 1984;15:621–57.
6. Oka K, Rhoton AL Jr, Barry M, Rodriguez R. Microsurgical anatomy of the superficial veins of the cerebrum. Neurosurgery. 1985;17:711–48.
7. Browning H. The confluence of dural venous sinuses. Am J Anat. 1953;93:30–29.
8. Stolz E, Babacan SS, Bodeker RH, Gerriets T, Kaps M. Interobserver and intraobserver reliability of venous transcranial color-coded flow velocity measurements. J Neuroimaging. 2001;11:385–92.
9. Stolz E, Kaps M, Dorndorf W. Assessment of intracranial venous hemodynamics in normal individuals and patients with cerebral venous thrombosis. Stroke. 1999;30:70–5.
10. Stolz E, Kaps M, Kern A, Dorndorf W. Frontal bone windows for transcranial color-coded duplex sonography. Stroke. 1999;30:814–20.
11. Saposnik G, Barinagarrementeria F, Brown RD Jr, et al. Diagnosis and management of cerebral venous thrombosis: a statement for healthcare professionals from the American Heart Association/American Stroke Association. Stroke. 2011;42:1158–92.
12. Wardlaw JM, Vaughan GT, Steers AJ, Sellar RJ. Transcranial Doppler ultrasound findings in cerebral venous sinus thrombosis. Case report. J Neurosurg. 1994;80:332–5.
13. Valdueza JM, Schultz M, Harms L, Einhaupl KM. Venous transcranial Doppler ultrasound monitoring in acute dural sinus thrombosis. Report of two cases. Stroke. 1995;26:1196–9.
14. Becker G, Bogdahn U, Gehlberg C, Frohlich T, Hofmann E, Schlief MD. Transcranial color-coded real-time sonography of intracranial veins. Normal values of blood flow velocities and findings in superior sagittal sinus thrombosis. Stroke. 1995;26:1196–9.
15. Ries S, Steinke W, Neff KW, Hennerici M. Echo contrast enhanced transcranial color-coded sonography for the diagnosis of transverse sinus venous thrombosis. Stroke. 1997;28:696–700.
16. Stolz E, Gerriets T, Bodeker RH, Hugens-Penzel M, Kaps M. Intracranial venous hemodynamics is a factor related to a favorable outcome in cerebral venous thrombosis. Stroke. 2002;33:1645–50.
17. Baumgartner RW, Gonner F, Arnold M, Muri RM. Transtemporal power- and frequency-based colour-coded duplex sonography of cerebral veins and sinuses. Am J Neuroradiol. 1997;18:1771–81.
18. Valdueza JM, Hoffmann O, Weih M, Mehraein S, Einhaupl KM. Monitoring of venous hemodynamics in patients with cerebral venous thrombosis by transcranial Doppler ultrasound. Arch Neurol. 1999;56:229–34.
19. Zhao JZ, Yu LB. The application of ultrasound in the management of cerebral arteriovenous malformation. Neurosci Bull. 2008;24:387–94.
20. Chen YW, Jeng JS, Liu HM, et al. Diagnosis and follow-up of carotid cavernous fistulas by carotid duplex sonography and transcranial color Doppler imaging. Ultrasound Med Biol. 1996;22:1155–62.
21. Chen YW, Jeng JS, Liu HM, Hwang BS, Lin WH, Yip PK. Carotid and transcranial color-coded duplex sonography in different types of carotid-cavernous fistula. Stroke. 2000;31:701–6.

22. Zakharkina MV, Chechetkin AO, Krotenkova MV, Konovalov RN. Ultrasound diagnostics of a spontaneous arteriovenous fistula of the head and neck. J Ultrason. 2017;17:217–21.
23. Busch KJ, Kiat J, Stephen M, Simons M, Avolio A, Morgan MK. Cerebral hemodynamics and the role of transcranial Doppler applications in the assessment and management of cerebral arteriovenous malformations. J Clin Neurosci. 2016;30:24–30.
24. Murayama Y, Usami S, Hata Y, et al. Transvenous hemodynamic assessment of arteriovenous malformations and fistulas. Preliminary clinical experience in Doppler guidewire monitoring of embolotherapy. Stroke. 1996;27:1358–64.
25. Meila D, Lisseck K, Jacobs C, Lanfermann H, Brassel F, Feldkamp A. Cranial Doppler ultrasound in Vein of Galen malformation. Neuroradiology. 2015;57:211–9.
26. American College of Radiologist. ACR-AIUM-SPR-SRU Practice parameter for the performance of transcranial Doppler ultrasound. 2017; Res.33.
27. Stolz E, Gerriets T, Babacan SS, Jauss M, Kraus J, Kaps M. Intracranial venous hemodynamics in patients with midline dislocation due to postischemic brain edema. Stroke. 2002;33:479–85.
28. Asil T, Uzunca I, Utku U, Berberoglu U. Monitoring of increased intracranial pressure resulting from cerebral edema with transcranial Doppler sonography in patients with middle cerebral artery infarction. J Ultrasound Med. 2003;22:1049–53.
29. Mursch K, Wachter A, Radke K, et al. Blood flow velocities in the basal vein after subarachnoid haemorrhage. A prospective study using transcranial duplex sonography. Acta Neurochir. 2001;143:793–9.
30. Lindegaard KF, Nornes H, Bakke SJ, Sorteberg W, Nakstad P. Cerebral vasospasm diagnosis by means of angiography and blood velocity measurements. Acta Neurochir. 1989;100:12–24.
31. Connolly F, Schreiber SJ, Leithner C, Bohner G, Vajkoczy P, Valdueza JM. Assessment of intracranial venous blood flow after subarachnoid hemorrhage: a new approach to diagnose vasospasm with transcranial color-coded duplex sonography. J Neurosurg. 2017;15:1–7.
32. Schoser BG, Riemenschneider N, Hansen HC. The impact of raised intracranial pressure on cerebral venous hemodynamics: a prospective venous transcranial Doppler ultrasonography study. J Neurosurg. 1999;91:744–9.
33. Robba C, Cardim D, Tajsic T, et al. Ultrasound non-invasive measurement of intracranial pressure in neurointensive care: a prospective observation study. PLoS Med. 2017;14:e1002356.

Chapter 29
Arteriovenous Malformation (AVM) and Arteriovenous Fistula in the ICU: Contributions of Transcranial Doppler (TCD/TCCS) to Diagnosis

Eva Bartels

Key Points

1. Arteriovenous malformations (AVMs) or fistulas can also be the cause of intracranial bleeding with headaches, intracerebral hemorrhage, and focal seizures are possible manifestations.
2. The hemodynamic phenomena caused by AVMs can be detected by transcranial Doppler sonography (TCD/TCCS). The most important parameters are the maximum and mean arterial flow velocities (MFV), the pulsatility index of the Doppler spectrum, and the cerebrovascular reserve capacity (autoregulatory reserve).
3. The sonographic diagnosis (TCCS) of an AVM is not based on an exact anatomic presentation of the pathological structures, but on the ability of the color-coded Doppler signal to show the pathological flow phenomena in real time.
4. The following flow values can serve as guidelines: maximal systolic blood flow velocity >140 cm $s^{-}1$, end-diastolic blood flow velocity >100 cm s^{-1}, and pulsatility index <0.6.
5. The use of echo contrast agents can increase the diagnostic success rate, particularly for those located in an unfavorable temporal acoustic bone window.
6. Errors can occur in the transcranial duplex sonography diagnosis of AVMs when there are convolutes of elongated arteries. Multiple color signals in the vascular loops can give the appearance of a malformation.
7. Transcranial color-coded duplex sonography (TCCS) is a valuable, noninvasive method for the diagnosis of intracranial vascular malformations and the assessment of the hemodynamic situation.

E. Bartels (✉)
Neurologist, Center for Neurological Vascular Diagnostics, Munich, Germany

Educational Coordinator - ESNCH, Oslo, Norway
e-mail: bartels.eva@t-online.de

C. N. Rodríguez et al. (eds.), *Neurosonology in Critical Care*,
https://doi.org/10.1007/978-3-030-81419-9_29

29.1 Introduction

Intracranial hemorrhage can occur as a complication of various vascular diseases and make treatment in an intensive care unit necessary. The bleeds can be epidural, intra- or subdural, subarachnoid, or intracerebral. Using ultrasound to visualize intracerebral hematomas or the vasospasm typically seen following the subarachnoid hemorrhage of a ruptured intracranial aneurysm is described in other chapters of this book. Arteriovenous malformations or fistulas can also be the cause of intracranial bleeding. The aim of this chapter is to present their characteristic appearance in color-coded duplex sonograms.

29.2 TCD/TCCS: Arteriovenous Malformation (AVMs)

An arteriovenous malformation (AVM, synonym arteriovenous angioma) is a congenital malformation with familial predisposition [1]. Headaches, intracerebral hemorrhage, and focal seizures are possible manifestations of an AVM. The first symptoms can appear in young adults [2]. Magnetic resonance imaging (MRI), MR angiography (MRA), computerized tomography (CT), CT angiography (CTA), and digital subtraction angiography (DSA) are currently used to make the final diagnosis.

An arteriovenous angioma consists of a pathological connection between the arterial and venous system bypassing the capillary bed [3]. The hemodynamic phenomena caused by this can be detected by transcranial Doppler sonography (TCD) [4–6]. The most important parameters are the maximum and mean arterial flow velocities (MFV), the pulsatility index of the Doppler spectrum, and the cerebrovascular reserve capacity (autoregulatory reserve) [7, 8].

The cerebrovascular reserve capacity can be determined by CO_2 reactivity or with the acetazolamide (Diamox®) test. The apnea test [9] can be used for an initial evaluation. Autoregulation is reduced in arteriovenous malformations, since the vessels in the angioma are already maximally dilated [10, 11].

In conventional transcranial Doppler sonography, the Doppler signal is only evaluated using indirect criteria, that is, flow direction, depth of the detected signal, position of the probe, and perhaps response to compression. This can lead to difficulties in assigning the signals to the individual basal arteries. With transcranial color-coded duplex sonography (TCCS), the Doppler signal can be assigned to the anatomical site under visual control, which allows a better assessment of pathological cerebrovascular processes [12].

There are fundamental methodological differences between color-coded duplex sonography and other imaging techniques such as MRI and MRA in the visualization of arteriovenous malformations. The sonographic diagnosis of an AVM is not based on an exact anatomic presentation of the pathological structures, but on the ability of the color-coded Doppler signal to show the pathological flow phenomena in real time [13, 14].

The center of an AVM is a nidus around which are located numerous vascular loops of afferent and efferent vessels. Their caliber is abnormally large, and they can form arteriovenous short circuits. They drain through one or several veins, which are characterized by a typical arterial Doppler spectrum [15]. After switching to color-coding, individual vascular loops are revealed by the multicolor pattern induced by the aliasing phenomenon caused by the increased flow velocities. The colors vary over the entire range from turquoise to dark blue, black and red to light yellow. Using different sectional planes through the angioma, one can recognize the various vascular loops in the malformation and identify those with blood flow toward and those with flow away from the transducer by the abrupt color shift from red over black to blue and vice versa (Fig. 29.1).

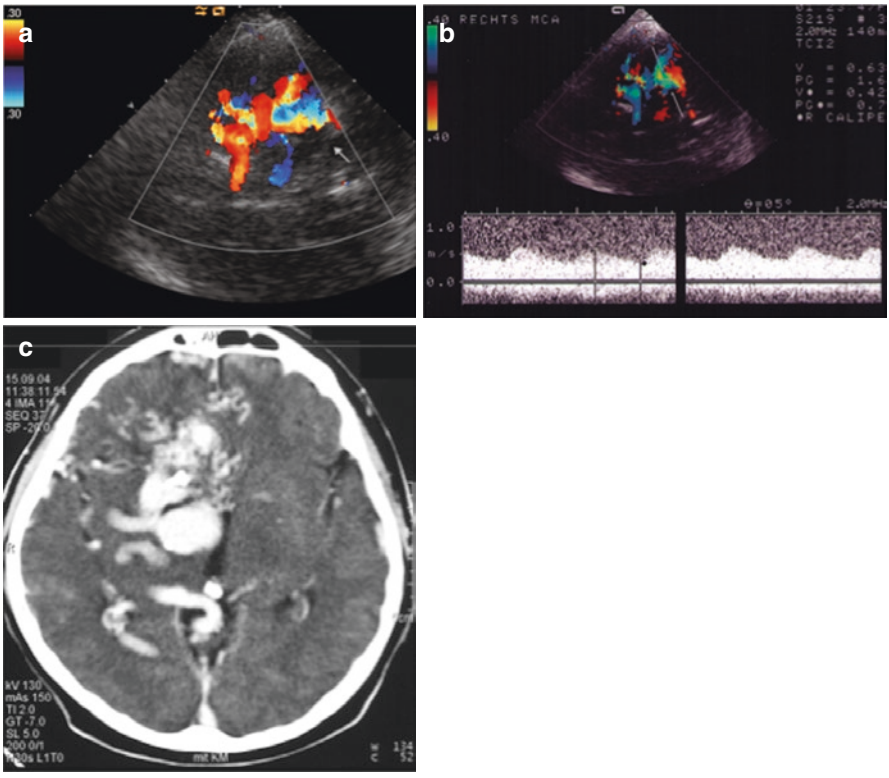

Fig. 29.1 Visualization of an extensive basal arteriovenous malformation with color-coded duplex sonography
An arteriovenous malformation located bilaterally in the basal brain region in a 65-year-old patient with epileptic seizures
(**a**) Multicolored signal due to aliasing, which coincides with the vascular convolutes of the malformation and are immediately recognizable
(**b**) Typical Doppler spectrum of the arteriovenous malformation. Low pulsatility with an elevated diastolic flow velocity due to the low vascular resistance is characteristic of an AVM
(**c**) Computer tomographic image of the arteriovenous malformation in the axial plane

Positioning the sample volume under visual guidance in different areas of the vascular convolution reveals a typical Doppler spectrum with markedly increased flow velocities and with a disturbed flow. Due to the reduced peripheral resistance in an angioma, the diastolic component of the Doppler spectrum is increased more relative to the systolic component, which leads to the typical low pulsatility index.

The hemodynamic changes are more pronounced the closer the transducer is to the angioma. For this reason, it is not possible to define the exact hemodynamic criteria that define an artery supplying an angioma. The following flow values can serve as guidelines [12]:

- Maximal systolic blood flow velocity >140 cm s^{-1}.
- End-diastolic blood flow velocity >100 cm s^{-1}.
- Pulsatility index <0.6.

An important finding is a lateral difference in the arterial flow velocities of greater than 20% which can indicate a steal mechanism. Using these parameters, one can also determine which other arteries of the circle of Willis located outside the angioma are involved in its blood supply. The most important indirect diagnostic criterion is not the absolute value of the flow velocity but the relationship between the maximal systolic and the end-diastolic velocities, which is indicated by the pulsatility of the Doppler spectrum, that is, in the resistance or pulsatility index.

The pulsatility of the Doppler spectrum is also decisive in the examination of the brain supplying arteries in the neck, since the flow velocities alone can be in the normal range.

The location plays a large role when visualizing arteriovenous malformations [16]. In a 6-year prospective study, we employed sonography to assess 54 patients with an intracranial AVM confirmed by angiography. We were able to confirm the results of the digital subtraction angiography in 42 of the 54 patients (77.8%) by sonography [17]. The results of our study showed that AVMs located in the basal regions (temporo-, parieto-, and frontobasal) were particularly easy to visualize with an 88.9% success rate. They lie in the axial plane, which is a good location for transcranial duplex sonography. The vascular convolutes can often be immediately detected by their multicolored appearance. Subcortical (frontal, parietal, occipital) or cerebellar AVMs are more difficult to visualize for technical reasons because they lie outside the field accessible by the beam.

The size of an AVM plays a less important role than a favorable location when it comes to visibility in ultrasound imaging. In our patient collective, the smallest AVM visualized in the axial plane had a diameter of 1.3 cm. Subcortical and cerebellar angiomas are more difficult to image even if their diameter is greater. Employing the axial diencephalic or coronal plane can prove useful in such cases [18]. The use of echo contrast agents can increase the diagnostic success rate, particularly for those located in an unfavorable temporal acoustic bone window [19–24].

Transcranial Doppler sonography is convenient for postoperative follow-up examinations [25, 26]. Hemodynamic changes can be detected more clearly postoperatively or following embolization using transcranial color-coded duplex

ultrasonography [27, 28]. If it is not possible to directly image an AVM, an indirect diagnosis can be made by visualizing the arteries feeding the angioma. As mentioned above, the typical hemodynamic pattern of these vessels, that is, high flow velocities and low pulsatility are more pronounced the closer to the angioma the examination is (Fig. 29.2).

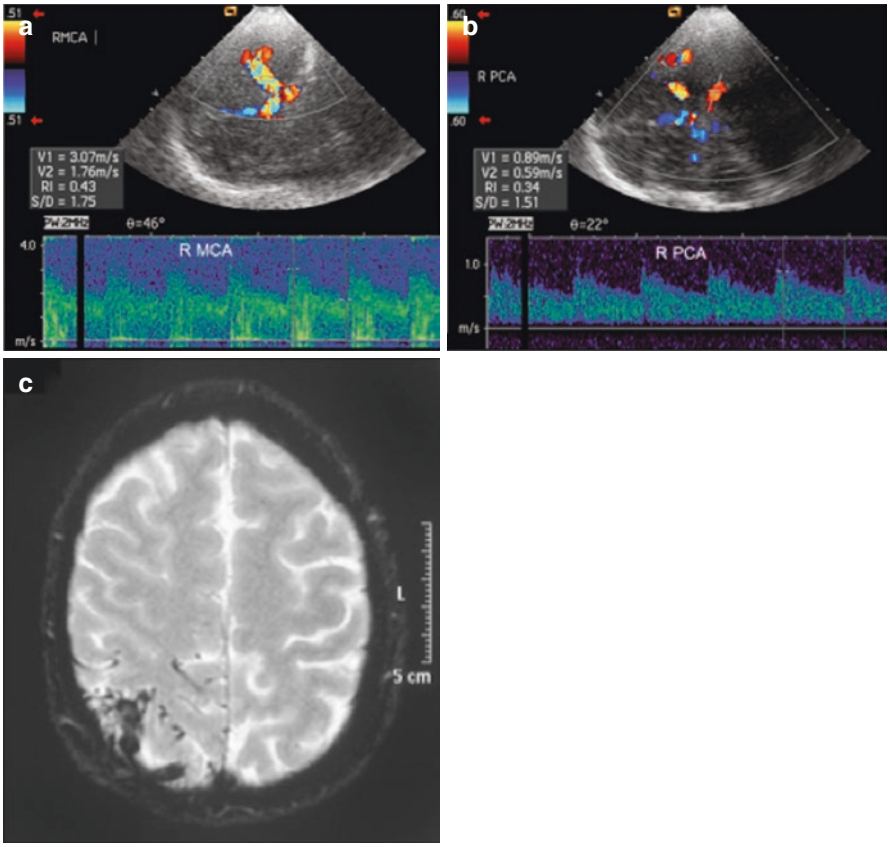

Fig. 29.2 Arteriovenous malformation with imaging of the vessels supplying the angioma
A 43-year-old patient with a right parieto-occipital, subcortical arteriovenous malformation
(**a**) The AVM cannot be directly imaged. The Doppler spectrum of the feeding middle cerebral artery is pathologically altered. Indirect indications of its involvement in the supply to the subcortical AVM are elevated flow velocities (systolic ca. 300 cm s^{-1}, diastolic ca. 180 cm s^{-1}), and a lowered resistance index (RI = 0.43) in the imaged arteries. In addition, an aliasing phenomenon due to the increased flow velocities with markedly increased flow volume
(**b**) The hemodynamic changes are less pronounced in the posterior circulation than in the right middle cerebral artery. The Doppler spectrum of the right posterior cerebral artery also exhibits a slight increase in the flow velocity and a lower pulsatility as a sign that the posterior circulation is involved in the supply to the AVM
Red arrow in Figs. (**a**, **b**): The aliasing phenomenon is still discernable after extending the color scale, which indicates an increased flow velocity in the imaged vessel
(**c**) Magnetic resonance image of the right parieto-occipital AVM

29.3 TCD/TCCS and Arteriovenous Malformation: Pitfalls

Errors can occur in the transcranial duplex sonography diagnosis of AVMs, for example, when there are convolutes of elongated arteries. Multiple color signals in the vascular loops can give the appearance of a malformation. This error can be avoided by a careful analysis of the Doppler spectrum.

Differentiating AVMs from vascularized tumors is not difficult because the tumor arteries are not as highly perfused, and there is no indication of the increased flow volume seen in angiomas.

29.4 TCD/TCCS: Arteriovenous Fistula

An arteriovenous fistula can either be inborn or can occur after a direct injury of the vessel wall. As in AVMs there is a pathological short circuit between the arterial and venous system bypassing the capillary bed. The characteristic hemodynamic changes are an increased flow volume, increased systolic and end-diastolic flow velocities, and a decreased peripheral flow resistance, which is manifested as a low resistance index. The flow in the efferent veins is distinctly pulsatile and essentially arterialized.

29.4.1 Carotid-Cavernous Fistula (CCF)

Carotid-cavernous fistula is a trauma-related abnormal communication between the internal carotid artery and the cavernous sinus. The typical hemodynamic changes and the color-coded duplex sonography findings are shown in Fig. 29.3. A high frequency bruit, typically a machine-like murmur, is characteristic of a fistula. The orbital veins are highly perfused in an intra- to extracranial direction, and the venous Doppler spectrum is arterial in character. Clinical signs are a pulsatile proptosis and chemosis. Paresis of the external eye muscles and impaired vision are secondary ocular effects, while the steal effect of a high flow through the fistula can cause hypoperfusion of the ipsilateral hemisphere.

29.4.2 Dural Arteriovenous Fistulas

Dural arteriovenous fistulas are abnormal connections between dural arteries and veins, which are primarily supplied by the external carotid artery. They occur close to the skull, which makes them difficult to image with transcranial color-coded

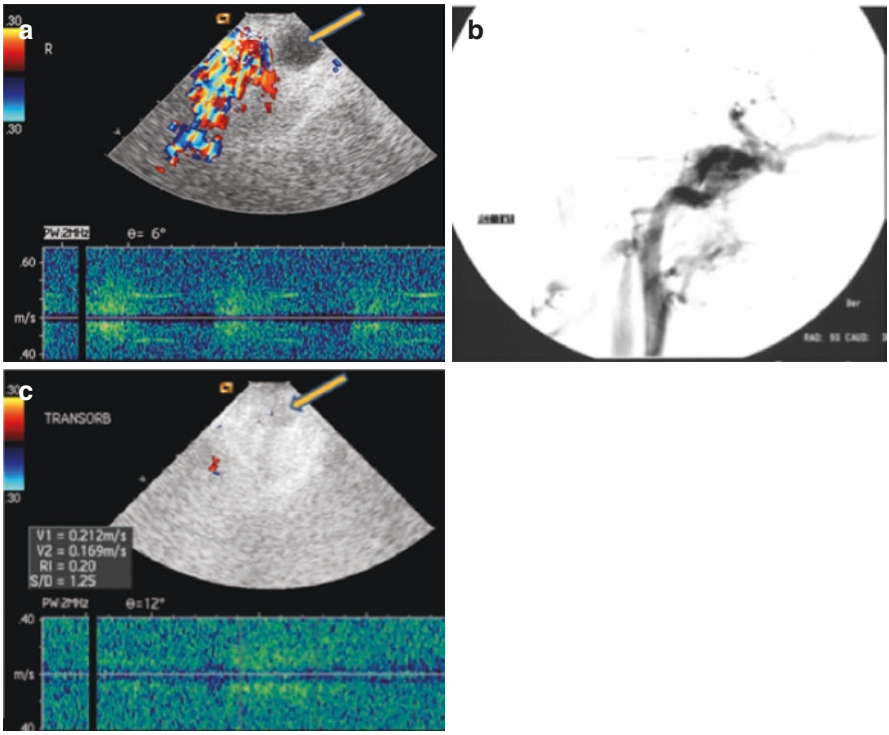

Fig. 29.3 Right carotid–cavernous fistula in a 45-year-old patient with traumatic brain injury
A pathological connection between the cavernous sinus and the carotid artery causes an increased flow volume in the involved vessels
(**a**) Sonographic findings before embolization. The fistula is revealed in the sonogram by a conspicuous mosaic pattern. The increased shunt volume manifests itself in a characteristic flow phenomenon in the Doppler spectrum of the orbital veins, and in the typical audible bruit, the so called "machine-noise". Inspection showed a pulsating exophthalmus
(**b**) Angiogram of the carotid-cavernous fistula (Diagnostische und interventionelle Neuroradiologie, Universitätsmedizin Göttingen)
(**c**) Sonographic findings after extracranial closure of the right internal carotid artery. After an attempt at complete occlusion of the fistula by endovascular embolization was unsuccessful, blood flow in the fistula was interrupted by extracranial closure of the right internal carotid artery. Transorbital ultrasound only shows a minimal fistula flow signal
Arrow: Orbit

duplex sonography. The sonographic diagnosis is made indirectly based on extracranial changes in the branches of the external carotid artery, particularly the occipital artery, that indicate a more cranially located decrease in vascular resistance with increased flow volume. The veins draining the fistula exhibit a Doppler spectrum more typical of arteries. A dural arteriovenous fistula can present as a pulse-synchronous tinnitus with or without focal deficits. It can be treated by endovascular embolization [29].

29.5 Conclusion

Transcranial color-coded duplex sonography (TCCS) is a valuable, noninvasive method for the diagnosis of intracranial vascular malformations and the assessment of the hemodynamic situation. It should not be used for screening, but as method complementary to other imaging techniques such as MRI, MRA, and CT. TCCS is well suited for noninvasive follow-ups after surgery or embolization. Decisions on further therapeutic measures with vascular malformations are based on digital subtraction angiography, still the preferred diagnostic method.

References

1. Yokoyama K, Asano Y, Murakawa T, Takada M, Ando T, Sakai N, Yamada H, Iwata H. Familial occurrence of arteriovenous malformations of the brain. J Neurosurg. 1991;74:585–98.
2. Berlit P, Berg-Dammer E, Nahser HC, Kühne D. Zerebrale arteriovenöse Malformationen (AVM). Diagnostik, Klinik und Therapie. Nervenarzt. 1994;65:226–37.
3. McCormick WF. The pathology of vascular ("arteriovenous") malformations. J Neurosurg. 1994;24:807.
4. Hassler W. Hemodynamic aspects of cerebral angiomas. Acta Neurochir. 1986;37(suppl): 1–136.
5. Lindegaard KF, Grolimund P, Aaslid R, Nornes H. Evaluation of cerebral AVM's using transcranial Doppler ultrasound. J Neurosurg. 1986;65:335–44.
6. Nornes H, Grip A. Hemodynamic aspects of cerebral arteriovenous malformations. J Neurosurg. 1980;53:456–64.
7. Kremkau FW. Sonography. In: Principles and instruments. 9th ed. Elsevier; 2016.
8. Kaps M, v. Reutern G-M, Stolz E, v. Büdingen HJ. Sonografie in der Neurologie. Thieme; 2017.
9. Widder B, Görtler MW. Duplexsonographie der hirnversorgenden Arterien. 7. Auflage. Springer; 2004.
10. Batjer HH, Devous MD Sr. The use of acetazolamide-enhanced regional cerebral blood flow measurement to predict risk to arteriovenous malformation patients. Neurosurgery. 1992;31:213–7.
11. Diehl RR, Henkes H, Nahser HC, Kühne D, Berlit P. Blood flow velocity and vasomotor reactivity in patients with arteriovenous malformations. A transcranial Doppler study. Stroke. 1994;25:157–80.
12. Bartels E. In: 2nd, editor. Color-Coded Duplex Ultrasonography of the Cerebral Vessels/ Atlas and Manual; Farbduplexsonographie der hirnversorgenden Gefäße/Atlas und Handbuch. Schattauer Stuttgart; 2018.
13. Becker GM, Winkler E, Hoffmann E, Bogdahn U. Imaging of cerebral arteriovenous malformations by transcranial colour-coded real-time sonography. Neuroradiology. 1990;32:280–8.
14. Baumgartner RW, Mattle HP, Schroth G. Transcranial colour-coded duplex sonography of cerebral arteriovenous malformations. Neuroradiology. 1996;38:734–7.
15. Bartels E. Aneurysms and Arteriovenous Malformations (AVMs). In: Bogdahn U, Becker G, Schlachetzki F, editors. Echoenhancers and Transcranial Color Duplex Sonography. Blackwell Berlin; 1998. p. 276–97.
16. Bartels E. Evaluation of arteriovenous malformations with transcranial color-coded duplex ultrasonography. Does the location of an AVM influence its ultrasonic detection? J Ultrasound Med. 2005;24:1511–7.

17. Bartels E, Knauth M. Möglichkeiten und Grenzen der transkraniellen Farbduplexsonographie bei der Darstellung intrakranieller arteriovenöser Malformationen. Fortschr Röntgenstr. 2006;178:64–70.
18. Bartels E. The axial imaging plane – the main domain of the transcranial color-coded duplex ultrasonography? Eur J Ultrasound. 2002;16:47–57.
19. Uggowitzer MM, Kugler C, Riccabona M, et al. Cerebral arteriovenous malformations: diagnostic value of echo-enhanced transcranial Doppler sonography compared with angiography. AJNR Am J Neuroradiol. 1999;20:101–6.
20. Schreiber SJ, Franke U, Doepp F, et al. Doppler sonographic measurement of global cerebral circulation time using echo contrast-enhanced ultrasound in normal individuals and patients with arteriovenous malformations. Ultrasound Med Biol. 2002;28:453–8.
21. Droste DW, Boehm T, Ritter MA, Dittrich R, Ringelstein EB. Benefit of echocontrast-enhanced transcranial arterial color-coded duplex ultrasound. Cerebrovasc Dis. 2005;20:332–6.
22. Bartels E. Contrast ultrasound in cerebrovascular disease and stroke management. In: Lencioni R, editor. Enhancing the Role of Ultrasound with Contrast Agents. Springer; 2006. p. 131–44.
23. Seidel G, Meairs S. Ultrasound contrast agents in ischemic stroke. Cerebrovasc Dis. 2009;27(suppl 2):25–39.
24. Sidhu PS, Cantisani V, Dietrich CF, Gilja OH, Saftoiu A, Bartels E, et al. The EFSUMB guidelines and recommendations for the Clinical Practice of Contrast-Enhanced Ultrasound (CEUS) in non-hepatic applications: update 2017. Ultraschall Med. 2018;39:2–44.
25. Batjer HH, et al. Evidence of redistribution of cerebral blood flow during treatment for an intracranial arteriovenous malformation. Neurosurgery. 1989;25:599–605.
26. Petty GW, Massaro AR, Tatemichi TK, Mohr JP, Hilal SK, Stein BM, Solomon RA. Transcranial Doppler ultrasonographic changes after treatment for arteriovenous malformations. Stroke. 1990;21:260–6.
27. Klötzsch C, Henkes H, Nahser HC, Kühne D, Berlit P. Transcranial color-coded duplex sonography in cerebral arteriovenous malformations. Stroke. 1995;12:2298–301.
28. Bartels E. Transcranial color-coded duplex ultrasonography in routine cerebrovascular diagnostics. In: Bartels E, Bartels S, Poppert H, editors. New trends in neurosonology and cerebral hemodynamics – an update. Perspectives in medicine 2012, vol. 1. München: Elsevier; 2012. p. 325–30.
29. Arning C, Grzyska U, Lachenmayer L. Lateral cranial dural fistula. Detection with Doppler and duplex ultrasound. Nervenarzt. 1997;68:139–46.

Chapter 30
Stroke Prognosis: Monitoring the Hemodynamics and Blood Pressure by TCD/TCCS

Ricardo Varela, José Coelho, Sara Bernardo-Castro, Fernando Silva, and João Sargento-Freitas

Key Points

1. Recanalization, reperfusion, collateral circulation influence neuronal resistance to ischemia.
2. After recanalization, cerebral blood flow (CBF) should be assessed for hyperperfusion.
3. Blood pressure management in acute stroke is dependent on recanalization status.
4. Neurosonological techniques can provide continuous assessment of the patients' hemodynamic status.

30.1 Introduction

An updated definition of stroke for the twenty-first century establishes that central nervous system infarction be defined as a brain, spinal cord, or retinal cell death attributable to ischemia, based on neuropathological, neuroimaging, and/or clinical evidence of permanent injury [1]. Fortunately, long gone is the notion that stroke represents

R. Varela · J. Coelho · F. Silva
Neurosonology Laboratory, Centro Hospitalar e Universitário de Coimbra, Coimbra, Portugal

S. Bernardo-Castro
Neurosonology Laboratory, Centro Hospitalar e Universitário de Coimbra, Coimbra, Portugal

Faculdade de Medicina da Universidade de Coimbra, Coimbra, Portugal

J. Sargento-Freitas (✉)
Neurologist, Neurosonology Laboratory, Centro Hospitalar e Universitário de Coimbra, Coimbra, Portugal

Faculdade de Medicina da Universidade de Coimbra, Coimbra, Portugal

Committee Member - ESNCH, Oslo, Norway
e-mail: jsargentof@hotmail.com

C. N. Rodríguez et al. (eds.), *Neurosonology in Critical Care*,
https://doi.org/10.1007/978-3-030-81419-9_30

an unmodifiable illness by its nature, and acute therapeutic approaches represent the mainstay approach to this infirmity. In an oversimplistic way, we could settle that the mainstay of acute stroke therapy is to reverse the neurological deficit by reopening the culprit vessel by endovascular procedures or intravenous fibrinolysis. Furthermore, the clinical course of stroke may include either spontaneous improvements or deterioration related to dynamic changes in brain perfusion. These changes may include spontaneous thrombolysis, hyperperfusion, reocclusion, microembolism, thrombus propagation, or collateralization [2]. The intricate complexity of these mechanisms helps understand the impact of the other approved therapeutic action: admission to a stroke unit. This represents the holistic approach of targeting treatments to specific needs of each individual patient and at a specific time point. Acute classic semiological assessment falls short in this setting, and active vasculature status may be acquired with current imaging modalities, which include digital subtraction angiography (DSA), contrast-enhanced CT angiography (CTA), and magnetic resonance angiography (MRA). However, these methods are impractical and difficult to obtain serially. In this setting, it is becoming widely accepted that transcranial Doppler (TCD) is an alternative noninvasive, nonionizing, and inexpensive method of assessing patterns of cerebral circulation that could help to achieve the previously stated acute stroke aims. Furthermore, its bedside availability, convenience to the patient, and serial or even continuous monitoring options reinforce its clinical value in an emergency scenario.

The single value of each hemodynamic assessment is limited taking into account the main clinical picture of an acute stroke patient. The primary clinical challenge lays in the active correlation of clinical scenario (age, time of symptoms, vascular syndrome), acute therapy, recanalization status, and general hemodynamic and oxygen delivery variables such as blood pressure and peripheral oxygen saturation.

We aim in this chapter to highlight further the acute hemodynamic status assessment and management that current stroke therapy demands, reinforcing the value of TCD assessment in this comprehensive approach. A comprehensive clinical case will also be presented reinforcing the real-world application of the described concepts.

30.2 Concepts on Stroke Hemodynamics

30.2.1 Collateral Circulation

The extracranial (carotid and vertebral arteries) and intracranial arteries (composing the circle of Willis) represent a dynamic system intrinsically designed to compensate for dynamic changes, acute or chronic, to its normal flow. The latter is represented by an integrated activation of a collateral system hierarchically composed of primary (such as anterior and posterior communicating arteries) and secondary pathways (such as ophthalmic artery and leptomeningeal vessels).

Collateral circulation is a crucial element for preserving cerebral blood flow in the setting of acute or chronic vessel occlusion [3]. Several studies have established the importance of collateral flow in predicting stroke outcome by correlating the degree of collateral circulation with infarct volume and functional status [4].

Conventional angiography sets the gold standard by providing the most accurate information about the circle of Willis and leptomeningeal collaterals status [5], although it may be easily stated that its applicability is limited by its availability, invasive nature, and associated risks of this diagnostic procedure. TCD appears to be an excellent alternative to DSA, in fact, this accessible, reliable, noninvasive, replicable, and dynamic tool is quite useful in the indirect assessment of collaterals and is, therefore, recommended by the American Academy of Neurology for the evaluation of the collateral pathways in the condition of an internal carotid artery (ICA) occlusion [6].

TCD can be useful in assessing the previously described primary and secondary systems in addition to others related to posterior circulation stroke syndromes, mainly flow changes enrolling the basilar and vertebral arteries.

We describe each of the arterial segments and flow pattern modification in response to hemodynamic insults in distinct arterial vessels below and in Table 30.1.

Table 30.1 Summary of collateral mechanisms in response to different occluded vessels

Occluded artery	Collateral pathway	Vessel	TCD findings
ICA	AComA	MCA	↓ ipsilateral MFV and pulsatility; normal contralateral values. No change in the MFV by compression of the ipsilateral CCA; ↓MFV with compression of the contralateral one
		ACA	Reversed flow in the proximal segment of the ipsilateral. 1.2↑ of contralateral MFV. No change in the MFV by compression of the ipsilateral CCA; ↓MFV with compression of the contralateral one
	PComA	ICA and PCA	Consistent flow sign directing flow from P1-PCA into ICA
		BA	Accelerated flow in all its course with PSV usually over 70 cm/s
		PCAs	Asymmetry between their PSV with an increased velocity ipsilateral to the culprit side
	OA	OA	Retrograde flow moving away from a transorbital placed probe, with a low pulsatility index at a 40–60 mm depth
MCA	Leptomeningeal vessels	ACA and PCA	Increased flow velocity and decreased flow resistance at the ACA and PCA ipsilateral to occluded vessel
BA	PCAs	BA	Inversion of the distal BA demonstrated in suboccipital window
		PCA	Inversion of one or both P1 segments of PCAs
		ICA	Similar vertical systolic flow acceleration indicating anterior circulation flow origin at the top of the BA
Proximal Subclavian artery	VA	VA	Retrograde blood flow from the ipsilateral VA into the subclavian artery distal to the occlusion. The contralateral VA feeds this reversed flow

30.2.1.1 Collateral Flow Through the Anterior Communicating Artery (AComA)

First, it should be stated that TCD is unable to individually assess the AComA due to its small diameter and length. Thereby, TCD can only determine flow findings related to the anterior cerebral artery cross-filling via the AComA [7]. Taking into account the previous criteria, a high correlation was found between DSA and TCD when assessing the AComA [8].

30.2.1.2 Collateral Flow Through the Posterior Communicating Artery (PComA)

The PComA is responsible for connecting the posterior and anterior cerebral arterial systems. Increasing degrees of internal carotid artery (ICA) stenosis will increase flow from the P1 segment of posterior cerebral artery (PCA), through the PComA into the distal, post-stenotic ICA, with reported sensitivity of 79% and specificity of 86% in the setting of over 70% ICA stenosis and absent reliable flow changes under that [7, 9–11].

The AComA appears to be activated firstly in the setting of a proximal anterior occlusion/stenosis in relation to the PComA resulting in an increased sensitivity of flow changes from the first related to the later [12, 13]. Additionally, it was also described that a single PComA collateral support constitutes a sign of deteriorated cerebral perfusion. Hence, a small or absent PComA can be considered as a significant risk factor for watershed infarction [14].

30.2.1.3 Collateral Flow from a Reversed Ophthalmic Artery (OA)

The OA is reversed in the setting of ICA occlusion or severe stenosis (>80%) proximal to the OA origin [15]. Adding the previous findings to a delayed systolic flow acceleration in the ipsilateral MCA reinforces the degree of suspicion for an ICA stenosis/occlusion, making it quite likely by the simultaneous detection of at least one first-order collateral channel (AComA or PComA). Supratrochlear flow assessment, occasionally easier than OA evaluation, is also a reliable marker for ICA disease and is equally reversed in the setting of its occlusion/high degree stenosis.

As a second-order collateral system, OA flow reversal often happens in the setting of an impaired or suboptimal cerebral perfusion and possibly impaired intracranial vasomotor reactivity, which, globally, encompasses a poor prognosis. Therefore, a reversed OA flow in the setting of asymptomatic stenosis may place the patient in a higher risk group for future ischemic events [15].

30.2.1.4 Collateral Flow from Leptomeningeal Vessels

In the setting of proximal MCA occlusion, the single reliable mechanism to compensate for the perfusion deficit relies on the leptomeningeal vessels arising from the ACA and PCA. It is readily understood that the distal pressure lowering from the MCA branches creates a gradient between the ones that are distal to the ACA and PCA; therefore, establishing a hemodynamic drive to the opening of this collateral system that, because of the more prominent number of cortical arterial anastomoses, appears to be more useful for the former vessel (ACA) than for the latter.

An understanding of this mechanism is vital to integrate how TCD can help to assess the effectiveness of this collateral system, in the way that it somehow works with induction markers of its establishment, mainly an increased flow velocity and decreased flow resistance at the ACA and PCA. This mechanism is the foundation of the somehow vague concept of flow diversion (FD). The ambiguity derives mainly from the discrepancy across the literature regarding the affected or nonaffected side used as reference. As the comparison of affected MCA flow and ipsilateral ACA may overestimate the FD, the comparison of both ACAs, using as cut-off a discrepancy over 30%, appears to be a good predictor of FD [16].

Leptomeningeal circulation appears to be an independent predictor of stroke outcome, where patients with FD are more likely to have a good outcome (defined as a modified Rankin score between 0 and 2), and TCD can provide a noninvasive and reliable evaluation of its effectiveness [17].

30.2.1.5 Collateral Flow from Reversed Basilar Artery (BA)

Acute BA occlusion is an ominous disease with potentially disastrous results. BA flow reversal happens in the setting of a proximal BA occlusion creating a pressure gradient between the anterior and posterior cerebral arterial systems, therefore moving the system from the increased pressure side (anterior) to the one in deficit by the PCA's. This phenomenon can happen not only in the setting of a proximal BA occlusion but also, expectedly to a lesser extent, in a critical bilateral vertebral disease [18]. This collateral flow detection is quite useful in the setting of assessing a continuing perfusion of vital brain structures and is associated with lower stroke severity and better outcome after acute proximal BA occlusion [19].

30.2.1.6 Collateral Flow from Reversed Vertebral Artery (VA)

The most common cause of VA artery reversal happens as a surrogate marker of proximal subclavian occlusion or stenosis as a compensatory mechanism to ensure the distal patency of this arterial segment. This was first described by Contorni and Reivich in 1960 as the subclavian steal syndrome [20, 21]. In this setting, the

obstruction is bypassed by retrograde blood flow from the ipsilateral VA into the subclavian artery distal to the occlusion, and the contralateral vertebral artery feeds this reversed flow. If there is a joint pathology of the contralateral VA, other collateral circulation can arise from external carotid branches (occipital artery) that anastomose with muscular branches of the VA.

30.2.2 Recanalization

With the diffusion of different acute stroke therapies, which include intravenous or intra-arterial procedures, came the need for a real-time assessment of the vascular status of acutely treated stroke patients. As it will be developed further, despite some misuse across the literature, recanalization and reperfusion have different meanings although, commonly in ideal post-treatment conditions, they may overlap.

For the matter of this chapter, we will define recanalization as the restoration of vessel patency at the site of the occlusion.

As we may expect, a myriad of imaging techniques shares the ability to demonstrate this hemodynamic status, mainly DSA, CTA, or magnetic resonance angiography (MRA). It is also stated as a common grounding factor that they also work by non-longitudinally assessing stroke patients by means of its availability, cost, and practicality. In this context, TCD emerges as the ideal noninvasive, real-time bedside tool for evaluation of cerebral vessels, despite initially being demonstrated for endovenous thrombolysis [2], TCD preserved its ability to assess patients treated with other modalities, mainly endovascular procedures as they had broad and unanimous approval.

As defined for thrombolysis, TIBI score ranges from 0 to 5, being 0 synonym of flow absence and 5 of normal blood efflux, as defined elsewhere (stroke reference). Emergent TIBI classification by TCD correlates with initial stroke severity, clinical recovery, and mortality in stroke patients submitted to endovenous fibrinolysis. There is also a positive and significant correlation between flow-grade improvement and clinical benefit. In the thrombectomy era, TIBI score retained its clinical significance by demonstrating an overall accuracy of 89% and a sensitivity/specificity of 88/89% when predicting recanalization status against DSA, used as the gold standard [22].

30.2.3 Reperfusion

As stated before, recanalization and reperfusion are not absolute synonyms despite the potential overlap. In fact, reperfusion refers to anterograde perfusion of patent microvasculature supplying a target tissue after recanalization. One could easily argue that a tissue is also perfused through collateral supply working in a retrograde

manner; therefore, angiographic reperfusion distinctly involves perfusion of distal territory in an anterograde manner following recanalization.

As described, tools and scoring systems designed to characterize reperfusion need to encompass different variables that extrapolate recanalization status, as ideally, they should address collateral flow, be readily applicable, reproducible, and encompass a prognostic significance and a correlation with clinical outcome [23].

As an intrinsic part of mechanical thrombectomy, DSA offers the most comprehensive when assessing the previous variables, as it allows evaluation of the occlusion site, potentially the length of the vessel harboring the clot, extent of collateral supply, as well as post-intervention characterization of vessel patency, rate of blood flow, reperfusion territory, distal occlusion/embolization, and early venous shunting.

Ideally, a DSA acute stroke scoring system should easily encompass the previous variables. Despite the establishment of different scoring systems including the TIMI score [24], the Mori reperfusion scale [25], the Qureshi scale [26], and the most currently used TICI scale [27], a definite system is still lacking. One of the most notable features lacking in the latter is the lack of a collateral flow scoring system, which has a demonstrated relation with clinical outcome [28]. One could bypass this by also using the American Society of Intervention and Therapeutic Neuroradiology/Society of Interventional Radiology Collateral Flow Grading Scale, but the integration of different scoring systems in an emergency setting as the one elicited by stroke approach makes its clinical diffusion more challenging.

30.2.4 Hypoperfusion

Throughout the twentieth century, prevailed the concept that embolization and hypoperfusion were entirely independent and different hemodynamic stroke mechanisms. Even now, the boundaries between them appear to be more established then what, in fact, they appear to be.

Regarding hypoperfusion, clearly, in all circumstances, a prolonged failure to deliver oxygen and sugar-rich blood to brain tissue causes cell death. This may happen by the blockage of a microscopic-sized penetrating artery causing severe local decreased perfusion to the small region supplied by the obstructed penetrating artery, which constitutes the nuclear founder of small vessel disease pathology, or by blockage of a distal branch of an intracranial artery by embolic material, which causes infarction of the limited tissue supplied by that branch and represents the primary mechanism of embolism.

The culprit mechanism by which a hypoperfusion resulting from a diminished blood flow at a distance from vulnerable brain tissue resulting, for instance, from a stenotic carotid disease does not seem so clear as the previous ones [29]. Grounding this argument is the established notion that most patients with severe stenosis or occlusion of the carotid or vertebral arteries in the neck do not develop severe strokes. Adding to this, the ICA occlusion is often asymptomatic and the annual rate

of stroke in patients with even severe asymptomatic ICA occlusive disease is only 2–3% [30].

The ongoing concept that hypoperfusion and embolization probably interact synergistically is further reinforced by the common knowledge that non-embolic carotid artery dissection is associated mainly with transient focal symptoms and that the definite ones are overall linked to an embolus traveling intracranially. As previously established, this is probably linked by the hemodynamic adapting mechanisms encompassed by the ECA (by the ophthalmic artery), ACA, AComA, PCA, PComA, and BA as explained in the collateral section of this chapter. Further evidence from a synergistic interaction between hypoperfusion and embolization comes from the fact that HITS, or high-intensity transient signals, as collected by DTC in the setting ICA atheromatous disease, tend to have a direct connection between their number and stenotic severity [31].

As an epiphenomenon of embolization, HITS, and MCA stenosis share the same connection pattern, as demonstrated by Wong et al. where patients with severe MCA stenosis had more than twice the frequency of HITS detection compared to those with slight to moderate stenosis [32]. The necropsy evidence that the watershed regions of patients with severe carotid stenosis are composed mainly of infarcted brain tissue infiltrated by cholesterol crystals and white platelet emboli further reinforces this concept [33], as the evidence that most patients with watershed lesions have any type of embolic source [34]. The previous evidence, at least, settles the ground for a plausible doubt regarding the not so by chance co-occurrence of hypoperfusion mechanisms and embolization, as they appear to act synergically in the stroke genesis.

30.2.5 Hyperperfusion, Cerebral Hyperperfusion Syndrome, and Cerebral Reperfusion Injury

Failure to improve after an intravenous or intra-arterial procedure may happen even in the setting of a documented recanalization. As seen before, different and dynamic variables play a crucial role in the interface between vessel reopening and clinical benefit, namely, hypoperfusion or no perfusion, for instance. Counterintuitively, the non-improvement scenario is not only fed by an absent hemodynamic response, as a matter of fact, clinical worsening may happen in the setting of excessive and uncontrolled blood supply into a vascular unit.

Throughout the medical literature, one may find hyperperfusion, cerebral hyperperfusion syndrome, and cerebral reperfusion injury used interchangeably. Despite the lack of absolute consensus, one can argue that they may represent a continuum between recanalization and no clinical benefit or even worsening status.

Cerebral hyperperfusion has been described as a sudden rapid rise in cerebral blood flow in excess of metabolic demand. One strict approach defines hyperperfusion as an increase in CBF relative to preocclusion values (>100%). This definition

is useful in elective surgery with adequate workup, but it is often impractical in a post-acute stroke, as pre-ischemic CBF measurements are almost always absent. Here, a practical approach may define hyperperfusion as a significant increase in CBF relative to the homologous area of the contralateral hemisphere [35]. Isolated hyperperfusion may be asymptomatic as immediately documented in 20–40% of the patients submitted to carotid endarterectomy [36]. When becoming symptomatic, hyperperfusion may manifest as cerebral hyperperfusion syndrome, which is characterized by an ipsilateral headache, hypertension, seizures, and focal neurological deficits, and if not treated properly, it can result in severe brain edema, intracerebral or subarachnoid hemorrhage, and death [37].

Despite some overlapping throughout medical literature, cerebral reperfusion injury appears to be an even more general entity as it is defined as a biochemical cascade causing further worsening of ischemic brain tissue that concomitantly reverses the benefits of restoring cerebral circulation following systemic thrombolysis or mechanical thrombectomy for acute ischemic stroke [38]. The hyperperfusion and hemorrhagic transformation may configure subsets of reperfusion injury, but other clinical elements take place in this setting as no-reflow phenomenon (no reperfusion despite recanalization); leukocyte, reactive oxygen species, complement activation and platelet-mediated injury; and blood-brain barrier disruption.

Clinicians must be aware of these dynamic events in acute stroke setting, as they may be determinant in clinical outcome.

30.2.6 Acute Hypertensive Response

Acute hypertensive is defined as the elevation of blood pressure relative to normal or premorbid levels that occurs within the first 24 hours of symptom onset in patients with acute ischemic stroke. The 2003 World Health Organization (WHO)/International Society of Hypertension (ISH) statement [39] settles a highly sensitive definition of acute hypertensive response, as "systolic ABP >140 mm Hg or diastolic ABP of >90 mm Hg demonstrated on 2 recordings taken 5 minutes apart within 24 hours of symptom onset" can be seen in approximately 75% of patients with acute ischemic stroke. The authors argue that such a definition should prevail as a uniform standard across literature, not necessarily being associated with a modulation of therapeutical approaches, and potentially conditioning an overrepresentation of this phenomenon with reports of over 60% of patients with acute stroke [40].

Despite its ubiquity, the acute hypertensive response appears to be an independent prognostic factor, as demonstrated in a systematic review of 18 studies that demonstrated that patients with stroke and high initial ABP were at a 1.5- to 5.0-fold increased risk of death or dependency and clinical deterioration [41].

Taking into account the classic vascular risk factors that act as a preamble for stroke, one could argue that the acute hypertensive response is merely a reflection of inadequately treated or undetected chronic hypertension [42], but several concomitant evidence highlights the specific nature of intrinsic hypertensive stroke mechanisms: New-onset high blood pressure happens in as much as 20% of patients with acute stroke [43]; spontaneous reduction of blood pressure (by an average of 20/10 mm Hg) within 10 days after the acute event without any specific antihypertensive therapy [44]; spontaneous reduction of blood pressure is often observed after vessel recanalization [45].

Classically, the relationship between systolic ABP and clinical outcome was described as U or J shaped, with both high and low values of ABP being independent prognostic factors for poor outcome [46]. Such an assumption was made disregarding recanalization status; therefore, in an increasingly growing acute stroke endovenous and intra-arterial therapy era, our center tried to further explore the relationship between clinical outcome and blood pressure in recanalized and non-recanalized patients. After enrolling 674 acute stroke patients submitted to either endovenous, intra-arterial, or a combination of both treatment with <24 h vessel status assessment, we concluded that systemic ABP in the first 24 hours after ischemic stroke influences functional outcome in patients with acute stroke depending on the recanalization state. In the non-recanalized group, a J-shaped association is observed. However, in the recanalized group, the association is linear, and low ABP is associated with the best outcome [47].

30.3 Methods to Assess Acute Stroke Hemodynamics

30.3.1 Neurosonology

Neurosonologists are often tempted to overemphasize the role of TCD/TCCS study in stroke patients in a perpetual talk that compares the virtues of Christian Doppler works to the ones from René Laennec and his historical creation. In fact, in vascular neurology field, by the merits of its ubiquity, ease of use, noninvasiveness, and every-time use, TCD may configure our clinical equivalent to the stethoscope.

In a simplified approach, one could state that the culprit stroke vessel may, at any time of its clinical course, be occluded, entirely or partially compensated by collateral flow despite being occluded, partially or totally recanalized in a spectrum that may include hypo, normal, or hyperperfusion. One may comprehensively argue that a strict hemodynamic approach falls short in the complexity of tissue pathology related to stroke, but in what relates to acute stroke care and therapeutical approach, this live hemodynamic longitudinal assessment reveals as a critical element to the chain of decision (Fig. 30.1).

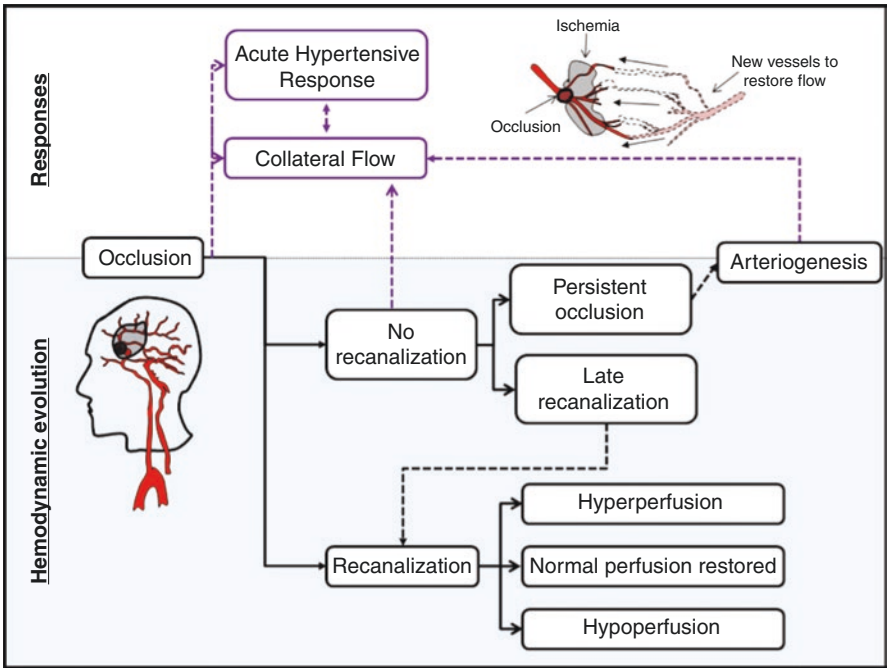

Fig. 30.1 intends to highlight the core hemodynamic concepts and its neurosonological correlates relevant to the active assessment of acute stroke patients. Schematic representation of the possible hemodynamic evolutions after acute ischemic stroke

30.3.2 Magnetic Resonance Imaging

MRI is more time consuming and less available than CT but has significantly higher sensitivity and specificity in the diagnosis of acute ischemic infarction in the first few hours after onset. In acute stroke setting, an MRI protocol may be designed as a set of individual image acquisitions that each have different signal contrast weightings, assembled with the goal of detecting pathology comprehensively. Invaluable clinical information may derive from an MRI acute stroke application, as possible active ischemia, hemorrhage, and occluded vessels, and insight regarding the size and location of the core infarct as well as the extent of surrounding tissue that potentially can be salvaged (the ischemic penumbra) [48].

A conventional acute stroke MRI protocol comprehends diffusion-weighted imaging (DWI), fluid-attenuated inversion recovery (FLAIR), MRA, perfusion-weighted imaging (PWI), and T2-weighted imaging. Different imaging behaviors are expected according to the time of symptom onset, site of occlusion, infarcted tissue extension, collateralization, and hemodynamic complications [49].

The following table summarizes the main concepts behind each of the imaging acquisitions in the acute stroke phase (Table.30.2).

Table 30.2 Summary of the main features of each MRI sequence and its interpretation in the context of acute ischemic stroke

MRI sequence	Clinical and imagiological concepts
T1&2-weighting	Lacks sensitivity to the immediate effects of cerebral ischemia
DWI	Highly sensitive to ischemia; increased signal in minutes following vessel occlusion, highlighting early cytotoxic edema and sodium-potassium pump early failure in the setting of acute ischemia; four to five times more sensitive for detecting acute stroke than is non-contrast CT(49)
FLAIR	Increased signal within 3 hours of stroke onset; Combination of DWI and FLAIR signal interpretation may estimate time from symptom onset in an unknown setting
MRA	Non-invasive method to screen for vessel occlusions, stenosis, or malformations; Non-contrasted, 3DTOF (three-dimensional time-of-flight angiography), and contrasted modalities, CE-MRA (contrast-enhanced magnetic resonance angiography), may be used, but not interchangeably, as the first provides an easier and safer acquisition, but has less contrast and is more sensitive to flow hemodynamics change; the latter provides a better image from intra and extracranial vessel and may provide "beyond the lumen" information, as in symptomatic atherosclerotic plaques
PWI	Semi-quantitative perfusion maps are obtainable from this examination that estimate cerebral blood volume, the mean transit time (MTT, the average time required by the bolus of contrast agent to cross the capillary network), the cerebral blood flow; combined with DWI provide information about the ischemic core and penumbra
T2	Acute hemorrhage detection with equivalent accuracy to CT; Microbleeds, indicative of multiple types of microangiopathy, detection

Despite financial and time-to-perform limitations, MRI in the acute stroke appears to be highly valuable. The time from symptom onset evocable by the DWI&FLAIR profile concept was recently explored in the WAKE-UP trial—MRI-guided thrombolysis for stroke with unknown time of onset [50]—which concluded that in patients with acute stroke with an unknown time of onset, "intravenous alteplase guided by a mismatch between diffusion-weighted imaging and FLAIR in the region of ischemia resulted in a significantly better functional outcome and numerically more intracranial hemorrhages than placebo at 90 days."

30.3.3 Cerebral Autoregulation in Stroke

As seen in other chapters of this book and above, cerebral autoregulation (CA) plays a crucial part in the viability of brain tissue after an acute ischemic stroke, trying to assure the maintenance of flow velocities in response to blood pressure variations.

There are several strategies to evaluate CA, that simplistically are all based in the concept of quantifying cerebral blood flow during induced or spontaneous blood pressure changes. Examples of externally modulated variations are a quick deflation of bilateral thigh cuffs, Valsalva maneuver, hand grip, or sit-to-stand method.

Response to vasodilatory stimulus as acetazolamide or CO_2 is more specific for evaluating endothelial function.

The autoregulatory index (ARI) assessed using the thigh cuff maneuver approximates the rate of recovery of cerebral blood flow compared with 10 rates. When ARI is less than 4, it is considered that cerebral autoregulation is impaired.

The mean flow velocity and the arterial blood pressure can be used to measure CA in frequency domain—transfer function analysis (TFA).

Mx is calculated as the correlation coefficient between slow spontaneous fluctuations of cerebral perfusion pressure and cerebral blood flow velocity. One strategy to estimate noninvasively Mx is by using finger plethysmograph arterial blood pressure with simultaneous transcranial Doppler [51]. In this technique, TCD assumes a fundamental task as it can evaluate cerebral blood flow velocity.

30.3.4 Other Neuroimaging Techniques

The use of cerebral perfusion CT in the context of acute ischemic stroke to determine the volume of irreversible lesion is advancing, with increased clinical applicability drawn from recent endovascular trials (DAWN and DEFFUSE-3) where this exam was used to guide indication for thrombectomy outside conventional time-based decision windows [52, 53].

Cerebral perfusion CT interpretation is simplistically based in three parameters:

(a) Cerebral blood flow (CBF)—defined as the volume of blood passing through a given amount of brain tissue per unit of time.
(b) Cerebral blood volume (CBV)—defined as the volume of blood in a given amount of brain tissue.
(c) Mean transit time (MTT)—corresponds to the average time, in seconds that red blood cells spend within a determinate volume of capillary circulation.

With these parameters, it is possible to define the infarct core and the penumbra area of salvageable tissue. The concept is based on autoregulation, since in the setting of acute occlusion, there is a compensatory cerebral vasodilatation. This results in a normal value or even an elevation of the cerebral blood volume while the cerebral blood flow is reduced. In opposition, irreversible tissue presents both decrease in CBF and CBV indicating the inability of the tissue's microvessels to vasodilate in response to the hypoperfusion (CBF reduction) thus causing reduced CBV. These new reperfusion trials used an automatic software to read the perfusion CT. This software was named RAPID and had the objective of standardizing the evaluation of the core lesion: Ischemic core is defined as the volume of tissue that shows a severely reduced cerebral blood flow (<30% of that in normal tissue), whereas a perfusion delay of more than 6 seconds represents hypoperfused tissue or tissue at risk. The two trials both used the concept of ischemic core based on RAPID quantification and differed slightly on the definition of tissue at risk. In the DAWN trial, this was assed based on NIHSS and patients' age, whereas DEFUSE-3 used a strictly neuroimaging definition based on the volume of tissue with perfusion delay. It has the advantage of being applicable to MRI DWI studies.

The concepts behind the perfusion techniques are related to the physiologic response of brain tissue to acute occlusion. In this setting, there is an immediate reduction of flow in the affected brain tissue. This results in a reduction of the cerebral blood flow defined above. Cerebral autoregulation promotes vasodilatation to compensate the flow reduction, resulting in normal or higher levels of cerebral blood volume.

PET scan has allowed to understand the flow and metabolic thresholds critical for the maintenance of brain function and morphology. This concept is no more than the concept of penumbra presenting in other imaging studies [54, 55].

Near-infrared spectroscopy is a technique that allows the evaluation of brain oxygenation. It was recently validated in acute stroke setting [56].

30.4 Integration of Blood Pressure, Stroke Hemodynamics, and Clinical Decisions

Up to 84% of patients presenting with acute ischemic stroke in emergency room have high blood pressure [40]. Historically, a U-shaped relationship was documented between outcomes and the admission ABP in the acute setting [46]. In other words, very low ABP is associated with worst outcomes presumably due to reduced flow in penumbral areas, whereas very high ABP is associated with increased risk of hemorrhagic transformation. In other words, a very low BP value is associated with worse outcomes due to reduced flow in the penumbra zone; whereas a high ABP value is associated with a higher risk of hemorrhagic transformation. However, with the increased use of intravenous and endovascular reperfusion therapies, as well as the possibility of assessing vascular status, the understanding of the effects of ABP on stroke is evolving. In fact, more recent studies demonstrated that the impact of systemic ABP in the first 24 hours after ischemic stroke is dependent on recanalization status, with recanalized patients showing a linear association between systolic blood pressure and clinical outcome [47, 57] whereas non-recanalized patients show the classical curvilinear association (Fig. 30.2).

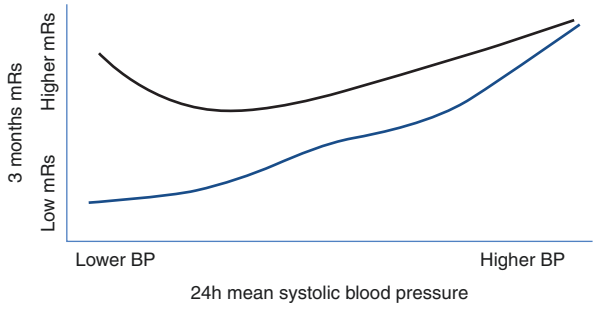

Fig. 30.2 Association of Blood Pressure (BP) and clinical outcome according to recanalization. Black line revealing the classic curvilinear association relation in non-recanalized patients between clinical outcome and blood pressure. Blue line reveals the linear relation that occurs in patients recanalized

The valuable use of transcranial ultrasound in the setting of acute ischemic stroke is largely established [58]. This allows to verify the recanalization status, the existence of collateral flow, and the existence of hyperperfusion in the symptomatic artery. Patients with successful recanalization who deteriorate should be assessed for hyperperfusion syndrome [59]. Specifically, the early use of neurovascular ultrasound can identify patients with hyperperfusion syndrome before being clinically evident. This may allow a more aggressive blood pressure approach.

The above examples demonstrate the major advantage of using TCCS in the setting of acute ischemic stroke.

30.5 Clinical Vignette

30.5.1 Case 1

A 72-year-old man presented to the emergency room with global aphasia, right hemianopia, and right hemiparesis (NIHSS: 18) that had started 1 hour before. In the cerebral CT, ASPECTS was 10. Since there were no absolute contraindications, rtPA bolus was administered. A cerebral angio CT was performed revealing an absent flow in the M1 segment of the left middle cerebral artery and excellent leptomeningeal collaterals.

While performing rtPA perfusion, endovascular thrombectomy was performed, and after 45 minutes, a final TICI of 3 was obtained. He was admitted to the stroke unit. A carotid and transcranial ultrasound was performed at 12 hours after symptom onset and a left middle cerebral arterial hyperflow was observed (Fig. 30.3). At that time, blood pressure was 175/102 mmHg. Intravenous beta-blocker was started to maintain systolic blood pressure below 140 mmHg, and patient was left in rest with head elevation at 45°. The next day hyperflow was still present and the previous described measures were maintained. At day 2, there was a symmetric flow between the left and right M1 segment of cerebral middle artery. A control CT demonstrated only minor reperfusion injury with petechial intralesion hyperdensities (type 1 hemorrhagic infarction, according to the ECASS II definition) [60].

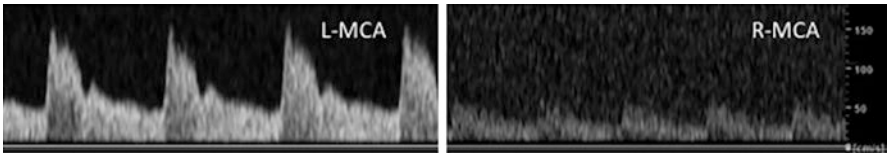

Fig. 30.3 Flow velocities after thrombectomy of the left middle cerebral artery (PI: 1.29; Mean velocity: 84 cm/s) and right middle cerebral artery (PI:0.75; Mean velocity: 45.7 cm/s) respectively

This case highlights the importance of TCD in a stroke unit both acutely and during follow-up. The demonstration of an elevated flow velocity in the whole MCA after successful recanalization indicates the impairment of autoregulatory mechanisms with potential to cause reperfusion injury. As such, measures to address hyperperfusion (still without clinical symptoms) were initiated (bed elevation and aggressive blood pressure control). Notably, if the elevated velocities were registered only in a short segment of the MCA, this finding would probably be associated with residual thrombus or intracranial stenosis (also to be clarified in subsequent exams).

30.5.2 Case 2

A 53-year-old woman patient presenting to the emergency room for headache associated with palpebral ptosis with onset on the previous day. In the neurological examination, it was noted a left Horner sign, mild right hemiparesis, and difficulty naming objects. A cerebral CT was performed with no acute changes. A cervical and transcranial ultrasound was performed, identifying a high resistance flow in the left common carotid artery and a pencil-tapering occlusion of the ipsilateral internal carotid artery (ICA), suggestive of dissection. The transcranial ultrasound revealed permeability of all arteries, with an asymmetric flow between middle cerebral arteries (Fig. 30.4a). Systemic blood pressure was 135/84 mmHg. She was admitted to the stroke unit and maintained in supine position and endovascular fluids were administered to raise blood pressure. She recovered in a few hours. She repeated ultrasound assessment that maintained occlusion of ICA, with a higher systolic peak velocity in the symptomatic MCA, that was still asymmetrical and maintained a low resistance flow (Fig. 30.4b). She was kept on bed rest. At day 7, transcranial ultrasound revealed a symmetrical flow velocity in the MCAs with a small pulsatility reduction in the left MCA (Fig. 30.4c, d). At this time, head position was gradually elevated and she started getting up after a few days. This case represents the importance of ultrasound in accessing cerebral hemodynamics and adapts our strategies for blood pressure and positioning management in the context of different hemodynamic status, specifically due to its unique possibility of continuous reassessments.

30.6 Conclusion

The real-time visualization of recanalization status, and the presence of hyperperfusion, allows for an optimization of acute stroke hemodynamics. In Fig. 30.5, we present a proposed algorithm for the management of acute stroke hemodynamics.

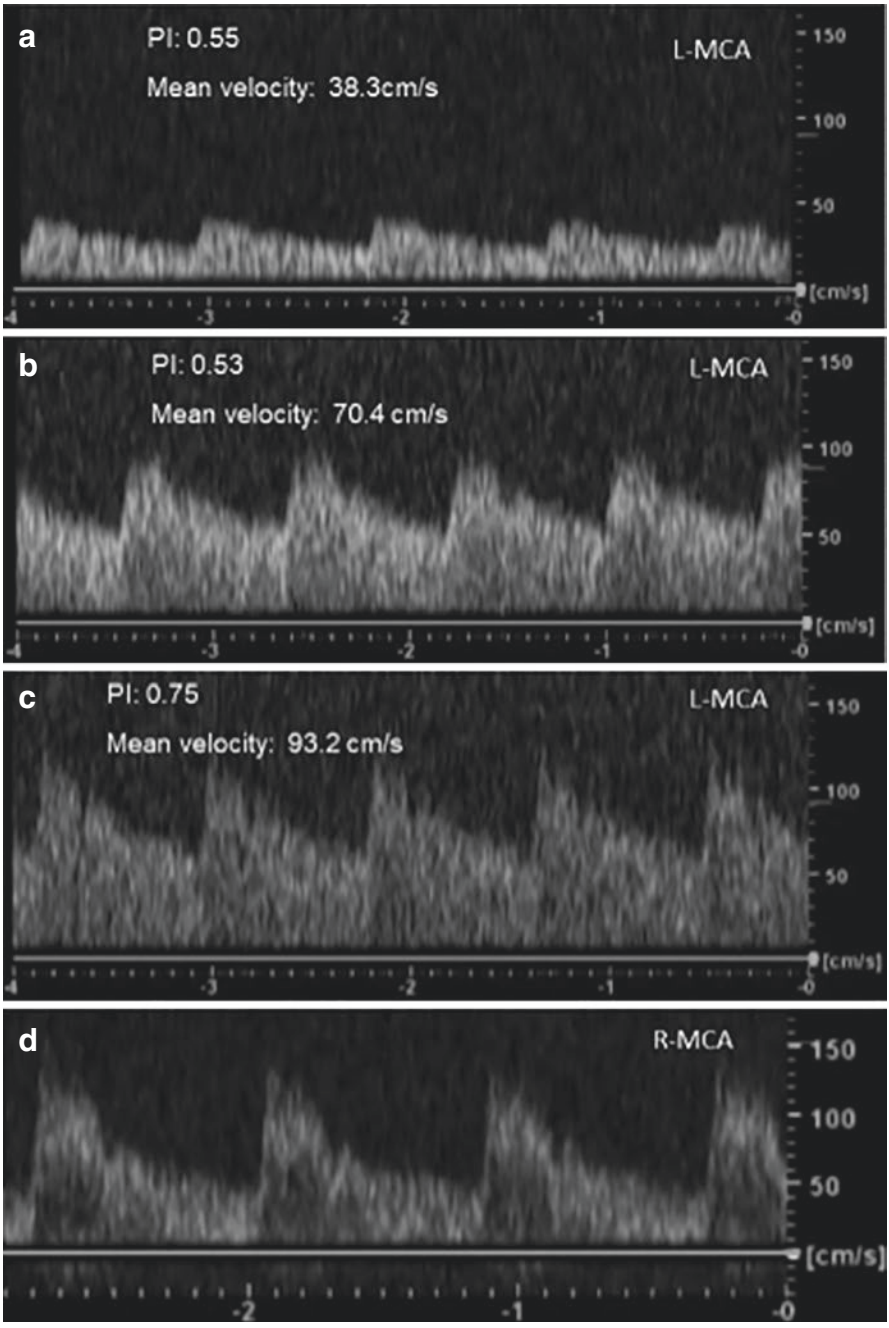

Fig. 30.4 (**a**) Left middle cerebral artery with a low flow and a low resistance, consequence of a dissection of ipsilateral internal carotid artery. (**b**) Next day after the exam shown in Fig. 30.5. A, we can verify a better flow velocity yet with a low resistance index. (**c**) Middle cerebral artery with normal flow and normal resistance. (**d**) Right middle cerebral artery that was identical during the three evaluations. PI: 1.10: Mean velocity 78 cm/s

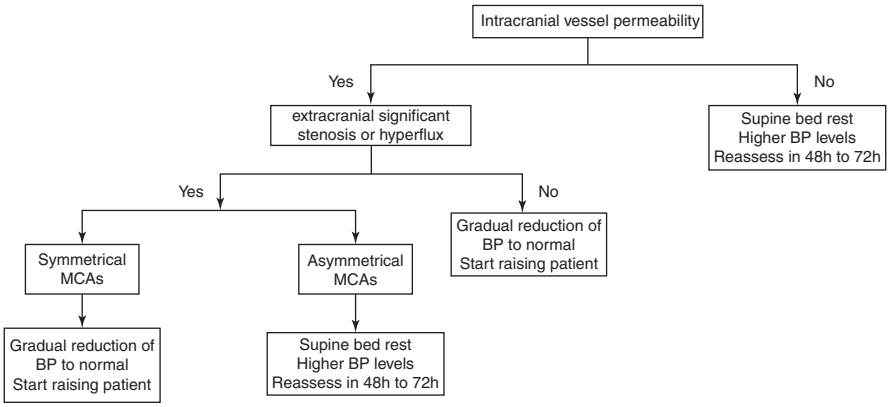

Fig. 30.5 A proposed algorithm for approaching patients with acute ischemic stroke. This is based in the authors personal experience and in the conclusions of the AVERT trial

References

1. Sacco RL, Kasner SE, Broderick JP, Caplan LR, Connors JJ, Culebras A, et al. An updated definition of stroke for the 21st century: a statement for healthcare professionals from the American heart association/American stroke association. Stroke. 2013;44(7):2064–89.
2. Akopov S, Whitman GT. Hemodynamic studies in early ischemic stroke: serial transcranial Doppler and magnetic resonance angiography evaluation. Stroke. 2002;33(5):1274–9.
3. Liebeskind DS. Understanding blood flow: the other side of an acute arterial occlusion. Int J Stroke. 2007;2(2):118–20.
4. Lau AYL, Wong EHC, Wong A, Mok VCT, Leung TW, Wong KSL. Significance of good collateral compensation in symptomatic intracranial atherosclerosis. Cerebrovasc Dis. 2012;33(6):517–24.
5. Awad I, Little JR, Modic MT, Furlan AJ. Intravenous digital subtraction angiography: an index of collateral cerebral blood flow in internal carotid artery occlusion. Stroke. 1982;13(4):469–72.
6. Report of the American Academy of Neurology Therapeutics and Technology Assesment Subcommittee. Assessment: Transcranial Doppler. Neurology. 1990;40:680–1.
7. Qureshi AI, Alexandrov AV, Tegeler CH, Hobson RW, Dennis Baker J, Hopkins LN. Guidelines for screening of extracranial carotid artery disease: a statement for healthcare professionals from the Multidisciplinary Practice Guidelines Committee of the American Society of Neuroimaging; cosponsored by the society of vascular and interven. J Neuroimaging. 2007;17(1):19–47.
8. Muller M, Hermes M, Bruckmann H, Schimrigk K. Transcranial Doppler ultrasound in the evaluation of collateral blood flow in patients with internal carotid artery occlusion: correlation with cerebral angiography. Am J Neuroradiol. 1995;16(1):195–202.
9. Christou I, Felberg RA, Demchuk AM, Grotta JC, Scott Burgin W, Malkoff M, et al. A broad diagnostic battery for bedside transcranial Doppler to detect flow changes with internal carotid artery stenosis or occlusion. J Neuroimaging. 2001;11(3):236–42.
10. Guan J, Lu Z, Zhou Q, Li C, Zhang S. Usefulness of transcranial Doppler ultrasound in evaluating cervical-cranial collateral circulations. Interv Neurol. 2014;2(1):8–18.
11. Zachrisson H, Fouladiun M, Blomstrand C, Holm J, Volkmann R. Functional assessment of high-grade ICA stenosis with duplex ultrasound and transcranial Doppler. Clin Physiol Funct Imaging. 2012;32(3):241–6.

12. Herdera P, Bujdáková J, Traubner P. Effect of collateral flow patterns on outcome of carotid occlusion. Eur J Neurol. 1995;35:212–6.
13. Von Reutern GM, Goertler MW, Bornstein NM, Del Sette M, Evans DH, Hetzel A, et al. Grading carotid stenosis using ultrasonic methods. Stroke. 2012;43:916–21.
14. Kluytmans M, Van Der Grond J, Van Everdingen KJ, Klijn CJM, Kappelle LJ, Viergever MA. Cerebral hemodynamics in relation to patterns of collateral flow. Stroke. 1999;30(7):1432–9.
15. Telman G, Kouperberg E, Sprecher E, Hoffman A, Yarnitsky D. Assessment of ophthalmic artery collateral pathway in the hemispheric cerebral hemodynamics in patients with severe unilateral carotid stenosis. Neurol Res. 2003;25(3):309–11.
16. Alexandrov A, Demchuk A, Wein T, Grotta J. Yield of transcranial Doppler in acute cerebral ischemia. Stroke. 1999;30(8):1604–9.
17. McVerry F, Liebeskind DS, Muir KW. Systematic review of methods for assessing leptomeningeal collateral flow. AJNR Am J Neuroradiol. 2012;33:576–82.
18. Brandt T, Knauth M, Wildermuth S, Winter R, Von Kummer R, Sartor K. CT angiography and Doppler sonography for emergency assessment in acute basilar artery ischemia. Stroke. 1999;30(3):606–12.
19. Ribo M, Garami Z, Uchino K, Song J, Molina CA, Alexandrov AV. Detection of reversed basilar flow with power-motion Doppler after acute occlusion predicts favorable outcome. Stroke. 2004;35(1):79–82.
20. Controni L. II circolo collaterale vertebro-vertebro nell obhterazione dell'artena succlavia alia sua ongine. Minerva Chir. 1960;15:268–71.
21. Reivich M, Holling HE, Roberts B, Toole JF. Reversal of blood flow through the vertebral artery and its effect on cerebral circulation. N Engl J Med. 1961;265(18):878–85.
22. Tsivgoulis G, Ribo M, Rubiera M, Vasdekis SN, Barlinn K, Athanasiadis D, et al. Real-time validation of transcranial Doppler criteria in assessing recanalization during intra-arterial procedures for acute ischemic stroke an international, multicenter study. Stroke. 2013;44(2):394–400.
23. Zaidat OO, Yavagal DR. Endovascular acute ischemic stroke therapy. Neurology. 2012;79(13 Supplement 1):S1 LP-S2.
24. Chesebro JH, Knatterud G, Roberts R, Borer J, Cohen LS, Dalen J, et al. Thrombolysis in myocardial infarction (TIMI) trial, phase I: a comparison between intravenous tissue plasminogen activator and intravenous streptokinase. Clinical findings through hospital discharge. Circulation. 1987;76(1):142–54.
25. Mori E, Yoneda Y, Tabuchi M, et al. Intravenous recombinant tissue plas- minogen activator in acute carotid artery territory stroke. Neurology. 1992;42(5):976–82.
26. Qureshi AI. New grading system for angiographic evaluation of arterial occlusions and recanalization response to intra-arterial thrombolysis in acute ischemic stroke. Neurosurgery. 2002;50(6):1405–15.
27. Higashida RT, Furlan AJ, Assessment T. Trial design and reporting standards for intraarterial cerebral thrombolysis for acute ischemic stroke. J Vasc Interv Radiol. 2003;14(9 PART 2).
28. Bang OY, Saver JL, Kim SJ, Kim G-M, Chung C-S, Ovbiagele B, et al. Collateral flow predicts response to endovascular therapy for acute ischemic stroke. Stroke. 2011;42(3):693–9.
29. Caplan LR, Ka SW, Gao S, Hennerici MG. Is hypoperfusion an important cause of strokes? If so, how? Cerebrovasc Dis. 2006;21(3):145–53.
30. Hennerici M, Hulsbomer H, Hefter H, Lammerts D, Rautenberg W. Natural history of asymptomatic extracranial arterial disease. Brain. 1987;110:777–91.
31. Orlandi G, Parenti G, Bertolucci A, Murri L. Silent cerebral microembolism in asymptomatic and symptomatic carotid artery stenosis of low and high degree. Eur Neurol. 1997;38:39–43.
32. Wong KS, Gao S, Chan YL, Hansberg T, Lam WWM, Droste DW, et al. Mechanisms of acute cerebral infarctions in patients with middle cerebral artery stenosis: a diffusion-weighted imaging and microemboli monitoring study. Ann Neurol. 2002;52(1):74–81.

33. Masuda J, Yutani C, Ogata J, Kuriyama Y, Yamaguchi T. Atheromatous embolism in the brain: a clinicopathlogic analysis of 15 autopsy cases. Neurologia. 1994;44(7):1231–7.
34. Belden JR, Caplan LR, Pessin MS, Kwan E. Mechanisms and clinical features of posterior border-zone infarcts. Neurology. 1999;53(6):1312.
35. Marchal G, Young AR, Baron JC. Early postischemic hyperperfusion: pathophysiologic insights from positron emission tomography. J Cereb Blood Flow Metab. 1999;19(5):467–82.
36. Schoser BGH, Heesen C, Eckert B, Thie A. Cerebral hyperperfusion injury after percutaneous transluminal angioplasty of extracranial arteries. J Neurol. 1997;244(2):101–4.
37. Van Mook WNKA, Rennenberg RJMW, Schurink GW, Van Oostenbrugge RJ, Mess WH, Hofman PAM, et al. Cerebral hyperperfusion syndrome. Lancet Neurol. 2005;4(12):877–88.
38. Bai J, Lyden PD. Revisiting cerebral postischemic reperfusion injury: new insights in understanding reperfusion failure, hemorrhage, and edema. Int J Stroke. 2015;10(2):143–52.
39. Whitworth J. 2003 World Health Organization (WHO)/International Society of Hypertension (ISH) statement on management of hypertension. J Hypertens. 2003;21:1983–92.
40. Qureshi AI, Ezzeddine MA, Nasar A, Suri MFK, Kirmani JF, Hussein HM, et al. Prevalence of elevated blood pressure in 563 704 adult patients with stroke presenting to the ED in the United States. Am J Emerg Med. 2007;25(1):32–8.
41. Willmot M, Leonardi-Bee J, Bath PMW. High blood pressure in acute stroke and subsequent outcome a systematic review. Hypertension. 2004;43(1):18–24.
42. Arboix A, Roig H, Rossich R, Martínez E, García-Eroles L. Differences between hypertensive and non-hypertensive ischemic stroke. Eur J Neurol. 2004;11(10):687–92.
43. Rodríguez-Yáñez M, Castellanos M, Blanco M, García MM, Nombela F, Serena J, et al. New-onset hypertension and inflammatory response/poor outcome in acute ischemic stroke. Neurology. 2006;67(11):1973–8.
44. Wallace JD. Blood pressure after stroke. JAMA J Am Med Assoc. 1981;246(19):2177–80.
45. Mattle HP, Kappeler L, Arnold M, Fischer U, Nedeltchev K, Remonda L, et al. Blood pressure and vessel recanalization in the first hours after ischemic stroke. Stroke. 2005;36(2):264–8.
46. Leonardi-Bee J, Bath PMW, Phillips SJ, Sandercock PAG. Blood pressure and clinical outcomes in the International Stroke Trial. Stroke. 2002;33(5):1315–20.
47. Martins AI, Sargento-Freitas J, Silva F, Jesus-Ribeiro J, Correia I, Gomes JP, et al. Recanalization modulates association between blood pressure and functional outcome in acute ischemic stroke. Stroke. 2016;47(6):1571–6.
48. MacIntosh BJ, Graham SJ. Magnetic resonance imaging to visualize stroke and characterize stroke recovery: a review. Front Neurol. 2013;4(60):1–14.
49. Chalela JA, Kidwell CS, Nentwich LM, Luby M, Butman JA, Demchuk M, et al. MRI and CT in emergency assessment of Pat w/ suspected acute stroke a prospective comparison. Methods. 2007;369(9558):293–8.
50. Thomalla G, Simonsen CZ, Boutitie F, Andersen G, Berthezene Y, Cheng B, et al. MRI-guided thrombolysis for stroke with unknown time of onset. N Engl J Med. 2018:NEJMoa1804355.
51. Lavinio A, Schmidt EA, Haubrich C, Smielewski P, Pickard JD, Sci FM, et al. Noninvasive evaluation of dynamic cerebrovascular autoregulation using Finapres plethysmograph and transcranial Doppler. Stroke. 2007;38(2):402–4.
52. Nogueira RG, Jadhav AP, Haussen DC, Bonafe A, Budzik RF, Bhuva P, et al. Thrombectomy 6 to 24 hours after stroke with a mismatch between deficit and infarct. N Engl J Med. 2018;378(1):11–21.
53. Albers GW, Marks MP, Kemp S, Christensen S, Tsai JP, Ortega-Gutierrez S, et al. Thrombectomy for stroke at 6 to 16 hours with selection by perfusion imaging. N Engl J Med. 2018;NEJMoa1713973.
54. Zaro-Weber O, Moeller-Hartmann W, Heiss WD, Sobesky J. MRI perfusion maps in acute stroke validated with 15O-water positron emission tomography. Stroke. 2010;41(3):443–9.
55. Heiss WD. PET imaging in ischemic cerebrovascular disease: current status and future directions. Neurosci Bulletin. 2014:713–32.

56. Moreau F, Demchuk AM, Dunn JF. Near-infrared measurements of brain oxygenation in stroke. Naurophotonics. 2016;3(3):1–8.
57. Maier IL, Tsogkas I, Behme D, Psychogios M. High systolic blood pressure after successful endovascular treatment affects early functional outcome in acute ischemic stroke. Cerebrovasc Dis. 2018;(January).
58. Levi C, Zareie H, Parsons M. Transcranial Doppler in acute stroke management — a 'real-time' bed-side guide to reperfusion and collateral flow. Pers Med. 2012;1(1):185–93.
59. Backhaus R, Ulrich B. Hyperperfusion syndrome after MCA embolectomy – a rare complication ? Am J Case Rep. 2013;141:513–7.
60. Hacke W, Kaste M, Fieschi C, Von Kummer R, Davalos A, Meier D, et al. Randomised double-blind placebo-controlled trial of thrombolytic therapy with intravenous alteplase in acute ischaemic stroke (ECASS II). Lancet. 1998;352(Ecass Ii).

Chapter 31
Acute Ischemic Stroke in ICU: Monitoring of Arterial Recanalization After Endovascular Treatment (EVT) by Transcranial Doppler (TCD/TCCS)

José I. Suárez

Key Points

1. TCD/TCCS is an important complementary tool in the evaluation and management of patients with acute ischemic stroke.
2. The most important indications for the use of TCD/TCCS in acute ischemic stroke are the detection of arterial occlusions, collateral circulation, arterial stenosis, microembolic signals, and re-occlusions or arterial rethrombosis after post-thrombolysis or post-thrombectomy reperfusion.
3. The addition of TCD/TCCS can lead to changes in therapeutic behavior in 20% of cases with acute ischemic stroke.
4. Sonothrombolysis is not recommended in the management and treatment of patients with acute ischemic stroke.
5. TCD/TCCS is a useful diagnostic test when sufficient resources are not available for the acquisition of advanced diagnostic images or when patients present with clinical instability that makes transfer very difficult.
6. The reliability of the TCD/TCCS depends on the operator and a good acoustic window.

J. I. Suárez (✉)
Division of Neurosciences Critical Care, Departments of Anesthesiology and Critical Care Medicine, Neurology, and Neurosurgery, The Johns Hopkins University School of Medicine, Baltimore, MD, USA
e-mail: jsuarez5@jhmi.edu

C. N. Rodríguez et al. (eds.), *Neurosonology in Critical Care*,
https://doi.org/10.1007/978-3-030-81419-9_31

31.1 Introduction

Transcranial Doppler and transcranial color-coded duplex sonography (TCD/TCCS) are common tools and have has become fundamental elements of the armamentarium in diagnostic and research of neurocritical care and stroke units [1]. TCD/TCCS are noninvasive ultrasound clinical diagnostic methods, which allow determining the speed and direction of local blood flow in the proximal segments of the larger intracranial arteries. As is well known, and analogous to other methods based on ultrasound, the results and interpretation of these depend largely on the operator, and as a corollary, it is important to ensure good training and expertise to obtain reliable results. In most hospitals and academic centers, TCD is operated by technicians or trained medical personnel, and the results are interpreted by vascular neurologists or radiologists specialized in the subject.

The greatest usefulness of TCD/TCCS is in the management and therapeutic decision-making of patients with cerebrovascular diseases or alterations of the intracranial dynamics that entail important alterations of the cerebral blood flow (CBF). All the initial TCD/TCCS validation studies have used cerebral angiography, an invasive method that is not without important risks, as a gold standard and reference in the evaluation of the diameter and permeability of the cerebral arteries and in the measurement of the different degrees of stenosis [2–4]. It follows that TCD/TCCS offer significant advantages for daily clinical practice, among which the following could be listed:

A. The TCD/TCCS examination can be carried out at the patient's bedside as the equipment is portable.
B. Studies can be repeated as required.
C. Continuous monitoring of cerebral blood flow velocities (CBFV) is possible.
D. TCD/TCCS are cheaper than cerebral angiography and associated with minimal risks to the patient.
E. Does not require intravenous contrast (when the acoustic bone window is accessible).

It is also relevant to present the limitations of TCD/TCCS:

A. The results depend on the operator. The operator's expertise is important as in many techniques.
B. It can only measure the CBFV in the most proximal segments of the cerebral arteries. However, changes in the morphology of the CBF velocity waves may suggest distal stenosis or obstruction.
C. It is difficult to obtain reliable results in patients with poor acoustic window.

Finally, it should be noted that other diagnostic modalities, such as CT angiography, also present limitations in the evaluation of the most distal segments of the cerebral vasculature.

In this chapter, we will describe in a practical way the possible indications for TCD/TCCS monitoring in patients who require medical attention after ischemic stroke and emphasize the cases in which endovascular therapy is necessary (Table 31.1).

Table 31.1 Common indications of TCD/TCCS monitoring in patients with acute ischemic stroke

Evidence of cerebral artery occlusion
Detection of microembolic signals
Confirm reperfusion during thrombolysis or endovascular therapy
Monitor the permeability of cerebral arteries
Diagnosis of cerebral artery stenosis

31.2 TCD/TCCS in Acute Ischemic Stroke

TCD/TCCS may be very useful in the evaluation of patients with acute ischemic stroke. The most important findings are the presence of arterial occlusions, collateral circulation, arterial stenosis, microembolic signals, and re-occlusions or arterial re-thrombosis after post-thrombolysis or post-thrombectomy reperfusion.

31.2.1 Acute Cerebral Infarction

TCD/TCCS can serve as an aid to traditional diagnostic imaging tests in the diagnosis and treatment of large caliber cerebral artery occlusions, especially in hospitals with limited resources. A middle cerebral artery occlusion can be detected with a sensitivity and specificity of more than 90% [5]. Although TCD/TCCS have a lower sensitivity than CT angiography for the detection of thrombosis of the terminal segment of the carotid and basilar arteries (33–75%), it is equally specific to CT for the identification of middle cerebral artery occlusion (99–100%).

During the first 4.5 hours of management of patients with ischemic stroke, TCD/TCCS may be an important complement to more advanced imaging techniques. It has been shown that TCD/TCCS can lead to changes in therapeutic behavior in 20% of cases [6]. For example, TCD/TCCS can detect thrombosis of the middle cerebral artery not adequately visualized in CT angiography.

31.2.2 Detection of Microembolic Signals

TCD/TCCS plays an important role in the diagnosis of paradoxical embolism in patients with patent foramen ovale and arteriovenous pulmonary vascular bed fistulas as described in other chapters of this book. To summarize, the test consists of the injection of an ultrasonic contrast medium, usually agitated saline, while the patient, in a dorsal decubitus position, is asked to perform a Valsalva maneuver. If there is a reversal of blood flow from right to left, the TCD/TCCS transducer will detect microembolic signals in the middle cerebral arteries (Table 31.2).

It has been observed that TCD/TCCS is as good as other diagnostic methods for the detection of the patent ovale foramen [7, 8].

Table 31.2 Characteristics of microembolic signals (MES) detected by TCD/TCCS

Characteristic acoustic sound
High intensity amplitude and at least 3 decibels greater than the basal spectrum
Transient signals of short duration and usually less than 300 milliseconds
Unidirectional signals
Detected within the flow spectrum

TCD/TCCS has a higher sensitivity, though less specificity, than echocardiography and allows for a 15–25% additional diagnosis. In other pathologies where microembolic signals can be detected, such as cardioembolic phenomena or carotid stenosis, TCD can be used to monitor these patients [9–11]. It has been shown that up to 43% of patients with symptomatic carotid stenosis present microembolic signals, as opposed to 10% of patients with asymptomatic lesions. In addition, the presence of microembolic signals is an important predictor of stroke 1 year after its discovery by TCD/TCCS even in patients with asymptomatic lesions. The CARESS study (Clopidogrel and Aspirin for Reduction of Emboli in Symptomatic Carotid Stenosis) showed that in 43.8% of patients with symptomatic carotid stenosis and those receiving antiplatelet therapy with aspirin and clopidogrel, microembolic signals could be detected, while in those who only received aspirin, the frequency was 73% [12]. Similar reductions have been reported in patients after endarterectomy [13]. The results of the CARESS study (Clopidogrel and Aspirin for Reduction of Emboli in Symptomatic Carotid Stenosis) showed that in 43.8% of patients with symptomatic carotid stenosis and those receiving antiplatelet therapy with aspirin and clopidogrel microembolic signals could be detected, while in those who only received aspirin, the frequency was 73% [12]. Similar reductions have been reported in patients after endarterectomy [13].

31.2.3 Monitoring During Thrombolysis or Endovascular Therapy

Thrombolytic and endovascular therapies with thrombectomy are established as the most effective for improving the clinical outcomes of patients with ischemic stroke [14, 15]. The role of TCD/TCCS is primarily in the detection of middle cerebral artery occlusion, its reperfusion, and re-occlusion, monitoring of microembolic signals, and documentation and follow-up of cerebral artery stenosis. Initial results from clinical trials using sonothrombolysis, the idea that TCD increases the fibrinolytic effect of rt-PA, demonstrated favorable effects in patients with acute ischemic stroke [4]. However, more recent clinical trials have shown neutral results with respect to clinical improvement, death, and adverse effects compared to the control groups. The use of sonothrombolysis is not recommended in the latest treatment guidelines for patients with acute ischemic stroke [15].

This author recommends the use of TCD/TCCS at the beginning of the evaluation of the patient with acute ischemic stroke to document the initial findings and once treatment is received, intermittent evaluation is continued to ensure that the state of the cerebral vessels has not changed.

31.3 Conclusion

TCD/TCCS may be very useful in the evaluation of patients with acute ischemic stroke. The role of TCD/TCCS is primarily in the detection of middle cerebral artery occlusion, its reperfusion and re-occlusion, monitoring of microembolic signals, and documentation and follow-up of cerebral artery stenosis.

Algorithm

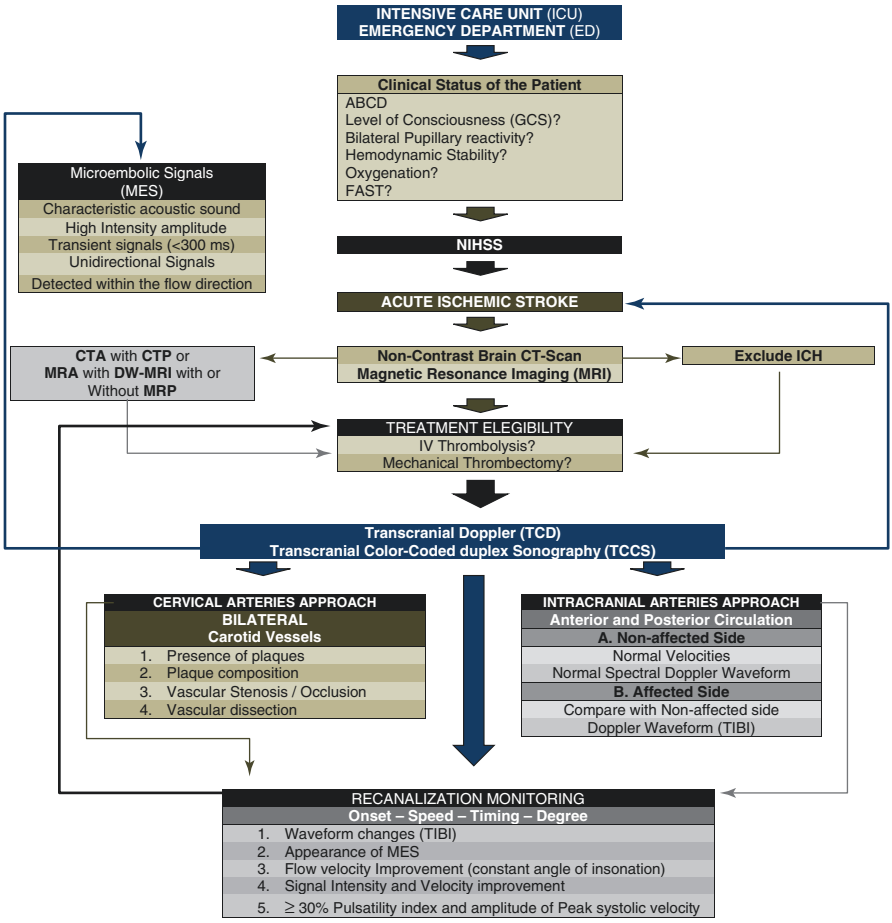

FAST Facial-Arm-Speech-Time, *CTA* Computed tomography angiography, *MRA* Magnetic resonance angiography, *DW-MRI* Diffusion Weighted-Magnetic resonance imaging, *MRP* Magnetic resonance perfusion, *ICH* Intracerebral hemorrhage,*TIBI* Thrombolysis in Brain ischemia, *MES* Microembolic signals

References

1. Sloan MA, Alexandrov AV, Tegeler CH, et al. Assessment: transcranial Doppler ultrasonography: report of the Therapeutics and Technology Assessment Subcommittee of the American Academy of Neurology. Neurology. 2004;62:1468–81.
2. Kargiotis O, Psychogios K, Safouris A, et al. The role of transcranial Doppler monitoring in patients with multi-territory acute embolic strokes: a review. J Neuroimaging. 2019;0:1–14.
3. Kilburg C, McNally JS, de Havenon A, et al. Advanced imaging in acute ischemic stroke. Neurosurg Focus. 2017;42:1–8.
4. Bor-Seng-Shu, et al. Sonothrombolysis for acute ischemic stroke: a systematic review of randomized controlled trials. Neurosurg Focus. 2012;32:1–6.
5. Tsivgoulis G, Sharma VK, Lao AY, Malkoff MD, Alexandrov AV. Validation of transcranial Doppler with computed tomography angiography in acute cerebral ischemia. Stroke. 2007;38:1245–9.
6. Brunser AM, Mansilla E, Hoppe A, Olavarría V, Sujima E, Lavados PM. The role of TCD in the evaluation of acute stroke. J Neuroimaging. 2016;26:420–5.
7. de Havenon A, Moore A, Sultan-Qurraie A, Majersik JJ, Stoddard G, Tirschwell D. Ischemic stroke patients with active malignancy or extracardiac shunts are more likely to have a right-to-left shunt found by TCD than echocardiogram. Transl Stroke Res. 2015;6:361–4.
8. Katsanos AH, et al. Transcranial Doppler versus transthoracic echocardiography for the detection of patent foramen ovale in patients with cryptogenic cerebral ischemia: a systematic review and diagnostic test accuracy meta-analysis. Ann Neurol. 2016;79:625–35.
9. Ritter MA, Dittrich R, Thoenissen N, Ringelstein EB, Nabavi DG. Prevalence and prognostic impact of microembolic signals in arterial sources of embolism. A systematic review of the literature. J Neurol. 2008;255:953–61.
10. Safouris A, Katsanos AH, Kerasnoudis A, et al. Statin pretreatmentand microembolic signals in large artery atherosclerosis. Stroke. 2018;49:1992–5.
11. King A, Markus HS. Doppler embolic signals in cerebrovascular disease and prediction of stroke risk: a systematic review and meta-analysis. Stroke. 2009;40:3711–7.
12. Markus HS, et al. Dual antiplatelet therapy with clopidogrel and aspirin in symptomatic carotid stenosis evaluated using Doppler embolic signal detection: the Clopidogrel and Aspirin forReduction of Emboli in Symptomatic Carotid Stenosis (CARESS) trial. Circulation. 2005;111:2233–40.
13. van Zuilen EV, Moll FL, Vermeulen FE, Mauser HW, van Gijn J, Ackerstaff RG. Detection of cerebral microemboli by means of transcranial Doppler monitoring before and after carotid endarterectomy. Stroke. 1995;26:210–3.
14. National Institute of Neurological Disorders and Stroke rt-PA Stroke Study Group. Tissue plasminogen activator for acute ischemic stroke. N Engl J Med. 1995;333:1581–7.
15. Powers WJ, et al. Guidelines for the early management of patients with acute ischemic stroke: 2019 update to the 2018 guidelines for the early management of acute ischemic stroke: a guidelines for healthcare professionals from the American Heart Association/American Stroke Association. Stroke. 2019;50:e344–418.

Chapter 32
Transcranial Doppler (TCD) and Transcranial Color-Coded Duplex Sonography (TCCS): Defining Collateral Cerebral Blood Flow

Maher Saqqur

Key Points

1. TCD/TCCD may have an important role in defining collateral blood flow (CF) in stroke patients and monitoring of CBF.
2. It is a noninvasive technique and can be utilized repeatedly allowing for changes in the blood flow dynamics as treatment is delivered.
3. The criteria of CBF on TCD and TCCD have been developed and verified.
4. TCD/TCCD is unique monitoring tool of CBF in an acute stroke setting.
5. TCD/TCCD has an evolving role as monitoring tool of therapeutic efficacy in CBF augmentation.

32.1 Introduction

An acute occlusion of the blood flow to the brain leads to rapid and irreversible neuronal injury. The duration of the occlusion and the extent of collateral flow are two of the most important determinants of tissue viability following an acute stroke. Thrombolysis with intravenous (IV) recombinant tissue plasminogen activator (rt-PA) was first shown to be effective in an acute stroke in the mid-1990s and is the most important advance in the management of acute stroke [1–3]. Recently, several major trials utilizing interventional mechanical thrombectomy in properly selected patients with an acute stroke have shown that reperfusion and restoration of blood flow can be offered beyond the time window used for IV rt-PA trials [4–8]. In all trials with IV rt-PA or with mechanical thrombectomy, the response to treatment has

M. Saqqur (✉)
Division of Neurology, Department of Medicine and Department of Radiology, Mackenzie Health Sciences Centre, University of Alberta, Edmonton, AB, Canada

Neuroscience Institute, Hamad General Hospital Doha, Doha, Qatar
e-mail: msaqqur@ualberta.ca

C. N. Rodríguez et al. (eds.), *Neurosonology in Critical Care*,
https://doi.org/10.1007/978-3-030-81419-9_32

been variable with some patients showing excellent recovery, while in others, there was very little or no improvement. The presence of good pial collaterals is one of the most important factors contributing to a better outcome in patients with a successful recanalization [5].

In the endovascular treatment for small core and anterior circulation proximal occlusion with emphasis on minimizing computed tomography (CT) to recanalization time (ESCAPE) trial, the presence of moderate to good collateral flow (CF) defined as the filling of 50% or more of the ipsilateral MCA pial arterial circulation on CT angiography (CTA) when compared to contralateral hemisphere pial vessels was one of the major criteria for inclusion in the study [5]. Several additional studies have also shown that collateral blood flow plays a major role in predicting outcome and saving the arterial bed until the artery is opened with IV thrombolysis or mechanical thrombectomy [9–13].

There are several imaging modalities that can be utilized in defining collateral blood flow at baseline in patients with acute ischemic stroke [14]. Digital subtraction angiography offers the best means for the detection of the pial collateral vessels in patients with acute stroke, but because of its invasive nature, it did not gain widespread popularity. New imaging techniques, especially CTA, can be proven very useful in identifying the pial collaterals [15–19]. CTA, however, is a "snap shot in time," making it difficult to be utilized as a monitoring tool in an acute stroke setting.

Magnetic resonance imaging/MR angiography (MRI/MRA) of the brain has been utilized in defining collateral blood flow in the acute stroke setting [20]. For an example, the Flair hyperintensity and magnetic resonance angiography have been used to grade collateral status and its relation to outcome [21, 22]. The distal hyperintense vessels have a serpentine appearance and might be an indicator of slow retrograde collateral flow [23–25]. However, MRI and MRA are not available in all centers, time consuming and still snap shot in time.

Transcranial Doppler ultrasound (TCD) is an excellent bedside monitoring tool that has the ability to provide noninvasive continuous monitoring of the arterial status while the patient is being treated with IV rt-PA [26–30]. TCD can, in real time, very quickly determine if an occlusion is present [27, 31–33] or if recanalization has been achieved [29, 30, 34]. In addition, there is some suggestion that continuous TCD monitoring may augment the t-PA-induced arterial recanalization effect with a trend toward an increased rate of recovery from the acute stroke [35, 36].

The role of TCD and transcranial color-coded duplex sonography (TCCS) in understanding the flow dynamics following an acute ischemic stroke is evolving [37–42]. In this review, we highlighted the role of TCD and TCCS in detecting collateral flow following an acute ischemic stroke. We also highlighted if the use of TCD and TCCS is helpful in decision-making regarding the type of treatment offered to the patients and if this predicts outcome and long-term prognosis in an acute stroke setting.

32.2 Anatomy of Collateral Blood Flow

There are three principal anatomical features that underlie the collateral perfusion to the brain. The first one consists of extracranial to intracranial collateral communication mainly seen in the presence of internal carotid severe stenosis or occlusion. One of the important collateral circuits includes flow through the ophthalmic (retrograde) and superficial temporal arteries to the intracranial vessels, normally supplied by the internal carotid artery [43]. In the posterior circulation, many anastomoses do exist between the vertebral arteries and the muscular branches at the cervical level. The anterior and posterior spinal arteries also communicate with branches of the proximal intracranial arteries supplying the medulla and pons [44]. Another type of collateral is the persistent trigeminal artery, which is a fetal arterial communication between the basilar and cavernous carotid arteries. This provides collateral flow in the presence of basilar artery occlusion [45]. Only the ophthalmic artery can be imaged by the TCD and TCCS, whereas the rest of the CF are difficult to image.

The second type of collateral blood flow is the circle of Willis CF. This is unique collateral system because there are four major arteries coalesce to form an equalizing distributor, the circle of Willis, which can redistribute blood flow in the event of a sudden occlusion of a parent vessel. The anatomy of the circle of Willis varies between patients and is an important determinant of how well blood flow diversion can occur in the presence of an arterial occlusion. Roughly 50% of individuals have a normal or complete configuration of the circle of Willis. Common variations are, in order of frequency, atretic or string-like anterior or posterior communicating arteries, triplication or duplication of vessels, and a fetal origin of one or both posterior communicating arteries [46]. The presence of any of these abnormalities, particularly atretic communicating vessels, can seriously compromise ability to compensate for sudden occlusions [44]. This type of collateral can be imaged well with TCCS and measured with TCD with confidence. However, there is quite bit of variety in imaging based on the type of anomaly present.

The third type of collateral blood flow is the leptomeningeal or pial anastomoses which potentially provide arterial blood supply to the cortical surface [9, 14, 47]. In these vessels, blood can flow in both directions as a function of the hemodynamic and metabolic needs of the two territories that they connect. The leptomeningeal anastomoses linking distal sections of the major cerebral arteries are small arteriolar connections (~50–400 μm) that allow retrograde perfusion of the adjacent territories [46, 47]. They are important routes for collateral flow, especially in times of acute vascular occlusion. These arteriolar anastomoses join the middle cerebral artery (MCA) with both the anterior cerebral artery (ACA) and posterior cerebral artery (PCA). Anastomoses from the ACA potentially supply the superior or anterior divisions of the MCA, with most collateral flow of posterior or inferior divisions of the MCA arising from the PCA. These pial collaterals are difficult to image with TCCS but can be measured indirectly by TCD.

32.3 Defining Collateral Blood Flow (CF) on TCD/TCCS

A number of studies have reported on the role of TCD in defining changes in CF in the presence of cervical internal carotid artery (ICA) critical stenosis or occlusion [39, 42]; however, data on the utility of TCD in evaluating the blood flow dynamics in patients with acute proximal MCA occlusion is limited [41, 48]. In general, in the absence of an acute or chronic extra cranial or intracranial arterial occlusion, the CF cannot be imaged on TCCS or measured by TCD. Other imaging techniques (DSA, CTA, and MRA) are also handicapped in evaluation of the pial collateral status as these vessels are in a remnant state in the absence of an acute or chronic arterial occlusion [14, 49]. However, when an extracranial or intracranial occlusion or stenosis occurs, a gradient develops in the flow of blood between two arterial beds that have anastomosis [9, 50]. This results in the opening of collateral vascular channels that can be insonated by routine TCD and imaged by TCCS.

Four types of CF can be defined on TCD and TCCS: primary CF, secondary CF, extracranial source of CF, and other types of collateral blood flow [9, 43, 51, 52].

32.4 Primary CF (Circle of Willis Collateral)

32.4.1 Anterior Cross Filling [Anterior Communicating Artery (AcomA)] (Fig. 32.1, Panel a–c)

Anterior communicating artery is one of the main cross filling collateral of the circles of Willis between the bilateral anterior cerebral arteries. It does play major role as an anterior circulation collateral in the presence of ICA critical stenosis or occlusion or terminal ICA occlusion by shifting blood flow from contralateral donor ACA to the ipsilateral reverse ACA into the ipsilateral MCA. Several anomalies can be seen in the AcomA ranging between normal and absent AcomA [53]. Other AcomA anomalies include duplication, triplication, oblique course, hypoplastic, plexiform, dimple, and fused AcomA. In the case of azygous ACA artery, the right and left anterior cerebral arteries joined together to form a single trunk, which entered the median fissure. The detection of congenital abnormalities in the circle of Willis is important. Hypoplasia or the absence of the AcomA can compromise blood flow to the affected hemisphere and may lead to higher risk of stroke due to ICA critical stenosis or occlusion [60, 61].

The presence of anterior cross filling collateral (AcomA) is one of the diagnostic criteria of ICA stenosis or occlusion on TCD [27, 41, 54–56]. The first sign of ICA

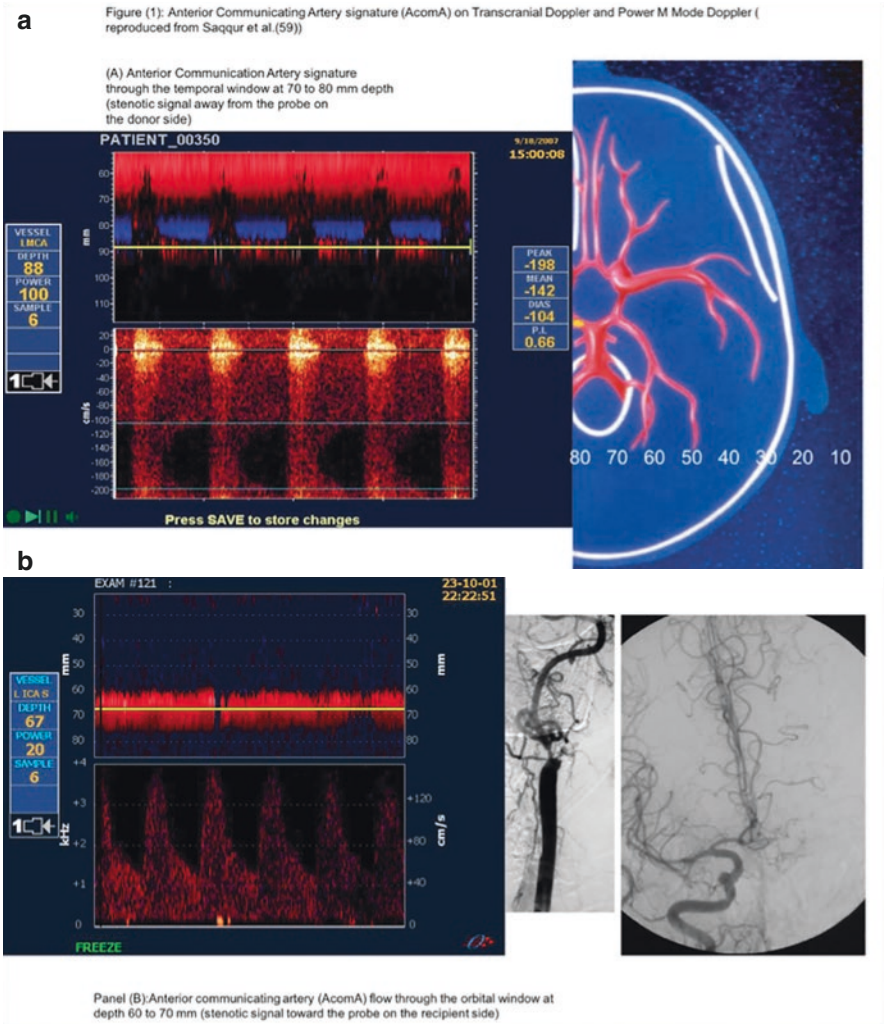

Fig. 32.1 Anterior Communicating Artery signature (AcomA) on Transcranial Doppler and Power M Mode Doppler; Panel (**a**) Anterior Communication Artery signature through the temporal window at 70–80 mm depth (stenotic signal away from the probe on the donor side); Panel (**b**): AcomA flow through the orbital window at depth 60–70 mm (stenotic signal toward the probe on the recipient side); Panel (**c**): Collateral blood flow through anterior communicating artery in the presence of internal carotid artery critical stenosis: (a) delayed flow acceleration of ipsilateral middle cerebral artery (MCA), (b) ipsilateral reverse anterior cerebral artery (ACA) flow, (c) AcomA flow, (d) normal flow in the contralateral MCA, (e) donor ACA

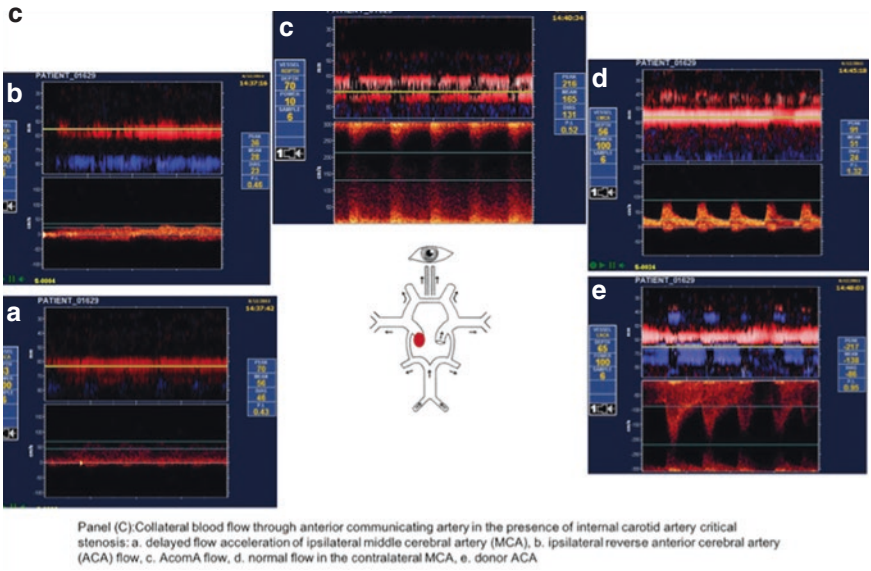

Fig. 32.1 (continued)

critical stenosis or occlusion on TCCS is the reversal of ipsilateral A1 ACA due to anterior cross filling through AcomA from the donor ACA [57] (Fig. 32.1, Panel c).

The AcomA is a small vessel and is not easily be defined on routine TCD. In addition, especially when very small, it may not be functional in many individuals with normal cerebral circulation. Interestingly, in the presence of critical ICA stenosis or occlusion, there is an increase in the flow of blood through the AcomA as it becomes the collateral route of blood supply to the ipsilateral MCA and ACA making it easier to insonate [41, 51, 58]. In addition, AcomA can be defined on power M mode TCD through the temporal window as a stenosis signal at midline at a depth of 70–75 mm or at a depth of 60–65 mm through the orbital window [59] (Fig. 32.1, Panel a, b).

On TCCS, the AcomA has the shape of hourglass. The diameter is smaller in the midsection of the artery than at the junction of A1 segment [57]. On TCCS, the threshold's diameter, allowing for anterior cross flow through the primary collateral arteries of the circle of Willis, is below 1 mm, whereas the threshold for functional AcomA collateral is 0.4 and 0.6 mm [62].

The TCCS with common carotid artery (CCA) compression test allows a real-time evaluation of the AcomA CF [63]. CCA compression test can be performed to evaluate the presence of functional AcomA or PcomA in the absence of ICA disease [56]. Functional AcomA is defined on the CCA compressing test by reversal of the blood flow in the A1 ipsilateral to the compressed CCA, combined with an enhanced blood flow velocity in the contralateral A1 ACA. Both A1 ACA segments can be evaluated by compressing the bilateral CCA vessels.

The CCA compression test can be applied low in the neck just proximal to the sternal head of the clavicle for a maximum of four cardiac cycles. It is important to rule out any significant atherosclerotic disease in the CCA prior to preforming the test, mainly to avoid dislodging plaque during the test [57, 62, 64].

The diagnostic accuracy of AcomA on TCD and TCCS has been tested in several studies. Muller et.al did correlate the CF on TCD with cerebral angiography in the presence of ICA disease [41]. The TCD sensitivity of identifying AcomA was 95%, and specificity, 100%. On TCCS, the sensitivity and specificity for TCCS evaluation of AcomA cross-flow were 100% in one study [64]. In another one, the sensitivity of TCCS for the detection of AComA CF in patients with occlusive carotid artery disease was 98%, specificity was 100%, positive predictive value was 100%, and negative predictive value was 98% [63].

The technical recommendations for defining AComA CF on TCD/TCCS and PMD TCD are summarized in (Table 32.1) [27, 31, 41, 63, 64].

32.4.2 Posterior Communicating Artery (PcomA) (Fig. 32.2, Panel a, b)

The PcomA does originate embryonically from the ICA and connects with the PCA. It plays a major role as a posterior collateral blood flow in the presence of ICA critical stenosis or occlusion or basilar artery occlusion. The PcomA varies extensively in length, diameter, and course. In one autopsy study, the PcomA has a mean outer diameter of 1.2 mm and a mean length of 12.6 mm [65]. In 33% of the cases, the vessel exists only unilaterally, and in more than 50%, abnormalities such as aplasia, hypoplasia, or duplication are demonstrable [66].

On TCD, the blood flow in the PcomA is usually low resistance and directed toward the probe and located posterior to the ICA bifurcation when insonated through the temporal window (it is consistently detected at the depth of 58–68 mm) [27, 31] (Fig. 32.2, Panel a). It can also be visualized through the orbital window on power M Mode (PMD) TCD at the depth of 70–80 mm (Fig. 32.2, Panel b). Its flow can be directed toward or away from the problem depending on the location of the arterial occlusion. However, one of the major challenges in identifying PcomA signal is differentiating between PComA, terminal ICA, and compensatory velocity increase in the posterior cerebral artery (PCA).

In the presence of terminal ICA occlusion beyond the PcomA branching from the ICA, the PcomA flow will usually be away from the probe when insonating through the orbital window since the flow through the siphon ICA will be diverted toward the posterior circulation instead of the anterior circulation due to complete distal ICA occlusion after the PcomA branch (Fig. 32.2, Panel b). Whereas flow will be toward the probe through the temporal window in the presence of cervical ICA critical stenosis or occlusion since the PcomA will be functioning as a posterior

Table 32.1 TCD and TCCS criteria for collateral blood flow

Type of CF	TCD	TCCS	PMD
AcomA (Fig. 32.2 Panel a–c)	1. Elevated A1 ACA MFVs on donor side (iACA > iMCA) or (iACA MFVs ≥1.2 times cACA MFV) + stenotic-like flow at depths 72–78 mm directed away from donor side. A normal or low MFV in A1 ACA of recipient side with or without A1 flow reversal [27, 31]. 2. The CCA compression test demonstrate drop in the iMCA MFV to the occulted ICA side [64].	Reverse iACA on obstructed ICA side. If iACA was missed, iMCA decreased during manual compression of the contralateral CCA [63, 64]	Blue (donor side) and red (affected side) stenotic signal with turbulence flow at depth 75–80 mm through the temporal window aiming anterior
PcomA (Fig. 32.2 Panel e, f)	1. Stenotic signal at depth 55–70 mm via the transtemporal approach when the sonographer switches from ICA bifurcation posteriorly to locate the PCA 2. PSV in P1 PCA > mean value + 2 SD of normal; (C) Ratio of PSV iP1 to PSV P2 PCA > mean ratio + 2 SD of normal 3. Ratio of iP1 PSV to c/l P1 PSV > mean ratio + 2 SD of normal 4. PSV BA > mean value + 2 SD of normal [64]. 5. Anterior to posterior collateral (BA occlusion), flow is directed away from the probe, whereas posterior to anterior collateral (ICA critical stenosis or occlusion), flow is directed towards the probe	1. Color-coded signal of the vessel between the ICA and the precommunicating segment of the PCA 2. Evidence of a pulsatile Doppler signal within the supposed vessel [68]	Blue (donor side) and red (affected side) stenotic signal with turbulence flow at depth 55–70 mm through the temporal window aiming midline Red signal or blue signal through orbital window at depth 80–85 mm

Table 32.1 (continued)

Type of CF	TCD	TCCS	PMD
Reverse BA	1. Detecting low resistance flow signal toward the probe through the transforaminal window at depth 80–110 mm 2. Absent, minimal, dampened or blunted blood flow signal at proximal BA (depth 80–90 mm) indicative of proximal BA occlusion [77]. 3. High-resistance antegrade blood flow in both vertebral arteries 4. Transmitted signals in the PComA and/or the BA in response to CCA tapping in the neck 5. Detection of Doppler signal through temporal or orbital window, PcomAs signals towards the posterior circulation (away from the probe)	1. Color-coded signal of vessel with flow towards the probe at depth 80–100 mm though transforaminal window 2. Evidence of a pulsatile Doppler signal within the supposed vessel	Red signal at depth 80–100 mm through transforaminal window
LMCs	Indirectly measured by flow diversion to iACA or iPCA. (iACA or iPCA >30% analogous artery of contralateral side) and low resistance (pulsatility index <1.2)	1. Color-coded signal of vessel with flow away from the probe at depth <30 mm though temporal window 2. Evidence of a pulsatile low resistance Doppler signal within the supposed vessel	Low resistance blue signal in the distal <30 mm depth on PMD might be an indicative of LMC through temporal window
Reverse OA	1. Low pulsatility flow directed away from the probe via transorbital window at 40–60 mm depth 2. Additional findings may include no substantial difference in MFVs detected in the OA and ICA siphon, high velocities in the ICA siphon, suggesting either a high-grade proximal ICA and/or siphon stenosis, and no flow signals at depths ≥60 mm, suggesting an ICA occlusion proximal to OA origin	Color-coded signal of vessel with flow away from the probe at depth 40 to 60 mm though orbital window and confirmed with conventional Doppler sampling	Low resistance blue signal (flow away from probe) at depth 40 to 60 mm though orbital window

(continued)

Table 32.1 (continued)

Type of CF	TCD	TCCS	PMD
Lenticulostriate Perforator's collaterals	A low-resistance flow at proximal M1 MCA in the presence of abnormal or absent distal M1 or M2 MCA signals Flow is away from the probe and below the baseline on traditional TCD	Color-coded signal of vessel with flow away from the probe at depth 45 to 55 mm though temporal window and confirmed with conventional Doppler sampling as low resistance flow	Low resistance blue signal at depth 45–55 through temporal window
Reverse VA	*Difference in BP between arms of ≥20 mmHg*. At rest: systolic flow reversal (alternating flow signal or absent diastolic flow) in the "stealing" VA as well as a low resistance flow in the donor VA *BP difference between the arms is 10–20 mmHg* and the steal waveforms are not present at rest or flow reversal is incomplete. Hyperemia test: reversal of VA flow during systole or entire cycle		Intermittent red signal in the middle of low resistance blue signal through the transforaminal window
Cerebellar collaterals	Low resistance flow toward the probe were picked up at depth 75–80 mm and 80–90 mm when the probe in the lateral position through transforaminal window	Color coded signal (toward the probe at depth 75–80 mm and 80–90 mm through transforaminal window	Red signal at depth 75–80 mm and 80–90 mm through transforaminal window

MCA middle cerebral artery, *M1* MCA M1 branch, *M2* MCA M2 branch, *ACA* anterior cerebral artery, *PCA* posterior cerebral artery, *P1* PCA P1 branch, *P2* MCA P2 branch, *BA* basilar artery, *VA* vertebral artery, *CCA* common carotid artery, *ICA* internal carotid artery, *OA* ophthalmic artery, *AComA* Anterior communicating artery, *PComA* posterior communicating artery, *LMCs* Leptomeningeal collaterals, *MFV* mean flow velocity, *PSV* peak systolic velocity, *iMCA* ipsilateral MCA, *iACA* ipsilateral ACA, *cACA* contralateral ACA, *CF* collateral flow, *PMD* power M mode Doppler, *SD* standard deviation, *BP* blood pressure

circulation collateral from the basilar artery (BA) to the anterior circulation due to cervical ICA occlusion before the PcomA branching (Fig. 32.2, Panel a).

If PcomA cannot be visualized or measured directly on TCD, it can be defined indirectly as shown by Reinhard et al. [67]. In their study, they defined PcomA indirectly by the presence of increased flow velocity of 50% in the P1 segment of PCA ipsilateral to the ICA stenosis when compared to the contralateral P1 PCA.

On TCCS, the arterial threshold diameter allowing for PcomA collateral flow through the circle of Willis lies between 0.4 and 0.6 mm [57]. In addition, quite often

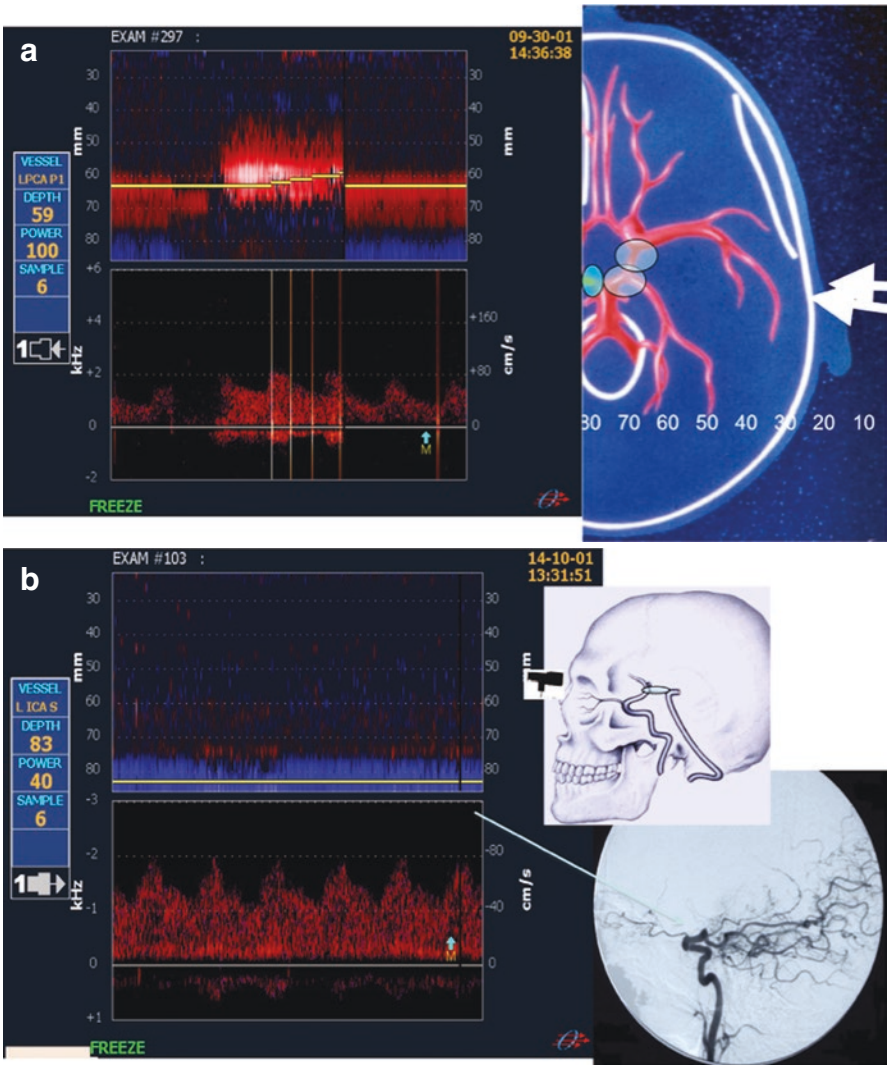

Fig. 32.2 Posterior Communicating Artery signature (PcomA) on Transcranial Doppler and Power M Mode Doppler: Panel (**a**) PcomA signature through the temporal window at depth 50–60 mm (Stenotic signal toward the probe on the affected side); Panel (**b**) Retrograde PcomA Signature through the orbital window in the presence of terminal internal carotid artery occlusion (Stenotic blue signal at depth >80 mm)

the diameter of the PcomA is slightly larger than the AcomA on TCCS. But in general, several studies have shown that communicating arteries with diameter of <0.5 mm should be considered as hypoplastic vessels and difficult to image with TCCS [57].

On TCCS, the functional patency of the PcomA is defined by a peak systolic velocity (PSV) increase of 20% in the PCA P1 ipsilateral to the compressed

CCA. This value is twice as much as would be expected from normal variations seen with physiological activities and related to measurement error [56]. The PSV increase is always measured over the highest peaks on the Doppler spectrum. If the PSV increase in the PCA P1 is less than 20%, the PcomA will be defined as hypofunctional. Velocity measurements are taken proximally in the A1 and P1 with the sample volume set as narrow as possible. It is recommended that measurements in the P1 are taken as close as possible to the top of the basilar artery since this is more informative of the P1 PCA feeding segment to the PcomA than the distal PCA.

One of the pitfalls of TCCS is a misdiagnosis of the anterior choroidal artery for the PcomA. This was less likely because this vessel, which originates close to the PcomA just below the ICA bifurcation, is very small (mean OD, 0.78 mm).

The sensitivity of TCD for the detection of CF via the BA through the PcomA in the presence of ICA stenosis or occlusion was 87% and specificity was 95% [41].

The sensitivity of TCCS for detection of collateral flow through the PcomA in patients with occlusive carotid artery disease was 84%, specificity was 94%, positive predictive value was 94%, and negative predictive value was 84% [63].

The technical recommendations for defining PComA CF on TCD TCCD and PMD TCD are summarized in Table 32.1 [64, 68].

32.4.3 Reverse Basilar Artery Sign and Other Form of Posterior Circulation Collateral

TCD can be used to detect BA occlusion in an acute stroke setting [27]. It can detect flow reversal in the distal part of the BA. This finding is an indicative of collateralization of flow through the posterior communicating arteries and accounts for lower national institute of health stroke scale (NIHSS) at baseline and better outcome at 3 months.

The normal signal of the basilar artery is usually away from the probe via the trans-occipital window at depth 80–110 mm. In the presence of proximal BA occlusion, a pressure gradient developed between carotid anterior circulation and bilateral PCAs and superior cerebellar arteries through the BA blood flow. This leads to flow reversal from the ICA through the PcomAs bilaterally to the BA in order to supply blood to the "distal bed" of the occluded BA. A similar mechanism to improve basilar flow can also develop in the presence of acute bilateral vertebral artery occlusions [69]. Reversal BA sign has also been described in the presence of subclavian steal syndrome due to subclavian artery stenosis or occlusion [70].

The presence of good posterior circulation collateral blood flow is an important determinant for better outcome with interventional and clot retraction [71–73]. The collateral flow to the distal basilar artery comes from the PcomA and this can be insonated with TCD. This "reverse basilar artery sign" as seen on TCD is indicative of good outcome as shown in several studies [74].

Ribo et al. found that patients with reversed BA flow showed lower NIHSS scores on admission (median 4 vs. 15.5, $P = 0.009$), on discharge (2 vs. 21.5, $P = 0.03$) and did not experience neurological deterioration during hospital stay (n = 0 vs. 4, $P = 0.05$) in comparison to patients with BA occlusion who did not have this sign [74]. In addition, there was a trend toward better outcome at 3 months in their study's sample (mRS 1 vs. 4, $P = 0.07$). They concluded that the detection of reversed flow in the distal BA with Power M Mode TCD is associated with lower stroke severity and better outcome after acute basilar artery occlusion.

There are several types of posterior circulation collaterals that can be seen in the presence of BA stenosis or occlusion [75]. Alqadri et al. classified the reverse BA sign into different grading system:

1. *Grade I* represents the presence of retrograde filling of the basilar artery through PCA with filling of the superior cerebellar artery.
2. *Grade II* represents the presence of retrograde filling of the basilar artery through the PCA but no filling of the superior cerebellar artery.
3. *Grade III* is when there are bilateral anastomoses of cerebellar arteries or PCAs.
4. *Grade IV* is when there are unilateral anastomoses of cerebellar arteries or PCAs [75].

Unfortunately, routine TCD is not capable of looking into these variables and TCCS through sub-occipital window might play this role in the future.

Along with reverse BA sign, other variables like increased flow as collateral blood supply in the presence of other type of occlusion can be seen. Zhong et al. studied the increased flow in the basilar artery instead of the reversal BA. They found that increased peak systolic velocity in the BA aside from intrinsic BA stenosis was seen frequently in the presence of ICA or VA stenosis and was suggestive of good collateral blood flow [76].

The technical recommendations for defining reversal BA sign are summarized in Table 32.1 [77].

32.5 Leptomeningeal or Pial Collateral Blood Flow in Acute Stroke (Fig. 32.3, Panel a, b).

The leptomeningeal collaterals (LMCs) are an important source of blood flow to the ischemic brain during acute stroke secondary to occlusion of the proximal MCA or terminal ICA [5, 78–81]. In the presence of anterior circulation proximal arterial occlusion (MCA or terminal ICA), the perfusion pressure in the distal arterial bed drops significantly in comparison to the ipsilateral ACA or PCA. This leads to pressure gradient between these vessels that facilitate the opening of leptomeningeal collateral channels. The speed with which the ischemic tissue progresses to infarction is directly depended on LMCs. Patients with poor collaterals show imaging signs of irreversible ischemic tissue injury very early compared to patients with good collaterals where the injury may not be evident for hours after the insult [14].

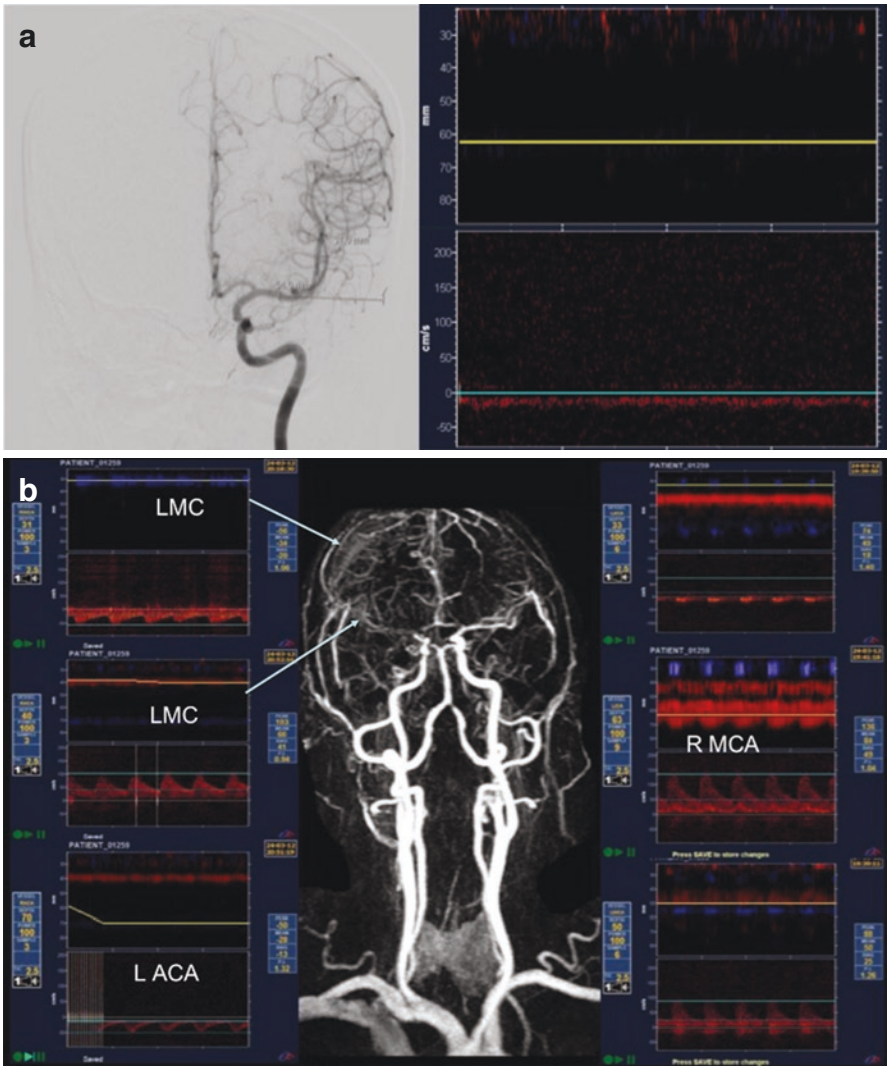

Fig. 32.3 Panel (**a**) (a) CT angiogram axial sections; (b) Cerebral Angiography: left internal carotid injection; demonstrating the vessels insonated at the depths of 20–40 mm on Transcranial Doppler (TCD); (c) the green and orange horizontal bars demonstrates the depths of 30–40 mm and 20–30 mm respectively on TCD. Panel (**b**) Right terminal internal carotid artery occlusion, no ipsilateral anterior cerebral artery flow diversion but patient has Leptomeningeal collaterals (LMC) at the depth of 31 mm and 40 mm. R right, L left, MCA middle cerebral artery, ACA anterior cerebral artery

The correct identification of the LMCs allows for planning of reperfusion therapies and for proper patient's selection for endovascular treatment [5]. The presence of good LMCs also allows for fewer patients to develop thrombolysis-related intracerebral hemorrhage (ICH) [82]. The extent of LMCs can only be identified in the presence of a proximal large vessel intracranial occlusion. It is best identified with conventional digital angiography, CTA, or MRA [16, 24, 83].

TCD/TCCS may be helpful in the bedside evaluation of LMCs in acute stroke. Whereas LMCs cannot be visualized directly on routine TCD, they can be evaluated indirectly by measuring changes in the diverted blood flow to the ipsilateral ACA and PCA that probably supply the LMCs [32, 51, 79]. Kim et al. studied the relation between flow diversion (FD) into the ipsilateral ACA and PCA and leptomeningeal collateral circulation in the presence of proximal MCA occlusion [79]. They defined flow diversion as ipsilateral ACA or PCA flow velocity >30% higher than the analogous artery on the contralateral side with low resistance (pulsatility index <1.2). They found that the sensitivity of flow diversion to ACA or PCA in detecting LMCs was 81%, specificity 76.7%, positive predictive value 70.8%, and negative predictive value 85.2% in comparing to gold standard cerebral angiography. In addition, Kim et al.'s study found that flow diversion showed good correlation with the presence of LMCs in patients with MCA stenosis ($r = 0.568$, $P < 0.001$). Zareie et al. did correlation between flow diversion to ACA in acute ischemic stroke and infarct core on CT perfusion [84]. They found that the presence of flow diversion to ACA (30% increase in flow velocity in comparison to contralateral ACA) and good collateral flow on computed tomography angiography were both independent predictors of admission infarct core volume and 24 hours infarct volume on CT perfusion.

The main limitation of TCD/TCCS in such situations is if the ipsilateral ACA or the PCA are hypoplastic. In such situations, the increased flow velocity may be misinterpreted as collateral flow whereas it is more of dominant ACA or PCA flow. In the presence of dominant ACA or PCA vessel, usually the blood flow will be increased normally to supply both hemispheres. However, this shortcoming can be overcome by putting the TCD finding into clinical contest of acute MCA stroke syndrome.

TCD studies may also be helpful in the study of LMCs in patients with chronic occlusion of the neck arteries. Reinhard et al. studied the spontaneous LMCs in the presence of cervical carotid disease. They found that a mean flow velocity increase of >30% in the P2 segment of the PCA ipsilateral to the ICA stenotic side compared with the P2 segment of the contralateral PCA was an indicator of good LMC and, at the same time, a reduced pulsatility with a side-to-side difference of more than 30% [67]. They did avoid the ACA flow diversion since there was higher chance of the presence of hypoplastic ACA than PCA flow.

The technical recommendations for defining LMCs on TCD and TCCS are summarized in Table 32.1.

32.6 Extracranial Source of Collateral Blood Flow (CF)

32.6.1 Reverse Ophthalmic Artery (Fig. 32.4)

In normal conditions, the flow direction of ophthalmic artery (OA) is antegrade since the internal carotid artery feeds it. In the presence of critical ICA stenosis or occlusion, OA becomes a collateral channel from the external carotid artery to the internal carotid artery and imaged by TCD as reverse OA sign. A reversal of flow in the OA reflects opening of collateral vessels and was first described by Moniz et al. among patients with ICA disease. This sign can be identified easily with TCD [85]. The transorbital approach is used for insonation of the OA and carotid siphon [86]. This window can be reliably insonated in all patients unlike the transtemporal bone window, which may be absent in up to 15%.

The OA can be insonated through the orbital window at a depth of 40–60 mm (Fig. 32.4). However, at shallower depths (<40 mm), interpretation of the imaging can become less reliable as the readings may be from the insonation of OA branch arteries.

A previous transcranial color duplex ultrasonography study in the non-acute setting suggested that a reversed OA flow is specific in predicting ICA stenosis greater than 80% [87]. A single gate spectrogram study of reversed OA flow revealed 48% sensitivity and 100% specificity for identifying ICA stenosis greater than 70% [88].

Fig. 32.4 Normal and reversed Ophthalmic Artery (OA) on Power M Mode (PMD) and spectrogram. Reversed OA flow through the orbital window: Low pulsatility flow directed away from the probe (blue signal) via transorbital window at 40–60 mm depth. The signal is obtained through the orbital window by aiming the probe medially

In a study from our group, reversed OA sign was evident on TCD monitoring in 70.5% of the cases with ICA occlusion [27].

Wilterdink et al. studied a battery of seven TCD findings in patients with various degree of ICA stenosis (reversed ipsilateral OA, reversed flow in the ipsilateral ACA, elevated flow velocity (> 80 cm/s) in the contralateral ACA, absence of Doppler signal in the ipsilateral OA or carotid siphon, and diminished pulsatility index or flow acceleration in the ipsilateral MCA). They found that reversed OA and absent OA had the highest specificity (100%) among these parameters with 48% and 3% sensitivity, respectively, for ICA stenosis >70% [88]. However, the combination of reversed OA sign with the other TCD parameters had a much higher sensitivity (95%) than any one investigatory measure alone. Finally, Kisler et al. studied TCD criteria for hemodynamically significant ICA stenosis based on residual lumen diameter calculated from en bloc endarterectomy specimens [89]. They found that for the transorbital approach, the strongest indicator of a residual lumen diameter <1.5 mm was the reversed flow in the ipsilateral OA and a >50% peak systolic velocity difference between the carotid siphons (distal ICAs) in patients with unilateral ICA origin stenosis.

Our group demonstrated the utility of the TCD orbital window at depth of 50–60 mm for identifying a reversed OA in acute stroke setting with higher specificity (100%) and sensitivity (75%) for ICA occlusion or critical stenosis than the previous studies [59]. In addition, we did demonstrate a unique TCD finding that when the OA flow direction is antegrade, the MFV and PI could discriminate patients who have critical carotid stenosis or occlusion. The pathophysiology is related to the arterial flow patterns. When the ICA is occluded, antegrade flow through the OA is from the anterior and/or posterior communicating arteries which provides low-volume and low-pressure flow resulting in a low MFV and PI.

It is important to remember that the reverse flow in the OA can change over time. A longitudinal study of collateral flow patterns in the circle of Willis and OA in patients with symptomatic ICA occlusion, completed by Rutger et al. [90], showed that most of patients with unilateral ICA occlusion had reversed OA sign in the first 6 months after the ischemic event. In the follow-up investigation of these patients, this percentage decreased significantly.

Few studies have shown that the OA flow is a major contributor to cerebral circulation [91]. However, other studies suggested that the reverse OA flow is the last resort of collateral blood flow circulation in ICA disease [92, 93] and that it may be an indicator of a poor long-term prognosis [94].

The technical recommendations for defining reverse OA sign on TCD/TCCS and PMD are summarized in Table 32.1.

Common sources of error include shallow or deep OA insonation, vessel identification problems (vein, branching and anastomosing arteries in the orbit), ICA dissection with considerable residual flow, terminal ICA occlusion distal to the OA origin, and retrograde filling of the ICA siphon with normal OA direction. Furthermore, a normal OA direction does not rule out the proximal ICA stenosis.

32.7 Other Types of Cerebral Collaterals that Can Be Measured by TCD/TCCS

32.7.1 Reverse Vertebral Artery

The direction and pattern of flow in the vertebral artery (VA) can be very helpful in determining the presence of collaterals in the posterior circulation. The transforaminal window is used for the insonation of the VA and the BA. Insonation performed at a depth of 75 mm depth to locate the terminal VA and BA. Insonation of the BA is performed distally along its course (range 80–100 mm), followed by assessment of the more proximal left and right VAs at depths of 50–80 mm by lateral probe positioning. The normal signal of VA is usually low resistance flow away from the probe.

The presence of subclavian artery or innominate artery severe stenosis or occlusion results in a reversal of the blood flow in the VAs to feed the subclavian artery distal to the stenosis or occlusion (subclavian steel syndrome) [95–97]. A few cases have been documented where a reversal of the BA flow was also seen as a collateral blood flow from the anterior circulation that diverted to the distal subclavian arterial bed. This occurred most often in the presence of contralateral VA stenosis or hypoplasia [70, 98]. However, Harper et al. have demonstrated that the intracranial anterior circulation flow via the BA is an infrequent contributor to the collateral blood flow in the distal subclavian artery stenosis or occlusion. The majority of blood is diverted from the unaffected vertebral artery [98]. Rarely, especially in the presence of contralateral hypoplastic or occulted VA, collateral blood flow can develop from the external carotid artery branches including the occipital, thyrocervical, and costocervical trunks through the muscle branch to the ipsilateral VA [97]. However, these branches cannot be insonated by TCD or TCCS.

TCD can be very useful in the diagnosis of subtle subclavian steal syndrome. The "provocative ischemia test" is ischemia induced in the arm ipsilateral to the site of subclavian steal by the inflation of a brachial blood pressure cuff to supra-systolic pressure for 1–3 minutes. After the 3-minute period, the cuff is deflated while the ipsilateral vertebral and basilar artery velocities' waveforms are monitored for 30 seconds to 1 minute to document any changes in the velocity or direction of the blood flow in comparison to baseline. In normal circumstances, no change in the VA or BA flow is noted. Whereas, in the presence of subclavian artery stenosis or occlusion, a reversal VA or BA flow will be noted.

The severity of subclavian artery stenosis can be estimated based on the TCD findings. In the presence of mild to moderate subclavian artery stenosis, VA flow may be normal. In the presence of moderate subclavian artery stenosis, systolic deceleration of the VA or reversal of flow direction during the systolic period is evident. In addition, reversal of VA flow may be seen only during the provocative ischemia testing. Finally, in the presence of severe stenosis or occlusion of subclavian artery stenosis, the VA flow is reversed during the entire cardiac cycle.

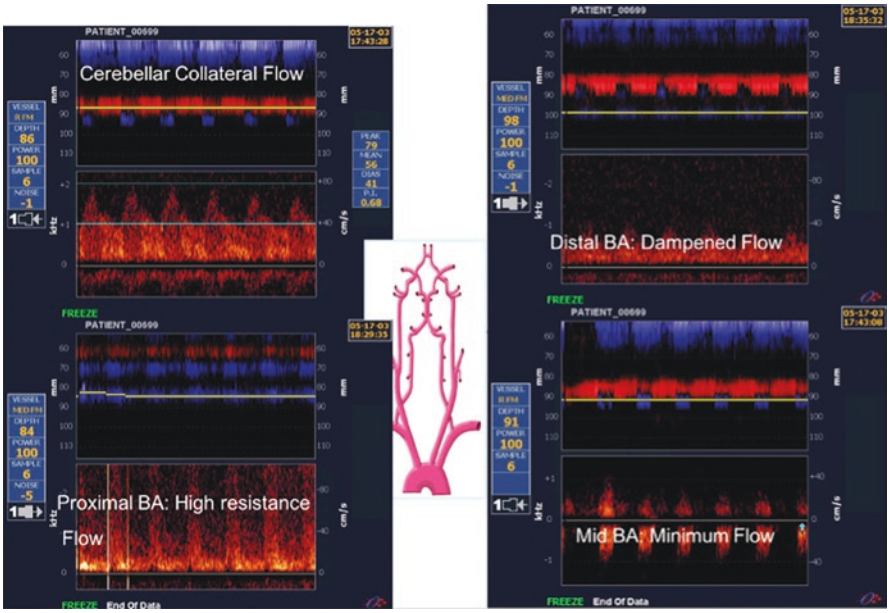

Fig. 32.5 Power M Mode/Transcranial Doppler showed mid basilar artery (BA) occlusion: cerebellar collateral arteries are seen at depth 84 mm (most likely from anterior inferior cerebellar artery branch)

The technical recommendations for defining reverse OVA signs on TCD/TCCS and PMD are summarized in Table 32.1.

32.7.2 Cerebellar Collaterals (Fig. 32.5)

Cerebellar collaterals through the augmentation of blood flow in the SCA AICA and PICA vessels usually developed in the presence of chronic BA occlusion [99]. TCD/TCCS and PMD-TCD may be helpful in determining the existence of such collaterals [75, 99].

The technical recommendations for defining cerebellar collaterals on TCD/TCCS and PMD are summarized in Table 32.1.

32.7.3 Lenticulostriate Perforator's Collaterals (LPC) (Fig. 32.6)

The presence of lenticulostriate collateral arteries is well described in the presence of Moyamoya disease as well as in the presence of proximal MCA occlusion as flow diversion to the perforators [27, 100].

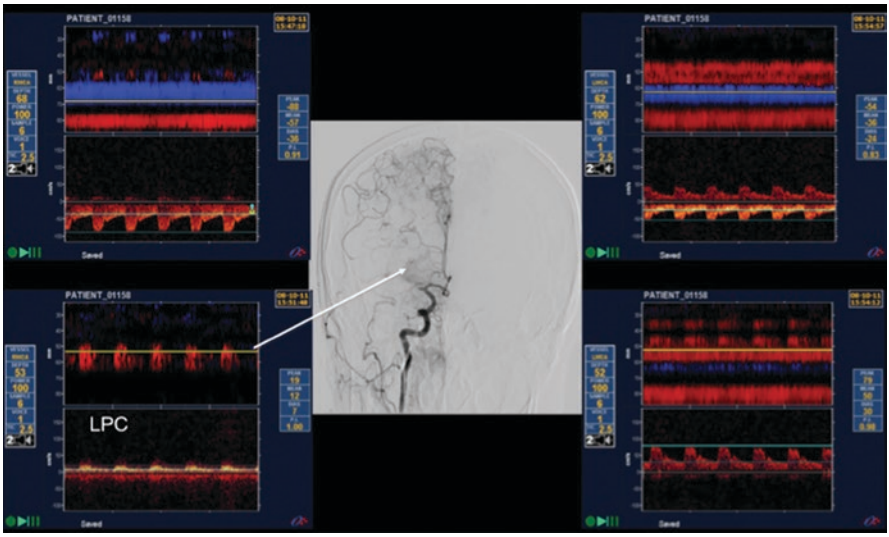

Fig. 32.6 Right Middle Cerebral Artery occlusion with flow diversion in the Anterior cerebral artery and lenticulostriate Perforator's collaterals (LPC) seen at depth 50 mm as low resistance blood flow below baseline

The technical recommendations for defining LPC on TCD/TCCS and PMD are summarized in Table 32.1.

32.8 The Limitations of Routine TCD/TCCS in Defining Collateral Blood Flow

TCD is very useful in defining blood flow in large vessels. However, there are situations where TCD may not allow for evaluation of the local circulation and blood flow. TCD is of limited value in the presence of poor or absent temporal window.

The role of TCCS is well established in defining CF in patients with limited temporal window. The images of TCCS can be enhanced by using echo contrast material [101]. Ghan et al. showed that echo-enhanced TCCS enables the study of collateral blood flow through the communicating arteries of the circle of Willis with high sensitivity and specificity in patients with obstructions of the internal carotid artery and limited acoustic bone windows [101]. They found that the echo-enhanced TCCS detected the collateral blood flow through the anterior communicating artery in 16 of 18 patients (sensitivity 89%, 95% CI: 65–99%). For the posterior communicating artery, sensitivity was 11/14 (79%, 95% CI: 49–95%) and specificity was 15/16 (94%, 95% CI: 70–100%).

In addition, TCCS combined with (CCA) compression tests allows real-time evaluation of the collateral ability of the circle of Willis as mentioned above [57, 63, 102, 104].

Hoksbergen et al. did study the CF on TCCS with the CCA compression test in correlation to autopsy [57, 103]. In their study, the CCA test was performed in the

absence of ICA critical stenosis or occlusion [56]. They found that the threshold diameter allowing for cross-flow through the primary collateral arteries of the circle of Willis is between 0.4 and 0.6 mm on TCCS.

32.9 The Role of TCD/TCCS as Monitoring Tool of Collateral Blood Flow

In an acute ischemic stroke (AIS) setting, TCD and TCCS can play a major role in defining and monitoring arterial occlusion and CF and as a monitoring tool of CF during the augmentation therapy.

32.9.1 TCD/TCCS as a Diagnostic Tool of Arterial Occlusion and Collateral Flow in an AIS

TCD and TCCS is a better tool than other imaging modalities for the monitoring of CF in an acute stroke setting [105–111]. After defining an arterial occlusion, CF can be quickly defined and monitored during thrombolysis.

For an example, in the presence of proximal MCA occlusion, TCD and TCCS can easily define the type of flow at the occlusion site and flow diversion to the ipsilateral vessels in few minutes as long as the patient has adequate temporal windows [26, 38].

In the presence of ICA occlusion, usually the TCD test takes longer since more CF vessels need to be defined (AcomA, PcomA, reverse ACA, reverse OA) [112].

In the presence of VB occlusion, the diagnostic accuracy varies based on the position of the patient and if he is on ventilator or not where it is difficult to flex the neck in order to obtain good sub-occipital window imaging. The main CFs that can be monitored is the reverse BA, reverse VA, and possible cerebellar collateral.

In Table 32.2, we summarized the recommended TCD and TCCS protocol to perform in an acute stroke setting to define arterial occlusion and CF based on the type of occlusion.

32.9.2 TCD/TCCS Predicts Outcome in an AIS Based on Collateral Flow

TCD and TCCS have unique role in monitoring the CF in an acute stroke setting noninvasively and this can play role in predicating clinical outcome and final infarct volume in an acute ischemic stroke based on CF finding on TCD as it showed in several studies [14, 18, 37, 38, 113–115]. In addition, the presence or absence of good CF in an acute ischemic stroke does predict response to IV thrombolysis and risk of hemorrhagic transformation after IV thrombolysis [18].

Table 32.2 The recommended TCD and TCCS protocol to perform in an acute stroke setting to define collateral flow (CF) based on the type of occlusion

Type of arterial occlusion	CF on TCD TCCS PMD
Proximal MCA	Flow diversion to iACA, iPCA LPC LMC
Cervical ICA	Reverse OA AcomA PcomA Donor ACA Reverse iACA
Terminal ICA	Absent OA AcomA PcomA (from post circulation to anterior circulation) LMC
BA	PcomA (from anterior circulation to posterior circulation) Reverse BA Cerebellar collaterals (through SCA AICA and possible PICA)
VA	Reverse VA Cerebellar collateral (through PICA)
SCA stenosis	Reverse iVA at rest or during hyperemia test

MCA middle cerebral artery, *ACA* anterior cerebral artery, *PCA* posterior cerebral artery, *BA* basilar artery, *VA* vertebral artery, *PICA* posterior inferior cerebellar artery, *AICA* anterior cerebellar artery, *SCA* superior cerebellar artery, *ICA* internal carotid artery, *OA* ophthalmic artery, *AComA* Anterior communicating artery, *PComA* posterior communicating artery, *LMCs* Leptomeningeal collaterals, *LPC* lenticulostriate Perforator's collaterals, *iMCA* ipsilateral MCA, *iACA* ipsilateral ACA, *iVA* ipsilateral VA, *PMD* Power M Mode, *CF* collateral flow

Labiche et al. examined 75 patients with proximal MCA on TCD pre-IV rt-PA and for up to 2 hours thereafter to determine the recanalization rate [37]. They found that patients with detectable residual flow signal at the occlusion site before the administration of IV rt-PA bolus were twice as likely to have complete recanalization (41%) compared with those with no detectable residual flow (19%). This earlier reperfusion was associated with reduced infarct volume and improved clinical outcome.

Kim et al. showed that patients with proximal MCA occlusion and flow diversion to both the anterior and posterior circulation had a greater early recovery when treated with IV rt-PA than the ones without flow diversion [79].

Our group has previously studied the role of residual blood flow at the occlusion site measured by the TIBI grading system in predicting short- and long-term outcome in IV rt-PA-treated patients [38]. We found that the pretreatment residual flow at the intracranial occlusion predicts the likelihood of complete recanalization, time of recanalization, and long-term clinical outcome. The lack of detectable residual flow at the occlusion's site is indicative of less chance of achieving recanalization and recovery with systemic thrombolysis. The findings in the present study are in keeping with the observations from our previous research. Patients who had augmentation of their residual blood flow at the occlusion's site had better outcome compared to those without similar augmentation. We proposed that the presence of

residual blood flow at the occlusion site most likely feeds into the lenticulostriate arteries as a form of collateral blood flow or the distal ischemic bed beyond the clot.

Defining CF noninvasively in an acute stroke setting is very critical in planning further interventional therapy [6, 15, 80, 116]. For an example, in the presence of proximal arterial occlusion on TCD and lack of good CF, this is an indicative of poor chance of response to mechanical therapy as shown in several studies [13, 80, 117]. Whereas in the presence of proximal arterial occlusion with good CF on TCD is an indicative of a good response to interventional therapy. This hypothesis needs to be tested in future prospective studies with multiple imaging modalities.

In addition, several studies have shown that the hemodynamic of CF in an acute stroke is not of static condition and varies with the timing from stroke onset and might lead to collateral failure [118]. These changes in the collateral blood flow, which sustain brain viability distal to arterial occlusion, may impact infarct evolution and final infarct volume [119]. TCD is an ideal tool in that case since the CF can be monitored on a continuous base and not just a snap shot in time. Future studies are needed where CF can be monitored in an acute ischemic stroke and define the term of collateral failure on TCD as a major cause of clinical deterioration and enlargement of the infarct volume.

32.9.3 TCD/TCCS as a Monitoring Tool for Therapeutic Augmentation of CF in AIS Setting

Lately, there has been an evolving interest in developing new modalities of treatment by enhancing CF in an acute stroke setting with the main aim of avoiding collateral failure and save the distal ischemic bed until the artery open [120–122]. One of the major challenges is finding a homodynamic imaging modality that can monitor the CF during augmentation. It needs to be at bedside, noninvasive, and able to be repeated frequently. TCD is an ideal in this condition as long as the CF measurements are consistent, accurate, and not operator dependent.

One of the examples regarding TCD role in monitoring treatment's efficacy in enhancing CF is the role of TCD in the NeuroFlo™ device. The NeuroFlo™ device is an intravascular catheter that partially restricts the lumen of the abdominal aorta in stroke patients who failed to respond to thrombolysis [120, 123, 124].

In our small study, we demonstrated that TCD could measure changes in blood flow while the NeuroFlo™ device is being inflated in the abdominal aorta [123]. In this study, patients with neurological deficits following thrombolysis were treated with partial aortic occlusion. TCD was used to measure arterial flow velocities at baseline, before, and during balloon inflation at the occlusion site.

We showed that if there is an increase in blood flow at the occlusion site during the procedure, this might predict better recovery (Fig. 32.7). Patients in whom MFV increased by at least 35% at the site of occlusion had good clinical outcome at 90 days. In contrast, the change in MFV at the occlusion site in patients with poor outcome was always <15%.

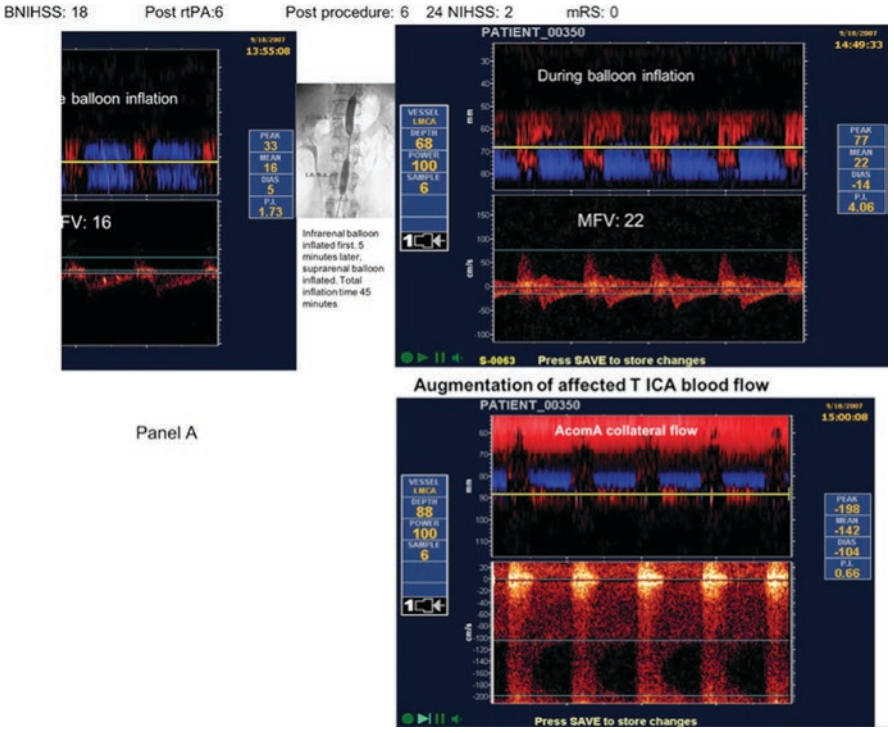

Fig. 32.7 Two examples of patients with terminal internal carotid artery (TICA) occlusion that treated with intravenous (IV) tissue plasminogen activator (tPA), then intra Aorta Balloon procedure (IABP) as augmentation collateral blood flow method
Panel (A) Patient had left TICA occlusion: He underwent IV tPA then IABI collateral blood flow procedure with good long-term outcome (3 months mRS = 0). Anterior communicating artery (AcomA) collateral blood flow developed during the IABI procedure with augmentation in the blood flow at the occlusion site. MFV Mean flow velocity, mRS modified Rankin scale

In our study's sample, three patients developed anterior cross filling collaterals (anterior communicating artery) during the procedure, and two of them had good long-term outcome.

Our case series suggests several potential mechanisms whereby the NeuroFlo™ device may increase blood flow to the ischemic tissue:

1. Augmenting the blood flow through the lenticular striatal arterial collaterals: The affected MCA EDV was augmented during the balloon inflation, which may be an objective measure of enhanced flow through the lenticular striatal collaterals. In our case series, this was indicative of good outcome.
2. Augmenting the blood flow at the site of the clot: The MFV at the occlusion's site was augmented during balloon inflation, which may suggest enhancement of blood flow to the distal bed beyond the clot.
3. Augmenting the blood flow through the circle of Willis collateral (AcomA and PcomA).

4. The NeuroFlo™ device may enhance the blood flow through the leptomeningeal collateral by augmenting the contralateral MCA blood flow or ipsilateral ACA or PCA blood flow.

Out study provides a very good example where TCD measurements of CF were used as a surrogate marker of the successful collateral flow augmentation in an acute stroke setting [123]. The invasive nature of our NeuroFlo™ device might make it more applicable as an adjunct therapy in the future interventional treatment for augmenting collateral tool in an acute stroke setting. Ideally, adjunct TCD can help monitor the efficacy of this model of treatment.

There are several noninvasive tools that have been tested regarding enhancing cerebral blood flow. One of these tools is the external counterpulsation device (ECP), which is a noninvasive method of improving the brain's perfusion. It operates by applying ECG-triggered diastolic pressure of approximately 250 mm Hg to the lower extremities by means of air-filled cuffs. The diastolic augmentation of the blood flow and the simultaneously decreasing systolic afterload therefore increases blood flow to the heart, brain, and kidneys [125]. This device has been tested lately in a randomized crossover trial of ECP treatment consisted of 35 daily 1-hour sessions and it did show that ECP-induced brain perfusion augmentation may subsequently result in a favorable outcome when applied early week 1–7 after ischemic stroke than later [122]. The possible mechanism is that ECP may increase collateral perfusion either by releasing vasodilating factors, such as nitric oxide, or by factors related to angiogenesis, such as vascular endothelial growth factors [126]. This model of treatment has never been tested with TCD or TCCS and is worthwhile considering for future trials.

32.10 TCD AND TCCS Role in Subacute Stroke

TCD and TCCS can play a role in defining CF in the subacute stroke setting mainly by predicting stroke recurrence and clinical outcome.

First, defining CF on TCD and TCCS by itself in subacute stroke can play role in predicting short and long-term outcome in the presence of arterial occlusion. Previous studies have shown that the presence of CF on cerebral angiography is associated with less risk of stroke or TIA in the presence of ICA stenosis [127]. In addition, the development of border zone stroke in the presence of ICA critical stenosis or occlusion does correlate with the presence of CF mainly AcomA and PcomA [127–129].

From that prospective, defining CF on TCD can help in predicting outcome in the presence of ICA stenosis or dissection.

For an example, in the presence of ICA dissection, the presence of CF can predict outcome as shown in Silvestrini et al.'s study [130]. In their study, TCD was used to investigate collateral blood vessels in a study of 66 patients with cervical arterial dissection. Flow velocity was systematically measured within the ophthalmic, anterior, and posterior communicating arteries. Good collateral status was

reported if two or all three vessels were recruited within 24 h of the stroke onset. The researchers used TCD to judge collateral status within 24 h of a stroke secondary to carotid dissection and showed how this noninvasive technique could help to establish the long-term prognosis in such patients. Forty of 66 patients had good collaterals, and less than 5% of these patients had a score on the modified Rankin scale of more than one at 90 days, compared with 77% of patients with poor collaterals. Patients with good collaterals were younger, were more likely to be men, and had a lower NIHSS at time of admission than those with poor collaterals.

Second, in patients with TIA or stroke associated with internal carotid artery (ICA) occlusion, the risk of (recurrent) stroke before the era of rigid control of vascular risk factors was reported to be 5–6% per year [131]. This risk was estimated to be two times higher in patients in whom hemodynamic compromise was demonstrated [132]. TCD and TCCS do play role in evaluating cerebral autoregulation in the presence of ICA stenosis or intracranial stenosis [60, 67, 133]. The hemodynamic reserve can be estimated by measuring cerebrovascular reactivity induced by breathing CO_2 and pressure autoregulation by analyzing spontaneous slow fluctuation in arterial pressure and MCA blood flow velocity.

In the presence of ICA critical stenosis or occlusion, autoregulation of the distal intracranial vasculature will maximally dilate the cerebral arterioles to maintain cerebral blood flow to compensate for the proximal occlusion. With further reduction in cerebral perfusion pressure and maximally dilated arterioles, the cerebral blood flow will also decrease and potentially increase the risk of stroke. A recent meta-analysis on cerebrovascular reserve capacity and the risk of future stroke in symptomatic and asymptomatic patients with carotid stenosis or occlusion demonstrated an association between CO_2 reactivity and the risk of future ischemic events [134]. In addition, the CO_2 reactivity correlates well with the presence of white matter disease as it is shown in one study [135].

There have been two main approaches to measuring cerebral vasomotor reactivity (VMR). One approach attempts direct cerebral blood flow measurements of the brain tissue with flow sensitive imaging techniques such as positron emission tomography, nuclear medicine techniques, CT perfusion, or MR perfusion before and after a vasodilator stimulus. The second approach involves transcranial Doppler measurement of flow velocities (typically in the middle cerebral artery) distal to a lesion both before and after a vasodilator stimulus with the increased flow velocity considered a surrogate for CVR. Vasodilator stimuli include increasing levels of CO_2 (such as with breath-holding or inhalation of CO_2 gas mixtures) and pharmacological challenge with acetazolamide [136–138].

Vernieri et al. did evaluate the relationships between type and number of collateral pathways, cerebral vasomotor reactivity (VMR), and outcome of patients with carotid occlusion [139]. In their study, the cerebral VMR to hypercapnia was evaluated by means of the breath-holding index (BHI) at the beginning of the observation period. The index is obtained by dividing the percent increase in mean flow velocity (MFV) that occurs during breath-holding by the length of time (30 seconds) that subjects hold their breath after a normal inspiration (Eq. 32.1):

$$\left[\left(\text{MFV at the end of breath} - \text{holding} - \text{rest MFV}\right) / \text{rest MFV}\right] \times 100 / \text{seconds of breath} - \text{holding}. \tag{32.1}$$

They did evaluate the presence of following CF: reverse OA, AcomA, and PcomA. In their sample, patients with normal VMR and full collateral development; in this group, no patient experienced an ischemic event. On the other hand, an impaired VMR and increased probability of experiencing a stroke were found in patients without collateral pathways. The annual risk of ipsilateral stroke in this group was 32.7%. Patients with one or two collateral pathways showed a different VMR ranging from normal to strongly reduced BHI values. The ipsilateral stroke event risk was 17.5% in patients with one collateral vessel and 2.7% in patients with two collateral pathways. In these cases, the risk of cerebrovascular events occurring during the follow-up period was significantly related to VMR.

The VMR was not only reduced in the presence of extracranial ICA steno-occlusive disease but also in the presence of intracranial disease as shown by Lee et al. [134]. They measured the VMR in the presence of MCA stenosis, by using the BHI with MCA MFV measurement at depth 50–60 mm on TCD. In their study, the MFV of MCA were recorded at 10 s before rebreathing (pre-MFV) and at a steady state (post-MFV) where end-expiratory CO_2 levels reached a plateau of 45% or more.

The VMR was calculated as percentage MFV changes: (Eq. 32.2)

$$\left[\left(\text{Post} - \text{MFV} - \text{pre} - \text{MFV}\right) / \text{pre} - \text{MFV}\right] \times 100 \tag{32.2}$$

They found that the VMR was reduced in patients with MCA stenosis without ipsilateral ICA stenosis. The decrement of VMR was well correlated with the severity of stenosis and MCA stenosis per se was an independent predictor of reduced VMR.

In conclusion, a novel role of TCD and TCCS, as defining CF in an acute stroke setting and monitoring that, is evolving. It is a noninvasive technique and can be utilized repeatedly allowing for changes in the blood flow dynamics as treatment is delivered in an acute stroke setting. The utilities of defining CF in an acute stroke setting plays a role not only in predicting clinical outcome but also in monitoring the treatment efficacy of the augmentation of CF. Further studies are needed to support that novel role.

32.11 Conclusion

TCD/TCCS may have an important role in defining collateral blood flow (CF) in stroke patients. It is a noninvasive technique and can be utilized repeatedly allowing for changes in the blood flow dynamics as treatment is delivered.

Algorithm

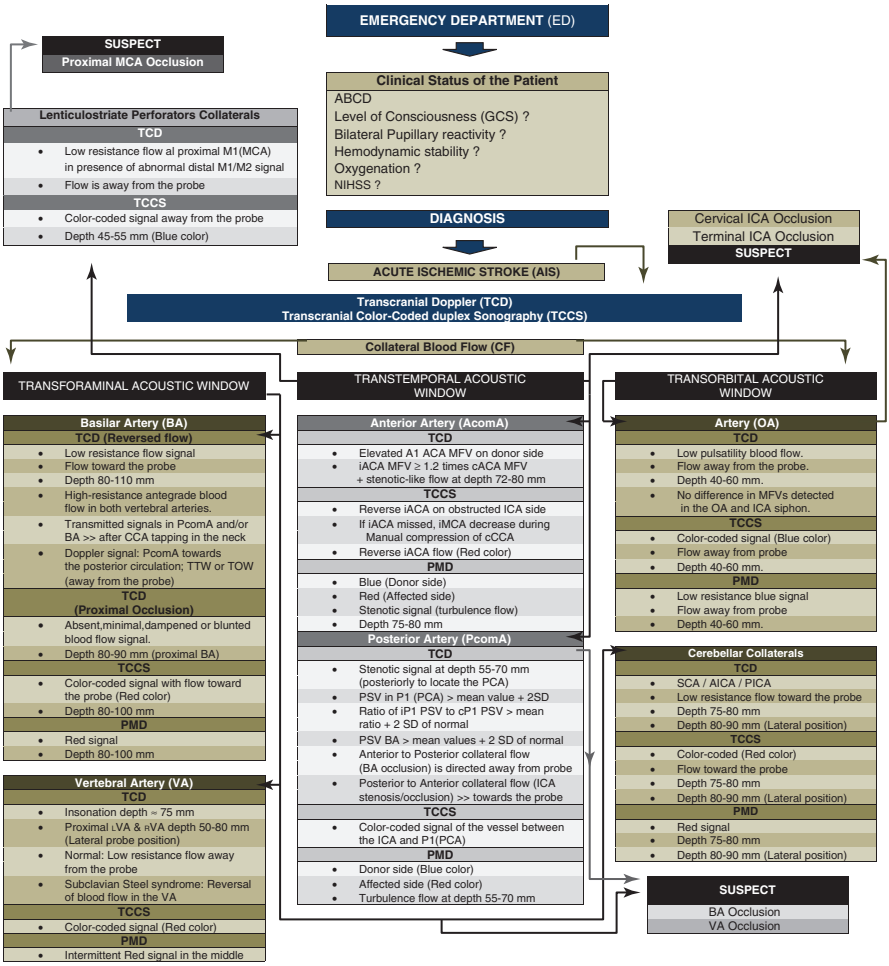

ABCD Airway-breathing-circulation-disability, *PMD* Power M mode doppler, *SD* Standard deviation, *cCCA* contralateral Common carotid artery, *iMCA* ipsilateral middle cerebral artery, *iACA* ipsilateral anterior cerebral artery, *PCA* Posterior cerebral artery, *PICA* Posteroinferior cerebellar artery, *AICA* Anteroinferior cerebellar artery, *SCA* Superior cerebellar artery, $_{L}VA$ Left vertebral artery, $_{R}VA$ Right vertebral artery, *iP1* ipsilateral P1 segment, *ICA* internal carotid artery, *A1* segment of ACA, *TTW* transtemporal window, *TOW* Transorbital window

References

1. Tissue plasminogen activator for acute ischemic stroke. The national institute of neurological disorders and stroke rt-pa stroke study group. N Engl J Med. 1995;333:1581–7.

2. Broderick JP, Palesch YY, Demchuk AM, et al. Endovascular therapy after intravenous t-pa versus t-pa alone for stroke. N Engl J Med. 2013;368:893–903.
3. Saqqur M, Uchino K, Demchuk AM, et al. Site of arterial occlusion identified by transcranial Doppler predicts the response to intravenous thrombolysis for stroke. Stroke. 2007;38:948–54.
4. Fransen PS, Beumer D, Berkhemer OA, et al. Mr. clean, a multicenter randomized clinical trial of endovascular treatment for acute ischemic stroke in the Netherlands: Study protocol for a randomized controlled trial. Trials. 2014;15:343.
5. Goyal M, Demchuk AM, Menon BK, et al. Randomized assessment of rapid endovascular treatment of ischemic stroke. N Engl J Med. 2015;372:1019–30.
6. Demchuk AM, Goyal M, Menon BK, et al. Endovascular treatment for small core and anterior circulation proximal occlusion with emphasis on minimizing ct to recanalization times (escape) trial: methodology. Int J Stroke. 2015;10:429–38.
7. Campbell BC, Mitchell PJ, Kleinig TJ, et al. Endovascular therapy for ischemic stroke with perfusion-imaging selection. N Engl J Med. 2015;372:1009–18.
8. Saver JL, Goyal M, Bonafe A, et al. Stent-retriever thrombectomy after intravenous t-pa vs. T-pa alone in stroke. N Engl J Med. 2015;372:2285–95.
9. Liebeskind DS. Collateral circulation. Stroke. 2003;34:2279–84.
10. Liebeskind DS. Collateral therapeutics for cerebral ischemia. Expert Rev Neurother. 2004;4:255–65.
11. Liebeskind DS, Kim D, Starkman S, Changizi K, Ohanian AG, Jahan R, Vinuela F. Collateral failure? Late mechanical thrombectomy after failed intravenous thrombolysis. J Neuroimaging. 2010;20:78–82.
12. Liebeskind DS, Sanossian N. How well do blood flow imaging and collaterals on angiography predict brain at risk? Neurology. 2012;79:S105–9.
13. Liebeskind DS, Tomsick TA, Foster LD, et al. Collaterals at angiography and outcomes in the interventional management of stroke (ims) iii trial. Stroke. 2014;45:759–64.
14. Shuaib A, Butcher K, Mohammad AA, Saqqur M, Liebeskind DS. Collateral blood vessels in acute ischaemic stroke: a potential therapeutic target. Lancet Neurol. 2011;10:909–21.
15. Menon BK, d'Esterre CD, Qazi EM, et al. A new tool for the imaging triage of patients with acute ischemic stroke. Radiology. 2015;275:510–20.
16. Menon BK, O'Brien B, Bivard A, et al. Assessment of leptomeningeal collaterals using dynamic ct angiography in patients with acute ischemic stroke. J Cereb Blood Flow Metab. 2013;33:365–71.
17. Seeta Ramaiah S, Churilov L, Mitchell P, Dowling R, Yan B. The impact of arterial collateralization on outcome after intra-arterial therapy for acute ischemic stroke. Am J Neuroradiol. 2014;35:667–72.
18. Brunner F, Tomandl B, Hanken K, Hildebrandt H, Kastrup A. Impact of collateral circulation on early outcome and risk of hemorrhagic complications after systemic thrombolysis. Int J Stroke. 2014;9:992–8.
19. Angermaier A, Langner S, Kirsch M, Kessler C, Hosten N, Khaw AV. Ct-angiographic collateralization predicts final infarct volume after intra-arterial thrombolysis for acute anterior circulation ischemic stroke. Cerebrovasc Dis. 2011;31:177–84.
20. Liebeskind DS, Alexandrov AV. Advanced multimodal CT/ MRI approaches to hyperacute stroke diagnosis, treatment, and monitoring. Ann N Y Acad Sci. 2012;1268:1–7.
21. Ichijo M, Iwasawa E, Numasawa Y, et al. Significance of development and reversion of collaterals on MRI in early neurologic improvement and long-term functional outcome after intravenous thrombolysis for ischemic stroke. Am J Neuroradiol. 2015;36:1839–45.
22. Hong D, Seo HS, Lee YH, Kim KJ, Suh SI, Jung JM. Leptomeningeal enhancement on magnetic resonance imaging as a predictor of hemodynamic insufficiency. J Comput Assist Tomogr. 2015;39:307–12.
23. Lee KY, Latour LL, Luby M, Hsia AW, Merino JG, Warach S. Distal hyperintense vessels on flair: an MRI marker for collateral circulation in acute stroke? Neurology. 2009;72:1134–9.

24. Karadeli HH, Giurgiutiu DV, Cloonan L, et al. Flair vascular hyperintensity is a surrogate of collateral flow and leukoaraiosis in patients with acute stroke due to proximal artery occlusion. J Neuroimaging. 2016;26:219–23.
25. Forster A, Wenz H, Kerl HU, Al-Zghloul M, Habich S, Groden C. Flair vascular hyperintensities and dynamic 4d angiograms for the estimation of collateral blood flow in posterior circulation occlusion. Neuroradiology. 2014;56:697–707.
26. Alexandrov AV, Sloan MA, Tegeler CH, et al. Practice standards for transcranial Doppler (TCD) ultrasound. Part II. Clinical indications and expected outcomes. J Neuroimaging. 2012;22:215–24.
27. Demchuk AM, Christou I, Wein TH, Felberg RA, Malkoff M, Grotta JC, Alexandrov AV. Specific transcranial Doppler flow findings related to the presence and site of arterial occlusion. Stroke. 2000;31:140–6.
28. Demchuk AM, Burgin WS, Christou I, et al. Thrombolysis in brain ischemia (TIBI) transcranial Doppler flow grades predict clinical severity, early recovery, and mortality in patients treated with intravenous tissue plasminogen activator. Stroke. 2001;32:89–93.
29. Christou I, Felberg RA, Demchuk AM, et al. Intravenous tissue plasminogen activator and flow improvement in acute ischemic stroke patients with internal carotid artery occlusion. J Neuroimaging. 2002;12:119–23.
30. Burgin WS, Malkoff M, Felberg RA, et al. Transcranial Doppler ultrasound criteria for recanalization after thrombolysis for middle cerebral artery stroke. Stroke. 2000;31:1128–32.
31. Demchuk AM, Christou I, Wein TH, et al. Accuracy and criteria for localizing arterial occlusion with transcranial Doppler. J Neuroimaging. 2000;10:1–12.
32. Alexandrov AV, Demchuk AM, Burgin WS. Insonation method and diagnostic flow signatures for transcranial power motion (m-mode) Doppler. J Neuroimaging. 2002;12:236–44.
33. Saqqur M, Hill MD, Alexandrov AV, et al. Derivation of power m-mode transcranial Doppler criteria for angiographic proven MCA occlusion. J Neuroimaging. 2006;16:323–8.
34. Alexandrov AV, Burgin WS, Demchuk AM, El-Mitwalli A, Grotta JC. Speed of intracranial clot lysis with intravenous tissue plasminogen activator therapy: sonographic classification and short-term improvement. Circulation. 2001;103:2897–902.
35. Alexandrov AV, Demchuk AM, Burgin WS, Robinson DJ, Grotta JC. Ultrasound-enhanced thrombolysis for acute ischemic stroke: phase i. findings of the clotbust trial. J Neuroimaging. 2004;14:113–7.
36. Alexandrov AV, Demchuk AM, Felberg RA, et al. High rate of complete recanalization and dramatic clinical recovery during TPA infusion when continuously monitored with 2-mhz transcranial Doppler monitoring. Stroke. 2000;31:610–4.
37. Labiche LA, Malkoff M, Alexandrov AV. Residual flow signals predict complete recanalization in stroke patients treated with TPA. J Neuroimaging. 2003;13:28–33.
38. Saqqur M, Tsivgoulis G, Molina CA, Demchuk AM, Shuaib A, Alexandrov AV. Residual flow at the site of intracranial occlusion on transcranial doppler predicts response to intravenous thrombolysis: a multi-center study. Cerebrovasc Dis. 2009;27:5–12.
39. Zachrisson H, Fouladiun M, Blomstrand C, Holm J, Volkmann R. Functional assessment of high-grade Ica stenosis with duplex ultrasound and transcranial Doppler. Clin Physiol Funct Imaging. 2012;32:241–6.
40. van Everdingen KJ, Visser GH, Klijn CJ, Kappelle LJ, van der Grond J. Role of collateral flow on cerebral hemodynamics in patients with unilateral internal carotid artery occlusion. Ann Neurol. 1998;44:167–76.
41. Muller M, Hermes M, Bruckmann H, Schimrigk K. Transcranial Doppler ultrasound in the evaluation of collateral blood flow in patients with internal carotid artery occlusion: correlation with cerebral angiography. Am J Neuroradiol. 1995;16:195–202.
42. Russell SM, Woo HH, Siller K, Panasci D, Leroux PD. Evaluating middle cerebral artery collateral blood flow reserve using acetazolamide transcranial doppler ultrasound in patients with carotid occlusive disease. Surg Neurol. 2008;70:466–70.

43. Krishnaswamy A, Klein JP, Kapadia SR. Clinical cerebrovascular anatomy. Catheter Cardiovasc Interv. 2010;75:530–9.
44. Liebeskind DS. Neuroprotection from the collateral perspective. Investig Drugs J. 2005;8:222–8.
45. Willinsky R, Lasjaunias P, Berenstein A. Intracavernous branches of the internal carotid artery (ica). Comprehensive review of their variations. Surg Radiol Anat. 1987;9:201–15.
46. Vander Eecken HM. Morphological significance of leptomeningeal anastomoses confined to the territory of cerebral arteries. Acta Neurol Psychiatr Belg. 1954;54:525–32.
47. Brozici M, van der Zwan A, Hillen B. Anatomy and functionality of leptomeningeal anastomoses: a review. Stroke. 2003;34:2750–62.
48. Qureshi AI, El-Gengaihi A, Hussein HM, Suri MF, Liebeskind DS. Occurrence and variability in acute formation of leptomeningeal collaterals in proximal middle cerebral artery occlusion. J Vasc Interv Neurol. 2008;1:70–2.
49. Martinon E, Lefevre PH, Thouant P, Osseby GV, Ricolfi F, Chavent A. Collateral circulation in acute stroke: assessing methods and impact: a literature review. J Neuroradiol. 2014;41:97–107.
50. Liebeskind DS. Collaterals in acute stroke: beyond the clot. Neuroimaging Clin N Am. 2005;15:553–73.
51. Guan J, Zhang S, Zhou Q, Li C, Lu Z. Usefulness of transcranial doppler ultrasound in evaluating cervical-cranial collateral circulations. Interv Neurol. 2013;2:8–18.
52. Alexandrov AV, Sloan MA, Wong LK, et al. Practice standards for transcranial Doppler ultrasound: part i--test performance. J Neuroimaging. 2007;17:11–8.
53. Kardile PB, Ughade JM, Pandit SV, Ughade MN. Anatomical variations of anterior communicating artery. J Clin Diagn Res. 2013;7:2661–4.
54. Baracchini C, Meneghetti G, Manara R, Ermani M, Ballotta E. Cerebral hemodynamics after contralateral carotid endarterectomy in patients with symptomatic and asymptomatic carotid occlusion: a 10-year follow-up. J Cereb Blood Flow Metab. 2006;26:899–905.
55. Byrd S, Wolfe J, Nicolaides A, Stansby G, Cheshire N, Thomas D, Mansfield A. Vascular surgical society of Great Britain and Ireland: transcranial doppler ultrasonography as a predictor of haemodynamically significant carotid stenosis. Br J Surg. 1999;86:692–3.
56. Chaudhuri R, Padayachee TS, Lewis RR, Gosling RG, Cox TC. Non-invasive assessment of the circle of Willis using transcranial pulsed Doppler ultrasound with angiographic correlation. Clin Radiol. 1992;46:193–7.
57. Hoksbergen AW, Fulesdi B, Legemate DA, Csiba L. Collateral configuration of the circle of Willis: transcranial color-coded duplex ultrasonography and comparison with post-mortem anatomy. Stroke. 2000;31:1346–51.
58. Hendrikse J, Klijn CJ, van Huffelen AC, Kappelle LJ, van der Grond J. Diagnosing cerebral collateral flow patterns: accuracy of non-invasive testing. Cerebrovasc Dis. 2008;25:430–7.
59. Saqqur M, Demchuk AM, Hill MD, et al. Bedside emergency transcranial doppler diagnosis of severe carotid disease using orbital window examination. J Neuroimaging. 2005;15:138–43.
60. Ringelstein EB, Weiller C, Weckesser M, Weckesser S. Cerebral vasomotor reactivity is significantly reduced in low-flow as compared to thromboembolic infarctions: the key role of the circle of willis. J Neurol Sci. 1994;121:103–9.
61. Hedera P, Bujdakova J, Traubner P, Pancak J. Stroke risk factors and development of collateral flow in carotid occlusive disease. Acta Neurol Scand. 1998;98:182–6.
62. Orosz L, Hoksbergen AW, Molnar C, et al. Clinical applicability of a mathematical model in assessing the functional ability of the communicating arteries of the circle of willis. J Neurol Sci. 2009;287:94–9.
63. Baumgartner RW, Baumgartner I, Mattle HP, Schroth G. Transcranial color-coded duplex sonography in the evaluation of collateral flow through the circle of Willis. Am J Neuroradiol. 1997;18:127–33.

64. Baumgartner RW, Baumgartner I, Schroth G. Diagnostic criteria for transcranial colour-coded duplex sonography evaluation of cross-flow through the circle of willis in unilateral obstructive carotid artery disease. J Neurol. 1996;243:516–21.
65. Lang J, Schaffrath H, Fischer G. Further findings on the diencephalic artery branches. Neurochirurgia. 1987;30:103–7.
66. Ross MR, Pelc NJ, Enzmann DR. Qualitative phase contrast MRA in the normal and abnormal circle of willis. Am J Neuroradiol. 1993;14:19–25.
67. Reinhard M, Muller T, Guschlbauer B, Timmer J, Hetzel A. Dynamic cerebral autoregulation and collateral flow patterns in patients with severe carotid stenosis or occlusion. Ultrasound Med Biol. 2003;29:1105–13.
68. Klotzsch C, Popescu O, Berlit P. Assessment of the posterior communicating artery by transcranial color-coded duplex sonography. Stroke. 1996;27:486–9.
69. Lee SI, Yang HD, Son IH, Han SJ. Recovery of reversed basilar artery flow as seen by transcranial sonography and MRA source images for vertebral dissection. J Neuroimaging. 2008;18:451–3.
70. Mayberg MR, Howard MA 3rd, Le Roux PD, Newell DW, Richard WH. Reversible basilar artery blood flow in subclavian steal syndrome. J Stroke Cerebrovasc Dis. 1991;1:103–8.
71. Brandt T. Diagnosis and thrombolytic therapy of acute basilar artery occlusion: a review. Clin Exp Hypertens. 2002;24:611–22.
72. Brandt T, Baloh RW. Rotational vertebral artery occlusion: a clinical entity or various syndromes? Neurology. 2005;65:1156–7.
73. Brandt T, von Kummer R, Muller-Kuppers M, Hacke W. Thrombolytic therapy of acute basilar artery occlusion. Variables affecting recanalization and outcome. Stroke. 1996;27:875–81.
74. Ribo M, Garami Z, Uchino K, Song J, Molina CA, Alexandrov AV. Detection of reversed basilar flow with power-motion Doppler after acute occlusion predicts favorable outcome. Stroke. 2004;35:79–82.
75. Alqadri S, Adil MM, Watanabe M, Qureshi AI. Patterns of collateral formation in basilar artery steno-occlusive diseases. J Vasc Interv Neurol. 2013;6:9–13.
76. Zhong J, Chen XY, Leung TW, et al. Significance of raised flow velocity in basilar artery in patients with acute ischemic stroke: focal stenosis, coexistent stenosis, and collateral flow. J Neuroimaging. 2015;25:922–6.
77. Grolimund P, Seiler RW, Aaslid R, Huber P, Zurbruegg H. Evaluation of cerebrovascular disease by combined extracranial and transcranial doppler sonography. Experience in 1,039 patients. Stroke. 1987;18:1018–24.
78. Sheth SA, Liebeskind DS. Collaterals in endovascular therapy for stroke. Curr Opin Neurol. 2015;28:10–5.
79. Kim Y, Sin DS, Park HY, Park MS, Cho KH. Relationship between flow diversion on transcranial Doppler sonography and leptomeningeal collateral circulation in patients with middle cerebral artery occlusive disorder. J Neuroimaging. 2009;19:23–6.
80. Menon BK, Campbell BC, Levi C, Goyal M. Role of imaging in current acute ischemic stroke workflow for endovascular therapy. Stroke. 2015;46:1453–61.
81. Spiessberger A, Federau C, Guggenberger R, Kollias S. Influence of leptomeningeal collateral pattern on the prognostic value of mismatch in acute anterior circulation stroke. J Comput Assist Tomogr. 2015;39:213–6.
82. Calleja AI, Cortijo E, Garcia-Bermejo P, et al. Collateral circulation on perfusion-computed tomography-source images predicts the response to stroke intravenous thrombolysis. Eur J Neurol. 2013;20:795–802.
83. Frolich AM, Wolff SL, Psychogios MN, et al. Time-resolved assessment of collateral flow using 4d ct angiography in large-vessel occlusion stroke. Eur Radiol. 2014;24:390–6.
84. Zareie H, Quain DA, Parsons M, et al. The influence of anterior cerebral artery flow diversion measured by transcranial Doppler on acute infarct volume and clinical outcome in anterior circulation stroke. Int J Stroke. 2013;8:228–34.

85. Schneider PA, Rossman ME, Bernstein EF, Ringelstein EB, Otis SM. Noninvasive assessment of cerebral collateral blood supply through the ophthalmic artery. Stroke. 1991;22:31–6.
86. Ward JB, Hedges TR 3rd, Heggerick PA. Reversible abnormalities in the ophthalmic arteries detected by color Doppler imaging. Ophthalmology. 1995;102:1606–10.
87. Reynolds PS, Greenberg JP, Lien LM, Meads DC, Myers LG, Tegeler CH. Ophthalmic artery flow direction on color flow duplex imaging is highly specific for severe carotid stenosis. J Neuroimaging. 2002;12:5–8.
88. Wilterdink JL, Feldmann E, Furie KL, Bragoni M, Benavides JG. Transcranial doppler ultrasound battery reliably identifies severe internal carotid artery stenosis. Stroke. 1997;28:133–6.
89. Can U, Furie KL, Suwanwela N, et al. Transcranial doppler ultrasound criteria for hemodynamically significant internal carotid artery stenosis based on residual lumen diameter calculated from en bloc endarterectomy specimens. Stroke. 1997;28:1966–71.
90. Rutgers DR, Klijn CJ, Kappelle LJ, van Huffelen AC, van der Grond J. A longitudinal study of collateral flow patterns in the circle of Willis and the ophthalmic artery in patients with a symptomatic internal carotid artery occlusion. Stroke. 2000;31:1913–20.
91. Countee RW, Vijayanathan T. External carotid artery in internal carotid artery occlusion. Angiographic, therapeutic, and prognostic considerations. Stroke. 1979;10:450–60.
92. Tatemichi TK, Chamorro A, Petty GW, et al. Hemodynamic role of ophthalmic artery collateral in internal carotid artery occlusion. Neurology. 1990;40:461–4.
93. Anzola GP, Gasparotti R, Magoni M, Prandini F. Transcranial doppler sonography and magnetic resonance angiography in the assessment of collateral hemispheric flow in patients with carotid artery disease. Stroke. 1995;26:214–7.
94. Hu HH, Wang S, Chern CM, Yeh HH, Sheng WY, Lo YK. Clinical significance of the ophthalmic artery in carotid artery disease. Acta Neurol Scand. 1995;92:242–6.
95. Contorni L. The vertebro-vertebral collateral circulation in obliteration of the subclavian artery at its origin. Minerva Chir. 1960;15:268–71.
96. Rozsa A, Lipcsey A. Subclavian steal syndrome examined by transcranial doppler sonography. Orv Hetil. 1991;132:2265–9.
97. Huang Y, Gao S, Wang B, Li S. The evaluation of intra- and extra-cranial circulation in subclavian steal syndrome. Chin Med J. 1997;110:286–8.
98. Harper C, Cardullo PA, Weyman AK, Patterson RB. Transcranial Doppler ultrasonography of the basilar artery in patients with retrograde vertebral artery flow. J Vasc Surg. 2008;48:859–64.
99. Karacostas D, Ioannides P, Balamoutsos G, Artemis N. Rich collaterals in clinically unsuspected basilar artery occlusion-as good as it gets. J Neuroimaging. 2012;22:89–91.
100. Lee WJ, Jung KH, Lee KJ, et al. Sonographic findings associated with stenosis progression and vascular complications in moyamoya disease. J Neurosurg. 2015:1–9.
101. Gahn G, Hahn G, Hallmeyer-Elgner S, et al. Echo-enhanced transcranial color-coded duplex-sonography to study collateral blood flow in patients with symptomatic obstructions of the internal carotid artery and limited acoustic bone windows. Cerebrovasc Dis. 2001;11:107–12.
102. Hoksbergen AW, Legemate DA, Ubbink DT, de Vos HJ, Jacobs NJ. Influence of the collateral function of the circle of Willis on hemispherical perfusion during carotid occlusion as assessed by transcranial colour-coded duplex ultrasonography. Eur J Vasc Endovasc Surg. 1999;17:486–92.
103. Hoksbergen AW, Legemate DA, Csiba L, Csati G, Siro P, Fulesdi B. Absent collateral function of the circle of willis as risk factor for ischemic stroke. Cerebrovasc Dis. 2003;16:191–8.
104. Droste DW, Jurgens R, Weber S, Tietje R, Ringelstein EB. Benefit of echocontrast-enhanced transcranial color-coded duplex ultrasound in the assessment of intracranial collateral pathways. Stroke. 2000;31:920–3.
105. Moehring MA, Spencer MP. Power m-mode Doppler (pmd) for observing cerebral blood flow and tracking emboli. Ultrasound Med Biol. 2002;28:49–57.

106. Ribo M, Molina CA, Alvarez B, Rubiera M, Alvarez-Sabin J, Matas M. Transcranial doppler monitoring of transcervical carotid stenting with flow reversal protection: a novel carotid revascularization technique. Stroke. 2006;37:2846–9.
107. Vernieri F, Tibuzzi F, Pasqualetti P, et al. Transcranial Doppler and near-infrared spectroscopy can evaluate the hemodynamic effect of carotid artery occlusion. Stroke. 2004;35:64–70.
108. Zachrisson H, Blomstrand C, Holm J, Mattsson E, Volkmann R. Changes in middle cerebral artery blood flow after carotid endarterectomy as monitored by transcranial doppler. J Vasc Surg. 2002;36:285–90.
109. Visser GH, Wieneke GH, van Huffelen AC, Eikelboom BC. The use of preoperative transcranial Doppler variables to predict which patients do not need a shunt during carotid endarterectomy. Eur J Vasc Endovasc Surg. 2000;19:226–32.
110. Fearn SJ, Picton AJ, Mortimer AJ, Parry AD, McCollum CN. The contribution of the external carotid artery to cerebral perfusion in carotid disease. J Vasc Surg. 2000;31:989–93.
111. Valdueza JM, Hoffmann O, Weih M, Mehraein S, Einhaupl KM. Monitoring of venous hemodynamics in patients with cerebral venous thrombosis by transcranial doppler ultrasound. Arch Neurol. 1999;56:229–34.
112. Bisschops RH, Klijn CJ, Kappelle LJ, van Huffelen AC, van der Grond J. Collateral flow and ischemic brain lesions in patients with unilateral carotid artery occlusion. Neurology. 2003;60:1435–41.
113. Riva M, Pappada GB, Papadakis M, et al. Hemodynamic monitoring of intracranial collateral flow predicts tissue and functional outcome in experimental ischemic stroke. Exp Neurol. 2012;233:815–20.
114. Beyer SE, Thierfelder KM, von Baumgarten L, et al. Strategies of collateral blood flow assessment in ischemic stroke: prediction of the follow-up infarct volume in conventional and dynamic cta. Am J Neuroradiol. 2015;36:488–94.
115. Umemura A, Yamada K, Masago A, Kanda Y, Matsumoto T, Shimazu N. Hemodynamic flow patterns evaluated by transcranial color-coded duplex sonography after sta-mca bypass for internal carotid artery occlusion. Cerebrovasc Dis. 2002;14:143–7.
116. Menon BK, Qazi E, Nambiar V, et al. Differential effect of baseline computed tomographic angiography collaterals on clinical outcome in patients enrolled in the interventional management of stroke iii trial. Stroke. 2015;46:1239–44.
117. Nambiar V, Sohn SI, Almekhlafi MA, et al. CTA collateral status and response to recanalization in patients with acute ischemic stroke. Am J Neuroradiol. 2014;35:884–90.
118. Beard DJ, McLeod DD, Logan CL, et al. Intracranial pressure elevation reduces flow through collateral vessels and the penetrating arterioles they supply. A possible explanation for 'collateral failure' and infarct expansion after ischemic stroke. J Cereb Blood Flow Metab. 2015;35:861–72.
119. Campbell BC, Christensen S, Tress BM, et al. Failure of collateral blood flow is associated with infarct growth in ischemic stroke. J Cereb Blood Flow Metab. 2013;33:1168–72.
120. Emery DJ, Schellinger PD, Selchen D, et al. Safety and feasibility of collateral blood flow augmentation after intravenous thrombolysis. Stroke. 2011;42:1135–7.
121. Wojner-Alexander AW, Garami Z, Chernyshev OY, Alexandrov AV. Heads down: flat positioning improves blood flow velocity in acute ischemic stroke. Neurology. 2005;64:1354–7.
122. Han JH, Leung TW, Lam WW, et al. Preliminary findings of external counterpulsation for ischemic stroke patient with large artery occlusive disease. Stroke. 2008;39:1340–3.
123. Saqqur M, Ibrahim M, Butcher K, Khan K, Emery D, Manawadu D, Derksen C, Schwindt B, Shuaib A. Transcranial Doppler and cerebral augmentation in acute ischemic stroke. J Neuroimaging. 2013;23:460–5.
124. Hussain MS, Bhagat YA, Liu S, et al. Dwi lesion volume reduction following acute stroke treatment with transient partial aortic obstruction. J Neuroimaging. 2010;20:379–81.
125. Bonetti PO, Barsness GW, Keelan PC, et al. Enhanced external counterpulsation improves endothelial function in patients with symptomatic coronary artery disease. J Am Coll Cardiol. 2003;41:1761–8.

126. Bonetti PO, Holmes DR Jr, Lerman A, Barsness GW. Enhanced external counterpulsation for ischemic heart disease: What's behind the curtain? J Am Coll Cardiol. 2003;41:1918–25.
127. Henderson RD, Eliasziw M, Fox AJ, Rothwell PM, Barnett HJ. Angiographically defined collateral circulation and risk of stroke in patients with severe carotid artery stenosis. North American symptomatic carotid endarterectomy trial (nascet) group. Stroke. 2000;31:128–32.
128. Miralles M, Dolz JL, Cotillas J, et al. The role of the circle of Willis in carotid occlusion: assessment with phase contrast MR angiography and transcranial duplex. Eur J Vasc Endovasc Surg. 1995;10:424–30.
129. Schomer DF, Marks MP, Steinberg GK, et al. The anatomy of the posterior communicating artery as a risk factor for ischemic cerebral infarction. N Engl J Med. 1994;330:1565–70.
130. Silvestrini M, Altamura C, Cerqua R, et al. Early activation of intracranial collateral vessels influences the outcome of spontaneous internal carotid artery dissection. Stroke. 2011;42:139–43.
131. Klijn CJ, Kappelle LJ, Algra A, van Gijn J. Outcome in patients with symptomatic occlusion of the internal carotid artery or intracranial arterial lesions: a meta-analysis of the role of baseline characteristics and type of antithrombotic treatment. Cerebrovasc Dis. 2001;12:228–34.
132. Grubb RL Jr, Derdeyn CP, Fritsch SM, et al. Importance of hemodynamic factors in the prognosis of symptomatic carotid occlusion. J Am Med Assoc. 1998;280:1055–60.
133. Lee JY, Lee YS. Vasomotor reactivity in middle cerebral artery stenosis. J Neurol Sci. 2011;301:35–7.
134. Gupta A, Chazen JL, Hartman M, et al. Cerebrovascular reserve and stroke risk in patients with carotid stenosis or occlusion: a systematic review and meta-analysis. Stroke. 2012;43:2884–91.
135. Fu JH, Lu CZ, Hong Z, Dong Q, Ding D, Wong KS. Relationship between cerebral vasomotor reactivity and white matter lesions in elderly subjects without large artery occlusive disease. J Neuroimaging. 2006;16:120–5.
136. Wiart M, Berthezene Y, Adeleine P, et al. Vasodilatory response of border zones to acetazolamide before and after endarterectomy: an echo planar imaging-dynamic susceptibility contrast-enhanced MRI study in patients with high-grade unilateral internal carotid artery stenosis. Stroke. 2000;31:1561–5.
137. Ogasawara K, Ogawa A, Yoshimoto T. Cerebrovascular reactivity to acetazolamide and outcome in patients with symptomatic internal carotid or middle cerebral artery occlusion: a xenon-133 single-photon emission computed tomography study. Stroke. 2002;33:1857–62.
138. Eicke BM, Bahr RR, Buss E, Doberenz C, Paulus W. Quantitative volumetry in patients with carotid disease–effects of acetazolamide. J Neuroimaging. 2001;11:13–7.
139. Vernieri F, Pasqualetti P, Matteis M, et al. Effect of collateral blood flow and cerebral vasomotor reactivity on the outcome of carotid artery occlusion. Stroke. 2001;32:1552–8.

Chapter 33
Reversed Robin Hood Syndrome and Ischemic Stroke: Usefulness of Transcranial Doppler (TCD/TCCS) to Real-Time Monitoring

Sanjeev Sivakumar and Ryan Hakimi

Key Points

1. Reversed Robin Hood syndrome (RRHS) is the term used to describe clinical manifestations in the presence of sonographic observations on TCD/TCCS of a paradoxical decrease in the cerebral blood flow velocity in blood vessels supplying ischemic areas of the brain, during episodes of hypercapnia.
2. Reversed Robin Hood phenomenon is accompanied by an expected increase in cerebral blood flow velocity in the nonaffected cerebral vessels with hypercarbia leading to the analogy "rob the poor to feed the rich."
3. RRHS most often affects younger male patients with persistent proximal arterial occlusions and places them at risk for ipsilateral ischemic stroke.
4. Spencer's curve depicts the relationship between mean flow velocity, degree of stenosis, and cerebral blood flow.
5. Vasomotor reactivity (VMR) can be used to risk stratify patients with carotid occlusive disease and in poststenotic arterial segments or arteries with residual flow due to an acute occlusion. This is most easily assessed using the breath-holding index (BHI).
6. RRHS and hemodynamic steal can be found in 7–14% of patients presenting with stroke and who have persisting arterial occlusions. TCD can noninvasively

S. Sivakumar
Department of Neurology, University of South Carolina-Greenville School of Medicine, Greenville, SC, USA
e-mail: Sanjeev.Sivakumar@prismahealth.org

R. Hakimi (✉)
Neuro ICU, TCD Services, Prisma Health-Upstate, Greenville, SC, USA

Department of Medicine (Neurology), USC School of Medicine-Greenville, Greenville, SC, USA

American Society of Neuroimaging (ASN), Minneapolis, MN, USA
e-mail: ryan.hakimi@prismahealth.org

C. N. Rodríguez et al. (eds.), *Neurosonology in Critical Care*,
https://doi.org/10.1007/978-3-030-81419-9_33

demonstrate the hemodynamic phenomenon and can be used to determine the steal magnitude, thereby identifying patients at risk for cerebral ischemia and infarction.

33.1 Introduction

In 2007, Andrei Alexandrov and colleagues coined the term reversed Robin Hood syndrome (RRHS) based on clinical manifestations that accompany sonographic observations of a paradoxical decrease in the cerebral blood flow velocity in blood vessels supplying ischemic areas of the brain, during episodes of hypercapnia [1]. This phenomenon occurred concurrently, with an expected increase in cerebral blood flow velocity in the nonaffected cerebral vessels with hypercapnia. The analogy "rob the poor to feed the rich" was thus used to term this syndrome. RRHS and hemodynamic steal can be found in 7–14% of patients presenting with stroke and who have persisting arterial occlusions [2]. RRHS has been described most often in younger male patients with persistent proximal arterial occlusions and excessive sleepiness (a 1-point increase in the Epworth Sleepiness Scale was independently associated with increased likelihood of RRHS of 36%) [2, 3]. RRHS is independently associated with ipsilateral ischemic stroke recurrence [4]. This chapter provides an overview of cerebral vasomotor reactivity and blood flow dynamics in pathologic states and sonographic findings seen in RRHS.

33.2 Cerebral Vasomotor Reactivity and Cerebral Blood Flow Autoregulation

Alveolar ventilation (AV) is defined by the volume of air per minute that enters the respiratory zones and is available for gas exchange [5]. A portion of this volume remains in areas of the lung, where gases do not diffuse into the blood stream (dead space); thus, alveolar ventilation can be determined using the following equation (Eq. 33.1):

$$\mathrm{AV} = \text{Respiratory rate}\left(\mathrm{RR}\right) \times \left(\text{Volume tidal}\left[\mathrm{V_T}\right] - \text{Volume dead space}\left[\mathrm{V_{DS}}\right]\right)\left[5\right] \tag{33.1}$$

Hyperventilation results in an increase in alveolar ventilation. Since alveolar ventilation has an inverse relationship with alveolar CO_2, as AV increases, the alveolar CO_2 levels decrease. [6] Alveolar CO_2 has a direct association with partial pressure of arterial CO_2 ($PaCO_2$), which reflects a balance between CO_2 production and elimination. Several factors such as diet, exercise, hormonal activity (thyroid), and temperature affect the cellular production of CO_2 [5]. The normal $PaCO_2$ values

typically fluctuate between 35 and 45 mmHg (4.7–6 kPa) at normal body temperature and at sea level, with a barometric pressure of 760 mmHg [6]. If the body temperature decreases, $PaCO_2$ decreases by about 4.5% for each degree Celsius decrease, due to increased solubility of CO_2 [7]. At high altitudes, the barometric pressure decreases and stimulates AV, thereby decreasing $PaCO_2$ levels [8].

Autoregulation of cerebral blood flow is primarily achieved by changes in the arteriolar resistance via dilation and contraction of pial arterioles in response to changes in arterial blood pressure, metabolic demand, blood viscosity, and gases [9, 10]. CO_2 reactivity is the ability of cerebral arterioles to dilate or contract in response to changes in $PaCO_2$. Cerebral vasodilation occurs when $PaCO_2$ rises above 44 mmHg, and cerebral vasoconstriction occurs when $PaCO_2$ decreases below 35 mmHg [11–15]. Overall, vascular reactivity occurs when $PaCO_2$ ranges between 20 and 60 mmHg [16]. Figure 33.1 illustrates the cerebral autoregulation curves depicting CBF according to shifts in $PaCO_2$ [12, 17]. If $PaCO_2$ increases to 80 mmHg, the resulting cerebral vasodilation can increase CBF by 100–200%, which can increase metabolic activity. For every 1 mmHg decrease in $PaCO_2$, CBF decreases by 3% and $PaCO_2$ levels between 20 and 25 mmHg are associated with

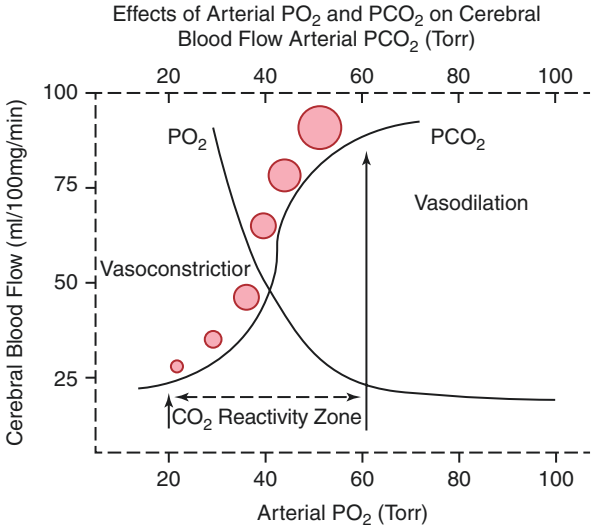

Fig. 33.1 Effects of arterial PO_2 and PCO_2 on cerebral blood flow. The Monro-Kellie Doctrine states that the sum of volumes of the brain, cerebrospinal fluid (CSF) and intracerebral blood is constant [19, 20]. Since the cranial cavity has a fixed volume, an increase in the mass of one of these compartments (e.g. cerebral edema, hematoma, and tumor) can cause a critical elevation in the intracranial pressure (ICP). This elevation in ICP can impair cerebral perfusion and result in ischemia. Hypercapnia induces vasodilation, which leads to an increase in CBV and a subsequent increase in ICP, while hypocapnia triggers vasoconstriction leading to a decrease in CBV and a resultant decrease in ICP. The induction of hypocapnic alkalosis decreases cerebral blood volume resulting in a decreased in the volume of cranial contents by means of potent cerebral vasoconstriction. This results in lowering of intracranial pressure. This forms the basis for transient induced hypocapnia in the management of intracranial hypertension [21]

CBF reduction of 40–50% [13, 16]. Normal cerebral blood volume (CBV) is 3–4 mL per 100 g of brain parenchyma [13]. Any changes in CBV with hypercapnia or hypocapnia can be attributed to changes in arteriolar diameter, as veins and capillaries do not react to fluctuations in $PaCO_2$ [18].

33.3 Ischemic Stroke: Stenosis, Vasospasm, and Vasomotor Reactivity

The TOAST (trial of Org 10,171 in Acute Stroke Treatment) stroke subtype classification is widely used in clinical trials and practice to delineate the mechanism of stroke [22]. This denotes five subtypes of stroke, namely, large-artery atherosclerosis, cardioembolism, small-vessel occlusion, stroke of other determined etiology, and undetermined etiology. Regardless of stroke etiology, cerebral blood flow in the presence of hemodynamically significant stenosis of the intracranial circulation can be noninvasively monitored using transcranial Doppler ultrasound. The correlation between mean flow velocity (MFV) and stenosis was first described by Spencer and Reid but is often referred to as Spencer's curve (Fig. 33.2) [23, 24].

When the degree of vessel stenosis increases, the velocity increases. Further considerations of hemodynamic changes with arterial stenosis or spasm are described in Tables 33.1 and 33.2 [25].

33.4 Vasomotor Reactivity (VMR) and Breath-Holding Index (BHI)

Vasomotor reactivity (VMR) is useful for risk stratification in patients with carotid occlusive disease and in poststenotic arterial segments or arteries with residual flow due to an acute occlusion. VMR testing utilizes one of three approaches: (i) dose-controlled CO_2 inhalation, (ii) intravenous acetazolamide injection, or (iii) breath-holding index (BHI). The changes in CBF with vasodilation and vasoconstriction also affect the velocity and waveform morphology in the proximal branches of the circle of Willis. The middle cerebral artery (MCA) MFV changes by 3–4% per mmHg change in end tidal CO_2 [26]. Markus and Harrison described a practical method to estimate vasomotor reactivity (VMR), termed breath-holding index (BHI) [27]. The VMR is measured by the MFV's response to 30 seconds of breath holding (Eq. 33.2).

$$\mathrm{BHI} = \left(\mathrm{MFV}_{\mathrm{end}} - \mathrm{MFV}_{\mathrm{baseline}} / \mathrm{MFV}_{\mathrm{baseline}}\right) \times \left(100 / \mathrm{s\,of\,breath - holding}\right) \tag{33.2}$$

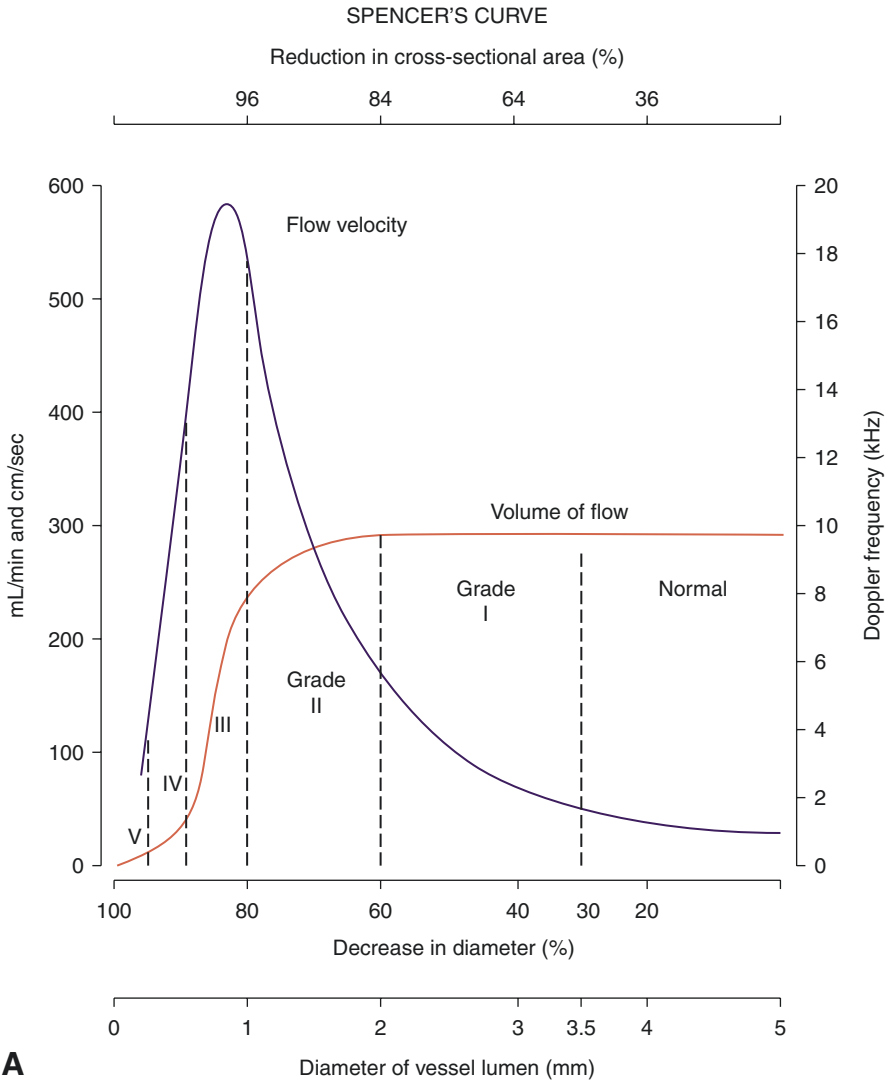

Fig. 33.2 Spencer's Curve. (Courtesy Andrei Alexandrov, MD)

Table 33.1 Degree of Vessel stenosis

	Degree	Length	BP	TCD (CBFV)	Interpretation
STENOSIS	↑	Unchanged	Unchanged	↑	FSP
	↓	Unchanged	Unchanged	↓	FSR

↑ denotes increase, ↓ decrease, *CBFV* Blood flow velocity, *FSP* Focal stenosis progression, *FSR* Focal stenosis regression, *BP* Blood pressure

Table 33.2 Degree of Vessel Spasm

	Length	Degree	BP	TCD (BFV)	Interpretation
SPASM	↑	Unchanged	Unchanged	Unchanged or ↓	DVS
	↓	Unchanged	Unchanged	Unchanged or ↑	FVS

↑ denotes increase, ↓ decrease, *BFV* Blood flow velocity, *DVS* Diffuse vasospasm, *FVS* Focal vasospasm, *BP* Blood pressure

where MFV_{end} represents the Doppler mean flow velocity toward the end of breath holding and $MFV_{baseline}$ represents the Doppler mean flow velocity toward the beginning of breath holding.

Assessment of the intracranial response is expressed as a percentage change from baseline to poststimulus over baseline, with or without adjustment for time it took for this response to develop. Using the BHI, prospective clinical trials have shown that impaired VMR can identify patients with asymptomatic carotid stenosis or previously symptomatic carotid occlusion who are at higher risk for stroke [28, 29].

33.5 Collateral Blood Flow Adaptation to Stenosis and Occlusion

In normal cerebral circulation, the cerebral blood flow is maintained at relatively constant levels over a wide range of blood pressures in normotensive individuals (Lassen curve) via intrinsic autoregulatory mechanisms that modulate vascular resistance. Autoregulation is accomplished by metabolic (imbalance between supply-demand) or myogenic (vascular smooth vessel response to transmural pressure, Bayliss effect) mechanisms [25]. These mechanisms prevent cerebral hyperperfusion during sudden increases in systemic blood pressure. Both VMR and cerebral autoregulation can coexist and override one another. Cerebral autoregulation decreases distal vascular resistance when a proximal arterial occlusion develops. When these distal vessels dilate to a physiological maximum in order to compensate for proximal stenosis or occlusion, no vasomotor response is induced by breath holding, and a significant drop in systemic blood pressure can cause cerebral hypoperfusion and ischemic injury [30].

Blood flow in a bifurcation involved as collateral channels is triggered when a lesion is located proximal to its origin and a pressure gradient develops between the donor and recipient arteries. Some of the factors which can affect cerebral autoregulation include systemic blood pressure, cardiac output, blood viscosity, platelet function, and increased vascular resistance due to tissue edema. When the velocity in branching vessel increases with constant velocity in the stem with bifurcations, the velocity proximal to clot decreases due to collateral channels "escape hatch," increased resistance. As an example, in case of a distal M1-middle cerebral artery (MCA) occlusion, the anterior cerebral artery (ACA) serves as collateral channel to

deliver blood to MCA territory via transcortical collaterals. The lenticulostriate arteries deliver blood to internal capsule and distally via ascending branches which can act as "escape hatch" for flow proximal to occlusion. Thus, distal M1-MCA occlusion may not always cause significant proximal velocity decrease [25].

33.6 Hemodynamic Phenomenon in Reversed Robin Hood Syndrome (RRHS)

For a given systemic blood pressure, an increase in the degree of intracranial arterial stenosis results in a decrease in vasomotor reactivity [25] (Table 33.3).

A decrease in vasomotor reactivity or intracerebral steal can suggest a failure of collateral flow to adapt to a progression in intracranial stenosis. In such situations, hypercapnia can lead to a paradoxical reduction in flow velocities distal to a persisting arterial occlusion, while resulting in normal vasodilation and velocity increase in the unaffected blood vessels [1]. In such an event, the velocity reduction indicates a "steal" phenomenon (reversed Robin Hood phenomenon), where blood flow is diverted from vessels that are already affected by ischemia to normal vessels that have the capacity to vasodilate. This has been described as the hemodynamic steal mechanism that can result in clinical deterioration. The analogy "rob the poor to feed the rich" is applicable and led to Alexandrov coining the term reversed Robin Hood syndrome. This typically occurs 15–25 seconds from the beginning of breath holding (Eq. 33.3).

$$\text{Steal magnitude}\left(\text{SM},\%\right) = \left(\text{MFV}_{\text{min}} - \text{MFV}_{\text{baseline}} \,/\, \text{MFV}_{\text{baseline}}\right) \times 100 \quad (33.3)$$

where MFV_{min} is the minimal flow velocity at the time of vasodilation and velocity increase in unaffected vessels. The steal magnitude can range from −15% to −43% [1].

33.6.1 Reversed Robin Hood Syndrome (RRHS): Clinical Relevance

Hyperventilation has historically been advocated as a therapy for patients with acute stroke, which can reduce intracranial pressure and induce inverse steal in ischemic areas of the brain, and to correct acidosis in the zones around ischemic tissue.

Table 33.3 Intracranial arterial stenosis and vasomotor reactivity

Degree of spasm	Blood viscosity	Degree of stenosis	Clinical result
Unchanged	Unchanged	↑	VMR ↓

↑ Increase, ↓ Decrease, *VMR* vasomotor reactivity

However, this has not been demonstrated to yield improved outcomes. In patients with RRHS, hypercapnia causes a paradoxical reduction in flow velocities distal to a persistent arterial occlusion, while producing normal vasodilation and velocity increase in unaffected blood vessels. This steal phenomenon suggests exhausted vasomotor reactivity and a "failed" vasodilatory reserve. This can predict who is "at risk" for cerebral infarction in patients with critical intracranial stenosis or occlusive disease who become symptomatic with hypercapnia. Studies have replicated findings of this steal phenomenon with Technetium-99 m hexamethyl propylenamine oxime single-photon emission tomography (Tc-99 m-HMPAO-SPECT) with acetazolamide challenge demonstrating reduction in cerebral perfusion after acetazolamide injection [25, 31].

33.6.2 TCD/TCCS: Real-Time Monitoring

A 2-MHz TCD probe is used to insonate the bilateral transtemporal windows, to identify the bilateral MCAs, ACAs, and posterior cerebral arteries (PCAs). The transducer is then placed over the suboccipital window to obtain the vertebral arteries and the basilar artery waveforms, followed by insonation of the transorbital window at 10% reduced power to identify the carotid siphon. The peak systolic velocity (PSV), end diastolic velocity (EDV), and the TAMM mean flow velocity of the anterior and posterior circulation are calculated across different depths. The PI, resistivity index (RI), and markers of downstream resistance in the cerebral circulation are also calculated. Note the depth of insonation of the proximal MCA. The transducer is then secured in place at this depth using a hands-free headframe.

Vasomotor reactivity is then assessed by breath-holding index (BHI) during simultaneous TCD monitoring of both MCAs using Eq. (33.1). In this equation, a patient is subject to minimum of 24 seconds of breath holding; MFV_{end} is measured 4 seconds after the patient starts breathing. The normal response should consist of a mean flow velocity increase from baseline, after 30 sec of breath holding. However, the mean flow velocity in the pathological hemisphere with reversed Robin Hood phenomenon will demonstrate a paradoxical velocity reduction toward end of voluntary breath holding, suggesting an exhausted vasomotor reactivity or failed vasodilatory drive. The steal magnitude can then be calculated using Eq. (33.2).

33.6.3 Illustrative Case

A 54-year-old female with diabetes mellitus and dyslipidemia presented with recurrent episodes of left sided weakness. The patient also reported mild headaches and lethargy upon awakening which would resolve 1 hour following awakening. Her neurological examination was unremarkable, and she did not have any signs or

symptoms of obstructive sleep apnea. Her MRA of the head revealed absence of flow within the right MCA distribution (Fig. 33.3).

TCD was obtained as part of determination of vasomotor reserve via BHI calculation (Fig. 33.4).

Additional supporting information was obtained in the form of SPECT scan following injection of IV acetazolamide (Fig. 33.5).

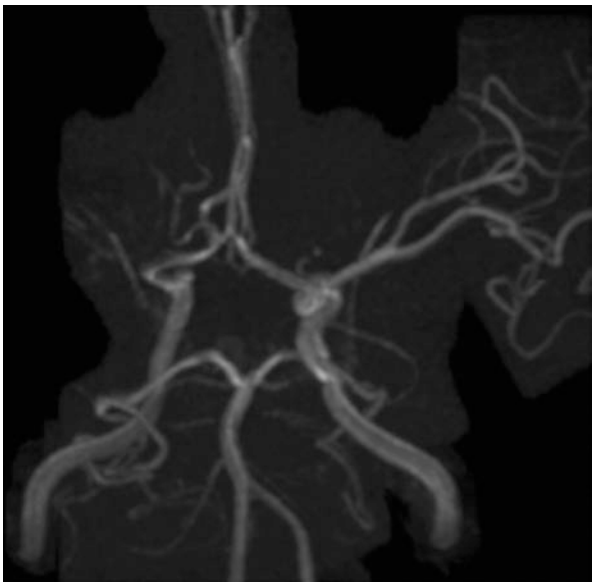

Fig. 33.3 Brain MRA revealing absence of flow signal in the right MCA distribution. (Courtesy: Vijay Sharma, MD)

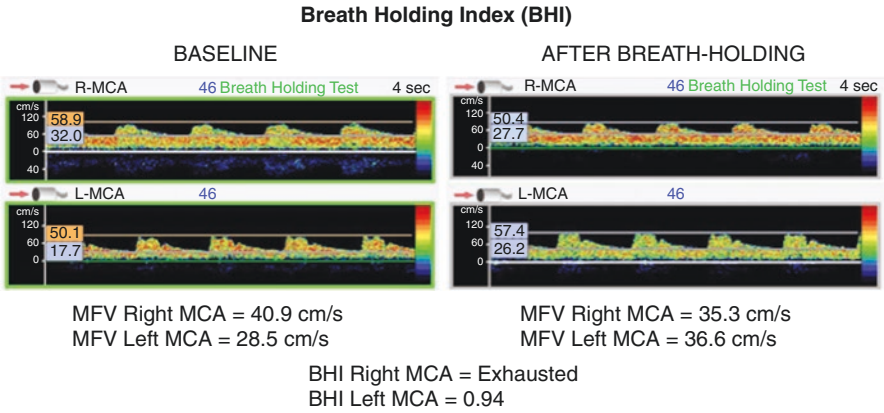

Fig. 33.4 BHI calculated via TCD demonstrating absence of vasomotor reserve in the right MCA. (Courtesy: Vijay Sharma, MD)

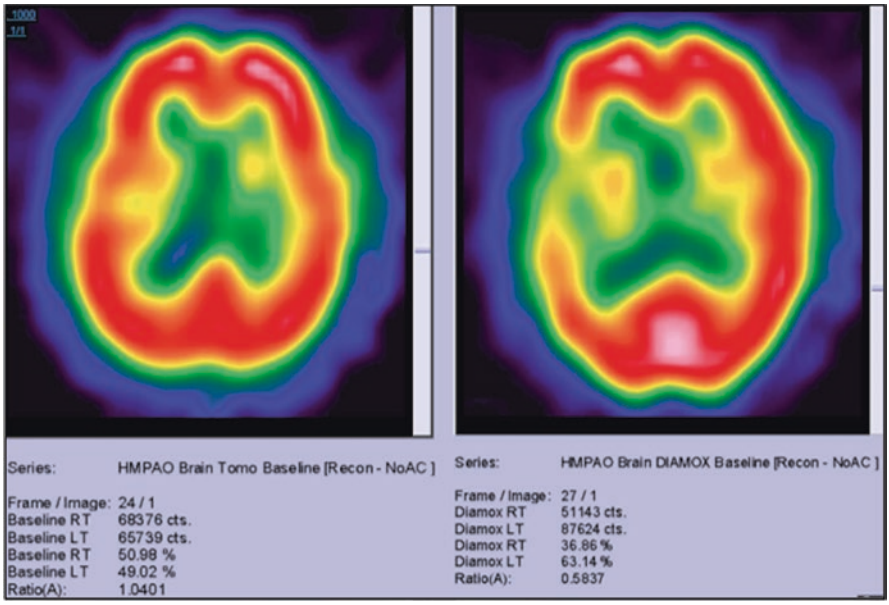

Fig. 33.5 Acetazolamide-challenged HMPAO-SPECT. Baseline SPECT shows nearly symmetrical metabolic perfusion in both hemispheres (right 50.98%, left 49.02%). However, after acetazolamide challenge, markedly reduced metabolic perfusion is noted in the right hemisphere (right 36.86%, left 63.14%; net perfusion deficit = 28.24%). (Courtesy: Vijay Sharma, MD)

Overall, the patient's symptoms were referable to loss of vasomotor reserve in the right MCA distribution which would manifest as left hemiparesis.

33.7 Conclusion

RRHS and hemodynamic steal can be found in 7–14% of patients presenting with stroke and who have persisting arterial occlusions. Transcranial Doppler can noninvasively demonstrate this hemodynamic phenomenon and can be used to determine the steal magnitude, thereby identifying patients at risk for cerebral ischemia and infarction.

References

1. Alexandrov AV, Sharma VK, Lao AY, Tsivgoulis G, Malkoff MD, Alexandrov AW. Reversed Robin Hood syndrome in acute ischemic stroke patients. Stroke. 2007;38:3045–8.
2. Alexandrov AV, Nguyen HT, Rubiera M, et al. Prevalence and risk factors associated with reversed Robin Hood syndrome in acute ischemic stroke. Stroke. 2009;40:2738–42.

3. Barlinn K, Alexandrov AV. Sleep-disordered breathing and arterial blood flow steal represent linked therapeutic targets in cerebral ischaemia. Int J Stroke. 2011;6:40–1.
4. Palazzo P, Balucani C, Barlinn K, et al. Association of reversed Robin Hood syndrome with risk of stroke recurrence. Neurology. 2010;75:2003–8.
5. West JB, Luks AM. Respiratory physiology: the essentials. 10th ed. Wolters Kluwer: Philadelphia; 2016.
6. Laffey JG, Kavanagh BP. Hypocapnia. N Engl J Med. 2002;347:43–53.
7. Stoelting RK, Hillier SC. Acid-base balance. In: Stoelting RK, Hillier SC, editors. Pharmacology and physiology in anesthetic practice. Philadelphia: Lippincott Williams and Wilkins; 2006. p. 794–802.
8. Kellogg RH. Altitude acclimatization, a historical introduction emphasizing the regulation of breathing. Physiologist. 1968;11:37–57.
9. Aaslid R, Lindegaard KF, Sorteberg W, Nornes H. Cerebral autoregulation dynamics in humans. Stroke. 1989;20:45–52.
10. Czosnyka M, Brady K, Reinhard M, Smielewski P, Steiner LA. Monitoring of cerebrovascular autoregulation: facts, myths, and missing links. Neurocrit Care. 2009;10:373–86.
11. Raichle ME, Plum F. Hyperventilation and cerebral blood flow. Stroke. 1972;3:566–75.
12. Heffner JE, Sahn SA. Controlled hyperventilation in patients with intracranial hypertension. Application and management. Arch Intern Med. 1983;143:765–9.
13. Brian JE Jr. Carbon dioxide and the cerebral circulation. Anesthesiology. 1998;88:1365–86.
14. Stocchetti N, Maas AI, Chieregato A, van der Plas AA. Hyperventilation in head injury: a review. Chest. 2005;127:1812–27.
15. Curley G, Kavanagh BP, Laffey JG. Hypocapnia and the injured brain: more harm than benefit. Crit Care Med. 2010;38:1348–59.
16. Cold GE. Cerebral blood flow in acute head injury. The regulation of cerebral blood flow and metabolism during the acute phase of head injury, and its significance for therapy. Acta Neurochir Suppl (Wien). 1990;49:1–64.
17. Harper AM, Glass HI. Effect of alterations in the arterial carbon dioxide tension on the blood flow through the cerebral cortex at normal and low arterial blood pressures. J Neurol Neurosurg Psychiatry. 1965;28:449–52.
18. Ito H, Ibaraki M, Kanno I, Fukuda H, Miura S. Changes in the arterial fraction of human cerebral blood volume during hypercapnia and hypocapnia measured by positron emission tomography. J Cereb Blood Flow Metab. 2005;25:852–7.
19. Monro A. Observations on the structure and functions of the nervous system. William Creech: Edinburgh; 1783.
20. Kellie G. On Death from Cold and on Congestions of the Brain. An account of the appearances observed in the dissection of two of three individuals presumed to have perished in the storm of the 3rd, and whose bodies were discovered in the vicinity of Leith on the morning of the 4th, November 1821: with some reflections on the pathology of the brain. Transactions of the Medico-Chirurgical Society of Edinburgh. 1824;1:84–169.
21. Carney N, Totten AM, O'Reilly C, et al. Guidelines for the management of severe traumatic brain injury, fourth edition. Neurosurgery. 2017;80:6–15.
22. Adams HP Jr, Bendixen BH, Kappelle LJ, et al. Classification of subtype of acute ischemic stroke. Definitions for use in a multicenter clinical trial. TOAST. Trial of Org 10172 in Acute Stroke Treatment. Stroke. 1993;24:35–41.
23. Spencer MP, Reid JM. Quantitation of carotid stenosis with continuous-wave (C-W) Doppler ultrasound. Stroke. 1979;10:326–30.
24. Alexandrov AV. The Spencer's curve: clinical implications of a classic hemodynamic model. J Neuroimaging. 2007;17:6–10.
25. Alexandrov AV. Cerebrovascular ultrasound in stroke prevention and treatment. 2nd ed. Hoboken, NJ: Wiley- Blackwell; 2011.
26. Giller CA, Bowman G, Dyer H, Mootz L, Krippner W. Cerebral arterial diameters during changes in blood pressure and carbon dioxide during craniotomy. Neurosurgery. 1993;32:737–41; discussion 41–2.

27. Markus HS, Harrison MJ. Estimation of cerebrovascular reactivity using transcranial Doppler, including the use of breath-holding as the vasodilatory stimulus. Stroke. 1992;23:668–73.
28. Silvestrini M, Vernieri F, Pasqualetti P, et al. Impaired cerebral vasoreactivity and risk of stroke in patients with asymptomatic carotid artery stenosis. JAMA. 2000;283:2122–7.
29. Vernieri F, Pasqualetti P, Matteis M, et al. Effect of collateral blood flow and cerebral vasomotor reactivity on the outcome of carotid artery occlusion. Stroke. 2001;32:1552–8.
30. Ringelstein EB, Weiller C, Weckesser M, Weckesser S. Cerebral vasomotor reactivity is significantly reduced in low-flow as compared to thromboembolic infarctions: the key role of the circle of Willis. J Neurol Sci. 1994;121:103–9.
31. Sharma VK, Teoh HL, Paliwal PR, Chong VF, Chan BP, Sinha AK. Reversed Robin Hood syndrome in a patient with luxury perfusion after acute ischemic stroke. Circulation. 2011;123:e243–4.

Chapter 34
Ischemic Stroke in the ICU: Bedside Monitoring of the Cerebral Autoregulation Status by Transcranial Doppler (TCD/TCCS) in the Acute Stage

Pedro Castro and Ricardo Soares-dos-Reis

Key Points

1. Cerebral autoregulation is regarded as the capability of cerebral flow to regulate itself irrespective to cerebral perfusion pressure changes.
2. Cerebral autoregulation can be measured with pressure manipulation or using spontaneous fluctuations of blood pressure (arterial line or plethysmography) and cerebral flow velocity (transcranial Doppler).
3. A headframe is necessary to ensure fixation of the 2-Mhz probes is always needed since the slightest probe sliding will affect results.
4. Transfer function characterizes cerebral autoregulation in frequency domain by three parameters: phase, gain, and coherence. Higher coherence, lower gain, and phase different from zero represent more effective autoregulatory response.
5. Cerebral autoregulation is related to hemorrhagic transformation risk, larger infarcts, and worse outcome in ischemic stroke.

P. Castro (✉)
Department of Clinical Neurosciences and Mental Health, Faculty of Medicine of University of Porto, Porto, Portugal

Department of Neurology and Stroke Unit, Centro Hospitalar Universitário de São João, E.P.E., Porto, Portugal
e-mail: pedromacc@gmail.com

R. Soares-dos-Reis
Department of Clinical Neurosciences and Mental Health, Faculty of Medicine of University of Porto, Porto, Portugal

Department of Neurology, Centro Hospitalar Universitário de São João, E.P.E., Porto, Portugal

C. N. Rodríguez et al. (eds.), *Neurosonology in Critical Care*,
https://doi.org/10.1007/978-3-030-81419-9_34

34.1 Introduction

Measuring cerebral autoregulation (CA), on par with cerebrovascular reactivity, tests different properties of the cerebrovascular system, thus providing a window into the ability of the cerebral circulation to react to variations in pressure/flow, metabolites, and gases. CA evaluation, in particular, assesses the changes in cerebrovascular resistance in response to perfusion pressure changes. If CA is impaired, systemic arterial blood pressure (ABP) fluctuations are directly transmitted to the brain parenchyma, resulting in either hypoperfusion or brain edema [1, 2]. This is especially important in the setting of acute ischemic stroke, where there should be a balance between perfusing the ischemic penumbra and minimizing the risk of hemorrhagic reperfusion [2, 3].

34.2 Cerebral Autoregulation: General Outline

Despite the various methods that can be used to assess CA, only a few can be applied during the acute phase of stroke due to the lack of patient cooperation and/or contraindications arising from the patient's clinical situation. At our center, we use continuous transcranial Doppler (TCD) recording of the M1 segment of the middle cerebral artery (MCA) cerebral blood flow velocities (CBFVs), as a CBF surrogate, and measure peripheral ABP noninvasively with a Finapres® device (which can be replaced by an arterial line, should the patient have one).

We then synchronously record ABP and CBFV continuous beat-to-beat time series, during at least 5 minutes, which is then evaluated off-line by dedicate software. This approach assumes that the MCA diameter is constant during monitoring, which has been shown to be true for this method. Furthermore, to ensure test reliability, CO_2 levels should be constant. These can be monitored by capnography measurements of end-tidal CO_2.

In patients with severe conditions, who carry an intracranial pressure (ICP) catheter, another index – the pressure-reactivity index (PRx) – can be derived. This obviates the need for TCD monitoring and is outside the scope of this chapter.

34.3 Cerebral Autoregulation Measurement: Method

Evaluations should be carried out in supine resting position with the bed at 0° during the 10 minutes of recording. The instrumentation of the patient is carried out as follows:

- TCD with 2-MHz monitoring probes are secured with a standard headband; CBFVs are recorded bilaterally from the M1 segment of MCA (depth of 50–55 mm) as shown in Fig. 34.1.

Fig. 34.1 Setting of a patient to measure CA
The patient lies supine with bed close to 0°. A thin pillow provides comfort to TCD apparatus avoiding pain and agitation throughout the monitoring. TCD probes (1) are bilaterally secured with a headframe (2). A nasal cannula (3) is also put in place and secured in the headframe. A facial mask might be needed in patients breathing through the mouth. Three electrodes (4) are used to get a lead-II electrocardiographic line. Note that the height pressure corrector (5) that comes coupled with the plethysmography is located at heart level; this corrects possible drifts in ABP caused by unwilling hand movement of the patient. Continuous blood pressure measurement with finger plethysmography (6), in this case Finometer® device (FMS, Amsterdam, The Nederland), in which we can observe the arterial blood pressure curve beat-to-beat

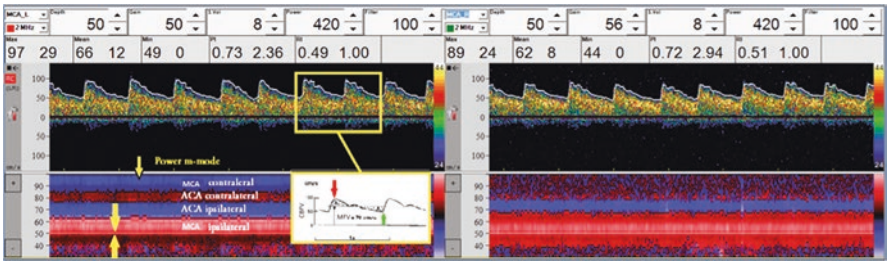

Fig. 34.2 Transcranial Doppler display of BoxX® (DWL, Singen, Germany)
In the upper panels, we observed two spectra (right and left) Doppler signal of a bilateral monitoring of the middle cerebral arteries (MCA). Under the spectrum, there is the envelope (white line), from which we can calculate the values of cerebral systolic blood flow velocities (red arrow), diastolic (green arrow) and average for each cardiac cycle. The yellow-bounded miniature represents schematically the various cerebral blood flow velocities to be calculated (systolic, diastolic and mean). In the lower panels, we can see the appearance of the Power M-Mode mode. Here, the scale refers to the depth (mm) and shows the directional flow (by convention the red is towards the probe and the blue in the opposite direction of the probe). Among the yellow arrows, the white line corresponds to the sampling depth of the upper panel's flow spectrum

- TCD display (Fig. 34.2) is inspected to ensure that the envelope of the Doppler spectrum correctly outlines maximum velocity and has no artifacts; this is a crucial step to have enough continuous good-quality data to further analyze CA; at least 5 minutes of continuous undisturbed TCD CBFV will be needed.
- ABP is continuously monitored with a finger cuff in the unaffected side, as shown in Fig. 34.3. Usually, some time is needed to stabilize ABP through the automated calibration of the device; keep the patient's hand or height corrector (coupled with the plethysmography device) at heart level.

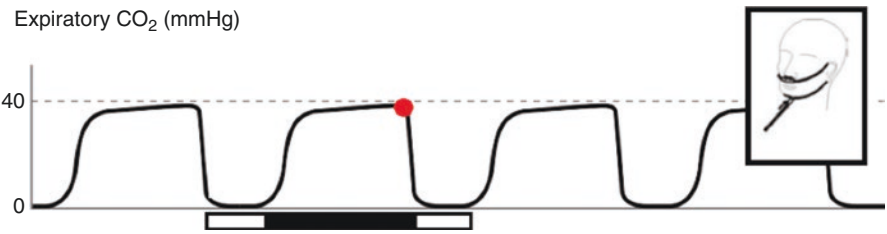

Fig. 34.3 Capnography nasal line for non-invasive end-tidal CO_2 measurement
After an inspiratory stage (white bar), in which the flow in the cannula is not stopped, the device detects a sudden increase of carbon dioxide (CO_2) after expiration starts, eventually reaching a plateau stage in which there is a alveolar equilibrium of $PaCO_2$. Thus, the end-tidal value of CO_2 ($EtCO_2$) approximates the actual value $PaCO_2$

- Heart rate (HR) is assessed from lead II of a standard 3-lead electrocardiogram as shown in Fig. 34.3.
- End-tidal carbon dioxide (CO_2) is continuously recorded using a nasal cannula attached to a capnograph (Nonin, Amsterdam, the Netherlands). This is not actually needed to calculate CA indexes, but it is an important physiological parameter that can influence CBFV and its average value should be reported during monitoring (Fig. 34.3).
- All data are synchronized and digitized in an analogue-digital converter like Powerlab (AD Instruments, Oxford, UK) and stored for offline analysis.

34.4 Cerebral Autoregulation Measurement: Technical Tips

A few technical details are important whenever assessing CA:

- A headframe to ensure fixation of the 2-Mhz probes is always needed since the slightest probe sliding will affect results.
- Take your time to stabilize Doppler probes to ensure that the envelope is correctly determined despite some head movement. It is critical to have a good envelope of CBFV curve to minimize artifacts.
- Finger cuffs used with plethysmography will not detect ABP curve properly if the hand is cold. You can overcome this by keeping a warm room temperature as well as applying a rubber glove filled with heated water or a hot pack (e.g., those commonly used for muscle pain therapy) close to the hand with the cuff.
- ABP measurement with plethysmography is usually performed at heart level. If the patient is in supine position, this is the same as the brain level. However, if the subject is seated, the ABP at brain level will be lower in an amount equivalent to the difference of hydrostatic pressure between the cuff and the probe (usually

20 cm H_2O, or approximately 15 mm Hg). In practice, you need to measure with a common ruler the distance between the finger and the Doppler probe and subtract this to the actual ABP measured. Consider that 1 mm Hg = 1.36 cm H_2O.

- Additionally, blood pressure should be assessed with an oscillometric cuff to provide standard mean ABP values; this might be used during the data analysis to correct mean ABP values calculated in the ABP curve of plethysmography.

34.5 Cerebral Autoregulation Measurement: Data Analysis

This analysis is usually done in noncommercial software like MATLAB®.

All signals are inspected and artifacts removed by linear interpolation. Mean flow velocities (MFV) and mean arterial pressure (MAP) are calculated beat-to-beat as shown in Fig. 34.4. Transfer function analysis (TFA) is used to assess dynamic CA by calculating coherence, gain, and phase parameters from beat-to-beat spontaneous oscillations in MFV and MAP (Fig. 34.5). In order to do this, we use a minimum of 5 minutes of normalized data interpolated at 100 Hz into a uniform time basis; the averaged periodogram is calculated by the Welch method with a Hanning window of 30 seconds, with 50% overlap [4].

The approach we describe above provides an adequate assessment of dynamic CA, with no need for patient collaboration or hemodynamic challenges, relying instead on the response of CBF(V) to spontaneous ABP fluctuations. In this setting, ABP fluctuations can be regarded as an input and the subsequent CBFV response as an output of this system. The relationship between both parameters can be

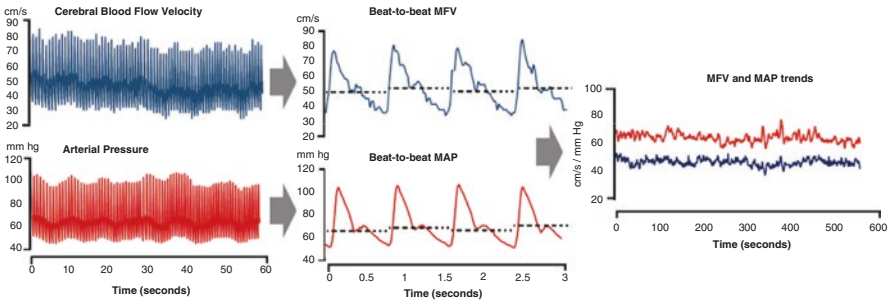

Fig. 34.4 Spontaneous oscillation of systemic and cerebral hemodynamic signals
Graphical representation of blood pressure obtained by Finometer® and cerebral blood flow by transcranial Doppler. On the left, note spontaneous oscillation over 1 minute of monitoring. In the center, an inspection of 4 cardiac cycles is observed, calculating the means of both signals (MAP and MFV, respectively), beat-to-beat. Further to the right, we observe the variation of the MFV and MAP over almost 10 minutes of monitoring. These oscillations allow the calculation of cerebral autoregulation, for example, by the transfer function analysis

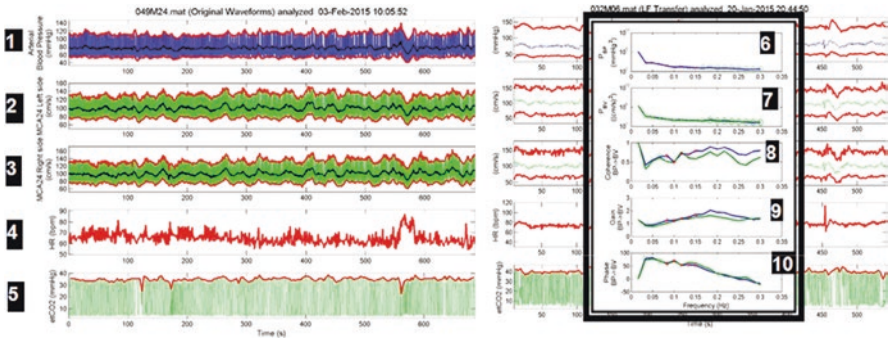

Fig. 34.5 Transfer Function Analysis
From the time series of continuous monitoring of blood pressure (1) and cerebral blood flow velocity (2, 3) we derive their mean values (MFV and MAP, respectively). Note the spontaneous oscillation of these physiological variables. The transfer function analysis (TFA) verifies the influence of the MAP (input) on the MFV (output) in the frequency domain from its spectra (6 and 7, respectively). The TFA produces 3 parameters: coherence (8), gain (9) and phase shift (10). In this case, we note that autoregulation functions as a high-pass filter, with a slower MAP oscillation (<0.2 Hz), manifested by a higher damping (decrease of gain (9)) and higher (increase of phase (10)). Personal data, unpublished, calculated with private software based on Matlab®

adequately analyzed by a method called TFA, which had its origin in electronics and relates to linear control systems theory. Claasen and colleagues, on behalf of the International Cerebral Autoregulation Research Network [4], have produced a white paper establishing a standardization of parameters and settings which should be adopted for using TFA in dynamic CA studies. In this paper, they describe standardized testing conditions and recommendations regarding the off-line computations required to obtain *gain*, *phase,* and *coherence*. These three parameters can be simplistically regarded as the difference in amplitude between the CBFV and ABP wave amplitude (*gain*), the time shift between the ABP stimulus and CBFV response (phase shift), and the squared correlation coefficient (coherence), which is helpful in assessing measurement reliability and noise. Coherence is calculated between input auto-spectra of ABP over cross-spectra of CBFV/ABP, and transfer functions of phase and gain are determined by dividing the cross-spectrum by the input auto-spectrum. Coherence is the coefficient of correlation between the signals; higher coherence between the oscillations is reflective of less effective CA. Gain quantifies the damping effect of CA on the magnitude of ABP oscillations. Phase shift represents the time delay between ABP and CBFV oscillations. Lower gain and higher phase represent tighter, more effective autoregulatory response. A schematic representation of the physiological interpretation of CA phase and gain is depicted in (Fig. 34.6). Values are reported in three frequency bands: very low (VLF

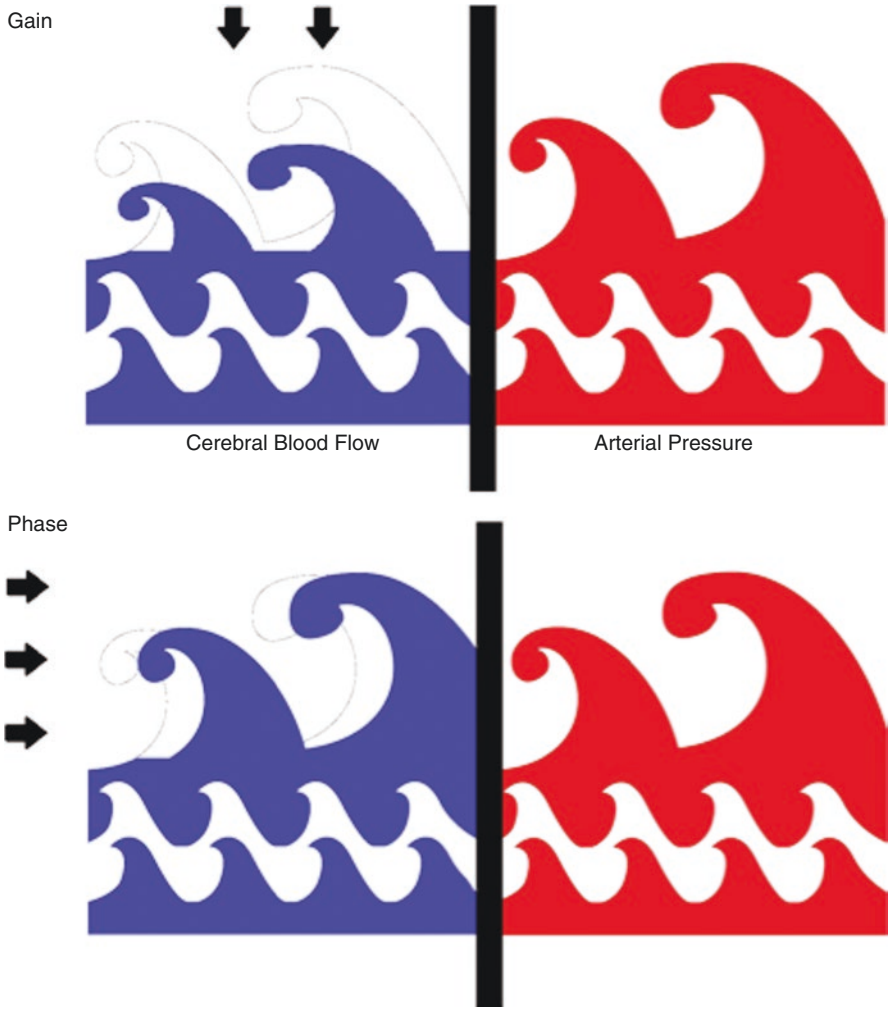

Fig. 34.6 Schematic representation of the gain and phase effect

0.02–0.07 Hz), low (LF 0.07–0.20 Hz), and high (HF 0.20–0.50 Hz) frequency ranges.

Other indexes of CA can be calculated, such as the autoregulatory index (ARI) [5, 6] or Mx (Fig. 34.7). To assess ARI, the actual CA response, after applying an inverse discrete Fourier transform of amplitude (gain) and phase, is compared to 10 predefined responses, allowing for classification of the autoregulatory index (ARI) from 0 to 9 (higher numbers represent better CA) [1].

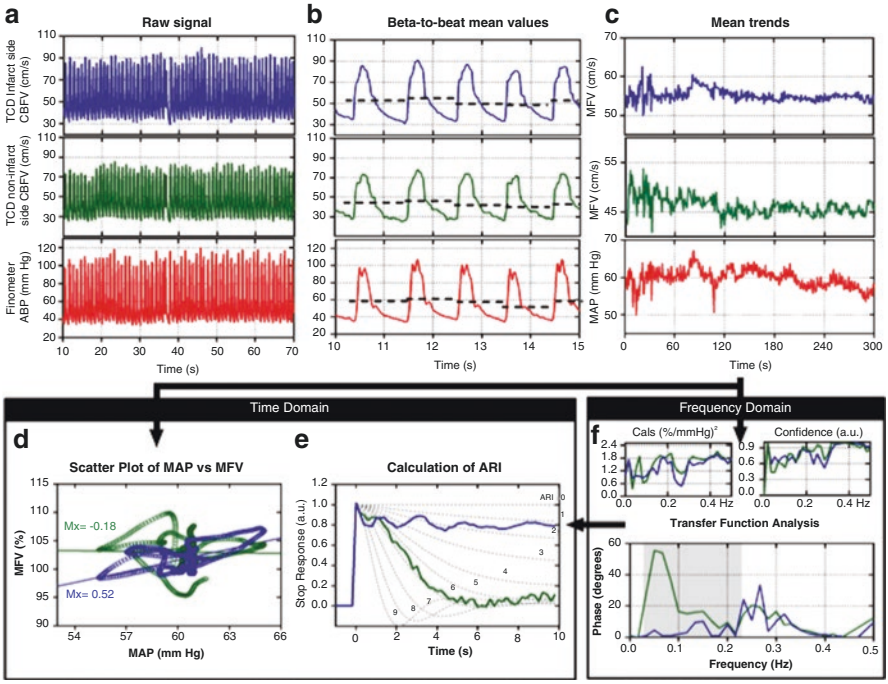

Fig. 34.7 Calculation of various CA indexes within 6 hours of stroke onset with total affection of the MCA territory. (**a**) The continuous signals of transcranial Doppler (TCD) cerebral blood flow velocity (CBFV) and arterial blood pressure (ABP, red) from affected (blue) and unaffected (green) MCA hemispheres are inspected and mean values calculated (MFV and MAP, respectively) (**b**). From 300 seconds of these time-series (**c**), CA can be calculated in time and frequency domains. In the first case (**d**, **e**), MFV is plotted against MAP and a Pearson's correlation coefficient is obtained (Mx). Note that Mx = 0.52 in infarct hemisphere while Mx = − 0.18 in the contralateral side, meaning worse CA in affected side. In frequency domain (**f**) TFA analysis outputs are coherence, gain and phase. Phase is higher within CA range (VLR + LF bands, 0.03 – 0.2 Hz, shaded area) at contralateral versus ipsilateral side (7 versus 41 degrees). From the inverse Fourier transform of the transfer function we come back to time domain to depict MFV step response to an impulse of MAP. The actual response is compared to ten predefined responses (dashed gray lines) from ARI = 0 to 9. In the affected side, the response is very slow (ARI = 2.1), but in the contralateral side the response is faster (ARI = 7.0). CA is highly impaired at the affected side. The patient had hemorrhagic transformation at 24 hours and remained bedridden (3 months modified Rankin scale of 5). (Published with permission of Castro et al. [5])

So far, our approach has relied on frequency analysis of ABP and CBVF waveforms. However, one can also perform a time-domain analysis by using the correlation coefficient between 30 consecutive 10-s averages of TCD CBFV and ABP; this coefficient is referred to as Mx [5, 7].

34.6 Cerebral Autoregulation Assessment: Interpretation of the Results

In CA, coherence and gain are reduced and phase shift is increased during transition from HF to LF, resulting in dampened and delayed repercussion of ABP oscillations to the cerebral vessels, and therefore desynchronization between ABP/CBFV fluctuations, similarly to a high-pass filter. Since vasomotor adaptation is slow and requires at least 6–10 s, CA is most likely to operate at low frequencies. Although a validated cutoff between normal and abnormal CA does not exist, a phase shift of less than 30 degrees [8] has been proposed to represent CA failure. This closely matches the cutoff that was obtained in a cohort of ischemic stroke patients that had worse outcome [3].

An ARI <4 has been proposed as a threshold for impaired CA [6].

Concerning Mx, a correlation approaching 0 denotes that CBF is unaffected by ABP variation and, therefore, CA is preserved. On the contrary, values greater than 0.3 denote an impaired CA. This method has the advantage that it is suitable even when linearity is not present. However, care should be taken to ensure adequate measurements are taken, as lack of correlation may be purely due to insufficient data quality.

34.7 Clinical Relevance

Studying dynamic CA in the acute phase of stroke is extremely relevant and may establish a foundation for personalization of ABP goals during the acute phase of stroke. Several recent studies have shown that CA is impaired in the acute phase of stroke. We have assessed CA in a cohort of 46 adult stroke patients within 6 h of symptom onset, when cerebral perfusion changes are most likely important. Our analysis showed that low phase in the affected hemisphere correlated with hemorrhagic transformation and edema, larger infarct sizes, and worse 3-month outcome, as assessed by the mRankin scale. This CA dysregulation resolved within 3 months. Other authors have published data in agreement the hypothesis of impaired CA during the acute phase of stroke. Reinhardt and colleagues have indeed shown that CA is impaired as assessed by TFA and Mx, in the affected hemisphere, and that it correlates with higher NIHSS, infarct size, and mRankin scale. In addition, Saeed demonstrated that cortical infarcts had a greater impairment than subcortical ones. Interestingly, work by Guo and colleagues has demonstrated that, while in larger infarcts, CA impairment is unilateral; in lacunar infarcts, there is bilateral CA dysregulation. Challenging those findings, Xiong and others have compared phase difference in 60 acute stroke patients and 16 healthy controls. They have shown that

CA is bilaterally impaired in stroke patients, when compared with control values, and that this impairment is symmetrical. In this study, coexisting small-vessel disease correlated with an even greater impairment of CA. Llwyd and colleagues have found, by amalgamating 143 ischemic stroke patients, that CA was similarly impaired in the affected hemisphere, regardless of stroke severity and subtype. Nevertheless, the same authors published a subsequent report of 55 stroke patients where they reported larger loss of CA in moderate and severe strokes, correlating with a worse functional outcome. In summary, most studies to date show CA impairment in patients with ischemic stroke [5].

This impairment is more frequently focal with large-vessel strokes and global in small-vessel strokes, which usually happen in the setting of cerebral microangiopathy, which induces a more global pattern of impaired CA. Nevertheless, some study results are still conflicting, and there is an urge for widespread standardization of CA assessment in the setting of acute stroke. Standardization of CA monitoring, right from stroke onset, should establish the foundations for clinical trials analyzing the impact of CA-oriented ABP management.

34.8 Conclusion

Cerebral autoregulation can be measured spontaneously with pressure manipulation using spontaneous fluctuations of blood pressure and cerebral flow (velocity). Noninvasively, the usual apparatus consists in a plethysmography device and transcranial Doppler to assess continuous blood pressure and cerebral blood flow velocity. Impairment of cerebral autoregulation appears to be involved in the pathophysiology of acute ischemic stroke. A less effective cerebral autoregulation (reduced phase) in acute ischemic stroke puts brain tissue at risk of progression to cerebral edema or hemorrhagic transformation. These complications are associated with an inappropriate vasodilator response in the acute phase which also suggests vasomotor dysfunction. A less effective cerebral autoregulation (reduced phase) in acute ischemic stroke is associated with larger-volume infarcts at 24 hours, probably due to ischemic progression in the penumbra area.

In summary, dynamic brain self-regulation has been shown to play a considerable role in the study and evaluation of acute cerebral ischemia. The results obtained encourage the development of different lines of research with potential therapeutic interest that may benefit the prognosis of patients with acute ischemic stroke.

References

1. Azevedo E, Castro P. Cerebral autoregulation. Cambridge: Cambridge University Press; 2016.
2. Castro P, Azevedo E, Serrador J, Rocha I, Sorond F. Hemorrhagic transformation and cerebral edema in acute ischemic stroke: link to cerebral autoregulation. J Neurol Sci. 2017;372:256–61.

3. Castro P, Serrasor JM, Rocha I, Sorond F, Azevedo E. Efficacy of cerebral autoregulation in early ischemic stroke predicts smaller infarcts and better outcome. Front Neurol. 2017;8:113.
4. Claassen JA, Meel Van den Abeelen AS, Simpson DM, Panerai RB. Transfer function analysis of dynamic cerebral autoregulation: a white paper from the International Cerebral Autoregulation Research Network. J Cereb Blood Flow Metab. 2016;36:665–80.
5. Castro P, Azevedo E, Sorond F. Cerebral autoregulation in stroke. Curr Atheroscler Rep. 2018;20:37.
6. Panerai RB, Haunton VJ, Hanby MF, Salinet AS, Robinson TG. Statistical criteria for estimation of the cerebral autoregulation index (ARI) at rest. Physiol Meas. 2016;37:661–72.
7. Reinhard M, Rutsch S, Lambeck J, Wihler C, Czosnyka M, Weiller C, et al. Dynamic cerebral autoregulation associates with infarct size and outcome after ischemic stroke. Acta Neurol Scand. 2012;125:156–62.
8. Diehl RR. Cerebral autoregulation studies in clinical practice. Eur J Ultrasound. 2002;16:31–6.

Chapter 35
Sonothrombolysis: Usefulness of Transcranial Doppler Ultrasonography (TCDU)

Jose C. Navarro, Cyrus G. Escabillas, and Vijay K. Sharma

Key Points

1. Acute ischemic stroke may not be a common occurrence in the ICU; however, vigilance should still be exercised to identify these patients for immediate treatment following existing guidelines.
2. Intravenous recombinant tissue plasminogen activator is still the mainstay in treatment of ischemic stroke for immediate recanalization of the cerebral vessels.
3. The addition of ultrasound (sonothrombolysis) would further augment the rate of recanalization of occluded vessel.
4. Additional information could be provided by the transcranial Doppler ultrasound, such as occlusion, recanalization, and re-occlusion in real time and noninvasively.
5. Rapid advancement in the design of therapeutic TCD devices and microbubbles holds promise for establishing a better future for patients with acute ischemic stroke.

J. C. Navarro (✉)
Jose R. Reyes Memorial Medical Center, Department of Neurology, Institute of Neurosciences, St Luke's Medical Center, University of Santo Tomas, University of Santo Tomas Hospital, Manila, Philippines
e-mail: josecnavarromd@gmail.com

C. G. Escabillas
Jose R. Reyes Memorial Medical Center, Manila, Philippines

V. K. Sharma
Division of Neurology, National University Health System, Singapore and Yong Lo Lin School of Medicine, National University of Singapore, Singapore, Singapore
e-mail: mdcvks@nus.edu.sg

C. N. Rodríguez et al. (eds.), *Neurosonology in Critical Care*,
https://doi.org/10.1007/978-3-030-81419-9_35

35.1 Introduction

The development of intensive care units (ICUs) in 1952 has tremendously improved the care of critically ill patients [1]. This allowed patients with multiple organ failure or complex systemic diseases to attain longer survival with a better functional status. In the United States, approximately 55,000 patients are treated in ICU each day [2]. Most patients admitted in the ICU often develop several complications such as infections, organ failure, and neurologic dysfunction, which are often associated with poor outcomes [3].

Undoubtedly, patients admitted in the ICU may also develop acute ischemic stroke (AIS). Multiple conditions, such as vascular risk factors, coagulopathy [4], diabetes mellitus [5], and infections [6], and medications, such as hormonal replacement therapy [7], anticoagulants [8], amphetamine, and cocaine [9], may predispose patients for developing AIS. AIS occurring in the ICU may result in worsening of the existing medical condition and affect the long-term outcome. To date, there is a very limited data on the incidence of AIS in the ICU. Unfortunately, because of little awareness and limited attention given to patients who are at risk for AIS in the ICU, the condition is not immediately and well recognized. In a 10-year retrospective study by Wijdicks et al., only 19 patients with critical illness experienced stroke, 10 of which were ischemic and 9 were hemorrhagic in nature. Although the number of stroke occurring in the ICU remains small, the mortality among these patients is significant, reported to be as high as 89% [10].

Management of AIS even in the ICU setting must follow internationally recognized guidelines. Critically ill patients, especially when on mechanical ventilation, are unable to complain of weakness, slurring of speech, and sensory deficit. Hence, the nurses and physicians in ICU must remain extra vigilant about the neurological status. A regular round the clock neurological examination must be performed among high-risk patients to recognize any neurological deterioration.

Intravenously administered recombinant tissue plasminogen activator (IV-rTPA) remains the only approved drug therapy for achieving arterial recanalization in AIS. However, its use is limited by a narrow therapeutic time window (up to 4.5 hours of symptom onset), strict inclusion criteria, and the associated risk of bleeding. More importantly, the intracranial arterial recanalization rates are often unsatisfactory [11]. Consequently, there has been an ongoing quest for exploring additional interventions that could further enhance the thrombolytic action of IV-rTPA. Accordingly, continuous monitoring with the conventional 2-MHz transcranial Doppler (TCD) ultrasound during systemic thrombolysis (sonothrombolysis) demonstrated safety and efficacy in terms of early recanalization [12–14]. Furthermore, addition of ultrasound contrast agents (microbubbles) was also reported to enhance the thrombolytic effect of IV-rTPA. We summarize the available experimental and clinical data on the potentials, failures, and current status of sonothrombolysis.

35.2 AIS: Intravenous Thrombolysis with IV-rTPA

In 1995, a clinical trial funded by the National Institute of Neurological Diseases and Stroke (NINDS) showed the benefit of IV-rTPA within 3 hours after AIS [15]. Subsequent clinical trials established the efficacy of IV thrombolysis up to 4.5 hours of symptom onset [16]. Interestingly, this was predicted from the pooled analysis of initial six randomized clinical trials of IV-rTPA in Europe and the United States [17–20]. An important finding of the pooled analysis indicated that the onset to treatment time was inversely associated with the likelihood of favorable functional outcome at 3 months.

35.3 Ultrasound-Enhanced Thrombolysis

The term sonothrombolysis is used to describe the ultrasound-assisted clot lysis during intravenous thrombolysis for AIS. Ultrasound-assisted thrombolysis, sonothrombolysis, has shown promise for becoming a rapidly available, noninvasive, and portable tool in the armamentarium of the stroke neurologists.

35.4 In Vitro Models: Understanding the Mechanism of Sonothrombolysis

Ultrasound waves in the range of MHz-KHz frequency are known to enhance the therapeutic efficacy of IV-rTPA [21]. Ultrasound, being a mechanical and pressure wave, leads to transient and repeated thinning of the fibrin threads. Such exposure potentially separates the strands of fibrin and creates micro-streaming of blood flow though the clot, thereby enhancing better and faster clot lysis. Ultrasound exposure leads to some conformational changes like reversible disaggregation of uncrossed-linked fibrin fibers. Other plausible mechanisms responsible for the ultrasound-assisted thrombolysis are micro-cavity formation in the shallow layers of thrombus, superficial vasodilation, and promoting nitric oxide release. The aforementioned mechanisms increase the penetration of rTPA into clot, leading to residual flow enhancement, clot lysis, and reduction in infract size [21].

The effects of sonothrombolysis were studied by Zhou et al. in an in vitro experiment [22]. Blood clots were prepared from horse blood and used to create occlusions in the silicone tubing, mimicking the intracranial arteries, in an in vitro, water tank with controlled temperature. Then, the authors evaluated the relationship between the effect of ultrasound-assisted thrombolysis and age of the clot as well as

the cholesterol content. The clots were aged by repeated replacement of serum by fresh blood. Cholesterol content of the clot was increased by adding the commercially available chemical cholesterin. Clots were placed in the closed-loop silicone tube model in which normal saline flowed in a pulsatile fashion. Commercially available rTPA was added (equivalent to the therapeutic dose for AIS thrombolysis) to the saline, and clot was exposed to the diagnostic 2-MHz transcranial Doppler ultrasound for 1 hour continuously. The clot lysis was evaluated by measuring the weight of the clot at the end of the experiment and surface electron microscopy. The study found that sonothrombolysis induced greater reduction in clot size with younger age and higher cholesterol content.

The property of ultrasound to enhance clot lysis was first demonstrated around the 1970s [23, 24] and was subsequently investigated on animals and in vitro models [25, 26]. However, these mechanisms of ultrasound to facilitate clot dissolution have not been well understood [27]. Several mechanisms of action have been proposed to explain its enhanced-lytic effect. The pressure wave effect created by ultrasound may accelerate the enzymatic dissolution of clot by way of nonthermal action in increasing the transport of drug to the clot [28]. Cavitation of the thrombus by the ultrasound wave also plays a significant role in ultrasound-enhanced thrombolysis [29]. Another plausible mechanism of sonothrombolysis is microstreaming, which promotes the movement of fluid around the thrombus [30].

35.5 Sonothrombolysis in AIS: Human Studies

Ultrasound in Kilo-Hertz frequencies is known to penetrate better into the human soft tissue [27, 31]. It was tested in the transcranial low-frequency ultrasound-mediated thrombolysis in brain ischemia (TRUMBI) trial in Germany [32]. The trial included only 26 AIS patients treated within 6 hours of symptom onset. This multicenter trial evaluated the effect of 90-minute exposure of the occluded intracranial artery by using 300-kHz frequency ultrasound in duplex system. This study was stopped prematurely due to very high incidence of symptomatic intracranial hemorrhage (SICH) in the combined treatment (ultrasound+IV-rTPA) arm (93%) as compared to the IV-rTPA only arm (42%). No definite mechanism was elucidated for this observation. However, authors hypothesized that reverberations of long wavelength ultrasound inside the head lead to resonance and development of hotspots to be responsible for very high incidence of hemorrhages in the infarcted tissues as well as in remote locations. Furthermore, the configuration of the ultrasound waves used in the trial could have caused mechanical damage and distortion of micro vessels [33].

CLOTBUST trial looked at the safety and feasibility of the use of routinely used diagnostic 2-MHz ultrasound in enhancing the action of systemic thrombolysis [34]. The study enrolled 126 patients: 63 randomized to continuous ultrasound

exposure for 2 hours, while 63 patients were allocated to the placebo arm. Patients randomized into the placebo arm underwent intermittent TCD to evaluate the arterial patency. Robust primary outcome included complete recanalization on TCD or dramatic clinical recovery within 2 hours after the administration of the rTPA bolus, or reduction in National Institute of Health Stroke Scale (NIHSS) score by 10 points or a total NIHSS 3 points at the end of 2 hours. Interestingly, the primary end point was achieved by 49% patients in target group as compared with 30% patients in the control group (P = 0.03), without any increase in SICH in the ultrasound group. This study also showed nonsignificant (13% absolute) increase in patients with modified Rankin Scale (mRS) of 0–1 point at 3 months (42% vs. 29%, p value for trend 0.2). An example of the change in TCD flow spectra during IV-rTPA infusion is shown in Fig. 35.1.

Synthetic microbubbles were initially used as contrast agents to improve the quality of ultrasound images. The microbubbles (microspheres) oscillate and cavitate when exposed to pulsed wave ultrasound, thereby releasing more energy along

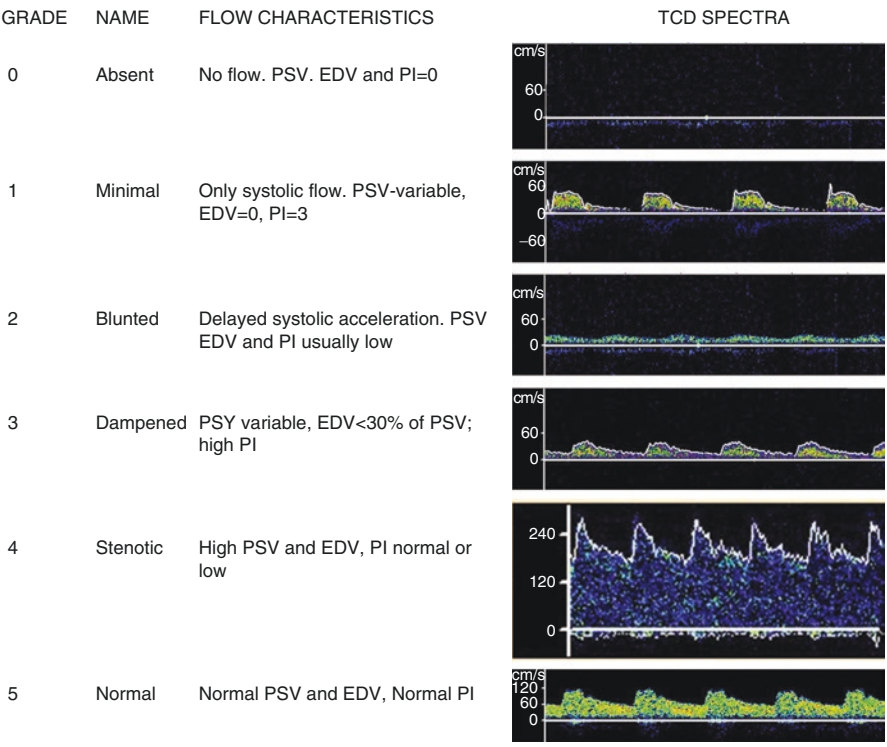

Fig. 35.1 Thrombolyis in Brain Ischemia (TIBI) grading system. TIBI grading system represents the patency and flow characteristics in an intracranial artery. Flow spectra determined by peak systolic velocity (PSV), end-diatolic velocity (EDV) and pulsatility index (PI) are represented for each TIBI grade

the insonated tissues. The momentum of bubble movement can potentially increase residual flow around and through the thrombus, thus helping in mechanical degradation of clot and promoting recanalization [35]. The role played by microbubbles in improving the efficacy of IV-rTPA in humans AIS was described by Molina et al. by using galactose-based microbubbles [36]. In this study of 111 patients, three different arms were tested in AIS patients presenting within 3 hours from symptom onset. IV-rTPA alone was compared with IV-rTPA plus 2-MHz ultrasound as well as IV-rTPA plus ultrasound plus microbubbles. Microbubbles were shown to be safe with no increase in SICH and resulted in improving the recanalization rates (54%).

Newer generation microbubbles use phospholipid molecules. These microbubbles have a median size of 1.2 micron or lesser in diameter [37]. When injected, these bubbles are activated by ultrasound waves, and the induced pulsations break their phospholipid shell, releasing the inert gas in their core. The thrombus surface undergoes cavitation, increases the surface area for the action of rTPA, and increases lysis of the clot. Higher recanalization rates, with no increase in SICH, were observed in a clinical trial that used the third-generation Perflutren-lipid microbubbles, which permeate beyond occlusions [38]. The transcranial ultrasound in clinical sonothrombolysis (TUCSON) trial evaluated the safety of IV-rTPA plus 2-MHz ultrasound plus escalating doses of intravenous microspheres. The trial was terminated after three subjects developed SICH in the second dose tier, and the financial support was withdrawn by the sponsor. Interestingly, a dose of one vial of microsphere use (Tier 1) demonstrated 67% recanalization rate with no increase in SICH [39].

A recent comprehensive review and meta-analysis evaluated the role of sonothrombolysis in AIS [40]. It identified six randomized (total 224 patients) and three nonrandomized (total 192 patients) relevant studies. There were no safety concerns as the pooled rate of SICH did not show any increase with the use of sonothrombolysis. Furthermore, complete recanalization rates were higher in patients receiving sonothrombolysis (37.2%; 95% CI, 26.5–47.9%) compared with patients treated with IV-rTPA alone (17.2%; 95% CI, 9.5–24.9%). Similarly, eight studies for sonothrombolysis with 2-MHz TCD, with or without microspheres, were associated with higher likelihood of complete recanalization (pooled OR 2.99; 95% CI, 1.7–5.25; $p = 0.0001$) as compared to intravenous rTPA alone.

AIS patients with NIHSS scores $\geq$10 points and proximal intracranial occlusions appeared to benefit more from sonothrombolysis [41]. Results of the previous studies warranted the need for an efficacy trial for sonothrombolysis. However, a major hurdle was the operator dependency of TCD machines and limited availability of adequately trained neurosonologists for a timely completion of a proposed clinical trial. To overcome this limitation, a novel therapeutic device was developed, which did not require operator targeting of target vessels. The configuration ensured sufficient ultrasound exposure of various branches of the circle of Willis. Safety of this device was established in stroke-free volunteers in a phase II study [42, 43]. This device did not require any ultrasound training for the stroke neurologists and could be placed on the head by following various anatomic landmarks.

Using the above-mentioned operator-independent headframe, a prospective, multicenter, randomized, double-blind, placebo-controlled clinical trial (CLOTBUST-ER) was initiated [44]. The headframe employed 16 transducers fixed into three different arrays (two temporal and one transforaminal/suboccipital – similar to the conventional acoustic windows employed for diagnostic TCD) to transmit sequential ultrasound energy to the principal intracranial regions to the various major branches of the circle of Willis [45]. Subjects were allocated in 1:1 ratio to the target group (active ultrasound + IV-rTPA) or the control group (sham ultrasound + IV-rTPA) using web-based central randomization. Adult patients with AIS (premorbid functioning in community) aged 18–80 years and with a baseline NIHSS score ≥10 points and within 4.5 hours of symptom-onset (3 hours for the United States and Canada) were included in the trial. All patients received standard stroke care in addition to trial treatment. The primary outcome was assessed on the modified Rankin Scale (mRS) at 90 days from randomization. Safety outcomes included SICH within 24 hours of IV-rTPA bolus and an overall analysis of adverse events. The trial was terminated prematurely in March 2015 upon recruitment of 675 out of the target sample of 830 subjects, due to the futility of the study in a preliminary analysis (results announced at European Stroke Organization Conference 2015 at Barcelona, Spain). Details of the study results are awaited.

In 2008, Eggers et al. reported the findings of a randomized controlled trial combining tPA and transcranial color-coded sonography (TCCS) [46]. A 1.8-MHz continuous ultrasound for 1 hour was used in patients, while controls were treated with intravenous thrombolysis alone. Complete/partial recanalization was seen in 58% of patients with rTPA and TCCS and 22% recanalization in rTPA alone. Improvement of NIHSS was also observed from day 1 to 4, and mRS ≤1 was seen in four subjects after 90 days in the treatment group and none in the control group. Furthermore, a Barthel Index of ≥95 was also observed in eight patients in the treatment group and none in the control group. However, the recently published Norwegian Sonothrombolysis in Acute Stroke Study (NOR-SASS) reported no benefits of contrast-enhanced sonothrombolysis [47]. In this randomized clinical trial, 183 patients were randomly assigned to either contrast-enhanced sonothrombolysis (93 patient) or sham ultrasound treatment (90 patients). The rates of SICH or mortality were not similar in the two groups. Neurological improvement at 24 hours and functional outcome at 90 days were similar in the two groups both in the intention-to-treat analysis and in the per-protocol analysis. However, an important limitation of this trial is the low median NIHSS scores (only 4 points in the active arm and 5 points in the sham treatment arm). We strongly feel that the trial did not include appropriate patients who could benefit from sonothrombolysis (i.e., patients with at least a moderate stroke and intracranial arterial occlusion). Probably influenced by the results of NOR-SASS and CLOTBUSTER trials, the American Heart Association/American Stroke Association (AHA/ASA) downgraded the level of recommendation for sonothrombolysis to "No clear benefit" in the recently updated guidelines for the early treatment of AIS [48].

35.6 TCD Monitoring: Arterial Occlusion, Recanalization, and Re-Occlusion

Several TCD studies have shown that the dynamic process of acute proximal occlusions can be followed up in real time following systemic thrombolysis (Figs. 35.1 and 35.2). Moreover, the beginning of recanalization can be timed and quantified using the Thrombolysis in Brain Ischemia (TIBI) criteria (Fig. 35.1) [49]. Dissolution of clot and subsequent flow improvement can also be monitored with additional changes indicating clot lysis such as intensity of flow signals, presence of microembolization, changes in mean flow velocity, and changes in the pulsatility index. These changes follow the TIBI flow pattern for occlusion and recanalization (Fig. 35.2).

The beginning of recanalization, for example, speed and completeness of clot dissolution, can be established by monitoring the following parameters: a change in the waveform by 1 or more TIBI residual flow grade (absent to minimal, minimal to blunted, and minimal to normal flow), microembolic signal starts to appear (high-intensity transient signals, HITSs), improvement of the mean flow velocity by almost 30% and more with constant angle of insonation, skull-probe interface and gain/sample volume/scale setting, and Doppler signals indicating changes (30% or more) in the pulsatility indexes and amplitude of the systolic peaks [50]. The appearance of highest TIBI flow grade is an indication of complete recanalization.

The appearance of recanalization, complete or partial, has also been described as "sudden" in which there is an abrupt appearance of normal or stenotic flow;

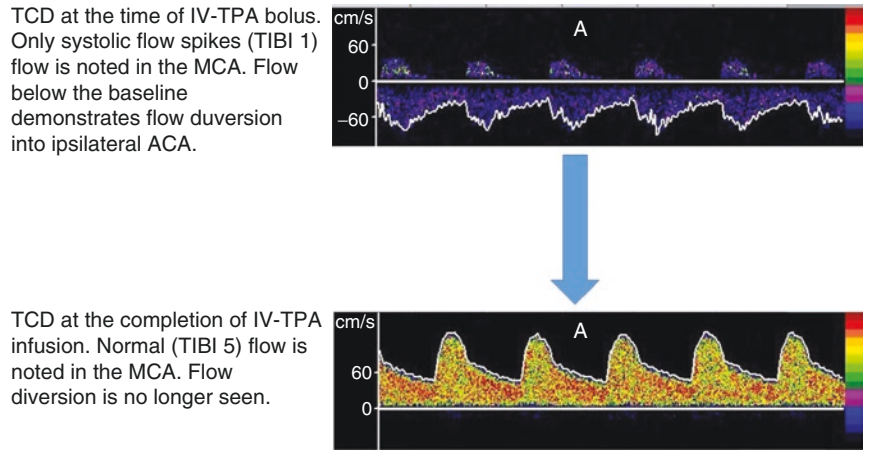

Fig. 35.2 Real-time monitoring of complete recanalization in a patient with proximal MCA occlusion treated with sonothrombolysis. Baseline TIBI: Grade 1 (**a**); TIBI at the end of 2 hour TCD monitoring: Grade V (**b**)

"stepwise" where flow improvement is observed over 1–29 minutes and slow wherein recanalization is observed in more than 30 minutes. Following this speed of clot lysis, it has been observed that rapid or sudden recanalization is associated with better short-term improvement, while slow (30 minutes or more) or partial flow improvement with dampened TIBI signals has less favorable outcome [51].

Spontaneous complete recanalization has been observed at an average rate of 18.8% during the first 6 hours of symptom onset in a complete occlusion of the MCA. Others have also reported spontaneous recanalization at different rates [52–54]. However, IV thrombolysis can further increase the recanalization rate of about 44% in M2 MCA occlusion. Patients receiving IV-rTPA begin to recanalize around the median time of 17 minutes, and maximum TIBI flow grades at 35 minutes after the bolus of rTPA. It has a mean duration of recanalization of 23 ± 16 minutes. In one study, recanalization was "sudden" in 12%, "stepwise" in 53%, and "slow" in 35% of patients [55]. NIHSS scores of 0–3 at 24 hours in these respective groups were noted to be 80%, 30%, and 13%. In partial recanalization where flow velocity was low and dampened, 53% of patients had an NIHSS score of ≥10 at 24 hours [56, 57]. It has also been observed that about a third of patients with early recanalization will not result in immediate clinical improvement even with complete recanalization. However, a third of this patients with silent recanalization even recover completely after 3 months. Cerebral stunning has been postulated to explain this phenomenon [58].

Aside from the above TIBI flow grading, ultrasound-screening criteria for lesions amenable for intervention have also been proposed (Table 35.1) [59]. Since

Table 35.1 Ultrasound screening criteria for lesions amenable for intervention

Lesion location	TCD criteria (at least one present)	CD criteria
MI/M2 MCA	Primary: thrombolysis in brain infarction (TIBI) grades 0–4 (absent, minimal, blunted, dampened, or stenotic) at depths <45 mm (M2) and 45–65 mm (M1) *Secondary:* flow diversion to ACA, PCA, or M2. Increased resistance in unilateral TICA. Embolic signals in MCA. Turbulence, disturbed flow at stenosis. Non-harmonic and harmonic covibrations (bruit or pure musical tones)	Extracranial findings may be normal or show decreases CIA velocity unilateral to lesion
TICA	*Primary:* TIBI grades 0–4 at 60–70 mm. Increased velocities suggest anterior cross-filling of collateral flow in posterior communicating artery *Secondary:* embolic signals in unilateral MCA. Blunted unilateral MCA, MFV >20 cm/s	Decreased ICA velocity unilateral to lesion or normal extracranial findings

(continued)

Table 35.1 (continued)

Lesion location	TCD criteria (at least one present)	CD criteria
Proximal ICA	*Primary:* increased flow velocities suggest anterior cross-filling through anterior communicating artery or collateral flow through posterior communicating artery. Reversed 0A. Delayed systolic flow acceleration in or blunted ipsilateral MCA, MFV >20 cm/s *Secondary:* Embolic signals in unilateral MCA. Normal 0A direction because of retrograde filling of siphon	B-mode evidence of a lesion in ICA ± CCA; Flow imaging evidence of no flow or residual lumen ICA >50% stenosis PSV >125 cm/s; EDV >40 cm/s; ICA/CCA PSV ration >2 ICA near-occlusion or occlusion. Blunted, minimal, reverberating, or absent spectral Doppler waveforms in ICA
Tandem ICA/MCA stenosis/ occlusion	*Primary:* TIBI grade 0–4 *and* increased velocities in contralateral ACA, MCA or unilateral posterior communicating artery *or* reversed unilateral 0A *Secondary:* delayed systolic flow acceleration in proximal MCA or TICA. Embolic signals in proximal MCA or TICA	B-mode evidence of a lesion in ICA ± CCA *or* flow imaging evidence of residual lumen or no flow. ICA >50% stenosis; PSV >125 cm/s; EDV >40 cm/s; ICA/CCA PSV ratio > 2 ICA near-occlusion or occlusion. Blunted, minimal, reverberating, or absent spectral Doppler waveforms in ICA
Basilar artery	*Primary:* TIBI flow grade 0–4 at 75–100 mm *Secondary:* flow velocity increase in terminal VA and branches, MCAs, or posterior communicating arteries. High resistance flow signals in VA(s). Reversed flow direction in distal basilar artery (85 mm)	Extracranial findings may be normal or showing decreased VA velocities of VA occlusion
Verterbral artery	*Primary* (intracranial VA occlusion): TIBI flow grades 0–4 at 40–75 Primary (extracranial VA occlusion): Absent, minimal, or reversed high resistance flow signals in unilateral terminal VA *Secondary:* embolic signals. Increased velocities or low pulsatility in contralateral VA	Extracranial findings may be normal (intracranial VA lesion) or showing decreased VA velocities or VA occlusion

thrombosis is a dynamic process, even after recanalization especially those with partial or incomplete process, reocclusion is prone to occur and it may be seen in about 25% of patients treated with rTPA [60, 61]. Two thirds of patients who would deteriorate clinically after recanalization developed arterial reocclusion. Reocclusion occurred at an average time of 65 minutes after the initial rTPA bolus. Even after reocclusion, there is a 33% chance of favorable outcome at 3 months, and about 50% of patients will have favorable outcome if there is stable recanalization.

35.7 Sonothrombolysis: Procedural Steps

TCD emits high-frequency 2-MHz pulsed-wave ultrasound through a portable probe during sonothrombolysis. To provide optimize delivery of ultrasound energy, a stable and functional headframe is used. It can be easily adjusted and helps in ensuring a constant angle of insonation on the vessel of interest. Of the routinely used transcranial acoustic windows, the temporal window has been utilized the most to monitor MCA in clinical trials. Other acoustic windows may also be used if other intracranial arteries are acutely occluded. The squamous portion of the cranium is the thinnest among the various acoustic windows, permitting the transmission of maximum ultrasound energy for sonothrombolysis (Fig. 35.3). The following step-by-step procedure should be systematically followed for an optimal approach:

- Set the machine to following: 2-MHz frequency, power at 100%, and gate setting of 15 mm (this is for standard fast-track insonation protocol).
- Patients must be carefully screened for the inclusion and exclusion criteria for IV thrombolysis. If possible, a baseline TCD exam should be done before initiating IV thrombolysis. This would help in establishing the diagnosis of steno-occlusive

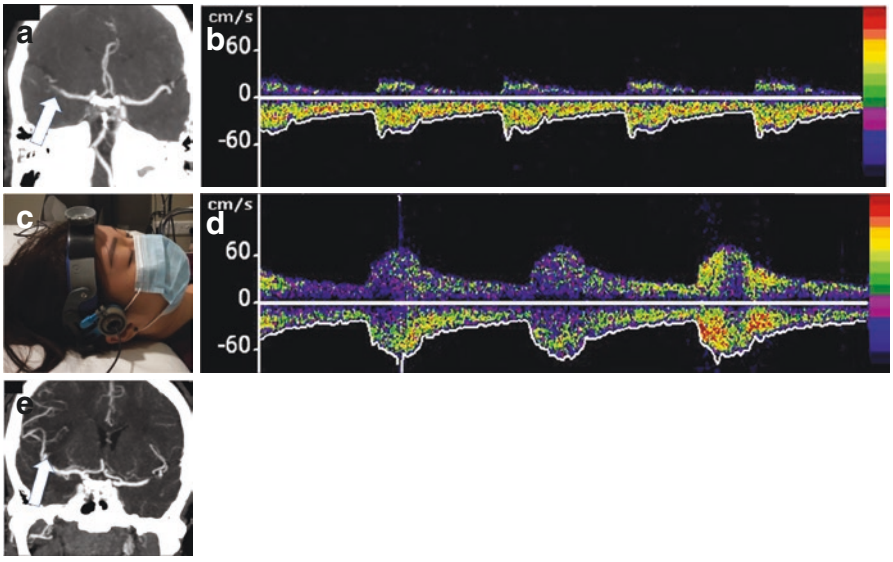

Fig. 35.3 Shows the procedure for sonothrombolysis using CLOTBUST methodology. (1) The patient's CT angiography showed an occlusion of the distal right MCA (**a**). The site of intracranial occlusion is located by a fast track TCD protocol. TCD Doppler spectra obtained from the site of MCA occlusion shows TIBI grade 1 flow at the time of IV-TPA bolus (**b**). Spencer's head frame (**c**) is fixed to ensure constant insonation. (2) Continuous TCD is insonation is performed and flow spectra are recorded continuously. TCD demonstrated TIBI grade 5 (normal) flow spectra at the completion of IV-TPA infusion, suggestive of complete recanalization. This was confirmed by CT angiography performed on day 2 (**e**).

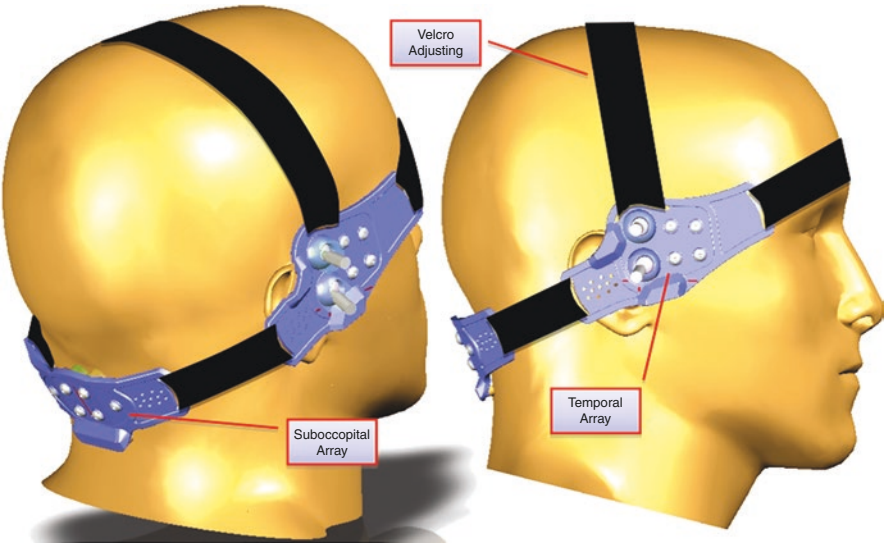

Fig. 35.4 Hands-free sonothrombolysis device with three diamond-shaped sets of probes for transcranial insonation of proximal arteries of Willis

lesion and baseline TIBI grade. The baseline examination will also help in locating the best acoustic window.

- Ensure proper fixation of the monitoring probe that can be adjusted for a reliable and continuous ultrasound exposure.
- Set the depth of the TCD to the segment of the vessel with lowest TIBI. Sufficient amount of gel should be applied to ensure firm contact between the skin and monitoring probe (Fig. 35.4) and to have an optimize transmission of ultrasound energy to the occluded vessel.
- The continuous TCD monitoring should be performed for 120 minutes, while signals received should be digitally stored every 30 minutes to observe for worsening or improvement of TIBI flow grades.
- A repeat examination of baseline TCD monitoring is recommended after completion of IV thrombolysis and at 24 hours. This may help in establishing a persistent recanalization, partial recanalization, or re-occlusion.

35.8 Ultrasound Without Thrombolysis – Sonolysis

Some AIS patients in the intensive care unit may not satisfy the inclusion criteria of IV thrombolysis. In such cases, isolated (without administration of IV thrombolytic agent) TCD exposure has been tried. In a study by Eggers et al., patients

exposed to continuous TCD achieved significantly better NIHSS. Continuous TCD monitoring promoted recanalization in the anterior circulation ischemia [62]. This was also analyzed by the group of Skoloudik et al. and confirmed both the safety and efficacy of sonolysis with continuous TCCD monitoring using with 2–4 MHz pulsed-wave ultrasound. Accelerated MCA recanalization rates were noted at 6 and 24 hours as compared to the control group (69.2% vs. 7.7% and 92.3 vs. 61.5%) [63].

35.9 Sonothrombolysis: Limitations

Sonothrombolysis influences the thrombolytic activity of IV-tPA. However, the optimal frequency of therapeutic TCD remains debatable. The temporal bone attenuates almost 86% of the currently used 2-MHz ultrasound energy. Insufficient temporal acoustic window leads to an inability of monitoring the intracranial arteries in a fair proportion of patients, especially among Asians. Temporal bone window failure is reported in 8–29% [64, 65]. Hyperostosis is a possible reason for this observation, especially in elderly females, observed in 6–12% of adult women of all ages and in >50% of those more than 60 years of age (compared with only 1% of men) [66].

35.10 Conclusion

Sonothrombolysis is a promising treatment approach in acute ischemic stroke patients treated with intravenous thrombolysis, due to its portable nature and ease of use, especially in the peripheral health centers. Although robust data exist to support the efficacy, the conclusive evidence for sonothrombolysis remains awaited. A new phase III clinical trial is being planned to use a better designed operator-independent headframe. Sonothrombolysis may play a pivotal role for AIS patients with distal arterial occlusions, which are not amenable to endovascular thrombectomy. In other patients, continuous monitoring of the occluded proximal intracranial artery by TCD may help in an early selection of patients for various endovascular interventions. Rapid advancements in the designs of therapeutic TCD devices and microbubbles hold promise for establishing a better level of recommendation from AHA/ASA and a better future for patients with acute ischemic stroke.

Algorithm

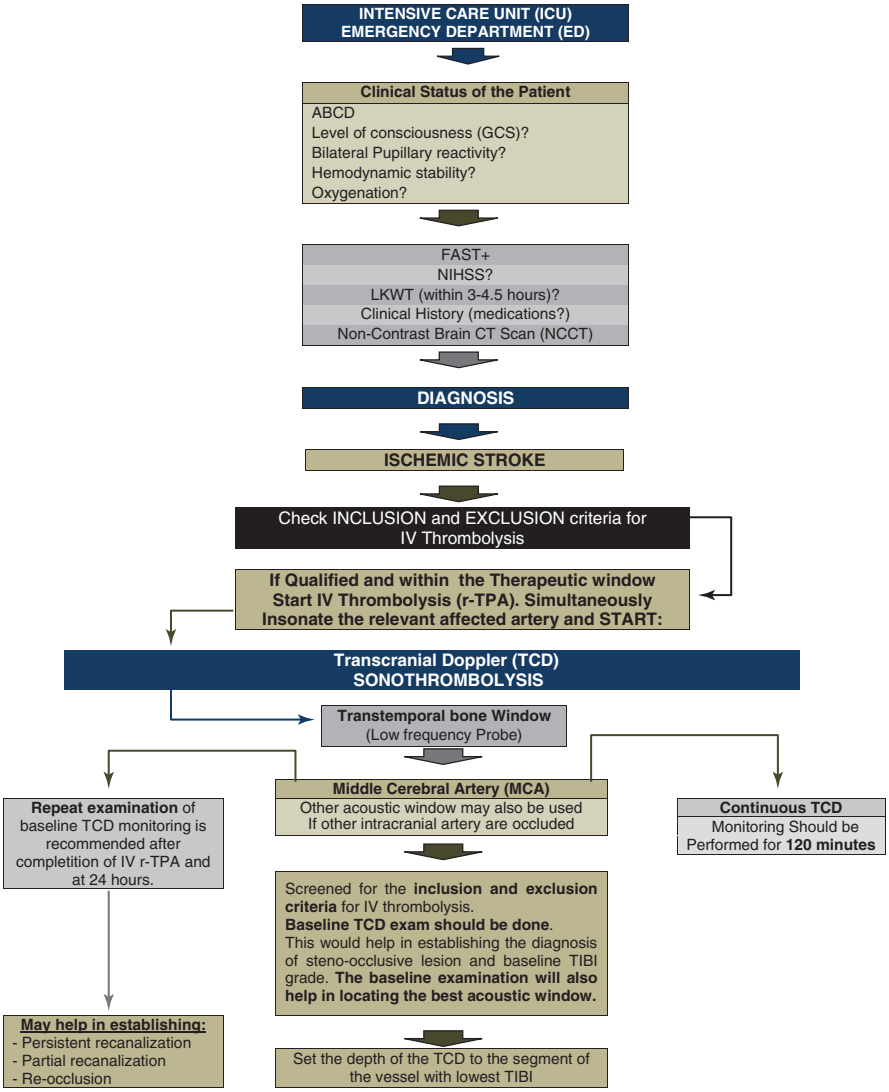

FAST Face-Arm-Speech-Time, *NIHSS* National Institute of Health Stroke Scale, *NCCT* Non-Contrast Computed Tomography, *LKWT* Last Know Well Time, *ABP* Arterial Blood Pressure, *MCA* Middle Cerebral Artery

References

1. Kelly FE, Fong K, Hirsch N, Nolan JP. Intensive care medicine is 60 years old: the history and future of the intensive care unit. Clin Med (Lond). 2014;14:376–9.
2. Hopkins RO, Jackson JC. Long-term neurocognitive function after critical illness. Chest. 2006;130:869–78.
3. Howard RS, Kullmann DM, Hirsch NP. Admission to neurological intensive care: who, when, and why? J Neurol Neurosurg Psychiatry. 2003;74 Suppl 3:iii2–9.
4. Rogers LR. Cerebrovascular complications in cancer patients. Neurol Clin. 2003;21:167–92.
5. Finney SJ, Zekveld C, Elia A, Evans TW. Glucose control and mortality in critically ill patients. JAMA. 2003;290:2041–7.
6. Emsley HC, Hopkins SJ. Acute ischaemic stroke and infection: recent and emerging concepts. Lancet Neurol. 2008;7:341–53.
7. Billeci AM, Paciaroni M, Caso V, Agneli G. Hormone replacement therapy and stroke. Curr Vasc Pharmacol. 2008;6:112–23.
8. Murthy SB, Gupta A, Merkler AE, Navi BB, Mandava P, Iadecola C, et al. Restarting anticoagulant therapy after intracranial hemorrhage: a systematic review and meta-analysis. Stroke. 2017;48:1594–600.
9. Westover AN, McBride S, Haley RW. Stroke in young adults who abuse amphetamines or cocaine: a population-based study of hospitalized patients. Arch Gen Psychiatry. 2007;64:495–502.
10. Wijdicks EF, Scott JP. Stroke in the medical intensive-care unit. Mayo Clin Proc. 1998;73:642–6.
11. Bhatia R, Hill MD, Shobha N, Menon B, Bal S, Kochar P, Watson T, et al. Low rates of acute recanalization with intravenous recombinant tissue plasminogen activator in ischemic stroke: real world experience and a call for action. Stroke. 2010;41:2254–8.
12. Tsivgoulis G, Culp WC, Alexandrov AV. Ultrasound-enhanced thrombolysis in acute arterial ischemia. Ultrasonics. 2008;48:303–11.
13. Tsivgoulis G, Alexandrov AV. Ultrasound-enhanced thrombolysis in acute ischemic stroke: potential, failures, and safety. Neurothrapeutics. 2007;4:420–7.
14. Tsivgoulis G, Alexandrov AV. Utrasound-enhanced thrombolysis: application in acute cerebral ischemia. J Clin Neurol. 2007;3:1–8.
15. NINDS rt-PA stroke study group. Tissue plasminogen activator for acute ischemic stroke. N Engl J Med. 1995;333:1581–7.
16. The ATLANTIS, ECASS, and NINDS rt-PA Study Group Investigators. Association of outcome with early stroke treatment: pooled analysis of ATLANTIS, ECASS, and NINDS rt-PA stroke trials. Lancet. 2004;363:768–74.
17. Hacke W, Kaste M, Fieschi C, Toni D, Lesaffre E, von Kummer R, et al for the ECASS Study Group. Intravenous thrombolysis with recombinant tissue plasminogen activator for acute hemispheric stroke: the European Cooperative Acute Stroke Study (ECASS). JAMA 1995;274:1017–25.
18. Hacke W, Kaste M, Fieschi C, von Kummer R, Davalos A, Meier D, et al. Randomized double-blind placebo controlled trial of thrombolytic therapy with intravenous alteplase in acute ischemic stroke (ECASS II). Lancet. 1998;352:1245–51.
19. Clark WM, Albers GW, Madden KP, et al. The rt-PA (alteplase) 0- to 6-hour acute stroke trial, part A (A0267g): results of a double blind, placebo-controlled, multicenter study. Stroke. 2000;31:811–6.

20. Clark WM, Wissman S, Albers GW, Jhamandas JH, Madden KP, Hamilton S. Recombinant tissue-type plasminogen activator (alteplase) for ischemic stroke 3 to 5 hours after symptom onset: the ATLANTIS study- a randomized controlled trial. JAMA. 1999;282:2019–26.
21. Alexandrov AV, Barlinn K, Strong R, Alexandrov AW, Aronowski J. Low-power 2 MHz pulsed-wave transcranial Doppler reduces ischemic brain damage in rat. Transl Stroke Res. 2011;2:376–81.
22. Zhou Y, Murugappan SK, Sharma VK. Effect of clot aging and cholesterol content on ultrasound-assisted thrombolysis. Transl Stroke Res. 2014;5:627–34.
23. Trubestein R, Bernard HR, Etzel F, Sobbe A, Cremer A, Stumpff U. Thrombolysis by ultrasound. Clin Sci Mol Med. 1976;51:697–8.
24. Tachibana K, Tachibana S. Ultrasonic vibration for boosting fibrinolytic effects of urokinase in-vivo. Thrombo Haemost. 1981;46:211.
25. Suchkova VN, Baggs RB, Francis CW. Effect of 40-Hz ultrasound on acute thrombotic ischemia in rabbit femoral artery thrombosis model: enhancement of thrombolysis and improvement in capillary muscle perfusion. Circulation. 2000;101:2296–301.
26. Kimura M, Iijima S, Kobayashi H, Furuhata H. Evaluation of the thrombolytic effect of tissue-type plasminogen activator with irradiation: in-vitro experiment involving assay of the fibrin degradation products from the clot. Biol Pharm Bull. 1994;17:126–30.
27. Akiyama M, Ishibashi T, Yamada T, Furuhata H. Low-frequency ultrasound penetrates the cranium and enhances thrombolysis in-vitro. Neurosurgery. 1998;43:828–32.
28. Polak JF. Ultrasound energy and the dissolution of Thrombus. N Engl J Med. 2004;351:2154–5.
29. Sakharov DV, Barret-Bergshoeff M, Hekkenberg RT, Rijken DC. Fibrin-specificity of a plasminogen activator affects efficiency of fibrinolysis and responsiveness to ultrasound: comparison of nine plasminogen activators in-vitro. Thromb Haemoast. 1999;81:605–12.
30. Behrens S, Spengos K, Daffertshofer M, Schroeck H, Dempfle. Low frequency, low-intensity ultrasound accelerates thrombolysis through the skull. Ultrasound Med Biol. 2001;27:1683–9.
31. Suchkova V, Siddiqi FN, Carstensen EL, Dalecki D, Child S, Francis CW. Enhancement of fibrinolysis with 40-kHz ultrasound. Circulation. 1998;98:1030–5.
32. Daffertshofer M, Gass A, Ringleb P, Sitzer M, Sliwka U, Els T, et al. Transcranial low-frequency ultrasound-mediated thrombolysis in brain ischemia: increased risk of hemorrhage with combined ultrasound and tissue plasminogen activator: results of a phase II clinical trial. Stroke. 2005;36:1441–6.
33. Cintas P, Nguyen F, Boneu B, Larrue V. Enhancement of enzymatic fibrinolysis with 2-MHz ultrasound and microbubbles. J Thromb Haemost. 2004;2:1163–6.
34. Alexandrov AV, Molina CA, Grotta JC, Garami Z, Ford SR, Alvarez-Sabin J, et al. Ultrasound-enhanced systemic thrombolysis for acute ischemic stroke. N Engl J Med. 2004;351:2170–8.
35. Molina CA, Ribo M, Rubiera M, Montaner J, Santamarina E, Delgado-Mederos R, et al. Microbubble administration accelerates clot lysis during continuous 2-MHz ultrasound monitoring in stroke patients treated with intravenous tissue plasminogen activator. Stroke. 2006;37:425–9.
36. Sharma VK, Tsivgoulis G, Lao AY, Malkoff MD, Alexandrov AW, Alexandrov AV. Quantification of microspheres appearance in brain vessels: implications for residual flow velocity measurements, dose calculations, and potential drug delivery. Stroke. 2008;39:1476–81.
37. Alexandrov AV, Mikulik R, Ribo M, Sharma VK, Lao AY, Tsivgoulis G, et al. A pilot randomized clinical safety study of sonothrombolysis augmentation with ultrasound-activated perflutren-lipid microspheres for acute ischemic stroke. Stroke. 2008;39:1464–9.
38. del Zoppo GJ, Higashida RT, Furlan AJ, Pessin MS, Rowley HA, Gent M. PROACT: a phase II randomized trial of recombinant pro-urokinase by direct arterial delivery in acute middle cerebral artery stroke. PROACT Investigators. Prolyse in Acute Cerebral Thromboembolism. Stroke. 1998;29:4–11.
39. Molina CA, Barreto AD, Tsivgoulis G, Sierzenski P, Malkoff MD, Rubiera M, et al. Transcranial ultrasound in clinical sonothrombolysis (TUCSON) trial. Ann Neurol. 2009;66:28–38.

40. Saqqur M, Tsivgoulis G, Nicoli F, Skoloudik D, Sharma VK, Larrue V, et al. The role of sonolysis and sonothrombolysis in acute ischemic stroke: a systematic review and meta-analysis of randomized controlled trials and case-control studies. J Neuroimaging. 2014;24:209–20.
41. Barlinn K, Tsivgoulis G, Barreto AD, Alleman J, Molina CA, Mikulik R, et al. Outcomes following sonothrombolysis in severe acute ischemic stroke: subgroup analysis of the CLOTBUST trial. Int J Stroke. 2014;9:1006–10.
42. Barlinn K, Barreto AD, Sisson A, Liebeskind DS, Schafer ME, Alleman J, et al. CLOTBUST-hands free: initial safety testing of a novel operator-independent ultrasound device in stroke-free volunteers. Stroke. 2013;44:1641–6.
43. Barreto AD, Alexandrov AV, Shen L, Sisson A, Bursaw AW, Sahota P, et al. CLOTBUST-hands free: pilot safety study of a novel operator-independent ultrasound device in patients with acute ischemic stroke. Stroke. 2013;44:3376–81.
44. Schellinger PD, Alexandrov AV, Barreto AD, Demchuk AM, Tsivgoulis G, Kohrmann M, et al. Combined lysis of thrombus with ultrasound and systemic tissue plasminogen activator for emergent revascularization in acute ischemic stroke (CLOTBUST-ER): design and methodology of a multinational phase 3 trial. Int J Stroke. 2015;10:1141–8.
45. Saqqur M, Uchino K, Demchuk AM, Molina CA, Garami Z, Calleja S, et al. Site of arterial occlusion identified by transcranial Doppler predicts the response to intravenous thrombolysis for stroke. Stroke. 2007;38:948–54.
46. Eggers J, Konig IR, Koch B, Handler G, Seidel G. Sonothrombolysis with transcranial color-coded sonography and recombinant tissue-type plasminogen activator in acute middle cerebral artery main stem occlusion: results from a randomized study. Stroke. 2008;39:1470–5.
47. Nacu A, Kvistad CE, Naess H, Øygarden H, Logallo N, Assmus J, et al. NOR-SASS (Norwegian Sonothrombolysis in Acute Stroke Study): randomized controlled contrast-enhanced sonothrombolysis in an unselected acute ischemic stroke population. Stroke. 2017;48:335–41.
48. Powers WJ, Rabinstein AA, Ackerson T, Adeoye OM, Bambakidis NC, Becker K, et al. 2018 guidelines for the early management of patients with acute ischemic stroke: a guideline for healthcare professionals from the American Heart Association/American Stroke Association. Stroke. 2018;
49. Demchuck AM, Burgin Scott W, Chistou I, Felberg RA, Barber PA, Hill MD, et al. Thrombolysis in Brain Ischemia (TIBI)- Transcranial Doppler flow grades predict clinical severity, early recovery and mortality in patients treated with intravenous tissue plasminogen activator. Stroke. 2001;32:89–93.
50. Sharma VK, Yeo LL, Teoh HL. How an occluded artery recanalizes during acute stroke thrombolysis. J Cardiovasc Ultrasound. 2015;23:56–7.
51. Christou I, Alexandrov AV, Scott Burgin W, Wojner AW, Felberg RA, Malkoff M, et al. Timing of recanalization after tissue plasminogen activator therapy determined by transcranial Doppler correlates with clinical recover from ischemic stroke. Stroke. 2000;31:1812–6.
52. Molina C, Montaner J, Abilleira S, Ibarra B, Romero F, Arenillas JF, et al. Timing of spontaneous recanalization and risk of hemorrhagic transformation in acute cardioembolic stroke. Stroke. 2001;32:1078–84.
53. Scot Burgin W, Malkoff M, Felberg RA, Demchuck AM, Christou I, Grotta JC, et al. Transcranial Doppler ultrasound criteria for recanalization after thrombolysis for middle cerebral artery stroke. Stroke. 2000;31:1128–32.
54. Furlan A, Higashida R, Wechsler L, Gent M, Rowle H, Kase C, et al. Intra-arterial prourokinase for acute ischemic stroke-the PROACT II study: a randomized controlled study. JAMA. 1999;282(21):2003–11.
55. Rha JH, Saver JL. The impact of recanalization on ischemic stroke outcomes: a meta-analysis. Stroke. 2007;38:967–73.
56. Alexandrov AV, Scott Burgin W, Demchuck AM, El-Mitwali A, Grotta JC. Speed of intracranial clot lysis with intravenous tissue plasminogen activator therapy: sonographic classification and short term improvement. Circulation. 2001;103:2897–902.

57. Toni D, Fiorelli M, Zanette EM, Sacchetti ML, Salerno A, Argentino C, et al. Early spontaneous improvement and deterioration of ischemic stroke patients: a serial study with transcranial Doppler ultrasonography. Stroke. 1998;29:1144–8.
58. Alexandrov AV, Demchuck AM, Felberg RA, Christou I, Barber P, Scott Burgin W, et al. High rate of recanalization and dramatic clinical recovery during tPA infusion when continuously monitored with 2-MHz transcranial Doppler monitoring. Stroke. 2000;31:610–4.
59. Alexandrov AV, Hall CE, Labiche LA, Wojner AW, Grotta JC. Ischemic stunning of the brain: early recanalization without immediate clinical improvement in acute ischemic stroke. Stroke. 2004;35:449–52.
60. Alexandrov AV, Demchuck AM, Felberg RA, Grotta JC, Krieger D. Intracranial clot dissolution is associated with embolic signals on transcranial Doppler. J Neuroimaging. 2000;10:27–32.
61. Alexandrov AV, Grotta JC. Arterial reocclusion in stroke patients treated with intravenous tissue plasminogen activator. Neurology. 2002;59:862–7.
62. Eggers J, Seidel G, Koch B, König IR. Sonothrombolysis in acute ischemic stroke for patients ineligible for rt-PA. Neurology. 2005;64:1052–4.
63. Sloudik D, Bar M, Skoda O, Vaclavik D, Hradilek P, Allendoerfer J, et al. Safety and efficacy of the sonographic acceleration of the middle cerebral artery recanalization: results of the pilot thrombotripsy study. Ultrasound Med Biol. 2008;34:1775–82.
64. Lindsay BD, Nicoletto HA, Bennett ER, Laskowitz DT, Smith SW. Simultaneous bilateral real-time 3-D transcranial ultrasound imaging at 1 Mhz through poor acoustic windows. Ultrasound Med Biol. 2013;39:721–34.
65. Wijnhoud AD, Franckena M, van der Lugt A, Koudstall PJ, Dippel ED. Inadequate acoustical temporal bone window in patients with transient ischemic attack or minor stroke: role of skull thickness and bone density. Ultrasound Med Biol. 2008;34:923–9.
66. Eden A. Transcranial Doppler ultrasonography and hyperostosis of the skull. Stroke. 1988;19:1445–6.

Chapter 36
Neurosonology in ICU: Transcranial Doppler (TCD/TCCS) and Microemboli Detection

Branko Malojcic

Key Points

1. Cerebral microemboli are small solid or gaseous particles within the blood stream travelling towards cerebral arteries. They can be easily detected with transcranial Doppler ultrasound.
2. Cerebral microemboli can be used as a surrogate marker of stroke risk and of therapeutic effects in stroke and surgical patients.
3. Transcranial Doppler (TCD) ultrasound systems with or without probe holders for bilateral monitoring provide automatic detection of microembolic signals, but to have a reliable and comparable finding, individual training is necessary as well as compliance to published standards of insonation.

36.1 Introduction

Cerebral microemboli are small solid or gaseous particles within the blood stream travelling towards cerebral arteries. Transcranial Doppler (TCD) ultrasound is used to monitor blood flow in the arteries at the base of the brain. Backscatter of ultrasound energy from microemboli is higher than the backscatter from normal blood particles (mostly erythrocytes), and this transient increase of backscattered energy caused by passage of microemboli through ultrasound beam appears as high-intensity transient signals (HITSs, or microembolic signals (MESs) used interchangeably) within the spectrograms of transcranial Doppler (TCD) ultrasound systems (Fig. 36.1).

B. Malojcic (✉)
Director of TIA Centre, Department of Neurology, University Hospital Center Zagreb, Zagreb School of Medicine, Zagreb, Croatia

Secretary - ESNCH, Oslo, Norway
e-mail: bmalojcic@gmail.com

C. N. Rodríguez et al. (eds.), *Neurosonology in Critical Care*,
https://doi.org/10.1007/978-3-030-81419-9_36

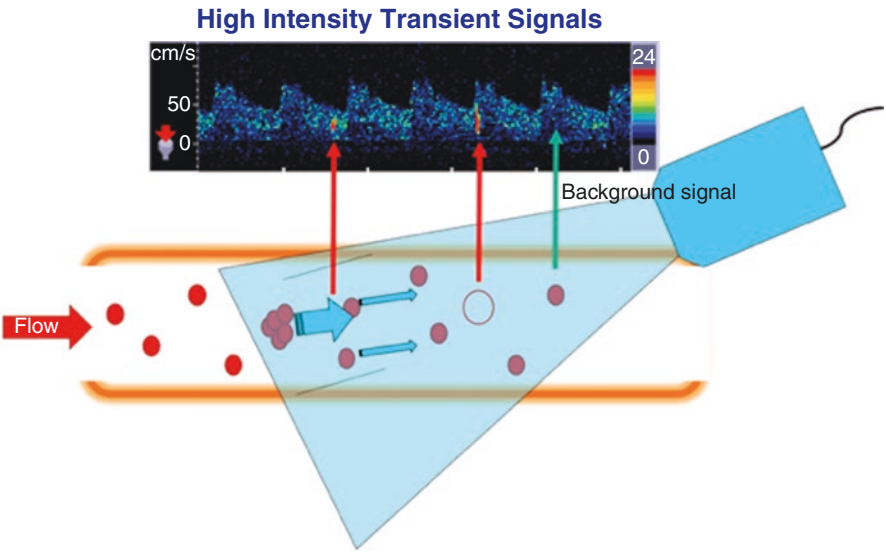

Fig. 36.1 Transcranial Doppler ultrasound systems emit and detect ultrasound energy backscattered from blood cells as a background signal within the blood flow spectra (green arrow). Transient increases of backscattered energy from solid or gaseous particles are visualized as high-intensity transient signal (red arrows) within Doppler spectrograms

From a clinical point of view, microemboli are in most cases asymptomatic, but it has been proven in a large number of studies that their number is proportional to stroke risk. Microemboli detection might be used to detect probable source of stroke, such as from an unstable plaque, a right-to-left shunt or a cardiac source. Additionally, it might be used to evaluate the effect of antithrombotic drugs or as to monitor invasive procedures (endovascular or surgical).

In order to properly use this tool in daily routine, neurosonologists should be trained properly and comply with standards of performing the examination.

36.2 Technical Considerations

A standard setup for HITS detection is bilateral monitoring of blood flow in both middle cerebral arteries (MCAs) through transtemporal window using probe holder which allows maintaining fixed position of the 2 MHz TCD probes during the insonation period. Of course, HITS may be detected with transcranial colour-coded sonography (TCCS) probes held in hand and other arteries might be insonated as well, such as anterior cerebral (ACA), vertebral (VA) or posterior cerebral arteries (PCA), depending on the clinical situation. Also depending on the clinical scenario, a patient might be supine or sitting upright and special TCD holters enable monitoring even while a patient is active. To prevent movement artefacts of uncooperative patients, temporary sedation might be required.

The influence of US system settings on the detectability of MES is extremely important, and the setup should be standardized in order to make studies relevant. The methodology for detecting MES was established and defined by the International Consensus Group on Microembolus Detection in 1997, which suggested that all future studies should report microemboli detection protocols uniformly [1]. Automated detection protocols can be time saving, but their sensitivity and specificity still fail to meet requirements for routine clinical use.

All of the relevant TCD producing companies offer probe holders (frames) for their systems, and system software contains MES detection in the most of standard packages. These standard monitoring packages are set up by manufacturers by their best experience to discriminate between HITS and artefacts, to count the number of HITS automatically and to allow manual offline review of the recordings. However, some basic knowledge is mandatory to optimize recordings and interpretation as the automatic HITS detection still may overestimate or underestimate the real number of events (Fig. 36.2).

Generally, to get the best results, detection threshold should be in range from 3 to 9 dB. Higher detection thresholds will result in lower sensitivity and higher specificity of detection. Each system might be calibrated individually against normal controls or by interpatient analysis. Another parameter which should be taken care of is the axial length of the sample volume. In most cases, it should be between 3 and 10 mm to optimize measurements of relative intensity increase. For the MCA, optimal insonation depth is between 55 and 45 mm as at the depth of terminal internal carotid artery (ICA) or the syphon turbulence, and bilateral direction of microemboli movement may impede reliability of HITS detection. Gain should be kept minimal and standard recording time should be 30 min to 1 h.

Multi-gating can help in HITS detection. If two sample volumes are positioned within the same vessel at a distance of at least 5 mm, a time delay between HITS appearance in deeper sample (in case of MCA insonation) and shallower sample confirms this is an embolus contrary to an artefact which will appear in both depths simultaneously. Another useful tool is the power motion mode Doppler (M-mode or PMD) signal which covers the full insonation depth of 6 or more cm in steps of 2 mm and gives information on the direction of blood flow at each 2 mm steps. As microemboli move within the blood stream towards (MCA) or from (ACA), the probe high power slopes appear within the M-mode traces, while artefacts appear as vertical high-power lines (Fig. 36.3).

	Microembolic Signals	**Artefacts**
Time length	Short (<300ms)	Variable duration
Itensity	≥3dB	Variable (high intensity)
Appearance	Random (any part of cardiac cycle)	Random
Signal tracing	Inside the Doppler-spectrum	Outside the Doppler-spectrum
Direction	Unidirectional	Bidirectional
Sound effects	Bloop or chirp	No specific sound effects

Fig. 36.2 Differences between microembolic signals and artefacts

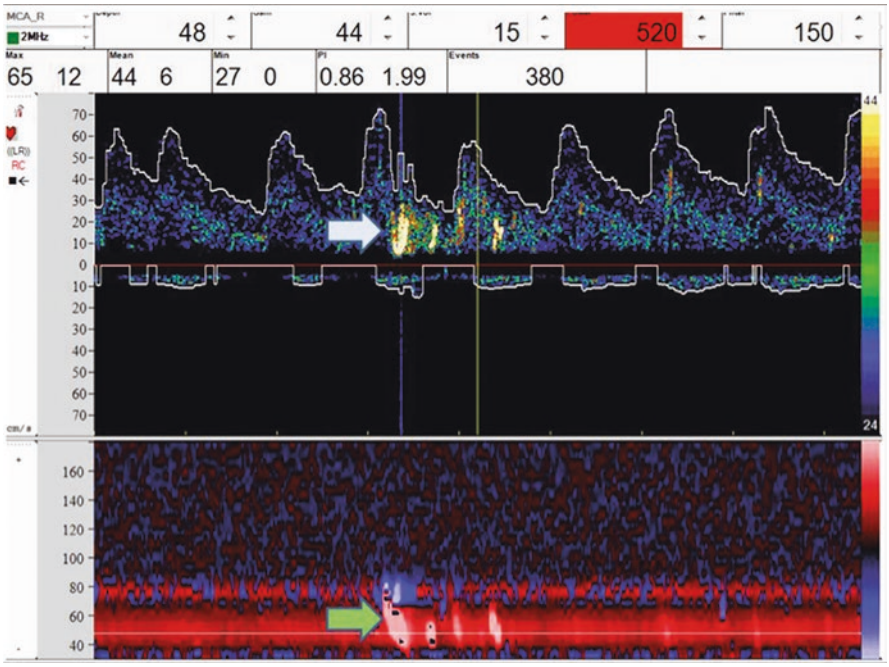

Fig. 36.3 The appearance of four consecutive HITS within the spectrum of TCD monitoring of MCA blood flow (white arrow). Note the high-power inclined slopes within the M-mode traces that correspond to movement of microemboli through different depths of MCA

Although distinguishing solid and gaseous emboli is in the focus for many years now and double frequency probes may have achieved the best results so far, the reliability of this method is still not fully confirmed. There are even less results in differentiation of other microembolic sources such as particles of atheroma or platelet aggregates.

As the MES detection protocols require significant time to perform the examination and to analyse the results, training and experience of neurosonologists is required to shorten this commitment as much as possible. Certifications of physicians and sonographers, quality control and continuing medical education can promote wider use and benefits of MES detection in ultrasound laboratories and ICUs.

36.3 Clinical Applications

36.3.1 Detection of Patent Foramen Ovale

Around 25% of the general population are reported to have patent foramen ovale (PFO), and PFO prevalence in young patients with cryptogenic stroke might be even higher [2]. Detection of microbubbles within agitated saline with TCD (bubble test)

is highly specific and sensitive method for PFO detection. Transesophageal echocardiography (TEE), on the other hand, still has the advantage of analysing additional characteristics of PFO such as its morphology and the existence of atrial septal aneurysm. However, as TEE is unpleasant and some patients find it difficult to swallow the probe, TCD offers a reliable screening method which will prevent unnecessary exposure to TEE.

In the standard protocol, 2 MHz probes are placed on the transtemporal bone window and held there with probe holder or manually if only one probe is used. The insonation depth should be 50–60 mm. If in doubt, initial monitoring of at least 20 min should be done to exclude other possible causes of spontaneous emboli (such as atrial fibrillation). The patient should be in a supine position with arms put horizontally (although a sitting position may be acceptable, and it may provide higher sensitivity of the test) [3]. Intravenous line (18- or 20-gauge needle) with a short flexible line to a three-way stopcock should be positioned preferably in the right cubital vein.

Contrast agent is prepared from saline and air mixture (agitated saline, microbubbles). In one of the two syringes, 9 mL of saline is drawn and 1 mL of air is drawn into the other. Both syringes are connected to stopcock to back and forth exchange their content for at least 10 times. To increase homogeneity of the mixture, additional 0.5 mL of patient's blood may be added and mixed with agitated saline for a few more times.

Immediately after preparation of the mixture, a bolus injection should follow, and in the case of right-to-left shunt is confirmed, HITS will appear in both MCAs some 10 s after injection. Permanent shunting is confirmed if HITS appears spontaneously. If they do not, the test is repeated asking the patient to perform Valsalva manoeuvre (VM) 5–6 s after the injection and to hold it for at least 5–10 s. It is advisable to check the correct performance of VM before the preparation of agitated saline. If a patient performs VM adequately, there will be a drop of the MCA peak systolic velocity during VM and a compensatory increase immediately afterwards.

The result of PFO detection test should be evaluated in terms of the number of HITS, delay of their appearance in the MCAs after the injection of microbubbles and spontaneous or VM-induced appearance. Relation of the number of HITS to the size of right-to-left shunt is shown in Table 36.1 [4]. The size of right-to-left shunt doesn't have to be related to the size of PFO estimated with echocardiography as there can be other factors that influence blood flow through the shunt.

Table 36.1 Relation of the number of HITS to the size of right-to-left shunt

Negative result (category I)	No HITS
Small PFO (category II)	1–10 HITS
Large PFO (category III)	>10 HITS
Curtain effect (category IV)	Shower of microbubbles (a single microbubble cannot be detected)

36.3.2 Risk Stratification in Patients with Internal Carotid Artery Stenosis

Estimation of the risk from ICA stenosis is getting more important as the new evidence is emerging, which confirms that the surgical treatment is indicated only in high-risk patients, while optimal medical therapy may be sufficient even for high-grade stenosis if the stroke risk is low. In asymptomatic stenosis, there is a significant difference in the number of HITS between 30% and 69% and between 70% and 99%, although total number of HITS positive findings can be relatively low (3% vs. 12%, respectively). In symptomatic patients, positive HITS findings are present in 19% vs. 48%, again a highly significant difference [5]. Presence of HITS rises stroke risk up to nine times in both symptomatic and asymptomatic ICA stenosis.

Since the studies on the effectiveness of antiaggregant therapies require large patient populations and long observation periods to reach clinical endpoint, detection of MES has been used as a surrogate marker of therapeutic efficiency. Dual antiplatelet therapy significantly reduced the number of MES vs. single antiplatelet therapy when it was given early after ischemic event (lower number of MES was observed already on the day 1, and on the seventh day, a highly significant difference in the number of MES was achieved) [6] (Fig. 36.4).

We present here a case of patient which was referred to our department with symptomatic in-stent restenosis (recurrent TIAs) 6 months after carotid artery stenting (CAS). At the time of presentation, she was treated with low molecular heparin and aspirin. CT angiography and carotid ultrasound confirmed formation of a thrombus within the stent lumen. DWI showed foci of restricted diffusion and TCCS detected frequent HITS. As both surgical (due to previous ipsilateral endarterectomy) and endovascular (due to fresh thrombotic material) procedures carried high risk, we immediately added loading dose of clopidogrel. On the next day, the patient was completely symptom free, there were no MESs in 1-h TCD detection, and 3 days later, CT angiography showed significant regression of stenosis. We believe that this case nicely presents how HITS detection may help in clinical judgment, how well it relates to DWI positive TIAs and how it can be a surrogate marker of therapeutic efficiency.

A question which still remains unanswered is for how long the patients should be monitored. Standard procedure, which was used in most of the studies, requires 1 h of continuous monitoring. This time frame is challenged by the fact that microemboli appear randomly and that the absolute number of MES can be low even in longer monitoring periods.

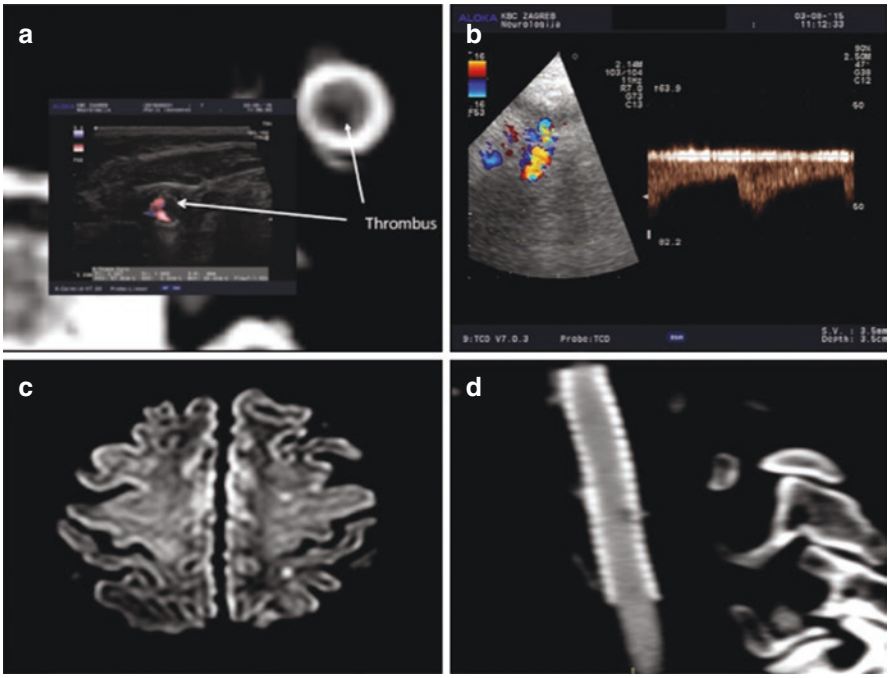

Fig. 36.4 A patient with aspirin resistance. (**a**) Carotid duplex and CT angiography show formation of in-stent thrombus in left ICA. (**b**) TCCS examination of ICA through submandibular window detects HITS. (**c**) DWI imaging reveals zones of signal restriction ipsilateral to in-stent thrombosis. (**d**) Resolution of thrombus in CTA 3 days after initiation of dual antiplatelet therapy

36.3.3 Monitoring of Invasive Procedures

Surgical and endovascular procedures generate microemboli of thrombotic, gaseous, tissue, or surgical material origin. Microemboli reach cerebral circulation from direct arterial manipulation or, if PFO is present, from paradoxical embolism. As perioperative stroke is one of major concerns in many types of invasive procedures, HITS detection has become one of the strategies to control the quality of procedures and to prevent neurological deficit.

Monitoring of carotid endarterectomies detected MES at the time of shunting and after clamp release. If the number of MES served as quality control to surgeons by making them adjust the operative technique, it has been shown that the risk for neurologic complications decreased from 7% to 2% [7].

Our group used HITS detection to compare single and multiple aortic clamping during coronary artery bypass grafting (CABG). As the outcome measures, the number of HITS and neurocognitive status were evaluated. Data acquisition was performed preoperatively, early postoperatively and at the 4-month follow-up. Intraoperative HITS monitoring was used to quantify the embolic load in relation to different aortic clamping strategies. Single clamping group patients had fewer embolization signals (270 ± 181 vs 465 ± 160, $p < 0.0001$). Early postoperative neurocognitive results were depressed in comparison to preoperative values in both groups ($p < 0.05$ for multiple comparisons). The magnitude of this cognitive depression was greater in the multiple clamping group ($p < 0.05$ for multiple comparisons). In conclusion, the embolic burden was significantly lower in the single clamping group. This outcome was translated into fewer early cognition deficits and superior late restoration of function [8].

36.3.4 Prognostic Value

A prospective multicentre study of consecutive patients with ischemic stroke and occlusion of anterior circulation vessels after successful thrombectomy assessed the microemboli by 30 minutes of transcranial Doppler monitoring within 72 hours of the last-seen-well time. Major outcomes included mRankin Scale at 90 days and infarct volume on head computed tomography at 24 hours. They also assessed recurrence of stroke, transient ischemic attack or systemic embolism within 90 days. The occurrence of MES was not associated with a significant difference in modified Rankin Scale nor in functional independence but predicted new embolic events (adjusted Cox hazard ratio, 6.78 [95% CI, 1.63–27.8] $P = 0.01$) within 90 days [9].

36.4 Conclusion

Although there is a still ongoing debate on the clinical importance of MES, as the most of detected signals are asymptomatic, there is sufficient evidence that confirms they can be used to stratify stroke risk, define stroke aetiology, monitor invasive procedures and confirm therapeutic efficiency of antiaggregant drugs.

Being time demanding, long-term monitoring of surgical or stroke patients requires adequately trained ultrasonographers as online analysis significantly improves reliability of the results. On the other side, PFO detection with TCD is a reliable and sensitive test for right-to-left shunt which can be used in a daily routine as it can be done in very short period of time.

There are ongoing trials which will try to confirm clinical significance of HITS detection in large number of controlled patients and standardized procedures. Once obtained, these results will most probably enable consideration of HITS detection for official stroke guidelines, and then, we can expect to have it in all standards of care.

Algorithm

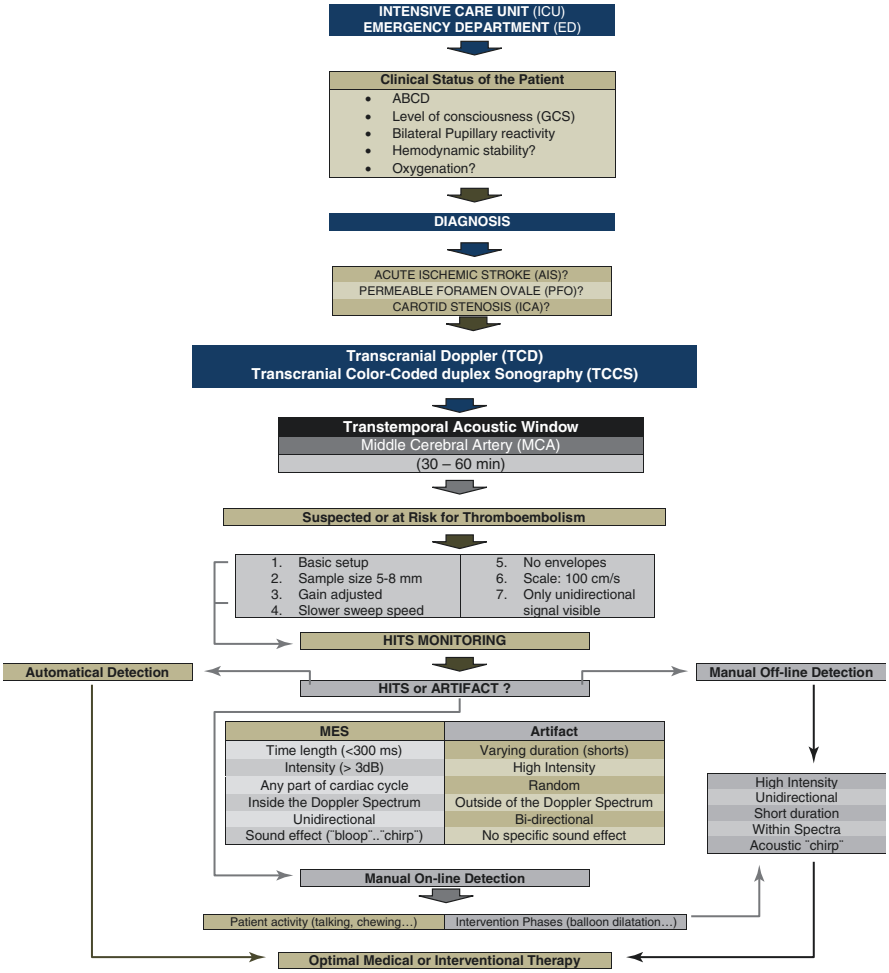

ABCD Airway-Breathing-Circulation-Disability, *GCS* Glasgow coma Scale, *MES* Microemboli signals, *HITS* High Intensity Transient Signal

References

1. Ringelstein EB, Droste DW, Babikian VL, Evans DH, Grosset DG, Kaps M, et al. Consensus on microembolus detection by TCD. International Consensus Group on Microembolus Detection. Stroke. 1998;29(3):725–9.
2. Lechat P, Mas JL, Lascault G, Loron P, Theard M, Klimczac M, et al. Prevalence of patent foramen ovale in patients with stroke. N Engl J Med. 1988;318(18):1148–52.

3. Lao AY, Sharma VK, Tsivgoulis G, Malkoff MD, Alexandrov AV, Frey JL. Effect of body positioning during transcranial Doppler detection of right-to-left shunts. Eur J Neurol. 2007;14(9):1035–9.
4. Jauss M, Zanette E. Detection of right-to-left shunt with ultrasound contrast agent and transcranial Doppler sonography. Cerebrovasc Dis. 2000;10(6):490–6.
5. Ritter MA, Dittrich R, Thoenissen N, Ringelstein EB, Nabavi DG. Prevalence and prognostic impact of microembolic signals in arterial sources of embolism. A systematic review of the literature. J Neurol. 2008;255(7):953–61.
6. Markus HS, Droste DW, Kaps M, Larrue V, Lees KR, Siebler M, et al. Dual antiplatelet therapy with clopidogrel and aspirin in symptomatic carotid stenosis evaluated using Doppler embolic signal detection: the Clopidogrel and Aspirin for Reduction of Emboli in Symptomatic Carotid Stenosis (CARESS) trial. Circulation. 2005;111(17):2233–40.
7. Spencer MP. Transcranial Doppler monitoring and causes of stroke from carotid endarterectomy. Stroke. 1997;28(4):685–91.
8. Gasparovic H, Borojevic M, Malojcic B, Gasparovic K, Biocina B. Single aortic clamping in coronary artery bypass surgery reduces cerebral embolism and improves neurocognitive outcomes. Vasc Med. 2013;18(5):275–81.
9. Sheriff F, Diz-Lopes M, Khawaja A, Sorond F, Tan CO, Azevedo E, Franceschini MA, Vaitkevicius H, Li K, Monk AD, Michaud SL, Feske SK, Castro P. Microemboli after successful thrombectomy do not affect outcome but predict new embolic events. Stroke. 2020;51(1):154–61.

Chapter 37
Stroke and Right-to-Left Shunt in ICU: Role of the Transcranial Doppler (TCD/TCCS)

Edoardo Vicenzini and Chiara Izzo

Key Points

1. Select patients for right-to-left shunt (RLS) diagnosis: cryptogenic stroke/transient ischemic attack (TIA), symptomatic decompressive signs, and symptoms in divers. Being patent *foramen ovale* very frequent (up to 25–35%) in asymptomatic population, avoid unnecessary screening.
2. Prepare peripheral elbow vein line for contrast bolus injection.
3. Set middle cerebral artery monitoring for emboli identification and count with transcranial Doppler.
4. Have an echographic equipment to perform trans-thoracic echocardiography to collect data on anatomy and to differentiate cardiac and pulmonary shunts.
5. Prepare a concise medical report, clearly stating basal and Valsalva maneuver-induced entity of the shunt.

37.1 Introduction

The identification of right-to-left shunt (RLS) and *patent foramen ovale* (PFO) is a very frequent question addressed in everyday clinical practice, for neurologists, cardiologists, and anesthesiologists. As a matter of fact, paradoxical embolism could

E. Vicenzini (✉)
Department of Neurosciences and Mental Health, Neurosonology, Sapienza, University of Rome, Rome, Italy

Member - ESNCH, Oslo, Norway
e-mail: edoardo.vicenzini@uniroma1.it

C. Izzo
Department of Neurosciences and Mental Health, Neurosonology, Sapienza, University of Rome, Rome, Italy

C. N. Rodríguez et al. (eds.), *Neurosonology in Critical Care*,
https://doi.org/10.1007/978-3-030-81419-9_37

be responsible for stroke and for signs and symptoms of decompression sickness in divers and high altitude pilots.

Transcranial Doppler (TCD), trans-thoracic echocardiography (TTE), and trans-esophageal echocardiography (TEE) techniques with first generation contrast agents – that is – those agents not able to pass the pulmonary filter – have been compared regarding their sensitivity and specificity in the RLS diagnosis [1–3], with the following final conclusions: (1) TCD has a very high sensitivity for RLS detection, better than TTE, since the capability to detect the emboli is higher; however, the specificity for PFO diagnosis is lower, considering that in up to 10–15% of cases, RLS may be related to extra cardiac passages such as in pulmonary fistulae, in which a PFO is not necessarily present; (2) TCD and TEE have similar sensitivity for RLS detection, TEE though being invasive with a obviously higher specificity for PFO detection and morphological description, it is able to directly visualize the interatrial septum; and (3) TTE is a highly specific technique for shunt detection, whose major advantage is the ability to detect large RLSs, particularly if associated with an atrial septal aneurysm, but with less capacities than TCD to quantify the shunt. Consequently, it has been advised that TCD should be nowadays recommended as the first choice examination for RLS screening, because of its simplicity, non-invasive character, low cost, and high sensitivity [4].

37.2 Regional Anatomy

The interatrial septum begins to form during the second month of fetal life in different steps. At first, the "septum primum" starts to grow from the posterior part of the atria and increases in volume and length, but without fully occluding the atria communication (Fig. 37.1a). This residual opening is called the "*ostium primum*" and it allows the blood to be shunted from the right to the left circulation, thus excluding the immature lungs. With the growth of the *septum primum* – before it completely occludes the atria communication – a second hole opens in the inferior part of the septum; this is called the "*ostium secundum*," and still allows the blood shunting, escaping the pulmonary fetal circulation (Fig. 37.1b). Later, anteriorly to the *septum primum*, the "*septum secundum"* starts growing, leaving a small opening in its lower part, called the "*foramen ovale,"* which may come in continuity with the *ostium secundum* of the *septum primum* (Fig. 37.1c). Gradually, the *septum secundum* increases in size and thickness and the *septum primum* becomes a thin membrane, covering with a tiny flap the *foramen ovale* and forming a small valve, opening and closing in relation to the pressure gradients in the two atria: a left atrium increase of pressure will determine the closing of the communication, while the right atrium pressure increase will open the valve. During fetal life, non-active lungs result in higher pulmonary circulation pressure that induces the flap to be opened in direction of the left circulation. Finally, when the lungs expand at birth, pressure becomes higher in the left heart sections and the valve closes, with permanent septa fusion within 2 years in 70–75% of infants (Fig. 37.1d) [5, 6].

Septum development fails are very common, resulting in an atrial septal defect.

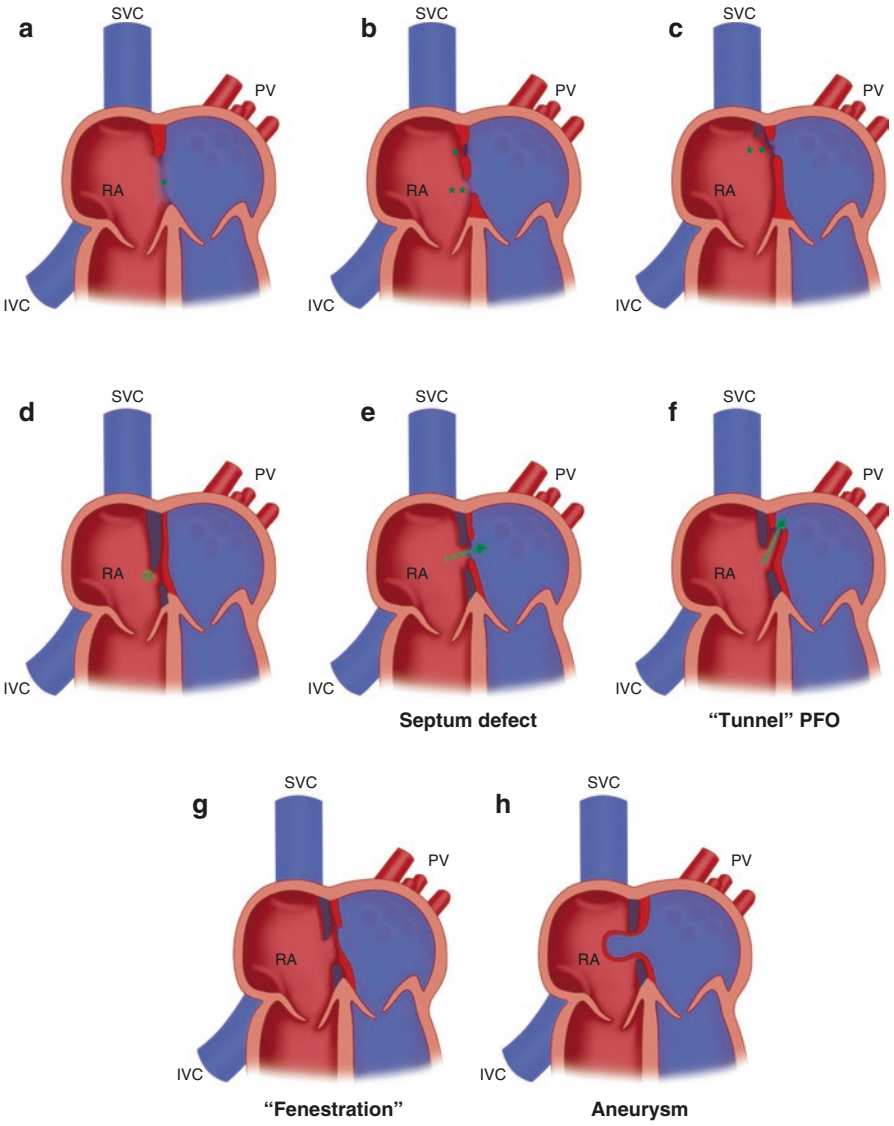

Fig. 37.1 (**a**–**h**) Embryogenesis and development of interatrial septum. *Septum primum* (red) and *septum secundum* (blue), *ostium primum* (*), *ostium secundum* (**), and *fossa ovale* (°). Green arrow in E shows the shunt through a "true" *patent foramen ovale*, in F depicts the shunt through the "tunnel" foramen ovale, derived by the lack of fusion between the *septum primum* and the *septum secundum*. Red dotted lines in G shows the "fenestration" of the flap in *the septum secundum* and the red bulge in H shows aneurysm of the interatrial septum. Further explanation in the text. Legend: RA: right atrium; SVC: superior vena cava; IVC: inferior vena cava; PA: pulmonary veins

When the persistence of the interatrial communication between the two septa occurs at the level of the *ostium secundum,* the hole being at the overlap with the *foramen ovale,* we refer to a true atrial septum defect and patent *foramen ovale* (Fig. 37.1d). More frequently, even though the septa have been formed completely, the lack of fusion between the two septa occurs: in this case the *foramen ovale* may not be really "patent" (Fig. 37.1e), but the *septum primum* continues to act as a one-way valve, blocking the flow backwards to the right atrium. When the right atrial pressure overrides the left atrial pressure, blood may shunt from the right to the left circulation, through a "tunnel" of variable length, formed by the exceeding part of the valve consistent with tiny membrane of the septum *primum* (Fig. 37.1f). The frequency of interatrial communication may reach up to 25–40% of routine heart anatomy, even in asymptomatic patients. Another condition of septum discontinuity is the presence of one or several fenestrations in the flap of the *septum primum* covering the *foramen ovale (*of the *septum secundum*) (Fig. 37.1g). The *entire septum primum* flap can also be large and redundant with a higher mobility and bulge throughout the two atria, even developing aneurysms of 15–20 mm size (Fig. 37.1h) [7, 8].

Different defects occur in Down's syndrome, with the failure of the *septum primum* to fuse to the endocardium, thus leaving open the *ostium primum*. In this case, the shunt occurs initially from the left to the right atrium and it may be asymptomatic until, over time, pulmonary hypertension and right ventricular hypertrophy develop, reversing the shunt again backwards to right atrium (Eisenmenger syndrome) [5, 6].

37.3 Right-Left Shunt Diagnosis: Technique

After the first consensus in 2000 on the TCD guidelines for RLS diagnosis [9], several recommendations have been published to standardize the methodology and to obtain more reliable and sensitive results [10, 11].

37.3.1 Transcranial Doppler

Use standard TCD systems for the RLS detection. The images of this chapter were obtained with a DWL/Compumedics MultiDop Digital X equipment and one 2 MHz probe fixed with a probe holder (Marc 600, Spencer Technologies), insonating the right middle cerebral artery, at the depth of 46–54 mm, in supine position. Multigate Doppler with standard presets for emboli detection software was used and Doppler spectrum was recorded continuously throughout the examination for the off-line

analysis. Acoustic threshold for microembolic signal (MES) identification have been set at 9 dB and signals counted both manually and automatically. Literature suggests bilateral monitoring to increase emboli detection sensitivity, but since no side-differences have been clearly reported, this approach may be more time consuming.

Transcranial color-coded duplex sonography (TCCS) machines may also be used for this purpose, directly imaging the middle cerebral artery and using the pulsed wave (PW)-Doppler. However, some considerations have to be taken into account: (1) while with the TCD with the head-frame you obtain a stable signal and you can perform all the procedure alone, with the TCCS you will need a second person, one for holding the probe and the second for contrast bolus administration; moreover, during the Valsalva maneuver (VM) you may have difficulties in holding the probe firmly and to keep a stable signal, especially if you are working in emergency settings and the patient is not fully cooperative; (2) TCCS machines usually do not allow long Doppler spectra recordings, and using a slow swipe of the spectrum and the cine-loop scrolling, modality may reduce the sensibility to individually count the MES, especially when the count is performed off-line; (3) TCCS machines are not able to perform the "multigate" sampling – that is – recording the Doppler Signal at two or more different depths – thus neither automatic MES count nor true automatic embolus and artifact detection and differentiation is possible (see section below on data interpretation); and (4) bilateral and simultaneously monitoring is not possible with TCCS.

37.3.2 Contrast Agent Preparation and Administration

Air-saline injections should be performed, according to literature [9, 10], with a mixture of saline 9 ml and air 1 ml, rapidly shaken at least ten times through a three-way stopcock, and bolus injected into an antecubital vein line, prepared with a 20 Gauge Venflon with the patient lying down in the bed, and not in upward sit position. Choice of right or left arm could vary according to your facilities. If you will then plan to perform the TTE, consider the right side preferential, since when the patient will be laying on the left side for the TTE, it will be easier to access the right arm for the contrast administration. The bolus should be repeated at least three times: the first time at rest and another two times followed by a 5" Valsalva maneuver, starting 5″ after the injection, each with a 3–4 minutes interval. The Valsalva maneuver is a fundamental step for the RLS identification, since it increases the intrathoracic and right heart section pressure, facilitating the right-to-left shunt. Hemodynamically, at TCD monitoring, it will result in an initial blood flow velocities reduction followed by an increase in blood flow velocities that will confirm that the Valsalva had been performed correctly [12].

37.3.2.1 Tips and Pitfalls for Contrast Preparation and Injection

Air-saline contrast shaking [13] should be done directly at the arm, connecting the syringes to the stop cock screwed to the Venflon. To prevent vein traumatism from the repeated shaking in the unavoidable uncomfortable operator position, you can use the small connection tubes available in the market. To avoid casual disconnection of the syringes from the stop cock, you can use one or two Luer-Lock syringes, with the locking screw edge connected to the freeways of the stop cock.

Guidelines also suggest adding 1 ml of fresh blood, retrieved from the patient's line just before the solution shaking, to obtain a more stable "foam." Even though no contraindications or side effects have been reported with this approach, we tend to consider it less hygienic and less practical, both for the blood manipulation during the shaking, as well as for the possible disconnection of the syringe from the stop cock with the result to have very low hygienic results.

37.3.2.2 Contrast Preparation with Air-Gelatin Solutions

To achieve a better visualization of the right heart chambers during echocardiography cardiologists also are used to add gelatins – plasma expanders – to prepare the air-saline mixture, thus obtaining a more dense and stable preparation than air-saline alone [14–16]. The concept is similar to that of the blood addition. The air-gelatin mixture preparation at the bedside is faster, much easier and already stable after three shakes through the stopcock, with the result of a long-lasting contrast agent, preserving the principal air-saline characteristics meant for the PFO diagnosis with TCD, that is, not to pass the pulmonary filter. In echocardiography, it has been indeed demonstrated as superior, with a higher sensitivity in respect to air-saline, for the visual identification of the shunt in PFO [15, 16]. Our group also has recently published data on the increase of RLS sensitivity with TCD and air-gelatin mixture at rest, even in patients in whom air-saline mixture fails to identify the shunt [17]. Several concentrations of gelatins can be added to the solution, up to a total gelatin-air mixture, better results being obtained with saline 8 ml, gelatin 1 ml, and air 1 ml.

37.3.3 Transcranial Color-Coded Duplex Sonography (TCCS)

Approach the transtemporal insonation with a sector array probe (2–3.5 MHz) and specific TCCS imaging presets. Images presented in this review have been obtained with a Siemens S2000 apparatus. Focus on the middle cerebral artery segment adapting the sample volume without the need of reducing it as much as possible and reducing the swipe of the Doppler spectrum, to have the visualization of at least 5–6 seconds on the screen during freeze.

37.3.4 Trans-Thoracic Echocardiography

Use the cardiac sector array probe (2–3.5 MHz) in B-Mode with four chambers projection. Use long clips (60–90″) to obtain the overall view of the procedure. Images presented in this review have been obtained with a Siemens S2000 apparatus with specific cardiac settings.

37.3.5 Data Interpretation

In the middle cerebral artery Doppler spectrum, the small microbubbles escaping the pulmonary filter will strongly reflect the ultrasound beam with a very high frequency and intensity signal deriving from high ultrasound reflection and burst of the bubbles. These can be easily displayed and recognized for the typical sound as "high intensity transient signals – HITS," referred to as "chirps" or "microembolic signals – MES." They are visualized as white spots in the Doppler spectrum and as "comma-shaped" signals in the power-M-Mode, displaying the multigate Doppler shift of the different depths on a single line – as the M-Mode in the heart – but according to the red-blue direction color coding (Fig. 37.2).

According to literature [9, 10, 18–20], to achieve the highest sensitivity and specificity for considering TCD positive for a PFO-related RLS, at least 1 MES had to be detected within 40 seconds or sooner after the start of injection. Later MES were interpreted as of possible extracardiac origin. With air-saline, RLS was graded counting the number of MES: (a) 0; (b) 1–10; (c) >10, countable with shower effect; and d) curtain effect with too numerous MES for a single identification [10]. Consider the count *per side* when applying bilateral monitoring. Figure 37.2 reports the TCD images during basal and after Valsalva maneuver and with the different shunt entity (see Figure legend for explanation).

MES can be easily differentiated from artifacts on Doppler spectrum, generally provoked by movements of the patient or for the ultrasound gel "crackling" under the probe, since the multigate insonation allows the identification of the same acoustic wave originating from the embolus in two different times, earlier on deeper sample volumes and then moving later to more superficial depths (Fig. 37.3a). In power M-Mode imaging, displaying the Doppler shift of different depths on a single line according to the red-blue direction color-coding, this will cause a "comma-"shaped signal, appearing first at higher depths and then moving along the vessels course (Fig. 37.2). On the other hand, artifacts have a straight appearance throughout the power-M mode scan (Fig. 37.3b,c), allowing the systems to automatically consider it an artifact and reject it from the embolus count. However, in RLS TCD examination, automatic count has less importance than their direct recognition, since the time of execution of the exam is very short and different from that of the long-lasting sessions for MES monitoring in other diseases.

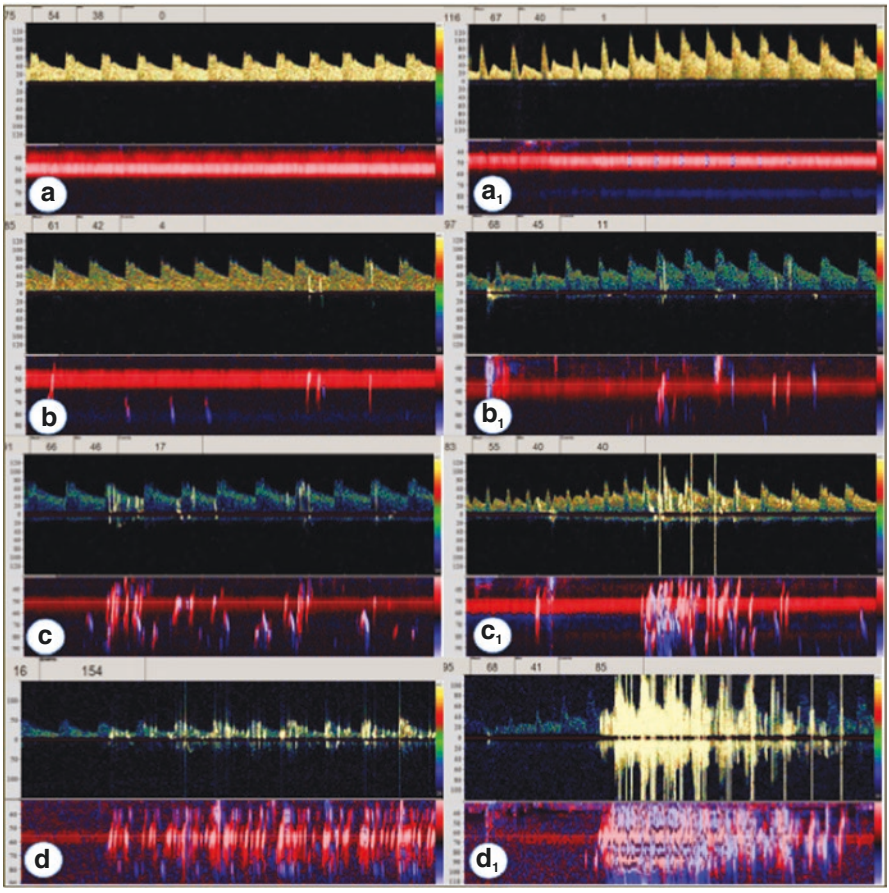

Fig. 37.2 TCD right-to-left shunt identification and severity grading. Left side, basal condition: Absent (**a**): 0 embolic signals. Light (**b**): 1-10 embolic signals. Moderate (**c**): > 10 embolic Signals, countable and with "shower" effect. Severe (**d**): massive shunt (>30 MES) with MES uncountable. Right side, Valsalva maneuver: Absent ($\mathbf{a}_1$): 0 embolic signals. Light ($\mathbf{b}_1$): 1-10 embolic signals. Moderate ($\mathbf{c}_1$): > 10 embolic Signals, countable and with "shower" effect. Severe ($\mathbf{d}_1$): massive shunt (>30 MES) with "curtain" effect (MES uncountable). In the Power M-Mode, note the "comma-shaped" signal referred to the embolus (see text)

Data could also be identified with TCCS (Fig. 37.4), but in considering that the multi-gate options to differentiate emboli from artifacts will not be available and that – generally – ultrasound machines allow recording of only short Doppler spectra. However, experienced examiners will easily recognize artifact signals from those of the true emboli. Moreover, as stated above, while examinations with TCD and helmet probe holder could be carried on by a single examiner, TCCS will require instead a second person, one for holding the probe and the second to perform the contrast bolus.

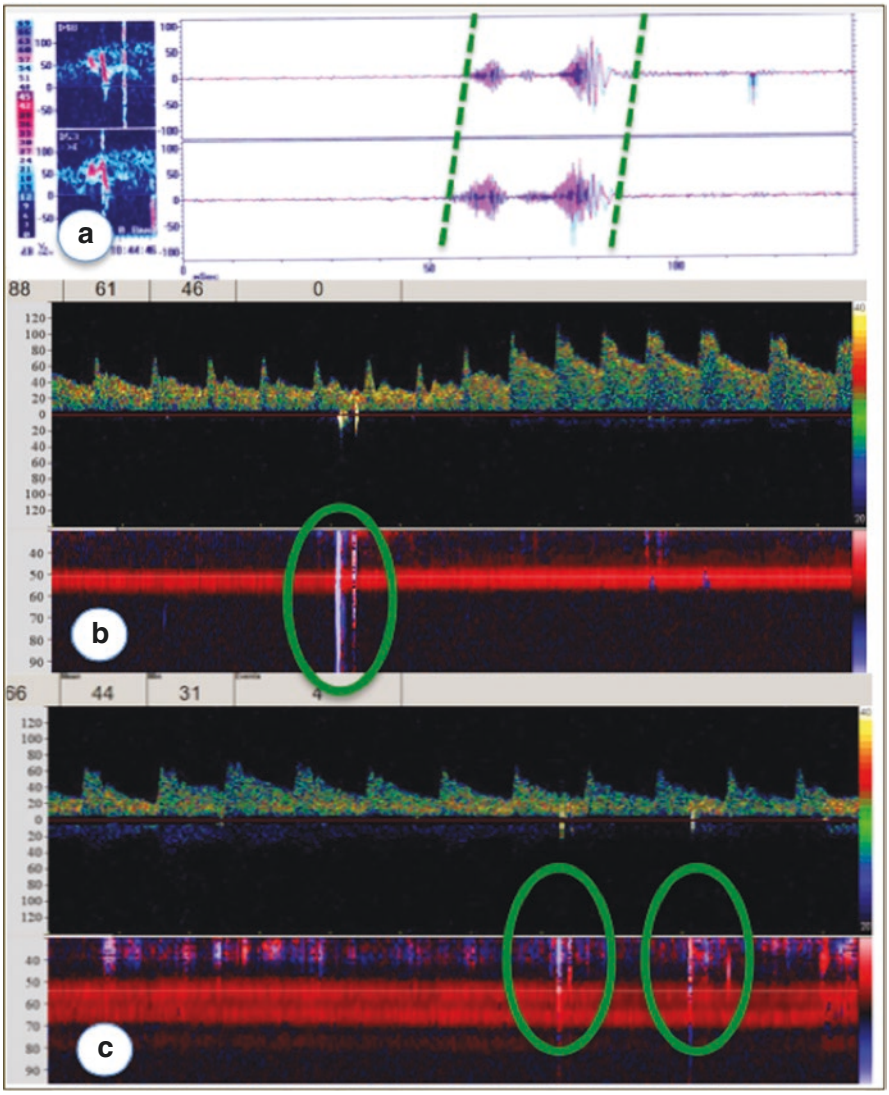

Fig. 37.3 TCD differentiation of emboli and artifacts: note the signal progression when visualized as sound waves (**a**, green lines), and the straight appearance in the power M-Mode of the artifacts (**b**, green circle, **c**), compared with the "comma-shaped" signal of the true emboli in Fig. 37.2

TTE can be interpreted on digital clips of 90–120 seconds, recorded during the contrasts administrations. With some manual skills, a single operator could perform both TTE and contrast agent administration, though cooperation of a second person is advisable. Cardiac RLS originating from the *patent foramen ovale* can be diagnosed when the shunt is directly visualized from the interatrial septum or when the

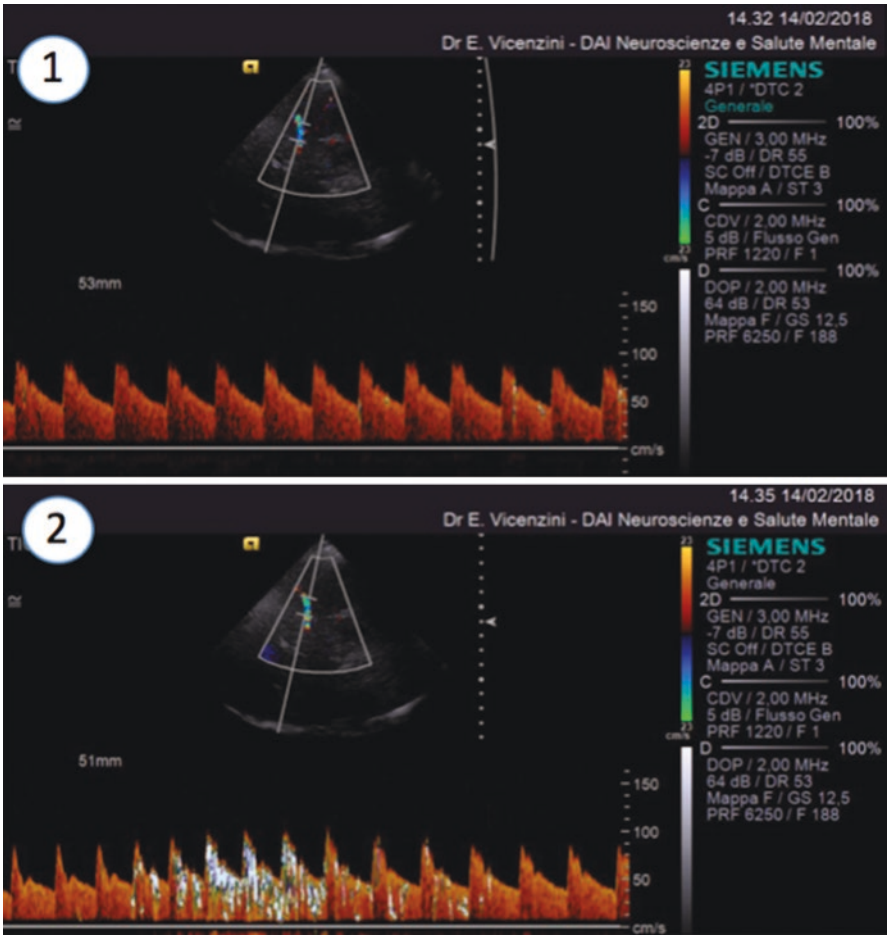

Fig. 37.4 Example of TCCS with saline to RLS identification, detected only after Valsalva maneuver: (1) basal; (2) Valsalva maneuver. MES are identical to those observed with TCD on the Doppler spectrum, but with short monitoring time and lack of power M-Mode

bubbles are visualized in the left heart sections within the third (fourth in case of bradycardia) heartbeat after contrast arrival in the right heart chambers (Fig. 37.5a). Later shunts, detected from the left side of the left atrium and originating from the pulmonary veins, are considered related to pulmonary passage (Fig. 37.5b). It has to be noticed that the Valsalva maneuver, when performed correctly with a deep inspiration, may hamper the heart visualization, thus missing the first heartbeats after contrast arrival, reducing sensibility to detect shunts only after the Valsalva maneuver.

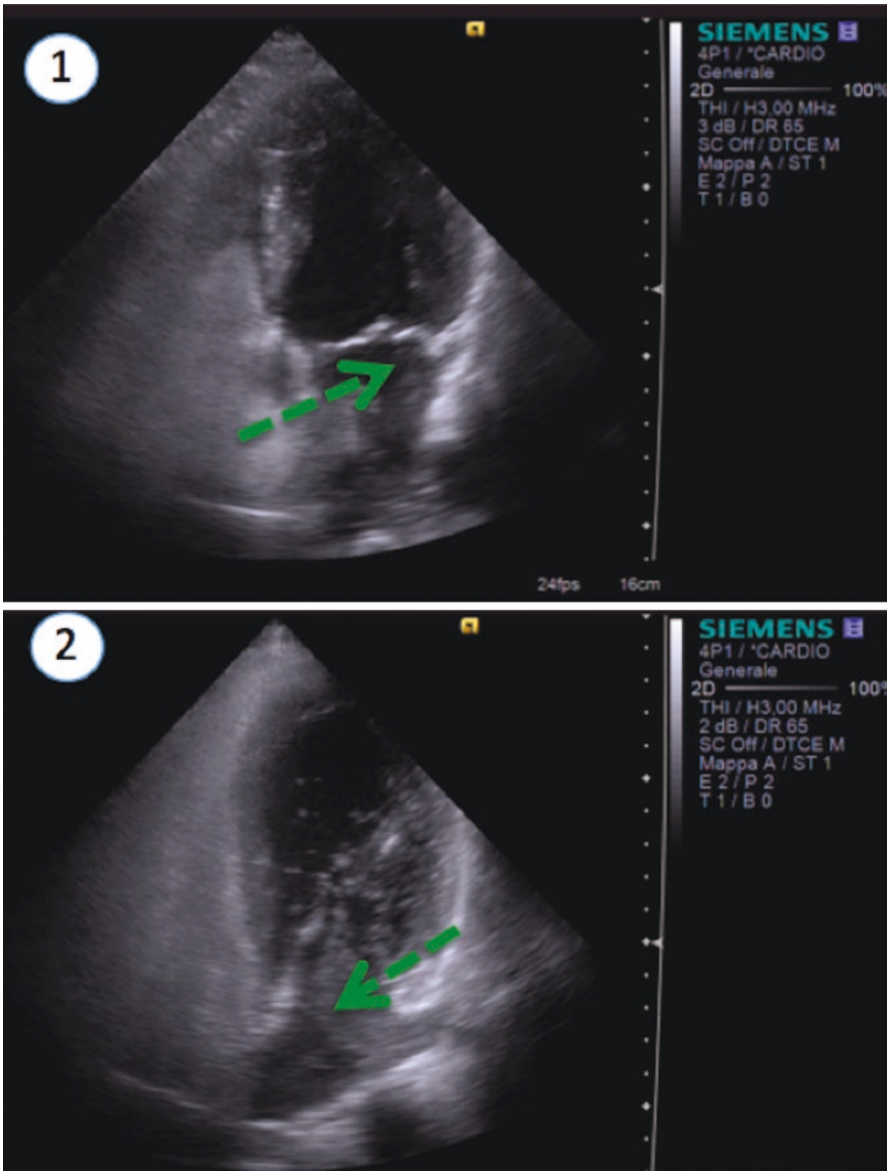

Fig. 37.5 Trans-thoracic echocardiography to discriminate cardiac and pulmonary shunt. TTE shows the passage of the microbubbles within the 3rd heart beat from contrast arrival in the right heart section in PFO, and later when arising from pulmonary veins and pulmonary fistulae Note the different origin of the bubble jet in the PFO (1), from right atrium, in respect to the pulmonary shunt (2), clearly originating from the pulmonary veins

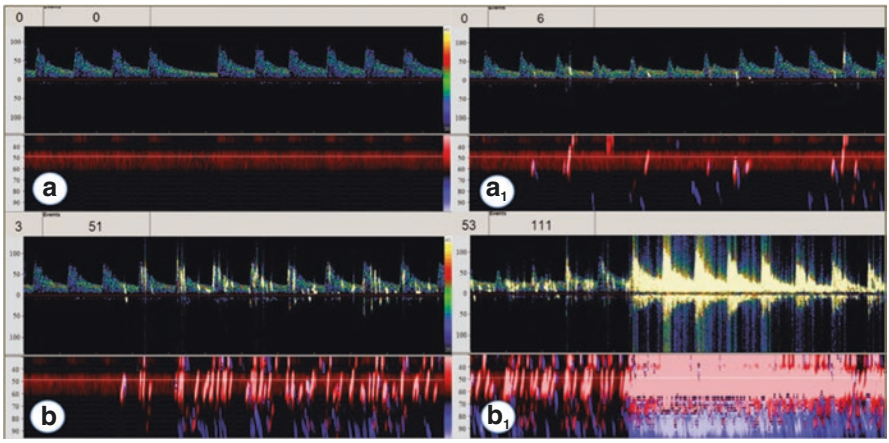

Fig. 37.6 Right-to-left shunt detection with saline (**a**) and gelofusine (**b**) air-mixed contrast agents. With the saline alone, patient shows no shunt in basal condition (**a**) and light shunt after VM (**a**$_1$). Contrast preparation with gelofusine 1 ml reveals instead the shunt also in basal condition (**b**), markedly increased after the VM (**b**$_1$). Thus, in uncooperative patients and emergency settings, gelofusine-air contrast could be helpful to reveal the shunt already in basal conditions and without the need of VM

As regards to the sensitivity increase for RLS detection with TCD and air-gelatin solution, we have observed that in patients with RLS only after VM, air gelatin may facilitate and reveal the shunt even in basal conditions, even in patients in whom air-saline mixture gives negative basal results. This could be helpful in emergency settings and in uncooperative patients unable to perform correctly the VM [17] (Fig. 37.6).

37.4 Usefulness of the Clinical Study

Transcranial Doppler with saline contrast agents is the easiest and non-invasive way to identify RLS, and it is up-to-date considered the first-line screening test. However, being an interatrial communication present – and asymptomatic – in up to 35–40% of the world population, it is crucial to select those patients in whom to explore the RLS presence and in whom its casual identification will change the medical follow-up.

Multiple studies have reported a significant association – up to 45% – between migraine, particularly with aura, and the presence of patent *foramen ovale* [21–23]. It had been indeed hypothesized that peripheral circulation neurotransmitters shunt through the PFO without pulmonary passage as well as the recurrence of microembolism could trigger spreading depression in migraine. However, the role of PFO in

migraine remains poorly understood and recent results have clearly shown no benefits from its closure and migraine symptoms [24, 25]. Consequently, investigating PFO routinely in migraine seems to be useless, even from the subsequent migraine management. The white matter abnormalities commonly observed in migraine does not appear to be related to repeated embolism and the association of migraine symptoms with cerebral autosomal dominant arteriopathy with subcortical infarcts and leukoencephalopathy (CADASIL) – a hereditary microangiopathy caused by mutation in the Notch3 gene – suggesting the presence of an intrinsic cerebral endothelial vulnerability and susceptibility in migraine states, that could be responsible both for clinically apparent stroke or "silent" white matter disease.

The association of cryptogenic stroke and PFO has been largely debated in clinical trials. Except the cases in whom the paradoxical embolism is evident for the detection of the peripheral embolic source and the temporal correlation with the stroke onset, studies on PFO closure and stroke risk reduction are controversial, with up to now three published studies showing negative effects [26–28] and three showing positive effects [29–31]. It is true that PFO may be considered as an embolic source per se, even causing cardiac arrhythmias when associated to interatrial aneurism, but when it is isolated the causality of the ischemic event with PFO have to be considered cautiously. Other comorbidities and other vascular risk factors, such as the presence of an altered hypercoagulable state, should be taken into account to identify the cause and the source of the embolus that crossed the septum to reach the brain and the peripheral arterial circulation. However, PFO should be investigated in patients with TIA and stroke in the young and in cryptogenic stroke.

The presence of RLS is on the other hand strongly associated to decompressive sickness (DCS) in divers with neurological, inner ear, and cutaneous forms [32–38]. In this case the gaseous emboli arising in the peripheral venous circulation represent our peripheral embolic source. This suggests that RLS identification should be always investigated in divers after DCS, excluding musculoskeletal and atypical localizations. However, recent evidences show that RLS identification is not a reliable predictor of DCS occurrence [39], thus limiting the value of RLS screening before DCS had occurred. On the other hand, residual shunt identification after PFO closure may be important to understand which already symptomatic DCS subjects may be declared able to dive again [39].

As regards to the long distance flights, the "economy class syndrome" has been defined to describe the risk of pulmonary embolism during air travelling, with an increased risk, up to 150 fold, in those who travel by air for more than 5000 km or spend approximately 6 hours or more in flight [40]. Up to 10% of healthy air travelers develop indeed deep vein thrombosis without clinical symptoms after long flights [41]. Matching the information that PFO is highly prevalent in the normal population and this high frequency of asymptomatic deep vein thrombosis, it is reasonable to hypothesize that among long distance travelers there could be and increased PFO-related stroke risk. This has been described in literature as the

"economy class stroke" [42–44], especially in patients with other vascular risk factors and susceptibility to thrombotic state. Again, the idea to perform RLS mass screening in those who are supposed to travel long distance flights is not advisable, but it may be strongly recommended that the preventive strategies for avoiding deep vein thrombosis should be observed, with correct leg exercise during the flight and, eventually, short-term ASA premedication.

37.5 Complications

No side effects have been reported in literature from the procedure using air-saline contrast solution, nor in our series of patients using air-gelatins solutions. A case of anaphylaxis – periorbital edema – to gelatins has been described in literature during echocardiography with gelatins [45], though with a single bolus of 8 ml of gelofusine, expression of already described allergy to plasma expanders [46, 47].

37.6 Conclusion

PFO with paradoxical RLS may be related to several neurovascular injures. TCD with saline contrast agents is nowadays the first-line examination to investigate and detect the RLS, to be evaluated also with echocardiography – considering transesophageal when mechanical closure becomes the treatment option. Since up to one fourth of the world's population may have PFO, it is crucial to identify those subjects in whom it should be investigated and in whom it really had become symptomatic, in order not to overdiagnose a paraphysiological condition. The question still to be cleared is: "If PFO opens a "back-door" for clots to go to the brain, where do these clots come from?" Biomarkers of embolic risk as well as not yet completely identified hypercoagulable and thrombophilic conditions identification, will help in the definition of the patient "at true risk" of paradoxical embolism in PFO presence.

Algorithm

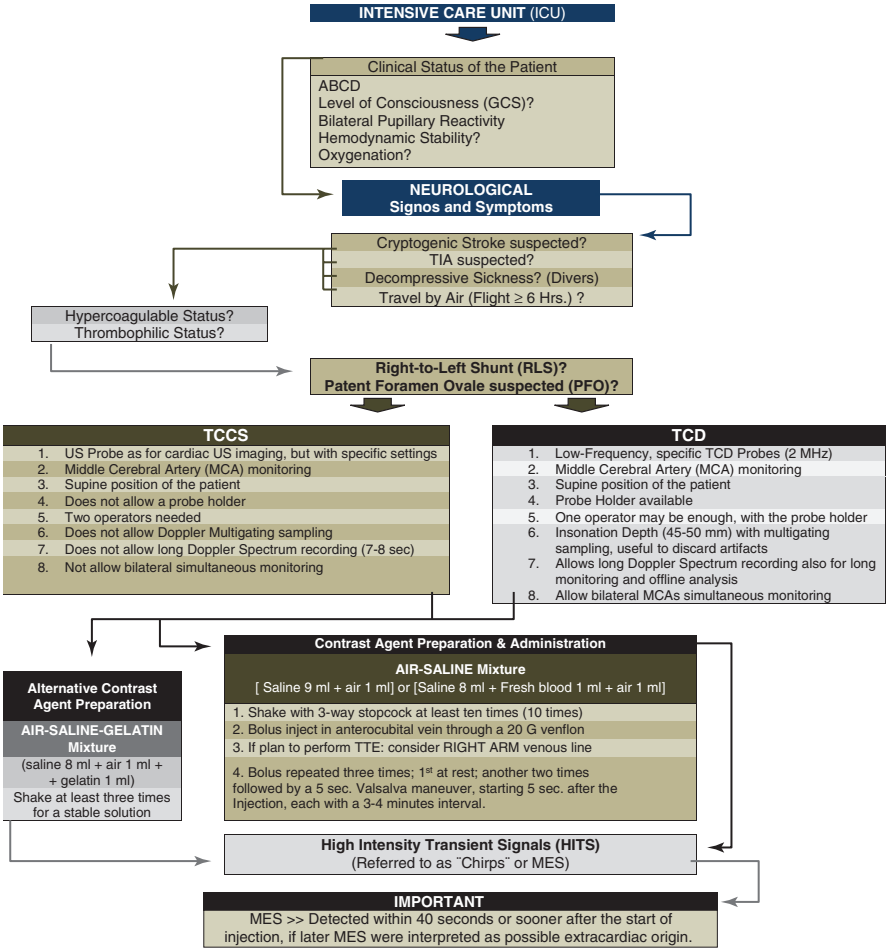

References

1. Zito C, Dattilo G, Oreto G, Di Bella G, Lamari A, Iudicello R, et al. Patent foramen ovale: comparison among diagnostic strategies in cryptogenic stroke and migraine. Echocardiography. 2009;26(5):495–503.
2. Mojadidi MK, Roberts SC, Winoker JS, Romero J, Goodman-Meza D, Gevorgyan R, et al. Accuracy of transcranial Doppler for the diagnosis of intracardiac right-to-left shunt: a bivariate meta-analysis of prospective studies. JACC Cardiovasc Imaging. 2014;7:236–50.

3. González-Alujas T, Evangelista A, Santamarina E, Rubiera M, Gómez-Bosch Z, Rodríguez-Palomares JF, et al. Diagnosis and quantification of patent foramen ovale. Which is the reference technique? Simultaneous study with transcranial Doppler, transthoracic and transesophageal echocardiography. Rev Esp Cardiol. 2011;64:133–9.
4. Komar M, Olszowska M, Przewłocki T, Podolec J, Stępniewski J, Sobień B, et al. Transcranial Doppler ultrasonography should it be the first choice for persistent foramen ovale screening? Cardiovasc Ultrasound. 2014;22:12–6.
5. Anatomy G's. The anatomical basis of clinical practice. 39th ed; 2005.
6. Anderson RH, Brown NA, Webb S. Development and structure of the atrial septum. Heart. 2002;88:104–10.
7. Rana BS, Shapiro LM, McCarthy KP, Ho SY. Three-dimensional imaging of the atrial septum and patent foramen ovale anatomy: defining the morphological phenotypes of patent foramen ovale. Eur J Echocardiogr. 2010;11:19–25.
8. Klimek-Piotrowska W, Hołda MK, Koziej M, Piątek K, Hołda J. Anatomy of the true interatrial septum for transseptal access to the left atrium. Ann Anat. 2016;205:60–4.
9. Jauss M, Zanette E. Detection of right-to-left shunt with ultrasound contrast agent and transcranial Doppler sonography. Cerebrovasc Dis. 2000;10:490–649.
10. Droste DW, Schmidt-Rimpler C, Wichter T, Dittrich R, Ritter M, Stypmann J, et al. Right-to-left-shunts detected by transesophageal echocardiography and transcranial Doppler sonography. Cerebrovasc Dis. 2004;17:191–6.
11. Uzuner N, Horner S, Pichler G, Svetina D, Niederkorn K. Right-to-left shunt assessed by contrast transcranial Doppler sonography: new insights. J Ultrasound Med. 2004;23:1475–82.
12. Droste DW, Jekentaite R, Stypmann J, Grude M, Hansberg T, Ritter M, et al. Contrast transcranial Doppler ultrasound in the detection of right-to-left shunts: comparison of Echovist-200 and Echovist-300, timing of the Valsalva maneuver, and general recommendations for the performance of the test. Cerebrovasc Dis. 2002;13:235–41.
13. Gentile M, De Vito A, Azzini C, Tamborino C, Casetta I. Adding blood to agitated saline significantly improves detection of right-to-left shunt by contrast-transcranial color-coded duplex sonography. Ultrasound Med Biol. 2014;40:2637–41.
14. Soliman OI, Geleijnse ML, Meijboom FJ, Nemes A, Kamp O, Nihoyannopoulos P, et al. The use of contrast echocardiography for the detection of cardiac shunts. Eur J Echocardiogr. 2007;8:S2–12.
15. Buttignoni SC, Khorsand A, Mundigler G, Bergler-Klein J, Heger M, Zehetgruber M, et al. Agitated saline versus polygelatine for the echocardiographic assessment of patent foramen ovale. J Am Soc Echocardiogr. 2004;17:1059–65.
16. Santoso T, Roelandt J, Mansyoer H, Abdurahman N, Meltzer RS, Hugenholtz PG. Myocardial perfusion imaging in humans by contrast echocardiography using polygelin colloid solution. J Am Coll Cardiol. 1985;6:612–20.
17. Puledda F, Toscano M, Pieroni A, Veneroso G, Di Piero V, Vicenzini E. Right-to-left shunt detection sensitivity with air-saline and air-succinil gelatin transcranial Doppler. Int J Stroke. 2016;11:229–38.
18. Droste DW, Silling K, Stypmann J, Grude M, Kemény V, Wichter T, et al. Contrast transcranial doppler ultrasound in the detection of right-to-left shunts: time window and threshold in microbubble numbers. Stroke. 2000;31:1640–5.
19. Droste DW, Kriete JU, Stypmann J, Castrucci M, Wichter T, Tietje R, et al. Contrast transcranial Doppler ultrasound in the detection of right-to-left shunts: comparison of different procedures and different contrast agents. Stroke. 1999;30:1827–32.
20. Droste DW, Reisener M, Kemény V, Dittrich R, Schulte-Altedorneburg G, Stypmann J, et al. Contrast transcranial Doppler ultrasound in the detection of right-to-left shunts. Reproducibility, comparison of 2 agents, and distribution of microemboli. Stroke. 1999;30:1014–8.
21. Takagi H, Umemoto T. A meta-analysis of case-control studies of the association of migraine and patent foramen ovale. J Cardiol. 2016;67:493–503.

22. Lip PZY, GYH L. Patent foramen ovale and migraine attacks: a systematic review. Am J Med. 2014;127:411–20.
23. Del Sette M, Angeli S, Leandri M, Ferriero G, Bruzzone GL, Finocchi C, et al. Migraine with aura and right-to-left shunt on transcranial Doppler: a case-control study. Cerebrovasc Dis. 1998;8:327–30.
24. Finocchi C, Del Sette M. Migraine with aura and patent foramen ovale: myth or reality? Neurol Sci. 2015;36(S1):61–6.
25. Tobis JM, Charles A, Silberstein SD, Sorensen S, Maini B, Horwitz PA, et al. Percutaneous closure of patent foramen ovale in patients with migraine: the PREMIUM trial. J Am Coll Cardiol. 2017;70(22):2766–74.
26. Mas JL, Derumeaux G, Guillon B, Massardier E, Hosseini H, Mechtouff L, et al. Patent foramen ovale closure or anticoagulation vs. antiplatelets after stroke. N Engl J Med. 2017;377:1011–21.
27. Saver JL, Carroll JD, Thaler DE, Smalling RW, MacDonald LA, Marks DS, et al; RESPECT Investigators. Long-term outcomes of patent foramen ovale closure or medical therapy after stroke. N Engl J Med 2017; 377:1022–32.
28. Søndergaard L, Kasner SE, Rhodes JF, Andersen G, Iversen HK, Nielsen-Kudsk JE, et al; Gore REDUCE Clinical Study Investigators. Patent foramen ovale closure or antiplatelet therapy for cryptogenic stroke. N Engl J Med 2017; 377:1033–1042.
29. Furlan AJ, Reisman M, Massaro J, Mauri L, Adams H, Albers GW, et al; CLOSURE I Investigators. Closure or medical therapy for cryptogenic stroke with patent foramen ovale. N Engl J Med 2014; 366:991–9.
30. Carroll JD, Saver JL, Thaler DE, Smalling RW, Berry S, MacDonald LA, et al; RESPECT Investigators. Closure of patent foramen ovale versus medical therapy after cryptogenic stroke. N Engl J Med 2013; 368:1092–100.
31. Meier B, Kalesan B, Mattle HP, Khattab AA, Hildick-Smith D, Dudek D, et al; PC Trial Investigators. Percutaneous closure of patent foramen ovale in cryptogenic embolism. N Engl J Med 2013; 368:1083–91.
32. Cantais E, Louge P, Suppini A, Foster PP, Palmier B. Right-to-left shunt and risk of decompression illness with cochleovestibular and cerebral symptoms in divers: case control study in 101 consecutive dive accidents, Crit. Care Med. 2003;31:84–8.
33. Gempp E, Blatteau JE, Stephant E, Louge P. Relation between right-to-left shunts and spinal cord decompression sickness in divers. Int J Sports Med. 2009;30:150–3.
34. Gempp E, Louge P. Inner ear decompression sickness in scuba divers. Eur Arch Otorhinolaryngol. 2012;270:1831–7.
35. Wilmshurst P, Bryson P. Relationship between the clinical features of neurological DCI and its causes. Clin Sci. 2000;99:65–75.
36. Germonpré P, Dendale P, Unger P, Balestra C. Patent foramen ovale and decompression sickness in sports divers. J Appl Physiol. 1998;84:1622–6.
37. Moon RE, Camporesi EM, Kisslo JA. Patent foramen ovale and decompression sickness in divers. Lancet. 1989;333:513–4.
38. Wilmshurst PT, Morrison WL, Walsh KP. Comparison of the size of persistent foramen ovale and atrial septal defects in divers with shunt-related decompression illness and in the general population. Diving Hyperb Med. 2015;45:89–93.
39. Gempp E, Lyard M, Louge P. Reliability of right-to-left shunt screening in the prevention of scuba diving related-decompression sickness. Int J Cardiol. 2017;48:155–8.
40. Lapostolle F, Surget V, Borron SW, Desmaizières M, Sordelet D, Lapandry C, et al. Severe pulmonary embolism associated with air travel. N Engl J Med. 2001;345:779–83.
41. Scurr JH, Machin SJ, Bailey-King S, Mackie IJ, McDonald S, Smith PD. Frequency and prevention of symptomless deep-vein thrombosis in long-haul flights: a randomised trial. Lancet. 2001;357:1485–9.

42. Foerch C, Kessler KR, Steinmetz H, Sitzer M. Economy class stroke syndrome. Neurology. 2002;59(6):962–3. author reply 963.
43. Isayev Y, Chan RK, Pullicino PM. “Economy class” stroke syndrome? Neurology. 2002;58(6):960–1.
44. Ayo-Martin O, Garcia-Garcia J, Sopelana D, Segura T. Traveler’s stroke: it is not just flying that does it. Cerebrovasc Dis. 2008;26:566–8.
45. Dubrey SW, Dahdal G, Grocott-Mason R. Severe anaphylaxis to Gelofusine during a transthoracic echo bubble study. Eur J Echocardiogr. 2008;9:303.
46. Vervloet D, Senft M, Dugue P, Arnaud A, Charpin J. Anaphylactic reactions to modified fluid gelatins. J Allergy Clin Immunol. 1983;71:535–40.
47. Apostolou E, Deckert K, Puy R, Sandrini A, de Leon MP, Douglass JA, Rolland JM, O'hehir RE. Anaphylaxis to Gelofusine confirmed by in vitro basophil activation test: a case series. Anaesthesia. 2006;61:264–8.

Chapter 38
Neuro-Orbital Ultrasound: Ocular Color-Coded Duplex Sonography (OCCS)

Camilo N. Rodríguez, Milija Mijajlovic, and Juan Diego Ciro

Key Points

1. Ocular color-coded duplex sonography (OCCS) is a noninvasive technique with high potential for diagnosis of pathologies associated with raised intracranial pressure and cerebral vascular alterations.
2. The ultrasound equipment should be adjusted for orbital sonography according to the ALARA principle. The examination time should be less than a minute for each eye.
3. The Spectral-Doppler waveform analysis of the orbital vessels (OA and CRA) is very important for the interpretation in the alteration of the flow patterns (PSV/MFV).
4. During the interpretation of the results, consider the trend of the measurements is very important to correctly interpret the results obtained, not the absolute values alone.
5. ONSD had a strong correlation with ETD, and ONSD/ ETD index might provide more reliable data than ONSD itself as a marker of ICP.

C. N. Rodríguez (✉)
Intensive Care Medicine, Hospital Nacional Prof. Dr. A. Posadas, University of Buenos Aires (UBA), Neurointensive Care Section - ESICM, Neurointensive Care Section - AMCI, Neurointensive Care Committee - FEPIMCTI. Member of ESNCH, Buenos Aires, Argentina
e-mail: camilo.rodriguez@nesccco.com

M. Mijajlovic
Clinical Case Reports Journal, EAN Neurosonology Scientific Panel, Neurology Clinic, Clinical Center of Serbia, Faculty of Medicine, University of Belgrade, Belgrade, Serbia

Member At-Large - ESNCH, Oslo, Norway

J. D. Ciro
Anesthesiology – Intensive Care Medicine, ICU Department, Clínica Las Américas, Medellin, Colombia

Neurointensive Care Section – AMCI, Bogotá, Colombia

C. N. Rodríguez et al. (eds.), *Neurosonology in Critical Care*,
https://doi.org/10.1007/978-3-030-81419-9_38

6. Papilledema (there is disagreement about the optimal cutoff for this distance) and optic nerve sheath diameter (ONSD) should be integrated at the time to be interpreted it.

38.1 Introduction

Ocular color-coded duplex sonography (OCCS) is a noninvasive technique with high potential for diagnosis in the diseases with raised intracranial pressure (ICP) and vascular diseases affecting the eye in a wide range of neurological disorders. Among the main applications of OCCS are the following two factors:

1. Bed side estimation of ICP
2. Evaluation of the ophthalmic and central retinal arteries blood flow velocities

The high rate of reproducibility and the easy documentation of the ultrasound (US) results make it a very convincing technique and a very valuable tool to guide clinical decisions in real time.

Ocular color-coded duplex sonography (OCCS) is a noninvasive technique with high potential for diagnosis of pathologies associated with raised ICP and cerebral hemodynamic alterations.

38.2 Neuro-Vascular Orbital Anatomy

The most clinically relevant orbital anatomic structures for OCCS are as follows (Figs. 38.1 and 38.2):

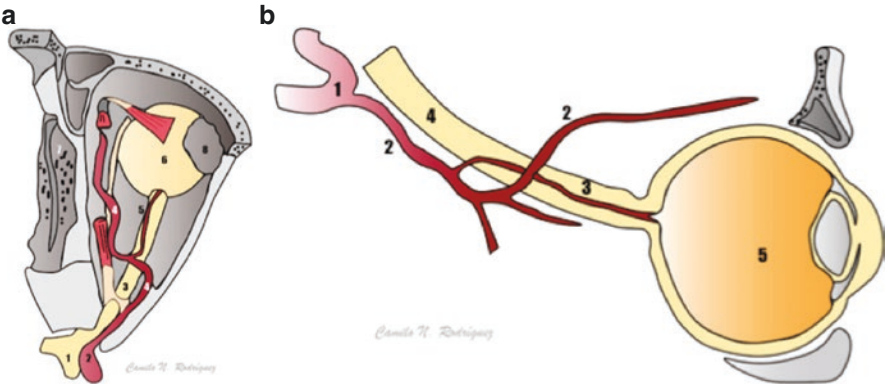

Fig. 38.1 (**a**) Schema: Anatomy of the Intraocular vessels and Optic Nerve, Upper visión of right orbit; (1) Optic Chiasma, (2) Internal Carotid Artery, (3) Optic Nerve, (4) Ophthalmic Artery, (5) Central retinal Artery, (6) Eyeball, (7) Cribiform sheet of etmoid bone and (8) Lacrimal gland. (**b**) Schema: Anatomy of thr Intraocular vessels and Optic Nerve, Lateral vision of right orbit; (1) Internal carotid artery, (2) Ophthalmic artery, (3) Central retinal artery, (4) Optic Nerve, (5) Vitreous body

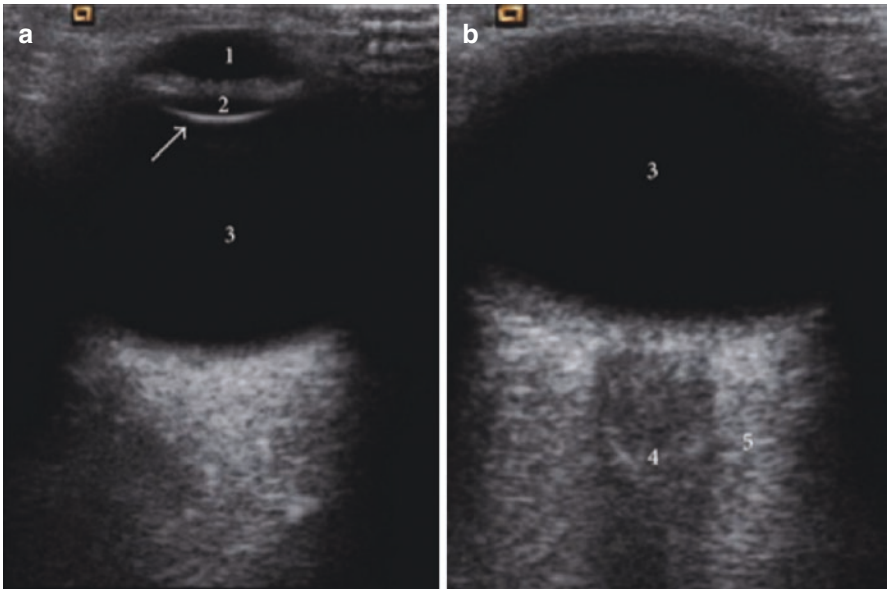

Fig. 38.2 OCCS: Axial (Transverse) B-Mode ultrasound image that shows normal anatomy of ocular structures; (**a**) (1) Anterior chamber, (2) Lens and (3) Vitreous body; (**b**) (3) Vitreous body (bulbus), (4) Optic nerve sheath complex and (5) Retrobulbar fat. (Courtesy: Jiménez Aragón et al. [32])

1. Pupil
2. Eye globe
3. Papilla
4. Optical nerve (ON)
5. Intraorbital vessels (central retinal artery (CRA)/ophthalmic artery (OA)/posterior ciliary artery)

38.2.1 Pupil

Assessment of pupillary shape, size, and pupillary light reflex (PLR) is a standard diagnostic procedure in the intensive care unit (ICU) and emergency room (ER) and is an important part of the basic neurological examinations. Clinical examination of pupillary function typically includes estimation of pupillary diameters and its response to light stimulus [1].

38.2.2 Papilla (Optical Disc)

The papilla (optical disc) is the origin of the ON and has a diameter of around 1.5 mm [2].The central retinal artery and vein run through the papilla. Intracranial hypertension leads to episodes of papillary swelling (papilledema) as an estimation of ICP.

38.2.3 Optic Nerve (ON)

The length of the ON is 4 cm, where the intraorbital portion is 2.5 cm. The ON is sheathed by the optic nerve sheath (conformed by three sheets: dura mater, subarachnoid, and pia mater). The optic nerve sheath communicates with the subarachnoidal space of the brain. The optic nerve sheath diameter is 5–7 mm and could differ between right and left eye [2] (Fig. 38.1).

38.2.4 Intraorbital Vessels

The two most clinically relevant intraorbital vessels are as follows:

1. The ophthalmic artery (OA): First branch of the internal carotid artery (ICA) located within the inferolateral area of the OA
2. The central retinal artery (CRA): First branch of the OA

   Both arteries can be approached with OCCS in the posterior pole of the eyeball (Fig. 38.1).

38.3 OCCS: Ultrasound Protocol

For a pragmatic and complete OCCS study, we suggest the following technique and approach:

38.3.1 General Approach: Steps of the Procedure

38.3.1.1 Probe Selection

Linear array transducer (6–12 MHz)

38.3.1.2 Patient Positioning

Place patient in supine position (head at 30° aligned with the body) with both of their eyelids closed. Apply sufficient gel on the eyelids to examine. We recommend covering the eye with a transparent dressing to avoid corneal irritation [3].

38.3.1.3 Ultrasound Machine Setting: (Safety Procedure)

We strongly recommend using the prespecified orbital setting available in the ultrasound machine to ensure a safe procedure for the patient [4].

- *Mechanical Index (MI):* < 0.23
- *Thermal Index (TI):* < 0.2

38.3.1.4 Operator/Probe Positioning

The operator could be positioned to the right, left, or behind the patient's head with the ultrasound machine in front of the examiner. The probe should be held with one hand placing the heel of the hand on the skull of the patient to avoid applying pressure on the eyeball. Place the probe on the temporal part of the closed upper eyelid in an oropharygeal direction.

38.3.1.5 Examination

Both eyes must be examined. Locate the complete eye globe and the proximal portion of the ON in the center of the screen and freeze the image to make the corresponding measurements [reduce insonation time – as low as reasonably achievable (ALARA) principle] [4, 5].

Freeze the image and elevate the transducer from the eye to reduce insonation time.

Remember that in those patients with the Bell's phenomenon (an upward and outward movement of the eye), the ON might look curved.

38.3.1.6 Documentation Data

Record the data obtained from both eyes in the clinical notes. Analyze the data obtained within the clinical context of the patient. Document measurement trends.

38.4 OCCS: Safety Aspects

The ultrasound settings should be adjusted for orbital sonography, following the as low as reasonably achievable (ALARA) principle. The main biological adverse effects would be cavitation and temperature increase [4–6] (Table 38.1).

Table 38.1 Safe Orbital Color-Coded Sonography (OCCS)

Values to monitor	Suggested value	Biological effects
Mechanical Index value (MI)	0–1.0 (<0.23)	Cavitation (formation/activity of gas filled bubbles)
Thermal Index value (TIS)	0–0.3 (<0.2)	Temperature Rise
ISPTA (Spatial-peak temporal-average intensity)	<17 mW/ cm^3	Power/Intensity (increase with frequency, exposure duration and pulse repetition frequency)
Examination Time: Less than a minute for each aye		

For certain clinical situations, (e.g.,color Doppler) we can increase the power beyond these limits (MI, TIS, ISPTA) for a short time

38.5 OCCS: Optic Nerve Sheath Diameter (ONSD)

Patients with acute neurological injury are expected to show dynamic ICP changes. Prompt recognition and treatment are necessary to prevent long-term neurological deficits, knowing the changes and trends of the ICP in real-time (goal ICP <22 mmHg) [7] in the ICU and emergency department (ED), allowing physicians to make therapeutic decisions to maintain adequate cerebral oxygen delivery and cerebral blood flow (CBF) [8, 9].

Invasive ICP monitors remain the gold standard in ICU patients (intraventricular devices), but may not always be available and/or feasible (e.g., coagulopathy, thrombocytopenia, neurosurgical access limited, etc.).

Measurement of optic nerve sheath diameter (ONSD) is a noninvasive bedside cost-effective alternative tool, which makes it an alternative of great value to estimate and monitor the ICP changes trends.

The utility of transbulbar ultrasound by B-Mode of the optic nerve (as alternative approach) for estimating raised ICP in patients requiring neurocritical care has been demonstrated [8, 10]. Moreover, such technique has been characterized as having a high intra- and interobserver reliability [11–13].

The cut-off values for ONSD correlating to elevated ICP should be established and standardized for diverse subgroups of patients, based on age, gender, and clinical condition. OCCS may not be appropriate in certain clinical situations such as local surgical wounds and anatomical alterations of the orbit due to trauma (e.g., head and facial trauma) [14].

38.5.1 ONSD: Steps of the Procedure

38.5.1.1 Machine Setting: (Safety Procedure)

- *Mechanical Index (MI):* < 0.23
- *Thermal Index (TI):* < 0.2

38.5.1.2 Examination

Both eyes must be examined. Identify the eye globe in full and position of the proximal portion of the ON in the center of the screen (less than 1 minute per eye). Then, proceed to freeze the image for the corresponding measurements (reduce insonation time – ALARA principle) [5].

B-Mode

The ON is detected as a retrobulbar hypoechoic structure surrounded by retrobulbar fat (hyperchoic). Then, the ONSD is measured 3 mm behind the papilla (Fig. 38.3a,b).

Measurements: B-Mode Ultrasound [13]

- *Ultrasound depth*: 4 cm
- *Machine setting*: Freeze and store de image
- *Measured:* Both eyes.
- *Measuring planes:* Sagittal plane (M1) and Axial (Transverse) plane (M2) (Eq. 38.1; Fig. 38.4).

$$\textbf{ONSD} = \left[\left(\mathrm{M1} + \mathrm{M2\,RE}\right) + \left(\mathrm{M1} + \mathrm{M2\,LE}\right)\right] / 4 \tag{38.1}$$

(RE: Right Eye/LE: Left Eye)

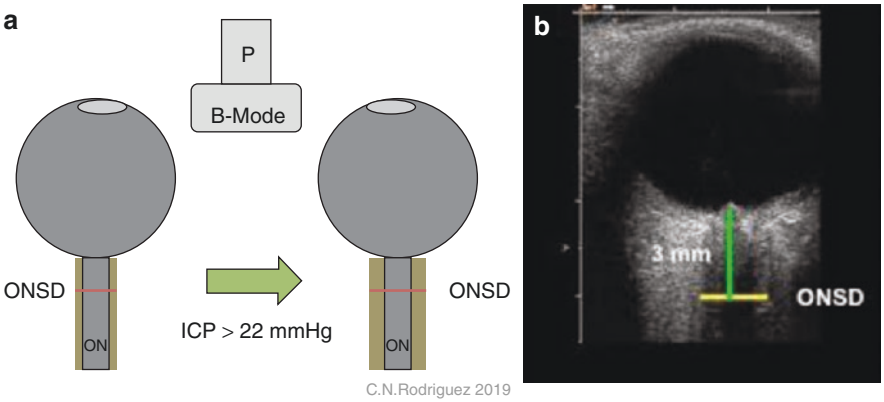

Fig. 38.3 (**a**) Schema: Anatomy of ONSD; (ON) Optic nerve, (ONSD) Optic nerve sheath diameter, (Green arrow) ICP rise; (**b**) Orbital Ultrasound: (Green Line) Distance between papilla and measurement sector of the ONSD, (Yellow line) ONSD measurement

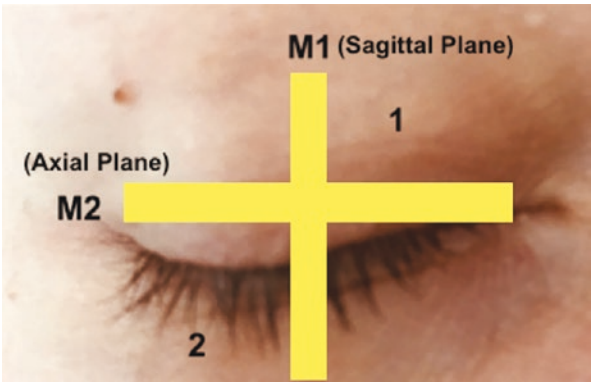

Fig. 38.4 ONSD Approach: Measuring planes; (M1) Sagittal plane, (M2) Axial (Transverse) plane, (1) Upper eyelid and (2) Lower eyelid

38.5.1.3 Documentation

The ONSD should be documented for each eye separately. Remember, you must freeze the screen before taking the measurements.

- *ONSD cut-off value*: <5 mm [15, 16]
- *ONSD right eye*: M1 and M2 planes
- *ONSD left eye*: M1 and M2 planes
- *Mechanical Index*
- *Thermal Index*

38.5.1.4 Interpretation:

Estimate the dynamic changes in ICP (real time). Compare both eyes over time and document the values trends. Consider the clinical context of the critically ill patient [17].

The ONSD is a highly accurate noninvasive technique for the detection of intracranial hypertension (invasive ICP >22 mmHg) [7]. A diameter of 5.7–6.0 mm corresponds well with symptomatically increased ICP (>20 cmH_2O) [23]. This technique can be performed by intensivists at the bedside, using point-of-care ultrasound (POCUS) machines that are already widely available [18].

38.5.2 ONSD: Utility in Other Clinical Contexts

38.5.2.1 Hyponatremia

Hyponatremia (<135 mEq/L) is the most common electrolyte disorder in the neuro-ICU, occurring in 30% of patients with subarachnoid hemorrhage (SAH) and may be associated with cerebral edema.

The patient with symptomatic hyponatremia may suffer changes in the ONSD most commonly than asymptomatic patients. Therefore, variations in the ONSD results (increase) appear to reflect consistent with intracranial pressure (ICP) and serum sodium changes [33].

38.5.2.2 Cerebral Venous Thrombosis

Cerebral venous thrombosis (CVT), difficult to diagnose, is a rare presentation form of stroke carrying high mortality and morbidity. Then, a change in ICP is to be expected (raise). Therefore, the changes in the size of the papilla (papilledema) could be reflect this ICP variations [34].

38.5.2.3 Spontaneous Intracranial Hypotension (SIH)

Spontaneous intracranial hypotension (SIH) is an recognized neurologic syndrome commonly caused by cerebrospinal fluid (CSF) leakage, where the hallmark symptom is orthostatic headache. OCCS is a simple, costeffective, non-invasive, and repeatable diagnostic tool that would aid in diagnosis, follow-up, and understanding of the pathophysiology of SIH would be useful, through optic nerve sheath diameter (ONSD) measurement during changes position of the patient [38].

38.6 OSSC: Examination of the Papilla

Patients with acute neurological injury are expected to show dynamic changes of the ICP (raise). The ultrasound of the papilla (papilledema) may be useful to detect acute increases in ICP.

38.6.1 Papilla: Steps of the Procedure

38.6.1.1 Machine Setting: (Safety Procedure)

- *Mechanical Index (MI):* < 0.23
- *Thermal Index (TI):* < 0.2

38.6.1.2 Examination

Both eyes must be examined. Identify the bulbus (Hypoechoic) in the center of the screen (less than 1 minute per eye). Then, proceed to freeze the image for the corresponding measurements (reduce insonation time – ALARA principle) [5].

B-Mode

The origin of the ON could serve as a landmark. Optimizing the image (zoom), the plane with the maximum papilla elevation is selected and freeze. We recommend marking it with a circle (surrounding the bulbus) which allow definition of papilla position (Fig. 38.5a). This maneuver allows measurement the distance between the circle and papilla prominence.

Measurements: B-Mode Ultrasound

- *Ultrasound depth*: 4 cm
- *Machine setting*: Freeze and store de image

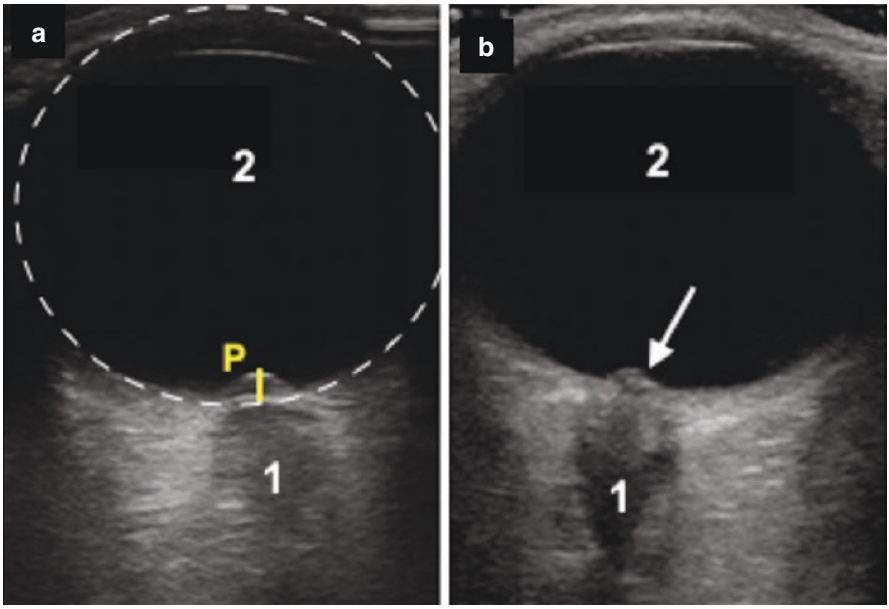

Fig. 38.5 OCCS: B-Mode Ultrasound of the papilla through Axial (transverse) plane: (**a**) (1) Optic nerve, (2) Bulbus (eyeball), (Dotted line) circle to define the papilla, (P) Papilla prominence (papilledema) and (yellow line) Distance between the circle and papilla prominence; (**b**) (1) Optic nerve, (2) Bulbus (eyeball) and (arrow) Papilla prominence (papilledema)

- *Measured:* Optic disc edema in both eyes
- *Measuring planes:* Axial (transverse)

38.6.1.3 Documentation

The papilla should be documented for each eye separately. Remember, you must freeze the screen before taking the measurements. The method is optimal to estimate the ICP and control the therapeutic effects through measurement of the prominence of the papilledema. Measure and document together with the ONSD measurement [35–37].

- *Probe*: Linear probe MHz
- *Papilla prominence cut-off value*: < 0.5 mm
- (disagreement about the optimal cutoff)
- *Papilla prominence right eye*: Axial plane (Transverse) (Fig. 38.5b)
- *Papilla prominence left eye*: Axial plane (Transverse)
- *ONSD right eye*
- *ONSD left eye*
- *Mechanical Index*
- *Thermal Index*

38.6.1.4 Interpretation

- *Papilledema*: Papilledema refers to edema of the retinal disc caused by elevated ICP. Ultrasound can detect papilledema.
  - *Caution*: The changes of the papilla may be slower than ONSD. Papilledema can take some time to develop (once acute ICP has raised acutely) and restore it (once therapy was installed).
- *Pseudopapilledema*: Refers to anything causing optic nerve edema other than ICP elevation.
  - *Inflammation:* This is often unilateral, which may help differentiate it from papilledema (optic neuritis, systemic lupus erythematosus, etc.).
  - *Optic disc drusen:* These are essentially bits of calcium within the optic disc.

Papilledema (there is disagreement about the optimal cutoff for this distance) and optic nerve sheath diameter (ONSD) should be integrated at the time to be interpreted it (Table 38.2).

Table. 38.2 Papilla and ONSD measurements and clinical interpretation

Papilledema	ONSD	Clinical interpretation
Absence	Normal	Normal
Absence	Enlarged	Hyperacute ICP elevation
Presence	Normal	Pseudopapilledema
Presence	Enlarged	ICP elevation

38.7 OCCS: ONSD/ETD Index

The OSND/Eye Globe Transverse Diameter (ETD) Index approach may be a complementary tool to estimate an acute raise of ICP in the critically ill patient [26] (Eq. 38.2).

A large number of studies tested the utility of optic nerve sheath diameter (ONSD) measured by US to predict intracranial hypertension [17, 27]. But the isolated measurement of the ONSD may present some limitations for its correct interpretation as surrogate of an acute raise of the ICP [28].

$$\textbf{ONSD / ETD Index} = \mathrm{ONSD}(\mathrm{mm}) / \mathrm{ETD}(\mathrm{mm}) \tag{38.2}$$

38.7.1 ONSD/ETD Index Approach

38.7.1.1 Machine Setting: (Safety Procedure)

- *Mechanical Index (MI):* < 0.23
- *Thermal Index (TI):* < 0.2

38.7.1.2 Examination

Bilateral examination is recommended. Locate the complete eyeball and the proximal portion of the ON in the center of the screen and freeze the image to make the corresponding measurements (reduce insonation time – ALARA principle) [5, 26].

B-Mode

The eye globe is detected as a hypoechoic-rounded structure in the middle of the screen. The simultaneous appearance of lens and optic nerve meant that the ultrasound probe was on the best plane.

The ONSD (hyperechoic structure) is measured 3 mm behind the papilla.

Measurements

- *Ultrasound depth*: 4 cm
- *Machine setting*: Freeze and store de image
- *Measured:* Both eyes
- *Measuring planes:* Placed horizontally over the upper closed eyelid to insonate through axial plane

38.7.1.3 Documentation

The ONSD/ETD index should be documented for each eye separately. Remember, you must freeze the screen before taking the measurements.

- *Probe:* Type of probe (Linear probe)
- *Insonates eye*: Right and Left
- *ONSD/ETD Index normal values*: 0.18–0.25 [26, 29–31].
- *ONSD/ETD Index abnormal value*: >0.25 [26, 29–31].
- *Mechanical Index*
- *Thermal Index*

38.7.1.4 Interpretation

Clinical relevance: The ONSD/ETD index offers an estimation of dynamic changes in the rise of ICP (real time).

It is a highly accurate noninvasive technique for the detection of intracranial hypertension (invasive ICP > 22 mmHg) [7]. This technique can be performed by intensivists at the bedside, using point-of-care ultrasound (POCUS) machines that are already widely available [18].

In different studies, the ONSD had a strong correlation with ETD, and ONSD/ETD ratio might provide more reliable data than ONSD itself as a marker of ICP [26, 29–31]. Ultrasound-ONSD/ETD may be a reliable indicator for predicting intracranial hypertension in traumatic brain injury (TBI) and non-TBI patients.

However, further studies are required (more variety of population and race) before the ONSD/ETD index can be used to make clinical decisions.

38.8 OCCS: Pupillary Ultrasound

Examining pupillary reactivity through the ipsilateral and consensual pupillary light reflex (PLR) is a fundamental part of the neurological examination in the neurocritical care patient [1, 19]. Pupillary evaluation is often performed in a subjective manner, with a penlight testing reactivity to light stimuli. Common ambiguous

terminologies are used to describe the pupillary light reflex (PLR) and pupil size bedside: nonreactive, dilated, brisk, sluggish, and nonreactive (these terms may have a different interpretation among clinicians).

The B-mode ultrasound is an objective tool for the quantitative approach of pupillary function. Measurements of pupil size and reactivity are considered to be of prognostic importance for patients with critical conditions.

It is useful in a variety of settings where eyelid retraction is impeded (eyelid edema or hematoma) or when pupillometry is unavailable [20, 21] (Fig. 38.6b).

38.8.1 Pupillary Ultrasound: Steps of the Procedure

38.8.1.1 Machine Setting: (Safety Procedure)

- *Mechanical Index (MI):* < 0.23
- *Thermal Index (TI):* < 0.2

38.8.1.2 Examination Technique

Both eyes must be examined. Operator should spend at least 5–10 minutes in the room before testing to adapt to the light level of the room (reduce insonation time – ALARA principle) [5].

Approach: B-Mode/M-Mode

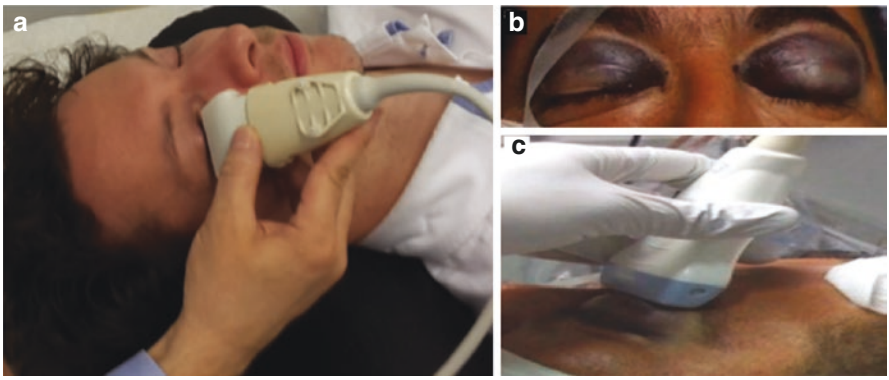

Fig. 38.6 (**a**) Acoustic window ultrasound: Lower eyelid approach. (Modified from Schmidt et al. [20]); (**b**) Skull base fracture ("Raccoon Eyes"): where eyelid retraction is impeded or when pupillometry is unavailable; (**c**) Acoustic window ultrasound: Upper eyelid approach. (Courtesy: Sangsyan et al. [22])

B-Mode

The pupil is detected in the proximal pole of the globe.

Each pupil was visualized with the probe positioned flatly on the lower closed eyelid or upper closed eyelid (Fig. 38.6a,c).

Activate penlight in front of each closed eyelid during a few seconds to measure the pupillary light reflex (PLR) [22] (Fig. 38.7).

M-Mode

Each pupil is visualized with the probe positioned flatly on the lower closed eyelid or upper closed eyelid.

Activate penlight in front of each closed eye during some seconds for the measurement of PLR. Use simultaneously B-mode and M-mode. Capability to plot the pupillary diameter versus time. (M-mode) [22] (Fig. 38.8).

38.8.1.3 Documentation

The PLR and pupillary constriction time (PCT) should be documented for each eye separately and in conjunction. Remember, you must freeze the screen before taking the measurements (Fig. 38.7).

- *Probe*: Type of probe (Linear probe)
- *Insonated eye*: Right and left
- *PLR* (mm): Rest and after light stimulus
- *PCT*(ms): After light stimulus
- *Mechanical index*
- *Thermal index*

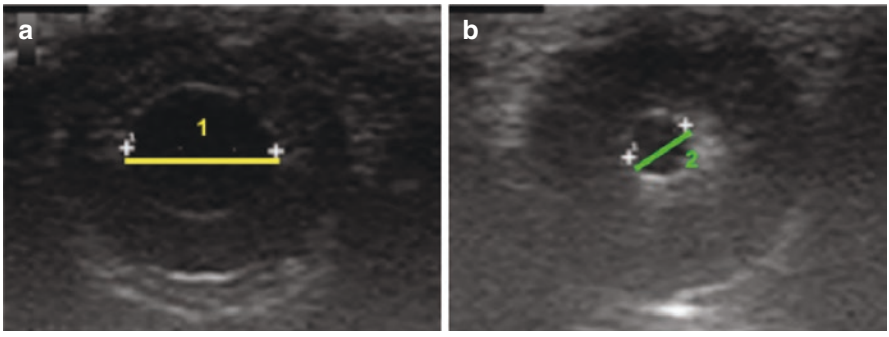

Fig. 38.7 Pupillary B-mode Ultrasound: Pupillary light reflex (PLR); (**a**) Standard dimmed light conditions and (Yellow line) (1) Measure of pupillary diameter (mm); (**b**) Ipsilateral Ligth stimulus, (Green line) (2) Measure of pupillary diameter after light stimulus. (Courtesy: Schmidt et al. [20])

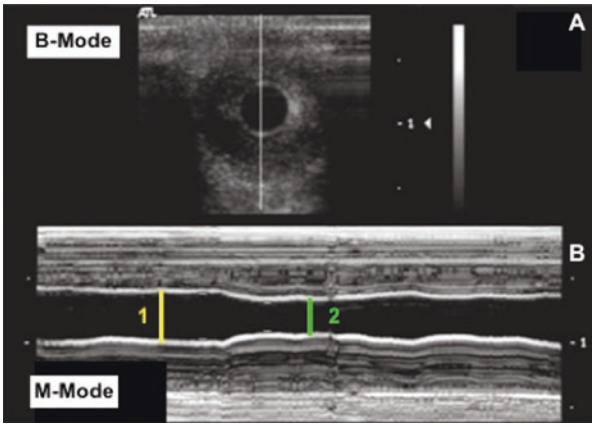

Fig. 38.8 (**a**) B-Mode Ultrasound: Measure of pupillary diameter; (**b**) M-Mode: (Yellow) Measure of pupillary diameter before light stimulus (mm) and (Green) Measure of pupillary diameter after light stimulus (mm). (Courtesy: Sangsyan et al. [22])

Table 38.3 Normal Mean values of Pupillary diameters (PD) and Pupillary constriction time (PCT). European population [20]

		PLR			
Pupillary function	Rest (mm)	I_{LS} (mm)	C_{LS} (mm)	PCT_i (ms)	PCT_c (ms)
Right Eye	4.5 ± 0.8	2.7 ± 0.6	2.6 ± 0.5	967 ± 220	963 ± 189
Left Eye	4.7 ± 0.8	2.8 ± 0.6	2.7 ± 0.6	970 ± 271	993 ± 192

I_{LS} Ipsilateral Light stimulus, C_{LS} Contralateral Light Reflex, PCT_i Ipsilateral Pupillary constriction time, PCT_c Contralateral Pupillary constriction time

38.8.1.4 Interpretation

Estimation of dynamic changes in ICP (real time). Compare both eyes over time and document the values trends. Consider the clinical context of the critically ill patient.

The cut-off values for pupillary diameters (before and after light stimulus) and the pupillary constriction time (PCT) (Table 38.3), both associated with elevated ICP or worsening neurological condition, should be established and standardized for diverse subgroups of patients, based on age, gender, and condition. In (Table 38.4), show some pupillary ultrasound values to have as reference [20].

Rather than taking into account the measured absolute values, it is very important to consider the trends (real-time changes of mm and/or ms and compare its over time) of the values obtained when analyzing the clinical context of the patient.

Table 38.4 Pupillary Light Reflex (PLR): pupillary measurement variables

Pupillary Light Reflex (PLR)	Eye	Ultrasound
Left Pupillary diameter (mm)	Ipsilateral	B-mode
Right Pupillary diameter (mm)	Ipsilateral	B-mode
Left Pupillary diameter (mm)	Contralateral (Consensual reflex)	B-mode
Right Pupillary diameter (mm)	Contralateral (Consensual reflex)	B-mode
Right & Left Pupillary diameter (mm)	Ipsilateral / Contralateral	M- mode
Pupillary constriction Time (ms)	Bilateral	B-mode
ALARA (As Low As Reasonable Achievable)		

mm milimeters, *ms* miliseconds

38.9 OCCS: Orbital Vessels Ultrasound (OVU)

38.9.1 OVU: Steps of the Procedure

38.9.1.1 Machine Setting: (Safety Procedure)

- *Mechanical Index (MI):* < 0.23
- *Thermal Index (TI):* < 0.2

38.9.1.2 Examination

Both eyes must be examined.

Locate the complete eye globe and the proximal portion of the ON in the center of the screen and freeze the image to make the corresponding measurements (reduce insonation time – ALARA principle) [5].

38.9.1.3 Color Doppler [23]

Vessels to Insonate:

- *Central Retinal Artery* (CRA) (Fig. 38.9).
- Distal branch of the OA. Enters to the Optic nerve 1–1.5 cm distal from the posterior pole of the eyeball coming from dorsolateral direction.
- *Ophthalmic Artery* (OA) (Fig. 38.10).
- *Posterior Ciliary Artery* (PCA) (Fig. 38.11).

PW Doppler

- *Central Retinal Artery (CRA)*
- Spectral Doppler waveform
- *Ophthalmic Artery (OA)*
- Spectral Doppler waveform

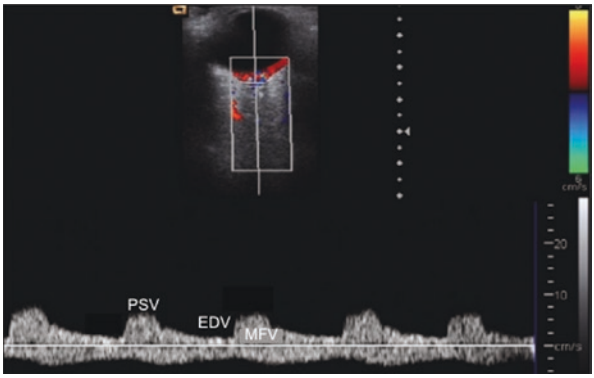

Fig. 38.9 OCCS: Typical waveform of CRA obtained by PW Doppler that shows a curve above the zero axis with rounded peak systolic and continuous flow during diastole, (PSV)Peak systolic velocity, (MFV) Mean flow velocity and (EDV) Diastolic flow velocity. (Courtesy: Jiménez Aragón et al. [32])

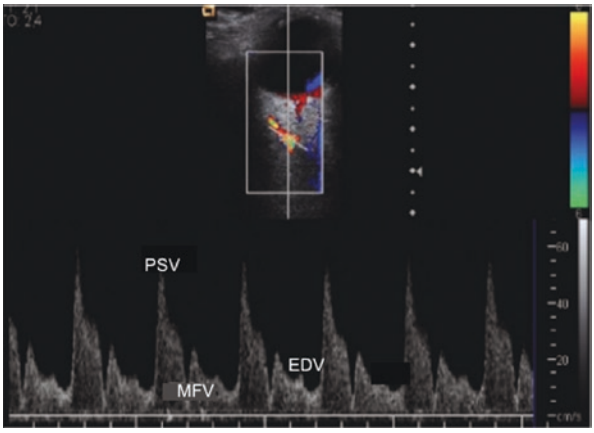

Fig. 38.10 OCCS: Ophthalmic Artery insonation and spectral doppler wave; Typical OA waveform obtained by PW Doppler that shows a Sharp peak systolic, a dicrotic notch, ans a relatively Little flow in diástole. [Alaising effect], (MFV) Mean flow veocity, (PSV) Peak systolic flow velocity and (EDV) diastolic flow velocity. (Courtesy: Jiménez Aragón et al. [32])

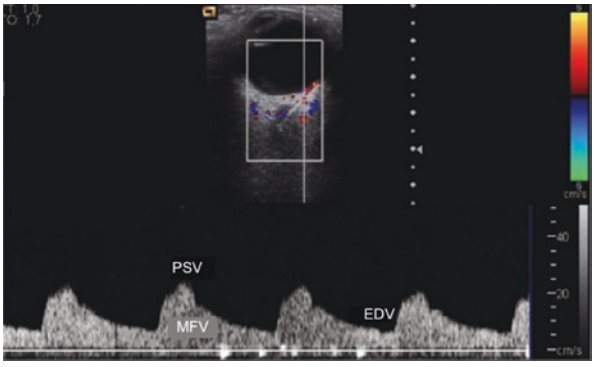

Fig. 38.11 OCCS: PCA in the retrobulbar fat; Typical PCA waveform obtained by PW Doppler shows a blunted peak systolic and low to moderate flow velocity during diástole; (PSV)Peak systolic velocity, (MFV) Mean flow velocity and (EDV) Distolic flow velocity. (Courtesy: Jiménez Aragón et al. [32])

- *Posterior Ciliary Artery (PCA)*
- Spectral Doppler waveform

38.9.1.4 Documentation

The OA, CRA, and PCA blood flow velocities should be documented for each eye separately. Remember, you must freeze the screen before analyze and document of the spectral Doppler waveform.

- *Probe*: Type of probe (Linear probe)
- *Insonated eye*: Right and Left
- *Velocities*: PSV, EDV, and MFV (Table 38.5).
- *Mechanical Index*
- *Thermal Index*

38.9.1.5 Interpretation

Estimation of dynamic changes in ICP (real time) and the hemodynamic changes in the internal carotid artery (ICA). Compare both eyes over time and document the values trends. Consider the clinical context of the critically ill patient.

- *Spectral Doppler Waveform Analysis* [24] (Figs. 38.9, 38.10, and 38.11):

  Occlusion?/stenosis?/hemodynamic changes in the ICA? [25]
  Analyze the spectral waveform trends in the clinical context of the patients

38.10 Conclusion

The orbit color-coded sonography (OCCS) is a very practical tool in the bedside evaluation in the ICU or ED, and is a noninvasive ultrasound procedure which permits simultaneous gray scale imaging of structure and color-coded imaging of blood vessels and their hemodynamics in real time. In a difficult clinical situations where invasive ICP monitoring is not possible (contraindications of the patient and/or

Table 38.5 Orbital Vessels: normal blood velocity values [23]

Orbital vessel	PSV (cm/s)	MFV (cm/s)
Ophthalmic Artery (OA)	40–41	30–31
Central Retinal Artery (CRA)	11–12	10–11
Posterior Ciliary Artery (PCA)	15–17	11–13

PSV Peak systolic velocity blood flow, *MFV* Mean velocity blood flow

non-accessibility to invasive monitoring), the OCCS becomes a useful alternative tool to take therapeutic decisions in real time.

Algorithm

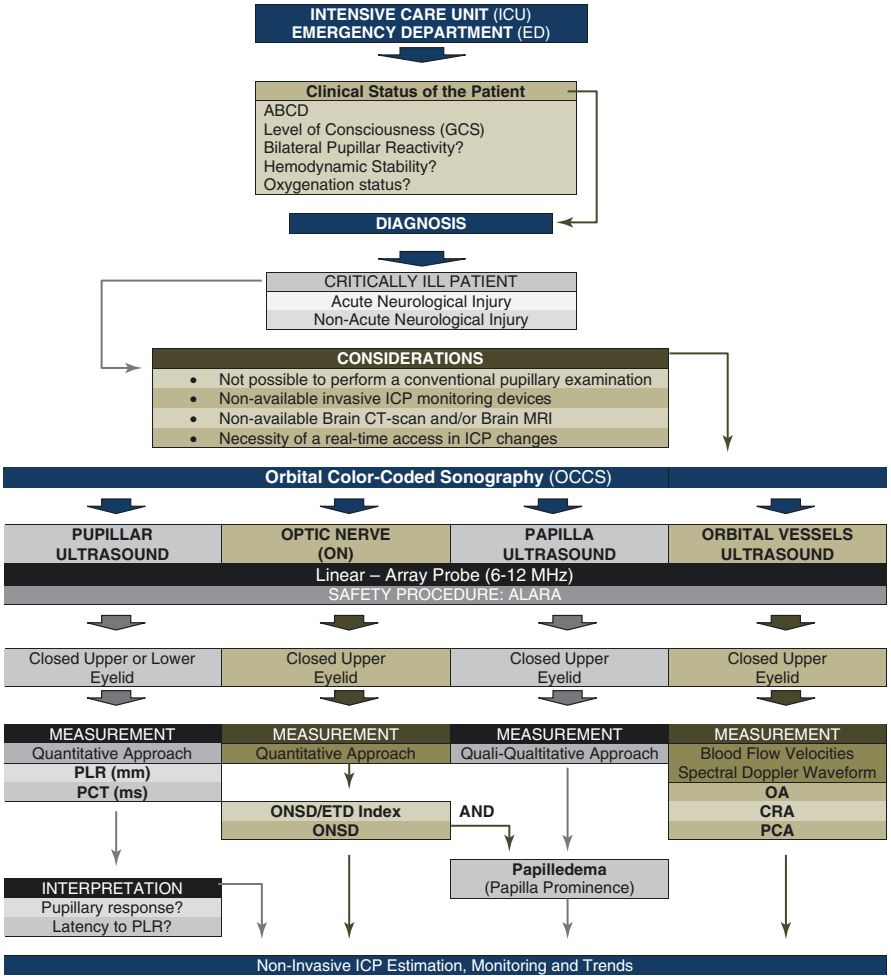

ABCD airway-breathing-circulation-disability, *GCS* Glasgow coma scale, *ICP* Intracranial Pressure, *CT* Computed Tomography, *MRI* Magnetic Resonance Imaging, *ALARA* As Low As Reasonable Achievable, *ETD* Eyeball Transverse Diameter, *ONSD* optic nerve sheath diameter, *PLR* pupillary light réflex, *PCT* Pupillary constriction time, *OA* ophthalmic artery, *CRA* central retinal artery, *PCA* posteiror ciliary artery

References

1. Wilhelm H. Neuro-ophthalmology of pupillary function- practical guidelines. J Neurol. 1998;245(9):573–83.
2. Gray's Anatomy, Williams & Warwick; 36th edition, volumen II. Salvat Publisher.
3. Hylkema C. Optic nerve sheath diameter ultrasound and the diagnosis of increased intracranial pressure. Crit Care Nurs Clin N Am. 2016;28:95–9.
4. Food and Drug Administration. Information for manufacturers seeking clearance of diagnostic ultrasound system and transducers; 2008.
5. The British Medical Ultrasound Society (BMUS). Guidelines for the safe use of diagnostic ultrasound equipment; 2009.
6. European Federation of Societies for Ultrasound in Medicine and Biology (EFSUMB). Newsletter, 2003.
7. Guidelines for the Management of Severe Traumatic Brain Injury 4th Edition. 2016.
8. Bäuerle J, Nedelmann M. B-mode sonography of the optic nerve in neurological disorders with altered intracranial pressure. Pers Med. 2012;1:404–7.
9. Darsie ME, Moheet AM. The pocket guide to neurocritical care. NCS; 2017.
10. Moretti R, Pizzi B. Ultrasonography of the optic nerve in neurocritically ill patients. Acta Anaesthesiol Scand. 2011;55:644–52.
11. Ballantyne SA, O'Neill G, Hamilton R, Hollman AS. Observer variation in the sonographic measurement of optic nerve sheath diameter in normal adults. Eur J Ultrasound. 2002;15(3):145–9.
12. Bäuerle J, Lochner P, Kaps M, Nedelmann M. Intra- and inter- observer reliability of sonographic assessment of the optic nerve sheath diameter in healthy adults. J Neuroimaging. 2012;22(1):42–5.
13. Soldatos T, et al. Optic nerve sonography in the diagnostic evaluation of adult brain injury. Crit Care. 2008;12:R67.
14. Hassen GW, et al. Accuracy of optic nerve sheath diameter measurement by emergency physicians using bedside ultrasound. J Emerg Med. 2015;48:450–7.
15. Blaivas M, et al. Elevated intracranial pressure detected by bedside emergency ultrasonography of the optic nerve sheath. Acad Emerg Med. 2003;
16. Zeiler FA, et al. A unique model for ONSD part II: inter/intra-operator variability. Can J Neurol Sci. 2014;41(4):430–5.
17. Robba C, et al. Ultrasound non-invasive measurement of intracranial pressure in neurointensive care: a prospective observational study. PLoS Med. 2017;14(7)
18. Rajajee V, Vanaman M, Fletcher JJ, Jacobs TL. Optic nerve ultrasound for the detection of raised intracranial pressure. Neurocrit Care. 2011;15:506–15.
19. Chestnut RM, Ghajar J, Maas AI, Marion DW, Servadei F, Teasdale GM. Part 2: early indicators of prognosis in severe traumatic brain injury. J Neurotrauma. 2000;17:557–627.
20. Schmidt FA, et al. B-mode ultrasound assessment of pupillary function: feasibility, reliability and normal values. PLoS One. 2017;12(12):e0189016.
21. Harris A, et al. Ultasound assessment of extraocular movements and pupillary light réflex in ocular trauma. Am J Emerg Med. 2010;28:956–9.
22. Sangsyan AE, et al. Ultrasonic evaluation of pupillary light réflex. Crit Ultrasound J. 2009;1:53–7.
23. Ertl M, et al. Ocular color-coded sonography-a promising tool for neurologists and intensive cara physicians. Ultraschall Med. 2014;35:422–31.
24. Tranquart FO, et al. Color doppler imaging of orbital vessels: personal experience and literature review. J Clin Ultrasound. 2003;31:258–73.
25. Hong SP, et al. Usefulness of the Doppler flow of the ophthalmic artery in the evaluation of carotid and coronary atherosclerosis. Korean Circ J. 2014;44(6):406–14.

26. Jie D, et al. Ratio of optic nerve sheath diameter to eyeball transverse diameter by ultrasound can predict intracranial hypertension in traumatic brain injury patients: a prospective study. Neurocrit Care. 2019.
27. Toscano M, et al. Optic nerve sheath diameter ultrasound evaluation in intensive care unit: possible role and clinical aspects in neurological critical patients' daily monitoring. Biomed Res Int. 2017;2017:1621428.
28. Rajajee V, Williamson CA, Fontana RJ, et al. Noninvasive intracranial pressure assessment in acute liver failure. Neurocrit Care. 2018;29:280–90.
29. Bekerman I, Sigal T, Kimiagar I, Vaiman M. Initial evaluation of the intracranial pressure in cases of traumatic brain injury without hemorrhage. J Neurol Sci. 2016;368:285–9.
30. Vaiman M, Sigal T, Kimiagar I, Bekerman I. Noninvasive assessment of the intracranial pressure in non-traumatic intracranial hemorrhage. J Clin Neurosci. 2016;34:177–81.
31. Kim DH, et al. Ultrasonographic measurement of the optic nerve sheath diameter and its association with eyeball transverse diameter in 585 healthy volunteers; 2017.
32. Jimenez-Aragón F, et al. Role of color Doppler imaging in early diagnosis and prediction of progression in glaucoma. BioMed Research International; 2013.
33. Demir TA, Yılmaz F, Sönmez BM, Karadaş MA, Okudan RN, Keskin O. Association of optic nerve sheath diameter measurement with hyponatremia in emergency department. Am J Emerg Med. 2019;37(10):1876–9.
34. Arthur J, Duran-Gehring P, Kumetz C, Chadwick S, McIntosh M. Cerebral venous thrombosis: an uncommon cause of papilledema on bedside ocular ultrasound. J Emerg Med. 2019;56(3):288–93.
35. Lochner P, et al. Feasibility and usefulness of ultrasonography in idiopathic intracranial hypertension or secondary intracranial hypertension. BMC Neurol. 2016;16:85.
36. Bäuerle J, Nedelmann M. Sonographic assessment of the optic nerve sheath in idiopathic intracranial hypertension. J Neurol. 2011;258(11):2014–9.
37. Geeraerts T, Merceron S, Benhamou D, Vigue B, Duranteau J. Non-invasive assessment of intracranial pressure using ocular sonography in neurocritical care patients. Intensive Care Med. 2008;34:2062–7.
38. Fichtner J, Ulrich CT, Fung C, et al. Management of spontaneous intracranial hypotension - Transorbital ultrasound as discriminator. J Neurol Neurosurg Psychiatry. 2016;87(6):650–5.

Chapter 39
Death by Neurological Criteria (DNC) in ICU: Usefulness of Transcranial Doppler (TCD)

José María Domínguez Roldán, Claudio García Alfaro, and Rosa Elena de la Torre Gómez

Key Points

1. To determine brain death, a patient has to have suffered a medically and surgically irreversible structural brain injury.
2. Transcranial Doppler is very useful to support the diagnosis of cerebral circulatory arrest that accompanies the determination of Death by Neurological Criteria (DNC).
3. In order to establish the diagnosis of cerebral circulatory arrest by means of TCD/TCCS, we must contemplate the study of the anterior and posterior cerebral circulation.
4. There are three sonographic patterns compatible with the diagnosis of cerebral circulatory arrest: a) diastole-systole separation pattern, b) reverberant blood flow velocity pattern, and c) isolated systolic spike pattern. The absence of insonation in patients who had previously been insonated is considered by some to be compatible with the diagnosis of cerebral circulatory arrest.
5. Transcranial Doppler (TCD), like other auxiliary studies that estimate cerebral blood flow through blood flow velocities, has its main limitation in patients in whom there is no cranial hermetism (craniectomy, external ventricular drain, etc.).
6. Ancillary tests for the DNC (including Transcranial Doppler) have their main indication when the concept of global brain death is being used or it is not possible to complete the neurological examination and/or apnea test.

J. M. Domínguez Roldán (✉)
Intensive Care Department, Hospital Universitario Virgen del Rocío, Seville, Spain
e-mail: jmdominguez@telefonica.net

C. G. Alfaro
University Hospital of Virgen del Rocío, Seville, Spain

R. E. de la Torre Gómez
National Medical Center of Western IMSS, Guadalajara, Mexico

C. N. Rodríguez et al. (eds.), *Neurosonology in Critical Care*,
https://doi.org/10.1007/978-3-030-81419-9_39

39.1 Introduction

Defining and determining death as the loss of circulatory-respiratory or cardiopulmonary function enjoys near-universal acceptance, across cultures and religious traditions. A more recent way of defining and determining death (brain death or Death by Neurological Criteria) has a fairly broad international acceptance as a medically valid and legal way to determine and define death, but there is a lack of international consensus about what diagnostic criteria are appropriate.

In 1968, from the Ad Hoc Committee of the Harvard Medical School, the concept of "brain death" was born [1], although this term probably tries to define "the death of the person based on neurological criteria." In 2010, the American Academy of Neurology (AAN) updated a practice guideline to outline the necessary examination to evaluate a patient for brain death.

The diagnosis of brain death is one of the most important and relevant tasks to intensive care unit (ICU) physicians following severe brain injury. In order to determine Death by Neurological Criteria (DCN), a patient has to have suffered a medically and surgically irreversible structural brain injury.

39.2 Concepts of Death by Neurological Criteria (DNC)

There are currently three main concepts of death based on neurological criteria. This translates into three different concepts of brain death: a) global brain death, b) brainstem death, and c) neocortical death.

39.2.1 Whole Brain Death

Whole brain death (WBD) is the standard for determining death used in the United States and most European countries. WBD is defined as the irreversible cessation of all functions of the entire brain, including the brain stem, except the spinal cord. In order to establish this diagnosis, a clinical examination must be carried out to demonstrate the absence of brainstem activity, as well as an instrumental test that demonstrates the existence of some of the brain phenomena associated with brain death (cessation of brain bioelectrical activity, cerebral circulatory arrest). Global encephalic death occurs either in supratentorial processes in which a face-flow deterioration is produced or in posterior fossa processes that initially produce a deterioration in the activity of the brain stem that follows a complete and irreversible cessation of brain activity.

39.2.2 Brainstem Death

Brainstem death is the standard for neurological death used in Canada, India, and the United Kingdom. Brainstem death is the irreversible loss of the capacity for consciousness combined with the irreversible loss of the capacity to breathe. It is based on proving the irreversible absence of the brainstem function. The diagnosis of brainstem death is based on the clinical examination [2]. In order to establish this diagnosis, it is not necessary to prove the absence of brain functions, so it is not necessary to perform instrumental tests. Brainstem death may occur as a consequence of the facial-caudal deterioration due to supratentorial lesions, although it may also occur as a consequence of primary lesions of the cerebellum and brain stem culminating in a complete cessation of the brain activity, without requiring rostral-caudal deterioration with involvement of the supratentorial structures.

39.2.3 Neocortical Death

It is based on the fact that the content of consciousness is the key defining element of human life [3]. Therefore, in those circumstances in which there is a complete and irreversible absence of the content of the consciousness, the diagnosis of death could be established based on neurological criteria. A clinical state equivalent to neocortical death would be the situation of a permanent vegetative state with apathetic syndrome.

Of the three concepts mentioned, the most developed at present are: the concept of global encephalic death and the concept of brainstem death.

39.3 Determination of Death by Neurological Criteria (DNC)

When the concept of whole brain death is used, the diagnosis of brain death is based on the demonstration of the irreversible absence of neurological activity of the central nervous system, except for the spinal cord, as well as the demonstration of some of the intracranial phenomena closely associated with brain death, such as the cessation of brain bioelectrical activity or cerebral circulatory arrest.

To establish the irreversible absence of central nervous system functions, a complete clinical examination of the neurological functions with an anatomical substrate in the brain stem is essential.

These criteria apply to adults only in the context of the primary principles:

1. Determination of structural and irreversible cause of brain injury.
2. Determination of the medical and surgical futility.

3. Exclude confounders.
4. Determination of the brainstem reflexes.
5. Test of apnea.

Prior to the complete diagnosis of brain death, it is necessary to rule out the presence of factors that could confuse the diagnosis and thus fulfill certain prerequisites, among which are arterial hypotension, severely induced hypothermia, the effects of muscle relaxant drugs or central nervous system depressant drugs, and electrolyte disorders. All these factors must be corrected before beginning the clinical and/or auxiliary diagnosis.

In order to establish the diagnosis of brain death, the complete and irreversible absence of brainstem activity must be confirmed. This requires a complete clinical examination of the brain stem, which should include the presence or absence of the following brainstem reflexes:

All components of the examination must be tested after all confounders have been excluded.

1. Photomotor reflex (absence of pupillary response in both eyes).
2. Corneal reflex.
3. Occulocephalic reflex.
4. Occulovestibular reflex.
5. Absence of facial muscle movements to a noxious stimulus.
6. Absence of pharyngeal and tracheal reflex:
    1. Absence of the gag reflex.
    2. Absence of cough response.

It is also necessary to demonstrate the absence of ventilatory activity by means of the apnea test. Stimulation of the respiratory center should be performed by increasing carbon dioxide (CO2) levels to more than 20 mmHg (arterial blood) above the patient's baseline values [4–6].

When the concept of death is used by Neurological Criteria based on the irreversible absence of brainstem activity (brainstem death), it is only necessary to confirm the absence of clinical activity by means of a complete clinical examination of the brain stem, and it is not necessary to prove the existence of other intracranial phenomena associated with brainstem death, since these refer fundamentally to supratentorial phenomena, which are essentially brain based.

When, on the contrary, we are using the concept of global encephalic death, it is necessary not only to carry out a complete clinical examination that demonstrates the absence of activity of the encephalic trunk, but it is also necessary to confirm the absence of brain activity. At this point, since the brain stem has no activity, it is not possible by clinical methods to access knowledge of brain function, so it is essential to use auxiliary methods that explore the phenomena associated with brain death.

39.4 Intracranial Phenomena and Death by Neurological Criteria

The mechanism most frequently involved in the development of brain death (although not the only one) is intracranial hypertension, which causes the cessation of intracranial circulation. As a consequence of this, a global encephalic ischemia is produced, with underlying metabolic disorders that compromise neurotransmission (more edema and more intracranial hypertension), to later produce an irreversible global brain damage. That is why as phenomena intimately associated with encephalic death (especially when the concept of global encephalic death is used), there is the cessation of intracranial circulation as the main actor, the cessation of brain bioelectrical activity, and the development of profound metabolic disorders due to the resulting ischemic-anoxic process.

Cerebral circulatory arrest, one of the phenomena most frequently associated with brain death, is sometimes the mechanism generating brain death, while on other occasions it is a consequence of it. Thus, in primary vascular processes, such as occlusion of the large arteries at the base of the skull, brain death occurs as a consequence of global brain ischemia. In other cases, the existence of large space-occupying lesions or a large cerebral edema is responsible for the cessation of intracranial circulation. In these patients, the increase in intracranial pressure, equal to the average blood pressure, makes the cerebral perfusion insufficient to meet the encephalic metabolic needs, and consequently triggers, irreversibly, the cessation of all central nervous system functions.

Cerebral circulatory arrest is a progressive phenomenon, not an instantaneous one. It is also often asymmetrical when the phenomenon is compared in the two cerebral hemispheres. Depending on the mechanism of cessation of circulation, an asymmetry of circulatory arrest can also be observed in the period before brain death is established when supratentorial regions are compared with infratentorial regions.

Therefore, it is important to remember that TCD (in the dynamic evaluation of cerebral hemodynamics) is based on the phenomenon of recording systolic patterns in intracranial arteries (circle of Willis) without evidence of diastolic flow to determine a pattern of cessation in cerebral circulation.

39.5 Transcranial Doppler (TCD): Utility and Prerequisites

Before using the TCD as an ancillary test for DNC diagnosis, the following prerequisites must be present:

1. Coma with a known cause that is irreversible.
2. Imaging that explains the comatose state.
3. Absence of spontaneous respirations.

4. Exclusion: Hypothermia, major correctable metabolic or endocrine disturbance, toxics, sedative medications, neuromuscular blocking agents.
5. Achievement of normal systolic blood pressure.

39.5.1 Preliminary Clinical Examination

Given that a complete clinical examination of the brain stem is essential for the diagnosis of brain death, evidencing the absence of brain activity, it is recommended that a clinical examination be performed prior to the use of Doppler. The use of Doppler would not make sense if clinical data of brainstem activity still persist, since in no case could the diagnosis of death be made.

The diagnostic accuracy of transcranial Doppler for brain death has not been confirmed in all settings [7].

39.5.2 Intracranial Pressure Stability

The stability of the intracranial pressure is also an essential element for the diagnosis, since it is possible to observe, in a transitory way, phenomena of cerebral circulatory arrest coinciding with intracranial hypertension waves which give way when these hypertension waves are controlled. It is true that on many occasions, stable and maintained intracranial hypertension accompanies brain death, and on many instances, this is the main physiopathological mechanism that generates it [8].

39.6 TCD as Ancillary Test: Determination of Cerebral Circulatory Arrest in DNC

If a clinical examination with apnea test is consistent with brain death, an ancillary test is not required. The insonation of the blood flow velocities in cerebral basal arteries (circle of Willis) for determination of brain death does not differ initially from the TCD insonation techniques described for other pathologies:

1. Probe:
   Low-frequency probe (2 MHz).
2. Initial acoustic window:
   Transtemporal window (bilateral)
3. Insonation depth:
   Middle cerebral artery (MCA) is between 45–65 mm and 70–100 mm for the basilar artery (BA). The depth will be shallower (30–50 mm) when performing

sounding [9, 10] in children. It is important to take into consideration the depth at which the scan is performed, the direction and sense of the signal detected, and also the response of the sounded artery to the compression maneuvers of the carotid arteries at neck level.

However, for the diagnosis of cerebral circulatory arrest in order to establish the diagnosis of DNC, it is essential to take into consideration a series of prerequisites that will avoid the misinterpretation of the results (blood flow velocities and spectral Doppler waveform) from the TCD. It is also necessary to take into account some specific technical strategies in the case of cerebral circulatory arrest, since in certain circumstances the insonation of intracranial arteries in patients where intracerebral flow has ceased requires alternatives to standard insonation techniques [11].

When ancillary test is utilized, only one test is required for the determination of DNC.

39.7 TCD: Sonography Patterns of Cerebral Circulatory Arrest and DNC

The diagnosis of cerebral circulatory arrest through TCD is supported by the appearance of at least one blood flow velocity pattern characteristic of cerebral circulatory arrest in all insonated intracranial vessels [12, 13]. It is important to note that although these patterns are usually associated with increased pulsatility index, and increased resistance index, these values are not really relevant for diagnosis. It is important to consider the trends in the flow patterns of the circle of Willis. The most important aspect for the diagnosis of cerebral circulatory arrest is the existence of *zero blood flow* velocity at the end of the diastole (absence of flow at the end of the diastole in spectral Doppler wave). In the telediastolic period, in a situation of circulatory arrest, no blood enters into the brain, so the cerebral perfusion pressure (CPP) is abolished.

39.7.1 Description of the Sonographic Patterns

The use of the TCD has allowed us to verify how the cessation of cerebral circulation until brain death is a process that begins (especially in supratentorial pathology that occurs with endocranial hypertension) with a progressive decrease in the diastolic blood flow velocity. This is followed by a separation of the diastolic wave (at the end of the diastole) and the systolic wave, an inversion of the diastolic blood flow velocity wave (reverberant flow), and a disappearance of the diastolic velocity wave with persistence only of the systolic spike (CPP $\approx$ zero) [14].

39.7.1.1 The Diastole-Systole Separation Blood Flow Pattern (Fig.39.1)

It is characterized by the absence of positive blood flow velocity (flow to the probe) at the end of the diastole. This pattern is the least frequent of the three patterns compatible with circulatory arrest, is usually of short duration, and represents the beginning of the cessation of arterial circulation in the vessel examined.

39.7.1.2 The Reverberant Blood Flow Pattern (Figs. 39.2, 39.3, and 39.4)

It is characterized by the presence of a retrograde blood flow velocity (moving away from the tube) in the diastolic period. It represents retrograde blood flow with no effective diastole (increased brain impedance) preventing adequate CPP. It is usually a pattern that precedes the isolated systolic spike pattern.

39.7.1.3 The Systolic Spike Blood Flow Pattern (Fig. 39.5)

It is characterized by the existence of antegrade cerebral blood flow velocity (CBFV) (which is directed toward the probe) during the systolic phase, with the absence of diastolic blood flow velocity (end-diastolic volume (EDV)). (CPP ≈ zero). This pattern represents the final hemodynamic stage of cerebral circulatory arrest.

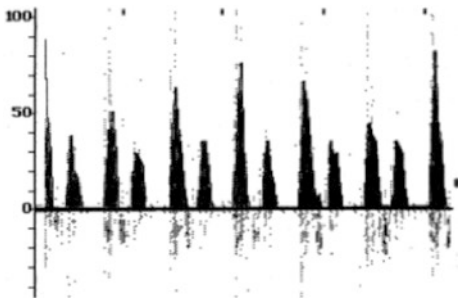

Fig. 39.1 TCD of Middle cerebral artery (MCA): Diastole-systole blood flow velocity separation pattern

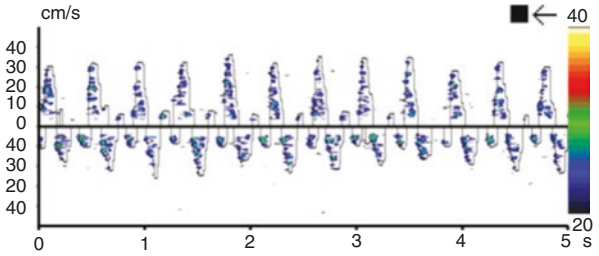

Fig. 39.2 TCD of MCA: Transition between the diastole-systole separation and reverberant blood flow velocities patterns

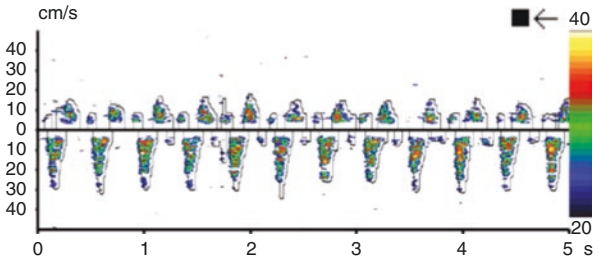

Fig. 39.3 TCD of the basilar artery (BA): Transition between the diastole-systole separation pattern and the reverberant blood flow velocity patterns

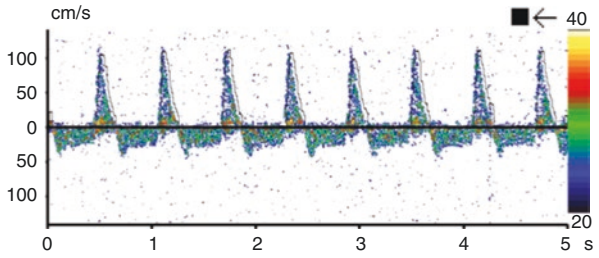

Fig. 39.4 TCD of MCA: Reverberant blood flow velocity pattern

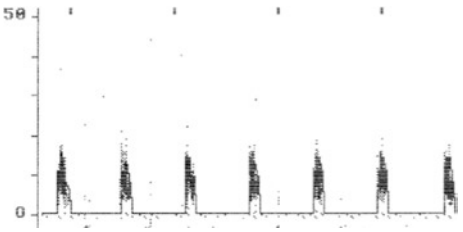

Fig. 39.5 TCD of MCA: Systolic spikes blood flow velocity pattern

Several hours, or days, after circulatory arrest is established, it is often impossible to insulate the arteries at the base of the skull in any period of the circulatory cycle. However, the absence of flow in a patient in whom flow had previously been recorded is considered by some groups to be a sonographic finding compatible with the diagnosis of brain death.

To complete the diagnosis of cerebral circulatory arrest, it is necessary that all intracranial vessels have one of the three blood flow velocity patterns compatible with circulatory arrest [15]. It is not necessary for the establishment of the diagnosis of circulatory arrest that all the sonographic patterns are similar in the insonated arteries.

There is no standard recording duration for each of the arteries, although some authors recommend a recording duration of 30 seconds. However, what is really important is that the blood pressure is normalized and the intracranial pressure stabilized, avoiding recording during transient elevations of intracranial pressure [16].

39.8 Transcranial Doppler and Death by Neurological Criteria: Some Limitations

There are several situations that must be considered when using Transcranial Doppler as an ancillary test:

39.8.1 Transient Cerebral Circulatory Arrest

Cerebral circulatory arrest is the pathophysiological result of an interaction between mean blood pressure (mean arterial pressure (MAP)) and intracranial pressure (ICP), variables that define CPP, in a closed compartment such as the skull. Under certain circumstances, for example, severe arterial hypotension or the presence of transient increases in intracranial pressure (Lundberg waves) [17, 18], a phenomenon of transient cerebral circulatory arrest may occur, which can be demonstrated by means of Transcranial Doppler and which only shows the interrelationship between mean arterial pressure and pressure within the intracranial compartment, this being neither a situation of irreversible cerebral circulatory arrest nor a false positive of TCD in the diagnosis of brain death.

39.8.2 Cerebral Circulatory Arrest Is Not Synonymous with Brain Death

It is important to note that no single instrumental test is sufficient, by itself, to establish the diagnosis of brain death. The absence of cerebral blood flow velocities and the absence of cerebral bioelectrical activity are phenomena intimately associated with brain death. However, none of these phenomena are synonymous with brain death. They must be supported by a complete clinical examination that explores and evidences the absence of brainstem activity. Currently, there is no instrumental test that is synonymous with brain death that can replace the clinical diagnosis used to establish the diagnosis of brain death.

39.8.3 Patients with Primary Injury Limited to the Brain Stem

In some cases of patients in whom the neurological impairment is not face-flow, but ascending (the initial neurological damage occurs in the posterior fossa), it is possible to observe the persistence of blood flow velocities at the level of the anterior

circulation in patients who meet clinical criteria for brain death. This is due to the absence of intracranial hypertension in the supratentorial territory, and should not be interpreted as a false negative of ultrasound diagnosis but as an inadequate interpretation and indication of the TCD; conceptually, when the concept of brainstem death is used it is not necessary to demonstrate the absence of supratentorial activity.

39.8.4 Closed-Vault Defects

The existence of a defect in the skull (fractures, hemi-craniectomy, etc.) may cause the normal balance between intracranial and extracranial pressures to be modified; this may influence the results of the instrumental tests used for the diagnosis of brain death, especially those that indirectly explore the cerebral blood flow (or blood flow velocities), causing them to lose diagnostic accuracy.

Flowers et al. [19] determine as possible causes of persistent cerebral blood flow accompanying the situation of brain death:

1. External or internal drains of the cerebrospinal fluid (CSF).
2. Decompressive craniectomies.
3. Large fractures of the base of the skull.
4. In children, the existence of open fontanelles.

Therefore, in these circumstances the use of tests that attempt to estimate brain blood flow, such as TCD by blood flow velocities' measurement, may determine a false negative result for the diagnosis of brain death and the diagnosis of brain death should not be excluded. Ancillary tests that measure other physiological variables associated with brain death, such as brain electrical activity, are suggested [10, 20].

39.9 TCD and DNC: Technical Difficulties

There are some clinical situations in which TCD insonation for the diagnosis of brain death is especially difficult:

39.9.1 Elderly Women

In this cohort of patients, in addition to the difficulties inherent in insonation for brain death, there is also the difficulty of finding an appropriate acoustic window, in the general population, there will be 15–20% of patients who will not have an adequate transtemporal acoustic window.

39.9.2 Inadequate Hemodynamic and Intracranial Conditions

For reliable TCD insonation, optimization of the patient's blood pressure and intracranial pressure is important. A TCD study to complement the brain death study should not be performed if the patient does not have an optimized systemic blood pressure.

It is also important to avoid performing studies during transitory elevations of intracranial pressure (Lundberg waves), since with these it is possible to have a transitory cerebral circulatory arrest in the cerebral artery with reversible cessation of cerebral blood flow velocities.

39.10 TCD and DNC: Technical Issues to Consider

When performing TCD for the support of diagnosis of brain death, in addition to the limitations mentioned above, certain technical aspects of the equipment used should be taken into account that will not only facilitate insonation but also increase the diagnostic accuracy of the technique.

39.10.1 Filter Control

When a TCD is performed in order to establish the persistence or absence of diastolic blood flow velocity, a key element in the diagnosis of cerebral circulatory arrest, it is important to avoid the existence of a phenomenon such as signal hyperfiltration. When high filter levels are used, it is possible not to detect the existence of the diastolic blood flow (in the case that it is low) because it is masked by the filtering of the equipment.

39.10.2 Optimization of the Power Ultrasound Beam

During the diagnosis of brain death by TCD, it is important to increase the diagnostic sensitivity of the test to the maximum. To do this, and especially in those patients with a difficult acoustic window, it is advisable to increase the power of the ultrasound beam during the first phase of the test until the sonographic location of the artery is made, and the power can be decreased once the artery is located, and until the best quality of insonation is achieved.

39.10.3 Orbital Acoustic Window

In cases where it is impossible to sound the arteries of the anterior circulation through the temporal window, the use of the orbital window is suggested in order to establish the absence of blood flow velocities at the level of the carotid artery [21, 22]. To do this, the standardized rules for insonation of the carotid artery through this acoustic window must be followed, and the optimization of the sample volume is important in order to isolate, from a sonographic point of view, the different sections of the carotid siphon. The absence of telediastolic blood flow velocity at the level of both carotid siphons suggests the absence of blood flow in anterior circulation.

39.11 Transcranial Doppler in the Diagnosis of Brain Death: Evidence

According to the Task Force Group on Cerebral Death of the Neurosonology Research Group of the World Federation of Neurology, transcranial Doppler is a reliable method for the diagnosis of brain death [15].

The transcranial Doppler technique has been used for the diagnosis of brain death for more than 20 years [23]. In general, the sensitivity and specificity of the technique for brain death ranges from 91 to 100% and 97 to 100%, respectively [24–27].

In a systematic review of 859 patients [28] (56.1% of whom had confirmed brain death using clinical criteria), the diagnostic sensitivity of transcranial Doppler was 0.90 (95% CI.0.87–0.92) and the overall specificity was 0.98 (95% CI.0.96–0.99).

39.12 Transcranial Doppler in the Diagnosis of Brain Death: Advantages and Disadvantages

The use of TCD in the diagnosis of brain death has advantages and disadvantages over other techniques used for the same purpose.

39.12.1 Advantages

1. It is performed at the patient's bedside. Transcranial Doppler devices are portable.
2. The TCD shows the cerebral circulatory arrest as a process. It is not uncommon to observe asynchronies in cerebral circulatory arrest in different intracranial

territories. It is possible to see circulatory arrest in one hemisphere, without it having yet been completed in the contralateral; or circulatory arrest in supratentorial territory [29], without it having yet manifested itself in infratentorial territory.

In either case, it should be taken into account that to complete the diagnosis of brain death, by this auxiliary test, the absence of circulation in all intracranial arterial territories must be confirmed.

3. It is a technique of simple interpretation. It is sufficient to observe the absence of telediastolic blood flow velocity in all intracranial territories (presence of some of the three sonographic patterns compatible with absence of blood flow velocity).
4. It is a technique of easy replication. The technique can be performed repeatedly without the need to mobilize the patient outside the intensive care unit (ICU).
5. Blood flow velocity rate measurements per se with the TCD are not interfered by central nervous system depressant drugs.

39.12.2 Disadvantages

1. Possible existence of blood flow velocity rates by TCD in patients who are in a situation of brain death; that is to say, a "false negative" for the diagnosis of brain death. This may occur in cases of absence of cranial hermetism due to decompressive craniectomies, external or internal drainage of the cerebrospinal fluid, or large base fractures of the skull. These potential disadvantages are shared with other instrumental tests that analyze cerebral blood flow in similar circumstances.
2. The absence of acoustic window. This is especially possible in older female patients, or in any patient where several days have elapsed since the cessation of intracranial arterial circulation. The use of the orbital window for carotid siphon insonation [21] may be a suitable option to overcome this problem when anterior circulation cannot be insonated through the transtemporal window.
3. Dependence on the operator technique. There are no significant differences in sonographic findings between two operators adequately trained in TCD.

39.13 Conclusion

Transcranial Doppler is an extraordinarily useful technique to support the diagnosis of Death by Neurological Criteria (DNC). As other diagnostic techniques, it requires adequate operator training to be performed correctly.

In order to know the usefulness of the technique, its indication must be clearly established, and it must be fundamentally used in the diagnosis of brain death when

the concept of whole brain death is being used. An adequate physiopathological knowledge of the intracranial phenomena associated with whole brain death helps to understand the sonographic expression of the circulatory arrest that accompanies brain death.

Algorithm

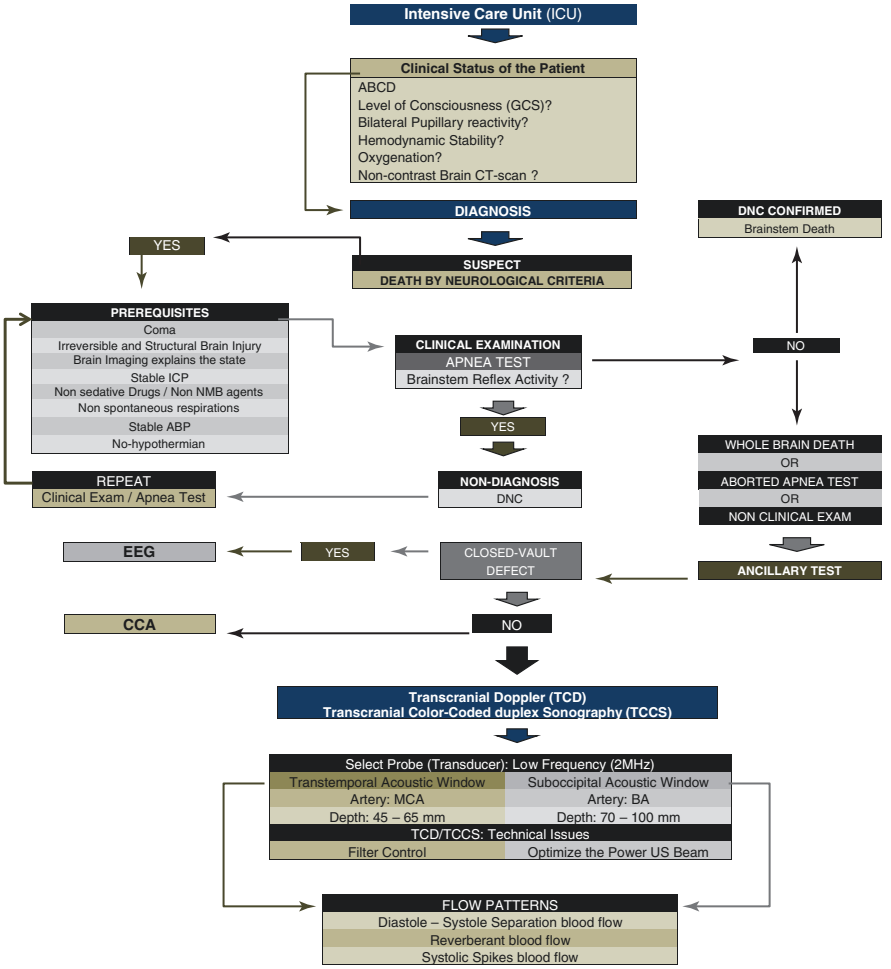

ABCD Airway-Breathing-Circulation-Disability, *ABP* Arterial blood pressure, *EEG*: Electroencephalogram, *ICP* Intracranial pressure, *NMB* Neuromuscular blockers, *CCA* Cerebral circulatory arrest, *MCA* Middle cerebral artery, *BA* Basilar artery, US Ultrasound

References

1. A definition of irreversible coma. Report of the Ad Hoc Committee of the Harvard Medical School to Examine the Definition of Brain Death. JAMA. 1968;205(6):337–40.
2. Pallis C. ABC of brain stem death. Prognostic significance of a dead brain stem. Br Med J (Clin Res Ed). 1983;286(6359):123–4.
3. Brierley JB, Graham DI, Adams JH, Simpsom JA. Neocortical death after cardiac arrest. A clinical, neurophysiological, and neuropathological report of two cases. Lancet. 1971;2(7724):560–5.
4. Practice parameters for determining brain death in adults (summary statement). The Quality Standards Subcommittee of the American Academy of Neurology. Neurology. 1995;45(5):1012–4.
5. Dominguez-Roldan JM, Barrera-Chacon JM, Murillo-Cabezas F, Santamaria-Mifsut JL, Rivera-Fernandez V. Clinical factors influencing the increment of blood carbon dioxide during the apnea test for the diagnosis of brain death. Transplant Proc. 1999;31(6):2599–600.
6. Wijdicks EF, Varelas PN, Gronseth GS, Greer DM. Evidence-based guideline update: determining brain death in adults: report of the Quality Standards Subcommittee of the American Academy of Neurology. Neurology. 2010;74(23):1911–8.
7. Cestari M, Gobatto ALN, Hoshino M. Role and limitations of transcranial Doppler and brain death of patients on veno-arterial extracorporeal membrane oxygenation. ASAIO J. 2018;64(4):e78.
8. Li Y, Liu S, Xun F, Liu Z, Huang X. Use of transcranial Doppler ultrasound for diagnosis of brain death in patients with severe cerebral injury. Med Sci Monit. 2016;22:1910–5.
9. Lobo CL, Cancado RD, Leite AC, Dos Anjos AC, Pinto AC, Matta AP, et al. Brazilian Guidelines for transcranial doppler in children and adolescents with sickle cell disease. Rev Bras Hematol Hemoter. 2011;33(1):43–8.
10. Verlhac S. Transcranial Doppler in children. Pediatr Radiol. 2011;41 Suppl 1:S153–65.
11. Sloan MA, Alexandrov AV, Tegeler CH, Spencer MP, Caplan LR, Feldmann E, et al. Assessment: transcranial Doppler ultrasonography: report of the Therapeutics and Technology Assessment Subcommittee of the American Academy of Neurology. Neurology. 2004;62(9):1468–81.
12. Rajagopal R, Gupta A. Transcranial Doppler flow patterns in brain death: "Storm before the calm". Neurol India. 2017;65(3):671–2.
13. Hashemian SM, Delavarkasmaei H, Najafizadeh K, Mojtabae M, Ardehali SH, Kamranmanesh MR, et al. Role of transcranial Doppler sonography in diagnosis of brain death: a single center study. Tanaffos. 2016;15(4):213–7.
14. Dominguez-Roldan JM, Murillo-Cabezas F, Munoz-Sanchez A, Santamaria-Mifsut JL, Villen-Nieto J. Changes in the Doppler waveform of intracranial arteries in patients with brain-death status. Transplant Proc. 1995;27(4):2391–2.
15. Sharma D, Souter MJ, Moore AE, Lam AM. Clinical experience with transcranial Doppler ultrasonography as a confirmatory test for brain death: a retrospective analysis. Neurocrit Care. 2011;14(3):370–6.
16. Latin American consensus on the use of transcranial Doppler in the diagnosis of brain death. Rev Bras Ter Intensiva. 2014;26(3):240–52.
17. Kirkham FJ, Levin SD, Padayachee TS, Kyme MC, Neville BG, Gosling RG. Transcranial pulsed Doppler ultrasound findings in brain stem death. J Neurol Neurosurg Psychiatry. 1987;50(11):1504–13.
18. Steinmetz H, Hassler W. Reversible intracranial circulatory arrest in acute subarachnoid haemorrhage. J Neurol Neurosurg Psychiatry. 1988;51(10):1355–6.
19. Flowers WM Jr, Patel BR. Persistence of cerebral blood flow after brain death. South Med J. 2000;93(4):364–70.
20. Cabrer C, Dominguez-Roldan JM, Manyalich M, Trias E, Paredes D, Navarro A, et al. Persistence of intracranial diastolic flow in transcranial Doppler sonography exploration of patients in brain death. Transplant Proc. 2003;35(5):1642–3.

21. Dominguez-Roldan JM, Jimenez-Gonzalez PI, Garcia-Alfaro C, Rivera-Fernandez V, Hernandez-Hazanas F. Diagnosis of brain death by transcranial Doppler sonography: solutions for cases of difficult sonic windows. Transplant Proc. 2004;36(10):2896–7.
22. Algin O, Gundogdu G, Izdes S, Keles GE, Solaroglu I. Diagnosis of brain death by orbital Doppler ultrasound: a comparative research study. Turk Neurosurg. 2015;25(2):256–62.
23. Hadani M, Bruk B, Ram Z, Knoller N, Spiegelmann R, Segal E. Application of transcranial doppler ultrasonography for the diagnosis of brain death. Intensive Care Med. 1999;25(8):822–8.
24. Hassler W, Steinmetz H, Pirschel J. Transcranial Doppler study of intracranial circulatory arrest. J Neurosurg. 1989;71(2):195–201.
25. Zurynski Y, Dorsch N, Pearson I, Choong R. Transcranial Doppler ultrasound in brain death: experience in 140 patients. Neurol Res. 1991;13(4):248–52.
26. Hassler W, Steinmetz H, Gawlowski J. Transcranial Doppler ultrasonography in raised intracranial pressure and in intracranial circulatory arrest. J Neurosurg. 1988;68(5):745–51.
27. Petty GW, Mohr JP, Pedley TA, Tatemichi TK, Lennihan L, Duterte DI, et al. The role of transcranial Doppler in confirming brain death: sensitivity, specificity, and suggestions for performance and interpretation. Neurology. 1990;40(2):300–3.
28. Chang JJ, Tsivgoulis G, Katsanos AH, Malkoff MD, Alexandrov AV. Diagnostic accuracy of transcranial Doppler for brain death confirmation: systematic review and meta-analysis. AJNR Am J Neuroradiol. 2016;37(3):408–14.
29. Dominguez-Roldan JM, Garcia-Alfaro C, Jimenez-Gonzalez PI, Rivera-Fernandez V, Hernandez-Hazanas F, Perez-Bernal J. Brain death due to supratentorial masses: diagnosis using transcranial Doppler sonography. Transplant Proc. 2004;36(10):2898–900.

Chapter 40
Intracerebral Hemorrhage in ICU: Dynamic Monitoring by Transcranial Color-Coded Duplex Sonography (TCCS)

Pol Camps-Renom

Key Points

1. Several radiological features, such as hematoma volume and midline shift, are related to poor outcome following an intracerebral hemorrhage and can be measured using transcranial color-coded duplex sonography (TCCS).
2. TCCS shows an excellent correlation with computed tomography in assessing the hematoma volume, midline shift, and the third ventricle diameter in patients with intracerebral hemorrhage.
3. TCCS allows a noninvasive monitoring of the hematoma characteristics as well as hemodynamic changes related to the mass effect such as the pulsatility index of the middle cerebral arteries (MCAs).
4. Hematoma volume measured with TCCS is a predictor of a poor outcome.

40.1 Introduction

Spontaneous intracerebral hemorrhage (ICH) represents approximately 15% of all strokes and is a major cause of morbidity and mortality [1]. Half of the events related to case fatality occur within the first 48 hours [2] and thus, identifying variables that contribute to early neurological deterioration and mortality is of enormous importance. An early estimation of the prognosis is crucial for deciding upon a treatment plan and properly informing families and relatives. There are several clinical features, such as the severity of the neurological deficit or the Glasgow Coma Scale (GCS) score, which are robustly associated with poor prognosis.

P. Camps-Renom (✉)
Department of Neurology, Hospital de la Santa Creu i Sant Pau, Universitat Autònoma de Barcelona, Barcelona, Spain

Biomedical Research Institute Sant Pau (IIB-Sant Pau), Barcelona, Spain
e-mail: pcamps@santpau.cat

C. N. Rodríguez et al. (eds.), *Neurosonology in Critical Care*,
https://doi.org/10.1007/978-3-030-81419-9_40

However, neuroimaging adds valuable information that complements the clinical judgment and is nowadays essential to give an accurate prognosis. In this chapter, we will discuss the main radiological features related to poor prognosis following an ICH, and how transcranial color-coded duplex sonography (TCCS) allows a non-invasive bedside monitoring of most of them.

40.2 ICH: Radiological Prognostic Factors

There are several ICH characteristics related to poor prognosis that can be assessed by brain imaging with either computed tomography (CT) or magnetic resonance imaging (MRI). Despite MRI having a higher resolution and sensitivity to detect and characterize ICH, its availability in the emergency departments is scarce, and thus, CT has become the most used technique to assess them. Several studies have demonstrated that some features, such as hematoma volume (HV), hematoma enlargement, midline shift (MLS), and intraventricular hemorrhage (IVH) [3–9], are related to poor functional outcome and mortality following and ICH. Therefore, all these radiological features should be assessed in the setting of an ICH. However, ICH is a dynamic process and some of these characteristics will change over time. Baseline CT in the emergency department may allow the first diagnosis and prognostic approach but is insufficient to predict how ICH is going to evolve. In the early stages, it can be difficult to monitor these prognostic radiological features with repeated CT scans due to the clinical and/or hemodynamic state of the patient (frequently intubated in the intensive care unit (ICU)), and the risk of radiation overexposure.

40.3 ICH: Role of the TCCS

TCCS is a noninvasive technique that provides simultaneous two-dimensional (2D) imaging of brain parenchyma and hemodynamic information from the main cerebral arteries. The role of TCCS is well established in the assessment of ischemic stroke, but its usefulness in the setting of acute ICH has been reported in only a few studies [10–16].

Visualization of acute ICH with TCCS is feasible [10–12]. Additionally, TCCS allows the assessment of the third ventricle (IIIV), the lateral ventricles (LV), MLS, and the presence of IVH [13–16]. Some studies have found an excellent correlation between CT scan and TCCS when measuring these characteristics. This begot interest in TCCS, which may represent a viable, noninvasive alternative to CT scan. In addition, TCCS may have some potential advantages, including its feasibility of performance at the bedside as many times as necessary, and regardless of the hemodynamic situation of the patient. From now on, we will describe the methodology to assess the main ICH characteristics using TCCS.

40.3.1 TCCS: Machine Setup

To evaluate ICH, we will use a 2–5 MHz range sectorial probe. For the exploration, the probe should be set up at 5 MHz and placed through the contralateral temporal bone window with a penetration depth of 14–16 cm. The transductor is skewed approximately 10° upward to scan axially and to visualize the contralateral skull bone and the midbrain in the center of the image. Image brightness, contrast, and time gain compensation should be adjusted to get the best image (Fig. 40.1).

40.3.2 TCCS: Hematoma Volume (HV)

ICH is visualized as a hyperechogenic mass and it should be assessed from the contralateral temporal bone. Deep supratentorial ICH is easier to identify, while lobar ICH is sometimes difficult to visualize properly. Extreme frontal or occipital lobe ICH as well as ICH from the convexity is usually inaccessible. Likewise, infratentorial ICH in adult patients is inaccessible with TCCS. Therefore, TCCS may be a useful tool to monitor the ICH volume mainly in supratentorial ICH affecting deep or lobar structures in the brain, excluding the convexity and the extreme frontal and occipital poles.

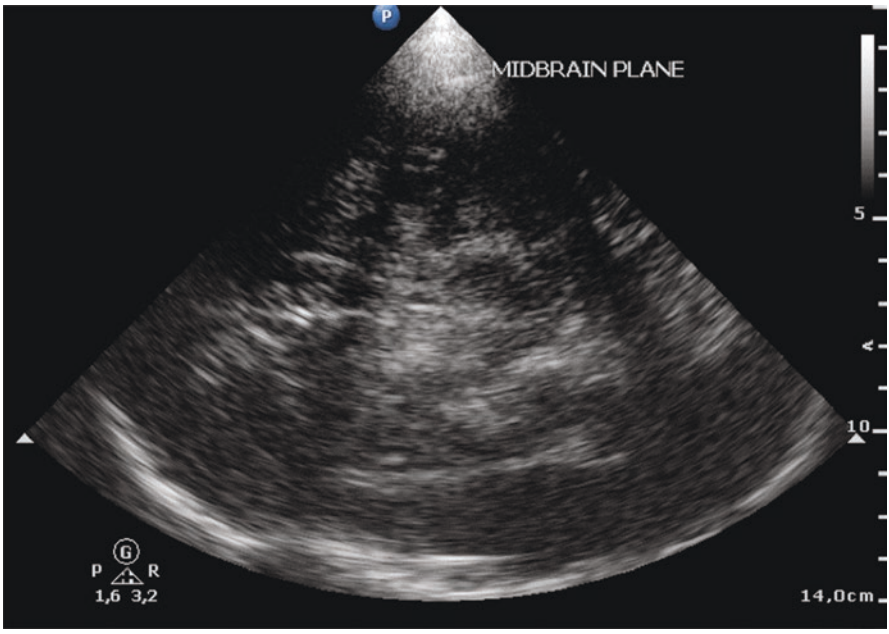

Fig. 40.1 Mesencephalic plane (midbrain plane) obtained from the temporal bone window

ICH should be assessed first in the axial plane skewing the transducer upward and downward to identify the greater diameter. In the axial plane, we will measure the longitudinal (*A*) and the axial (*B*) diameters (Fig. 40.2). Finally, we will turn the transducer 90° cranially and we will also measure the coronal (*C*) diameter. HV is calculated then with the formula $A \times B \times C/2$ [17]. In a prospective study, baseline HV assessed with TCCS and calculated with the formula of irregular volumes ($A \times B \times C/2$) was independently associated with the risk of early neurological deterioration and mortality [16]. In this study, investigators reported an excellent correlation between the baseline TCCS examination and the CT scan when measuring the HV ($r = 0.791$, $p < 0.001$), and separately the longitudinal ($r = 0.711$, $p < 0.001$), the axial ($r = 0.768$, $p < 0.001$), and the coronal diameters ($r = 0.754$, $p < 0.001$). Interestingly in the agreement analysis with Bland-Altman Plots, despite showing a good agreement, a systematic bias was detected between both the techniques: TCCS tended to overestimate the volumes of smaller ICH, and, contrariwise, to underestimate volumes in larger ICH.

Hyperechogenicity of ICH decreases over time due to the progressive transformation of hemoglobin and it may be difficult to visualize the hematoma beyond 72 hours. Thus, HV should be measured with TCCS in the acute phase, ideally within 2 hours from the baseline CT. Then, posterior examinations may be performed at bedside to detect the probable hematoma growth. Unfortunately, no studies have addressed the question of how frequently consecutive TCCS examinations should be performed.

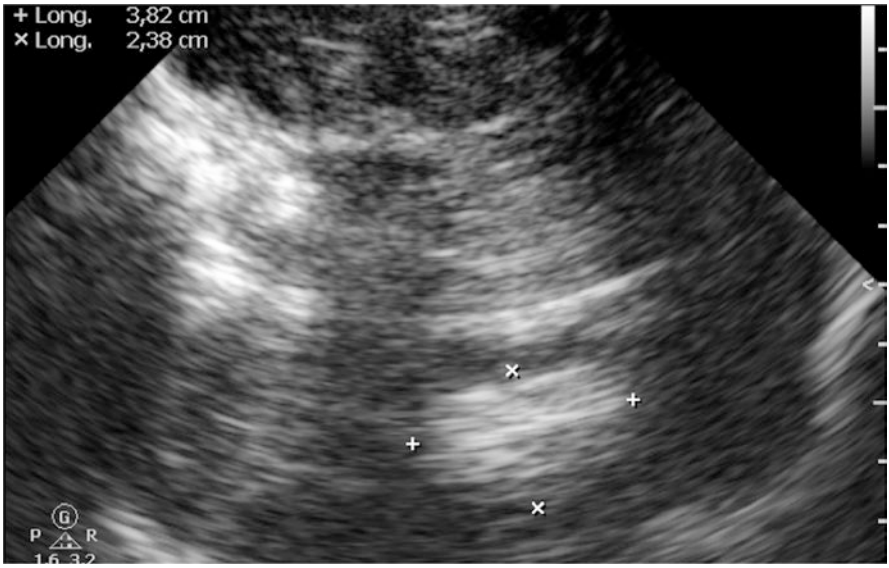

Fig. 40.2 ICH is visualized as a hyperechogenic mass (asterisks). This image shows the measurement of the axial and longitudinal diameter of a deep ICH

40.3.3 TCCS: Third Ventricle Diameter

The third ventricle (IIIV) diameter may be reliably measured with TCCS. The third ventricle diameter may increase in the setting of an ICH when there is intracranial hypertension. Visualizing the third ventricle is important not only to measure its diameter but also to measure MLS (see the next paragraph). To identify the third ventricle, we will slightly skew the transducer upward from the initial midbrain plane. The third ventricle is visualized at a depth of 6–8 cm and identified by its parallel hyperechogenic margins in front of a hyperechogenic rounded structure corresponding to the pineal gland. We can also see the surrounding hypoechogenic thalami [13] (Fig. 40.3). In this position, we will measure its maximum diameter. Some studies have reported an excellent correlation between TCCS and CT scan when measuring the third ventricle diameter [13, 16].

40.3.4 TCCS: Midline Shift (MLS)

ICH causes a mass effect in the surrounding cerebral tissue. This mass effect will be greater as greater will be the hematoma volume (HV). This phenomenon can be reported radiologically by the MLS and is associated with a poor outcome [3, 4]. The midline is defined by CT scan, as the distance between the skull and the central

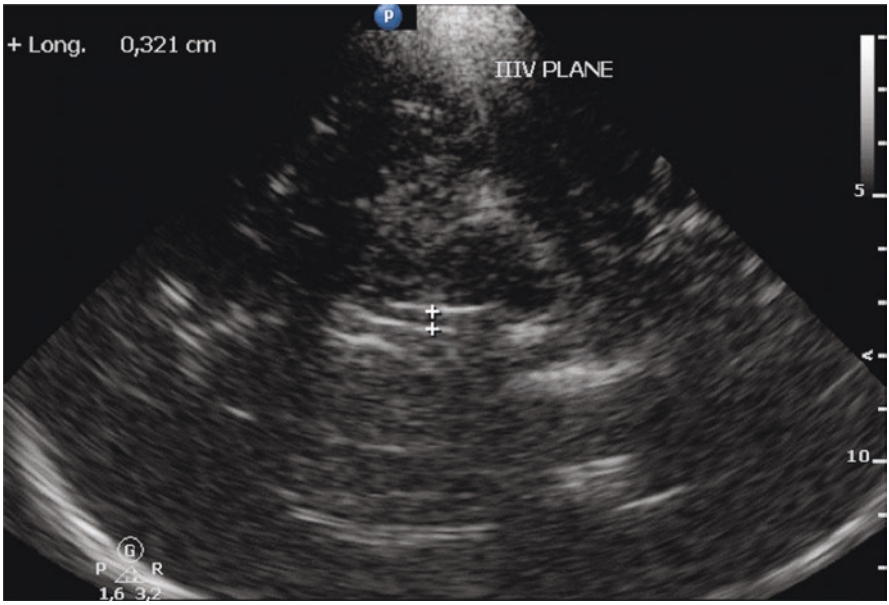

Fig. 40.3 Third ventricle (IIIV) is visualized as two hyperechogenic margins surrounded by the hypoechogenic thalami

point in the middle of the third ventricle. When there exists a mass effect, the IIIV shifts toward the contralateral hemisphere. This MLS may be calculated with the formula $(A - B)/2$ (A and B being the distances between each side of the skull and the IIIV). TCCS also allows the measurement of this shift. As described in some studies [16], once identified as the III ventricle, the midline shift (MLS) may be calculated with the same formula $(A - B)/2$ (A and B being the distances between the transducer and the IIIV, on each side of the skull) (Fig. 40.4).

40.3.5 TCCS: Lateral Ventricles Diameter

Similar to the IIIV, lateral ventricles (LV) diameter may increase in the setting of an ICH complicated with hydrocephalus. Thus, the monitoring of the LV diameters may identify patients with incipient hydrocephalus [14]. To identify the LV, we will skew the transducer upward from the IIIV plane approximately 10°. LV appear as two hyperechogenic margins (Fig. 40.5). However, the measurement of the LV diameter may be difficult, depending on the temporal bone window. In addition, the LV are visualized diagonally, instead of axially like the CT scan. These technical difficulties result in considerable variability in the measures [16]. In fact, some studies reported a poor correlation between the TCCS measures of the LV and the brain-CT scan [16].

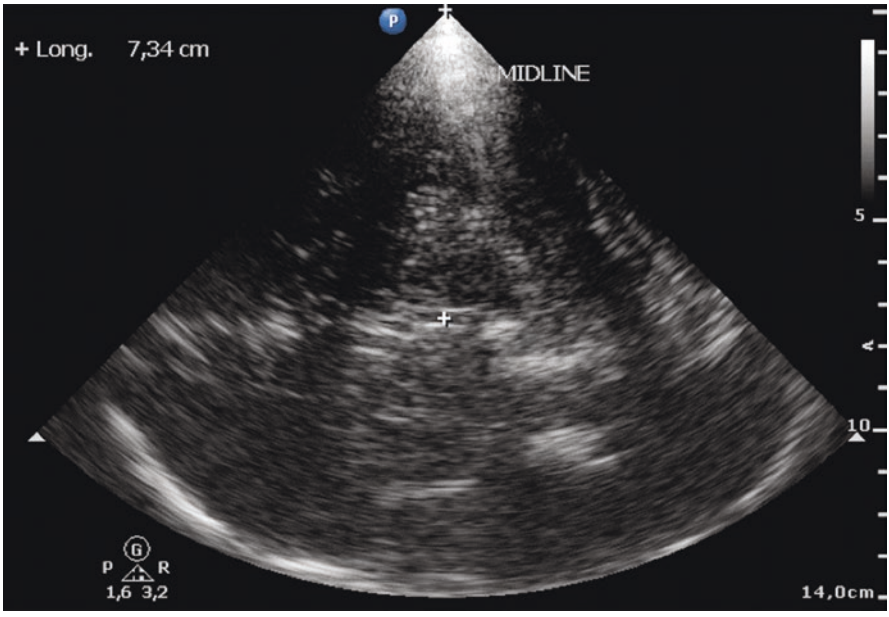

Fig. 40.4 MLS may be calculated with TCCS using the formula $(A - B)/2$ (A and B being the distances between the transducer and the third ventricle, on each side of the skull)

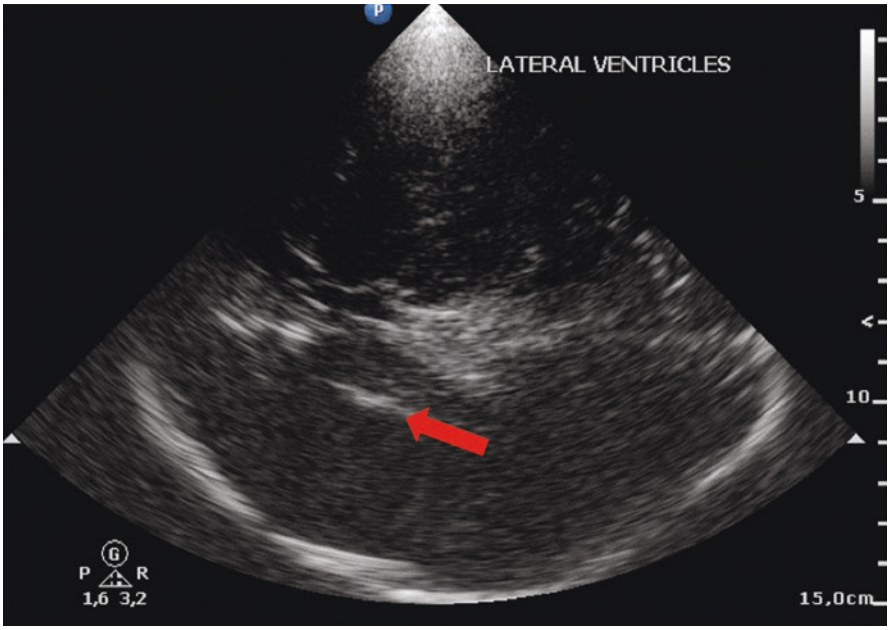

Fig. 40.5 LV appear as two hyperechogenic margins when skewing the transducer upward from the IIIV plane

40.3.6 TCCS: Intraventricular Hemorrhage (IVH)

IVH is associated with poor outcome following an ICH. This radiological characteristic is included in some of the most widely used prognostic scores [5]. In some patients, IVH can be identified by TCCS as a hyperechogenic content inside the LV (Fig. 40.6). However, the difficulty in visualizing the LV with TCCS is a clear drawback to using this technique to assess the presence of intraventricular hemorrhage (IVH).

40.3.7 TCCS: Pulsatility Index (PI)

Besides the morphological evaluation, TCCS provides hemodynamic information from the main cerebral arteries. This hemodynamic information may be helpful to detect a fearsome complication of ICH: intracranial hypertension. The exact intracranial pressure measurement is obtainable only by an invasive intracranial pressure device. Some studies have reported a good correlation between the intracranial pressure measured with invasive devices and the pulsatility index (PI) of the middle cerebral arteries (MCAs) [18]; however, others have provided evidence of poor

association between PI and ICP [20]. PI assesses the relationship between the systolic and the diastolic velocities through the formula (peak systolic velocity – end diastolic velocity)/mean velocity. In the context of an increase of the intracranial pressure, the peak of systolic velocity tends to increase in order to overcome the high resistance, while the diastolic velocity is likely to decrease. These changes lead to an increase of the PI. Some studies have found an association between this increase of the PI in the MCAs and a higher risk of mortality in the setting of an ICH [16, 19].

To measure the pulsatility index in both MCAs, we will start from the midbrain plane activating the color Doppler to visualize the circle of Willis (Fig. 40.7). To properly identify the MCA, sometimes it is necessary to skew slightly the transducer upward. It is advisable to measure the velocities in the proximal segment of the MCA prior to bifurcation, usually placed in a depth between 5.5 and 4.5 cm, in a region without curvatures to avoid flow accelerations (Fig. 40.7).

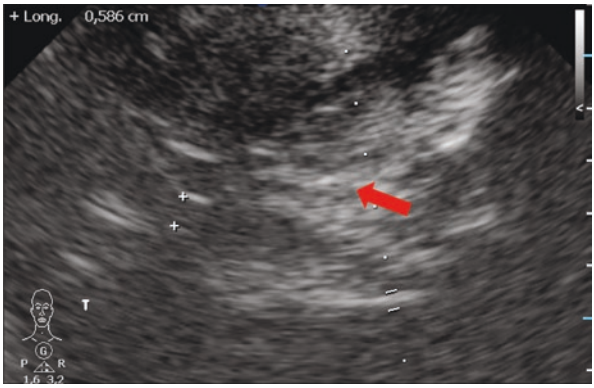

Fig. 40.6 Anterior hyperechogenic margins correspond to the LV. The red arrow points the hyperechogenic content inside the LV corresponding to IVH

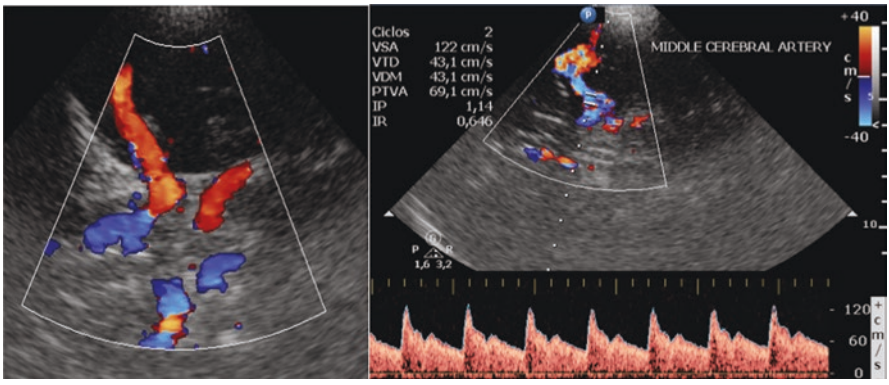

Fig. 40.7 Pulsatility index of the MCA is calculated with the formula (peak systolic velocity – end diastolic velocity)/mean velocity

40.4 Conclusion

There exists a good correlation between TCCS and CT scan in measuring HV, MLS, and the IIIV diameter. Conversely, its usefulness to assess LV diameter and IVH is controversial. In addition to the morphological information, TCCS allows the assessment of some hemodynamic parameters, such as the pulsatility index.

TCCS has some important limitations, including the examiner dependency and the susceptibility to an insufficient temporal bone window. Additionally, some specific limitations arise when assessing ICH, including the loss of echogenicity of the blood over time, and the difficulty in evaluating ICH in some locations like infratentorial structures. These drawbacks designate TCCS as a complementary diagnostic tool and CT scan remains the most reliable examination in the setting of an acute ICH. However, a TCCS examination following the baseline CT scan may allow the monitoring of some ICH characteristics at the bedside.

Algorithm

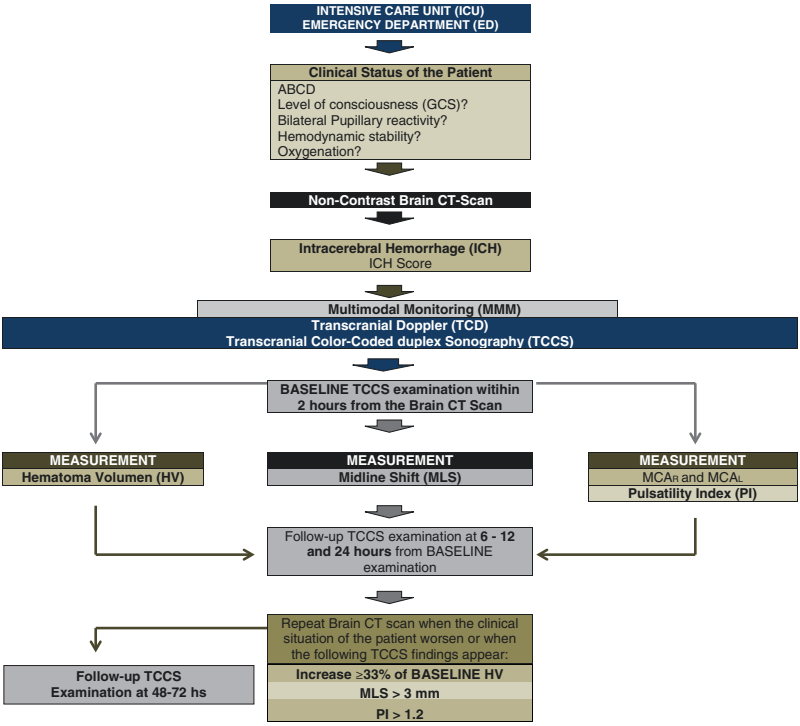

Algorithm for the noninvasive monitoring of ICH with TCCS.
ABCD Airway-breathing-circulation-disability MCA_R Right middle cerebral artery, MCA_L Left middle cerebral artery

References

1. Van Asch CJ, Luitse MJ, Rinkel GJ, et al. Incidence, case fatality, and functional outcome of intracerebral haemorrhage over time, according to age, sex, and ethnic origin: a systematic review and meta-analysis. Lancet Neurol. 2010;9:167–762.
2. Balami JS, Buchan AM. Complications of intracerebral haemorrhage. Lancet Neurol. 2012;11:101–18.
3. Leira R, Dávalos A, Silva Y, et al. Early neurologic deterioration in intracerebral hemorrhage: predictors and associated factors. Neurology. 2004;63:461–7.
4. Mayer SA, Sacco RL, Shi T, et al. Neurologic deterioration in noncomatose patients with supratentorial intracerebral hemorrhage. Neurology. 1994;44:1379–84.
5. Hemphill JC, Bonovich DC, Besmertis L, et al. The ICH score: a simple, reliable grading scale for intracerebral hemorrhage. Stroke. 2001;32:891–7.
6. Rost NS, Smith EE, Chang Y, et al. Prediction of functional outcome in patients with primary intracerebral hemorrhage: the FUNC score. Stroke. 2008;39:2304–9.
7. Davis SM, Broderick J, Hennerici M, et al. Hematoma growth is a determinant of mortality and poor outcome after intracerebral hemorrhage. Neurology. 2006;66:1175–81.
8. Tuhrim S, Horowitz DR, Sacher M, et al. Volume of ventricular blood is an important determinant of outcome in supratentorial intracerebral hemorrhage. Crit Care Med. 1999;27:617–21.
9. Brott T, Broderick J, Kothari R, et al. Early hemorrhage growth in patients with intracerebral hemorrhage. Stroke. 1997;28:1–5.
10. Becker G, Winkler J, Hofmann E, et al. Differentiation between ischemic and hemorrhagic stroke by transcranial color-coded real-time sonography. J Neuroimaging. 1993;3:41–7.
11. Pérez ES, Delgado-Mederos R, Rubiera M, et al. Transcranial duplex sonography for monitoring hyperacute intracerebral hemorrhage. Stroke. 2009;40:987–90.
12. Kiphuth IC, Huttner HB, Breuer L, et al. Sonographic monitoring of midline shift predicts outcome after intracerebral hemorrhage. Cerebrovasc Dis. 2012;34:297–304.
13. Seidel G, Kaps M, Gerriets T, et al. Evaluation of the ventricular system in adults by transcranial duplex sonography. J Neuroimaging. 1995;5:105–8.
14. Kiphuth IC, Huttner HB, Struffert T, et al. Sonographic monitoring of ventricular enlargement in posthemorrhagic hydrocephalus. Neurology. 2011;76:858–62.
15. Becker G, Bogdahn U, Strassburg HM, et al. Identification of ventricular enlargement and estimation of intracranial pressure by transcranial color-coded real-time sonography. J Neuroimaging. 1994;4:17–22.
16. Camps-Renom P, Mendez J, Granell E, et al. Transcranial Duplex sonography predicts outcome following an intracerebral hemorrhage. AJNR Am J Neuroradiol. 2017;38:1543–1549.
17. Kothari RU, Brott T, Broderick JP, et al. The ABCs of measuring intracerebral haemorrhage volumes. Stroke. 1996;27:1304–5.
18. Martí-Fàbregas J, Belvıs R, Guardia E, et al. Prognostic value of pulsatility index in acute intracerebral hemorrhage. Neurology. 2003;61:1051–6.
19. Bellner J, Romner B, Reinstrup P, et al. Transcranial Doppler sonography pulsatility index (PI) reflects intracranial pressure (ICP). Surg Neurol. 2004;62:45–51.
20. Zweifel C, Czosnyka M, Carrera E, de Riva N, Pickard JD, Smielewski P. Reliability of the blood flow velocity pulsatility index for assessment of intracranial and cerebral perfusion pressures in head-injured patients. Neurosurgery. 2012;71(4):853–6.

Chapter 41
Transcranial Doppler (TCD/TCCS) and Traumatic Brain Injury (TBI): Is There a Role?

Pierre Bouzat and Pierluigi Banco

Key Points

1. TCD/TCCS is increasingly used at the initial phase of severe TBI.
2. TCD is helpful for tailoring therapeutic management at the bedside.
3. TCD may rule out intracranial hypertension.
4. After mild-to-moderate TBI, TCD helps in the triage of patients at risk of neurologic worsening.
5. TCD is also useful in the intensive care unit (ICU) to assess brain autoregulation.

41.1 Introduction

Traumatic brain injury (TBI) is a global medical, economic, and social challenge. In Europe, 2.1 million patients over one year suffered from TBI, accounting for 82 000 deaths. It is estimated that 37% of injury-related deaths are due to TBI, occurring mostly in young patients [1]. Traumatic brain injury has diverse clinical presentations; only 15% patients are considered as severe according to the Glasgow Coma Scale (GCS, lower than 9), whereas 85% are mild-to-moderate TBI (GCS between 9 and 15).

P. Bouzat (✉)
CHU Grenoble Alpes, Grenoble Institut of Neurosciences, Grenoble, France
e-mail: pbouzat@chu-grenoble.fr

P. Banco
Anesthesiology and Intensive Care Medicine, CHU Grenoble Alpes Trauma Center, Grenoble, France
e-mail: pbanco@chu-grenoble.fr

C. N. Rodríguez et al. (eds.), *Neurosonology in Critical Care*,
https://doi.org/10.1007/978-3-030-81419-9_41

The initial severity of brain lesions and the occurrence of secondary cerebral damage directly affect neurological outcomes after TBI [2]. Its management is based upon the treatment and the prevention of secondary cerebral injuries that may be caused by the imbalance between oxygen supply and demand into the brain tissue [3]. One of the main causes of this imbalance is brain ischemia, that is, unadapted cerebral blood flow (CBF). Brain tissue oxygen pressure ($P_{bt}O_2$), microdialysis parameters, and jugular venous oxygen saturation ($SjvO_2$) are used in the intensive care unit as a bedside multimodal monitoring to detect and treat ischemia [4]. The therapeutic strategy is to manipulate the cerebral blood flow (CBF) at the bedside to sustain cerebral oxygen demand mirrored by multimodal monitoring parameters within normal ranges [5]. However, none of these parameters are direct measurements of CBF per se. Perfusion magnetic resonance imaging (MRI) and perfusion computed tomography (CT) scan are validated imaging methods to measure CBF, but cannot be used as monitoring tools and may be hazardous for unstable TBI patients [6]. The challenge in the ICU field is to find a reliable, bedside, and easy-to-use method that would ensure a real-time CBF monitoring while following the efficacy of therapeutic interventions such as osmotherapy and blood pressure optimization.

The transcranial Doppler (TCD) and the Transcranial color-coded Duplex sonography (TCCS) can be used to monitor real-time cerebral blood flow velocities from basal cerebral arteries and have been studied in anesthesia and intensive care [7–10]. Contrary to laser Doppler and thermal diffusion probes, this method is noninvasive. First introduced in 1982 by Aaslid et al., TCD has been initially used to screen vasospasm in patients with subarachnoid hemorrhage [11], before its usage being widespread to monitor cerebral autoregulation and help in the acute stroke diagnosis, the carotid stenting treatment, the brain death evaluation, and intracranial hypertension (ICH) management [12]. Recently, interest for TCD after TBI care has grown and this technology has been implemented in French national guidelines for the acute management of severe TBI. In this chapter, we explore the specific role of TCD after TBI in different settings:

1. At the acute phase, in the trauma bay, for severe TBI management
2. For the estimation of noninvasive intracranial pressure (ICP) before ICP monitoring
3. In the emergency department for the triage of mild-to-moderate TBI patients
4. For the screening of posttraumatic internal carotid artery dissection
5. In the ICU to assess autoregulation

41.2 Severe Traumatic Brain Injury (TBI): TCD/TCCS-Guided Therapy

Aggressive management of low brain perfusion episodes has a key role to prevent secondary brain injuries. Intracranial pressure monitoring is not always available at the early phase of severe TBI and clinical signs are usually associated with brain

herniation, that is, a final stage of brain hypoperfusion. In this context, guidelines suggest to maintain blood pressure for brain perfusion pressure management at the early phase of severe TBI, but uniform targets of blood pressure might not be adapted for all patients depending on disrupted/disturbed autoregulation [13]. Even if available, ICP monitoring may not be specific enough to detect brain hypoperfusion, since increase in ICP is not always associated with decreased CBF [14] and normal ICP cannot exclude brain ischemia [5]. Conversely, in severe TBI patients without impaired CBF, bleeding injuries and cerebral vasogenic edema might be worsened by an increase in mean arterial blood pressure (MAP) [15–18].

Impaired TCD/TCCS blood flow velocities at the early phase of severe TBI were associated with cerebral ischemia and had good prognostic value to identify patients at risk of poor neurologic long-term outcome [19–21]. For instance, Ziegler et al. demonstrated that patients with a pulsatility index (PI) higher than 1.4 and end-diastolic velocity (EDV) lower than 20 cm/sec on admission had a mortality rate of 98.6% [22]. As a consequence, TCD-based therapies may be implemented in the prehospital setting and/or in the trauma bay to optimize CBF at the bedside before ICP measurement or brain herniation signs. These therapies may include osmotherapy to decrease intracranial pressure and restore CBF, and/or hemodynamic optimization with volume expansion and norepinephrine infusion, in order to increase cerebral perfusion pressure. The ultimate goal of such therapies is to reduce the number and the duration of cerebral ischemia episodes before invasive cerebral monitoring availability [13].

In the prehospital setting, TCD/TCCS identified patients with impaired TCD values with subsequent bad neurologic outcome. Using a PI cut-off higher than 1.4, prehospital physicians optimized end-tidal CO_2 (EtCO2) and mean arterial blood pressure with norepinephrine infusion in order to improve CBF. Osmotherapy was also used if TCD/TCCS remained abnormal after hemodynamic optimization. Using this bundle of care, the authors normalized five out of nine patients in the abnormal TCD group. Interestingly, patients who did not correct their TCD values using this strategy died within the first 48 hours [23].

Ract et al. used TCD for CBF-directed therapy on admission at the trauma bay for 24 severe TBI patients. After adjusting the partial pressure of carbon dioxide ($PaCO_2$) between 35 and 40 mmHg and raising the MAP above 75 mmHg using norepinephrine titration, TCD was considered abnormal in severe TBI patients, if two of these three measurements were found: a mean blood flow velocity (MFV) lower than 30 cm/sec, end-diastolic blood flow velocity (EDV) lower than 20 cm/s, and PI higher than 1.4. A typical pattern of low CBF is shown in (Fig. 41.1). TCD goal-directed therapy included: the increase of cerebral perfusion by rising MAP and/or the decrease of cerebral edema with osmotherapy and if needed, emergency neurosurgical procedure. A second TCD was performed when invasive cerebral monitoring was obtained. The authors showed that, out of 24 patients, 11 patients had an abnormal TCD on admission and obtained a specific treatment in order to increase CBF, and all except two patients normalized their TCD. No patient in the normal TCD group required osmotherapy or emergency neurosurgical procedure. Interestingly, when invasive cerebral monitoring was obtained, ICP was higher in

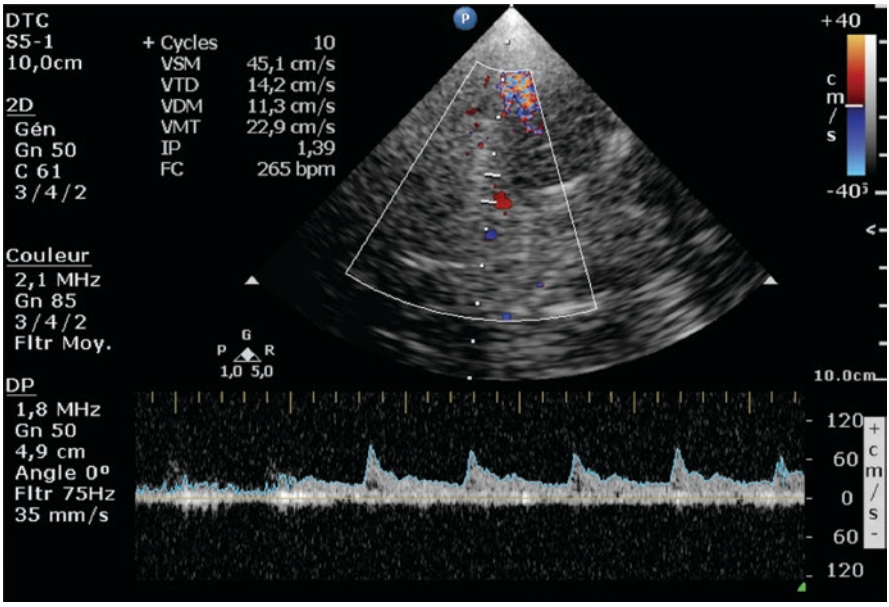

Fig. 41.1 Transcranial Doppler (TCD/TCCS) recording from the middle cerebral artery after severe TBI. Decrease in end-diastolic velocity (EDV) and increase in pulsatility Index (PI) are related to a rise in distal cerebrovascular resistance, which may be due to increased intracranial pressure (ICP)

the abnormal TCD group (32 +/−13 mmHg vs 22+/−10 mmHg), while cerebral perfusion pressure (CPP) (73 +/−15 mmHg vs 71 +/− 14 mmHg) and $SjvO_2$ (67 +/−2 mmHg vs 72 +/−9 mmHg) were within normal ranges [21].

41.3 TCD/TCCS: Noninvasive Assessment of ICP

Continuous ICP monitoring is a fundamental monitoring tool to detect intracranial hypertension that may induce decreased CBF. Elevated ICP was associated with poor neurologic outcome including death in several studies highlighting the need for ICP measurement as soon as possible. The gold standard of ICP measurement is the invasive measurement with an intraventricular catheter, but a more common alternative is possible using intraparenchymal probes. Such devices can induce intracerebral complications such as intraventricular infection for the intraventricular catheter or intracerebral hemorrhage for both devices. Moreover, intraparenchymal catheter may not be accurate due to measurement drifting, as it cannot be calibrated once inserted. Their implementation may also be delayed by ongoing posttraumatic coagulopathy [24]. As a result, access to an invasive ICP measurement may be cumbersome, and obtaining an ICP catheter can take up to 3 hours, potentially delaying specific treatments.

Studies regarding noninvasive ICP (nICP) monitoring using TCD/TCCS have started since 1987 [25], and relied upon three methods: ICP measurement based on PI, ICP measurement based on the calculation of noninvasive cerebral perfusion pressure, and ICP measurement based on mathematical models. A later review on the subject from Cardim et al. [26] suggested that TCD-based nICP methods presented an acceptable correlation with measured ICP (with the exceptions for PI-based methods) with an overall accuracy of +/− 12 mmHg. Rasulo et al. [27] showed in a prospective pilot study including 38 acute brain injury patients including 20 TBI patients that TCD-based ICP estimation correlated with invasive ICP values. Using an equation proposed by Czosnyka et al. (CPPe = MAP × EDV/MFV + 14) [28], TCD measured nICP had a 100% sensitivity in excluding an intracranial hypertension defined by an invasive ICP over 20 mmHg. TCD-based ICP values overestimated ICP by 6.2 mmHg on average. However, the correlation between invasive ICP and noninvasive ICP values is not perfect since decreased CBF might occur in patients with normal ICP, as demonstrated by hyperventilation. In conclusion, TCD/TCCS is able to assess changes in ICP but it is unable to give us absolute ICP values in relation to important variability in the reported accuracy.

41.4 Mild to Moderate Traumatic Brain Injury: TCD/TCCS-Guided Therapy

Early triage and management of mild-to-moderate TBI is a daily challenge in the emergency room (ER). These patients represent more than 80% of TBI patients [29] and are exposed to a rapid and sudden secondary neurologic worsening described by some authors as “talk and die” patients [30–32]. Even in mild TBI, up to 10% of patients will present neurologic worsening, requiring emergency neurosurgical procedures [33–35]. Neurologic worsening is usually caused by diverse intracerebral complications such as cerebral edema, intracerebral or subdural hematoma, extradural hematoma, subarachnoid hemorrhage, and/or hydrocephalus.

Prediction of neurologic status of mild-to-moderate TBI patients is based on clinical examination, biomarkers, and brain CT scan. The prognostic value of biomarkers such as protein S100 or neuron-specific enolase is beyond the scope of this chapter and warrants further investigation, whereas the prognostic value of CT scan is only demonstrated in patients with no or severe intracerebral injuries [31, 36, 37]. The triage of patients with moderate initial intracerebral lesion is still challenging in the ER and systematic CT scan monitoring is often done even in patients with no clinical sign of neurologic worsening [38, 39].

Recently, TCD/TCCS has been assessed for the prediction of neurologic worsening after mild-to-moderate TBI. A threshold of 1.25 for PI and/or 25 cm/sec EDV predicted neurologic worsening up to Day 7, with a 91% sensitivity and a 90% specificity in 98 patients [40]. Interestingly, moderate lesion on brain CT scan only predicted neurologic worsening in 47% of these patients. In a later multicenter

observational prospective study, Bouzat et al. [41] confirmed their first finding in a cohort of 369 patients with mild-to-moderate TBI and moderate CT scan lesions. Using the same thresholds, they found a 98% negative predictive value (NPV) for neurologic worsening. Abnormal TCD/TCCS pattern was also associated with a worse neurological outcome at Day 28 based on the disability rating score (DRS).

On the one hand, Bouzat et al. concluded that TCD could have an impact on intrahospital triage, since patients with normal TCD might not require repeated CT scanning and might be discharged home early. On the other hand, the authors did not show that abnormal TCD is accurate enough for predicting neurologic worsening. This result might be explained by the fact that clinicians were not blinded for TCD measurements, probably resulting in management strategies that might have prevented neurologic worsening. Moreover, PI depends on systemic pulse pressure amplitude, which is higher in elderly patients due to an aortic insufficiency or loss in vessel compliance.

41.5 Posttraumatic Internal Carotid Artery Dissection: TCD/TCCS Role

Post-traumatic internal carotid artery dissection (TICAD) is rare, with a prevalence of around 2% [42–44]. TICAD has a high morbidity and mortality when untreated [44–47]. These injuries are most commonly found in the trauma patient population with high-energy injury mechanisms to the head, neck, and thorax. The current guidelines [48, 49] recommend that only clinical signs and radiologic risk factors dictate screening by either CT angiography or MR angiography. The delay between the time of injury and initial neurological symptoms can extend up to one week [50], and 30% of blunt cerebrovascular injuries detected on CT angiography have no clinical or radiologic associated signs [51].

TCD/TCCS could be a useful tool for the screening of TICAD on admission, as it could enhance the accuracy of screening protocols and optimize the use of diagnostic imaging. An asymmetry superior to 25% in peak systolic flow velocities (PSVs) between the two middle cerebral arteries and a PI lower than 0.8, creating a demodulated velocity waveform, was correlated to an ipsilateral traumatic carotid dissection [52–54] (Fig. 41.2). This particular waveform is explained by the fact that PSV reflects the upstream vascular blood flow that is reduced by any obstruction. Without carotid stenosis, TCD/TCCS might not be modified and TCD is only helpful when TICAD induces a reduction in carotid diameter.

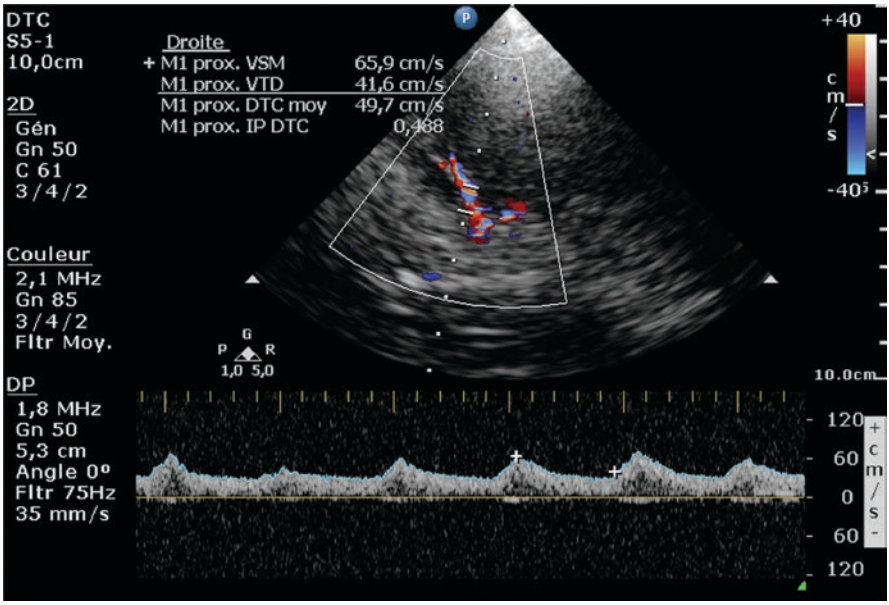

Fig. 41.2 Typical transcranial Doppler (TCD) recording from the middle cerebral artery after traumatic internal carotid artery dissection (TICAD)

41.6 Cerebral Autoregulation in TBI: TCD/TCCS Role

After severe TBI, the assessment of the autoregulation status is part of standard management. Autoregulation and vasoreactivity impairments were directly correlated with poor neurological outcome, as patients did not have an important protective mechanism and possibly an inadequate brain perfusion [55, 56]. While CT perfusion, positron emission tomography, and functional MRI methods have been described for vasoreactivity assessment, these methods are not appropriate for severe and unstable TBI patients, whereas TCD/TCCS can be used as a point-of-care tool for assessing cerebral autoregulation in TBI patients [57]. Different methods using TCD have been described in the literature:

1. The autoregulatory index (ARI) using the thigh cuff deflation technique relies on measuring changes in the MCA cerebral blood flow velocities induced by MAP drop followed by normalization [58]. After bilateral thigh cuffs' inflation and deflation, the strength of autoregulation was graded with a scale from 0 to 9 using a mathematical model. Autoregulation is defined as abnormal and passive below 4.

2. The autoregulatory index by transfer function analysis (TF ARI): using transfer function analysis to quantify the relationship between mean arterial blood pressure/CPP and cerebral blood flow velocities, inverse Fourier transform was used to obtain the cerebral blood flow velocity (CBFV) impulse response in time. The response was then fitted to the ARI models proposed by Tiecks [59].
3. The transient hyperemic response test [60]: using transient MCA hyperemia after ipsilateral carotid compression, this method defined an increase in PSV higher than 10% (after a steady and stable rise of MCA baseline values during compression) as a sign of intact autoregulatory capacity.
4. The TCD-based calculation of the mean flow index (Mx): using continuously CPP and MFV_{MCA} monitoring, a Pearson's correlation coefficient between these values is calculated to provide Mx between −1 and +1 [61]. A Mx lower than 0.05 indicated good autoregulation, and that higher than 0.3 is considered a sign of impaired autoregulation [62].

41.7 Conclusion

TCD is a noninvasive technique available at the bedside to improve the management of patients with severe TBI. This technique can be used at the early phase of TBI before invasive monitoring is available. It may help diagnose brain ischemia to tailor CBF manipulation at the bedside. This technology is also helpful to assess the risk of intracranial hypertension after severe TBI and/or the risk of early neurological worsening after mild-to-moderate TBI. An algorithm for early TBI management is proposed. In the ICU, TCD can be used as a dynamic tool to assess brain autoregulation. Taken together, all these roles further highlight the potential beneficial effect of TCD monitoring after TBI for daily clinical management.

Algorithm

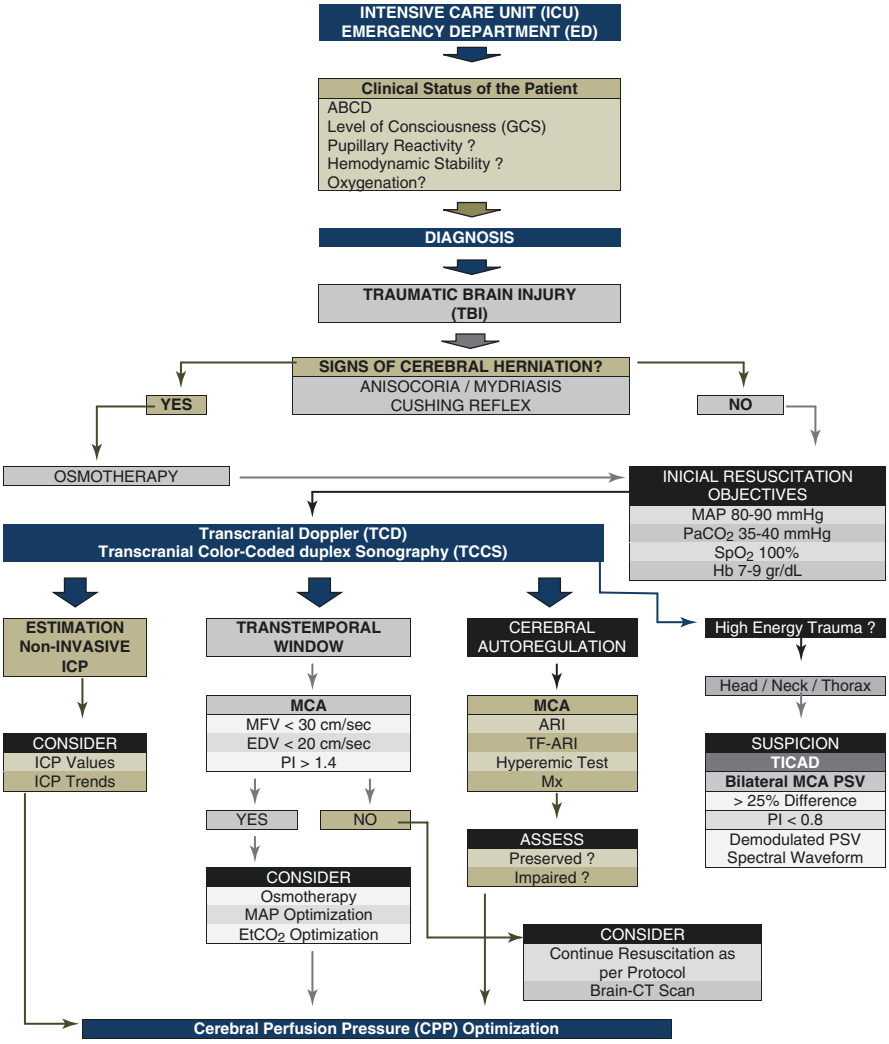

ABCD Airway-Breathing-Circulation-Disability, *PSV* Peak systolic Flow velocities, PI Pulsatility Index, *MCA* Middle cerebral artery, *MFV* Mean flow velocity, *EDV* End-Diastolic flow velocity, *ARI* Autoregulation index, *TF-AR* autoregulatory index by transfer function analysis, *Mx* Mean flow index, *MAP* Mean arterial pressure, *TICAD* Traumatic internal carotid dissection.

References

1. Maas A. Traumatic brain injury: changing concepts and approaches. Chin J Traumatol. 2016;19(1):3–6.
2. Maas AI, Stocchetti N, Bullock R. Moderate and severe traumatic brain injury in adults. Lancet Neurol. 2008;7(8):728–41.
3. Bouzat P, Sala N, Payen JF, Oddo M. Beyond intracranial pressure: optimization of cerebral blood flow, oxygen, and substrate delivery after traumatic brain injury. Ann Intensive Care. 2013;3(1):23.
4. Oddo M, Villa F, Citerio G. Brain multimodality monitoring: an update. Curr Opin Crit Care. 2012;18(2):111–8.
5. Coles JP. Regional ischemia after head injury. Curr Opin Crit Care. 2004;10(2):120–5.
6. Haacke EM, Duhaime AC, Gean AD, et al. Common data elements in radiologic imaging of traumatic brain injury. J Magn Reson Imaging. 2010;32(3):516–43.
7. White H, Venkatesh B. Applications of transcranial Doppler in the ICU: a review. Intensive Care Med. 2006;32(7):981–94.
8. Moppett IK, Mahajan RP. Transcranial Doppler ultrasonography in anaesthesia and intensive care. Br J Anaesth. 2004;93(5):710–24.
9. Bhatia A, Gupta AK. Neuromonitoring in the intensive care unit. I. Intracranial pressure and cerebral blood flow monitoring. Intensive Care Med. 2007;33(7):1263–71.
10. Saqqur M, Zygun D, Demchuk A. Role of transcranial Doppler in neurocritical care. Crit Care Med. 2007;35(5 Suppl):S216–23.
11. Lindegaard KF, Nornes H, Bakke SJ, Sorteberg W, Nakstad P. Cerebral vasospasm after subarachnoid haemorrhage investigated by means of transcranial Doppler ultrasound. Acta Neurochir Suppl (Wien). 1988;42:81–4.
12. Kalanuria A, Nyquist PA, Armonda RA, Razumovsky A. Use of Transcranial Doppler (TCD) ultrasound in the Neurocritical Care Unit. Neurosurg Clin N Am. 2013;24(3):441–56.
13. Vigue B, Ract C, Benayed M, et al. Early SjvO2 monitoring in patients with severe brain trauma. Intensive Care Med. 1999;25(5):445–51.
14. Bouzat P, Marques-Vidal P, Zerlauth JB, et al. Accuracy of brain multimodal monitoring to detect cerebral hypoperfusion after traumatic brain injury*. Crit Care Med. 2015;43(2):445–52.
15. Wintermark M, Chiolero R, van Melle G, et al. Relationship between brain perfusion computed tomography variables and cerebral perfusion pressure in severe head trauma patients. Crit Care Med. 2004;32(7):1579–87.
16. Tuor UI, Edvinsson L, McCulloch J. Catecholamines and the relationship between cerebral blood flow and glucose use. Am J Phys. 1986;251(4 Pt 2):H824–33.
17. Revell M, Porter K, Greaves I. Fluid resuscitation in prehospital trauma care: a consensus view. Emerg Med J. 2002;19(6):494–8.
18. Kroppenstedt SN, Kern M, Thomale UW, Schneider GH, Lanksch WR, Unterberg AW. Effect of cerebral perfusion pressure on contusion volume following impact injury. J Neurosurg. 1999;90(3):520–6.
19. Chan KH, Miller JD, Dearden NM. Intracranial blood flow velocity after head injury: relationship to severity of injury, time, neurological status and outcome. J Neurol Neurosurg Psychiatry. 1992;55(9):787–91.
20. van Santbrink H, Schouten JW, Steyerberg EW, Avezaat CJ, Maas AI. Serial transcranial Doppler measurements in traumatic brain injury with special focus on the early posttraumatic period. Acta Neurochir. 2002;144(11):1141–9.
21. Ract C, Le Moigno S, Bruder N, Vigue B. Transcranial Doppler ultrasound goal-directed therapy for the early management of severe traumatic brain injury. Intensive Care Med. 2007;33(4):645–51.
22. Ziegler D, Cravens G, Poche G, Gandhi R, Tellez M. Use of transcranial Doppler in patients with severe traumatic brain injuries. J Neurotrauma. 2017;34(1):121–7.

23. Tazarourte K, Atchabahian A, Tourtier JP, et al. Pre-hospital transcranial Doppler in severe traumatic brain injury: a pilot study. Acta Anaesthesiol Scand. 2011;55(4):422–8.
24. Brain Trauma F, American Association of Neurological S, Congress of Neurological S, et al. Guidelines for the management of severe traumatic brain injury. VII. Intracranial pressure monitoring technology. J Neurotrauma. 2007;24 Suppl 1:S45–54.
25. Klingelhofer J, Conrad B, Benecke R, Sander D, Markakis E. Evaluation of intracranial pressure from transcranial Doppler studies in cerebral disease. J Neurol. 1988;235(3):159–62.
26. Cardim D, Robba C, Donnelly J, et al. Prospective study on noninvasive assessment of intracranial pressure in traumatic brain-injured patients: comparison of four methods. J Neurotrauma. 2016;33(8):792–802.
27. Rasulo FA, Bertuetti R, Robba C, et al. The accuracy of transcranial Doppler in excluding intracranial hypertension following acute brain injury: a multicenter prospective pilot study. Crit Care. 2017;21(1):44.
28. Czosnyka M, Matta BF, Smielewski P, Kirkpatrick PJ, Pickard JD. Cerebral perfusion pressure in head-injured patients: a noninvasive assessment using transcranial Doppler ultrasonography. J Neurosurg. 1998;88(5):802–8.
29. Thornhill S, Teasdale GM, Murray GD, McEwen J, Roy CW, Penny KI. Disability in young people and adults one year after head injury: prospective cohort study. BMJ. 2000;320(7250):1631–5.
30. Marshall LF, Toole BM, Bowers SA. The National Traumatic Coma Data Bank. Part 2: patients who talk and deteriorate: implications for treatment. J Neurosurg. 1983;59(2):285–8.
31. Lobato RD, Rivas JJ, Gomez PA, et al. Head-injured patients who talk and deteriorate into coma. Analysis of 211 cases studied with computerized tomography. J Neurosurg. 1991;75(2):256–61.
32. Davis DP, Kene M, Vilke GM, et al. Head-injured patients who "talk and die": the San Diego perspective. J Trauma. 2007;62(2):277–81.
33. Stiell IG, Wells GA, Vandemheen K, et al. The Canadian CT Head Rule for patients with minor head injury. Lancet. 2001;357(9266):1391–6.
34. af Geijerstam JL, Britton M. Mild head injury - mortality and complication rate: meta-analysis of findings in a systematic literature review. Acta Neurochir. 2003;145(10):843–50. discussion 850
35. Fabbri A, Servadei F, Marchesini G, et al. Which type of observation for patients with high-risk mild head injury and negative computed tomography? Eur J Emerg Med. 2004;11(2):65–9.
36. Livingston DH, Lavery RF, Passannante MR, et al. Emergency department discharge of patients with a negative cranial computed tomography scan after minimal head injury. Ann Surg. 2000;232(1):126–32.
37. Thiruppathy SP, Muthukumar N. Mild head injury: revisited. Acta Neurochir. 2004;146(10):1075–82. discussion 1082-1073
38. Sifri ZC, Homnick AT, Vaynman A, et al. A prospective evaluation of the value of repeat cranial computed tomography in patients with minimal head injury and an intracranial bleed. J Trauma. 2006;61(4):862–7.
39. Brown CV, Zada G, Salim A, et al. Indications for routine repeat head computed tomography (CT) stratified by severity of traumatic brain injury. J Trauma. 2007;62(6):1339–44. discussion 1344-1335
40. Bouzat P, Francony G, Declety P, et al. Transcranial Doppler to screen on admission patients with mild to moderate traumatic brain injury. Neurosurgery. 2011;68(6):1603–9. discussion 1609-1610
41. Bouzat P, Almeras L, Manhes P, et al. Transcranial Doppler to predict neurologic outcome after mild to moderate traumatic brain injury. Anesthesiology. 2016;125(2):346–54.
42. Berne JD, Reuland KS, Villarreal DH, McGovern TM, Rowe SA, Norwood SH. Sixteen-slice multi-detector computed tomographic angiography improves the accuracy of screening for blunt cerebrovascular injury. J Trauma. 2006;60(6):1204–9. discussion 1209-1210

43. Schneidereit NP, Simons R, Nicolaou S, et al. Utility of screening for blunt vascular neck injuries with computed tomographic angiography. J Trauma. 2006;60(1):209–15. discussion 215-206
44. Biffl WL, Ray CE Jr, Moore EE, Mestek M, Johnson JL, Burch JM. Noninvasive diagnosis of blunt cerebrovascular injuries: a preliminary report. J Trauma. 2002;53(5):850–6.
45. Carrillo EH, Osborne DL, Spain DA, Miller FB, Senler SO, Richardson JD. Blunt carotid artery injuries: difficulties with the diagnosis prior to neurologic event. J Trauma. 1999;46(6):1120–5.
46. Fabian TC, Patton JH Jr, Croce MA, Minard G, Kudsk KA, Pritchard FE. Blunt carotid injury. Importance of early diagnosis and anticoagulant therapy. Ann Surg. 1996;223(5):513–22. discussion 522-515
47. Bruce LM, Croce MA, Santaniello JM, Miller PR, Lyden SP, Fabian TC. Blunt renal artery injury: incidence, diagnosis, and management. Am Surg. 2001;67(6):550–4. discussion 555-556
48. Biffl WL, Cothren CC, Moore EE, et al. Western Trauma Association critical decisions in trauma: screening for and treatment of blunt cerebrovascular injuries. J Trauma. 2009;67(6):1150–3.
49. Bromberg WJ, Collier BC, Diebel LN, et al. Blunt cerebrovascular injury practice management guidelines: the Eastern Association for the Surgery of Trauma. J Trauma. 2010;68(2):471–7.
50. Yang ST, Huang YC, Chuang CC, Hsu PW. Traumatic internal carotid artery dissection. J Clin Neurosci. 2006;13(1):123–8.
51. Bruns BR, Tesoriero R, Kufera J, et al. Blunt cerebrovascular injury screening guidelines: what are we willing to miss? J Trauma Acute Care Surg. 2014;76(3):691–5.
52. Romner B, Sjoholm H, Brandt L. Transcranial Doppler sonography, angiography and SPECT measurements in traumatic carotid artery dissection. Acta Neurochir. 1994;126(2–4):185–91.
53. Achtereekte HA, van der Kruijk RA, Hekster RE, Keunen RW. Diagnosis of traumatic carotid artery dissection by transcranial Doppler ultrasound: case report and review of the literature. Surg Neurol. 1994;42(3):240–4.
54. Bouzat P, Francony G, Brun J, et al. Detecting traumatic internal carotid artery dissection using transcranial Doppler in head-injured patients. Intensive Care Med. 2010;36(9):1514–20.
55. Lee JH, Kelly DF, Oertel M, et al. Carbon dioxide reactivity, pressure autoregulation, and metabolic suppression reactivity after head injury: a transcranial Doppler study. J Neurosurg. 2001;95(2):222–32.
56. Budohoski KP, Reinhard M, Aries MJ, et al. Monitoring cerebral autoregulation after head injury. Which component of transcranial Doppler flow velocity is optimal? Neurocrit Care. 2012;17(2):211–8.
57. Zeiler FA, Cardim D, Donnelly J, Menon DK, Czosnyka M, Smielewski P. Transcranial Doppler systolic flow index and ICP-derived cerebrovascular reactivity indices in traumatic brain injury. J Neurotrauma. 2018;35(2):314–22.
58. Tiecks FP, Lam AM, Aaslid R, Newell DW. Comparison of static and dynamic cerebral autoregulation measurements. Stroke. 1995;26(6):1014–9.
59. Liu X, Czosnyka M, Pickard JD, Varsos GV, Nasr N, Smielewski P. Derangement of cerebral blood flow autoregulation during intracranial pressure plateau waves as detected by time and frequency-based methods. Acta Neurochir Suppl. 2016;122:233–8.
60. Giller CA. A bedside test for cerebral autoregulation using transcranial Doppler ultrasound. Acta Neurochir. 1991;108(1–2):7–14.
61. Czosnyka M, Smielewski P, Kirkpatrick P, Menon DK, Pickard JD. Monitoring of cerebral autoregulation in head-injured patients. Stroke. 1996;27(10):1829–34.
62. Sorrentino E, Budohoski KP, Kasprowicz M, et al. Critical thresholds for transcranial Doppler indices of cerebral autoregulation in traumatic brain injury. Neurocrit Care. 2011;14(2):188–93.

Chapter 42
Sickle Cell Disease (SCD): Usefulness of Transcranial Doppler (TCD/TCCS) Monitoring

Juan Fernando Gómez Castro

Key Points

1. Acute stroke in patients with sickle cell disease (SCD) is a major complication and generates irreversible sequelae.
2. The pathophysiological mechanisms that lead to stroke are defined in SCD, some of which are potentially reversible and have key implications for prevention.
3. The different neurodiagnostic strategies in SCD seek to estimate the risk of acute stroke and have been key to its prevention.
4. Transcranial Doppler (TCD/TCCS) is the most widely used tool in the assessment of acute stroke risk in children with SCD, with clear indications as well as advantages over other diagnostic alternatives.
5. The existing recommendations for the performance and interpretation of TCD in SCD are defined. However, some technical aspects such as its use in older individuals are subject to investigation.

42.1 Introduction

Transcranial Doppler (TCD) is an ultrasound technique that, by using a low-frequency transducer applied to an acoustic window (head and/or neck), allows rapid, noninvasive, real-time detection of flow velocities in the basal cerebral arteries (circle of Willis) in different cerebrovascular diseases and traumatic brain injuries [1].

Another important advantage of TCD is to provide a continuous monitoring of cerebral hemodynamics, and for this reason TCD has become a very useful tool in ICU settings [2], with well-defined roles in the early identification and management of certain brain pathologies, such as vasospasm after posttraumatic subarachnoid

J. F. G. Castro (✉)
Pediatric Neurology Department, Hospital Universitario Valle del Lili, Cali, Colombia
e-mail: jfgomezcastro@gmail.com

C. N. Rodríguez et al. (eds.), *Neurosonology in Critical Care*,
https://doi.org/10.1007/978-3-030-81419-9_42

hemorrhage or after rupture of aneurysms, as well as the assessment of hemodynamic changes after acute stroke. Equally important applications include the detection of microembolic signals during cardiopulmonary bypass or in right-to-left cardiac shunts, as well as cerebral hemodynamics assessment in suspected brain death.

Despite its multiple applications, the use of TCD is still limited because it requires intensive training and appropriate equipment [3]. Moreover, its predictive accuracy should be improved, especially when combined with other physiological monitoring techniques such as EEG, cerebral tissue oxygen monitoring, and cerebral microdialysis. This would allow the validation of new criteria and critical values for conditions such as vasospasm, among others [4].

TCD/TCCS has proven to be an excellent diagnostic tool also in children, with some limitations specific to this group [5, 6]. There is one condition, namely SCD, in which TCD/TCCS has proven to be useful as a predictive tool of cerebrovascular complications (CVS) becoming an integral part of the guidelines for the approach and management of children affected by this disease.

42.2 Sickle Cell Disease (SCD)

In its homozygous form, SCD is one of the leading causes of acute ischemic stroke (AIS) in children, with a risk 410 times greater than the general population, and the consequent high prevalence of associated disability and mortality (10% of total deaths in SCD and a reduction of approximately 25 years in life expectancy) [7–9]. However, there are differences between the frequency of this complication according to the genotypes of hemoglobinopathy ¨S¨ present, being approximately 6 times lower in patients with sickle cell trait or sickle cell/thalassemic trait, when compared to the homozygous form of the disease [10].

In homozygous individuals for the “allele B” gene responsible for the synthesis of hemoglobin B chain, the formation of hemoglobin “SS” occurs, which, in conditions of low oxygenation, metabolic acidosis, or dehydration, polymerizes irreversibly changing the structure of the erythrocyte that contains it, leading to a defective function (ineffective oxygenation, inflammation of the vascular endothelium, and all subsequent events of the disease) [11]. The process of polymerization of the defective hemoglobin also leads, through its interaction with the endothelium and the various inflammatory cascades, to progressive vascular occlusion, which is ultimately responsible for events such as painful crises, acute chest syndrome, splenic sequestration, CVC, etc. (vaso-occlusive crisis).

Several studies have determined the overall incidence for the first AIS according to age, being lower for pediatric patients in the under-2 year group, higher between 2 and 5 years, and remaining high but stable from 6 to 29 years of age [12]. Those affected have been found to be at increased risk of AIS recurrence after the first event [13]. Environmental or personal factors such as low socioeconomic or

educational status in the child's social environment [14], and male gender [15] further contribute to the vulnerability of sickle cell patients to these and other complications.

42.3 Sickle Cell Disease: Pathophysiology

There are a number of conditions specific to SCD that increase the risk of vascular occlusion and therefore CVC, including [16].

1. Chronic hypoxia (associated with decreased oxygen saturation and/or decreased hemoglobin)
2. Occlusive cerebral vasculopathy acting simultaneously with increased blood flow, due to anemia and increased hemoglobin S which in turn decreases the cerebrovascular reserve
3. Increased metabolic demand on the brain, associated with fever or infection
4. Presence of previous ischemic brain injury, which increases risk, even in spite of appropriate management
5. Sudden increases in hemoglobin, associated with transfusion therapy
6. Cardiovascular risk factors common to the general population

These factors interact dynamically in the microcirculation, as shown in (Fig. 42.1).

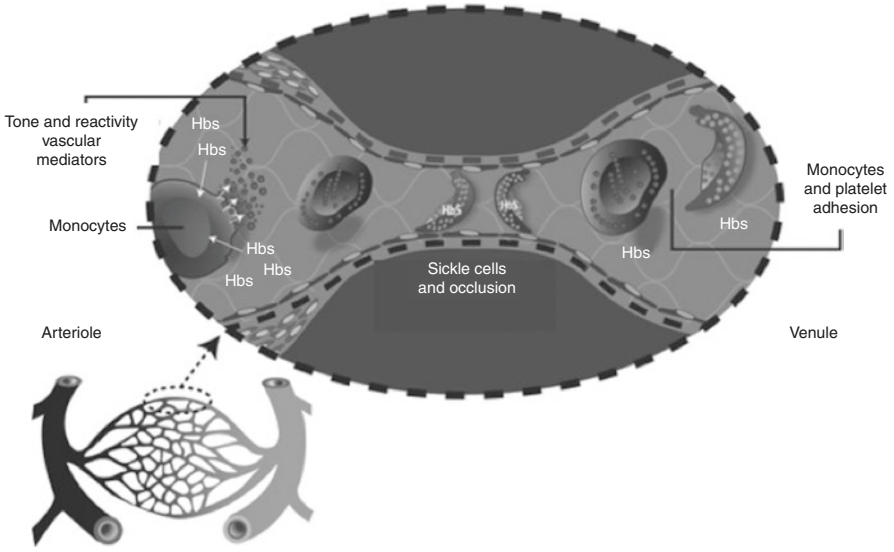

Fig. 42.1 Pathophysiology of capillary vascular occlusion in sickle cell disease

However, this series of events is not entirely applicable to explain the vascular occlusion observed in the large arteries of the cerebral circulation. Therefore, explanatory models have been devised that fuse these concepts of microvascular lesion as the events that lead to endothelial injury and, over time, progressive occlusion of the main cerebral vessels [17]. In these models, it is presumed that a number of molecules, including inflammation mediators, adhesion mediators, growth factors, and vascular reactivity among others, promote the activation and adhesion of leukocytes and platelets; which in turn activate or damage the cells of the large vessel endothelium, being replaced by vascular smooth muscle cells that migrate and proliferate uncontrollably along with the inflammatory and adhesion cascade described, to finally lead to a slow and progressive narrowing of the vascular lumen that can be detected by TCD/TCCS and which, if not reversed, will lead to an acute vascular occlusion (vascular-occlusion crisis). These models also suggest that early management before complete occlusion is generated and symptoms appear can gradually and progressively reverse the occlusion in the large cerebral vessels.

42.4 Cerebrovascular Complications (CVC): Estimation of Risk

Knowledge and understanding of CVC in SCD emphasizes the importance of estimating risk in affected children. Early therapeutic interventions such as chronic red blood cell transfusion have been shown to be useful in preventing CVC and/or recurrences of CVC [18]. Primary prevention depends on finding a way to identify as many individuals as possible who are at risk and potentially benefit from the treatments described.

To this end, some risk factors have been identified: (a) a lower hemoglobin value and (b) history of transient ischemic events or acute chest syndrome, among others. However, none of these factors have allowed the generation of a predictive model applicable to clinical risk assessment for CVC [19].

Brain imaging studies were initially considered as a good alternative. They would allow a direct visualization of the brain parenchyma (MRI) or blood vessels (angiography and/or angio-MRI). However, their use has proven impractical in children because they are either invasive or require anesthesia. Moreover, MRI, documenting cerebral infarctions, even if asymptomatic, is contrary to the preventive purpose of these studies [19, 20].

The above analysis and the obvious advantage of identifying intracerebral vessel stenosis made evident the application and usefulness of TCD/TCCS in estimating the risk of CVC.

The STOP trials provided evidence that TCD/TCCS is the method of choice for staging specific risk of CVC and indicating an appropriate management in each case.

42.5 Role of Doppler – STOP Trials

Despite the advantages of ultrasound over MRI or angio-MRI, it was necessary to demonstrate that this tool had similar or superior utility in establishing the degree of vascular stenosis/occlusion associated with CVC.

TCD/TCCS was chosen over cervical Doppler, since most vascular occlusions are found in the proximal segments of the middle cerebral artery (MCA), whereas the internal carotid artery is rarely involved in SCD [19]. Therefore, blood flow velocities of MCA were measured through population sampling; (a) healthy children and (b) SCD children without previous CVC history. This allowed the collection of flow velocity ranges in different clinical scenarios, correlating critical values of ultrasound flow velocities with the presence of severe stenosis/occlusion as documented by angio-MRI (Table 42.1) [21].

For patients with blood flow velocities suggestive of severe stenosis/occlusion, a higher risk of CVC was demonstrated at 12 months, than in other groups. This allowed to establish a CVC risk classification, according to the values of MCA velocities measured by TCD [22]:

(a) Low risk: <170 cm/s
(b) Moderate risk: 170–199 cm/s
(c) High risk: >200 cm/s

The STOP trial was conducted looking at the prevention of CVC in children with SCD. It was conducted in 14 centers in several countries over approximately 5 years. This trial was terminated prematurely because high-risk children were found to have a higher incidence of CVC when they were not given regular transfusions, compared to those who were given regular transfusions (greater than 90% reduction in risk when chronic transfusion was indicated by estimating the risk of CVC). This allowed the scientific associations to recommend research with TCD as well as prophylactic transfusion in cases of high risk due to altered flow rates [22–24].

A second clinical trial, STOP II, was conducted to evaluate the clinical and ultrasound behavior in children who were withdrawn from transfusion therapy after documenting improvement in flow rates in MCAs (approximately 50% went to low risk and 17% to moderate risk with the use of chronic transfusions). Again this trial

Table 42.1 Blood flow velocities values in the MCA

Cerebral blood flow velocity values	
Healthy child	79 cm/s ± 13
Child with SCD without stenosis/occlusion	133 cm/s ± 19
Child with SCD with severe stenosis/occlusion	190 cm/s
Child with SCD with critical stenosis/occlusion	<70 cm/s

SCD sickle cell disease

was stopped, when it was found that most of the children who were withdrawn from transfusions returned to high risk for CVC due to a rapid increase in flow rates detected by TCD, while those who continued transfusion therapy remained at low or moderate risk.

What was evident after the STOP I and STOP II studies was the change in morbidity and mortality rates due to CVC in children with SCD. This remarkable result was achieved by TCD, which since then has been incorporated into the protocols for periodic assessment in children with SCD, because it was recognized as one of the most effective tools for prevention and stratification of CVC [25]. Further surveillance has showed sustained lower incidence of AIS among patients with available follow-up implemented, and resurgence of CVC in whom protocols had not been properly implemented for diagnosis or treatment decisions [26].

An additional clinical trial, TCD with Transfusions Changing to Hydroxyurea (TWiTCH) [27], has compared chronic transfusions with the use of hydroxyurea as a measure to prevent CVC, and it has shown that this therapeutic intervention is as effective as chronic transfusion therapy in preventing deterioration in blood flow rates measured by TCD, as well as avoiding CVC. Benefits of hydroxyurea have also been proved using TCD, showing reduced TCD velocities and prevention of primary AIS using lower doses of medication than those used in STOP protocols [28]. Unexpected findings like a lower rate of TCD abnormalities for selected ethnic groups, as compared with values internationally reported, have been useful for raising questions about the need for identifying another risk factor and its importance through specific populations [29].

42.6 Detection of Cerebrovascular Complications: Limitations of TCD/TCCS

Despite the value of the TCD in the assessment of patients at risk of CVC and SCD, its universal application has not been possible, even in centers that participated in the original clinical trials [25]. This is due to institutional limitations in following established protocols, as well as difficulties in locating and monitoring patients, not only during childhood, but also in the transition period toward adulthood. In addition to these circumstances, which are inevitable even in more efficient health systems than ours, there are factors specific to the TCD procedure that deserve to be analyzed in order to avoid them in daily practice:

1. *Inadequate results:*
   These refer to those TCD where it is not possible to accurately measure the flow rate in the main vessels. The prevalence of this difficulty ranges from 8 to 16% and has a bimodal presentation.

   1.1 More frequent in children under 3 (due to poor cooperation from the child) and those over 16 (due to inadequate bone window).

1.2 The use of portable equipment for TCD also influences the difficulty in detecting measurable flow rates.
1.3 The presence of prior CVC is another circumstance that generates inadequate results, and it is for this reason, among others, that risk values for TCD results in patients with a history of such a complication cannot be estimated, since their outcome would not be interpretable based on existing protocols [30].

2. *Techniques:*
These include comparing TCD not associated with vascular imaging with TCCS, which is a common variation from original protocols of the STOP study [31]. Although the benefits of adequate measurement would seem obvious when using a technique that adds visualization of the vessel being studied, the velocities collected by TCCS have shown to be only slightly lower: approximatetly 9% for MCA and 10% for the distal internal carotid [32]. In short, the sonographer's experience should guide the choice of the different modality, TCD or TCCS, taking into account these small differences.
3. *Velocities:*
Some controversy has arisen as to whether risk values should be set according to the mean peak flow velocity or peak systolic velocity data, since this value is more commonly used in TCD/TCCS equipment, particularly TCCS. Although there are trials that have sought to match the values of both measurements and the risk prediction described in the STOP studies [33], to date no modifications have been made to the existing protocols, so the mean flow velocity value should be recorded and reported. If the TCD/TCCS equipment does not incorporate such a measurement, it can be extrapolated using the following formula:

$$\mathrm{MFV} = \left(\mathrm{PSV} - \mathrm{EDV}\right)/3 + \mathrm{EDV}$$

4. *Comparison of utility against other techniques:*
Despite benefits of TCD over brain MRI or angio-MRI (as discussed before), there are some settings where these techniques can be useful, such as inadequate or incomplete TCD assessment, and the fact that TCD is operator-dependent and therefore not allowed to second-reading or interpretation. Angio-MRI is also a tool to identify brain silent infarcts, even for patients without any vascular abnormalities or when TCD results are in low-risk values [34], which need to be kept in consideration for patients with long-term transfusions for SCD [35]. Correlations between TCD and hematologic test such as traditional hematocrit, red cell distribution width (RDW), or new techniques like red blood cell rigidity may provide more accurate pictures of the patient blood/vascular status rather than the blood viscosity alone and could be a future tool for the detection of stroke risk among SCD patients who cannot gain access even to a test like TCD ultrasound [36].

5. *Long-term follow-up / adults:*
   The role of TCD/TCCS has been evaluated in the follow-up of SCD patients, once the risk has been defined as well as the need for long-term management with transfusion therapy or other interventions. This affirmation, however, posts several points to consider. First, there is evidence of low adherence to periodic TCD, especially for patients seen first at the emergency department [37], therefore there is an opportunity for increased screening as to whether new efforts point toward recruiting new patients and continue educating personnel at these specific clinical settings [38].

   Secondly, although the risk of ischemic cerebrovascular disease (CVD) persists low over time, it has been documented that vasculopathy associated with SCD does not always regress and may even worsen in the adult, as shown by angio-MRI [39, 40]. The formation of multiple vessel stenoses and/or aneurysms/pseudoaneurysms, the higher rate of hemorrhagic CVC as well as the lack of established "risk" values for such a complication in the adult limit the application of TCD/TCCS measurements in this age group [41]. This opens up an opportunity to carry out clinical trials in the adult population in order to correlate mean flow velocity (MFV) values with risk of the different types of CVC, as well as studies to measure the impact that new drugs such as hydroxyurea might have on the paraclinical variables and final outcomes.

42.7 Conclusion

TCD/TCCS has proven to be a very reliable, easy-to-use, and cost-effective tool in pediatric SCD patients, providing risk stratification for CVD and indicating proper management. TCD/TCCS monitoring is also crucial for verifying treatment efficacy and disease modifications (new stenosis, worsening of known stenosis, etc.) during follow-up.

Algorithm

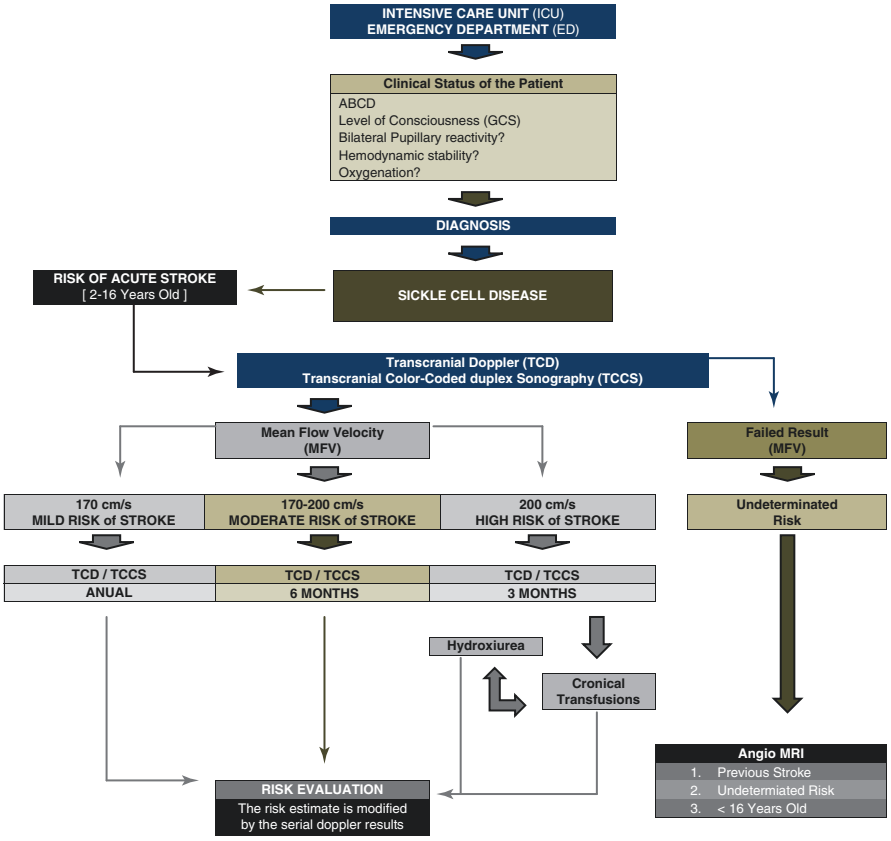

References

1. Antonello D, et al. Transcranial Doppler ultrasound: physical principles and principal applications in Neurocritical Care Unit. J Cardiovasc Echogr. 2016;26(2):29–41.
2. Saqqur M, et al. Role of transcranial Doppler in neurocritical care. Crit Care Med. 2007;35(5 Suppl):S216–23.
3. Bulas D, et al. Transcranial Doppler: applications in neonates and children. Ultrasound Clin. 2009;4:533–51.
4. Naqvi J, et al. Transcranial Doppler ultrasound: a review of the physical principles and major applications in critical care. Intl J Vasc Med. 2013;1:1–13.
5. Winkler P, et al. Major Pitfalls in Doppler investigations, with particular reference to the cerebral vascular system. Pediatr Radiol. 1990;20:219–28.
6. Fujioka K, et al. Anatomy and free hand examination techniques. In: Newell D, editor. Transcranial Doppler. New York: Raven Press; 1992. p. 9–31.

7. Switzer J, et al. Pathophysiology and treatment of stroke in sickle-cell disease: present and future. Lancet Neurol. 2006;5:501–12.
8. Gladwin MT, et al. Cardiovascular complications and risk of death in sickle-cell disease. Lancet. 2016;387:2565–74.
9. Rodrigues D, et al. Genetic determinants and stroke in children with sickle cell disease. J Pediatr (Bra). 2016;92(6):602–8.
10. Ohene-Frempong K, et al. Cerebrovascular accidents in sickle cell disease: rates and risk factors. Blood. 1998;91(1):288–29.
11. Conran N, et al. Newer aspects of the pathophysiology of sickle cell disease vaso-occlusion. Hemoglobin. 2009;33:1–16.
12. Balkaran B, et al. Stroke in a Cohort of patients with homozygous sickle cell disease. J Pediatr. 1992;120:360–6.
13. Powars D, et al. The natural history of stroke in sickle cell disease. Am J Med. 1978;65:461–71.
14. Sabarense A, et al. Characterization of mortality in children with sickle cell disease. J Pediatr (Bra). 2015;91:242–7.
15. Golomb M, et al. International Pediatric Stroke Study Group. Male predominance in childhood ischemic stroke. Stroke. 2009;40:52–7.
16. DeBaun M, et al. Central nervous system complications and management in sickle cell disease. Blood. 2016;127(7):829–83.
17. Platt O, et al. Preventing stroke in sickle cell anemia. N Engl J Med. 2005;353(26):2743–5.
18. Russell M, et al. Effect of transfusion therapy on arteriographic abnormalities and on recurrence of stroke in sickle cell disease. Blood. 1984;63(1):162–9.
19. Adams R. Big Strokes in Small Persons. Arch Neurol. 2007;64(11):1567–74.
20. Pavlakis S, et al. Brain infarction in sickle cell anemia: magnetic resonance imaging correlates. Ann Neurol. 1988;23(2):125–30.
21. Adams R, et al. Transcranial Doppler correlation with cerebral angiography in sickle cell disease. Stroke. 1992;23(8):1073–7.
22. Goldstein L, et al. Primary prevention of ischemic stroke: a statement for healthcare professionals from the Stroke Council of the American Heart Association. Stroke. 2001;32(1):280–99.
23. Adams R, et al. Stroke prevention trial in sickle cell anemia. Control Clin Trials. 1998;19(1):110–29.
24. Fullerton H, et al. Declining rates in Californian children with sickle cell disease. Blood. 2004;104(2):336–9.
25. Adams R, et al. Transcranial doppler re-screening of subjects who participated in STOP and STOP II. Am J Hematol. 2016;91:1191–4.
26. Kwiatkowski J, et al. Ischemic stroke in children and young adults with sickle cell disease in the post-STOP era. Am J Hematol. 2019;94:1335–43.
27. Ware R, et al. Hydroxycarbamide versus chronic transfusion for maintenance of transcranial doppler flow velocities in children with sickle cell anaemia - TCD With Transfusions Changing to Hydroxyurea (TWiTCH): a multicentre, open-label, phase 3, non-inferiority trial. Lancet. 2016;387:661–70.
28. Opoka R, et al. Hydroxyurea to lower transcranial Doppler velocities and prevent primary stroke: the Uganda NOHARM sickle cell anemia cohort. Haematologica. 2020;105(6):e272–5.
29. Wali Y, et al. Distribution of sickle cell disease and assessment of risk factors based on transcranial Doppler values in the Gulf region. Hematology. 2020;25(1):55–62.
30. Greenwood S, et al. The significance of inadequate transcranial Doppler studies in children with sickle cell disease. PLoS One. 2017;12(7):e0181681.
31. Schlenz A, et al. Practice patterns for stroke prevention using transcranial Doppler in sickle cell anemia: DISPLACE Consortium. atr Blood Cancer. 2020;67:e28172.
32. Bulas D, et al. Transcranial Doppler (TCD) screening for stroke prevention in sickle cell anemia: pitfalls in technique variation. Pediatr Radiol. 2000;30(11):733–8.
33. Jones A, et al. Can peak systolic velocities be used for prediction of stroke in sickle cell anemia? Pediatr Radiol. 2005;35(1):66–72.

34. Alshehri E, et al. The role of MRA in pediatric sickle cell disease with normal transcranial Doppler imaging velocities. J Stroke Cerebrovasc Dis. 2020;29(7):104864.
35. Estcourt L, et al. Interventions for preventing silent cerebral infarcts in people with sickle cell disease. Cochrane Database Syst Rev. 2020;4:CD012389.
36. Cardoso A. An experimental erythrocyte rigidity index (Ri) and its correlations with Transcranial Doppler velocities (TAMMV), Gosling Pulsatility Index PI, hematocrit, hemoglobin concentration and red cell distribution width (RDW). PLoS One. 2020;15(2):e0229105.
37. Weisman J, et al. Transcranial Doppler screening adherence among children with sickle cell anemia seen in the emergency department. J Pediatr. 2019;10:1–5.
38. Inusa B, et al. An educational study promoting the delivery of transcranial Doppler ultrasound screening in paediatric sickle cell disease: a European Multi-Centre Perspective. J Clin Med. 2020;9:44.
39. Seibert J, et al. Transcranial Doppler, MRA and MRI as a screening examination for cerebrovascular disease in patients with sickle cell anemia: an 8 year study. Pediatr Radiol. 1998;28(7):546.
40. Sheehan V, et al. Transcranial Doppler velocity and brain MRI/MRA changes in children with sickle cell anemia on chronic transfusions to prevent primary stroke. Pediatr Blood Cancer. 2013;60(9):1499–502.
41. Silva G, et al. Brain magnetic resonance imaging abnormalities in adult patients with sickle cell disease: correlation with transcranial Doppler findings. Stroke. 2009;40(7):2408–12.

Part IV
Neurosonology: Beyond Usual Monitoring

Chapter 43
Comatose Patient in ICU: Early Resuscitation Guided by Transcranial Doppler (TCD/TCCS)

Francisco Tamagnone and Ezequiel Luna

Key Points

1. Coma is a serious, multifactorial pathology that must be treated adequately and promptly. Therefore, after the initial medical stabilization, practitioners must find the cause to guide the therapy.
2. Transcranial Doppler (TCD)/transcranial color-coded duplex sonography (TCCS) are tools that may be useful in these comatose patients to estimate intracranial pressure (ICP), cerebral blood flow (CBF), and cerebral perfusion pressure (CPP) and to make a diagnosis of brain death.
3. Most of these pathologies are accompanied, as an underlying physiopathological mechanism, by an increase in intracranial pressure (ICP), through ischemia, edema, and herniation of encephalic structures. Therefore, TCD/TCCS could show us patterns of hypoperfusion (PI > 1,4 and EDV <20 cm/s) and thus gives us the opportunity to intervene in real time, minimizing secondary brain injury.
4. We propose to perform ultrasound-guided cerebro-cardiovascular resuscitation (US-CCaRE), with the aim of decreasing the extent of secondary injury and thus improve the prognosis of patients with cerebral hypoperfusion ([US-CCaRE]: English adaptation of the spanish acronym RECCUS).

F. Tamagnone (✉)
Intensive Care Medicine, Critical Care Ultrasound, University of Buenos Aires (UBA), Buenos Aires, Argentina

Bernardino Rivadavia Hospital, Buenos Aires, Argentina
e-mail: franciscotamagnone@hotmail.com

E. Luna
Intensive Care Medicine, Sanatorio Güemes, Buenos Aires, Argentina

University of Buenos Aires (UBA), Buenos Aires, Argentina

C. N. Rodríguez et al. (eds.), *Neurosonology in Critical Care*,
https://doi.org/10.1007/978-3-030-81419-9_43

43.1 Introduction

Disorders of consciousness, particularly coma, can be a reason for admission and a complication in the intensive care unit (ICU). Coma can be defined as the absence of eye opening or wakefulness and verbal or motor response for at least 1 hour [1].

The ascending reticular activating system (ARAS) is responsible for the waking state while the cerebral cortex and its subcortical connections are responsible for the consciousness state. For a coma to occur, the function of the ARAS or the cerebral cortex must be impaired or altered bilaterally [1].

Alterations in consciousness such as coma are serious conditions that must be treated appropriately and quickly (Fig. 43.1). The great challenge that this entity represents is that it can be caused by multiple causes of traumatic and nontraumatic origin [3] (Table 43.1).

Therefore, intensive care and emergency department physicians must act quickly. First, stabilize the patient, following the ABCDE international guidelines [4–6], and then arrive at a diagnosis of certainty in order to provide the patient with adequate treatment.

43.2 Neurological Exam in Coma: Usefulness?

The neurological examination is important for the localization and identification of the cause of coma. Serial examinations to assess dynamic changes are equally important. Systematic vital signs assessments and neurologic checks are the norm in patients admitted to the ICU. We recommend the use of standardized scales to assess disorders of consciousness (i.e., GCS or FOUR).

Many times, this step in the evaluation of the coma patient is impossible to perform in the ICU and ED. In this clinical scenario, the presence of a noninvasive neuromonitoring tool such as TCD/TCCS is useful for the assessment of intracerebral hemodynamic status for real-time resuscitation decisions.

We must consider that these patients suffer a primary injury and then are vulnerable to increased damage as a result of the secondary Injury such as ischemia, edema, or cerebral metabolic disorders.

Traumatic brain injury (TBI) is an important cause of coma. Mortality in these patients is approximately 30% [7]. Of the survivors, only 25% regain long-term

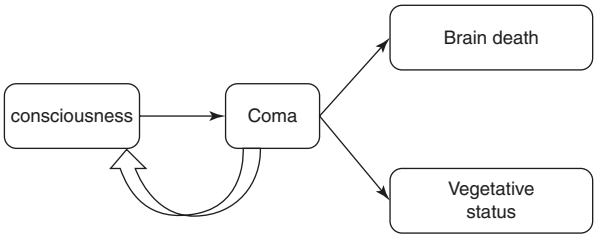

Fig. 43.1 Clinical evolution of coma

Table 43.1 Causes of coma

Traumatic causes	
Traumatic brain injury (TBI)	
Nontraumatic Causes	
Hyponatremia/hypernatremia	Elevated intracranial pressure
Hypercalcemia	Strokes
AKI >> uremia	Anoxic/hypoxic injury
Acute liver failure (ALF)	Subdural hematoma
Hyperammonemia	Hydrocephalus
Intoxications	CNS infection
Hypothermia/hyperthermia	NCSE/seizures
Hypercapnia	Sepsis
Hyperthyroid/hypothyroid state	Hypoglycemia
Sedatives/anesthetics/opioids	Hyperglycemia/ketoacidosis
AEDs/antipsychotic/hypnotics	Methemoglobinemia
Carbon monoxide poisoning	Herbicides/pesticides/rodenticides

NCSE nonconvulsive status epilepticus, *AKI* acute kidney injury, *CNS* central nervous system, *AEDs* antiepileptic drugs

functional independence [8–10] and 5–15% are discharged in a vegetative state, where only 50% regain consciousness with some neurological sequelae [9–11].

For patients in nontraumatic coma, the evidence is more heterogeneous. Some series place mortality between 25 and 48% [12, 13], others between 25 and 87% depending on the study and its cause. Overall, these studies show that acute ischemic stroke (AIS) is the cause of coma with the highest mortality (60–95%), followed by post-cardiorespiratory arrest anoxia-hypoxia injury (54–89%), and with the lowest mortality rates being intoxications / poisoning (0–7%) and nonconvulsive epileptic status (NCSE) (0–10%) [2].

Some causes of coma are reversible and have low morbidity and mortality, while others have a poor prognosis. Salahuddin et al. [14], in a prospective trial, included patients who, after showing resolution of their underlying pathology, remained in a coma after 48 hours off sedation. They underwent a brain CT scan, and the optic nerve sheath diameter (ONSD) was measured for signs of intracranial hypertension (IHT). Of the 102 patients included, 31 (30%) showed signs of IHT on CT scan. This group did not receive adequate treatment in a timely manner, which worsened their prognosis.

For all the above reasons, it is very useful to have a method that allows us to assess, in this group of patients, whether the estimated cerebral blood flow (by measuring the flow velocities in the intracerebral arteries) is adequate for the patient's clinical condition. The aim is to avoid, in real time, situations of ischemia or hyperemia.

43.3 TCD/TCCS: Neuromonitoring Tool

Some of the benefits of TCD/TCCS within the neuromonitoring of comatose patients are as follows:

(a) Noninvasive intracranial pressure (ICP) estimation

(b) Cerebral blood flow velocities measurement
(c) Noninvasive cerebral perfusion pressure (CPP) estimation
(d) Brain death determination

43.3.1 Noninvasive Intracranial Pressure (nICP) Estimation

We can estimate nICP by ultrasound, using the formula described by **Bellner**: (Eq. 43.1)

$$\text{ICP} = 10.93 \times \text{Pulsatility Index}\left[\text{PI}\right] - 1.28. \tag{43.1}$$

Equation (43.1) shows an important relationship between nICP and PI [15].

When the ICP starts to rise, the first variable to alter is the PI which rises >1.6 [15], then the end-diastolic flow velocity (EDV) falls, and finally the mean flow velocity (MFV). If the increase in ICP continues, the patterns of cerebral circulatory arrest will begin to appear (Fig. 43.2):

1. Reverberant blood flow
2. Systolic spike
3. Absence of flow

Another ultrasound method that can estimate noninvasive ICP is the measurement of the optic nerve sheath diameter (ONSD); this technique will be discussed in the corresponding chapter.

43.3.1.1 Pulsatility Index

It is important to keep in mind that PI does not depend exclusively on cerebral vascular resistance (CVR) but is the result of an interrelation of some variables such as: cerebral perfusion pressure (CPP), blood pressure pulse amplitude (A_1), cerebral vascular resistance (CVR), and cerebrovascular compliance (Ca).

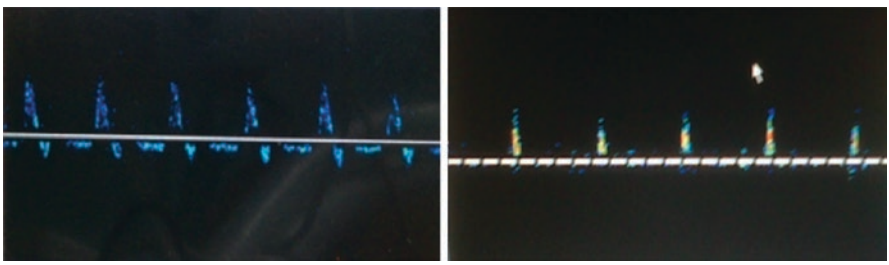

Fig. 43.2 Spectral Doppler (TCD): Left: Reverberant blood flow; Right: Systolic spikes

For this reason, some authors point out the possibility of obtaining an inverse, nonlinear relationship between CPP and PI, using the Doppler spectral PI to interpret the clinical situation. This is defined as the first harmonic of the flow velocity pulse wave divided by the mean flow velocity. The following relationship between PI and CPP is proposed [17, 20] (Eq. 43.2):

$$\mathrm{PI} = A_1 / \mathrm{CPPm} \times \left[\sqrt{\left(\mathrm{CVR} \times \mathrm{Ca}\right)^2 \times \mathrm{HR}^2 \times \left(2\pi\right)^2 + 1} \right] \tag{43.2}$$

PI: pulsatility index, A_1: first harmonic of arterial blood pressure, CPPm: media of cerebral perfusion pressure, CVR: cerebrovascular resistance, Ca: cerebral arteries compliance, HR: heart rate.

Although these measurements do not have sufficient evidence to replace invasive ICP monitoring, which is the gold standard, they are very useful complementary monitoring and estimation tools at the bedside of the critical patient when invasive monitoring is contraindicated or not available.

43.3.2 Intracranial Blood Flow Velocities Measurement

We can analyze the flow waveform in the arteries of the circle of Willis, especially the middle cerebral artery (MCA), evaluating their changes and morphology in real time. The classic MCA waveform has a low resistance pattern (Fig. 43.3).

43.3.3 Noninvasive Cerebral Perfusion Pressure (CPP) Estimation

Cerebral perfusion pressure (CPP) can also be estimated by this noninvasive monitoring technique. It depends on the ICP and mean arterial pressure (MAP); therefore, any factor that alters this relationship, increased ICP and/or decreased MAP, puts patients at risk of developing cerebral ischemia.

These alterations in CPP generate changes in the cerebral blood flow estimated by TCD/TCCS, with a decrease in the end-diastolic blood flow velocity (EDV) and a stable peak systolic blood flow velocity (PSV), increasing the value of the PI. Czosnyka et al. [16] developed a formula to estimate CPP (Eq. 43.2), which, although it has limitations to predict the value of CPP, allows us to objectify ¨real time¨ changes and take immediate action for their optimization.

Equation descripted by **Czosnyka**: (Eq. 43.3)

$$\mathrm{CPP} = \mathrm{MAP} \times \left(\mathrm{EDV} / \mathrm{MFV}\right) + 14 \tag{43.3}$$

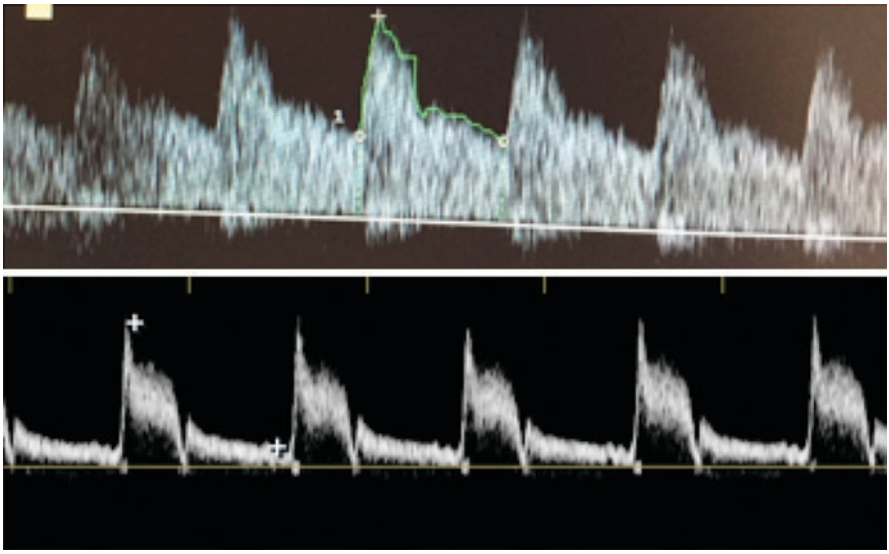

Fig. 43.3 UP: Spectral Doppler waveform of MCA (low resistance spectral pattern). Down: Spectral Doppler waveform of external carotid artery (ACE) (high resistance spectral pattern)

Descripted by **Belfort**: (Eq. 43.4)

$$\mathrm{CPP} = \left(\mathrm{MFV} / \mathrm{EDV}\right) \times \left(\mathrm{MAP} / \mathrm{DAP}\right) \tag{43.4}$$

CPP values below 60 mmHg should alert us; however, values above 60 mmHg cannot always be interpreted as safe for all patients.

In a study, da Riva et al. [17] showed that PI correlates better with CPP than with ICP values. Other authors also observe a good relationship between PI and CPP, especially when the latter falls below 70 mmHg [18].

Ursino et al. [19] used a mathematical model to observe the behavior of CPP with respect to flow rate. In patients with CPP > 70 mmHg, there is no decrease in the MFV, but when the CPP values begin to decrease, the PI increases. When CPP is between 40 and 70 mmHg, the MFV begins to decrease while the PI continues to increase. With CPP values below 40 mmHg, the MFV starts to decrease rapidly while the PI increases. These changes occur due to increases in the ICP and decreases in the MAP.

It is important to bear in mind that all of the above methods have their limitations and are not intended to replace invasive ICP measurement. However, they would allow us, in the case of not having the possibility of invasive ICP measurement, which is contraindicated or in pathologies without clear indication of invasive ICP monitoring, to obtain a parameter that can guide us in making decisions at the bedside of the critically ill patient.

In the Van Santbrink et al. trial [21], where patients with severe TBI were monitored early with TCD/TCCS, it was shown that the lowest mean MFV of MCA were

observed in the first 8 h of trauma. The decrease in MFV was accompanied by an increase in PI, where this group showed the worst evolution.

Vigué et al. [22] observed that in patients with severe TBI, 7 h elapsed from the time of trauma to the start of neurological monitoring, where it was initially performed with jugular bulb venous oxygen saturation ($SjvO_2$). In only 37% of these patients, the initial $SvjO_2$ was 55%, with MAP of 80 mmHg or more, so resuscitation of these patients could have been performed earlier. Resuscitation times would have been shorter if a rapid, noninvasive method of neurological monitoring had been available to estimate CPP at the bedside for earlier accurate resuscitation.

It is in these clinical scenarios where TCD/CCTS becomes a useful alternative for making decisions regarding resuscitation and/or initial treatment in coma patients.

The intention of this chapter is to review the available literature and to objectively assess whether TCD/TCCS has a place in the early resuscitation of comatose patients in ICU and emergency department (ED). For practical purposes, we will divide the analysis of this monitoring technique and its possible applications, in patients with traumatic and nontraumatic coma.

43.4 TCD/TCCS and Traumatic Coma

After a TBI, the brain suffers damage that depends on the mechanism and kinetics of the primary injury. It is then vulnerable to secondary injury due to edema and/or cerebral ischemia. Ischemia is the most important poor prognostic factor in patients with TBI [23–25].

With the aim of acting early, supported by the Van Santbrink [21] and Vigué [22] trials, which demonstrate low CPP in the first hours after trauma (8 hours) and delayed CPP monitoring (7 hours), respectively, it is very useful to have a noninvasive, reproducible and portable method of neurological monitoring. In this regard, the TCD/TCCS meets all the conditions.

In the clinical resuscitation scenario, whether in the intensive care unit (ICU) and/or the emergency department (ED), all patients are resuscitated according to international guidelines [5, 6], following the ABCDE sequence (A: airway, B: ventilation, C: circulation, D: neurological deficit, and E: body exposure).

The point ¨C¨ (circulation) of the current recommendation (ABCDE) is to maintain a systolic blood pressure (SBP) between 90 and 110 mmHg.

Having a noninvasive method of neuromonitoring and estimation of CPP such as TCD/TCCS would allow us to select patients who would benefit from a higher MAP (risk of cerebral ischemia) or simply a more conservative approach (risk of hyperemia).

Tazarourte et al. [26] conducted a study involving 18 patients with severe TBI. They were given prehospital TCD/TCCS within 90 minutes of the trauma. Fifty percent had abnormal TCD/TCCS with an PI > 1.4 in the MCA, interpreted as a patient at risk for cerebral ischemia. These patients received targeted treatment; in

the case of presenting MAP <80 mmHg, norepinephrine was initiated, and if the MAP was >80 mmHg, mannitol was used. A new TCD/TCCS was performed at the time of admission to the emergency department. Hundred percent of patients who persisted with abnormal TCD/TCCS did not survive. Those patients with normal TCD/TCCS (9/18) initially did not suffer clinical or ultrasound deterioration; of these nine patients, only one died due to uncontrolled bleeding. Although this is a small nonrandomized study, it allows us to think that this noninvasive neuromonitoring tool used promptly could guide an early and directed treatment to the clinical moment of the patient.

Ract et al. [27] in a prospective, nonrandomized study included 24 patients with severe TBI who underwent bilateral MCA TCD/TCCS on admission and post-admission under invasive ICP and $SvjO_2$ monitoring. The delay from the time of trauma to hospital admission was 45 minutes to 7.5 hours. The first TCD/TCCS was performed between 7 and 29 minutes from admission and the second was performed between 2 and 6 hours. Brain ultrasound was considered abnormal with two of the following criteria:

1. MFV < 30 cm/s
2. EDV < 20 cm/s
3. PI > 1.4

Forty-six percent of the patients presented with an abnormal initial brain ultrasound, so they received vasopressor drugs, mannitol, and/or emergency neurosurgery. TCD/TCCS values were normalized in all but two patients. After treatment, this group of patients showed ICP values >10 mmHg with respect to the group with normal initial brain ultrasound. However, no significant differences were observed in CPP and $SvjO_2$. The corollary to this is that patients at risk of ischemia were detected early. Therefore, the time that the brain was subjected to the secondary insult was reduced thanks to timely and targeted treatment. The conclusion of the authors is that TCD/TCCS is a suitable method to identify the patient at risk of cerebral hypoperfusion allowing a guided and optimal therapy. Randomized studies with a larger number of patients are necessary since the parameters that should be used to define TCD/TCCS as abnormal are not yet well defined.

Ziegler et al. [28] conducted a study of 255 patients with severe TBI who underwent TCD/TCCS on days 1, 2, 3, and 7 and were divided into three groups: (a) normal measurements (45%), (b) cerebral hypoperfusion (28%), and (c) cerebral vasospasm (27%). Of the patients in group (a), 43 patients were discharged, 55 were referred to chronic care centers, and 16 died (14% mortality). Of the patients in group (b), 71 patients died (98% mortality) (65 by brain death and 6 by withdrawal of support); the surviving patient presented moderate functional dependence. Of the patients in group (c), 12 were discharged, 35 went to chronic care centers, and 22 died (32% mortality).

We can observe, in a study with greater statistical power, the difference in the evolution of patients with normal TCD/TCCS, signs of hypoperfusion or vasospasm. It has been shown that patients with hypoperfusion have a high probability of death and unfavorable functional outcome. One is left to wonder what the result would have been like if therapy and resuscitation with TCD/TCCS had been guided by TCD/TCCS.

43.5 TCD/TCCS and Nontraumatic Coma

The challenge is to arrive at an early diagnosis, since many causes of coma are low risk and can reverse spontaneously without leaving sequelae and others present high morbidity and mortality, if not treated properly and in time.

This group can be divided into the following:

1. Patients who are admitted to the ICU in a coma.
2. Patients who evolve with this pathology during their stay in the ICU.

Within group (2) we find those who, after suspending sedation/analgesia, do not present a neurological response. Here the intensivists pose the following questions: (a) The lack of response is due to a slowed down metabolism of these drugs (after suspension) or (b) during the period of sedoanalgesia, some acute neurologic event occurred that explains the coma. We must do what is necessary to quickly reach a diagnosis and initiate specific treatment without delay, which would worsen the patient's prognosis.

The only study that evaluated resuscitation of comatose patients with both traumatic and nontraumatic causes is that of Tamagnone et al. [28]. The study included patients in coma (Glasgow ≤8), without criteria for emergency surgery or bilateral irritable mydriasis. Twenty-eight patients were enrolled, who underwent TCD as early as possible, before imaging studies. The reported diagnoses were: 6 intracerebral hemorrhage (ICH); 6 TBI; 6 metabolic encephalopathies; 3 meningitis; 3 acute ischemic stroke; 1 SAH; 1 brain tumor; 1 acute hydrocephalus; and 1 acute liver failure (ALF). Doppler was considered abnormal if:

1. Pulsatility index >1.4
2. EDV < 20 cm/s

This group was resuscitated with saline (0,9%) and norepinephrine to reach an MAP of 110 mmHg, if it was less than 100 mmHg. Responders were considered those who increased the EDV > 20 cm/s. Thirty-two percent presented normal results and 69% (19 patients) abnormal results. After treatment, the TCD values were normalized in 13 patients (13/19 (68%)). Overall mortality was 46% (13 patients) and that of the abnormal TCD group was 68%, being significantly higher in nonresponders (6/6; 100%) compared to responders (7/13; 53%). The group with normal TCD the mortality was 0%.

43.5.1 Nontraumatic Causes of Coma

43.5.1.1 Encephalopathy Due to Acute Liver Failure (ALF)

Approximately 50% of patients with ALF present clinical signs of cerebral edema and intracranial hypertension (IHT) and have an associated high mortality. This is due to cerebral ischemia and herniation in 38–81% of cases [30–32]. The increase in ICP as well as the decrease in CPP in this pathology may be correlated with

changes in the morphology of the cerebral blood flow velocity waveform obtained by TCD/TCCS spectral Doppler. Similar to IHT secondary to trauma, in liver pathology the waves follow a pattern of progressive decrease in EDV until it is reversed, leaving only a PSV [31]. In this condition, invasive ICP monitoring is not routinely validated. Patients often present with coagulopathies, increasing the risk of bleeding during placement of invasive ICP-monitoring devices and an increased risk of infection. This makes TCD/TCCS an ideal method for monitoring and for estimating ICP and CPP, while providing a useful guide to therapy of these patients.

43.5.1.2 Central Nervous System (CNS) Infection

As a cause of nontraumatic coma, bacterial meningitis carries high mortality (10–30%) and a high risk of developing neurological disability. It is associated with cerebral edema and increased ICP, which can lead to cerebral herniation. This would explain the poor prognosis that it presents, even with adequate treatment [33], and unfortunately invasive monitoring is not a standard of care. Müller et al. [38] described the findings obtained with TCD in patients with meningitis; what they observed was an increase in MFV in patients with Glasgow >9 and a decrease in MFV and increase in PI in patients with Glasgow ≤9, with a statistically significant difference. These data suggest that these patients might benefit from early and targeted resuscitation using TCD/CCTS in the early stages of this disease [34].

43.5.1.3 Cardiac Arrest (Anoxic/Hypoxic Injury)

In patients who are comatose survivors after cardiac arrest, the fundamental determinant of prognosis is the time of cardiopulmonary resuscitation (CPR). Even if return of spontaneous circulation (ROSC) is achieved, brain perfusion does not immediately recover; this is known as post-resuscitation syndrome. This was documented through assessment of cerebral hemodynamic status by TCD as well as through metabolic status by measuring cerebral O_2 extraction with $SvjO_2$. It was observed that during the first 24 hours, cerebral hypoperfusion predominates. This was evidenced by elevated PI (>1.4) and decreased MFV (<30 cm/s) in TCD monitoring. After the first 24 hours, cerebral hemodynamic patterns normalized in some cases and became hyperemic (low PI and increased MFV) in other cases. It seems that during the hypoperfusion phase (first 24 hours), there is an opportunity to try to optimize cerebral blood flow (CBF) through the information obtained from noninvasive neurological monitoring by TCD/TCCS [35–37].

43.5.1.4 Nonconculsive Status Epilepticus (NCSE)

Comatose patients due to NCSE have a high morbidity and mortality. Merceron et al. [38] observed that these patients had increased ICP as determined by measurements of the optic nerve sheath. This study shows a correlation between the

presence of signs of IHT with the consequent risk of cerebral ischemia. Therefore, the TCD/TCCS (changes in the PI and flow velocities of the MCA) could inform us that cerebral blood flow varies, estimated through the variability in intracerebral flow velocities, thus allowing us to try to optimize these cerebral hemodynamic alterations in real time.

43.5.1.5 Other Causes of Coma

Other pathologies can produce coma: those that generate an intracranial mass effect (intracerebral hematoma, extra and subdural hematoma, intracerebral tumors, brain abscesses, SAH, AIS, etc.). All of these share the physiopathological mechanism of increased ICP, with hemodynamic alterations corresponding to IHT being expressed in TCD/TCCS monitoring. Its main complications would be the generation of edema, ischemia, and herniation of encephalic structures. This is where TCD/TCCS could show us patterns of hypoperfusion (PI > 1.4 and EDV < 20 cm/s) and thus give us the opportunity to intervene, trying to avoid or minimize secondary brain injury.

43.6 Resuscitation Guided by TCD/TCCS

There are multiple pathologies, traumatic and nontraumatic in origin, that could lead to coma. These share the same physiopathology:

Cerebral Edema ⇔ Decrease of CPP ⇔ Cerebral Ischemia ⇔ Herniation syndromes

This physiopathological outcome determines the need for accurate diagnosis and early and timely treatment. The TCD/TCCS is a tool that allows us to estimate in a noninvasive way, and in real time, the CPP and the changes in the ICP. This is a tool that allows us to anticipate if the patient is undergoing a secondary brain injury or is at risk of developing one.

The literature is scarce, but there is a handful of small clinical studies that provide support to the notion of TCD/TCCS-guided brain resuscitation, mainly in patients with traumatic coma. In our opinion, the results of these studies are promising and would allow us to quickly separate patients at risk of further deterioration and damage to the central nervous system from those who simply recover spontaneously (e.g., patients with remnants of sedation). We therefore propose that when faced with a patient in a coma, from whatever cause, either on admission to the ICU or during their stay in the ICU, we use the TCD/TCCS in the following way:

1. Initial resuscitation as indicated by international guidelines [5, 6] (ABCDE).

   In point (D), when assessing the neurological deficit, we will add the performance of TCD/TCCS and thus divide the patients between those with normal and abnormal results

This last group is defined: (hypoperfusion pattern)

(a) EDV < 20 cm/s
(b) PI > 1.4

43.6.1 Ultrasound Protocol Proposal: Ultrasound-guided Cerebro-Cardiovascular Resuscitation (US-CCaRE)

The different causes of coma share the same physiopathology of a decrease in CPP, either by a decrease in MAP or an increase in ICP. Based on this premise, we designed a treatment algorithm guided by TCD/TCCS. To do so, we will subdivide the group of patients with altered ultrasonographic parameters into the following [29]:

1. Patients admitted to the ICU for coma (Group 1)
2. Patients who evolve with coma during ICU hospitalization (Group 2)

Both groups will be resuscitated according to the ABCDE established by the international guidelines already mentioned [5, 6]. By performing the TCD/TCCS at point (D) and obtaining abnormal results, our first goal will be to optimize the arterial blood pressure (ABP). As mentioned above, the recommendations tell us to maintain a systolic blood pressure (SBP) between 90 and 110 mmHg.

Group 1 (Protocol)

1. Increase MAP by 10% with respect to basal values using saline 0.9% expansion and/or norepinephrine infusion.
2. After increasing the MAP by 10%, we will evaluate the CPP with the TCD/TCCS. If the estimated values continue to be altered, the MAP should be increased by another 10% and so on until the TCD/TCCS is normalized or a MAP of 120 mmHg is reached, provided that the patient has no contraindications (e.g., active bleeding). If so, the MAP limit will be 90 mmHg.
3. If, despite reaching the new MAP target, the brain ultrasonographic values remain altered, we will focus on serum sodium concentration. Recommendations are to keep the latter values between 145 and 155 mEq/L [39, 40]. If the value is unknown or less than 145 mEq/L, a rapid infusion of hypertonic solution (3% sodium chloride) should be performed. The other link in hyperosmolar therapy is represented by mannitol, used in doses of 0.25–1 g/kg, once the SBP is optimized above 90 mmHg [6].
4. After optimizing MAP and serum sodium concentration, with still abnormal TCD/TCCS values, mannitol 20% 0.7 gr/kg will be administered [26, 27] and new measurements will be obtained with TCD/TCCS. If these are normalized, we will have achieved our objective; otherwise, the patient will be classified as nonresponsive to treatment.

Group 2 (Protocol)
In group 2 patients, the treatment algorithm will be similar:

1. Increase of MAP with titratable drugs (norepinephrine), since these are patients who were previously hospitalized, and we can assume that they are not hypovolemic, except in particular cases where the treating physician may opt for the use of crystalloid solutions as a first choice. Caution should be exercised, since the positive fluid balance (hyper-resuscitation) in both septic patients [41, 42] and neurocritical patients [40, 43, 44] increases their morbid-mortality.

   Therefore, in patients in both groups, and in particular group 2, we must be cautious in the use of fluids. Each physician will use the resuscitation parameters and fluid response predictors that he or she best manages and/or has available.

   The application of the US-CCaRE should never delay invasive ICP monitoring (gold standard), complementary studies (e.g., brain CT scan), and/or emergency neurosurgery. This technique does not seek to exclude the tools of standard care, but attempts to engage in resuscitation as a complementary tool of monitoring, treatment, and follow-up.

43.7 Conclusion

There are several algorithms for the treatment of the comatose patient, both traumatic and nontraumatic, and all focus on initial stabilization and finding the cause of the coma. During the performance of the history, laboratory and imaging results, TCD/TCCS would allow us to estimate whether the brain perfusion is adequate, beyond the underlying cause. As we previously analyzed, the physiopathology (cerebral edema—decreased CPP—cerebral ischemia—encephalic herniation) is similar in all etiologies. This allows us, in the event of CPP alterations, to optimize it.

Another point to take into account is the prognosis of these patients, since in many cases the pathologies may present signs that can simulate brain death. Here the TCD/TCCS shows us if the patient presents or not patterns of circulatory arrest and if these do not revert with resuscitation. In this way, we would make a more accurate prognosis.

In addition, the TCD/TCCS is a portable monitoring method that can be used in the prehospital and/or at the patient's bedside. It is reproducible, innocuous, not too costly, most institutions have ultrasound equipment and a 2 MHz transducer, and its learning curve is not too long.

We believe that this form of ultrasound-guided cerebro-cardiovascular resuscitation (US-CCaRE) could complement existing protocols such as ATLS, providing more information about patients' cerebral hemodynamics and guiding therapy in a more targeted and individualized way.

We must also define the parameters to determine whether TCD/TCCS is abnormal, since these are arbitrary and not well defined. Therefore, it would be interesting to design studies with an adequate number of patients, randomized and prospective, to define the parameters of abnormal TCD/TCCS and whether US-CCaRE manages to decrease mortality and improve the results.

Algorithm

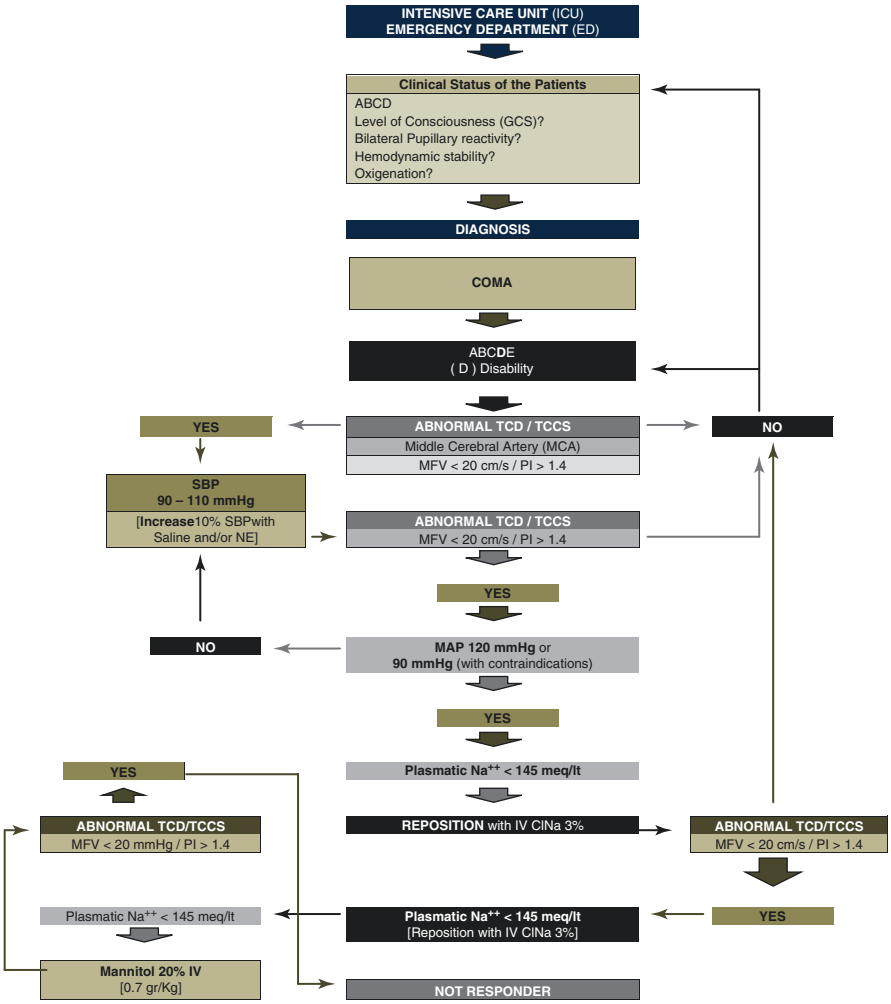

ABCD Arway-breathing-circulation-disability, *IMV* Invasive mechanical ventilation, *GCS* Glasgow coma scale, *TCD* Transcranial Dopples, *TCCS* Transcranial color-coded duplex Sonography, *PI* Pulsatility index, *MFV* Mean flow velocity, *SBP* Systolic blood pressure, *MAP* Mean arterial pressure, *Na++* Sodium, *NE* Norepinephrine, *IV* intravenous

References

1. Stevens RD, Bhardwaj A. Approach to the comatose patient. Crit Care Med. 2006;34(1):31–41.
2. Horsting MW, Franken MD, Meulenbelt J, van Klei WA, de Lange DW. The etiology and outcome of non-traumatic coma in critical care: a systematic review. BMC Anesthesiol. 2015;15:65.

3. Weiss N, et al. Causes of coma and their evolution in the medical intensive care unit. J Neurol. 2012;259(7):1474–7.
4. Kortbeek JB, et al. Advanced trauma life support, 8th edition, the evidence for change. J Trauma. 2008;64(6):1638–50.
5. Advanced trauma life support, ATLS, 10ma edición, 2017.
6. Carney N, et al. Guidelines for the management of severe traumatic brain injury, 4th Edition. Neurosurgery. 2016;80:6.
7. McMillan TM, Teasdale GM, Weir CJ, Stewart E. Death after head injury: the 13 year outcome of a case control study. J Neurol Neurosurg Psychiatry. 2011;82(8):931.
8. Schreiber MA, Aoki N, Scott BG, Beck JR. Determinants of mortality in patients with severe blunt head injury. Arch Surg. 2002;137(3):285.
9. Jiang JY, Gao GY, Li WP, Yu MK, Zhu C. Early indicators of prognosis in 846 cases of severe traumatic brain injury. J Neurotrauma. 2002;19(7):869.
10. Rosner MJ, Rosner SD, Johnson AH. Cerebral perfusion pressure: management protocol and clinical results. J Neurosurg. 1995;83(6):949.
11. Levin HS, et al. Vegetative state after closed-head injury. A Traumatic Coma Data Bank report. Arch Neurol. 1991;48(6):580–5.
12. Forsberg S, Hojer J, Enander C, Ludwigs U. Coma and impaired consciousness in the emergency room: characteristics of poisoning versus other causes. Emerg Med J. 2009;26(2):100–2.
13. Weiss N, et al. Causes of coma and their evolution in the medical intensive care unit. J Neurol. 2012;259(7):1474–7.
14. Salahuddin N, et al. The incidence of increased ICP in ICU patients with non-traumatic coma as diagnosed by ONSD and CT: a prospective cohort study. BMC Anesthesiol. 2016;16(1):106.
15. Bellner J, Romner B, Reinstrup P, Kristiansson KA, Ryding E, Brandt L. Transcranial Doppler sonography pulsatility index (PI) reflects intracranial pressure (ICP). Surg Neurol. 2004;62:45–51.
16. Czosnyka M, Matta BF, Smielewski P, Kirkpatrick PJ, Pickard JD. Cerebral perfusion pressure in head-injured patients: a noninvasive assessment using transcranial Doppler ultrasonography. J Neurosurg. 1998;88(5):802–8.
17. de Riva N, et al. TRanscranial Doppler pulsatility index: what it is and what it isn't. Neurocrit Care. 2012;17(1):58–66.
18. Chan KH, Miller JD, Dearden NM. The effect of changes in cerebral perfusion pressure upon middle cerebral artery blood flow velocity and jugular bulb venous oxygen saturation after severe brain injury. J Neurosurg. 1992;77:55–61.
19. Ursino M, Giulioni M, Lodi CA. Relationship among cerebral perfusión pressure, autoregulation and transcranial Dopplerwaveform: a modeling study. J Neurosurg. 1998;89(2):255–66.
20. Calviello LA, et al. Between brain pulsatility and cerebral perfusion pressure: replicated validation using different drivers of CPP change. Neurocrit Care. 2017;27(3):392–400.
21. van Santbrink H, Schouten JW, Steyerberg EW, Avezaat CJ, Maas AI. Serial transcranial Doppler measurements in traumatic brain injury with special focus on the early posttraumatic period. Acta Neurochir. 2002;144(11):1141–9.
22. Vigue B, et al. Early SjvO2 monitoring in patients with severe brain trauma. Intensive Care Med. 1999;25:445–51.
23. Chesnut RM, et al. The role of secondary brain injury in determining outcome from severe head injury. J Trauma. 1993;34:216–22.
24. Jones PA, et al. Measuring the burden of secondary insults in head-injured patients during intensive care. J Neurosurg Anesthesiol. 1994;6:4–14.
25. Stocchetti N, Furlan A, Volta F. Hypoxemia and arterial hypotension at the accident scene in head injury. J Trauma. 1996;40:764–7.
26. Tazarourte K, et al. Pre-hospital transcranial Doppler in severe traumatic brain injury: a pilot study. Acta Anaesthesiol Scand. 2011;55(4):422–8.
27. Ract C, Le Moigno S, Bruder N, Vigué B. Transcranial Doppler ultrasound goal-directed therapy for the early management of severe traumatic brain injury. Intensive Care Med. 2007;33(4):645–51.

28. Ziegler D, Cravens G, Poche G, Gandhi R, Tellez M. Use of transcranial Doppler in patients with severe traumatic brain injuries. J Neurotrauma. 2017;34(1):121–7.
29. Tamagnone F, Martínez E, Blejman SD, Rubianes JI, Previgliano IJ. A pilot study of transcranial Doppler-guided initial resuscitation of traumatic and non-traumatic comatose patients. Minerva Anestesiol. 2014;80(9):1012–7.
30. Bindi ML, Biancofiore G, Esposito M, Meacci L, Bisà M, Mozzo R, et al. Transcranial doppler sonography is useful for the decision-making at the point of care in patients with acute hepatic failure: a single centre's experience. J Clin Monit Comput. 2008;22:449e52.
31. Aggarwal S, Brooks DM, Kang Y, Linden PK, Patzer JF. Noninvasive monitoring of cerebral perfusion pressure in patients with acute liver failure using transcranial doppler ultrasonography. Liver Transpl. 2008;14:1048e57.
32. Abdo A, et al. Cerebral hemodynamics patterns by transcranial Doppler in patients with acute liver failure. Transplant Proc. 2015;47(9):2647–9.
33. Glimåker M, Johansson B, Grindborg Ö, Bottai M, Lindquist L, Sjölin J. Adult bacterial meningitis: earlier treatment and improved outcome following guideline revision promoting prompt lumbar puncture. Clin Infect Dis. 2015;60(8):1162–9.
34. Müller M, Merkelbach S, Hermes M, Schimrigk K. Transcraneal Doppler sonography at the early stage of acute central nervous system infections in adults. Ultrasound Med Biol. 1996;22(2):173–8.
35. van den Brule JM, Vinke E, van Loon LM, van der Hoeven JG, Hoedemaekers CW. Middle cerebral artery flow, the critical closing pressure, and the optimal mean arterial pressure in comatose cardiac arrest survivors-an observational study. Resuscitation. 2017;110:85–9.
36. Lemiale V, et al. Changes in cerebral blood flow and oxygen extraction during post-resuscitation syndrome. Resuscitation. 2008;76(1):17–24.
37. Buunk G, van der Hoeven JG, Frölich M, Meinders AE. Cerebral vasoconstriction in comatose patients resuscitated from a cardiac arrest? Intensive Care Med. 1996;22(11):1191–6.
38. Merceron S, Geeraerts T, Montlahuc C, Bedos JP, Resche-Rigon M, Legriel S. Assessment of cerebral blood flow changes in nonconvulsive status epilepticus in comatose patients: a pathophysiological transcranial Doppler study. Seizure. 2014;23(4):284–9.
39. Chapman SA, et al. Serum sodium response to hypertonic saline infusion therapy in traumatic brain injury. J Clin Neurosci. 2018;48:147–52.
40. Fletcher JJ, Bergman K, Blostein PA, Kramer AH. Fluid balance, complications, and brain tissue oxygen tension monitoring following severe traumatic brain injury. Neurocrit Care. 2010;13(1):47–56.
41. Vincent JL, et al. Sepsis in European intensive care units: results of the SOAP study. Crit Care Med. 2006;34(2):344–53.
42. Acheampong A, Vincent JL. A positive fluid balance is an independent prognostic factor in patients with sepsis. Crit Care. 2015;19:251.
43. Zhao Z, et al. Analysis of the association of fluid balance and short-term outcome in traumatic brain injury. J Neurol Sci. 2016;364:12–8.
44. Gantner D, Moore EM, Cooper DJ. Intravenous fluids in traumatic brain injury: what's the solution? Curr Opin Crit Care. 2014;20(4):385–9.

Chapter 44
Post-cardiac Arrest Care: Usefulness of Transcranial Doppler (TCD/TCCS) in Cerebral Hemodynamic Monitoring After Resuscitation

C. Hoedemaekers

Key Points

1. Post-cardiac arrest care is an essential part in the chain of survival after cardiac arrest.
2. An increased cerebrovascular resistance decreases cerebral blood flow early after cardiac arrest, with a concomitant decrease in oxygen demand of the brain.
3. During the first days after cardiac arrest, cerebral blood flows restore toward normal values in survivors after the arrest.
4. In non-survivors after cardiac arrest, gradual loss of vascular tone results in vasoplegia and cerebral hyperemia.
5. Disturbances in cerebral autoregulation renders the brain more at risk for cerebral hypo- and hyperperfusion.

44.1 Introduction

Cardiac arrest is a leading cause of mortality and morbidity. The incidence of cardiac arrest in Europe and North America ranges between 19 and 104 per 100.000 people per year with an overall survival to hospital discharge of 10–11% [1, 2]. In a large cohort study from the Netherlands, the rate of survival with a favorable neurological outcome has increased over a period of 7 years, largely because of improved outcome rates among patients with a shockable first rhythm [3]. This increased

C. Hoedemaekers (✉)
Department of Intensive Care, Radboud University Medical Center, Nijmegen, The Netherlands
e-mail: astrid.hoedemaekers@radboudumc.nl

C. N. Rodríguez et al. (eds.), *Neurosonology in Critical Care*,
https://doi.org/10.1007/978-3-030-81419-9_44

survival occurred at all stages of care in the chain of survival, that is, survival to emergency department admission, survival to hospital admission, and survival to hospital discharge, with the largest increase in survival during the prehospital phase. This increased survival is largely due to an increased use of automated external defibrillators at the site of the arrest, thus decreasing the time to restoration of spontaneous circulation (ROSC) [3].

After admission to the intensive care unit (ICU), approximately 60% of patients die before hospital discharge [4–6]. Neurological injury, leading to severe post-anoxic encephalopathy is responsible for the majority of deaths [5, 7]. Most survivors after cardiac arrest have a good neurological recovery. Although cognitive decline and psychiatric symptoms frequently occur in survivors after cardiac arrest, the majority of the survivors maintain their independence and have a good quality of life 1 year after the arrest [8, 9]. Survival with a severe disability or in a vegetative state occurs in approximately 10% of the survivors after cardiac arrest [4, 10].

Post-cardiac arrest care is an important link in the chain of survival after cardiac arrest and aims at restoration of the extensive pathophysiological derangements caused by the whole-body ischemia and reperfusion. Improvement of post-cardiac arrest care can considerably improve the outcome after cardiac arrest [11]. Institution of protocolized post-cardiac arrest care including treatment with targeted temperature therapy, coronary angiography, and percutaneous coronary interventions significantly improved survival in patients with a shockable rhythm after cardiac arrest [12].

44.2 Post-cardiac Arrest Syndrome (PCAS)

The post-cardiac arrest syndrome is a combination of pathophysiological processes and consists of four components: post-cardiac arrest brain injury, myocardial dysfunction, systemic ischemia/reperfusion response, and the underlying disease that caused the cardiac arrest [13]. The brain is highly vulnerable to ischemia due to its high metabolic rate in combination with the limited capacity for anaerobic metabolism and energy stores. Excitotoxicity, disrupted calcium homeostasis, free radical formation, pathological protease cascades, inflammation, and activation of cell-death signaling pathways can induce secondary brain injury that develops in the hours to days after ROSC.

Post-cardiac arrest myocardial dysfunction is characterized by low cardiac index, left ventricular systolic and diastolic dysfunction, and/or right ventricular failure [14, 15]. This usually transient cardiac dysfunction occurs in two-thirds of the patients after ROSC, even in the absence of underlying cardiac pathology. In the hours after ROSC, the low output state gradually evolves to a vasodilatory state with increasing cardiac index and decreased systemic vascular resistance and capillary leak, mimicking septic shock [14, 16]. The underlying pathology accounting for the cardiac arrest may further aggravate circulatory failure in patients after ROSC.

Whole-body ischemia and subsequent reperfusion causes an inflammatory response with activation of the immune system and coagulation pathways. The activation of the immune system results in release of cytokines, adhesion molecules, and other inflammatory factors, similar to the response in sepsis [16]. Ischemia/reperfusion activates the coagulation cascade without adequate activation of the fibrinolytic pathways, resulting in a procoagulant state that further aggravates the microcirculatory failure in post-cardiac arrest patients [17, 18].

44.3 Post-cardiac Arrest: Cerebral Blood Flow (CBF)

Restoration of circulation does not automatically restore cerebral blood flow (CBF). In animal models of cardiac arrest, cerebral perfusion after ROSC is characterized by early hyperemia followed by hypoperfusion and, finally, restoration of normal blood flow. Furthermore, the blood flow is heterogeneous, with areas of no flow, low flow, and increased flow at the level of the microcirculation [19]. The hypoxia-induced low flow and vasoparalysis occurs in the first 20 minutes after cardiac arrest [20] and is suggested to result from an imbalance between vasodilatory and vasoconstrictive mediators such as adenosine and nitric oxide [21, 22]. The hypoperfusion phase develops between 20 min and 12 h after ROSC and is characterized by an approximately 50% decrease in CBF [23, 24]. The arachidonic metabolites hydroxyeicosatetraenoic acids (HETEs) and epoxyeicosatrienoic acids (EETs) are potent vasoactive compounds and are considered to play an important role in this phase [25]. Finally, after 12–72 h, CBF returns toward normal values, remains low, or increases [26].

In humans, CBF after cardiac arrest is mainly studied by transcranial Doppler (TCD)/TCCS. Cerebral blood flow velocities (CBFV) are reduced in the first hours after ROSC and gradually return toward normal or increased values during the following 72 h [5, 27, 28].

Upon admission, the CBFV is similar in survivors versus non-survivors. In survivors after cardiac arrest, the CBFV increases to values similar to those in healthy volunteers, whereas in non-survivors, an overshoot in CBFV develops [29]. This relative hyperemia is most likely the result of a loss in vascular tone, resulting in a decrease in cerebrovascular resistance in these non-survivors.

During the first 72 h, the pulsatility index (PI) decreases, suggestive of a decrease in cerebrovascular resistance in parallel to the increase in CBFV [30]. At the same time, endothelin levels are high after ROSC, with gradually decreasing nitrate levels and gradually increasing cGMP levels [28]. This imbalance between local vasodilators and constrictors induces active vasoconstriction with consequent cerebral hypoperfusion during this so-called “delayed hypoperfusion phase” after cardiac arrest.

Further evidence for active vasoconstriction in the first hours after cardiac arrest is provided by estimation of the critical closing pressure (CrCP). The CrCP is a method to describe and quantify characteristics of the cerebrovascular bed in more

detail and is defined as the lower limit of arterial blood pressure below which vessels collapse and flow ceases [31, 32]. Because the CrCP cannot be measured directly, a model of cerebral impedance has been developed by Varsos et al. using TCD and arterial blood pressure as input data [33]. The CrCP is a valuable and clinically relevant tool in cerebrovascular research, as it allows to estimate changes in cerebrovascular tone and minimal cerebral perfusion pressure to prevent collapse of vessels and ischemia [34–36]. The CrCP gradually decreases in humans during the first 72 h after cardiac arrest, mainly as a result of a decrease in cerebrovascular resistance. Taken together, these results indicate that after cardiac arrest, the vasomotor tone gradually changes from vasoconstriction to vasodilation, allowing the CBF to restore towards normal levels.

44.4 Post-cardiac Arrest: Regulation of Cerebral Blood Flow (CBF)

Strict regulation of CBF is essential for the maintenance of constant nutrient and oxygen supply to the brain. The partial pressure of arterial carbon dioxide ($PaCO_2$), mean arterial pressure (MAP), cerebral metabolism, and the autonomic nervous system are the principal regulators of CBF [37].

Brain perfusion is highly sensitive to changes in $PaCO_2$. Arterial hypocapnia results in cerebrospinal fluid alkalosis, which decreases CBF, cerebral oxygen delivery, and, to a lesser extent, cerebral blood volume [38]. The cerebrovascular reactivity to changes in $PaCO_2$ is preserved after cardiac arrest [27, 39]. This has important clinical implications, since prolonged or severe hypocapnia during the post-resuscitation phase renders the brain at risk for secondary ischemia due to cerebral vasoconstriction.

Cerebral autoregulation aims to maintain a constant CBF despite changes in arterial blood pressure. Cerebral autoregulation can be evaluated by measuring changes in cerebral blood flow in response to a steady-state change in blood pressure (static method) or by measuring the response to a rapid change in blood pressure (dynamic method). While static measurements mainly evaluate the overall effect (efficiency) of the autoregulatory action, the dynamic responses also yield information about the speed in which the CBF can adapt to changes in cerebral perfusion pressure [37].

Static cerebral autoregulation was measured by TCD during the delayed hypoperfusion phase in 18 patients after cardiac arrest using noradrenalin for induction of a stepwise increase in blood pressure [40]. In 8 patients, CBF autoregulation was absent, and in 5 patients, the lower limit of autoregulation was significantly right shifted. Cerebral autoregulation was compromised in the majority of patients after cardiac arrest, rendering the brain more vulnerable to periods of reduced perfusion pressure.

Continuous TCD and near-infrared spectroscopy (NIRS) together with beat-to-beat arterial blood pressure monitoring allows quantification of the dynamic relation between cerebral blood flow derivates and arterial blood pressure. This dynamic

autoregulation is under control of different pathophysiological control mechanisms compared to static autoregulation [41] and may behave differently in disease states. NIRS is a noninvasive technology that can measure relative changes in oxygenated and deoxygenated blood. Dynamic cerebral autoregulation can be assessed in the time domain by calculation of a moving correlation coefficient between the mean arterial pressure and the ratio between oxygenated versus deoxygenated blood (COx) [42]. Dynamic cerebrovascular autoregulation was disturbed in one-third of patients after cardiac arrest [43], mainly in patients with a history of chronic arterial hypertension, suggesting an adaptive shift of the autoregulatory curve to the right. Abnormal cerebral autoregulation was independently associated with a poor neurological outcome, most likely because this renders the brain more vulnerable to rapid changes in blood pressure with subsequent risk of hypo- and hyperperfusion [43, 44].

After ROSC, CBF is initially low and restores toward normal values in the first 72 h after cardiac arrest. This hypoperfusion may cause a mismatch between cerebral oxygen supply and demand, resulting in ischemia and secondary brain injury. The oxygen extraction fraction can be calculated from the arterial and jugular bulb venous oxygen content. Despite the decreased CBF in the first hours after cardiac arrest, the cerebral oxygen extraction fraction remained in a normal range, strongly suggesting a decrease in oxygen consumption [27, 28, 30]. In addition, there was no evidence of tissue hypoxia [45]. These data indicate that cerebral metabolism is decreased, especially in the first hours after cardiac arrest. It is yet unclear whether hypoperfusion follows the inactivity of the brain or the neurons (temporarily) decrease their activity as a response to low CBF.

There is ample evidence for autonomic failure after cardiac arrest. To evaluate the autonomic nervous system, continuous monitoring of the CBFV by TCD and arterial blood pressure is required. These continuous signals can be evaluated in the time domain, using the coefficient of variation or in the frequency domain by measurement of the average spectral power in different frequency bands. The spontaneous variability of the CBFV signal measured by TCD and the arterial blood pressure was low after cardiac arrest, mainly in non-survivors [46]. In addition, the spectral power of both the CBFV and the blood pressure signals in the (very) low frequency domain was low, strongly suggesting failure of the (autonomic) nervous system in regulation of cerebrovascular tone or intrinsic myogenic failure of the cerebral blood vessels. Similarly, the heart rate variability is reduced in both low and high frequency power spectra in survivors and non-survivors after cardiac arrest, also suggesting a decrease in autonomic cardiovascular control [47, 48].

44.5 Post-cardiac Arrest: Clinical Implications

Besides the standard care that applies to all critically ill patients, optimal treatment of the post-cardiac arrest patients comprises a number of specific therapeutic strategies.

Targeted temperature treatment after cardiac arrest significantly improves survival after cardiac arrest [49, 50]. Targeting a body temperature of 33 °C has similar outcomes in terms of mortality and neurological outcome as compared to targeting a temperature of 36 °C [51]. Use of mild therapeutic hypothermia has no profound effect on restoration of CBF after cardiac arrest [52]. Although mild therapeutic hypothermia decreases the metabolic demand of the brain compared to patients treated with strict normothermia, temperature by itself is not a major determinant in restoration of CBF toward normal values [52].

The preserved cerebrovascular reactivity to changes in $PaCO_2$ emphasizes the importance of strict control of mechanical ventilation, as hypocapnia may exacerbate the neurological injury. Repeated transcranial Doppler and jugular bulb oximetry may assist in monitoring of the CBF and cerebral oxygenation during mechanical ventilation to prevent cerebral hypoperfusion and ischemia.

The optimal cerebral perfusion pressure target after cardiac arrest remains to be established. Observational data suggest that a mean arterial pressure <65 mmHg in the first days after the arrest is associated with an increased mortality, independent of the level of vasopressor support [53]. A similar threshold was found in another observational cohort, in which a threshold mean arterial pressure of >70 mmHg had the strongest association with a favorable neurological outcome [54]. In this cohort, higher mean arterial blood pressure thresholds were not associated with better outcome. A MAP below the optimal autoregulatory range during the first 48 hours after cardiac arrest was associated with worse outcomes compared to patients with higher blood pressures [55].

Large prospective intervention trials on the optimal blood pressure target are lacking. In addition, observational data suggesting blood pressure thresholds apply to populations, but these thresholds may not be appropriate for individual patients. To determine the optimal blood pressure range for patients after cardiac arrest, the strength of the autoregulation should be taken into account. TCD/TCCS is an important tool for the determination of dynamic cerebral autoregulation after cardiac arrest: a moving correlation coefficient between CBFV and arterial blood pressure can determine the dynamic autoregulation in the time domain (Mx) [56]. This moving correlation coefficient expresses the dynamic cerebral autoregulation as absolute values in the range between −1 (intact autoregulation) and +1 (defect autoregulation). The correlation coefficient reacts to changes in cerebral perfusion pressure, and the perfusion pressure at which the correlation coefficient is at its lowest point is considered as optimal cerebral perfusion pressure. Blood pressure below the optimal cerebral perfusion pressure is associated with poor outcome in patients with acute brain injury [57].

44.6 Post-cardiac Arrest: Future Perspectives

A universal target for cerebral perfusion pressure is unlikely to be optimal for all individual patients. Instead, an adaptive cerebral perfusion pressure target, based on

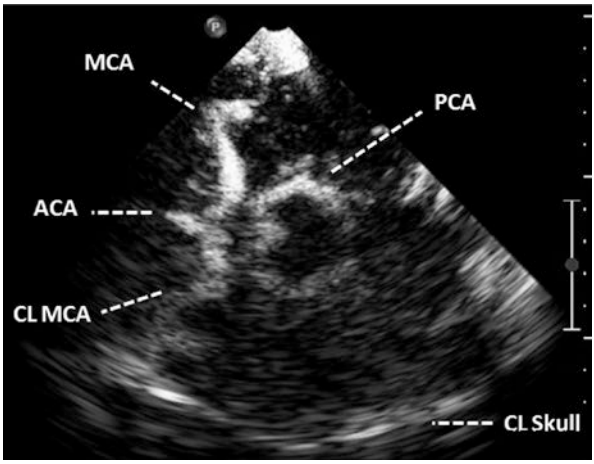

Fig. 44.1 Transcranial contrast enhanced ultrasound view through the transtemporal bone window (B-Mode): ACA anterior cerebral artery, MCA middle cerebral artery, PCA posterior cerebral artery, CLMCA contralateral middle cerebral artery, CLSkull contralateral skull bone

the autoregulatory status of the patient, may be an alternative target based on cerebrovascular characteristics of individual patients. In patients with traumatic brain injury, large retrospective cohort studies suggest that an individual target blood pressure strategy based on the current strength of the cerebrovascular autoregulation is associated with improved outcomes compared to conventional static blood pressure targets [57]. It is feasible in post-cardiac arrest patients to determine an optimal blood pressure target [43]. Whether this approach is beneficial remains to be determined in a prospective trial. TCD is an important tool as it allows for the determination of the optimal cerebral perfusion pressure.

Post-cardiac arrest research mainly focuses on the pathophysiological changes in the macrocirculation. The microcirculation is an essential part of the cerevasculature and consists of arterioles, capillaries, and post-capillary venules and is responsible for the exchange of oxygen and nutrients and plays an important role in the regulation of microvascular perfusion. Sublingual microvascular flow is impaired in post-cardiac arrest patients, similar to that in patients with sepsis [58]. It is likely that the microcirculation plays a key role in the pathophysiology of acute brain injury, such as post-anoxic encephalopathy [56, 60]. Currently available monitoring techniques are unable to measure the microvascular and macrovascular CBF simultaneously, require transportation of the patient outside the intensive care unit, or are invasive in nature. Contrast-enhanced ultrasound is a promising bedside technique for the quantification of macrovascular and microvascular CBF with a favorable safety profile [61]. Changes in perfusion are detectable with this technique [62]. This technique may be used to examine the pathophysiological changes in the cerebral microcirculation during the post-cardiac arrest syndrome and to monitor the effect bedside and immediately of interventions such as blood pressure changes [59–62] on the flow in the micro and macrocirculation (Fig. 44.1).

44.7 Conclusion

The cerebral blood flow and cerebral autoregulation are altered after cardiac arrest, most notably in patients with a poor outcome. TCD/TCCS plays an essential role in the clinical monitoring of patients after cardiac arrest, as it allows early detection of changes in cerebral perfusion and autoregulation and monitoring of treatment effects such as blood pressure manipulations. In addition, it is a valuable tool for research purposes that has greatly increased our current knowledge on cerebral blood flow and autoregulation in patients after cardiac arrest.

Algorithm

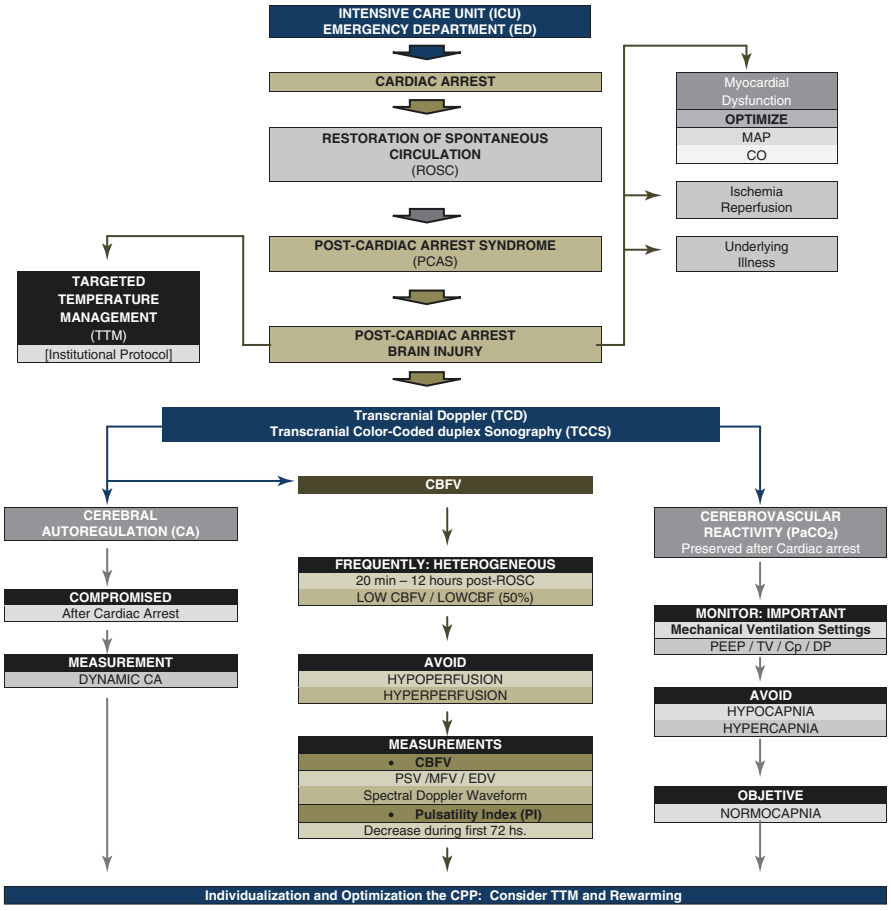

CPP Cerebral Perfusion Pressure, *MAP* Mean Arterial Pressure, *CO* Cardiac output, *CBFV* Cerebral Blood Flow Velocity, *PSV* Peak systolic flow velocity, *MFV* Mean flow velocity, *EDV* end-Diastolic flow velocity, *ABP* Arterial Blood Pressure, *CA* Cerebral Autoregulation, *TV* Tidal volumen, *Cp* Pulmonar compliance, *DP* Driving pressure.

References

1. Benjamin EJ, Blaha MJ, Chiuve SE, et al. Heart disease and stroke statistics-2017 update: a report from the American Heart Association. Circulation. 2017;135:e146–603.
2. Grasner JT, Lefering R, Koster RW, et al. EuReCa ONE-27 Nations, ONE Europe, ONE Registry: a prospective one month analysis of out-of-hospital cardiac arrest outcomes in 27 countries in Europe. Resuscitation. 2016;105:188–95.
3. Blom MT, Beesems SG, Homma PC, et al. Improved survival after out-of-hospital cardiac arrest and use of automated external defibrillators. Circulation. 2014;130:1868–75.
4. Bouwes A, Binnekade JM, Kuiper MA, et al. Prognosis of coma after therapeutic hypothermia: a prospective cohort study. Ann Neurol. 2012;71:206–12.
5. Lemiale V, Dumas F, Mongardon N, et al. Intensive care unit mortality after cardiac arrest: the relative contribution of shock and brain injury in a large cohort. Intensive Care Med. 2013;39:1972–80.
6. Sasson C, Rogers MA, Dahl J, Kellermann AL. Predictors of survival from out-of-hospital cardiac arrest: a systematic review and meta-analysis. Circ Cardiovasc Qual Outcomes. 2010;3:63–81.
7. Laver S, Farrow C, Turner D, Nolan J. Mode of death after admission to an intensive care unit following cardiac arrest. Intensive Care Med. 2004;30:2126–8.
8. Lilja G, Nielsen N, Friberg H, et al. Cognitive function in survivors of out-of-hospital cardiac arrest after target temperature management at 33 degrees C versus 36 degrees C. Circulation. 2015;131:1340–9.
9. Smith K, Andrew E, Lijovic M, Nehme Z, Bernard S. Quality of life and functional outcomes 12 months after out-of-hospital cardiac arrest. Circulation. 2015;131:174–81.
10. Dragancea I, Horn J, Kuiper M, et al. Neurological prognostication after cardiac arrest and targeted temperature management 33 degrees C versus 36 degrees C: results from a randomised controlled clinical trial. Resuscitation. 2015;93:164–70.
11. Lund-Kordahl I, Olasveengen TM, Lorem T, Samdal M, Wik L, Sunde K. Improving outcome after out-of-hospital cardiac arrest by strengthening weak links of the local Chain of Survival; quality of advanced life support and post-resuscitation care. Resuscitation. 2010;81:422–6.
12. Spaite DW, Bobrow BJ, Stolz U, et al. Statewide regionalization of postarrest care for out-of-hospital cardiac arrest: association with survival and neurologic outcome. Ann Emerg Med. 2014;64:496–506 e1.
13. Neumar RW, Nolan JP, Adrie C, et al. Post-cardiac arrest syndrome: epidemiology, pathophysiology, treatment, and prognostication. A consensus statement from the International Liaison Committee on Resuscitation (American Heart Association, Australian and New Zealand Council on Resuscitation, European Resuscitation Council, Heart and Stroke Foundation of Canada, InterAmerican Heart Foundation, Resuscitation Council of Asia, and the Resuscitation Council of Southern Africa); the American Heart Association Emergency Cardiovascular Care Committee; the Council on Cardiovascular Surgery and Anesthesia; the Council on Cardiopulmonary, Perioperative, and Critical Care; the Council on Clinical Cardiology; and the Stroke Council. Circulation 2008;118:2452–83.
14. Laurent I, Monchi M, Chiche JD, et al. Reversible myocardial dysfunction in survivors of out-of-hospital cardiac arrest. J Am Coll Cardiol. 2002;40:2110–6.
15. Ruiz-Bailen M, Aguayo de Hoyos E, Ruiz-Navarro S, et al. Reversible myocardial dysfunction after cardiopulmonary resuscitation. Resuscitation. 2005;66:175–81.
16. Adrie C, Adib-Conquy M, Laurent I, et al. Successful cardiopulmonary resuscitation after cardiac arrest as a "sepsis-like" syndrome. Circulation. 2002;106:562–8.
17. Adrie C, Monchi M, Laurent I, et al. Coagulopathy after successful cardiopulmonary resuscitation following cardiac arrest: implication of the protein C anticoagulant pathway. J Am Coll Cardiol. 2005;46:21–8.

18. Bottiger BW, Motsch J, Bohrer H, et al. Activation of blood coagulation after cardiac arrest is not balanced adequately by activation of endogenous fibrinolysis. Circulation. 1995;92:2572–8.
19. Iordanova B, Li L, Clark RSB, Manole MD. Alterations in cerebral blood flow after resuscitation from cardiac arrest. Front Pediatr. 2017;5:174.
20. Lee SK, Vaagenes P, Safar P, Stezoski SW, Scanlon M. Effect of cardiac arrest time on cortical cerebral blood flow during subsequent standard external cardiopulmonary resuscitation in rabbits. Resuscitation. 1989;17:105–17.
21. Humphreys SA, Koss MC. Role of nitric oxide in post-ischemic cerebral hyperemia in anesthetized rats. Eur J Pharmacol. 1998;347:223–9.
22. Sciotti VM, Van Wylen DG. Increases in interstitial adenosine and cerebral blood flow with inhibition of adenosine kinase and adenosine deaminase. J Cereb Blood Flow Metab. 1993;13:201–7.
23. Kagstrom E, Smith ML, Siesjo BK. Local cerebral blood flow in the recovery period following complete cerebral ischemia in the rat. J Cereb Blood Flow Metab. 1983;3:170–82.
24. Safar P, Stezoski W, Nemoto EM. Amelioration of brain damage after 12 minutes' cardiac arrest in dogs. Arch Neurol. 1976;33:91–5.
25. Roman RJ. P-450 metabolites of arachidonic acid in the control of cardiovascular function. Physiol Rev. 2002;82:131–85.
26. Sterz F, Leonov Y, Safar P, et al. Multifocal cerebral blood flow by Xe-CT and global cerebral metabolism after prolonged cardiac arrest in dogs. Reperfusion with open-chest CPR or cardiopulmonary bypass. Resuscitation. 1992;24:27–47.
27. Bisschops LL, Hoedemaekers CW, Simons KS, van der Hoeven JG. Preserved metabolic coupling and cerebrovascular reactivity during mild hypothermia after cardiac arrest. Crit Care Med. 2010;38:1542–7.
28. Buunk G, van der Hoeven JG, Frolich M, Meinders AE. Cerebral vasoconstriction in comatose patients resuscitated from a cardiac arrest? Intensive Care Med. 1996;22:1191–6.
29. van den Brule JM, Vinke E, van Loon LM, van der Hoeven JG, Hoedemaekers CW. Middle cerebral artery flow, the critical closing pressure, and the optimal mean arterial pressure in comatose cardiac arrest survivors-an observational study. Resuscitation. 2017;110:85–9.
30. Lemiale V, Huet O, Vigue B, et al. Changes in cerebral blood flow and oxygen extraction during post-resuscitation syndrome. Resuscitation. 2008;76:17–24.
31. Burton AC. On the physical equilibrium of small blood vessels. Am J Phys. 1951;164:319–29.
32. Dewey RC, Pieper HP, Hunt WE. Experimental cerebral hemodynamics. Vasomotor tone, critical closing pressure, and vascular bed resistance. J Neurosurg. 1974;41:597–606.
33. Varsos GV, Richards H, Kasprowicz M, et al. Critical closing pressure determined with a model of cerebrovascular impedance. J Cereb Blood Flow Metab. 2013;33:235–43.
34. Varsos GV, Budohoski KP, Czosnyka M, et al. Cerebral vasospasm affects arterial critical closing pressure. J Cereb Blood Flow Metab. 2015;35:285–91.
35. Varsos GV, Czosnyka M, Smielewski P, et al. Cerebral critical closing pressure in hydrocephalus patients undertaking infusion tests. Neurol Res. 2015;37:674–82.
36. Varsos GV, de Riva N, Smielewski P, et al. Critical closing pressure during intracranial pressure plateau waves. Neurocrit Care. 2013;18:341–8.
37. Willie CK, Tzeng YC, Fisher JA, Ainslie PN. Integrative regulation of human brain blood flow. J Physiol. 2014;592:841–59.
38. Laffey JG, Kavanagh BP. Hypocapnia. N Engl J Med. 2002;347:43–53.
39. Buunk G, van der Hoeven JG, Meinders AE. Cerebrovascular reactivity in comatose patients resuscitated from a cardiac arrest. Stroke. 1997;28:1569–73.
40. Sundgreen C, Larsen FS, Herzog TM, Knudsen GM, Boesgaard S, Aldershvile J. Autoregulation of cerebral blood flow in patients resuscitated from cardiac arrest. Stroke. 2001;32:128–32.
41. Tiecks FP, Lam AM, Aaslid R, Newell DW. Comparison of static and dynamic cerebral autoregulation measurements. Stroke. 1995;26:1014–9.
42. Brady KM, Lee JK, Kibler KK, et al. Continuous time-domain analysis of cerebrovascular autoregulation using near-infrared spectroscopy. Stroke. 2007;38:2818–25.

43. Ameloot K, Genbrugge C, Meex I, et al. An observational near-infrared spectroscopy study on cerebral autoregulation in post-cardiac arrest patients: time to drop 'one-size-fits-all' hemodynamic targets? Resuscitation. 2015;90:121–6.
44. Pham P, Bindra J, Chuan A, Jaeger M, Aneman A. Are changes in cerebrovascular autoregulation following cardiac arrest associated with neurological outcome? Results of a pilot study. Resuscitation. 2015;96:192–8.
45. Hoedemaekers CW, Ainslie PN, Hinssen S, et al. Low cerebral blood flow after cardiac arrest is not associated with anaerobic cerebral metabolism. Resuscitation. 2017;120:45–50.
46. van den Brule JM, Vinke EJ, van Loon LM, van der Hoeven JG, Hoedemaekers CW. Low spontaneous variability in cerebral blood flow velocity in non-survivors after cardiac arrest. Resuscitation. 2017;111:110–5.
47. Dougherty CM, Burr RL. Comparison of heart rate variability in survivors and nonsurvivors of sudden cardiac arrest. Am J Cardiol. 1992;70:441–8.
48. Huikuri HV, Linnaluoto MK, Seppanen T, et al. Circadian rhythm of heart rate variability in survivors of cardiac arrest. Am J Cardiol. 1992;70:610–5.
49. Bernard SA, Gray TW, Buist MD, et al. Treatment of comatose survivors of out-of-hospital cardiac arrest with induced hypothermia. N Engl J Med. 2002;346:557–63.
50. Hypothermia after Cardiac Arrest Study G. Mild therapeutic hypothermia to improve the neurologic outcome after cardiac arrest. N Engl J Med. 2002;346:549–56.
51. Nielsen N, Wetterslev J, Cronberg T, et al. Targeted temperature management at 33 degrees C versus 36 degrees C after cardiac arrest. N Engl J Med. 2013;369:2197–206.
52. Bisschops LL, van der Hoeven JG, Hoedemaekers CW. Effects of prolonged mild hypothermia on cerebral blood flow after cardiac arrest. Crit Care Med. 2012;40:2362–7.
53. Bro-Jeppesen J, Annborn M, Hassager C, et al. Hemodynamics and vasopressor support during targeted temperature management at 33 degrees C versus 36 degrees C after out-of-hospital cardiac arrest: a post hoc study of the target temperature management trial*. Crit Care Med. 2015;43:318–27.
54. Kilgannon JH, Roberts BW, Jones AE, et al. Arterial blood pressure and neurologic outcome after resuscitation from cardiac arrest*. Crit Care Med. 2014;42:2083–91.
55. Lee JK, Brady KM, Chung SE, et al. A pilot study of cerebrovascular reactivity autoregulation after pediatric cardiac arrest. Resuscitation. 2014;85:1387–93.
56. Czosnyka M, Smielewski P, Kirkpatrick P, Menon DK, Pickard JD. Monitoring of cerebral autoregulation in head-injured patients. Stroke. 1996;27:1829–34.
57. Needham E, McFadyen C, Newcombe V, Synnot AJ, Czosnyka M, Menon D. Cerebral perfusion pressure targets individualized to pressure-reactivity index in moderate to severe traumatic brain injury: a systematic review. J Neurotrauma. 2017;34:963–70.
58. Omar YG, Massey M, Andersen LW, et al. Sublingual microcirculation is impaired in post-cardiac arrest patients. Resuscitation. 2013;84:1717–22.
59. Dalkara T, Arsava EM. Can restoring incomplete microcirculatory reperfusion improve stroke outcome after thrombolysis? J Cereb Blood Flow Metab. 2012;32:2091–9.
60. Meairs S, Kern R. Intracranial perfusion imaging with ultrasound. Front Neurol Neurosci. 2015;36:57–70.
61. Vinke EJ, Kortenbout AJ, Eyding J, et al. Potential of contrast-enhanced ultrasound as a bedside monitoring technique in cerebral perfusion: a systematic review. Ultrasound Med Biol. 2017;43:2751–7.
62. Vinke EJ, Eyding J, de Korte C, Slump CH, van der Hoeven JG, Hoedemaekers CWE. Quantification of macrocirculation and microcirculation in brain using ultrasound perfusion imaging. Acta Neurochir Suppl. 2018;126:115–20.

Chapter 45
Large Hemispheric Infarction (LHI): Usefulness of Transcranial Doppler (TCD/TCCS)

Claudio E. Scherle Matamoros

Key Points

1. The preferred technique to follow-up of a patient with a large hemispheric infarction (LHI) is transcranial color-coded duplex sonography (TCCS).
2. In the patient with LHI, with confirmation by brain CT and/or MRI, the neurosonology (TCCS) acquires a special relevance in the diagnosis of the site of arterial occlusion.
3. The pulsatility index (PI) measured by TCCS can be used to detect and estimate, in a noninvasive manner, the increase in intracranial pressure in the hemisphere contralateral to the cerebral infarction, which could have an impact on the patient's prognosis.
4. The use of transcranial color-coded duplex sonography (TCCS) may be helpful in the early detection of midline shift.

45.1 Introduction

The clinical manifestations and consequences of cerebral ischemic lesions depend on their extent and the functional expression of the cerebral parenchymal damage [1]. Thus, we will assist patients with evidence of a stroke only detectable by brain image (silent infarctions) and in other cases with great disability, caused by a great volume of infarction [2]. Such is the case of large hemispheric infarction (LHI), a term used by Hacke et al. in 1996 to define the ischemic lesion affecting the entire territory of the middle cerebral (MCA), accompanied by mass effect and generally catastrophic prognosis [3] (Fig. 45.1).

C. E. Scherle Matamoros (✉)
Department of Neurology, Stroke Unit, Eugenio Espejo Hospital, Quito, Ecuador
e-mail: cscherle62@gmail.com

C. N. Rodríguez et al. (eds.), *Neurosonology in Critical Care*,
https://doi.org/10.1007/978-3-030-81419-9_45

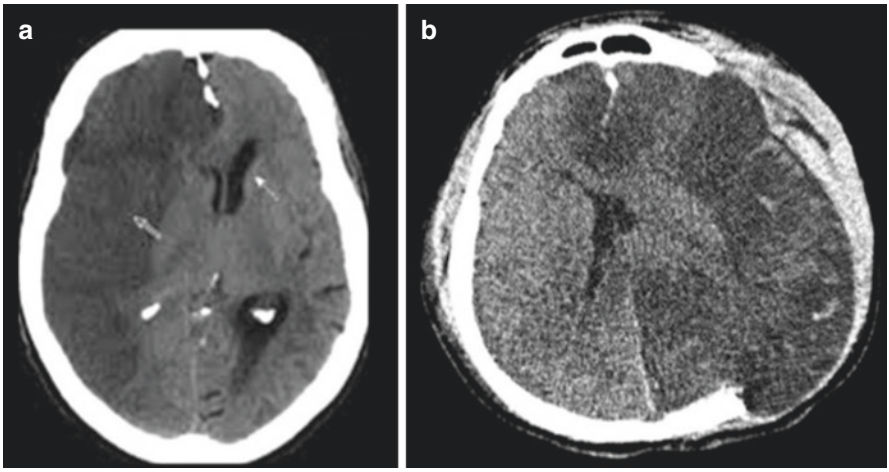

Fig. 45.1 Large hemispheric Infarction (LHI) of right middle cerebral artery (MCA_R). (**a**) Subfascial hernia and displacement to the left of the ventricular system. (**b**) Large hemispheric infarction of the left middle cerebral artery (MCA_L) and decompressive craniotomy. Extension of ischemia to the territory of the two ACA arteries and transcalvarial hernia

LHI occurs in at least 10% of supratentorial strokes [2], in which mortality used to exceed 80% [4]. However, nowadays, thanks to stroke units, multidisciplinary care and early decompressive craniotomy, mortality has been reduced to 25–40% [5, 6].

The most frequent etiology is embolic occlusion of the proximal segment of the MCA (M1). The atherothrombotic or embolic mechanism of the intracranial terminal segment of the internal carotid artery (ICA) can be considered another pathophysiological pathway [1–3].

Clinically, it manifests as a hemispheric syndrome:

- Hemiparesis
- Gaze deviation
- Language disturbances
- Visual disturbance

The NIHSS scale can be >20 points when the commitment is from the left hemisphere and ≥15 when the commitment is from the right [7].

In LHI, the alterations that occur after arterial obstruction are based on cytotoxic edema developed in the first 72 hours as a result of cell necrosis. Simultaneously, with the decrease in tissue in the penumbra and the increase in the area of necrosis, there is rupture of the blood-brain barrier, leading to vasogenic edema [8]. Therefore, with the progression of edema, the pressure on the underlying tissues increases, distorting the cerebral parenchyma.

Once the intracranial adaptive mechanisms are exhausted, intracranial pressure (ICP) begins to rise. When the mean arterial pressure (MAP) is exceeded by the ICP, the cerebral perfusion pressure (CPP) is compromised and the self-regulatory mechanism deteriorates. Therefore, this intensifies ischemia and cerebral edema,

increasing the risk of herniations and extension of ischemia to other arterial territories (Fig. 45.1b) [8, 9].

45.2 Occlusion Arterial Segment: Localization by Cerebral Ultrasound

The transcranial Doppler (TCD) and TCCS have demonstrated an excellent diagnostic correlation with arteriography to define the existence of arterial occlusion [10, 11]. Unlike MR-angiography (MRA), they do not require full patient collaboration and in contrast to CT-angiography; they provide real-time information on the state of the vessel and intracranial circulation.

During the first 6 hours, it is possible to detect arterial occlusion in more than 70% of patients with acute ischemic stroke. Although these data come from research based on digital subtraction angiography (DSA), studies conducted with TCD/TCCS show results that compared to arteriography have a sensitivity of 80% and a specificity greater than 94% [12].

45.3 TCD/TCCS: Arterial Occlusion Criteria

The main sonographic finding characteristic of arterial obstruction is an attenuated blood flow velocity wave (spectral Doppler waveform) in the segment where the thrombus is located. Depending the proximity and location of the probe to the clot and the degree of permeability to arterial blood flow, the spectral Doppler waveform varies between absence and different degrees of attenuation [12] (Fig. 45.2).

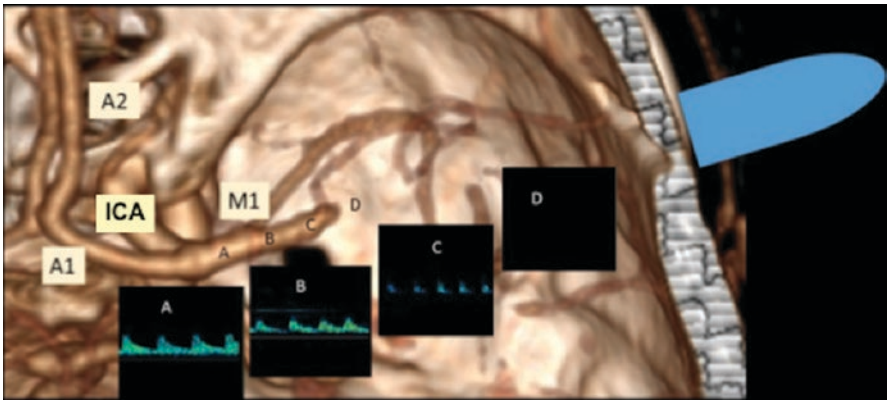

Fig. 45.2 CT-Angiography (CTA) shows the occluded right M1 segment. Attenuation of the flow spectral waves (A to D) in relation to the approximation to the site of the occlusion

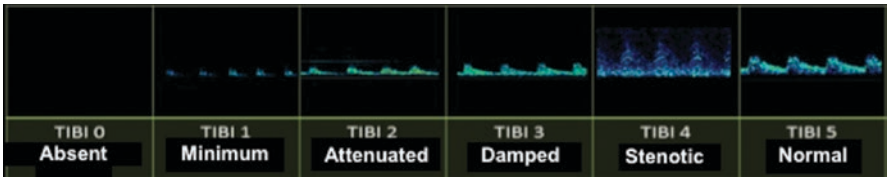

Fig. 45.3 TIBI degrees (thrombolysis in brain ischemia). TIBI 1: Systolic waves of variable velocity and duration in which the diastole may be inverted (reverberant flow). TIBI 2: Flattening of the systole-wave of variable duration and pulsatility (PI) is less than 1.2. TIBI 3: Progressively, the systole acquires normal acceleration and the diastole is positive, but there is a difference of more than 30% with respect to the mean flow velocity (vmf) with the homologous artery [13]. To establish in which segment of the MCA the occlusion is located, the depth at which the worst residual flow signal is detected (degree TIBI 0-1) should be considered [14]

These arterial blood flow variations have been classified according to residual flow in TIBI degrees. This scale is useful both for the initial assessment of the patient with acute ischemic stroke and for follow-up after recanalization treatment [13] (Fig. 45.3).

If we do not measure the MCA flow velocity and other vessels are identified deeper, from the anterior portion of the circle of Willis, it can be established that there is an occlusion in the proximal segment of the MCA. On the other hand, the detection of a <0.6 ratio between the mean flow velocity (MFV) of the affected MCA and the contralateral MCA is an indicator of proximal occlusion. In contrast, if flow velocity is recorded in the MCA proximal to the carotid bifurcation, the depth is reduced to identify if there is any more distal attenuated flow pattern in segment M1 [14]. It is recommended to start the exploration on the unaffected side so that we can establish the normal blood flow velocity waveform and velocity in the MCA, in order to be able to compare with the affected side (Fig. 45.4).

In a patient with LHI and signs of intracranial hypertension and without decompressive craniotomy, distortion of intracranial structures may make it difficult to locate the MCA with TCD. In this situation, the TCCS provides advantages, with the visual support offered by B-mode and the angiographic effect of the color-coded sonography facilitating the exploration.

The main diagnostic criterion by TCCS of an occlusion of the M1 segment of the MCA is the absence of color signal and the alteration of the doppler spectrum (TIBI 0–1) [15], being perceived the signal corresponding to the middle cerebral vein (MCV), the ACA (A1), the ipsilateral PCA, and the contralateral anterior circulation. Tandem occlusion of the ICA is diagnosed when flow signals are absent in M1 segment, A1 segment, and in the intracranial segment of internal carotid artery. By combining an anterior coronal plane with an axial plane at the protuberance level, the terminal portion of the ICA [16] can be accessed. If we use a TCD machine, it is possible to access the terminal portion of the carotid artery through the temporal acoustic window and the carotid siphon through the ophthalmic acoustic window [17].

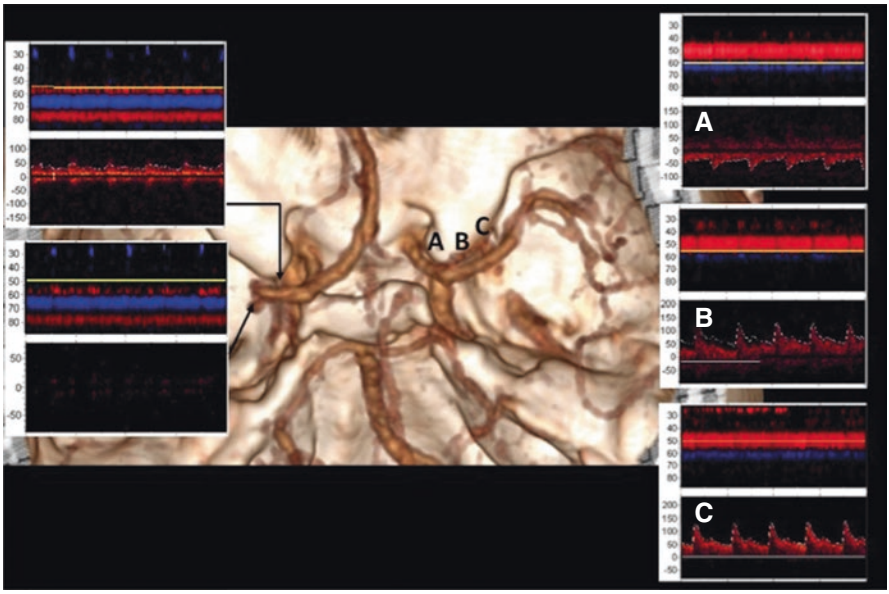

Fig. 45.4 Correlation between angio-TC and TCD. Absence of flow signal at 50 mm depth on the left side. Asymmetry between flow velocities in both MCAs and a smaller representation in mode M of the occluded side. On the right side, normal sonograms are presented (A: Corresponds to segment A1 of the anterior cerebral artery. B: Middle cerebral artery near the bifurcation. C: Middle cerebral sonogram near segment M2)

In 2009, a committee of TCCS experts proposed to reduce the TIBI criteria to a grading of four categories, resulting in the COGIF (Consensus on Grading Intracranial Flow obstruction) criteria [18]:

1. **COGIF 1** would imply complete vessel occlusion (TIBI 0).
2. **COGIF 2** represents the absence of diastolic flow (equivalent to TIBI 1).
3. **COGIF 3**, low systolic and diastolic velocities coexist, suggesting partial recanalization (equivalent to 2–3 TIBI).
4. **COGIF 4** corresponds to complete perfusion, including this group of three subcategories:

   4.1 Normal flow.
   4.2 Stenotic flow (TIBI 4).
   4.3 Increased flow in a segment or hyperperfusion (encompasses the TIBI 4–5 criteria).

45.4 Large Hemispheric Infarction (LHI): Intracranial Hypertension Monitoring

In 1974, Gosling and King introduced the concept of pulsatility index (PI) in the study of cerebral hemodynamics. It is a parameter that describes and quantifies the relationship between the peak velocity, the end-diastolic velocity, and the mean flow velocity. This index estimates the degree of resistance to flow (cerebral impedance) that exists in arterioles [19].

As the ICP increases, the CPP decreases, which translates into an initial decrease in the end-diastolic velocity (spectral Doppler waveform with resistive pattern) and a progressive increase in the PI. High pulsatility (PI between 1.2 and 1.6) correlates with moderate intracranial hypertension (ICH). PI >3 correlates with a severe increase in ICP and cerebral circulation arrest [20, 21]. This is true under condition that MAP is normal and patient is not hypocapnic [22]. Pulsatility index may be affected by hemodynamic, respiratory, and hematological factors, so its instant value is not always sufficient to characterize intracranial hemodynamic conditions [22].

For the measurement of the Gosling's index, flow velocity measurement is usually performed in the MCA. In the context of the LHI, in which the artery is occluded and the arterioles have undergone structural changes, it is reasonable to find that the resistance indices (PI and RI) are increased not necessarily as an expression of the increase in ICP but rather of the occlusion of the vessel.

Studies in patients with intracerebral hemorrhage (ICH) evaluated with TCD/TCCS have found that increased PI in the unaffected hemisphere correlates with 30-day mortality, with 80% sensitivity and 94% specificity [23, 24]. Therefore, measurement of PI in the contralateral hemisphere can provide prognostic data.

45.5 Large Hemispheric Infarction: Midline Shift Diagnosis

The monitoring of changes in the cerebral midline through the TCCS over time (trends) is very useful in the follow-up of these patients, especially after 16 hours of evolution. It is a rapid and reliable diagnostic method of herniation, which is useful for identifying the group of patients at risk who may benefit from a decompressive craniectomy [24].

Determination of midline shift needs to be done with TCCS. The neurocritical patient is approached:

1. *Patient position:* Supine
2. *Select the probe:* Low frequency (2.5 mHz)
3. *Selection of acoustic window:* Transtemporal window (with orbital direction, above the zygomatic arch)

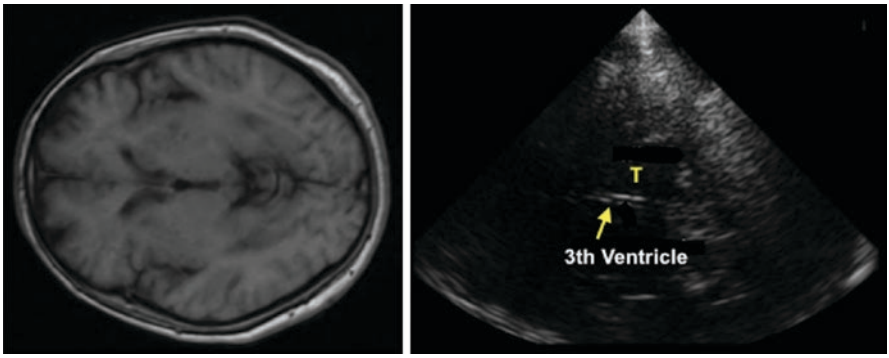

Fig. 45.5 Correlation between MRI and TCCS: Left: Brain MRI. Right: TCCS ventricular plane ((T): thalamus; Arrow: third ventricle)

4. *Select the initial insonation plane:* Mesencephalic plane (the hypoecogenic image of the midbrain surrounded by the cerebrospinal fluid is first identified)
5. *Ultrasound equipment setting*: Image depth of 14–16 cm, so that the contralateral temporal bone is identified.
6. *Selection of insonation plane for midline shift measurement*: Ventricular plane. By gently tilting the transducer approximately 10° in the cephalic direction, it is possible to identify the two hyperecogenic lines corresponding to the walls of the third ventricle between the two thalamus (hypoechoic) (Fig. 45.4). The distance between the transducer and the center of the third ventricle is measured in a perpendicular line on both sides. The midline deviation is calculated by subtracting the ipsilateral measure (A) from the contralateral measure (B) divided by 2 [25]. (Fig. 45.5) (For more details, see Chap. 62 on cerebral parenchyma and ultrasound.)

45.6 LHI: Optic Nerve Sheath Diameter (ONSD)

The optic nerve is sheathed by the dura, arachnoidea, and pia sheath. There is a liquor communication to the arachnoidal space of the brain. If the ICP increases, the NO sheath is edematized and swollen, which can be measured with ultrasound. The normal value of ONSD is <5 mm; if it is larger, it may be related to an increase in ICP greater than 20 mm Hg [26].

Transorbital exploration should be performed with the patient in a supine position, the head elevated from 20 to 30 degrees and with the eyelids closed. A thin layer of ultrasound gel is applied to the transducer, which is then placed on the temporal side of the eye in a transverse position to the longitudinal axis of the body, to reach an axial plane of the eyeball, papilla, and optic nerve in their longitudinal course (Fig. 45.6).

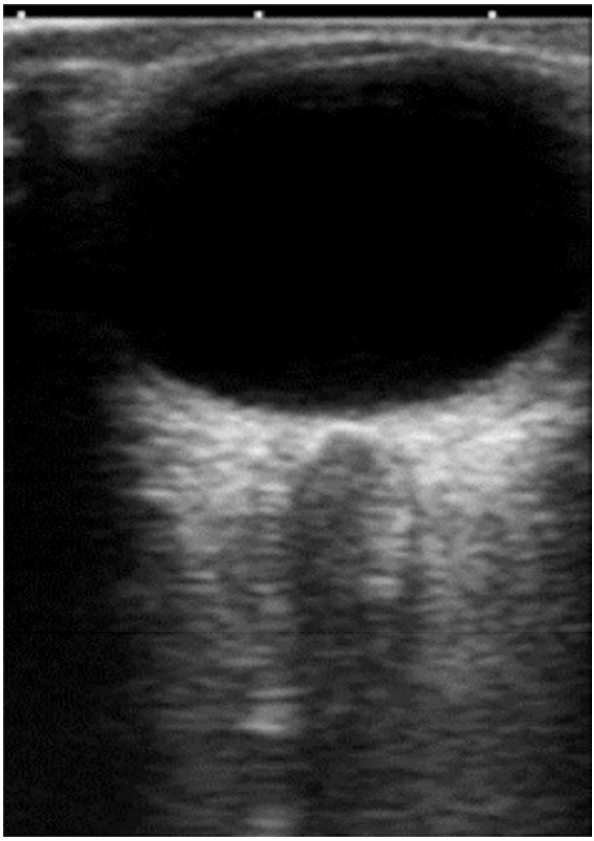

Fig. 45.6 ONSD ultrasound: axial plane

Pressing the eyeball should be avoided at all times so as not to cause pain or to modify the intraocular pressure and thus avoid arterial or venous hemodynamic variations.

45.7 Conclusion

The different techniques of neurosonology are diagnostic tools that should be used in the evaluation of the patient with an LHI of the middle cerebral artery. Their use helps to establish the severity of the patient and the selection of therapeutic measures.

Algorithm

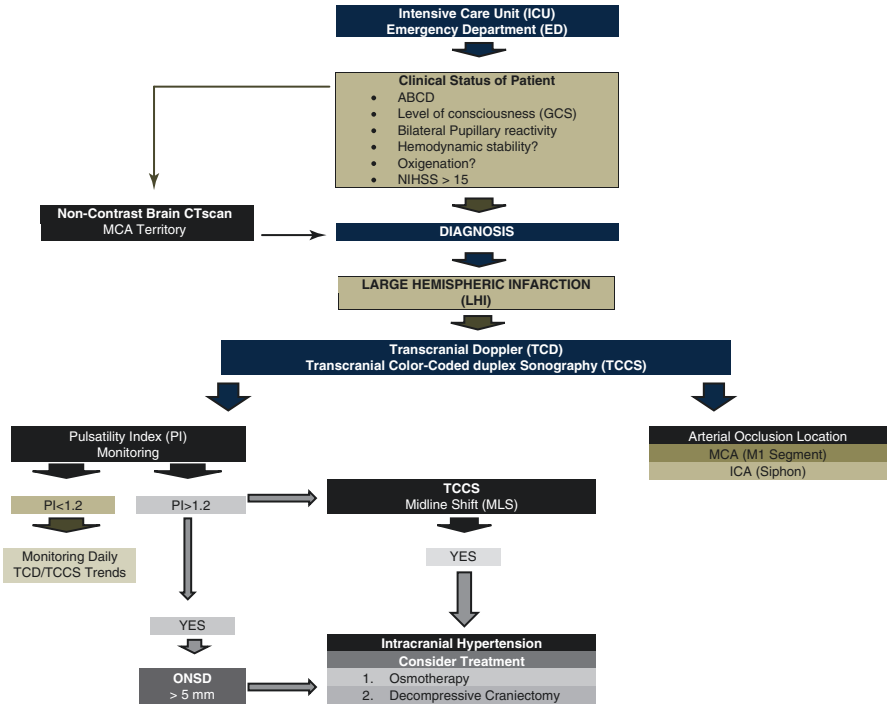

ABCD Airway-breathing-circulation-disability, *GCS* Glasgow coma scale, *NIHSS* National Institute of Healt Stroke Scale, *ICA* Internal Carotid Artery, *MCA* Middle Cerebral Artery, *ONSD* Optic Nerve Sheath Diameter, *CT* Computed Tomography.

References

1. Godoy D, Piñero G, Cruz-Flores S, Alcalá Cerra G, Rabinstein A. Infarto hemisférico maligno de la arteria cerebral media. Consideraciones diagnósticas y opciones terapéuticas. Neurologia. 2016;31(5):332–43.
2. Huttner HB, Schwab S. Malignant middle cerebral artery infarction: clinical characteristics, treatment strategies, and future perspectives. Lancet Neurol. 2009;8(10):949–58.
3. Hacke W, Schwab S, Horn M, Spranger M, De Georgia M, Von Kummer R. The malignant middle cerebral artery territory infarction: clinical course and prognostic signs. Arch Neurol. 1996;53(4):309–15.
4. Jüttler E, et al. Hemicraniectomy in older patients with extensive middle-cerebral-artery stroke. N Engl J Med. 2014;370:1091–100.

5. Kirkman MA, Citerio G, Smith M. The intensive care management of acute ischemic stroke: an overview. Intensive Care Med. 2014;40:640–53.
6. Taylor B, Lopresti M, Appelboom G, Sander Connolly E Jr. Hemicraniectomy for malignant middle cerebral artery territory infarction: an updated review. J Neurosurg Sci. 2015;59(1):73–8.
7. Albert AF, Kirkman MA. Clinical and radiological predictors of development and outcomes. J Stroke Cerebrovasc Dis. 2017;26(11):2671–9.
8. Heiss WD, Malignant MCA. Infarction: pathophysiology and imaging for early diagnosis and management decisions. Cerebrovasc Dis. 2016;41(1–2):1–7.
9. Treadwell SD, Thanvi B. Malignant middle cerebral artery (MCA) infarction: pathophysiology, diagnosis and management. Postgrad Med J. 2010;8s6(1014):235–42.
10. Suwanwela NC, Phanthumchinda K, Suwanwela N. Transcranial Doppler sonography and CT angiography in patients with atherothrombotic middle cerebral artery stroke. AJNR Am J Neuroradiol. 2002;23(8):1352–5.
11. Guan J, Zhou Q, Ouyang H, Zhang S, Lu Z. The diagnostic accuracy of TCD for intracranial arterial stenosis/occlusion in patients with acute ischemic stroke: the importance of time interval between detection of TCD and CTA. Neurol Res. 2013;35(9):930–6.
12. Demchuk AM, et al. Accuracy and criteria for localizing arterial occlusion with transcranial Doppler. J Neuroimaging. 2000;10(1):1–12.
13. Demchuk AM, et al. Thrombolysis in brain ischemia (TIBI) transcranial Doppler flow grades predict clinical severity, early recovery, and mortality in patients treated with intravenous tissue plasminogen activator. Stroke. 2001;32(1):89–93.
14. Demchuk AM, et al. Specific transcranial Doppler flow findings related to the presence and site of arterial occlusion. Stroke. 2000;31(1):140–6.
15. Nedelmann M. et al; TCCS Consensus Group. Consensus recommendations for transcranial color-coded duplex sonography for the assessment of intracranial arteries in clinical trials on acute stroke. Stroke. 2009;40(10):3238–44.
16. Eggers J, Pade O, Rogge A, Schreiber SJ, Valdueza JM. Transcranial color-coded sonography successfully visualizes all intracranial parts of the internal carotid artery using the combined transtemporal axial and coronal approach. AJNR. 2009;30(8):1589–93.
17. Bathala L, Mehndiratta MM, Sharma VK. Transcranial doppler: technique and common findings (part 1). Ann Indian Acad Neurol. 2013;16(2):174–9.
18. Nedelmann M, et al. Consensus recommendations for transcranial color-coded duplex sonography for the assessment of intracranial arteries in clinical trials on acute stroke and for the TCCS consensus group. Stroke. 2009;40(10):3238–44.
19. Gosling RG, King DH. Arterial assessment by Doppler-shift ultrasound. Proc R Soc Med. 1974;67(6 Pt 1):447–9.
20. Bellner J, Romner B, Reinstrup P, Kristiansson KA, Ryding E, Brandt L. Transcranial Doppler sonography pulsatility index (PI) reflects intracranial pressure (ICP). Surg Neurol. 2004;62(1):45–51.
21. Perez-Nellar J, Scherle C, Machado C. TCD systolic spikes in a malignant MCA infarct. Neurocrit Care. 2009;11(1):94–6.
22. de Riva N, Budohoski KP, Smielewski P, et al. Transcranial Doppler pulsatility index: what it is and what it isn't. Neurocrit Care. 2012;17(1):58–66.
23. Martí-Fàbregas J, et al. Prognostic value of Pulsatility Index in acute intracerebral hemorrhage. Neurology. 2003;61:1051–6.
24. Kiphuth IC, Huttner HB, Dörfler A, Schwab S, Köhrmann M. Doppler pulsatility index in spontaneous intracerebral hemorrhage. Eur Neurol. 2013;70(3–4):133–8.
25. Gerriets T, et al. Sonographic monitoring of midline shift in space-occupying stroke: an early outcome predictor. Stroke. 2001;32(2):442–7.
26. Hylkema C. Optic nerve sheath diameter ultrasound and the diagnosis of increased intracranial pressure. Crit Care Nurs Clin North Am. 2016;28(1):95–9.

Chapter 46
Non-Convulsive Status Epilepticus (NCSE) in ICU: Bedside Usefulness of TCD in Comatose Patient Diagnosis. When the EEG Is Too Far

Alshimaa Shaban Othman and Foad Abd-Allah

Key Points

1. Nonconvulsive status epilepticus (NCSE) is an important cause for unexplained impairment of consciousness, particularly in the intensive care unit (ICU).
2. Generation of abnormally prolonged or repeatedly recurrent brain electrical activity represents a metabolic burden not only on the neurons but also on the glial cells. This should be coupled by increase in cerebral blood flow (CBF).
3. The merits of the TCCS (transcranial color-coded duplex sonography) are being available, fast, bedside, safe, repeatable, and not interfering with continuous monitoring in the ICU.
4. TCCS assessment can help not only in diagnosis and follow-up of NCSE/IIC, but also in identifying the underlying etiology: arterial stenosis as a cause of acute ischemic stroke (AIS), dural venous sinus thrombosis, hydrocephalus, increased of ICP (by MLS, ONSD, and papilledema measurements) as in cases caused of space-occupying lesions (SOLs) (neoplasms, intra- and extra-axial hematoma, etc.).
5. Indirect assessment of cerebral blood flow (CBF) through cerebral blood flow velocities (CBFVs) measurement using TCD/TCCS was the most studied application of neurosonology in epileptic seizures, due to its ability to provide real-time evaluation at bedside.
6. EEG is the gold standard for diagnosis of NCSE/IIC; however, it can be unavailable or not conclusive enough. In these cases, vascular imaging can help to establish the diagnosis.

A. S. Othman · F. Abd-Allah (✉)
Kasr-Alainy School of Medicine, University of Cairo, Cairo, Egypt
e-mail: alshimaa.s.othman@kasralainy.edu.eg; foadneuro@hotmail.com

C. N. Rodríguez et al. (eds.), *Neurosonology in Critical Care*,
https://doi.org/10.1007/978-3-030-81419-9_46

46.1 Introduction

Nonconvulsive status epilepticus (NCSE) is an important cause for unexplained impairment of consciousness, particularly in the intensive care unit (ICU). However, the diagnosis is frequently missed, with negative impact on patient's outcome [1]. This can be partly explained by lack/paucity of prominent motor manifestations in NCSE, which was demonstrated in the new report of the international league against epilepsy (ILAE) about definition and classification of SE (Table 46.1).

Also, NCSE have several mimics, which further make the diagnosis challenging [3]. Another important point is that the diagnosis of NCSE heavily relies on the availability of electroencephalogram (EEG). According to the modified Salzburg criteria (mSCNC), a compatible clinical manifestations of ≥10 min and EEG changes of ≥10 s is required for the diagnosis of NCSE (Fig. 46.1).

Unfortunately, EEG and/or experienced EEG interpreter are not always available along the hour in some centers [3]. Also, some equivocal patterns might be demonstrated in EEG, with uncertain risk of neuronal injury and, thus the decision to initiate/escalate AED is controversial [1]. In these situations, there is an urge for other investigatory modality which can be used at bedside to estimate the risk of seizure activity and/or neuronal injury, justifying the use of AED and even continuous IV anesthetic drug infusion.

46.2 NCSE: ICU Epidemiology

NCSE as heterogeneous and complex electroclinical condition (electrographic seizure activity without clear clinical convulsive activity) is common among critically ill patients in the ICU, ranging from 10% to 67% with high morbidity and mortality rates (approximately 18% [5]), and must therefore be diagnosed promptly. Homeostatic derangement, brain injury, and the use of polypharmacy makes those

Table 46.1 Classification of nonconvulsive status epilepticus (NCSE) [2]

Status epilepticus without prominent motor features; nonconvulsive status epilepticus (NCSE)
1. NCSE with coma (i.e., subtle SE)
2. NCSE without coma:
2a. Generalized NCSE without coma (i.e., absence SE)
2b. Focal NCSE without coma, without consciousness impairment (i.e., aura continua with preserved awareness)
2c. Focal NCSE without coma, without consciousness impairment, with language impairment, i.e., aphasic SE
2d. Focal NCSE without coma, with consciousness impairment (i.e., aura continua with impaired awareness)
2e. NCSE without coma, unknown focal or generalized (i.e., autonomic SE)

NCSE nonconvulsive status epilepticus, *SE* status epilepticus

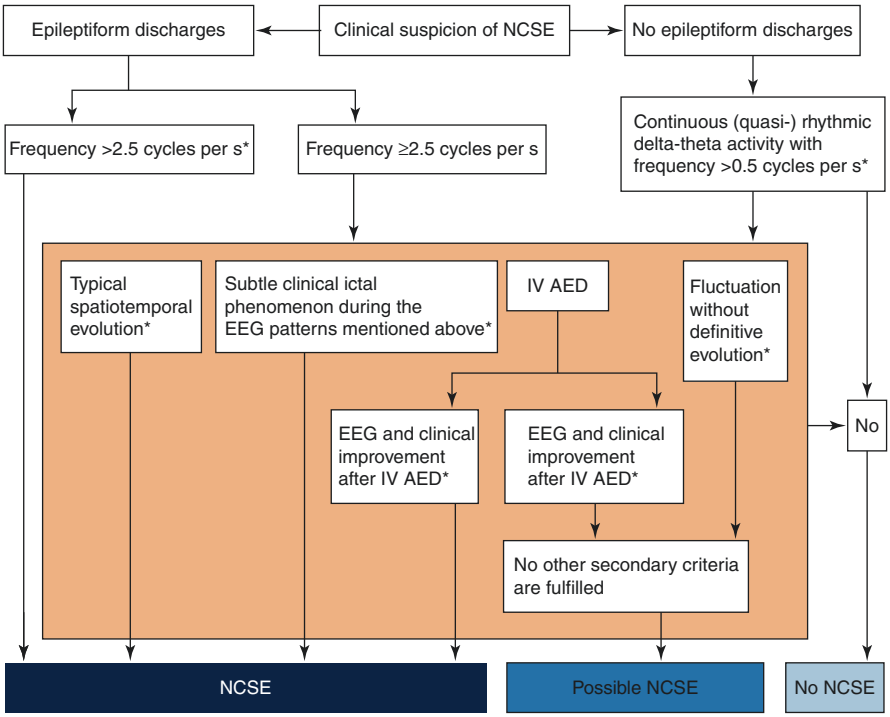

Fig. 46.1 Modified Salzburg consensus criteria for the diagnosis of NCSE (mSCNC). AED antiepileptic drugs, NCSE nonconvulsive status epilepticus. (Courtesy: Leitinger et al. [4])

patients highly susceptible to the development of NCSE [1]. The occurrence of NCSE prolongs the duration of ICU stay, ventilator dependency, and thus increases the risk of infection, negatively impacting the outcome. Nevertheless, both the clinical suspicion and EEG diagnosis are challenging within the noisy environment of ICU [1]. Multiple EEG-related factors add to the diagnostic difficulty including:

1. Unavailability of EEG. Particularly in resource-limited centers.
2. Possible NCSE, which was regarded as a gray land of debate among some authors [6].
3. Lack of surface EEG discharge compatible with mSCNC, in highly suspicious clinical situations, and where depth electrodes cannot be used/are unavailable [3].
4. Some equivocal EEG patterns may improve after IV benzodiazepines, though they are not of epileptic nature [3].
5. Metabolic/septic/drug-induced encephalopathy or encephalopathy associated with acute brain injury with epileptiform EEG discharges [2].
6. Differentiating post-ictal confusion from confusion due to NCSE following CSE [7].
7. Demonstration of one or more patterns of the ictal-interictal continuum (ICC) [1, 8].

46.2.1 Ictal-Interictal Continuum (IIC)

The widespread use of continuous EEG monitoring in the ICU has enabled recognition of some equivocal patterns that do not meet the proposed criteria for NCSE, but they possess some ictal/pre-ictal behavior. They represent a state of unstable metabolic demands, with risk of neuronal injury, depending on the patient's biological background, and thus the institution of AEDs should be individually evaluated [1, 8]. These patterns include lateralized or generalized (quasi-) periodic discharge (PD), lateralized or generalized (quasi-) rhythmic delta activity (RDA), burst suppression (BS), stimulus-induced rhythmic/periodic ictal discharge {SIRP(I)Ds}, brief (potentially ictal) rhythmic discharges {B(I)RDs}, extreme delta brush, and sharp waves with triphasic morphology (TM) [1].

46.3 NCSE: Cerebral Hemodynamics Changes

Hauf M et al. (2009) [9] shows regional cortical perfusion changes in patients with NCSE by perfusion CT (PCT). Regional hyperperfusion during seizure activity (increased CBF and CBV) and reduction of regional perfusion in post-ictal stage.

Generation of abnormally prolonged or repeatedly recurrent seizure activity represents a metabolic burden not only on the neurons but also on the glial cells. This should be coupled by increase in cerebral blood flow (CBF) to meet the needs of the hyperactive brain and clean the resultant waste products, according to the neurovascular coupling concept [10].

According to this concept, the state of hyperperfusion demonstrated in vascular and perfusion studies in cases of NCSE and IIC can be understood [8, 11–13]. However, with prolonged and persistent epileptic activity, the increase of CBF becomes insufficient to meet the metabolic needs of the exhausted tissue, with progressive mitochondrial and energy failure and uncoupling state or homeostatic failure ensues, which participates in secondary neuronal injury, perpetuating the epileptic activity. This can also explain the hypoperfusion state late in the course of SE or post-ictally [11]. An important observation is that while initial hyperperfusion is usually localized in the epileptogenic zone, this is not always the case for the delayed/post-ictal hypoperfusion, which sometimes occur across multiple vascular territories, a condition that might denote the involvement of more widespread dysfunction with prolonged ictal activity [14].

46.4 TCD/TCCS: Usefulness in the NCSE Diagnosis at Bedside

Neurosonology assessment includes sequential application of three modes: color Doppler, B-mode, and pulsed-wave Doppler. Whenever Doppler is combined with B-mode, we get a duplex study [15].

In addition to the several advantages of TCD/TCCS, the most concerning for NCSE/IIC are their bedside availability to continuous monitoring, providing real-time relationship to clinical and EEG changes.

TCD/TCCS assessment can help not only in diagnosis and follow-up of NCSE/IIC, but also in identifying the underlying etiology [1]: arterial stenosis as a cause of acute ischemic stroke (AIS), dural venous sinus thrombosis, hydrocephalus, increased of ICP (by MLS, ONSD, and papilledema measurements) as in cases caused of space-occupying lesions (neoplasms, intra- and extra-axial hematoma, etc.).

Merceron et al. (2014) [11] have assessed optic nerve sheath diameter (ONSD) using ocular sonography in ICU patients with suspected NCSE, and they found that all the examined population had increased ONSD, with no significant difference between those with and those without NCSE. However, their cohort consisted of comatose patients with meningitis, traumatic brain injury (TBI), and stroke, in addition to status epilepticus (SE). They concluded that the underlying cause of the coma, rather than the presence of SE per se, was responsible for elevation of ICP, which was reflected by the increase in ONSD in both study groups [11].

According to the neurovascular coupling principle, it is expected to have a state of hyperperfusion during ictal activity. Hyperperfusion means increase in cerebral blood flow (CBF), which is well represented by flow velocities of the cerebral basal arteries, particularly the middle cerebral artery (MCA), being the largest and most studied intracranial artery [16, 17]. This is the basis of assessment by TCD/TCCS in epilepsy, seizures, or suspected ictal activity. In the boundary conditions (e.g., IIC and possible NCSE), the presence of epileptic discharge co-localizing with hyperperfusion defines electro-perfusive SE [8].

Merceron, et al. (2014) [11] used TCD to estimate CBF through CBFVs measurements in comatose patients with NCSE in the ICU, whereas several trials have used TCD to estimate CBFVs changes during brief or recurrent epileptic seizures. Most of these studies were preplanned in patients with recurrent seizures, which enabled obtaining a baseline reference for comparison, using different formulas. The most used parameter was mean flow velocity of the middle cerebral artery (MCA MVF), via the transtemporal window at depth 50–60 mm, using the 2 MHz pulsed wave probe, with the patient lying supine [18, 16, 19–22]. However, sometimes this is not always feasible in comatose patients suspected of having NCSE/IIC, because the clinical state may be alternant without free period for baseline assessment. This might require comparison with CBFV values from a healthy control-patient, if available.

The accuracy of TCD in helping to diagnose NCSE in comatose patients was addressed by Merceron et al. (2014), who recruited 38 comatose patients (GCS $\leq$9) admitted to the ICU for continuous EEG monitoring and ICP monitoring [11], where 26.3% had NCSE by continuous EEG monitoring. TCD performed routinely in the minutes after EEG monitoring initiation. TCD was performed on the right and left mean cerebral arteries (MCAs) through transtemporal acoustic window; peak systolic velocity (PSV), end-diastolic velocity (EDV), and mean flow velocity (MFV) were recorded. Also, the pulsatility index (PI) was calculated.

Their results showed that TCD CBFVs were higher in those with NCSE (26.3%) than those without NCSE (73.7%), reflecting cerebral hyperperfusion in patients with NCSE where mean PSV was 116 cm/s (55% more) and mean EDV was 45 cm/s

(73% more). The difference of pulsatility index (PI) values was not statistically significant, which may be explained by the elevation of all CBFVs. The authors recommended that TCD can be used as an ancillary tool to investigate the possibility of NCSE in comatose ICU patients, but not as a primary diagnostic tool.

46.5 NCSE/IIC: TCD/TCCS Insonation Protocol

Whenever the diagnosis of NCSE is questionable, apply TCD/TCCS protocol as demonstrated in (Table 46.2). The primary goal is to demonstrate a state of hyperperfusion with increased CBFVs, co-localized/co-lateralized with the hypothesized

Table 46.2 Proposed setting for TCD/TCCS in NCSE [11, 23, 24]

Position of the patient	Supine
Patient state	According to the clinical context (disorders of consciousness/coma)
Probe	2 MHz-pulsed wave (low frequency)
Acoustic window	Transtemporal (most frequently used) and/or other windows
Artery	Bilateral: MCA, ACA, PCA, OA, BA, VA, intracranial ICA, and extracranial)
TCD (depth (mm))	According to the insonated artery: 50–60 mm for MCA. Consider monitoring the other arteries
TCCS (depth (mm))	14–16 mm: To insonate circle of Willis and contralateral bone skull
Measurements (cm/s)	MFV, PSV, EDV. Spectral Doppler waveform analysis
Hemodynamic indexes	PI, RI, BHI, LR
Brain parenchymal structures	MLS, 3th ventricle, lateral ventricles, space-occupying lesions, ONSD
TCD/TCCS: Protocol	1. Compare measurements values with baseline values of the patient himself (if available). If not, compare for age and sex-matched with healthy controls 2. Serial/continuous insonation may be needed 3. Always compare one hemisphere hemodynamic measurements to the other 4. Consider the structural brain imaging (for spatial co-localization and secondary effect on CBFVs) 5. Search for spatial co-localization with the EEG 6. If the decision to escalate AEDs was made, follow-up the previously documented parameters to check response to treatment 7. Consider the trends of the hemodynamic measured values and evaluate them with the clinical situation of the critically ill patient

TCD transcranial Doppler, *NCSE* nonconvulsive status epilepticus, *IIC* ictal-interictal continuum, *MCA* middle cerebral artery, *ACA* anterior cerebral artery, *PCA* posterior cerebral artery, *OA* ophthalmic artery, *BA* basilar artery, *ICA* internal carotid artery, *MFV* mean flow velocity, *PSV* peak systolic velocity, *EDV* end diastolic velocity, *PI* pulsatility index, *RI* resistivity index, *BHI* breath holding index, *LR* Lindegaard ratio, *AED* antiepileptic drugs, *MLS* midline shift
Sufficient data are not available regarding the proposed length/frequency of monitoring. Accordingly, this might be tailored on a case-by-case basis

epileptogenic zone, identified based on semiology, structural imaging, and EEG (if available).

The following cutoffs could be adopted from Merceron et al. trial, where areas under ROC curves compare the accuracy of cutoff values of the different MCA hemodynamic parameters:

1. Mean systolic velocity (mean PSV) at 95 cm/s
2. Maximal systolic velocity (max PSV) at 105 cm/s
3. Mean end-diastolic velocity (mean EDV) at 31 cm/s
4. Maximal end-diastolic velocity (maximal EDV) at 40 cm/s

The best performance was found for mean PSV at a cutoff value of 95 cm/s and maximal PSV of 105 cm/s, with superior performance of the mean PSV cutoff value, with no statistically significant difference between velocity parameters on both sides, consistent with the generalized ictal activity demonstrated by the EEG [11]. Pulsatility index (PI) was measured in middle cerebral arteries (MCA) bilaterally, with no statistically significant difference between patients with and without NCSE. However, segmental changes in flow velocity within a single artery usually co-localized with the epileptogenic zone during the hyperperfusion (ictal) state [18].

In TCD monitoring of focal seizures (with/without impairment of consciousness), increase in CBFVs was always higher on the seizure onset side (19–184% higher than the contralateral side); these changes usually started few seconds (1–7 s) after EEG onset [18, 22].

Follow up the trends and relationship between clinical and EEG progression/resolution [22]. Progressive increase of CBFVs might denote seizure activity. The development of hypoperfusion in context of clinical and/or EEG improvement might be taken as a marker of good response to treatment, particularly if co-localized in the initial area of hyperperfusion. Whereas the development of generalized hypoperfusion might denote widespread neuronal injury, which could be an indication for treatment escalation, especially with active EEG changes.

Changes in CBFVs usually return to baseline within 47 ± 7 s [18, 22]. Monitoring could be stopped if the subject and/or EEG/TCD parameters recover to normal/baseline condition from a seizure [18].

46.6 Conclusion

1. NCSE is an important cause of disorders of consciousness and/or coma in the ICU, with diverse presentations, and thus should always be kept in mind as a possible differential diagnosis.
2. EEG is the gold standard for diagnosis of NCSE/IIC; however, it can be unavailable or not conclusive enough. In these cases, vascular imaging can help to establish the diagnosis.
3. Hyper-perfusion is the cerebral hemodynamic pattern, which can be assessed non-invasively measuring the CBFVs by TCD/TCCS in the focus of seizure activity (epileptogenic zone).

4. The transition from hyperperfusion to hypoperfusion may denote treatment success, or exhaustion of the neurons, depending on the clinical scenarios.
5. TCCS can help in the diagnosis of NCSE/IIC and estimation of possible causes (brain parenchyma, MLS, ONSD, etc.).
6. More trials are needed to establish TCD/TCCS as useful tool to diagnose NCSE/IIC.

Algorithm

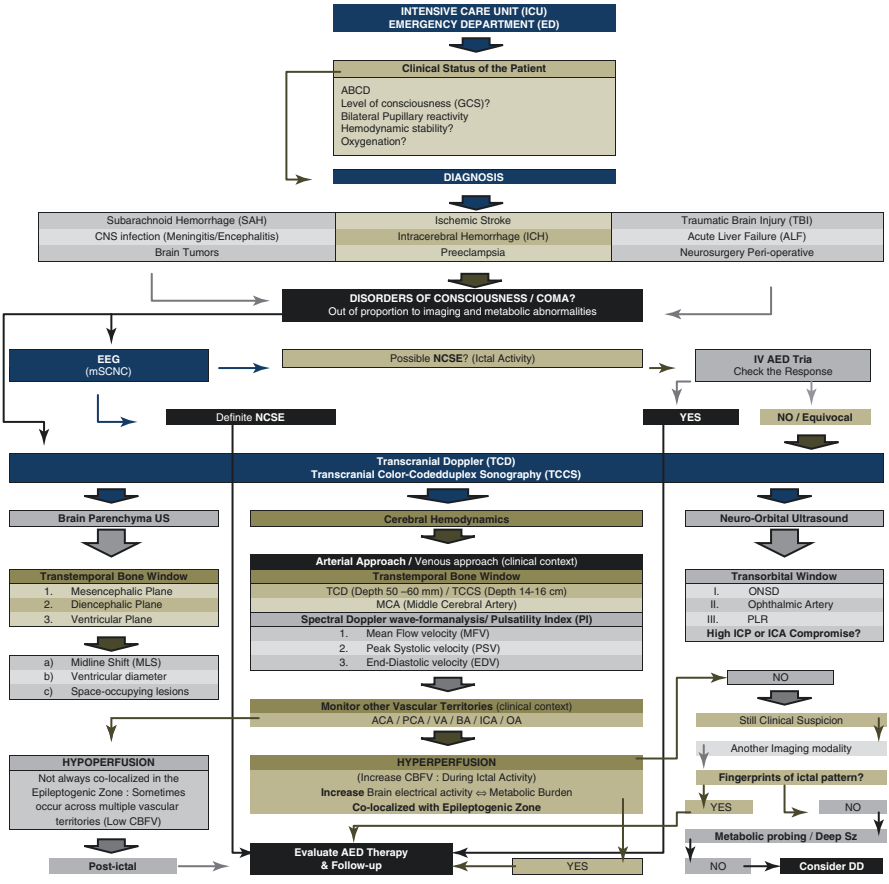

mSCNC: modified Salzburg criteria; ONSD: Optic Nerve Sheat Diameter; ACA: Anterior Cerebral Artery; PCA: Posterior Cerebral Artery; VA: Vertebral Artery; BA: Basilar Artery; ICA: Internal Carotid Artery; OA: Ophthalmic Artery; Sz: Seizure; DD: Differential Diagnosis; AED: Antiepilectic Drug; NCSE: Non-Convulsive Status Epileptic; EEG: Electroencephalogram; ICP: Intracranial Pressure.; CBFV: Cerebral Blood Flow Velocity; (1) Consider AED; PLR: Pupillary light reflex.

mSCNC modified Salzburg criteria, *ONSD* optic nerve sheath diameter, *ACA* anterior Cerebral artery, *PCA* posterior cerebral artery, *VA* vertebral artery, *BA* basilar artery, *ICA* internal carotid artery, *OA* ophthalmic artery, *Sz* seizure, *DD* differential diagnosis, *AED* antiepileptic drug, *NCSE* nonconvulsive status epileptic, *EEG* electroencephalogram, *ICP* intracranial pressure, *CBFV* cerebral blood flow velocity, (1) Consider AED, *PLR* pupillary light reflex

References

1. Kinney MO, Kaplan PW. An update on the recognition and treatment of non-convulsive status epilepticus in the intensive care unit. Expert Rev Neurother. 2017;17(10):987–1002.
2. Trinka E, Cock H, Hesdorffer D, Rossetti AO, Scheffer IE, Shinnar S, et al. A definition and classification of status epilepticus – report of the ILAE task force on classification of status epilepticus. Epilepsia. 2015;56(10):1515–23.
3. Kinney MO, Craig JJ, Kaplan PW. Non-convulsive status epilepticus: mimics and chameleons. Pract Neurol. 2018;18(4):291–305.
4. Leitinger M, Trinka E, Gardella E, Rohracher A, Kalss G, Qerama E, et al. Diagnostic accuracy of the Salzburg EEG criteria for non-convulsive status epilepticus: a retrospective study. Lancet Neurol. 2016;15(10):1054–62.
5. Shneker BF, Fountain NB. Assessment of acute morbidity and mortality in nonconvulsive status epilepticus. Neurology. 2003;61:1066–73.
6. Othman AS, Meletti S, Giovannini G. The EEG diagnosis of NCSE: concordance between clinical practice and Salzburg Criteria for NCSE. Seizure. 2020;79:1–7.
7. Shorvon S, Trinka E. Nonconvulsive status epilepticus and the postictal state. Epilepsy Behav. 2010;19(2):172–5.
8. Kapinos G, Trinka E, Kaplan PW. Multimodal approach to decision to treat critically ill patients with periodic or rhythmic patterns using an ictal–interictal continuum spectral severity score. J Clin Neurophysiol. 2018;35(4):314–24.
9. Hauf M, Slotboom J, Nirkko A, von Bredow F, Ozdoba C. Wiest cortical regional hyperperfusion in nonconvulsive status epilepticus measured by dynamic brain perfusion CT. Am J Neuroradiol. 2009;30(4):693–8.
10. Schwartz TH. Neurovascular coupling and epilepsy: hemodynamic markers for localizing and predicting seizure onset. Epilepsy Curr. 2007;7(4):91–4.
11. Merceron S, Geeraerts T, Montlahuc C, Bedos JP, Resche-Rigon M, Legriel S. Assessment of cerebral blood flow changes in nonconvulsive status epilepticus in comatose patients: a pathophysiological transcranial Doppler study. Seizure. 2014;23(4):284–9.
12. Witsch J, Morris NA, Roh D, Frey H-P, Claassen J. Multimodality monitoring correlates of seizures. In: Varelas P, Claassen J, editors. Seizures in critical care. Cham: Springer; 2017. p. 91–102.
13. Cole AJ. Status epilepticus and periictal imaging. Epilepsia. 2004;45(Suppl. 4):72–7.
14. Farrell JS, Gaxiola-Valdez I, Wolff MD, David LS, Dika HI, Geeraert BL, et al. Postictal behavioural impairments are due to a severe prolonged hypoperfusion/hypoxia event that is COX-2 dependent. elife. 2016;5:e19352.
15. Viski S, Olah L. Use of transcranial Doppler in intensive care unit. J Crit Care Med. 2017;3(3):99–104.
16. De Simone R, Placidi F, Diomedi M, Marciani MG, Silvestrini M. Inter-hemispheric asymmetry of cerebral flow velocities during generalized spike-wave discharges. J Neurol. 2002;249(9):1191–4.
17. Kirkham FJ, Angiology U, Hospital G. Transcranial measurement of blood velocities in the basal cerebral arteries using pulsed Doppler ultrasound: velocity as an index of flow. Ultrasound Med Biol. 1986;12(I):15–21.
18. Yao Y, Lu Q, Jin LR, Zhou XQ, Huang Y, Xu WH. Real-time TCD-vEEG monitoring for neurovascular coupling in epilepsy. Seizure. 2015;29:1–3.
19. Bode H. Intracranial blood flow velocities during seizures and generalized epileptic discharges. Eur J Pediatr. 1992;151(9):706–9.
20. Saito S, Yoshikawa D, Nishihara F, Morita T, Kitani Y, Amaya T, et al. The cerebral hemodynamic response to electrically induced seizures in man. Brain Res. 1995;673(1):93–100.
21. Diehl B, Knecht S, Deppe M, Young C, Stodieck SRG. Cerebral hemodynamic response to generalized spike-wave discharges. Epilepsia. 1998;39(12):1284–9.

22. Niehaus L, Wieshmann UC, Meyer BU. Changes in cerebral hemodynamics during simple partial motor seizures. Eur Neurol. 2000;44(1):8–11.
23. Robba C, Taccone FS. How i use transcranial Doppler. Crit Care. 2019;23(1):1–4.
24. Blanco P, Abdo-Cuza A. Transcranial Doppler ultrasound in the ICU: it is not all sunshine and rainbows. Crit Ultrasound J. 2018;10(1):4.

Chapter 47
Patient with Preeclampsia in ICU: Usefulness of the Transcranial Doppler (TCD/TCCS) to Monitor and Predict the Most Common Neurological Complications

Teelkien Van Veen and Ronney B. Panerai

Key Points

1. Preeclampsia/eclampsia is a heterogeneous systemic disorder, characterized by new-onset hypertension and proteinuria in pregnancy after the 20th week of pregnancy.
2. Cerebral involvement of preeclampsia is one of the most feared complications as it can lead to death or significant short- or long-term morbidity.
3. Normal pregnancy leads to increased cerebral perfusion pressure, decreased cerebral resistance, and redistribution of cerebral blood flow to the posterior circulation. Dynamic cerebral autoregulation is enhanced when compared to healthy nonpregnant women.
4. Preeclampsia can lead to increased cerebral blood flow velocity/volume and decreased resistance. However, cerebral perfusion pressure can be either normal, decreased, or increased.
5. Dynamic cerebral autoregulation is impaired in most women with preeclampsia, and most severely impaired in women with chronic hypertension who develop superimposed preeclampsia.

T. Van Veen (✉)
Department of Obstetrics and Gynecology, University of Groningen, Groningen, The Netherlands
e-mail: teelkien@gmail.com

R. B. Panerai
Department of Cardiovascular Sciences, University of Leicester, Leicester, UK
e-mail: rp9@leicester.ac.uk

C. N. Rodríguez et al. (eds.), *Neurosonology in Critical Care*,
https://doi.org/10.1007/978-3-030-81419-9_47

47.1 Introduction

During pregnancy, approximately 10% of women are diagnosed with some form of hypertension [1]. This incidence is rising due to changes in maternal characteristics, such as increasing number of mothers with advanced maternal age, presence of comorbidities, and higher prepregnancy weight [2, 3]. Although appropriate prenatal care has reduced the number of poor outcomes, hypertensive disorders of pregnancy are still among the leading causes of maternal mortality and severe morbidity in both developed [4] and developing countries [1, 5], accounting for more than 50,000 maternal deaths annually [2]. While the absolute mortality is much lower in developed countries, hypertension has nevertheless been implicated in approximately 20% of maternal deaths [5, 6], with cerebrovascular complications being the primary cause in over 50% [4, 6]. Both the incidence of hypertension and the morbidity/mortality rate are affected by geographic, social, economic, and racial differences [6, 7]. Although rare, eclampsia, the onset of seizures or coma in a preeclamptic woman, is still the most feared pregnancy complication, with a mortality rate of approximately 1% in developed countries [4], but as high as 26% in developing countries [8].

47.2 Hypertensive Disorders of Pregnancy

Hypertensive disorders of pregnancy range in a spectrum from chronic hypertension (CHTN) to gestational hypertension (GHTN), preeclampsia (PEE), and superimposed preeclampsia in the setting of chronic hypertension (SiPEE) [9]. All are part of a dynamic process, where CHTN can progress to SiPEE, and GHTN to PEE, and patients can deteriorate rapidly [9].

47.2.1 Preeclampsia (PEE)

Preeclampsia is a systemic disorder that is typically characterized by new-onset hypertension and proteinuria in pregnancy after the 20th week of pregnancy in a previously normotensive woman. If a woman with chronic hypertension develops proteinuria after 20 weeks of gestation, this is called superimposed preeclampsia. In case of baseline proteinuria, SiPEE is defined by a sudden increase in proteinuria, worsening or resistant hypertension in the last half of pregnancy or development of signs and symptoms of severe preeclampsia [10].

Preeclampsia can develop up to 4 weeks postpartum, but most cases of postpartum preeclampsia occur in the first 48 h. In the absence of proteinuria, PEE is diagnosed as hypertension with new development of thrombocytopenia, impaired liver function, renal insufficiency, pulmonary edema, or cerebral or visual disturbances [9].

Involvement of the brain can cause eclampsia: grand mal seizures or coma in a woman with preeclampsia, in the absence of other neurologic conditions that could account for the seizure [7]. Recurrent seizures can lead to hypoxia, maternal injury, aspiration pneumonia, and status epilepticus. While the incidence of eclampsia is 1 in 2000 in high-income countries, it is estimated to be 1 in 100 to 1 in 1700 deliveries in low- and middle-income countries [11].

Despite being the focus of many studies, the exact pathophysiology of preeclampsia remains unclear. It is a heterogeneous disorder, characterized by two major subtypes:

(a) Placental subtype (placental ischemic–hypoxic stress, followed by systemic maternal inflammation)
(b) Maternal subtype (metabolic–immunologic)

These two subtypes have different etiologies and phenotypes. The placental subtype usually causes early-onset preeclampsia and fetal growth restriction. The maternal subtype typically develops later, due to endothelial dysfunction and microvascular damage. Immune dysregulation plays a substantial role in both subtypes [12], and leads to generalized maternal endothelial dysfunction and, hence, symptomatic clinical disease, by which the fetus, central nervous system, lungs, liver, kidneys, systemic vasculature, coagulation, and the heart may be affected [13].

47.2.1.1 Management of Preeclampsia/Eclampsia

The only definite cure for preeclampsia is delivery. However, for women who are remote from term (<34 weeks gestation), expectant management can be attempted until development of maternal or fetal indications for delivery. In case of severe disease or eclampsia, magnesium sulfate should be started to prevent (further) seizures and antihypertensives (often intravenous) to lower pressures. In case of eclampsia, first priority is to support respiratory and cardiovascular functions. After this initial stabilization, the maternal and fetal condition needs to be evaluated and a plan regarding the need for delivery or observation has to be made [13].

47.3 Cerebrovascular Complications of Hypertension in Pregnancy

While multiple maternal organs can be affected, cerebral involvement is one of the most feared complications as it can lead to death or significant short- or long-term morbidity [6]. The risk of cerebrovascular complications during pregnancy is increased in all hypertensive disorders [14–16] but is most pronounced in severe preeclampsia [15, 16].

The neurological complications range from headache, visual disturbances, and hyperreflexia to tonic-clonic seizures, coma, and stroke. Gross and microscopic histopathology have demonstrated intracerebral hemorrhage, petechiae, cerebral edema, vasculopathy, ischemic brain damage, microinfarcts, and fibrinoid necrosis [17, 18]. Magnetic resonance imaging (MRI) has shown abnormal scans with nonspecific foci of increased signal in the deep cerebral white matter on T2-weighted images in 50% of the women with severe preeclampsia [19]. Widespread diffuse cerebral edema or localized hypodense lesions have been found with computed tomography (CT) imaging. This combination of radiologic anomalies and clinical symptoms is also known as posterior reversible leucoencephalopathy syndrome (PRES). In the absence of serious neurological symptoms, imaging is predominantly unremarkable [17].

Recent studies show promising results on the detection of cerebral biomarkers (S100B, neuron-specific enolase (NSE), neurofilament light chain (NfL), and tua) to diagnose cerebral complications at onset or before onset of preeclampsia [11].

The pathophysiology of these cerebrovascular complications remains poorly understood. Two opposing theories are both based on endothelial dysfunction and poor cerebral autoregulation:

1. Vasoconstriction/hypoperfusion
2. Hypertension/hyperperfusion [20]

The first theory suggests that endothelial dysfunction, caused by systemic toxicity, leads to vasoconstriction, ischemia, and subsequent brain edema due to increased permeability of endothelium [20]. This theory is supported by the vasospasm seen on cerebral angiograms in some women with eclampsia [21, 22], the fact that vasogenic edema is typically found in the watershed zones [23], and the systemic vasoconstriction seen in preeclampsia [13].

The second theory is based on loss of cerebral autoregulation. In the presence of endothelial dysfunction, sudden elevations in systemic blood pressure may exceed the cerebrovascular autoregulatory capacity, leading to forced dilatation of cerebral arteries, causing hyperperfusion, blood-brain barrier disruption, and edema [24, 25]. Interestingly, 20–40% of eclamptic patients never develop overt hypertension prior to convulsions or a stroke [26–28], suggesting an important role for autoregulatory dysfunction in the underlying pathophysiology.

It remains unclear why the parietooccipital lobes are most often involved [24, 25, 29], but it is hypothesized that the decreased sympathetic innervation of the vertebrobasilar arteries, as compared to that of the internal carotid artery system, plays a role [30]. Although the exact role of the autonomic nervous system on the regulation of cerebral blood flow remains controversial [31], recent studies do suggest an autonomic, mainly sympathetic, role in cerebral blood flow control [32, 33], protecting the brain from autoregulation breakthrough and loss of integrity of the blood-brain barrier [34, 35]. The decreased sympathetic innervation in the vertebrobasilar region may allow autoregulatory breakthrough at a lower pressure than in other more densely innervated areas during acute hypertension [30, 36].

47.4 Cerebral Hemodynamics in Pregnancy

The systemic cardiovascular changes in pregnancy are characterized by a significant fall in peripheral vascular resistance, leading to a drop in mean arterial pressure with a nadir at 20–24 weeks. The cardiac output and plasma volume both will increase by 40–50%. This maternal accommodation to pregnancy begins shortly after conception, driven by circulating hormones, with changes noted as early as 5–6 weeks gestation, and is necessary for normal growth and development of the fetal-placental unit.

The cerebral circulation is dependent on a constant blood supply and relative intolerant to increases or decreases in blood volume. Its adaptation to the systemic hemodynamic changes seen in pregnancy is therefore unique from other organs, which undergo substantial increase in perfusion. The cerebral arteries react to pregnancy through several mechanisms, including changes in vascular structure, blood-brain barrier properties, and counteracting the effect of circulating vasoactive factors in order to maintain brain homeostasis [37].

Animal models have been used to study the structural changes in the cerebral vasculature. In pregnant rats, both the lower and upper limits of the cerebral blood flow (CBF) autoregulation curve are extended [37], protecting the brain in cases of acute hypotension (e.g., after excessive blood loss postpartum) and hypertension (e.g., in acute hypertension or peripartum stress). Also in rats, parenchymal arteries undergo outward hypertrophic remodeling, which may cause autoregulatory breakthrough in acute hypertension [38].

In pregnant women, mainly transcranial Doppler ultrasound (TCD/TCCS) and MRI have been applied to study the changes in maternal cerebral blood flow. The flow velocity, flow volume, and resistance index (RI) in the middle and anterior cerebral artery (MCA and ACA) seem to be decreased in late pregnancy when compared to nonpregnant women. However, the cerebral perfusion pressure (CPP), global blood flow, and diastolic velocity in the posterior cerebral artery are increased [39–43]. This suggests that during normal pregnancy, there may be

some degree of redistribution of cerebral blood flow from the MCA and ACA territory to that of the PCA, explaining the vulnerability of the posterior circulation in preeclampsia [17, 44]. This is in line with the attenuated sympathetic innervation seen in the posterior cerebral circulation (vertebrobasilar arteries) when compared with the anterior circulation (MCA and ACA, arising from internal carotid arteries) [30].

The dynamic cerebral autoregulation of both the MCA and PCA is enhanced in the second half of pregnancy, when compared to nonpregnant fertile women [45, 46].

47.5 Cerebral Hemodynamics in Preeclampsia

Several neuroradiological imaging techniques have been used to improve the understanding of cerebrovascular hemodynamic changes and the association with neurological symptoms seen in preeclampsia. Both TCD/TCCS and MRI have shown increased cerebral blood flow velocity/volume and decreased resistance [47–50] in the MCA and PCA of women with preeclampsia when compared to normotensive controls [23, 48, 51], which persisted up to 10 days postpartum [52] but had returned to normal at 6–8 weeks after delivery [51] (Table 47.1).

Since preeclampsia is a heterogeneous condition, the extent of these hemodynamic changes is also diverse. It can lead to either normal, under-, or overperfusion (as indicated by CPP and compared to 95% confidence intervals for normal pregnancy); 52% of women with mild preeclampsia have underperfusion and 59% of women with severe preeclampsia have overperfusion [53]. Furthermore, preeclamptic women with headache were much more likely to have abnormal CPP than those without headache [54, 55]. The severity of preeclampsia seems to correlate with the degree of any TCD/TCCS abnormality, in a way that patients with severe preeclampsia or superimposed preeclampsia have the highest CPP or CBFV [47, 54, 55].

Table 47.1 Tendency of values according to gestational age: cerebral blood flow velocities, pulsatility index (PI), cerebral perfusion pressure (CPP), and ICA blood flow

	MCA	MCA	MCA	MCA	MCA	ICA
	PSV	EDV	MFV	PI	CPP	CBF
Gestational age	cm/s	cm/s	cm/s	–	mmHg	ml/min
8–20 weeks	97–102	31–47	60–71	0.92–1.0	37–50	318 ± 40.6
22–32 weeks	91–100	37–43	55–62	0.81–1.07	41–60	
≥36 weeks	86–92	37–44	55–58	0.76–0.91	46–63	381 ± 50

CPP cerebral perfusion pressure (mmHg), *CBF* cerebral blood flow, *PI* pulsatility Index, *ICA* internal carotid artery, *PSV* peak systolic velocity, *EDV* end-diastolic velocity, *MFV* mean flow velocity [39–41, 65]

Dynamic cerebral autoregulation (CA) is impaired in preeclampsia, and even more so in superimposed preeclampsia when compared to pregnant controls [56, 57]. These studies did not find a correlation between the autoregulatory index (ARI) and blood pressure, and impaired autoregulation could not be identified based on clinical symptoms such as headache or visual disturbances. The largest degree of impairment is seen in women with superimposed preeclampsia who required two or more antihypertensive drugs to control their blood pressure [57].

Very little is known about the cerebral autoregulation in eclampsia. Only one study, by Oehm et al., based on transfer function analysis of arterial blood pressure (ABP) and CBF velocity (TCD/TCCS), showed a severely reduced phase shift and elevated gain in two patients with eclampsia [58]. These changes are highly suggestive of an impaired dynamic CA in these patients.

47.6 TCD/TCCS: For Prediction of Preeclampsia

Although there is no proven effective method for the prevention of preeclampsia, identifying women at risk would allow individually tailored antenatal care and early delivery if needed, thereby reducing the risk of developing severe complications.

Previous studies have used different risk factors including clinical history, complete blood count, and biochemical markers to predict preeclampsia, but none are highly predictive [13].

The use of transcranial Doppler for this purpose also has shown conflicting results. A large prospective study showed that transcranial Doppler indices of low resistance in the MCA in the second trimester are predictive of the subsequent development of preeclampsia in a low-risk, ethnically homogeneous population [59, 60]. The autoregulation index of normotensive women does not seem to be predictive of the development of preeclampsia [46, 56, 60].

However, women with chronic hypertension who subsequently experienced preeclampsia had lower ARIs compared with those who did not. Their ARI was comparable to patients who already had superimposed preeclampsia [56]. Whether the lower ARI is due to preexistent differences or early affected cerebral circulation in pregnant women with chronic hypertension remains to be determined.

47.7 TCD/TCCS: Approach for Bedside Monitoring

In the setting of acute severe preeclampsia or eclampsia, stabilization of the maternal condition, by starting antihypertensives and magnesium sulfate, and support respiratory and cardiovascular functions, is the first priority. The exact mechanism by which magnesium sulfate decrease the risk of eclampsia is not known, nor is it clear what the effect of the different antihypertensive agents is on the cerebral vasculature.

In small studies, TCD/TCCS has been used to determine the effect of labetalol, magnesium sulfate, and nimodipine on the CPP. Labetalol and magnesium sulfate decreased CPP 180 min after administration [61, 62], while nimodipine showed a trend toward increase [62]. Another study showed decrease in CPP after magnesium sulfate in those women with high baseline CPP, but a small increase in those with normal range CPP [63]. If this will be confirmed in bigger studies, and the effect on cerebral autoregulation is examined, transcranial Doppler may have a role in guiding the choice of any one antihypertensive agent over another.

Another application for TCD/TCCS might be the evaluation of dynamic cerebral autoregulation to predict short- and long-term cerebral complications (as has been studied in stroke patients [64]), such as eclampsia, neurological complications, impaired cognitive function, and stroke [11].

47.8 Conclusion

Preeclampsia/eclampsia is a heterogenous systemic disorder, with cerebral complications being a significant factor in maternal morbidity and mortality. The TCD/TCCS anomalies are usually characterized by increased cerebral blood flow velocity/volume, cerebral perfusion pressure, and decreased resistance. However, the flow and perfusion pressure can also be normal, decreased, or increased, possibly reflecting the different etiologies of this heterogenous disorder.

It is not yet possible to predict those who might have an eclamptic seizure, nor the long-term outcome after cerebral involvement. Future research should focus on this topic, which will also contribute to the understanding of this heterogenic disease. Because of the systemic nature and the heterogeneity, collaboration should be sought with different disciplines, and probably peripheral biomarkers and in vitro studies should be added to the cerebral imaging.

A second important aim should be to examine the effect on the cerebral circulation of different antihypertensive drugs administered to treat acute severe hypertension. TCD/TCCS is especially suitable for this purpose, because of its efficiency and bedside application.

This potential new knowledge might considerably change the way we see and treat preeclampsia.

Algorithm

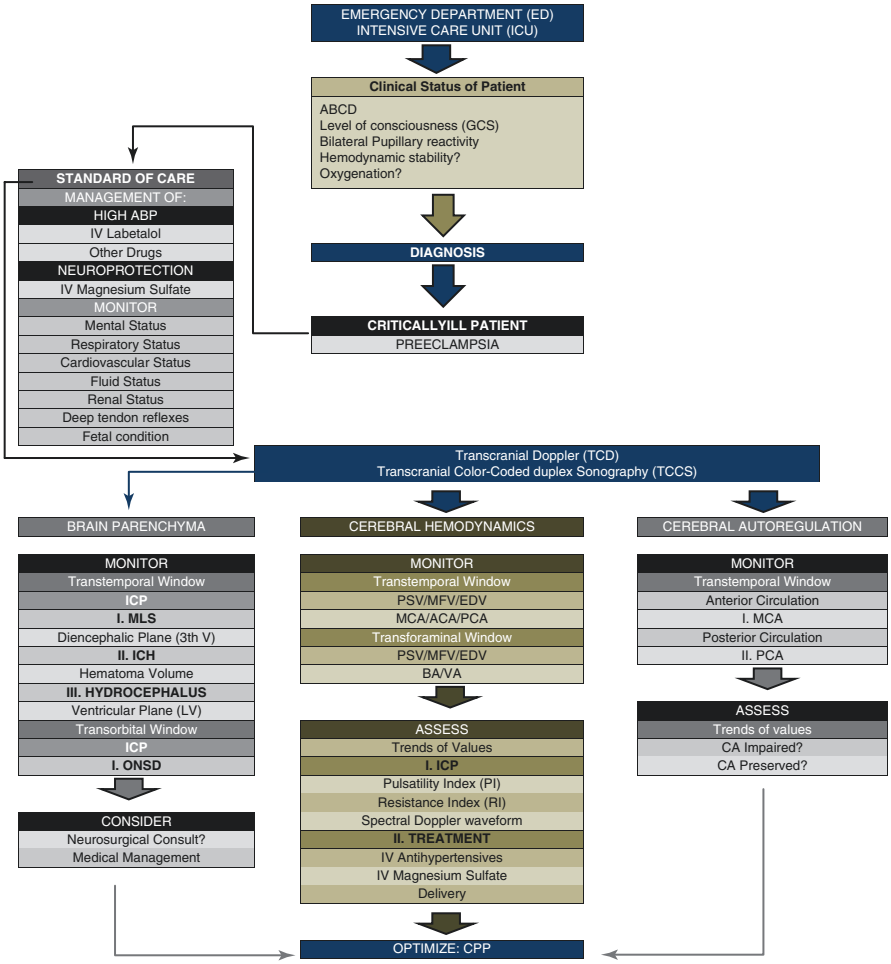

ABCD airway-breathing-circulation-disability, *MLS* midline shift, *ICP* intracranial pressure, *CA* cerebral autoregulation, *ICH* Intracerebral hemorrhage, *3rd* V third ventricle, *LV* lateral ventricles, *ONSD* optic nerve sheath diameter, *PSV* peak systolic velocity, *MFV* mean flow velocity, *EDV* end-diastolic velocity, *CPP* cerebral perfusion pressure, *MCA* middle cerebral artery, *ACA* anterior cerebral artery, *PCA* posterior cerebral artery, *BA* basilar artery, *VA* vertebral artery, *ABP* arterial blood pressure

References

1. Duley L. The global impact of pre-eclampsia and eclampsia. Semin Perinatol. 2009;33:130–7.
2. Hutcheon JA, Lisonkova S, Joseph KS. Epidemiology of pre-eclampsia and the other hypertensive disorders of pregnancy. Best Pract Res Clin Obstet Gynaecol. 2011;25:391–403.
3. Berg CJ, Mackay AP, Qin C, Callaghan WM. Overview of maternal morbidity during hospitalization for labor and delivery in the United States: 1993–1997 and 2001–2005. Obstet Gynecol. 2009;113:1075–81.
4. Centre for Maternal and Child Enquiries (CMACE). Saving mothers' lives: reviewing maternal deaths to make motherhood safer: 2006–08. The Eighth Report on Confidential Enquiries into Maternal Deaths in the United Kingdom. BJOG. 2011;118(Suppl. 1):1–203.
5. Khan KS, Wojdyla D, Say L, Gulmezoglu AM, Van Look PF. WHO analysis of causes of maternal death: a systematic review. Lancet. 2006;367:1066–74.
6. MacKay AP, Berg CJ, Atrash HK. Pregnancy-related mortality from preeclampsia and eclampsia. Obstet Gynecol. 2001;97:533–8.
7. ACOG Committee on Practice Bulletins–Obstetrics. ACOG practice bulletin. Diagnosis and management of preeclampsia and eclampsia. Number 33, January 2002. Obstet Gynecol. 2002;99:159–67.
8. Miguil M, Chekairi A. Eclampsia, study of 342 cases. Hypertens Pregnancy. 2008;27:103–11.
9. Anonymous hypertension in pregnancy: executive summary. Obstet Gynecol. 2013;122:1122–31.
10. American College of Obstetricians and Gynecologists. ACOG practice bulletin no. 125: chronic hypertension in pregnancy. Obstet Gynecol. 2012;119:396–407.
11. Bergman L, Torres-Vergara P, Penny J, Wikstrom J, Nelander M, Leon J, et al. Investigating maternal brain alterations in preeclampsia: the need for a multidisciplinary effort. Curr Hypertens Rep. 2019;21:72-019-0977-0.
12. Geldenhuys J, Rossouw TM, Lombaard HA, Ehlers MM, Kock MM. Disruption in the regulation of immune responses in the placental subtype of preeclampsia. Front Immunol. 2018;9:1659.
13. Steegers EA, von Dadelszen P, Duvekot JJ, Pijnenborg R. Pre-eclampsia. Lancet. 2010;376:631–44.
14. James AH, Bushnell CD, Jamison MG, Myers ER. Incidence and risk factors for stroke in pregnancy and the puerperium. Obstet Gynecol. 2005;106:509–16.
15. Kuklina EV, Ayala C, Callaghan WM. Hypertensive disorders and severe obstetric morbidity in the United States. Obstet Gynecol. 2009;113:1299–306.
16. Bateman BT, Schumacher HC, Bushnell CD, Pile-Spellman J, Simpson LL, Sacco RL, Berman MF. Intracerebral hemorrhage in pregnancy: frequency, risk factors, and outcome. Neurology. 2006;67:424–9.
17. Zeeman GG. Neurologic complications of pre-eclampsia. Semin Perinatol. 2009;33:166–72.
18. Richards A, Graham D, Bullock R. Clinicopathological study of neurological complications due to hypertensive disorders of pregnancy. J Neurol Neurosurg Psychiatry. 1988;51:416–21.
19. Digre KB, Varner MW, Osborn AG, Crawford S. Cranial magnetic resonance imaging in severe preeclampsia vs eclampsia. Arch Neurol. 1993;50:399–406.
20. Bartynski WS. Posterior reversible encephalopathy syndrome, part 2: controversies surrounding pathophysiology of vasogenic edema. AJNR Am J Neuroradiol. 2008;29:1043–9.
21. Sengar AR, Gupta RK, Dhanuka AK, Roy R, Das K. MR imaging, MR angiography, and MR spectroscopy of the brain in eclampsia. AJNR Am J Neuroradiol. 1997;18:1485–90.

22. Trommer BL, Homer D, Mikhael MA. Cerebral vasospasm and eclampsia. Stroke. 1988;19:326–9.
23. Naidu K, Moodley J, Corr P, Hoffmann M. Single photon emission and cerebral computerised tomographic scan and transcranial Doppler sonographic findings in eclampsia. Br J Obstet Gynaecol. 1997;104:1165–72.
24. Easton JD. Severe preeclampsia/eclampsia: hypertensive encephalopathy of pregnancy? Cerebrovasc Dis. 1998;8:53–8.
25. Schwartz RB, Feske SK, Polak JF, DeGirolami U, Iaia A, Beckner KM, et al. Preeclampsia-eclampsia: clinical and neuroradiographic correlates and insights into the pathogenesis of hypertensive encephalopathy. Radiology. 2000;217:371–6.
26. Douglas KA, Redman CW. Eclampsia in the United Kingdom. BMJ. 1994;309:1395–400.
27. Mattar F, Sibai BM. Eclampsia. VIII. Risk factors for maternal morbidity. Am J Obstet Gynecol. 2000;182:307–12.
28. Katz VL, Farmer R, Kuller JA. Preeclampsia into eclampsia: toward a new paradigm. Am J Obstet Gynecol. 2000;182:1389–96.
29. Hinchey J, Chaves C, Appignani B, Breen J, Pao L, Wang A, et al. A reversible posterior leukoencephalopathy syndrome. N Engl J Med. 1996;334:494–500.
30. Lincoln J. Innervation of cerebral arteries by nerves containing 5-hydroxytryptamine and noradrenaline. Pharmacol Ther. 1995;68:473–501.
31. Seifert T, Secher NH. Sympathetic influence on cerebral blood flow and metabolism during exercise in humans. Prog Neurobiol. 2011;95:406–26.
32. Zhang R, Zuckerman JH, Iwasaki K, Wilson TE, Crandall CG, Levine BD. Autonomic neural control of dynamic cerebral autoregulation in humans. Circulation. 2002;106:1814–20.
33. Hamner JW, Tan CO, Tzeng YC, Taylor JA. Cholinergic control of the cerebral vasculature in humans. J Physiol. 2012;590:6343–52.
34. Faraci FM, Mayhan WG, Werber AH, Heistad DD. Cerebral circulation: effects of sympathetic nerves and protective mechanisms during hypertension. Circ Res. 1987;61:II102–6.
35. Sadoshima S, Heistad D. Sympathetic nerves protect the blood-brain barrier in stroke-prone spontaneously hypertensive rats. Hypertension. 1982;4:904–7.
36. Cipolla MJ, Bishop N, Chan SL. Effect of pregnancy on autoregulation of cerebral blood flow in anterior versus posterior cerebrum. Hypertension. 2012;60:705–11.
37. Johnson AC, Cipolla MJ. The cerebral circulation during pregnancy: adapting to preserve normalcy. Physiology (Bethesda). 2015;30:139–47.
38. Cipolla MJ, Sweet JG, Chan SL. Cerebral vascular adaptation to pregnancy and its role in the neurological complications of eclampsia. J Appl Physiol (1985). 2011;110:329–39.
39. Belfort MA, Tooke-Miller C, Allen JC Jr, Saade GR, Dildy GA, Grunewald C, et al. Changes in flow velocity, resistance indices, and cerebral perfusion pressure in the maternal middle cerebral artery distribution during normal pregnancy. Acta Obstet Gynecol Scand. 2001;80:104–12.
40. Lindqvist PG, Marsal K, Pirhonen JP. Maternal cerebral Doppler velocimetry before, during, and after a normal pregnancy: a longitudinal study. Acta Obstet Gynecol Scand. 2006;85:1299–303.
41. Nevo O, Soustiel JF, Thaler I. Maternal cerebral blood flow during normal pregnancy: a cross-sectional study. Am J Obstet Gynecol. 2010;203:475.e1–6.
42. Bergersen TK, Hartgill TW, Pirhonen J. Cerebrovascular response to normal pregnancy: a longitudinal study. Am J Physiol Heart Circ Physiol. 2006;290:H1856–61.
43. van Veen TR, Haeri S, Sangi-Haghpeykar H, Belfort MA. Changes in maternal posterior and anterior cerebral artery flow velocity during pregnancy and postpartum–a longitudinal study. J Clin Ultrasound. 2013;41:532–7.

44. Loureiro R, Leite CC, Kahhale S, Freire S, Sousa B, Cardoso EF, et al. Diffusion imaging may predict reversible brain lesions in eclampsia and severe preeclampsia: initial experience. Am J Obstet Gynecol. 2003;189:1350–5.
45. van Veen TR, Panerai RB, Haeri S, van den Berg PP, Zeeman GG, Belfort MA. Changes in cerebral autoregulation in the second half of pregnancy and compared to non-pregnant controls. Pregnancy Hypertens. 2016;6(4):380–3.
46. Janzarik WG, Ehlers E, Ehmann R, Gerds TA, Schork J, Mayer S, et al. Dynamic cerebral autoregulation in pregnancy and the risk of preeclampsia. Hypertension. 2014;63:161–6.
47. Demarin V, Rundek T, Hodek B. Maternal cerebral circulation in normal and abnormal pregnancies. Acta Obstet Gynecol Scand. 1997;76:619–24.
48. Riskin-Mashiah S, Belfort MA. Preeclampsia is associated with global cerebral hemodynamic changes. J Soc Gynecol Investig. 2005;12:253–6.
49. Williams KP, Wilson S. Persistence of cerebral hemodynamic changes in patients with eclampsia: a report of three cases. Am J Obstet Gynecol. 1999;181:1162–5.
50. Riskin-Mashiah S, Belfort MA, Saade GR, Herd JA. Cerebrovascular reactivity in normal pregnancy and preeclampsia. Obstet Gynecol. 2001;98:827–32.
51. Zeeman GG, Hatab MR, Twickler DM. Increased cerebral blood flow in preeclampsia with magnetic resonance imaging. Am J Obstet Gynecol. 2004;191:1425–9.
52. Janzarik WG, Jacob J, Katagis E, Markfeld-Erol F, Sommerlade L, Wuttke M, Reinhard M. Preeclampsia postpartum: impairment of cerebral autoregulation and reversible cerebral hyperperfusion. Pregnancy Hypertens. 2019;17:121–6.
53. Belfort MA, Grunewald C, Saade GR, Varner M, Nisell H. Preeclampsia may cause both overperfusion and underperfusion of the brain: a cerebral perfusion based model. Acta Obstet Gynecol Scand. 1999;78:586–91.
54. Belfort MA, Saade GR, Grunewald C, Dildy GA, Abedejos P, Herd JA, Nisell H. Association of cerebral perfusion pressure with headache in women with pre-eclampsia. Br J Obstet Gynaecol. 1999;106:814–21.
55. Lee YJ, Lee S, Jo HN, Kim JM, Kwon BS, Joo JK, et al. Alterations in transcranial Doppler indices of pregnant women with complicated preeclampsia. Pregnancy Hypertens. 2019;15:189–94.
56. van Veen TR, Panerai RB, Haeri S, Singh J, Adusumalli JA, Zeeman GG, Belfort MA. Cerebral autoregulation in different hypertensive disorders of pregnancy. Am J Obstet Gynecol. 2015;212:513.e1–7.
57. van Veen TR, Panerai RB, Haeri S, Griffioen AC, Zeeman GG, Belfort MA. Cerebral autoregulation in normal pregnancy and preeclampsia. Obstet Gynecol. 2013;122:1064–9.
58. Oehm E, Hetzel A, Els T, Berlis A, Keck C, Will HG, Reinhard M. Cerebral hemodynamics and autoregulation in reversible posterior leukoencephalopathy syndrome caused by pre-/eclampsia. Cerebrovasc Dis. 2006;22:204–8.
59. Belfort M, Van Veen T, White GL, Kofford S, Allred J, Postma I, Varner M. Low maternal middle cerebral artery Doppler resistance indices can predict future development of pre-eclampsia. Ultrasound Obstet Gynecol. 2012;40:406–11.
60. Riskin-Mashiah S, Belfort MA, Saade GR, Herd JA. Transcranial doppler measurement of cerebral velocity indices as a predictor of preeclampsia. Am J Obstet Gynecol. 2002;187:1667–72.
61. Belfort MA, Tooke-Miller C, Allen JC Jr, Dizon-Townson D, Varner MA. Labetalol decreases cerebral perfusion pressure without negatively affecting cerebral blood flow in hypertensive gravidas. Hypertens Pregnancy. 2002;21:185–97.
62. Belfort MA, Saade GR, Yared M, Grunewald C, Herd JA, Varner MA, Nisell H. Change in estimated cerebral perfusion pressure after treatment with nimodipine or magnesium sulfate in patients with preeclampsia. Am J Obstet Gynecol. 1999;181:402–7.

63. Belfort M, Allred J, Dildy G. Magnesium sulfate decreases cerebral perfusion pressure in preeclampsia. Hypertens Pregnancy. 2008;27:315–27.
64. Salinet AS, Silva NC, Caldas J, de Azevedo DS, et al. Impaired cerebral autoregulation and neurovascular coupling in middle cerebral artery stroke: influence of severity? J Cereb Blood Flow Metab. 2018;39(11):2277–85.
65. Batur Caglayan HZ, et al. Assessment of maternal cerebral blood flow velocity by transcranial Doppler ultrasound before delivery and in the early postpartum period. J Matern Fetal Neonatal Med. 2019;32(4):584–9.

Chapter 48
ECMO Patient in Intensive Care Unit: Usefulness of Neurosonology in Neurologic Monitoring

Loïc Le Guennec and Alain Combes

Key Points

1. Nonpulsatile blood flow caused by the ECMO pump might affect cerebral autoregulation through the alteration of the myogenic response.
2. The addition of an IABP influences CBF depending on the systolic antegrade blood flow by spontaneous cardiac function. It decreases CBF in patients with cardiac stun because of transient end-diastolic reversal of intracranial blood flow induced by this device.
3. Too-rapid hypercapnia correction after VV ECMO cannulation might lead to cerebral vasoconstriction and cerebrovascular complications.
4. No correlation has been made yet, neither between MES and ECMO flow rate nor between MES and neurological outcome.
5. TCD/TCCS is a good tool to assess cerebral circulatory arrest during ECMO only in patients with an LVEF higher than 20%.

L. Le Guennec (✉)
Intensive Medicine Neurologic Reanimation, Hôpital Pitié-Salpêtrière, Paris, France

Sorbonne University, Paris, France
e-mail: loic.leguennec@yahoo.fr

A. Combes
Reanimation Service, Institute of Cardiology, Groupe Hospital Pitié–Salpêtrière, Public Assistance – Hospital of Paris, Paris, France

Sorbonne University, UPMC University Paris 06, Institute of Cardiometabolism and Nutrition, Paris, France
e-mail: alain.combes@psl.aphp.fr

C. N. Rodríguez et al. (eds.), *Neurosonology in Critical Care*,
https://doi.org/10.1007/978-3-030-81419-9_48

48.1 Introduction

Extracorporeal membrane oxygenation (ECMO) is an emergency support procedure used to provide cardiac and/or pulmonary support in patient refractory to conventional therapies [1]. Over recent years, the number of patients treated with ECMO has increased [2, 3] and risk–benefit balance ratio has improved [3, 4]. ECMO circuit is either in a veno-venous (VV) configuration or in a veno-arterial (VA) configuration. It is associated to a centrifugal pump, which provides a continuous flow in the circuit, and to a membrane oxygenator. VV ECMO is used in acute respiratory distress syndrome (ARDS), and VA ECMO in refractory cardiogenic shock and cardiac arrest.

In VA ECMO, the circuit includes an inflow cannula, which drains blood from the venous system, and an outflow cannula, which delivers the warmed oxygenated blood back into the arterial system in order to restore a circulatory flow [5]. It is used for refractory cardiac dysfunction, regardless of the underlying cardiac pathology (myocarditis, cardiomyopathy, postcardiotomy heart failure, primary graft failure after heart transplantation, ventricular dysfunction in patients with acute coronary syndrome, acute intoxications due to cardiotropic drugs, cardiac arrest) [5]. Intra-aortic balloon pump (IABP) is often added in those patients to protect against hydrostatic pulmonary edema [6], or to improve coronary bypass graft flows and cardiac function in refractory postoperative cardiogenic shock [7, 8]. It reduces left ventricular afterload, improves coronary perfusion, and provides a pulsatile blood flow [9, 10].

In VV ECMO, the outflow cannula delivers oxygenated and decarboxylated blood to the vena cava and the right atrium. The aim of this configuration is to insure a normal blood gas exchange during ARDS refractory to conventional therapy [5, 11].

The Extracorporeal Life Support Organization (ELSO) collects data since 2002 from 359 centers managing with ECMO worldwide [12]. ELSO reported overall outcomes in 2018 in 35,632 adult patients, among which 15,686 were VV ECMO with a survival rate of 66% and 15,201 were VA ECMO with a survival rate of 55%; there were also 4745 extracorporeal cardiopulmonary resuscitation with a survival rate of 38% [12]. These data show that survival rate is higher in VV than in VA ECMO.

Use of ECMO is associated with several cerebrovascular complications (anoxic cerebral injury, ischemic stroke and cerebral hemorrhage, epileptic seizures, coma and brain death) [13–15], responsible for high morbidity and mortality [13, 16]. Many pre-ECMO factors are associated with neurological injury, but during the course of ECMO, the modality used is also diversely associated to nervous system complication. Stroke occurs mainly during VA ECMO [15], whereas cerebral

hemorrhage is mostly observed during VV ECMO [14, 17]. These complications have an important impact in terms of outcome, and consequently on multidisciplinary team decisions.

It is likely that both VA and VV ECMO affect cerebral blood flow (CBF) and impact cerebral hemodynamics, resulting in neurological impairment [15, 17–20]. IABP might also play a role in CBF modification in patients with cardiac failure [10]. Early detection and specific care for neurological complications could improve the prognosis of these patients. Indeed, because of the critical condition of those patients and the use of deep sedation and anesthesia, it can be difficult to diagnose a neurological event under ECMO. Moreover, those neurological complications may be underestimated because of the difficulty to transfer these patients to other wards and to perform neuroimaging examinations.

As transcranial Doppler (TCD)/transcranial color-coded duplex sonography (TCCS) is a noninvasive monitoring procedure able to detect cerebral hemodynamic changes in real-time, microembolism, and has been used extensively in neurological and neurosurgical patients to monitor CBF velocities, there is an increasing literature about its usefulness in ECMO patients to detect as soon as possible ECMO-related cerebrovascular complication.

The aim of this chapter is to review literature concerning dynamic monitoring of CBF by TCD during ECMO and to give practical considerations.

48.2 Cerebral Hemodynamics

48.2.1 Physiological Mechanisms

The three processes responsible of cerebral hemodynamics regulation are the cerebrovascular responses to: (1) brain metabolism, called neurovascular coupling; (2) autonomic neurogenic regulation; and (3) changes in cerebral perfusion pressure (CPP), called cerebral autoregulation (CA).

Neurovascular coupling aim is to increase the CBF in response to regional or global brain metabolic demands. This metabolic regulation is effected by vasoactive mediators concentration changes in the perineuronal space such as CO_2, O_2, lactate, NO, K^+, Ca^{2+}, H^+, and adenosine [21–24].

Neurogenic regulation of the vascular tone is triggered by perivascular sympathetic and cholinergic nerves that originate from peripheral nerve ganglia and intrinsic brain neurons [25]. This mechanism depends on autonomic nervous system reactivity and, for example, plays an important role in the pathophysiology of the migraine [26].

CA is the ability of cerebral arterioles to maintain stable CBF while mean arterial blood pressure (MAP) and CPP vary [27]. The CPP is defined as the difference between the MAP and the intracranial pressure, which is the pressure of the cerebrospinal fluid in the subarachnoid space. The constant CBF is obtained by vasodilation and vasoconstriction of cerebral arterioles. This mechanism allows to maintain proper brain perfusion and to supply the brain with the necessary oxygen and energy substrates under physiological and pathological conditions. Indeed, changes in perfusion pressure occur under normal conditions, as exercise or during a change in posture, or may result from pathological conditions such as subarachnoid hemorrhage (SAH), traumatic brain injury, stroke, or drugs administration. The myogenic response observed in CA process is the intrinsic ability of small arteries and pial arterioles smooth muscle cells to respond to changes in transmural vascular pressure resulting from MAP or CPP modification. This innate myogenic mechanism is not regulated by the autonomic nervous system. It is responsible for myogenic tone and subsequently cerebral vascular resistance.

Segmental and regional heterogeneity within the brain can result in varying levels of CBF in different regions of the brain, over the same range of CPP [28].

In pathological conditions, cerebral hemodynamics may become dysfunctional. Several disease states resulting in impaired CA are known, such as traumatic brain injury [29, 30], ischemic stroke [31, 32], intracerebral hemorrhage [33, 34], and subarachnoid hemorrhage [35, 36].

48.2.2 Regulation During ECMO

In adult patients, there is limited literature about CA impairment during ECMO.

Although pre-ECMO factors, such as hypoxia, hypercapnia, hypoperfusion, or hypertension, can disrupt systemic blood flow regulation, leaving the brain vulnerable to changes in blood pressure [37], it has been shown that cannulation of great blood vessels and alterations of pulsatile flow during the course of ECMO also affect CA [38, 39]. Most of those studies have been done in pediatric patients and have used near infrared spectrophotometry (NIRS) to assess this impairment. Thus, both pre- and ECMO factors may contribute to cerebrovascular complications commonly seen in ECMO.

48.2.2.1 VA ECMO

Various factors can alter CBF during ECMO. One of the main hypotheses is that the laminar blood flow caused by the ECMO pump affects CA through the myogenic response. The effect of nonpulsatile flow on the brain has been of concern first in

cardiopulmonary bypass (CPB). An experimental animal study in the 1980s compared pulsatile and nonpulsatile bypass in a canine stroke model and found that pulsatile flow increased CBF significantly over nonpulsatile flow, showing the importance of pulsatile blood flow in ischemic brain disease [40]. In adult patients undergoing CPB, the mean lower limit of autoregulation, under which a drop in CPP results in a loss of CBF, has been found to be the MAP at 66 mmHg [41], but instead of targeting a specific MAP, CA monitoring using cerebral oximetry index to individualize optimal blood pressure is widely used to prevent neuronal injury [42].

During VA ECMO, CA has been evaluated in the early 1990s in newborn lambs [43]. Nonpulsatile roller-pump were used in this work. CA was evaluated during the course of ECMO by lowering the CPP via an increase in intracranial pressure through infusion of artificial cerebrospinal fluid into the lateral ventricle. CA was found to be impaired in lamb on VA ECMO (flow rates of 120–150 mL/kg/min) compared to control animals with right jugular vein and carotid artery ligation.

Multiple studies using NIRS and neuroimaging have shown abnormal CA in infants undergoing VA ECMO [20, 44, 45], but those studies are lacking in adult patients. Indeed, in neonates, the outflow arterial cannulation site can be the carotid artery, which can itself impact on CBF, whereas outflow arterial cannulation site in adult is often the femoral artery. However, when the outflow arterial cannula is the femoral artery, clinicians fear that the brain receives hypoxemic and undercarboxylated blood ejected from a residual activity of the left ventricle, in patient with poor lung function. This upper body differential hypoxemia defined as "Harlequin syndrome" [46] is usually detected by the monitoring of oxygen saturation within the right upper limb and could also impact CA.

The addition of an IABP in conjunction with VA ECMO to protect against hydrostatic pulmonary edema [6], or to improve coronary bypass graft flows and cardiac function in refractory postoperative cardiogenic shock [7, 8, 47], has also been shown to modify cerebral hemodynamics. Indeed, one study has shown, in patients with refractory cardiogenic shock after cardiac surgery requiring VA ECMO, that the addition of an IABP influences CBF depending on the systolic antegrade blood flow by spontaneous cardiac function. In this study, the addition of an IABP to VA ECMO support decreased the CBF in patients with cardiac stun, and it increased CBF in patients without cardiac stun [48].

48.2.2.2 VV ECMO

The main metabolic factors known to cause significant changes in CBF are $PaCO_2$ and pH. These parameters can rapidly change during VV ECMO [49]. Intracranial bleeding is the most frequent cerebrovascular complication during VV ECMO, and

it has been found that a decrease in $PaCO_2$ after ECMO cannulation was independently associated with this complication [17]. However, because rapid decrease in $PaCO_2$ leads to cerebral vasoconstriction, the relationship between $PaCO_2$ change and cerebral bleeding is difficult to understand. One hypothesis could be that those cerebral bleeding was in fact secondary hemorrhagic transformation after cerebral infarction due to a cerebral vasoconstriction induced by VV ECMO.

Another factor that could impair cerebral hemodynamic during VV ECMO is the internal jugular vein occlusion due to the inflow cannula, which can cause cerebral venous hypertension, resulting in a decreased CBF within the first hours of cannulation, as it has been described in newborn [50]. In those studies, this effect tends to disappear after 24 h of VV ECMO, with normalization of the CBF [50, 51].

We can see that various factors can alter CBF during both VA and VV ECMO, and noninvasive monitoring procedures able to detect those cerebral hemodynamic changes in real time might be useful in everyday medical practice.

48.3 Transcranial Doppler Monitoring

TCD/TCCS is the reference tool to monitor CBF velocities. It is broadly used by neurointensivists. Briefly, it emits pulse wave ultrasounds that penetrate brain parenchyma and are reflected back after being scattered by circulating red blood cells. The frequency of this echo is then proportional to red blood cells velocity. Measurement of the pulsatility index (PI) (calculated as systolic velocity – diastolic velocity)/mean velocity), which reflects vascular resistance, is then performed to evaluate cerebral blood. In physiological condition, PIs ranges approximately from 0.8 to 1.4 depending on patient's age.

Studies looking at TCD/TCCS on adult patients treated with ECMO are very limited in literature. However, this tool can be useful to assess CA during ECMO and has numerous advantages compared to other modalities, as it is a noninvasive technique, available at bedside, and repeatable without any risk of radiation.

48.3.1 VA ECMO

In 2016, a study in eight VA ECMO patients without IABP, implanted for cardiogenic shock or cardiac arrest, has shown a correlation between lowering of PIs and left ventricular ejection fraction (LVEF) [19]. Indeed, as the heart systolic function gives rise to the upstroke observed on TCDs, patients with a severely reduced LVEF displayed lower or noncomputable PIs. In this study, an ejection fraction (EF) of

less than 10% resulted in a nonpulsatile TCD waveform. Moreover, in those patients, the measurement of the diastolic phase during TCD for calculation of PIs corresponded to the nonpulsatile flow generated by the ECMO circuit. In an expected manner, when the EF increased during recovery or following placement of total artificial heart and ECMO decannulation, the systolic upstroke increases in amplitude, resulting in higher PIs values, and returns to normal. This study shows that low or noncomputable PIs and lack of systolic upstroke should not be mistaken with cerebral vasodilation in VA ECMO patients with laminar flow, and that rising of their PIs during the course of ECMO can be related to a cardiac recovery. However, focal or asymmetrical PIs modifications still suggest changes of vascular resistance and should evoke cerebrovascular disease [52, 53].

As IABP is increasingly used in addition to VA ECMO to improve coronary bypass graft flows and cardiac function, and protects against hydrostatic pulmonary edema in critically ill patients [6–8], some studies have evaluated the impact of this combination on CBF. As a reminder, the effect of IABP alone on CBF is controversial, and there are some examples of contradictions in literature. For example, a study in patients with IABP support alone after cardiac surgery found that this device caused a small but significant increase in systolic antegrade mean flow velocity in the middle cerebral artery, but because 30% of those patients displayed transient end-diastolic reversal of intracranial blood flow induced by this device, the resulting average flow velocity was not influenced by the IABP [54]. An older study has also shown in 56 patients on IABP assistance alone a reduction of 11.6% in the ocular blood flow measured by ocular pneumoplethysmography [55].

However, the effect of the combination of VA ECMO and IABP on the CBF is not well known. Only one prospective study has investigated with TCD the effect of IABP in addition to VA ECMO on the CBF, analyzing the blood flow of the bilateral middle cerebral arteries [48].

In this work, 12 adult patients receiving VA ECMO and IABP support for refractory postcardiotomy cardiogenic shock after coronary artery bypass were analyzed. The IABP was implanted before VA ECMO. The CBF velocity were measured once every 12 h, under “turned on” IABP and “turned off” IABP support. Patients provided their own control values through the “turned off” IABP condition. All 12 patients were successfully weaned from the IABP and VA ECMO, 8 patients were able to be discharged from the hospital, and survival rate was 66.7%. Cerebrovascular complications were not observed in this study. Concerning their CBF, no statistically significant differences for the mean CBFs were observed between VA ECMO alone and VA ECMO with IABP support, but the authors divided patients into two groups, considering their cardiac functional state and their basal pulsatile pressure without IABP support. Their conclusions were that the addition of an IABP to VA ECMO significantly decreased the mean CBF in patients with basal pulsatile pressure under 10 mmHg and led to a significant increase in the mean CBF values in patients with basal pulsatile pressure higher than 10 mmHg. The CBF decrease in

cardiac-stunned patient with VA ECMO and IABP seems to be due to the diastolic inflation of the IABP, which might intermittently compromise the retrograde flow, as it has been described in patients with cardiogenic shock and IABP alone [54].

Finally, in a recent retrospective study performed in 20 VA ECMO patients implanted for cardiogenic shock and/or cardiac arrest, 4 different TCD/TCCS waveform were correlated to LVEF values and IABP support [56]: (1) double systolic peak pattern in patients with both cardiac systole and IABP waves detectable; (2) Normal waveform pattern in patient with detectable cardiac systole wave with no IABP or IABP turned off; (3) systolic IABP peak into a continuous demodulate waveform pattern in patient with undetectable cardiac systolic wave; (4) continuous and nonpulsatile flow corresponding to VA ECMO flow in patient without detectable cardiac systole and no IABP, or IABP turned off. In that study, cardiac systolic peaks could be detected by TCD/TCSS when LVEF was above 20%.

Figure 48.1 shows patterns of TCD/TCCS waveforms of VA ECMO with IABP from our center.

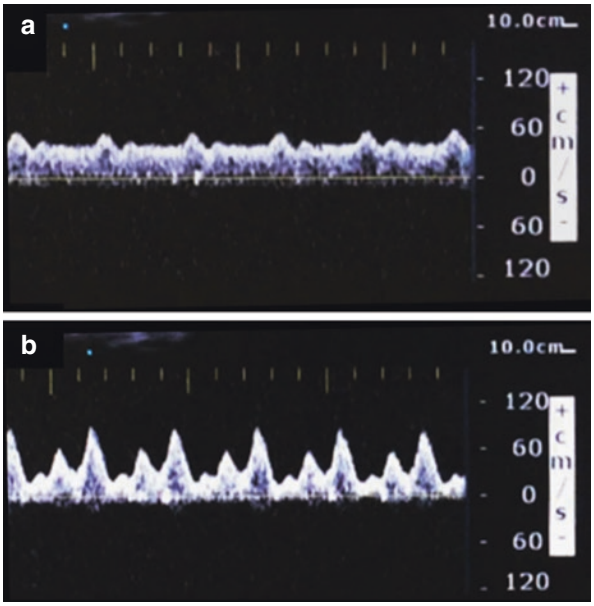

Fig. 48.1 Patterns of TCD waveforms of VA ECMO and VA ECMO with IABP patients, depending on their LVEF. Patient with LVEF of 30% and PP of 20 mmHg with VA ECMO and IABP. TCD monitoring of the right proximal segment of the middle cerebral artery of the right median cerebral artery showing (**a**) IABP off: Detectable cardiac systolic peak within a continuous demodulate waveform pattern. (**b**) IABP on: Double systolic peak corresponding to cardiac systole and IABP peak. ECMO extracorporeal membrane oxygenation, VA veno-arterial, LVEF left ventricular ejection fraction, PP pulsatile pressure, IABP intra-aortic balloon pump

48.3.2 VV ECMO

Concerning VV ECMO, a pediatric study [51] has shown in 19 newborns infants, among which 1 developed intracranial hemorrhage, that, except in this case of cerebral hemorrhage where the velocity in each of the cerebral arteries was higher compared with cases without cerebral complications, the CBF was either maintained or gradually increased before and during ECMO. Because most of these newborns were treated with double-lumen cannula, introduced into the right internal jugular vein, CBF trends to decrease within the first hours of cannulation, probably because of a transitory cerebral venous hypertension [50]. As described before, this effect trends to disappeared in the first day of VV ECMO, with normalization of the CBF.

48.4 TCD/TCCS: Cerebrovascular Complications During ECMO

ECMO use is associated with cerebrovascular diseases. In this paragraph, we focus on ischemic stroke and cerebral hemorrhage during ECMO and the contribution of TCD/TCCS in their early detection and specific care. We also discuss about brain death, even if this complication is mainly due to pre-ECMO factors, because of the specific management of brain-dead donor supported by this device, and the potential usefulness of TCD/TCCS in this particular situation. Algorithm resumes TCD/TCCS patterns depending on ECMO type.

48.4.1 Ischemic Stroke

48.4.1.1 VA ECMO

Ischemic strokes are more commonly observed in VA ECMO patients [15]. In 2016, a series of 137 patients with VA ECMO reported its incidence, diagnosed by brain imaging, at 10% [57]. However, this number was estimated at 50% in a 2006 study in which a cerebral magnetic resonance imaging (MRI) was performed systematically during the longitudinal follow-up of survivors, with median follow-up at 5 years [15]. Finally, in a study of 84 patients undergoing VA ECMO, where a brain autopsy was performed in 25% of non-survivors (10 patients), ischemic brain lesions were found in 70% of them, although neurological disorder was not notified during their stay [13].

Regarding the risk factors for ischemic stroke, a recent study of 171 patients including 80% of VA ECMO reported that a lactate level >10 mmol/L before ECMO cannulation was an independent risk factor of their occurrence [58].

48.4.1.2 VV ECMO

Ischemic stroke is less common in patients with VV ECMO compared to VA ECMO. The largest cohort that investigates neurological complications in patients undergoing VV ECMO has reported its incidence at 2% [17]. In this study, ischemic strokes occurred after a median of 21 days after ECMO implantation [17].

In 2006, a study in which a brain MRI was performed in survivors, no ischemic injury was found [15]. Studies with brain autopsy of patients undergoing VV ECMO have not been published so far.

48.4.1.3 Pathophysiological Mechanisms and TCD/TCCS Contribution

Mechanisms responsible for ischemic strokes are most likely to be different depending on the ECMO type. Regarding the mechanism of ischemic injury in patients undergoing VA ECMO, no study has analyzed their origin, but considering that these patients are more prone to ischemic stroke because of their underlying heart disease that motivates ECMO cannulation, the main cause seems to be cardioembolic stroke.

The role of the ECMO circuit itself in those strokes remains unclear, but it is likely that, regardless of the underlying disease, the presence of an ECMO may itself be a source of embolism. Indeed, the shear stress imposed by the flow pump generates an increased platelet activation, which causes their aggregation [59]. This is particularly observed with centrifugal pumps, widely used nowadays because of a decreased hemolysis compared to old roller-pump systems [59].

Another mechanism that can explain the high frequency of ischemic stroke in VA ECMO patients is cerebral hypoperfusion during initial cardiogenic shock. In this situation, cerebral infarctions have a particular topography, called "watershed cerebral infarction," also known as "border zone infarcts," because they occurred at the border between cerebral vascular territories where the tissue is farthest from arterial supply, and thus most vulnerable to reductions in perfusion. They are observed at the level of anastomoses between the different cerebral arterial territories, anterior, middle, and posterior.

For patients under VV ECMO, stroke physiopathology is less obvious than for VA ECMO. A mechanism involving a paradoxical embolism, responsible for 2% of ischemic strokes [60], could be evoked during VV ECMO, especially in ARDS patients with elevation of right atrial pressures induced by ultraprotective mechanical ventilation and high level of positive end-expiratory pressure, responsible for a reopening of their foramen ovale, and therefore, a higher risk of venous thromboembolism toward the arterial circulation. Finally, too-rapid correction of hypercapnia can result in respiratory alkalemia in these patients and may be responsible for cerebrovascular vasoconstriction and reduction in CBF that may cause ischemic injury [61].

TCD/TCCS can be used to identifying vessel occlusions and to monitor stroke response to treatment [62]. It is also used for microembolic signals (MES) detection [63]. MES are high-intensity transient signals detected by TCD/TCCS and have been shown to correspond to microemboli made of air, platelet, fibrinogen, or atheromatous material [63]. Their detection is correlated with recurrent ischemic stroke in patient with acute cerebral infarction [64]. They are also used as predictors of cerebral events in patients with symptomatic and asymptomatic carotid disease [65].

As cerebral infarctions might be caused by microemboli created in the arterial line during the ECMO support, studies have investigated if TCD/TCCS can aid in detecting microemboli arising from the ECMO circuit [66, 67]. In a 2010 study, six VA ECMO patients were evaluated for MES [66]. Among them, four had refractory postcardiotomy cardiogenic shock, and two were implanted because of cardiac arrest. All patients were assisted with IABP and with continuous renal replacement therapy. The authors reported a correlation between MES count and high flow rate of ECMO support (≥4 l/min). In 2016, a largest study in 55 patients with VA, VV ECMO, and extracorporeal CO_2 removal ($ECCO_2R$) had been performed and investigated if MES could be correlated to neurological outcome [67]. In this study, MES count was higher in VA ECMO patient than other, but no correlation was made, neither between MES and ECMO flow rate nor between MES and neurological outcome.

48.4.2 Intracerebral Hemorrhage

It is important to note that it can be difficult to distinguish between primary cerebral hemorrhage and secondary hemorrhagic transformation after cerebral infarction, which is correlated with the size of cerebral infarction [68].

48.4.2.1 VA ECMO

In 2013, the ELSO registry reported a rate of intracranial hemorrhage of 2% in patients undergoing VA ECMO. In 1999, a retrospective study searching for risk factors of cerebral hemorrhage during VA ECMO reported that neither the underlying disease nor the site of cannulation was associated with an increased risk of cerebral hemorrhage, as well as MAP, ECMO flow rate, or ECMO duration [69]. In addition, there was no evidence of a link between high activated clotting time (ACT) or low prothrombin time (PTT) and intracranial hemorrhage. In contrast, thrombocytopenia <50,000/mm^3 was an independent risk factor associated with a high risk of cerebral hemorrhage. Acute renal failure and hemodialysis were also associated with risk of intracranial bleeding. Unexpectedly, female sex was an independent risk factor for cerebral hemorrhage [69].

48.4.2.2 VV ECMO

In 2013, the ELSO registry reported a higher rate of HIC in patients under VV ECMO at 4% [14], and this number was up to 15% in a recent study with 25 patients [70]. The largest series specifically dealing with cerebrovascular complications in VV ECMO reported a rate of brain bleeding of 7.5% [17]. In this study, the average duration of onset of cerebral bleeding was 3 days after VV ECMO implantation. Intracranial hemorrhage was independently associated with acute renal failure upon admission to intensive care, too-rapid correction of $PaCO_2$ upon VV ECMO initiation, and was not associated with patient's age or hemostasis disorders.

48.4.2.3 Pathophysiological Mechanisms and TCD/TCCS Contribution

In the same way as for ischemic stroke, it is likely that pathophysiological mechanisms causing brain bleeding are different depending on the type of ECMO.

In VA ECMO patients, sudden restoration of brain flow could lead to intracranial edema, equivalent to a cerebral hyperperfusion syndrome, leading to hemorrhagic transformation, particularly in patients with previous ischemic stroke, by analogy with what is observed in patients undergoing carotid endarterectomy [71].

For VV ECMO, rapid correction of hypercapnia is an independent factor of the occurrence of cerebral hemorrhage [17]. Cerebral vasoconstriction induced by this too-rapid decline in $PaCO_2$ at the initiation of VV ECMO could be responsible for cerebral edema, with initial ischemic lesions evolving rapidly to and hemorrhagic transformation [61].

No study has yet investigated the usefulness of TCD/TCCS to prevent and monitor intracranial hemorrhage during VA or VV ECMO.

48.4.3 Brain Death During ECMO

Brain death is in 84% of cases directly related to pre-ECMO factors and cerebral edema secondary to cardiac arrest in ECMO patients [72]. Other causes are represented by ischemic strokes or intracranial bleeding occurring during ECMO support, representing respectively 4% and 12% of brain death during ECMO [72]. Patients on ECMO, and particularly patients implanted for refractory cardiac arrest, are increasingly regarded as potential organ donors, but high plasma levels of sedative drugs and hypothermia in those critically ill patients can make electroencephalogram examination unreliable and can delay brain death confirmation of brain death, as well as neurovascular imaging, because of the difficulty to transport these patients to radiology. TCD/TCCS could overcome all these limitations. To confirm a cerebral circulatory arrest with TCD/TCCS, several patterns are mandatory as a

reverberating flow, systolic spikes, and absence of signal, while mean flow velocity value detection is not required [73].

In 2018, a retrospective analysis has been performed in 25 patients (20 VA ECMO and 5 CPB) to evaluate the feasibility of cerebral circulatory arrest diagnosis by TCD during the circulatory support [56]. Indeed, TCD/TCCS is a worldwide accepted technique for cerebral circulatory arrest diagnosis for brain death confirmation [74]. In that study, brain death occurred in five patients. Those patients with VA ECMO were either assisted with IABP or had a LVEF higher than 20%. TCD/TCCS brain death patterns were found in all five patients. The lack of brain dead patients without IABP or with very low cardiac output in this study is highlighted by their authors as a major limitation to conclude whether TCD/TCCS can be used to confirm cerebral circulatory arrest in patients with laminar, nonpulsatile arterial flow.

48.5 Practical Considerations and Limitations

The specific management of these cerebrovascular complications remains the same as that of brain-damaged patients [75]. However, the evolution of patients on ECMO support during their stay in intensive care unit includes events that impose several constraints, for example, on patient's coagulation and oxygenation state, thus limiting specific therapeutic possibilities of these cerebrovascular complications. Even if TCD/TCCS is a practical tool to be informed about cerebral hemodynamics state in patients on ECMO support, the therapeutic impact of TCD/TCCS monitoring can be limited due to the many restrictions imposed by this circulatory device. Indeed, the heterogeneity of patients under ECMO requires individualized therapeutic strategies concerning ECMO flow rate or IABP use, which can rely on extra-neurological failures.

In the following paragraphs, we will exemplify two situations where TCD/TCCS findings should not be followed by circulatory device support parameter changes.

48.5.1 VA ECMO

As said previously, IABP is often added to VA ECMO, particularly in nonpulsatile patient with very low LVEF, in order to off-load the left ventricle and to protect against hydrostatic pulmonary edema [6]. TCD/TCCS has shown that in this subpopulation, IABP activation decreases CBF due to a transient end-diastolic reversal of intracranial blood flow during the diastolic inflation of the IABP [48]. Common sense should therefore avoid this device in patient with cardiac stun, but without an IABP, the probability that those VA ECMO patients develop severe hydrostatic

pulmonary edema and ARDS is high. During the cardiac recovery process on ECMO, the heart might eject desaturated blood from the left ventricle, and evolve toward an "Harlequin syndrome" [46] which is deleterious for the brain, and might be responsible for hypoxic-ischemic encephalopathy.

Therefore, IABP should be added in those VA ECMO patients with cardiac stun, even if TCD/TCCS finds a reduction in CBF.

48.5.2 VV ECMO

Some severe ARDS patients develop severe hypercapnia with respiratory acidosis and consequently, display cerebral vasodilatation patterns and a decreased CBF on TCD/TCCS monitoring [76]. After VV ECMO cannulation of these patients, common sense would tend to restore a normal $PaCO_2$ in order to restore a physiological pH and a normal CBF, but as told previously, intracranial bleeding is the most frequent cerebrovascular complication during VV ECMO, associated with rapid hypercapnia correction due to too-high extracorporeal gas flow on the circuit after cannulation [17].

Therefore, hypercapnia after cannulation should be respected within the first hours of VV ECMO, even if TCD/TCCS shows a vasodilatation pattern with a decreased CBF.

48.6 Conclusion

TCD/TCCS studies of patient undergoing ECMO are mandatory, and due to the lack of evidence regarding its usefulness during this circulatory report, it is not yet recommended as a regular and systematic monitoring tool during the follow-up of those patients for early detection or specific care of ECMO-induced neurological complications.

However, TCD/TCCS can represent a useful bedside tool to detect cerebral hemodynamic changes in real time in sedated and critically ill patients, in which clinical examination can hardly diagnose a neurological complication. Indeed, some medical centers, as "Baylor St. Luke's Medical Center" in Houston (Texas, USA), have established a neuromonitoring protocol for patients on ECMO support, in which daily TCD/TCCS are performed [77].

Algorithm

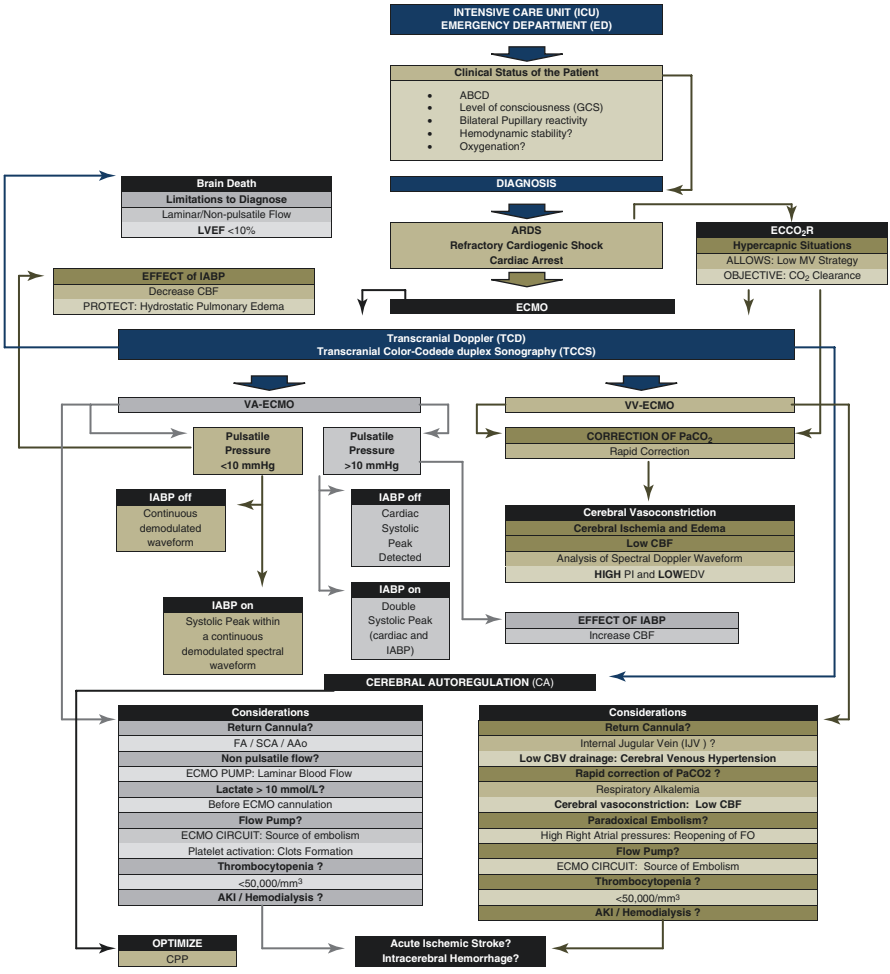

ABCD airway-breathing-circulation-disability, *GCS* Glasgow coma score, *LVEF* left ventricular ejection fraction, *CBF* Cerebral blood flow, *MV* mechanical ventilation, *IABP* Intra-aortic blood pump, *PI* pulsatility index, *EDV* end-diastolic velocity, *FA* femoral artery, *SCA* subclavian artery, *AAo* aortic, *CBV* cerebral blood volume, *FO* foramen ovale, *AKI* acute renal injury, *CPP* cerebral perfusion pressure

References

1. Davies A, et al. Extracorporeal membrane oxygenation for 2009 influenza A(H1N1) acute respiratory distress syndrome. JAMA. 2009;302(17):1888–95.
2. Luyt CE, et al. Long-term outcomes of pandemic 2009 influenza A(H1N1)-associated severe ARDS. Chest. 2012;142(3):583–92.
3. Combes A, et al. Position paper for the organization of extracorporeal membrane oxygenation programs for acute respiratory failure in adult patients. Am J Respir Crit Care Med. 2014;190(5):488–96.
4. Abrams D, et al. Position paper for the organization of ECMO programs for cardiac failure in adults. Intensive Care Med. 2018;44(6):717–29.
5. Marasco SF, et al. Review of ECMO (extra corporeal membrane oxygenation) support in critically ill adult patients. Heart Lung Circ. 2008;17(Suppl 4):S41–7.
6. Brechot N, et al. Intra-aortic balloon pump protects against hydrostatic pulmonary oedema during peripheral venoarterial-extracorporeal membrane oxygenation. Eur Heart J Acute Cardiovasc Care. 2018;7(1):62–9.
7. Madershahian N, et al. The acute effect of IABP-induced pulsatility on coronary vascular resistance and graft flow in critical ill patients during ECMO. J Cardiovasc Surg. 2011;52(3):411–8.
8. Madershahian N, et al. The impact of intraaortic balloon counterpulsation on bypass graft flow in patients with peripheral ECMO. J Card Surg. 2009;24(3):265–8.
9. Ma P, et al. Combining ECMO with IABP for the treatment of critically ill adult heart failure patients. Heart Lung Circ. 2014;23(4):363–8.
10. Chung ES, et al. Results of extracorporeal membrane oxygenation (ECMO) support before coronary reperfusion in cardiogenic shock with acute myocardial infarction. Korean J Thorac Cardiovasc Surg. 2011;44(4):273–8.
11. Combes A, et al. Extracorporeal membrane oxygenation for severe acute respiratory distress syndrome. N Engl J Med. 2018;378(21):1965–75.
12. Extracorporeal Life Support Organization. Registry report for all ECLS cases.
13. Mateen FJ, et al. Neurological injury in adults treated with extracorporeal membrane oxygenation. Arch Neurol. 2011;68(12):1543–9.
14. Mehta A, Ibsen LM. Neurologic complications and neurodevelopmental outcome with extracorporeal life support. World J Crit Care Med. 2013;2(4):40–7.
15. Risnes I, et al. Cerebral outcome in adult patients treated with extracorporeal membrane oxygenation. Ann Thorac Surg. 2006;81(4):1401–6.
16. Lewandowski K, et al. High survival rate in 122 ARDS patients managed according to a clinical algorithm including extracorporeal membrane oxygenation. Intensive Care Med. 1997;23(8):819–35.
17. Luyt CE, et al. Brain injury during venovenous extracorporeal membrane oxygenation. Intensive Care Med. 2016;23:23.
18. O'Brien NF, Hall MW. Extracorporeal membrane oxygenation and cerebral blood flow velocity in children. Pediatr Crit Care Med. 2013;14(3):e126–34.
19. Kavi T, et al. Transcranial Doppler changes in patients treated with extracorporeal membrane oxygenation. J Stroke Cerebrovasc Dis. 2016;25(12):2882–5.
20. Papademetriou MD, et al. Multichannel near infrared spectroscopy indicates regional variations in cerebral autoregulation in infants supported on extracorporeal membrane oxygenation. J Biomed Opt. 2012;17(6):067008.
21. Lassen NA, Christensen MS. Physiology of cerebral blood flow. Br J Anaesth. 1976;48(8):719–34.
22. Kuschinsky W, Wahl M. Local chemical and neurogenic regulation of cerebral vascular resistance. Physiol Rev. 1978;58(3):656–89.
23. Winn HR, et al. Brain adenosine production in rat during sustained alteration in systemic blood pressure. Am J Phys. 1980;239(5):H636–41.

24. Wei EP, Kontos HA. Increased venous pressure causes myogenic constriction of cerebral arterioles during local hyperoxia. Circ Res. 1984;55(2):249–52.
25. Hamel E. Perivascular nerves and the regulation of cerebrovascular tone. J Appl Physiol (1985). 2006;100(3):1059–64.
26. Waeber C, Moskowitz MA. Migraine as an inflammatory disorder. Neurology. 2005;64(10 Suppl 2):S9–15.
27. McHenry LC, et al. Cerebral autoregulation in man. Stroke. 1974;5(6):695–706.
28. Faraci FM, Mayhan WG, Heistad DD. Segmental vascular responses to acute hypertension in cerebrum and brain stem. Am J Phys. 1987;252(4 Pt 2):H738–42.
29. Bouma GJ, et al. Blood pressure and intracranial pressure-volume dynamics in severe head injury: relationship with cerebral blood flow. J Neurosurg. 1992;77(1):15–9.
30. Czosnyka M, et al. Cerebral autoregulation following head injury. J Neurosurg. 2001;95(5):756–63.
31. Powers WJ, et al. Autoregulation after ischaemic stroke. J Hypertens. 2009;27(11):2218–22.
32. Panerai RB, et al. Dynamic cerebral autoregulation following acute ischaemic stroke: comparison of transcranial Doppler and magnetic resonance imaging techniques. J Cereb Blood Flow Metab. 2016;36(12):2194–202.
33. Oeinck M, et al. Dynamic cerebral autoregulation in acute intracerebral hemorrhage. Stroke. 2013;44(10):2722–8.
34. Ma H, et al. Temporal course of dynamic cerebral autoregulation in patients with intracerebral hemorrhage. Stroke. 2016;47(3):674–81.
35. Budohoski KP, et al. Impairment of cerebral autoregulation predicts delayed cerebral ischemia after subarachnoid hemorrhage: a prospective observational study. Stroke. 2012;43(12):3230–7.
36. Otite F, et al. Impaired cerebral autoregulation is associated with vasospasm and delayed cerebral ischemia in subarachnoid hemorrhage. Stroke. 2014;45(3):677–82.
37. Short BL. The effect of extracorporeal life support on the brain: a focus on ECMO. Semin Perinatol. 2005;29(1):45–50.
38. Liem KD, et al. Cerebral oxygenation and hemodynamics during induction of extracorporeal membrane oxygenation as investigated by near infrared spectrophotometry. Pediatrics. 1995;95(4):555–61.
39. Fenik JC, Rais-Bahrami K. Neonatal cerebral oximetry monitoring during ECMO cannulation. J Perinatol. 2009;29(5):376–81.
40. Tranmer BI, et al. Pulsatile versus nonpulsatile blood flow in the treatment of acute cerebral ischemia. Neurosurgery. 1986;19(5):724–31.
41. Joshi B, et al. Predicting the limits of cerebral autoregulation during cardiopulmonary bypass. Anesth Analg. 2012;114(3):503–10.
42. Hori D, et al. Hypotension after cardiac operations based on autoregulation monitoring leads to brain cellular injury. Ann Thorac Surg. 2015;100(2):487–93.
43. Short BL, et al. Impairment of cerebral autoregulation during extracorporeal membrane oxygenation in newborn lambs. Pediatr Res. 1993;33(3):289–94.
44. Tian F, et al. Impairment of cerebral autoregulation in pediatric extracorporeal membrane oxygenation associated with neuroimaging abnormalities. Neurophotonics. 2017;4(4):041410.
45. Tian F, et al. Wavelet coherence analysis of dynamic cerebral autoregulation in neonatal hypoxic-ischemic encephalopathy. Neuroimage Clin. 2016;11:124–32.
46. Cakici M, et al. Controlled flow diversion in hybrid venoarterial-venous extracorporeal membrane oxygenation. Interact Cardiovasc Thorac Surg. 2018;26(1):112–8.
47. Doll N, et al. Five-year results of 219 consecutive patients treated with extracorporeal membrane oxygenation for refractory postoperative cardiogenic shock. Ann Thorac Surg. 2004;77(1):151–7. discussion 157
48. Yang F, et al. Effects of intra-aortic balloon pump on cerebral blood flow during peripheral venoarterial extracorporeal membrane oxygenation support. J Transl Med. 2014;12:106.
49. Meng L, Gelb AW. Regulation of cerebral autoregulation by carbon dioxide. Anesthesiology. 2015;122(1):196–205.

50. Weber TR, Kountzman B. The effects of venous occlusion on cerebral blood flow characteristics during ECMO. J Pediatr Surg. 1996;31(8):1124–7.
51. Fukuda S, et al. Comparison of venoarterial versus venovenous access in the cerebral circulation of newborns undergoing extracorporeal membrane oxygenation. Pediatr Surg Int. 1999;15(2):78–84.
52. Taylor GA, et al. Intracranial flow patterns in infants undergoing extracorporeal membrane oxygenation: preliminary observations with Doppler US. Radiology. 1987;165(3):671–4.
53. van de Bor M, et al. Extracorporeal membrane oxygenation and cerebral blood flow velocity in newborn infants. Crit Care Med. 1990;18(1):10–3.
54. Schachtrupp A, et al. Influence of intra-aortic balloon pumping on cerebral blood flow pattern in patients after cardiac surgery. Eur J Anaesthesiol. 2005;22(3):165–70.
55. Gee W, et al. Assessment of intra-aortic balloon pumping by ocular pneumoplethysmography. Am Surg. 1986;52(9):489–91.
56. Marinoni M, et al. Retrospective analysis of transcranial Doppler patterns in veno-arterial extracorporeal membrane oxygenation patients: feasibility of cerebral circulatory arrest diagnosis. ASAIO J. 2018;64(2):175–82.
57. Nasr DM, Rabinstein AA. Neurologic complications of extracorporeal membrane oxygenation. J Clin Neurol. 2015;11(4):383–9.
58. Omar HR, et al. Incidence and predictors of ischemic cerebrovascular stroke among patients on extracorporeal membrane oxygenation support. J Crit Care. 2016;32:48–51.
59. Meyer AD, et al. Platelet-derived microparticles generated by neonatal extracorporeal membrane oxygenation systems. ASAIO J. 2015;61(1):37–42.
60. Foster PP, et al. Patent foramen ovale and paradoxical systemic embolism: a bibliographic review. Aviat Space Environ Med. 2003;74(6 Pt 2):B1–64.
61. Stocchetti N, et al. Hyperventilation in head injury: a review. Chest. 2005;127(5):1812–27.
62. Brunser AM, et al. The role of TCD in the evaluation of acute stroke. J Neuroimaging. 2016;26(4):420–5.
63. Muehrcke DD, et al. Complications of extracorporeal life support systems using heparin-bound surfaces. The risk of intracardiac clot formation. J Thorac Cardiovasc Surg. 1995;110(3):843–51.
64. Jiang J, et al. Microembolic signal monitoring of TOASTclassified cerebral infarction patients. Mol Med Rep. 2013;8(4):1135–42.
65. Best LM, et al. Transcranial Doppler ultrasound detection of microemboli as a predictor of cerebral events in patients with symptomatic and asymptomatic carotid disease: a systematic review and meta-analysis. Eur J Vasc Endovasc Surg. 2016;52(5):565–80.
66. Zanatta P, et al. Microembolic signals and strategy to prevent gas embolism during extracorporeal membrane oxygenation. J Cardiothorac Surg. 2010;5:5.
67. Marinoni M, et al. Cerebral microemboli detected by transcranial doppler in patients treated with extracorporeal membrane oxygenation. Acta Anaesthesiol Scand. 2016;60(7):934–44.
68. Hornig CR, Dorndorf W, Agnoli AL. Hemorrhagic cerebral infarction–a prospective study. Stroke. 1986;17(2):179–85.
69. Kasirajan V, et al. Risk factors for intracranial hemorrhage in adults on extracorporeal membrane oxygenation. Eur J Cardiothorac Surg. 1999;15(4):508–14.
70. Martucci G, Lo Re V, Arcadipane A. Neurological injuries and extracorporeal membrane oxygenation: the challenge of the new ECMO era. Neurol Sci. 2016;19:19.
71. Hingorani A, et al. Causes of early post carotid endartectomy stroke in a recent series: the increasing importance of hyperperfusion syndrome. Acta Chir Belg. 2002;102(6):435–8.
72. Giani M, et al. Apnea test during brain death assessment in mechanically ventilated and ECMO patients. Intensive Care Med. 2016;42(1):72–81.
73. Sloan MA, et al. Assessment: transcranial Doppler ultrasonography: report of the Therapeutics and Technology Assessment Subcommittee of the American Academy of Neurology. Neurology. 2004;62(9):1468–81.

74. Wahlster S, et al. Brain death declaration: practices and perceptions worldwide. Neurology. 2015;84(18):1870–9.
75. Pugin D, Woimant F. Stroke care in the ICU: general supportive treatment. Experts' recommendations. Rev Neurol (Paris). 2012;168(6–7):490–500.
76. Atkinson JL, Anderson RE, Sundt TM. The effect of carbon dioxide on the diameter of brain capillaries. Brain Res. 1990;517(1–2):333–40.
77. Kazmi SO, et al. Cerebral pathophysiology in extracorporeal membrane oxygenation: pitfalls in daily clinical management. Crit Care Res Pract. 2018;2018:3237810.

Chapter 49
Neuro-ICU: Usefulness of Transcranial Doppler (TCD/TCCS) to Monitoring of Neurological Impact from Mechanical Ventilation and Prone Position in ARDS Patients

Anna Teresa Mazzeo, Giulia Catozzi, Simone Caccia, and Luciana Mascia

Key Points

1. An intense brain-lung interconnection is described in the neurological critically ill patients for whom acute respiratory distress syndrome represents the most common non-neurologic organ dysfunction.
2. Maintaining adequate cerebral blood flow (CBF) to meet metabolic demands after a neurological insult is critical to prevent secondary brain injury. Several factors influence CBF and in turn affect intracranial pressure.
3. Adequate oxygenation and tight CO_2 control, avoiding hypoxemia and hypercapnia, represent the main target of the ventilatory management of neurocritical patients.
4. In case of refractory hypoxemia, prone position represents an important option for critically ill patients to improve oxygenation.
5. Transcranial Doppler (TCD/TCCS) can be useful in acute brain injured patients with acute respiratory distress syndrome to monitor the effects induced by mechanical ventilation on cerebral hemodynamics.

A. T. Mazzeo (✉)
Department of Adult and Pediatric Pathology, University of Messina, AOU Policlinico G. Martino, Messina, Italy
e-mail: anna.mazzeo@unito.it

G. Catozzi · S. Caccia
Department of Surgical Sciences, Division of Anesthesia and Intensive Care, University of Turin, Turin, Italy
e-mail: giulia.catozzi@edu.unito.it

L. Mascia
Dipartimento di Scienze Biomediche e Neuromotorie, University of Bologna, Bologna, Italy
e-mail: luciana.mascia@unibo.it

C. N. Rodríguez et al. (eds.), *Neurosonology in Critical Care*,
https://doi.org/10.1007/978-3-030-81419-9_49

49.1 Introduction

The presence of a brain-lung cross-talk has been increasingly recognized in the critical care setting and may affect management of the neurologically critically ill patient developing respiratory complications.

Acute brain injured patients are at risk to develop extracerebral dysfunctions, with adverse effects on distal organs and systems, and increased morbidity and mortality. A high incidence of respiratory failure has been in particular described and may adversely affect outcome.

The aim of this chapter is to describe the main factors responsible for the development of acute respiratory distress syndrome (ARDS) after acute brain injury and the main ventilatory strategies for its treatment. Furthermore, patients developing ARDS may frequently present a compromise of cerebral autoregulation mechanisms, which can be studied with the use of transcranial Doppler (TCD/TCCS) monitoring.

49.2 Neuro-ICU: Acute Respiratory Distress Syndrome

ARDS is an acute diffuse, inflammatory lung injury, presenting with increased pulmonary vascular permeability, increased lung weight, and loss of aerated lung tissue.

According to the Berlin definition, the clinical hallmarks of ARDS are hypoxemia and bilateral radiographic opacities (not fully explained by effusions, lobar/lung collapse, or nodules), associated with increased venous admixture, increased physiological dead space, and decreased lung compliance [1] (Table 49.1).

It has been recently observed that 10% of all patients admitted to the intensive care unit (ICU) and 23% of mechanically ventilated patients have ARDS, with 46% mortality in the subgroup of patients with severe ARDS [2].

Table 49.1 ARDS Berlin Definition

Timing	<1 week of a known clinical insult or new/worsening respiratory symptoms
Chest imaging (chest radiograph or computed tomography scan)	Bilateral opacities not fully explained by effusions, lobar/lung collapse, or nodules
Origin of edema	Respiratory failure not fully explained by cardiac failure/fluid overload; need objective assessment to exclude hydrostatic edema if no risk factor present
Mild ARDS	200 mmHg < PaO_2/FiO_2 ≤300 mmHg with PEEP ≥5 cmH_2O
Moderate ARDS	100 mmHg < PaO_2/FiO_2 ≤200 mmHg with PEEP ≥5 cmH_2O
Severe ARDS	PaO_2/FiO_2 ≤100 mmHg with PEEP ≥5 cmH_2O

FiO_2 fraction of inspired oxygen, *PaO_2* partial pressure of arterial oxygen, *PEEP* positive end-expiratory pressure

In neurocritically ill patients, ARDS is the most common non-neurologic organ dysfunction, occurring in the early phase after severe acute brain injury, with a reported incidence of 10–20%.

Developing ARDS after traumatic brain injury (TBI) involves low partial pressure of oxygen in brain tissue, worse neurologic outcomes, and higher healthcare costs [3].

Pulmonary complications are commonly seen in neurologically critically ill patients with mechanical ventilation, and it has been observed that ARDS occurs in up to 20–38% of cases of subarachnoid hemorrhage (SAH), TBI, and spontaneous intracerebral hemorrhage, with a 35% reported incidence in a mixed cohort of neurologically critically ill patients [4].

Despite the clinical importance of ARDS after TBI, predicting which patients are at highest risk to develop ARDS is difficult and little has been discovered about the factors driving this association [3]. Major underlying ARDS risk factors are aspiration pneumonia, atelectasis, and lung contusion. Even the severity of brain injury seems to play an important role, and a severely and globally altered initial brain computed tomography (CT) scan and low Glasgow Coma Scale (GCS) have been reported as potential risk factors for the development of ARDS in patients with acute brain injury. The need for prolonged mechanical ventilation, frequent procedural and operative interventions, and patient comorbidities are conditions posing further risk for developing ARDS [5].

In addition, other interventions, such as exposure to blood products, may potentiate pulmonary injury in a susceptible host or lead directly to transfusion-related ARDS [3]. Induced hypertension and positive fluid balance, frequently required for the management of cerebral perfusion pressure (CPP) in patients with elevated intracranial pressure (ICP), has also been associated with an increased incidence of ARDS.

ARDS has a great impact on morbidity and is a major contributor to mortality in patients suffering from brain injury. It is associated with longer duration of mechanical ventilation and longer ICU length of stay, and it also worsens long-term neurologic outcome [6, 7].

The presence of a brain-lung interconnection has been increasingly hypothesized in the critical care scenario and represents a leading event in the emerging and clinically relevant field of organ cross-talk. It has been shown that brain injured patients are at risk to develop extracerebral dysfunctions, thus determining adverse effects on distal organs and systems, with a high incidence of respiratory failure. The physiopathological mechanism of ARDS has been described by the “double hit model” [8], presuming that the catecholamine storm and the systemic production of inflammatory mediators following TBI (first hit) set up a systemic inflammatory environment responsible for the increased lung susceptibility to injurious strategies of mechanical ventilation, infections, or invasive therapies (second hit) (Fig. 49.1).

At respiratory level the two mechanisms proposed to explain ARDS occurring after acute brain injury are a massive increase in sympathetic activity and an increased production of pro-inflammatory cytokines released into the systemic

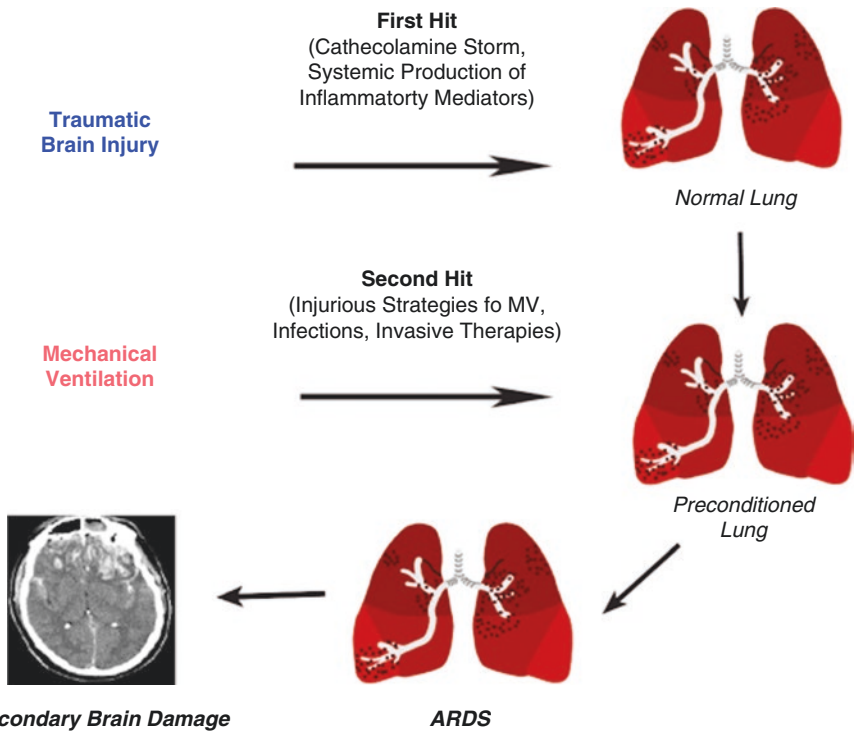

Fig. 49.1 Double hit model. The catecholamine storm and the systemic production of inflammatory mediators following traumatic brain injury (*first hit*) set up a systemic inflammatory environment responsible for the increased lung susceptibility to injurious strategies of mechanical ventilation, infections, or invasive therapies, as blood products transfusions (*second hit*). MV mechanical ventilation, ARDS acute respiratory distress syndrome, TBI traumatic brain injury

circulation, which play a central role in the development of this potentially life-threatening complication [9].

Catecholamine storm originating in the central nervous system following head trauma, causing high blood levels of catecholamines with high levels of norepinephrine in the vicinity of organs via sympathetic endings, caused by an acute increase in ICP ("blast injury theory"). This induces an increase in vascular hydrostatic pressure and pulmonary endothelial damage with a consequent increase in capillary permeability allowing outflow of protein-rich plasma into the interstitium and alveoli, producing ARDS. Using a dual tracer approach to measure the rate of extravascular protein accumulation in the lung in the event of increased ICP, McClellan et al. [10] observed that ICP elevation led to a nearly threefold rise in protein leak index, a measure of pulmonary vascular protein permeability. This was associated with an increase in systemic and pulmonary pressures, suggesting a role for autonomic nervous system activation in the development of neurogenic pulmonary edema. Therefore, it is important to distinguish increase in permeability from the effect of increase in pulmonary microvascular pressure [10].

However, acting alone or in combination with the above described blast injury model, a significant role has recently been suggested for neuroinflammation, in the genesis of ARDS following TBI. A complex network of inflammatory mediators, in fact, plays a central role in this mechanism and, while neuroinflammatory response represents initially a coordinated effort to protect the brain after injury, it may then become dysregulated and be responsible for the activation of the secondary injury cascade leading to single or multiple organ dysfunction [11] (Fig. 49.2).

There is a strict relationship between lung and brain injury in mechanically ventilated neurocritical patients. On one side, respiratory dysfunction is a potentially deleterious factor responsible for secondary insults to the brain, associated with poor neurologic outcome. Maintenance of respiratory homeostasis throughout an adequate mechanical ventilation strategy is, thus, a critical factor in the care of brain injured patients. On the other side, the occurrence of ARDS after brain injury is increasingly recognized, and represents the most frequent among extracranial complications of brain injury, increasing per se morbidity and mortality [9].

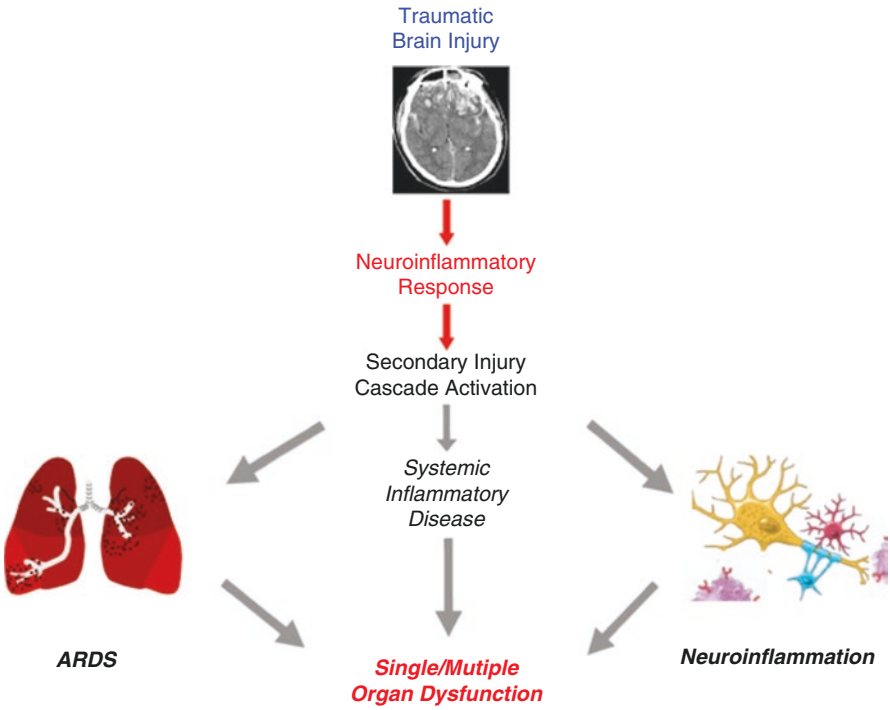

Fig. 49.2 Role of neuroinflammatory response. A complex network of inflammatory mediators plays a central role in the genesis of ARDS following TBI. Neuroinflammatory response represents initially a coordinated effort to protect the brain after injury, then it may become dysregulated and be responsible for the activation of the secondary injury cascade leading to single or multiple organ dysfunction. ARDS acute respiratory distress syndrome

49.3 Carbon Dioxide and Cerebral Blood Flow

Human brain is characterized by an intense metabolic activity. It receives 10–15% of cardiac output (CO) at rest, and it consumes about 20% of the total oxygen content present in the body, even though representing only 1–2% of body weight. Therefore, the high cerebral metabolic demand entails the need for a constant cerebral blood flow (CBF), although CBF determinants are subject to a wide range of possible variations. At the level of cerebral parenchyma CPP is the difference between the intra-arterial pressure and the venous pressure. Venous pressure is usually around 2–5 mmHg and is directly influenced by ICP. As a consequence CPP is calculated as the difference between mean arterial pressure (MAP) and ICP.

Autoregulation of CBF is defined as the ability of the arterial circulation to maintain relatively constant blood flow through changes in diameter of the cerebral vessels, in order to meet the metabolic needs, despite changes in CPP. In a CPP range of 50–150 mmHg, CBF is kept at about 50 ml per 100 g of tissue per minute. If CPP moves above or below this range, cerebral autoregulation mechanisms lose effectiveness and CBF becomes passively dependent on CPP, and consequently on MAP, in a linear manner.

Initially this reduction of flow is compensated by an increase in the rate of oxygen extraction by cerebral parenchyma; once this compensation mechanism is no longer able to satisfy the metabolic brain requests, pathological changes characteristics of ischemia will start to occur. CBF control mechanisms, therefore, ensure that blood supply is kept constant with changes in the systemic arterial pressure and that it is adequate for quantitative variations in excess or defect of toxic metabolites and energy substrates.

Cerebral autoregulation is the mechanism that maintains a stable CBF by modifying the caliber of arterial vessels, for a given level of cerebral metabolism, despite fluctuations of CPP. It is graphically visualized as the correlation between CBF and CPP or MAP in which the three key elements of the curve are represented by the lower limit, the upper limit, and the plateau (Fig. 49.3).

Cerebral autoregulation is based on the reactivity of cerebral vessels which undergo dilatation in response to a reduction in CPP, and constriction in response to a CPP increase.

It is however essential to consider that cerebrovascular tone is not controlled exclusively by CPP, but it is the result of the interaction of flow-related factors (MAP, ICP) and flow-independent factors ($PaCO_2$, PaO_2, pH, hemoglobin, hematocrit, temperature), each one playing a fundamental role in defining the limits of autoregulation curve.

Cerebral autoregulation of the arterial flow is based on variations in vascular resistance, a mechanism known as "cerebrovascular reactivity."Among different factors, $PaCO_2$ is considered to be the most powerful one, which is able to modulate the complex control mechanism of CBF regulation. Indeed variations in $PaCO_2$

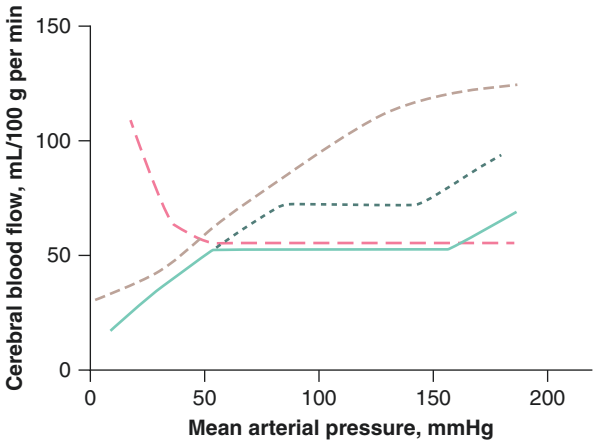

Fig. 49.3 Cerebral autoregulation. Green continuous line: cerebral autoregulation curve in normocapnia conditions; Red dotted line: CBF response to hypoxia; gray dotted line: CBF response to hypercapnia; blue dotted line: cerebral autoregulation curve in hypercapnia conditions. PaO_2 under 50 mmHg determines an important acceleration of CBF, up to a possible maximum increase of 400% for PaO_2 values under 20 mmHg (hypoxic vasodilation). For $PaCO_2$ values between 20 and 80 mmHg, CBF increases from 2% to 4% for each mmHg increase in $PaCO_2$, so that hypocapnia induces vasoconstriction, while hypercapnia induces vasodilation. Hypercapnic conditions result in a plateau width reduction of the autoregulation curve, which is proportional to hypercapnia severity

result in significant cerebrovascular responses: an increase in $PaCO_2$ (hypercapnia) causes a dilation of cerebral arteries leading to an increase in CBF, while reduction in $PaCO_2$ (hypocapnia) causes vasoconstriction and therefore a reduction of CBF [12], maintaining the cerebral and cerebrospinal fluid pH constant (Fig. 49.3).

Blood oxygen content is also fundamentally important in the regulation of CBF, since one of the fundamental goals of cerebral perfusion is oxygen delivery. Oxygen regulates CBF both alone and via an integrated mechanism that involves interplay with carbon dioxide, perfusion pressure, and maybe other physiological processes [13].

Under hypercapnia condition, the plateau of the autoregulation curve undergoes a reduction in amplitude proportional to hypercapnia severity.

Cerebrovascular reactivity to CO_2 represents a protective mechanism of cerebral homeostasis aimed at guaranteeing pH stability in front of $PaCO_2$ variations. It is evident that this mechanism can compromise the functionality of cerebral autoregulation by limiting the possibility to modulate the caliber of cerebral arteries [13].

49.4 ARDS: Mechanical Ventilation Management

The choice of the optimal ventilatory strategy to avoid the occurrence of injurious events, primarily to the lung and then to other organs, is essential in any critically ill patient. Modern respiratory management of head injury patient affected by ARDS aims to avoid secondary insults both to the damaged brain and to the injured lungs, with the consciousness that the two affected systems are tightly interconnected [9].

However, there is no published recommendation on which ventilator setting, in terms of tidal volume, respiratory rate, and positive end-expiratory pressure (PEEP) levels, should be used to obtain the safest respiratory targets. The standard of care for these critically ill patients consists in the use of low tidal volume ventilation, defined as "protective mechanical ventilation" [14].

Since the occurrence of ARDS in brain injured patients is not rare, the application of protective ventilation strategies in neurointensive care unit (NICU) is increasingly proposed. Mechanical ventilation is an integral part in the care of neurologic critically ill patients, and tight control of respiratory variables, such as PaO_2 and $PaCO_2$, remains the main goal of therapy.

Data on the effect of protective mechanical ventilation on NICU patients is still lacking, either for the prevention of VILI or for the treatment of coexisting ARDS [9], but several reviews have been published describing the importance of optimal ventilatory strategies in the management of acute brain injured patients [9, 11, 15–17].

Critical care management of such patients aims, on the one side, brain protection and, on the other, lung protection. Since it is well known that brain and lung treatment strategies can be in conflict, at least for the acute phase of the injury, the assertion "one size does not fit all" well explains this difficult task. Hence individualized treatment is mandatory, and, over time, priorities may change, shifting from "brain over lung" to "lung over brain." For this reason, a unique agreement on which may be considered the most effective ventilatory strategy in these patients has not been achieved. The main target of mechanical ventilation after acute brain injury is maintaining optimal oxygenation and tight control of $PaCO_2$, even if there is no published recommendation on which ventilatory settings should be applied to obtain these goals [9].

The new Brain Trauma Foundation guidelines on TBI [18] stated that normal ventilation is currently the goal for severe TBI patients in the absence of cerebral herniation and normal $PaCO_2$ ranges from 35 to 45 mmHg. They also stated that severe TBI patients receive mechanical ventilation, which can tightly regulate $PaCO_2$ levels through rate and tidal volume adjustments, but no precise indications are presented.

Conventional targets of mechanical ventilation in TBI patients are represented by the application of adequate tidal volumes to maintain lower range of normocapnia and adequate levels of PEEP to optimize oxygenation while preserving central venous drainage.

In order to prevent lung injury in acute brain injured patients, a combination of protective ventilation together with tight CO_2 control is essential. The injurious

effects of both severe hyper- and hypo-capnia on cerebrovascular system demand a continuous monitoring of CO_2 levels to avoid critically dangerous values. $PaCO_2$ should be maintained at approximately 35 mmHg and hyperventilation, applied in case of severe intracranial hypertension, should be avoided during the first 24 h after injury when CBF is often critically reduced [11].

Optimal ventilatory management of ARDS providing reduced tidal volumes and minute ventilation is often accompanied by an increase in $PaCO_2$, defined "permissive hypercapnia" which is usually well-tolerated in the non-neurologically ill patient, but in case of intracranial hypertension, it can have deleterious effects and should be avoided. However, It remains unclear if the outcome benefits of lung-protective ventilation (low tidal volume) reported in other populations would also be seen in brain injured ones [19].

Application of PEEP is part of the protective mechanical ventilatory strategy and it permits to recruit previously collapsed alveoli. Improvement in arterial oxygenation and reduction of respiratory system elastance, can be safely obtained by intensivists applying PEEP, in front of some mandatory conditions, represented in (Fig. 49.4).

It has been demonstrated that if the value of PEEP is lower than ICP, the associated increase in intrathoracic pressure does not translate into an increase in ICP [20].

Nowadays it is unknown if there is an optimal PEEP level for acute brain injury patients.

Neurointensivists face two competing priorities: on the one hand, the need to ensure the best care for the injured brain through tight CO_2 control and adequate

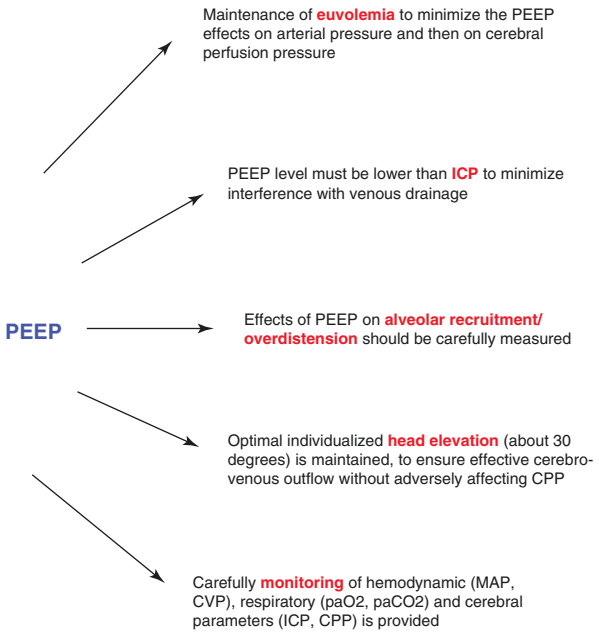

Fig. 49.4 Safe application of PEEP. Application of PEEP is part of the protective mechanical ventilatory strategy and it permits to recruit previously collapsed alveoli. Improvement in arterial oxygenation and reduction of respiratory system elastance can be safely obtained by neurointensivists applying PEEP, in front of some mandatory conditions, including patient euvolemia, not exceed ICP level, measurement of respiratory system mechanics, patient head elevation, and careful hemodynamic, respiratory, and cerebral monitoring

PaO_2 targets to prevent secondary cerebral ischemia, and, on the other hand, the need to prevent or mitigate VILI, using low tidal volumes, plateau pressure <30 cmH_2O, and adequate PEEP levels, which is, however, a ventilatory strategy with potential adverse effects on cerebral hemodynamics [9].

Since there is a potential conflict, a compromise needs to be achieved to set the optimal treatment strategy.

In a recent large international survey on the respiratory management and ventilatory strategies of TBI patients admitted to ICU, low tidal volumes with a $PaCO_2$ target of 36–40 mmHg were utilized, and lower levels of PEEP in the case of intracranial hypertension. In the case of refractory respiratory failure, the most frequent rescue therapy was the use of neuromuscular blocking agent, followed by recruitment maneuvers and prone position [21]. In this survey it was evident that the concept of lung protective ventilation is spreading also in the particular setting of acute brain injury patients [21]. The importance of neuromonitoring (in particular ICP, brain oxygenation, and TCD monitoring) while applying protective mechanical ventilation to titrate effects of ventilatory strategies on cerebral hemodynamics and to avoid adverse effect on cerebral homeostasis has been underlined in literature [15]. The use of neuromonitoring will in fact help to optimize the use of protective ventilation in acute brain injured patients, especially in cases complicated with ARDS.

49.4.1 Physiological Consequences of PEEP

PEEP has a fundamental role in improving pulmonary mechanics, increasing functional residual capacity, minimizing recruitment-derecruitment of the lung, decreasing pulmonary shunt, and improving arterial oxygenation, but can also have a potentially deleterious impact on many physiologic functions influencing cerebral circulation and ICP through hemodynamic and CO_2-mediated mechanisms.

From a hemodynamic point of view, PEEP application results in an increased central venous pressure (CVP) and a decreased MAP, due to the hindered cerebral venous drainage and reduced cardiac output. The decrease in MAP can diminish CBF in patients with impaired cerebral autoregulation, leading to a MAP-dependent cerebral perfusion with a higher risk of ischemia. Euvolemia need to be guaranteed to avoid cerebral hypoperfusion [22]. On the other hand, the increase in CVP may be responsible for an increase in cerebral blood volume and a deleterious rise in ICP.

Mechanical ventilation can also affect cerebral circulation through a CO_2-induced mechanism. The increase in $PaCO_2$ directly causes vasodilation of cerebral arteries increasing cerebral blood volume and rising ICP, especially if intracranial compliance is reduced [23]. If application of PEEP predominantly determines alveolar recruitment, pulmonary elastance decreases, and $PaCO_2$ is lowered because of the reopening of previously collapsed and perfused areas, reducing shunt without effects on ICP and CPP. Conversely, if application of PEEP predominantly determines hyperinflation of normal alveoli, pulmonary elastance and respiratory dead space increase and a rise in $PaCO_2$ will show, consequently increasing ICP.

McGuire et al. [20] studied in a cohort of 18 neurosurgical intensive care subjects, including post-traumatic brain injury, SAH, obstructive hydrocephalus, and intracerebral hemorrhage patients, the application of PEEP up to 15 cmH_2O. In a group with ICP elevation (>15 mmHg), no significant change in ICP occurred at any PEEP level applied, while in a second group with normal ICP values, elevation of PEEP levels at 10 and 15 cmH_2O produced a significant increase in ICP of 1.9 and 1.5 mmHg, respectively. It is possible that PEEP application induces significant ICP elevation only in patients with low cerebral compliance. The PEEP effect on ICP is variable when applied to patients with neurologic injuries; however, the overall impact is considered to be modest [19].

Interestingly for our discussion, Boone et al. [24], in a large population of 341 subjects with acute brain injury and varying categories of acute lung injury, investigated PEEP application and found a significantly relationship between PEEP and both ICP and CPP in the severe lung injury cohort (defined as $PaO_2/FiO_2<100$, according to the Berlin criteria for ARDS [1]), even though the increase was not clinically meaningful. In fact, a rise of 5 cmH_2O in PEEP produced a 1.6 mmHg augmentation and a 4.3 mmHg decrease in ICP and CPP, respectively, suggesting that PEEP can be applied safely in patients with acute brain injury without clinically significant effect on ICP or CPP.

In the end there is a complex interaction between mechanical ventilation and cerebral hemodynamics, which is affected by respiratory elements and patient-specific variables, tightly interconnected to each other, including level of applied PEEP, effectiveness of cerebral autoregulation, patient position, cardiovascular and volemic status, and basal ICP level.

Though application of PEEP in patients with brain injury remains controversial, a judicious adaption of PEEP to the demand in patients with lung injury is feasible.

Since in the event of ARDS complicating TBI, a combination of a protective strategy of ventilation together with tight CO_2 control becomes essential, an "open lung approach" consisting of low tidal volume ventilation to avoid overdistension of the lung, ventilation with elevated PEEP levels to avoid collapse of lung parenchyma, and reopening of the collapsed alveoli through recruiting maneuvers has been positively evaluated in the care of neurosurgical patients with concomitant lung injury [25].

49.4.2 Prone Position

Ventilation provided in the prone position could have beneficial effects on patient oxygenation, and it is independently correlated with positive outcomes in ARDS patients [26–28].

Prone position improves gas exchange with several mechanisms including alveolar recruitment, redistribution of ventilation toward dorsal areas that remain well perfused, homogenization of tidal volume distribution, and possible improved postural drainage of secretions [29] (Table 49.2).

Table 49.2 Prone position benefits and adverse effects

Benefits	Adverse Effects
Extent and duration of severe hypoxemia is reduced Decreased propensity to ventilator-induced lung injury Diminished occurrence of nosocomial or ventilator-associated pneumonia	Inadvertent extubation and risk of a potentially catastrophic hypoxemia episode Inadvertent bronchial intubation, worsening hypoxemia and increasing risk of barotrauma (e.g., pneumothorax) Development of pressure sores Ocular complications Intracranial hypertension, potentially compromising cerebral circulation

This technique is beneficial, showing outcome improvement, to patients with moderate to severe ARDS when used for prolonged periods of 16 h or more each day, in a 180° prone position [30, 31].

The actual recommendation for adult patients with severe ARDS is to receive prone positioning for more than 12 h per day [32, 33].

Since patient positioning has a great impact on ICP, supine 30° head-up posture is recommended to achieve the lowest ICP. However, in patients with severe respiratory insufficiency and hypoxemia, the situation can be different because, theoretically, an improved gas exchange and arterial oxygenation can result in lower ICP, given the beneficial effect of improved oxygen transport to the damaged brain [34].

The effect of ventilation in the prone position on head injured patients may also be considered.

Only a few studies with a small number of patients have provided data of the influence of prone position on ICP and CPP, leading to contradictory results, with only one study from Reinprecht et al. including patients with ARDS. In this study it was demonstrated that prone positioning was associated with a significant improvement of arterial oxygenation and cerebral tissue oxygenation, and that these beneficial effects on cerebral tissue oxygenation resulting from increased arterial oxygenation appeared to outweigh the expected adverse effect on cerebral tissue oxygenation by decreasing CPP in ARDS patients [19, 35].

At present, there are insufficient data to distinguish benefits and risks of prone positioning in patients with increased ICP. A raised ICP is regarded as a contraindication to prone positioning, so that this therapeutic measure is often withheld in patients suffering from acute brain injury [36].

It may be possible that head rotation could have an impact on the venous drainage during prone positioning, leading to elevated ICP. Furthermore, the neurological examination of patients with acute brain injury is difficult during this therapeutic position [36].

In conclusion, prone position could be considered to improve oxygenation in NICU patients, when needed, even in the presence of acute brain injury, but caution and implementation of neuromonitoring are advised during the treatment.

49.5 TCD/TCCS: ARDS Patient

Transcranial Doppler (TCD/TCCS) sonography represents a useful additional instrument among all the monitoring tools available in the critical care scenario. It is safe, inexpensive, repeatable, and well suited for routine clinical use, allowing a series of physiological bedside measurements. Specifically, TCD/TCCS allows the measurement of blood flow velocities of the large cerebral arteries, without exposing the patient to any kind of risk. It may be useful when invasive tools are not indicated (in case of mild-moderate degrees of TBI), contraindicated (patients with hemostatic disorders), unavailable (such as in general ICU), or as daily monitoring [37]. TCD/TCCS is operator-dependent, and training is necessary to reliably assess the examination of cerebral arteries.

TCD/TCCS is able to detect relevant changes in cerebrovascular system dynamics associated with ICP increase due to mechanical ventilation treatment, playing a primary role in assessing the alteration of CBF associated with changes in ICP [37].

CBF is influenced by several physiological factors, among which are the partial pressures of oxygen and carbon dioxide. Acute respiratory pathological conditions, such ARDS, imply a severe alteration of pulmonary function, seriously compromising gas exchange. This fact determines deranged values of PaO_2 and $PaCO_2$ in ARDS patients, and, since CBF is strictly affected by these variables, cerebral perfusion may be compromised, leading to potentially harmful events. Furthermore, the physiological mechanism of cerebral autoregulation may be pathologically affected because of acute severe modification in oxygenation and carbon dioxide removal.

TCD/TCCS monitoring in the neurocritically ill patients provides the clinician with several data which can guide clinical management. The study of cerebral autoregulation is one of these.

Noninvasive assessment of dynamic cerebral autoregulation is possible through a mathematical analysis of the correlation between changes in flow velocity at the level of the middle cerebral artery (MCA), and fluctuations of MAP. Mean flow velocity in MCA can be obtained by TCD/TCCS, while MAP is obtained through invasive monitoring of arterial pressure [38].

In particular, a TCD/TCCS-derived index, Mx Index, has been employed as a method to predict dynamic autoregulation of the patient, since it represents a linear regression correlation coefficient defining the dependence of oscillations in mean flow velocity in the MCA from oscillations in CPP.

Mx has been cross-validated with other methods of autoregulation assessment, and it showed a good performance in predicting dynamic autoregulation in response to temporary hemodynamic changes [39]. Another useful TCD/TCCS-derived index is Mxa, a correlation coefficient which takes into consideration the arterial blood pressure (ABP) rather than CPP, indicating the correlation between mean flow velocity and ABP. High Mxa values suggest high dependence of CBF velocity from ABP, hence an impaired autoregulation [40]. Furthermore, Mxa formula implies a completely noninvasive method from a cerebral point of view, as ABP

detection doesn't require ICP invasive measurement, but only the placement of an arterial catheter.

Cerebral autoregulation mechanism can be compromised or abolished in different pathological conditions, both affecting primarily the central nervous system and other organs, particularly when admission in ICU is required, such as ARDS. Patients suffering from severe ARDS develop an impairment of respiratory gas exchange. Given the close relationship between PaO_2 and $PaCO_2$ with CBF, this condition characterized by hypoxemia and hypercapnia can negatively affect, and even compromise CBF autoregulation. In this clinical scenario TCD/TCCS represents a valid monitoring tool; measuring mean-CBF velocity in MCA (MFV_{MCA}) on ARDS patients through trans-temporal acoustic window initially, it is possible, through TCD/TCSS-derived autoregulation calculated indices (e.g., Mx and Mxa), to realize a real-time, bedside cerebral autoregulation diagnostic assessment.

A few authors have studied TCD/TCCS as a useful bedside monitoring tool for the assessment of CBF velocity and its correlation with cerebrovascular reactivity, in different clinical scenario.

When ICP increases, or MAP and CPP decrease, CBF velocity is subject to linear reduction, with end-diastolic velocity (EDV) falling more than peak-systolic velocity (PSV) [41]. This leads to an augmentation in systolic-diastolic velocity difference and increase in TCD/TCCS-derived pulsatility index (PI), calculated as the ratio between systolic-diastolic flow velocity difference and mean flow velocity [41]. In healthy individuals, PI ranges between 0.8 and 1.2 and increases with age. PI, in fact, is the most widely used surrogate indicator for ICP and it is recognized to positively correlate with ICP increase [42–45]. It is important to note that as opposed to CBF velocities, PI is not influenced by the angle of insonation of the probe. As such, it is considered a more robust predictor of ICP.

Increased intrathoracic pressure and subsequent ICP elevation produces specific changes in the cerebral artery blood flow velocity waveform that can be seen as decreasing EDV and increasing PI. In mild to moderate TBI, PI values >1.25 or EDV <25 cm/s are considered signs of a pathological cerebral condition since they are associated to secondary neurological deterioration [37].

Cigada et al. [46] tested cerebral CO_2 vasoreactivity in 21 healthy subjects by adding CO_2 to inspiratory gases to achieve a hypercapnic state. The healthy volunteers were connected through a mouthpiece to a mechanical ventilator set in the intermittent positive pressure ventilation mode and fed by two tanks, one of which contained 5% CO_2; the examiner varied inspiratory CO_2 concentration from 0% to 5% at fixed time intervals and measured end-tidal CO_2 ($EtCO_2$) at the mouthpiece. TCD/TCCS of MCA was continuously performed through the duration of the test, and mean flow velocity and PI were recorded every 10 s together with $EtCO_2$, non-invasive arterial blood pressure (ABP), and heart rate. Cerebral CO_2 vasoreactivity was calculated as the percentage change in mean flow velocity or PI for mmHg change in $EtCO_2$ (assuming normal $EtCO_2$ = 40 mmHg). Authors found a linear correlation between CO_2 changes (represented by end-tidal CO_2 values) and mean flow velocity and PI: whether $EtCO_2$ was increased by 15.3 ± 2.9 mmHg (range 11 ± 21) from the initial value of 30.0 ± 2.1 mmHg, a highly significant increase in mean flow velocity of 60 ± 9 cm/s was noted; PI showed a lower but yet significant

increase of 0.90 ± 0.11. This is consistent with findings presented by Kirkham et al. [47] and Eng et al. [48], who reported a very good linear correlation between CBF velocity and $EtCO_2$ over a wide range of CO_2 values (20 ± 60 mmHg).

In 21 patients with severe head injury or SAH, who required mechanical ventilation and ICP monitoring, Caricato et al. [49] applied in random sequence 0, 5, 8, and 12 cmH_2O of PEEP, and observed, together with a CPP reduction, a significant decrease in MCA blood flow velocity (from 73.1 ± 27.9 to 67.4 ± 27.1 cm/s), likely due to a cerebral autoregulation impairment, but only in patients with normal respiratory system compliance. While, no significant variation in ICP and cerebral compliance was observed.

Mascia et al. [22] studied 12 severely head injured patients with acute lung injury, who underwent random PEEP application of 0, 5, and 10 cmH_2O. Patients with pretest ICP values lower than 10 mmHg or higher than 15 mmHg were excluded, to prevent PEEP from being transmitted through cerebral veins and to avoid increase in $PaCO_2$. Furthermore, all the subjects were nursed with 30° head position. TCD/TCCS measurements at the level of the MCA were recorded during periods of hemodynamic stability after PEEP application. The rise in ICP was paralleled by a significant increase in mean flow velocity (from 53 ± 4 to 59 ± 5 cm/s) in those patients where application of PEEP induced predominantly alveolar hyperinflation, confirming the CO_2-induced cerebral vasodilation; when the predominant effect was the alveolar recruitment, no change in ICP and mean flow velocity was showed.

Schramm et al. [40] studied the relationship between PEEP and autoregulation in 20 patients with ARDS by means of TCD-derived Mxa index. CBF velocity and Mxa were recorded at baseline and then PEEP was applied with progressive increments of 1 cmH_2O, each followed by a 5 min period of stabilization. TCD measurements were repeated after an optimal level of PEEP was reached, defined as the individual PEEP level obtained after an increase in peripheral oxygen saturation. CBF velocity and ABP for Mxa calculation were recorded over a period of 1 h and the time-averaged values were calculated. Positive values of Mxa represent correlation between ABP and CBF velocity, which implies autoregulation impairment as cerebral blood flow depends on ABP. Negative values of Mxa, or null Mxa, express active cerebrovascular response to blood pressure changes, hence a preserved autoregulation. Elevation of PEEP from 9.2 ± 1 to 14.3 ± 1 cmH_2O did not affect CBF velocity to a clinically relevant extent, as well as the rise in Mxa from 0.317 ± 0.35 to 0.414 ± 0.32 was found to be without clinical relevance, since a relevant difference between two Mxa values should be greater than 0.2. A plausible explanation is that autoregulation impairment, defined as Mxa >0.3, was already present at baseline, hence PEEP elevation did not further influence autoregulation in these patients. Likewise, there was no correlation between $PaCO_2$ elevation and autoregulation impairment. Therefore, in this study, application of PEEP and elevation of $PaCO_2$ in ARDS patients did not further impair cerebral autoregulation.

The adjustment of PEEP to an optimal level in patients with respiratory failure seems to be safe with regard to CBF velocity and autoregulation. Furthermore, the impaired autoregulation in the majority of the ARDS patients should be considered when ranges for MAP/CPP management are set in these patients to avoid cerebral hypoperfusion or hyperperfusion [40].

Another interesting application of TCD/TCCS in acute brain injured patients complicated with respiratory failure is the study of cerebral blood flow velocities (CBFV) in patients ventilated in prone positioning, known the potential adverse effects of this position on intracranial hypertension.

Robba et al. studied patients undergoing spine surgery and suggested that TCD/TCCS, with its derived indices, can be a useful, safe, quick, and easy technique to noninvasively detect ICP, since it may be increased in prone position. In critically ill patients with both elevated ICP and respiratory illness treated with ventilation in the prone position (such as patients with ischemic stroke and brain swelling complicated by aspiration pneumonia leading to ARDS), a noninvasive ICP monitoring through TCD could be a valid option to monitor intracranial hypertension [50].

49.6 Conclusion

In conclusion TCD/TCCS allows to continuously monitor the effects of several respiratory treatments for ARDS patients in ICU, on the central nervous system. Its usefulness varies between several experimental settings of application, investigating physiological variables, such as CBFV, cerebral autoregulation and cerebrovascular reactivity, and their interactions with mechanical ventilation and its parameters, adjustable from the critical care physician (tidal volume, respiratory rate, PEEP). TCD/TCCS has the potential to provide insight if PEEP, recruitment maneuvers, and prone positioning are causing pathological changes in cerebral hemodynamics [37].

Being an easily available monitoring tool, TCD allows the clinician to perform cerebral hemodynamic assessment routinely in the ICU/NICU. It can be useful to monitor the different cerebral hemodynamic response to the same ventilator setting and strategy between different patients, and also to monitor how the same patient adapts his cerebral physiology over time, day by day, during all the mechanical ventilation period.

The use of TCD/TCCS in neurocritically ill patients allows the clinician to have a comprehensive picture, not only of cerebral physiology but also of the possible effects of respiratory failure on cerebral pathophysiology, and, most importantly, it allows to study the effect of some intensive/aggressive respiratory treatments on cerebrovascular physiology.

TCD could potentially be used to guide mechanical ventilation and at the same time to monitor simultaneous relevant cerebrovascular physiological variables. These data taken altogether address relevant clinical aspects of the patient treatment and can guide our objectives like tolerance of recruitment maneuvers, set the appropriate value of PEEP, and decide the minimum tolerable minute ventilation [37].

Even if a clinical validation for routine TCD use in this setting is still lacking, nevertheless, a growing clinical interest and preliminary results from literature encourage an increasingly promising application of TCD in the routine NICU scenario.

Therefore, nowadays, TCD/TCCS can be considered a modern, useful, low-cost bedside monitoring tool that can offer important information in the neurologically critically ill patients complicated by ARDS and other types of respiratory failure.

Algorithm

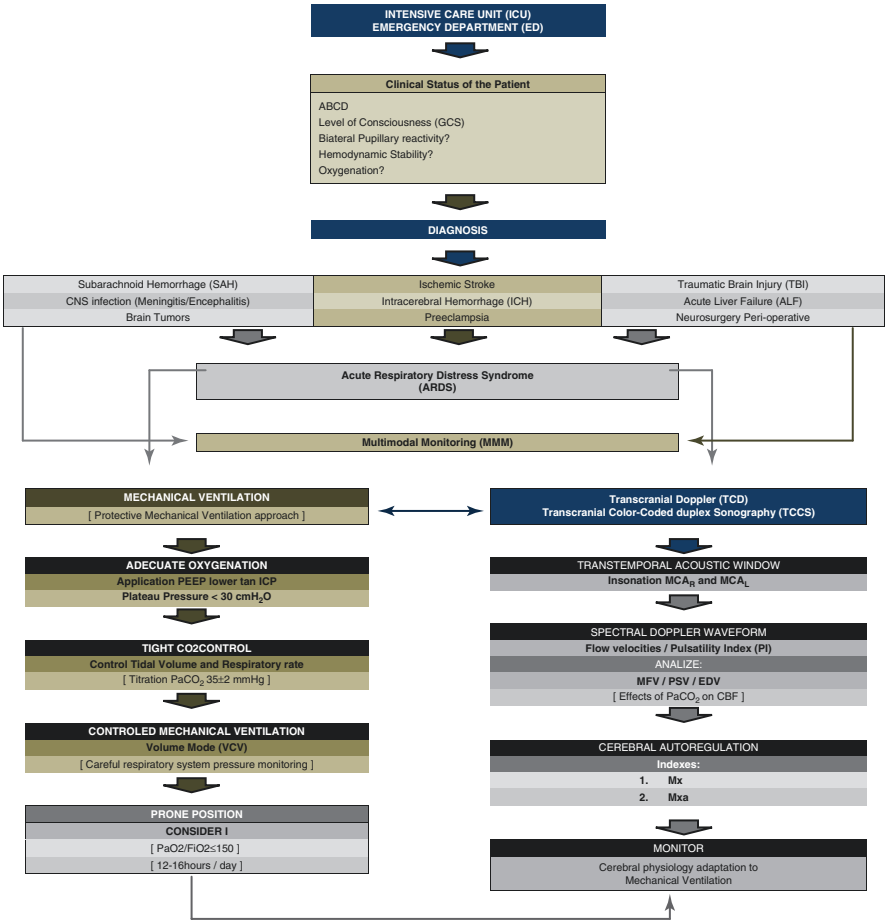

MFV Mean flow Velocity, *PSV* Peak systolic flow velocity, *EDV* End-diastolic flow velocity, *CBF* Cerebral Blood Flow, MCA_R Right Middle Cerebral Artery, MCA_L Left Middle cerebral artery, *ICP* Intracranial Pressure, *Mx* Mean flow index, *ICP* Intracranial pressure

References

1. Force ADT, et al. Acute respiratory distress syndrome: the Berlin definition. JAMA. 2012;307(23):2526–33.
2. Bellani G, et al. Epidemiology, patterns of care, and mortality for patients with acute respiratory distress syndrome in intensive care units in 50 countries. JAMA. 2016;315(8):788–800.
3. Hendrickson CM, et al. The acute respiratory distress syndrome following isolated severe traumatic brain injury. J Trauma Acute Care Surg. 2016;80(6):989–97.
4. Tejerina E, et al. Association between ventilatory settings and development of acute respiratory distress syndrome in mechanically ventilated patients due to brain injury. J Crit Care. 2017;38:341–5.
5. Veeravagu A, et al. Acute lung injury in patients with subarachnoid hemorrhage: a nationwide inpatient sample study. World Neurosurg. 2014;82(1–2):e235–41.
6. Bratton SL, Davis RL. Acute lung injury in isolated traumatic brain injury. Neurosurgery. 1997;40(4):707–12. discussion 712
7. Holland MC, et al. The development of acute lung injury is associated with worse neurologic outcome in patients with severe traumatic brain injury. J Trauma. 2003;55(1):106–11.
8. Mascia L. Acute lung injury in patients with severe brain injury: a double hit model. Neurocrit Care. 2009;11(3):417–26.
9. Mazzeo AT, Fanelli V, Mascia L. Brain-lung crosstalk in critical care: how protective mechanical ventilation can affect the brain homeostasis. Minerva Anestesiol. 2013;79(3):299–309.
10. McClellan MD, Dauber IM, Weil JV. Elevated intracranial pressure increases pulmonary vascular permeability to protein. J Appl Physiol (1985). 1989;67(3):1185–91.
11. Mascia L, Mazzeo AT. Ventilatory management in head injury patients. Is there any conflict? Trends Anaesth Crit Care. 2011;1(3):168–74.
12. Kety SS, Schmidt CF. The effects of altered arterial tensions of carbon dioxide and oxygen on cerebral blood flow and cerebral oxygen consumption of normal young men. J Clin Invest. 1948;27(4):484–92.
13. Meng L, Gelb AW. Regulation of cerebral autoregulation by carbon dioxide. Anesthesiology. 2015;122(1):196–205.
14. Acute Respiratory Distress Syndrome Network. Ventilation with lower tidal volumes as compared with traditional tidal volumes for acute lung injury and the acute respiratory distress syndrome. N Engl J Med. 2000;342(18):1301–8.
15. Oddo, et al. ARDS in the brain-injured patient: what's different? Intensive Care Med. 2016;42:790–3.
16. Young N, et al. Ventilatory strategies for patients with acute brain injury. Curr Opin Crit Care. 2010;16(1):45–52.
17. Della Torre V, et al. Acute respiratory distress syndrome in traumatic brain injury: how do we manage it? J Thorac Dis. 2017;9(12):5368–81.
18. Carney N, et al. Guidelines for the management of severe traumatic brain injury. Neurosurgery. 2017;80(1):6–15.
19. Piran P, Stevens RD. Lung-protective ventilation and adjunctive strategies to manage respiratory failure: are they safe in the neurological patient? Curr Opin Crit Care. 2021;26:115–9.
20. McGuire G, et al. Effects of varying levels of positive end-expiratory pressure on intracranial pressure and cerebral perfusion pressure. Crit Care Med. 1997;25(6):1059–62.
21. Picetti E, et al. VENTILatOry strategies in patients with severe traumatic brain injury: the VENTILO Survey of the European Society of Intensive Care Medicine (ESICM). Crit Care. 2020;24(1):158.
22. Mascia L, et al. Cerebro-pulmonary interactions during the application of low levels of positive end-expiratory pressure. Intensive Care Med. 2005;31(3):373–9.
23. Pinsky MR, Desmet JM, Vincent JL. Effect of positive end-expiratory pressure on right ventricular function in humans. Am Rev Respir Dis. 1992;146(3):681–7.

24. Boone MD, et al. The effect of positive end-expiratory pressure on intracranial pressure and cerebral hemodynamics. Neurocrit Care. 2017;26(2):174–81.
25. Wolf S, et al. The safety of the open lung approach in neurosurgical patients. Acta Neurochir Suppl. 2002;81:99–101.
26. Gattinoni L, et al. Effect of prone positioning on the survival of patients with acute respiratory failure. N Engl J Med. 2001;345(8):568–73.
27. Mure M, Lindahl SG. Prone position improves gas exchange–but how? Acta Anaesthesiol Scand. 2001;45(2):150–9.
28. Venet C, et al. Prognostic factors in acute respiratory distress syndrome: a retrospective multivariate analysis including prone positioning in management strategy. Intensive Care Med. 2003;29(9):1435–41.
29. Guerin C. Ventilation in the prone position in patients with acute lung injury/acute respiratory distress syndrome. Curr Opin Crit Care. 2006;12(1):50–4.
30. Guerin C, Reignier J, Richard JC. Prone positioning in the acute respiratory distress syndrome. N Engl J Med. 2013;369(10):980–1.
31. Sud S, et al. Effect of prone positioning during mechanical ventilation on mortality among patients with acute respiratory distress syndrome: a systematic review and meta-analysis. CMAJ. 2014;186(10):E381–90.
32. Fan E, et al. An official American thoracic society/European society of intensive care medicine/society of critical care medicine clinical practice guideline: mechanical ventilation in adult patients with acute respiratory distress syndrome. Am J Respir Crit Care Med. 2017;195(9):1253–63.
33. Hu SL, et al. The effect of prone positioning on mortality in patients with acute respiratory distress syndrome: a meta-analysis of randomized controlled trials. Crit Care. 2014;18(3):R109.
34. Nekludov M, Bellander BM, Mure M. Oxygenation and cerebral perfusion pressure improved in the prone position. Acta Anaesthesiol Scand. 2006;50(8):932–6.
35. Reinprecht A, et al. Prone position in subarachnoid hemorrhage patients with acute respiratory distress syndrome: effects on cerebral tissue oxygenation and intracranial pressure. Crit Care Med. 2003;31(6):1831–8.
36. Roth C, et al. Does prone positioning increase intracranial pressure? A retrospective analysis of patients with acute brain injury and acute respiratory failure. Neurocrit Care. 2014;21(2):186–91.
37. Corradi F, Robba C, Tavazzi G, Via G. Combined lung and brain ultrasonography for an individualized “brain-protective ventilation strategy” in neurocritical care patients with challenging ventilation needs. Crit Ultrasound J. 2018;10(1):24.
38. Doczi TP. Comparison of static and dynamic cerebral autoregulation measurements. Stroke. 1995;26(12):2372–3.
39. Zweifel C, et al. Continuous time-domain monitoring of cerebral autoregulation in neurocritical care. Med Eng Phys. 2014;36(5):638–45.
40. Schramm P, et al. Influence of PEEP on cerebral blood flow and cerebrovascular autoregulation in patients with acute respiratory distress syndrome. J Neurosurg Anesthesiol. 2013;25(2):162–7.
41. Chan KH, et al. The effect of changes in cerebral perfusion pressure upon middle cerebral artery blood flow velocity and jugular bulb venous oxygen saturation after severe brain injury. J Neurosurg. 1992;77(1):55–61.
42. Bellner J, et al. Transcranial Doppler sonography pulsatility index (PI) reflects intracranial pressure (ICP). Surg Neurol. 2004;62(1):45–51. discussion 51
43. Wang Y, et al. Middle cerebral arterial flow changes on transcranial color and spectral Doppler sonography in patients with increased intracranial pressure. J Ultrasound Med. 2014;33(12):2131–6.
44. Prunet B, et al. Noninvasive detection of elevated intracranial pressure using a portable ultrasound system. Am J Emerg Med. 2012;30(6):936–41.

45. Wakerley BR, et al. Usefulness of transcranial Doppler-derived cerebral hemodynamic parameters in the noninvasive assessment of intracranial pressure. J Neuroimaging. 2015;25(1):111–6.
46. Cigada M, et al. Cerebral CO2 vasoreactivity evaluation by transcranial Doppler ultrasound technique: a standardized methodology. Intensive Care Med. 2000;26(6):729–32.
47. Kirkham FJ, et al. Transcranial measurement of blood velocities in the basal cerebral arteries using pulsed Doppler ultrasound: velocity as an index of flow. Ultrasound Med Biol. 1986;12(1):15–21.
48. Eng C, et al. The influence of propofol with and without nitrous oxide on cerebral blood flow velocity and CO_2 reactivity in humans. Anesthesiology. 1992;77(5):872–9.
49. Caricato A, et al. Effects of PEEP on the intracranial system of patients with head injury and subarachnoid hemorrhage: the role of respiratory system compliance. J Trauma. 2005;58(3):571–6.
50. Robba C, et al. Effects of prone position and positive end-expiratory pressure on noninvasive estimators of ICP: a pilot study. J Neurosurg Anesthesiol. 2017;29(3):243–50.

Chapter 50
Acute Liver Failure (ALF) in ICU: Usefulness of Transcranial Doppler (TCD/TCCS)

Anselmo A. Abdo-Cuza

Key Points

1. Acute liver failure (ALF) is a potentially serious syndrome characterized by liver dysfunction (altered liver biochemistry plus coagulopathy) and encephalopathy.
2. Brain edema and intracranial hypertension complicate 75–80% of patients diagnosed with ALF and grade III or IV hepatic encephalopathy (HE), and are the leading cause of death.
3. Invasive intracranial pressure measurement has been considered the gold standard method of monitoring intracranial hypertension accompanying HE in ALF.
4. Noninvasive neuromonitoring is a suitable alternative without the adverse events of invasive techniques.
5. The study of cerebral hemodynamics by TCD/TCCS allows us to establish five hemodynamic patterns (hypoperfusion, high resistance, hyperemia, vasospasm, or cerebral circulatory arrest) with prognostic and therapeutic implications.
6. The use of TCD/TCCS together with jugular bulb venous oxygen saturation ($SjvO_2$) monitoring (cerebral hemodynamic-metabolic monitoring) could help to understand the pathophysiology of HE.

50.1 Introduction

Acute liver failure (ALF) is a potentially serious syndrome that occurs more often in young people without a history of liver disease, with an incidence of fewer than ten cases per million people. It is characterized by liver dysfunction (altered liver biochemistry plus coagulopathy) and encephalopathy. The most frequent etiologies are viral

A. A. Abdo-Cuza (✉)
Medical Surgical Research Center, La Habana, Cuba
e-mail: aaabdo@infomed.sld.cu

C. N. Rodríguez et al. (eds.), *Neurosonology in Critical Care*,
https://doi.org/10.1007/978-3-030-81419-9_50

infections (hepatitis A, B, and E viruses) and drug toxins [1, 2]. In theory, it is a reversible condition but 60–95% of patients (with non-acetaminophen-related etiology) progress to multiorgan failure and death if they do not undergo liver transplantation.

50.2 Hepatic Encephalopathy

It is the brain dysfunction secondary to liver failure. The clinical spectrum of presentation may range from apparent normality detectable only by neuropsychological or electrophysiological studies, to coma [3]. The time between the onset of jaundice and the appearance of encephalopathy has diagnostic and prognostic implications. In the hyperacute presentation (less than 7 days), cerebral edema, and intracranial hypertension are highly frequent, but the prognosis for recovery is more favorable than in the subacute form (more than 7 days), in which the appearance of even low-grade encephalopathy implies a worse outcome.

50.3 Hepatic Encephalopathy: Pathophysiology

The most recent studies involve increased ammonium concentrations and a cytokine-mediated inflammatory component (IL-1, IL-6, TNF) associated or not with sepsis, as the main mechanisms responsible for the neurological dysfunction that characterizes hepatic encephalopathy (HE) [4].

High levels of blood ammonia cross the blood–brain barrier (BBB), where it is metabolized by astrocytes to glutamine. It is the accumulation of glutamine that causes astrocyte edema with the consequent increase in intracranial pressure (ICP) and decrease in cerebral perfusion pressure (CPP).

In relation to hemodynamics and brain metabolism, a wide spectrum of possibilities has been described, from a decrease in cerebral blood flow (CBF), which in early phases is coupled with a decrease in brain metabolism, to high CBF values. In advanced phases and in a progressive manner, alteration of cerebral autoregulation favors an excessive CBF for the metabolic demand and the increased probability of cerebral edema with a decrease in cerebral perfusion down to a complete cessation of cerebral circulation accompanying brain death. Brain edema and intracranial hypertension complicate 75–80% of patients diagnosed with ALF and grade III or IV HE and are the leading cause of death.

50.4 Acute Liver Failure: Invasive Intracranial Pressure Monitoring

Neurological function in patients with ALF has been conventionally assessed by clinical and electroencephalographic tests. Imaging studies that are accessible to critically ill patients make it possible to rule out visible structural lesions, including

intracranial hemorrhage (ICH). High-level centers have been using the gold standard technique for ICP monitoring: intracranial placement of catheters for invasive measurement [5, 6]. The US ALF Study Group published an article in 2005 examining the experience on 332 patients diagnosed with severe HE and ALF (grades III and IV) at 25 centers in the USA [7]. Invasive ICP was monitored in 28% of patients, with variability across centers. Fresh frozen plasma (FFP) was used in 91% of preprocedure actions, while post-procedure ICH appeared in 10%. Performance in the two groups differed in relation to greater use of mannitol, barbiturates, and vasopressors in the study group whose ICP was monitored invasively. Survival at 30 days among patients who received liver transplantation was 85% in the two groups. The authors conclude that, although the incidence of ICH has decreased over time, serious complications related to the procedure are real. There was a more aggressive treatment of intracranial hypertension in the invasively monitored group and the results in survival warrant further studies with longer observation time, before a recommendation on its usefulness can be made.

In 2017 Rajajee et al. [8] published a single-center study in a hospital with a large volume of liver transplantation. The authors show the results from 24 patients out of 37 diagnosed with ALF who were monitored invasively for ICP. They present a preprocedure protocol where they administered activated factor VII; they only use intraparenchymal catheters and then perform computed tomography (CT) scans to evaluate bleeding complications, which were present in only one case. In the noninvasively monitored group, 15% died in brain death, compared to 4% in the invasively monitored group. The author of this chapter notes that out of 37 patients in the study diagnosed with ALF, 80% had contraindications for liver transplantation, which is the treatment of choice for most patients in this clinical situation.

Although the authors conclude that ICP monitoring according to the protocol described in the research is a procedure with a low incidence of complications and associated with superior results, they propose future studies with noninvasive methods such as ultrasound of the optic nerve and transcranial Doppler.

50.5 Acute Liver Failure: Noninvasive Intracranial Pressure Monitoring

The use of noninvasive methods to monitor ICP has been one of the chimeras of intensive care. Noninvasiveness would eliminate the main complications associated with the invasive method: bleeding and infection of the central nervous system. Moreover, some of the methods tested are less expensive and use traditional hospital equipment, features that make them desirable for intensive care units (ICUs) in developing countries. Today, although there has been progress, the invasive method remains the gold standard. Among the noninvasive methods of ICP estimation are the following: the cochlear fluid pressure analyzer by tympanic membrane displacement, tissue oxygenation monitoring by near infrared spectroscopy, fontanometry in neonates and the one that currently arouses most interest in emergency medicine

and ICU, the transorbital ultrasound measurement of the diameter of the optic nerve sheath [9, 10]. In general, these methods are attractive but even if they show a good correlation with invasive ICP measurement (a situation not unanimously achieved) they provide limited information that requires the complement of other methods, an action known as multimodal monitoring [11, 12].

50.6 Acute Liver Failure: Monitoring of Hemodynamics and Brain Metabolism

Most of the initial trials were performed by a few groups which used for the CBF evaluation, the Xenon 133 washing technique with the Kety-Schmidt equation. Brain metabolic activity was determined according to the arteriovenous oxygen difference ($AVDO_2$) between jugular bulb venous oxygen saturation ($SjvO_2$) obtained through blood from the jugular vein and arterial blood sample.

Aggarwal et al. [13] conducted a study to determine the incidence of patients diagnosed with ALF in five phases of hemodynamics and brain metabolism, which they established according to previous studies. The authors describe a phase one characterized by decreased CBF and normal ICP values. Phases two and three are characterized by elevated CBF with normal and elevated ICP, respectively. Phase four with decreased CBF and increased ICP; and Phase five: brain death. The phases describe the theory that changes in CBF precede and contribute to increased ICP and brain edema. The measurement of CBF was performed by the Xenon-133 brain clearance technique and ICP was monitored with a fiberoptic catheter placed in the epidural space. The results show that in the first evaluation of the patients under study, there were 10 patients in phase one (decreased CBF and normal ICP), 8 patients in phase two, and 8 patients in phase three; both phases were characterized by increased CBF. Among patients who received only medical treatment, 9 out of 11 survived in phase one or two, while all those in phase three and four died. The criterion for cerebral ischemia was defined according to $AVDO_2$ evaluation. In eight patients with CBF below 20 ml/100 g/min, no ischemia was evident due to flow-metabolism coupling. Similarly, by means of $AVDO_2$ analysis, 80.8% of patients were diagnosed with hyperemia pattern and by means of CBF measurement it was diagnosed in 65.4%. This research was published in 2005 in the journal *Liver Transplantation* and as far as we know, there is no publication that replicates the data presented with similar methodology.

50.7 Acute Liver Failure: Cerebral Hemodynamics Monitoring by TCD/TCCS

The introduction of Transcranial Doppler (TCD) in 1982 by Rune Aaslid represented an important step in the study of cerebral hemodynamics in a noninvasive way and at the patient's bedside. Through three acoustic windows (transtemporal,

transorbital, and transoccipital) the brain vessels that constitute the Circle of Willis can be insonated, using a low frequency transducer (e.g. 2 MHz pulsed Doppler). A fourth window, the submandibular window, allows the assessment of the hemodynamics of the distal extracranial segments of the carotid arteries, using the same transducer. At the end of the 1980s and favored by technological advances in ultrasound machines and transducers, transcranial color-coded duplex sonography (TCCS) was introduced in the adult population: this technique combines the acquisition of color and spectral images by transcranial Doppler together with two-dimensional images [14].

Since the introduction of transcranial Doppler, several studies have validated the technique as a reliable indirect measurement of CBF at baseline and under changing physiological conditions. In order to make the measurements comparable at the time of interpretation, it is necessary to know the variables that can modify cerebral blood flow velocities and the pulsatility index (Table 50.1).

PI has been evaluated as a reflection of cerebral vascular resistance (CVR), although there is research that demonstrates its dependence on multiple cerebral hemodynamic factors, such as blood pressure amplitude, compliance, and cerebral arterial bed resistance, among others, which make its interpretation complex [15]. Some authors have suggested that it more accurately reflects cerebral perfusion pressure (CPP) than ICP.

One of the first studies using TCD in patients with ALF was published by Strauss et al. [16] in 2001, where they evaluated the variability of a group of measurements in eight patients during normoventilation and hyperventilation. They report a modification of the values of CBF (ml/100 g/min) from 43 to 32; right mean blood flow velocity [MFV_{RMCA}] (cm/sec.) from 52 to 43; $SjvO_2$ (%) from 68 to 55 and mean arterial blood pressure [MAP] (mmHg) from 80 to 71. The correlation between CBF and MFV_{RMCA} was poor ($r = 0.30$). The authors concluded that TCD can be used in the monitoring of patients with ALF but its interpretation is recommended together with $SjvO_2$.

Table 50.1 Most frequent factors that can change the mean flow velocity (MFV) and Pulsatility index (PI) values

Mean flow velocity (MFV)		Pulsatility Index (PI)	
Increase	Decrease	Increase	Decrease
Diminished vessel area (vasospasm and stenosis) Anemia Hyperthermia Hypervolemia High ABP Hypercapnia Hypoxemia Volatile anesthetics	Age Hyperviscosity Dehydration Low cardiac output Low blood pressure Hypothermia Sedative and hypnotic drugs	IHT Hypocapnia Aortic insufficiency Chronic high ABP Leukoaraiosis	Hypercapnia AVM Post-stenotic vasodilation Hyperemia Hypervolemia

ABP Arterial blood pressure, *IHT* Intracranial hypertension, *AVM* Arterio-venous malformation

In 2010 Kawakami et al. [17] published a small series of six patients with ALF and reported high PI values in those with unfavorable evolution without possibility of transplantation, in contrast with those who had spontaneous recovery or received liver transplantation, who presented PI within normal range. The authors suggested that PI can be used as a prognostic factor and indicator for transplantation.

Abdo et al. [18, 19] presented in 2003 a series of five severe patients with ALF who underwent a TCD/TCCS study of cerebral hemodynamics on admission to the ICU and were compared with a control group of neurocritical patients of different etiologies. In the study group, a pattern of cerebral hypoperfusion with significantly altered MFV_{RMCA} and PI values was observed more often than in the control group. The same group of researchers published in 2015 an extension of the series with 21 patients. The sonographic patterns of cerebral hemodynamics were as follows: low-flow, 12 patients (57.1%); high resistance, 5 patients (23.8%); and hyperemic, 4 patients (19%). Death was associated with hypoperfusion and high brain resistance patterns, while the hyperemic pattern was associated with survival.

If a distribution of patients according to the phases of hemodynamics and brain metabolism described by Aggarwal et al. [13] is carried out as a theoretical exercise, and CBF is replaced by MFV_{RMCA} while ICP by PI, we would find different results: 52.4% of patients in phase four (decreased CBF, elevated ICP), 23.9% in a situation not recognized by the original study (normal CBF, elevated ICP), and only 19% in phases two or three (hyperemia). CBF monitoring, perhaps more reliable but logistically complex in ICUs, finds a predominance of hyperemia situation (defined by $AVDO_2$ measurements) and associates this pattern with worse outcome. The use of TCD/TCCS, a method available at the bedside, reproducible and noninvasive, shows a predominance of hypoperfusion pattern with high resistance, which was associated with worse outcome.

At the present time (data collection phase) in our working group, with the introduction of ultrasound-guided retrograde catheterization of the jugular vein, we incorporate new variables into the analysis of cerebral hemodynamics. We incorporated $SjvO_2$ and cerebral oxygen extraction fraction (O_2EF), the latter providing greater accuracy on the transport-consumption-metabolism relationship, than $AVDO_2$, used in the pioneering studies on the subject.

In the opinion of the author of this chapter, the data provided by TCD/TCCS on cerebral hemodynamics allow the formation of a pathophysiological sequence on HE secondary to ALF that can be initiated by a high resistance pattern (elevated PI with normal MFV_{RMCA}), expression of ammonium-glutamine damage in the astrocyte that generates cerebral edema; or initiated by a hyperemic pattern with normal PI, expression of increased CBF secondary to vasodilation by increased cytokines or self-regulatory disorders or motor vessel reactivity. The hyperemic pattern, according to its pathophysiology, can be associated with better survival, given the possibilities of action in the ICU. In more advanced stages, associated with worse prognosis, patients have a decreased CBF (assessed by MFV_{RMCA}) and increased ICP (assessed by PI). Patients with a hypoperfusion pattern would have a worse prognosis and less chance of surviving while waiting for transplantation, than patients with a hyperemic pattern, who would have a better chance.

Another utility of the TCD/TCCS study in patients with ALF lies in the assessment of contraindications to transplantation in patients with severe neurological impairment. Traditionally there have been two situations related to cerebral hemodynamics that contraindicate liver transplantation. These are the presence of ICP values above 40 mmHg or CPP values below 50 mmHg, for at least 2 hours. In 2008, Bindi et al. [20] presented three HE patients with clinically impaired ALF (three-point Glasgow Coma Scale) and severe electroencephalographic impairment, at a time when a decision on transplantation had to be made thanks to an available organ. The group took into account the results of MFV_{RMCA} and PI by TCD: patient 1 (low MFV: 36 cm/s, high PI: 2.8), patient 2 (low MFV: 18 cm/s, high PI: 4), patient 3 (low MFV: 20 cm/s, high PI: 4). Liver transplantation was successfully performed in all three patients who slowly recovered consciousness, even in the presence of severe clinical deterioration. These results suggest the usefulness of TCD to correctly evaluate the feasibility of liver transplantation without the need of invasive ICP or CPP measurement.

50.8 Acute Liver Failure: TCD/TCCS Protocol

Once the patient is admitted to the ICU, hemodynamic and metabolic stabilization will be performed if necessary. A brain CT/MRI is necessary to rule out any neurological complications associated with HE (cerebral infarction, ICH).

Prior to performing a neuroimaging and TCD, the following prerequisites should be checked: MAP >65 mmHg; blood oxygen pressure (PO_2) 60–110 mmHg; carbon dioxide pressure (PCO_2) 35–45 mmHg; body temperature 35–38 °C; hemoglobin >7 g/L; and pulse oximetry saturation >92%. TCD will be performed with the patient in a supine position. The vessels to be explored will be insonated with a 2 MHz pulsed Doppler transducer. The sample volume, gain, and power will be kept constant during the investigation. The right and left MCA sonograms will be displayed bilaterally through the time window in depths between 45 and 55 mm. Side-to-side asymmetry of MCA blood flow velocity values will be considered if the difference is greater than 20%.

For patients with high mean CBF velocities, the distal extracranial portion of the ipsilateral internal carotid artery (ICA) will be explored through the submandibular window at a depth between 30 and 55 mm, with the 2 MHz transducer in pulsed Doppler mode, in order to record its mean velocity and calculate the Lindegaard index (ratio between the MFV_{MCA} and MFV_{ICA}).

The flow tracing (velocity and spectral waveform) must be kept constant for at least 30 seconds per isolated artery, before the values of the parameters under study (MFV_{MCA}, PI) are recorded and collected.

Brain hemodynamic patterns are defined as follows:

1. Normal: MFV_{MCA} and PI within the reference values.
2. Hypoperfusion or low flow: MFV_{MCA} below the reference values, regardless of the PI.

3. Hyperemic: MFV_{MCA} greater than reference values, with Lindegaard index <3, regardless of PI.
4. Vasospasm: MFV_{MCA} greater than the reference values, with Lindegaard Index >3, independent of the PI.
5. High resistance: PI greater than the reference values.
6. Cerebral Circulatory Arrest (CCA): reverberant flow, isolated systolic spikes, or "disappearance" of previously detected flows. To certify this diagnosis, both MCA (anterior circulation) and the basilar artery (BA) or intracranial vertebral arteries (VA) (posterior circulation) must show similar spectra. To confirm the irreversibility of the CCA, it is necessary to have two measurements separated by at least 30 minutes. In the event that adequate acoustic windows are not found, the insonation of extracranial portion of ICAs (submandibular window) is acceptable, although it should be clarified that the appearance of CCA patterns in this artery occurs later (although very specific) than in the intracranial arteries.

50.8.1 Clinical Case

A 19-year-old female patient, diagnosed with ALF secondary to Hepatitis E virus infection. According to her clinical evaluation, she was classified as having HE grade II–III (Fig. 50.1b). TCD was performed and the patient was diagnosed with

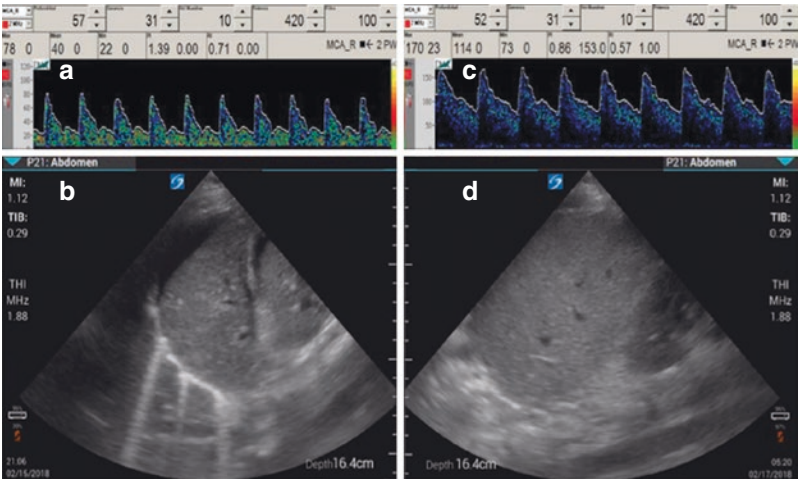

Fig. 50.1 (**a**) Middle cerebral artery Doppler spectrum (MCA) compatible with high resistance pattern (PI: 1.39), obtained in a transtemporal window at 57 mm depth, in a patient diagnosed with acute liver failure (ALF). In (**b**), small liver and ascitic fluid are observed, in correspondence with the ALF picture. (**c**) Doppler spectrum of MCA compatible with hyperemic pattern, obtained in transtemporal window at 52 mm depth, in the same patient after liver transplantation. (**d**) shows the ultrasound image of the transplanted liver

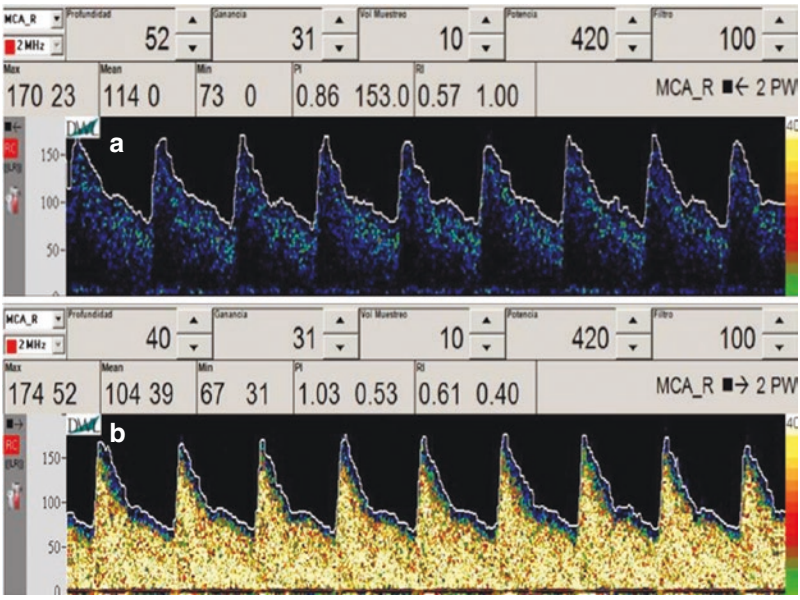

Fig. 50.2 Calculation of the lindegaard index (LI) The MFV in the middle cerebral artery (MCA) in (**a**). is 114 cm/sec, while in the extra-cranial portion of internal carotid artery (ICA) in (**b**)., is 104 cm/sec. The LI is obtained as MFV_{MCA}/ MFV_{ICA}, in this case 114/104 = 1.1; indicating that the increase in velocities in the MCA is due to hyperemia and not to cerebral vasospasm

high resistance cerebral hypoperfusion (Fig. 50.1a). General measures for the treatment of intracranial hypertension (IHT) were continued, mannitol treatment was initiated and mean arterial blood pressure (MAP) was maintained at 90 ± 5 mmHg. According to the criteria of the King College, the patient was placed on an emergency list for liver transplantation (Fig. 50.1d), which was achieved 48 hours later. In the initial post-transplant evaluation a high velocity pattern was obtained, (Fig. 50.1c), which was classified as hyperemic as the Lindegaard index was less than 3, (Fig. 50.2). The general measures of IHT prophylaxis/treatment were maintained, mannitol was removed and the MAP target was set at 65–70 mmHg. Adequate awareness was achieved and the patient was extubated within 24 hours of transplantation with good clinical and laboratory progress.

50.9 Conclusion

The study of cerebral hemodynamics by TCD/TCCS allows to establish five hemodynamic patterns (hypoperfusion, high resistance, hyperemia, vasospasm, cerebral circulatory arrest) with prognostic and therapeutic implications in patients with ALF.

Algorithm

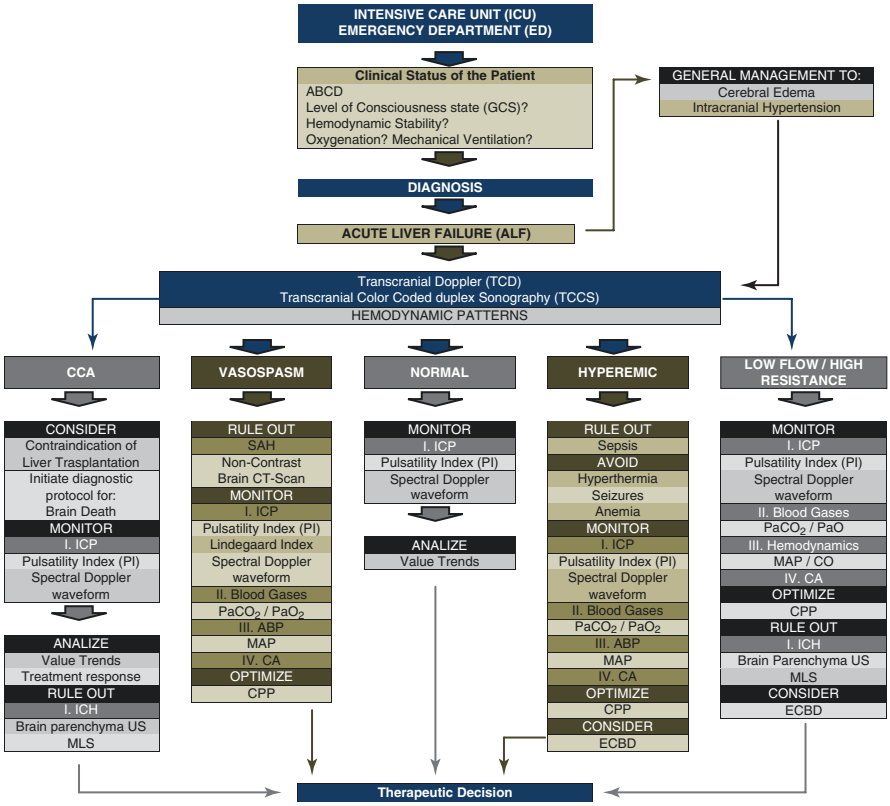

ABCD Airway-breathing-circulation-disability, *SAH* Subarachnoid hemorrhage, *ICP* Intracranial pressure, *ABP* Arterial blood pressure, *CA* Cerebral autoregulation, *CPP* cerebral perfusión pressure, *ICH* Intracerebral hemorrhage, *MLS* Midline shift, *US* Ultrasound, *MAP* mean arterial pressure, *CO* Cardiac output, *ECBD* Extracorporeal blood depuration, *CCA* Cerebral circulatory arrest

References

1. Rajaram P, Subramanian R. Acute Liver Failure. Semin Respir Crit Care Med. 2018;39(5):513–22.
2. Squires JE, McKiernan P, Squires RH. Acute liver failure: an update. Clin Liver Dis. 2018;22(4):773–805.
3. Ryu AJ, Rahimi RS, Leise MD. The current hepatic encephalopathy pipeline. J Clin Exp Hepatol. 2020;10(4):377–85.
4. Liere V, Sandhu G, DeMorrow S. Recent advances in hepatic encephalopathy. F1000Res. 2017;6:1637.
5. Wendon JA, Larsen FS. Intracranial pressure monitoring in acute liver failure. A procedure with clear indications. Hepatology. 2006;44(2):504–6.

6. Bernuau J, Durand F. Intracranial pressure monitoring in patients with acute liver failure: a questionable invasive surveillance. Hepatology. 2004;44(2):502–4.
7. Vaquero J, Fontana RJ, Larson AM, Bass NM, Davern TJ, Shakil AO, et al. Complications and use of intracranial pressure monitoring in patients with acute liver failure and severe encephalopathy. Liver Transpl. 2005;11(12):1581–9.
8. Rajajee V, Fontana RJ, Courey AJ, Patil PG. Protocol based invasive intracranial pressure monitoring in acute liver failure: feasibility, safety and impact on management. Crit Care. 2017;21(1):178.
9. Robba C, Cardim D, Tajsic T, Pietersen J, Bulman M, Donnelly J, et al. Ultrasound non-invasive measurement of intracranial pressure in neurointensive care: a prospective observational study. PLoS Med. 2017;14(7):e1002356.
10. Rajajee V, Williamson CA, Fontana RJ, Courey AJ, Patil PG. Noninvasive intracranial pressure assessment in acute liver failure. Neurocrit Care. 2018;29(2):280–90.
11. Lazaridis C, Robertson CS. The role of multimodal invasive monitoring in acute traumatic brain injury. Neurosurg Clin N Am. 2016;27(4):509–17.
12. Paschoal FM Jr, Nogueira RC, Ronconi Kde A, de Lima OM, Teixeira MJ, Bor-Seng-Shu E. Multimodal brain monitoring in fulminant hepatic failure. World J Hepatol. 2016;8(22):915–23.
13. Aggarwal S, Obrist W, Yonas H, Kramer D, Kang Y, Scott V, et al. Cerebral hemodynamic and metabolic profiles in fulminant hepatic failure: relationship to outcome. Liver Transpl. 2005;11(11):1353–60.
14. Blanco P, Abdo-Cuza A. Transcranial Doppler ultrasound in neurocritical care. J Ultrasound. 2018;21(1):1–16.
15. Calviello LA, de Riva N, Donnelly J, Czosnyka M, Smielewski P, Menon DK, et al. Relationship between brain pulsatility and cerebral perfusion pressure: replicated validation using different drivers of CPP change. Neurocrit Care. 2017;27(3):392–400.
16. Strauss GI, Møller K, Holm S, Sperling B, Knudsen GM, Larsen FS. Transcranial Doppler sonography and internal jugular bulb saturation during hyperventilation in patients with fulminant hepatic failure. Liver Transpl. 2001;7(4):352–8.
17. Kawakami M, Koda M, Murawaki Y. Cerebral pulsatility index by transcranial Doppler sonography predicts the prognosis of patients with fulminant hepatic failure. Clin Imaging. 2010;34(5):327–31.
18. Abdo A, López O, Fernández A, Santos J, Castillo J, Castellanos R, et al. Transcranial Doppler sonography in fulminant hepatic failure. Transplant Proc. 2003;35(5):1859–60.
19. Abdo A, Pérez-Bernal J, Hinojosa R, Porras F, Castellanos R, Gómez F, Gutiérrez J, et al. Cerebral hemodynamics patterns by transcranial Doppler in patients with acute liver failure. Transplant Proc. 2015;47(9):2647–9.
20. Bindi ML, Biancofiore G, Esposito M, Meacci L, Bisà M, Mozzo R, et al. Transcranial doppler sonography is useful for the decision-making at the point of care in patients with acute hepatic failure: a single centre's experience. J Clin Monit Comput. 2008;22(6):449–52.

Chapter 51
Sepsis in the ICU: Usefulness of Transcranial Doppler (TCD/TCCS) to Cerebral Hemodynamic Monitoring

Ilaria Alice Crippa and Fabio Silvio Taccone

Key Points

1. Sepsis-associated brain dysfunction is the most frequent sepsis-related organ dysfunction and is associated with mortality. In survivors, neurological consequences of sepsis extend beyond ICU stay, affecting quality of daily life.
2. Hypoperfusion and ischemia contribute to sepsis-associated brain dysfunction, both as a primary pathophysiological mechanism and as a secondary brain injury.
3. Transcranial Doppler (TCD/TCCS), although not able to quantify cerebral blood flow, can detect real-time changes in cerebrovascular hemodynamics.
4. Sepsis-related modifications in cerebral circulation have been investigated in humans with controversial results. Overall, cerebral autoregulation seems impaired early during the course of sepsis; impaired cerebral autoregulation is associated with neurological dysfunction and the degree of inflammation.
5. Along with impairment in cerebral autoregulation, an increase in cerebrovascular resistance may occur during sepsis.
6. Whether cerebrovascular reactivity to carbon dioxide is preserved during sepsis is not clear, as well as the influence of carbon dioxide levels on cerebral autoregulation.
7. To date, studies investigating cerebral hemodynamics in large cohort of septic patients are lacking. Moreover, the variety of methods in cerebral hemodynamics assessment in published literature makes comparison between studies difficult.

I. A. Crippa
Department of Intensive Care, University of Brussels, Erasme Hospital, Brussels, Belgium

F. S. Taccone (✉)
Emergency Medicine, University Libre of Brussels, Brussels, Belgium

Department of Intensive Care, Laboratory of Experimental Research, Erasme Hospital, Brussels, Belgium
e-mail: ftaccone@ulb.ac.be

C. N. Rodríguez et al. (eds.), *Neurosonology in Critical Care*,
https://doi.org/10.1007/978-3-030-81419-9_51

51.1 Introduction

Sepsis-associated encephalopathy (SAE) is the most frequent sepsis-related organ dysfunction [1]. It appears early during the course of infection, often before any other organ involvement [2], in up to 70% of hospitalized septic patients [3]. SAE is described as the diffuse cerebral dysfunction that accompanies the abnormal inflammatory response during an infection, in absence of direct central nervous system involvement. Clinical presentation of SAE resembles that of delirium, defined as an acute disturbance in attention, cognition, and awareness that tends to fluctuate in severity during the day and that is not explained by another preexisting, established, or evolving neurological disorder. Sometimes considered a subtype of delirium, SAE can vary in severity, ranging from behavioral alterations to coma [4]. Development of SAE is associated with mortality; in a prospective study on 50 patients, Eidelman et al. showed an inverse relationship between GCS on admission and ICU mortality (16% for GCS 15 up to 63% for GCS 3–8) [3]. Moreover, SAE can negatively impact the quality of life (QoL) of survivors, who may present persistent cognitive impairment, functional disability, and physical, sensory, and emotional alterations [5]. Because of the absence of specific clinical findings, SAE is a diagnosis of exclusion based on clinical examination.

51.2 Sepsis-Associated Brain Dysfunction (SAE): Pathophysiology

SAE is a multifactorial syndrome whose multiple pathophysiological mechanisms might be involved to different degrees depending on patient characteristics (e.g., age, preexisting cognitive status), medications, environmental factors (e.g., sleep deprivation), or metabolic alterations (e.g., fever, hypo-hyperglycemia) [6]. A synthetic, non-exhaustive representation of pathophysiology of SAE is reported in Fig. 51.1. Along with small hemorrhagic lesions, multiple ischemic lesions have been described in post-mortem analysis of septic shock patients, suggesting that alterations in cerebral blood flow (CBF) are involved in the development of SAE. Ischemic lesions were not only found in brain areas traditionally considered sensitive to ischemia (i.e., hippocampus, basal ganglia, frontal cortex), but also in the nuclei of the autonomic nervous system (i.e., amygdala, anterior and posterior hypothalamus, locus coeruleus), which seems to be specific to sepsis [7]. These brain areas are all involved in the development of the broad spectrum of SAE symptoms. Polito et al. investigated 71 septic patients through MRI during the first 7–14 days from diagnosis. They identified two prevalent patterns of brain injury: diffuse leukoencephalopathy and ischemic strokes. Leukoencephalopathy was attributed to blood–brain barrier (BBB) disruption and subsequent vasogenic edema, while ischemic strokes were attributed to cytotoxic edema due to cerebral hypoperfusion. Hemodynamic instability frequently characterizes early sepsis and septic

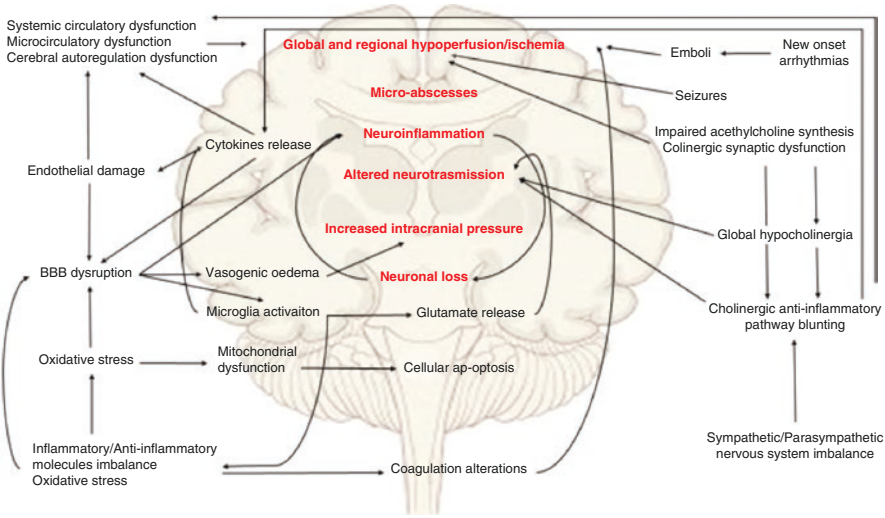

Fig. 51.1 Pathophysiology of sepsis-associated brain dysfunction

patients are potentially extremely vulnerable to hypotension. Cerebral oxygen demand is directly proportional the complexity of brain activity and even though the cerebral blood flow is only slightly reduced in septic patients [8], this reduction could be enough to impair superior cognitive functions. In case of nonconvulsive seizures and periodic epileptiform discharges, which may occur in septic patients [9], such reduction can determine an oxygen supply-demand imbalance. Such pathophysiological considerations underline the importance of optimizing brain perfusion during sepsis, in order to avoid secondary brain injury.

51.3 Transcranial Doppler (TCD/TCCS): Cerebral Perfusion During Sepsis

As for most organs in the body, the adequacy of oxygen supply-demand balance is far more important than the absolute value of oxygen delivery itself. It follows that the ability to regulate the CBF is more important than its absolute value in preventing hypoxic/ischemic episodes to the brain. Furthermore, there are evidences that cerebral autoregulation curve is modified under specific circumstances. For example, cerebral autoregulation is impaired early during the course of diabetic disease [10] and hypertensive patients have cerebral autoregulation curve shifted to the right [11]. The existence of such comorbidities in septic ICU patients cannot be neglected, so that monitoring of adequate oxygen supply to the brain while avoiding excessive flow, which would contribute to vasogenic edema, is of great importance in preventing neurological complications.

There are several methods to evaluate cerebral blood flow in humans. However, to date, there has been no consensus on which one is most accurate. Trans-cranial Doppler (TCD/TCCS), although not able to quantify CBF, is a suitable tool to investigate the cerebrovascular hemodynamics. Its affordable costs, absence of risk and discomfort for the patient also during long-time monitoring, portability and real-time detection of changes in cerebrovascular hemodynamics at bedside make it a most attractive option for cerebral circulation investigation in clinical practice. Sepsis-related modifications in cerebral circulation have been investigated by TCD/TCCS in humans with alternative results. In 1998, Smith et al. investigated a small cohort of septic patients ($n = 15$) and nonseptic controls ($n = 9$). They used Doppler blood flow velocity in common carotid artery to estimate CBF and found that it was directly proportional to the cardiac index in patients with septic shock, concluding that the cause must have been the loss of autoregulation of cerebral blood flow [12]. On the opposite, Matta and Stow investigated cerebral autoregulation (CA) by modifying mean systemic arterial pressure with phenylephrine infusion in 10 patients with altered mental status and on mechanical ventilation, during early sepsis (<24 hours from diagnosis): they found that raising mean systemic arterial pressure (MAP) from 75 to 98 mmHg did not induce modification in middle cerebral artery blood flow velocity measured by transcranial Doppler, concluding that CA was intact in that MAP range [13]. Taccone et al. reported that cerebral autoregulation was altered in 66% of 21 patients affected by septic shock [14]. Pfister et al. assessed cerebral autoregulation in 16 patients within 48 hours from diagnosis of sepsis. They assessed CA by Mxa and sepsis-associated delirium by CAM-ICU. Despite similar systemic hemodynamics parameters, in 12 patients diagnosed with SAE mean Mxa was higher than in patients who did not show signs of altered mental status, meaning an association between altered CA and occurrence of SAE [15]. Moreover, patients with SAE had higher C-reactive protein levels, which in turn were associated with increasingly altered autoregulation, suggesting a role of inflammation in altering CA [16]. There are evidence that cerebral autoregulation in septic patients is impaired early during the course of sepsis, but improves over time. Schramm et al. investigated CA in 30 patients during the first 4 days after sepsis or septic shock diagnosis. CA was impaired in 83% of patients. Mxa was highest on day 1 and then the value decreased during the first 72 hours (from 0.42 to 0.3), suggesting an improvement in CA over time. A significant association between CA impairment at day 1 and sepsis-associated delirium diagnosed at day 4 was found, suggesting that altered CA might influence the development of sepsis-associated delirium [17]. Unfortunately, due to the different methods of assessment on cerebral autoregulation, a pooled analysis of the patients included in the published studies has not been possible [18].

Pierrakos et al. calculated the pulsatility index (PI)—which is positively related to changes in vascular resistance [19]—in 38 patients during the first 72 hours from sepsis diagnosis. More than half of patients (55%) showed signs of SAE during

ICU stay, as assessed by CAM-ICU. PI >1.3 on the first day of assessment was independently associated with the development of neurological symptoms during their ICU stay up to a maximum of 10 days follow-up [20]. Straver et al. showed that mild intracranial vasospasm may occur in septic shock, as demonstrated by a Lindegaard ratio above 2 in 20 patients [21]. A recent meta-analysis [18] conducted on four studies [22–25] reported an increased PI in septic patients ($n = 92$) compared to healthy controls ($n = 86$). Taken together, these studies suggest altered basal vascular tone in cerebral circulation during sepsis with possible vasoconstriction.

Being carbon dioxide the main determinants of vascular tone, its influence on cerebral autoregulatory capacity has been hypothesized [26]. Animal studies showed that hypercapnia shifts the autoregulation curve to the right [27] and reduces the plateau [28]. On the other hand, pressure regulation prevails on carbon dioxide reactivity during hypotension [16, 26]. Matta and Stow tested carbon dioxide reactivity in a small sample of 10 sedated septic patients and found it to be within normal limits during early sepsis (<24 hours) [13]. In 2007, Thees et al. showed a normal cerebrovascular reactivity on a small sample ($n = 10$) of mechanically ventilated patients investigated during late sepsis (>48 hours) [29]. On the opposite, Bowie et al. found that cerebrovascular reactivity to active modifications of carbon dioxide (from normocapnia to hypocapnia and then hypercapnia) was reduced in 7 and increased in 2 out of 12 sedated and mechanically ventilated patients in late sepsis (>24 hours), while only 3 patients had normal cerebrovascular reactivity [30]. These results were consistent with those by Terborg et al. on eight septic patients [31] and those by Fülesdi et al. on 16 septic patients after administration of acetazolamide [23]. A composite effect of carbon dioxide and MAP on cerebral autoregulation cannot be excluded, so that comprehensive understanding of CA should take into account the integrated effect of multiple mechanisms. The effect of carbon dioxide levels on cerebral autoregulation has been tested by Taccone et al., who investigated the modification of middle cerebral artery blood flow velocity in response to a vasopressor-induced MAP challenge in 21 patients during the first 3 days of septic shock. CA was more frequently altered in patients with hypercapnia (pCO_2 >40 mmHg), suggesting that carbon dioxide levels may alter the responsiveness of cerebral arteries to arterial pressure changes [14]. Hence, there is the chance that even small changes in plasmatic carbon dioxide levels during studies exploring cerebral perfusion and autoregulation may obscure the effects of any investigated intervention or mechanism. These results have not been confirmed later by Berg et al., who showed no difference in frequency-domain analysis of cerebral autoregulation after modification in carbon dioxide levels in seven mechanically ventilated septic patients within 72 hours from diagnosis [32]. However, the sample size in this latter study does not allow any definite conclusions. Overall, in most of those studies cerebral autoregulation appeared to be altered in septic patients, more severely in patients affected by SAE (Table 51.1).

Table 51.1 Prospective studies using transcranial Doppler to monitor the brain in septic patients

Study	Year	Sample size	Diagnosis	Evaluation time	Methods of assessment	Results
Berg et al. [32]	2016	7	Severe sepsis or septic shock	<72 hrs	TFA after modifications of pCO_2 through respiratory settings	CO_2R preserved in septic patients
Berg et al. [33]	2015	9 HV with IV LPS 6 septic patients	Sepsis and septic shock	<72 hrs	RoR after thigh-cuff deflation-induced changes in MAP, where RoR = (ΔCVC/Δtime)/ΔMAP, where CVC=VACM/MAP	CA enhanced in healthy volunteers; results inconclusive on septic patients
Pierrakos et al. [20]	2014	38	Sepsis and septic shock	<24 hrs and >71 hrs	PI (PI = (PSV-EDV)/MFV) on 10-seconds recordings	PI was increased at >24 hrs and decreased/normalized at >72 hrs. Positive association between PI at day 1 and SAE during ICU stay
Fülesdi et al. [23]	2012	16	Sepsis and severe sepsis	<24 hrs	PI automatically calculated during 20-minutes recordings with acetazolamide test	PI was increased in the sepsis group compared to healthy controls during the whole recording
Schramm et al. [17]	2012	30	Sepsis or septic shock	1–4 days	Mx (ICM+ software)	CA impaired at day 1 and then improving; impaired CAR at day 1 associated with SAE at day 4
Szatmári et al. [24]	2010	34	Sepsis with altered mental status	–	PI automatically calculated during 20-minutes recordings with acetazolamide test	PI increased in the sepsis group compared to healthy controls
Taccone et al. [14]	2010	21	Septic shock	<72 hrs	CAI = ΔMAP%/ ΔCVR% where CVR = MAP/VMCA.	CA altered in 66% of patients. All patients with pCO_2 >40 had altered CA.
Pfister et al. [15]	2009	16	Sepsis and septic shock	<48 hrs	Mx (ICM+ software)	Altered CA in patients with SAE compared to septic patients without SAE
Thees et al. [29]	2007	10	Severe sepsis and abnormal EEG	>48 hrs	CCP extrapolated y regression analysis of arterial pressure/VMCA plots during modifications of pCO_2 through respiratory settings	Preserved CO_2R

Bowie et al. [30]	2003	12	Severe sepsis and septic shock	<24 hrs	CO_2R = VMCA at hypocapnia – VMCA at hypercapnia expressed as a % of the baseline VMCA per kPa change in $ETCO_2$	Inconstant CO_2R reactivity
Terborg et al. [31]	2001	8	Severe sepsis and septic shock	–	CO_2R = ΔVMCA% for 1% increase in $ETCO_2$	Decreased CO_2R
Smith et al. [12]	1998	15	Septic shock	12–48 hrs	Changes in blood flow in ICA was compared to changes in CI using 4 to 5 seconds recordings	Blood flow in Ica was positively related to cardiac index, implying loss of CA
Matta and Stow [13]	1996	10	Sepsis and septic shock	<24 hrs	IOR = ΔCVRe%/ΔMAP% where CVRe = MAP/VMCA and IOR. To determine CO_2R regression lines were constructed for paired pCO_2 /VMCA	Normal CA
Straver et al. [21]	1996	20	Septic shock	–	Lindegaard ratio	Mild vasospasm in septic patients

CAI Cerebral autoregulation index, *CA* Cerebral autoregulation, *CCP* Critical closing pressure, *CI* Cardiac index, *CO_2R* Carbon dioxide reactivity, *CVC* Cerebro-vascular conductance, *CVR* Cerebro-vascular resistance, *CVRe* Estimated cerebral vascular resistance, *EDV* End-diastolic velocity, *EEG* Electroencephalography, *$ETCO_2$* End-tidal CO_2, *hrs* hours, *MAP* Mean arterial pressure, *ICA* Internal carotid artery, *IOR* Index of autoregulation, *MFV* Mean velocity, *pCO_2* Carbon dioxide arterial partial pressure, *PI* Pulsatility index, *RoR* Rate of regulation, *PSV* Peak systolic velocity, *VMCA* Velocity in the middle cerebral artery, *TFA* Transfer function analysis

Whether cerebrovascular reactivity to carbon dioxide is preserved during sepsis is not clear, while an influence of carbon dioxide levels on cerebral autoregulation performance during sepsis cannot be excluded.

One last technical consideration about cerebral autoregulation assessment in septic patients is due. As explained in the dedicated chapter, cerebral autoregulation may be assessed by different methods. The mean flow index (Mxa) is an index of cerebral autoregulation previously used in septic and non-septic patients [34] and relies on prolonged TCD/TCCS monitoring, which allows CA assessment using spontaneous fluctuations in mean arterial pressure [35]. Use of spontaneous MAP fluctuations is a validated method to assess CA while limiting potentially stressful procedural and/or pharmacological interventions (e.g., pain during thigh-cuff test) and interfere with the homeostasis of CA itself. Such fluctuations have been observed in healthy subjects and patients affected by intracranial disease [36]. They occur spontaneously at very low frequency or as a physiologic response to variations in intra-thoracic pressures [37] and depend on intact neuronal pathways mainly located in the brain stem [38]. Unfortunately, the presence and amplitude of such spontaneous fluctuations in septic patients has not been determined yet.

51.4 Conclusion

Sepsis-associated brain dysfunction is one of the most common organ dysfunction during sepsis and is associated with poor outcome. Moreover, acute brain dysfunction is an important risk factor for long-term cognitive impairment among survivors. Brain hypoperfusion may contribute to the development of sepsis-associated brain dysfunction and transcranial Doppler (TCD/TCCS), although not able to quantify cerebral blood flow, can be helpful to detect changes in cerebrovascular hemodynamics, to assess cerebral autoregulation and to evaluate the status of cerebrovascular resistance. Further studies should evaluate therapeutic strategies aiming at optimizing cerebral perfusion using transcranial Doppler and the effects of such interventions on the occurrence and severity of sepsis-associated brain dysfunction.

Algorithm

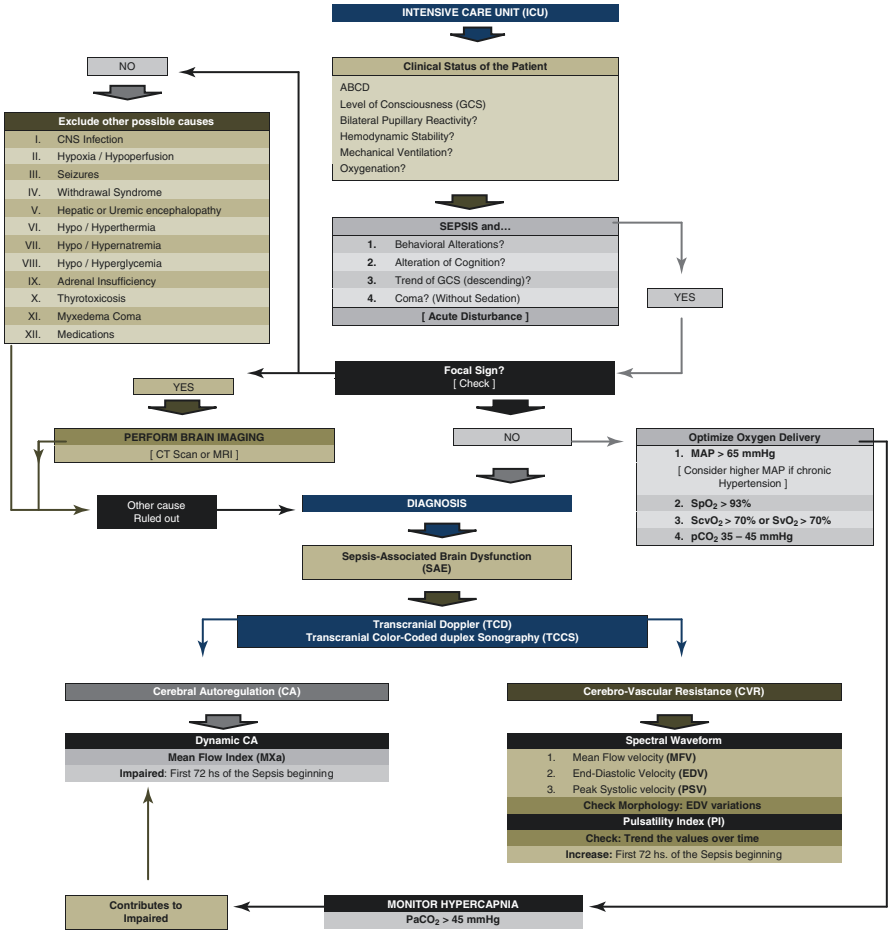

ABCD Airway-breathing-circulation-disability, *CNS* Central nervous system, *MAP* Mean arterial pressure, SpO_2 peripheral capillary Oxygen saturation, pCO_2 Carbon dioxide arterial partial pressure, $ScvO_2$ Central venous oxygen saturation, SvO_2 Mixed venous oxygen saturation

References

1. Papadopoulos MC, Davies DC, Moss RF, Tighe D, Bennett ED. Pathophysiology of septic encephalopathy: a review. Crit Care Med. 2000;28:3019–24.
2. Bolton CF, Young GB, Zochodne DW. The neurological complications of sepsis. Ann Neurol. 1993;33:94–100.
3. Eidelman LA. The spectrum of septic encephalopathy. JAMA. 1996;275:470.
4. Gofton TE, Young GB. Sepsis-associated encephalopathy. Nat Rev Neurol. 2012;8:557–66.

5. Annane D, Sharshar T. Cognitive decline after sepsis. Lancet Respir Med. 2015;3:61–9.
6. Sonneville R, Rauturier C, Klein IF, Wolff M. Understanding brain dysfunction in sepsis. Ann Intensive Care. 2013;3:1.
7. Sharshar T, Annane D, de la Grandmaison GL, Brouland JP, Hopkinson NS, Françoise G. The neuropathology of septic shock. Brain Pathol. 2004;14:21–33.
8. Bowton DL, Bertels NH, Prough DS, Stump DA. Cerebral blood flow is reduced in patients with sepsis syndrome. Crit Care Med. 1989;17:399–403.
9. Hosokawa K, Gaspard N, Su F, Oddo M, Vincent J-L, Taccone FS. Clinical neurophysiological assessment of sepsis-associated brain dysfunction: a systematic review. Crit Care. 2014;18:1–12.
10. Kim Y-S, Immink RV, Stok WJ, Karemaker JM, Secher NH, van Lieshout JJ. Dynamic cerebral autoregulatory capacity is affected early in Type 2 diabetes. Clin Sci (London, England: 1979). 2008;115:255–62.
11. Barry DI. Cerebral blood flow in hypertension. J Cardiovasc Pharmacol. 1985;7 Suppl 2:S94–8.
12. Smith SM, Padayachee S, Modaresi KB, Smithies MN, Bihari DJ. Cerebral blood flow is proportional to cardiac index in patients with septic shock. J Crit Care. 1998;13:104–9.
13. Matta BF, Stow PJ. Sepsis-induced vasoparalysis does not involve the cerebral vasculature: indirect evidence from autoregulation and carbon dioxide reactivity studies. Br J Anaesth. 1996;76:790–4.
14. Taccone FS, Castanares-Zapatero D, Peres-Bota D, Vincent J-L, Berre J, Melot C. Cerebral autoregulation is influenced by carbon dioxide levels in patients with septic shock. Neurocrit Care. 2010;12:35–42.
15. Pfister D, Siegemund M, Dell-kuster S, et al. Cerebral perfusion in sepsis-associated delirium. Crit Care. 2008;12:1–9.
16. Harper AM, Glass HI. Effect of alterations in the arterial carbon dioxide tension on the blood flow through the cerebral cortex at normal and low arterial blood pressures. J Neurol Neurosurg Psychiatry. 1965;28:449–52.
17. Schramm P, Klein KU, Falkenberg L, et al. Impaired cerebrovascular autoregulation in patients with severe sepsis and sepsis-associated delirium. Crit Care (London, England). 2012;16:R181.
18. de Azevedo DS, Salinet ASM, de Lima OM, Teixeira MJ, Bor-Seng-Shu E, de Carvalho Nogueira R. Cerebral hemodynamics in sepsis assessed by transcranial Doppler: a systematic review and meta-analysis. J Clin Monit Comput. 2016:1–10.
19. Naqvi J, Yap KH, Ahmad G, Ghosh J. Transcranial Doppler ultrasound: a review of the physical principles and major applications in critical care. J Vasc Med. 2013;2013.
20. Pierrakos C, Attou R, Decorte L, et al. Transcranial Doppler to assess sepsis-associated encephalopathy in critically ill patients. BMC Anesthesiol. 2014;14:45.
21. Straver JS, Keunen RW, Stam CJ, et al. Transcranial Doppler and systemic hemodynamic studies in septic shock. Neurol Res. 1996;18:313–8.
22. Pierrakos C, Antoine A, Velissaris D, et al. Transcranial doppler assessment of cerebral perfusion in critically ill septic patients: a pilot study. Ann Intensive Care. 2013;3:28.
23. Fülesdi B, Szatmári S, Antek C, et al. Cerebral vasoreactivity to acetazolamide is not impaired in patients with severe sepsis. J Crit Care. 2012;27:337–43.
24. Szatmári S, Végh T, Csomós A, et al. Impaired cerebrovascular reactivity in sepsis-associated encephalopathy studied by acetazolamide test. Crit Care. 2010;14:R50.
25. Kadoi Y, Saito S, Kawauchi C, Hinohara H, Kunimoto F. Comparative effects of propofol vs dexmedetomidine on cerebrovascular carbon dioxide reactivity in patients with septic shock. Br J Anaesth. 2008;100:224–9.
26. Meng L, Gelb AW. Regulation of cerebral autoregulation by carbon dioxide. Anesthesiology. 2015;122:196–205.
27. Häggendal E, Johansson B. Effects of arterial carbon dioxide tension and oxygen saturation on cerebral blood flow autoregulation in dogs. Acta Physiol Scand Suppl. 1965;258:27–53.

28. Ekström-Jodal B, Häggendal E, Linder LE, Nilsson NJ. Cerebral blood flow autoregulation at high arterial pressures and different levels of carbon dioxide tension in dogs. Eur Neurol. 1971;6:6–10.
29. Thees C, Kaiser M, Scholz M, et al. Cerebral haemodynamics and carbon dioxide reactivity during sepsis syndrome. Crit Care. 2007;11:R123.
30. Bowie RA, O'Connor PJ, Mahajan RP. Cerebrovascular reactivity to carbon dioxide in sepsis syndrome. Anaesthesia. 2003;58:261–5.
31. Terborg C, Schummer W, Albrecht M, Reinhart K, Weiller C, Röther J. Dysfunction of vasomotor reactivity in severe sepsis and septic shock. Intensive Care Med. 2001;27:1231–4.
32. Berg RMG, Plovsing RR. Effects of short-term mechanical hyperventilation on cerebral blood flow and dynamic cerebral autoregulation in critically ill patients with sepsis. Scand J Clin Lab Invest. 2016;76:226–33.
33. Berg RMG, Plovsing RR, Bailey DM, Holstein-Rathlou N-H, Møller K. Dynamic cerebral autoregulation to induced blood pressure changes in human experimental and clinical sepsis. Clin Physiol Funct Imaging. 2016;36(6):490–6.
34. Goodson CM, Rosenblatt K, Rivera-Lara L, Nyquist P, Hogue CW. Cerebral blood flow autoregulation in sepsis for the intensivist: why its monitoring may be the future of individualized care. J Intensive Care Med. 2018;33(2):63–73.
35. Czosnyka M, Smielewski P, Kirkpatrick P, Menon DK, Pickard JD. Monitoring of cerebral autoregulation in head-injured patients. Stroke. 1996;27:1829–34.
36. Lang EW, Diehl RR, Timmermann L, et al. Spontaneous oscillations of arterial blood pressure, cerebral and peripheral blood flow in healthy and comatose subjects. Neurol Res. 1999;21:665–9.
37. Zweifel C, Dias C, Smielewski P, Czosnyka M. Continuous time-domain monitoring of cerebral autoregulation in neurocritical care. Med Eng Phys. 2014;36:638–45.
38. Lang EW, Mudaliar Y, Lagopoulos J, et al. A review of cerebral autoregulation: assessment and measurements. In: Australasian Anaesthesia; 2005. p. 161–72.

Chapter 52
Infective Endocarditis and Stroke: Active Embolization Risk Monitoring by Transcranial Doppler (TCD/TCCS)

Carla Venegas, Leilani Johnson, and Aarti Sarwal

Key Points

1. Patients with infective endocarditis (IE) are at high risk of developing an embolic stroke, but up to 30% of patients may fail to meet the definite modified Duke criteria. Demonstration of embolic phenomena on transcranial Doppler (TCD) emboli monitoring, especially in echocardiographic negative cases, may qualify as minor criteria to assist in definitive diagnosis.
2. Presence of embolic phenomena on TCD may predict the risk of ischemic as well as hemorrhagic stroke in patients with IE. This may be useful for screening patients for risk of initial or recurrent stroke.
3. Presence or persistence of high-intensity transient signals (HITS) on TCD in a patient with IE may be a useful guide to tailor therapeutic interventions including antibiotic duration, prolonged antibiotic prophylaxis, early valvular surgery, or vacuum-assisted vegetation extraction.

C. Venegas
Critical Care Medicine, Mayo Clinic, Jacksonville, FL, USA

L. Johnson
Neurology, Wake Forest School of Medicine, Winston-Salem, NC, USA
e-mail: lljohnso@wakehealth.edu

A. Sarwal (✉)
Neurology, Wake Forest School of Medicine, Winston-Salem, NC, USA

Neurocritical Care Society (NCS), Chicago, IL, USA
e-mail: asarwal@wakehealth.edu

C. N. Rodríguez et al. (eds.), *Neurosonology in Critical Care*,
https://doi.org/10.1007/978-3-030-81419-9_52

52.1 Introduction

Patients with left-sided infective endocarditis (IE) may present with central nervous system (CNS) emboli manifesting as acute ischemic or hemorrhagic stroke in up to 55% of cases [1]. The diagnosis of underlying endocarditis rests on the modified Duke criteria that includes major and minor criteria, with one of the minor criteria being the presence of embolic events. Up to 14% of patients with definitive criteria and 41% of patients meeting possible IE diagnostic criteria may have no echocardiographic evidence of vegetation diverting the focus of stroke workup to alternate etiologies as well as influencing rigor of continuing antibiotic therapy [2].

Transcranial Doppler (TCD) is a noninvasive method for cerebral hemodynamic assessment using low frequency (2 MHz) pulsed sound to detect vasospasm, intracranial stenosis, or emboli in patients with acute cerebrovascular disease. TCD with emboli monitoring has shown potential in predicting the risk of stroke in carotid and intracranial disease [3]. Detection of high-intensity transient signals (HITS) as Doppler manifestations of emboli may be used as minor criteria to diagnose IE [3]. Emerging studies have suggested that emboli monitoring may be useful in predicting the risk of initial and recurrent stroke in patients with IE [2].

52.2 Infective Endocarditis: Epidemiology of Stroke

Over the past decade, the incidence of IE has increased due to a rise in the use of implantable cardiac devices, an increasing number of hospital-acquired cases, and opioid use [4]. Acute ischemic stroke may occur in 20–55% of patients with left-sided IE and may be silent in a majority of patients [1]. After initiation of appropriate antimicrobial therapy, frequency of new stroke rapidly declines, falling from 4.82 of 1000 patient-days in the first week to 1.71 of 1000 patient-days in the second week [5]. IE patients with coincidental or subsequent episode of cardioembolism continue to be at increased risk for both recurrent clinical and subclinical ischemic events [6].

While ischemic stroke is clinically apparent in approximately 40–56% of these patients, up to 82% of patients with IE may experience asymptomatic cerebral lesions as visualized on neuroimaging [7, 8]. A study based mainly on neuroimaging has shown that one-third of patients may have evidence of embolic phenomena change the diagnosis to “definite” or “possible” IE [7]. Other neurological complications like cerebral microbleeds, mycotic aneurysms, cerebritis, and abscesses have been proposed to be a sequelae of embolic complications [9, 10].

52.3 Infective Endocarditis: Pathophysiology of Stroke

Acute stroke occurs due to thromboembolic phenomenon associated with the vegetation characteristic of left-sided IE or thrombus associated with it. Right-sided IE may result in embolic phenomenon in the presence of a right-to-left shunt [4]. The distribution of such strokes is usually punctate across multiple arterial territories, but it may also cause large vessel occlusions. Risk factors like anticoagulant therapy, vegetation larger than 3 cm, *S. aureus* infection, and mitral valve involvement predict increased risk of neurological complications in patients with left-sided IE. Protective factors against further embolization include initiation of appropriate antimicrobial therapy as early as within the first week of treatment [5].

Other complications caused by IE include cerebral microhemorrhages, mycotic aneurysm, vasculitis/venulitis, and superficial siderosis. The embolized vegetation becomes established in the cerebral vessels and can cause endarteritis with resultant additional ischemic or hemorrhagic strokes [10].

52.4 Infective Endocarditis: Management of Stroke

The mainstay of definitive therapy in IE is appropriate antibiotics and preventing further embolization of the infectious source by eliminating the cardioembolic vegetation through valvular surgery [2]. For acute presentations of stroke, thrombolytic therapy decisions may be challenging in known IE due to high risk of intracerebral hemorrhage [2]. In the setting of IE, valvular surgical repair is indicated in the presence of heart failure or anatomical heart destruction, highly resistant microorganisms, relapsing prosthetic valve endocarditis, and persistent infection or recurrent embolic events despite appropriate antibiotic therapy [2]. Serial brain imaging may be needed in patients with left-sided IE in order to rule our stroke or intracranial bleeding, especially in settings of surgical intervention, general anesthesia, or perioperative systemic anticoagulation. Cerebral mycotic aneurysm may further delay surgical repair due to associated risk of intracranial hemorrhage with systemic anticoagulation [2].

Patients with ischemic stroke secondary to IE are also at higher risk for hemorrhagic transformation with reported worse prognosis; hence, the efficacy of antithrombotic agents in stroke related to IE is debatable. Aspirin does not appear to be beneficial and may have a tendency to increase risk of bleeding [4]. The evidence is insufficient regarding benefit and safety of recommending anticoagulation therapy, and indications may differ depending on whether IE occurs in native valve versus prosthetic valve. In cases that have a high risk of cardioembolic stroke due to another clinical indication like atrial fibrillation, pacemakers or presence of mechanical valve requiring anticoagulation therapy may be continued after screening for mycotic aneurysm with close neurological monitoring or serial brain imaging to

exclude hemorrhagic transformation. If a patient develops an intracerebral hemorrhage while anticoagulated, anticoagulation should be fully reversed according with the severity of the bleed and the anticoagulant agent in use.

52.5 Transcranial Doppler (TCD/TCCS): Active Embolization Monitoring Role

TCD is an emerging, noninvasive diagnostic application used to assess embolic phenomena, such as vasospasm or intracranial stenosis, in patients with acute cerebrovascular disease. TCD can detect embolic phenomena, which are indicated by HITS, critical for an early diagnosis of IE. TCD monitoring can play several roles in evaluation and management of IE including diagnosis in echocardiographic negative cases, predicting stroke risk and guiding escalation for definitive therapies in patients with persistent HITS [11, 12].

HITS represent solid or gaseous microemboli that can be detected on TCD. These solid or gaseous microemboli are characterized by unidirectional short-term intensity increases, at least 3 dB above the background intensity level, accompanied by an audible "whistling" sound (Fig. 52.1) [13]. Most of these

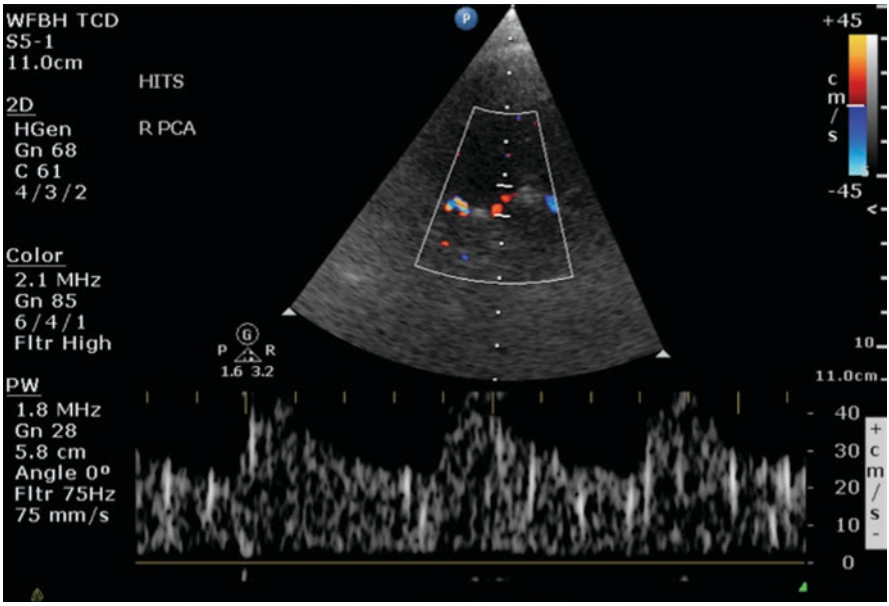

Fig. 52.1 An example of high-intensity transient signals (HITS) visualized on transcranial Doppler imaging of posterior cerebral artery. HITS are solid or gaseous microemboli within the blood flow and are represented by unidirectional short-term intensity increases

microembolic signals are clinically asymptomatic, but represent an increased risk of stroke. HITS have been shown to predict complications and recurrent stroke in carotid and intracranial thromboembolic disease, pointing toward needs for more aggressive therapy [3].

Many studies have shown a relationship between HITS and patients with cardioembolic source. A small but significant number of patients may not meet echocardiographic criteria for a definitive diagnosis of IE [2]. This may dissuade pursuance of IE treatments and initiate diagnostic workup for alternate etiologies. Presence of HITS on TCD may be the only evidence of septic brain embolization in these patients. TCD/TCCS can play several roles in evaluation and management and, may complement MRI in the diagnosis of apparent asymptomatic patients. Studies assessing correlation of HITS with occurrence of stroke have found the prevalence of HITS to be highest in patients with IE [3]. Results showed that neurological complications occurred in 83% of patients with HITS compared to 33% of patients without HITS ($P = 0.021$). The most common neurological complication was ischemic stroke, present in 69% of patients. Additionally, there was a trend toward higher in-hospital mortality in patients with HITS [11]. This suggests the role of inclusion of TCD with emboli monitoring on initial diagnostic testing in evaluation of IE where initial cardioembolic etiology may not be visualized via echocardiography [11, 12, 14].

Patients found with HITS on TCD/TCCS have 2.5 times higher incidence of stroke, compared with patients without HITS, also have been associated with higher mortality [3]. The presence of HITS in IE patients with no neurological manifestations may suggest the need for early initiation of therapy (e.g., antibiotics) in high clinical suspicion of IE, but no documentation of vegetation or evaluation for more aggressive therapies like valvular surgery or vacuum-assisted vegetation extraction. It may be pertinent to assess for alternate comorbidities like presence of atrial fibrillation and carotid stenosis that may also cause HITS on TCD. Further studies are needed to investigate the role of antithrombotic therapy in conjunction with antibiotic treatment to prevent further strokes in patients with HITS. Imaging to rule out mycotic aneurysms or angiographic evidence of endarteritis may be necessary if antithrombotics are initiated.

Persistent HITS despite antibiotic can play several roles in evaluation, and management therapy can also play a role in escalating urgency for earlier surgical interventions. In patients with left-sided IE, severe valve disease, and large vegetation, one randomized controlled trial showed a significantly reduced risk of death and embolic events in those who underwent early surgery versus conventional treatment [15]. Demonstration of persistent HITS, a known precursor to strokes, might sway the evidence needed to assess risk-benefit ratios of earlier surgical intervention. Emboli monitoring may also assess early triage of high-risk patients with high perioperative risk for open valvular surgery for procedures like vacuum-assisted vegetation extraction.

An increasing number of studies have suggested adding cerebral microbleeds, mycotic aneurysms, cerebritis, and abscesses to the spectrum of phenomenon included in septic embolization. Thus, making it worthwhile to investigate the correlation of these phenomena on angiographic and MRI with HITS can play several roles in evaluation and management visualized on TCD emboli monitoring. Since these phenomena correlate with risk of hemorrhagic stroke as well, embolic monitoring may provide a critical opportunity to assess risk of hemorrhagic stroke in these patients as well as the safety of prophylactic or therapeutic anticoagulation.

52.6 Conclusion

Neurologic complications are common in patients with left-sided IE and may be initially clinically silent in a significant number of patients. Despite advances in clinical diagnosis and surgical options, in-hospital mortality rates of patients who suffer neurological complications from IE continues to be high. Thus, any interventions targeted toward early diagnosis and detection of neurological complications can have an impact on outcomes. In the absence of a visualized cardioembolic source on echocardiography, demonstration of HITS on TCD monitoring may be considered a surrogate for cardioembolic phenomena and facilitate earlier definitive diagnosis of IE. The detection of HITS may also predict a higher risk for neurological complications and may guide decisions for appropriate and aggressive medical and surgical treatment.

Algorithm

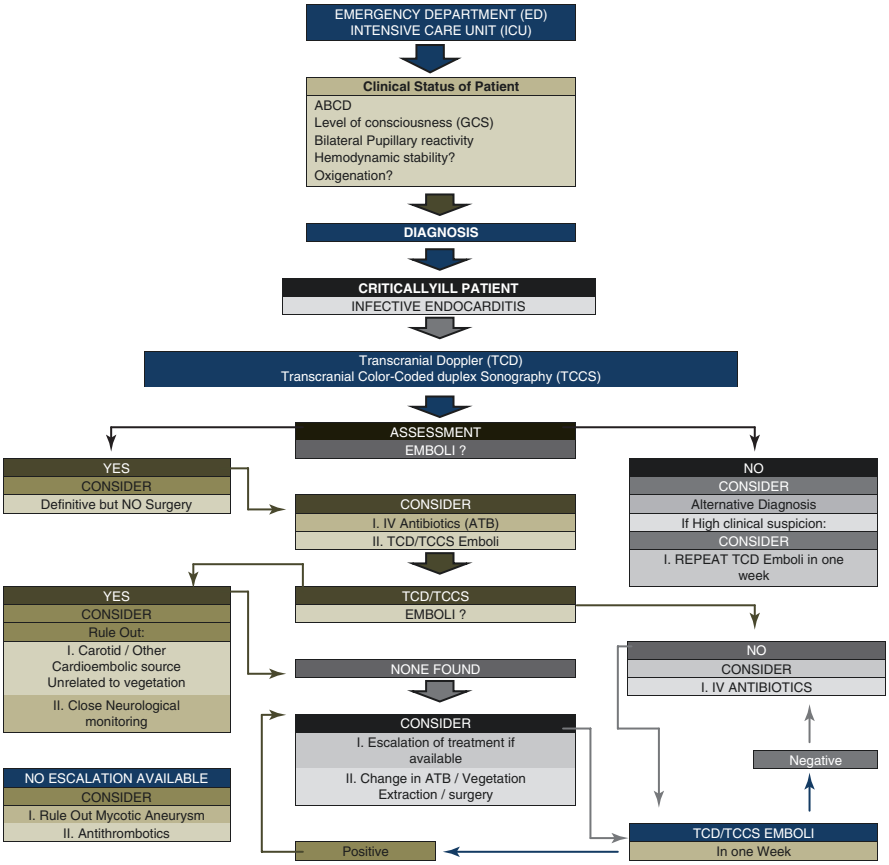

ABCD Arway-breathing-circulation-disability, *ATB* Antibiotics, *IV* Intravenous

References

1. García-Cabrera E, Fernández-Hidalgo N, Almirante B, Ivanova-Georgieva R, Noureddine M, Plata A, et al. Neurological complications of infective endocarditis: risk factors, outcome, and impact of cardiac surgery: a multicenter observational study. Circulation. 2013;127(23):2272–84.
2. Habib G, Lancellotti P, Antunes MJ, Bongiorni MG, Casalta JP, Del Zotti F, et al. 2015 ESC Guidelines for the management of infective endocarditis: The Task Force for the Management of Infective Endocarditis of the European Society of Cardiology (ESC). Endorsed by: European Association for Cardio-Thoracic Surgery (EACTS), the European Association of Nuclear Medicine (EANM). Eur Heart J. 2015;36(44):3075–128.

3. Huang G, Johnson LL, Peacock JE Jr, Tegeler C, Davis K, Sarwal A. Transcranial Doppler emboli monitoring for infective endocarditis. J Neuroimaging. 2020;30(4):486–92.
4. Cahill TJ, Baddour LM, Habib G, Hoen B, Salaun E, Pettersson GB, et al. Challenges in infective endocarditis. J Am Coll Cardiol. 2017;69(3):325–44.
5. Dickerman SA, Abrutyn E, Barsic B, Bouza E, Cecchi E, Moreno A, et al. The relationship between the initiation of antimicrobial therapy and the incidence of stroke in infective endocarditis: an analysis from the ICE Prospective Cohort Study (ICE-PCS). Am Heart J. 2007;154(6):1086–94.
6. Kargiotis O, Psychogios K, Safouris A, Magoufis G, Zervas PD, Stamboulis E, et al. The role of transcranial Doppler monitoring in patients with multi-territory acute embolic strokes: a review. J Neuroimaging. 2019;29(3):309–22.
7. Duval X, Iung B, Klein I, Brochet E, Thabut G, Arnoult F, et al. Effect of early cerebral magnetic resonance imaging on clinical decisions in infective endocarditis: a prospective study. Ann Intern Med. 2010;152(8):497–504, w175.
8. Thuny F, Avierinos J-F, Tribouilloy C, Giorgi R, Casalta J-P, Milandre L, et al. Impact of cerebrovascular complications on mortality and neurologic outcome during infective endocarditis: a prospective multicentre study. Eur Heart J. 2007;28(9):1155–61.
9. Bakshi R, Wright PD, Kinkel PR, Bates VE, Mechtler LL, Kamran S, et al. Cranial magnetic resonance imaging findings in bacterial endocarditis: the neuroimaging spectrum of septic brain embolization demonstrated in twelve patients. J Neuroimaging. 1999;9(2):78–84.
10. Malhotra A, Schindler J, Mac Grory B, Chu SY, Youn TS, Matouk C, et al. Cerebral microhemorrhages and meningeal siderosis in infective endocarditis. Cerebrovasc Dis. 2017;43(1–2):59–67.
11. Georgiadis D, Lindner A, Manz M, Sonntag M, Zunker P, Zerkowski HR, et al. Intracranial microembolic signals in 500 patients with potential cardiac or carotid embolic source and in normal controls. Stroke. 1997;28(6):1203–7.
12. Sliwka U, Job FP, Wissuwa D, Diehl RR, Flachskampf FA, Hanrath P, et al. Occurrence of transcranial Doppler high-intensity transient signals in patients with potential cardiac sources of embolism. A prospective study. Stroke. 1995;26(11):2067–70.
13. Sliwka U, Diehl RR, Meyer B, Schondube F, Noth J. Transcranial Doppler "High Intensity Transient Signals" in the acute phase and long-term follow-up of mechanical heart valve implantation. J Stroke Cerebrovasc Dis. 1995;5(3):139–46.
14. Dittrich R, Ringelstein EB. Occurrence and clinical impact of microembolic signals (MES) in patients with chronic cardiac diseases and atheroaortic plaques–a systematic review. Curr Vasc Pharmacol. 2008;6(4):329–34.
15. Kang DH, Kim YJ, Kim SH, Sun BJ, Kim DH, Yun SC, et al. Early surgery versus conventional treatment for infective endocarditis. N Engl J Med. 2012;366(26):2466–73.

Chapter 53
Neurosurgical Patient in ICU: Usefulness of Transcranial Doppler (TCD/TCCS) in Postoperative Monitoring

Camilo N. Rodríguez and Thomas Geeraerts

Key Points

1. The basic principle of neurosurgical patient management is to ensure adequate brain tissue perfusion, maintaining a sufficient blood flow to supply energy and oxygen to the brain parenchyma.
2. If neuroworsening occurs after a neurosurgical procedure, prompt recognition is essential because it may be the first indication of potential complications.
3. In many clinical scenarios during neurosurgical postoperative period, TCD/TCCS may have a transcendent role in diminished gap between neurological clinical examination and other investigations that may be invasive or require patient transport outside of the ICU.
4. Midline shift (MLS) monitoring is important for preventing neurological worsening and assess early neurosurgical intervention. Keep in mind that any amount of midline shift is considered abnormal.
5. Measurement of volume of Intracerebral Hematoma (ICH) is a very useful monitoring tool in the daily bedside following, and thus contribute to therapeutic decisions in real time interpreting the clinical trends.
6. The most used approach, to diagnose hydrocephalus by TCCS, is the measurement of the diameter of the third ventricle through the transtemporal window.
7. It is critical to interpret and integrate hemodynamic qualitative and quantitative trends (not only the absolute value) of the Spectral Doppler wave (blood flow velocity patterns) with the clinical context of the patient.

C. N. Rodríguez (✉)
Intensive Care Medicine, Hospital Nacional Prof. Dr. A. Posadas, University of Buenos Aires (UBA), Neurointensive Care Section - ESICM, Neurointensive Care Section - AMCI, Neurointensive Care Committee - FEPIMCTI, Member of ESNCH, Buenos Aires, Argentina
e-mail: camilo.rodriguez@nesccco.com

T. Geeraerts
Department of Anesthesiology and Intensive Care, University Hospital of Toulouse, Toulouse NeuroImaging Center (ToNIC), Inserm, Toulouse, France

C. N. Rodríguez et al. (eds.), *Neurosonology in Critical Care*,
https://doi.org/10.1007/978-3-030-81419-9_53

8. TCD/TCCS allows to calculate indexes of cerebral autoregulation (CA); mean velocity index (Mx); and systolic velocity index (Sx) in search of the optimal CPP during postoperative period.

53.1 Introduction

Neurosurgical patients frequently require admission to ICU, either for postoperative management or for treating complications (including traumatic brain injury (TBI), intracerebral spontaneous hematomas (ICH), ischemic strokes, subarachnoid hemorrhages (SAH), or elective surgeries). One of the primary goals of neurosurgeon, anesthesiologist, and intensive care physicians during perioperative care is to minimize complications, where they contribute substantially to increased morbidity and mortality in patients after neurosurgical procedures. Despite that the admission of all neurosurgical patients to the ICU was questioned by recent studies, admission to ICU has shown better clinical outcomes [1]. Hence, the immediate postoperative management of these patients is based on maintaining an optimal cerebral perfusion pressure (CPP) ensuring a correct cerebral oxygenation.

Numerous studies describe different rates of complications in the neurosurgical postoperative period. Rolston et al. [2] have reported the postoperative period complication rate of neurosurgical procedures is approximately 14%. While Manninen et al. [3] have reported the incidence of immediate postoperative period complications occurring from 3% up to 30% and Siqueira Pires et al. [4] describe a difference in the rate of complications, discriminating between immediate (45–52%) and late (71–79%) neurosurgical postoperative period. Therefore, it must be considered that postoperative complications are relatively high, where it seems that in non-elective neurosurgical procedures (emergency situation) intracranial hypertension and pupillary reactivity changes are the top of clinical manifestations [4]. The indication for ICU admission may be due to postoperative admission for an intervention, to an altered level of consciousness requiring clinical or multimodal monitoring, to requiring mechanical ventilation (MV) for airway protection, or to postsurgical medical complications [5].

Transcranial Doppler (TCD) and transcranial color-coded duplex sonography (TCCS), adopted as goal-directed at the bedside, are noninvasive patient bedside monitoring techniques which facilitate management and monitoring of acute neurological injury clinical evolution including immediate (<24 hrs) and/or late (>24 hrs) neurosurgical postoperative complications.

As Robba et al. highlight in the review of 2017 [8], the need of real-time patient bedside neurological diagnosis and monitoring of cerebrovascular evolution in the ICU convert TCD/TCCS on the stethoscope for the brain.

53.2 Neurosurgical Postoperative Period: General Management Goals

The basic principle of neurosurgical patient management is to ensure an optimal cerebral perfusion pressure (CPP), maintaining an adequate blood flow to supply energy and oxygen to the brain parenchyma. During postoperative neurosurgery in ICU, elevated ICP may be the final common pathway of space-occupying pathology. Prompt recognition and treatment is necessary to prevent neurologic deficit and/or death.

Postoperative neurosurgical patients are at risk of developing complications. Therefore, neurological and systemic monitoring is used to identify deteriorating patients for the purpose of treat the underlying cause and minimize the impact on final outcomes [9]. Then, we must consider monitoring systemic and neurological parameters [7] (Table 53.1).

1. Systemic parameters monitoring (Table 53.2)

An exhaustive clinical examination is crucial to detect minimal changes in the physiologic parameters that allow us to anticipate a clinical deterioration, as a cause or consequence of neuroworsening.

Table 53.1 Bed side postoperative neurosurgical patient assessment in ICU: Systemic and neurological examination integrative approach

Examination	
TCD/TCCS	1. Hemodynamic parameters
	CBFVs
	Spectral Doppler waveform analysis
	Hemodynamic indexes (PI, LR…)
	2. Brain parenchyma parameters
	Midline Shift (MLS)
	Size: 3th Ventricle/Lateral ventricles
	Space-occupying lesions
	3. Ocular color-coded sonography (OCCS)
	ONSD
	Pupillary light reflex (PLR)
Neurological	Glasgow coma scale/FOUR Scale
	Pupillary reactivity
	Motor deficit
	Sensitiv deficit
	Behavior
	Cranial nerves deficit
	Language
	Seizures
	MMM

(continued)

Table 53.1 (continued)

Systemic	Fast-Hug-Bid
	Respiratory pattern and rate
	SpO2/EtCO2
	Heart rate/ECG/ABP
	CO/EVLWI/SVV
	RASS/CPOT
	Electrolytes/Glucose/Hematology
POCUS	BLUE Protocol
	RUSH Protocol
	FALLS Protocol

TCD/TCCS Transcranial Doppler and transcranial color-coded duplex sonography, *POCUS* Point-of-care ultrasound, *RUSH* Rapid ultrasound in shock, *BLUE* Bedside lung ultrasound in emergency, *FALLS* Fluid administration limited by lung sonography

Table 53.2 Systemic parameters

Systemic parameters: Monitoring				
Clinical surveillance	Hemodynamics	Oxygenation	Lab. examination	Medications
FAST HUG BID [91]	ABP (invasive, noninvasive)	SpO_2	ABG	RASS [89] /BPS/ CPOT [88]
Respiratory rate	MAP	Pulmonary US [90]	Hematology	Drugs: CO/ABP
Respiratory pattern	CO / EVLWI / GEDVI / SVV [21]	Cardiac US [90]	Coagulation status	Steroids
Dyspnea	ECG	MV settings [12]	Glucose	ATB/Fluids
Heart rate	$EtCO_2$	O_2: FiO_2	$[Na^{++}]p$	Anticoagulation
Temperature	Cardiac US [90]			
Nausea/ vomiting	Pulmonary US [90]			
Blurred vision				
Shivering				
Headache				

FAST HUG Feeding, analgesia, sedation, thromboembolic prophylaxis, Head-of-bed elevation, stress ulcer prevention, and glucose control, *ABP* Arterial blood pressure, *MAP* Mean arterial pressure, *CO* Cardiac output, *SpO_2* Peripheral capillary oxygen saturation, *EKG* Electrocardiogram, *ELWI* Extrapulmonary lung water index, *GEDI* Global end-diastolic volume index, *SVV* Stroke volume variation, *MV* Mechanical ventilation, *RASS* Richmond agitation sedation scale, *BPS* Behavioral pain scale, *CPOT* Critical-care pain observation tool, *ATB* Antibiotics, *ABG* Arterial blood gases, *$[Na^{++}]p$* plasmatic sodium, *US* Ultrasound

1. FAST HUG BID [91]
   - Once a day
2. Central venous cannulation:
   - Internal Jugular Vein
   - Asymmetric drainage (right-side dominance (80%)) [10]
   - Main outflow of the cerebral blood flow (73%) [87]
3. Sedation-analgesia monitoring:
   1. Allow (if possible) "Neurological examination windows" [13]
   2. Neurological parameters monitoring (Table 53.3)

A detailed clinical examination will be performed evaluating the level of consciousness through the Glasgow Coma Scale (GCS), pupil size and reactivity (pupillometry (NPi)/ultrasound (US)), and/or the FOUR scale [14].

Table 53.3 Neurological parameters

Neurological parameters: Monitoring					
Clinical surveillance	Multimodal monitoring: Brain specific monitoring				
LoC (GCS/FOUR)	TCD/TCCS	Oxygenation	Other	ICP	Hemodynamics
Pupillary reactivity	CBFV	$P_{bt}O_2$	CMD	EVD	CPP
Cranial nerves deficit	Pulsatility Index	$SjvO_2$	EEG	ONSD	
Nystagmus	Resistance Index	NIRS	SSEPs	Pupillometry (NPi)	
Dysarthia/Aphasia	Lindegaard Index				
Photophobia	CA				
CAM-ICU	Midline Shift[a]				
Motor response	Lateral Ventricles[a]				
Sensitivity response	Third ventricle[a]				
Seizure activity	Intraaxial collection[a]				
Ocular fundus Nuchal Rigidity	Extraaxial collection[a]				

LoC Level of consciousness, *CBFV* Cerebral blood flow velocity, *CA* Cerebral autoregulation, $P_{bt}O_2$ Brain tissue oxygenation tension, $SjvO_2$ Jugular bulb venous oxygenation, *NIRS* Near-infrared spectroscopy, *CMD* Cerebral mycrodialysis, *EEG* Electroencephalogram, *ICP* Intracranial pressure, *EVD* External ventricular drain, *ONSD* Optic nerve sheath diameter, *CPP* cerebral perfusion pressure, *NPi* Neurologic pupil index, *SSEPs* Somatosensory evoked potentials

[a]They do not strictly belong to multimodal monitoring, but will be considered in the post-operative neurological complications assessment if high ICP is suspected

If abrupt and/or sustained changes are present in the neurological exploration (the evaluation of trends is important), the need to perform, if possible, an imaging (Gold standard), either a brain CT/MRI scan, in search of intracranial complications [15] should be considered.

Repeated clinical and neurological examination is probably the most important and cost-effective monitor in the postoperative setting [9]. Hence, the implementation of a neurosurgical Postoperative Checklist as a standard and reproducible tool for the ICU staff is recommended to reduce the rate of complications and improve patient safety and quality of postoperative care [16, 17].

53.3 Neurosurgical Postoperative Period: Neuromonitoring

It is common that craniotomy patients are admitted to an intensive care unit (ICU) for the first 12–24 hrs and transferred out of the ICU on the day after, a common situation in elective and noncomplicated neurosurgical procedure. In other clinical scenarios, patients have a high risk of neurological complications, where the neurological procedures are complicated or are performed during emergency situations, and the time-of-care in the ICU is much longer [18]. When a patient is admitted to ICU physicians should first stabilize all vital signs (ABC) and do a thorough physical examination to assess the general condition and severity of the patient. Sometimes the neurological examination is not possible or is not enough, and hence advance neurological monitoring is necessary.

53.3.1 Modality of Neuromonitoring

53.3.1.1 Multimodal Monitoring (MMM)

A variety of advanced techniques are used to monitor systemic and neurophysiological parameters to identify real-time changes and guide patient directed treatment before clinical deterioration in the ICU [19].

53.3.2 Focus of Postoperative Neuromonitoring: Real-Time Decisions

The goal of postoperative period of neurosurgery in the ICU is to provide continuity of patient care to detect and prevent neurological worsening (Table 53.4) while stabilizing systemic and neurological homeostasis, which requires a planning that begins in the preoperative period with a multidisciplinary team involved [20].

Table. 53.4 Neurosurgical postoperative complications: Potential causes of neurological deterioration

Neuroworsening: Possible causes of deterioration
1. Intracranial hypertension: High ICP
1.1 Cerebral edema
1.2 Expanding intracranial mass lesion
1.2.1 Intra or extra-axial hemorrhage (ICH, SDH, SAH, etc.)
1.2.2 Intra or extra-axial collection (abscess, empyema, etc.)
1.3 Acute hydrocephalus
1.4 Seizures
1.5 Hyperthermia
2. Acute ischemic stroke
3. CSF leak
4. Acid-base and electrolyte disturbances
4.1 $PaCO_2$ disturbance
4.2 Hyponatremia/Hypoglycemia
5. Systemic hypotension (Low SBP and Low MAP)
6. CNS infection
7. Hypoxemia/Tissue hypoxia
8. Seizures (consider NCSE)
9. Vasospasm (DCI)
10. Medication effect (sedation, analgesia, etc)
11. Tension pneumocephalus

ICP Intracranial pressure, *ICH* Intracerebral hemorrhage, *SDH* Subdural hematoma, *SAH* Subarachnoid hemorrhage, *CSF* Cerebral-spinal fluid, *SBP* Systolic blood pressure, *MAP* Mean arterial pressure, *CNS* Central nervous system, *NCSE* Non-convulsive status epilepticus, *DCI* Delayed cerebral ischemia

53.3.3 Goals of Postoperative Neuromonitoring: Guided-Therapeutic Decisions

Prevention, identification, monitoring, and directed treatment of secondary brain injury (brain edema and intracranial hypertension, cerebral hypoxia/ischemia, brain energy dysfunction, convulsive/nonconvulsive seizures) occur after the initial insult and surgical intervention (sometimes subclinical presentation) [21] and thus impact functional recovery and outcome of the patients.

If clinical and/or neurologic deterioration occurs, prompt recognition is crucial because it may be the first indication of a serious and potentially fatal complication [3, 4, 22]. Meticulous attention of these is essential as poor management can profoundly affect neurological outcome (Fig. 53.1).

In this chapter we will focus on the measurement and analysis of cerebral blood flow velocities (CBFV) through TCD/TCCS as monitoring of neurological deterioration secondary to postoperative complications and in those neurophysiological parameters related to this technique.

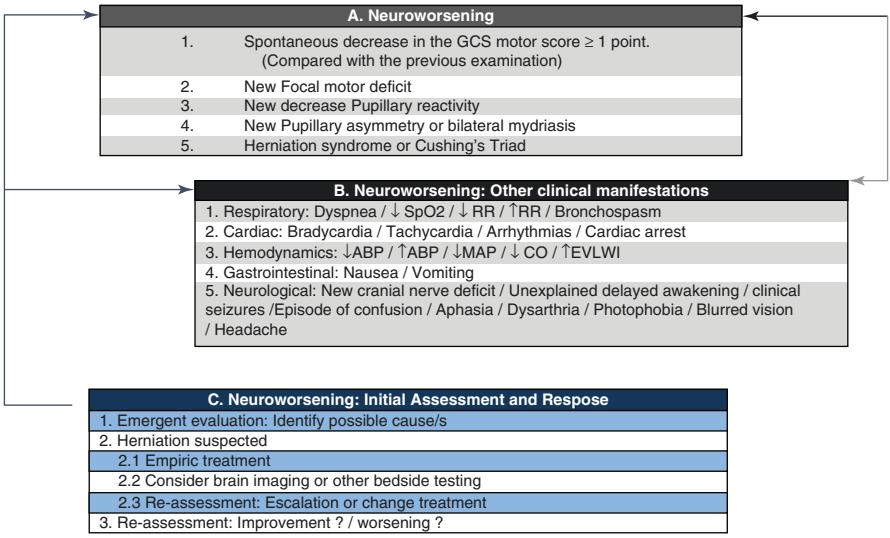

Fig. 53.1 Neuro-worsening: Monitoring the neurological deterioration [7, 11]. (A, B) Demonstrate the clinical presentation of neurologic deterioration; (C) Demonstrate the emergent assessment and response. ↓ Low, ↑ High, *ABP* Arterial blood pressure, *RR* Respiratory rate, *MAP* Mean arterial pressure, *CO* Cardiac output, *EVLWI* Extravascular lung water index

53.4 Transcranial Doppler (TCD/TCCS): Neurosurgical Postoperative Neurological Monitoring

In intensive care unit (ICU), TCD/TCCS has particular value in patients with an insufficient or incomplete neurologic examination. Hence, can help the clinician in making decisions and potential real-time clinical interventions. The assistance relevance of this goal-directed approach, 24 hours and 7 days a week, allows availability, repeatability, immediate interpretation, and quick clinical integration [23].

In patients who are unconscious or early postoperative recovering, there often exists a diagnostic gap between the yield of the bedside neurologic examination (even in conscious patients, sometimes it is not enough) and other investigations that may be invasive or require patient transport outside of the ICU. In many clinical scenarios during neurosurgical postoperative, TCD/TCCS may have a transcendent role in diminishing this gap. We should keep in mind that some proportion of the patients transported out of the ICU (complementary studies such as brain CT scan, CT angiography, or MRI) had secondary injuries post-transfer [24, 25].

In this chapter, we will focus on neurological monitoring of postoperative neurosurgical complications through TCD/CCTS at the bedside in the ICU. The rest of the neurological parameters will be briefly developed to complement the understanding of the interaction with TCD/TCCS. Transcranial perfusion monitoring provides early and real-time warning of impending brain ischemia and/or ICP changes, as a secondary brain insult clinical manifestation, and may be used to guide

management of an optimal cerebral perfusion pressure (CPP) and brain oxygenation [26]. During postoperative of neurosurgery in ICU, elevated ICP may be the final common result related with space-occupying brain lesions, hypoperfusion, and ischemia, hence we will focus on cerebral hemodynamic bedside monitoring through TCD/TCCS to estimate real-time ICP changes as a trigger of clinical manifestation of complications. However, the noninvasive assessment of the ICP should be integrated with systemic and neurological monitoring parameter to interpret and take the better point-of-care therapeutic decision (Fig. 53.1).

In certain clinical scenarios, transcranial Doppler (TCD/TCCS) may have a role in bridging this gap, and helping the bedside physician decide whether investigations such as brain CT scan, CT angiography (CTA), or MRI are necessary, or if intracranial pressure (ICP) monitoring or other surgical interventions are required.

The main objectives of neurological monitoring in ICU, during the postoperative period of neurosurgical procedures, through the TCD/TCCS are to ensure adequate cerebral perfusion pressure (CPP) and brain oxygenation. Therefore, to make therapeutic decisions integrating the different clinical and monitoring findings, TCD/TCCS has the following goals (Fig. 53.2):

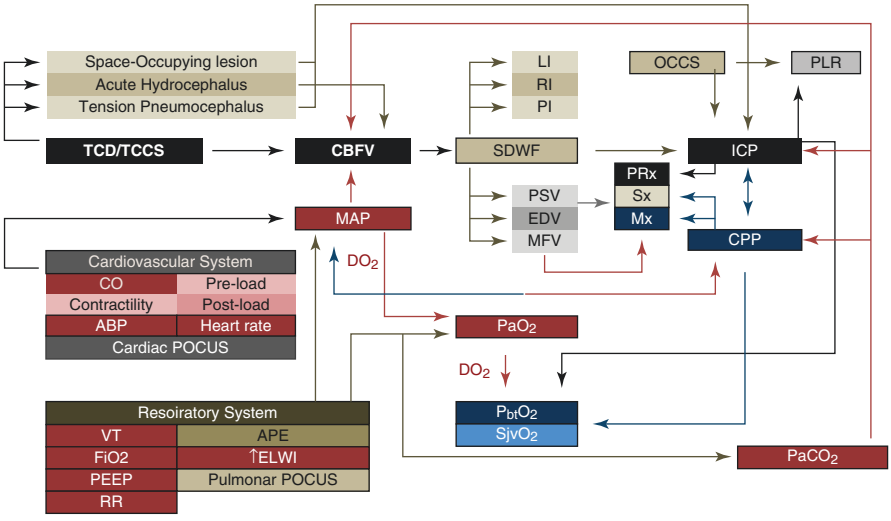

Fig. 53.2 Schema of multimodal monitoring oriented to TCD/TCCS: Usefulness of neurological monitoring by TCD/TCCS to estimate ICP changes and the influence from clinical and neurologic parameters during interpret a neuro-worsening during postoperative period. *CO* cardiac output, *ABP* Arterial blood pressure, *VT* Tidal volume, FiO_2 Inspired oxygen fraction, *PEEP* Positive end-expiratory pressure, *RR* Respiratory rate, *APE* Acute pulmonary edema, *ELWI* Extrapulmonar lung water index, *POCUS* Point-of-care ultrasound, *ICP* Intracranial pressure, *CPP* Cerebral perfusion pressure, *CBFV* Cerebral blood flow velocity, *PI* Pulsatility index, *RI* Resistance index, *LI* Lindegaard index, *MAP* Mean arterial pressure, $P_{bt}O_2$ Brain tissue oxygen tension, *OCCS* Ocular color-coded sonography, *PLR* Pupillary light reflex, *SDWF* Spectral Doppler wave form, DO_2 Delivery oxygen, *PSV* Peak systolic velocity, *EDV* End-distolic velocity, *MFV* Mean flow velocity, *Mx* Mean velocity index, *PRx* Pressure reactivity index

1. Estimation of intracranial pressure (ICP)
2. Estimation an optimal noninvasive CPP
3. Detection of cerebral ischemia

*53.4.1 Intracranial Pressure (ICP): Monitoring and Estimation***

Elevated ICP may be the final result of disequilibrium (in context of compensatory mechanisms depleted) between the volume of intracranial components in a rigid vault as skull (Monro-Kellie doctrine). The ICP depends, in other words, on arterial inflow volume and partial pressure of each component (Eq. 53.1) [27].

$$ICP = P_{Brain} + P_{Blood} + P_{CSF} \tag{53.1}$$

P_{Brain} = Pressure generated by brain parenchyma volume
P_{Blood} = Pressure generated by equilibrium between inflow and outflow volume
P_{CSF} = Pressure generated by equilibrium between production volume and reabsorption
** For more details, see Chap. 2.

53.4.1.1 Invasive Approach: Gold Standard Monitoring

There are a variety of device options to monitor ICP when indicated:

- *Intraventricular probe*
  - Allows: CSF diversion (EVD)
- *Intraparenchymal probe*
  - Allows: Regional oxygenation monitoring ($P_{bt}O_2$)
  - Allows: Cerebral microdialysis (CMD)

53.4.1.2 Invasive Approach: Interpretation

The ICP is more than a number. Morphological analysis of the ICP pulse waveform is crucial. Integrate the parameters.

- Absolute ICP value (NV*: 7–15 mmHg)
- ICP waveform analysis (assess brain compliance)
- Response to ICP therapy (asses brain compliance) [27]

*NV: Normal value

53.4.1.3 Noninvasive Approach: Estimation of ICP

Intracranial hypertension is a frequent and deleterious complication of brain injury (secondary to diffuse (cerebral edema) or focal changes (space-occupying lesions) of the parenchymal brain), where noninvasive ICP estimation would be helpful, especially in clinical situations where the risk benefit balance of invasive ICP monitoring is unclear or when ICP monitoring is not immediately available or is even contraindicated. There are two noninvasive methods to estimate noninvasive ICP at bedside [28]:

- *TCD* approach
  - Mode: Pulsed wave spectral Doppler
  - Mode: M-mode (PMD)
- *TCCS* approach
  - Mode: Pulsed spectral Doppler and color-coded
  - Mode: B-mode (grayscale)
- *OCCS* (Optical color-coded sonography)
  - Mode: B-mode (ONSD)
  - Mode: B-mode (PLR**)

  ** Pupillary light reflex

53.4.1.4 Noninvasive Approach: ICP Interpretation

Elevation of ICP may be the common denominator in the clinical evolution of neurological impairment during the neurosurgical postoperative period, in response to mechanical complication (occupying-effect lesion) and in response to cerebral or systemic hemodynamic involvement. Therefore, the estimation and monitoring of ICP is crucial.

Changes in the CBFV are observed with ICP increases as well as when cerebral perfusion pressure (CPP) decreases, usually manifested on TCD/TCCS as decreasing EDV and MFV, and thus an elevation of the pulsatility index (PI). The integration of clinical findings, B-mode images, blood flow velocities, and PI may help to differentiate patients with intracranial hypertension and/or cerebral hypoperfusion at bedside, providing ICU staff an individualize diagnostic and treatment approach [29] (Fig. 53.3). Bedside neurosonology is more practical for situations where information regarding serial temporal changes of intracranial parameters are required [30].

- *TCD/TCCS* (general settings)
  - *ICP: Noninvasive estimation*

    Hemodynamic manifestation

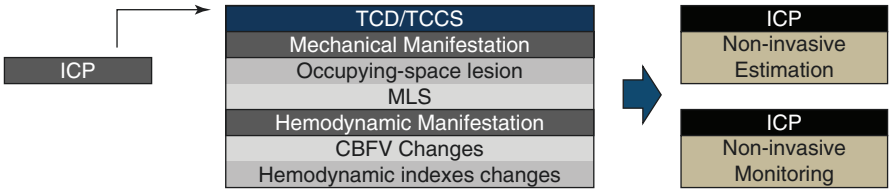

Fig. 53.3 TCD/TCCS approach: Non-invasive estimation and monitoring of the ICP through sonographic mechanical and hemodynamic manifestations. *MLS*: Midline shift, *CBFV* Cerebral blood flow velocity, *ICP* Intracranial pressure

- *Acoustic window:* Transtemporal (first step) and transforaminal
- *Modes*:

  TCD: PW Doppler flow and power-motion mode Doppler (PMD)
  TCCS: Color Doppler flow imaging and duplex

- *Depth of insonation:*

  TCCS: 14–16 cm [6, 23] (to recognize the hyperechoic contralateral skull)
  TCD: According to the insonated vessel

- *Arterial CBFV*:

  MCA / ACA / PCA / ICA / BA / VA
  Measurements (cm/s)

  - Spectral Doppler wave
  - PSV (peak systolic velocity)
  - MFV (mean flow velocity)
  - EDV (end-diastolic velocity)

In clinical practice, MCA is the most frequently insonated intracranial vessel, because it is easy delineated through the transtemporal acoustic window. It collects approximately 60–70% of the internal carotid artery (ICA) blood flow. Then its evaluation can be taken to represent almost total blood flow to one hemisphere.

Start the insonation protocol with the measurement of the CBFV, pulsatility index (PI), and analysis of the spectral waveform contour of the middle cerebral artery (MCA), through the transtemporal acoustic window. Consider, performing a sonographic assessment aimed at bedside clinical findings.

The CPP is maintained in both systole and diastole, as shown by the systolic and diastolic component of the TCD/TCCS spectral waveform, where the brain is being a low-resistance system. Therefore, the adequacy of cerebral perfusion can be assessed by evaluating the diastolic component (EDV) of the TCD/TCCS waveform and ensuring that its amplitude is approximately half of the peak systolic (PSV) amplitude [31].

- *Spectral Doppler morphology analysis*
  - TCCS: Angle correction(1)

    More exact measurement of flow velocity. (Positioning the cursor of the sample volume as parallel as possible to the flow lines)
  - TCD: No angle correction
- *Qualitative waveform changes* [32]
  - Shape of wave (Blood flow velocity pattern)
  - Differences in pulsatility amplitudes between PSV and EDV. (Characterized by a high diastolic component)
- *Quantitative waveform changes*
  - EDV measurement
  - MFV measurement
  - Hemodynamic indexes
- *Hemodynamic patterns:*
  1. Hypoperfusion: EDV < 20 cm/s, MFV < 30 cm/s and PI >1.4 [33, 34]
  2. Hyperemia: CBFV above normal reference values, LR < 3 (anterior circulation), and LR < 2 (posterior circulation) [35]
  3. High resistance: high pulsatility index and normal CBFV [35]
  4. Vasospasm: CBFV above normal reference values, LR > 3 (Anterior circulation), and LR > 2 (Posterior circulation) [35].
  5. Cerebral circulatory arrest (Assess flow trends): Reverberating flow, systolic spikes, and/or absence of flow [35]
- *Assess CBFV hemodynamic indexes*:
  - Gosling Pulsatility Index (PI)(2): Normal value: 0.8–1.2 [32]
  - Pourcelot Resistivity Index (RI)
  - Lindegaard ratio (LR): Anterior circulation (MFV_{MCA}/MFV_{ICA})

    Hyperemia (LR < 3)
    Vasospasm (LR > 3)
  - Lindegaard ratio (LR): Posterior circulation (MFV_{BA}/MFV_{VA}) [35]

    Hyperemia (LR < 2)
    Vasospasm (LR > 2)

The pulsatility of the waveform reflects the amount of resistance in the distal cerebral blood vessels. In addition to the isolated values, TCCS-derived hemodynamic parameters and PI could serve as a reliable guide for detecting intracranial hypertension in the ICU, provided that trends are sought rather than the use of

individual measurements [85, 86]. TCD/TCCS PI-derived ICP values should be considered as estimates, and an intracranial invasive monitor (gold standard) should be placed to confirm. However, estimation of ICP through PI measurement is crucial to make individualized therapeutic decisions at bedside in real-time, especially when the patient cannot access to invasive ICP monitoring (Eq. 53.2).

$$\mathrm{PI} = \left(\mathrm{PSV} - \mathrm{EDV}\right) / \mathrm{MFV} \tag{53.2}$$

PI is not affected by the angle of insonation. With the estimation of ICP, we can obtain the CPP value (CPP = ICP – MAP). The target value is to maintain a CPP > 60 mmHg; lower levels have been associated with worse outcome [36]. The PI can be converted to an estimate of ICP through the following formula [23] with a sensitivity of 89%, and specificity of 92%, where a PI of >2.13 would correlate to an ICP > 22 mmHg [37, 38] (Eq. 53.3).

$$\mathrm{ICP} = \left(10.93 \times \mathrm{PI}\right) - 1.28 \tag{53.3}$$

(1) More details, see Chap. 15.
(2) More details, see Chap. 21.

Please keep in mind that the prediction of ICP with PI is relatively large, as the 95% confidence interval of the prediction has been described to be ±4.2 mmHg [38].It is also critical the interpretation and integration of the hemodynamic qualitative and quantitative trends (not only the absolute value) of the Spectral Doppler wave (blood flow velocity patterns) with the clinical context of the patient [33].

Finally, as a home message, when interpreting the increase (or trend) of PI we must consider that it can increase in two important clinical circumstances: (1) rising of ICP (rising cerebrovascular changes resistance), and/or (2) changes in cerebral perfusion (CPP) (hemodynamic changes) [39]

- *Venous/sinuses CBFV* (1) [92]
  - dMCV(2)/Vein of Galen/Basal vein (Rosenthal)(3)
- Transtemporal acoustic window
  - Transverse sinus
- Transtemporal acoustic window
  - Straight sinus(4)
- Transtemporal acoustic window
- Transforaminal acoustic window
  - Measurements (cm/s)

    PSV
    EDV
    MFV

(3) 78–100% detection rate through transtemporal acoustic window [40].

(4) 48–83% detection rate through transtemporal acoustic window [40].

In general, venous TCCS is a less commonly used method to estimate, at the bedside, the increase in ICP. Elevation of ICP causes venous hemodynamic changes (changes in blood flow velocities and pulsatility), as this low-pressure system is the most sensitive to these ICP variations. Therefore, compression of this compartment behaves as a compensatory mechanism to intracranial pressure changes [41]. Therefore, venous blood may be pooled toward larger venous vessels (straight sinus and Basal vein) or straight sinus is compressed by rising ICP (with constant blood flow) causing an increase in venous flow velocity.

Intracranial venous flow velocities have a better correlation with cerebral blood flow (CBF) than arterial cerebral blood flow velocities, because they are less influenced by active diameter changes (vasoreactivity) and a thinner vascular wall (anatomy).

Intracranial venous Doppler signals show a low pulsatility. Therefore, the most accessible hemodynamic measurements are the peak systolic (PSV) and end-diastolic (EDV) blood flow velocities, where sometimes the measurement of mean flow velocity (MFV) is difficult in the context of poor spectral enveloped wave of venous pulsed Doppler. Due to this, the automatic calculation of the pulsatility index may be difficult [42].

Stolz et al. [42] applied venous TCCS to estimate of intracranial venous hemodynamic response in a clinical context of a midline dislocation due to postischemic brain edema. Basal vein (Rosenthal), vein of Galen, and straight sinus insonation showed that the change caused in the midline (hemispheric cerebral edema) determined a change in ICP. This increase in ICP was manifested through changes in venous blood flow velocities, especially in the vein of Galen (increase venous PSV_{VG}), basal vein (decrease venous PSV_{bv}), and straight sinus (increase venous PSV_{SRS}). Therefore, the decrease of venous PSV_{BV} may be due to compression of the basal veins in the midbrain cistern (anatomical layout) and/or possible cuffing of the vein of Galen joining the straight sinus. Other venous TCCS parameters (venous resistance index and systolic/diastolic ratio) may not be good estimators of ICP.

Schoser et al. [11] applied venous TCCS for estimation of ICP, finding a linear relationship between rising ICP and increasing straight sinus peak systolic velocity (PSV_{SRS}). Finally, Robba et al. [30] demonstrated that a method based on the combination of two correlated parameters (ONSD + PSV_{SRS}) perform promising value for the diagnosis of intracranial hypertension, and a strong correlation with invasive ICP monitoring (AUC: 0.93 for prediction of ICP above 20 mmHg). The best ONSD and PSV_{SRS} cut-off values for prediction of intracranial hypertension were 5.85 mm and 38.50 cm/s, respectively.

Despite of venous MFV measurements are difficult, Valdueza et al. [41] describe the usefulness of the venous TCCS in the monitoring of venous collateral pathways in superior sagittal sinus thrombosis (SSST). An increase in MFV was demonstrated in the basal vein (collateral venous pathway). This great venous capacitance (collateral) determines a favorable prognosis.

(1)More details, see Chaps. 7 and 28.

(2)Deep middle cerebral vein.

- *TCCS* (General settings)
  - *ICP: Noninvasive estimation*

    Parenchymal manifestation
  - *Acoustic window*: Transtemporal through diencephalic (Thalamic) plane to measure third ventricle
  - *Modes*:

    TCCS: B-mode

The harmonic tissue imaging (THI) generates images that contain fewer artifacts improving conventional grayscale images quality (B-mode) [43].

- *Depth of insonation:*
  - TCCS: 14–16 cm [6, 23] (To recognize the hyperechoic contralateral skull)
- *Brain midline shift* (MLS): >0.35–0.5 cm [44–46] (Fig. 53.4)

Diagnosis of midline shift is important both for preventing further secondary neurological injury by early neurosurgical intervention. Any amount of midline shift is considered abnormal, where poor neurological outcome can be associated with a clinically significant midline shift ≥0.5 cm [45]. MLS measurements on ultrasound have correlated well with CT findings, and have been predictive of poor outcome during clinical evolution of acute neurologic injury [46, 47].

One of the first and most straightforward clinical applications of TCCS is to identify the presence of MLS, where the technique includes third ventricle measurement with B-mode sonography through transtemporal acoustic window by diencephalic plane [48]. TCCS can be regarded as a reliable tool for monitoring the midline shift in patients with acute supratentorial brain lesions. Approximately, 5–20% of patients will have difficult views leading to uninterpretable TCCS images [37]. The MLS can be measured by the following formula (Eq. 53.4, Fig. 53.4) [23, 37].

$$\text{MLS} = \left(\text{distance A} - \text{distance B}\right) / 2 \tag{53.4}$$

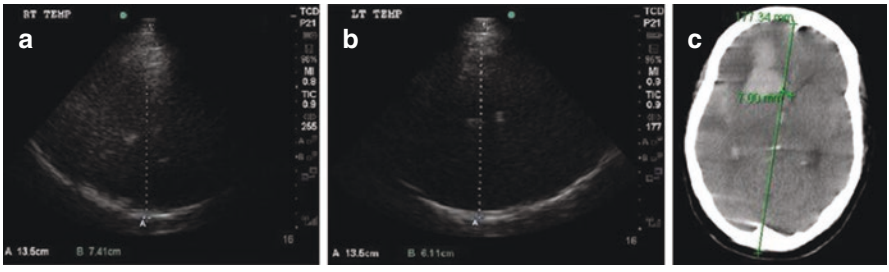

Fig. 53.4 Transcranial imaging for midline shift. (**a**) Insonation from right temporal bone to third ventricle, representing distance A (7.41 cm). (**b**) Insonation from left temporal bone to third ventricle, representing distance B (6.11 cm). (**c**) Follow-up CT scan post TCD which reveals midline shift to be 7 mm. (Courtesy: Lau VI, Arntfield RT. Crit Ultrasound J, 2017;9:21)

MLS (>0.4 cm) can be a good independent predictor of clinical outcome in patients with intracerebral hemorrhage [49]. With the increase of ICP and/or space-occupying lesions, MLS measured at the level of the third ventricle increases linearly with time as ICP increases. Therefore, periodic measurement of MLS (trends) is as important as the absolute value [42, 48]. Clinical utilization of TCD/TCCS for MLS should incorporate integration of measured CBFV and PI between right and left anterior circulation. The trends and asymmetry findings in CBFV and PI are the main indicators of potential midline shift. Consider that in some circumstances, such as bone defects (decompressive craniectomy) or temporal cephallohematomas, the use of the aforementioned method of midline shift measurement may be imprecise [50].

As a tip to take home, the presence of hydrocephalus of the third ventricle does not affect MLS measurement, as the measurements are done to the center of the third ventricle, not to its outer walls [51].

- *TCCS*
- General settings and considerations
- *Space-occupying lesion (mass effect)*
- Parenchymal manifestation (mechanical changes)

If there is evidence of clinical deterioration and signs of increased ICP (CBFV, spectral Doppler waveform, and hemodynamic indexes changes), it is prudent to investigate changes in the cerebral parenchyma with the goal of finding potentially treatable postoperative complications. However, the space-occupying lesion effect on the midline does not necessarily indicate raised ICP [46].

- *Acoustic window*: Transtemporal (axial planes and coronal plane)
- *Modes:*
- TCCS: B-mode
- *Depth of insonation*:
- TCCS: 14–16 cm (to recognize the hyperechoic contralateral skull)
- *Brain Midline Shift* (MLS): >0.35–0.50 cm [44, 46]
- Transtemporal acoustic window through diencephalic plane to measure third ventricle

During the neurosurgical postoperative period, clinical and/or neurological worsening may result from midline deviation secondary to space-occupying injury, resulting in an episode of elevated and sustained ICP. These lesions may present as: (1) Infra-axial collections (intracerebral hematoma, abscess, SAH), (2) extra-axial collections (subdural hematoma, empyema, hygromas, pneumo-encephalus), and (3) hemispheric cerebral edema (post-ischemic brain edema).

The abnormalities that can evidence through TCD/TCCS associated with elevated ICP secondary to space-occupying lesion, in the context of external compression of the cerebral vessels and brain parenchymal structure dislocation, are characteristic alterations in the spectral Doppler tracing (changes in the spectral Doppler waveform and CBFVs) and/or space-occupying effect (midline shift), respectively. Hence, we must keep in mind that any amount of midline shift is considered abnormal.

- Intracranial hemorrhage

- *Intracerebral hematoma (ICH)* (Fig. 53.5)
- *Subdural hematoma (SDH)* (Fig. 53.6)
- *Epidural hematoma (EDH)* (Fig. 53.7)
- Intracerebral hematoma (ICH) [52, 53]
  - Parenchymal manifestations: Mass effect and midline shift
- *Acoustic window*: Transtemporal
  - Axial planes (supratentorial)
  - Axial plane (infratentorial): Upper pons**
  - Coronal plane: (90° turn from mesencephalic plane with probe mark toward cephalic)

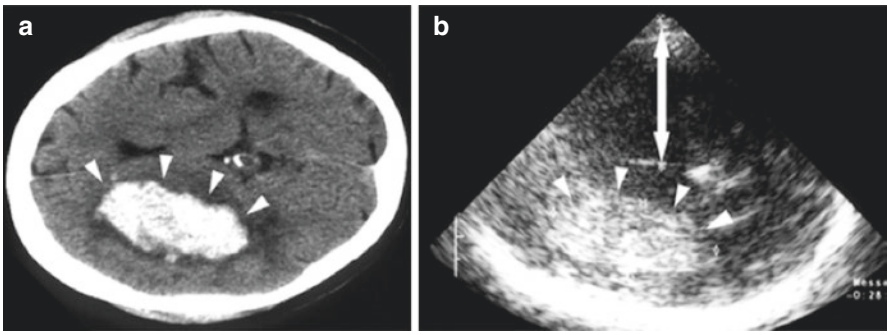

Fig. 53.5 TCCS axial brain scan at thalamus level showing a large intracerebral hematoma: (**a**) Computed tomography (CT) image corresponding to the TCCS image shown in (**b**). The triangles indicate the hematoma. (**b**) TCCS image showing the hyperechoic hematoma in the acute phase. (Courtesy: Uwe Walter. Transcranial sonography of the cerebral parenchyma: Update on clinically relevant applications, Perspectives in Medicine (2012))

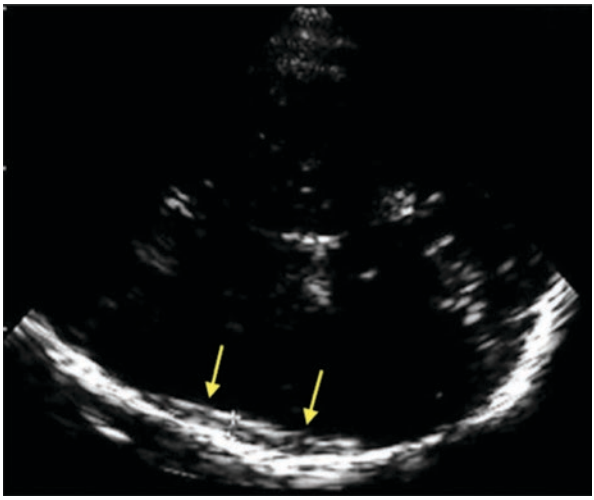

Fig. 53.6 The figure shows the highly echogenic skull opposite to the probe and a highly echogenic membrane clearly distinctable from the skull as sonographic correlate of the dural border of the arachnoid and as a sign of subdural space enlargement (yellow arrows). (Courtesy: Niesen WD, et al. Front Neurol 2018;9:374)

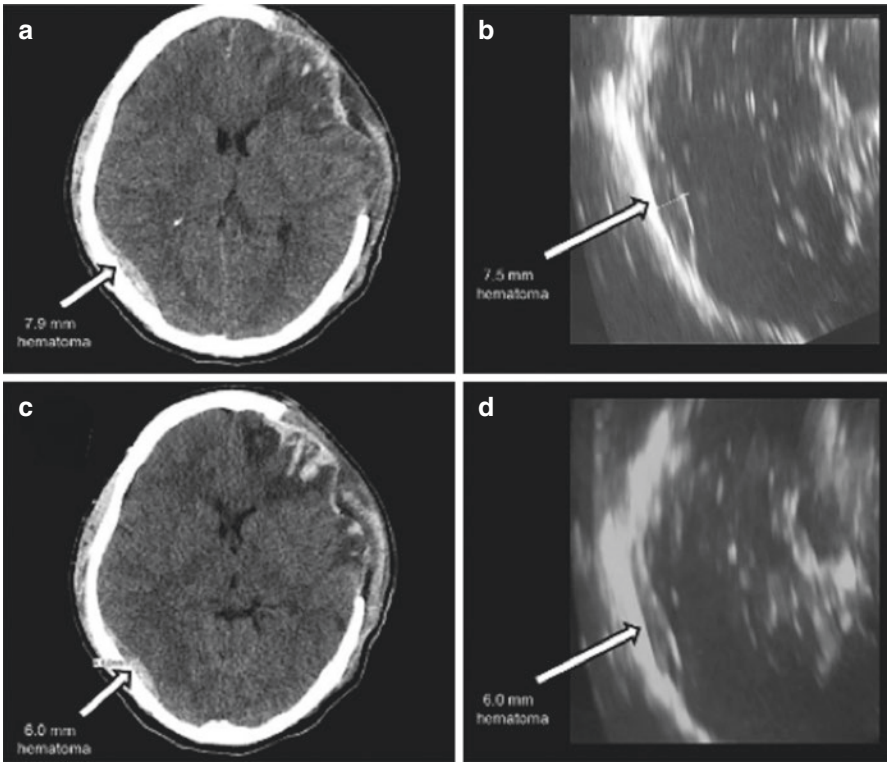

Fig. 53.7 Brain CT-scan and TCCS (B-mode): (**a**) CT-scan showing persistent diffuse edema and epidural hemorrhage, approximately 7.9 mm diameter; (**b**) TCCS showing an epidural hematoma with 7.5 mm diameter; (**c**) CT- scan showing an epidural hematoma with 6 mm diameter; (**d**) TCCS showing a 6 mm diameter epidural hematoma (EDH). (Courtesy: Lacerda FH, Rahhal H, Soares LJ, Ureña FDRM, Park M. Rev. Bras Ter Intensiva. 2017;29(2):259–260)

** May be useful for a cerebellar hematoma.

The calculation of hematoma volume by TCCS needs transtemporal axial view to measure anteroposterior (cm) and transverse dimensions (cm), and coronal view to measure height dimension (cm). Using the same equation as the one used for the estimation of intracerebral hematoma volume routinely through CT. The formula is: (Eq. 53.5) [53].

$$\mathrm{HV} = \left(\mathrm{A} \times \mathrm{B} \times \mathrm{C}\right) / 2 \tag{53.5}$$

HV: Hematoma volume.

There are three important determinants of the effectiveness of TCCS in the diagnosis and monitoring of hematomas: size, location, and sonographic appearance. Thus, parietal and frontal hematomas are the most difficult to locate [54]. Small hematoma may be detected if the location is within reach of ultrasound. Finally, the hematomas (intra- and extra-axial) are changing their sonographic appearance (grayscale) over the days. In an acute phase (<5 days) they are insonated as

hyperechogenic structures, while beyond 5 days hematoma becomes hypoechogenic with a peripheral reinforcement. Therefore, in acute stages the TCCS presents a better accuracy [53].

This technique is a very useful monitoring tool for intracranial hematomas [55]. It contributes to the interpretation of clinical trends and real-time therapeutic decision making at the bedside.

- *Subdural hematoma* (SDH) [52, 53, 56] (Fig. 53.6)
  - Parenchymal manifestations: Mass effect and midline shift
- *Acoustic window*: Transtemporal (through bilateral approach)
  - Axial planes (supratentorial)
- *Depth of insonation*:
  - TCCS: 14–16 cm

(To recognize the hyperechoic contralateral skull)

SDH can be visualized from the side opposite to the pathology confirmed by brain CT scan. Demonstration of a hyperechoic membrane distinguishable (detached hyperechoic line) from opposing skull is defined as the dural border of the arachnoid showing a subdural space enlargement (the echogenicity depends on the evolution time of the collection) on transcranial grayscale imaging (B-mode). SDH is quantized by measuring (mm or cm) the distance between the skull and the dural border of the arachnoid (hyperechogenic membrane).

- *Mode*:
  - *TCCS*: B-mode (tissue harmonic imaging (THI) could be an alternative)

Brain CT scan currently is the method of choice to monitor (Gold standard) [75]. Subdural hematoma (SDH) are potential life-threatening complications. If undetected and untreated, they may lead to progressive transtentorial herniation with loss of consciousness, pupillary dilation, and further neurologic deficits [50].

TCCS, through grayscale (B-mode), demonstrated sufficient resolution for diagnosis and monitoring the extent of hematoma with high correlation with brain CT scan, showing sensitivity of 90.9% and a specificity of 93.8% to predicting surgical evacuation (>13.2 mm), in particular, by measuring the distance between the skull and the dural border of the arachnoid, described as a hyperechoic membrane [56–58].

However, small cortical hemorrhages could not easily be distinguished [53, 56]. Mostly, in critically ill patients, serial brain CT scan is performed leading to patient transportation out of the ICU, which may place patients at risk. Thus, TCCS may represent a possible method for noninvasively monitoring early hematoma growth at the bedside of patients.

- *Epidural hematoma* (EDH) [59] (Fig. 53.7)
  - Parenchymal manifestations: Mass effect and midline shift

- *Acoustic window*: Transtemporal (through bilateral approach)
  - Axial planes (supratentorial)
- *Mode*:
  - TCCS: B-mode (tissue harmonic imaging (THI) could be an alternative)
- *Depth of insonation*:
  - TCCS: 14–16 cm

(To recognize the hyperechoic contralateral skull)

The EDH is a hyperechoic collection in the epidural space, which is located between the inner table of the skull and the dura mater. Epidural hematomas may be characterized clinically by a lucid interval, in which the patient is asymptomatic or not critically ill. However, once the epidural hematoma reaches a large enough size, it may exert significant mass effect. Therefore, patients with an epidural hematoma identified should be taken to the operating room for emergency evacuation. EDH is quantized by measuring the distance (mm or cm) between the skull and the dura mater by transcranial grayscale imaging (B-mode) (Fig. 53.7).

- *Extra-axial collections*
- *Tension pneumocephalus*
  - Parenchymal manifestation: Mass effect and herniation
- *Acoustic window:* Transtemporal and frontal(1)
- *Mode*:
  - TCCS: B-mode (tissue harmonic imaging (THI) could be an alternative)
- *Depth of insonation*: Bilateral approach
  - TCCS: 14–16 cm

(To recognize the hyperechoic contralateral skull)

(1) Is not described, but with adequate experience it could be useful.

Remember, an unexplained difficulty of accessing cerebral basal arteries in follow-up TCD/TCCS examinations may suggest pneumocephalus [60].

Patients operated in sitting or semi-sitting positions are at risk of developing pneumocephalus. Large amount of air trapping results in altered level of consciousness, seizures, and coma. Tension pneumocephalus requires urgent decompression [61].

Tension pneumocephalus: Entry of air through a dural defect and subsequent air expansion in the subdural, epidural, intraventricular, or intraparenchymal spaces (brain CT scan: Mount Fuji sign) [62]. A high degree of clinical suspicion is needed to recognize this life-threatening neurological emergency (brain parenchyma compression), which must be made by prompt resolution [63]. Sometimes, in the context of neurosurgical postoperative period, an unexplained difficulty of accessing cerebral basal arteries in follow-up TCD/TCCS examinations may suggest

pneumocephalus as a differential diagnosis [60]. The frontal acoustic window may be another window to search it, if suspected. TCD/TCCS is not a gold standard for diagnosis; however, it is a useful alternative tool in clinical situations where the clinical suspicion is high and moving out the patient from the ICU is not possible.

Keep in mind that the sudden eruption of an intracranial mass (Dynamics diseases) displaces brain tissue and can induce an increase in ICP, where all of these complications potentially increase mass effect, finally resulting in neurologic deterioration.

- *Hydrocephalus* [64] (Fig. 53.8)
  - Parenchymal manifestations: Herniation (mass effect)
- *Acoustic window*: Transtemporal through diencephalic plane to measure third ventricle [65, 66], and through ventricular plane to measure lateral ventricles (frontal horns) [51]

The advantages of TCCS, as a daily alternative monitoring tool (studies with larger number of patients should be performed), to follow hydrocephalus could encompass:

(a) Low cost
(b) Safe technique
(c) No radiation risk
(d) Daily monitoring
(e) Bedside imaging

It is difficult to determine a cut-off point (as a predictor) from which the patient may suffer neurological impairment. However, diameters of the third ventricle have been described in a normal population measured by TCCS (0.39 +/− 0.25 cm) [67]. Therefore, daily monitoring of changes in third ventricle diameter through TCCS appears to be of greater clinical utility than a single absolute value. The most used approach is the measurement of the diameter of the third ventricle through the transtemporal window, where TCCS and computed tomography findings correlated better for the third ventricle that right and left frontal horns of the lateral ventricles [65, 66]. Therefore, direct measurement of lateral ventricles is more difficult because of the angle with respect to the ultrasound probe. However, Kiphuth et al. [51] have described that the resulting estimated optimal cut-off value of 5.5 mm in ventricle width after clamping (CSF drainage system) has a high sensitivity (100%) and a high negative predictive value (100%). TCCS offers a valuable alternative to repeated CT scans in the ICU in patients with hydrocephalus.

- *TCD/TCCS*
- Space-occupying lesion *(mass effect)*
  - Hemodynamic manifestations
- *Acoustic window:* Transtemporal (first step) and transforaminal
- *Modes*:

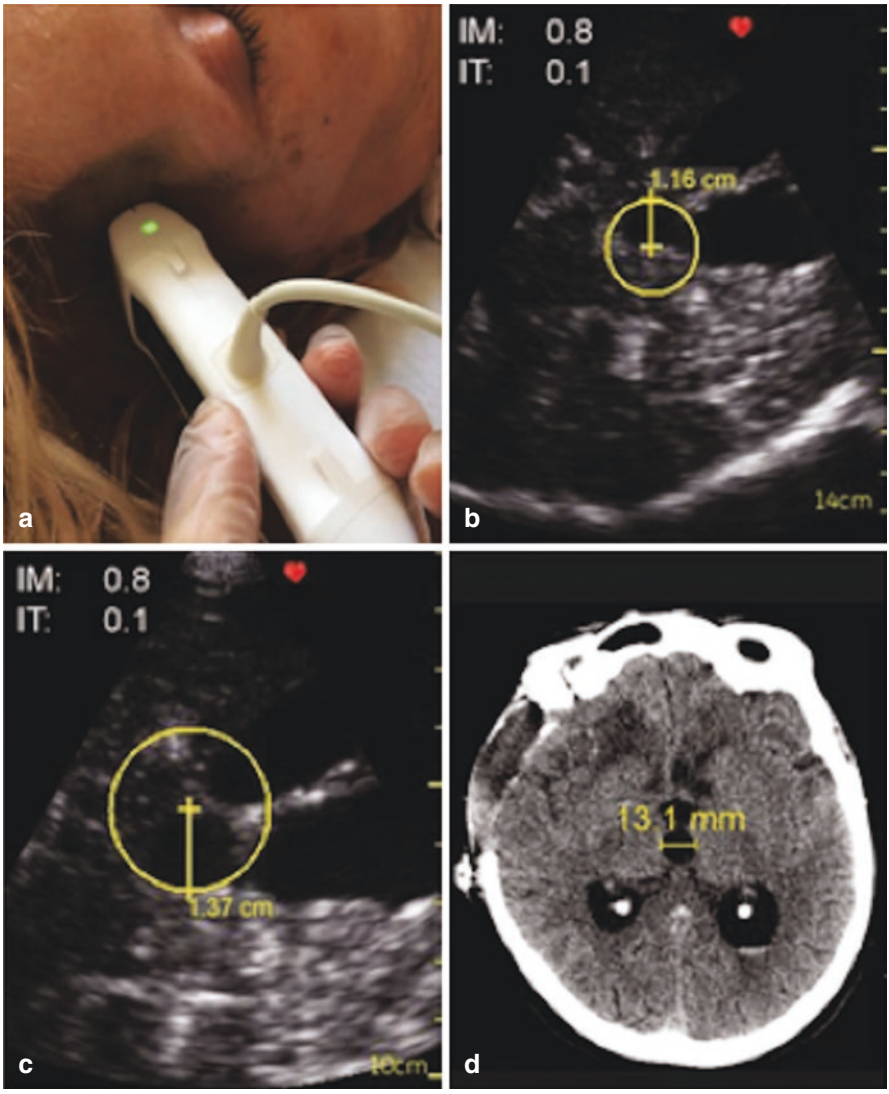

Fig. 53.8 (**a**) TCCS: Transtemporal acoustic window. (**b**) TCCS showed a measurement of the third ventricle at around 1.16 cm. (**c**) TCCS showed a dilated third ventricle measuring 1.37 cm. (**d**) CT scan showed a dilated third ventricle measuring 13.1 mm. (Courtesy: Najjar et al. Crit Ultrasound J (2017) 9:17)

  - TCD: PW Doppler flow and power-motion mode Doppler (PMD)
  - TCCS: Color Doppler flow imaging and PW Doppler

- *Depth of insonation:*
  - TCCS: 14–16 cm [6, 23]
  - TCD: According to the insonated vessel

(To recognize the hyperechoic contralateral skull)

Sudden eruption of an intracranial mass (Dynamics diseases) displaces brain tissue and can induce an increase in ICP, where all of these complications potentially increase mass effect, finally resulting in neurologic deterioration. Increased ICP and resulting decreased cerebral perfusion pressure (CPP) give rise to typical changes in the spectral Doppler waveform obtained by TCD/TCCS (decrease of EDV and an increase in the PI) [68].

- *Spectral Doppler morphology analysis*
  - Middle cerebral artery (MCA)
  - Bilateral insonation
  - Consider trends of measurements
- *Qualitative waveform changes* [32]
  - Shape of wave (blood flow velocity pattern)
  - Differences in pulsatility amplitudes between PSV and EDV (Characterized by a high diastolic component)
- *Quantitative waveform changes*
  - EDV measurement
  - MFV measurement
  - Hemodynamic indexes

    Pulsatility index
  - Hemodynamic patterns

The rise of ICP (mass effect) is represented, hemodynamically, by an initial increase in MCA velocity during systole and a corresponding decrease in velocity during diastole in both brain hemispheres. When ICP is severely elevated, diastolic flow may be absent or reversed. As PSV rises and EDV falls, PI (and therefore ICP) increases. Additionally, analysis of MCA spectral Doppler waveform always provides clinically useful information to address changes of the hemodynamic patterns in real-time [23, 68].

- *OCCS*: Ocular color-coded sonography**
- *ICP: Noninvasive estimation*
  - Parenchymal manifestations: ONSD and pupillary light reflex (PLR)
- *Acoustic window:* Bilateral approach
  - Transorbital: Through sagittal (M1) and transverse plane (M2)
- *Mode*:
  - OCCS: B-mode

Optic nerve sheath diameter (ONSD) ultrasound is a safe and noninvasive method of estimation ICP with high sensitivity and specificity (Eq. 53.6). However,

diagnostic criteria of rising ICP-based ultrasonographic ONSD have not been established. Hence, after many studies, the 4.8–5.2 mm cut-off [69, 70], as optimal ONSD for the detection of increasing ICP might be a good approach. These threshold values provide a qualitative indication of increased ICP. However, some studies have used ultrasonographic ONSD to quantitatively (mathematical formula) assess ICP values [71, 72] (Eq. 53.7). This technique might be helpful for screening patients with rise ICP, especially when invasive ICP monitoring is contraindicated.

$$\mathrm{ONSD} = \left(\mathrm{M1} + \mathrm{M2}\right) + \left(\mathrm{M1} + \mathrm{M2}\right) / 4 \tag{53.6}$$

$$\mathrm{ICP} = \left(77.36 \times \mathrm{ONSD}\right) - 111.92\left(\mathrm{mmH_2O}\right) \tag{53.7}$$

In the other hand, evaluation of pupillary shape and size as well as of the pupillary light reflex (PLR) is a standard diagnostic procedure in neurological examinations. Clinical examination of pupillary function typically includes estimation from both eyes of pupillary diameter and testing the PLR with a penlight.

B-mode ultrasound an objective method for the quantitative assessment of pupillary function, which is useful where eyelid retraction is impeded or a pupillometry device is unavailable [73]. Ultrasonography pupillary assessment has high Pearson's correlation coefficient (r) with infrared pupillometer ($r = 0.92$ right eye and $r = 0.96$ left eye) in critically ill patients [84] (Fig. 53.9).

** More details, see Chap. 38.

- *ICP:* Noninvasive estimation
  - Hemodynamic manifestations **: Ophthalmic artery (OA), central retinal artery (CRA), and carotid siphon
- *Acoustic window:* Bilateral approach
  - Transorbital: Through transverse plane

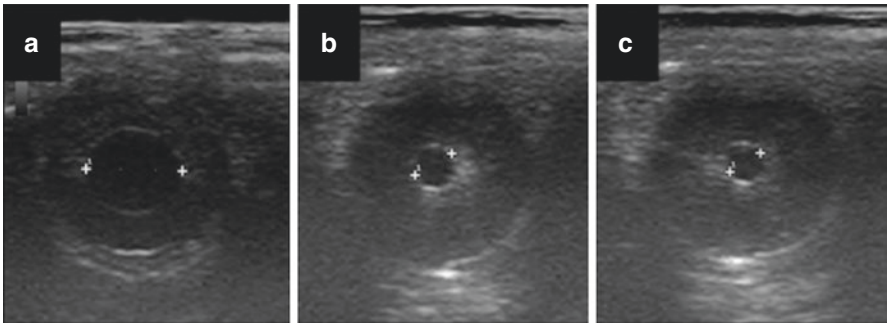

Fig. 53.9 Example of pupillary diameter [PD] assessment in the closed eye by B-mode ultrasound. (**a**) PD at rest under standard dimmed light conditions of the ultrasound study room. (**b**) PD during ipsilateral light stimulus [Lstim]. (**c**) PD during contralateral Lstim. Crosses represent the markers set by the examiner for measuring the PD. (Courtesy: Schmidt FA, et al. PLoS ONE 2017;12(12): e0189016)

- *Mode*:
  - OCCS: Color-coded duplex and PW Doppler
- *Measurement* (cm/s): PSV and MFV

Consider that the blood flow of the ophthalmic artery is orthograde (red color) with a characteristic flow pattern of high resistance (as a peripheral vessel). When assessing the orbital vessels, the operator must integrate the hemodynamic findings (changes in flow velocities, spectral Doppler waveform, and direction of flow) with the patient's clinical findings.

** More details, see Chap. 38.

53.4.2 Estimation of an Optimal Noninvasive CPP

Adequate cerebral blood flow (CBF) is dependent on three components [74]:

A. Cardiovascular (ABP)
B. Intracranial pressure components (ICP)
C. Cerebrovascular (CVR)

$$\mathrm{CBF} = \left(\mathrm{ABP} - \mathrm{ICP}\right) / \mathrm{CVR} \tag{53.8}$$

These three regulatory components of CBF can be monitored and corrected at the patient's bedside in the ICU. Focusing on noninvasive neurological monitoring through TCCS, we focus on noninvasive estimation of the ICP (intracranial content) and the cerebrovascular component (CVR, through active change in the diameter of the regulating vessels) to integrate the third cardiovascular component to select an optimal CPP goal [74].

A. Cardiovascular: Monitoring MAP
   (a) Technique: Artery line
B. Intracranial components: Estimation and monitoring ICP
   (a) TCD/TCCS: Hemodynamic manifestations
   (b) TCSS: Parenchymal manifestations
C. Cerebrovascular: Cerebral autoregulation assessment
   (a) TCD/TCCS: Dynamic approach (Mx and Sx) [75, 76]

Cerebral perfusion pressure (CPP) is the driving pressure gradient for blood flow to the brain, which depends on the changes in the values of the ICP and the MAP (Fig. 53.10).

$$\mathrm{CPP} = \mathrm{MAP} - \mathrm{ICP} \tag{53.9}$$

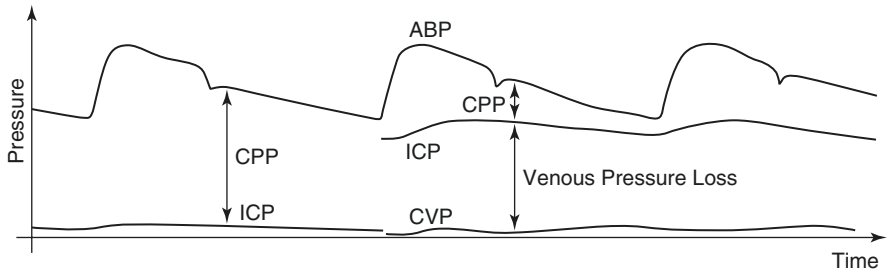

Fig. 53.10 Definition of cerebral perfusion pressure (CPP). ABP is the blood pressure in the aorta. In the left half of tracing the intracranial pressure (ICP) is normal. To the right the ICP is elevated. Then the difference between ICP and central venous pressure (CVP) is causing venous collapse and increased outflow resistance. (Courtesy: Aaslid R, Lindegaard KF, Cerebral hemodynamic. Springer nature 1986)

ICP: Intracranial pressure

MAP: Mean arterial pressure

CPP goal: ≥ 60 mmHg. This value should be adjusted (individualized) based on neuromonitoring data and the cerebral autoregulation status of the patient [92].

Noninvasive estimation of CPP by using TCD/TCCS may be of value in situations in which monitoring relative changes in CPP is required without invasive measurement of intracranial pressure.

Patients are at risk of increasing ICP and of sudden changes in ABP or CPP that may require immediate clinical intervention. Low CPP is associated with potential instances of cerebral ischemia; conversely, high CPP is associated with brain edema [77].

Focusing on the monitoring and noninvasive estimation of CPP through TCD/TCCS, Czosnyka et al. [78] describe the utility and good correlation (r = 0.73) between CPP (MAP minus invasive ICP) and eCPP (noninvasive) since the insonation of the MCA (Eq. 53.10).

$$\mathrm{eCPP} = \mathrm{MAP} \times \left(\mathrm{EDV} / \mathrm{MFV}\right) + 14 \tag{53.10}$$

eCPP: Estimated CPP

EDV: End-diastolic velocity

MFV: Mean flow velocity

Robotic TCD recordings have a more continuous CPP estimation, though further research is required [79]. Combining TCD/TCCS measured CPP with noninvasive TCD cerebrovascular reactivity indices, such as $\mathrm{Sxa}^{(1)}$ or $\mathrm{Mxa}^{(2)}$ (acquired using TCD/TCCS in conjunction with continuous MAP), one could in theory obtain optimal CPP through an entirely noninvasive means.

1. Systolic flow index based on MAP (correlation between PSV and MAP)
2. Mean flow index based on MAP (correlation between MFV and MAP)

It is important to keep in mind that preserved cerebral autoregulation (CA) is an important tool when selecting optimal CPP. Therefore, brain perfusion becomes dependent on CPP when autoregulatory mechanisms that maintain cerebral blood flow fail, where it is important to know the "cerebral hemodynamic moment" to position the patient outside of hypo- or hyperperfusion clinical situation to optimizing CPP. It can be useful to calculate two indexes of autoregulation with stronger association between it, called mean flow index (Mx) and systolic flow index (Sx) [8, 79], where zero or negative correlation indicates preserved CA.**

** More details, see Chap. 16.

53.4.3 Detection of Cerebral Ischemia

The pathophysiology of brain injury can be thought of in terms of primary and secondary events. Secondary insults consist of a wide range of ischemic, metabolic, and inflammatory insults. The etiology of these secondary events is diverse and can include systemic and intracranial phenomena such as hypotension, hypoxemia, intracranial hypertension, or edema. The goal of neurological monitoring is to detect potentially harmful pathophysiologic events.

Ischemia is defined as a decrease in blood flow below the level necessary to sustain normal cell structure and function. Ischemia can be global (intracranial hypertension) or focal as in occlusion or narrowing of an intracranial vessel (embolism, thrombus, or vasospasm).

We will focus the monitoring and manifestation of cerebral ischemia, through TCD/TCCS in two pathologies that can manifest complications during the postoperative period in the ICU, after its neurosurgical treatment.

53.4.3.1 Aneurysmal Subarachnoid Hemorrhage (SAH)

Patient in poor neurologic condition (Modified Fisher scale, Hunt & Hess scale and/or WFNS scale) frequently develop intracranial hypertension and vasospasm with delayed neurologic deficit and/or cerebral infarction. However, other causes of neurological worsening should be excluded.

Arterial vasospasm (angiographic evidence and/or sonographic suspicion) is considered the most common cause of ischemia and clinical deterioration; specially delayed cerebral ischemia (DCI) (30%), although pathophysiology leading remains unclear [80], sometimes is reversible but may also progress to cerebral infarction [81]. The excellent sensitivity (90%) and high negative predictive value (92%) makes TCD/TCCS an ideal screening tool for detecting vasospasm in SAH [31].

The hemodynamic manifestation of TCD/TCCS is: high MFV (cm/s), which may correspond to hyperemia or vasospasm.

- *TCD/TCCS*:**
  - *B-mode*: Color-coded duplex and PW Doppler
  - *Acoustic window:* Transtemporal, submandibular, and transforaminal
  - *Arterial CBFV*: Vasospasm [82]

    MCA
    ICA
    Measurements (anterior circulation)

    - MFV_{MCA}*
      - Mild: 120–159 cm/s
      - Moderate: 160–199 cm/s
      - Severe: ≥200 cm/s

Once a spectral Doppler tracing has been obtained by tracing the envelope of the spectrum corresponding to one cardiac cycle (VTI: velocity time integral). The ultrasound machine will then generate a series of values, the most important of which is the MFV (TAV: time-average velocity or TAMAX: time-average maximum velocity). Progressive or persistent increase in blood flow velocity in a given vessel suggests focal vasospasm [23, 54] and may be associated with DCI [80].

- *Lindegaard ratio* (LR)
  - LR: <3 (suggestive of hyperemia)
  - LR: 3–6 (mild to moderate vasospasm)
  - LR: > 6 (severe vasospasm)

  * MFV of middle cerebral artery

- Measurements (posterior circulation)
  - *BA* (MFV > 95 cm/s)(1)
  - *VA* (Right or left)
  - *Sviri ratio* (SR) [83, 93] (MFV_{BA} / MFV_{VA})(2)

    SR: 2 (Hyperemia)
    SR: 2–2.49 (possible vasospasm)
    SR: 2.5–2.99 (moderate vasospasm)
    SR: ≥ 3 (severe vasospasm)

1. Specificity up to 100%
2. Accuracy is lower to identify vasospasm in the BA [83]

Digital subtraction angiography (DSA) is traditional gold standard imagings for detecting of vasospasm.

** More details, see Chaps. 22 and 23.

53.4.3.2 Acute Ischemic Stroke (AIS)

Acute ischemic stroke results in focal neurological deficit, referable to a particular cerebral arterial territory, due to steno-occlusive extracranial and/or intracranial arterial disease. Early diagnosis is highly relevant for acute treatment strategies. Therefore, in clinical context of new neurological deficit, we focus on a key question to begin the assessment:

1. Suspecting an AIS: extracranial and/or intracranial stenosis/occlusion disease?
    1. Rapid detection of arterial steno-occlusive disease:

- Technique: Fast-Track insonation protocol
- *Cervical duplex ultrasound (CDU)*
  - Blood flow parameters
  - Anatomic features
- *TCD/TCCS*
  - Real-time flow findings
  - Parenchymal ultrasound
- Protocol: [94, 95]

A. *Anterior circulation*: Transtemporal window/transorbital window/submandibular window.

Step1: TCD/TCCS
1. Insonation MCA (M1) in non-affected side. Compare with the affected side.
2. Insonation MCA (M1) in affected side. Insonation of ACA and PCA (flow diversion?). Compare waveform shape and systolic acceleration.
3. Insonation OA: Measure flow direction and PI. Insonation of ICA-siphon.
4. If motor or sensory deficit: Evaluate BA and VA (V4).

Step 2: CDU/vertebral duplex
1. Insonation affected side: B-mode, color, or power mode. Identify CCA
2. ICA: document if it has lesion (B-mode) and disturbance on flow
3. PW-Doppler of CCA, ICA, and ECA (spectral velocity)
4. Affected side: If motor or sensory deficit, insonate the cervical portion of the VA by B-mode and PW-Doppler
5. Non-affected side: Insonation of cervical arteries

B. *Posterior circulation*: Transtemporal window/transforaminal window/submandibular window

Step1: TCD/TCCS
1. CBFV: BA and VA

2. If abnormal CBFV values: Insonate VA (V4) on the affected and non-affected sides to compare
3. Bilateral insonation of PCA: Possible collateral flow through PcomA
4. Bilateral insonate of ACA and MCA: Assess possible compensatory velocity increase as indirect sign of BA occlusion

Step 2: CDU/vertebral duplex

1. Insonation affected side: B-mode. Identify CCA
2. Bilateral insonation of VA: Spectral Doppler
3. Bilateral duplex insonation of: CCA, ICA, and ECA

Note that to reduce the protocol-time of insonation, we may use IV echo-contrast (1–2 ml) [94]. This fast-track insonation protocol is a great complementary monitoring tool, especially in patients with contraindications to angiographic methods and in clinically less affected patients.

53.4.3.3 Traumatic Brain Injury (TBI)[(1)]

Secondary cerebral ischemia is very common after TBI, where impaired CA and elevated ICP can contribute with poor outcome.

The goals of TCD/TCCS, in these patients are monitoring and/or estimation of (1) ICP, (2) CPP, and (3) posttraumatic cerebral artery vasospasm. We focus on the last of these.

- TCD/TCCS
- *B-mode*: Color-coded duplex and PW Doppler
- *Acoustic window:* Transtemporal
- *Arterial CBFV*: Oligoemia
  - MCA: Decrease of MFV(cm/s) and increase PI
- *Arterial CBFV:* Vasospasm/hyperemia
  - MCA
  - ICA
  - Measurements (anterior circulation)
- MFV_{MCA}*
  - Mild: 120–159 cm/s
  - Moderate: 160–199 cm/s
  - Severe: ≥200 cm/s
- *Lindegaard ratio* (LR)
  - LR: <3 (suggestive of hyperemia)

  - LR: 3–6 (mild to moderate vasospasm)
  - LR: >6 (severe vasospasm)
- *Gosling Pulsatility Index*
  - MCA (spectral Doppler waveform)

* MFV of middle cerebral artery

Posttraumatic cerebral artery vasospasm may occur up to 50% of patients typically 12 hours to 5 days after primary injury. TCD/TCCS might be helpful for screening patients with rise ICP and/or potential oligoemic or hyperemic CBFV patterns, specially which invasive ICP monitoring is contraindicated or is not possible.

The hemodynamic changes and considerations in clinical context of decompressive craniectomy are reviewed in Chap. 55.

(1) More details, see Chap. 41.

53.5 Conclusion

1. The neurosurgical patient requires a comprehensive postoperative management with dynamic monitoring (real time) depending on their clinical situation.
2. During postoperative period, a complete and frequent neurological exploration must be performed to detect early appearance of some type of deficits in the ICU.
3. In sedated patients where a complete clinical examination is not possible, multimodal monitoring will be considered to help us optimize management and detect the appearance of complications.
4. The need of real-time, especially in certain clinical scenarios where the transport of the patient and/or invasive monitoring is not possible, patient bedside neurological diagnosis and monitoring of cerebrovascular evolution in the ICU convert TCD/TCCS on the stethoscope for the brain and make individual therapeutic decisions immediately.

Algorithm

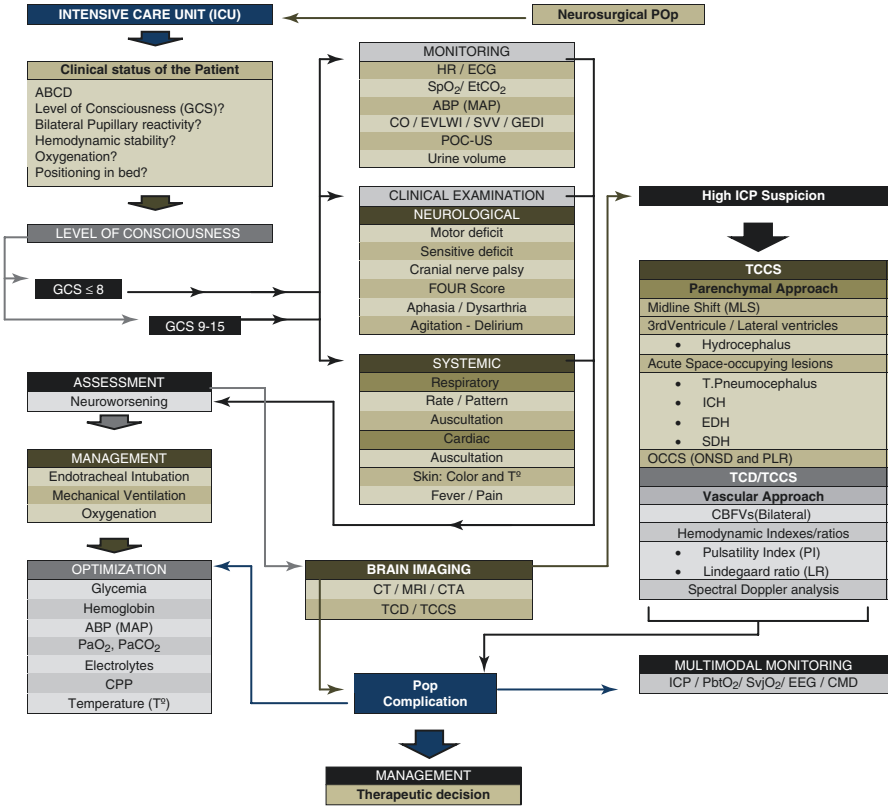

ABCD Airway-breathing-circulation-disability, *GCS* Glasgow coma scale, *Pop* Post-operative, *ICP* Intracranial pressure, *TCD* Transcranial Doppler, *TCCS* Trabscranial color-coded duplex sonography, *CPP* Cerebral perfusion pressure, *ABP* Arterial blood pressure, *MAP* Mean arterial pressure, *CBFVs* Cerebral blood flow velocites, *HR* Heart rate, *ECG* Electrocardiogram, *SpO_2* Peripheral capillary oxygen saturation, *$EtCO_2$* End-tidal CO_2, *CO* Cardiac output, *POC-US* Point-of-cara ultrasound, *OCCS* Ocular color-coded sonography, *EVLWI* Extravascular lung water index, *ICH* Intracerebral hematoma, *EDH* Extradural hematoma, *SDH* Subdural hematoma, *GEDI* Global end-diastolic index, *SVV* Stroke volume variation, *CMD* Cerebral microdialysis, *CTA* Computed tomography angiography, *PRL* Pupillary light index

References

1. Jeong JH, Bang J, Jeong W, Yum K, Chang J, Hong JH, Lee K, Han MK. A dedicated neurological intensive care unit offers improved outcomes for patients with brain and spine injuries. J Intensive Care Med. 2019;34(2):104–8.
2. Rolston JD, Han SJ, Lau CY, Berger MS, Parsa AT. Frequency and predictors of complications in neurological surgery: national trends from 2006 to 2011. J Neurosurg. 2014;120:736–45.
3. Manninen PH, Raman SK, Boyle K, EI-Beheiry H. Early postoperative complications following neurosurgical procedures. Can J Anesth. 1999;46(1):7–14.
4. Pires Siqueira EM, Diccini S. Postoperative complications in elective and non-elective neurosurgery. Acta Paul Enferm. 2017;30(1):101–8.
5. Howard R, Kullmann D, Hirsch N. Admission to neurological intensive care: who, when, and why? J Neurol Neurosurg Psychiatry. 2003;74(Suppl 3):iii2–9.
6. Bartels E. Transcranial color-coded duplex ultrasonography in routine cerebrovascular diagnostics. Pers Med. 2012;1:325–30.
7. Walter U. Transcranial sonography of the cerebral parenchyma: update on clinically relevant applications. Pers Med. 2012;1:334–43.
8. Robba C, Cardim D, Sekhon M, Budohoski K, Czosnyka M. Transcranial Doppler: a stethoscope for the brain-neurocritical care use. J Neuro Res. 2018;96:720–30.
9. Pfister D, Strebel SP, Steiner LA. Postoperative management of adult central neurosurgical patients: systemic and neuro-monitoring. Best Pract Res Clin Anaesthesiol. 2007;21(4):449–63.
10. Lobato EB, Sulek CA, Moody RL, Morey TE. Cross-sectional area of the right and left internal jugular veins. J Cardiothorac Vasc Anesth. 1999;13(2):136–8.
11. Doepp F, Schreiber SJ, von Münster T, Rademacher J, Klingebiel R, Valdueza JM. How does the blood leave the brain? A systematic ultrasound analysis of cerebral venous drainage patterns. Neuroradiology. 2004;46(7):565–70.
12. Swain A, Bhagat H, Sahni N, Salunke P. Mechanical ventilation in neurological and neurosurgical patients. Neurol India. 2016;64(3):485–93.
13. Srivastava VK, Agrawal S, Kumar S, Mishra A, Sharma S, Kumar R. Comparison of dexmedetomidine, propofol and midazolam for short-term sedation in postoperatively mechanically ventilated neurosurgical patients. J Clin Diagn Res. 2014;8(9):GC04–7.
14. Wijdicks EF, Bamlet WR, Maramattom BV, Manno EM, McClelland RL. Validation of a new coma scale: the FOUR score. Ann Neurol. 2005;58(4):585–93.
15. Williamson C, Morgan L, Klein JP. Imaging in Neurocritical care practice. Semin Respir Crit Care Med. 2017;38(6):840–52.
16. Hall AJ, Toner NS, Bhatt PM. The introduction of a Neurosurgical Postoperative Checklist improved quality of care and patient safety. Br J Neurosurg. 2019;33(5):495–9.
17. Haynes AB, Weiser TG, Berry WR, Lipsitz SR, Breizat AH, Dellinger EP, Safe Surgery Saves Lives Study Group. A surgical safety checklist to reduce morbidity and mortality in a global population. N Engl J Med. 2009;360(5):491–9.
18. de Almeida CC, Boone MD, Laviv Y, Kasper BS, Chen CC, Kasper EM. The utility of routine intensive care admission for patients undergoing intracranial neurosurgical procedures: a systematic review. Neurocrit Care. 2018;28(1):35–42.
19. Roh D, Park S. Brain multimodality monitoring: updated perspectives. Curr Neurol Neurosci Rep. 2016;16(6):56.
20. Wan ZakariaWan A, Luoma AMV. Postoperative care of neurosurgical patients: general principles. Anaesth Intensive Care Med. 2020;21(7):349–55.
21. Algahtani R, Merenda A. Multimorbidity and critical care neurosurgery: minimizing major perioperative cardiopulmonary complications. Neurocrit Care. 2020:1–15.
22. Chesnut R, Aguilera S, Buki A, Bulger E, Citerio G, Cooper DJ, et al. A management algorithm for adult patients with both brain oxygen and intracranial pressure monitoring: the Seattle International Severe Traumatic Brain Injury Consensus Conference (SIBICC). Intensive Care Med. 2020;46(5):919–29.

23. Lau VI, Jaidka A, Wiskar K, Packer N, Tang JE, Koenig S, et al. Better with ultrasound: transcranial Doppler. Chest. 2020;157(1):142–50.
24. Andrews PJ, Piper IR, Dearden NM, Miller JD. Secondary insults during intrahospital transport of head-injured patients. Lancet. 1990;335(8685):327–30.
25. Kaups KL, Davis JW, Parks SN. Routinely repeated computed tomography after blunt head trauma: does it benefit patients? J Trauma. 2004;56(3):475–80.
26. Smith M. Perioperative uses of transcranial perfusion monitoring. Neurosurg Clin N Am. 2008;19(3):489–502.
27. Messerer M, Daniel RT, Oddo M. Neuromonitoring after major neurosurgical procedures. Minerva Anestesiol. 2012;78(7):810–22.
28. Carney N, Totten AM, O'Reilly C, Ullman JS, Hawryluk GW, Bell MJ, et al. Guidelines for the management of severe traumatic brain injury, fourth edition. Neurosurgery. 2017;80(1):6–15.
29. Robba C, Cardim D, Tajsic T, Pietersen J, Bulman M, Donnelly J, et al. Ultrasound non-invasive measurement of intracranial pressure in neurointensive care: a prospective observational study. PLoS Med. 2017;14(7):e1002356.
30. Lee SJ, Ahn JH, Hong JM. Neurosonology for unconscious or neurocritically ill patients. J Neurosonol Neuroimag. 2019;11(1):46–61.
31. Hakimi R, Alexandrov AV, Garami Z. Neuro-ultrasonography. Neurol Clin. 2020;38(1):215–29.
32. Kalanuria A, Nyquist PA, Armonda RA, Razumovsky A. Use of Transcranial Doppler (TCD) ultrasound in the Neurocritical Care Unit. Neurosurg Clin N Am. 2013;24(3):441–56.
33. Bouzat P, Oddo M, Payen JF. Transcranial Doppler after traumatic brain injury: is there a role? Curr Opin Crit Care. 2014;20(2):153–60.
34. Ract C, Le Moigno S, Bruder N, Vigué B. Transcranial Doppler ultrasound goal-directed therapy for the early management of severe traumatic brain injury. Intensive Care Med. 2007;33(4):645–51.
35. Blanco P, Abdo-Cuza A. Transcranial Doppler ultrasound in neurocritical care. J Ultrasound. 2018;21(1):1–16.
36. Kirkman MA, Smith M. Intracranial pressure monitoring, cerebral perfusion pressure estimation, and ICP/CPP-guided therapy: a standard of care or optional extra after brain injury? Br J Anaesth. 2014;112(1):35–46.
37. Lau VI, Arntfield RT. Point-of-care transcranial Doppler by intensivists. Crit Ultrasound J. 2017;9(1):21.
38. Bellner J, Romner B, Reinstrup P, Kristiansson KA, Ryding E, Brandt L. Transcranial Doppler sonography pulsatility index (PI) reflects intracranial pressure (ICP). Surg Neurol. 2004;62(1):45–51.
39. Czosnyka M, Richards HK, Whitehouse HE, Pickard JD. Relationship between transcranial Doppler-determined pulsatility index and cerebrovascular resistance: an experimental study. J Neurosurg. 1996;84(1):79–84.
40. Schreiber SJ, Stolz E, Valdueza JM. Transcranial ultrasonography of cerebral veins and sinuses. Eur J Ultrasound. 2002;16(1–2):59–72.
41. Valdueza JM, Schultz M, Harms L, Einhäupl KM. Venous transcranial Doppler ultrasound monitoring in acute dural sinus thrombosis. Report of two cases. Stroke. 1995;26(7):1196–9.
42. Stolz E, Gerriets T, Babacan SS, Jauss M, Kraus J, Kaps M. Intracranial venous hemodynamics in patients with midline dislocation due to postischemic brain edema. Stroke. 2002;33(2):479–85.
43. Puls I, Berg D, Mäurer M, Schliesser M, Hetzel G, Becker G. Transcranial sonography of the brain parenchyma: comparison of B-mode imaging and tissue harmonic imaging. Ultrasound Med Biol. 2000;26(2):189–94.
44. Llompart Pou JA, Abadal Centellas JM, Palmer Sans M, Pérez Bárcena J, Casares Vivas M, Homar Ramírez J, et al. Monitoring midline shift by transcranial color-coded sonography in traumatic brain injury. A comparison with cranial computerized tomography. Intensive Care Med. 2004;30(8):1672–5.

45. Seidel G, Gerriets T, Kaps M, Missler U. Dislocation of the third ventricle due to space-occupying stroke evaluated by transcranial duplex sonography. J Neuroimaging. 1996;6(4):227–30.
46. Motuel J, Biette I, Srairi M, Mrozek S, Kurrek MM, Chaynes P, et al. Assessment of brain midline shift using sonography in neurosurgical ICU patients. Crit Care. 2014;18(6):676.
47. Quattrocchi KB, Prasad P, Willits NH, Wagner FC Jr. Quantification of midline shift as a predictor of poor outcome following head injury. Surg Neurol. 1991;35(3):183–8.
48. Stolz E, Gerriets T, Fiss I, Babacan SS, Seidel G, Kaps M. Comparison of transcranial color-coded duplex sonography and cranial CT measurements for determining third ventricle midline shift in space-occupying stroke. AJNR Am J Neuroradiol. 1999;20(8):1567–71.
49. Yang WS, Li Q, Li R, Liu QJ, Wang XC, Zhao LB, et al. Defining the optimal midline shift threshold to predict poor outcome in patients with supratentorial spontaneous intracerebral hemorrhage. Neurocrit Care. 2018;28(3):314–21.
50. Caricato A, Pitoni S, Montini L, Bocci MG, Annetta P, Antonelli M. Echography in brain imaging in intensive care unit: state of the art. World J Radiol. 2014;6(9):636–42.
51. Kiphuth IC, Huttner HB, Struffert T, Schwab S, Köhrmann M. Sonographic monitoring of ventricle enlargement in posthemorrhagic hydrocephalus. Neurology. 2011;76(10):858–62.
52. Matsumoto N, Kimura K, Iguchi Y, Aoki J. Evaluation of cerebral hemorrhage volume using transcranial color-coded duplex sonography. J Neuroimaging. 2011;21(4):355–8.
53. Seidel G, Kaps M, Dorndorf W. Transcranial color-coded duplex sonography of intracerebral hematomas in adults. Stroke. 1993;24(10):1519–27.
54. Blanco P, Blaivas M. Applications of transcranial color-coded sonography in the emergency department. J Ultrasound Med. 2017;36(6):1251–66.
55. Ovesen C, Christensen AF, Krieger DW, Rosenbaum S, Havsteen I, Christensen H. Time course of early postadmission hematoma expansion in spontaneous intracerebral hemorrhage. Stroke. 2014;45(4):994–9.
56. Niesen WD, Rosenkranz M, Weiller C. Bedsided transcranial sonographic monitoring for expansion and progression of subdural hematoma compared to computed tomography. Front Neurol. 2018;9:374.
57. Besenski N. Traumatic injuries: imaging of head injuries. Eur Radiol. 2002;12(6):1237–52.
58. Niesen WD, Burkhardt D, Hoeltje J, Rosenkranz M, Weiller C, Sliwka U. Transcranial grey-scale sonography of subdural haematoma in adults. Ultraschall Med. 2006;27(3):251–5.
59. Heit JJ, Iv M, Wintermark M. Imaging of intracranial hemorrhage. J Stroke. 2017;19(1):11–27.
60. Lee EJ, Lee MY, Hung YC. The application of transcranial Doppler sonography in patients with chronic subdural haematoma. Acta Neurochir. 1999;141(8):835–9.
61. Panda NB, Mahajan S, Chauhan R. Management of postoperative neurosurgical patients. J Neuroanaesthesiol Crit Care. 2019;6:80–6.
62. Clement AR, Palaniappan D, Panigrahi RK. Tension pneumocephalus. Anesthesiology. 2017;127(4):710.
63. Harvey JJ, Harvey SC, Belli A. Tension pneumocephalus: the neurosurgical emergency equivalent of tension pneumothorax. BJR Case Rep. 2016;2(2):20150127.
64. Najjar A, Denault AY, Bojanowski MW. Bedside transcranial sonography monitoring in a patient with hydrocephalus post subarachnoid hemorrhage. Crit Ultrasound J. 2017;9(1):17.
65. Becker G, Bogdahn U, Straßburg HM, Lindner A, Hassel W, Meixensberger J, et al. Identification of ventricular enlargement and estimation of intracranial pressure by transcranial color-coded real-time sonography. J Neuroimag. 1994;4:17–22.
66. Seidel G, Kaps M, Gerriets T, Hutzelmann A. Evaluation of the ventr1cular system 1n adults by transcranial duplex sonography. J Neuroimag. 1995;5:105–8.
67. Hernández NL, Escrivá AG, Jordà JM. Study of the diameter of the third ventricle with transcranial sonography. Neurologia. 2007;22(8):507–10.
68. Martí-Fàbregas J, Belvís R, Guàrdia E, Cocho D, Martí-Vilalta JL. Relationship between transcranial Doppler and CT data in acute intracerebral hemorrhage. AJNR Am J Neuroradiol. 2005;26(1):113–8.

69. Rajajee V, Vanaman M, Fletcher JJ, Jacobs TL. Optic nerve ultrasound for the detection of raised intracranial pressure. Neurocrit Care. 2011;15(3):506–15.
70. Moretti R, Pizzi B. Optic nerve ultrasound for detection of intracranial hypertension in intracranial hemorrhage patients: confirmation of previous findings in a different patient population. J Neurosurg Anesthesiol. 2009;21(1):16–20.
71. Wang LJ, Yao Y, Feng LS, Wang YZ, Zheng NN, Feng JC, et al. Noninvasive and quantitative intracranial pressure estimation using ultrasonographic measurement of optic nerve sheath diameter. Sci Rep. 2017;7:42063.
72. Wang LJ, Chen HX, Chen Y, Yu ZY, Xing YQ. Optic nerve sheath diameter ultrasonography for elevated intracranial pressure detection. Ann Clin Transl Neurol. 2020;7(5):865–8.
73. Schmidt FA, Ruprecht K, Connolly F, Maas MB, Paul F, Hoffmann J, et al. B-mode ultrasound assessment of pupillary function: feasibility, reliability and normal values. PLoS One. 2017;12(12):e0189016.
74. Donnelly J, Budohoski KP, Smielewski P, Czosnyka M. Regulation of the cerebral circulation: bedside assessment and clinical implications. Crit Care. 2016;20(1):129.
75. Budohoski KP, Reinhard M, Aries MJ, Czosnyka Z, Smielewski P, Pickard JD, et al. Monitoring cerebral autoregulation after head injury. Which component of transcranial Doppler flow velocity is optimal? Neurocrit Care. 2012;17(2):211–8.
76. Czosnyka M, Smielewski P, Kirkpatrick P, Menon DK, Pickard JD. Monitoring of cerebral autoregulation in head-injured patients. Stroke. 1996;27(10):1829–34.
77. de Riva N, Budohoski KP, Smielewski P, Kasprowicz M, Zweifel C, Steiner LA, et al. Transcranial Doppler pulsatility index: what it is and what it isn't. Neurocrit Care. 2012;17(1):58–66.
78. Czosnyka M, Matta BF, Smielewski P, Kirkpatrick PJ, Pickard JD. Cerebral perfusion pressure in head-injured patients: a noninvasive assessment using transcranial Doppler ultrasonography. J Neurosurg. 1998;88(5):802–8.
79. Zeiler FA, Czosnyka M, Smielewski P. Optimal cerebral perfusion pressure via transcranial Doppler in TBI: application of robotic technology. Acta Neurochir. 2018;160(11):2149–57.
80. Chang JJ, Triano M, Corbin MJ, Desale S, Liu AH, Felbaum DR, et al. Transcranial Doppler velocity and associations with delayed cerebral ischemia in aneurysmal subarachnoid hemorrhage. J Neurol Sci. 2020;415:116934.
81. Vergouwen MD, Vermeulen M, van Gijn J, Rinkel GJ, Wijdicks EF, Muizelaar JP, et al. Definition of delayed cerebral ischemia after aneurysmal subarachnoid hemorrhage as an outcome event in clinical trials and observational studies: proposal of a multidisciplinary research group. Stroke. 2010;41(10):2391–5.
82. Bonow RH, Young CC, Bass DI, Moore A, Levitt MR. Transcranial Doppler ultrasonography in neurological surgery and neurocritical care. Neurosurg Focus. 2019;47(6):E2.
83. D'Andrea A, Conte M, Scarafile R, Riegler L, Cocchia R, Pezzullo E, et al. Transcranial Doppler ultrasound: physical principles and principal applications in neurocritical care unit. J Cardiovasc Echogr. 2016;26(2):28–41.
84. Yic CD, Prada G, Paz SI, Moraes L, Pontet JC, Lasso ME, et al. Comparison of ultrasonographic versus infrared pupillary assessment. Ultrasound J. 2020;12:38.
85. Wakerley BR, Sharma VK. Transcranial Doppler derived pulsatility index in the assessment of intracranial pressure: the trend is your friend. Neurosurgery. 2013;72(2):E319–20.
86. Schoser BG, Riemenschneider N, Hansen HC. The impact of raised intracranial pressure on cerebral venous hemodynamics: a prospective venous transcranial Doppler ultrasonography study. J Neurosurg. 1999;91(5):744–9.
87. Devlin JW, Skrobik Y, Gélinas C, Needham DM, Slooter AJC, Pandharipande PP, et al. Clinical practice guidelines for the prevention and management of pain, agitation/sedation, delirium, immobility, and sleep disruption in adult patients in the ICU. Crit Care Med. 2018;46(9):e825–73.

88. Celis-Rodríguez E, Díaz Cortés JC, Cárdenas Bolívar YR, Carrizosa González JA, Pinilla DI, Ferrer Záccaro LE, et al. Evidence-based clinical practice guidelines for the management of sedoanalgesia and delirium in critically ill adult patients. Med Intensiva. 2020;44(3):171–84.
89. Bilotta F, Dei Giudici L, Lam A, Rosa G. Ultrasound-based imaging in neurocritical care patients: a review of clinical applications. Neurol Res. 2013;35(2):149–58.
90. Nair AS, Naik VM, Rayani BK. FAST HUGS BID: modified mnemonic for surgical patient. Indian J Crit Care Med. 2017;21(10):713–4.
91. Stolz E, Kaps M, Kern A, Babacan SS, Dorndorf W. Transcranial color-coded duplex sonography of intracranial veins and sinuses in adults. Reference data from 130 volunteers. Stroke. 1999;30(5):1070–5.
92. Picetti E, Rossi S, Abu-Zidan FM, et al. WSES consensus conference guidelines: monitoring and management of severe adult traumatic brain injury patients with polytrauma in the first 24 hours. World J Emerg Surg. 2019;14:53.
93. Sviri GE, Ghodke B, Britz GW. Transcranial Doppler grading criteria for basilar artery vasospasm. Neurosurgery. 2006;59:360–6.
94. Conolly F, Rohl JE, Guthke C, Wengert O, Valdueza JM, Schreiber SJ. Emergency room use of ¨fast track¨ ultrasound in acute stroke: an observational study. Ultrasound Med Biol. 2019;45(5):1103–11.
95. Chernyshev OY, Garami Z, Calleja S, et al. Yield and accuracy of urgent combined carotid/transcranial ultrasound testing in acute cerebral ischemia. Stroke. 2005;36:32–7.

Chapter 54
Perioperative Cardiovascular Surgery: Transcranial Doppler (TCD/TCCS) As a Tool in Predicting Neurological Outcome

Leandro Aguirre and Francisco Klein

Key Points

1. Neurological complications in the context of cardiovascular surgery range from 1% to 5% for stroke, 15% for delirium, and up to 32% for postoperative cognitive dysfunction.
2. Transcranial Doppler neuromonitoring allows evaluation of cerebral hemodynamics and detection of microembolic signals.
3. During carotid endarterectomy it allows to evaluate perfusion during clamping and the need for shunting.
4. During cardiac surgeries it allows to evaluate the embolic load.
5. In aortic arch surgery, it allows to identify and correct states of cerebral malperfusion.

54.1 Introduction

Transcranial Doppler/transcranial color-coded duplex sonography **(TCD/TCCS) is a cost-effective and practical noninvasive tool that allows for real-time evaluation of cerebral hemodynamics.

L. Aguirre (✉)
Favaloro Foundation University Hospital, Buenos Aires, Argentina
e-mail: laguirre@ffavaloro.org

F. Klein
Neuroscience Institute, Hospital Universitario Fundación Favaloro, Buenos Aires, Argentina
e-mail: fklein@ffavaloro.org

C. N. Rodríguez et al. (eds.), *Neurosonology in Critical Care*,
https://doi.org/10.1007/978-3-030-81419-9_54

Noninvasive monitoring during endarterectomy can identify those patients who are developing ischemia during surgery [1].

Brain ultrasound demonstrates in real time what mechanism is involved in the development of it, by embolism, hypoperfusion, thrombosis, or hyperperfusion [2].

Neuropsychological involvement is a common complication of carotid vascular surgeries, whether these are carotid endarterectomies or angioplasties with stenting. It is also a complication of cardiac surgeries, both aortic arch, valvular, or myocardial revascularization by coronary pass.

** TCCS is not a tool for continuous monitoring.

54.2 Post-Cardiovascular Surgery Neurological Dysfunction

Neurological complications have been a major concern in the history of cardiovascular surgery. Three pathophysiological mechanisms cause injury to brain tissue in the context of cardiovascular surgery:

1. Mechanical injury by cerebral embolisms.
2. Alterations in the blood flow and reperfusion injury.
3. Environmental, pharmacological, or "patient-related" factors influencing the postoperative state [3, 4].

Currently, minimally invasive technology and techniques are available for the repair of vascular, valve, and coronary pathology. Therefore, endovascular therapeutics and advances in coronary bypass surgeries are provided in a safer environment today [5].

However, despite these advances, post-cardiovascular surgery complications do occur, including ischemic stroke, delirium, and cognitive impairment.

Ischemic stroke and delirium occur in 1– 5% of patients undergoing myocardial revascularization surgery and 24–70% of behavioral abnormalities have been documented on neuropsychological testing.

With respect to carotid endarterectomy, to maintain benefits over medical therapy, the incidence of complications should be kept below 5–6% for symptomatic internal carotid disease and less than 3% for asymptomatic ones.

With regard to repair procedures for dissection of the ascending aorta and aortic arch, the incidence of focal neurological injury varies between 1% and 11% with a consequent increase in mortality. In addition, delirium, agitation, and confusion are collectively referred to as postoperative neurological dysfunction (PND), accounting for 9–32% of patients with long-term deleterious consequences [7].

54.2.1 Perioperative Stroke

A recent study reports postoperative stroke rates of myocardial revascularization surgery (MRS) between 1% and 5%. Diabetic patients have an increased risk of post-MRS stroke of 2–5% at 5 years [8]. Valve surgeries have an increased risk of perioperative stroke of 4–8% after isolated aortic valve replacement, 8.8% after mitral replacement surgery, and 9.7% after double mitral and aortic valve replacement surgery. Perioperative strokes can be divided into early and late:

1. Early:
   Present at the time of extubation (mainly intraoperative).
2. Late:
   It happens after extubation.

The choice of MRS compared to percutaneous coronary interventions has been associated with more stroke events, but fewer combined cardiac or cerebrovascular major adverse events [9–11].

When the comparison of "off-pump" cardiovascular surgery versus "on-pump" cardiovascular surgery was performed, no difference was found in the incidence of stroke and 30-day mortality. This and other studies suggest that cardiopulmonary bypass does not contribute to the risk of perioperative stroke.

Pharmacological treatment with aspirin, statins, and aggressive anticoagulation and electrical cardioversion treatments of atrial fibrillation have contributed to reducing both the risk of perioperative stroke and other non-neurological complications.

Intraoperative management to minimize stroke includes optimization of blood pressure, mild to moderate hypothermia, hemodilution and transfusions of blood products, strict glycemic control, and primarily neuromonitoring [7].

54.2.2 Neurocognitive Complications: Delirium and Cognitive Impairment

Neurocognitive sequelae in the perioperative period of cardiovascular surgery, including delirium and postoperative cognitive dysfunction (POCD), are still quite common and affect more than half of the patients.

54.2.2.1 Delirium

The question of whether delirium and postoperative cognitive dysfunction represent two clinical forms of a continuum or represent two different forms of brain injury remains unclear.

Delirium is an acute change in mental status characterized by confusion and inattention with a poorly defined pathophysiology. It can be classified as either hyperactive or hypoactive.

The incidence of delirium in one study by Arenson was approximately 15% and the factors associated with its development were: (a) age over 65 years, (b) postoperative stroke, (c) mechanical ventilation for more than 24 hours, (d) postoperative renal failure, (e) blood product transfusions, (f) combined valvular and coronary surgery, and (g) the use of postoperative benzodiazepines [12].

But despite identifying these risk factors the physiopathology of postoperative delirium remains unclear.

54.2.2.2 Postoperative Cognitive Dysfunction (POCD)

Defined as a decline in pre- and postoperative neuropsychological test scores, this is a controversial syndrome, although clearly associated with reduced quality of life and higher annual mortality. It indicates that it is a major problem affecting a certain group of patients [6].

Increasing evidence indicates that there is a relationship between a decrease in cerebral perfusion pressure (CPP) and cognitive impairment in conditions unrelated to cardiovascular surgery (CVSU) [13].

Similarly, a decrease in preoperative blood flow in the dominant hemisphere, that is, a decrease in the cerebral blood flow velocities measured by transcranial Doppler (TCD/TCCS), has been associated with both early and late post CVSU cognitive impairment [14].

54.3 Intraoperative Monitoring of Cardiovascular Procedures

The occurrence of adverse neurological events has encouraged the development of methods to monitor both brain function and circulation in a noninvasive way in order to detect electrophysiological or hemodynamic alterations.

An ideal neuromonitoring system should provide continuous, real-time information about brain function and circulation.

Currently available methods of functional neuromonitoring include electroencephalogram (EEG) and somatosensory evoked potentials (SSEPs), while hemodynamic/circulatory information can be provided by near-infrared spectroscopy (NIRS) and transcranial Doppler ultrasonography (TCD/TCCS) [7].

The objective of this chapter is to describe the characteristics of transcranial Doppler, both for intraoperative management and the evaluation of neurological prognosis in cardiovascular surgery [15].

54.3.1 Transcranial Doppler (TCD/TCCS)

The TCD/TCCS measures only the velocity of local blood flow (velocity and direction) in the proximal portions of the large intracranial arteries (circle of Willis).

Assuming that arterial blood pressure (ABP) and PCO_2 are stable, changes in these measured velocities reflect changes in the cerebral blood flow (CBF).

TCD/TCCS monitoring of the middle cerebral artery (MCA) does not provide direct information on hemodynamic changes that occur in the collateral vessels and in the distal microcirculation that irrigates the ischemic areas.

Hemodynamic compromise can be estimated when there is a reduction or increase in the mean flow velocity.

In addition, the TCD/TCCS can detect microembolic signals that reflect the presence of gaseous or particulate material in the cerebral artery that is not sounded (Fig. 54.1).

Such gaseous, lipid, or solid material has different acoustic impedances with respect to the surrounding red blood cells generating reflection or scattering of the sound beam at the blood-embolus interface which generates an increase in the

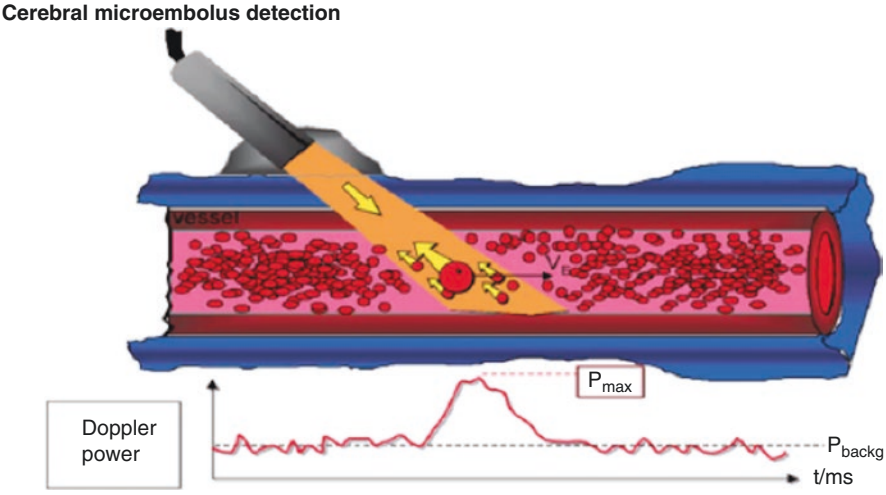

Fig. 54.1 Detection of cerebral microembolism using ultrasound showing an increase in the power or intensity of the reflected ultrasound (P max) caused by an embolus, compared to the background intensity (P back) caused by the erythrocytes. (Courtesy: Rusell D. J Neurol Sci. 2002;203–204:211–4) [16]

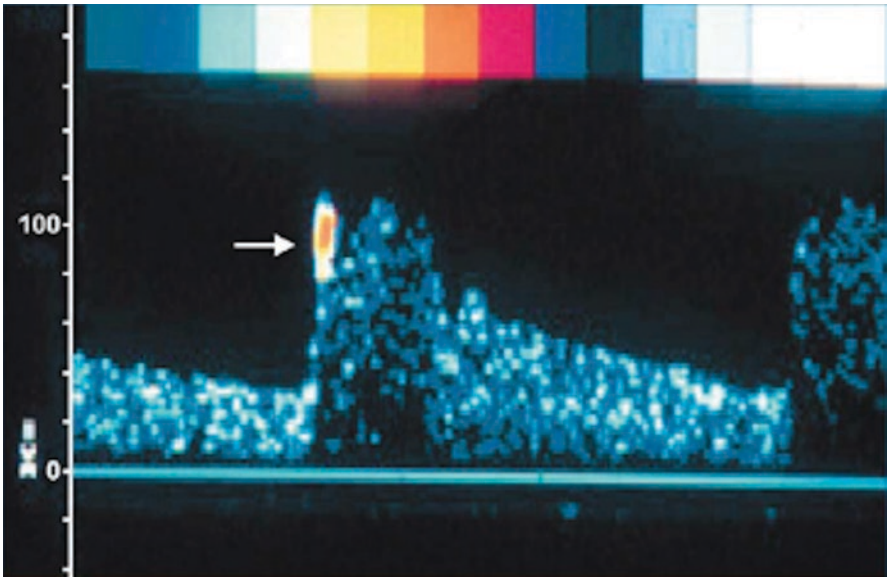

Fig. 54.2 A cerebral microembolus (HIT) (White arrow) passing through the middle cerebral artery in a cardiac cycle color scale: decibels (top); embolus (red); erythrocytes (blue); horizontal axis = time. Vertical axis = velocities (cm/s). (Courtesy: Rusell D. J Neurol Sci. 2002;203–204:211–4) [16]

intensity of the signal received (high intensity transient signals (HITS)) on the spectral Doppler wave [16] (Fig. 54.2).

54.4 Usefulness of TCD/TCCS in Carotid Endarterectomy (CE) and Carotid Angioplasty (CAP)

In the presurgical stage, TCD/TCCS is a useful method of evaluation:

1. Intracranial stenoses.
2. To detect high-risk patients with asymptomatic carotid lesions.
3. Evaluate right-left short circuit stroke.

The detection of embolisms and the presence of a substantial short circuit allow the definition of the need for a CE, Cap, or closure procedure of an interauricular communication [17, 18].

In the intervention stage, the occurrence of stroke in the context of a carotid procedure can be by both hemodynamic and embolic mechanisms, the latter being the main mechanism at the site of intervention [19].

Transcranial Doppler monitoring allows:

1. Real-time monitoring of changes in blood flow velocities rates in the basal arteries.
2. The detection of microembolic signals (HITS) that correspond to both particulate material (plungers and/or atheroma plates) and bubbles

54.4.1 Carotid Endarterectomy (CE)

The monitoring of hemodynamic variations expressed as changes in flow rates during carotid endarterectomy requires more attention mainly at three stages of the procedure:

54.4.1.1 Presurgical Evaluation

In addition to the degree of stenosis, TCD/TCCS allows the detection of microembolic signals, this possibility of detecting asymptomatic embolization in patients with asymptomatic carotid lesions allows the identification of patients with a higher risk of stroke or transient ischemic accidents and the definition of a surgical indication [20, 21].

54.4.1.2 Clamping

Flow rates correlate with pressure in the area of the distal stump to clamping which depends on the collateral circulation provided by the circle of Willis [22]. During intraoperative use of TCD/TCCS allows detection of hypoperfusion at the time of carotid clamping which has indicated the need for shunting in up to 44% of procedures [23]. The TCD/TCCS allows measurement of the average blood flow velocity in the middle cerebral artery during the occlusion test (by balloon in angioplasty or clamping in endarterectomy) and has been shown to be highly predictive of the capacity of collateral circulation (Fig. 54.3), although an optimal cut-off point has not yet been determined at which the collateral circulation is considered inadequate and increases the possibility of neurological adverse events.

In a study by Eckert et al., using a 20-minute occlusion test of the internal carotid artery (ICA) and measurement of mean flow velocity (MFV) in the MCA, the authors reported that a drop of more than 50% from baseline is critical for the development of silent ischemia and the occurrence of neurological symptoms [24]. Other authors with different clamping times also conclude that an abrupt 50–60% drop in MFV in MCA exposes the patient to the risk of neurological complications and some shunting is recommended [25]. Contralateral occlusion or stenosis is a risk factor for difficulty in having an adequate shunt; with this in mind, Telman et al.

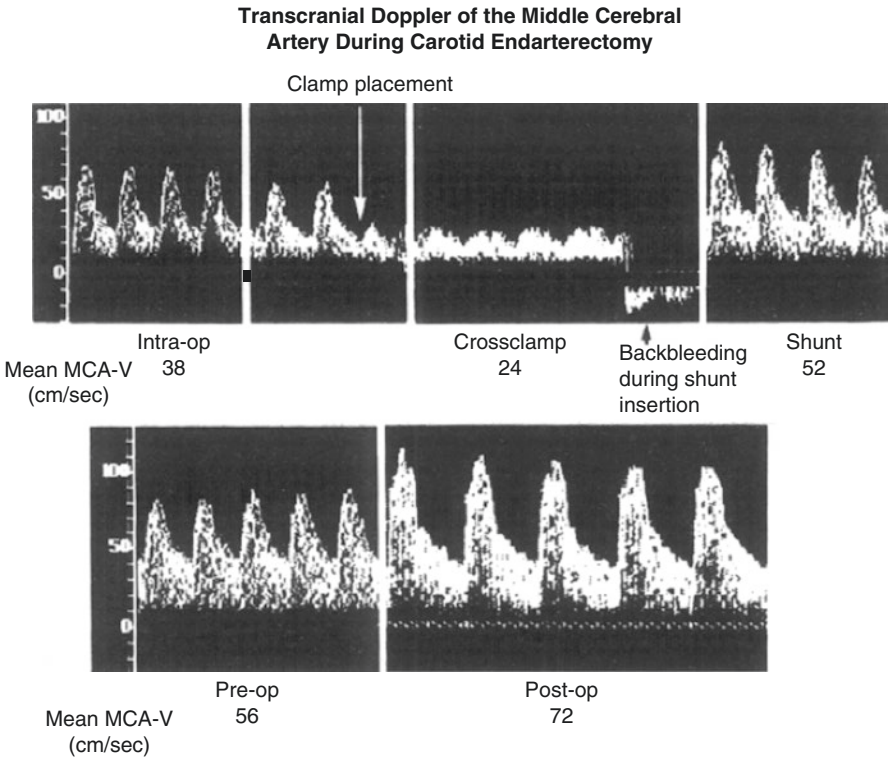

Fig. 54.3 Carotid clamping with insufficient collateral circulation from the posterior communicating with recovery of flow with shunt placement. (Courtesy: Schneider PA, et al. J Vasc Surg. 1988;7(2):223–31) [31]

used acetazolamide as a vasodilator stimulus to evaluate cerebrovascular hemodynamic reserve in 76 patients with unilateral stenosis undergoing carotid endarterectomy. Based on their experience the ability to predict the need for shunt was 80% [26]. The presence of reverse ophthalmic flow as an expression of last-spring collateral flow may mean per se a depleted cerebrovascular vasomotor reserve [27].

54.4.1.3 After Declamp

The hemodynamic changes include an improvement in the average speed of the middle, anterior and ophthalmic cerebral arteries, a resolution of the "side to side" asymmetries in the flow rates occurs and the vasoreactivity to CO_2 is recovered (Fig. 54.4).

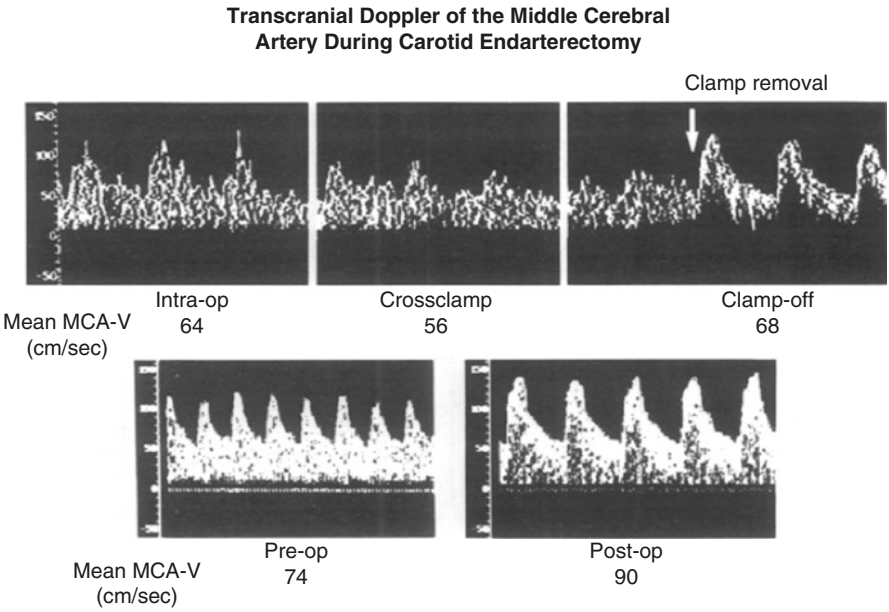

Fig. 54.4 Carotid clamping with collateral circulation from adequate posterior communicator. No shunt was required. Removal of the clamp shows increased velocities (hyperflow). (Courtesy: Schneider PA, et al. J Vasc Surg. 1988;7(2):223–31) [31]

54.4.1.4 Postoperative

An increase in velocities of more than 150% with respect to pre-clamping is indicative of a hyperperfusion syndrome with risk of encephalopathy or intracerebral hemorrhage [28].

In this sense, postsurgical monitoring with TCD/TCCS during the first 7 days allows the detection of patients with hyperperfusion syndrome, with the highest velocities up to day 2 postsurgery, averaging more than 32% compared to presurgical velocities [29, 30] (Fig. 54.5).

54.4.2 Carotid Angioplasty (CAP)

Proximal protection systems that involve stopping or reversing the flow as a protective measure of distal embolization significantly reduce the embolic load in carotid angioplasties.

Given the inherent inability of this procedure to perform a shunt, these protective systems require collateral circulation to the ipsilateral hemisphere with the consequent risk of hypoperfusion if the collateral is not sufficient.

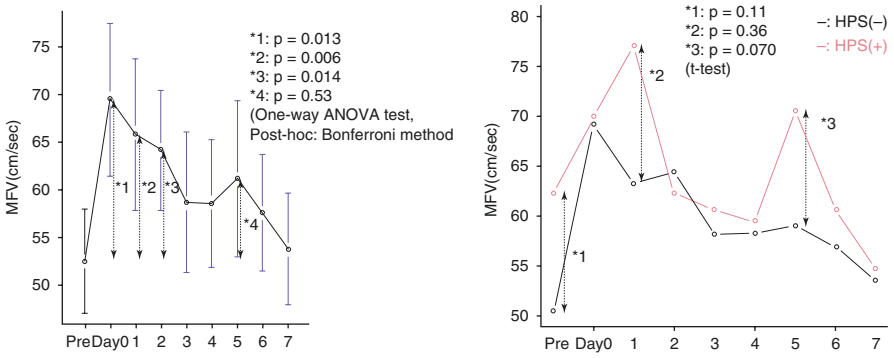

Fig. 54.5 Daily trend of MFV in ipsilateral MCA to CE. The graph on the right shows the trend in the groups with and without probable hyperperfusion syndrome (HPS). Mean velocities were higher in the probable hyperperfusion syndrome group with high velocities up to the second postoperative day. (Courtesy: Koizumi S, et al. World Neurosurg. 2018;110:e710–4] [29]

In a record of approximately 1300 patients, Stabile et al. trial reported that 20% of patients undergoing angioplasty had clinical intolerance at the time of aspiration [32], Even if hypoperfusion exists, the clearance capacity of the emboli is diminished at the time of balloon deflation [33].

The TCD provides the operator with a continuous assessment of brain blood flow. But unlike endarterectomy, where the TCD helps predict tolerance to clamping, during proximal guarded angioplasty there are specific differences that require further investigation; first the inability to shunt forces patients with absent or insufficient contralateral flow to become a distal guarded procedure.

In conclusion, TCD/TCCS is an excellent method of providing a real-time view of cerebral hemodynamics. Despite some promising data indicating its ability to help predict those patients with compromised hemodynamic reserve, its use in carotid angioplasty for the prediction of silent ischemia needs to be further studied.

54.5 Usefulness of TCD/TCCS in Cardiac Surgery (MRS and Valve Surgery)

54.5.1 Myocardial Revascularization Surgery (MRS)

Neurological complications after myocardial revascularization surgery may manifest themselves as:

1. Acute stroke.
2. Postoperative cognitive dysfunction (POCD).

Postoperative cognitive dysfunction is common and clinically presented as a combination of (a) fine motor function deficit, (b) attention deficit, memory consolidation, and (c) psychomotor impairment. The etiology is still unclear, but a multifactorial cause is postulated that includes embolic events, inflammatory processes, hypoperfusion, cerebral edema, and hyperthermia. They probably play a role in the neurocognitive impairment seen in up to 50–70% of patients in postsurgical cardiac surgery [14, 16, 34, 35].

The TCD/TCCS is a sensitive tool in the detection of embolism during MRS; however, there are contradictory observations regarding the occurrence of high intensity embolism signals (HITS) and the occurrence of postsurgical cognitive dysfunction (POCD).

In a study by Stroobant et al. the embolic load was evaluated by detecting HITS, during MRS in two groups of patients, 32 of them under extracorporeal circulation pump (ECP) and 18 of them without ECP. Cerebral blood flow rate and brain vasoreactivity were studied both preoperatively and postoperatively (early (6 days) and late (6 months)) during neurocognitive tests.

Although a greater number of HITS were observed in the group of patients undergoing ECP (especially at the time of aortic cannulation) and a trend toward less favorable results on neurocognitive tests at 6 months, the number of HITS showed no significant correlation with the degree of cognitive impairment in the early or late postoperative period [36].

Another Gasparovich et al. trial compared the differences in embolic loads (HITS) according to the type of strategy of single transverse or multiple lateral clamping of the aorta, with higher embolic loads in those with multiple clamps, which translated into lower early cognitive deficits and higher levels of late restoration of cognitive functions [37].

In contrast, Pugsley finds data suggesting that neuropsychological deficits are related to the number of microemboli that occur during surgery [38]. On the other hand, Mascerotti et al. found suggestive findings that reduced blood flow rates on the left side may represent an independent risk factor for the development of postsurgical cognitive dysfunction [39]. On the other hand, Nathan et al. found no correlation between the number of embolisms detected intraoperatively and the occurrence of cognitive impairment in patients undergoing protective hypothermia [40]. Also an analysis of two studies conducted by Rodriguez et al. including 356 patients undergoing MRS found no correlation between the HITS count and the presence of POCD [41].

Although more studies are still needed to determine the correlation between microembolic events and the development of POCD, the available evidence would indicate that there is no strong association between HITS load or count and the presence of POCD.

54.5.2 Valvular Surgery (VS)

Valvular replacement surgery is a major risk factor for intraoperative microembolization compared to MRS. Abu Omar et al. found a 2100% increase in the number of microembolisms in patients undergoing valvular surgery (VS) compared to MRS [42].

But the comparison of the results of neurocognitive tests of both surgeries is not conclusive, regarding the association with the number of intraoperative microembolisms.

Neville et al. in a study of 193 patients found a significantly higher number of embolisms in the VS group compared to MRS, but not a correlation with an increased risk of adverse neurological events [43].

A trial from the University of Oslo compared the incidence of intraoperative microembolic signals with neurocognitive deficit in the postoperative period in both valve replacement surgeries and MRS. A higher number of microembolic signals was found in patients with cognitive deficits undergoing VS and not in patients undergoing MRS [44].

With respect to asymmetry in Zanatta and coli embolizations, they found that patients undergoing valve replacement surgery were more sensitive to the impairment of memory, psychomotor, and performance functions detected in the left middle cerebral artery (MCA_L) but not in the right MCA_R [39].

With regard to the transcatheter aortic valve implantation (TAVI), Erdoes et al. evaluated 44 patients by means of TCD/TCCS during the procedure, observing that the embolic load presents a peak during the deployment of the device, no difference being observed if the access is transfemoral or transapical. Despite the embolic load detected there were only two stroke events and no delirium events in the population studied [45].

54.6 Usefulness of TCD/TCCS in Aortic Arch Surgery (AOAS)

Neurological injury still remains a significant problem during the repair of acute aortic dissection type A, with incidences of stroke ranging from 1% to 11% and delirium or transient neurological dysfunction of 9–32% with consequent long-term disability.

Different neuroprotection techniques have been designed for this type of complex repair, within the methods to improve safety during circulatory arrest (e.g., cerebroplegia, antegrade perfusion via innominate artery and hypothermia). Retrograde cerebral perfusion:

1. Reverses the massive air embolism that can occur in this type of surgery.
2. Maintains cerebral blood flow.

Both neurological dysfunction and stroke are related to clinical or subclinical microembolism as well as to states of generalized cerebral malperfusion (defined as

a 50% reduction in the average speed of blood flow in the MCA with respect to the basal one determined by means of TCD/TCCS). Cerebral hypoperfusion states in the context of Aortic Arch pathology occur:

1. During an aortic dissection by compromise and progression of the dissection to the supra-aortic and intracranial vessels with consequent neurological damage.
2. Intraoperatively, during retrograde brain perfusion with hypothermia.

In this context the transcranial Doppler allows monitoring of cerebral blood flow:

(a) To evaluate the effectiveness of the reversal in the direction of blood flow in the M1 and M2 segments of the MCA.
(b) To identify and correct brain malperfusion states (i.e., guiding the selection of optimal brain retroperfusion blood flow) [30].

These interventions may improve neurological prognosis during the repair of acute aortic dissections type A.

A study by Estera et al. examined the occurrence of stroke and temporary neurological dysfunction in 56 patients undergoing aortic arch surgery for type A dissection. Fifty percent were monitored by TCD and guided retroperfusion as needed and the control group was given unmonitored conventional brain retroperfusion with a fixed flow of 500 ml/min.

In the monitoring group with TCD, 28% of cerebral malperfusion states were detected, allowing modification of the operative procedures in order to optimize the flow rates in MCA. Consequently, in this series, the incidence of transitory neurological dysfunction was significantly reduced in the group in study compared to the control group (14.8% vs 51.8% respectively; $p < 0.008$) [46].

On the other hand, Ghazy et al. in 2017 evaluated nine patients with aortic surgery and neuroprotection by unilateral selective antegrade brain perfusion and performed perfusion monitoring and HITS count. In this series of patients, TCD monitoring allowed optimization of perfusion through flow adjustments or eventual conversion to bilateral perfusion if insufficient collateral flow was detected. In addition, in one patient who was detected abundant bubble HITS, the stroke was observed in the postoperative period.

In conclusion, monitoring with TCD allowed the adaptation of the brain perfusion strategy or the need to optimize it as well as to evaluate the presence of embolisms (aerial or particulate) and thus achieve an interpretation of the postoperative neurological deficits [47].

54.7 Conclusion

As an increasing number of patients undergo some form of surgical or interventional procedure, including older patients or those with comorbidities, neurological complications remain a major source of concern for their increased morbidity and mortality.

Neuromonitoring through TCD/TCCS provides useful information during both intrathoracic and carotid vascular surgeries. This information complements and can help in decision making about intraoperative management, surgical techniques, and possibly improving the neurological evolution of these patients.

Algorithm

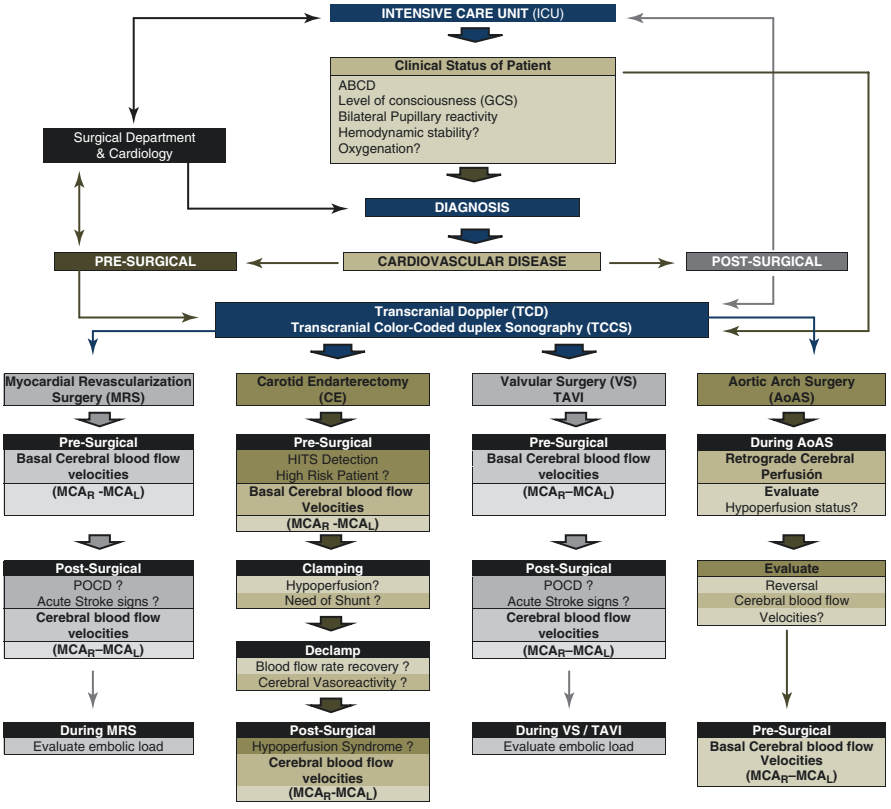

MCA$_R$ Right middle cerebral artery, *MCA$_L$* Left middle cerebral artery, *ABCD* Airway, breathing, circulation, disability, *TAVI* Transcatheter aortic valve Implantation, *POCD* Postoperative cognitive dysfunction, *GCS* Glasgow coma scale

References

1. Spacek M, Sorrell VL, Veselka J. Transcranial Doppler ultrasound in the current era of carotid artery stenting. Ultraschall der Medizin. 2015;36(4):337–41.

2. Sloan MA, Alexandrov AV, Tegeler CH, Spencer MP, Caplan LR, Feldmann E, et al. Assessment: Transcranial Doppler ultrasonography. Report of the Therapeutics and Technology Assessment Subcommittee of the American Academy of Neurology. Neurology; 2004.
3. Swain J. Cardiac surgery and the brain. N Engl J Med. 1993;329(20):1119–20.
4. Newman MF, Kirchner JL, Phillips-Bute B, Gaver V, Grocott H, Jones RH, et al. Longitudinal assessment of neurocognitive function after coronary-artery bypass surgery. N Engl J Med. 2001;344(6):395–402.
5. McDonagh DL, Berger M, Mathew JP, Graffagnino C, Milano CA, Newman MF. Neurological complications of cardiac surgery. Lancet Neurol. 2014;13(5):490–502.
6. Zabala JA. [Neurological complications of cardiac surgery]. Complic Neurol la Cir Card [Internet]. 2005;58(9):1003–6.
7. Sloan MA. Prevention of ischemic neurologic injury with intraoperative monitoring of selected cardiovascular and cerebrovascular procedures: roles of electroencephalography, somatosensory evoked potentials, transcranial Doppler, and near-infrared spectroscopy. Neurol Clin. 2006;24(4):631–45.
8. Tarakji KG, Sabik JF, Bhudia SK, Batizy LH, Blackstone EH. Temporal onset, risk factors, and outcomes associated with stroke after coronary artery bypass grafting. JAMA - J Am Med Assoc. 2011.
9. Lee JH, Lee SW. Strategies for multivessel revascularization in patients with diabetes. J Comp Eff Res. 2013;2(3):231–4.
10. Mohr FW, Morice MC, Kappetein AP, Feldman TE, Ståhle E, Colombo A, et al. Coronary artery bypass graft surgery versus percutaneous coronary intervention in patients with three-vessel disease and left main coronary disease: 5-year follow-up of the randomised, clinical SYNTAX trial. Lancet. 2013;381(9867):629–38.
11. Provenzano R, Wiecek A, Levin NW, Kaplan M, Macdougall IC, et al. Peginesatide in patients with anemia undergoing hemodialysis. N Engl J Med. 2013;368:307–19.
12. Arenson BG, MacDonald LA, Grocott HP, Hiebert BM, Arora RC. Effect of intensive care unit environment on in-hospital delirium after cardiac surgery. J Thorac Cardiovasc Surg [Internet]. 2013;146(1):172–8.
13. Marshall RS. Effects of altered cerebral hemodynamics on cognitive function. J Alzheimers Dis. 2012.
14. Messerotti Benvenuti S, Zanatta P, Valfrè C, Polesel E, Palomba D. Preliminary evidence for reduced preoperative cerebral blood flow velocity as a risk factor for cognitive decline three months after cardiac surgery: an extension study. Perfus (United Kingdom). 2012;27(6):486–92.
15. Crawford S, Channon S. Dissociation between performance on abstract tests of executive function and problem solving in real-life-type situations in normal aging. Aging Ment Heal. 2002;6(1):12–21.
16. Russell D. Cerebral microemboli and cognitive impairment. J Neurol Sci. 2002;203–204:211–4.
17. Spence JD. Transcranial Doppler: uses in stroke prevention. J Vasc Ultrasound. 2015;39(4):183–7.
18. Garami Z, Lumsden AB. Intra-operative TCD monitoring. In: Cerebrovascular ultrasound in stroke prevention and treatment. 2nd ed; 2011.
19. Gattuso R, Martinelli O, Alunno A, D'Angeli I, Felli M, Castiglione A, et al. Carotid stenting and transcranial doppler monitoring: indications for carotid stenosis treatment. Vasc Endovasc Surg. 2010;44(7):535–8.
20. Markus HS, King A, Shipley M, Topakian R, Cullinane M, Reihill S, et al. Asymptomatic embolisation for prediction of stroke in the Asymptomatic Carotid Emboli Study (ACES): a prospective observational study. Lancet Neurol. 2010;9(7):663–71.
21. Best LMJ, Webb AC, Gurusamy KS, Cheng SF, Richards T. Transcranial Doppler ultrasound detection of microemboli as a predictor of cerebral events in patients with symptomatic and asymptomatic carotid disease: a systematic review and meta-analysis. Eur J Vasc Endovasc Surg. 2016;52(5):565–80.

22. Spencer MP, Thomas GI, Moehring MA. Relation between middle cerebral artery blood flow velocity and stump pressure during carotid endarterectomy. Stroke. 1992;23(10):1439–45.
23. Cho JW, Jang JS. Near-infrared spectroscopy versus transcranial doppler-based monitoring in carotid endarterectomy. Korean J Thorac Cardiovasc Surg. 2017;50(6):448–52.
24. Eckert B, Thie A, Carvajal M, Groden C, Zeumer H. Predicting hemodynamic ischemia by transcranial Doppler monitoring during therapeutic balloon occlusion of the internal carotid artery. Am J Neuroradiol. 1998;19(3):577–82.
25. Giller CA, Mathews D, Walker B, Purdy P, Roseland AM. Prediction of tolerance to carotid artery occlusion using transcranial Doppler ultrasound. J Neurosurg. 1994.
26. Telman G, Kouperberg E, Nitecki S, Karram T, Schwarz HA, Sprecher E, et al. Preoperative cerebral hemodynamics and shunting during carotid endarterectomy in patients with severe unilateral carotid stenosis. J Clin Ultrasound. 2007.
27. Fearn SJ, Picton AJ, Mortimer AJ, Parry AD, CN MC. The contribution of the external carotid artery to cerebral perfusion in carotid disease. J Vasc Surg. 2000.
28. Jansen C, Sprengers AM, Moll FL, Vermeulen FEE, Hamerlijnck RPHM, van Gijn J, et al. Prediction of intracerebral haemorrhage after carotid endarterectomy by clinical criteria and intraoperative transcranial Doppler monitoring: results of 233 operations. Eur J Vasc Surg. 1994.
29. Koizumi S, Yamaoka Y, Matsuo T, Kimura T, Inoue T. Changes in blood flow velocity of the middle cerebral artery after carotid endarterectomy: daily assessment with transcranial color-coded sonography. World Neurosurg. 2018;110:e710–4.
30. Alexandrov AV. Cerebrovascular ultrasound in stroke prevention and treatment; 2008.
31. Schneider PA, Rossman ME, Torem S, Otis SM, Dilley RB, Bernstein EF. Transcranial Doppler in the management of extracranial cerebrovascular disease: implications in diagnosis and monitoring. J Vasc Surg. 1988;7(2):223–31.
32. Stabile E, Salemme L, Sorropago G, Tesorio T, Nammas W, Miranda M, et al. Proximal endovascular occlusion for carotid artery stenting. Results from a prospective registry of 1,300 patients. J Am Coll Cardiol. 2010.
33. Orlandi G, Fanucchi S, Gallerini S, Sonnoli C, Cosottini M, Puglioli M, et al. Impaired clearance of microemboli and cerebrovascular symptoms during carotid stenting procedures. Arch Neurol. 2005.
34. Stump DA, Rogers AT, Hammon JW, Newman SP. Cerebral emboli and cognitive outcome after cardiac surgery. J Cardiothorac Vasc Anesth. 1996;10(1):113–9.
35. Liu YH, Wang DX, Li LH, Wu XM, Shan GJ, Su Y, et al. The effects of cardiopulmonary bypass on the number of cerebral microemboli and the incidence of cognitive dysfunction after coronary artery bypass graft surgery. Anesth Analg. 2009;109(4):1013–22.
36. Stroobant N, Van Nooten G, Van Belleghem Y, Vingerhoets G. Relation between neurocognitive impairment, embolic load, and cerebrovascular reactivity following on- and off-pump coronary artery bypass grafting. Chest. 2005;127(6):1967–76.
37. Gasparovic H, Borojevic M, Malojcic B, Gasparovic K, Biocina B. Single aortic clamping in coronary artery bypass surgery reduces cerebral embolism and improves neurocognitive outcomes. Vasc Med (United Kingdom). 2013;18(5):275–81.
38. Pugsley W, Klinger L, Paschalis C, Treasure T, Harrison M, Newman S. The impact of microemboli during cardiopulmonary bypass on neuropsychological functioning. Stroke. 1994;25(7):1393–9.
39. Zanatta P, Benvenuti SM, Valfrè C, Baldanzi F, Palomba D. The role of asymmetry and the nature of microembolization in cognitive decline after heart valve surgery: a pilot study. Perfusion. 2012;27(3):199–206.
40. Boodhwani M, Rubens F, Wozny D, Rodriguez R, Nathan HJ. Effects of sustained mild hypothermia on neurocognitive function after coronary artery bypass surgery: a randomized, double-blind study. J Thorac Cardiovasc Surg. 2007;134(6).

41. Rodriguez RA, Rubens FD, Wozny D, Nathan HJ. Cerebral emboli detected by transcranial doppler during cardiopulmonary bypass are not correlated with postoperative cognitive deficits. Stroke. 2010;41(10):2229–35.
42. Abu-Omar Y, Cifelli A, Matthews PM, Taggart DP. The role of microembolisation in cerebral injury as defined by functional magnetic resonance imaging. In: European Journal of Cardiothoracic Surgery; 2004.
43. Neville MJ, Butterworth J, James RL, Hammon JW, Stump DA. Similar neurobehavioral outcome after valve or coronary artery operations despite differing carotid embolic counts. J Thorac Cardiovasc Surg. 2001;121(1):125–36.
44. Braekken SK, Reinvang I, Russell D, Brucher R, Svennevig JL. Association between intraoperative cerebral microembolic signals and postoperative neuropsychological deficit: comparison between patients with cardiac valve replacement and patients with coronary artery bypass grafting. J Neurol Neurosurg Psychiatry. 1998;65(4):573–6.
45. Erdoes G, Basciani R, Huber C, Stortecky S, Wenaweser P, Windecker S, et al. Transcranial doppler-detected cerebral embolic load during transcatheter aortic valve implantation. Eur J Cardio Thoracic Surg. 2012;41(4):778–84.
46. Estrera AL, Garami Z, Miller CC, Sheinbaum R, Huynh TTT, Porat EE, et al. Cerebral monitoring with transcranial Doppler ultrasonography improves neurologic outcome during repairs of acute type A aortic dissection. J Thorac Cardiovasc Surg. 2005;129(2):277–85.
47. Ghazy T, Darwisch A, Schmidt T, Fajfrova Z, Zickmüller C, Masshour A, et al. Transcranial doppler sonography for optimization of cerebral perfusion in aortic arch operation. Ann Thorac Surg. 2016.

Chapter 55
Decompressive Craniectomy in the ICU: Usefulness of Transcranial Doppler (TCD/TCCS) in the Monitoring of Hemodynamic Changes

Sebastián Vásquez, Juliana Mendoza Mantilla, María Natalia Suárez, Luis A. Bustamante, Joffre Guzman, and Andrés M. Rubiano

Key Points

1. TCD/TCCS is a noninvasive monitoring technique in patients with acute neurological injury and/or neurosurgical pathology. TCD/TCCS is safe, which facilitates the study of cerebral blood flow velocities (CBFVs) and allows detection of possible complications.
2. TCCS allows visualization of possible anatomical changes of the brain parenchyma and blood vessels, and achieves a greater accuracy measures of CBFVs compared with TCD method (blind technique), pre- and post-craniectomy.
3. TCD/TCCS allows assessment of cerebral hemodynamic changes in real time during the intracranial hypertension management, as well as the hemodynamic changes due to decompressive craniectomy (DC).

S. Vásquez
Neurology Department, Rosario University, Bogotá, Colombia

Neuroscience Institute, El Bosque University, INUB – Meditech Research Group, Bogotá, Colombia

J. M. Mantilla · J. Guzman
Neuroscience Institute, El Bosque University, INUB – Meditech Research Group, Bogotá, Colombia

M. N. Suárez
Health Faculty, South-Colombian University, Neiva, Colombia

L. A. Bustamante
Trauma Intensive Care Unit, San Fernando/Valle Salud Clinic, Cali, Colombia

A. M. Rubiano (✉)
Neuroscience Institute, El Bosque University, INUB – Meditech Research Group, Bogotá, Colombia

Trauma Intensive Care Unit, San Fernando/Valle Salud Clinic, Cali, Colombia
e-mail: andresrubiano@aol.com

C. N. Rodríguez et al. (eds.), *Neurosonology in Critical Care*,
https://doi.org/10.1007/978-3-030-81419-9_55

4. Decompressive craniectomy is considered a life-saving surgical technique to improve refractory intracranial hypertension, where ICP elevation is not controlled with medical management. TCD/TCCS provides useful information during clinical evolution and could contribute to determining the neurological prognosis of the critically ill patient.

55.1 Introduction

Transcranial Doppler/transcranial color-coded duplex sonography (TCD/TCCS) are noninvasive and reproducible monitoring tools that facilitate the study of the cerebral hemodynamics, allowing for the assessment in real time the CBFV variations and its association with clinical changes at bedside [1]. These noninvasive monitoring techniques are part of the diagnostic arsenal to provide timely and directed-therapy. Therefore, TCD/TCCS measurements can provide information to individualize interventions adjusted to the clinical needs of each patient [1].

TCCS, compared to other monitoring techniques, provides images of the brain parenchyma anatomical (B-mode) and cerebral blood vessels in real time, enabling a more accurate acoustic access [2, 3].

In patients with traumatic brain injury (TBI), TCD/TCCS provides information on the cerebral hemodynamic status. Hyperemia and vasospasm are pathological conditions present during TBI. These clinical situations can be differentiated from each by calculating the Lindegaard ratio [6]. If the latter is elevated, then vasospasm is the most likely reason for the elevated CBFVs. The vasospasm and CBFV changes (spectral Doppler waveform analysis) may precede the clinical manifestations of neurological worsening (e.g., delayed cerebral ischemia). Therefore, TCD/TCCS is a useful technique to anticipate neurological worsening at bedside [4, 5]. It has been described that vasospasm findings evidenced by TCD/TCCS predict and are associated with documented vasospasm through invasive angiography (CTA, DSA) [6].

A three-phase CBF pattern has been described after TBI [6]. Initially, overall CBF is reduced leading to a hypoperfusion status followed by a hyperperfusion phenomenon in the following 24–72 hours [5, 6].

There are patterns for rapid and simple recognition of CBF disturbances (e.g., hyperflow, cerebral circulatory arrest), which can be identified in the interpretation of spectral Doppler waveform analysis and hemodynamic indexes (pulsatility indexes (PI), resistance index (RI)) derived from it [2], thus facilitating rapid real-time therapeutic decision (Fig. 55.1).

55.2 TCD/TCCS Technique

TCD technique uses a low-frequency transducer (2 MHz), and TCCS uses phased array transducer whose frequency oscillates between 1 and 5 MHz, being automatically configured at frequencies 1 and 2 MHz when the B-mode is selected [1, 2, 38].

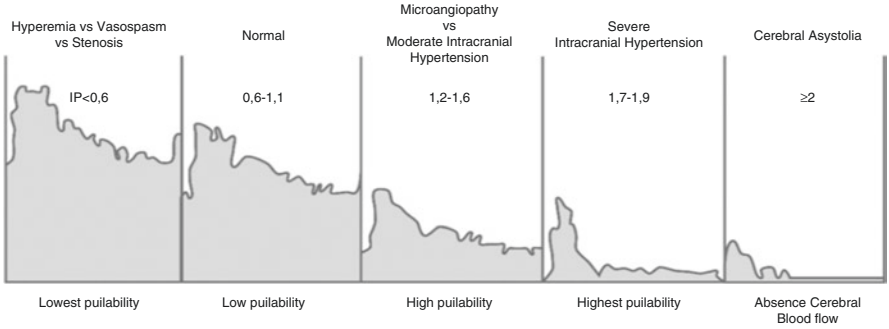

Fig. 55.1 Morphological spectrum of waves reflecting cerebral blood flow velocities and PI documented by transcranial Doppler and examples of relevant conditions. HIC Intracranial hypertension, PI Pulsatility index ([Maximum systolic flow velocity – minimal diastolic flow velocity/ Mean flow velocity])

CBFVs should be measured with an insonation angle less than 60 degrees. The following precaution is recommended [1]:

1. Importance of keeping the correct insonation angle-correction. It can increase 20–30% in CBFVs measurement (more details see Chap. 72).

One of the impediments for an adequate transcranial insonation of CBFVs is the absence of transtemporal and suboccipital acoustic windows (prevalent in elderly women). Therefore, in craniectomized patients [1, 38, 39], the evaluation of cerebral basal arteries is easier.

55.3 Descompressive Craniectomy (DC)

The utility of DC to manage intracranial hypertension syndrome has been well described. A space-occupying lesion (intracerebral hemorrhage, subdural hematoma, etc.) or diffuse lesions (brain edema) may generate midline shift and/or different classic herniation syndromes. According to the classical Monro-Kellie doctrine, intracranial components shift to compensate the ICP changes to maintain adequate brain oxygen delivery and cerebral perfusion pressure (CPP). The following have been described as compensatory mechanisms: cerebrospinal fluid (CSF) redistributes from skull into the spinal canal (less production and increase reabsorption), venous systems compression (increase venous outflow), and arterial system compression (decrease blood entering the skull). These mechanisms are only temporarily effective. Hence, when these compensatory mechanisms are exhausted, neurological worsening ensues [4, 5, 17].

DC is a surgical procedure whereby a bone fragment with a diameter of at least 12–15 cm (supratentorially) is temporarily removed. This provides additional space for brain tissue expansion, thus restoring some balance of intracranial pressures [14, 15], to decrease ICP and CPP [3, 8]. After this procedure, the pressure gradient

generated by the displacement of brain structures decreases according to the Monro-Kellie doctrine, therefore avoiding brain edema, cerebral hypoperfusion, and brain herniation syndromes [4, 16, 19, 20, 22, 23].

ICP control through DC leads to a theoretical improvement of cerebral hemodynamics and maintain adequate brain oxygen delivery due to optimization of CBF [10–12]. TCD/TCCS has a potential as a diagnostic and monitoring tool to indirectly record these hemodynamic changes, to obtaining real-time information and make crucial and individualized therapeutic decisions to optimize CPP, as well as its usefulness in the post-DC follow-up [3–8].

DC is employed when intracranial hypertension is refractory to medical treatment, such as in cases of severe TBI, acute ischemic stroke (AIS), aneurysmal subarachnoid hemorrhage (aSAH), CNS infections, and venous sinus thrombosis [3, 4], and can be classified in two ways: chronological and initial vs add-on therapy [26, 27] (Table 55.1).

In general, there are two types of surgical techniques for DC (Table 55.2).

Table 55.1 Classification of decompressive craniectomy (DC)

Medical management	DC procedure time
Early primary: Carried out in patients with limited access to multimodal neuromonitoring and indicated as first line control of tissue damage, as long as the patient is under sedation and with availability of neuroimaging control [13] *Primary:* Also known as prophylactic, performed simultaneously with a cranial surgical procedure, such as post-traumatic mass-effect lesion evacuation, for the prevention of subsequent ICP increase [13, 26]; it is estimated that edema increases after 4-5 days, so the bone is removed before this timeframe *Secondary:* Also known as therapeutic, performed as second-line therapy in the management of medically-refractory increased intracranial pressure [3, 19, 20] Useful in centers with multimodal neuromonitoring resources [26]	*Early:* Carried out in the first hours after the trauma in ranges from 4 to 24 hours [27] *Late:* Carried out after 24–48 hours post-trauma [28]. DC is not recommended after 4-5 days of trauma

Table 55.2 Types of surgical techniques for DC

Bifrontal	Hemispheric
In frontal lobes edema with or without associated injury [21]	In the presence of unilateral focal lesion with mass-effect (i.e malignant MCA ischemic stroke) [4]
Diffuse brain edema with posterior basal cistern compression (quadrigeminal) [4]	Diffuse brain edema with basal cistern compression (ambiens and crural) [4]
Anterior-posterior trauma vector	Latero-lateral trauma vector
Technique: Frontal and temporal bones are removed up to 2–3 cm preceding the coronal suture bilaterally. The superior sagittal sinus and the falx cerebri can be ligated to allow anterior expansion [23]	*Technique*: The frontal, temporal and parietal bones are removed from one or both sides, obtaining a bone flap of at least 12–15 cm, with subsequent dural opening [24, 25]

55.4 Neurological Syndromes and Decompressive Craniectomy: The ¨Open Box¨ Concept

When a bone flap is removed, the skull or "closed box," becomes an "open box" [3, 5, 29, 31, 32, 36]. Therefore, once swollen brain tissue herniates through the craniectomy defect, ICP and midline shift (mass effect) are immediately reduced, responding to the Monro-Kellie doctrine [29, 32]. After DC, the neurosurgical team and ICU team should pay attention to the new "invisible" variable, atmospheric pressure [37].

The "open box" concept has particular pathophysiological features. The lateral ventricle can migrate to the craniectomy defect. However, it is not clear whether this represents a localized effect of ex-vacuo hydrocephalus, altered CSF dynamics, or a combination of both phenomena [32, 37]. Hence, a disturbance of CSF dynamics may occur, including a "siphon effect" and subsequent reduction of CBF. This may be due to both the venous return disturbance and the subarachnoid space obliteration due to direct pressure on the brain parenchyma that compromise regional CPP [32].

Different neurological syndromes (some early and some late) associated with DC has been described [29, 32, 37], resulting from external and/or internal forces, such as pathophysiological consequences on intracranial compartments (Tables 55.3 and 55.4, Figs. 55.2 and 55.3).

Table 55.3 Intracranial and extracranial forces. Open box concept (Fig. 55.2)

Intracranial forces	
Cerebral spinal fluid (CSF) pressure	
Gravitational forces	
Physical properties	Brain compliance
	Masses
	Brain-bone interfaces
	Sites of dural insertions
Extracranial forces	
Galea aponeurotica	
Subgaleal fluid	
Atmospheric pressure	1 atm = 14.7 PSI = 1.033 cmH_2O

Table 55.4 Neurological syndromes associated with DC

Syndrome	Key feature
Syndrome of the trephined or post-traumatic syndrome	Headache, vertigo, tinnitus, insomnia, memory disturbances, hemiparesis, gait disturbances, epilepsy, mood swings, cognitive and behavioral disorders [30, 31]
Sinking flap syndrome	Focal neurological deficit in hemicraniectomies [33]
Motor syndrome of the trephined	Term focused on motor disorders [34, 35]
True syndrome of the trephined (similarities with sinking flap syndrome)	Focal deficit [29] Ex: Hemiparesis (resolves after cranioplasty)
Neurological susceptibility to the skull defect	Neurological symptoms after decompressive craniectomy with subsequent recovery with cranioplasty [3]

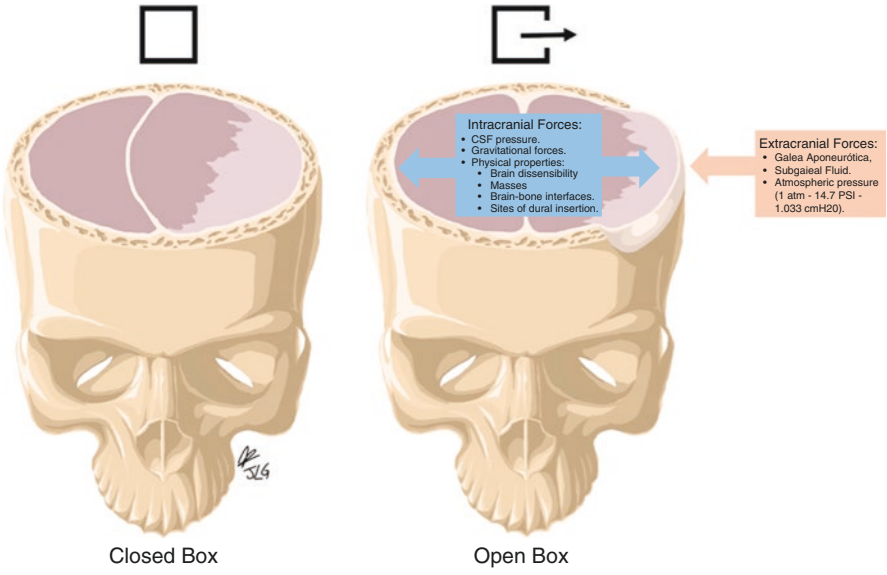

Fig. 55.2 Extracranial and intracranial forces in the "Open Box" concept

Consequently, the usefulness of TCD/TCCS in this clinical scenario, is real-time early detection of hemodynamic changes (CBFVs, spectral Doppler waveform, PI, etc.) to improve cerebral perfusion through individualized therapeutic decisions [30, 34] (Fig. 55.3).

55.5 TCD/TCCS: Hemodynamic Changes Associated with Decompressive Craniectomy

TCD/TCCS provides information for the evaluation of the hemodynamic changes of the "exposed" brain after bone window removal [5, 6], which facilitates the measurements.

After performing a DC, mechanical, systemic, and atmospheric pressure changes involved in cerebral perfusion must be considered [8, 29, 32, 42, 44]. The impact of cerebral hemodynamic changes (CBFVs and hemodynamic indexes) can be recorded by TCD/TCCS during post-DC follow-up in ICU (Table 55.5), as they are progressively restored.

Understanding the different cerebral hemodynamic patterns (pre- and post-DC), help the implementation of timely therapeutic decisions individualized to optimize CPP for each patient. Therefore, keep in mind that generalized treatment goals [17] can lead to hypo- or hyperperfusion phenomena, being deleterious for the patient [11, 12, 39, 40] (Figs. 55.4a–c and 55.5).

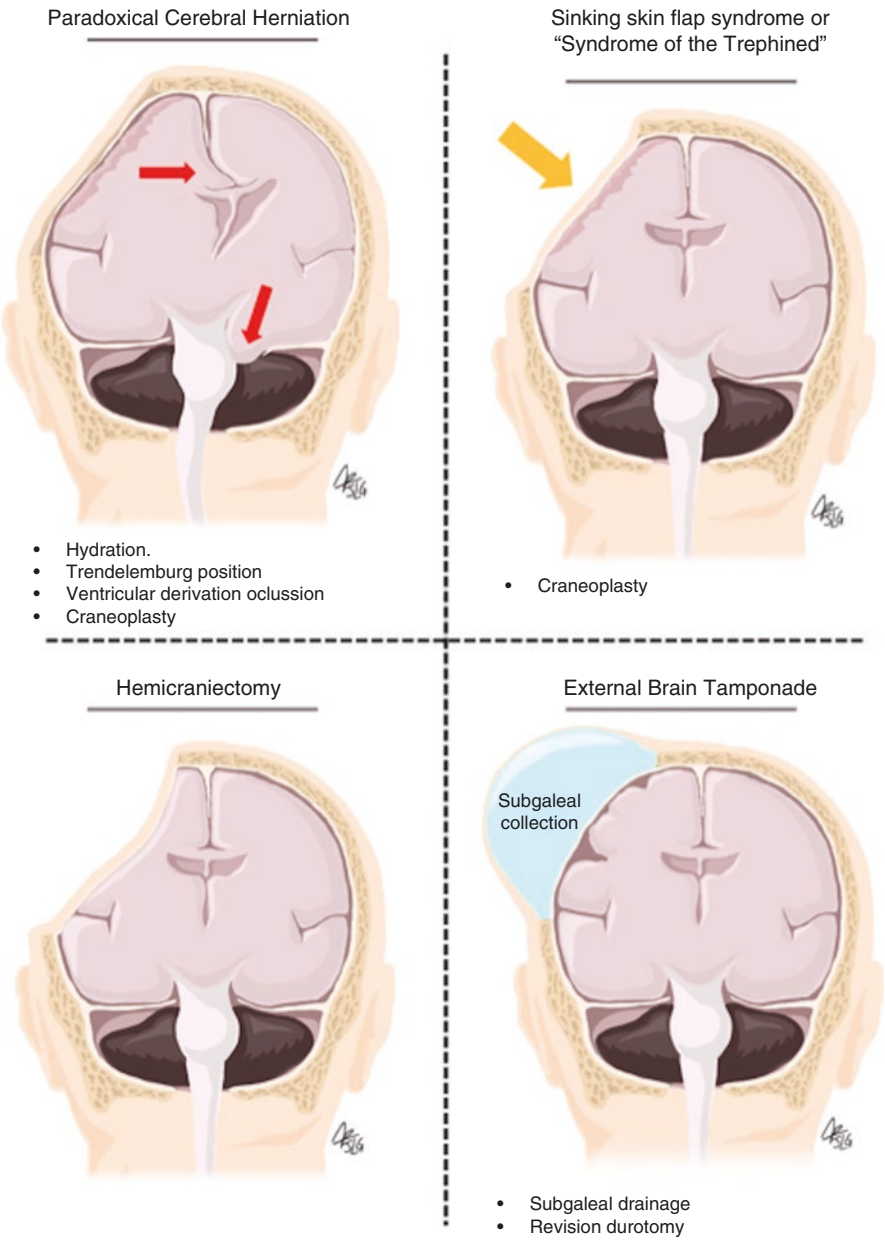

Fig. 55.3 Neurologic syndromes and potential treatments

Table 55.5 TCD/TCCS Patterns: Post-decompressive craniectomy

	TCD pattern				
	Normal	Intermediate /Transition	Oligemic	"Pure"Hyperemic (LI < 3)	Vasospasm (LI < 3)
PI	=	Normal/ ↑	Normal/ ↑	Normal/ ↑	Normal/ ↑
Wave morphology	=	Normal/ ↑	Hight resistance	↓	↓
MFV	=	Normal	↓	↑ ↑	↑ ↑ ↑
Congestion	=	Normal	Normal/	Normal/ ↓	Normal/ ↓

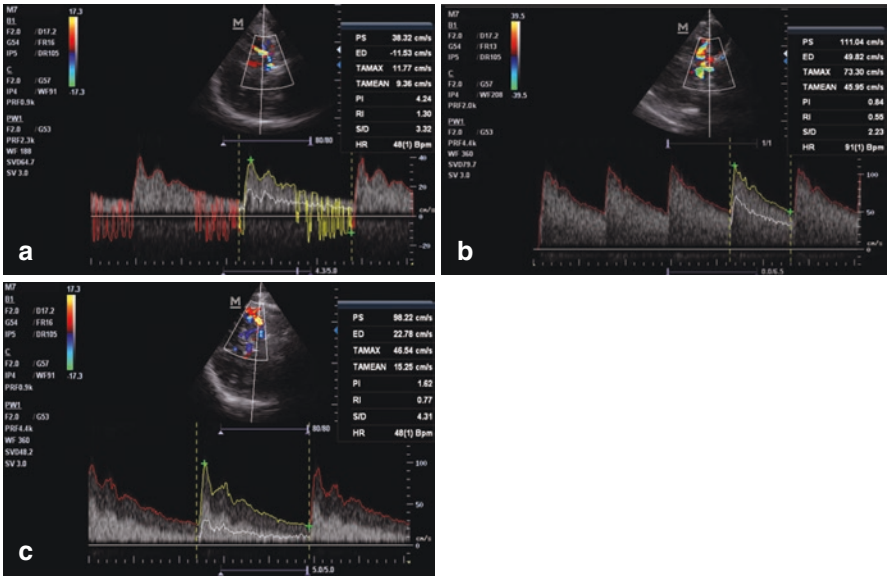

Fig. 55.4 (**a**) "Oligemic / hypoperfused" pattern in post-DC patient. This highlights an abnormally elevated PI and a very low amplitude of spectral Doppler wave, which in addition to low mean flow velocities (MFV, shown in the device screen as "TAMAX") in MCA (<40 cm/s) suggest severe intracranial hypertension. *ED* End-diastolic volume, *RI*Resistance index. (**b**) "Hyperemic/ hyperperfused" pattern in the patient of Fig. A, this time post-DC (48 hr). Although literature [40] has defined "hyperemia" with MCA MFV >100 cm/s, there is an increase in MCA MFV >30% in comparison with pre-DC values. Turbulent flow, vascular congestion, increasing spectral Doppler waveform amplitude and a marked decrease in PI are also shown, which suggests a possible "exacerbated" reperfusion phenomena of the vascular territories secondary to intracranial pressure reduction after DC. (**c**) "Intermediate" pattern post-DC (6 hr). Although it has been described as "non-specific" by some authors [40], in this particular context of early post-DC, we propose a transition pattern between oligemia and hyperemia, with a tendency to PI improving (but still increased), a normal spectral-waveform morphology and stable values of MFV, reflecting the importance of "normoperfusion" as a neuroprotective measure and treatment goal in the neurocritical patient

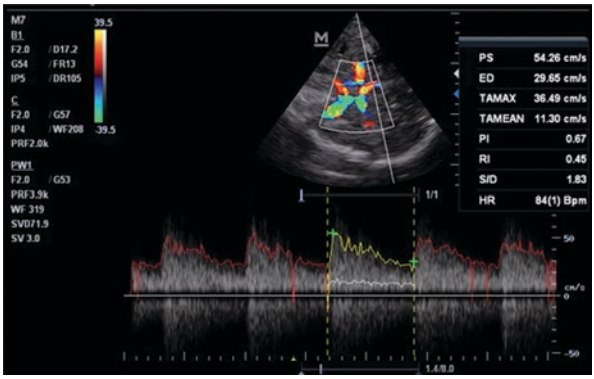

Fig. 55.5 Insonation of the posterior cerebral artery (P1) and associated findings. The PI normalization, spectral-waveform morphological changes, and also MFV normalization after DC had been also reflected in a global manner, as a response to intracranial pressure management and control

55.6 Conclusion

During follow-up of cerebral hemodynamic changes in patients with acute brain injury (ABI), it is important to prevent and identify disturbances that extend their hospital stay and determine unfavorable long-term outcomes [38]. In the context of refractory intracranial hypertension, DC is a crucial intervention to restore adequate cerebral perfusion and brain oxygenation delivery. TCD/TCCS is a noninvasive monitoring tool that provides useful information for hemodynamic parameters analysis and estimate cerebral prognosis of the critically ill patients with ABI [6, 22].

TCD/TCCS is an useful monitoring method to assess indirectly CBF in neurocritical patients to demonstrate its optimization after therapeutic interventions such as DC or external ventricular drain (EVD), providing data to follow-up and control of CPP and ICP changes derived from medical and surgical therapeutic interventions [8, 9]. However, the measurement of the hemodynamic variables by TCD/TCCS (CBFVs, spectral Doppler waveform, PI, etc.) is an operator- and/or acoustic window-dependent technique [6, 10]. Hence, it is vitally important to have high-expertise staff to reduce as much as possible the error rate on clinical interpretation of data [10, 38]. Although there is increasing knowledge about the hemodynamic and vascular perfusion changes during ABI after a DC (Table 55.5), the heterogeneous therapeutic results in this clinical scenario cannot be overlooked. Therefore, a careful, detailed and specific analysis of each clinical situation is required to make individualize decisions [5, 6, 8, 9, 10–12, 39, 40].

DC is currently considered as a "definitive" management to control intracranial hypertension. This data assure that this procedure is effective for the management of cerebral oligemia without necessarily implying a post-DC cerebral hemodynamic equilibrium [41, 42, 46]. This surgical procedure may cause secondary harmful effects by hyperemia (paradoxical increase of ICP and/or risk of bleeding) or oligemia (hypoperfusion, ischemia). These cerebral hemodynamic events are possible causes of perpetuous secondary brain injury [18].

In consequence, the need for early and protocolized management of these probable neurological worsening variables, (1) arterial hypertension, (2) hypervolemia status, (3) hyperdynamic states (exacerbate hyperemia), (4) dehydration status and ICP increases (worsen the oligemia), which are considered commonly as late causes of clinical deterioration. Hence, the cerebral hemodynamic repercussion of these physiological/pathophysiological variables can be assessed indirectly by TCD/TCCS through pre-post DC cerebral flow patterns analysis [6–8, 38–40]. In the specific case of patients with TBI, the metabolic crisis is not only the result of cerebral ischemia and hypoperfusion [39, 40] but even can occur under apparently normal conditions of cerebral blood flow assessed by TCD/TCCS.

Therefore, multimodal neuromonitoring (MMM) in ICU is crucial because microvascular alteration [41], cerebral excitotoxicity, electrical pathologic activity, and brain dysoxia [18, 39, 41] require the integration of different type of devices to arrive at a diagnosis, where information provided in real-time by TCD/TCCS at bedside is very useful to make-directed therapeutic decisions.

Finally, it is important to consider the skull multicompartmental theory at time to perform cerebral hemodynamic assess by TCD/TCCS [41, 46]. This theory refers to the fact that a patient with (or without) DC can develop hyperemia in one hemisphere and vasospasm in the contralateral hemisphere. These clinical conditions challenge classical management strategies, rendering them contradictory. However, bedside assessment by TCD/TCCS allows us to better understand these cerebral hemodynamic phenomena, motivating a more individualized treatment [37–41].

Algorithm

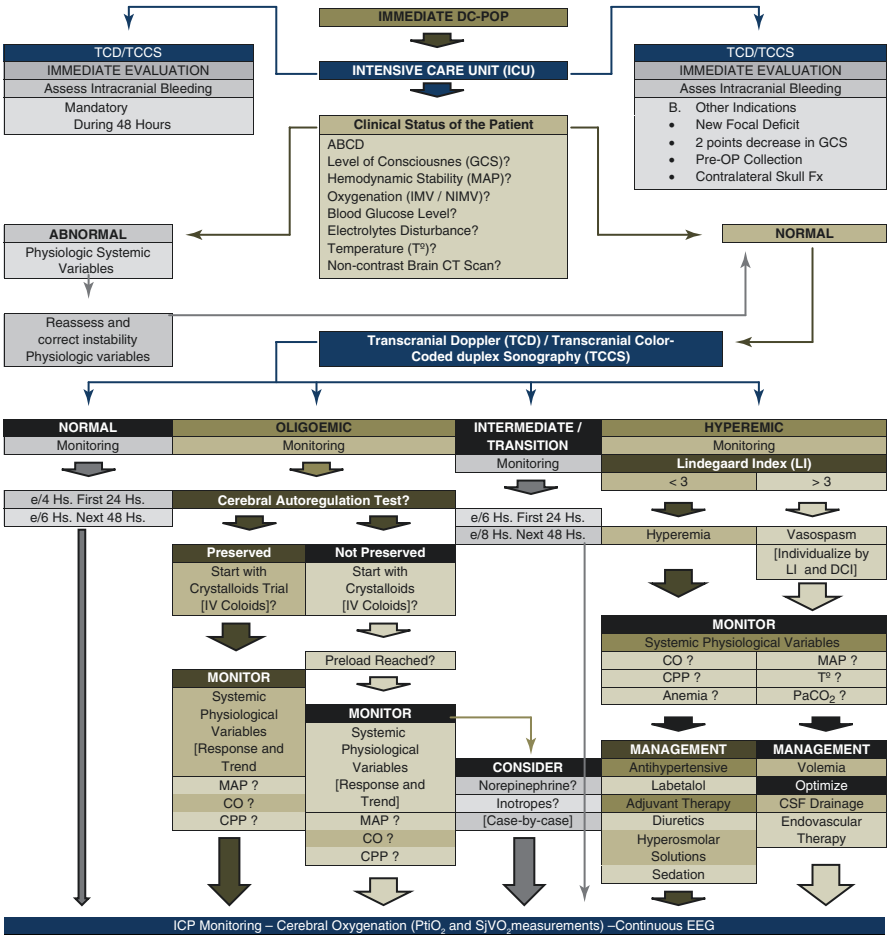

DC-POP Decompressive craniectomy postoperative, *ABCD* Airway-breathing-circulation-disability, *MAP* Mean arterial pressure, *IMV* Invasive mechanical ventilation, *NIMV* Non-invasive mechanical ventilation, *GCS* Glasgow coma scale, *Fx* Fracture, *IV* Intravenous, *CO* Cardiac output, *CPP* Cerebral perfusión pressure, *DCI* Delayed cerebral ischemia, *e/* Every, *Pre-OP* Pre-Operative

References

1. Fernández Domínguez J, et al. El Doppler Color Transcraneal en el estudio vascular cerebral. Elsevier Doyma. 2012;4(3):132–43.
2. Romero JA, Rivero OM. Chapter 19, Doppler transcraneal: Técnica y aplicaciones clínicas. In: Niño MC, Ferrer LE, editors. Neuroanestesia enfoque perioperatorio en el paciente neurológico, vol. 431–443. Editorial Distribuna; 2005.
3. Honeybul S, et al. Neurological susceptibility to a skull defect. Surg Neurol Int. 2014;5:83.
4. Lang S, et al. Monitoring and intraoperative management of elevated intracranial pressure and decompressive craniectomy. Elsevier; 2012. p. 289–310.
5. Song J, et al. Beneficial impact of early cranioplasty in patients with decompressive craniectomy: evidence from transcranial Doppler ultrasonography, vol. 156. Springer-Verlag Wien; 2013. p. 193–8.
6. Kalanuria A, Nyquist PA, Armonda RA, Razumovsky A, et al. Use of transcranial Doppler (TCD) ultrasound in the neurocritical care unit, vol. 24. Elsevier; 2013. p. 441–56.
7. Jaeger M, Soehle M, Meixensberger J, et al. Effects of decompressive craniectomy on brain tissue oxygen in patients with intracranial hypertension. J Neurol Neurosurg Psychiatry. 2003;74:513–5.
8. Daboussi A, et al. Cerebral hemodynamic changes in severe head injury patients undergoing decompressive craniectomy. J Neurosurg Anesthesiol. 2009;21:339–45.
9. Bor-Shen-Shu E, Jacobsen Teixeira M, Hirsch R, Ferreira de Andrade A, Marino R Jr, et al. Transcranial Doppler Sonography in tEwo patients who underwent Decompressive Craniectomy for Traumatic Brain Swelling. Arq Neuropsiquiatr. 2004;62(3-A)
10. Paredes I, et al. The effect of cranioplasty on cerebral hemodynamics as measured by perfusion computed tomography and Doppler ultrasonography. J Neurotrauma Mary Ann Liebert. 2006;33:1586–97.
11. Vicenzini E, et al. Transcranial Doppler for brain death after decompressive craniectomy: persistence of cerebral blood flow with flat EEG. 2010; Springer and ESICM. Intensive Care Med. 36:2163–4.
12. Lazaridis C, DeSantis SM, Vandergrift AW, Krishna V, et al. Cerebral blood flow velocity changes and the value of the pulsatility index post decompressive craniectomy. J Clin Neurosci. 2001;19:1052–4.
13. Rubiano AM, Villarreal W, Hakim EJ, Aristizabal J, Hakim F, Dìez JC, et al. Early decompressive craniectomy for neurotrauma: an institutional experience. Ulusal Travma ve Acil Cerrahi Dergisi = Turkish Journal of Trauma & Emergency Surgery: TJTES. 2009;15(1):28–38.
14. Guerra WK, Gaab MR, Dietz H, Mueller JU, Piek J, Fritsch MJ. Surgical decompression for traumatic brain swelling: indications and results. J Neurosurg. 1999;90:187–96.
15. Polin RS, Shaffrey ME, Bogaey CA, Tisdale N, Germanson T, Bocchicchio B, et al. Decompressive bifrontal craniectomy in the treatment of severe refractory posttraumatic cerebral edema. Neurosurgery. 1997;41:84–94.
16. Stocchetti N, Zanaboni C, Colombo A, et al. Refractory intracranial hypertension and "second-tier" therapies in traumatic brain injury. Intensive Care Med. 2008;34:461–7. 6.
17. Stocchetti N, Colombo A, Ortolano F, et al. Time course of intracranial hypertension after traumatic brain injury. J Neurotrauma. 2007;24:1339–46.
18. Stocchetti N, Maas AIR. Traumatic intracranial hypertension. N Engl J Med. 2014;370:2121–30.
19. Delashaw JB, Broaddus WC, Kassell NF, et al. Treatment of right hemispheric cerebral infarction by hemicraniectomy. Stroke. 1990;21:874–81.
20. Weiner GM, Lacey MR, Mackenzie L, et al. Decompressive craniectomy for elevated intracranial pressure and its effect on the cumulative ischemic burden and therapeutic intensity levels after severe traumatic brain injury. Neurosurgery. 2010;66:1111–8.
21. Kjellberg RN, Prieto A Jr. Bifrontal decompressive craniotomy for massive cerebral edema. J Neurosurg. 1971;34:488–93.

22. Larach DR, Larach DB, Larach MG. A life worth living: seven years after craniectomy. Neurocrit Care. 2009;11:106–11.
23. Cooper DJ, Rosenfeld JV, Murray L, et al. Decompressive craniectomy in diffuse traumatic brain injury. N Engl J Med. 2011;364:1493–502.
24. Vahedi K, Hofmeijer J, Juettler E, et al. Early decompressive surgery in malignant infarction of the middle cerebral artery: a pooled analysis of three randomised controlled trials. Lancet Neurol. 2007;6:215–22.
25. Michel P, Arnold M, Hungerbuhler HJ, et al. Decompressive craniectomy for space occupying hemispheric and cerebellar ischemic strokes: Swiss recommendations. Int J Stroke. 2009;4:218–23.
26. AI-Jishi, Saluja RS, AI-Jehani H, Lamoureux J, Maleki M, Marcoux J. Primary or secondary decompressive craniectomy: different indication and outcome. Can J Neurol Sci. 2011;38(4):612–20.
27. Wang R, Li M, Gao WW, Guo Y, Chen J, Tian HL. Outcomes of early decompressive craniectomy versus conventional medical management after severe traumatic brain injury: a systematic review and meta-analysis. Medicine (Baltimore). 2015;94(43):e1733.
28. Van der Meer C, Van Lindert E, Petru R. Late decompressive craniectomy as rescue treatment for refractory high intracranial pressure in children and adults. Acta Neurochir Suppl. 2012;114:305–10.
29. Fodstad H, Love JA, Ekstedt J, Fridén H, Liliequist B. Effect of cranioplasty on cerebrospinal fluid hydrodynamics in patients with the syndrome of the trephined. Acta Neurochir. 1984;70:21–30.
30. Granthan E, Landis H. Cranioplasty and the post traumatic syndrome. J Neurosurg. 1947;5:19–22.
31. Grant FC, Norcross NC. Repair of cranial defects by cranioplasty. Ann Surg. 1939;110:488–512.
32. Stiver SI, Wintermark M, Manley GT. Reversible monoparesis following decompressive hemicraniectomy for traumatic brain injury. J Neurosurg. 2008;109:245–54.
33. Yamaura A, Makino H. Neurological deficits in the presence of the sinking skin flap following decompressive craniectomy. Neurol Med Chir (Tokyo). 1977;17:43–53.
34. Schiffer J, Gur R, Nisim U, Pollak L. Symptomatic patients after craniectomy. Surg Neurol. 1997;47:231–7.
35. Segal DH, Oppenheim JS, Murovic JA. Neurological recovery after cranioplasty. Neurosurgery. 1994;34:729–31.
36. Gordon WA, Zafonte R, Cicerone K, Cantor J, Brown M, Lombard L, et al. Traumatic brain injury rehabilitation: state of science. Am J Phys Med Rehabil. 2006;85:343–82.
37. Akins P, Guppy KH. Sinking skin flaps, paradoxical herniation, and external brain tamponade: a review of decompressive craniectomy management. Neurocrit Cara. 2008;9:269–76.
38. Blanco P, Abdo-Cuza A. Transcranial Doppler ultrasound in neurocritical care. J Ultrasound. 2018;21:1–16.
39. Chang T, et al. Transcranial Doppler ultrasonography for the management of severe traumatic brain injury after decompressive craniectomy. World Neurosurg. 2019;126:e116–24.
40. Bor-Seng-Shu E, de-Lima-Oliveira M, Nogueira RC, Almeida KJ, EHA P, Paschoal FM Jr. Decompressive craniectomy for traumatic brain injury: postoperative TCD cerebral hemodynamic evaluation. Front Neurol. 2019;10:354.
41. Czosnyka M, Brady K, Reinhard M, Smielewski P, Steiner LA. Monitoring of cerebrovascular autoregulation: facts, myths, and missing links. Neurocrit Care. 2009;10:373–86.

Chapter 56
Therapeutic Hypothermia (TH) in ICU: Cerebral Hemodynamics Monitoring by Transcranial Doppler (TCD/TCCS)

Sanjeev Sivakumar and Christos Lazaridis

Key Points

1. The changes in MFV as visualized by TCD in the main cerebral arteries strongly reflect changes in cerebral blood flow (CBF) following return of spontaneous circulation after cardiopulmonary resuscitation and during therapeutic hypothermia.
2. Early post-cardiac arrest hypoperfusion syndrome is characterized by low MFV_{MCA} and high PI. MFV_{MCA} gradually increases over 72 h and during mild hypothermia toward normal values and continues to increase post rewarming.
3. The relationship between CPP and MFV can be estimated using an index (Mx), which can be used in the monitoring of cerebral autoregulation and establish treatment thresholds.
4. Among patients with acute brain injury, rewarming can acutely increase cerebral metabolic rate of oxygen ($CMRO_2$), inducing cerebral vasodilation and increase of cerebral blood volume and flow indicated by increase in MFV_{MCA}, with a rebound increase in ICP and sustained increase of PI.
5. A linear relationship between PI and ICP has been described; an upward trend in PI during hypothermia or rewarming represents reduced intracranial compliance, high ICP and potentially a low CPP. Refractory ICP can lead to cerebral circulatory arrest, represented on TCD/TCCS by loss of diastolic flow, appearance of retrograde diastolic flow, systolic spikes, and finally no detectable flow in the cerebral arteries.

S. Sivakumar
Department of Neurology, University of South Carolina-Greenville School of Medicine, Greenville, SC, USA
e-mail: Sanjeev.Sivakumar@prismahealth.org

C. Lazaridis (✉)
Neurocritical Care, Departments of Neurology and Neurosurgery, University of Chicago, Chicago, IL, USA
e-mail: lazaridis@uchicago.edu

C. N. Rodríguez et al. (eds.), *Neurosonology in Critical Care*,
https://doi.org/10.1007/978-3-030-81419-9_56

56.1 Introduction

Targeted temperature management (TTM) and therapeutic hypothermia (TH) are modalities with a recognized utility in critical care, particularly in the setting of post-resuscitative care [1–3]. Therapeutic hypothermia involves treatment to achieve and maintain a target body temperature for specific durations of time aimed at improving neurologic outcomes or mitigating secondary brain injury. Hypothermia can have significant effects on cerebral hemodynamics and cerebral blood flow (CBF).

With growing evidence on the benefits of hypothermia for a broad range of cerebrovascular diseases, TCD/TCCS has found utility for the noninvasive monitoring of cerebral hemodynamics during TH and TTM. Recent literature describing novel uses of TCD that can be applied in the setting of HT include estimation of intracranial pressure (ICP) and cerebral perfusion pressure (CPP) and monitoring of cerebrovascular reactivity to $PaCO_2$ after cardiac arrest [4].

In this chapter, we review the physiology of brain temperature regulation, the effects of temperature on cerebral hemodynamics, and use of TCD/TCCS for noninvasive monitoring of cerebral hemodynamics during therapeutic hypothermia in the intensive care unit.

56.2 Brain Temperature Regulation: Physiology and Effects of Temperature on Cerebral Hemodynamics

The core body temperature is maintained at 37 °C under normal conditions. The brain is highly metabolically active, and consumes 25% of total body glucose and 20% of total body oxygen for ATP production [5]. Blood entering the brain is at core temperature, which is lower than brain temperature. The gradient between brain and body temperature ranges from 0.3 °C to 1.1 °C, and is usually higher in the brain. While there is a correlation between brain and body temperature, the brain-body temperature gradient may be reversed with brain hyperthermia or hypothermia [6].

Cerebral metabolic rate of oxygen ($CMRO_2$) and regional cerebral blood flow (CBF) are important determinants of brain temperature. Variations in these parameters can change or reverse the gradient between brain and core temperatures. By modulation of the diameter of cerebral vasculature, $CMRO_2$ is physiologically coupled to CBF [7]. Reduced CBF and oxygen extraction with induction of hypothermia and subsequent increase of CBF during rewarming has been demonstrated [8]. Increase in $CMRO_2$ results in vasodilation and increase in CBF, which in turn leads to increase in cerebral blood volume (CBV). When the cerebral autoregulatory mechanisms are intact, increase in CBV is compensated by cerebrospinal fluid (CSF) outflow from the cranium and collapse of low pressure cerebral veins. Upon exhaustion of these mechanisms, the ICP increases. Increase in ICP can result in secondary brain injury due to ischemia resulting from reduction in CPP.

Fever has been associated with metabolic distress. Increase in ICP with fever has been observed among patients with acute brain injury [9, 10]. Likewise, a decline in ICP with fever defervescence has been demonstrated [9, 11, 12]. Increase in ICP can be associated with increased "fuel" delivery, to compensate for metabolic demand during fever. Cerebral microdialysis studies have demonstrated preservation of the lactate/pyruvate ratio (LPR) during fever, which is indicative of adequate substrate delivery for aerobic metabolism [10]. Cerebral energy crisis at a cellular level ensues once maximal cerebral vasodilation occurs, after which a further increase in $CMRO_2$ may not be compensated by further increases in CBF. Transcranial Doppler can be used to noninvasively monitor the hemodynamic changes during hypothermia, by measuring cerebral blood flow velocity, ICP, and CPP.

56.3 Cerebrovascular Hemodynamics Parameters: Utility of Monitoring Therapeutic Hypothermia

The conventional parameters obtained using TCD/TCCS include peak systolic velocity (PSV), end-diastolic velocity (EDV), and mean flow velocity (MFV) represented by the time average mean of maximum velocity or TAMAX. The Pourcelot resistivity index (RI) and Gosling pulsatility index (PI) give an estimation of downstream resistance in the cerebral circulation.

$$\mathrm{PI} = \left(\mathrm{PSV} - \mathrm{EDV}\right) / \mathrm{MFV} \tag{56.1}$$

Normal PI in the MCA varies between 0.69 ± 0.10 at 55 mm and 0.71 ± 0.13 at 30 mm. PI has been shown to correlate with ICP; PI variation of 2.4% is reflected by a 1 mmHg shift of ICP in the same direction [13–15].

The Pourcelot resistivity index (RI) is calculated using the following formula (Eq. 56.2):

$$\mathrm{RI} = \left(\mathrm{PSV} - \mathrm{EDV}\right) / \mathrm{PSV} \tag{56.2}$$

Estimation of CBF using TCD/TCCS-measured cerebral blood flow velocity (CBF-V) has been described in literature using the following equation [16] (Eq. 56.3):

$$\mathrm{CBF} = \left[\left(60 \times \alpha \times \mathrm{K} \times \mathrm{A}\right) / \mathrm{T}\right] \times \mathrm{CBF} - \mathrm{V} \tag{56.3}$$

CBF measured in mL/100 g/min, *alpha* cosine of angle of insonation, *K* constant, *A* cross-sectional area of vessel in cm2, *T* territory of vessel supply in 100 g of brain tissue, *CBF-V* cerebral blood flow velocity in cm/s.

Noninvasive measurement of ICP and CPP using TCD/TCCS have been proposed and validated in numerous studies. Estimation of CPP using TCD-measured

CBF-V and Near-Infrared Spectroscopy (NIRS)-based measurements of cerebral oxygen saturation (rSO_2) have been proposed in recent studies [17, 18]. Using serial estimations of MFV_{MCA} and diastolic flow velocities, the estimated CPP (eCPP) is calculated using the following formula (Eq. 56.4):

$$\text{eCPP} = \left(\text{MAP} \times \text{EDV}_{\text{MCA}}\right) / \left(\text{MFV}_{\text{MCA}} + 14\right)[17] \tag{56.4}$$

TCD/TCCS-based estimation of ICP(ICPtcd) has also been described. In patients with TBI who have invasive ICP monitoring (external ventricular drain or bolt), the acoustic window ipsilateral to the ICP bolt is preferably used to estimate the ICP, using the following equation (Eq. 56.5):

$$\textbf{ICPtcd} = \textbf{MAP} - \textbf{eCPP}[17] \tag{56.5}$$

TCD/TCCS-based eCPP has been validated to estimate cerebral perfusion after TBI and cardiac arrest and has prognostic implications. A significantly lower eCPP was found among non-survivors of cardiac arrest when compared to survivors [18]. Applications of TTM and TH in neurointensive care unit are shown in Table 56.1.

56.4 TCD/TCCS: Monitoring of Cerebral Hemodynamics in Therapeutic Hypothermia

56.4.1 TCD/TCCS: Baseline Cerebral Hemodynamic Values

The ideal target population for noninvasive cerebrovascular monitoring are comatose survivors (GCS ≤8) after successful resuscitation following cardiac arrest, and after acute brain injury. All eligible patients are cooled to 32–36 °C by rapid infusion of cold IV crystalloids followed by external cooling, or using intravascular temperature management systems. Temperature is monitored continuously using rectal temperature probes. All patients are sedated with midazolam and/or propofol and fentanyl. In case of shivering, patients are paralyzed using intravenous rocuronium or cisatracurium. All patients are intubated and mechanically ventilated to obtain an adequate PaO_2 > 75 mmHg and $PaCO_2$ between 35 and 40 mmHg. Alpha-stat is used for pH maintenance. Central venous and arterial catheters are routinely used for ICU patients. In addition, patients with severe TBI have invasive ICP monitoring, often in addition to brain tissue oxygenation monitoring and less commonly cerebral microdialysis (CMD). End-tidal volume CO_2 is monitored in all patients. Once the patient has been stabilized, the ideal first step is to obtain a baseline TCD study.

A 2 MHz TCD probe is used to insonate the transtemporal window bilaterally and identify the middle (MCA), anterior (ACA), and posterior (PCA) cerebral arteries. The MCA is chosen for continuous monitoring as this vessel perfuses

Table 56.1 Guidelines for the use of therapeutic hypothermia and targeted temperature management in neurocritical care

Clinical indication	Level of evidence (where available)
Comatose survivors after successful cardiopulmonary resuscitation (CPR) [1] 1. TH (32–34° C for 24 hours) for VT/VF arrest 2. TTM (36° C for 24 hours, 8 hours rewarming to 37 and temperature management for 72 hours) for VT/VF or PEA/asystole arrest is an acceptable alternative to TH 3. VF arrest, insufficient evidence to support or refute 32 °C vs 34 °C	1. Highly likely and effective in improving neurological outcome and survival compared to non-TH. Level A 2. As effective as TH in improving neurological outcomes and survival; acceptable alternative. Level B 3. Lack of evidence. Class III, Level U
Traumatic brain injury 1. Early (within 2.5 hours), short-term (48 hours post injury), prophylactic hypothermia is not recommended to improve outcomes, in patients with diffuse injury [19] 2. Hypothermia can lower ICP in patients with TBI [20–23]	1. Level II B
Subarachnoid hemorrhage 1. Induced hypothermia during aneurysm surgery 2. Surface/intravascular cooling when antipyretics fail for fever control, during at-risk period for delayed cerebral ischemia (DCI)	1. Not routinely recommended but may be reasonable in selected cases. Class III (no benefit) Level B (Single RCT) [24] 2. Low quality of evidence, strong recommendation [25]
Acute ischemic stroke 1. Induced hypothermia for ischemic stroke 2. Hypothermia for cerebral edema management	1. Benefit not established. Only in context of clinical trials. Class IIb (weak), Level B-R (Moderate quality, 1 or more RCT) [26] 2. No benefit (Class III) [26]
Hypothermic cardiopulmonary bypass (CPB) Hypothermic CPB is associated with abnormal CBF– blood pressure autoregulation, which can lead to increased incidence of stroke. Impaired autoregulation is worsened with rewarming. TCD can be used for continuous monitoring of CBF-blood pressure autoregulation during CPB [27].	No recommendation for a guideline concerning optimal temperature for weaning from CPB due to insufficient published evidence

approximately 80% of the cerebral hemisphere and its accessibility is easy and reproducible. Trends in cerebral hemodynamics are most accurate when TCD measurements are taken at the same depth and insonation angle. The transducer is held at this depth using a headframe, which will allow for serial monitoring during induction and maintenance of hypothermia. Time integrated arterial blood pressure and TCD data are sampled. The PI, RI, CBF velocities, and eCPP (in patients without invasive ICP monitoring) can be calculated using equations 56.1–56.5. Arterial blood pressure data and TCD signals can be sampled with an analog-to-digital converter at 60 Hz. Processing these data with ICM+ software (University of Cambridge, Cambridge, UK) has been previously described [28, 29].

Time domain analysis of slow wave changes in TCD-derived CBF velocity in response to spontaneous changes in arterial blood pressure has been validated as means for continuous monitoring of CBF autoregulation [28, 29]. The TCD signals can be time integrated as nonoverlapping 10-s mean values. Correlation between MAP and TCD CBF velocities can then be calculated. The relationship between CPP and TCD measured-CBF velocity is given by the mean velocity index (Mx). When CBF and arterial blood pressure autoregulate, this index is near 0 or negative; when the index approaches 1.0 (high correlation), blood pressure is outside autoregulatory limits. A continuous correlation coefficient can be calculated between MAPs and TCD flow velocities obtaining a mean flow velocity index. Absolute Mx values ranging between 0.3 and 0.5 are indicative of impaired autoregulation [30, 31].

Post-resuscitation myocardial dysfunction can result in low cardiac output in the first hours after ROSC. Cardiac output can change CBF, independent of changes in MAP. Immediately after cardiac arrest the MFV_{MCA} as a parameter of CBF is low, with a high PI. This low flow state represents cerebral hypoperfusion phase of the post-cardiac arrest syndrome which has been shown to last up to 24 h, and is explained by increased cerebrovascular resistance due to imbalance of endothelin and cyclic guanosine monophosphate [32]. This phase is followed by normoperfusion, or hyperperfusion in several patients which can be associated with risk of brain swelling [33–35]. Lower MFV immediately following arrest, higher initial cerebrovascular resistance, gradual increase in MFV (opposed to pronounced increase in MFV_{MCA}), and concomitant change in cerebrovascular profile from vasoconstriction on admission to vasodilation after 72 h have been associated with increased survival in some studies, whereas others show no correlation with patient outcome [36]. A sufficiently high CPP should be maintained in the first hours after cardiac arrest to avoid secondary brain injury; MAP ranging from 85 to 105 mmHg has been suggested [37]. In contrast, a low PI and low MFV reflect inadequate cardiac output [38]. Preserved cerebrovascular reactivity to changes in $PaCO_2$ and disturbed cerebral autoregulation are described in many patients after cardiac arrest [34, 39]. These early changes in cerebral hemodynamics can be monitored by obtaining a baseline TCD/TCCS study post ROSC. An example of global hypoperfusion during the early hours after cardiac arrest monitored by TCCS is shown in Fig. 56.1.

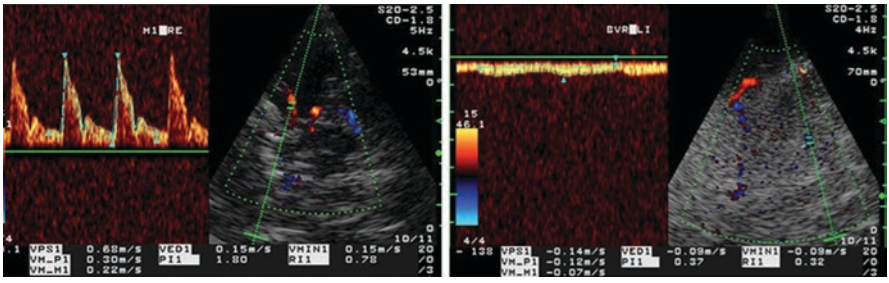

Fig. 56.1 Example of cerebral hypoperfusion 24 h after cardiac arrest. Left: blood flow in the right middle cerebral artery. Note the reduced mean blood flow velocity (MFV 30 cm/s) and increased pulsatility (pulsatility index: 1.8). Right: normal blood flow in the left basal vein of Rosenthal (MFV 12 cm/s). (Reprinted from Doepp Connolly et al. [43]. With permission from Elsevier)

56.4.2 TCD/TCCS: Monitoring of Cerebral Autoregulation During Hypothermia

Hypothermia (32–34 °C) and TTM (36 °C) using surface and/or intravascular cooling devices are typically initiated and maintained for 24 hours in the ICU post-cardiac arrest, followed by gradual rewarming (0.5 °C/h) to 37 °C. Hypothermia may be used for longer periods in patients with TBI. However, while hypothermia has been shown to reduce ICP, early prophylactic hypothermia is not recommended for TBI [22].

Upon induction of TTM or hypothermia in patients following cardiac arrest, the CBF velocities from bilateral proximal MCA are monitored using a headframe. Measurements are obtained at least twice daily to monitor trends at three time points: pre-hypothermia phase, hypothermia phase (12–24 h in cardiac arrest, longer in other diagnoses), and rewarming phase (12–48 h after body temperature reaches 36 °C). The mean flow velocity in the MCA, as a parameter of CBF, is low in the first hours after cardiac arrest and can decrease further during hypothermia, followed by gradual increase toward normal values with rewarming [33]. Jugular venous oxygenation has been demonstrated to be normal during hypothermia; together with low MFV_{MCA}, this suggests a decreased cerebral metabolism with hypothermia and TTM. CBF autoregulation is continuously monitored using Mx. Rewarming from mild or moderate hypothermia can be associated with impairment of CBF autoregulation denoted by an Mx $\geq$0.4 [27]. Impaired autoregulation may cause persistent increase of PI, and decreased MFV. During rewarming, a pressure passive CBF could have deleterious effects on cerebral perfusion. This is of particular significance in patients with cerebrovascular disease, as MAP can decrease during this phase. High PI in the rewarming phase can predict hypoperfusion and raised ICP, and is an indication to return to moderate hypothermia or optimize hemodynamic conditions. Presence of low PI with high MFV may reflect hyperemia, vasospasm, or stenosis. Impaired CBF autoregulation increases the risk of neurological complications, particularly ischemic stroke. When the Mx exceeds 0.3, arterial blood pressure is below the patient's lower autoregulatory "threshold" or "breakpoint." This should trigger targeted therapy to optimize MAP within the autoregulatory range, reflected by a decrease of Mx below 0.3, which means a lower risk of adverse cerebrovascular events.

In patients with TBI, impaired CBF autoregulation is a predictor of adverse neurological outcomes. Conversely, outcomes improve when arterial blood pressure is optimized within the autoregulatory range [28, 40]. In patients with reduced intracranial compliance, small changes in CBV can have an effect on ICP. The PI can increase during re-warming following prolonged hypothermia [41]. A linear relationship between PI and ICP has been described [13, 42]. In patients with diffuse TBI without invasive ICP monitoring, an upward trend in PI should alert the physician to reduced intracranial compliance, high ICP, and potentially a low CPP. In addition, high PI may predict inadequate reperfusion or hypoperfusion related to raised ICP. With refractory intracranial hypertension, brain herniation and cerebral circulatory arrest can ensue. This is represented by a pattern of loss of diastolic flow,

appearance of retrograde diastolic flow, or no detectable flow in the cerebral arteries on TCD. CBF velocity can vary despite a constant CPP; CPP can remain stable as MAP reduction is typically concurrent to ICP decrease during hypothermia.

In patients with severe TBI where hypothermia is used to control refractory ICP, the integration of TCD with multimodal monitoring allows for dynamic cerebral hemodynamic monitoring. Induction of hypothermia decreases $CMRO_2$. $CMRO_2$ is physiologically coupled to CBF via modulation of vessel diameter, and this results in a decrease in CBF and CBV. TCD is used to monitor CBF-V during this phase. Rewarming poses challenges in patients with severe diffuse brain injury with low intracranial compliance. Rewarming can acutely increase $CMRO_2$, inducing cerebral vasodilation and increase in CBV and CBF and a rebound increase in ICP. Preserved CO_2 reactivity has been demonstrated in early stages of hypothermia [34]. Changes in arterial $PaCO_2$ correlates with changes in MFV_{MCA} and prolonged decrease in $PaCO_2$ can reduce CBF resting in mismatch between cerebral oxygen demand and supply. Ventilator settings and serial arterial blood gases should be monitored. Monitoring CBF-V, PI, and Mx during rewarming allows the detection of the autoregulatory threshold, providing a target CPP value for treatment. In conjunction with brain tissue oxygen tension ($P_{bt}O_2$) and CMD, TCD/TCCS allows for individualizing CPP goals in patients with severe TBI. Identifying thresholds for temperature and physiologic interactions and targeted treatments to preserve CPP can prevent secondary brain injury. Treatment algorithm demonstrating use of TCD in the neuromonitoring of hypothermia is shown below.

56.5 Conclusion

Serial TCD/TCCS assessment of intracranial hemodynamics is a feasible diagnostic bedside tool in the acute phase after cardiac arrest, acute brain injury, and for neuromonitoring during targeted temperature management and therapeutic hypothermia.

Algorithm

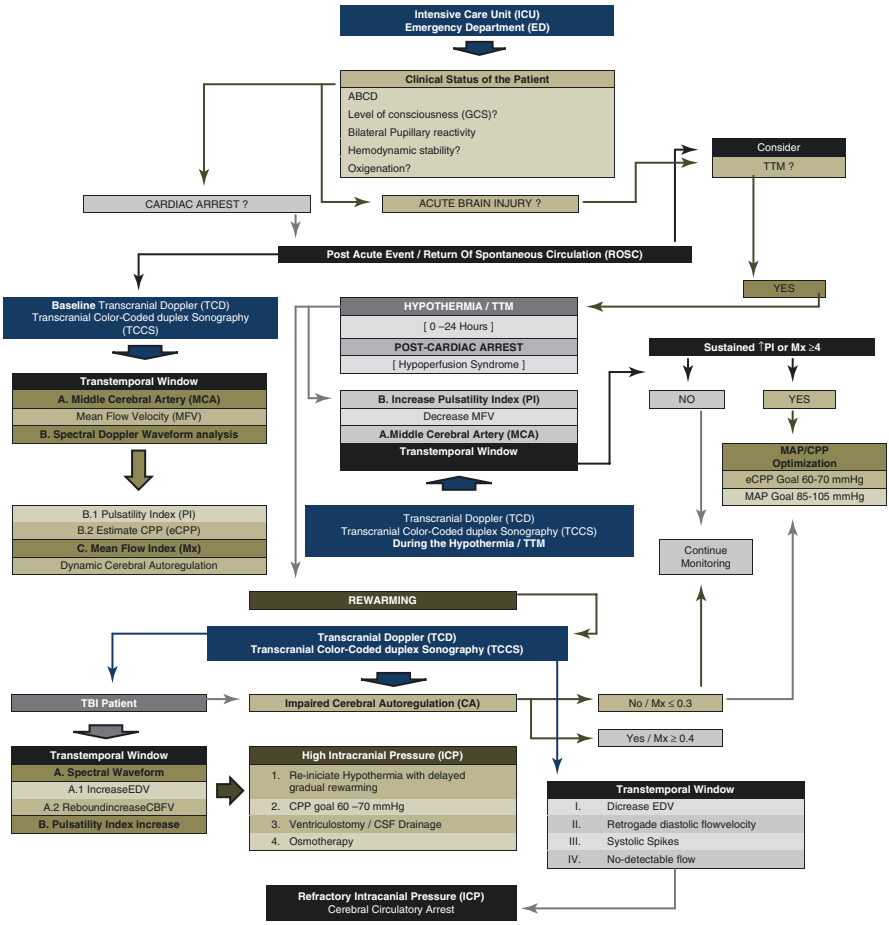

ABCD Airway-breathing-circulation-disability, *TTM* Target temperatura management, *ICP* Intracranial pressure, *EDV* End-distolic velocity, *CBFV* Cerebral blood flow velocity, *CSF* Cerebrospinal fluid, *CPP* cerebral perfusión pressure, *Mx* Mean flow index, ↑ Increase, *MAP* Mean arterial pressure

References

1. Geocadin RG, Wijdicks E, Armstrong MJ, et al. Practice guideline summary: reducing brain injury following cardiopulmonary resuscitation: report of the Guideline Development, Dissemination, and Implementation Subcommittee of the American Academy of Neurology. Neurology. 2017;88:2141–9.

2. Howes D, Gray SH, Brooks SC, et al. Canadian Guidelines for the use of targeted temperature management (therapeutic hypothermia) after cardiac arrest: a joint statement from The Canadian Critical Care Society (CCCS), Canadian Neurocritical Care Society (CNCCS), and the Canadian Critical Care Trials Group (CCCTG). Resuscitation. 2016;98:48–63.
3. Cariou A, Payen JF, Asehnoune K, et al. Targeted temperature management in the ICU: guidelines from a French expert panel. Anaesth Crit Care Pain Med. 2017.
4. Voicu S, Deye N, Malissin I, et al. Influence of alpha-stat and pH-stat blood gas management strategies on cerebral blood flow and oxygenation in patients treated with therapeutic hypothermia after out-of-hospital cardiac arrest: a crossover study. Crit Care Med. 2014;42:1849–61.
5. KG G. The cerebral blood supply. Energy metabolism of the brain. In: Go KG, editor. Cerebral pathophysiology. Amsterdam: Elsevier; 1991. p. 66–172.
6. Smith CM, Adelson PD, Chang YF, et al. Brain-systemic temperature gradient is temperature-dependent in children with severe traumatic brain injury. Pediatr Crit Care Med. 2011;12:449–54.
7. Lassen NA, Christensen MS. Physiology of cerebral blood flow. Br J Anaesth. 1976;48:719–34.
8. Lemiale V, Huet O, Vigue B, et al. Changes in cerebral blood flow and oxygen extraction during post-resuscitation syndrome. Resuscitation. 2008;76:17–24.
9. Rossi S, Zanier ER, Mauri I, Columbo A, Stocchetti N. Brain temperature, body core temperature, and intracranial pressure in acute cerebral damage. J Neurol Neurosurg Psychiatry. 2001;71:448–54.
10. Stocchetti N, Protti A, Lattuada M, et al. Impact of pyrexia on neurochemistry and cerebral oxygenation after acute brain injury. J Neurol Neurosurg Psychiatry. 2005;76:1135–9.
11. Oddo M, Frangos S, Milby A, et al. Induced normothermia attenuates cerebral metabolic distress in patients with aneurysmal subarachnoid hemorrhage and refractory Fever. Stroke. 2009;40:1913–6.
12. Puccio AM, Fischer MR, Jankowitz BT, Yonas H, Darby JM, Okonkwo DO. Induced normothermia attenuates intracranial hypertension and reduces fever burden after severe traumatic brain injury. Neurocrit Care. 2009;11:82–7.
13. Bellner J, Romner B, Reinstrup P, Kristiansson KA, Ryding E, Brandt L. Transcranial Doppler sonography pulsatility index (PI) reflects intracranial pressure (ICP). Surg Neurol. 2004;62:45–51; discussion.
14. Voulgaris SG, Partheni M, Kaliora H, Haftouras N, Pessach IS, Polyzoidis KS. Early cerebral monitoring using the transcranial Doppler pulsatility index in patients with severe brain trauma. Med Sci Monit. 2005;11:CR49–52.
15. Zweifel C, Czosnyka M, Carrera E, de Riva N, Pickard JD, Smielewski P. Reliability of the blood flow velocity pulsatility index for assessment of intracranial and cerebral perfusion pressures in head-injured patients. Neurosurgery. 2012;71:853–61.
16. Schatlo B, Glasker S, Zauner A, Thompson BG, Oldfield EH, Pluta RM. Continuous neuromonitoring using transcranial Doppler reflects blood flow during carbon dioxide challenge in primates with global cerebral ischemia. Neurosurgery. 2009;64:1148–54.
17. Rasulo FA, Bertuetti R, Robba C, et al. The accuracy of transcranial Doppler in excluding intracranial hypertension following acute brain injury: a multicenter prospective pilot study. Crit Care. 2017;21:44.
18. Taccone FS, Crippa IA, Creteur J, Rasulo F. Estimated cerebral perfusion pressure among post-cardiac arrest survivors. Intensive Care Med. 2018.
19. Carney N, Totten AM, O'Reilly C, et al. Guidelines for the Management of Severe Traumatic Brain Injury, Fourth Edition. Neurosurgery. 2017;80:6–15.
20. Lee HC, Chuang HC, Cho DY, Cheng KF, Lin PH, Chen CC. Applying cerebral hypothermia and brain oxygen monitoring in treating severe traumatic brain injury. World Neurosurg. 2010;74:654–60.
21. Qiu W, Zhang Y, Sheng H, et al. Effects of therapeutic mild hypothermia on patients with severe traumatic brain injury after craniotomy. J Crit Care. 2007;22:229–35.

22. Smrcka M, Vidlak M, Maca K, Smrcka V, Gal R. The influence of mild hypothermia on ICP, CPP and outcome in patients with primary and secondary brain injury. Acta Neurochir Suppl. 2005;95:273–5.
23. Zhao QJ, Zhang XG, Wang LX. Mild hypothermia therapy reduces blood glucose and lactate and improves neurologic outcomes in patients with severe traumatic brain injury. J Crit Care. 2011;26:311–5.
24. Connolly ES Jr, Rabinstein AA, Carhuapoma JR, et al. Guidelines for the management of aneurysmal subarachnoid hemorrhage: a guideline for healthcare professionals from the American Heart Association/american Stroke Association. Stroke. 2012;43:1711–37.
25. Diringer MN, Bleck TP, Claude Hemphill J 3rd, et al. Critical care management of patients following aneurysmal subarachnoid hemorrhage: recommendations from the Neurocritical Care Society's Multidisciplinary Consensus Conference. Neurocrit Care. 2011;15:211–40.
26. Powers WJ, Rabinstein AA, Ackerson T, et al. 2018 Guidelines for the Early Management of Patients With Acute Ischemic Stroke: A Guideline for Healthcare Professionals From the American Heart Association/American Stroke Association. Stroke. 2018;49:e46–e110.
27. Joshi B, Brady K, Lee J, et al. Impaired autoregulation of cerebral blood flow during rewarming from hypothermic cardiopulmonary bypass and its potential association with stroke. Anesth Analg. 2010;110:321–8.
28. Steiner LA, Czosnyka M, Piechnik SK, et al. Continuous monitoring of cerebrovascular pressure reactivity allows determination of optimal cerebral perfusion pressure in patients with traumatic brain injury. Crit Care Med. 2002;30:733–8.
29. Steiner LA, Coles JP, Johnston AJ, et al. Assessment of cerebrovascular autoregulation in head-injured patients: a validation study. Stroke. 2003;34:2404–9.
30. Czosnyka M, Brady K, Reinhard M, Smielewski P, Steiner LA. Monitoring of cerebrovascular autoregulation: facts, myths, and missing links. Neurocrit Care. 2009;10:373–86.
31. Brady KM, Lee JK, Kibler KK, et al. Continuous time-domain analysis of cerebrovascular autoregulation using near-infrared spectroscopy. Stroke. 2007;38:2818–25.
32. Nolan JP, Neumar RW, Adrie C, et al. Post-cardiac arrest syndrome: epidemiology, pathophysiology, treatment, and prognostication. A Scientific Statement from the International Liaison Committee on Resuscitation; the American Heart Association Emergency Cardiovascular Care Committee; the Council on Cardiovascular Surgery and Anesthesia; the Council on Cardiopulmonary, Perioperative, and Critical Care; the Council on Clinical Cardiology; the Council on Stroke. Resuscitation. 2008;79:350–79.
33. Bisschops LL, van der Hoeven JG, Hoedemaekers CW. Effects of prolonged mild hypothermia on cerebral blood flow after cardiac arrest. Crit Care Med. 2012;40:2362–7.
34. Bisschops LL, Hoedemaekers CW, Simons KS, van der Hoeven JG. Preserved metabolic coupling and cerebrovascular reactivity during mild hypothermia after cardiac arrest. Crit Care Med. 2010;38:1542–7.
35. Alvarez-Fernandez JA. Transcranial Doppler ultrasound use in post-cardiac arrest coma. Rev Neurol. 2011;53:545–54.
36. van den Brule JM, Vinke E, van Loon LM, van der Hoeven JG, Hoedemaekers CW. Middle cerebral artery flow, the critical closing pressure, and the optimal mean arterial pressure in comatose cardiac arrest survivors-An observational study. Resuscitation. 2017;110:85–9.
37. Ameloot K, Genbrugge C, Meex I, et al. An observational near-infrared spectroscopy study on cerebral autoregulation in post-cardiac arrest patients: time to drop 'one-size-fits-all' hemodynamic targets? Resuscitation. 2015;90:121–6.
38. Giller CA, Hodges K, Batjer HH. Transcranial Doppler pulsatility in vasodilation and stenosis. J Neurosurg. 1990;72:901–6.
39. Sundgreen C, Larsen FS, Herzog TM, Knudsen GM, Boesgaard S, Aldershvile J. Autoregulation of cerebral blood flow in patients resuscitated from cardiac arrest. Stroke. 2001;32:128–32.
40. Czosnyka M, Smielewski P, Kirkpatrick P, Menon DK, Pickard JD. Monitoring of cerebral autoregulation in head-injured patients. Stroke. 1996;27:1829–34.

41. Stretti F, Gotti M, Pifferi S, Brandi G, Annoni F, Stocchetti N. Body temperature affects cerebral hemodynamics in acutely brain injured patients: an observational transcranial color-coded duplex sonography study. Crit Care. 2014;18:552.
42. Brandi G, Bechir M, Sailer S, Haberthur C, Stocker R, Stover JF. Transcranial color-coded duplex sonography allows to assess cerebral perfusion pressure noninvasively following severe traumatic brain injury. Acta Neurochir. 2010;152:965–72.
43. Doepp Connolly F, Reitemeier J, Storm C, Hasper D, Schreiber SJ. Duplex sonography of cerebral blood flow after cardiac arrest – a prospective observational study. Resuscitation. 2014;85(4):516–21.

Chapter 57
Management of Brain Tumors in ICU: Monitoring the Neurological Impact by Transcranial Doppler (TCD/TCCS)

Mohammed F. Kananeh and Syed Omar Shah

Key Points

1. Transcranial Doppler and transcranial color-coded duplex sonography (TCD/TCCS) are useful tools that are underutilized in the NCCU in investigating these tumors.
2. TCD/TCCS are a quick, noninvasive study to aid in the evaluation of brain tumors both pre- and postoperatively.
3. The examiner has to be aware of several artifacts that might be interpreted as progressive or returning tumors. Air trapped in the resection site will result in increased echogenicity and can be mistaken for tumor tissue.
4. The use of TCD/TCCS is also hampered by the 10–15% rate of inadequate acoustic windows prevalent in African, Americans, Asians, and elderly women.

57.1 Introduction

The investigation of brain tumors involves analyzing the type, location, circumscribed vs invasive, extent of edema, and malignancy. In general, computed topography (CT) and magnetic resonance imaging (MRI) have long been the gold standard in examining brain tumors. Although CT scans are quick and cost-effective, their limitations including exposure to radiation, contrast administration, and difficulty interpreting some of the images obtained make them less than ideal. MRI, on the other hand, does not suffer from exposure to radiation but are affected by the high cost, long scans, and contraindication in patients with cardiac devices. In addition,

M. F. Kananeh · S. O. Shah (✉)
Department of Neurological Surgery, Vickie and Jack Farber Institute for Neuroscience, Thomas Jefferson University, Philadelphia, PA, USA
e-mail: Syed.Shah@jefferson.edu, syed.o.shah@jefferson.edu

C. N. Rodríguez et al. (eds.), *Neurosonology in Critical Care*,
https://doi.org/10.1007/978-3-030-81419-9_57

many critically ill patients in the neurocritical care unit (NCCU) are unable to tolerate transportation to the MRI/CT bay for scanning. These limits can affect the diagnosis and follow-up of patients with brain tumors.

The use of transcranial color-coded duplex sonography (TCCS) and transcranial Doppler (TCD) has advanced the investigation of brain tumors. TCD/TCCS are noninvasive and easily performed, so that follow-up investigations can be performed bedside at less expense compared with CT and MRI [1, 2]. As such, TCDs have great utilization in investigating brain tumors beyond the typical use for checking vasospasm in subarachnoid hemorrhage (SAH) [3].

Doppler ultrasonography can be used to assess tumor vascularity, plan the operative approach, and for follow-up postoperatively. It utilizes the Doppler effect, which is an observed frequency shift when an ultrasound (US) wave is reflected back to the transducer from moving particles, to determine the direction and relative velocity of fluid along the axis of the probe [4]. This provides real-time measurement of blood flow characteristics and cerebrovascular hemodynamics of brain tumors, which is useful for highly vascular tumors, like hemangioblastomas [2, 4].

57.2 TCD/TCCS: Use in Tumor Evaluation

Different types of Doppler ultrasonography exist and proper use can maximize the information gained about the tumor in question. Transcranial color-coded duplex Sonography (TCCS) is useful in examining highly vascular tumors like gliomas pre- and postoperatively. Color Doppler imaging relies on the magnitude of measured Doppler shift, which shows with color the direction of flow, either toward or away from the probe, overlaid on the 2D US image. Consequently, color Doppler is very much angle dependent: if the flow is perpendicular to the US waves, the Doppler shift is lost and no flow will be appreciated [2, 5]. Furthermore, color Doppler suffers from aliasing, an artifact in which areas of flow are represented with incorrect magnitude or direction as a result of transducer pulse rate limitations [5]. Lastly, color Doppler imaging is highly susceptible to noise, which may overwhelm the flow signal [6]. Power Doppler is an alternative to the frequency-coded signal as it relies on the power of the Doppler shift signal instead of the magnitude of the shift [5, 6]. Power Doppler has many advantages including less noise, less angle dependence, greater resolution of small vessels, and no aliasing [5, 6]. Additionally, power Doppler can be reconstructed into a 3D volume, which, as compared to magnetic resonance angiography (MRA), can simultaneously demonstrate arteries and veins, include small-caliber vessels [7–9]. However, power Doppler sacrifices information about flow direction and velocity [2, 5]. The power Doppler signal can exaggerate smaller vessels, so they appear larger on power Doppler imaging than they do on MRA [2, 5]. This high sensitivity of power Doppler may result in visualization of small vessels of limited relevance, thus diminishing intraoperative utility [2, 5]. Power Doppler is also limited by operator dependence, motion sensitivity artifacts, and overall poor resolution compared to other imaging modalities [2, 5].

Contrast-enhanced US delivers reliable intraoperative visualization of peritumoral and intratumoral vascularity [2, 10]. Strong contrast enhancement is seen in meningiomas, hemangioblastomas, and metastases, with less enhancement seen in gliomas and lymphomas [10]. US elastography is a new technology that is based on arterial pulsation to help to differentiate tumor from normal parenchyma. It is important to note that these images have only been compared with 2D US and not MRI or histopathology [11, 12]. Endonasal US is an emerging technology with studies conducted with the early rigid endonasal US probes suggested that US could identify pituitary tumors with 81% sensitivity [2]. In this book, we will concentrate on TCCS as it has the most applicability in the setting on the neurocritical care unit.

57.2.1 Sensitivity

It is important to note that the overall sensitivity of TCCS in tumor detection is inferior compared to CT and MRI [1, 13]. However, color Doppler is more sensitive than CT in detection of residual tumor and tumor regrowth [1, 14]. Solid tumors appear hyperechogenic on TCCS and the interspersed hypoechogenic areas represent necrotic or cystic tumor portions [13, 14]. In addition, comparison with histopathology revealed that TCCS are consistent with the demonstration of tumor extension, due to the distinct differences in echogenicity between tumor tissue and perifocal brain edema and normal brain tissue. Neither CT nor MRI can definitively differentiate between non-contrast enhancing tumor tissue and perifocal brain edema [13, 15, 16]. Postoperatively TCCS is more sensitive than CT in detecting residual tumor. In one study, 12 out of 20 patient who underwent operative removal of brain glioma displayed residual tissue on CT. Three out of the eight remaining designated "tumor free" patients were found to have residual tumor tissue on TCCS, which was confirmed by pathology [15, 17]. It is essential to determine the extent of any residual tumor tissue postoperatively. Albert et al. through MRI-controlled studies demonstrate that residual tumor tissue is the most predictive factor of survival in patients with supratentorial gliomas [18]. Additionally, complete tumor resection improved quality of life and renders adjuvant therapies, like chemotherapy and radiation, more effectively [19]. Neither CT nor TCCS is able to determine the total extension of an infiltrating tumor (including the infiltrating zone) precisely [14]. However, when compared to CT, TCCS can provide more reliable data on the location, residual, and regrowth of tumors**.**

57.2.2 Artifacts

The examiner has to be aware of several artifacts that might be interpreted as progressive or returning tumors. Air trapped in the resection site will result in increased echogenicity and can be mistaken for tumor tissue [14]. This artifact is usually

resolved after postoperative day 5. Moreover, hemorrhage along the resection site or within the resection cavity may also lead to a misinterpretation by TCCS in the early postoperative period. A CT scan would be more helpful to differentiate hemorrhage at the resection site or around the surgery site. In case CT imaging is difficult to obtain, then a follow-up color Doppler study is helpful to differentiate tumor tissue from hemorrhage. In general, the echogenicity of blood would decrease in size within the first 2 postoperative weeks [14].

57.2.3 Vasospasm Detection

TCD/TCCS are helpful in ruling out vasospasm and ischemia in conditions like subarachnoid hemorrhage and stroke. It is possible to observe vasospasm and ischemia after resection of intracranial tumors but this has not received extensive attention clinically [20]. Often, they are misdiagnosed and improperly treated as surgical brain damage or brain swelling. Some of the factors that appear to correlate with a higher incidence of postoperative vasospasm include a larger tumor size, the need for preoperative embolization indicating increased tumor vascularity, vessel encasement, displacement, and narrowing and increased intraoperative blood loss [20, 21]. It is likely that the presence of blood in the basal cisterns is responsible for this condition. Vasospasm should be considered in patients who are deteriorating after the surgical removal of a cerebral tumor. TCD/TCCS are indispensable in investigating vasospasm to help initiate the appropriate treatment.

57.3 TCD/TCCS: Limitations

TCD/TCCS carry some limitations, where the operator should be conscious of the resolution of ultrasonography (US), which is not uniform in every direction or every tissues. Because the appearance of tissue depends on the depth and angle of US waves insonation, it can be challenging both to interpret US images and to compare them to images from other modalities, such as MR and CT [2, 14]. Dense tissue like bone can create a shadow that diminishes signal of any tissue behind it. Fluids like blood can mimic tumor tissue due to its echogenicity, which can imply tumor extension [14]. TCD is highly operator dependent, with the handheld technique requiring detailed three-dimensional knowledge of cerebrovascular anatomy and its variations. The use of TCD/TCCS is also hampered by the 10–15% rate of inadequate acoustic windows prevalent in African Americans, Asians, and elderly women [1, 2].

57.4 Conclusion

TCD/TCCS are useful tools that are underutilized in the NCCU in investigating tumors. TCD/TCCS and sonography in general lack behind CT and MRI in the ability to initially diagnose brain tumors [1, 14]. But they are superior to CT in identifying tumor extension and regrowth. TCD is better than CT and MRI in differentiating between normal tissue and edema. TCD is an indispensable tool intraoperatively and provides multitude of information. It is very useful tool to monitor extension and regrowth of brain tumors, especially in patients who are unstable to undergo CT or MRI postoperatively. It is cheap and relatively easy to learn. With experience, TCD will be a crucial tool in investigating and understanding the progression of brain tumors in patients in the NCCU.

References

1. Meyer K, Seidel G, Knopp U. Transcranial sonography of brain tumors in the adult: an in vitro and in vivo study. J Neuroimaging. 2001;11(3):287–92.
2. Purkayastha S, Sorond F. Transcranial Doppler ultrasound: technique and application. Semin Neurol. 2013;32(4):411–20.
3. Naqvi J, Yap KH, Ahmad G, Ghosh J. Transcranial Doppler ultrasound: a review of the physical principles and major applications in critical care. Int J Vasc Med. 2013.
4. Sastry R, Bi WL, Pieper S, et al. Applications of ultrasound in the resection of brain tumors. J Neuroimaging. 2016;27(1):5–15.
5. Sloan MA, Alexandrov AV, Tegeler CH, et al. Therapeutics and Technology Assessment Subcommittee of the American Academy of Neurology. Assessment: transcranial Doppler ultrasonography: report of the Therapeutics and Technology Assessment Subcommittee of the American Academy of Neurology. Neurology. 2004;62(9):1468–81.
6. Lysakowski C, Walder B, Costanza MC, Tramer MR. Transcranial Doppler versus angiography in patients with vasospasm due to a ruptured cerebral aneurysm: a systematic review. Stroke. 2001;32(10):2292–8.
7. Lindegaard KF, Nornes H, Bakke SJ, Sorteberg W, Nakstad P. Cerebral vasospasm diagnosis by means of angiography and blood velocity measurements. Acta Neurochir. 1989;100(1–2):12–24.
8. Tsivgoulis G, Alexandrov AV, Sloan MA. Advances in transcranial Doppler ultrasonography. Curr Neurol Neurosci Rep. 2009;9(1):46–54.
9. Saqqur M, Zygun D, Demchuk A. Role of transcranial Doppler in neurocritical care. Crit Care Med. 2007;35(5):S216–23.
10. Serrador JM, Sorond FA, Vyas M, Gagnon M, Iloputaife ID, Lipsitz LA. Cerebral pressure-flow relations in hypertensive elderly humans: transfer gain in different frequency domains. J Appl Physiol. 2005;98(1):151–9.
11. Wijnhoud AD, Koudstaal PJ, Dippel DW. The prognostic value of pulsatility index, flow velocity, and their ratio, measured with TCD ultrasound, in patients with a recent TIA or ischemic stroke. Acta Neurol Scand. 2011;124(4):238–44.
12. Kelley RE, Chang JY, Suzuki S, Levin BE, Reyes-Iglesias Y. Selective increase in the right hemisphere transcranial Doppler velocity during a spatial task. Cortex. 1993;29(1):45–52.

13. Becker G, Krone A, Koulis D, Lindner A, Hofmann E, Roggendorf, et al. Reliability of transcranial color-coded real-time onography in the assessment of brain tumors: correlation between ultrasound, computerized tomography and biopsy findings. Neuroradiology. 1994:36585–90.
14. Becker G, Krone A, Schmitt K, et al. Preoperative and postoperative follow-up in high-grade gliomas: comparison of transcranial color coder real-time sonography and computed tomography findings. Ultrasound Med Biol. 1995;21:1123–35.
15. Enzmann DR, Wheat R, Marshall WH, Bird R, Murphy-Irwin K, Karbon K, et al. Tumors of the central nervous system studied by computed tomography and ultrasound. Radiology. 1985;154:393–9.
16. Gooding GA, Boggan JE, Weinstein PR. Characterisation of intracranial neoplasms by CT and intraoperative sonography. AJNR. 1984;5:517–20.
17. Burger PC, Heinz ER, Shibata T, Kleihues P. Topographic anatomy and CT correlations in the untreated glioblastoma multiforme. J Neurosurg. 1988;68:698–704.
18. Albert F, Forsting M, Sator K, Adams HP, Kunze S. Early postoperative magnetic resonance imaging after resection of malignant glioma: objective evaluation of residual tumor and its influence on regrowth and prognosis. Neurosurgery. 1994;34:45–61.
19. Ammirati M, Vick N, Liao Y, Ciri MM. Effect of extent of surgical resection on survival and quality of life in patients with supratentorial glioblastomas and anaplastic astrocytomas. Neurosurgery. 1987;2:201–6.
20. Kalanuria A, Nyquist PA, Armonda RA, Razumovsky A. Use of Transcranial Doppler (TCD) ultrasound in the Neurocritical Care Unit. Neurosurg Clin N Am. 2013;24:441–56.
21. Alotaibi NM, Lanzino G. Cerebral vasospasm following tumor resection. J Neurointerv Surg. 2012:1–6.

Chapter 58
Point-of-Care Ultrasound: Guidance for Lumbar Puncture

Camilo N. Rodríguez and Tiffany Fong

Key Points

1. Ultrasound guidance is a tool to increase procedural success and decrease complications of lumbar puncture.
2. Sonography in the transverse plane determines the position of the spinal midline while imaging in a longitudinal plane maps the lumbar spine levels to identify the most appropriate interspinous space. The intersection of these two lines establishes the needle insertion site.
3. Depth of needle insertion may be predicted by visualizing and measuring the distance to the ligamentum flavum.
4. The use of ultrasound guidance should always be considered to improve outcomes of lumbar puncture, particularly in patients with obesity or spinal landmarks that are difficult to palpate.

58.1 Introduction

Lumbar puncture (LP) is a core procedure for the diagnosis and management of critical neurologic pathology. During LP, cerebrospinal fluid (CSF) is removed from the lumbar subarachnoid space, below the termination of the spinal cord.

C. N. Rodríguez (✉)
Intensive Care Medicine, Hospital Nacional Prof. Dr. A. Posadas, University of Buenos Aires (UBA), Neurointensive Care Section - ESICM, Neurointensive Care Section - AMCI, Neurointensive Care Committee - FEPIMCTI, Member of ESNCH, Buenos Aires, Argentina
e-mail: camilo.rodriguez@nesccco.com

T. Fong
Division of Emergency Ultrasound, Department of Emergency Medicine, The Johns Hopkins University School of Medicine, Baltimore, MD, USA
e-mail: tfong3@jhmi.edu

C. N. Rodríguez et al. (eds.), *Neurosonology in Critical Care*,
https://doi.org/10.1007/978-3-030-81419-9_58

When LP is performed routinely by palpation of external landmarks, overall procedural success rate is reported to be 72% [1], with only 61.5% success at first attempt [2]. Obesity can present a significant obstacle to landmark palpation and has been shown to be a major contributor to failed LP [3, 4]. Such anatomic challenges are quite common; 30% of ED patients requiring LP have spinal landmarks that are difficult to identify [5]. One technique to promote the success and safety of LP is the use of point-of-care ultrasound guidance. This has been shown to improve procedural success rates, while reducing the time to successful LP, number of needle passes and redirections, patient pain scores, and risk of a traumatic LP [6–8]. Ultrasound guidance should always be considered in patients who have anticipated procedural challenges (e.g., obesity or abnormal spinal anatomy) or after multiple failed attempts using conventional palpation methods.

58.2 Descriptive Anatomy: Lumbar Spine

The lumbar spine is composed of five vertebrae (L1-L5). The vertebral body is the weight bearing portion of the vertebra, and connects to the pedicles, laminae, transverse processes, and spinous process (Fig. 58.1). The spinous process is palpable in the posterior midline of the spine, and the L2-L4 spinous processes are typically the most superficial.

The spinal cord ends at L1–L2 in most adult patients, with cadaveric and MRI studies demonstrating a range between T11 and L3 [9]. Generally, LP can be safely performed below the L2 vertebra. The L2–L3 and L3–L4 interspinous spaces are typically the widest. Using anatomic landmarks, the L4-L5 interspace is identified in the spinal midline at its intersection with Tuffier's line, which spans the superior aspects of both iliac crests.

Moving from superficial to deep, multiple layers are traversed by the spinal needle during lumbar puncture:

- Skin and subcutaneous tissue
- *Supraspinous ligament:*
  - Connects the tips of the midline spinous processes
- *Interspinous ligament:*
  - Connects the shafts of the spinous processes
- *Ligamentum Flavum (LF):*
  - Lies deep to the interspinous ligaments, connects the lamina, and lines the vertebral foramina
- Epidural space
- Dura mater

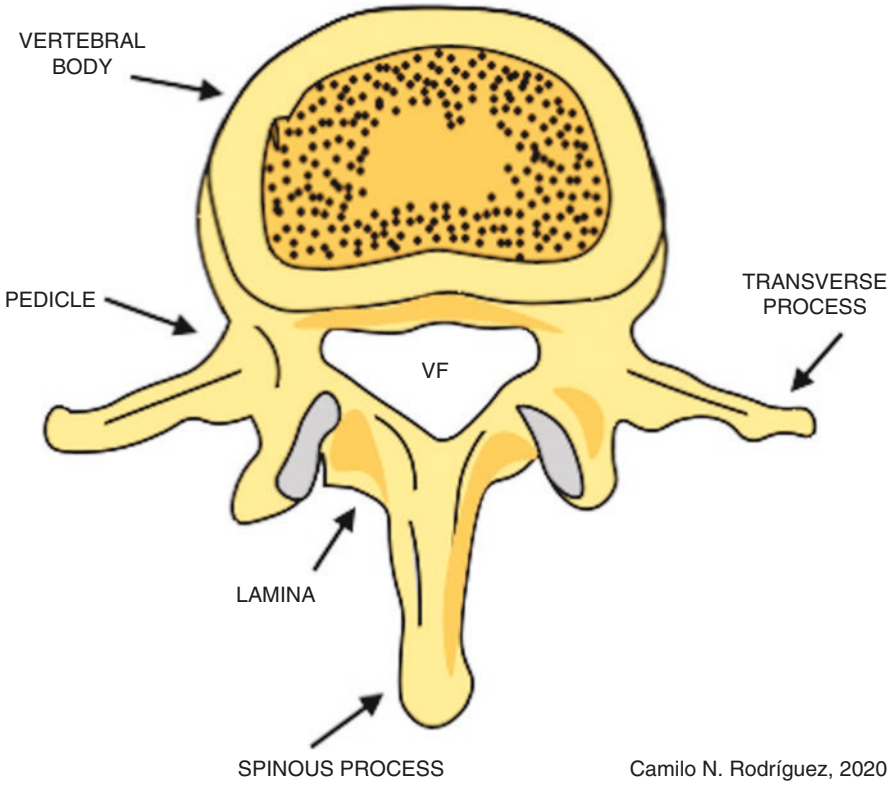

Fig. 58.1 Scheme: L2- vertebrae. (VF): vertebral foramen

Further stabilizing the spinal vertebra are the posterior longitudinal ligament and anterior longitudinal ligament. These structures are located deep to any areas that should be traversed during an LP procedure (Figs. 58.1 and 58.2a).

Lumbar puncture (LP) is most commonly performed using a midline approach (Fig. 58.2b). A paramedian approach with a needle trajectory through the interlaminar space may be used as an alternative.

58.3 Pre-procedure Considerations

58.3.1 Procedural Preparation to Reduce Complications of Lumbar Puncture

Thoughtful preparation prior to LP can help improve safety and reduce procedural complications [10, 11] (Table 58.1).

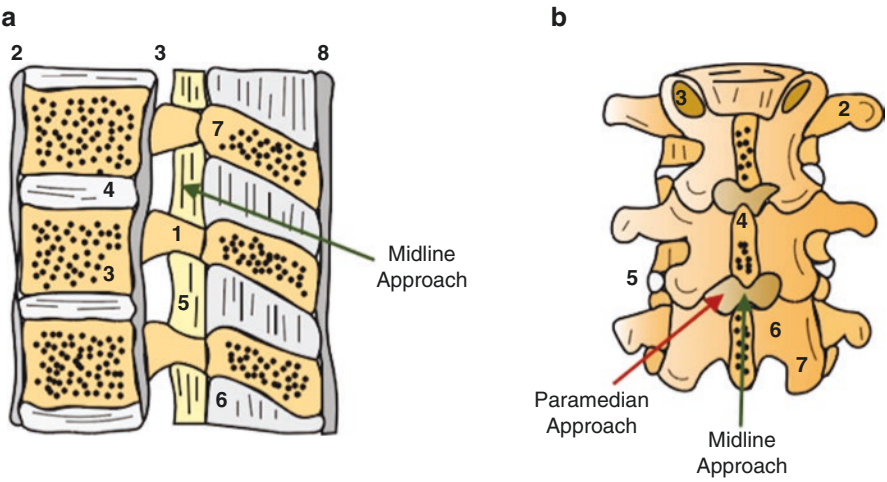

Fig. 58.2 Anatomy of the lumbar spine; (**a**) Sagittal view: (1) Lamina, (2) Anterior longitudinal ligament, (3) Posterior longitudinal ligament, (4) Intervertebral disk, (5) Ligamentum flavum, (6) Interspinous ligament, (7) Spinous process and (8) Supraspinous ligament; (**b**) Posterior view: (1) Lumbar vertebral body, (2) Transverse process, (3) Superior articular process, (4) Spinous process, (5) Intervertebral disk, (6) Lamina and (7) Inferior articular process; Red arrow: Trajectory of spinal needle during LP using a paramedian approach; Green arrow: Trajectory of spinal needle using a midline approach

Table 58.1 Modifiable factors to reduce complications of LP [10, 11]

Complication	Modifiable factor	Intervention
Post-dural puncture headache	Patient positioning	Lateral decubitus
	Needle tip	Pencil point (atraumatic)
	Needle size	Smallest bore possible, preferably smaller than 20G
	Needle position	Bevel parallel to long axis of spine
	CSF drainage	Passive drainage of no more than 30 ml CSF
Bleeding	Coagulopathy	Defer LP until INR <1.4
	Thrombocytopenia	Defer LP until platelet count is >50,000–80,000
	Use of anticoagulant medications	For elective LP, STOP anticoagulation prior to procedure: *Heparin drip*: 2–4 hours *LMWH*: 12–24 hours *Warfarin*: 5–7 days *NOAC*: 48 hours
Cerebral herniation	Assess for elevated intracranial pressure	Obtain CT scan first if: Altered mental status Focal neurologic signs Papilledema Seizure within 1 week Immunosuppression

LP Lumbar puncture, *LMWH* Low molecular weight heparin, *NOAC* Novel oral anticoagulants, *CSF* Cerebral spinal fluid, *INR* International normalized ratio

58.4 Patient Positioning

Lumbar puncture may be performed in either a lateral decubitus or upright seated position. The lateral decubitus position allows a more accurate measurement of opening pressure, but has lower success rate than an upright position. If an upright seated position is used, the patient's flexed upper body must be supported on a surface, and if possible a stool used to elevate the legs. This flexion of the back and hips serves to maximize interspinous distance. If a lateral decubitus position is used, the patient should flex the back as far as possible, raising the knees toward the chin and furthermore ensure that the hips and shoulders are aligned and perpendicular to the floor. The goal of positioning, whether lateral decubitus or upright, is to expand the interspinous space to facilitate needle passage. Choice of position should be dictated by clinical circumstance and patient tolerance.

58.5 Probe (Transducer) Selection

A low frequency (2–5 MHz) curvilinear transducer is preferred for obese patients (BMI >30), as it enables adequate penetration to visualize deeper structures where the bony landmarks are non-palpable. For nonobese patients (BMI <25), a high frequency (5–10 MHz) linear transducer will provide the highest resolution images of relevant anatomic structures at 6–9 cm in depth. A musculoskeletal exam preset should be chosen if available. A depth of 10–12 cm may be used as starting point, but should be adjusted to the specific patient. The probe marker should be oriented to the operator's left.

58.6 Ultrasound Technique

Point-of-care ultrasound is most commonly used for static guidance, in which key spinal landmarks are mapped to identify a needle insertion site prior to performing LP. Though real-time ultrasound needle guidance has been described in the literature, it is more technically challenging and less well studied. This chapter will focus on a midline approach using static guidance.

58.6.1 Midline Approach

58.6.1.1 Identify the Spinal Midline: Transverse View

Begin by placing the transducer over the sacrum, which is visible as a hyperechoic line with an irregular surface. Slide the probe cephalad to sequentially identify the lumbar spinous processes (L5-L4-L3-L2) [22, 23] (Figs. 58.3 and 58.5). Each

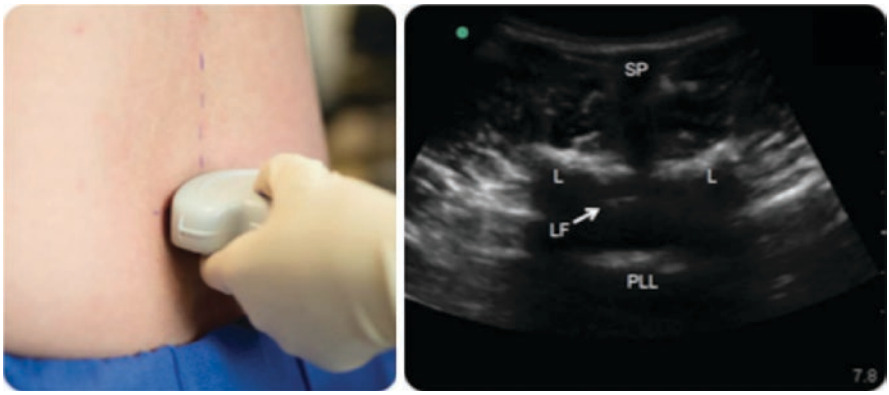

Fig. 58.3 Lumbar ultrasound: Transverse view; SP Spinous process, L Lamina, LF Ligamentum flavum, PLL Posterior longitudinal ligament. (Courtesy: Soni et al. Neurol Clin Pract, 2016)

spinous process will appear superficially as a small, thin hyperechoic structure with posterior acoustic shadowing. The laminae are seen deeper and more lateral to the spinous process, and the transverse processes can be visualized deeper and more lateral to the laminae.

The transducer position should be adjusted until the spinous process is centered on the screen and a skin marker used to mark the midline perpendicular to the transducer. The spinal midline should be marked over a minimum of two or three spinous processes [12, 13].

58.6.1.2 Map the Lumbar Interspinous Space: Longitudinal View

At the L3-L4 interspinous space, rotate the probe 90° into a longitudinal orientation over the spinal midline. The spinous processes will appear similar to a row of ¨tombstones¨. Slide the probe along the midline to identify the widest interspinous space. Once the transducer is centered over the widest space (most commonly L3-L4), use a marking pen to draw a line perpendicular the probe [12, 13] (Figs. 58.4 and 58.5).

58.6.1.3 Identify the Needle Entry Site

The needle entry site should be the intersection of the two marked lines, representing the spinal midline at the widest lumbar interspinous space (L3-L4).

The lumbar puncture may proceed using standard techniques. It must be emphasized that the patient must remain in the same position during both ultrasound and LP components of the procedure, to ensure that marked areas do not shift relative to underlying anatomy.

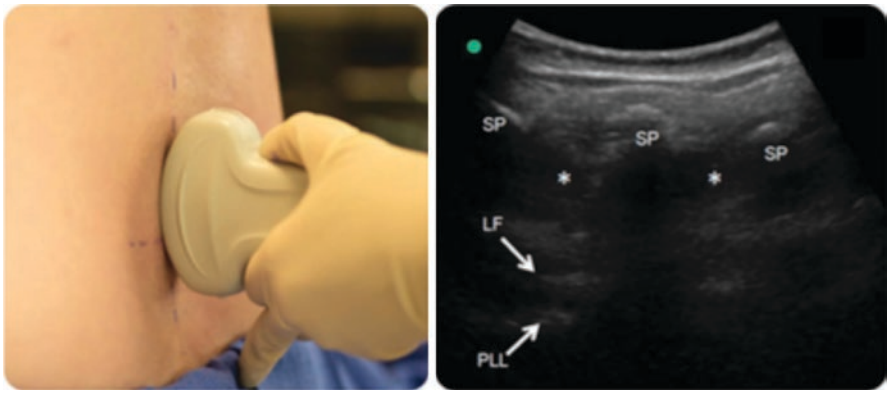

Fig. 58.4 Longitudinal view of lumbar spine at midline. (1) Spinous processes (Tombstone), (2) Lamina SP, LF Ligamentum flavum, PLL Posterior longitudinal ligament. (Courtesy: Soni et al. Neurol Clin Pract, 2016)

58.6.2 Paramedian Approach

A paramedian technique is an alternative approach to LP that utilizes a needle trajectory through the interlaminar space. Its advantages include a larger pathway to access the dura, and avoidance of the supraspinous and interspinous ligaments which may be calcified in elderly patients. This technique may also be assisted with ultrasound, and in addition to identifying a needle entry site, it allows the operator to estimate the distance that the needle must travel from skin to dural space (Fig. 58.8).

In a longitudinal plane, the operator slides the transducer to either a left or right paramedian position to identify the lamina of sequential lumbar vertebra (Figs. 58.6 and 58.7). Deep to the laminae in the interspinous space, the ligamentum flavum is visible as a hyperechoic linear structure. The dura lies just a few millimeters deep to the ligamentum flavum. Measuring the distance from the skin to the ligamentum flavum allows the operator to predict the necessary depth of needle insertion [13, 14, 23], and to ensure a needle of appropriate length is selected for the procedure.

In patients with challenging surface anatomy, the midline and paramedian views may be easily confused, leading to misidentification of spinous processes as laminae. A distinction can be made by sweeping the transducer form the patient's left to right and ensuring that both the spinous processes and laminae are visualized. Furthermore, the spinous processes should have only skin and subcutaneous tissue overlying, whereas erector spinae muscle fibers will be seen overlying the laminae.

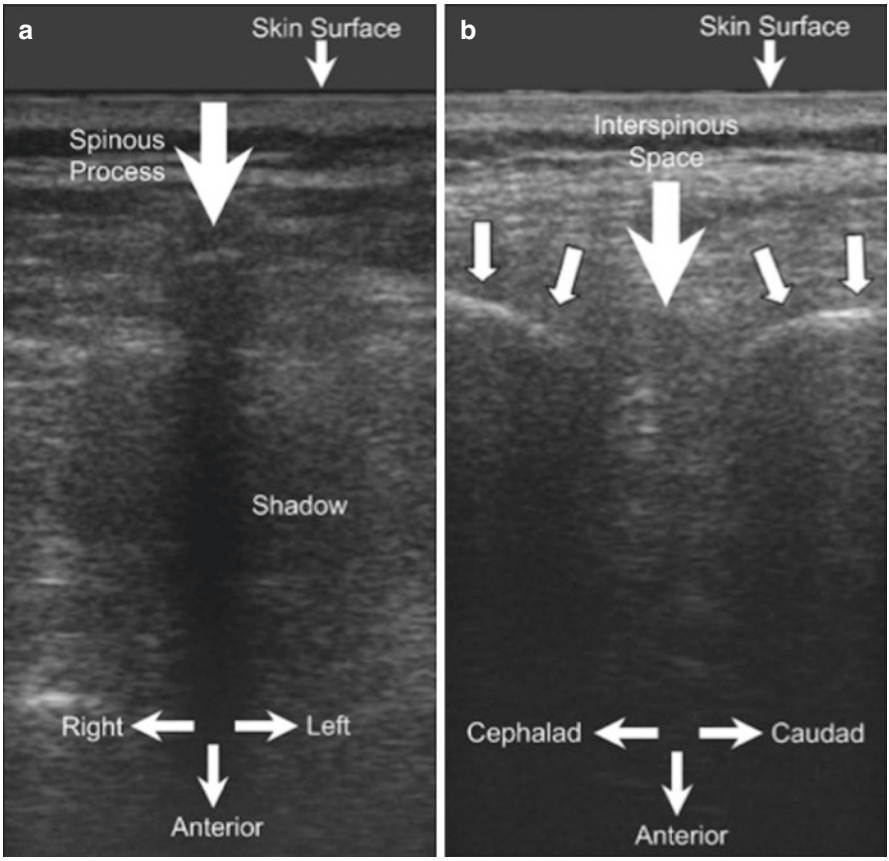

Fig. 58.5 (**a**) Transverse ultrasound view of midline lower back. (Shadow): Spinous process; (**b**) Longitdinal ultrasound view of the lower back over spine. (Small unlabeled arrows): Inidicate echogenic border of two spinous process. (Courtey: Peterson MA, et al. Acad Emerg Med 2014;21:130–136.) [19]

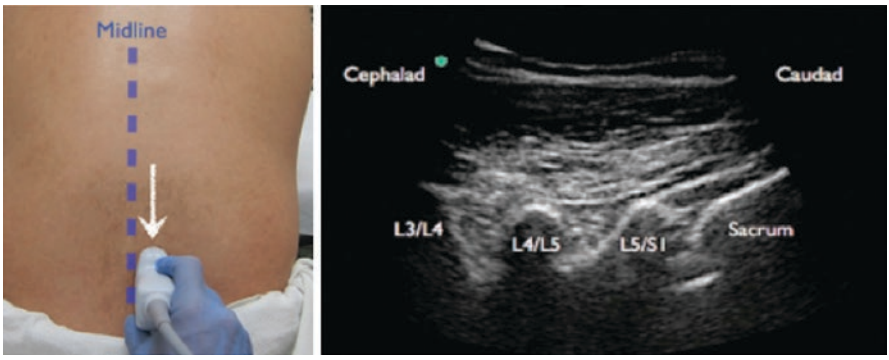

Fig. 58.6 Longitudinal view of lumbar spine (Paramedian approach): (Caudal) Sacrum, (Cephalad) L3/L4 articular processes (A lateral slight probe movement: From the transverse processes to articular process). (Courtesy: Nagdev Arun, et al. ACEP. 2014;33) [14]

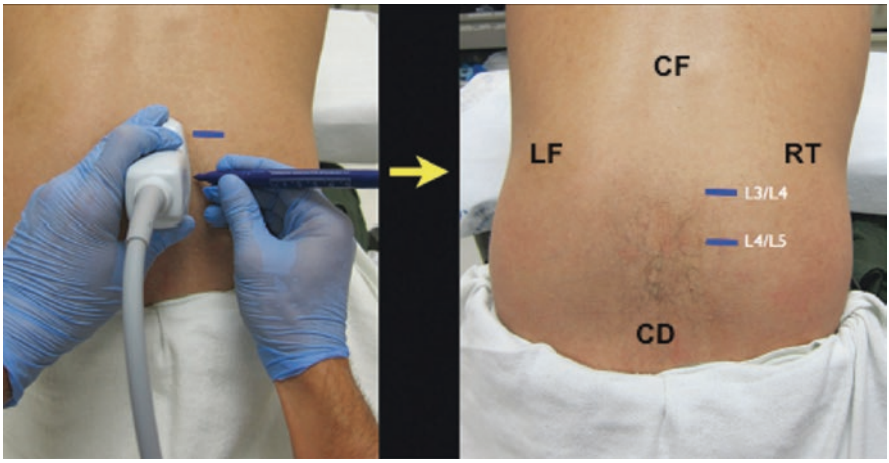

Fig. 58.7 Longitudinal view (Paramedian approach): Using marker, the interspaces are labeled lateral to the probe; CF Cepahlic, CD Caudal, LF Patient's left, RT Patient's right. (Courtesy: from Nagdev Arun, et al. ACEP. 2014;33) [14]

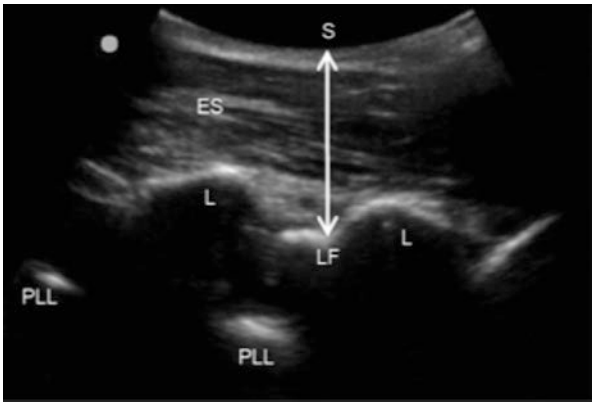

Fig. 58.8 Longitudinal paramedian view of lumbar spine. S Skin, ES Erector spinae muscle, L Lamina, LF Ligamentum flavum, PLL Posterior longitudinal ligament. The anechoic structure between LF and PLL is the dural sac filled with cerebral spinal fluid). (Arrow): Distance between skin and LF. (Courtesy: Soni et al. [13])

58.7 Lumbar Puncture Procedure: Advantages

Lumbar puncture (LP) mapping with ultrasound has the greatest benefit in patients with obesity or poorly palpable bony landmarks. Advantages of this technique are reviewed in Table 58.2.

Table 58.2 Ultrasound-guided lumbar puncture advantages

1. Decrease time wasting in the procedure [12, 18, 19, 27]
2. Increase ease of procedure in those patients whose spinal landmarks are either difficult to palpate or not palpable [12, 15, 16, 18]
3. Decrease pain scores [12, 27]
4. Fewer traumatic taps [7, 18, 19, 27]
5. Reduce the number failure procedures [1, 7, 16–19, 27]
6. Fewer needle redirection [7, 20]
7. Proper length spinal Needle selection (Depth: Skin to ligamentum flavum) [13, 20]
8. Decrease overall costs [1]

58.8 Ultrasound-Guided Lumbar Puncture: Training Considerations

Like all bedside procedures, learning curves for skill acquisition in ultrasound-guided LP are variable and should be adapted based on the operator's prior ultrasound experience.

It is recommended that novices learning ultrasound-guided LP should have a training program that includes didactics, simulation-based practice (if available), supervised practice by more experienced operators, and experiential and competency-based assessment for procedural credentialing and privileging. Various guidelines exist, and in general recommend performance of 10–20 supervised procedures [21, 24–26].

58.9 Conclusion

Ultrasound-guided lumbar puncture is associated with higher success rates, shorter time to successful LP, fewer needle attempts, fewer traumatic taps, and lower patient pain scores when compared to palpation techniques. Static ultrasound guidance maps spinal landmarks to identify an ideal needle puncture site, and allows the operator to predict needle trajectory and depth. Point-of-care ultrasound is excellent complementary tool to perform lumbar punctures, and should always be a considered as a procedural adjunct, especially in patients with obesity or difficult anatomy.

Algorithm

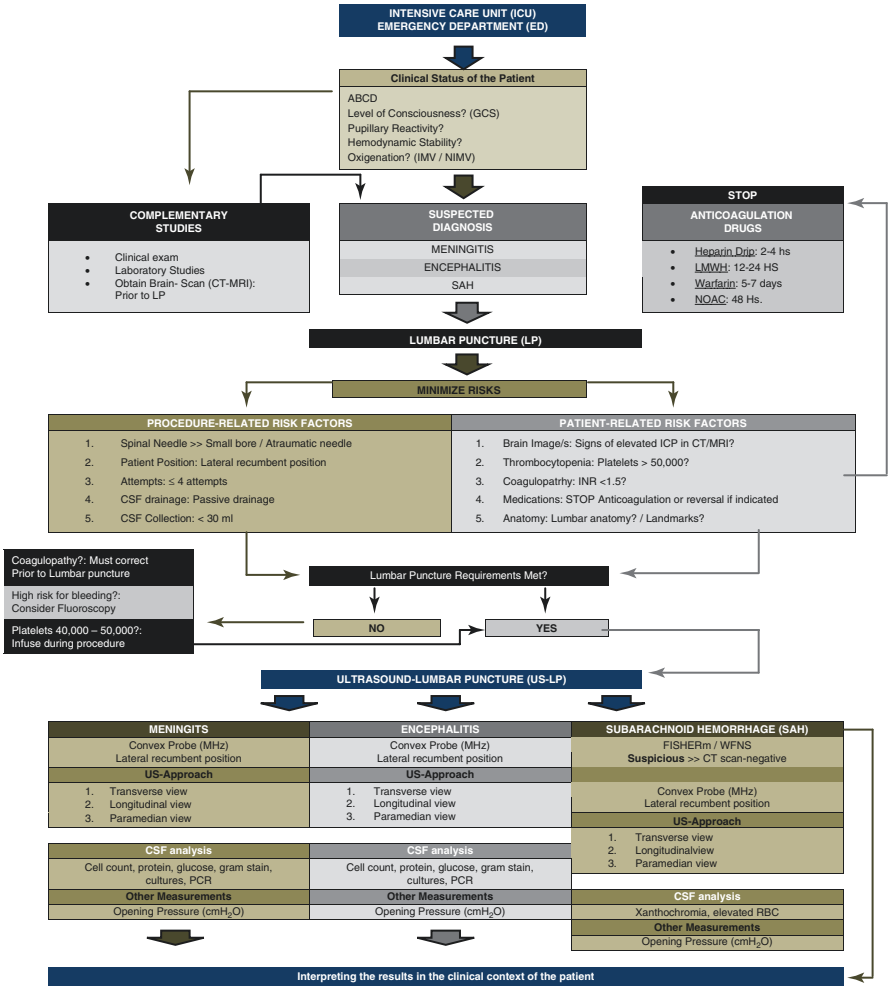

CSF Cerebral spinal fluid, *CT* Computed tomography, *MRI* Magnetic resonance image, *ABCD* Airway, breath, circulation, disability, *US* Ultrasound, *LMWH* Low molecular weight heparin, *NOAC* New oral antocoagulant

References

1. Williams P, Tait G, Wijeratne T. Success rate of elective lumbar puncture at a major Melbourne neurology unit. Surg Neurol Int. 2018;9:12.
2. de Filho GR, Gomes HP, da FMH, Hoffman JC, Pederneiras SG, Garcia JH. Predictors of successful neuraxial block: a prospective study. Eur J Anaesthesiol. 2002;19:447–51.

3. Edwards C, Leira EC, Gonzalez-Alegre P. Residency training: a failed lumbar puncture is more about obesity than lack of ability. Neurology. 2015;84:e69–72.
4. Stiffler KA, et al. The use of ultrasound to identify pertinent landmarks for lumbar puncture. AJEM. 2007;25:331–4.
5. Shah KH, McGillicuddy D, Spear J, Edlow JA. Predicting difficult and traumatic lumbar punctures. Am J Emerg Med. 2007;25(6):608–11.
6. Gottlieb M, Holladay D, Peksa GD. Ultrasound-assisted lumbar punctures: a systematic review and meta-analysis. Acad Emerg Med. 2018;26(1).
7. Shaikh F, et al. Ultrasound imaging for lumbar punctures and epidural catheterisations: systematic review and meta-analysis. BMJ. 2013;346:f1720.
8. Perlas A, Chaparro LE, Chin KJ. Lumbar neuraxial ultrasound for spinal and epidural anesthesia: a systematic review and meta-analysis. Reg Anesth Pain Med. 2016;41(2):251–60.
9. Boon JM, Abrahams PH, Meiring JH, Welch T. Lumbar puncture: anatomical review of a clinical skill. Clin Anat. 2004;17(7):544–53.
10. Engelborghs S, et al. Consensus guidelines for lumbar puncture in patient with neurological disease. Elsevier; 2017.
11. Straus SE, et al. How do I perform a lumbar puncture and analyze the results to diagnose bacterial meningitis? JAMA. 2006;296:2012–22.
12. Mofidi M, et al. Ultrasound guided lumbar puncture in emergency department: time saving and less complications. J Res Med Sci. 2013;18(4):303–7.
13. Soni NJ, et al. Ultrasound guidance for lumbar puncture. Neurol Clin Pract. 2016;6:358–68.
14. Nagdev A, et al. How to perform an ultrasound-assisted lumbar puncture. ACEP; 2014.
15. Pisupati D, Heyming TW, Lewis RJ, Peterson MA. Effect of ultrasonography localization of spinal landmarks on lumbar puncture in the emergency department. Ann Emerg Med. 2004;44:S83.
16. Nomura JT, Leech SJ, Shenbagamurthi S, et al. A randomized controlled trial of ultrasound-assisted lumbar puncture. J Ultrasound Med. 2007;26:1341–8.
17. Lee WS, Jeong WJ, Yi HY, Ryu S, Lee JW, Kim SW. The usefulness of ultrasound-assisted lumbar puncture on adult patients in the emergency center: comparison with classic lumbar puncture. J Korean Soc Emerg Med. 2008;19:562.
18. Cho YC, Koo DH, Oh SK, Jeong WJ, Lee WS, You YH. Comparison of ultrasound-assisted lumbar puncture with lumbar puncture using palpation of landmarks in aged patients in an emergency center. J Korean Soc Emerg Med. 2009;20:304.
19. Peterson MA, Pisupati D, Heyming TW, Abele JA, Lewis RJ. Ultrasound for routine lumbar puncture. Acad Emerg Med. 2014;21:130–6.
20. Perlas A. Evidence for the use of ultrasound in neuraxial blocks. Reg Anesth Pain Med. 2010;35:S43–6.
21. Ferre RM, Sweeney TW. Emergency physicians can easily obtain ultrasound images of anatomical landmarks relevant to lumbar puncture. Am J Emerg Med. 2007;25:291–6.
22. Darrieutort-Lafte C, Bart G, Planche L, et al. Usefulness of a pre-procedure ultrasound scanning of the lumbar spine before epidural injection in patients with a presumed dif cult puncture: a randomized controlled trial. Joint Bone Spine. 2015;82(5):356–61.
23. Soni NJ, Franco-Sadud R, Kobaidze K, Schnobrich D, Salame G, Lenchus J, et al. Recommendations on the use of ultrasound guidance for adult lumbar puncture: a position statement of the Society of Hospital Medicine. J Hosp Med. 2019:14(10).
24. Barsuk JH, Cohen ER, Caprio T, et al. Simulation-based education with mastery learning improves residents' lumbar puncture skills. Neurology. 2012;79(2):132–7.
25. Margarido CB, Arzola C, Balki M, Carvalho JC. Anesthesiologists' learn- ing curves for ultrasound assessment of the lumbar spine. Can J Anaesth. 2010;57(2):120–6.
26. Terblanche NC, Arzola C, Wills KE, et al. Standardised training program in spinal ultrasound for epidural insertion: protocol driven versus non-proto- col driven teaching approach. Anaesth Intensive Care. 2014;42(4):460–6.
27. Pouraghaei M, Tarzamani MK, Moharramzadeh P, Nikniaz S, Karimian S, Balafar M. Ultrasound guided lumbar puncture reduces failed punctures, spent time and number of attempts in emergency department. J Res Clin Med. 2020;8:20.

Chapter 59
Intensive Care Unit-Acquired Weakness (ICUAW): Usefulness of Bedside Ultrasound

Paolo Formenti, Michele Umbrello, and Davide Chiumello

Key Points

1. The principal causes of weakness include neuropathic and myopathic disorders, and mixed disorders that have been summarized in the term "ICU-acquired weakness" (ICUAW)
2. It is now recognized to be a very important factor in "difficult-to-wean" patients in the ICU setting with prolonged ICU stay.
3. The high-resolution ultrasounds now routinely available represent a valid tool to provide qualitative and quantitative details about muscle disease.
4. The ultrasonography has been reported to offer more accurate data with excellent reliability compared to the anthropometric measure (such as limb circumference).
5. The cross-sectional area (CSA), muscle layer thickness, echointensity and pennation angle are the parameters of the muscular architecture used during ultrasound (US) examination of the patient suspected of ICUAW.

P. Formenti (✉) · M. Umbrello
SC Anestesia e Rianimazione, Ospedale San Paolo – Polo Universitario, ASST Santi Paolo e Carlo, Milan, Italy
e-mail: paolo.formenti@asst-santipaolocarlo.it; Michele.umbrello@fastwebnet.it

D. Chiumello
SC Anestesia e Rianimazione, Ospedale San Paolo – Polo Universitario, ASST Santi Paolo e Carlo, Milan, Italy

Dipartimento di Scienze della Salute, Università degli Studi di Milano, Milan, Italy

Centro Ricerca Coordinata di Insufficienza Respiratoria, Università degli Studi di Milano, Milan, Italy
e-mail: Davide.chiumello@unimi.it

C. N. Rodríguez et al. (eds.), *Neurosonology in Critical Care*,
https://doi.org/10.1007/978-3-030-81419-9_59

59.1 Introduction

A generalized muscle weakness syndrome is experienced by many patients admitted to the intensive care unit (ICU) [1]. Since this syndrome occurs in the absence of pre-existing neuromuscular disease, it is believed to reflect illnesses or treatments occurring in the ICU [2]. The principal causes of weakness include neuropathic and myopathic disorders, and mixed disorders that have been summarized in the term "ICU acquired weakness" (ICUAW) [3]. Recent studies have demonstrated that a reduced excitability of the nerve and muscle cell membranes might contribute to weakness during the acute stages of the polyneuropathy and myopathy encountered in critically ill patients [4]. This has been found to be increasingly associated with a severe systemic response to infection with mortality rate up to 30% [5]. Moreover, it is now recognized to be a very important factor in "difficult-to-wean" patients in the ICU setting with prolonged ICU stay [1, 6]. In order to improve nutritional and rehabilitation strategies, different diagnostic methods to diagnose ICUAW at an early stage have been investigated and in part already reviewed elsewhere [7–9]. Among these, manual muscle strength using different scales (such as the Medical Research Council) has been applied, with a major limitation that patients need to be awake and cooperative for reliable assessment [10, 11]. That said, the high-resolution ultrasounds now routinely available represent a valid tool to provide qualitative and quantitative details about muscle disease.

The aim of this chapter is to describe the available literature knowing about the use of muscular ultrasound in detecting muscle weakness and its impact on patients' treatments and prognosis.

59.2 Critical Illness: ICU-Acquired Weakness (ICUAW)

Functional weakness is a common phenomenon after critical care affecting all ages [12–15]. Various causal factors for this functional incapacity have been proposed. Whereas both psychiatric and psychological dysfunction are common after intensive care [16, 17], these do not appear to be the cause of physical limitation. Altered pulmonary function and cardiac dysfunction secondary to sepsis) has been reported after critical illness and may contribute per se to exercise limitation [18–20]. Nerve conduction abnormalities have been demonstrated frequently in the critically ill patient, and emerging hypotheses for the pathophysiology include acquired channelpathies of voltage gated sodium channels, localizing the defect to the muscle membrane [21–23]. Despite this, critical illness neuropathy seems to be much less common than critical illness myopathy [4, 24], and its correlation with weakness seems inconsistently correlated with its symptoms [25]. Regarding the develop of ICUAW – even if this issue is not the purpose of this review and has been already

extensively discussed [3, 26] – it is important to briefly report that many factors play a key role, even if not completely understood at all. Among these, the patient-independent features – such as age and comorbidity [27] – associated with bed rest [28] and many pharmacological strategies (such as the practise of sedation, neuromuscular blocked agents (NMBAs) and steroids) used in the ICU as well as the metabolic approach seem to be all related with the reduction in muscular strength and mass (Fig. 59.1) [29].

59.3 Muscular Ultrasound: Is It a Surrogate for Strength?

The currently available tools for the assessment of skeletal muscle mass with the highest level of accuracy and reproducibility are represented by computerized tomography, magnetic resonance imaging and dual energy X-ray absorptiometry. Intuitively, all these methods are time-consuming and difficult to be performed especially in the ICU setting. Thus, a valid alternative to these imaging modalities able to early assess skeletal mass features is represented by ultrasonography. In fact, real-time ultrasound may allow visualization of muscle characteristics by detecting different parameters such as the cross-sectional area (CSA), the muscles layer thickness, the echo intensity grey-scale and the pennation angle. The reliability of ultrasound to measure skeletal muscle thickness and the size of trunk muscles compared to gold standard measurement tools has been already reviewed [30]. In particular, Reeves et al. [31] validated the reproducibility of the CSA in lower limb muscles compared to magnetic resonance imaging-based measurements and Miyatany [32] demonstrated the accuracy of estimating the volume of limb muscles using ultrasonographic muscle thickness in different muscle groups compared with magnetic resonance imaging. Specifically in the ICU scenario, newly Paris et al. [33] evaluated the qualities and challenges of using computed tomography and ultrasonography to specifically measure skeletal muscle. The authors showed how the ultrasound-based quadriceps' muscle layer thickness was positively correlated with CT-CSA. Finally, the ultrasonography has been reported to offer more accurate data with excellent reliability compared to anthropometric measure (such as limb circumference) [10].

59.4 Ultrasound Assessment: Muscular Features

As a non-invasive, painless technique, ultrasound may be used to identify skeletal muscle pathology. It offers several advantages compared with other tests in the evaluation of muscle features, allowing to quickly screen large areas of muscle at the bedside. In fact, healthy muscle tissue has a distinctive appearance on ultrasound

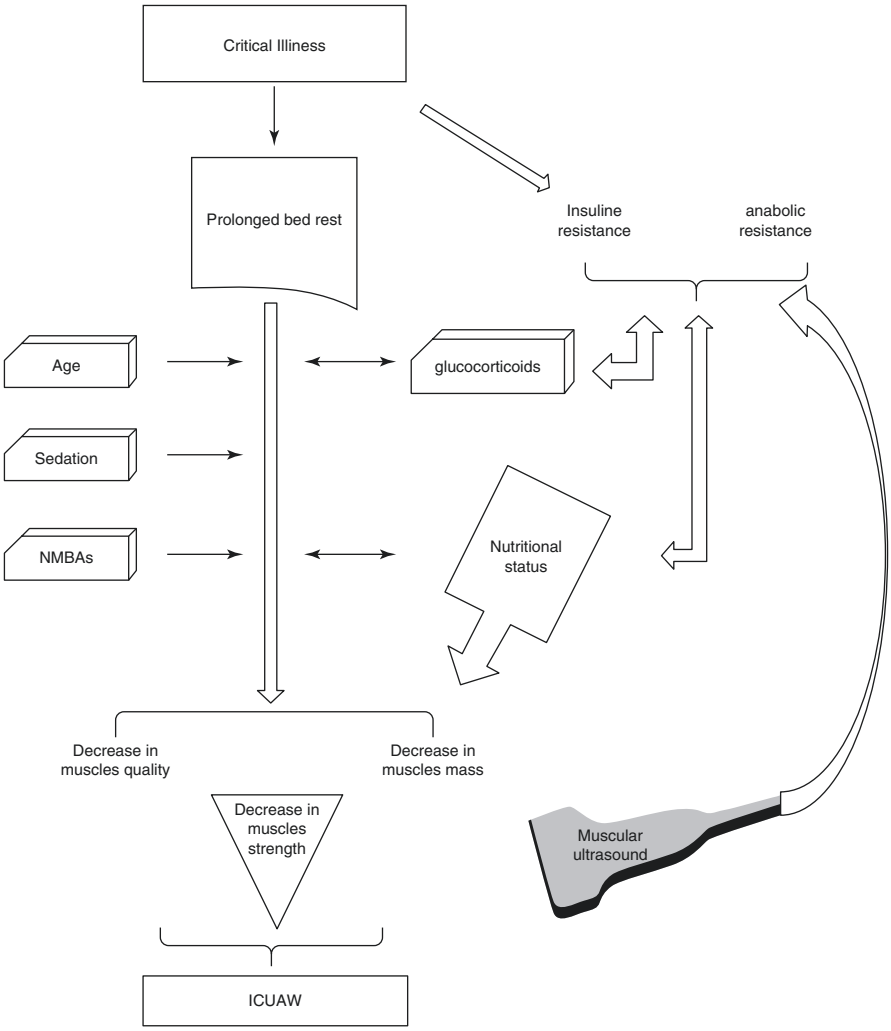

Fig. 59.1 A simplified diagram of ICUAW development. Critically ill patients are exposed to a variety of stimuli, which might impact upon muscle turnover, and the combination and intensity of these will vary with the background burden of disease, the nature and severity of the disease state causing admission, the therapies applied, the physiological response to disease and treatment. The prolonged bed rest, the use of specific pharmacological strategies need for the critical illness (such as sedative and neuromuscular blockade), as well as glucocorticoids and basal nutritional status, all interact in the balance between insulin resistance and anabolic resistance that influence per se the modulation of nutritional status. As consequence, a decrease in muscle quality and quantity (mass) might occur, determine a decrease of global muscle strength until the ICUAW. The muscular ultrasound (both peripheral and diaphragmatic) could play a role in the earlier detection of muscle strength reduction with the aim to improve

that readily distinguishes it from other tissues [34, 35]. To perform an adequate ultrasound examination of skeletal muscle, several technical components must be considered. First of all, muscle and subcutaneous fat are easily compressed. Thus, sufficient coupling gel combined with a minimal amount of pressure on the tissue with the ultrasound probe allow for the best imaging conditions. Additionally, obesity and subcutaneous oedema can significantly alter the appearance and quality of the ultrasound images of skeletal muscle. Therefore the examiner must be aware of the depth of the imaged tissue, the effects of attenuation of the ultrasound signal and the limitations of the ultrasound system. Manipulating the gain, the focal points and the compression may improve imaging of deep structures, but may also significantly alter the overall appearance of myofascial structures [31]. The probe orientation and muscle position can also radically alter the image appearance. The ultrasonographic brightness of the muscle is critically dependent on the relationship between the angle of the probe and the underlying pennation angle of the myofascial bands [36]. In fact, a pennate muscle is a muscle with fascicles that attach obliquely to its tendon. These types of muscles generally allow higher force production but smaller range of motion meaning that when a muscle contracts and shortens, the pennation angle increases. Thus, in a bipennate muscle (i.e. the rectus femoris) the superficial and deep portions of the muscle will alternately appear bright or dark as the probe angle is adjusted. Maintaining the probe angle perpendicular to the bone yields an image of the bone with a bright reflection.

59.5 Muscular Ultrasound: Parameters of Muscles Architecture

59.5.1 Cross-Sectional Area

The anatomical cross-sectional area is the area of the cross section of a muscle perpendicular to its longitudinal axis. The physiological CSA is the area of the cross section of a muscle perpendicular to its fibres, generally at its largest point. Both are used to describe the contraction properties of pennate muscles, and in a non-pennate muscle they coincide because the fibres are parallel to the longitudinal axis (Fig. 59.2). As the muscle strength is related to muscle volume, it is reflected by muscle CSA and thickness [37]. Because their measurements do not need muscle tension, they are often assessed instead of the muscle strength test. Thus, muscle substance can be measured by the CSA which variation is dependent on age, gender and muscle group [38]; the muscle atrophy can likely be assessed by measuring the muscle thickness that has to be compared with subcutaneous fat (approximately 2:1) even if the muscle-to-subcutaneous-fat ratio can be misleading in some patient categories (such as obese patients and infants) [39] determining that both quantitative and qualitative assessment of muscle thickness must be interpreted using standards adjusted for patient characteristics.

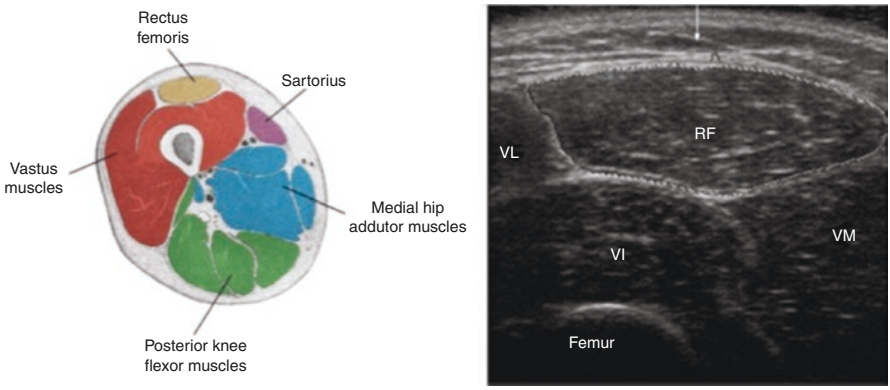

Fig. 59.2 Muscle cross-sectional area. The figure depict the cross sectional area of the rectus femoris perpendicular to its longitudinal axis

59.5.2 Muscle Layer Thickness

The muscle thickness is defined as the distance between two fascias easily determined with ultrasound. It has been shown that muscle loss of ICU patients could be monitored by thickness measurements of muscle rectus femoris and rectus intermedius [40]. Thus, in order to raise the accuracy, other indexes reflecting muscle strength should be added to that of muscle thickness. Concerning the reproducibility, muscle thickness measurements revealed the highest reproducibility in various muscles [41–43].

59.5.3 Echointensity

Information about the muscle composition can be gathered by quantification of muscle echogenicity [44]. The measure of the grey-scale of the image may reflect muscle composition: the increased echogenicity represents the more homogenous muscle [45]. Its value is calculated by performing grey-scale analysis of image pixels using the histogram feature of image-processing software. All of the pixels in the selected area of the muscle are categorized on a grey-scale configuration. It can be measured subjectively using a standard histogram function widely available in many commercially computer software programs for image editing (Fig. 59.3). Quantitative grey-scale analysis proved to be better than visual assessment alone of ultrasound images [35]. The ultrasonic echogenicity can be graded according with a score that differentiates ultrasonic echogenicity semi-quantitatively into four grades in which the higher grade of echostructure with reduced or lost bone signal correlates to the severity of muscle impairment [46]. This process has been shown to correlate with muscle pathologic findings on biopsy [44]. As for other measures, an echogenicity measurement seems to be highly influenced by observer-dependent

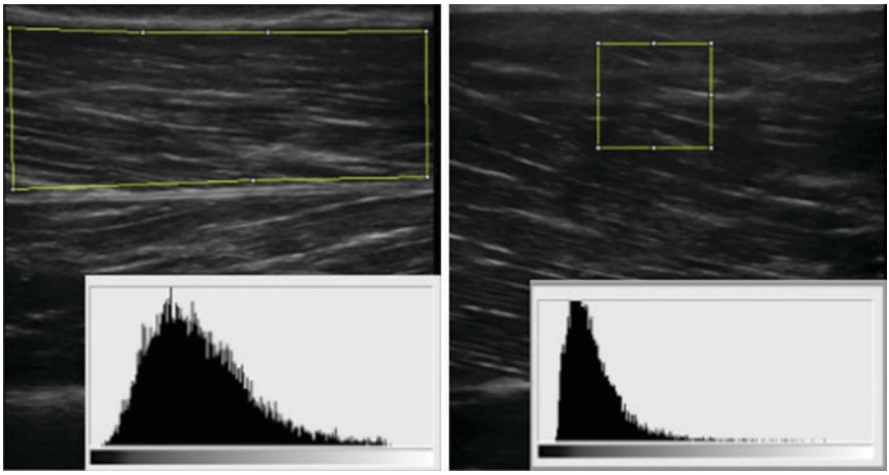

Fig. 59.3 The muscle ultrasound echointensity. Ultrasound images of two different ROIs used to measure muscle echo-intensity. A maximum ROI was defined for each image to include as much of the muscle as possible, avoiding bone and surrounding fasciae (right panel). A smaller ROI was positioned approximately at the center of the muscle image (left panel)

factors such as the adjustment of the ultrasound probe. Additionally, factors as for example the hydration balance of the muscle might also have an impact on echogenicity measurements. Only one study investigating reproducibility of echogenicity of muscle rectus femoris and intermedius in healthy individuals showed no inter-observer reproducibility for measurements of echogenicity [47]. Finally, this methodology is slightly more time-consuming and requires the establishment of normal values.

59.5.4 Pennation Angle

As mentioned above, muscle architecture can be described by the pennation angle, the angle of insertion of muscle fibres into muscle aponeurosis (Fig. 59.4). It gives information about muscle strength as the larger the pennation angle is, the more contractile material can be packed within a certain volume and thus increases the muscle's capacity to produce force [48]. Manini et al. [49] reported that muscle disuse results in altered composition, characterized by a significant increased accumulation of intramuscular fat, which is accompanied by a significant loss of muscle strength. Moreover, it has been already significantly correlated to the CSA [50]. Therefore, the angle of pennation is critical for determining force dynamics of muscle. Because pennation angle measurements are strongly influenced by adjustment of the ultrasound probe, difficulties in observer-dependent techniques were reported [51]. In particular, its reproducibility in other muscles of the quadriceps was generally worse [36]. Finally, the fascicle length (FL) can be derived from pennation

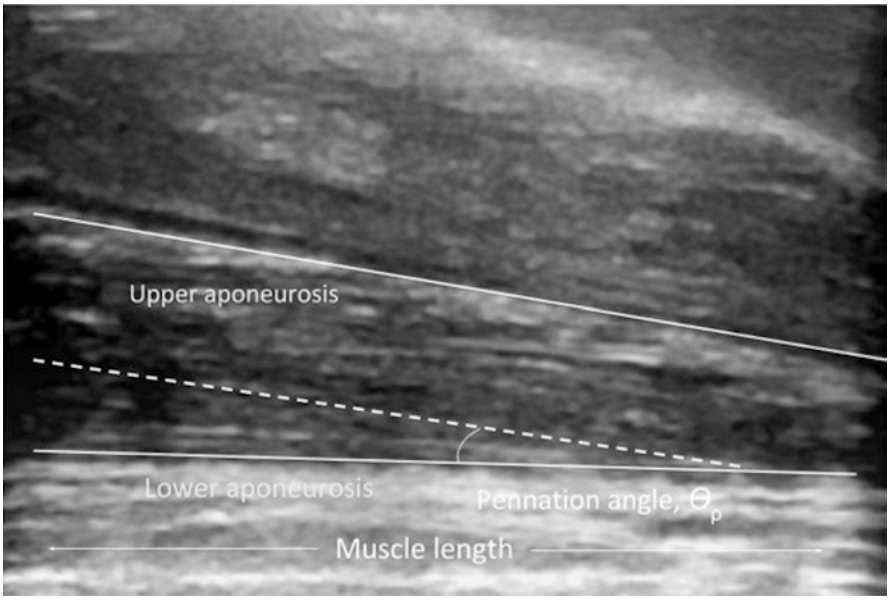

Fig. 59.4 The muscle ultrasound pennation angle. The figure represents a longitudinal view of quadriceps rectus femoris muscle. The pennation angle is calculated with the interception of fascicular path to the lower aponeurosis; additionally, the muscle length can be measure. The to variables may be use to determine the strength of the muscle, as the lower is the angle, the lower is the length, the lower is the strength. The fascicle length (FL) can be derived from pennation angle and muscle thickness using the following formula: FL = MT/(sin PA)

angle and muscle thickness as described elsewhere [39, 52] using the following formula: (Eq. 59.1)

$$\mathrm{FL} = \mathrm{MT} / \left(\sin \mathrm{PA}\right). \tag{59.1}$$

Muscles with larger pennation angles have greater muscle thickness by having greater numbers of sarcomeres in parallel to the direction of the fascicle. It may be that these parallel sarcomeres are lost first, causing loss of pennation angle and consequently loss of muscle thickness. In practical terms, a large pennation angle is able to pack more contractile components in parallel into a certain volume, and thus can generate greater force up to angles of 45° degrees, while a loss of angle leads to a loss of force generation.

59.6 Muscular Ultrasound: Clinical Practice

Among different regions of interest within the muscle, the quadriceps muscle is one of the greatest muscles groups of the lower limb, which can be explored using ultrasounds. Usually, the main image obtained permits the assessment of the muscle

pattern and layer thickness aspects, which can be useful in monitoring the effects of different types of contraction in muscular physiology and in pathology. In the following section, we will describe the literature knowledge of this method in healthy, COPD and critically ill patients (Table 59.1).

Table 59.1 Principal studies regarding peripheral muscular ultrasound

	Author	Design	Parameters	Main remarks
Healthy	Chi-Fishman 2004 [57]	9 patients with myositis vs. healthy subject	Maximal isometric contraction of the rectus femoris muscle in 2 knee-flexion positions (60°, 90°) during simultaneous ultrasound imaging and muscle force dynamometry	Ultrasonography provided a quantitative measure of change between relaxed and contracted state of muscle, which correlated with muscle force. Ultrasound identified significant differences in cross-sectional diameters between the myopathic and normal muscles sampled and may be useful for measuring muscle response to drug and exercise therapy
	Baldwin 2011[76]	40 healthy subjects	Diaphragm thickness and thicknesses of the mid-upper arm, mid-forearm and mid-thigh musculature	Ultrasound technique has good reliability in recumbent positions, making it useful for application to clinical populations
	E Lima 2012 [86]	15 healthy subjects	Cross-sectional area rectus femoris measurements, obtained by ultrasound, with two in two distinct regions performed in 2 days	There were significant differences between areas at 15 cm above the patella and at 50% of the thigh length, emphasizing the lack of uniformity of this value along the muscle
	Takai 2013 [54]	77 healthy subjects	Ultrasound muscle thickness (MT) measurements for predicting leg skeletal muscle mass (SM) vs. dual-energy X-ray absorptiometry (DXA)	The application of equation for the cross-validation group did not yield a significant difference between the measured or estimated LTM and systematic error. With the ultrasound approach, increasing the number of levels for MT measurements will improve the accuracy of LTM estimation
	Tillquist 2014 [55]	78 healthy volunteers	Evaluate the intra- and inter-reliability of muscle quadriceps muscle layer thickness (QMLT)	Excellent intra- and inter-rater reliability for ultrasound measurements of QMLT in healthy volunteers was observed; multivariate linear regression showed that sarcopenia, but not muscle index, was associated with decreased ventilator-free and ICU-free days

(continued)

Table 59.1 (continued)

	Author	Design	Parameters	Main remarks
	De Bruin 1997 [68]	9 asthmatic patients vs. healthy subjects	Forces generated by the respiratory (Diaphragm) and thigh muscles (rectus femoris) vs. with their dimensions assessed by ultrasound	Asthmatic patients had preserved quadriceps strength and Cross-sectional area of the relaxed rectus femoris muscle but moderately impaired maximum inspiratory pressure and thicker compared to normal subjects
COPD	Vivodtzev 2006 [87]	17 COPD with low BMI	Quadriceps muscle strength, total muscle mass (MM), exercise capacity with usual rehabilitation or plus muscular electrical stimulation (ES)	A significant relationship was found between changes in maximal voluntary contraction and changes in MM after training in the ES
	Seymour 2009 [70]	30 COPD vs. 26 healthy subjects	Rectus femoris muscle cross-sectional area (RFCSA) by US vs. whole-body free fatty mass by BIA	Mean RFCSA was reduced in patients with COPD by 25% of the mean value in healthy subjects; Ultrasound measurement of RFCSA is an effort-independent and radiation-free method of measuring quadriceps muscle cross-sectional area in patients with COPD that relates to strength
	Menon 2012 [67]	45 COPD	Ultrasound derived measures of quadriceps mass vs. dual energy x-ray absorptiometry (DEXA)	Serial ultrasound measurements of the quadriceps can detect changes in muscle mass. The technique has good reproducibility, and may be more sensitive to changes in muscle mass when compared to DEXA
	Hammond 2014 [66]	15 nondisabled subjects and 17 COPD	Measurements of rectus femoris cross-sectional area by using a curved array transducer vs. a linear-array transducer	In nondisabled subjects, the rectus cross-sectional area measured with the curved-array transducer by the novice and experienced operators was valid and reliable in COPD, both reliability and repeatability were high
	Campbell 1995 [88]	17 patients with MOF	Serial measurements of both muscle thickness (five limb and one trunk measurements) and mid-upper-arm circumference	In patients with MOF, muscle thickness showed a statistically significant decrease with time, which in general was not detectable from arm circumference. The muscle thicknesses that correlate best with lean body mass are measured over the biceps, anterior forearm, and anterior thigh

Table 59.1 (continued)

	Author	Design	Parameters	Main remarks
	Thomas 2012 [89]	45 CAD	Diameter of rectus femoris muscle US vs. muscle dimensions measured with CT scans	The absolute difference between both techniques was 0.01 ± 0.12 cm resulting in a typical percentage error of 4.4%. Muscle strength parameters were also significantly correlated with muscle diameter assessed with both techniques. Ultrasound imaging can be used as a valid and reliable measurement tool to assess the rectus femoris muscle diameter
	Moukas 2002 [90]	37 ICU hemiplegic patients	Low dose and short- term administration of corticosteroids vs. muscles relaxants on muscular mass (upper arm) and albumin detected by US (1th and tenth days)	Muscular atrophy of the ICU hemiplegic patients is significantly influenced by the synchronous treatment with muscle relaxants and corticosteroids at low doses and for short term
ICU	Reid 2004 [58]	50 ICU patients	Serial measurements of both mid-upper arm circumference (MAC) and muscle thickness, using ultrasound, were made at 1–3 day intervals	Muscle thickness decreased in almost every patients; ultrasound technique devised to identify muscle wasting in the presence of severe fluid retention works in the majority of patients; Energy balance made no difference to the rate of wasting
	Gruther 2008 [40]	118 ICU patients	Muscle layer thickness of the quadriceps femoris detected by US	Quadriceps femoris thickness showed a significant negative correlation with length of stay in ICU and seems to be higher during the first 2–3 weeks
	Gerovasili 2009 [91]	49 ICU patients	Electrical muscle stimulation effects on cross sectional diameter (CSD) of the vastus intermedius and the rectus femoris of the quadriceps muscle	The CSD of the right rectus femoris decreased significantly less in the EMS group and the CSD of the right vastus intermedius decreased significantly less in the EMS group
	Derde 2012 [92]	208 ICU patients	Markers of muscle atrophy and denervation vs. rectus abdominis and vastus lateralis; tissue and electrical physiological analysis	Both limb and abdominal wall skeletal muscles of prolonged critically ill patients showed down-regulation of protein synthesis at the gene expression level as well as increased proteolysis

(continued)

Table 59.1 (continued)

	Author	Design	Parameters	Main remarks
	Puthucheary 2013 [26]	63 ICU patients	Serial US measurement of the rectus femoris cross-sectional area (CSA) on days 1, 3, 7, and 10; histopathological analysis was performed	There were significant reductions in the rectus femoris CSA observed at day 10
	Cartwright 2013 79	16 ICU patients	Serial muscle ultrasound for thickness and gray-scale assessment of the tibialis anterior, rectus femoris, abductor digit, biceps, and diaphragm muscles over 14 days	The tibialis anterior and rectus femoris had significant decreases in gray-scale standard deviation when analyzed over 14 days. No muscles showed significant changes in thickness
	Grimm 2013 [78]	28 ICU septic patients vs. healthy	Biceps brachii and quadriceps femoris muscles, extensor muscles of the forearms and tibialis anterior muscle US, and nerve conduction studies on days 4 and 14 after sepsis	A significant difference in mean muscle echotexture between patients and controls was found at day 4 and day 14; day 4 to day 14, the mean grades of muscle echotexture increased in the patient group
	Baldwing 2014 [76]	16 ICU vs. 16 healthy	Diaphragm, upper arm, forearm, and thigh muscle thicknesses US; respiratory muscle strength by means of maximal inspiration. Fat-free body mass (FFM) measured by bioelectrical impedance spectroscopy	Patients' diaphragm thickness did not differ from that of the control group, Within the patient sample, all peripheral muscle groups were thinner compared with the diaphragm. Within the critically ill group, limb weakness was greater than the already-significant respiratory muscle weakness
	Moisey 2013 [6]	149 ICU trauma patients	CT Muscle cross-sectional area at the third lumbar vertebra quantified and related to clinical parameters including ventilator-free days, ICU-free days, and mortality	Increased muscle index was significantly associated with decreased mortality

Table 59.1 (continued)

	Author	Design	Parameters	Main remarks
	Puthucheary 2015 [93]	30 ICU patients	Vastus Lateralis histological specimens and ultrasound assessment of Rectus Femoris echogenicity	Change in muscle echogenicity was greater in patients who developed muscle necrosis. The area under receiver operator curve for ultrasound echogenicity's prediction of myofiber necrosis was 0.74. Myofiber necrosis and fascial inflammation can be detected noninvasively using ultrasound in the critically ill
	Parry 2015 [80]	22 ICU patients	Sequential quadriceps US images were obtained over the first 10 days	There was a 30% reduction in vastus intermedius thickness, rectus femoris thickness, and cross-sectional area within 10 days of admission. Muscle echogenicity scores increased for both RF and VI. There was a strong association between function and VI thickness and echogenicity
	Sarwal 2015 [51]	20 ICU patients	Diaphragm and quadricipites US muscle thickness and echogenicity	Excellent interobserver reliability was obtained for all measurement techniques regardless of expertise level
	Greening 2015 [82]	119 ICU COPD patients	Multivariate analysis between age, MRC dyspnea grade, home oxygen use, quadriceps (rectus femoris) cross-sectional area and hospitalization in the previous year	Patients with the smallest muscle spent more days in hospital than those with largest muscle. Smaller quadriceps muscle size, as measured by US in the acute care setting, is an independent risk factor for unscheduled readmission or death, which may have value both in clinical practice and for risk stratification
	Mueller 2016 [81]	102 ICU postsurgical	Rectus femoris cross-sectional area US	Diagnosis of sarcopenia by ultrasound predicts adverse discharge disposition in SICU patients equally well as frailty
	Turton 2016 [77]	22 ICU patients	Elbow flexor compartment, medial head of gastrocnemius and vastus lateralis muscle US at day 1,5 and 10th	No changes to the size of the elbow flexor compartment over 10 days. In the gastrocnemius, there were no significant changes to muscle. In the vastus lateralis, we found significant losses in muscle thickness

(continued)

Table 59.1 (continued)

	Author	Design	Parameters	Main remarks
	Seragan 2017 [84]	44 ICU patients	Muscle depth changes assessed by US on study days 1, 3, 5, 7, 12 and 14 in normal BMI vs. higher	Obese patients lost muscle depth in a comparable manner to non-obese patients, suggesting that BMI may not prevent muscle depth loss
	Annetta 2017 [83]	38 ICU trauma	Morphological changes of rectus femoris (RF) and anterior tibialis (AT) muscles up to 3 weeks	Progressive loss of muscle mass from day 0 to day 20, that was more relevant for the RF than for the AT; this was accompanied by an increase in echogenicity which is an indicator of myofibers depletion
	Valla 2017 [94]	73 PICU	Transverse and longitudinal axis measurements of quadriceps femoris anterior thickness	Femoris thickness decrease, proposed as a surrogate for muscle mass, is an early, frequent, and intense phenomenon in PICU. Quadriceps femoris ultrasonography is a reliable technique to monitor this process and in future could help to guide rehabilitation and nutrition interventions
	Hadda 2018 [85]	45 ICU patients	Arm muscle thickness US measured	There was an excellent intra- and inter-observer agreement among 5 observers for measurement of arm muscle thickness using bedside USG among patients with sepsis

59.6.1 Muscular Ultrasound: Healthy Patient

Skeletal muscle ultrasound became a standardized and accurate imaging technique that has entered in clinical practice for the diagnosis and follow-up of neuromuscular disorders since Pillen reviewed its usefulness in this field [53]. Before and after that, many studies in healthy subject focused principally on validation of the technique and its reliability as compared with standard methods. Takai et al. [54], compared the ultrasound muscle thickness measurements for predicting leg skeletal muscle mass with dual-energy X-ray absorptiometry in 77 older individuals. The lean tissue mass calculated by DEXA was used as a representative variable of leg skeletal muscle mass. The authors showed how the product of muscle thickness measured on the right leg at thigh anterior and posterior, lower leg anterior and posterior with limb length was a strong contributor for predicting the measured skeletal mass, as already reported by Miyatani [32]. Tillquist and colleagues [55]

showed an excellent intra- and inter-reliability for ultrasound measurements of muscle quadriceps muscle layer thickness measured at the border between the lower third and upper two-thirds between the anterior superior iliac spine and the upper pole of the patella, as well as the measurement of the midpoint between the anterior superior iliac spine and the upper pole of the patella. With a similar purpose, the reliability of the ultrasound CSA measurement of the rectus femoris muscle has been proved in a couple of studies in which CSA was measured in two distinct regions (15 cm above the patella and 50% of the thigh length) five times/day for two consecutive days. The authors pointed out a significant different values of CSA between the two sites due to the fact that with a longer length of the thigh, the image were obtained more distally and with a smaller anatomical CSA [56]. With a different purpose, the ultrasound CSA was correlated with strength measures detected by dynamometry during a relaxed and maximal isometric contraction of the rectus femoris muscle in 2 knee-flexion positions (60°, 90°) [57]. In this study the authors compared healthy muscles with those affected by myositis, and showed how the differences in CSA axes observed between the relaxed and contracted states of muscle correlated with muscle force, as measured by dynamometry. Moreover, the study highlighted how the rectus femoris could be considered the easiest for standardizing measurement location across subjects because it is the largest, most superficial and the only two-joint muscle in the quadriceps complex. Finally, there is only a study that validated the ultrasound application in the recumbent position considering how in in many clinical populations, including critically ill patients, the erect posture presents logistic difficulties [58]. Even if the main purpose was the study of the diaphragm thickness, the authors investigated also the feasibility of mid-upper arm thickness measured to the humerus, with the elbow extended and arm neutrally rotated in slight abduction alongside the body. Interestingly, there was greater variability in peripheral muscle thickness measured on the right body side compared with the left. However, the level of error reported could be accepted in the sub-acute phase of critical illness as patients with multiple organ failure suffer a reduction in the combined measurements of peripheral muscle thicknesses. These results are congruent with others reported in the early 1990s where muscle thicknesses measured over the biceps, anterior forearm and anterior thigh correlated best with lean body mass [59].

59.6.2 Muscular Ultrasound: COPD Patients

There are several studies that covered the muscular ultrasound investigation topic in a population – as the COPD is – in which generalized loss of weight and skeletal muscle mass might reduce the force generated both by respiratory and limb muscles. In particular, the disease is frequently accompanied by concomitant systemic manifestations among which skeletal muscle weakness is one of the major effects associated with the loss of lean body mass [60]. Therefore, the severity of

quadriceps weakness has been already showed to be associated with reductions in work capacity: across the spectrum of airflow obstruction all patients have both respiratory and peripheral muscle weakness [61], worsening dyspnoea and decreasing health-related quality of life, and increasing mortality [62]. In these terms, quadriceps strength, associated with CSA measured by CT and age, have been shown to be a powerful parameters to predict mortality [63, 64]. Moreover, it has been already observed that quadriceps wasting evaluated by ultrasound CSA exists in patients with mild and advanced COPD GOLD stages, and it is independently associated with physical inactivity [65]. Since ultrasound of the diaphragm has become a diagnostic technique of emerging interest among clinicians used to estimate muscle mass by measurement of muscle thickness and diagnose diaphragm weakness, some studies in COPD associated the two muscular components investigations. First of all, the methodological assessment of the rectus CSA has been validated measured with the curved-array transducer by the novice and experienced operators in terms of both reliability and repeatability (%TE: 7.6% and 9.8%) [66]. Moreover, Menon and colleagues [67] compared the responsiveness of ultrasound-derived measures of quadriceps mass against DEXA in patients with COPD and healthy controls following a program of high rehabilitation. This study showed how serial ultrasound measurements of the quadriceps was able detect changes in muscle mass in response to rehabilitation in COPD and how the technique had a good reproducibility and might be more sensitive to changes in muscle mass when compared to DEXA. In one of the first studies published with the aim of comparing the quality of diaphragm and limb muscles, De Bruin [68] compared the forces generated by the respiratory and thigh muscles with their dimensions assessed either by diaphragmatic thickness and CSA of the relaxed rectus femoris muscle ultrasound – obtained half-way between the major trochanter and the lateral joint-line of the knee – in chronic asthma patients and healthy subjects. The authors did not find any abnormality of the size and strength of the quadriceps muscle in asthmatic subjects and showed how the force generated by limb muscles was positively correlated to their ultrasound CSA as previously reported [38, 69]. Similarly, Saymur et al. [70] compared the rectus femoris CSA and whole-body free fatty mass estimated using electrical bioimpedance in 30 COPD patients and 26 healthy subjects, showing how in patients with COPD the quadriceps CSA was reduced by 25% as compared to healthy subjects. Moreover, a significantly higher echo-intensity of the rectus femoris has been observed in all stages of COPD patients with the quadriceps muscle thickness and CSA of the rectus femoris significantly decreased in COPD GOLD III–IV [71]. Very recently, a study in 285 stable COPD 85 failed to determine functionally relevant rectus femoris ultrasound CSA cut-points that identify patients with COPD unable to stand independently as compared with previous observations that identified functionally relevant cut-points for isometric quadriceps strength [72]. The identification of these patients in which muscular weakness is preponderant may guide early lifestyle and therapeutic interventions.

59.6.3 Muscular Ultrasound: ICU Setting

Many studies examined the association between muscle weakness and clinical outcome, and showed how muscle weakness was an independent predictor of mortality [73], associated with an increased ventilator dependent time [74] and ICU length of stay (LOS) [75]. In particular, a negative correlation between muscular thickness (in both upper and lower limb) with ICU LOS has been shown [40, 58, 59]. For these reasons, many papers focused on this topic have been published in the last two decades. Several studies investigated the alterations in anabolic and catabolic signalling and introduced the use of ultrasound in the detection of muscular characteristics with the aim of improving the pathophysiological knowledge and anticipating as much as possible its diagnosis. However, their interpretation result difficult because of significant methodological variability (such as small sample sizes and the standardization of imaging assessment) as well as the reliability of method was not the primary outcome. Moreover, we are currently unaware of how sex, age and presenting illness affect muscle mass loss in the critically ill. Most of the studies investigated the lower limb muscles for the reasons explained above, even if there are few studies that selected the upper arm as principal district, sometimes compared it with others. Among these, Reid [58] performed a serial measurement of both mid-upper arm thickness within the first 72 hours of ICU stay, showing how it decrease in almost every 50 patients enrolled independently of positive or negative energy balance. With similar purpose, more recently Baldwing et al. [76] investigated serial measurements of the thickness of the anterior mid–upper arm, midforearm in 16 septic ICU patients compared with healthy subject. As expected, septic patients were significantly weaker than control participants, with a significant difference in the thickness and thickness/Free Fatty Mass (FFM) of all peripheral muscles, suggesting that by 2 weeks of ICU admission, muscles of different functionalities may not be equally affected by a combination of insults that occur with critical illness. Finally, Turton et al. [77] investigated the elbow flexor compartment, the medial head of gastrocnemius and the vastus lateralis muscle at the admission and after 10 days in 22 ICU mechanically ventilated patients. Interestingly, this study showed no changes to the size of the elbow flexor compartment with a muscle thickness that indicated a mass loss occurred preferentially in the lower limb. This supports the validity of choosing the quadriceps as the most extensively studied peripheral muscle group in critically ill patients perhaps due to the fact that lower limb becoming earliest prone to disuse atrophy. Moreover, this was the first study that investigated the role of the pennation angle, addressing previous lack of knowledge. More specifically, patients who had a larger pennation angle at the day of admission had a greater percentage of their pennation angle reduction as well as muscle thickness.

Focusing largely on lower limb ultrasound investigation, most of the studies considered the muscle layer thickness and the CSA parameters, while only in few

papers the assessment of ultrasonic muscle echogenicity was the key parameter considered. With this regard, Grimm et al. [78] found significant alterations in muscle echostructure in the early stage of sepsis compared with healthy controls. Since those patients were septic and have a positive fluid balance, it is difficult to clarify whether oedema or muscle weakening may cause muscle echogenicity. However, as the authors pointed out, the significance of tissue oedema in the assessment of muscle echogenicity may be overestimated, since tissue oedema cannot alter the bone signal that is part of the echogenity score. Moreover, since the muscle echostructure score increased in the first 2 weeks with a concomitant decreasing in fluid balances, a specific structural damage in muscle architecture has been assumed. Cartwright and colleagues [79] found similar observation in echostructure changes over 2 weeks in both the tibialis anterior and rectus femoris muscles. Interestingly, these changes were similar to those seen in other myopathy conditions and included a significant increase in mean grey-scale value, indicating an increased muscle echogenicity and a decrease in grey-scale standard deviation, indicating that the muscle is more homogeneous. The use of grey-scale standard deviation to define muscle homogeneity is justified considering that the standard deviation decreases as the pixels in the region of interest become more uniform. However, once again, it is difficult to define if this pattern of change occurs because of muscle breakdown and loss of the normally well-organized muscle architecture or due to inflammation or fluid retention in the subcutaneous tissue and muscle. Since it is not clear if the ultrasonographic muscle changes correlate with strength, Parry et al. [80] addressed this topic showing how muscle echogenicity scores increased in quadriceps muscle (both rectus femoris and intermedious vastus) by 12% and 25%, suggesting deterioration in muscle quality with a strong association between function and echogenicity. Finally, in a recent prospective two-centre observational study, a comparison between sequential histological samples and ultrasound assessment of rectus femoris echogenicity was made [78]. This interesting paper showed how muscle echogenicity changes were greater in patients who developed muscle necrosis than in those who did not (8.2% vs −15.0%) and how the echogenicity's prediction of myofiber necrosis was 0.85. In a previous study [26], rectus femoris CSA and protein/DNA ratio were investigated showing that all decreased over the first week. This lower limb muscle wasting has been suggested as a consequence of both depressed muscle protein synthesis and an elevation in protein breakdown relative to protein synthesis, resulting in a net catabolic state. Unfortunately, muscle ultrasound significantly underestimated protein loss (as measured by the protein/DNA ratio), perhaps in part because of the presence of interstitial oedema. Moving forward on CSA studies, there is only one paper that integrated the ultrasound values into a sarcopenia and frailty prediction model, showing how the rectus fermoris CSA adjusted for sex and integrated with nutrition, comorbidities, depression and patient demographics data was able to predict adverse discharge disposition in surgical ICU patients [81]. With a similar purpose, looking at the risk of unscheduled readmission or death, Greening et al. [82] showed how smaller quadriceps muscle size described by CSA in the acute care setting was an independent risk factor for subsequent unscheduled re-admission. CSA have been also evaluated in selected critically ill populations – such as trauma and obese – confirming some previous

observation. In particular, the analysis of CSA and muscle diameter followed for 3 weeks in ICU trauma patients, showed how 100% experienced severe muscle mass loss and 45% of RF muscle mass was lost by day 20, together with a progressive increase in echogenicity score [83]. The muscle depth to measure muscle wasting was applied between obese, overweight and normal weight patients using a muscle ultrasound technique [84]. Compared with a previous study that used a similar methodology, the muscle depth loss was comparable and not statistically different between the obese groups at each of the time points. Lastly, the muscle thickness was investigated in many studies at different muscles group and the main results found that it is significantly reduced. Among these, as already mentioned, it has been shown to be decreased by 0.2–5.7% /day in the upper arm [58] and by a similar percentage in the lower limb [40]. Interestingly, the progression of this reduction was not uniform among the different quadriceps muscles, with a 30% reduction in RF and VI thickness and 14% reduction in VL [80]. Finally, very recently, in a cross-sectional observational study which included critically ill patients with sepsis, arm muscle thickness was measured with the aim of clarifying the intra- or inter-observer variations that were excellent as reported by other studies, concluding how there was an excellent intra- and inter-observer agreement among 5 observers for measurement of arm muscle thickness [85].

59.7 Conclusion

Skeletal muscle wasting in the critically ill has significant functional implications for patients who survive and the development of prophylactic or therapeutic interventions has been troubled by our lack of understanding of the pathophysiology driving the process of muscle wasting. Strong correlations have been demonstrated between muscle strength and indices of muscle mass, which can be easily detected by ultrasound with rectus femoris CSA and muscle limb thickness, both having highly functional relevance. Several studies have demonstrated that muscle ultrasound is able to reliably detect pathological changes; despite this, the interpretation of available studies is difficult because of significant methodological defects, inadequate sample sizes and lack of standardization of ultrasound methodology. Ideally, within the first 48 hours after the admission to the ICU, a first muscular ultrasound assessment should be performed. For simplicity, the evaluation should be confined to the rectus femoris of quadriceps muscle. Simultaneously, volitional strength evaluation should be performed as soon as cognitive impairment allows. The degree of possible cooperation should also be evaluated with validated scales for sedation, agitation level and delirium. Manual muscle testing, such as MRCS, reasonably achieved on average only 7–10 days after ICU admission, should be performed with a score in the normal range confirming the absence of ICUAW. When this is not accomplished, serial re-evaluations by muscular ultrasound may represent valuable tools. In particular, a reduction of 20% in muscle thickness, 10% of CSA, 5% of pennation angle and an increment in echo-intensity of at least 8% seem to be a reasonable indicators of ICUAW.

Algorithm

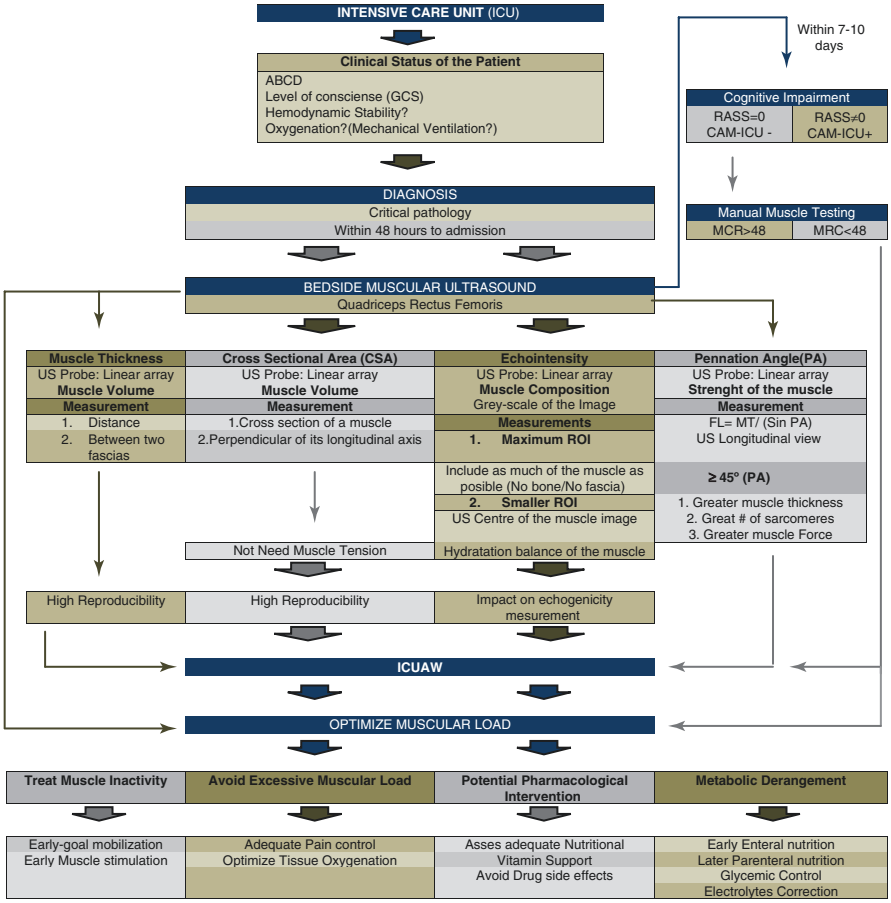

RASS Richmond agitation sedation scale, *CAM-ICU* Confusion assessment method for the ICU, *ICU* Intensive care unit, *MRC* Medical research council scale,; *TH* Muscle thickness, *CSA* Cross-sectional area, *ICUAW* ICU-acquired weakness

A flowchart suggests a protocol for early identification of ICUAW. Ideally, within the first 48 hours, a first muscle ultrasound assessment should be performed for a baseline description of patient muscle characteristics comprehensive of the quadriceps rectus femoris. It should include at least two or more of the following: muscle thickness (mTH), cross-sectional area (CSA), echointensity and pennation angle (PA). At the same time, the cognitive impairment should be evaluated using standard reproducible scales. If these scores are in the normal range, the application of manual muscle testing such as the medical research council scale is possible (MRCS). These first evaluations might be reconsidered within the first week after the admission in the ICU, and their modifications over time, integrated with each

other as well as with the re-evaluation of MRC scale, allow an accurate diagnosis of ICUAW and should be used to modify the different patient-dependent factors, such as pharmacological strategies, muscular over-loading or inactivity and metabolic derangements.

References

1. De Jonghe B, Bastuji-Garin S, Sharshar T, Outin H, Brochard L. Does ICU-acquired paresis lengthen weaning from mechanical ventilation? Intensive Care Med. 2004;30:1117–21.
2. Bednarík J, Vondracek P, Dusek L, Moravcova E, Cundrle I. Risk factors for critical illness polyneuromyopathy. J Neurol. 2005;252:343–51.
3. Hermans G, Van den Berghe G. Clinical review: intensive care unit acquired weakness. Crit Care. 2015;19:274.
4. Bednarik J, Lukas Z, Vondracek P. Critical illness polyneuromyopathy: the electrophysiological components of a complex entity. Intensive Care Med. 2003;29:1505–14.
5. Zhou C, Wu L, Ni F, Ji W, Wu J, Zhang H. Critical illness polyneuropathy and myopathy: a systematic review. Neural Regen Res. 2014;9:101–10.
6. Moisey LL, Mourtzakis M, Cotton BA, Premji T, Heyland DK, Wade CE, et al. Skeletal muscle predicts ventilator-free days, ICU-free days, and mortality in elderly ICU patients. Crit Care. 2013;17:R206.
7. Bittner EA, Martyn JA, George E, Frontera WR, Eikermann M. Measurement of muscle strength in the intensive care unit. Crit Care Med. 2009;37:S321–30.
8. Waak K, Zaremba S, Eikermann M. Muscle strength measurement in the intensive care unit: not everything that can be counted counts. J Crit Care. 2013;28:96–8.
9. Denehy L, de Morton NA, Skinner EH, Edbrooke L, Haines K, Warrillow S, et al. A physical function test for use in the intensive care unit: validity, responsiveness, and predictive utility of the physical function ICU test (scored). Phys Ther. 2013;93:1636–45.
10. Connolly BA, Jones GD, Curtis AA, Murphy PB, Douiri A, Hopkinson NS, et al. Clinical predictive value of manual muscle strength testing during critical illness: an observational cohort study. Crit Care. 2013;17:R229.
11. Hough CL, Lieu BK, Caldwell ES. Manual muscle strength testing of critically ill patients: feasibility and interobserver agreement. Crit Care. 2011;15:R43.
12. Cheung AM, Tansey CM, Tomlinson G, Diaz-Granados N, Matté A, Barr A, et al. Two-year outcomes, health care use, and costs of survivors of acute respiratory distress syndrome. Am J Respir Crit Care Med. 2006;174:538–44.
13. Cuthbertson BH, Roughton S, Jenkinson D, Maclennan G, Vale L. Quality of life in the five years after intensive care: a cohort study. Crit Care. 2010;14:R6.
14. Herridge MS, Cheung AM, Tansey CM, Matte-Martyn A, Diaz-Granados N, Al-Saidi F, et al. One-year outcomes in survivors of the acute respiratory distress syndrome. N Engl J Med. 2003;348:683–93.
15. Myhren H, Ekeberg Ø, Stokland O. Health-related quality of life and return to work after critical illness in general intensive care unit patients: a 1-year follow-up study. Crit Care Med. 2010;38:1554–61.
16. Hopkins RO, Weaver LK, Pope D, Orme JF, Bigler ED, Larson-LOHR V. Neuropsychological sequelae and impaired health status in survivors of severe acute respiratory distress syndrome. Am J Respir Crit Care Med. 1999;160:50–6.
17. Hopkins RO, Weaver LK, Collingridge D, Parkinson RB, Chan KJ, Orme JF. Two-year cognitive, emotional, and quality-of-life outcomes in acute respiratory distress syndrome. Am J Respir Crit Care Med. 2005;171:340–7.

18. Orme J, Romney JS, Hopkins RO, Pope D, Chan KJ, Thomsen G, et al. Pulmonary function and health-related quality of life in survivors of acute respiratory distress syndrome. Am J Respir Crit Care Med. 2003;167:690–4.
19. Rudiger A, Singer M. The heart in sepsis: from basic mechanisms to clinical management. Curr Vasc Pharmacol. 2013;11:187–95.
20. Rudiger A, Singer M. Mechanisms of sepsis-induced cardiac dysfunction. Crit Care Med. 2007;35:1599–608.
21. Allen DC, Arunachalam R, Mills KR. Critical illness myopathy: further evidence from muscle-fiber excitability studies of an acquired channelopathy. Muscle Nerve. 2008;37:14–22.
22. Novak KR, Nardelli P, Cope TC, Filatov G, Glass JD, Khan J, et al. Inactivation of sodium channels underlies reversible neuropathy during critical illness in rats. J Clin Invest. 2009;119:1150–8.
23. Teener JW, Rich MM. Dysregulation of sodium channel gating in critical illness myopathy. J Muscle Res Cell Motil. 2006;27:291–6.
24. Stevens RD, Dowdy DW, Michaels RK, Mendez-Tellez PA, Pronovost PJ, Needham DM. Neuromuscular dysfunction acquired in critical illness: a systematic review. Intensive Care Med. 2007;33:1876–91.
25. Herridge MS, Moss M, Hough CL, Hopkins RO, Rice TW, Bienvenu OJ, et al. Recovery and outcomes after the acute respiratory distress syndrome (ARDS) in patients and their family caregivers. Intensive Care Med. 2016;42:725–38.
26. Puthucheary ZA, Rawal J, McPhail M, Connolly B, Ratnayake G, Chan P, et al. Acute skeletal muscle wasting in critical illness. JAMA. 2013;310:1591–600.
27. Batt J, dos Santos CC, Cameron JI, Herridge MS. Intensive care unit-acquired weakness: clinical phenotypes and molecular mechanisms. Am J Respir Crit Care Med. 2013;187:238–46.
28. Babb T, Levine B, Philley J. ICU-acquired weakness: an extension of the effects of bed rest. Am J Respir Crit Care Med. 2012;185:230–1.
29. Nanas S, Kritikos K, Angelopoulos E, Siafaka A, Tsikriki S, Poriazi M, et al. Predisposing factors for critical illness polyneuromyopathy in a multidisciplinary intensive care unit. Acta Neurol Scand. 2008;118:175–81.
30. Dupont AC, Sauerbrei EE, Fenton PV, Shragge PC, Loeb GE, Richmond FJ. Real-time sonography to estimate muscle thickness: comparison with MRI and CT. J Clin Ultrasound. 2001;29:230–6.
31. Reeves ND, Maganaris CN, Narici MV. Ultrasonographic assessment of human skeletal muscle size. Eur J Appl Physiol. 2004;91:116–8.
32. Miyatani M, Kanehisa H, Ito M, Kawakami Y, Fukunaga T. The accuracy of volume estimates using ultrasound muscle thickness measurements in different muscle groups. Eur J Appl Physiol. 2004;91:264–72.
33. Paris MT, Mourtzakis M, Day A, Leung R, Watharkar S, Kozar R, et al. Validation of bedside ultrasound of muscle layer thickness of the quadriceps in the critically ill patient (VALIDUM study). JPEN J Parenter Enteral Nutr. 2017;41:171–80.
34. Peetrons P. Ultrasound of muscles. Eur Radiol. 2002;12:35–43.
35. Pillen S, van Keimpema M, Nievelstein RAJ, Verrips A, van Kruijsbergen-Raijmann W, Zwarts MJ. Skeletal muscle ultrasonography: Visual versus quantitative evaluation. Ultrasound Med Biol. 2006;32:1315–21.
36. Strasser EM, Draskovits T, Praschak M, Quittan M, Graf A. Association between ultrasound measurements of muscle thickness, pennation angle, echogenicity and skeletal muscle strength in the elderly. Age (Dordr). 2013;35:2377–88.
37. Akima H, Kubo K, Imai M, Kanehisa H, Suzuki Y, Gunji A, et al. Inactivity and muscle: effect of resistance training during bed rest on muscle size in the lower limb. Acta Physiol Scand. 2001;172:269–78.
38. Ikai M, Fukunaga T. Calculation of muscle strength per unit cross-sectional area of human muscle by means of ultrasonic measurement. Int Z Angew Physiol. 1968;26:26–32.

39. Abe T, Loenneke JP, Thiebaud RS. Morphological and functional relationships with ultrasound measured muscle thickness of the lower extremity: a brief review. Ultrasound. 2015;23:166–73.
40. Gruther W, Benesch T, Zorn C, Paternostro-Sluga T, Quittan M, Fialka-Moser V, et al. Muscle wasting in intensive care patients: ultrasound observation of the M. quadriceps femoris muscle layer. J Rehabil Med. 2008;40:185–9.
41. Miyatani M, Kanehisa H, Kuno S, Nishijima T, Fukunaga T. Validity of ultrasonograph muscle thickness measurements for estimating muscle volume of knee extensors in humans. Eur J Appl Physiol. 2002;86:203–8.
42. Blazevich AJ, Gill ND, Zhou S. Intra- and intermuscular variation in human quadriceps femoris architecture assessed in vivo. J Anat. 2006;209:289–310.
43. Thoirs K, English C. Ultrasound measures of muscle thickness: intra-examiner reliability and influence of body position. Clin Physiol Funct Imaging. 2009;29:440–6.
44. Reimers K, Reimers CD, Wagner S, Paetzke I, Pongratz DE. Skeletal muscle sonography: a correlative study of echogenicity and morphology. J Ultrasound Med. 1993;12:73–7.
45. Pillen S, van Dijk JP, Weijers G, Raijmann W, de Korte CL, Zwarts MJ. Quantitative gray-scale analysis in skeletal muscle ultrasound: a comparison study of two ultrasound devices. Muscle Nerve. 2009;39:781–6.
46. Heckmatt JZ, Leeman S, Dubowitz V. Ultrasound imaging in the diagnosis of muscle disease. J Pediatr. 1982;101:656–60.
47. Maurits NM, Bollen AE, Windhausen A, De Jager AEJ, Van Der Hoeven JH. Muscle ultrasound analysis: normal values and differentiation between myopathies and neuropathies. Ultrasound Med Biol. 2003;29:215–25.
48. Fukunaga T, Kawakami Y, Kuno S, Funato K, Fukashiro S. Muscle architecture and function in humans. J Biomech. 1997;30:457–63.
49. Manini TM, Clark BC, Nalls MA, Goodpaster BH, Ploutz-Snyder LL, Harris TB. Reduced physical activity increases intermuscular adipose tissue in healthy young adults. Am J Clin Nutr. 2007;85:377–84.
50. Rutherford OM, Jones DA. Measurement of fibre pennation using ultrasound in the human quadriceps in vivo. Eur J Appl Physiol Occup Physiol. 1992;65:433–7.
51. Sarwal A, Parry SM, Berry MJ, Hsu F-C, Lewis MT, Justus NW, et al. Interobserver reliability of quantitative muscle sonographic analysis in the critically ill population. J Ultrasound Med. 2015;34:1191–200.
52. Nasirzade A, Ehsanbakhsh A, Ilbeygi S, Sobhkhiz A, Argavani H, Aliakbari M. Relationship between sprint performance of front crawl swimming and muscle fascicle length in young swimmers. J Sports Sci Med. 2014;13:550–6.
53. Pillen S, Arts IMP, Zwarts MJ. Muscle ultrasound in neuromuscular disorders. Muscle Nerve. 2008;37:679–93.
54. Takai Y, Ohta M, Akagi R, Kato E, Wakahara T, Kawakami Y, et al. Validity of ultrasound muscle thickness measurements for predicting leg skeletal muscle mass in healthy Japanese middle-aged and older individuals. J Physiol Anthropol. 2013;32:12.
55. Tillquist M, Kutsogiannis DJ, Wischmeyer PE, Kummerlen C, Leung R, Stollery D, et al. Bedside ultrasound is a practical and reliable measurement tool for assessing quadriceps muscle layer thickness. JPEN J Parenter Enteral Nutr. 2014;38:886–90.
56. Delaney S, Worsley P, Warner M, Taylor M, Stokes M. Assessing contractile ability of the quadriceps muscle using ultrasound imaging. Muscle Nerve. 2010;42:530–8.
57. Chi-Fishman G, Hicks JE, Cintas HM, Sonies BC, Gerber LH. Ultrasound imaging distinguishes between normal and weak muscle. Arch Phys Med Rehabil. 2004;85:980–6.
58. Reid CL, Campbell IT, Little RA. Muscle wasting and energy balance in critical illness. Clin Nutr. 2004;23:273–80.
59. Freilich RJ, Kirsner RL, Byrne E. Isometric strength and thickness relationships in human quadriceps muscle. Neuromuscul Disord. 1995;5:415–22.
60. Maltais F, Decramer M, Casaburi R, Barreiro E, Burelle Y, Debigaré R, et al. An official American Thoracic Society/European Respiratory Society statement: update on limb

muscle dysfunction in chronic obstructive pulmonary disease. Am J Respir Crit Care Med. 2014;189:e15–62.
61. Singer J, Yelin EH, Katz PP, Sanchez G, Iribarren C, Eisner MD, et al. Respiratory and skeletal muscle strength in chronic obstructive pulmonary disease: impact on exercise capacity and lower extremity function. J Cardiopulm Rehabil Prev. 2011;31:111–9.
62. Decramer M, Rennard S, Troosters T, Mapel DW, Giardino N, Mannino D, et al. COPD as a lung disease with systemic consequences--clinical impact, mechanisms, and potential for early intervention. COPD. 2008;5:235–56.
63. Swallow EB, Reyes D, Hopkinson NS, Man WD-C, Porcher R, Cetti EJ, et al. Quadriceps strength predicts mortality in patients with moderate to severe chronic obstructive pulmonary disease. Thorax. 2007;62:115–20.
64. Marquis K, Debigaré R, Lacasse Y, LeBlanc P, Jobin J, Carrier G, et al. Midthigh muscle cross-sectional area is a better predictor of mortality than body mass index in patients with chronic obstructive pulmonary disease. Am J Respir Crit Care Med. 2002;166:809–13.
65. Shrikrishna D, Patel M, Tanner RJ, Seymour JM, Connolly BA, Puthucheary ZA, et al. Quadriceps wasting and physical inactivity in patients with COPD. Eur Respir J. 2012;40:1115–22.
66. Hammond K, Mampilly J, Laghi FA, Goyal A, Collins EG, McBurney C, et al. Validity and reliability of rectus femoris ultrasound measurements: comparison of curved-array and linear-array transducers. J Rehabil Res Dev. 2014;51:1155–64.
67. Menon MK, Houchen L, Harrison S, Singh SJ, Morgan MD, Steiner MC. Ultrasound assessment of lower limb muscle mass in response to resistance training in COPD. Respir Res. 2012;13:119.
68. de Bruin PF, Ueki J, Watson A, Pride NB. Size and strength of the respiratory and quadriceps muscles in patients with chronic asthma. Eur Respir J. 1997;10:59–64.
69. Young A, Stokes M, Crowe M. The size and strength of the quadriceps muscles of old and young men. Clin Physiol. 1985;5:145–54.
70. Seymour JM, Ward K, Sidhu PS, Puthucheary Z, Steier J, Jolley CJ, et al. Ultrasound measurement of rectus femoris cross-sectional area and the relationship with quadriceps strength in COPD. Thorax. 2009;64:418–23.
71. Ye X, Wang M, Xiao H. Echo intensity of the rectus femoris in stable COPD patients. Int J Chron Obstruct Pulmon Dis. 2017;12:3007–15.
72. Canavan JL, Maddocks M, Nolan CM, Jones SE, Kon SSC, Clark AL, et al. Functionally relevant cut point for isometric quadriceps muscle strength in chronic respiratory disease. Am J Respir Crit Care Med. 2015;192:395–7.
73. Sharshar T, Bastuji-Garin S, Stevens RD, Durand M-C, Malissin I, Rodriguez P, et al. Presence and severity of intensive care unit-acquired paresis at time of awakening are associated with increased intensive care unit and hospital mortality. Crit Care Med. 2009;37:3047–53.
74. De Jonghe B, Sharshar T, Lefaucheur J-P, Authier F-J, Durand-Zaleski I, Boussarsar M, et al. Paresis acquired in the intensive care unit: a prospective multicenter study. JAMA. 2002;288:2859–67.
75. Ali NA, O'Brien JM, Hoffmann SP, Phillips G, Garland A, Finley JCW, et al. Acquired weakness, handgrip strength, and mortality in critically ill patients. Am J Respir Crit Care Med. 2008;178:261–8.
76. Baldwin CE, Bersten AD. Alterations in respiratory and limb muscle strength and size in patients with sepsis who are mechanically ventilated. Phys Ther. 2014;94:68–82.
77. Turton P, Hay R, Taylor J, McPhee J, Welters I. Human limb skeletal muscle wasting and architectural remodeling during five to ten days intubation and ventilation in critical care - an observational study using ultrasound. BMC Anesthesiol. 2016;16:119.
78. Grimm A, Teschner U, Porzelius C, Ludewig K, Zielske J, Witte OW, et al. Muscle ultrasound for early assessment of critical illness neuromyopathy in severe sepsis. Crit Care. 2013;17:R227.

79. Cartwright MS, Demar S, Griffin LP, Balakrishnan N, Harris JM, Walker FO. Validity and reliability of nerve and muscle ultrasound. Muscle Nerve. 2013;47:515–21.
80. Parry SM, El-Ansary D, Cartwright MS, Sarwal A, Berney S, Koopman R, et al. Ultrasonography in the intensive care setting can be used to detect changes in the quality and quantity of muscle and is related to muscle strength and function. J Crit Care. 2015;30:1151.e9–14.
81. Mueller N, Murthy S, Tainter CR, Lee J, Riddell K, Fintelmann FJ, et al. Can sarcopenia quantified by ultrasound of the rectus Femoris muscle predict adverse outcome of surgical intensive care unit patients as well as frailty? A prospective, observational Cohort Study. Ann Surg. 2016;264:1116–24.
82. Greening NJ, Harvey-Dunstan TC, Chaplin EJ, Vincent EE, Morgan MD, Singh SJ, et al. Bedside assessment of quadriceps muscle by ultrasound after admission for acute exacerbations of chronic respiratory disease. Am J Respir Crit Care Med. 2015;192:810–6.
83. Annetta MG, Pittiruti M, Silvestri D, Grieco DL, Maccaglia A, La Torre MF, et al. Ultrasound assessment of rectus femoris and anterior tibialis muscles in young trauma patients. Ann Intensive Care. 2017;7:104.
84. Segaran E, Wandrag L, Stotz M, Terblanche M, Hickson M. Does body mass index impact on muscle wasting and recovery following critical illness? A pilot feasibility observational study. J Hum Nutr Diet. 2017;30:227–35.
85. Hadda V, Kumar R, Hussain T, Khan MA, Madan K, Mohan A, et al. Reliability of ultrasonographic arm muscle thickness measurement by various levels of health care providers in ICU. Clin Nutr ESPEN. 2018;24:78–81.
86. e Lima KMM, da Matta TT, de Oliveira LF. Reliability of the rectus femoris muscle cross-sectional area measurements by ultrasonography. Clin Physiol Funct Imaging. 2012;32:221–6.
87. Vivodtzev I, Pépin J-L, Vottero G, Mayer V, Porsin B, Lévy P, et al. Improvement in quadriceps strength and dyspnea in daily tasks after 1 month of electrical stimulation in severely deconditioned and malnourished COPD. Chest. 2006;129:1540–8.
88. Campbell IT, Watt T, Withers D, England R, Sukumar S, Keegan MA, et al. Muscle thickness, measured with ultrasound, may be an indicator of lean tissue wasting in multiple organ failure in the presence of edema. Am J Clin Nutr. 1995;62:533–9.
89. Thomaes T, Thomis M, Onkelinx S, Coudyzer W, Cornelissen V, Vanhees L. Reliability and validity of the ultrasound technique to measure the rectus femoris muscle diameter in older CAD-patients. BMC Med Imaging. 2012;12:7.
90. Moukas M, Vassiliou MP, Amygdalou A, Mandragos C, Takis F, Behrakis PK. Muscular mass assessed by ultrasonography after administration of low-dose corticosteroids and muscle relaxants in critically ill hemiplegic patients. Clin Nutr. 2002;21:297–302.
91. Gerovasili V, Stefanidis K, Vitzilaios K, Karatzanos E, Politis P, Koroneos A, et al. Electrical muscle stimulation preserves the muscle mass of critically ill patients: a randomized study. Crit Care. 2009;13:R161.
92. Derde S, Hermans G, Derese I, Güiza F, Hedström Y, Wouters PJ, et al. Muscle atrophy and preferential loss of myosin in prolonged critically ill patients. Crit Care Med. 2012;40:79–89.
93. Puthucheary ZA, Phadke R, Rawal J, McPhail MJW, Sidhu PS, Rowlerson A, et al. Qualitative ultrasound in acute critical illness muscle wasting. Crit Care Med. 2015;43:1603–11.
94. Valla FV, Young DK, Rabilloud M, Periasami U, John M, Baudin F, et al. Thigh ultrasound monitoring identifies decreases in quadriceps femoris thickness as a frequent observation in critically ill children. Pediatr Crit Care Med. 2017;18:e339–47.

Chapter 60
POCUS Application in Neurocritical Care Patients: Transcranial Doppler (TCD/TCCS) as a Part of POCUS, from the Brain Ultrasound to Monitoring the Systemic Complications

Raffaele Aspide, Chiara Robba, and Federico Bilotta

Key Points

1. The clinical applications of Ultrasound (US) in perioperative medicine have enormously expanded over the past decades and include US-guided central venous catheterization, cardiac US imaging, airways and lung ultrasound, and abdominal ultrasound.
2. Point-of-care ultrasonography can be performed rapidly with good quality in critically ill patients.
3. Point-of-care ultrasonography frequently can help to diagnose and manage patients in the ICU and therefore can potentially have a substantial impact on critical care practice.
4. In the specific context of neurocritical care, in addition to other applications, transcranial Doppler (TCD/TCCS) ultrasonography has gained particular interest as a non-invasive bedside monitoring technique that helps to evaluate cerebral blood flow hemodynamics in the intracranial arterial vessels.
5. Brain US also includes the assessment of optic nerve sheath diameter, midline shift, hydrocephalus, and intracranial hemorrhage for the bedside diagnosis of neurological complications.

R. Aspide (✉)
IRCCS Istituto delle Scienze Neurologiche di Bologna, Anesthesia and Neurointensive Care Unit, Bologna, Italy
e-mail: r.aspide@isnb.it

C. Robba
Department of Anaesthesia and Intensive Care, Ospedale Policlinico San Martino IRCCS, IRCCS for Oncology, University of Genoa, Genoa, Italy

Deputy Neurointensive Care section - ESICM, Brussels, Belgium

F. Bilotta
Department of Anesthesiology, Critical Care and Pain Medicine, Section of Neuroanaesthesia and Neurocritical Care, Sapienza University of Rome, Rome, Italy

C. N. Rodríguez et al. (eds.), *Neurosonology in Critical Care*,
https://doi.org/10.1007/978-3-030-81419-9_60

60.1 Introduction

The clinical applications of ultrasound in perioperative medicine have enormously expanded over the past decades. The use of ultrasound to assist physicians in vascular cannulation and regional anesthesia has been described in depth. Moreover, transesophageal echocardiography has been performed by anesthesiologists during cardiac surgery for over 20 years [1].

Since the advent of portable ultrasonography machines, many providers, including intensivists, have been adequately trained in point-of-care ultrasonography (POCUS). When point-of-care ultrasonography is performed with a focused clinical question and goal, it serves as a valuable adjunct to the clinical examination and can facilitate patient care and disease management, without subjecting the patient to excessive radiation or transfer risks [2].

Management of critically ill patients requires rapid and safe diagnostic techniques. Ultrasonography can help with early detection of neurological emergencies; it is of assistance in the diagnosis of abdominal, lung, and brain pathologies and provides real-time information on the cardiac performance of critically ill patients.

Point-of-care ultrasonography can be performed rapidly with adequate image quality in the majority of critically ill patients. Point-of-care ultrasonography frequently brings changes to diagnosis and management in the ICU and therefore can potentially have a substantial impact on critical care practices [3]. Whether such impact translates into an improvement in patient outcomes remains to be demonstrated, but a growing body of evidence seems to point in this direction: Point-of-Care ultrasound has the potential to enhance patient care in the ICU and should now be part of every critical care clinician's armamentarium [4].

There was strong agreement among several international experts with regard to the guidelines for the use of ultrasound in the ICU. These recommendations were published by the Society of Critical Care Medicine (SCCM). They defined Grade 1A as follows: ultrasound-guidance for pleural effusion, diagnosis of pneumothorax, ultrasound-guided internal jugular venous cannulation, and ultrasound guidance for femoral venous cannulation. Grade 1B includes the use of ultrasound to assist with the following: drainage, paracentesis, diagnosis of most proximal deep venous thrombosis, and diagnosis of lower extremity proximal deep venous thrombosis. In particular, for cardiac ultrasonography, SCCM authors included in Grade 1B, investigation of the following: preload responsiveness in mechanically ventilated patients, pulmonary hypertension, ventricular tachycardia/fibrillation, cardiac tamponade, pericardiocentesis, shock, prosthetic valve endocarditis, blunt chest trauma for the pericardium, pediatric reversible causes of cardiac arrest, and pediatric preload responsiveness [6].

In the specific context of neurocritical care, in addition to other applications, transcranial Doppler (TCD) ultrasonography has gained particular interest. TCD is a non-invasive bedside monitoring technique that helps to evaluate cerebral blood flow velocities (CBFVs) in the intracranial arterial vessels. TCD allows the assessment of linear cerebral blood flow velocity with a high temporal resolution and is

inexpensive, reproducible, and portable. In this chapter, besides the general applications of Ultrasound in critically ill patients, we will present an overview of the most commonly used TCD applications in neurocritical care settings. The latter include the evaluation of intra- and extra-cranial arterial and venous vascular flow as well as the ultrasound imaging of the cerebral parenchyma, the ventricles, and the optic nerve with its sheath [5, 78].

60.2 Evaluation of Neurocritical Care Patients: Use of Pocus

60.2.1 POCUS: US-Guided Central Venous Catheterization

The ultrasound guidance to cannulate venous access has revolutionized medical practice, reducing errors and improving outcome. In addition to central venous access, echoguide is also used for various peripheral venous approaches (Midline, PICC) and for arterial access [11]. Often neurocritical patients, both in intensive care and operating room settings, need central venous access, for example, for interventions in a sitting position or in patients needing hemodynamic support, prolonged parenteral nutrition, or when prolonged stay in intensive care is needed. The cannulation of the internal jugular vein, the femoral vein, and also the subclavian vein (the infraclavicular approach being more common than the supraclavicular) is facilitated by the use of ultrasound, reducing accidental arterial punctures and helping the operator in complex situations, such as in a neurocritical patient with cervical spine injury [7]. This technique aids the identification of possible anatomical variations and the assessment of vessel depth, vein patency, and the possible presence of venous thrombosis that may contraindicate venous access [8, 9]. A linear probe of 5–15 Mhz is generally used, which allows for color Doppler analysis. The approach may include pre-procedure use of ultrasound for the identification of the vessel, which is then cannulated "freehand" ("US-assisted" CVC placement), or the fully ultrasound-guided approach that follows the puncture and the needle during the insertion phase (Fig. 60.1a). This technique encompasses two methods: the "out-of-plane" method, which uses the short-axis on the transverse plane and is easier for the less experienced US-operator, and the "in-plane" method, which uses the long-axis on the longitudinal plane and allows the operator to follow the needle during the entire insertion phase avoiding punctures of the vessel's back wall (Fig. 60.1b).

From a recent systematic review and meta-analysis, it appears that the echo-guided technique for cannulation of the internal jugular vein significantly reduces complications, accidental arterial puncture and hematoma formation and increases the success of the procedure, aiding cannulation at the first puncture [10, 13].

In addition to the anatomical identification of the vein, the most commonly used algorithm for the echo-guided approach to central vein cannulation allows for testing of the compressibility of the vessel; exclusion of thrombosis; use of ultrasound

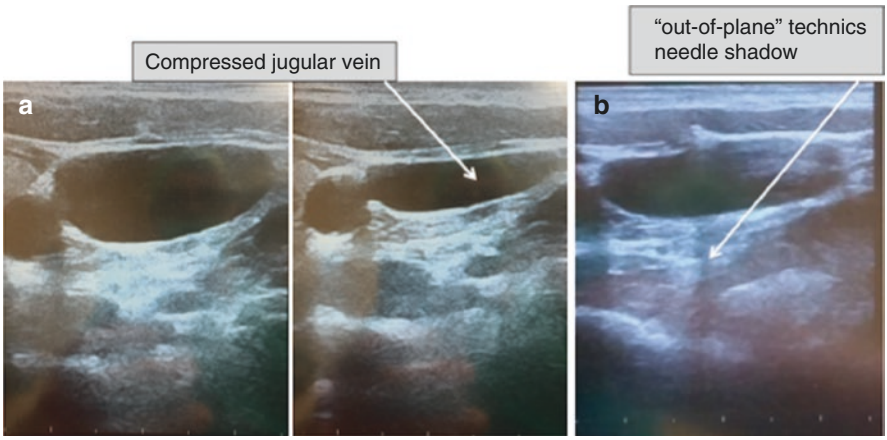

Fig. 60.1 B-Mode ultrasound of internal jugular vein: (**a**) compression maneuver; (**b**) needle insertion through transverse plane ("out-of-plane")

in real time in an aseptic and sterile environment during the puncture; and confirmation of correct needle positioning and correct direction of the wire and catheter (using both short-axis and long-axis) [12].

Despite the extensive evidence available, the actual worldwide use of the technique at bedside has yet to be fully implemented.

60.2.2 POCUS: Cardiac Ultrasound

Neurocritical care (NCC) patients can suffer from damage of the blood–brain barrier following stroke, subarachnoidal hemorrhage (SAH), or traumatic brain injury (TBI), but also as a consequence of brain tumors and other causes of increased intracranial pressure (ICP) [14]. This is mainly due to local brain inflammation, which produces endothelial damage in the vessels, increases oxidative stress, and promotes the release of cytokines and chemokines, activating the response of astrocytes, microglia, and macrophages. This mechanism can alter both the sympathetic and parasympathetic system regulation, activate the hypothalamic–pituitary–adrenal (HPA) axis, cause catecholamine surges, gut microbiome dysbiosis, as well as the release of microvesicles and microRNA. These phenomena can cause cardiac dysfunction, arrhythmias, and heart failure. These cardiac dysfunctions have been shown to be associated with an increased risk of death, delayed cerebral ischemia, and poor outcomes after SAH [15].

Specific cardiac diseases such as stress-induced cardiomyopathy – the Takotsubo syndrome (TTS) – have been found with a certain frequency among neurocritical patients. According to a retrospective study including over 2000 patients, 0.8% of patients with non-traumatic SAH may present with TTS. The causes and

pathogenesis of TTS, described by Japanese authors in the 1990s, remain to be clarified in detail. These patients mimic a myocardial infarction with severe left ventricle dysfunction, apical ballooning pattern, ST and troponin-I elevation, but with unharmed coronary arteries. They tend to recover in a few days or weeks. Some of them can present a left ventricular clot. TTS is linked to higher short-term and long-term mortality. The pathophysiological mechanism seems to be related to hormonal alterations and an increased bioavailability of catecholamines, which can induce coronary vasoconstriction.

These phenomena are currently the object of in-depth study within the medical sub-specialty now called neurocardiology. In this context, echocardiography allows even an intensivist without specific cardiological training to assess - with bedside point-of-care ultrasound (Fig. 60.2a) the size and function of the left ventricle, the transvalvular gradient, the pressure in the left atrium and, indirectly, the value of pulmonary artery pressure. Furthermore, the volume status can be assessed by calculating the degree of inspiratory collapse of the inferior vena cava [16].

Moreover, with echocardiography, it is possible to evaluate cardiac abnormalities such as atrial septal defect and patent foramen ovale, which can sometimes explain the source of emboli in patients with atrial fibrillation, as well as to assess the ventricular function and verify the presence of pericardial effusion/cardiac tamponade. In neurocritical patients, it is very important to avoid prolonged hypotension and hypoxia due to cardiac depression, as these can worsen patients' outcomes and increase the risk of both early and delayed cerebral injury. Finally, for example, pericardial tamponade is often present in polytrauma patients [14, 17].

Evaluation of the left ventricular function is performed with a 2D view of the four cardiac chambers: after freezing a good image, the operator freezes an image of the left ventricle in systole, with the caliper instrument delimiting the area of the

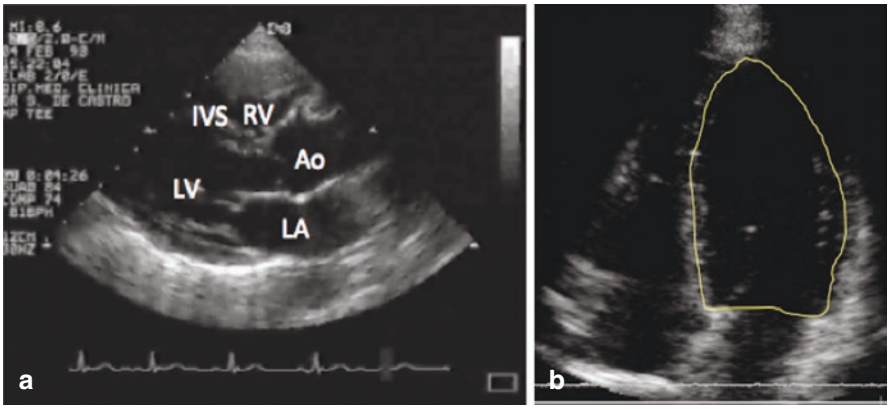

Fig. 60.2 Cardiac US: (**a**) Paraesternal long axys view; (IVS) Intraventricular septum, (LV) Left ventricle, (RV) Right ventricle, (LA) Left atrium, (Ao) Aortic valve; (**b**) Paraesternal short appical view (yellow line): Distolic area

ventricle, and the same measurement is repeated during the diastolic phase [18]; then fraction of ejection (EF) is calculated as:

$$\text{LVEF} = \left(\text{LVEDV} - \text{LVESV}\right) / \text{LVEDV} \qquad \left(\text{Fig. 60.2b}\right)$$

Once the interatrial septum is identified, with the color mode on, it is possible to highlight an abnormal flow if a defect is present. Indeed, with the rapid injection of intravenous microbubbles (1 milliliter of blood mixed with 9 milliliters of normal saline and some air), it is possible to highlight the passage of microbubbles through a patent oval foramen (a finding present in 25% of population) [77].

To prevent cerebral edema, an accurate fluid management strategy is very important. The volume status can be evaluated by comparing the two ventricles: if the right ventricle is as large as or larger than the left ventricle and a septal shift can be seen, it is likely that the patient is overloaded or suffers from pulmonary hypertension.

To implement tailored fluid therapy, ultrasound evaluation of the collapse of the inferior vena cava (IVC) can be very valuable: there is a poor relationship between central venous pressure (CVP) and blood volume, so the CVP/dCVP relationship has poor sensitivity in predicting the hemodynamic response to fluid challenge. The inspiratory collapse of the IVC, to be measured using the subcostal window, has shown good accuracy in predicting responsiveness to fluids. IVC diameter should be measured just proximally to the entrance of the hepatic veins. IVC diameter <2.1 cm that collapses >50% with an in-breath suggests normal right atrial (RA) pressure of 3 mm Hg (range 0–5 mm Hg); IVC diameter >2.1 cm that collapses <50% suggests high RA pressure of 15 mm Hg (range 10–20 mm Hg). In scenarios in which IVC diameter and collapse do not fit this paradigm, an intermediate value of 8 mm Hg (range 5–10 mm Hg) may be used [17, 19]. However, there are restrictions to the use of indicators such as IVC and its collapse in patients on the ICU: first, the IVC is commonly dilated and may not collapse in mechanically ventilated patients; and second, the IVC may be dilated in the presence of normal pressure in normal young athletes. However, measurement of changes in IVC dimensions after administration of an i.v. bolus of fluid is of particular interest, because of its technical simplicity.

60.2.3 POCUS: Airway and Lung Ultrasound

The use of US for assessment of the airways and the lungs is an important part of the point-of-care assessment in NCC patients. In particular, we recognize two main applications of lung US: the management of percutaneous tracheostomy and the study of lung parenchyma and pleurae. Many neurocritical patients may require mechanical ventilation by tracheostomy due to the persistence of neurological deficits. In percutaneous dilatational tracheostomy (PDT), we can distinguish a pre-procedural and an intra-procedural role for US [20]. Pre-tracheostomy US is used to

make anatomical assessments, to identify the vascular structures present and the location of the thyroid, and occasionally to exclude patients from the percutaneous tracheostomy pathway, allocating them to surgery. Pre-procedural US leads to tracheal puncture site change in 20–24% of cases and is associated with less bleeding during the procedure [21]. It can be very valuable to use US in the course of PDT, reducing the risk of accidental vascular punctures, stings of the first tracheal ring, puncture of the posterior tracheal wall, and upper misplacement of the tracheostomy [22]. Real-time US during PDT is very useful in the management of obese patients with difficult anatomy and in patients with cervical spine injury. Finally, the effects on systemic and cerebral hemodynamics can also be better modulated with the use of US during the procedure, a very valuable element in neurocritical patients [23].

Evaluation of the pulmonary parenchyma and pleurae can help us in the diagnosis of neurogenic pulmonary edema, a frequent scenario in NCC patients [24]. A linear or microconvex ultrasound probe works well on the chest surface, even with a grayscale-only machine. The evaluation must be performed with the patient in the supine position; the transducer is placed on the anterior chest wall in the second or third intercostal space in the longitudinal plane [25].

"Neurogenic" pulmonary edema complicates a fair share (10%) of cases of SAH. It seems to be mainly linked to hemodynamic changes due to alterations in the central neurovegetative control. Specifically, SAH is known to induce a stress of the sympathetic descending system with final depressive effects on the performance of the left ventricle. The absence of X-ray exposure and the simple reproducibility of the examination have made lung ultrasound a real point-of-care tool for the patients in ICU [28]. Fluids management in patients in NCC is very delicate and crucial in preventing cerebral edema; the search for specific signs with lung ultrasound can be an important guide. The use of the BLUE protocol [83] (Figs. 60.3 and 60.4)

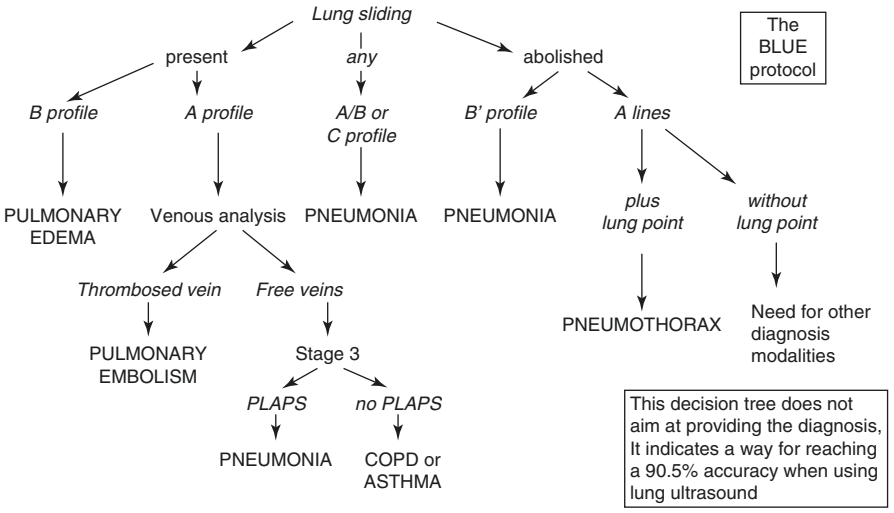

Fig. 60.3 Lung ultrasound: BLUE protocol. (Courtesy from Lichtenstein and Mezière [26])

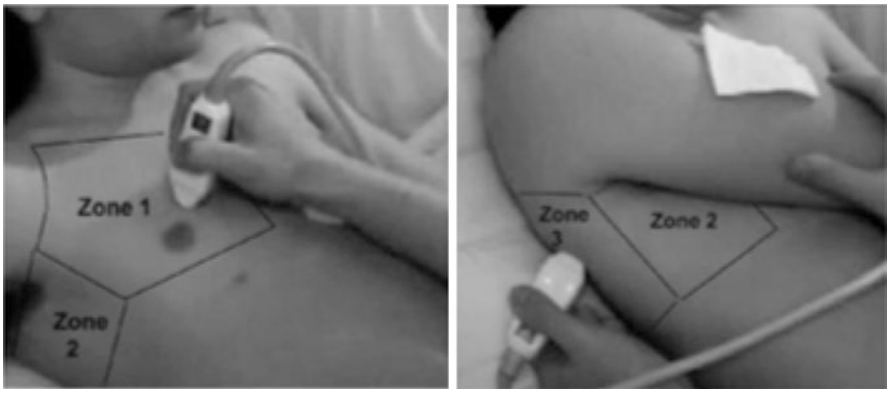

Fig. 60.4 BLUE protocol: ultrasound areas; (Zone1) anterior chest wall, (Zone 2) lateral wall and (Zone 3) posterolateral chest wall. (Courtesy from Lichtenstein and Mezière [26])

Table 60.1 Lung ultrasound: normal findings

Ultrasound findings	Definition	Clinical implications
Lung sliding	A movement in rhythm with respiration at the pleural line: Sliding of the visceral on parietal pleura	NO pneumothorax
Lung pulse	Absence of lung sliding, with perception of heart activity at pleural line	Atelectasis. NO Pneumothorax
A-lines	An horizontal line located below the pleural line, at the same distance of the skin from the pleura	NORMAL If present with lung sliding PNEUMOTHORAX If present with lung point, without lung sliding

(Bedside Lung Ultrasound in Emergency) [26], extended to include more specifically cardiac aspects in the fluid administration limited by lung sonography [84] (FALLS) protocol, is a good starting point. Possessing the skills to look for the top 10 ultrasound signs leads to a diagnostic accuracy between 90 and 100%. A normal lung surface is characterized by the presence of long sliding, bat sign, lung pulse, and A-lines. Abnormalities are identified by detecting lung point (absence of sliding), increase in pleural thickness (surface consolidation), vertical B-lines (lung rockets in interstitial syndromes), C-pattern in the consolidation areas, pleural effusion, and pneumothorax with a stratosphere sign and lung point (Table 60.1) [27].

The most common use of thoracic ultrasound is for the identification of the pneumothorax. Ultrasound sensitivity in the detection of the pneumothorax is very high; even a small apical or localized pneumothorax may be visualized.

60.2.4 POCUS: Abdominal Ultrasound: FAST

Among the various applications of ultrasound, the study of the abdomen is probably the most widespread. Neurocritical patients, and in particular TBI patients with polytrauma, require a prompt assessment of abdominal trauma at arrival in the Emergency Department (ED) [29]. Ultrasound can be a valuable point-of-care tool both to avoid moving such complex patients to radiological environments and to speed up management.

The aim of abdominal ultrasound examination in ED is to identify the presence and localization of blood (hemoperitoneum) and/or fluids. Blood and fluids tend to be located in the recess of the Morison for the supramesocolic regions, whereas from the suprapubic view the inframesocolic region is usually explored, which in women corresponds to the rectouterine space, known as Douglas' recess.

The most widespread and recognized protocol in ED is called FAST (focused assessment with sonography for trauma) and should include views of four different abdominal areas: the hepatorenal recess (or Morison's pouch) on the right, the perisplenic region on the left, the subxiphoid pericardial window centrally, and the Douglas pouch in the suprapubic window. In an extended version – the E-FAST examination – views of the bilateral hemithoraces and the upper anterior chest wall should also be performed [30, 31].

The main ultrasound examination of the abdomen includes four principal approaches. The areas should be examined using the probe on all available orthogonal planes: transverse, longitudinal, and coronal. FAST Protocol, step by step in the following order:

1. *The Pericardial View (Subcostal or Subxiphoid View)*:
   This view uses the liver as an acoustic window to detect pericardial effusion (fluid or blood). It is also possible to study the inferior vena cava (IVC) and the hepatic veins. IVC evaluation is also useful for the assessment of volume status and fluid responsiveness.
2. *The Right Upper Quadrant View*:
   Here, the liver is used as an ultrasound window to study the liver itself and the hepatorenal recess (Morison's pouch) for free fluid. In this view, it is also possible, by tilting the probe, to explore the dome of the liver and the diaphragm. From the same position, the right pleural space can also be explored. Finally, in the caudal direction, the upper pole of the right kidney can be viewed and the right paracolic gutter can be examined for the presence of free fluid.
3. *The Left Upper Quadrant View*:
   This allows examination of the spleen, the perisplenic space, the diaphragm, and the hepatorenal recess from the left. Above these, the left pleural space can be seen, and below them the upper pole of the left kidney and the left paracolic gutter can be identified.

4. *The Pelvic View*:

   Ideally, this evaluation is performed with a fluid-filled bladder (fluid can be inserted through a Foley catheter or trapped in the bladder by clamping the Foley catheter). This is the point of view of choice for the identification of free fluid in the peritoneum. The bladder should be studied on both the sagittal and transversal planes.

Acute hemorrhages appear as anechoic fluid collections. However, as the blood clots, often quite rapidly, these fluid collections may appear complex, hypoechoic, or even isoechoic to surrounding structures [32]. There are additional and more specific windows and training programs that exist for medical and non-medical ultrasound operators that are specific to each scientific company of reference and their guidelines. However, the interpretation of the exam must be performed exclusively by doctors. This is because the FAST examination has some limitations in identifying retroperitoneal hemorrhages and because the presence of free fluid in the abdomen can be due to concomitant causes, which are unrelated to trauma. Also bowel gas, obesity, subcutaneous emphysema, patient positioning, the degree of injury and rate of bleeding, adhesions from prior surgeries, and often in the patients who has pain or they are combative (secondary to traumatic injury), it can be difficult ultrasound diagnosis.

60.2.5 POCUS: Neurosonology

Already in the 50s, French and Leksell carried out several studies of the brain parenchyma, assessing the midline shift by using ultrasound images [33]. In 1982, Rune Aaslid from the University of Berne, Switzerland, developed the measurement of cerebral arteries' velocities flow through the Doppler effect, laying the foundations of our current knowledge [34]. By using a low-frequency–pulsed Doppler of 2 MHz over different acoustic windows – i.e., areas where cranial bones are thin – and the foramen magnum, Aaslid made use of the phenomenon described by physicist Christian Andreas Doppler in the nineteenth century: when a sound wave with a certain frequency strikes a moving object (such as red blood cells inside an artery), it is reflected with a different frequency - the Doppler shift - which is directly proportional to the velocity of the object (V). Echoes received by the transducer probe are processed in pulse or continuous mode to produce a spectral waveform with peak systolic and diastolic velocity values.

Over the years, this technique, integrated with US imaging, has found many fields of application not limited to neurocritical care but extending to a vast range of clinical scenarios, thus becoming a real point-of-care application [6, 35]. Common applications in NCC include the detection of vasospasm in patients with spontaneous or traumatic subarachnoid hemorrhage [36, 37, 83], cerebrovascular autoregulation [36, 38, 81, 82], as an adjunct in the clinical diagnosis of brain death [36–40], and many other scenarios [80]. The application of this technique in other clinical

areas – including liver failure, pregnancy in pre-eclampsia [41], and sepsis [42] – is undergoing further study, although at present there is not enough scientific evidence to incorporate it into daily practice.

60.2.5.1 Techniques

The traditional transcranial Doppler (TCD) equipment is commonly called "blind", and it usually uses a dedicated device that can only measure blood flow velocity through one or more types of probes, where the 2 MHz probe is the most commonly used. With the same type of equipment, it is possible to use the so-called bilateral continuous Doppler through a special helmet in which 2 MHz probes are usually inserted; this allows the continuous monitoring of flow velocities in the patient's brain vessels.

A development of this equipment is represented by the combination of ultrasound imaging (B-Mode) with color Doppler through the color-coded duplex mode: TCCS (transcranial color-coded duplex sonography). In many ultrasound devices there are pre-defined TCCS settings that allow, using a low-frequency 1.6–3.5 MHz probe, the one of 4 MHz normally used for echocardiography, visualization of basal cerebral arterial anatomy to measure blood flow velocities and to study brain parenchyma by combining B-mode ultrasound imaging and Doppler curves. If pre-set options are not present, the operator will need to ask a specialist or consult manufacturer's documentation in order to correctly set up the equipment's parameters to better visualize brain images. With the same probe, without using the Doppler effect and using the appropriate landmarks, it is possible to study the parenchymal structures of the brain in the B-mode exclusively.

To perform TCD, the operator should position her/himself behind the head of the supine patient, in a neutral position. A slow circular movement of the end of the transducer without change in contact may help find a signal. A signal identifying the middle cerebral artery (MCA) can usually be obtained at a starting focus depth of 55 mm. If a signal is not found, the probe is shifted more anteriorly toward the orbital rim. If a signal is still not found, the probe is moved upward at the crossing of the zygomatic bone and the lateral orbital margin. Approximately 10% of patients do not have a temporal window, and failure to find a signal cannot therefore be automatically attributed to technique [43]. The echo-Doppler monitor is normally on one side of the bed and it is useful to avoid that the probe cable impedes the operator's movements. Especially in the early stages of learning, a lot of endurance and tranquility are needed: just getting used to doing very fine movements, the evaluation might take a long time (about 20–30 minutes) [44, 45].

The aim of the examination is the insonation of the main structures of the brain, including mesencephalon, basal cisterns, lateral ventricles, third ventricle, and the Circle of Willis.

60.2.5.2 Neurosonology: Cerebral Blood Flow Velocities (CBFV)

The Circle of Willis has the shape of a heptagon with the following sides: frontally, the two anterior (right and left) cerebral arteries (ACA) that are connected via the anterior communicating artery (AcomA); posteriorly, the two posterior cerebral arteries (right and left) (PCA); between the anterior and posterior cerebral arteries of each side, the posterior communicating arteries (PcomA); and at the point of convergence between the posterior communicating artery and the anterior cerebral artery, the middle cerebral artery (MCA).

The classical didactic image of the circle of Willis, which sees the basal artery in the center, as the point of convergence of the two vertebral arteries, then the circle, must be mentally rotated by 90 degrees in lateral B-mode ultrasound. MCA is the vessel of largest caliber (approximately 3 mm), and is responsible for the 75% of the brain blood flow. It is the vessel of choice for most of the TCD-derived signals; it comes from the medial angle of the small wing of the sphenoid and approaches laterally and obliquely the surface of the temporal bone squama.

In daily practice, the four more common acoustic windows used to insonate the vessels are: transtemporal, suboccipital, transorbital, and submandibular.

TCD/TCCS: Basic and Advanced Methods to Measure CBFV and Indexes

Each of these fields of application requires significant dedication to the learning process. For all applications, solid knowledge of the local neuroanatomy and of the cerebrovascular anatomy in particular is essential; images of interventional neuroradiology may prove very useful in this respect.

Given the range of fields of application, learning to identify the main basic elements – flow velocities and pulsatility index (PI) – is essential for a practical and quick approach.

With reference to cerebral arteries, flow velocity is measured in cm/sec and indicated by CBFV. It comprises three components: cerebral flow peak systolic velocity (PSV), mean flow velocity (MFV), and end-diastolic velocity (EDV). Peak systolic flow velocity (PSV) is predominantly dependent on cardiac output.

In physiological conditions, CBFV is proportional to the cerebral blood flow (CBF). Although TCD/TCCS does not allow for the calculation of an absolute value of CBF, changes in CBFV over time are related to changes in CBF. Therefore, since TCD/TCCS provides a quantitative measurement of CBFV, the measurement of changes in CBFV provides an estimation of the changes in CBF. This means that TCD/TCCS is a very useful tool to follow up of a phenomenon. With CBFV it is possible to study, through the analysis of waveform, the CPP (Cerebral Perfusion Pressure) reduction due to rising ICP in TBI for example, and cerebrospinal fluid (CSF) dynamics related to arterial blood pressure (ABP) and increased ICP.

The PI, also known as Gosling's index, describes the cerebral vascular resistance through the interpretation of TCD/TCCS curves. Mathematically, PI is calculated as the relationship between the difference of PSV and EDV, divided by the mean flow velocity (MFV) [46].

PI has been used for the assessment of the distal cerebrovascular resistance (CVR), with greater PI values corresponding to higher CVR [47]; however, hypercapnia is known to alter CVR behavior [48]. Despite some the discordant findings in the literature, there is a positive correlation between PI and ICP (R = 0.94 $p < 0.05$) [49, 50, 58]. We can say that the sensitivity of PI in identifying a raised ICP is high, but its specificity is low. In addition, PI is dependent on a variety of factors, including ICP, ABP, CPP, and vascular tone (consequently CO_2).

During a TCD/TCCS exam, an obstructive lesion proximal to the insonation point produces a prolonged rise time and damping of the peak systolic and end-diastolic components due to the loss of pressure when crossing the proximal obstruction. Increased PI typically occurs proximal to the lesion, because maximal vasodilatation from intact autoregulation produces less resistance and therefore increased pulsation. Abnormalities in absolute values, a relative difference of more than 50% from each side, and turbulence producing a cracked or harsh sound and localized focal reversal of the signal should be noted.

ICP measurement is considered a milestone for many neuro-acute patients, and the gold standard is represented by the use of invasive techniques (intraparenchymal, intraventricular, subdural, and epidural probes), which carry a certain risk of hemorrhagic and infectious complications and whose indication is often dependent on the neurosurgeon's opinion. Non-invasive management of the ICP through TCD has been studied since the time of Aaslid, with not always encouraging results [51]. In view of the practical approach of this book, we wish to point out that from the studies by Czosnyka et al. in 1998 [52], the confirmations by Cardim et al. and other more recent literature too, we have learned that the non-invasive measurement of CPP, called nCPP, has a high predictive power (94%) for low CPP (<60 mm Hg) [53–55]. The formula is always nICP = ABP – nCPP. The most correlated parameter of the TCD waveform is undoubtedly the EDV. Having said that, we suggest that it is very important, once the operator has acquired sufficient mastery of the technique, that they keep themselves up to date on scientific developments in the field of non-invasive ICP (nICP) and its correlations with ABP, $EtCO_2$.

New non-invasive approaches have included cerebral venous oxygen monitoring [56] and venous transcranial Doppler ultrasonography for increased ICP: venous blood is pooled to larger venous vessels, and venous maximal blood flow velocity increases [57].

60.2.5.3 TCCS: Brain Parenchyma Ultrasound

Thanks to the refinement of ultrasound hardware in B-mode, it is possible to study, in addition to cerebral vessels, the parenchymal structures of the brain using the same windows of insonation. It is therefore possible, by exploiting the different echogenicities of parenchymal structures, to assess in more detail the characteristics of space-occupying pathologies, such as deep hemorrhages, subdural hematomas, and neoplasms. This approach is known as brain parenchyma sonography and is an expanding field of clinical application. The main US landmarks are represented by hyperechogenic parenchymal structures such as bone and perimesencephalic

cisterns where the liquid–solid interface generates echoes; these structures appear to be whiter than the surrounding parenchyma [59]. Other parenchymal structures, such as the substantia nigra and the lenticular nucleus, also appear hypercogenic and may be valuable landmarks. Vessels are also important landmarks and blood in the form of a hematoma also appears hyperechoic. However, if the normal parenchyma of the brain (called white and gray matter) is considered normoechogenic, the structures that are crossed by the ultrasound – that is the cerebrospinal fluid and the vacuum - appear black [60].

This kind of ultrasound study can be performed using the transtemporal window, modifying the inclination of the probe. It is possible to identify five different planes, which in the cranial-caudal direction are: the ventricular plane, the diencephalic (or third ventricle) plane, the mesencephalic plane, the upper pontine plane, and the lower pontine plane. We can mention a semi-coronal plane (45°), through the transtemporal window, which allows us to visualize the 4th ventricle and the cerebellum. It is part of the TCCS approach in movement disorders as a cerebellar plane (Parkinson Disease) [61, 62, 83].

In this type of exam, it is always essential to answer two questions: where are we and what are we insonating? The starting point for TCCS (B-mode) is the mesencephalic plane, in which the mesencephalon is shown as the main landmark, with its typical "butterfly-like" image. It is advisable to work with a probe depth of about 16 cm, to look for the midbrain at 7–10 cm of depth, using as a landmark the small wing of the concave and oblique sphenoid and the contralateral cranial theca inferiorly. The midbrain is surrounded laterally and anteriorly by the P_1 and P_2 traits of the posterior cerebral arteries and, at a closer look, the substantia nigra is visible in the anterior portion of the midbrain, and the red nucleus in its posterior-medial portion. An operator who is unfamiliar with TCCS (B-mode) will find it very useful to compare an ultrasound image and a CT image of the same patient, to identify correctly and more easily the parenchymal structures.

The mesencephalic plane can be further divided into three sections: lower, middle, and upper, which can be identified by means of micro movements of the probe of 2–3°. These three continuity planes follow the anatomical development that leads from the Varolio bridge to the cerebral peduncles, whereby the midbrain will appear oval in the lower plane, partially divided into two in the middle plane, and completely divaricated at the cerebral peduncles in the upper plane. Vessels and features of the cerebral lobes can become important anatomical landmarks.

For the diencephalic plane, it is essential to identify the third ventricle; this appears as a binary structure that is hypoechoic at the center and hyperechogenic externally with two lines representing the liquor–ependima interface. Posteriorly, the pineal gland appears often hyperechoic, outwardly and externally to the "white rails", making the overall image easily recognizable, with the oval shape identifying the two thalami. In front of the third ventricle and thalamus, it is possible to identify the frontal horns of the lateral ventricles. Sometimes in the posterior horn of the lateral ventricle, posterior hyperechogen elements appear, which represent the choroid plexi. Directing the probe cranially by another 20–30°, we reach the ventricular

plane, where it is possible to identify the frontal horns of lateral ventricles as two symmetrical hypoechoic strips.

Brain Parenchyma Ultrasound: Clinical Applications

Optic Nerve Sheath Diameter (ONSD)

In addition to brain parenchyma and cerebral vessels, nerves can also be studied with ultrasound techniques. In particular, the study of the optic nerve sheath diameter is becoming increasingly useful for the detection of raised intracranial pressure [58, 63, 73, 76]. The sheath of the optic nerve is continuous with the dura mater and contains CSF in the subarachnoid space [64]. The sheath of the optic nerve is distensible, whereby an increase in intracranial pressure corresponds to a transmission to the subarachnoid compartment of the nerve sheath, which can be measured as an increase in ONSD as in the case of papilledema [65]. Many studies have correlated these changes with ICP changes detected by other methods; the relationship seems to be linear and confirmed also through infusion studies (performed through EVD) and in the case of CO_2 variations [66–70]. The application of color-Doppler can refine the assessment technique [85].

Midline Shift

In the patient with neurotrauma or acute brain injury, the midline shift (MLS) often represents a life-threatening situation that requires urgent diagnosis and treatment. A shift ≥0.5 cm at CT scan is associated with poor neurological outcome and a shift ≥1 cm is associated with an increase in mortality [71, 72] (Fig. 60.5). Besides trauma, hematomas and intracranial masses can also cause midline shift, CT scan of the brain is the gold standard for diagnosis of MLS. However, this may not be immediately available, is not easily repeatable in a short time, presents side effects, and an uncompromising environment for critically ill patients undergoing all sorts of monitoring. For these reasons, several authors have begun to experiment with the use of ultrasound for the detection of MLS, with the aim to aid timely diagnosis and identify the need for aggressive treatment in neurocritical patients both in the ICU and in ED [71].

Hydrocephalus

There is significant scientific debate on the definition and diagnosis of hydrocephalus. The term hydrocephalus refers to an increase in the volume of CSF that occupies the cerebral ventricles. This increase in volume is due to a hydrodynamic disorder: alteration of the equilibrium between the ependymal production and the absorption of CSF. The effect of this is ventricular dilatation and partial discharge of CSF into the periventricular space, with consequent damage to the white substance and glial cells. The classification of hydrocephalus provides a distinction between non-communicating hydrocephalus, also known as obstructive (either

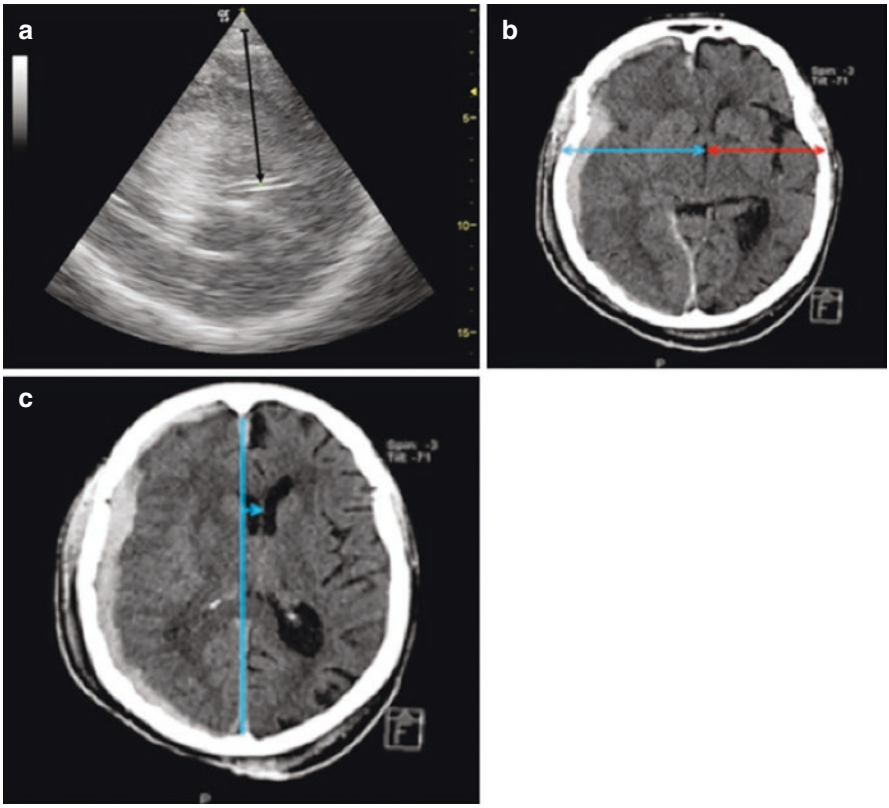

Fig. 60.5 Midline shift measurement (MLS): (**a**) MLS measurement by TCCS through transtemporal acoustic window: (arrow) distance between external bone table (skull) and the centre of third ventricle; (**b**) MLS measurement by brain-CT scan: (red and blue arrow) distance between the skull and the centre of the third ventricule; (**c**) MLS measurement by brain-CT scan: (blue line) ideal midline and (blue arrow) distance between ideal midline and the septum pellucidum. (Coutesy: Motuel et al. [72])

congenital or acquired), and communicating hydrocephalus, mainly due to increased CSF production. Different types of hydrocephalus can also be distinguished on the basis of accompanying intracranial pressure values: so, a hydrocephalus is distinguished from a "normal pressure hydrocephalus", linked to a characteristic syndrome. The causes of hydrocephalus can be many and the gold standard for diagnosis is the measurement of the ventricular diameters by CT scan.

In view of this, various authors compared the measurements taken with CT and ultrasound. On the diencephalic plane, the third ventricle and the frontal horns of the lateral ventricles are measured. The accepted physiological measures vary according to age: under 60 years, third ventricle 7 mm and frontal horns <17 mm; over 60 years, third ventricle <10 mm and horns <20 mm. On the ventricular plane, it is possible to measure the middle cell of the lateral ventricles; normal values are: under 60 years <19 mm; over 60 years <22 mm. A good correlation between the two methods was found for the measurement of the third ventricle; however,

measurement of the lateral ventricles proved more difficult with brain parenchymal ultrasound [71, 74]. Ultrasound measurement of the third ventricle for the evaluation of hydrocephalus can be a useful point-of-care tool for neurocritical patients, especially for follow-up and in the case of drainage patients with continuous monitoring of the ICP, as it is non-complex and easily repeatable.

In some studies, good correlation indices between US and CT measurements have been identified in patients undergoing decompressive craniectomy: $r = 0.978$ for the right lateral ($p < 0.001$); $r = 0.975$ for the left lateral ($p < 0.001$); and $r = 0.987$ for the third ($p < 0.001$) ventricle [72].

Intracranial Hemorrhage

Although in non-decompressed patients, ultrasound evaluation of hemorrhages and hematomas is very limited, through the temporal bone window it is possible to evaluate the presence of parenchymal blood lesions. Blood appears hyperechoic on cerebral ultrasonography. Thanks to blood hyperechogenicity, it is possible to accurately trace the limit between healthy brain parenchyma and a hematoma. It is therefore possible, by measuring thicknesses at different points, to study intra-parenchymal hematomas, such as hematomas below and above the dura.

It is also possible to use brain US to monitor the volume of intracranial bleeding. Some authors have studied the usefulness of US in a cohort of decompressed patients, correlating their measurements with those performed in CT (intraclass correlation coefficient 0.993, $p < 0.001$) [72]. According to other authors, the use of BPS in patients affected by stroke in whom a temporal bone window was present was useful to correctly differentiate ischemic from hemorrhagic areas in many cases [75, 78, 79].

60.3 Conclusion

Even for the neurocritical patient, ultrasound can be a very valuable tool. Specific theoretical notions, training courses for medical and nursing staff, are now indispensable, but only with daily practice under expert guidance, with the devices and the correct settings, it is possible to obtain reliable examinations:

- US-guided central and peripheral venous catheterization minimizes complication risks and standardizes procedures.
- POCUS echocardiography together with the measurement of the inferior vena cava can help the neuro intensivist to manage the use of catecholamines, to highlight specific dyskinesias and syndromes (i.e. Takotsubo) and together with TCD to diagnose the patency of the oval foramen(stroke or sitting position surgery).
- Airway ultrasound can facilitate the management and timing of percutaneous tracheostomy, avoiding maneuvers harmful to the neurological patient; lung US can anticipate diagnosis of overload or inflammatory processes.
- Abdominal US with E-FAST is now widely used in the emergency department on patients with polytrauma or even only with trauma brain injury.

- Transcranial Doppler (TCD/TCCS) ultrasonography is a cornerstone in neurointensive care and it is essential that a large group of the staff know how to do it. In addition to studying the velocities of the circle of Willis and assessment of vasospasms, neurosonology is now valuable for monitoring cerebral blood flow, noninvasive intracranial pressure, and cerebral autoregulation.
- Brain ultrasound (B-mode) is one of the specific applications of TCCS. It also includes the assessment of optic nerve sheath diameter, midline shift, hydrocephalus and cerebral hemodynamic monitoring through Doppler, which is very useful in the acute ICU patient.

Algorithm

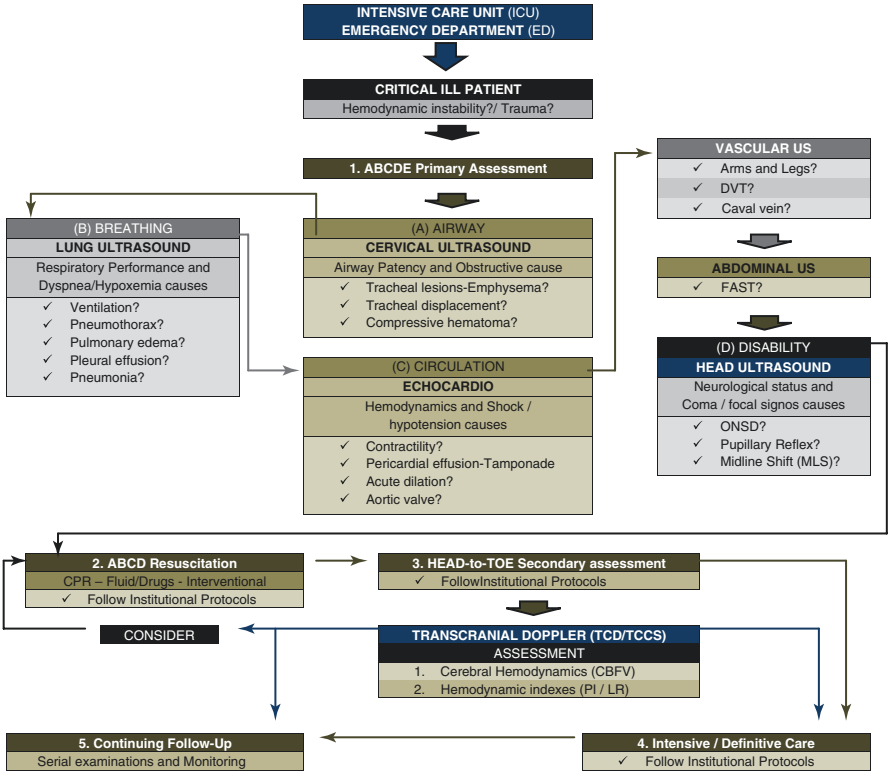

ABCDE Airway-breathing-circulation-disability-exposure, *ONSD* Optic nerve sheath diameter, *CPR* Cardio-pulmonary resuscitation, *DVT* Deep venous thrombosis, *FAST* Focused assessment with sonography in trauma, *CBFV* Cerebral blood flow velocity, *PI* Pulsatility index, *LR* Lindegaard ratio, *US* Ultrasound.

References

1. Cowie BS. Focused transthoracic echocardiography in the perioperative period. Anaesth Intensive Care. 2010;38:823–36.
2. Sekiguchi H. Tools of the trade: point-of-care ultrasonography as a stethoscope. Semin Respir Crit Care Med. 2016;37(1):68–87.
3. Manno E, Navarra M, Faccio L, Motevallian M, Bertolaccini L, et al. Deep impact of ultrasound in the intensive care unit: the "ICU-sound" protocol. Anesthesiology. 2012;117:801–9.
4. Bernier-Jean A, Albert M, Shiloh AL, Eisen LA, Williamson D, Beaulieu Y. The diagnostic and therapeutic impact of point-of-care Ultrasonography in the intensive care unit. J Intensive Care Med. 2017;32(3):197–203.
5. Bilotta F, Dei Giudici L, Lam A, Rosa G. Ultrasound-based imaging in neurocritical care patients: a review of clinical applications. Neurol Res. 2013;35(2):149–58.
6. Zieleskiewicz L, Muller L, Lakhal K, Meresse Z, Arbelot C, Bertrand PM, et al. Point-of-care ultrasound in intensive care units: assessment of 1073 procedures in a multicentric, prospective, observational study. Intensive Care Med. 2015;41(9):1638–47.
7. Slama M, Novara A, Safavian A, Ossart M, Safar M, Fagon JY. Improvement of internal jugular vein cannulation using an ultrasound-guided technique. Intensive Care Med. 1997;23(8):916–9.
8. Ablordeppey EA, Drewry AM, Beyer AB, Theodoro DL, Fowler SA, Fuller BM, et al. Diagnostic accuracy of central venous catheter confirmation by bedside ultrasound versus chest radiography in critically ill patients: a systematic review and Meta-analysis. Crit Care Med. 2017;45(4):715–24.
9. Yonei A, Nonoue T, Sari A. Real-time ultrasonic guidance for percutaneous puncture of the internal jugular vein. Anesthesiology. 1986;64:830–1.
10. Leung J, Duffy M, Finckh A. Real-time ultrasonographically- guided internal jugular vein catheterization in the emergency department increases success rates and reduces complications: a randomized, prospective study. Ann Emerg Med. 2006;48:540–7.
11. DeLemos C, Abi-Nader J, Akins PT. Use of peripherally inserted central catheters as an alternative to central catheters in neurocritical care units. Crit Care Nurse. 2011;31:70–5.
12. Kaye AD, Fox CJ, Hymel BJ, Gayle JA, Hawney HA, Bawcom BA, et al. The importance of training for ultrasound guidance in central vein catheterization. Middle East J Anesthesiol. 2011;21:61–6.
13. Livesley MA, Tebbs SE, Moss HA, Faroqui MH, Lambert PA, Elliott TS. Use of pulsed field gel electrophoresis to determine the source of microbial contamination of central venous catheters. Eur J Clin Microbiol Infect Dis. 1998;17:108–12.
14. Jefferson AL, Liu D, Gupta DK, Pechman KR, Watchmaker JM, Gordon EA, et al. Lower cardiac index levels relate to lower cerebral blood flow in older adults. Neurology. 2017;89:2327–34.
15. Frankel HL, Kirkpatrick AW, Elbarbary M, Blaivas M, Desai H, Evans D, et al. Guidelines for the appropriate use of bedside general and cardiac ultrasonography in the evaluation of critically ill patients-part I: general ultrasonography. Crit Care Med. 2015;43(11):2479–502.
16. Levitov A, Frankel HL, Blaivas M, Kirkpatrick AW, Su E, Evans D, et al. Guidelines for the appropriate use of bedside general and cardiac ultrasonography in the evaluation of critically ill patients-part II: cardiac ultrasonography. Crit Care Med. 2016;44(6):1206–27.
17. Vermeiren GL, Malbrain ML, Walpot JM. Cardiac Ultrasonography in the critical care setting: a practical approach to assess cardiac function and preload for the "non-cardiologist". Anaesthesiol Intensive Ther. 2015;47:89–104.
18. Heiberg J, El-Ansary D, Canty DJ, Royse AG, Royse CF. Focused echocardiography: a systematic review of diagnostic and clinical decision-making in anaesthesia and critical care. Anaesthesia. 2016;71(9):1091–100.

19. Chien-Chia Wu V, Takeuchi M. Three-dimensional echocardiography: current status and real-life applications. Acta Cardiol Sin. 2017;33(2):107–18.
20. Dinh VA, Farshidpanah S, Lu S, Stokes P, Chrissian A, Shah H, et al. Real-time sonographically guided percutaneous dilatational tracheostomy using a long-axis approach compared to the landmark technique. J Ultrasound Med. 2014;33(8):1407–15.
21. King D. Preventing bleeding complications in percutaneous tracheostomy--another role for portable ultrasound in intensive care. Br J Anaesth. 2003;91(4):607.
22. Flint AC, Midde R, Rao VA, Lasman TE, Ho PT. Bedside ultrasound screening for pretracheal vascular structures may minimize the risks of percutaneous dilatational tracheostomy. Neurocrit Care. 2009;11(3):372–6.
23. Mitra S, Kapoor D, Srivastava M, Sandhu H. Real-time ultrasound guided percutaneous dilatational tracheostomy in critically ill patients: a step towards safety! Indian J Crit Care Med. 2013;17(6):367–9.
24. Yin W, Li Y, Zeng X, Qin Y, Wang D, Zou T, et al. The utilization of critical care ultrasound to assess hemodynamics and lung pathology on ICU admission and the potential for predicting outcome. PLoS One. 2017;12:e0182881.
25. Bouhemad B, Zhang M, Lu Q, Rouby JJ. Clinical review: bedside lung ultrasound in critical care practice. Crit Care. 2007;11:205.
26. Lichtenstein DA, Mezière GA. Relevance of lung ultrasound in the diagnosis of acute respiratory failure: the BLUE protocol. Chest. 2008;134(1):117–25.
27. Alptekin B, Tran DT, Lisbon A, Kaynar AM. Bedside ultrasonography in the differential diagnosis of pulmonary pathologies in the intensive care unit. J Clin Anesth. 2006;18:534–6.
28. Ioos V, Galbois A, Chalumeau-Lemoine L, Guidet B, Maury E, Hejblum G. An integrated approach for prescribing fewer chest x-rays in the ICU. Ann Intensive Care. 2011;1:4.
29. Montoya J, Stawicki SP, Evans DC, Bahner DP, Sparks S, Sharpe RP, et al. From FAST to E-FAST: an overview of the evolution of ultrasound-based traumatic injury assessment. Eur J Trauma Emerg Surg. 2016;42(2):119–26.
30. Kirkpatrick AW, Sirois M, Laupland KB, Goldstein L, Brown DR, Simons RK, et al. Prospective evaluation of hand-held focused abdominal sonography for trauma (FAST) in blunt abdominal trauma. Can J Surg. 2005;48(6):453–60.
31. Kirkpatrick AW, Sirois M, Ball CG, Laupland KB, Goldstein L, Hameed M, et al. The hand-held ultrasound examination for penetrating abdominal trauma. Am J Surg. 2004;187(5):660–5.
32. Bahner D, Blaivas M, Cohen HL, Fox JC, Hoffenberg S, Kendall J, et al. SAIUM practice guideline for the performance of the focused assessment with sonography for trauma (FAST) examination. J Ultrasound Med. 2008;27(2):313–8.
33. Leksell L. Echo-encephalography. I. Detection of intracranial complications following head injury. Acta Chir Scand. 1956;110(4):301–15.
34. Aaslid R, Markwalder TM, Nornes H. Noninvasive transcranial Doppler ultrasound recording of flow velocity in basal cerebral arteries. J Neurosurg. 1982;57:769–74.
35. Edmonds HL Jr, Isley MR, Sloan TB, Alexandrov AV, Razumovsky AY. American Society of Neurophysiologic Monitoring and American Society of Neuroimaging joint guidelines for transcranial Doppler ultrasonic monitoring. J Neuroimaging. 2011;21(2):177–83.
36. Sloan MA, Alexandrov AV, Tegeler CH, et al. Assessment: transcranial Doppler ultrasonography: report of the Therapeutics and Technology Assessment Subcommittee of the American Academy of Neurology. Neurology. 2004;62:1468–81.
37. Marshall SA, Nyquist P, Ziai WC. The role of transcranial Doppler ultrasonography in the diagnosis and management of vasospasm after aneurysmal subarachnoid hemorrhage. Neurosurg Clin N Am. 2010;21:291–303.
38. Tsivgoulis G, Alexandrov AV, Sloan MA. Advances in transcranial Doppler ultrasonography. Curr Neurol Neurosci Rep. 2009;9:46–54.
39. Petty GW, Mohr JP, Pedley TA, et al. The role of transcranial Doppler in confirming brain death: sensitivity, specificity, and suggestions for performance and interpretation. Neurology. 1990;40:300–3.

40. Bode H, Sauer M, Pringsheim W. Diagnosis of brain death by transcranial Doppler sonography. Arch Dis Child. 1988;63:1474–8.
41. Robba C, Cardim D, Sekhon M, Budohoski K, Czosnyka M. Transcranial Doppler: a stethoscope for the brain-neurocritical care use. J Neurosci Res. 2018;96:720–30.
42. Pierrakos C, Antoine A, Velissaris D, Michaux I, Bulpa P, Evrard P, et al. Transcranial doppler assessment of cerebral perfusion in critically ill septic patients: a pilot study. Ann Intensive Care. 2013;3:28.
43. Newell DW, Aaslid R. Transcranial Doppler. New York: Raven Press; 1992.
44. Klinzing S, Steiger P, Schüpbach RA, Bèchir M, Brandi G. Competence for transcranial color-coded Duplex sonography is rapidly acquired. Minerva Anestesiol. 2015;81(3):298–304.
45. Teixidó-Martínez A, Adorna-Garralaga E, Marsillach AM. Doppler transcranial ultrasonography: a means of non-invasive monitoring at the patient's bedside. Enferm Intensiva. 1998;9(4):169–74.
46. Naqvi J, Yap KH, Ahmad G, Ghosh J. Transcranial Doppler ultrasound: a review of the physical principles and major applications in critical care. Int J Vasc Med. 2013;2013:629378.
47. Bouma GJ, Muizelaar JP, Bandoh K, Marmarou A. Blood pressure and intracranial pressure-volume dynamics in severe head injury: relationship with cerebral blood flow. J Neurosurg. 1992;77(1):15–9.
48. Czosnyka M, Richards HK, Reinhard M, Steiner LA, Budohoski K, Smielewski P, et al. Cerebrovascular time constant: dependence on cerebral perfusion pressure and end-tidal carbon dioxide concentration. Neurol Res. 2012;34(1):17–24.
49. Cardim D, Robba C, Bohdanowicz M, Donnelly J, Cabella B, Liu X, et al. Non-invasive monitoring of intracranial pressure using transcranial Doppler ultrasonography: is it possible? Neurocrit Care. 2016:1–19.
50. Bellner J, Romner B, Reinstrup P, Kristiansson KA, Ryding E, Brandt L. Transcranial Doppler sonography pulsatility index (PI) reflects intracranial pressure (ICP). Surg Neurol. 2004;62(1):45–51.
51. Prunet B, Asencio Y, Lacroix G, Montcriol A, Dagain A, Cotte J, et al. Noninvasive detection of elevated intracranial pressure using a portable ultrasound system. Am J Emerg Med. 2012;30(6):936–41.
52. Czosnyka M, Matta BF, Smielewski P, Kirkpatrick PJ, Pickard JD. Cerebral perfusion pressure in head-injured patients: a noninvasive assessment using transcranial Doppler ultrasonography. J Neurosurg. 1998;88(5):802–8.
53. Cardim D, Robba C, Donnelly J, Bohdanowicz M, Schmidt B, Damian M, et al. Prospective study on noninvasive assessment of intracranial pressure in traumatic brain-injured patients: comparison of four methods. J Neurotrauma. 2016;33(8):792–802.
54. Robba C, Donnelly J, Bertuetti R, Cardim D, Sekhon MS, Aries M, et al. Doppler non-invasive monitoring of ICP in an animal model of acute intracranial hypertension. Neurocrit Care. 2015;23(3):419–26.
55. Rasulo FA, Bertuetti R, Robba C, Lusenti F, Cantoni A, Bernini M, et al. The accuracy of transcranial Doppler in excluding intracranial hypertension following acute brain injury: a multicenter prospective pilot study. Crit Care. 2017;21(1):44.
56. Macmillan CS, Andrews PJ. Cerebrovenous oxygen saturation monitoring: practical considerations and clinical relevance. Intens Care Med. 2000;26:1028–36.
57. Schoser BG, Riemenschneider N, Hansen HC. The impact of raised intracranial pressure on cerebral venous hemodynamics: a prospective venous transcranial Doppler ultrasonography study. J Neurosurg. 1999;91:744–9.
58. Robba C, Cardim D, Tajsic T, Pietersen J, Bulman M, Donnelly J, et al. Ultrasound non-invasive measurement of intracranial pressure in neurointensive care: a prospective observational study. PLoS Med. 2017;14(7):e1002356.
59. Bartova P, Skoloudik D, Bar M, Ressner P, Hlustik P, Herzig R, et al. Transcranial sonography in movement disorders. Biomed Pap Med Fac Univ Palacky Olomouc Czech Repub. 2008;152(2):251–8.

60. Berardelli A, Wenning GK, Antonini A, Berg D, Bloem BR, Bonifati V, et al. Recommendations for the diagnosis of Parkinson's disease. Eur J Neurol. 2013;20(1):16–34.
61. Gaenslen A, Unmuth B, Godau J, Liepelt I, Di Santo A, Schweitzer KJ, et al. The specificity and sensitivity of transcranial ultrasound in the differential diagnosis of Parkinson's disease: a prospective blinded study. Lancet Neurol. 2008;7(5):417–24.
62. Berg D, Godau J, Walter U. Transcranial sonography in movement disorders. Lancet Neurol. 2008;7(11):1044–55.
63. Vaiman M, Sigal T, Kimiagar I, Bekerman I. Noninvasive assessment of the intracranial pressure in non-traumatic intracranial hemorrhage. J Clin Neurosci. 2016;34:177–81.
64. Puntis M, Reddy U, Hirsch N. Cerebrospinal fluid and its physiology. Anaesth Intensive Care Med. 2016;17:611–2.
65. Helmke K, Hansen HC. Fundamentals of transorbital sonographic evaluation of 14 optic nerve sheath expansion under intracranial hypertension. I. Experimental study. Pediatr Radiol. 1996;26:701–5.
66. Hansen HC, Helmke K. Validation of the optic nerve sheath response to changing cerebrospinal fluid pressure: ultrasound findings during intrathecal infusion tests. J Neurosurg. 1997;87:34–40.
67. Launey Y, Nesseler N, Le Maguet P, Malledant Y, Seguin P. Effect of osmotherapy on optic nerve sheath diameter in patients with increased intracranial pressure. J Neurotrauma. 2014;31:984–8.
68. Ballantyne J, Hollman AS, Hamilton R, et al. Transorbital optic nerve sheath ultrasonography in normal children. Clin Radiol. 1999;54:740–2.
69. Strumwasser A, Kwan RO, Yeung L, Miraflor E, Ereso A, Castro-Moure F, et al. Sonographic optic nerve sheath diameter as an estimate of intracranial pressure in adult trauma. J Surg Res. 2011;170:265–71.
70. Dubourg J, Javouhey E, Geeraerts T, Messerer M, Kassai B. Ultrasonography of optic nerve sheath diameter for detection of raised intracranial pressure: a systematic review and meta-analysis. Intensive Care Med. 2011;37:1059–68.
71. Seidel G, Kaps M, Gerriets T, Hutzelmann A. Evaluation of the ventricular system in adults by transcranial duplex sonography. J Neuroimaging. 1995;5:105–8.
72. Motuel J, Biette I, Srairi M, Mrozek S, Kurrek MM, Chaynes P, et al. Assessment of brain midline shift using sonography in neurosurgical ICU patients. Crit Care. 2014;18(6):676.
73. Blanco P, Matteoda M. Images in emergency medicine. Extra-axial intracranial hematoma, midline shift, and severe intracranial hypertension detected by transcranial color-coded duplex sonography. Ann Emerg Med. 2015;65(2):e1–2.
74. Bendella H, Maegele M, Hartmann A, et al. Cerebral ventricular dimensions after decompressive craniectomy: a comparison between bedside sonographic duplex technique and cranial computed tomography. Neurocrit Care. 2017;26:321–9.
75. Caricato A, Mignani V, Bocci MG, et al. Usefulness of transcranial echography in patients with decompressive craniectomy. Crit Care Med. 2012;40:1745–52.
76. Chelly J, Deye N, Guichard JP, Vodovar D, Vong L, Jochmans S, et al. The optic nerve sheath diameter as a useful tool for early prediction of outcome after cardiac arrest: a prospective pilot study. Resuscitation. 2016;103:7–13.
77. Damasceno BP. Neuroimaging in normal pressure hydrocephalus. Dement Neuropsychol. 2015;9(4):350–5.
78. Kiphuth IC, Huttner HB, Struffert T, Schwab S, Köhrmann M. Sonographic monitoring of ventricle enlargement in posthemorrhagic hydrocephalus. Neurology. 2011;76:858–62.
79. Gerriets T, Stolz E, König S, et al. Sonographic monitoring of midline shift in space-occupying stroke. An early otcome predictor. Stroke. 2001;32:442–7.
80. Alexandrov AV, Sloan MA, Tegeler CH, et al. Practice standards for transcranial Doppler (TCD) ultrasound, part II: clinical indications and expected outcomes. J Neuroimaging. 2012;22:215–24.

81. Aries MJH, Elting JW, De Keyser J, Kremer BPH, Vroomen PCAJ. Cerebral autoregulation in stroke: a review of transcranial Doppler studies. Stroke. 2010;41:2697–704.
82. Kumar G, Shahripour RB, Harrigan MR. Vasospasm on transcranial Doppler is predictive of delayed cerebral ischemia in aneurysmal subarachnoid hemorrhage: a systematic review and meta-analysis. J Neurosurg. 2016;124(5):1257–64.
83. Walter U, Školoudík D. Transcranial sonography (TCS) of brain parenchyma in movement disorders: quality standards, diagnostic applications and novel technologies. Ultraschall Med. 2014;35(4):322–31.
84. Lichtenstein D, Karakitsos D. Integrating lung ultrasound in the hemodynamic evaluation of acute circulatory failure (the fluid administration limited by lung sonography protocol). J Crit Care. 2012;27(5):533.e11–9.
85. Aspide R, Bertolini G, Albini Riccioli L, Mazzatenta D, Palandri G, Biasucci DG. A proposal for a new protocol for sonographic assessment of the optic nerve sheath diameter: the CLOSED protocol. Neurocrit Care. 2020;32(1):327–32.

Chapter 61
Intra-Aortic Balloon Pump (IABP) in ICU: Cerebral Hemodynamics Monitoring by Transcranial Doppler (TCD/TCCS)

Juliana Caldas and Ronney B. Panerai

Key Points

1. Intra-aortic balloon pump (IABP) modifies the pattern of arterial blood pressure pulsatility leading to concurrent changes in the cerebral blood flow (CBF) waveform during the cardiac cycle.
2. Transcranial Doppler ultrasound (TCD/TCCS) allows measurement of CBF velocity (CBFV) in the middle cerebral artery, or other large intracranial arteries, with considerable potential to identify cerebral hemodynamic disturbances in critically ill patients.
3. TCD can detect reversal of diastolic CBFV which is likely to be iatrogenic and should be minimized.
4. Microemboli produced by IABP should be evaluated with TCD to avoid neurological complications.
5. Patients suspected of clinical brain death need IABP to be on standby to allow a proper determination of the actual CBFV by TCD/TCCS.

J. Caldas (✉)
Department of Anesthesia, University of Sao Paulo, Butanta, Sao Paulo, Brazil

Critical Care Unit Hospital São Rafael Salvador, Salvador, Brazil
e-mail: caldas.juliana@usp.com

R. B. Panerai
Department of Cardiovascular Sciences, University of Leicester, Leicester, UK
e-mail: rp9@leicester.ac.uk

C. N. Rodríguez et al. (eds.), *Neurosonology in Critical Care*,
https://doi.org/10.1007/978-3-030-81419-9_61

61.1 Introduction

Intra-aortic balloon pump (IABP) remains the most widely used form of mechanical circulatory support in current clinical practice [1]. The accepted clinical indications for IABP use are wide ranging, but the available clinical evidence is largely limited to cardiogenic shock, myocardial infarction without shock, high-risk percutaneous coronary intervention, and perioperative of cardiac surgery [1]. In neurological critical care patients, IABP has been used in subarachnoid hemorrhage (SAH) [2–4].

The physiological premise underlying the utilization of IABP was first described by Kantrowitz in animal models in 1953, based on the diastolic augmentation of aortic root and coronary pressure [5]. Percutaneous IABP was first applied clinically in 1980 and remains the most widely used form of left ventricular mechanical support in most centers [6].

The IABP is a flexible balloon catheter with two lumens—one to allow flushing, aspiration, and for aortic pressure to be transduced; the other to allow inflation/deflation with the rapid shuttling of gas (usually helium) to and from the balloon [7]. Triggering of the insufflation and deflation is synchronized by the trace of the electrocardiogram (ECG) or the systemic arterial blood pressure (ABP) [8]. Of considerable relevance, the control of triggering can be changed to change the time delay when inflation takes place after the QRS complex of the ECG, leading to changes in the temporal pattern of the ABP waveform as it will be discussed later.

In this procedure, a balloon is placed into the aorta just distal to the left subclavian artery, generally via the femoral artery [6]. The balloon is connected to an external pump through a catheter. The pumping is timed so that the balloon inflates immediately after the aortic valve closes. Balloon inflation decreases diastolic aortic runoff and increases diastolic aortic pressure; these changes increase perfusion of the coronary arteries. The balloon deflates just before systole. Balloon deflation results in systolic unloading and a decrease in the aortic impedance to left ventricular ejection [1, 9] (Fig. 61.1). This combination causes relatively little change in the mean aortic pressure but decreases the left ventricular pressure by approximately 20% and increases coronary perfusion and cardiac output by up to 40%. As a consequence of these hemodynamic changes, cardiac workload and myocardial oxygen consumption are reduced in patients with a failing heart in cardiogenic shock or heart failure [10, 11].

IABP use is not free from complications. Postmortem examinations have shown multiple etiologies, including cerebral air embolism secondary to IABP rupture, compromised spinal cord blood supply due to mechanical trauma, dissecting hematoma of the thoracic aorta, spinal cord necrosis, microatheroembolism to radicular arteries, and other minor cerebrovascular events [12–15].

Given ongoing concerns about the effects of cardiac surgery on cognitive impairment and perioperative hypoperfusion stroke, the role of IABP on alterations of cerebral hemodynamic parameters is of considerable interest.

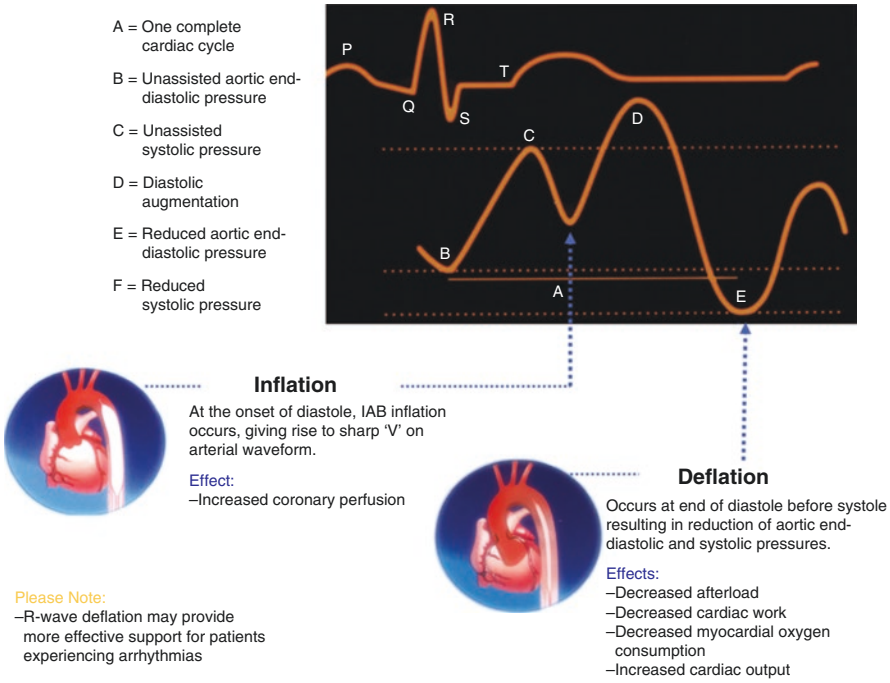

Fig. 61.1 The pressure waveform transduced from the tip of the IABP demonstrates a reduction in systolic pressure and augmentation of diastolic pressure with counterpulsation. (Courtesy: Murli and Zacharowski [51])

61.2 Neuro ICU: Intra-Aortic Balloon Pump (IABP)

In the neuro intensive care unit, the IABP has been used in patients with subarachnoid hemorrhage (SAH) [2, 4, 16] in two distinct clinical situations. The first one is the neurogenic stunned myocardium, that is, a severe condition characterized by reversible left ventricular dysfunction [17]. Neurogenic stunned myocardium following SAH occurs in 20–30% of SAH patients and may result in several complications such as cardiac arrhythmia, pulmonary edema, and prolonged intubation, which can negatively impact morbidity and mortality as well as long-term recovery [17]. Patient management remains basically supportive with case reports acknowledging the utility of contractility vasopressors such as dobutamine and milrinone [17]. Limited data also suggested the utility of IABP in patients who require hemodynamic support when neurogenic stunned myocardium is accompanied by cardiogenic shock [4, 18].

The second clinical situation reported is when patients develop refractory cardiogenic shock despite vasopressor use in cerebral vasospasm after SAH [2, 18]. Cerebral vasospasm is a major cause of morbidity and mortality following

aneurysmal SAH and contributes to delayed cerebral ischemia [19]. The combination of induced hypertension, hypervolemia, and hemodilution (triple-H therapy) is often used to improve cerebral perfusion pressure following cerebral vasospasm [20]. Although this approach has gained widespread acceptance over the past 20 years, the efficacy of triple-H therapy in the management of the acute phase of SAH may be questioned [19]. The IABP can improve the hemodynamic status of patients, who would probably die without such therapy and allow the continuing use of triple-H therapy [3].

TDC is a standard screening tool for vasospasm, but the predictive value of mean flow velocity (MFV) is likely inaccurate in the setting of an IABP, as the aforementioned alterations in the arterial waveform are reflected in the TCD velocity waveform (Fig. 61.1). There is just one study that explored this topic; Morris and colleagues reviewed cases of SAH that underwent same-day TDC and angiography [2]. TDC/TCCS waveforms were assessed for MFV, peak systolic velocity (PSV), balloon pump-augmented diastolic velocity, and a novel feature that they called "delta velocity" (balloon pump-augmented velocity—systolic velocity) [2]. The authors concluded that delta velocity, a novel transcranial Doppler flow velocity feature, may reflect vasospasm in patients with SAH with IABP support. The MFV, usually considered the most accurate TCD/TCCS measure of proximal vasospasm, was not significantly correlated with proximal vasospasm, although it was correlated with distal vasospasm [2]. However, these data are from a single, retrospective observational study. Clearly, interpretation of the waveform in patients with IABP for vasospasm detection requires further investigation.

61.3 Cerebral Blood Flow: IABP Effects

Although its benefits for improving cardiac function have been well documented, the effects of IABP on the cerebral circulation are still not well understood. Studies investigating the effects of IABP on the cerebral circulation provide conflicting results and have suggested that IABP either decreased, increased, or even transiently reversed cerebral blood flow [21–23]. What is clear though is that the use of IABP can change the temporal pattern of CBFV waveforms during the cardiac cycle, leading to characteristic double-peaked waveforms (Figs. 61.2 and 61.3) and the occurrence of transient reversed diastolic (i.e., negative) values of CBFV recorded with TCD [21, 24].

Cheung et al. reported in their study with 19 patients that IABP modified the pattern of CBFV in the middle cerebral artery (MCA) as measured by TCD but did not affect mean CBFV, even at different magnitudes of augmentation or trigger ratios [21]. They also concluded that IABP modified the phasic profile of cerebral blood flow to reflect the arterial pressure waveform (Figs. 61.2 and 61.3), and this pattern was not showing on standby mode.

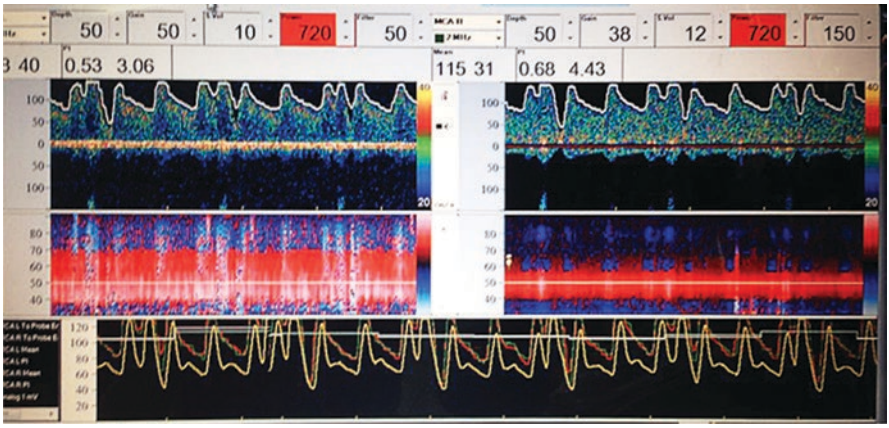

Fig. 61.2 Continuous recording of blood pressure (yellow tracing) and cerebral blood flow velocity (top, right and left middle cerebral arteries) from a 55-year-old male patient with IABP ratio 1:2 showing the double-peaked waveform

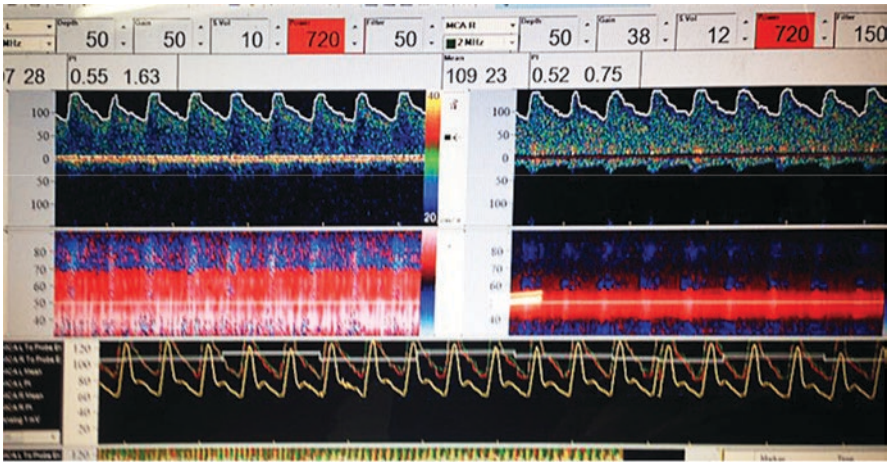

Fig. 61.3 Continuous recording of blood pressure (yellow tracing) and cerebral blood flow velocity (top, right and left middle cerebral arteries) from the same patient in Fig. 61.1 showing the IABP in standby mode

Notwithstanding some studies reported that the IABP device probably not changes the MFV. Currently, this device uses a square-wave function to control gas flow into the balloon [8], and with TCD, it may be possible to devise nonlinear inflation/deflation sequences for intra-aortic balloon pumps that can maximize forward blood flow in the intracranial circulation [24].

61.3.1 Transient Reversed Diastolic CBFV

Late diastolic IABP flow reversal in CBFV was first described in 1990 when TCD was used to evaluate CBF in three patients with an IABP [24]. This phenomenon is not uncommon; studies suggested that waveform flow reversal in intracranial vessels may occur in up to 35% of cardiac surgery patients supported by IABP [22].

Under normal conditions, forward CBFV is detected in both systole and diastole with TCD. The reversal of diastolic CBFV implies negative CBF in diastole (Fig. 61.4) and has also been described in other cerebrovascular conditions such as intracranial hypertension, intracranial circulatory arrest, in the first minutes after acute SAH, in metabolically compromised comatose patients, and, in the posterior circulation, the subclavian steal syndrome [24, 25]. However, the clinical significance of this dramatic alteration in the CBF waveform pattern is still unknown and more research on its implications is urgently needed [26].

Reversal of diastolic CBFV has been reported in a few case studies in the literature [27, 28]. The reversal or absence of diastolic flow at late diastole is probably due to diastolic pressure rapid reduction induced by deflation of IABP, so this phenomenon is a direct cause of IABP utilization (Fig. 61.4). These case reports suggest that reversal of diastolic CBFV is iatrogenic and it should be avoided. One

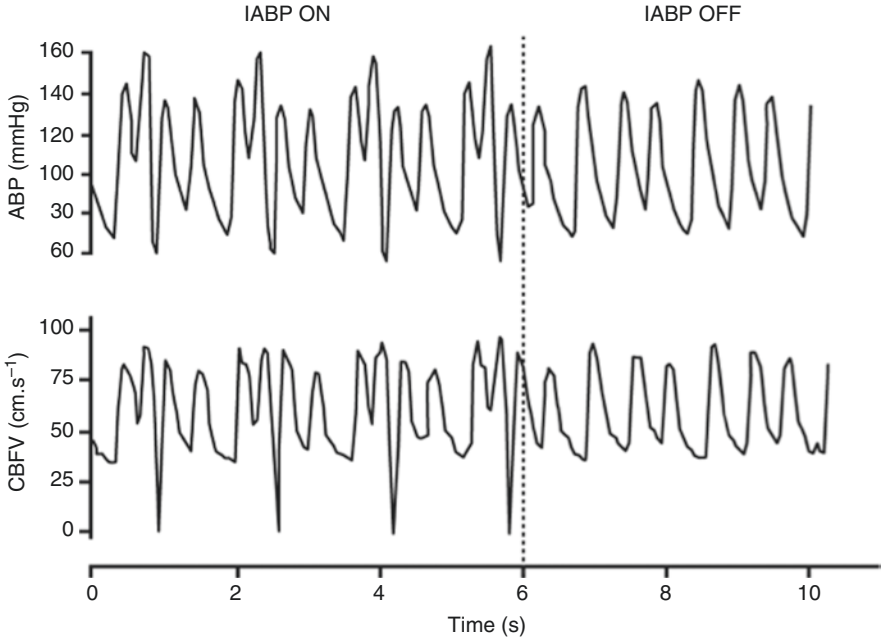

Fig. 61.4 Continuous recording of blood pressure and cerebral blood flow velocity from a 63 year-old male patient with IABP ratio 1:3 showing the transient reversed diastolic and the moment of balloon withdrawal (vertical dashed line). ABP Arterial blood pressure, CBFV Cerebral blood flow velocity, IABP Intra-aortic balloon pump. (Courtesy: Caldas et al. [37])

possible approach is to optimize the balloon inflation/deflation cycle, by moving deflation to the absolute end of diastole [24, 27]. Although the precise effects of CBFV diastolic reversal on cerebral hemodynamics are still unknown, its departure from normal physiological waveforms is likely to be undesirable and to have a negative effect on CA.

TDC available in ICU, as an easy-to-use, safe, and low-cost bedside tool, is advantageous to identify the reversal of diastolic CBFV in patients with IABP. Furthermore, it could be helpful to assess the hemodynamic response to changes in the balloon deflation timings to minimize the flow reversal phenomenon.

61.4 IABP: Cerebral Autoregulation

The main reason why IABP might disturb CBF and/or its regulatory mechanisms is due to observed changes in CBF temporal patterns. Chiefly among these regulatory mechanism is cerebral autoregulation (CA) that maintains cerebral perfusion within strict limits despite changes in mean ABP in the range 60–150 mmHg [29].

Assessments of CA are generally classified as being "static" or "dynamic" [30]. Static CA refers to the steady-state relationship between ABP and CBF [30, 31]. Dynamic CA reflects the transient response of CBF, often recorded as CBFV with TCD to rapid changes in ABP [31]. Impairment of CA renders the brain less tolerant to both low and high ABP, with increased risks of significant brain oligemia and hyperemia, respectively [32]. Assessment of CA in critical care patients and those with IABP could be an important bedside tool to avoid these complications [50].

There are numerous methods of quantification and assessment of CA in use at the current time, each with their own inherent assumptions, caveats, and specific analytical models. Importantly, no particular method is currently considered to be the "gold standard" [33].

Hypo- and hyper-perfusion, resulting from disturbances in cerebral autoregulation, are thought to be contributing factors in the neurological complications following cardiac surgery with cardiopulmonary bypass, and the use of IABP could also play a part in the development of these complications [34–36].

Hitherto, only two studies evaluated cerebral autoregulation in patients with IABP [37, 38]. These studies used different methods to assess cerebral autoregulation. Caldas et al. (2017) used transfer function analysis and the autoregulation index (ARI) to quantify the efficiency of CA [31, 37]. The second study (Bellapart 2010) was based on the time-delay between fluctuations in CBFV and ABP, estimated using a cross-correlation technique. Both studies found that cerebral autoregulation was intact in patients with IABP [37, 38].

One important corollary of these studies though was demonstrating the feasibility of performing bedside assessments of CA in critically ill patients requiring the use of IABP or different invasive support devices. Several critical care conditions were reported with impairment of cerebral autoregulation, such as sepsis, perioperative of cardiac surgery, ischemic heart disease, or SAH, and these conditions may be

requiring the use of IABP [39–44]. Patients who have manifested impairment of CA should have close monitoring and management of arterial blood pressure, to prevent ischemia or hyper-perfusion.

61.5 IABP and TCD/TCCS: Other Miscellaneous Conditions

61.5.1 Microemboli

Monitoring of the cerebral circulation with TCD can identify microemboli within the MCA during cardiopulmonary bypass procedures [45–47]. Similar techniques during the use of left ventricular assist devices may help identify occult cerebral embolization with IABP. Cerebral air embolism is a neurological emergency most commonly iatrogenic in origin [14]. It has been reported following invasive procedures such as cardiac catheterization, central venous catheter insertion, and cardiothoracic surgery. This complication, previously reported in patients with IABP when there is a rupture with gas embolization, is a rare but potentially fatal event [48].

61.5.2 Brain Death

The classical TCD pattern in brain death consists of three stages: oscillating or biphasic flow, systolic spike flow, and no flow [49]. With increasing intracranial pressure, diastolic flow ceases and systolic peaks become sharper. As cerebral perfusion pressure approaches zero, there is collapse of blood vessels during diastole, and so absent or reversed diastolic flow can be demonstrated.

The IABP can induce alterations in the pattern of CBFV measurements and the reversal of flow in late diastole may appear [24, 27]. Therefore, in a patient with an IABP, who is clinically brain dead, the IABP has to be on standby to allow a proper determination of the actual CBFV. The classic TCD pattern has to be detectable for at least 30 minutes [25] to confirm the diagnosis of brain death.

61.6 Conclusion

IABP significantly changes CBF temporal patterns in basal cerebral arteries. TCD provides valuable information about cerebral hemodynamics with intra-aortic balloon pumping, given the ability to measure subsecond changes in cerebral hemodynamics.

The IABP is an important resource to support the failing heart, in diverse clinical situations, but the alterations produced in the systemic circulation are transmitted to

the brain, resulting in alterations of the CBFV temporal pattern, whose implications still require more detailed investigation. The use of TCD for monitoring patients with IABP, and also performing a number of dedicated assessments, such as dynamic CA or brain death, is recommended.

Further studies are needed in patients with IABP to assess the extent of cerebral hemodynamic effects, particularly regarding the phenomenon of diastolic CBFV reversal.

Algorithm

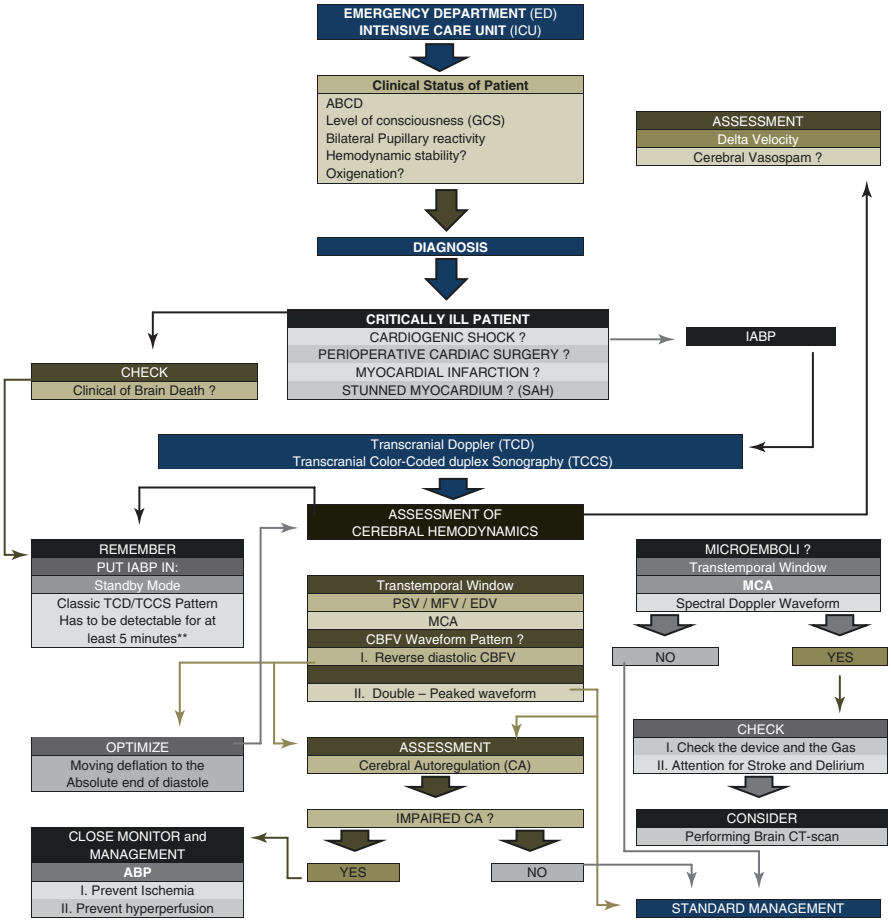

ABCD Airway-breathing-circulation-disability, *IABP* Intra-aortic balloon pump, *CA* Cerebral autoregulation, *ABP* Arterial blood pressure, *MCA* Middle cerebral artery, *CBFV* Cerebral blood flow velocity, *PSV* Peak systolic velocity, *MFV* Mean flow velocity, *EDV* End-diastolic velocity, *SAH* Subarachnoid hemorrhage; ** If the complementary exam is needed

References

1. White JM, Ruygrok PN. Intra-aortic balloon counterpulsation in contemporary practice where are we? Heart Lung Circ. 2015;24(4):335–41.
2. Morris NA, Manning N, Marshall RS, Connolly ES, Claassen J, Agarwal S, et al. Transcranial Doppler waveforms during intra-aortic balloon pump counterpulsation for vasospasm detection after subarachnoid hemorrhage. Neurosurgery. 2018;83(3):416–21.
3. Taccone FS, Lubicz B, Piagnerelli M, Van Nuffelen M, Vincent J-L, De Backer D. Cardiogenic shock with stunned myocardium during triple-H therapy treated with intra-aortic balloon pump counterpulsation. Neurocrit Care. 2009;10(1):76–82.
4. Ducruet AF, Albuquerque FC, Crowley RW, Williamson R, Forseth J, McDougall CG. Balloon-pump counterpulsation for management of severe cardiac dysfunction after aneurysmal subarachnoid hemorrhage. World Neurosurg. 2013;80(6):347.
5. Kantrowitz A. Experimental augmentation of coronary flow by retardation of the arterial pressure pulse. Surgery. 1953;34(4):678–87.
6. Vignola PA, Swaye PS, Gosselin AJ. Guidelines for effective and safe percutaneous intraaortic balloon pump insertion and removal. Am J Cardiol. 1981;48(4):660–4.
7. Klopman MA, Chen EP, Sniecinski RM. Positioning an intraaortic balloon pump using intraoperative transesophageal echocardiogram guidance. Anesth Analg. 2011;113(1):40–3.
8. Webb CAJ, Weyker PD, Flynn BC. Management of Intra-Aortic Balloon Pumps. Semin Cardiothorac Vasc Anesth. 2015;19(2):106–21.
9. Urschel CW, Eber L, Forrester J, Matloff J, Carpenter R, Sonnenblick E. Alteration of mechanical performance of the ventricle by intraaortic balloon counterpulsation. Am J Cardiol. 1970;25(5):546–51.
10. Williams DO, Korr KS, Gewirtz H, Most AS. The effect of intraaortic balloon counterpulsation on regional myocardial blood flow and oxygen consumption in the presence of coronary artery stenosis in patients with unstable angina. Circulation. 1982;66(3):593–7.
11. Kern MJ, Aguirre F, Bach R, Donohue T, Siegel R, Segal J. Augmentation of coronary blood flow by intra-aortic balloon pumping in patients after coronary angioplasty. Circulation. 1993;87(2):500–11.
12. Patel JJ, Kopisyansky C, Boston B, Kuretu ML, McBride R, Cohen M. Prospective evaluation of complications associated with percutaneous intraaortic balloon counterpulsation. Am J Cardiol. 1995;76(16):1205–7.
13. Beholz S, Braun J, Ansorge K, Wollert HG, Eckel L. Paraplegia caused by aortic dissection after intraaortic balloon pump assist. Ann Thorac Surg. 1998;65(2):603–4.
14. Cruz-Flores S, Diamond AL, Leira EC. Cerebral air embolism secondary to intra-aortic balloon pump rupture. Neurocrit Care. 2005;2(1):49–50.
15. Honet JC, Wajszczuk WJ, Rubenfire M, Kantrowitz A, Raikes JA. Neurological abnormalities in the leg(s) after use of intraaortic balloon pump: report of six cases. Arch Phys Med Rehabil. 1975;56(8):346–52.
16. Al-Mufti F, Morris N, Lahiri S, Roth W, Witsch J, Machado I, et al. Use of intra-aortic- balloon pump counterpulsation in patients with symptomatic vasospasm following subarachnoid Hemorrhage and neurogenic stress cardiomyopathy. J Vasc Interv Neurol. 2016;9(1):28–34.
17. Kerro A, Woods T, Chang JJ. Neurogenic stunned myocardium in subarachnoid hemorrhage. J Crit Care. 2017;38:27–34.
18. Lazaridis C, Pradilla G, Nyquist PA, Tamargo RJ. Intra-aortic balloon pump counterpulsation in the setting of subarachnoid hemorrhage, cerebral vasospasm, and neurogenic stress cardiomyopathy. Case report and review of the literature. Neurocrit Care. 2010;13(1):101–8.
19. Milinis K, Thapar A, O'Neill K, Davies AH. History of aneurysmal spontaneous subarachnoid hemorrhage. Stroke. 2017;48(10):e280–3.
20. Dumont AS, Dumont RJ, Chow MM, Lin C-L, Calisaneller T, Ley KF, et al. Cerebral vasospasm after subarachnoid hemorrhage: putative role of inflammation. Neurosurgery. 2003;53(1):123–33; discussion 133–135.

21. Cheung AT, Levy WJ, Weiss SJ, Barclay DK, Stecker MM. Relationships between cerebral blood flow velocities and arterial pressures during intra-aortic counterpulsation. J Cardiothorac Vasc Anesth. 1998;12(1):51–7.
22. Schachtrupp A, Wrigge H, Busch T, Buhre W, Weyland A. Influence of intra-aortic balloon pumping on cerebral blood flow pattern in patients after cardiac surgery. Eur J Anaesthesiol. 2005;22(3):165–70.
23. Pfluecke C, Christoph M, Kolschmann S, Tarnowski D, Forkmann M, Jellinghaus S, et al. Intra-aortic balloon pump (IABP) counterpulsation improves cerebral perfusion in patients with decreased left ventricular function. Perfusion. 2014;29(6):511–6.
24. Brass LM. Reversed intracranial blood flow in patients with an intra-aortic balloon pump. Stroke. 1990;21(3):484–7.
25. van der Naalt J, Baker AJ. Influence of the intra-aortic balloon pump on the transcranial Doppler flow pattern in a brain-dead patient. Stroke. 1996;27(1):140–2.
26. Caldas JR, Panerai RB, Passos R, et al. Is there still a place for transcranial Doppler in patients with IABP? Crit Care. 2020;24:625.
27. Gao Y-Z, Zhang M. Effect of intra-aortic balloon pump on reversal of diastolic cerebral flow: deflated too early? Neurocrit Care. 2018;29:313–4.
28. Schutt RC, Bhimiraj A, Estep JD, Guha A, Trachtenberg BH, Garami Z. Deflation timing influences intra-aortic balloon pump-mediated carotid blood flow reversal: a case report. Circ Heart Fail. 2016;9(9):e003474.
29. Paulson OB, Strandgaard S, Edvinsson L. Cerebral autoregulation. Cerebrovasc Brain Metab Rev. 1990;2(2):161–92.
30. Aaslid R, Lindegaard KF, Sorteberg W, Nornes H. Cerebral autoregulation dynamics in humans. Stroke. 1989;20(1):45–52.
31. Tiecks FP, Lam AM, Aaslid R, Newell DW. Comparison of static and dynamic cerebral autoregulation measurements. Stroke. 1995;26(6):1014–9.
32. Panerai RB. Transcranial Doppler for evaluation of cerebral autoregulation. Clin Auton Res. 2009;19(4):197–211.
33. Tzeng YC, Ainslie PN, Cooke WH, Peebles KC, Willie CK, MacRae BA, et al. Assessment of cerebral autoregulation: the quandary of quantification. Am J Physiol Circ Physiol. 2012;303(6):658.
34. Scolletta S, Taccone FS, Donadello K. Brain injury after cardiac surgery. Minerva Anestesiol. 2015;81(6):662–77.
35. Brown CH 4th, Faigle R, Klinker L, Bahouth M, Max L, LaFlam A, et al. The association of brain MRI characteristics and postoperative delirium in cardiac surgery patients. Clin Ther. 2015;37(12):2699.e9.
36. Koster S, Hensens AG, Schuurmans MJ, van der Palen J. Risk factors of delirium after cardiac surgery: a systematic review. Eur J Cardiovasc Nurs. 2011;10(4):197–204.
37. Caldas JR, Panerai RB, Bor-Seng-Shu E, Almeida JP, Ferreira GSR, Camara L, et al. Cerebral hemodynamics with intra-aortic balloon pump: business as usual? Physiol Meas. 2017;38(7):1349–61.
38. Bellapart J, Geng S, Dunster K, Timms D, Barnett AG, Boots R, et al. Intraaortic balloon pump counterpulsation and cerebral autoregulation: an observational study. BMC Anesthesiol. 2010;10:3.
39. Schramm P, Klein KU, Falkenberg L, Berres M, Closhen D, Werhahn KJ, et al. Impaired cerebrovascular autoregulation in patients with severe sepsis and sepsis-associated delirium. Crit Care. 2012;16(5):181.
40. Salinet AS, Panerai RB, Robinson TG. The longitudinal evolution of cerebral blood flow regulation after acute ischaemic stroke. Cerebrovasc Dis Extra. 2014;4(2):186–97.
41. Ma H, Guo ZN, Liu J, Xing Y, Zhao R, Yang Y. Temporal course of dynamic cerebral autoregulation in patients with intracerebral hemorrhage. Stroke. 2016;47(3):674–81.

42. Caldas JR, Panerai RB, Haunton VJ, Almeida JP, Ferreira GSR, Camara L, et al. Cerebral blood flow autoregulation in ischemic heart failure. Am J Physiol Regul Integr Comp Physiol. 2016;312:108–13.
43. Budohoski KP, Czosnyka M, Kirkpatrick PJ, Reinhard M, Varsos GV, Kasprowicz M, et al. Bilateral failure of cerebral autoregulation is related to unfavorable outcome after subarachnoid hemorrhage. Neurocrit Care. 2015;22(1):65–73.
44. Caldas JR, Haunton VJ, Panerai RB, Hajjar LA, Robinson TG. Cerebral autoregulation in cardiopulmonary bypass surgery: a systematic review. Interact Cardiovasc Thorac Surg. 2017;6
45. Kunt A, Atbas C, Hidiroglu M, Cetin L, Erdogan KE, Kucuker A, et al. Predictors and outcomes of minor cerebrovascular events after cardiac surgery: a multivariable analysis of 1346 patients. J Cardiovasc Surg. 2013;54(4):537–43.
46. Al-Atassi T, Lam K, Forgie M, Boodhwani M, Rubens F, Hendry P, et al. Cerebral microembolization after bioprosthetic aortic valve replacement comparison of warfarin plus aspirin versus aspirin only. Circulation. 2012;126(11):S239–44.
47. Barbut D, Yao FSF, Lo YW, Silverman R, Hager DN, Trifiletti RR, et al. Determination of size of aortic emboli and embolic load during coronary artery bypass grafting. Ann Thorac Surg. 1997;63(5):1262–7.
48. Furman S, Vijaynagar R, Rosenbaum R, McMullen M, Escher DJ. Lethal sequelae of intra-aortic balloon rupture. Surgery. 1971;69(1):121–9.
49. Ropper AH, Kehne SM, Wechsler L. Transcranial Doppler in brain death. Neurology. 1987;37(11):1733–5.
50. Caldas JR, Panerai RB, Bor-Seng-Shu E, et al. Intra-aortic balloon pump does not influence cerebral hemodynamics and neurological outcomes in high-risk cardiac patients undergoing cardiac surgery: an analysis of the IABCS trial. Ann Intensive Care. 2019;9(1):130.
51. Murli K, Zacharowski K. Principles of intra-aortic balloon pump counterpulsation. Contin Educ Anaesth Crit Care Pain. ScienceDirect. 2009;9(1):24–8.

Chapter 62
Brain Parenchyma: Usefulness of Transcranial Color-Coded Duplex Sonography (TCCS)

Silvana Svampa

Key Points

1. The combination of B-mode and spectral Doppler images allows the visualization of structures of the cerebral parenchyma and the vessels of the circle of Willis.
2. Measurement of arterial and venous blood flow velocities, as well as collateral circulation.
3. The most common axial insonation planes by TCCS: mesencephalic, diencephalic, and ventricular planes through transtemporal acoustic window.
4. Measurement and follow-up of midline shift (MLS).
5. TCCS allows the evaluation of changes in the third ventricle (hydrocephalus or intracranial hypertension).
6. TCCS is useful for locating, measuring, and following up intracerebral hematomas (ICH).

62.1 Introduction

Transcranial color-coded duplex sonography (TCCS) is an ultrasound monitoring method to produce a useful combination between two-dimensional images (B-Mode) and spectral Doppler images (duplex sonography) [1].

This combination allows the visualization of parenchymal structures (such as the third ventricle and midline) as well as the exact determination of the insonated vessel (arterial and venous), improving the angle of insonation and therefore the

S. Svampa (✉)
Intensive Care Medicine, CMIC Clinic, Neuquén, Argentina

Medical Foundation of Río Negro and Neuquén, Cipolletti, Río Negro, Argentina

SATI, Buenos Aires, Argentina
e-mail: silvanasvampa@gmail.com

C. N. Rodríguez et al. (eds.), *Neurosonology in Critical Care*,
https://doi.org/10.1007/978-3-030-81419-9_62

cerebral blood flow velocity (CBFV). It also detects hyperdense mass lesions, compared to other techniques such as computed tomography (CT).

However, in daily practice, its use is less frequent than TCD despite having been introduced in 1996 and sharing the same characteristics in terms of noninvasiveness, reproducibility, and the possibility of being performed at the bedside of the patient in a critical area where transfers for other complementary studies are risky.

62.2 TCCS: Probe and Acoustic Window Selection

TCCS requires the use of lower-frequency (2–2.5 MHz) sector transducer and the use of same acoustic window such as TCD [1].

62.2.1 Transtemporal Acoustic Window

Monitoring axial and coronal plans (Tables 62.1 and 62.2).

62.2.2 Suboccipital (transnuchal) Acoustic Window (Table 62.3)

Table 62.1 Axials approach

Axial plans of insonation	Intracerebral structure
1. Mesencephalon	Mesencephalon and basal cistern
2. Diencephalic	3rd ventricle and pineal gland
3. Ventricular	Anterior horns of lateral ventricules
4. Upper pons plane	ICA-siphon/sphenoid bone
5. Lower pons plane	Petrosal segment of internal carotid artery (ICA)

Table 62.2 Coronal approach

Coronal plans of insonation	Estructuras cerebrales
Anterior coronal plane	Distal ICA/bifurcation on middle cerebral artery (MCA) and anterior cerebral artery (ACA)
Posterior coronal plane	Distal segment of basilar artery(BA)/superior cerebellar arteries (SCA) and posterior cerebral artery (PCA)

Table 62.3 Suboccipital acoustic window

Structure	Identification
Foramen magnum	Round and hypoechoic
Vertebral arteries (VA)	V3/V4 segments
Basilar artery (BA)	Proximal segment

62.2.3 Trans-orbital Acoustic Window

Allows us the assess ophthalmic artery (OA) and central retinal artery (CRA) hemodynamic changes, and dynamic changes of optic nerve sheath diameter (ONSD).

62.2.4 Frontal Bone Window: B-Mode Sonography

For depiction of the parenchymal anatomy, an insonation depth of 14–16 cm should be chosen so that the contralateral skull becomes visible. Stolz et al. (1999) described two intonation views through frontal bone window (FBW): paramedian frontal bone window (PMFBW) and latero-frontal bone window (LFBW), whereas Sentenac et al. (2020) described three view zones through FBW: paramedian frontal zone (PMFZ), supraorbital zone (SOZ), and latero-frontal zone (LFZ) [3, 4].

Stolz (1999): FBW—Parenchymal and vascular structures

- *PMFBW*: Contralateral skull bone (hyperechoic), choroid plexus of the third ventricle (hyperechoic), third ventricle (hypoechoic), corpus callosum (hypoechoic), orbital roof (hyperechoic), and cerebellar tentorium (hyperechoic).
- *LFBW*: Rotated 90° outward and move horizontally from PMFBW, up to the latero-frontal zone: Sylvian fissure (hyper echoic), contralateral skull bone (hyperechoic), and mesencephalon (hypoechoic) as landmarks structures to assess the circle of Willis [3].

Sentenac (2020): FBW—Parenchymal and vascular structures

- *PMFZ*: Contralateral skull bone (hyperechoic), choroid plexus of the third ventricle (hyperechoic), third ventricle (hypoechoic), corpus callosum (hypoechoic), orbital roof (hyperechoic), and cerebellar tentorium (hyperechoic).
- *SOZ*: Insonation A2 segments of the ACA were recorded.
- *LFZ*: The A2 segments of the ACA were recorded, while only the A1 segments were measured by the TBW [4].

The FBW was able to insonate the ACA in 45% of patients admitted to ICU for brain injury. Combining transtemporal acoustic window with the FBW significantly enhanced the insonation rate of the ACA when compared to the transtemporal window alone [4].

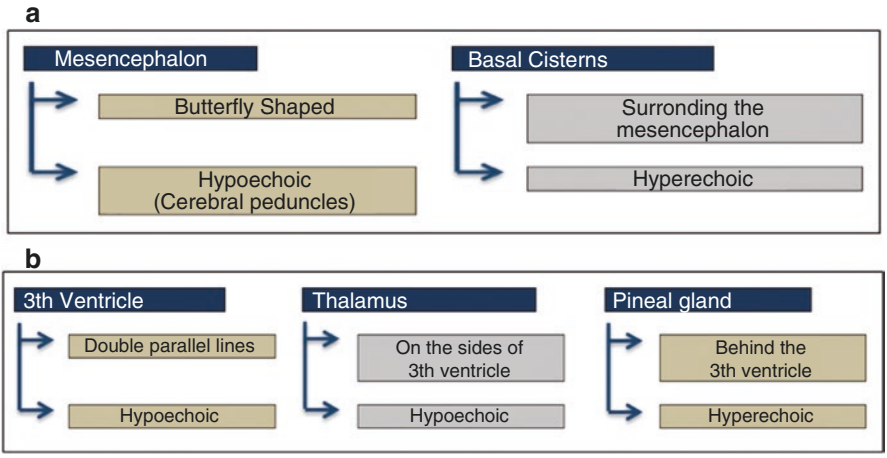

Fig. 62.1 (**a**) Schema of the brain structures visualized by ultrasound (B-Mode) through the mesencephalic plane. (**b**) Schema of brain structures visualized by ultrasound (B-Mode) through the diencephalic plane

62.3 TCCS B-Mode: Insonation Plans

62.3.1 Mesencephalic Plane (Fig. 62.1a)

1.1 Mesencephalon (hypoechoic)
1.2 Basal cisterns (hyperechoic)

62.3.2 Diencephalic Plane (Fig. 62.1b)

2.1 Third ventricle
2.2 Thalamus (hypoechoic)
2.3 Pineal gland (hyperechoic)

62.3.3 Ventricular Plane

3.1 Frontal horns of lateral ventricles (LV) (hypoechoic)

62.3.4 Upper Pons Plane

Ultrasound landmarks: Sphenoid bone anteriorly and petrosal bone posteriorly

4.1 Middle temporal fossa (hypoechoic)
4.2 Posterior fossa: Cerebellum (hypoechoic)
4.3 ICA-siphon (vascular structure)

62.3.5 Lower Pons Plane

Ultrasound landmarks: Sphenoid bone anteriorly and petrosal bone posteriorly

5.1 Middle temporal fossa (hypoechoic)
5.2 Posterior fossa: Cerebellum (hypoechoic)
5.3 ICA-petrosal segment (vascular structure)

62.4 TCCS: Advantages over TCD

1. TCCS allows to see cerebral basal arteries and deep cerebral venous, being able to locate accurately, quickly, and efficiently the insonated vessel, improving the insonation angle and, therefore, the CBFV that is higher than those from TCD.
2. It can improve the detection of collateral circulation, having greater sensitivity (S) and specificity (E).
3. It allows the visualization of parenchymal structures such as the third ventricle and can detect hydrocephalus due to its enlargement or intracranial hypertension (ITH) due to collapse.
4. The monitoring of the midline shift (MLS) allows you to detect signs of subfalcial herniation as an expression increase intracranial pressure (ICP).
5. TCCS can detect intra- (SAH, ICH, abscess, etc.) and extra-axial hemorrhages and/or space-occupying lesions (subdural hematoma, subdural empyema, epidural hematoma).

62.5 TCCS: Brain Parenchymal Approach

62.5.1 Insonation Protocol

A. *Window*: Transtemporal acoustic window
   Transtemporal acoustic window failure is found in 8–20% of patients [5].
B. *Planes*: Five axial insonation planes (rostro-caudal course)

1.1 *The midbrain (mesencephalic) plane*: can be identified as the typical image, "butterfly-shaped" (hypoechoic), surrounded by the hyperechoic basal cisterns. Circle of Willis can be located from this plane (Fig. 62.2a).

1.2 *The diencephalic plane*: can be identified in the same plane with a slight rotation of 10 ° upward, being able to locate the third ventricle by a double hyperechoic line, in front of pineal gland (hyperechoic posterior landmark). The normal values for the third ventricle are 4.8 ± 1.9 mm for those under 60 years and 7.6 ± 2.1 mm for those over 60 years (Fig. 62.2b).

1.3 *The ventricular plane*: where we can identify the hypoechoic frontal horns of lateral ventricles (LV), directing the transducer upward. The normal values for the lateral ventricles (frontal horns) are 16 ± 2.3 mm for under 60 years old people and 19 ± 2.9 mm for over 60 years old [6] (Fig. 62.3).

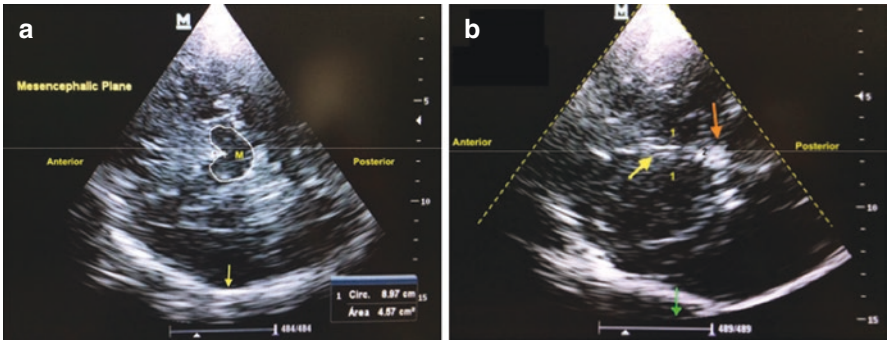

Fig. 62.2 (**a**) Mesencephalic plane and basal cisterns; (**b**) Diebcephalic plane where it's shown the third ventricle (arrow) and pineal gland (posterior hyperechoic structure close to third ventricle); C(s) contralateral skull

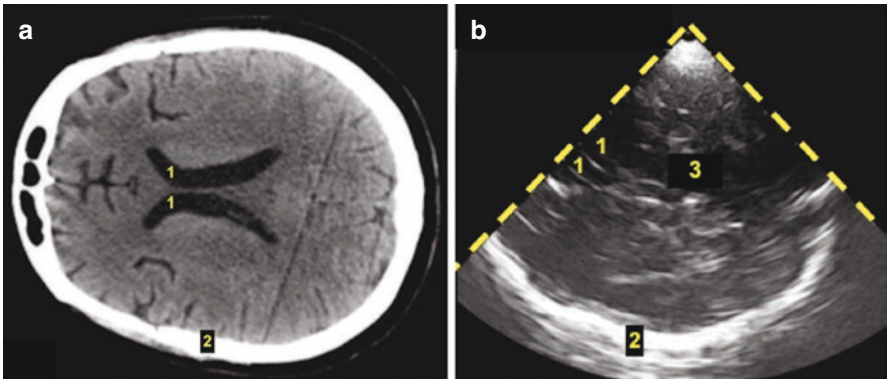

Fig. 62.3 Lateral ventricles: (**a**) Computed tomography (CT): (1) Frontal horns of lateral ventricles, (2) Skull bone; (**b**) TCCS: (1) Frontal horns of lateral ventricles are visualized as hypoechogenic structure. The three parallel lines correspond to lateral layers of ependima and septum pellucidum, (2) Contralateral skull bone and (3) Third ventricle

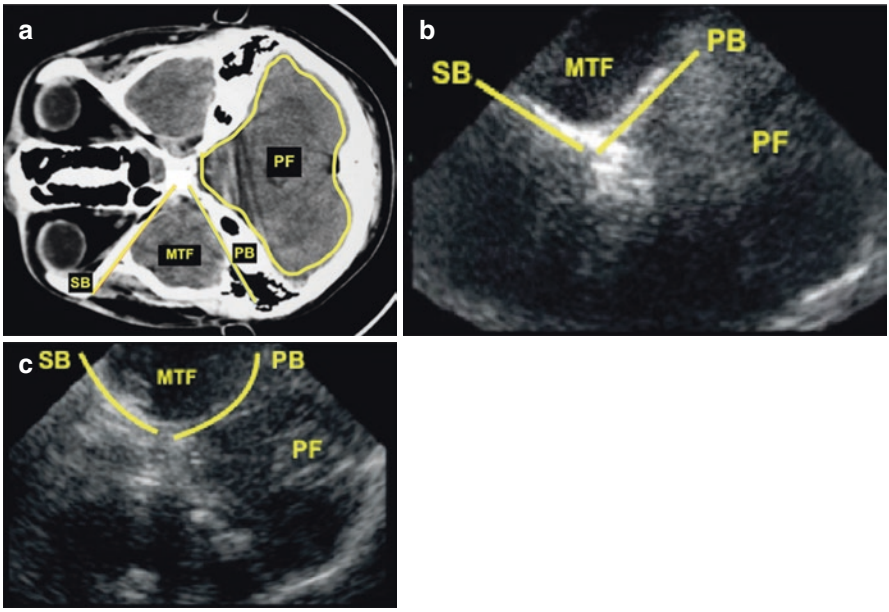

Fig. 62.4 (**a**) Non-contrast CT brain-scan; (**b**) Lower pons plane: TCCS by transtemporal acousitc window; (**c**) Upper pons plane: TCCS by transtemporal acoustic window. (SB) Sphenoidal bone, (PB) Petrosal bone, (MTF) Middle temporal fossa and, (PF) Posterior fossa (cerebellum)

1.4 *The upper pons plane*: from the mesencephalic lowering the insonation angle approximately 10°, where ultrasound landmarks are the sphenoid bone anteriorly and petrosal bone posteriorly (forming together the middle temporal fossa). ICA-siphon (hyperechoic) can be observed in the minor wing of the sphenoid. Here we can identify the ACA, MCA, and ICA (Fig. 62.4a, c).

1.5 *The low pons plane*: located below upper pons plane by an additional 10°, where ultrasound landmarks are the sphenoid bone anteriorly and petrosal bone posteriorly (forming middle temporal fossa). The hyperechoic distal ICA can be observed in its petrosal portion (Fig. 62.4b).

62.5.2 Other Insonation Planes

2.1 *Coronal planes* : Transtemporal acoustic window [7]

2.1.1 Anterior: Probe is rotated from the midbrain plane by 90° in temporal position.

– Frontal horns of lateral ventricle

– Third ventricle
– Contralateral bone skull

2.1.2 Posterior: Probe is rotated from the level of the PCA by 90° in temporal position.

– Vascular structure: Top of the basilar artery (BA)

2.2 *Sagittal plane*: Frontal bone window (FBW)

2.2.1 PMFBW/PMFZ [3, 4]:
Contralateral skull bone (hyperechoic), choroid plexus of the third ventricle (hyperechoic), third ventricle (hypoechoic), corpus callosum (hypoechoic), orbital roof (hyperechoic), and cerebellar tentorium (hyperechoic)

62.5.3 Midline Shift Measurement (MLS)

It can be measured in two different ways, always in the diencephalic plane:

3.1 Measure the distance between the two temporal bones to the middle of the third ventricle (Eq. 62.1; Fig. 62.5) [8]:

$$\text{MLS} = \text{Distance } A - \text{Distance } B / 2 \tag{62.1}$$

A is ipsilateral.
B is contralateral.

3.2 Measure the distance to the third ventricle and measure the distance between the two temporal bones (Eq. 62.2) [8]:

$$\text{MLS} = \text{Distance } C - \left(\text{Distance } D / 2\right) \tag{62.2}$$

C is ipsilateral.
D is distance between the two temporal bones.

If the MLS value is positive, it is by ipsilateral deviation. If it is negative, it is by contralateral deviation.

The MLS expresses “mass effect” and according to different authors has a very good correlation with the brain CT scan measurement ($r = 0.88$) [9].

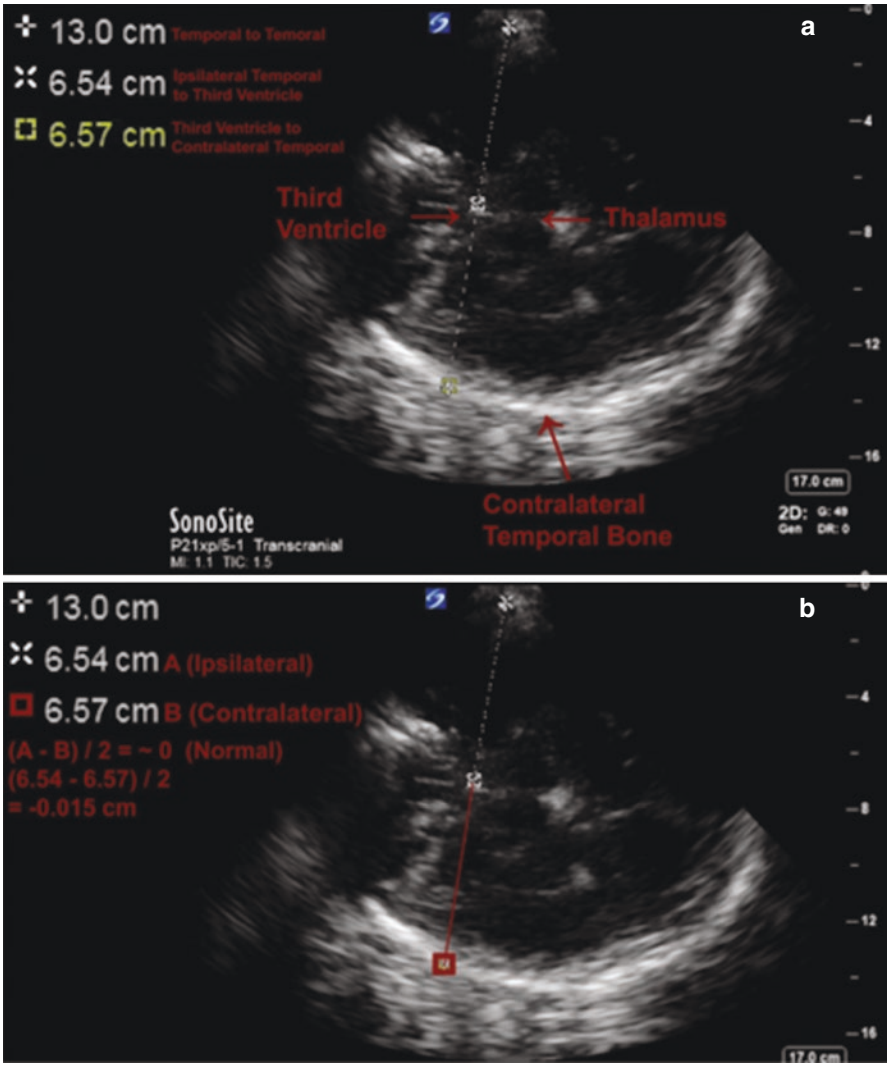

Fig. 62.5 Midline shift (MLS): Detecting midline shift; (**a**) First method to estimate midline shift. Measuring the distance from the ipsilateral temporal bone to the contralateral temporal bone (here 13.0 cm), and comparing it with the distance from the ipsilateral temporal bone to the third ventricle (here 6.54 cm). (**b**) Second method to estimate midline shift. Measuring the distance from the temporal bone to the third ventricle on one side (here 6.54 cm), and comparing it with the same measurement taken on the other side (not shown). (Courtesy: Lau et al. [8])

A deviation >2.5 mm is considered significant and suggests the need to repeat the brain CT scan [10].

MLS is not reliable when there are skull defects such as fractures and decompressive craniectomy (DC), the presence of cephalohematomas in the scalp, or changes in intracranial anatomy visualized through brain CT scan [2].

62.5.4 Measurement and Follow-Up of Third Ventricle (Fig. 62.4b)

The normal values described for the third ventricle, according to the age groups, are 4.8 ± 1.9 mm for those under 60 years and 7.6 ± 2.1 mm for those over 60 years.

Other authors consider hydrocephalus by TCCS when the size of third ventricle >9 mm and >19 mm for lateral ventricles, showing a very good correlation with brain CT scan.

Based on these data, the TCCS allows us to define the placement or removal of a ventricular drainage [2].

On the other hand, the reduction in the diameter of the third ventricle may express increase in the ICP.

In a paper published by Oliveira in 2017 comparing both methods (CT scan and TCD/TCCS) in patients with traumatic brain injury (TBI), it shows a correlation ($r = 0.93$) for MLS and ($r = 0.88$) for third ventricle [10].

62.5.5 Measurement and Follow-Up of Perimesencephalic Basal Cisterns (PBC) Size

The TCCS, through the mesencephalic plane, can measure and estimate if there is compression or not of the PBC with a 100% of sensitivity and 50% of specificity; this allows to estimate, as it can be seen in a brain CT scan, increase of ICP [10].

62.5.6 Measurement and Follow-Up of Intracerebral Hemorrhage (ICH)

The intracerebral hematoma (Fig. 62.6) [11] is usually identified as a hyperechoic mass in its acute stage (<5 days) and as hypoechoic with a hyperechoic halo around the hematoma (>5 days).

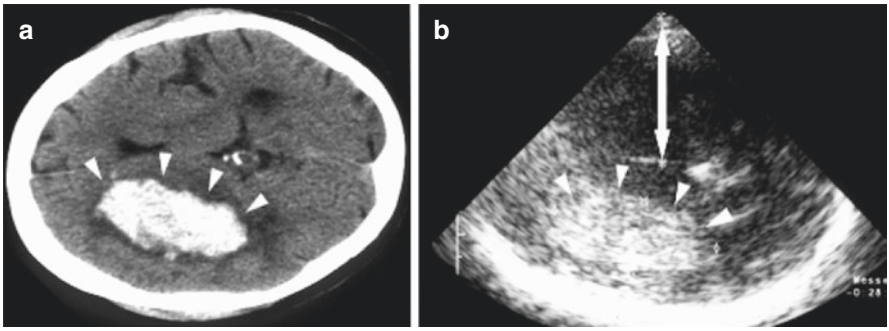

Fig. 62.6 TCCS axial brain scan at thalamus level showing a large intracerebral hematoma. (**a**) Computed tomography (CT) image corresponding to the TCS image shown in (**b**). The triangles indicate the hematoma. (**b**) TCS image showing the highly echogenic hematoma in the acute phase. The midline shift at level of third ventricle can be calculated after measuring the distance d of the temporally placed transducer face to the third ventricle (indicated by double arrow) from both sides: midline shift = $(d1 - d2)/2$. (Courtesy: Walter et al. [14])

The TCCS also allows the evaluation of the size of the third ventricle and LV, MLS, the presence of intraventricular hemorrhage (IVH), as well as measuring and follow-up of the volume of the intracerebral hematoma according to the equation (Eq. 62.3):

$$\text{Hematoma volume}\left(\text{HV}\right):\left(A\times B\times C\right)/2 \tag{62.3}$$

Camps et al. (2017) found that an average HV value of 21.8 ml measured by TCCS has a sensitivity of 88.9% and specificity of 80% in predicting early neurological deterioration and correlates very well with brain CT scan findings [12].

However, Camps et al. concluded that TCCS may overestimate the volume of small hematomas and underestimate large ones. The detection of intracerebral hematomas by TCCS depends more on location than size of it. It is easier to recognize deep hematomas than those located at the frontal or parietal level. A sensitivity of 94% and a specificity of 95% are described. Differential diagnosis should be made with arteriovenous malformation (AVMs) and brain tumors.

62.6 TCCS: Other Diagnostic Methods in ICU

Using the same acoustic windows as TCD. TCCS also achieves a two-dimensional image (B-mode) of the parenchymal brain. The anatomical details are inferior to the computed tomography (CT), but it allows to recognize the mass effects and midline shift (MLS).

62.6.1 Advantages Over Brain CT Scan

1.1 Noninvasive
1.2 Non-radiation
1.3 Fast
1.4 The patient should not be transported
1.5 It is reproducible
1.6 Allows monitoring of vasospasm, vessel stenosis, acute vascular occlusion, ICP changes, and the calculation of cerebral perfusion pressure (CPP)

62.7 Traumatic Brain Injury (TBI): Usefulness of TCCS

TCCS is a complementary monitoring tool in the acute phase of TBI. It allows the assessment of brain perfusion and response to secondary brain injury until the placement of invasive intracranial pressure monitoring.

It can detect patients with mild or moderate TBI at risk of neurological impairment.

According to different authors based on:

1. MLS: TCCS is a bedside technique that is valid for determining MLS in patients with TBI, where coefficient of correlation between MLS measured by CT and TCCS was 0.88 ($r = 0.88$) [13].
2. Third ventricle: Reduction of the size.

As described for TCD/TCCS, the decrease in end-diastolic flow velocity (EDV) < 20 cm/s, decreased mean flow velocity (MFV) < 30 cm/s, and increase in pulsatility index (PI) > 1.4 could be expressing cerebral hypoperfusion and are associated with poor results [14, 15].

62.8 Conclusion

Despite being a portable, accessible, noninvasive tool that provides more information than the TCCS (midline deviation, signs of brain herniation, intra- and extra-axial bleeding) by combining two-dimensional ultrasound images with spectral ones, it is a tool that is beginning to gain ground in the daily clinical practice of the ICUs as monitoring at the bedside of the critically ill patient in real time.

Algorithm

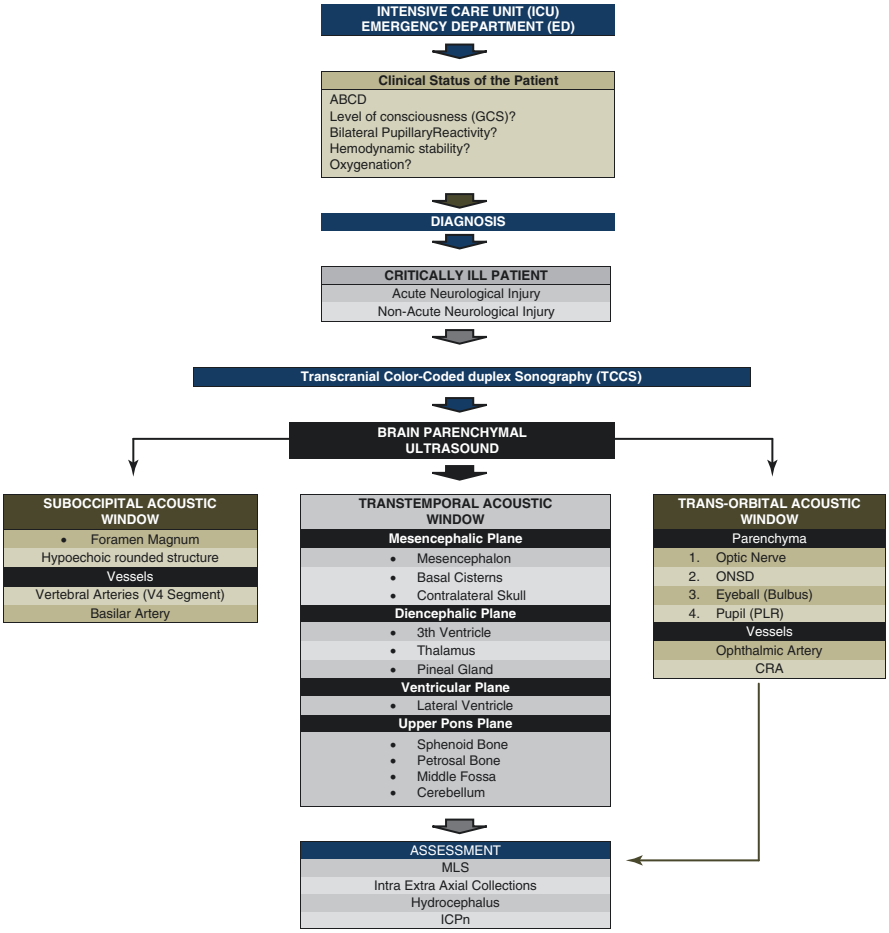

ABCD Airway-breathing-circulation-disability, *GCS* Glasgow coma scale, *MLS* Midline shift, *ICPn* Non-invasive ICP, *ONSD* Optic nerve sheath diameter, *PLR* Pupilar light reflex, *CRA* Central retinal artery

References

1. Vincent IL, Arntfield T. Point-of-care transcranial Doppler by intensivists. Crit Ultrasound J. 2017;9:21.
2. Abdo A, Castellanos R, et al. Transcranial Duplex sonography for measurement of third ventricle diameter and midline shift. Rev Cubana de Medicina Intensiva y Emergencias. 2017;16(4):21–30.

3. Stolz E, Kaps M, Kern A, Dorndorf W. Frontal bone windows for transcranial color-coded Duplex sonography. Stroke. 1999;30:814–20.
4. Sentenac P, Charbit J, Maury C, Bory P, Dagod G, Greco F, et al. The frontal bone window for transcranial Doppler ultrasonography in critically ill patients: validation of a new approach in the ICU. Neurocrit Care. 2020;33:115–23.
5. Lee CH, Jeon SH, Wang SJ, et al. Factors associated with temporal window failure in transcranial Doppler sonography. Neurol Sci. 2020;41:3293–9.
6. Seidel G, Kaps M, Gerriets T, Hutzelmann A. Evaluation of the ventricular system in adults by transcranial duplex sonography. J Neuroimaging. 1995;5(2):105–8.
7. Eggers J, Pade O, Rogge A, Schreiber SJ, Valdueza JM. Transcranial color-coded sonography successfully visualizes all intracranial parts of the internal carotid artery using the combined transtemporal axial and coronal approach. AJND Am J Neuroradiol. 2009;30:1589–93.
8. Lau VI, Jaidka A, Wiskar K, Packer N, Tang JE, Koenig S, et al. Better with ultrasound: transcranial Doppler. Chest. 2020;157(1):142–50.
9. Blanco P, Abdo-Cuza A. Transcranial Doppler ultrasound in de ICU: it is not all sunshine and rainbows. Crit Ultrasound J. 2018;10:2.
10. Oliveira RAG, et al. Comparison between brain computed tomography scan and transcranial sonography to evaluate third ventricle width, Peri-mesencephalic cistern, and Sylvian fissure in traumatic brain-injured patients. Front Neurol. 2017;8:44.
11. Uwe W. Transcranial sonography of the cerebral parenchyma: update on clinically relevant applications. Pers Med. 2012;1:334–43.
12. Camps-Renom P, Mendez J, et al. Transcranial duplex sonography predicts outcome following an intracerebral Hemorrhage. AJNR Am J Neuroradiol. 2017;38:1543–9.
13. Llompart Pou JA, Abadal Centellas JM, Palmer Sans M, et al. Monitoring midline shift by transcranial color-coded sonography in traumatic brain injury. Intensive Care Med. 2004;30:1672–5.
14. Walter U, Behnke S, Eyding J, Niehaus L, Postert T, Seidel G, et al. Transcranial brain parenchyma sonography in movement disorders: state of the art. Ultrasound Med Biol. 2007;33(1):15–25.
15. Bouzat P, Oddo M, Payen J-F. Transcranial Doppler after traumatic brain injury: is there a role? Curr Opin Crit Care. 2014;20:153–60.

Chapter 63
ICP Management by Osmotherapy with Mannitol and Hypertonic Saline in ICU: Real-Time Effect on Optic Nerve Sheath Diameter Monitoring by Ultrasound

Yoann Launey

Key Points

1. Optic nerve sheath diameter (ONSD) ultrasonography is a useful noninvasive and accurate tool to detect raised ICP.
2. The procedure requires a strict technique following safety rules to warrant quality images and patient safety.
3. Serial ONSD measurements may help to detect real-time changes in ICP such as the effect of osmotherapy.
4. ONSD may be a surrogate for ICP monitoring when invasive ICP monitoring is unavailable or contraindicated.
5. There is a need for additional research to validate ONSD use for tracking ICP changes in real time.

63.1 Introduction

Acute brain injuries result from the primary insult but may largely depend on secondary injuries induced by brain swelling, inflammation, intracranial hypertension, and consecutive reduced cerebral perfusion [1]. Specifically, in traumatic brain injuries (TBI), the management of the most severe patients includes intracranial pressure (ICP) monitoring [2]. A rapid detection of elevated ICP and subsequent management are crucial, as raised ICP is significantly associated with mortality and morbidity [3]. The reference method for estimating ICP includes invasive methods such as intraventricular catheterization and intraparenchymal probes. However,

Y. Launey (✉)
Intensive Care Unit, Department of Anaesthesia, Critical Care and Perioperative Medicine, Centre Hospitalier Universitaire de Rennes, Rennes, France
e-mail: yoann.launey@chu-rennes.fr

C. N. Rodríguez et al. (eds.), *Neurosonology in Critical Care*,
https://doi.org/10.1007/978-3-030-81419-9_63

these procedures may be delayed because of the absence of neurosurgeons, or intensive care units or complicated by hemorrhage or infection. In addition, ICP probe insertion is contraindicated in case of coagulation disorders. Accordingly, the need for noninvasive methods for rapid ICP assessment has increased and several emerging tools have been investigated. Specifically, the use of optic nerve sheath diameter (ONSD), measured by computed tomography (CT) or ultrasonography (US), has considerably gained interest over the past decade in intensive care units and emergency departments.

63.2 Optic Nerve: Anatomy and Physiology

The optic nerve is a part of the central nervous system (CNS). In its intraorbital part, the optic nerve extends from the eye globe to the optic canal and is surrounded with a dural sheath, which is an extension of the CNS meninges. The space delineated by this sheath (i.e., dura mater and arachnoid mater) allows communication between the perioptic nerve cerebrospinal fluid (CSF) and cerebral CSF [4] (Fig. 63.1). The

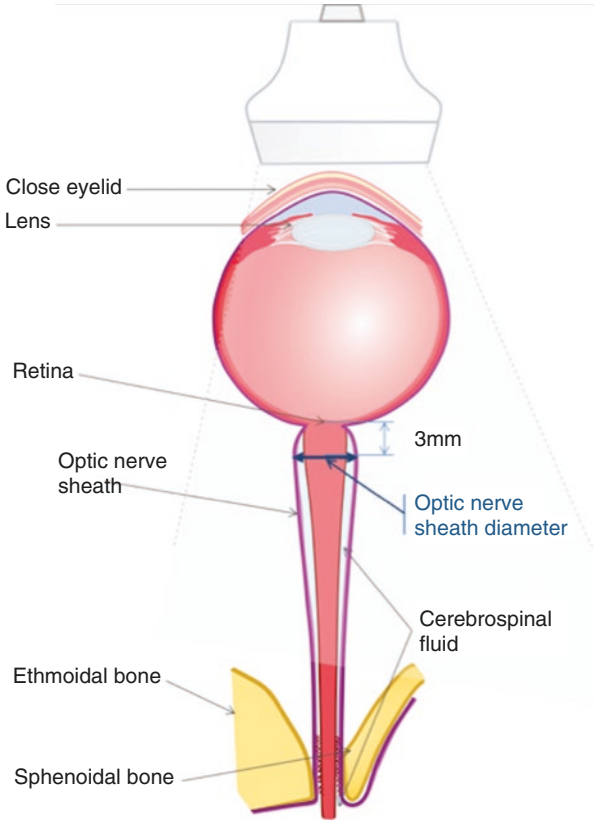

Fig. 63.1 Anatomical transverse view of eyeball and optic nerve. Optic nerve sheath diameter is measured 3 mm behind the retina

sheath is normally described to be loose near the eye globe, forming larger space between the optic nerve and the sheath than anywhere alongside its course, consequently appearing bulbous shape just behind the eyeball. Then, this space narrows in the region of the optic canal, with thick fibrous bands stretching from the dura mater to the pia mater of the optic nerve so that the space shapes a trabecular meshwork in the canal, where the subarachnoid and subdural spaces are reduced to almost a capillary size [5]. Communication between the subarachnoid spaces of the cranial cavity and of the sheath almost always exists. However, the extent of communication in the optic canal may widely fluctuate from one subject to another. Thus, during ICP increases due to limited intracranial compliance, CSF accumulates in the optic nerve sheath thereby widening its diameter. This dilation tends to reach a plateau at an ONSD of just over 7 mm (US measurement) [6]. As regards dynamics, previous human studies have demonstrated that this phenomenon occurs within minutes of acute upward changes of ICP and is reversible [7–9].

63.3 ONSD Sonography: Technique

The technique of ONSD US has been previously described [10–12] and its reproducibility seems good [13]. In detail, the patient is placed in supine position at 20–30° to horizontal. A thick layer of standard water-soluble ultrasound transmission gel is applied over the closed upper eyelid. The operator holds the transducer close to the contact surface, touching the patient's face with the fourth and/or the fifth finger for stability. The probe is placed only on the gel in the temporal area of the eyelid to prevent pressure being exerted on the eye. The transverse view with a front lateral approach allows avoiding the edge-shadowing artifact that in anteroposterior views obscures the peripheral zones of the vitreous humor and the globe wall near the equator. The oblique transverse view with optic disc and optic nerve head is the quickest and the most reproducible way to measure ONSD (Fig. 63.2a). From this view, ONSD can also be measured in sagittal plane by rotating the probe of 90° (Fig. 63.2b).

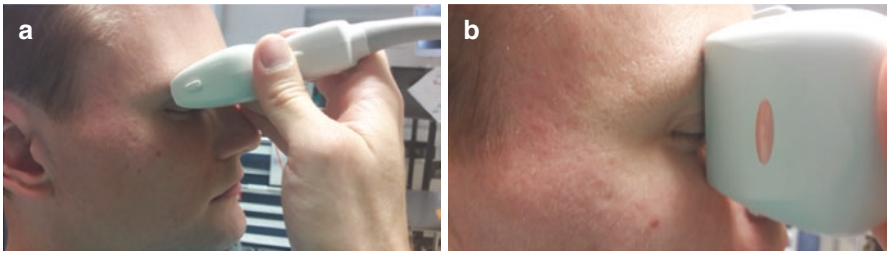

Fig. 63.2 Position of the probe for ultrasonographic neasurements of ONSD in transvere view (**a**) and parasagittal view (**b**)

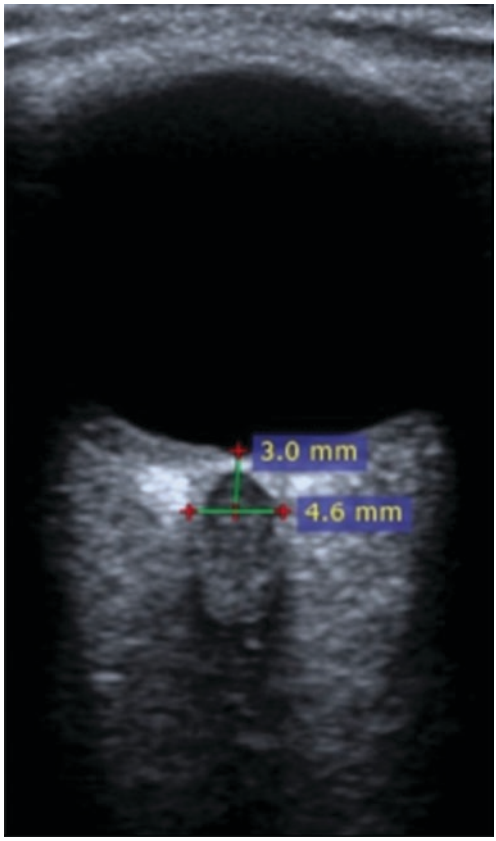

Fig. 63.3 Ultrasonogaphic view of eyeball and optic nerve sheath in transverse view. Optic nerve sheath diameter is measured at 3 mm behind the retina

The probe is placed laterally to the cornea so that the imaging plane bypasses the anterior structures (cornea, anterior chamber, ciliary body and the lens).The position of the probe is adjusted to give a suitable angle for displaying the entry of the optic nerve into the globe. Two-dimensional mode is used, and ONSD is measured 3 mm behind the globe where the optic nerve enter the globe (optic disc or optic papilla), using an electronic calliper along an axis perpendicular to the optic nerve (Fig. 63.3). A fair visualization of optic nerve assumes a straight forward gaze but may not possible in unconscious or sedated patients. If the patient is conscious and cooperative, he is asked to look straight ahead with eyes closed, without clenching the eyelids.

63.3.1 Ultrasonography Settings

Usually, the procedure requires the use of a high-resolution 7.5–12 MHz or higher linear array ultrasound transducer to ensure a sufficient resolution for superficial tissue such as the ocular globe. Before scanning the ocular globe, several different control settings need to be mentioned.

First, the following two have to be considered and continuously monitored to prevent adverse bioeffects of ultrasounds; both are available and displayed on the screen of modern machines:

1.1 *Mechanical index* (MI) roughly refers to the likelihood of the occurrence of cavitation. Its value is constantly updated by the scanner, according to the control settings.
1.2 *Thermal index* (TI) is defined as the ratio of the emitted acoustic power required to raise the temperature of tissue by 1 °C. In soft tissue insonation, TI should be limited to 1.0 [14].

Second, the following controls need to be set to optimize the MI and TI and image quality:

1.3 *Time-gain compensation* (TGC) or linear-in-dB gain: the purpose of TGC is to normalize the signal amplitude with time, compensating for depth. Roughly, this parameter adjustment allows to compensate the depth-related signal attenuation and to display similar tissue material with the same brightness.
1.4 *Depth*: usually this parameter is set to 4 cm which allows the visualization of the eyeball, its posterior part, and the first centimeter of the optic nerve including bulbous part. Depth should be adjusted so that the image of the eye fills the screen.
1.5 *Focus:* by adjusting the depth of focusing, this setting enhanced the image quality and beam focus at the focal zone. Focus should be set at the level of area of optic nerve measurement.
1.6 *Power output*: it refers to acoustic power emitted by the transducer. This control should be set at the optimal value to respect safe levels of MI and TI.

63.3.2 Normal Findings

A clear understanding of the normal range for ONSD and its associated factors is crucial to refine the interpretation of ONSD. The normal eye appears as a circular hypoechoic structure. The cornea is seen as a thin hypoechoic layer parallel to the eyelid. The anterior chamber is filled with anechoic fluid and is bordered by the cornea, iris, and anterior reflection of the lens capsule. The iris and ciliary body are seen as echogenic linear structures extending from the peripheral globe toward lens. The normal lens is anechoic. The normal vitreous chamber is filled with anechoic fluid. Sonographically, the normal retina cannot be differentiated from the other choroidal layers. The optic nerve is visible as a hypoechoic linear region radiating away from the posterior region of the globe, and the optic disc appears as an echogenic structure where the nerve meets vitreous without any interposition of thick echogenic layer of the posterior sclera.

63.3.3 Quality Criteria for Valid ONSD Imaging

Literature describing the quality criteria for ONSD measurements is scarce; however, some criteria may be suggested to warrant safety, reproducibility, and valid measurements:

1. The ultrasound plane should not include the lens on the image.
2. The image contrast should be optimized to view clearly the sonographic differentiation between the nerve and the wrapping arachnoid corresponding to CSF space.
3. Identification of the outer border of the arachnoid requires clear and well-focused images to allow confident measurements of the inner diameter of the dural sheath.
4. Ideal views should demonstrate the point of its penetration into the globe (optic disc).
5. Standardized measurements: the most distensible part of the sheath is located at 3 mm distance from the vitreoretinal interface. ONSD measurements must be performed at this level in a direction perpendicular to the nerve longitudinal axis. In extreme gaze deviations, this position may be hard to obtain and may require repeated attempt or adjustment of gaze if possible.
6. To warrant quality and valid measurements, ONSD should be measured bilaterally, in more than one image frame, ideally in sagittal and transverse views.
7. For ONSD monitoring the previous record with images must be reviewed to ensure similar views and measurements technique. Prior images should be available at bedside for reference. ONSD measured in sagittal planes should not be compared with ONSD from transverse planes.

63.4 ONSD Ultrasound: Safety Considerations

Despite an excellent safety record of ultrasound in clinical imaging, a prolonged exposure of tissues to high levels of ultrasound can potentially cause harmful adverse bioeffects [15], especially in ocular ultrasound procedures. Indeed, the eyes are fluid-filled structures containing large amounts of collagen which provides a perfect acoustic window, but make them efficient absorbers of ultrasound energy and, consequently, can potentiate an increase in local temperature in case of prolonged ultrasound exposure. Furthermore, in the context of acute traumatic brain injury (TBI), the orbital structures can be damaged by mechanical forces. Then, in case of unstable probe position or eyeball compression during probe positioning, incautious movements of the procedure performer or involuntary movements of the patient may be deleterious. Moreover, the use of irritant antiseptics for probe disinfection or inappropriate ultrasound gel can lead to chemical conjunctivitis. By contrast, the failure of appropriate probe disinfection or the use of inappropriate gel can

potentially be a way of accumulation of pathogenic flora in conjunctival sac. Hence, the three following safety sections should be considered to minimize risks of harmful effects:

63.4.1 Respect of the "As Low As Reasonably Achievable" (ALARA) Principle Which Relies On

1.1 Control of energy, meaning a low acoustic output levels, including TI ≤ 1.0 and MI ≤ 0.23. Check TI and MI upon each mode change; and before increasing output level, prefer optimizing two-dimensional gain, focus, and time-gain compensation.
1.2 Control of exposure time to ultrasound: minimize data redundancy, scan only while looking, and delay measurements after procedure.
1.3 Control scanning technique, which includes gaze control, minimizing movement, elimination of distraction, good ergonomics, using sufficient amount of gel, prioritization of views, control of total duration of the procedure, deferring secondary views to the end of the procedure.

63.4.2 Chemical and Biological Safety

2.1 Use of sonographic gel safe for human use and cleared for eye contact (safety datasheet).
2.2 Appropriate disinfection of the transducer (with 70% isopropyl or ethyl alcohol solution) and air-drying before gel application.
2.3 Respect hygiene rules: general skin hygiene and operator's hand hygiene including gloves.

63.4.3 Mechanical Safety

3.1 Stable and comfortable position of the operator before starting the procedure.
3.2 Adequate time for scanning must be available to avoid rush.
3.3 Use a good transducer manipulation technique: stable position including hand anchoring, use of bony prominences of the patient's periorbital area, and use of both hands as necessary to reliably control probe position and prevent transducer pressure at all times especially in trauma patient where a possibility of globe rupture exists.

63.5 ONSD: Clinical Applications

In clinical practice, ONSD US is a rapid and easily accessible bedside test. Indeed, growing evidences have shown that this procedure has high reproducibility and low intra- and inter-observer variability [13]. In addition, the learning curve has been shown finite for operators having performed more than 20 procedures [16]. Then, ONSD measurements may be a good choice to assess elevated ICP in clinical settings. For instance, ONSD US may be useful when invasive monitoring is contraindicated or unavailable, or in "borderline" situations in which the insertion of invasive monitoring is questioned but noninvasive ICP measurement helpful, such as nontraumatic subarachnoid or intracranial hemorrhage [17, 18]. Other applications of ONSD US rely on patients at risk of intracranial hypertension for non-neurosurgical causes (such as liver transplantation and intraoperative settings at risk of intracranial hypertension) [19, 20]. ONSD US may be a worthwhile screening tool in emergency departments in patients where the need for invasive ICP monitoring is questionable [11, 21].

Broadly, in intensive care medicine, ONSD US may be relevant to address two aspects of ICP-related issues: detection of raised ICP and monitoring rapid changes of ICP.

63.5.1 Detection of Raised ICP

ONSD measurement to detect raised ICP has been investigated in different environments, mainly in intensive care units and emergency departments. However, the optimal cutoff value for an abnormal ONSD indicating elevated ICP remains unclear, and ranges from 5.2 to 5.9 mm. The sensitivity ranges from 74% to 95% and the specificity from 74% to 100% to identify ICP >20 mmHg [22]. These variations may be due to the small number of subjects included in most of the studies on ONSD measurement. Furthermore, although previous studies considered demographic and physiological factors affecting ONSD, the results have been inconsistent or inconclusive due to a relatively wide interindividual range of ONSD which may be a result of ethnic diversity, or genetic differences. Another explanation could be attributed to the fact that ONSD reaches a plateau at some point of dilation, and further distension may be too small to measure or be due to technical issues because ONSD measurements in early clinical study have not been performed using refined methodology according to strict image quality criteria.

One-time ONSD measurements should be considered with caution, and cutoff values reported in literature should be used as "alert levels" to prompt additional attention to ICP. The clinician must also remember that any patient may have had a large ONSD before the current illness [23].

63.6 ONSD Ultrasound: Monitoring of Osmotherapy Effect

ONSD measurement may also be an interesting tool to track rapid changes in ICP in patients at risk of raised ICP or to confirm the effect of therapeutics in decreasing ICP (such as osmotherapy or ventricular CSF shunt placement). However, studies focused on investigating ONSD changes to monitor ICP trends remain limited.

Several lines of evidence come from in vivo studies led by Tamburrelli, Hansen, and Helmke. Indeed, using an intrathecal infusion of saline, Tamburrelli et al. found a "direct, biphasic, positive relation between diastolic ICP and optic nerve diameters" measured by A-scan sonography. The authors showed rapid changes of optic nerve diameters in response to variation of ICP [24]. Later, works from Hansen and Helmke were based on recording ONSD using B-scan mode sonography versus ICP data in an intrathecal infusion test [8]. Ultrasonography was performed at 2- to 4-minute intervals. Their data support a linear relationship between ICP and ONSD over a particular cerebrospinal fluid pressure interval. A noteworthy point is that this interval differed between patients: optic nerve sheath dilation started at pressure thresholds between 15 and 30 mmHg and in some patients saturation of the response (constant ONSD) occurred between 30 and 40 mmHg. The slope of ONSD versus ICP curve varied considerably by patient, making it impossible to infer an absolute ICP value from an ONSD without prior knowledge of the patient's ratio. Additionally, no temporal delay of the ONS response was found within this ICP interval. The only study comparing real-time ONSD data to gold-standard measurements of rapidly changing ICP in humans was performed by Maissan et al. in 2015 [25]. In 18 TBI patients monitored with intraparenchymal ICP probes, ONSD measurements were performed during endotracheal tube suctioning, a period of transiently ICP raising. Consecutive ONSD US measurements were performed 30–60 seconds prior to suctioning, during suctioning, and 30–60 seconds after suctioning.

Even during this very rapid time course, a strong correlation between ICP and ONSD measurements was demonstrated (correlation coefficient at 0.80). There was no perceptible "lag" in ONSD change during ICP alterations. Moreover, for an ONSD cutoff $\geq$5.0 mm, the sensitivity and specificity were 74% and 98%, respectively, with an area under the curve of 0.99 (95% CI 0.97–1.00) to detect raised ICP. But, an absolute change of less than 8–10 mm Hg in ICP did not affect ONSD, which is consistent with data collected by Hansen and Helmke.

Regarding ONSD measurements to assess decreasing ICP, the evidence is scant and addresses two kinds of treatment. First, in idiopathic intracranial hypertension (IIH), therapeutic lumbar puncture (LP) effect has been assessed: there are few case reports of ONSD US measurements performed before and after LP in patients with IIH. In the first, in 1989, Galetta et al. used A-scan US to measure pre- and post-LP ONSD in a woman with papilledema secondary to IIH. They found a significant reduction in ONSD bilaterally "within minutes" of performing the LP [26]. A second case report was published in 2015 by Singleton et al. They recorded ONSD

measurements 30 minutes pre- and post-LP in a woman who presented to the ED with symptoms from elevated ICP. After reduction of pressure via LP, they recorded a significant reduction in ONSD bilaterally [27]. Similarly, a recent case reported by Hassen et al. showed the first continuous real-time ONSD dynamic change measurement over 5–10 minutes during an LP for removing CSF in a patient with IIH. The ONSD changed from 7.8 to 5.7 mm at the end of the procedure [28].

Regarding the assessment of osmotherapy effect, only one study has specifically addressed the change of ONSD during osmotherapy infusion for ICP reduction [7]. Using B-mode US, the rate of ONSD change was measured in 13 patients with TBI or subarachnoid hemorrhage with raised ICP episodes (>25 mmHg) and 20 minutes following a 20% mannitol infusion. A significant ICP reduction was observed in all cases, but the variation of ONSD was not correlated to ICP variation suggesting the ONSD reversibility may be impaired after episodes of prolonged raised ICP or high ICP. To explain this impairment, Hansen and Helmke investigated the distensibility and elasticity optic nerve sheath using postmortem optic nerve preparations. They found a linear correlation between pressure increases of 5–45 mmHg and ONSD. However, they demonstrated that when ICP increased higher than 45 mmHg, false-positive ONSD findings occur, most likely because of structural changes within the optic nerve sheath. Their model of hysteresis curve may explain why ONSD remains widened despite a dramatic drop of ICP following therapeutic action [9]. Similarly, in 2012, Rajajee et al. [29] found that acute ICP fluctuation could affect the accuracy of ONSD measurements and proposed that delayed reversal of optic nerve sheath distension might be impaired following flare-ups of intracranial hypertension. Recently, in another clinical situation, Sahay et al. showed that ONSD increased when pneumoperitoneum was insufflated during laparoscopic surgery, but did not revert to baseline value after 5 minutes following disinflation [30]. Despite some limitations and the non-ICU patient population, this study supports the hypothesis of a hysteresis curve for ONSD changes in response to ICP trends, relying on the distensibility characteristics of the optic nerve sheath. Consequently, further clinical investigations are needed in living patients to clarify the value of ONSD especially when monitoring downward ICP trends.

63.7 Conclusion

Using an appropriate and rigorous technique, ONSD US values accurately reflect the anatomic dimension of the sheath at a specific point behind the retina. ONSD measurements may be an interesting tool to track rapid changes in ICP in patients at risk of raised ICP or to confirm the effect of therapeutics in decreasing ICP (such as osmotherapy or ventricular CSF shunt placement). However, one must keep in mind some limitations associated to ONSD use, which should make careful interpretation of ONSD variations when assessing effect of ICP reduction therapy especially in downward trends and warrant further clinical investigations to validate its use in tracking real-time ICP changes.

References

1. Kumar A, Loane DJ. Neuroinflammation after traumatic brain injury: opportunities for therapeutic intervention. Brain Behav Immun. 2012;26:1191–201.
2. Carney N, et al. Guidelines for the management of severe traumatic brain injury, fourth edition. Neurosurgery. 2017;80:6–15.
3. Güiza F, et al. Visualizing the pressure and time burden of intracranial hypertension in adult and paediatric traumatic brain injury. Intensive Care Med. 2015;41:1067–76.
4. Bruce BB. Noninvasive assessment of cerebrospinal fluid pressure. J Neuro-Ophthalmol. 2014;34:288–94.
5. Hayreh SS. Structure of the optic nerve in ischemic optic neuropathies. Berlin, Heidelberg: Springer; 2011. p. 7–34.
6. Hansen HC, Helmke K. The subarachnoid space surrounding the optic nerves. An ultrasound study of the optic nerve sheath. Surg Radiol Anat SRA. 1996;18:323–8.
7. Launey Y, Nesseler N, Le Maguet P, Yannick M, Philippe S. Effect of osmotherapy on optic nerve sheath diameter in patients with increased intracranial pressure. J Neurotrauma. 2014;31:984–8.
8. Hansen HC, Helmke K. Validation of the optic nerve sheath response to changing cerebrospinal fluid pressure: ultrasound findings during intrathecal infusion tests. J Neurosurg. 1997;87:34–40.
9. Hansen HC, Lagrèze W, Krueger O, Helmke K. Dependence of the optic nerve sheath diameter on acutely applied subarachnoidal pressure – an experimental ultrasound study. Acta Ophthalmol. 2011;89:e528–32.
10. Blaivas M, Theodoro D, Sierzenski PR. A study of bedside ocular ultrasonography in the emergency department. Acad Emerg Med. 2002;9:791–9.
11. Blaivas M, Theodoro D, Sierzenski PR. Elevated intracranial pressure detected by bedside emergency ultrasonography of the optic nerve sheath. Acad Emerg Med. 2003;10:376–81.
12. Geeraerts T, et al. Ultrasonography of the optic nerve sheath may be useful for detecting raised intracranial pressure after severe brain injury. Intensive Care Med. 2007;33:1704–11.
13. Dubourg J, Javouhey E, Geeraerts T, Messerer M, Kassai B. Ultrasonography of optic nerve sheath diameter for detection of raised intracranial pressure: a systematic review and meta-analysis. Intensive Care Med. 2011;37:1059–68.
14. British Medical Ultrasound Society. Guidelines for the safe use of diagnostic ultrasound equipment. Ultrasound. 2010;18:52–9.
15. Shankar H, Pagel PS. Potential adverse ultrasound-related biological effects: a critical review. Anesthesiology. 2011;115:1109–24.
16. Zeiler FA, et al. A unique method for estimating the reliability learning curve of optic nerve sheath diameter ultrasound measurement. Crit Ultrasound J. 2016;8:9.
17. Moretti R, Pizzi B, Cassini F, Vivaldi N. Reliability of optic nerve ultrasound for the evaluation of patients with spontaneous intracranial hemorrhage. Neurocrit Care. 2009;11:406–10.
18. Geeraerts T, Merceron S, Benhamou D, Vigué B, Duranteau J. Non-invasive assessment of intracranial pressure using ocular sonography in neurocritical care patients. Intensive Care Med. 2008;34:2062–7.
19. Helmke K, Burdelski M, Hansen HC. Detection and monitoring of intracranial pressure dysregulation in liver failure by ultrasound. Transplantation. 2000;70:392–5.
20. Robba C, et al. Effects of prone position and positive end-expiratory pressure on noninvasive estimators of ICP: a pilot study. J Neurosurg Anesthesiol. 2017;29:243–50.
21. Komut E, et al. Bedside sonographic measurement of optic nerve sheath diameter as a predictor of intracranial pressure in ED. Am J Emerg Med. 2016;34:963–7.
22. Rosenberg JB, Shiloh AL, Savel RH, Eisen LA. Non-invasive methods of estimating intracranial pressure. Neurocrit Care. 2011;15:599–608.
23. Lyon M, et al. Effect of history of mild traumatic brain injury on optic nerve sheath diameter changes after Valsalva Maneuver. J Neurotrauma. 2018;35:695–702.

24. Tamburrelli C, Anile C, Mangiola A, Falsini B, Palma P. CSF dynamic parameters and changes of optic nerve diameters measured by standardized echography. Ophthal Echogr. 1993;13:101–9.
25. Maissan IM, et al. Ultrasonographic measured optic nerve sheath diameter as an accurate and quick monitor for changes in intracranial pressure. J Neurosurg. 2015;123:743–7.
26. Galetta S, Byrne SF, Smith JL. Echographic correlation of optic nerve sheath size and cerebrospinal fluid pressure. J Clin Neuroophthalmol. 1989;9:79–82.
27. Singleton J, Dagan A, Edlow JA, Hoffmann B. Real-time optic nerve sheath diameter reduction measured with bedside ultrasound after therapeutic lumbar puncture in a patient with idiopathic intracranial hypertension. Am J Emerg Med. 2015;33:860.e5–7.
28. Hassen GW, Al-Juboori M, Koppel B, Akfirat G, Kalantari H. Real time optic nerve sheath diameter measurement during lumbar puncture. Am J Emerg Med. 2018;36:736.e1–3.
29. Rajajee V, Fletcher JJ, Rochlen LR, Jacobs TL. Comparison of accuracy of optic nerve ultrasound for the detection of intracranial hypertension in the setting of acutely fluctuating vs stable intracranial pressure: post-hoc analysis of data from a prospective, blinded single center study. Crit Care Lond Engl. 2012;16:R79.
30. Sahay N, et al. Effect of pneumoperitoneum and patient positioning on intracranial pressures during laparoscopy: a prospective comparative study. J Minim Invasive Gynecol. 2018;25:147–52.

Chapter 64
Neuroanesthesia: Usefulness of Transcranial Doppler (TCD)

Marta García-Orellana and Nicolás de Riva Solla

Key Points

1. Transcranial Doppler (TCD) is very useful in the operating room for neurosurgical interventions, but it has two main limitations: (1) The absence of an acoustic window in 10–20% of patients and the difficulty in keeping the probe fixed and (2) obtaining a continuous signal.
2. The most frequent uses in the operating room are (1) monitoring of cerebral hemodynamic function during neuroendoscopy and (2) neurosurgery in the sitting position for detection of the permeable foramen ovale (bubbling technique), detection of vascular air embolism, and carotid artery surgery.
3. The use of the robotic probes may make TCD a routine monitor in the future.

64.1 Introduction

As a noninvasive neuromonitoring system, transcranial Doppler (TCD) allows indirect estimation ("surrogate marker") of cerebral blood flow (CBF). In addition to its applications in critical care already explained in previous chapters, TCD can have a certain role in the operating room, although in this area it has two main limitations:

1. The absence of an adequate acoustic bone window in 10–20% of patients [1]
2. Difficulty in continuous monitoring during surgery, as slight movements of the probe significantly alter the recorded signal (the TCCS technique does not yet allow for a continuous monitoring approach)

M. García-Orellana · N. de Riva Solla (✉)
Neuroanesthesia Division, Anesthesiology Department, CLINIC Hospital, Barcelona, Spain
e-mail: nderiva@clinic.cat

C. N. Rodríguez et al. (eds.), *Neurosonology in Critical Care*,
https://doi.org/10.1007/978-3-030-81419-9_64

Therefore, intraoperative monitoring with TCD is really restricted to very specific surgeries and clinical research.

64.2 TCD: Usefulness in the Operating Room

As in the intensive care unit (ICU), we use a low frequency probe (2–2.5 MHz), and the most frequently used is the trans-temporal acoustic window. The probe is positioned in front of the swallow and above the zygomatic arch, and, once positioned, we can use different systems ("helmets") of fixation [2] in order to monitor continuously during the whole surgery (Fig. 64.1). The recent appearance of robotic probes in the market makes it easier to find, optimize, and maintain the TCD signal [3].

From the trans-temporal acoustic window, we can examine the different arteries of the circle of Willis. The most frequently monitored is the middle cerebral artery (MCA), easily identifiable (M1 segment) by its characteristic horizontal trace in the direction of the transducer (positive spectral wave) and with a velocity of around 50 ± 10 cm/s.

64.3 Most Common Uses in the Operating Room

64.3.1 Monitoring of Cerebral Hemodynamic Function During Neuroendoscopy

Neuroendoscopy (Fig. 64.2) is a minimally invasive neurosurgery that uses an endoscope to directly visualize deep brain structures through the ventricular system, and thus the treatment of various neurosurgical pathologies.

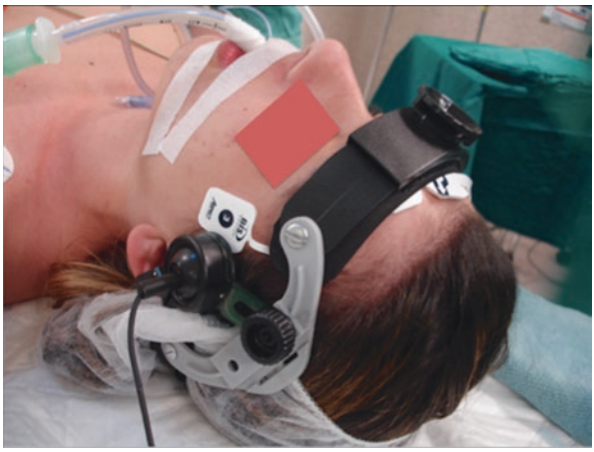

Fig. 64.1 Helmet for fixing the probe on the transtemporal acoustic window (bilateral insonation)

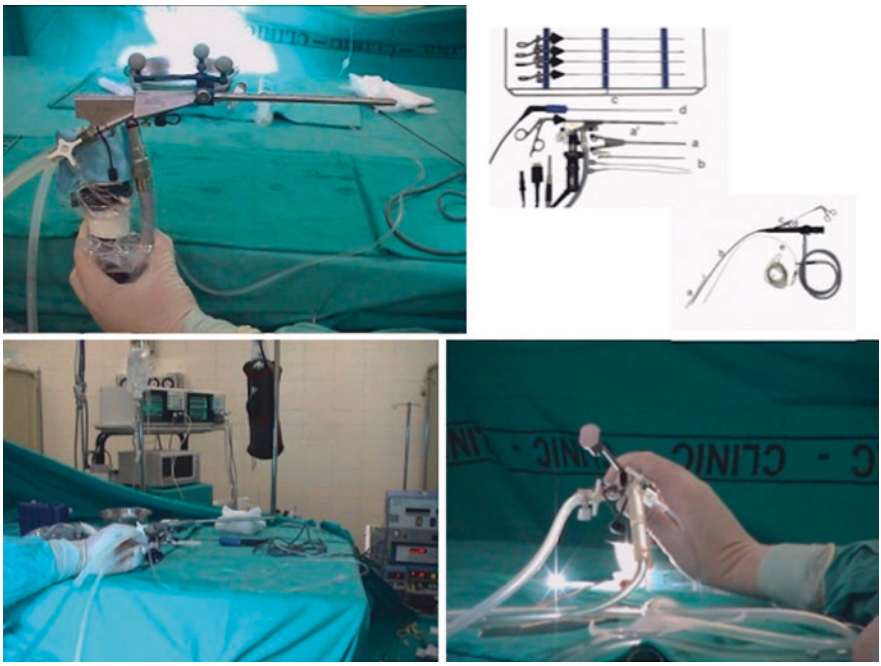

Fig. 64.2 Neuroendoscope

The classic indication for neuroendoscopy is the performance of a ventriculostomy on the floor of the third ventricle for the treatment of noncommunicating hydrocephalus [3]. This surgical approach also allows the performance of septostomies and/or foraminotomies, the fenestration or exeresis of colloid cysts, the biopsy or resection of intraventricular tumors, etc.

Each of these procedures has different complexity and duration, and consequently patients may present various perioperative complications related to the manipulation or injury of nearby brain structures, bleeding, nerve tract distension, or hypothalamic injury [4, 5].

To perform neuroendoscopic surgery, the patient is positioned in a supine position, slightly "in a hammock," with minimal neck flexion (10–20°), and fixing the head by means of a Mayfield type craniostat.

Then, the neuroendoscope is introduced through a trephine, which will be either rigid or flexible depending on the type of surgery. For greater safety, in some cases this device can be fixed to an articulated arm to avoid undesired movements.

Neuroendoscopy requires intermittent perfusion of fluid inside the ventricular system to facilitate visibility and keep it permeable. This infusion is usually of lactated Ringer's or sodium chloride 0.9% (heated to 37 °C) and is introduced under pressure through a lateral channel of the endoscope, whose connection is opened and closed at the discretion of the neurosurgeon.

The neuroendoscope also has a second channel for drainage-suction of the introduced fluid and a third channel (working) through which the different surgical instruments are introduced. The drainage of the irrigation fluid is very important to avoid an excessive increase of the intracranial pressure (ICP) due to the irrigation pressure and/or the accumulation of the perfusion solution.

Although neuroendoscopy is defined as a minimally invasive technique, it is a procedure that is associated with a high percentage of complications both intraoperatively (up to 50% depending on the series) [6–8] and post-operatively (6–12%) [9, 10], although with an estimated mortality rate of <1% [11].

64.3.2 Intraoperative Complications of Neuroendoscopy

64.3.2.1 Hemodynamics (up to 50%)

They are produced by surgical manipulation of brain structures or by sudden changes in ICP associated with intraventricular irrigation [6, 7]. They can manifest themselves both in the form of tachycardia and bradycardia-asystole, and in both cases may be associated (or not) with hemodynamic instability in the form of hypertension or hypotension.

64.3.2.2 Intracerebral Bleeding Related to Manipulation of the Endoscope

It is usually venous and easily controlled with irrigation solution and/or cauterization. In contrast, arterial bleeding due to injury of the basilar column or one of its branches is the most serious intraoperative complication of the technique and has a high mortality rate [4].

64.3.2.3 Intracranial Hypertension and Decreased Cerebral Perfusion Pressure (CPP)

Although it was initially assumed that the outlet of the irrigation fluid from the neuroendoscope prevented rapid increases in ICP, it has been shown that in up to 40% of cases these episodes of intracranial hypertension do occur [3, 4]. This significant increase in ICP can cause hemodynamic imbalance (changes in CPP) and even lead to cerebral circulatory arrest, although these alterations rapidly subside when the irrigation fluid is released.

Cerebral circulatory imbalance leads to perioperative cardiovascular complications and retinal bleeding, delayed awakening, transitory neurological focus, hydrocephalus, cognitive impairment, ionic disorders, rhythm disorders, vomiting, etc. [12].

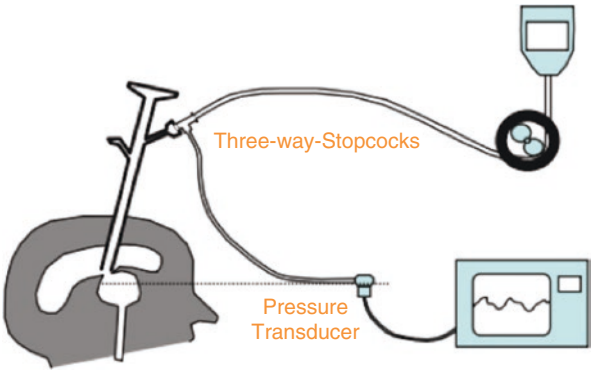

Fig. 64.3 Assembly for PIN monitoring [12]

Therefore, in addition to the intraoperative monitoring that we would have for a craniotomy, it is advisable to use as direct a monitoring of the cerebral blood flow and its behavior in real time as possible [4, 5].

The ICP can be measured indirectly and simply by continuously monitoring the value of "pressure inside the neuroendoscope" (PIN) [12]. This is done by connecting a pressure transducer at one end to a three-step tap located in the irrigation channel of the endoscope (via an extension tube filled with saline) and at the other end to the anesthesia monitor. The "zero" of this pressure is made at the level of the external auditory canal (Fig. 64.3).

In this context, the TCD allows us to detect severe drops in the cerebral perfusion pressure (through dynamic changes in blood flow velocities rates and Doppler spectral waveform) that do not have systemic repercussions. Moreover, it has been shown that there is a clear association between PIN values and changes in TCD blood flow velocities, so to avoid complications, it is recommended to keep PIN <30 mmHg and CPP >40 mmHg [4].

64.3.3 Neurosurgery in a Sitting Position

In neurosurgery, the seating position is used for occipital, posterior fossa, and posterior cervical approaches. In addition to improving surgical access to these anatomical structures, this position decreases venous bleeding, increases gravity drainage of the cerebrospinal fluid (CSF), and decreases ICP.

64.3.3.1 Permeable Foramen Ovale (PFO) Screening

Approximately 25% of healthy adults (with equal distribution between men and women) have a patent foramen ovale (PFO), but most are asymptomatic [4]. However, when the pressure in the right atrium increases and is higher than in the

left atrium (e.g., during a punctual Valsalva maneuver) a right-left shunt is produced through this foramen.

This direct passage of venous blood into the arterial circulation can cause a paradoxical embolism through the foramen, which could trigger a cerebral, coronary, or other systemic embolism with serious consequences. This fact becomes vitally important in surgeries with the patient in sedation, in which the difference in hydrostatic pressures may facilitate the entry of air through the venous sinuses of the dura mater when these are open.

Therefore, it is essential to rule out the existence of a PFO for surgeries performed on site. The gold standard is to perform a study with transesophageal echocardiography (TEE), but given the limited access to this possibility, a first screening can be done using the simple double bubbling technique [13, 14] and the performance of TCD before placing the patient in sedation. The test is performed using bolus-stirring saline through a central venous line while monitoring the flow in the MCA through the trans-temporal acoustic window (Fig. 64.4).

The test is first performed on normal controlled ventilation and then a moderate Valsalva maneuver (peak 25–30 cmH_2O) is performed. If PFO is present, microbubbles from the saline will be detected in the MCA "real-time" insonation. It is

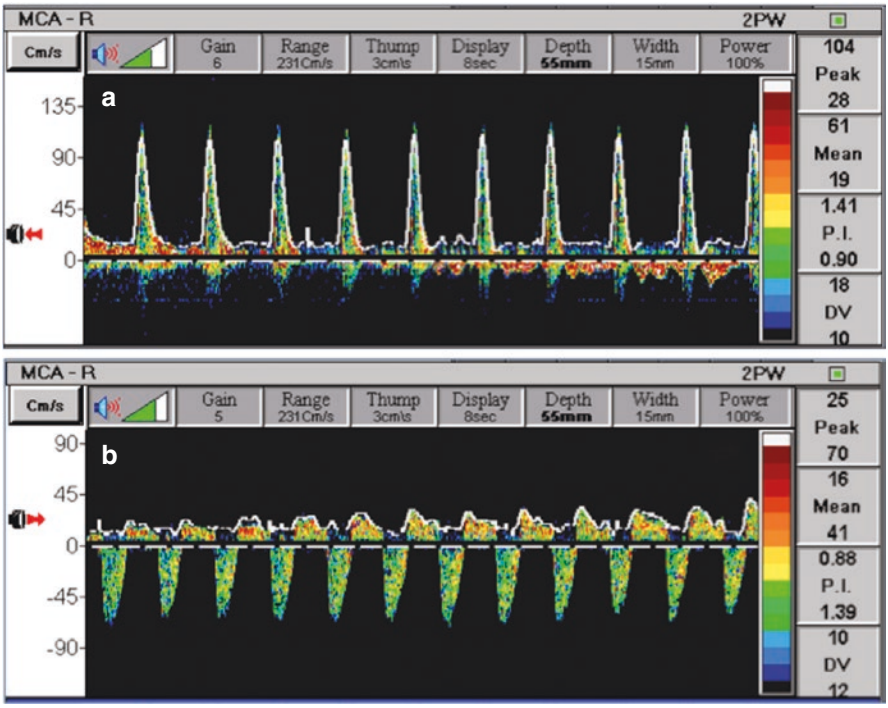

Fig. 64.4 Example of two intraoperative TCD records during neuroendoscopic procedures. (**a** panel) Systolic spicules; (**b** panel) Reverberant flow

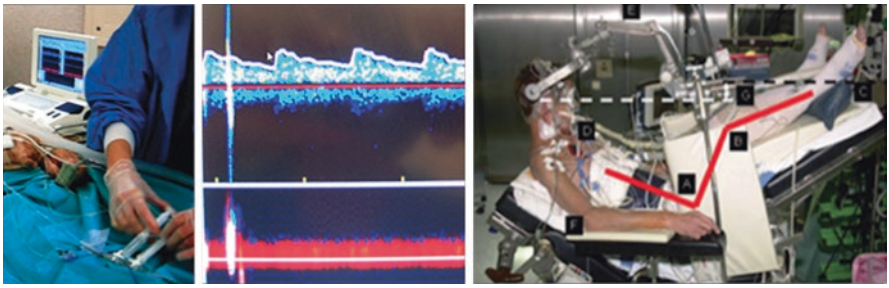

Fig. 64.5 Bubbling technique, high-intensity microsignals (HITS) in MCA and "modified Jadick" seating position

considered positive when high-intensity microsignals (HITS) are recorded in the MCA [15].

If a PFO is detected, it is advisable to inform the neurosurgical team and decide jointly on the patient's position during surgery, assessing the pros and cons on an individual basis [16]. Other possibilities for placement are the prone position or the "modified" seating by Jadick et al. (Fig. 64.5).

64.3.3.2 Detection of Air Embolism

Air embolism can occur in any surgery where the head is in a higher position than the chest, and air can be drawn into the venous bloodstream during ventilation. It has been described in neurosurgery but also in neck, shoulder, axilla, breast, and thyroid surgery [13].

The actual incidence of air embolism is difficult to determine, as its incidence varies greatly depending on the method of detection. In addition, many embolisms are subclinical and not reported.

Although the intraoperative use of precordial Doppler is indicated in sedation neurosurgery to detect possible venous air embolism, TCD could be another option in those cases where it can be applied [17]. An early diagnosis allows the neurosurgeon to be alerted so that he or she can apply the necessary measures to reduce the entry of air and, at the same time, inform the neuro-anesthesiologist so that he or she can aspirate the intravascular air through the central venous catheter inserted at the beginning of the surgery in anticipation of this intraoperative complication.

64.4 Conclusion

Today the TCD (maybe the transcranial color-coded duplex sonography (TCCS)) is the monitor that best estimates, indirectly, the CBF and its dynamic changes. Classically (through the cerebral blood flow velocity changes), it has been used in

experimental studies because of the limitation that exists when it comes to obtaining an uninterrupted signal [18]. Despite this, we have seen that it has real utility in intraoperative monitoring in neurosurgery, and in the future the potential of robotic probes could make it a monitor for routine use [3].

References

1. Naqvi J, Yap KH, Ahmad G, Ghosh J. Transcranial Doppler ultrasound: a review of the physical principles and major applications in critical care. Int J Vasc Med. 2013;2013:629378.
2. Lam AM. Intraoperative transcranial Doppler monitoring. Anesthesiology. 1995;82(6):1536–7.
3. Zeiler FA, Smielewski P. Application of robotic transcranial Doppler for extended duration recording in moderate/severe traumatic brain injury: first experiences. Crit Ultrasound J. 2018;10(1):16.
4. Salvador L, Hurtado P, Valero R, et al. Importancia de la monitorización de la "presión intracraneal dentro del neuroendoscopio" durante el tratamiento anestésico de la cirugía neuroendoscópica. Experiencia en 101 casos. Rev Esp Anestesiol Reanim. 2009;56:75–82.
5. Salvador L, Valero R, Carazo J, et al. Pressure inside the neuroendoscope: correlation with epidural intracranial pressure during neuroendoscopic procedures. J Neurosurg Anesthesiol. 2010;22(3):240–6.
6. Fàbregas N. Episodic high irrigation pressure during surgical neuroendoscopy may cause intermittent intracranial circulatory insufficiency. J Neurosurg Anesthesiol. 2001;13(2):152.
7. El-Dawlatly AA, et al. The incidence of bradycardia during endoscopic third ventriculostomy. Anesth Analg. 2000;91(5):1142.
8. Khan MB. Endoscopic third ventriculostomy for obstructive hydrocephalus: outcome analysis of 120 consecutively treated patients from a developing country. Int J Surg. 2016;26:69.
9. Feng H. Endoscopic third ventriculostomy in the management of obstructive hydrocephalus: an outcome analysis. J Neurosurg. 2004;100(4):626.
10. Hopf NJ. Endoscopic third ventriculostomy: outcome analysis of 100 consecutive procedures. Neurosurgery. 1999;44(4):795.
11. Amini A. Endoscopic third ventriculostomy in a series of 36 adult patients. Neurosurg Focus. 2005;19(6):E9.
12. Fàbregas N. Anesthetic management of surgical neuroendoscopies: usefulness of monitoring the pressure inside the neuroendoscope. J Neurosurg Anesthesiol. 2000;12(1):21.
13. Mirski MA, Lele AV, Fitzsimmons L, Toung TJK. Diagnosis and treatment of vascular air embolism. Anesthesiology. 2007;106(1):164–77.
14. Tornero Tornero C, Aliaga Font L. Anestesia: Fundamentos y Manejo Clínico. Editorial Médica Panamericana; 2015.
15. Schatlo B, Pluta RM. Clinical applications of transcranial Doppler sonography. Rev Recent Clin Trials. 2007;2(1):49–57.
16. Gracia I, Fabregas N. Craniotomy in sitting position: Anesthesiology management. Curr Opin Anaesthesiol. 2014;27(5):474–83.
17. Ishida K, Yamashita A, Matsumoto M. Role of transcranial Doppler ultrasonography in neuroanesthesia. In: Neuroanesthesia and cerebrospinal protection. Tokyo: Springer Japan; 2015. p. 193–213.
18. Marda MK, Prabhakar H. Transcranial Doppler. J Neuroanaesth Crit Care. 2015;2(3):215–20.

Chapter 65
Traumatic Brain Injury in Neuro-ICU: Usefulness and Experience of Robotic Transcranial Doppler (TCD)

Frederick A. Zeiler

Key Points

1. Current robotic TCD (rTCD) technology improves the ability to obtain extended duration uninterrupted recordings of cerebral blood flow velocity (CBFV).
2. Automated signal acquisition algorithms appear to reduce setup time for TCD in TBI.
3. Various functions exist to automatically alter probe position and insonation angle.
4. Tracking algorithms exist to automatically correct for probe shift and improve CBFV, further reducing the need for user input.
5. With further advances, high-quality uninterrupted signals obtained from rTCD could be utilized for continuous assessments of various other aspects of cerebral physiology.

65.1 Introduction

It is well known that dysfunction to CBF and cerebral autoregulation (CA) occurs after TBI and is associated with mortality in moderate/severe TBI and long-term functional outcome across the spectrum of TBI [1–5]. The application of transcranial doppler (TCD) in the neurocritical care unit (NCCU) can provide invaluable information regarding cerebral blood flow velocity (CBFV), a surrogate measure of cerebral blood flow (CBF). Thus, having a real-time assessment of CBFV in the NCCU can prove useful for the early detection of deficits in flow. Various vascular territories can be assessed via TCD, with bilateral assessment of the middle cerebral arteries (MCA) being the most common [6, 7]. Other territories include

F. A. Zeiler (✉)
Section of Neurosurgery, Department of Surgery, Department of Human Anatomy and Cell Science, Rady Faculty of Health Sciences, University of Manitoba, Winnipeg, MB, Canada
e-mail: frederick.zeiler@umanitoba.ca

C. N. Rodríguez et al. (eds.), *Neurosonology in Critical Care*,
https://doi.org/10.1007/978-3-030-81419-9_65

supraclinoid internal cerebral artery, ophthalmic artery, posterior cerebral artery, and basilar artery [6, 7].

However, standard TCD comes with limitations. The technique has classically involved intensive user input through probe application, obtaining the correct insonation position/angle, and correction for probe shift during the recording. This is even the case with commercially available probe holding systems. To further complicate matters, the NCCU care for those with moderate/severe TBI is complex, with numerous other invasive intracranial/extracranial devices and constant bedside care [8, 9]. As such, classically it has proven difficult to obtain long-duration uninterrupted TCD recording of the MCA in these critically ill TBI patients, with many studies reporting recording lengths of less than 1 hour [10, 11], not including interruptions due to probe shift.

Recent technological advancements have led to the development of robotic technology that has been integrated with TCD systems. Such systems allow for extended duration TCD recordings in TBI, with minimal signal interruption and user input. These advancements, though only preliminarily assessed to date in critically ill moderate/severe TBI patient populations [12, 13], open the doors to increased application of TCD monitoring in the NCCU TBI population. This short chapter reviews some of the aspects of this emerging technology.

65.2 Robotic TCD: Equipment and Technique

65.2.1 Equipment

Currently, there are few systems available on the market, with the most readily advertised systems including Delica EMS Robotic TCD Systems (Shenzen Delica Medical Equipment Co. Ltd., China; http://www.delicasz.com) and the Atys Robotic TCD-X Systems (Atys Medical, France; http://www.atysmedical.com). To date, only the Delica EMS 9D system has been evaluated in critically ill TBI patients [12, 13]. As such, the technique section will focus primarily on the Delica system, though the Atys system and other systems in development in theory should perform similarly.

65.2.1.1 Delica Systems

The Delica EMS 9D system is a rTCD system designed for simultaneous bilateral insonation of the MCA. Initially designed for less acute patients and the outpatient clinical setting, this device has been adapted and recently employed within the NCCU for monitoring critically ill TBI patients [12, 13]. The device consists of a headframe composed of both rigid plastic and Velcro, padded with Neoprene, allowing for ease of adjustment and comfort for the patient. Furthermore, a ratcheting system exists to reduce the need for headband and head manipulation during final adjustments. Figure 65.1a displays the headband with frontal ratchet system. A

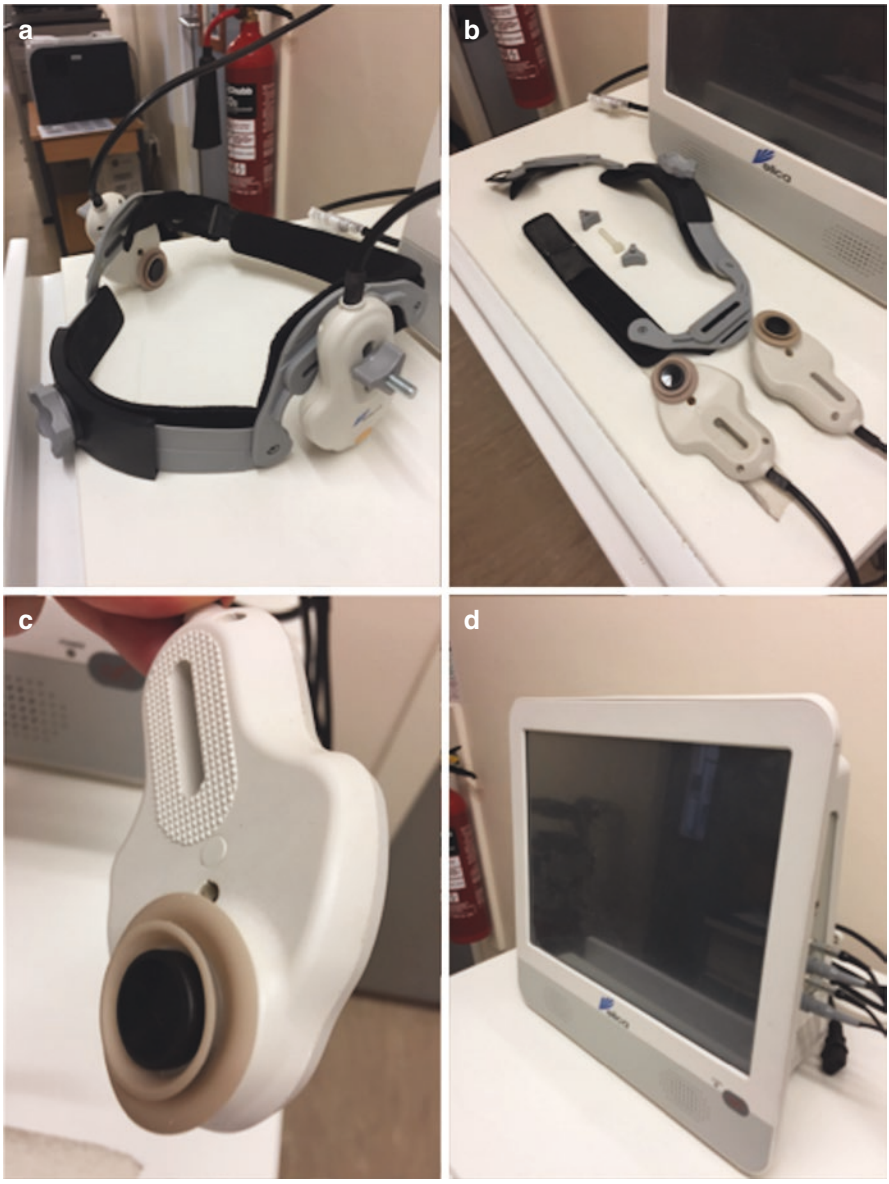

Fig. 65.1 Delica EMS 9D rTCD System. rTCD robotic transcranial Doppler. Panel (**a**) – Adjustable headband with ratchet system. Bilateral TCD probe/robotic construct attached. Panel (**b**) – Demonstrates ability to completely dismantle headband system, enabling reassembly around a patient's head. Panel (**c**) – TCD probe and robotic drive construct. Black 1–2 MHz TCD probe is surrounded by optional rubber ring, designed to retain ultrasound gel and reduced gel drying. Panel (**d**) – Delica EMS 9D rTCD monitor

particularly important aspect of this headband system is that it can be completely disassembled and reassembled around the patient's head, allowing for placement in those critically ill TBI patients in which excessive movement is not desired. Figure 65.1b displays the headband system dismantled.

The standard TCD system employs 1–2 MHz probes attached to robotic drives, with the entire construct encased in a plastic shell. These constructs are mounted to the headband via adjustable wing-nuts over the temporal windows. Figure 65.1c displays the TCD probe/robotic drive construct. The robotic drives allow millimeter-based adjustments in the TCD probe position and insonation angle, via a hands-free touch-screen interaction with the TCD device monitor (Fig. 65.1d). Two cables exit from the probe constructs leading to the TCD monitor. They are of sufficient length to allow placement of the entire device behind the bed and ventilator in the NCCU. All aspects of the system are easily cleaned via disinfectant wipes.

65.2.1.2 Atys Systems

Though this system has not been employed to monitory critically ill TBI patients, some aspects of this system deserve mentioning. The device is designed for the simultaneous bilateral insonation of the MCAs. The setup of the headband and probe constructs are similar to that described above, with the exception that the Atys system utilizes "glasses" with headband construct, instead of the pure headband system employed with the Delica. However, one good additional aspect is the TCD-Holter part of the Atys TCD-X system. This aspect allows for continuous recording of bilateral MCA CBFV on a Holter-like box attached to the TCD headframe, further increasing portability of the unit and eliminating the need for attachment to an external monitor.

65.2.2 Technique

Initially the headband has the robotic TCD probe constructs attached to each side. The Velcro headband is undone and slipped around the patient's head with minimal need to move or manipulate the head/neck position. Caution needs to be taken in those patients with unknown or existing cervical spine pathology. The straps are then tightened, with final adjustment via the frontal ratchet system. The TCD monitoring program on the device is then turned on with both probes activated. Ultrasound gel is applied to the probe faces, and the probes are than manipulated grossly by hand until there is initial capture of the MCA CBFV waveform. The wing-nut adjusters are then tightened, securing the robotic probe construct in place.

Using the touch-screen interface on the TCD monitor, the insonation depth, gain, and amplitude can be set (Fig. 65.2a). The screen displays mean flow velocity (MFV), peak systolic velocity (PSV), pulsatility index (PI), and heart rate for each side insonated. A look-ahead view of the probe can be seen on the left-hand side of the screen for each probe, providing CBFV waveforms at 40, 50, 60, 70, and 80 mm depth (Fig. 65.2b).

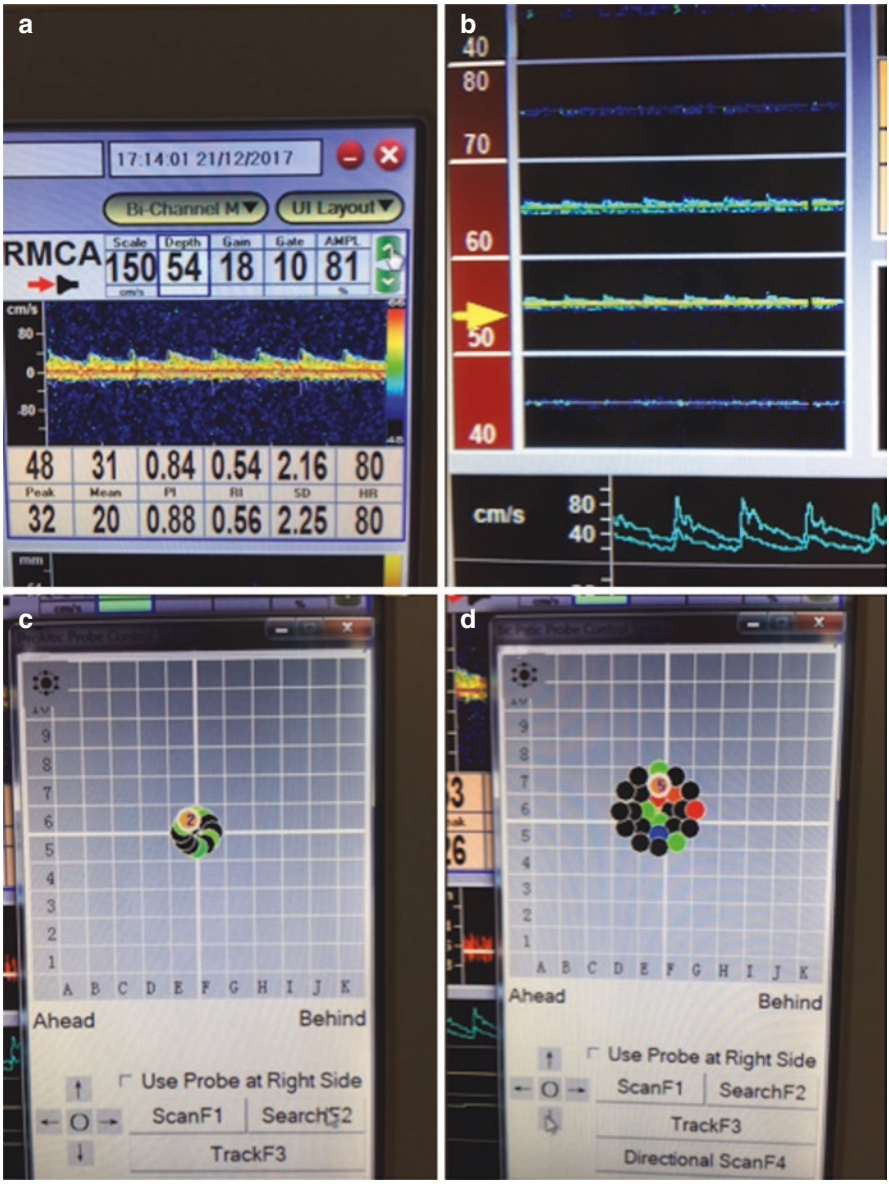

Fig. 65.2 Example of Delica EMS 9D rTCD Monitor display during insonation and robotic adjustment. rTCD robotic transcranial Doppler. Panel (**a**) – cerebral blood flow velocity (CBFV) waveform for right middle cerebral artery, with peak, mean, pulsatility index, depth, gain and amplitude displayed on adjustable touch screen. Panel (**b**) – "look-ahead" view of CBFV. Panel (**c**) – Search robotic adjustment algorithm, insonating in spinal pattern about current probe center. Color coding indicates insonation CBFV intensity with black indicating no flow detected and yellow/red indicating moderate/good signal intensity. Panel (**d**) – Directional scan robotic adjustment algorithm. Insonates about current probe axis, changing insonation angle to optimize signal intensity. Again, red indicates good CBFV signal intensity. (Figure reproduced in color with author permission from Zeiler and Smielewski [12])

To improve/optimize signal quality, the robotic control function is accessed. This allows access to the proprietary automatic robotic control system. All functions are designed to optimize the detected CBFV envelope. Within the Delica system, three main function exist. First, "Scan" produces a square grid about the current position, insonating at each spot, returning a color-coded signal strength indicated with red indicated strong signal and black indicated no signal. The algorithm then chooses the optimal position based on signal quality. Second, the "Search" function runs a spiral insonation pattern about the current position, producing a similar color pattern for signal quality (Fig. 65.2c), automatically choosing the optimal position. Finally, the "Directional Scan" function alters the probe face insonation angle to improve signal intensity (Fig. 65.2d), with color coding of each insonation position. In practice, the author has found it useful to manually find the initial position of the MCA, as described, followed by running the Scan, Search, and Directional Search functions in this sequence for optimal probe position. Occasionally, one is fortunate enough to manually manipulate the probe into a good position prior to robotic adjustments. In this case, the author finds it useful to only employ the Search and Directional Scan functions to optimize the signal intensity.

The final step prior to long-term bilateral insonation involves activating the automated tracking algorithm, which will correct for minor shifting in probe position. The algorithm involved is proprietary. After one obtains optimal position of the probe with satisfactory CBFV waveform, the "Track" function in the robotic control system window can be activated for each probe. In the author's experience, this function has enabled smooth continuous CBFV recording during bedside care, turning, portable chest X-rays, and chest tube placement. Figure 65.3 displays an

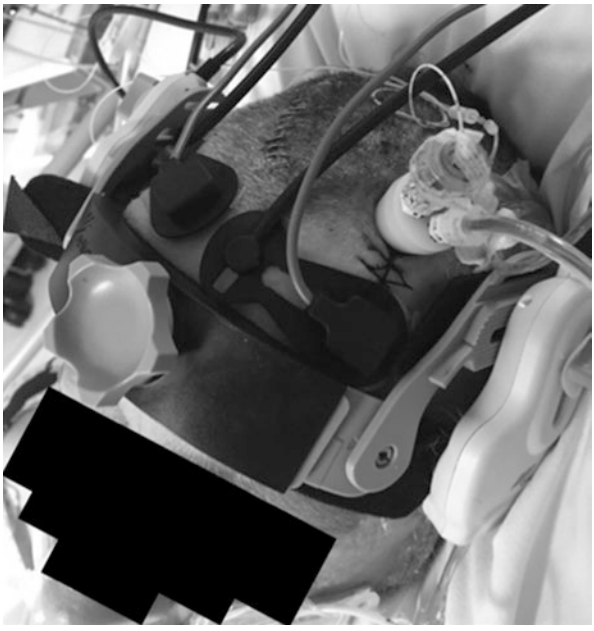

Fig. 65.3 Example of rTCD set-up with multi-modal monitoring. rTCD robotic transcranial Doppler. Figure demonstrates bilateral middle cerebral artery insonation via Delica EMS 9D rTCD system in the presence of left front triple bolt (intra-cranial pressure, microdialysis, and brain tissue oxygen monitoring) and bifrontal near infrared spectroscopy. (Figure reproduced with author permission from Zeiler and Smielewski [12])

example of patient setup for rTCD in the presence of numerous other invasive and noninvasive cranial multimodal monitoring devices (reproduced from Zeiler and Smielewski [12], with permission by authors).

65.3 rTCD: Applications

Though the current experience with rTCD systems in critically ill TBI populations is limited, there are some clear initial applications and some potential future applications.

65.3.1 Immediate Applications

65.3.1.1 Continuous CBFV and PI Monitoring

Current experience suggests the ability to obtain at least 4 hours of continuous uninterrupted signal recording, with the ability to push beyond this. Thus, with these rTCD systems, we now have the ability to continuously monitor bilateral CBFV and PI in TBI [7, 14–16] with reduced user input. Therefore, continuous monitoring of CBFV and PI symmetry, and assessment for posttraumatic cerebral vasospasm [17, 18], is possible, doing away with the previous intermittent/interrupted recordings from standard TCD devices. Figure 65.4a displays the continuous uninterrupted CBFV recordings obtained over a 4-hour period.

65.3.1.2 Continuous Invasive/Noninvasive Cerebrovascular Reactivity

The Delica EMS 9D system is currently integrated with the third-party ICM+ software (Cambridge Enterprise Ltd., Cambridge, UK, http://icmplus.neurosurg.cam.ac.uk), allowing for recording/archiving of digital CBFV signals from the TCD device and other NCCU monitors (cranial and systemic). With this software, all signals can be linked in time-series and processed in real time, or offline, for the assessment of other aspects of cerebral physiology [19]. Thus, aside from standard CBFV monitoring, one can now more continuously assess cerebrovascular reactivity via TCD in TBI patients. Such cerebrovascular reactivity indices have been evaluated in TBI in the past, with strong associations demonstrated between global patient outcome[10, 11, 20] and other more invasive autoregulation measurement techniques [11, 13, 20–22].

The premise behind these indices is that the moving correlation between vasogenic slow-wave fluctuations in CBFV and a driving pressure (such as mean arterial pressure (MAP) or cerebral perfusion pressure (CPP)) is representative of cerebrovascular reactivity [10, 20, 23]. TCD-based cerebrovascular reactivity indices that

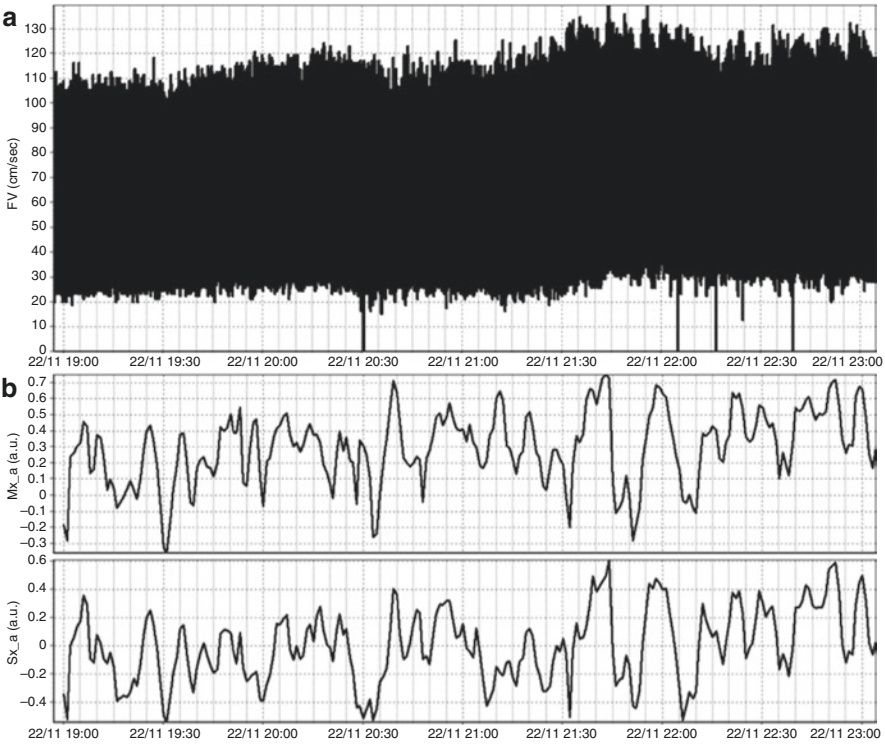

Fig. 65.4 Example of 4 hours of continuous rTCD recording and derived physiologic indices. a.u. arbitrary units, cm/s centimeters per second, FV flow velocity, Mx_a mean flow index (correlation between slow waves of mean flow velocity (MFV) and mean arterial pressure (MAP)), Sx_a systolic flow index (correlation between flow waves in Peak systolic flow velocity (PSV) and MAP). Panel (**a**) – example of 4 hours of continuous uninterrupted rTCD recording from Delica EMS 9D. Panel (**b**) – top and bottom plots show 4 hours of continuous cerebrovascular reactivity monitoring using non-invasive rTCD measures. (All signals captured from rTCD and arterial blood pressure line, with post acquisition processing via ICM+ software (Cambridge Enterprise Ltd., Cambridge, UK, http://icmplus.neurosurg.cam.ac.uk))

have been applied in TBI include mean flow index (Mx—moving correlation between mean CBFV and CPP) and systolic flow index (Sx—moving correlation between systolic CBFV and CPP). To date, critical thresholds associated with global patient outcome in TBI have been defined for both Mx and Sx [10, 11]. The advent of rTCD allows for continuous measurement in the NCCU.

Further to this, if one were to use MAP instead of CPP in the derivation of Mx or Sx, we then produce Mx_a (correlation between mean CBFV and MAP) and Sx_a (correlation between systolic CBFV and MAP). MAP can be derived from either invasive arterial lines or noninvasive continuous arterial blood pressure (ABP) monitoring. The Delica EMS rTCD systems offer an optional noninvasive continuous finger-cuff module (Finapres Nanocore, Finapres Medical Systems, Netherlands, http://www.finapres.com) for continuous ABP assessment during the TCD

recordings. With such noninvasive ABP systems and rTCD CBFV recordings, we can obtain continuous noninvasive cerebrovascular reactivity monitoring. This allows for subacute and outpatient assessments of cerebrovascular reactivity in TBI patients. To date, both Mx_a and Sx_a have been demonstrated to be closely related to the invasive "gold standard" continuous autoregulation pressure reactivity index (PRx—correlation between intracranial pressure (ICP) and MAP) [11, 13, 20–22, 24]. Figure 65.4b displays the continuous Mx_a and Sx_a derived over a 4-hour period of recording using rTCD.

65.4 rTCD: Potential Future Applications

Various other potential applications in TBI exist for uninterrupted CBFV signal obtained through rTCD devices. Such applications include noninvasive ICP and CPP assessments [25–30]. Various attempts/methods have been applied for the derivation of these measures, with moderate correlations obtained to invasively derived ICP and CPP measurements. The details of these methods are beyond the scope of this chapter, and, if interested, the reader should refer to the cited references [25–30]. However, with the long-duration CBFV signals from rTCD, the feasibility of noninvasive TCD-based ICP and CPP measurements is increased, potentially allowing us to get one step closer to more noninvasive monitoring in TBI care without the loss of physiologic information obtained through more invasive means.

65.5 rTCD: Advantages and Disadvantages

65.5.1 Main Advantages

Various advantages of rTCD systems exist over existing TCD systems for monitoring TBI patients in the NCCU. First, with rTCD one is able to obtain extended duration, uninterrupted CBFV recordings in critically ill TBI patients. While the current experience is limited in this population, the initial results are promising with recordings of 4 hours or longer obtained. This now allows for continuous assessment of CBFV, PI, and other aspects of cerebrovascular physiology via noninvasive TCD. Second, the setup time, in the author's experience, for bilateral MCA insonation is reduced with the robotic Scan, Search, and Directional Scan algorithms once some comfort is gained with the software and robotic control system. Third, the automated Track algorithm allows for hands-free correction for probe shift during insonation. This is a major step forward in TCD technology, reducing the need for constant user input and presence during recording. This is not only a time saver but reduces the need to have patient contact during TCD recording in a complex care environment. Finally, the system is easily cleaned, having Neoprene and plastic external components.

65.5.2 Main Disadvantages

Despite the initial results proving promising, there are some important disadvantages for existing systems. First, the current algorithms for optimization of CBFV signal intensity are good, but not perfect. Thus, during the setup phase, the user needs to pay attention to the algorithm selection of the optimal insonation position, as occasionally it selects a suboptimal position. This is easily corrected by selecting the proper position on the touch-screen interface. With newer renditions of the software, this algorithmic limitation has improved and will likely continue to improve further. Second, the Track autocorrection function works well for small shifts in probe position. It cannot correct for large gross shifts in the headframe. Thus, the user still needs to periodically check on the system during recording to ensure that bedside care or patient movement hasn't dislodged the headband and probes. Third, despite being able to disassemble the headframe with the Delica systems, there still is some degree of head manipulation to successfully place the headframe in the critically ill TBI patients. Thus, this may preclude its use in those with unstable cervical spines. Finally, in the author's personal experience, excessive soft-tissue injury on the scalp can trigger pain with the headband application if not properly sedated. This has led to an anecdotal increase in ICP in one patient recorded. Further application of these devices will show whether this is a recurring issue.

65.6 Conclusion

With the advent of rTCD technology, it is now possible to obtain extended duration, relatively uninterrupted, CBFV recordings in critically ill TBI patients with reduced operator input. This allows for continuous noninvasive recording of various aspects of cerebral physiology in the NCCU. The current experience with the technology in critically ill TBI is limited. As technology continues to advance, it is expected that this semiautomated technology will improve and become more readily accessible in NCCU's worldwide.

References

1. Czosnyka M, Smielewski P, Kirkpatrick P, Laing RJ, Menon D, Pickard JD. Continuous assessment of the cerebral vasomotor reactivity in head injury. Neurosurgery. 1997;41:11–7; discussion 17–19.
2. Sorrentino E, Diedler J, Kasprowicz M, Budohoski KP, Haubrich C, Smielewski P, et al. Critical thresholds for cerebrovascular reactivity after traumatic brain injury. Neurocrit Care. 2012;16:258–66.
3. Zeiler FA, Donnelly J, Calviello L, Smielewski P, Menon DK, Czosnyka M. Pressure autoregulation measurement techniques in adult traumatic brain injury, part II: a scoping review of continuous methods. J Neurotrauma. 2017;34:3224–37.

4. Mutch WAC, Ellis MJ, Ryner LN, McDonald PJ, Morissette MP, Pries P, et al. Patient-specific alterations in CO2 cerebrovascular responsiveness in acute and sub-acute sports-related concussion. Front Neurol. 2018;9:23.
5. Ellis MJ, Ryner LN, Sobczyk O, Fierstra J, Mikulis DJ, Fisher JA, et al. Neuroimaging assessment of cerebrovascular reactivity in concussion: current concepts, methodological considerations, and review of the literature. Front Neurol. 2016;7:61.
6. D'Andrea A, Conte M, Cavallaro M, Scarafile R, Riegler L, Cocchia R, et al. Transcranial Doppler ultrasonography: from methodology to major clinical applications. World J Cardiol. 2016;8:383–400.
7. Kalanuria A, Nyquist PA, Armonda RA, Razumovsky A. Use of transcranial Doppler (TCD) ultrasound in the neurocritical care unit. Neurosurg Clin N Am. 2013;24:441–56.
8. Georgiadis AL, Palesch YY, Zygun D, Hemphill JC, Robertson CS, Leroux PD, et al. Multimodality neuro-monitoring: conventional clinical trial design. Neurocrit Care. 2015;22:369–77.
9. Le Roux P, Menon DK, Citerio G, Vespa P, Bader MK, Brophy G, et al. The international multidisciplinary consensus conference on multimodality monitoring in neurocritical care: evidentiary tables: a statement for healthcare professionals from the Neurocritical Care Society and the European Society of Intensive Care Medicine. Neurocrit Care. 2014;21(Suppl 2):S297–361.
10. Sorrentino E, Budohoski KP, Kasprowicz M, Smielewski P, Matta B, Pickard JD, et al. Critical thresholds for transcranial Doppler indices of cerebral autoregulation in traumatic brain injury. Neurocrit Care. 2011;14:188–93.
11. Zeiler FA, Cardim D, Donnelly J, Menon DK, Czosnyka M, Smielewski P. Transcranial Doppler systolic flow index and ICP-derived cerebrovascular reactivity indices in traumatic brain injury. J Neurotrauma. 2018;35:314–22.
12. Zeiler FA, Smielewski P. Application of robotic transcranial Doppler for extended duration recording in moderate/severe traumatic brain injury: first experiences. Crit Ultrasound J. 2018;10(1):16.
13. Zeiler FA, Smielewski P, Stevens A, Czosnyka M, Menon DK, Ercole A. Non-invasive pressure reactivity index using Doppler systolic flow parameters: a pilot analysis. J Neurotrauma. 2018;36(5):713–20.
14. Bianciardi M, Toschi N, Polimeni JR, Evans KC, Bhat H, Keil B, et al. The pulsatility volume index: an indicator of cerebrovascular compliance based on fast magnetic resonance imaging of cardiac and respiratory pulsatility. Philos Transact A Math Phys Eng Sci. 2016;374:20150184.
15. Czosnyka M. Pulsatility index. J Neurosurg. 2001;94:685–6.
16. Calviello LA, de Riva N, Donnelly J, Czosnyka M, Smielewski P, Menon DK, et al. Relationship between brain pulsatility and cerebral perfusion pressure: replicated validation using different drivers of CPP change. Neurocrit Care. 2017;27:392–400.
17. Al-Mufti F, Amuluru K, Changa A, Lander M, Patel N, Wajswol E, et al. Traumatic brain injury and intracranial hemorrhage-induced cerebral vasospasm: a systematic review. Neurosurg Focus. 2017;43:E14.
18. Perrein A, Petry L, Reis A, Baumann A, Mertes P, Audibert G. Cerebral vasospasm after traumatic brain injury: an update. Minerva Anestesiol. 2015;81:1219–28.
19. Smielewski P, Lavinio A, Timofeev I, Radolovich D, Perkes I, Pickard JD, et al. ICM+, a flexible platform for investigations of cerebrospinal dynamics in clinical practice. Acta Neurochir Suppl. 2008;102:145–51.
20. Budohoski KP, Reinhard M, Aries MJH, Czosnyka Z, Smielewski P, Pickard JD, et al. Monitoring cerebral autoregulation after head injury. Which component of transcranial Doppler flow velocity is optimal? Neurocrit Care. 2012;17:211–8.
21. Zeiler FA, Donnelly J, Menon DK, Smielewski P, Zweifel C, Brady K, et al. Continuous autoregulatory indices derived from multi-modal monitoring: each one is not like the other. J Neurotrauma. 2017;34:3070–80.
22. Zeiler FA, Smieleweski P, Donnelly J, Czosnyka M, Menon D, Ercole A. Estimating pressure reactivity index using non-invasive Doppler based systolic flow index. J Neurotrauma. 2018;35(14):1559–68.

23. Zeiler FA, Donnelly J, Calviello L, Menon DK, Smielewski P, Czosnyka M. Pressure autoregulation measurement techniques in adult traumatic brain injury, part I: a scoping review of intermittent/semi-intermittent methods. J Neurotrauma. 2017;34:3207–23.
24. Zeiler FA, Donnelly J, Cardim D, Menon DK, Smielewski P, Czosnyka M. ICP versus laser Doppler cerebrovascular reactivity indices to assess brain autoregulatory capacity. Neurocrit Care. 2018;28(2):194–202.
25. Budohoski KP, Schmidt B, Smielewski P, Kasprowicz M, Plontke R, Pickard JD, et al. Non-invasively estimated ICP pulse amplitude strongly correlates with outcome after TBI. Acta Neurochir Suppl. 2012;114:121–5.
26. Cardim D, Robba C, Bohdanowicz M, Donnelly J, Cabella B, Liu X, et al. Non-invasive monitoring of intracranial pressure using transcranial Doppler ultrasonography: is it possible? Neurocrit Care. 2016;25:473–91.
27. Robba C, Donnelly J, Bertuetti R, Cardim D, Sekhon MS, Aries M, et al. Doppler non-invasive monitoring of ICP in an animal model of acute intracranial hypertension. Neurocrit Care. 2015;23:419–26.
28. Robba C, Cardim D, Tajsic T, Pietersen J, Bulman M, Donnelly J, et al. Ultrasound non-invasive measurement of intracranial pressure in neurointensive care: a prospective observational study. PLoS Med. 2017;14:e1002356.
29. Robba C, Bacigaluppi S, Cardim D, Donnelly J, Bertuccio A, Czosnyka M. Non-invasive assessment of intracranial pressure. Acta Neurol Scand. 2016;134:4–21.
30. Khan MN, Shallwani H, Khan MU, Shamim MS. Noninvasive monitoring intracranial pressure – a review of available modalities. Surg Neurol Int. 2017;8:51.

Chapter 66
Prehospital Transcranial Color-Coded Duplex Sonography (TCCS): Usefulness for the Diagnosis and Early Stroke Treatment

Felix Schlachetzki, Mustafa Kilic, Markus Webert, Michael Ertl, Dobri Baldaranov, and Sandra Boy

Key Points

1. Stroke scales are imperfect differentiating ischemic from hemorrhagic stroke, including selecting patients for endovascular embolectomy.
2. Prehospital ultrasound consists of transcranial color-coded sonography ideally with the aid of echo-enhancing agents for faster diagnosis, diagnostic confidence, and to overcome insufficient acoustic bone windows.
3. Prehospital TCCS is highly suitable to identify patients with middle cerebral artery occlusion with a consistent neurological finding and may justify bypass to the next comprehensive stroke center for endovascular embolectomy.

66.1 Introduction

Ischemic stroke is a time-critical vascular disease that affects neural function and is the leading cause of permanent disability in people in industrialized nations [1, 2]. Acute therapies include IV thrombolysis with a time window up to 4.5 h and interventional embolectomy with an extended time window up to 24 h [3, 4]. In

F. Schlachetzki (✉) · M. Kilic · M. Webert · D. Baldaranov
Department of Neurology, Center for Vascular Neurology and Neurointensive Care, University of Regensburg, medbo Bezirksklinikum Regensburg, Regensburg, Germany
e-mail: felix.schlachetzki@klinik.uni-regensburg.de; mustafa.kilic@medbo.de

M. Ertl
Department of Neurology, University Clinic Augsburg, Augsburg, Germany
e-mail: michael.ertl@klinikum-augsburg.de

S. Boy
Department of Neurology, Asklepios Clinic Bad Tölz, Bad Tölz, Germany
e-mail: s.boy@asklepios.com

C. N. Rodríguez et al. (eds.), *Neurosonology in Critical Care*,
https://doi.org/10.1007/978-3-030-81419-9_66

hemorrhagic stroke, this time window is less defined, and acute therapies in general aim to prevent hematoma enlargement and life-threatening secondary complications [5].

Rapid identification and etiopathological classification of stroke patients in the prehospital phase is critical for successful stroke therapy. Especially in rural areas secondary transports from regional stroke units to comprehensive stroke centers with interventional neuroradiology and neurosurgery resulted in unwanted therapeutic delays [6]. Specifically, prehospital stroke scales such as CPSS, FAST, MASS, LAPSS, PASS, FAST-ED, and RACE have not been consistently validated in the field by paramedics or first-aid doctors but, that is, after arrival in a stroke unit, after exclusion of brain hemorrhage, ischemic stroke database analysis, and by NIHSS-trained doctors and neurologists thus presenting a severe selection bias.

The current discussion in the field of acute stroke care addresses the question how to select patients for direct transfer to a comprehensive stroke center ("mothership") bypassing smaller stroke units thus potentially prolonging symptom-to-needle time for thrombolysis for faster time-to-groin time for endovascular embolectomy [6, 7]. To date, no scale predicted large vessel occlusion (LVO) with both high sensitivity and specificity to justify bypassing of primary stroke units, and more prospective studies are needed to assess the accuracy of LVO prediction instruments in the prehospital setting in all patients with suspected stroke, including patients with hemorrhagic stroke and stroke mimics [8].

Point-of-care diagnostics can significantly enhance stroke diagnosis and differentiation. Blood serum analysis has drawn significant interest in prehospital stroke care, and to date, only glial fibrillary acid protein level detection may separate hemorrhagic stroke from ischemic stroke and stroke mimics if this diagnostic is available in the field [9, 10]. Mobile stroke units (with computed tomography, clinical chemistry, and telemedical support) allow for prehospital thrombolysis with significant shorter symptom-to-needle times but are limited in range and require dedicated paramedics, X-ray technicians, and doctors [11, 12].

While the aforementioned strategies are either not available (GFAP) or limited in distance and costs (mobile stroke units), point-of-care ultrasound (POCUS) equipment has significantly gained attention over the years, has reached technical maturity, and is currently used for assessment for trauma patients, cardiac arrest, hemodynamic instability, respiratory failure, suspected abdominal aortic aneurysm, fetal monitoring, and vascular access [13]. A previous study using transcranial color-coded duplex sonography (TCCS) has demonstrated a sensitivity of 90% and specificity of 98% for the identification of middle cerebral artery (MCA) occlusion. We were able to demonstrate, in the hands of trained neurologists, improved identification of stroke patients with MCA occlusion [14]. In addition, other significant findings also included reversal of flow in the anterior cerebral artery but also high rates of patent cerebral arteries, probably excluding patients from interventional embolectomy [15].

66.2 Prehospital Ultrasound: Practical Guideline

Any prehospital diagnostic should not prolong transport to the target clinic—therefore ultrasound investigations should be performed during transport. However, experienced sonographers with a basic pathological concept (i.e., left-sided hemiparesis with gaze to the right ≥ suggestive of right hemispheric pathology) may be able to perform such an investigation under 5 min. This implies that only transcranial color-coded sonography (TCCS) can be performed as carotid, vertebral, or transnuchal sonography require more stable testing conditions (Fig. 66.1). Any portable color duplex ultrasound machine may be used for prehospital TCCS, yet the equipment should be easy to use and robust and the screen should be big enough not to miss subtle flow signals. Telemedical transfer of TCCS images to experienced neurologists may support the sonographer if not experienced and without emergency stroke knowledge.

Prehospital TCCS does not differ from TCCS in the clinic, and the use of ultrasound echo enhancers (UEE) such as Sonovue® (Bracco, Italy) significantly increases not only signal-to-noise ratio, helps in patients with insufficient temporal acoustic bone window, and therefore diagnostic confidence but significantly shortens scanning time [16–18]. Figure 66.2 depicts the normal intracranial arteries—investigations should be made from both sides starting with the presumed pathological hemisphere. However, the effort is not limited to detection of middle cerebral artery occlusion but can detect a variety of brain pathologies. The following findings can be made by the experienced sonographer (Table 66.1):

Fig. 66.1 Prehospital transcranial color-coded sonography through the left temporal bone window during ambulance transport to the stroke unit

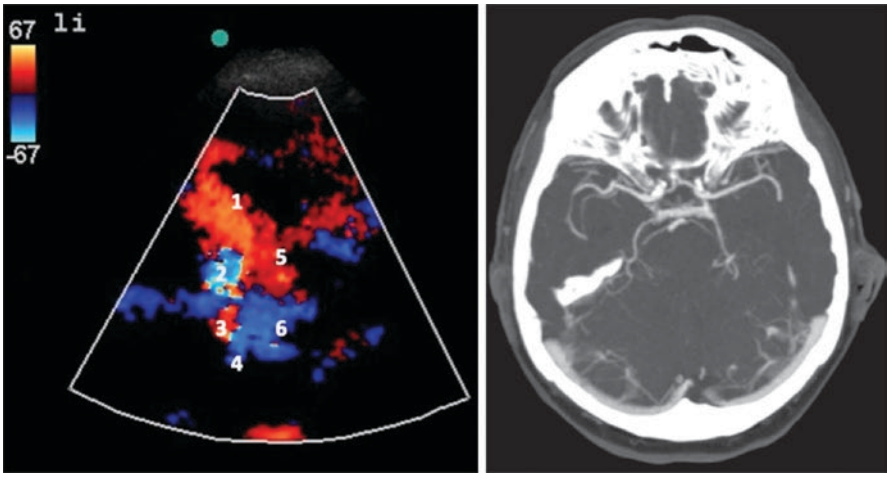

Fig. 66.2 Normal TCCS finding (left) with correlating CT-angio (right). For better correlation rotate left image 90° clockwise to match CT-angio. 1 – left MCA, 2 – left ACA, 3- right ACA, 4 – right MCA, 5 – left PCA, 6 – right PCA, for more pathological findings see open access article [14]

Table 66.1 TCCS Findings

Diagnosis	TCCS finding	Confirmation	Tips & limitation
MCA main stem occlusion	Absence of ipsilateral MCA color-coded in red	Visualization of the ipsi- and contralateral ACA (blue and red)	Perform flow measurements in order not to miss MCA low flow
Carotid-T-occlusion	Absence of ipsilateral MCA color-coded (red) and ACA (blue)	Visualization of the contralateral ACA (red) and ipsilateral PCA	
Basilar artery occlusion	Absence of both PCAs in the P1-segments (=top of the basilar)	Visualization of the anterior circulation (MCA, ACA)	Visualization of both P2-Segments in a non-commatose Patient may be due to fetal type origin of the PCA
ICA occlusion or high grade stenosis	Reversal of flow in the ipsilateral ACA	"Musical murmurs" in the anterior communicating artery	
Space occupying lesions, i.e. ICH, subdural hematoma or brain tumor	Midline displacement of the third ventricle	Increase of pulsatility index in the MCAs	Finding may be non-specific and should correlate with patients neurological status.
ICH	Hyperechoic mass lesion	Location in the basal ganglia and thalamus have highest sensitivity	Detection of ICH is difficult, as hyperacute ICH, cortical, cerebellar, frontal and occipital ICH can be missed

MCA Middle cerebral artery, *ACA* Anterior cerebral artery, *PCA* Posterior cerebral artery, *ICA* Extracranial internal carotid artery, *ICH* Intracerebral hemorrhage

66.3 Prehospital TCCS: Suitable for Selection for Embolectomy?

The strength of pre-hospital TCCS is the detection of MCA occlusion with a sensitivity of 90% and specificity of 98% in the hands of trained neurologists. Therefore, this ultrasound technique improves the identification of patients with stroke (high sensitivity and specificity) and middle cerebral artery (MCA) occlusion [14]. Figure 66.3 depicts the stroke detection algorithm that can be altered implementing prehospital TCCS especially in rural areas and limited capabilities for endovascular embolectomy.

66.4 Conclusion

High-end stroke diagnostics include cerebral computed tomography and magnetic resonance imaging with angiography or even perfusion imaging. The main advantage is that large vessel occlusion, early brain parenchyma ischemia, penumbra, and

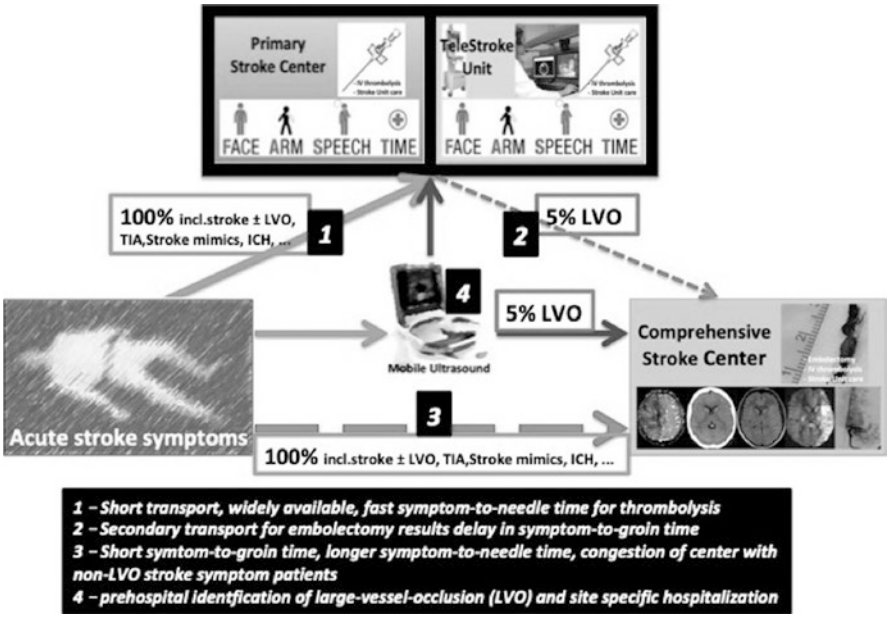

Fig. 66.3 Pre-hospital TCCS and stroke. ICH Intracerebral hemorrhage, LVO Larger vessel occlusion, TIA Transient ischemic attack

brain hemorrhage can be easily depicted even with only rudimental neurological information. Yet these diagnostics will not be widely available in the prehospital field and over long distances. Prehospital transcranial ultrasound such as TCCS in acute stroke patients is a highly promising tool identifying and excluding stroke patients with LVO. The application of prehospital TCCS was first described in a patient with middle cerebral artery territory ischemic stroke in high altitude leading the physicians to apply aspirin with diagnostic confidence and who monitored the cerebrovascular status until arrival in a hospital [19]. Since then only data from our group with neurologists in the field have been published, yet the main limitation of this approach next to the supporting application of echo-enhancing agents and training of the TCCS technique is the requirement of a fundamental pathophysiological concept in each stroke patient [14, 15, 20]. For example in a patient with pure motor stroke one does not expect MCA occlusion as this is the classical lacunar stroke syndrome with microangiopathic lesion in the internal capsule or pons. As most prehospital stroke scales cannot even differentiate between left and right hemispheric symptoms, the diagnostic confidence in any prehospital ultrasound finding will be low. However, telemedicine in the field can overcome this limitation, and thus the combination of live stream ultrasound images, video, and two-way audio streams to hospital-based specialists, which is currently studied in Scotland, has attracted widespread attention [21]. Thus far only healthy volunteers have been investigated using their sophisticated diagnostic setup [22].

Overall, prehospital ultrasound is still in a very early stage, yet the potential triaging stroke patients and thus improving outcome is as high as it is in trauma patients [23, 24]. Novel nonimaging ultrasound technique and machine-learning algorithms may help to implement the widespread use in prehospital stroke diagnostics for large vessel occlusion [25]. Still, well-trained physicians and first-aid personnel supplemented with telemedical support from neurovascular ultrasound specialists may elevate this diagnostic approach to more widespread brain diagnostics, that is, also in brain trauma and raised intracranial pressure.

Algorithm

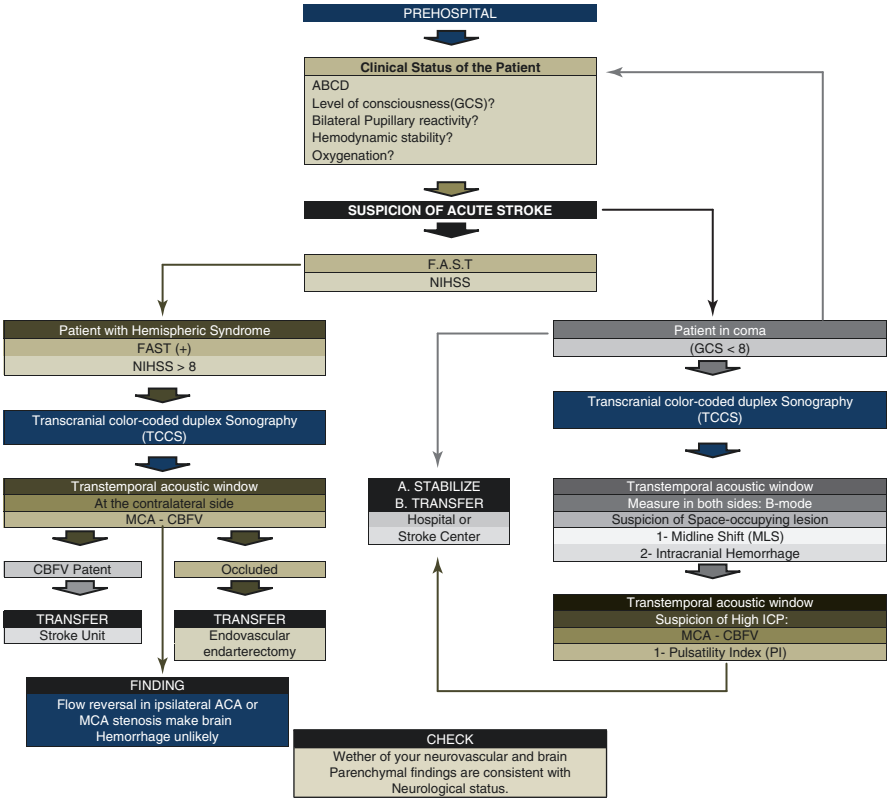

ABCD Airway-breathing-circulation-disability, *FAST* Face-arm-speech-time, *NIHSS* National institute of health stroke scale, *MCA* Middle cerebral artery, *ACA* Anterior cerebral artery, *CBFV* Cerebral blood flow velocity, *ICP* Intracranial pressure, *GCS* Glasgow coma scale

References

1. Rothwell PM, Coull AJ, Silver LE, et al. Population-based study of event-rate, incidence, case fatality, and mortality for all acute vascular events in all arterial territories (Oxford Vascular Study). Lancet. 2005;366:1773–83.
2. Prabhakaran S, Ruff I, Bernstein RA. Acute stroke intervention – a systemic review. JAMA. 2015;313:1452–61.
3. Campbell BCV, Donnan GA, Lees KR, et al. Endovascular stent thrombectomy: the new standard of care for large vessel ischaemic stroke. Lancet Neurol. 2016;14:846–54.
4. Nogueira RG, Jadhav AP, Haussen DC, et al. Thrombectomy 6 to 24 hours after stroke with a mismatch between deficit and infarct. N Engl J Med. 2018;378:11–21.
5. Cordonnier C, Demchuk A, Ziai W, et al. Intracerebral haemorrhage: current approaches to acute management. Lancet. 2018;392(10154):1257–68.

6. Milne MSW, Holodinsky JK, Hill MD, et al. Drip ‘n ship versus mothership for endovascular treatment modeling the best transportation options for optimal outcomes. Stroke. 2017;48:791–4.
7. Pérez de la Ossa N, Ribó M, Jiménez X, et al. Prehospital scales to identify patients with large vessel occlusion it is time for action. Stroke. 2016;47:2877–8.
8. Smith EE, Kent DM, Bulsara KR, et al. Accuracy of prediction instruments for diagnosing large vessel occlusion in individuals with suspected stroke. A systematic review for the 2018 guidelines for the early management of patients with acute ischemic stroke. Stroke. 2018;49:e111–22.
9. Foerch C, Niessner M, Back T, et al. Diagnostic accuracy of plasma glial fibrillary acidic protein for differentiating intracerebral hemorrhage and cerebral ischemia in patients with symptoms of acute stroke. Clin Chem. 2012;58:237–45.
10. Montaner J, Perea-Gainza M, Delgado P, et al. Etiologic diagnosis of ischemic stroke subtypes with plasma biomarkers. Stroke. 2008;39:2280–7.
11. Yperzeelea L, Van Hooffa RJ, De Smedta A, et al. Prehospital stroke care: limitations of current interventions and focus on new developments. Cerebrovasc Dis. 2014;38:1–9.
12. Ebinger M, Kunz A, Wendt M, et al. Effects of golden hour thrombolysis: a Prehospital Acute Neurological Treatment and Optimization of Medical Care in Stroke (PHANTOM-S) substudy. JAMA Neurol. 2015;72(1):25–30.
13. Nielsen MB, Cantisani V, Sidhu PS, et al. The use of handheld ultrasound devices – an EFSUMB position paper. Ultraschall Med. 2019;40:30–9.
14. Herzberg M, Boy S, Hölscher T, et al. Prehospital stroke diagnostics based on neurological examination and transcranial ultrasound. Crit Ultrasound J. 2014;6:3.
15. Schlachetzki F, Herzberg M, Hölscher T, et al. Transcranial ultrasound from diagnosis to early stroke treatment: part 2: prehospital neurosonography in patients with acute stroke: the Regensburg stroke mobile project. Cerebrovasc Dis. 2012;33:262–71.
16. Postert T, Braun B, Meves S, et al. Contrast-enhanced transcranial color-coded sonography in acute hemispheric brain infarction. Stroke. 1999;30:1819–26.
17. Gerriets T, Goertler M, Stolz E, et al. Feasibility and validity of transcranial duplex sonography in patients with acute stroke. J Neurol Neurosurg Psychiatry. 2002;73:17–20.
18. Schlachetzki F, Nedelmann M, Poppert H, et al. Neurosonology makes the difference in acute stroke care. Akt Neurol. 2017;44:1–8.
19. Wilson MH, Van Hooffa RJ, De Smedta A, et al. Stroke at high altitude diagnosed in the field using portable ultrasound. Wilderness Environ Med. 2011;22:54–7.
20. Hölscher T, Donford JV, Schlachetzki F, et al. Prehospital stroke diagnosis and treatment in ambulances and helicopters-a concept paper. Am J Emerg Med. 2013;31:743–7.
21. Mort A, Eadie L, Regan L, et al. Combining transcranial ultrasound with intelligent communication methods to enhance the remote assessment and management of stroke patients: framework for a technology demonstrator. Health Informatics J. 2016;22:691–701.
22. Eadie L, Mulhern J, Regan L, et al. Remotely supported prehospital ultrasound: a feasibility study of real-time image transmission and expert guidance to aid diagnosis in remote and rural communities. J Telemed Telecare. 2018;24:616–22.
23. Rudolpha SS, Sorensenb MK, Svanea C, et al. Effect of prehospital ultrasound on clinical outcomes of non-trauma patients—a systematic review. Resuscitation. 2014;85:21–30.
24. Sheppard JP, Mellor RM, Greenfield S, et al. The association between prehospital care and in-hospital treatment decisions in acute stroke: a cohort study. Emerg Med J. 2015;32:93–9.
25. Thorpe SG, Thibealt CM, Canac N. Decision criteria for large vessel occlusion using transcranial Doppler waveform morphology. Front Neurol. 2018;17(9):847.

Chapter 67
Transcranial Doppler (TCD/TCCD) and Ultrasonography: A Useful Tool in the Aeromedical Transport. What Should We Consider?

Anselmo Caricato and Eleonora Stival

Key Points

1. During air medical transport, the physical examination often is impeded by helicopter noise and vibration, distracting injuries, and altered consciousness. These limitations force clinicians to rely on other diagnostic tools for early diagnosis and management of patients, such as ultrasounds.
2. Many air critical care transport service incorporated prehospital ultrasounds in standard practice since it can be easily taught to flight clinicians and can improve identification and monitoring of injury during transport.
3. The improvement of image quality, together with the decreasing size and weight of portable devices, results in extended indications in air medical transport. Wireless probes can show high-quality images on tablet or mobile phone. Images can be quickly transferred to the hospital by telesonography system, and may have invaluable importance in life-threatening conditions.
4. Availability of transcranial Doppler "on the scene" and during flight transport in stroke patients has the potential of a better use of resources and increasing rate of candidates to treatment.
5. Transcranial Doppler and B-mode brain sonography may be useful to rule out intracranial hypertension during flight.

A. Caricato (✉) · E. Stival
Department of Anesthesia and Intensive Care, NeuroIntensive Care, IRCCS Policlinico Universitario "A. Gemelli", Rome, Italy
e-mail: anselmo.caricato@unicatt.it

C. N. Rodríguez et al. (eds.), *Neurosonology in Critical Care*,
https://doi.org/10.1007/978-3-030-81419-9_67

67.1 Introduction

Bedside point-of-care ultrasound in the emergency department has been routinely introduced more than two decades ago, particularly for trauma patients. This technique is now part of the initial diagnostic evaluation of in-hospital patients, and many guidelines consider ultrasound as a standard of care [1–4].

Advancements in technology offered the possibility to increase ultrasound applications in out-of-hospital settings by using a portable ultrasound machine. Prehospital ultrasound (PHUS) allows a faster and accurate management and treatment of life-threatening conditions, helping medical decision in prioritizing initial treatment and choosing the most appropriate destination. Many air critical care transport service incorporated PHUS in standard practice since it can be easily taught to flight clinicians and can improve identification and monitoring of injury during transport [5–7]. Price et al. were the first to illustrate the feasibility of PHUS during a helicopter transport, showing that ultrasound examination can be quickly conducted without interfering with helicopter avionics [8].

Although the application of PHUS is increasing, especially in aeromedical transport, there are moderate evidences in medical literature to assess the effect of PHUS on patient outcomes [7]. On the other side, the decreasing costs of the instruments and the improvement in image quality, together with the decreasing size and weight of portable devices, result in extended indications for PHUS also in austere settings. Based on recent data, the diagnostic accuracy of PHUS-focused assessment sonography in trauma (FAST) in aeromedical transport reaches a sensitivity from 50% to 78.6% compared with clinical examination or CT scan, and could be performed in about 3 min or less by a nonradiology clinician [3].

67.2 Flight Transport: Medical Consideration

Flight transport requires in-depth knowledge of several problems:

1. If a patient have to be transferred by helicopters, he should be prepared for the boarding. A strict attention should be paid to clothes that have to be restrained; any object placed on the patient may be sucked into the rotor blades and/or engines, and could be a potential serious danger.
2. If the patient is boarded, and the helicopter encounters spinning rotors, ground personnel must be trained to avoid the patient and the treating team being struck by the main or tail rotor. The danger is real; particularly if the landing zone is in the field (uneven terrain), where the rotor blades may be close to the ground.
3. Weight also has to be carefully calculated, in particular for helicopter transport, since the engines are only able to produce a finite amount of power. An aircraft that is overweight can end in disaster.
4. Physiologic changes due to altitude should be well known, in particular if fixed wing aircraft is used for the transport. In fact, when an aircraft ascends, any gas on board will increase in volume; thus, if a pneumothorax is present, it may have

an increase in the size if a chest drainage is not properly functioning. Furthermore, gas-filled cuffs, such as endotracheal tubes, should be considered. If the volume inside the cuff is allowed to expand, it could cause damage to the trachea including pressure necrosis. So, changing air with liquid is recommended, especially when a long flight at high altitude is expected.

During air medical transport, the physical examination often is impeded by helicopter noise and vibration, distracting injuries, altered consciousness, and intubation. These limitations force clinicians to rely on other diagnostic tools for early diagnosis and management of patients, such as ultrasound technique.

Since 2000, the availability of small portable ultrasound machine with high-quality images led to investigate the feasibility of ultrasound examination during helicopter transport. Price et al., using a 2.5 kg Sonosite 180, found that, in 21 cases, FAST was easy to perform during helicopter flight, and mean duration of exam was 3 min [8]. The most important limitation to the examination was patient positioning and sunlight on the screen. Recently, Yates, using a Sonosite M-Turbo device during helicopter flight on 190 trauma patients, obtained a positive predictive value of 100% and a negative predictive value of 98.3% for the identification of pneumothorax, hemothorax, and free abdominal fluid, if compared with CT imaging [9].

Technology has now further improved, and wireless probes of a few centimeters in length and a few grams in weight can show high-quality images on tablet or mobile phone. Images can be quickly transferred to the hospital by telesonography system, and may have invaluable importance in life-threatening conditions [10].

A remarkable limitation peculiar to helicopter flight is still the patient positioning, which depends on the vehicle model. In some setting, one of the patient sides is positioned against the wall, impeding not only clinical examination but also some ultrasound views. Knowing in advance these problems, we can properly position the patient, according to the side of the cabin where the patient was loaded, so to consent ultrasound examination. According to some authors, it may be very practical learning to scan with either hand [11]. A strict communication with pilot is mandatory to avoid problems with unanticipated turbulence.

Motion artifacts during flight were not considered an important limitation to the exam. Lyon et al., in 2012, collected a total of 104 images of sliding lung sign on M-mode obtained during 3 distinct phases of transport: without rotor rotation, with rotor rotation while on the ground, and at level flight [12]. Motion artifacts were noted in images taken during rotor rotation but these were not felt to affect the diagnostic utility of the M-mode ultrasound tracing.

67.3 Ultrasound During Flight: Diagnostic Indication

67.3.1 Airways

One of the most dangerous complications of prehospital intubation and transport of intubated patients is unrecognized endotracheal tube dislodgement. It is of paramount importance to acknowledge esophageal intubation as soon as possible, and the use of

ultrasounds aimed to visualize tracheal and cricothyroid could be a determinant in detecting the correct endotracheal tube position when capnography is not available [13]. In particular, during aeromedical transport, auscultation is not always feasible, and ultrasounds might be a considerable tool to assess the airways, able to discriminate between endotracheal and endobronchial position. According to some studies, sensitivity and specificity for identifying endotracheal intubation with ultrasound compared to esophageal intubation were nearly 100% in cadavers [14] and in live patients [15].

67.3.2 Cardiopulmonary Diseases

In case of respiratory failure or nontraumatic shock, clinicians must differentiate between a cardiac or pulmonary cause. Using structured protocols, ultrasounds have been proposed as a means to augment advanced cardiac life support algorithms [16, 17]. Lung ultrasound associated with echocardiography and assessment of inferior vena cava collapsibility give an invaluable help in rapid identification of acute hearth failure, massive pulmonary embolism, respiratory distress syndrome, cardiac tamponade, tension pneumothorax, and hypovolemia. In the flight setting, cardiovascular monitoring may be very poor, and even measurement of blood pressure can be challenging. Ultrasound can give us important information about hemodynamics, orienting to a life-threating condition's treatment decision.

67.3.3 Chest Traumatic Injury

Early detection of potentially lethal injuries has an important impact on mortality rates. In flight, pneumothorax and hemothorax diagnosis is quickly feasible, has a rapid learning curve, and permits to decide if performing a tube thoracostomy or activate massive transfusion protocol. In flight medicine, both helicopter and fixed wing aircraft, ultrasound was found to be safe and with a high accuracy similar to the emergency department radiology [18]. In a feasibility study, the agreement between providers and expert physicians in thoracic echography was very high when lung ultrasound was performed during flight [19]. With the in-flight limitations of auscultation, echography is extremely useful to identify life-threatening conditions, avoiding iatrogenic injury.

67.3.4 Abdomen Traumatic Injury

In traumatic shock, the extended FAST protocol has been validated in emergency department and in prehospital settings as the gold standard in detecting abdominal bleeding [1–4]. The sensitivity and specificity of PHUS-extended FAST are similar to in-hospital exams, and no significant difference in performing time had been

recorded. Some studies assessed the feasibility and quality of FAST images collected during air transport, demonstrating that FAST was possible and did not affect transport times [3].

67.4 Neurologic Emergencies: Ultrasound During Flight

67.4.1 Ischemic Stroke

Intravenous thrombolysis and endovascular thrombectomy are highly effective therapies for acute ischemic stroke, but only a minority of hospitals treating these patients may offer both these treatments [20]. Since the effect of these therapies diminishes over time, stroke systems of care need to rapidly identify patients with cerebral artery occlusion and transport them to proper hospitals as quickly as possible [21].

Flight transport had an increasing importance in last years, significantly reducing prehospital time, and increasing rate of patients who can benefit from stroke treatment. Recent data from 21,712 ischemic stroke patients registered in Austrian Stroke Unit Registry reported that thrombolysis rates were highest in 905 patients transported by helicopter (24%), when compared with remaining patients transported by ground ambulance with emergency physicians (18%) [22].

Actually, it is not only a problem of time. To increase the efficiency of stroke system, the identification of suspected stroke is of paramount importance, so to address resources where they really need. A recent systematic review observed that scale with scoring system had low sensitivity and low specificity to predict ischemic stroke [23]. Ultrasonography may play an important role in this setting.

Transcranial Doppler (TCD/TCCS) ultrasound is a reliable diagnostic tool for assessing the presence and severity of cerebral arteries occlusion [24], and has the additional advantages of being noninvasive, inexpensive, and portable. For these features, TCD may be very useful for prehospital diagnosis and assessment in stroke. Indeed, bedside TCD examinations to detect stenosed and/or occluded intracranial vessels are routinely conducted as standard of care at many comprehensive stroke centers [25]. Numerous studies have been published comparing TCD diagnosis of cerebral arterial occlusion with angio-CT imaging, reporting sensitivity and specificity ranging between 79 and 98% depending on occlusion location [26–29]. A limiting factor of these studies is the TCD operator's ability to locate and interpret the cerebral blood flow velocity waveform. Such challenges have contributed to TCD being critically underutilized for stroke assessment [30].

No study was specifically directed to a systematic investigation of reliability of TCD during flight. Nevertheless, an interesting pilot experience was conducted in Germany with a joint program for prehospital stroke diagnosis and treatment between the University of San Diego, California, and the University of Regensburg in Germany [31].

Herzberg et al. hypothesized that a neurologist equipped with a portable ultrasound device was able to achieve a similar diagnostic accuracy "in the field" as compared with in-hospital advanced neuroimaging, such as angio-CT or angio-MRI

[31]. Thus, a stroke team was sent together to the ground ambulance team when a stroke code was received from dispatch center. They observed that, with a combined neurological and neurosonological examinations, more than half of the patients seen after a stroke emergency call were identified as not suffering a stroke; actually, an occlusion in the territory of middle cerebral artery was identified with a sensitivity of 90% and a specificity of 98%. These results show that ultrasounds may help in a correct diagnosis of stroke directly in prehospital setting.

Availability of TCD "on the scene" and during flight transport has the potential for a better use of resources and increasing rate of stroke patients candidate to treatment.

67.4.2 Intracranial Hypertension

Brain ultrasound was suggested as a point-of-care method to rule out intracranial hypertension, to measure midline shift, as confirmatory test for cerebral circulatory arrest, and to assess cerebral ventricular enlargement [32]. In prehospital setting, some authors suggested to include brain ultrasound in whole body evaluation, extending established protocol as FAST for trauma patients. This approach is still not validated, and brain ultrasound is not included in critical care ultrasound competency statement. Nevertheless, several papers were published in the last years on this topic, and a lot of evidence suggest that this technique may be useful in emergency conditions [32–36].

In particular, many authors showed that transcranial Doppler could reliably exclude a condition of intracranial hypertension. Ract observed that intracranial hypertension on hospital admission was associated with abnormal TCD pattern, and that early brain-oriented therapy could restore normal TCD values [33]. Tazarourte confirmed these data in prehospital phase, showing that high pulsatility index and low diastolic velocity were both associated with intracranial hypertension and poor outcome [34]. A large multicentric study is ongoing on this topic, and is aimed to validate a mathematic formula based on TCD parameters to exclude intracranial hypertension [35].

Practical problems for a detailed execution of transcranial Doppler may arise in prehospital phase and during ground or air transport to the hospital. B-mode brain ultrasound can be easier in this setting, and optic nerve sheath diameter may be an important technique to give similar information about intracranial hypertension, even if Doppler is not available [37].

67.5 Conclusion

Several studies show that ultrasounds have an increasing importance in diagnosis and in addressing treatment in the prehospital phase. In this review, we report the features of flight transport, and highlight the usefulness of ultrasound in this setting.

We focused on neurological emergencies, and reviewed experiences where transcranial Doppler and B-mode ultrasounds were used for rapid and correct diagnosis and for a better use of resources.

Algorithm

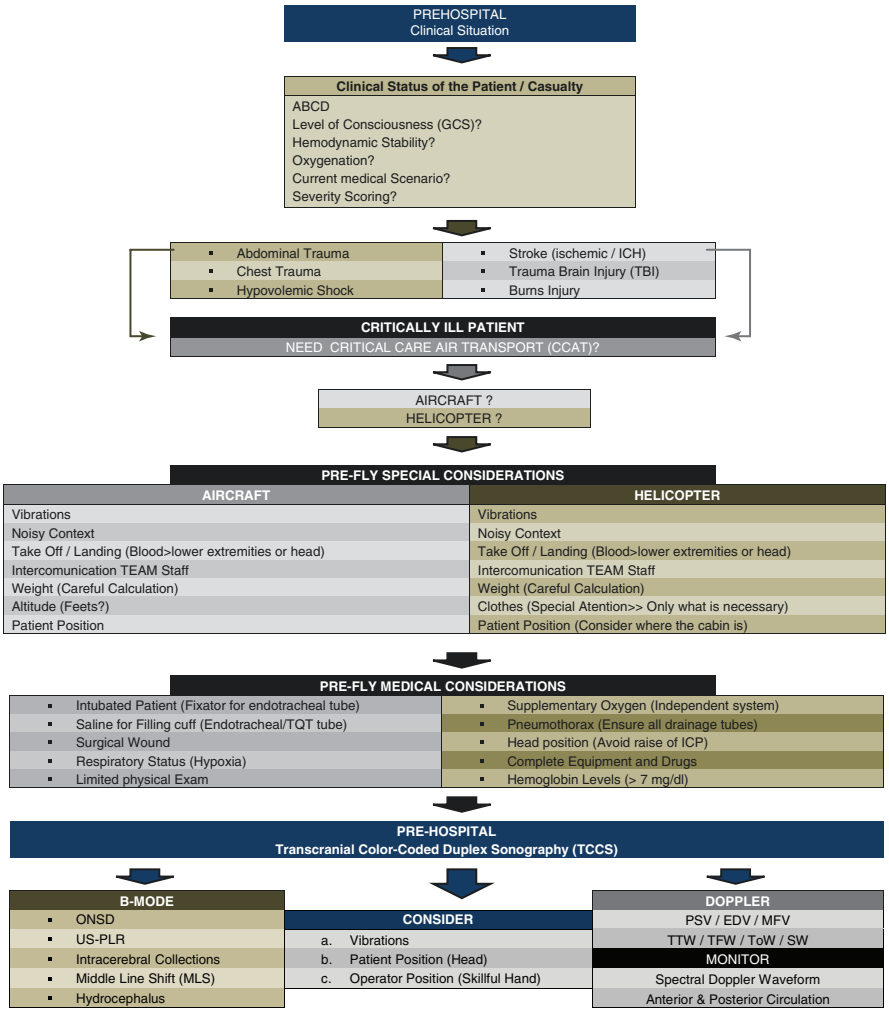

ABCD Airway-breathing-circulation-disability, *ICP* Intracranial pressure, *ONSD* Optic nerve sheath diameter, *US-PLR* Ultrasound pupillary light reflex, *PSV* Peak systolic velocity, *EDV* End-distolic velocity, *MFV* Mean flow velocity, *TTW* Transtemporal window, *TFW* Transforaminal window, *ToW* Transorbital window, *SW* SUbmandibular window

References

1. Montoya J, Stawicki SP, Evans DC, Bahner DP, Sparks S, Sharpe RP, et al. From FAST to E-FAST: an overview of the evolution of ultrasound-based traumatic injury assessment. Eur J Trauma Emerg Surg. 2016;42(2):119–26.
2. Williams SR, Perera P, Gharahbaghian L. The FAST and E-FAST in 2013: trauma ultrasonography: overview, practical techniques, controversies, and new frontiers. Crit Care Clin. 2014;30(1):119–50.
3. Stengel D, Rademacher G, Ekkernkamp A, Guthoff C, Mutze S. Emergency ultrasound-based algorithms for diagnosing blunt abdominal trauma. Cochrane Database Syst Rev. 2015;(9):CD004446.
4. Subcommittee on Advanced Trauma Life Support (ATLS) of the American College of Surgeons (ACS), Committee on Trauma. Advanced trauma life support course for physicians. 10th ed. Chicago: American College of Surgeons; 2017.
5. Ketelaars R, Hoogerwerf N, Scheffer GJ. Prehospital chest ultrasound by a Dutch helicopter emergency medical service. J Emerg Med. 2013;44(4):811–7.
6. MacDonald RD, Alqattan S. Articles that may change your practice: prehospital ultrasound. Air Med J. 2017;36(1):16–8.
7. Jørgensen H, Jensen CH, Dirks J. Does prehospital ultrasound improve treatment of the trauma patient? A systematic review. Eur J Emerg Med. 2010;17(5):249–53.
8. Price DD, Wilson SR, Murphy TG. Trauma ultrasound feasibility during helicopter transport. Air Med J. 2000;19(4):144–6.
9. Yates JG, Baylous D. Aeromedical ultrasound: the evaluation of point-of-care ultrasound during helicopter transport. Air Med J. 2017;36(3):110–5.
10. Marsh-Feiley G, Eadie L, Wilson P. Telesonography in emergency medicine: a systematic review. PLoS One. 2018;13(5):e0194840.
11. Mazur SM, Pearce A, Alfred S, Goudie A, Sharley P. The F.A.S.T.E.R. trial. Focused assessment by sonography in trauma during emergency retrieval: a feasibility study. Injury. 2008;39:512–8.
12. Lyon M, Shiver SA, Walton P. M-mode ultrasound for the detection of pneumothorax during helicopter transport. Am J Emerg Med. 2012;30(8):1577–80.
13. Weaver B, Lyon M, Blaivas M. Confirmation of endotracheal tube placement after intubation using the ultrasound sliding lung sign. Acad Emerg Med. 2006;13:239–44.
14. Ma G, Davis DP, Schmitt J, Vilke GM, Chan TC, Hayden SR. The sensitivity and specificity of transcricothyroid ultrasonography to confirm endotracheal tube placement in a cadaver model. J Emerg Med. 2007;32:405–7.
15. Milling TJ, Jones M, Khan T, Tad-y D, Melniker LA, et al. Transtracheal 2-D ultrasound for identification of esophageal intubation. J Emerg Med. 2007;32:409–14.
16. Hernandez C, Shuler K, Hannan H, Sonyika C, Likourezos A, et al. Cardiac arrest ultra-sound exam – a better approach to managing patients in primary non arrhythmogenic cardiac arrest. Resuscitation. 2008;76:198–206.
17. Jones AE, Tayal VS, Sullivan DM, Kline JA. Randomized, controlled trial of immediate versus delayed goal-directed ultrasound to identify the cause of nontraumatic hypotension in emergency department patients. Crit Care Med. 2004;32:1703–8.
18. Blaivas M, Lyon M, Duggal S. A prospective comparison of supine chest radiography and bedside ultrasound for the diagnosis of traumatic pneumothorax. Acad Emerg Med. 2005;12:844–9.
19. Roline CE, Heegaard WG, Moore JC, Joing SA, Hildebrandt DA, et al. Feasibility of bedside thoracic ultrasound in the helicopter emergency medical services setting. Air Med J. 2013;32:153–7.
20. Goyal M, Menon BK, van Zwam WH, Dippel DW, Mitchell PJ, Demchuk AM, et al. Endovascular thrombectomy after large-vessel ischaemic stroke: a meta-analysis of individual patient data from five randomized trials. Lancet. 2016;387:1723–31.

21. Saver JL, Goyal M, Hill MD, HERMES Collaborators. Time to endovascular thrombectomy for acute stroke: reply. JAMA. 2017;317:1175–6.
22. Reiner-Deitemyer V, Teuschl Y, Matz K, Reiter M, Eckhardt R, Seyfang L, et al. Helicopter transport of stroke patients and its influence on thrombolysis rates: data from the Austrian Stroke Unit Registry. Stroke. 2011;42(5):1295–300.
23. Smith EE, Kent DM, Bulsara KR, Leung LY, Lichtman JH, Reeves MJ, et al. Accuracy of prediction instruments for diagnosing large vessel occlusion in individuals with suspected stroke: a systematic review for the 2018 guidelines for the early management of patients with acute ischemic stroke. Stroke. 2018;49(3):e111–22.
24. Saqqur M, Uchino K, Demchuk AM, Molina CA, Garami Z, Calleja S, et al. Site of arterial occlusion identified by transcranial Doppler predicts the response to intravenous thrombolysis for stroke. Stroke. 2007;38:948–54.
25. Alberts MJ, Latchaw RE, Selman WR, Shephard T, Hadley MN, Brass LM, et al. Recommendations for comprehensive stroke centers: a consensus statement from the brain attack coalition. Stroke. 2005;36:1597–616.
26. Brunser AM, Lavados PM, Hoppe A, Lopez J, Valenzuela M, Rivas R. Accuracy of transcranial Doppler compared with CT angiography in diagnosing arterial obstructions in acute ischemic strokes. Stroke. 2009;40:2037–41.
27. Demchuk AM, Christou I, Wein TH, Felberg RA, Malkoff M, Grotta JC, et al. Accuracy and criteria for localizing arterial occlusion with transcranial Doppler. J Neuroimaging. 2000;10:1–12.
28. Saqqur M, Hill MD, Alexandrov AV, Roy J, Schebel M, Krol A, et al. Derivation of power M-mode transcranial Doppler criteria for angiographic proven MCA occlusion. J Neuroimaging. 2006;16:323–8.
29. Tsivgoulis G, Sharma VK, Lao AY, Malkoff MD, Alexandrov AV. Validation of transcranial Doppler with computed tomography angiography in acute cerebral ischemia. Stroke. 2007;38:1245–9.
30. Thorpe SG, Thibeault CM, Canac N, Wilk SJ, Devlin T, Hamilton RB. Decision criteria for large vessel occlusion using transcranial doppler waveform morphology. Front Neurol. 2018;9:1–1.
31. Herzberg M, Boy S, Hölscher T, Ertl M, Zimmermann M, Ittner KP, et al. Prehospital stroke diagnostics based on neurological examination and transcranial ultrasound. Crit Ultrasound J. 2014;6(1):3–15.
32. Lau VI, Arntfield RT. Point-of-care transcranial Doppler by intensivists. Crit Ultrasound J. 2017;9(21):1–11.
33. Ract C, Le Moigno S, Bruder N, Vigué B. Transcranial Doppler ultrasound goal-directed therapy for the early management of severe traumatic brain injury. Intensive Care Med. 2007;33(4):645–51.
34. Tazarourte K, Atchabahian A, Tourtier JP, David JS, Ract C, Savary D, et al. Pre-hospital transcranial Doppler in severe traumatic brain injury: a pilot study. Acta Anaesthesiol Scand. 2011;55(4):422–8.
35. Rasulo FA, Bertuetti R, Robba C, Lusenti F, Cantoni A, Bernini M, et al. The accuracy of transcranial Doppler in excluding intracranial hypertension following acute brain injury: a multicenter prospective pilot study. Crit Care. 2017;21(1):44.
36. Caricato A, Mignani V, Sandroni C, Pietrini D. Bedside detection of acute epidural hematoma by transcranial sonography in a head-injured patients. Intensive Care Med. 2010;36(6):1091–2.
37. Robba C, Santori G, Czosnyka M, Corradi F, Bragazzi N, Padayachy L, et al. Optic nerve sheath diameter measured sonographically as non-invasive estimator of intracranial pressure: a systematic review and meta-analysis. Intensive Care Med. 2018;44(8):1284–94.

Chapter 68
Cerebral Hemodynamic Monitoring and Renal Replacement Therapy (RRT) in ICU: Usefulness of the Transcranial Doppler (TCD/TCCS)

Camilo N. Rodríguez and Jorge Cerdá

Key Points

1. The central nervous system (CNS) and kidneys are tightly interconnected in an organ cross talk, "Brain-Kidney" connection.
2. The incidence of AKI in the intensive care unit (ICU) involves up to 50% of ICU admissions. Many of those patients require some type of renal replacement therapy (RRT).
3. Critical patients with acute brain injury (ABI) are part of a population of critical patients where the prescription of RRT must consider the risk of secondary brain injury and address main CNS physiological variables (CBF, CPP, and ICP).
4. During RRT, spectral Doppler waveform evaluation (PSV, EDV, and MFV) and the pulsatility index (PI) that is derived from it are very useful to estimate "in real time" possible modifications in regional cerebral blood flow.
5. The dialysis disequilibrium syndrome (DDS) can occur in any patient under RRT, but it is observed more frequently when patients are exposed to their first RRT session, when control of the rate of urea removal is crucial.

68.1 Introduction

Acute kidney injury (AKI) is a common and multifactorial syndrome characterized by rapid progressive loss of kidney excretory function, typically manifested by the

C. N. Rodríguez (✉)
Intensive Care Medicine, Hospital Nacional Prof. Dr. A. Posadas, University of Buenos Aires (UBA), Neurointensive Care Section - ESICM, Neurointensive Care Section - AMCI, Neurointensive Care Committee - FEPIMCTI, Member of ESNCH, Buenos Aires, Argentina
e-mail: camilo.rodriguez@nesccco.com

J. Cerdá
Nephrology Division, Department of Medicine, Albany Medical College, Albany, NY, USA

C. N. Rodríguez et al. (eds.), *Neurosonology in Critical Care*,
https://doi.org/10.1007/978-3-030-81419-9_68

accumulation of waste products of nitrogen metabolism (urea and creatinine), decreased production of urine, or both.

The onset of AKI imposes a heavy burden of disease (morbidity and mortality) and high health system costs (Fig. 68.1). In the intensive care unit, the incidence of AKI is as high as 30–65% of the admissions (15–60% mortality) and 50–70% of patients require some type of RRT during the ICU stay. Among patients hospitalized outside of the ICU, AKI incidence reaches 5–20% [1–6].

The central nervous system (CNS) and the kidneys have a strong interconnection as a "Brain-Kidney binominal". The CNS regulates renal blood flow, glomerular filtration rate (GFR), and affects renal water and sodium handling. Vasopressin hormone is secreted from the hypothalamo-pituitary axis and acts on the distal nephron to regulate water balance and serum osmolality [7, 8] (Tables 68.1 and 68.2;

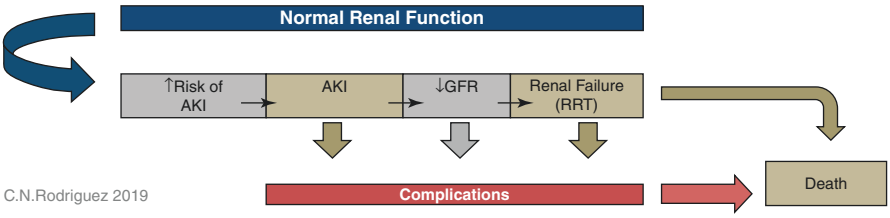

Fig. 68.1 Clinical evolution of AKI. GFR Glomerular filtration rate, AKI Acute kidney injury, RRT Renal replacement therapy

Table 68.1 How acute brain injury affects the kidney

Mechanism	Pathway	Clinical consequence
Neuroinflammation	Increase of cytokines	Cascade of Inflammatory events (Multiorgan failure, BBB damage, etc.)
Sympathetic activity	Increase of catecholamines	Systolic hypertension, haemolysis, red cell thrombi in the glomeruli
Hypothalamo-pituitary axis (HPA)	Decrease of vasopressin	Electrolyte and fluid disturbances: (Water balance and serum osmolality) Central neurogenic diabetes insipidus Inappropriate secretion of antidiuretic Cerebral salt-wasting syndrome

BBB Blood-brain-barrier, *ICP* Intracranial pressure, *AKI* Acute kidney injury

Table 68.2 How acute kidney injury (AKI) has its effect on Brain

Mechanism	Pathway	Clinical consequence
Inflammation (AKI)	Increase of cytokines	Cascade of inflammatory events (Multiorgan failure, BBB damage, endothelial injury)
Sympathetic activity	Increase of catecholamines	Systolic hypertension, encephalopathy, edema, ischemia, coma.
Acid-Base Disturbance	Uremia acidosis hyperosmolar status	Cerebral Edema (increase of ICP) Impairment of cerebral function Delirium, stupor, coma

BBB Blood-brain-barrier, *ICP* Intracranial pressure, *AKI* Acute kidney injury

Figs. 68.2 and 68.3). The incidence of acute renal dysfunction and renal failure after acute brain injury is reported to range between 8–23% and 0.5–0.8%, respectively [7].

Among AKI patients requiring RRT, current evidence has not demonstrated superiority of any modality of renal replacement therapy.

A large meta-analysis [9] comparing intermittent renal replacement therapy (IRRT) with continuous renal replacement therapy (CRRT) showed no significant differences between the two techniques on length of hospital stay, recovery of renal function, and mortality [1]. The choice of one modality over another should be based on the individual characteristics of each patient, their comorbidities, and local hospital expertise.

Within the intensive care unit (ICU), the patient with acute brain injury (ABI) (including ischemic stroke, intracerebral hemorrhage, subarachnoid hemorrhage, and traumatic brain injury) belongs to a population of critical patients in whom the management of AKI and the possible establishment of some type of RRT must consider the possibility of secondary brain injury and its pathophysiological variables:

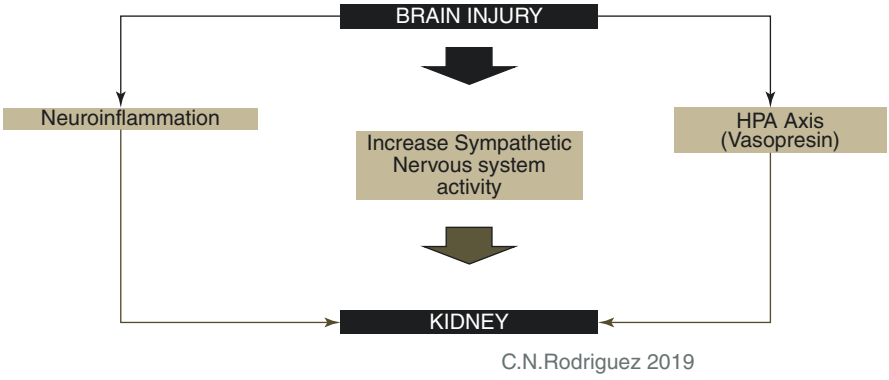

Fig. 68.2 Brain injury: Mechanisms of damage to the kidney. HPA Hypothalamic-pituitary-adrenal axis

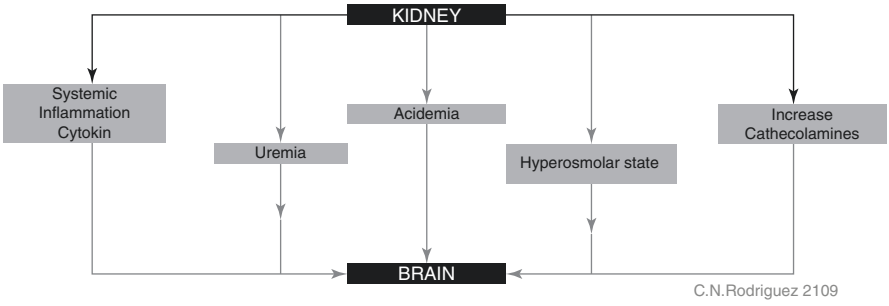

Fig. 68.3 Kidney dysfunction: Mechanism that affect the brain

cerebral blood flow (CBF), cerebral perfusion pressure (CPP), and intracranial pressure (ICP). These treatment end points can be seriously affected by RRT. Therefore, an adequate selection of RRT modality will contribute to avoid or worsen secondary brain injury, and therefore, severely impact clinical outcome [10].

In this chapter, we will highlight the changes in cerebral hemodynamic variations in direct relation with the application of RRT in the ICU, and the clinical and technical circumstances to be considered at the time of prescription and surveillance.

68.2 Acute Kidney Injury and Renal Replacement Therapy

The most frequent causes of AKI in the neuro-ICU are shown in Table 68.3.

After the diagnosis of AKI, the ICU multidisciplinary team should define the most appropriate therapeutic plan considering the clinical situation of the patient and its potential benefits and complications (Table 68.4) [14].

68.3 Renal Replacement Therapy and Changes in the Cerebral Blood Flow

One objective of dialysis treatment is to normalize the blood plasma electrolytes and remove waste products such as urea and creatinine from blood. RRT, in any of its modalities, will present an electrolyte modification that in time will directly affect cerebral hemodynamics, promoting clinically significant modifications for the patient with acute neurological injury.

Serum urea concentration declines rapidly in comparison to reduction in urea concentration in the brain (as time is required for urea to move across cell membranes through urea transporters). This osmolality gradient between serum and brain results in the movement of water down the concentration gradient, leading to cerebral edema.

Table 68.3 Most common causes for AKI in the Neuro-ICU (NICU) [11–13]

Causes of AKI	
Sepsis	Trauma Brain Injury (TBI)
Rhabdomyolysis	Other Acute brain Injury (SAH,ICH)
Propofol Infusion Syndrome (PRIS)	Hyperosmolar Therapy (Sodium)
Status Epilepticus	Hyperosmolar Therapy (Mannitol)
Pharmacology (Nephrotoxicity)	Hypotension (decrease MAP)

MAP Mean arterial pressure, *SAH* Subarachnoid hemorrhage, *ICH* Intracerebral hemorrhage, *AKI* Acute kidney Injury

Table 68.4 ICU multidisciplinary team checklist for RRT indication

Pathology	Neuro-critical patient Non neuro-critical patient Hemodynamic stability
Timing (classical criteria)	Hyperkalemia (>6.5 mmol/L or a rapid increase) Refractory fluid overload Metabolic acidosis Clinical signs of uremia Other causes (Intoxication)
Vascular access	RIJV (Elective) LIJV Subclavian Femoral
RRT modality	Intermittent Continuous Hybrid
Membrane	Patient's body surface and RRT Dose
Dialysate	$[Na^{++}]/[NaHCO_3^-]$
RRT dose	ml/kg/hour
Laboratory [Urea]p	[Urea]p Pre-RRT
Anticoagulation	Systemic (UFH-LMWH) Regional (Citrate) Without anticoagulation
Fluid Balance	With ultrafiltration/without ultrafiltration
Weaning of the RRT	Recovery of diuretic rhythm (>400 ml/day) Improvement of creatinine clearance (>20 ml/min)

RRT Renal replacement therapy, *UFH* Unfractioned heparin, *LMWH* Low molecular weight heparin, *[Urea]p* Urea plasmatic concentration, *RIJV* Right internal jugular vein, *LIJV* Left internal jugular vein

68.3.1 Worsening Cerebral Edema: Mechanism

Disequilibrium dialysis syndrome (DDS) can be an explanation of the cerebrovascular events and acute neurological deterioration resulting from the RRT [15]. Especially when the RRT efficiency is greater (elevated solutes and fluids removal rate). Although DDS-related mortality is not frequent, this syndrome can be a determining factor in the final outcome of the patient in certain clinical circumstances [16–18]:

1. *First session of RRT with sessions < 2 hours*
   (High urea removal rate: great changes in the [Urea]p*)
2. *RRT with high efficiency*
   Large area filters and aggressive removal of [Urea]p: High urea reduction ratio (URR) [Urea]p > 40% in 2 hours [18–21] (Eq. 68.1)

3. *Patient with chronic kidney disease (CKD)*
4. *Previous neurological impairment*
5. *[Urea]p > 175 mg/dl*

*[Urea]p: plasmatic urea concentration

Urea Reduction Ratio (URR):

$$\left(\text{Pre - dialysis}\left[\text{Urea}\right]\text{p} - \text{Post - dialysis}\left[\text{Urea}\right]\text{p}\right)**/\text{Pre - dialysis}\left[\text{Urea}\right]\text{p} \times 100 \tag{68.1}$$

Recommended value: < 0.4 (40%)

**Measured 5 minutes after the end of dialysis [22].

Due to a shift in plasma osmolarity, a rapid or excessive change in the electrolytes can lead to complications like cardiovascular instability, disequilibrium dialysis syndrome, cardiac arrhythmias, cerebral edema, etc., especially for critically ill patients in the ICU. Since the exchange velocity of the electrolytes mainly depends on the concentration gradients across the dialysis membrane between blood and dialysate, it can be controlled by an individualized composition of dialysate concentrations. In order to obtain a precise concentration gradient with the individualized dialysate, it is necessary to continuously monitor the plasma concentrations, which becomes more important when we are treating a neurocritical patient [22].

The most frequent clinical manifestations of DDS, in a conscious patient, are usually mostly neurological as a surrogate of intracranial hypertension: (a) nausea, (b) vomiting, (c) anorexia, (d) headache, (e) encephalopathy, (f) seizures, and (g) coma (herniation).

In the ICU, with the patient under sedation and analgesia, clinical interpretation is more difficult. However, the "real time" approach by TCCS neuroimaging next to the patient's bed is a valuable option.

In the DDS and its apparent pathophysiology (since there are no certainty mechanisms), we can define three dynamic situations that convert it into a multifactorial metabolic complication with clear cerebrovascular impact [15]:

A. Effects by the correction of the [Urea]p
   (It is important to know the plasmatic urea kinetics, which depends on the blood flow rate and the time of initiation of RRT) [21] (Fig. 68.4; Eq. 68.1)
B. Presence of ideogenous osmoles
   (In the neuron)
C. Intracerebral acidosis

RRT is associated with increased ICP in neurocritically ill patients. The magnitude of the increase in ICP may be related to higher initial plasma urea levels [23, 24].

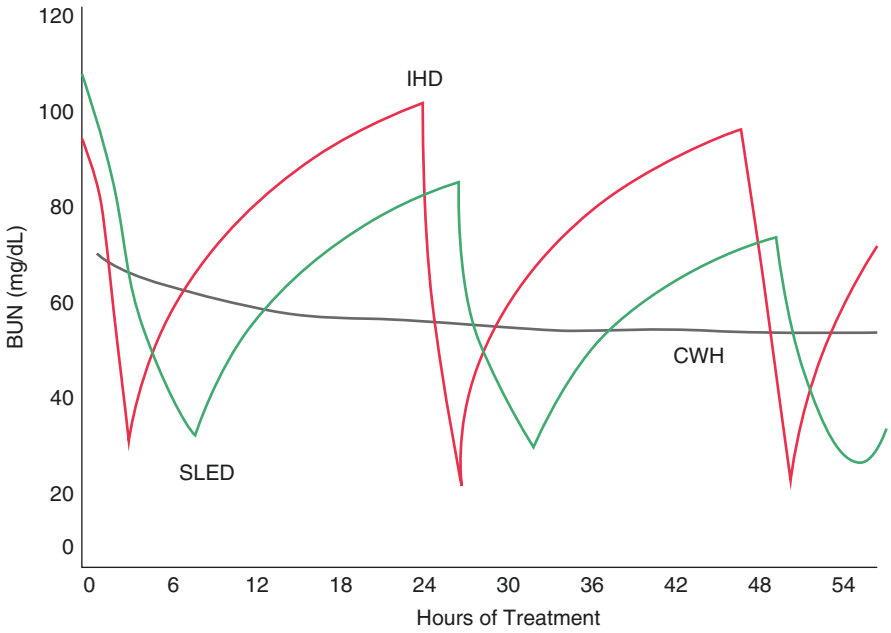

Fig. 68.4 Blood urea nitrogen (BUN) kinetic. SLED Sustained low efficiency dialysis (Green line), IHD Intermittent hemodialysis (Red line), CVVH Continuous veno-venous hemodialysis (Gray line)

68.3.2 Pathophysiological Mechanism of Disequilibrium Dialysis Syndrome

Although the mechanisms involved in the DDS are uncertain [25, 15], the pathophysiological events (hemodynamic and metabolic) are dynamically interrelated to contribute to the indirect changes in CBF and CPP, by means of direct changes in ICP in the patient with acute brain injury and AKI.

2.1 *Changes in the Osmotic Gradient and Modification of the CBF*

The efficiency of the RRT promotes a decrease in [Urea]p and an increase in [HCO_3-]p with the consequent decrease in pH in the cerebrospinal fluid (increase (↑) H_2O and increase (↑) CO_2), promoting cerebral edema (decrease intracellular pH with increase in H^+ and increase in ideogenous osmoles), then decrease in CPP, then increase in ICP with a fall of the CBF, then Ischemia, and greater cerebral edema [10, 21] (Fig. 68.5a, b).

The dialysate bicarbonate concentration also plays a potential role in cerebral edema and acute brain injury. During hemodialysis, as the serum bicarbonate level and arterial blood pH rise, there is paradoxical intracellular acidosis (Fig. 68.5a). The intracellular acidosis leads to neuron swelling and cerebral edema [26].

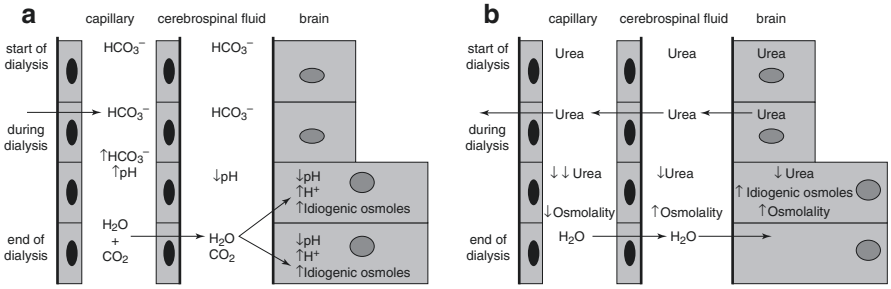

Fig. 68.5 Metabolic changes and Neurological impact during RRT: (**a**) During hemodialysis, plasma bicarbonate (HCO_3^-) level rapidly increases, but bicarbonate cannot readily pass across the BBB, whereas carbon dioxide (CO_2) diffuses rapidly. The initial increased passage of carbon dioxide into the CSF and brain leads to a reduction in pH (Henderson-Hasselbach equation), and intracellular acidosis results in the breakdown of intracellular proteins to create idiogenic osmoles that create an osmotic gradient for water movement into the brain. (**b**) Pathogenesis of dialysis disequilibrium syndrome caused by increased removal of plasma urea, with slower removal from CSF and brain tissue, thus setting up an osmotic gradient with passage of water from the relatively hypotonic plasma to the relatively hypertonic brain, causing brain edema. (Courtesy: Davenport [10]). BBB Brain blood barrier, CSF Cerebro-spinal fluid, RRT Renal replacement therapy

2.2 *Cerebral Edema: Pathophysiology*

Osmolar shift in dialysis. Secondary to the acute modification of plasma osmolarity by hemodialysis. Thus, this osmolar change causes an acute increase in brain water and a reduction in the distensibility of the brain parenchyma [27].

68.3.3 Differential Diagnosis

The symptoms of DDS that may present during the course of RRT are not specific to this syndrome, so alternative differential diagnoses should be considered:

(a) *Subdural hematoma*

Monitoring by TCCS: B-mode (brain parenchyma)

(b) Uremia

(c) Hyperosmolar nonketotic coma

(d) *Ischemic stroke/intracerebral hemorrhage*

Monitoring by TCCS: B-mode (brain parenchyma)

- Size of hematoma
- Location of hematoma
- Mass effect (midline shift)

Monitoring by TCCS: Color Doppler and spectral Doppler waveform

(e) Hypoglycemia

(f) Hypertensive emergency

(g) Hyponatremia
(h) Hypophosphatemia

In the clinical context of a critical patient, it is recommended to rule out any complications of primary neurological pathology or a secondary neurological complication before considering DDS as the primary cause of patient deterioration.

68.4 Pathophysiological Mechanism of RRT

68.4.1 Systemic Hemodynamics Changes: Impact on the CBF

1.1 Hemofiltration (many times without adequate fluid replenishment) during RRT promotes episodes of MAP drop with increase in rheological changes and plasma viscosity (η) with evidence of decrease in CPP with a consequent drop of regional CBF (CBF_R), then ischemia, and greater cerebral edema [28] (Fig. 68.5).
1.2 After MAP decreases (due to ultrafiltration) in a patient with impaired CA, CPP decrease is evidenced with a consequent drop of CBF_R, then ischemia, and greater cerebral edema occurs (Fig. 68.6).

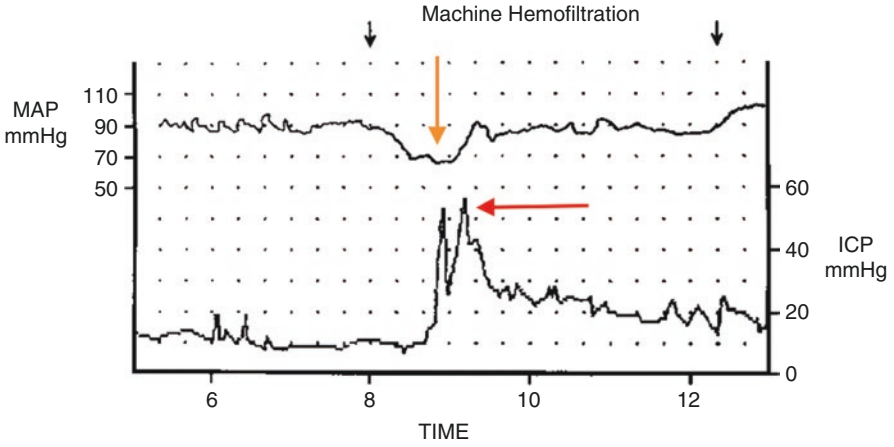

Fig. 68.6 Relationship of the mean arterial pressure (MAP) and the ICP during the session of intermittent RRT after hemofiltration. The arrow (orange) shows the MAP drop, which shows an increase in the ICP (red arrow). (Courtesy: Modified of AJKD, Davenport [10])

68.4.2 Clinical Results

The sum of the hemodynamic and metabolic events, secondary to the implementation of RRT in the patient with acute brain injury (ABI) and AKI, has as a clinical result the development and perpetuation (if treatment does not occur) of cerebral edema and its consequences at the cerebrovascular level (Fig. 68.7).

In the clinical context of a patient with acute brain injury, we must carefully analyze and evaluate the RRT modality selection and serum urea concentration.

Perform a real-time neurological monitoring by TCCS of cerebral hemodynamics pre-RRT, during RRT, and post-RRT.

2.1 *Maintenance of Cerebral Perfusion*

The cerebral perfusion pressure (CPP) is dependent on a stable mean arterial pressure and ICP changes (cerebral edema). RRT reduced CBF even in stable patients undergoing routine maintenance hemodialysis treatment (manifesting itself in cerebral blood flow velocities through TCD/TCCS). Maintenance of hemodynamic stability (avoidance of intradialytic hypotension) prevents further worsening of ABI. Thus, the ultrafiltration rate and total fluid volume need to be prescribed cautiously.

It has been postulated that the CT brain scan showed increased brain water content after IRRT (cerebral edema), whereas no such changes were observed after continuous renal replacement therapy (CRRT) [29].

2.2 *Cerebral Microembolism in Critically Ill Patient*

It is postulated that during intermittent renal replacement therapy (IRRT) and continuous renal replacement therapy (CCRT) used in intensive care units to support an AKI, there may be a greater predisposition to cerebral microembolism with a higher incidence of cerebrovascular injury (ischemic brain injury) and/or neurodegenerative disease.

There are two hypotheses (interrelated) about the physiopathology of cerebral microembolism during RRT:

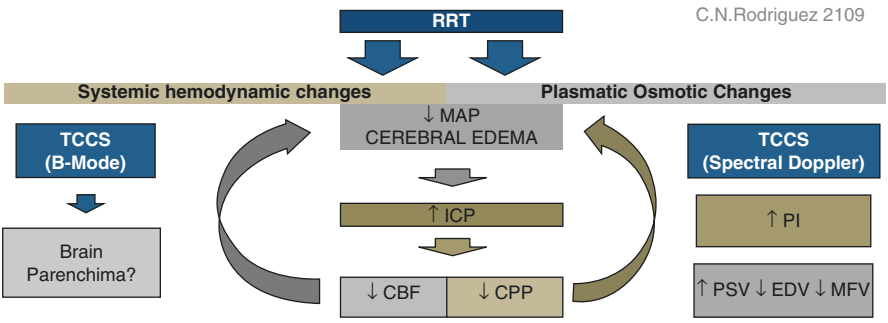

Fig. 68.7 Clinical repercussion of the Renal Replacement Therapy (RRT). CBF Cerebral blood flow, CPP Cerebral perfusion pressure, ICP Intracranial pressure, TCCS Transcranial color-coded duplex sonography, PI Pulsatility index, MAP Mean arterial pressure, EDV End diastolic flow velocity, MFV Mean flow velocity, PSV Peak systolic flow velocity, ↑ increase, ↓ decrease

2.2.1 *Microbubbles Generation*: (Gaseous)

The generation of microbubbles in the hemodialysis circuit is related to the blood flow rate and associated arterial and venous pressure changes (cavitation). Therefore, caution must be taken with the high blood flow rates and high dynamic pressure gradient.

2.2.2 *Clot Generation*: (Solid Particles [Fibrin])

Direct effect of microbubble in the microcirculation. High pressure on the endothelial cells results in activation of coagulation cascade and clot formation. These effects may contribute to, in some clinical situations, insufficient anticoagulation and/or altered biocompatibility.

These assumptions will be ratified or rectified with the forthcoming publication of the results of the COMET-AKI study [30].

- **TCD/TCCS**[(1)]
  - Detection of microembolic signals (MES) in the cerebral circulation

    Acoustic window: transtemporal
    Approach

    - Continuous (TCD head frame)
    - Intermittent (bilateral TCD/TCCS)

    Measurement: MCA

[(1)]For more details, see Chap. 37.

68.5 Neurocritical Patient and Renal Replacement Therapy (RRT)

ICU team and nephrologists should be familiar with prescription modifications that are important to safely provide dialysis care for such patients with acute brain injury, which is associated with risk of worsening cerebral edema. Prescription modifications could minimize changes in serum urea limiting water movement and brain edema.

The modalities of RRT most used today include intermittent (IRRT), continuous (CRRT), hybrid (HRRT), and peritoneal dialysis (PD).

The choice of one RRT modality over another requires analyzing some characteristics (Table 68.5):

1. *Technique*

   1.1 RRT modality
   1.2 Filter efficiency
   1.3 RRT dose
   1.4 RRT Intensity

Table 68.5 Considerations of the ICU multidisciplinary Team: Renal replacement therapy (RRT) in the neuro-critical patient

Considerations of AKI (RRT)	Variables (RRT)	Therapeutic considerations in the Neuro-critical patient
Modality/ Duration of RRT (Hours)	1. Intermittent (3–5 hours/ day) 2. Continuous (18–24 hours/ day) 3. Hybrid (8–12 hours/ day) 4. Peritoneal	Consider: The impact of the solute removal rate (solutes/ time) on plasma osmolarity. The CRRT is the most recommended in the critical patient with hemodynamic instability and in the Neuro-critical patient. The Hybrid modality can be a good alternative option in these patients population. Attention in the peritoneal dialysis (PD) where intra-abdominal instillation of large fluid volumes (>2 L) can compromise lung function (basal atelectasis) with decreased oxygenation (increase $PaCO_2$) and there are reports that increased intra-abdominal pressure may contribute to ICP increase [31].
Timing (When?)	1. Fluids overload (Resistant to Diuretics) 2. Hyperkalemia (>6.5 mmol/L) 3. Metabolic acidosis 4. Uremia 5. Oliguria/ Anuria 6. Sepsis 7. Intoxication 8. Electrolytes disturbance 9. Others	The classic indications to iniciate RRT should always be considered at the same time as the clinical status of the patient, his/her hemodynamic stability and his/her critical pathology to determine the most appropriate time of its onset and duration.
Permeability of membrane (Filter/flow)	1. High flow 2. Low flow 3. Surface area	Consider: Starting the RRT session with low flow and gradually increasing flow is a recommendation that allows monitoring in ¨real time¨ the patient's tolerance to the chosen therapy modality. Try to avoid large areas of filter surface initially.
Anticoagulation	1. Systemic (UFH-LMWH) 2. Regional (Citrate) 3. Without anticoagulation	Caution with systemic anticoagulation in patients with high probability of bleeding (SAH, ICH, TBI, ischemic stroke, etc.). Evaluate the most convenient type of coagulation (systemic vs. regional) or consider a modality that does not require anticoagulation. Systemic anticoagulation with heparin or similar agents should be avoided due to the high risk of bleeding and complications.
Dialysate solutions (Sodium and sodium bicarbonate)	$[Na^{++}]$/ $[NaHCO_3^-]$	An adequate $[Na^{++}]$ in the dialysate is very useful for intradialytic arterial hypotension management and thus obtain the least possible impact in the fall of the CBF and the CPP. Dialysate $[NaHCO_3^-]$ is a great osmotic determinant of intracerebral pH. A dialysate rich in $NaHCO_3^-$, increases the chances of developing cerebral edema and increased ICP.

Table 68.5 (continued)

Considerations of AKI (RRT)	Variables (RRT)	Therapeutic considerations in the Neuro-critical patient
Vascular access	1. Internal Jugular vein (R) 2. Internal Jugular vein (L) 3. Subclavian 4. Femoral	Evaluate the potential hemodynamic impact on drainage of the cerebral venous system through the internal jugular veins in the Neuro-critical patient. Jugular accesses can hinder cerebral venous drainage and promote an increase ICP, CBF compromise and decrease the CPP. Consider catheter placement under ultrasound guidance.
Ultrafiltration (ml/hour)	1. Yes 2. No	A high rate (ml/min) of ultrafiltration can predispose the patient to hemodynamic instability situation with drop in Cardiac Output (CO) and hypotension. Context that predisposes to CBF and CPP fall.
Filter performance	1. Efficiency 2. Intensity 3. Effectiveness	Carefully assess the Urea removal rate. A removal >40% of the basal [Urea]p in the first session can precipitate an increase the Cerebral volume (Cerebral Edema). ICP increase, CBF and CPP decrease.

RRT Renal replacement therapy, *SAH* Subaracnoid hemorrhage, *ICH* Intracerebral hemorrhage, *TBI* Trauma brain injury, *ICP* Intracranial pressure, *CPP* Cerebral perfusion pressure, *CBF* Cerebral blood flow, *[Urea]p* Plasmatic urea concentration, *UFH* Unfractioned heparin, *LMWH* Low-molecular Weight heparin, *CRRT* Continuous renal replacement therapy

2. *Administrative and management issues*

   2.1 Availability in the health center
   2.2 Experiences of medical staff

3. *Clinical status of the critical patient in ICU*

   3.1 Hemodynamic stability
   3.2 Comorbidities of the patient
   3.3 Type of critical pathology

Within the critical pathology of the patient, acute brain injury (subarachnoid hemorrhage, intracerebral hemorrhage, TBI, etc.) is a special clinical scenario. In this scenario, we must consider the secondary neurological injury when selecting the most appropriate RRT modality for the patient's clinical moment [32].

Fluid movement and osmotic changes usually occur through the blood-brain barrier (BBB) and the intravascular compartment during RRT, so patients with acute brain injury have a greater risk or susceptibility to changes in ICP.

The kinetics of urea and its plasmatic concentration changes during RRT lead the gradients that will determine the directions of the intravascular fluid movement to the cerebral parenchyma or vice versa.

68.5.1 Intermittent Renal Replacement Therapy (IRRT)

The IRRT is the most commonly used modality both in patients with CKD in hemodialysis and in patients with the AKI syndrome, inside or outside of the ICU.

The IRRT modality in its three most used modalities – hemodialysis, hemofiltration, and hemodiafiltration – is often the technique selected and considered at the beginning that adjusts to the experience and resources of the center.

IRRT utilizes the transport of solutes by simple diffusion, where the dialysate solution creates a concentration gradient across the semipermeable membrane of the filter. This technique is highly effective and rapid, resulting in sudden changes in the osmotic gradients and the plasma solutes concentration [33].

In most patients with AKI syndrome, inside or outside the ICU, IRRT is often the first choice of modality. However, we know that there are no significant differences in days of hospital stay, renal function recovery, and mortality with respect to CRRT [33]. But if the patient has a sustained severe acute brain injury, this choice becomes more complex, and special considerations have to be taken into account [10] (Table 68.6).

In this population of patients, the choice of the appropriate RRT and the objective of the treatment focus on the prevention and/or avoidance of precipitation of secondary brain injury, the adequate maintenance of cerebral hemodynamic parameters such as CBF and CPP, with an adequate control of the ICP. These treatment and monitoring objectives are affected by RRT. Patients with acute brain injury are very sensitive to abrupt changes in plasma osmolarity, which is why IRRT would be an inadequate treatment modality (cerebral edema, herniation, etc.) [34, 35].

In the neurocritical patient, the loss of the cerebral autoregulation is frequently impaired to a passive variation of CBF and CPP in the direction of MAP changes. In this context, episodes of arterial hypotension occurring during IRRT (due to either excessive ultrafiltration and/or inadequate dialysate solute concentration) produce a marked fall in CPP and a fall in velocities in the middle cerebral artery with an increase in ICP [28, 36].

Table 68.6 Strategy for IRRT

Strategy for IRRT
1. Smaller dialyzer surface area
2. Reduce blood and dialysate flow rates
3. Shorter session
4. Cooler dialysate temperature for better hemodynamic stability
5. Avoid high ultrafiltration to prevent hemodynamic instability (reduce CPP)
6. Regional Citrate (if anticoagulation is needed)
7. Consider frequent IRRT to maintain serum Urea at lower range and minimize rapidly changes
8. Lower dialysate bicarbonate to avoid the rapid rise in arterial pH
9. Higher dialysate sodium, calcium, and potassium for better hemodynamic and serum osmolality support.

CPP Cerebral perfusion pressure, *IRRT* Intermittent renal replacement therapy

However, the selection of one modality over the other should be based on the individual characteristics of each patient, their clinical status, and the experience of the center. The focus is on minimizing changes in serum osmolality and maintaining cardiovascular stability.

68.5.2 Continuous Renal Replacement Therapy (CRRT)

During admission and stay in the ICU, acute tubular necrosis (ATN) behaves as the most common cause of AKI in the hospital setting, with a multifactorial cause, whose pathophysiology results from ischemia and/or tubular nephrotoxicity. In the course of ATN (in its extension and/or maintenance phase), a percentage of patients at some point in its evolution will need RRT for the management of metabolic complications.

In most cases, the nephrologist, as a member of the ICU multidisciplinary team, will manage AKI with intermittent modality renal replacement therapy. One of the most prominent disadvantages is the risk of hypotension that occurs between 20% and 30% of the patients. However, there is a 10% of patients with AKI who do not tolerate the intermittent RRT modality (hemodynamic instability), so that continuous RRT becomes an option [37].

CRRT is a modality support that is indicated for the patient population in which intermittent therapy is not well tolerated.

Patients with AKI and acute neurologic injury (ischemic stroke, SAH, intracerebral hemorrhage, TBI, etc.), as well as those with hemodynamic instability, represent a critical patient population in which the planning of the RRT requires special considerations [1].

Treatment and support should be focused on preventing secondary brain injury, maintenance of an adequate CBF, and optimizing CPP as well as maintaining an adequate ICP, understanding that the RRT (whichever is chosen) can have a significant impact on these cerebrovascular variables.

Neurocritical patients are patients whose vascular-brain physiology is frequently altered, from proinflammatory processes in favor of cerebral edema and changes in the ICP (hence, the great sensitivity to plasma osmotic changes) to the loss of cerebral autoregulation and passive CBF changes following ABP changes, leading to ischemia or hyperemia.

We propose that CRRT should be the preferred RRT modality to support AKI in patients with acute neurological injury based on its neurological impact. The advantages and disadvantages of the modality are shown in Tables 68.7 and 68.8.

The selection of the RRT modality in the critically ill patient with acute neurological pathology should consider the prevention of secondary brain injury. The KDIGO guidelines recommend the use of CRRT for patients with ABI [38].

Table 68.7 AKI/ABI: Neurological impact of the CRRT

Continuous renal replacement therapy (CRRT)	
CRRT performance	Monitoring variable
Greater Hemodynamic Stability with less impact on Cardiac Output. *(More time per session: Less fluid removal rate)*	*MAP* (Greater control of hypotension) *CBF* (Less impact in cerebral hemodynamics)
Greater control of abrupt changes in plasma osmotic gradients. *(Control of [Urea]p, [Na^{++}]p, [$NaHCO_3^-$]p: Less water diffusion to the brain)*	*CPP* (Less impact in cerebral perfusion) *ICP* (Greater control of ICP increases: Decrease Cerebral Edema)
Greater control over secondary brain injury	

MAP Mean Arterial Pressure, *CBF* Cerebral Blood Flow, *CPP* Cerebral Perfusion Pressure, *ICP* Intracranial Pressure, *[$NaHCO_3^-$]p* Sodium bicarbonate plasmatic concentration, *[Na^{++}]p* Sodium plasmatic concentration

Table 68.8 CRRT: Advantages and disadvantages

Advantages	Disadvantages
Lower solute transport rate.	The patient persists immobilized. (Prevents the early mobilization of the critical patient in the ICU)
24 hours duration (Remove more solutes than the IRRT)	Need systemic anticoagulation (UFH – LMWH)
Fluid removal is slower (Greater hemodynamic control (lower episodes of hypotension) and better control of fluid balance)	Higher health costs (Average of U$s 474/day)
Ability to adjust the patient's treatment when required. (Ultrafiltration, TTM, etc.)	Medical/nursing ICU staff trained in the CRRT technique. (Attention: It is a continuous extracorporeal circulation technique.)

CRRT Continuous renal replacement therapy, *IRRT* Intermittent renal replacement therapy, *TTM* Target temperature management, *UFH* Unfractioned heparin, *LMWH* Low-molecular weight Heparin

68.5.3 Hybrid Renal Replacement Therapy (HRRT)

Hybrid renal replacement therapy (HRRT) is a combination of characteristics between IRRT and CRRT, becoming a very good alternative to the intolerance and/or inaccessibility to these techniques:

- Use of standard machines and supplies commonly used in the sessions programmed for the CKD patients.
- It is a "discontinuous" therapy, given that its duration generally ranges from 6 to 18 hours. (Will depend on dialysate flow and/or patient tolerance.)

- The therapy time is longer than in the IRRT. Removal of solutes and fluids slower than intermittent RRT and faster than continuous RRT. (It will be variable according to the "clinical moment" of the patient and their needs.)
- Less health costs.

3.1 *Type of HRRT most commonly used*
SLED (sustained low-efficiency dialysis)
3.2 *Characteristics of the HRRT* [39]

(a) *Adequate electrolyte and acid-base control*

(a.1) [Urea]p
(a.2) [$NaHCO_3^-$]p

(b) *Accuracy in ultrafiltration objectives without arterial hypotension*

(b.1) Great hemodynamic control
(b.2) Net ultrafiltration rate is determined by patient's need and hemodynamics stability

(c) *Good acceptance by the nursing staff*

(c.1) Nursing availability: patient in ICU can be 2:1
(Different with respect to continuous RRT that requires a 1:1 ratio.)

(d) *Less health costs*

(d.1) Less logistics

(e) *Possibility of night programming*

(e.1) Allows the possibility of working with the patient in ICU during the day

Hybrid RRT is a proven alternative for patients with acute brain injury where sudden changes in plasma osmolarity and urea concentration can deepen neurological damage [36].

Critical patients with hemodynamic instability also benefit from this type of renal replacement therapy over classic intermittent therapy.

68.5.4 Peritoneal Dialysis (PD)

Peritoneal dialysis is a technique of controversial utility in critically ill patients with acute brain injury and AKI. Although it is a technique with slower solute clearance than hemodialysis in all its versions, we must consider certain characteristics of the patient and/or the technique before its indication [40–42] (Table 68.9).

We cannot recommend the routine use of this RRT technique in the neurocritical patient. It could become a strong alternative if the ICU multidisciplinary does not have other RRT techniques. However, the ICU team must strictly control the technique implemented (time, replacement, volumes, etc.) and the patient's response.

Table 68.9 Peritoneal dialysis and some considerations

Considerations	
Pathology of the patient	In the patient with acute brain injury, neurological damage can be deepened by changes in abdominal, intrathoracic and cerebral pressures. We suggest that the ICU interdisciplinary team consider the costs and benefits of this technique in the patient with acute brain injury.
Dialysate solution	Important to consider: 1. [$NaHCO_3^-$]d 2. [Glusose]d 3. [Na^{++}]d The concentrations of these three solutes should be closely monitored. High levels of sodium bicarbonate, low levels of sodium and episodes of hyperglycemia (due to daily exposure) can promote secondary brain injury. Glucose can be changed by a more compatible option such as Icodextrin, which provides a lower glucose load.
Refill volumes	Consider the daily replacement volumes, where replacements with a volume >2 liters can have important hemodynamic repercussions due to the generation of an intraabdominal hypertension (IAH): 1. Reduction of intracerebral venous drainage. 2. Increment of the ICP and decrease of the CPP. 3. Reduction of venous return to the right atrium with the consequent fall in cardiac output and decrease in MAP; Decrease CPP. 4. Ventilation/Perfusion alterations with increase $PaCO_2$; Increase ICP. If the technique is used, replacement volumes <2 liters are recommended.
Replacement frequency	The frequency of refilling determines the time of exposure of the patient to the solutes of dialysate and their concentrations (hyperglycemia, hyponatremia, etc.) as well as repeated changes in intra-abdominal pressure. These changes of the internal environment and of the pressures (mechanical) can deepen the neurological lesion.

CPP Cerebral perfusion pressure, *ICP* Intracranial pressure, *MAP* Mean arterial pressure, *IAH* Intraabdominal hypertension, *$PaCO_2$* Arterial carbon dioxide, *[$NaHCO_3^-$]d* Sodium bicarbonate dialysate concentration, *[Na^{++}]d* Sodium dialysate concentrate, *[Glucose]d* Glucose dialysate concentration

Remember the potential cerebral hemodynamic changes through repeated intraabdominal pressure changes.

The strategy of selecting RRT for the patient with acute brain injury must be individualized for each patient and each clinical circumstances, accessibility, and experience of the center. The RRT modality that gives the patient the greatest benefits without precipitating the secondary brain injury should be considered.

68.6 Renal Replacement Therapy and Neurocritical Patient: Usefulness of TCD/TCCS

Transcranial color-coded duplex ultrasonography (TCCS) allows the visualization of intracerebral arteries and veins through the skull by color coding of blood flow velocity and the most important brain parenchyma structures by B-mode ultrasound.

On the other hand, the "blind" TCD technique is also used, where the scanning of the blood flow of the basal cerebral arteries is not performed under visible anatomical landmarks. We will focus on the TCCS technique as an important and very useful neuroimaging method.

For the development of this technique, the attending physician must follow a protocol (see Chap. 14 of the TCCS protocol for more details) to obtain a complete study directed to what is sought.

The patient with acute brain injury and AKI should not follow a different protocol at the time of conducting the study by TCCS, but we must consider specific situations in these critical patients. Summary, we expect that the ICU TCCS operator will continue with the following steps [43] (Table 68.10):

Table 68.10 TCD/TCCS examination technique (Steps to follow) [45–49]

A. TCD/TCCS steps		
1. Select the probe	Sector transducer	Low frequency (2–3.5 MHz)
2. Select the 1st acoustic window	Transtemporal	Axial planes
3. Depth	Transtemporal	140–160 mm
B. TCCS steps (B-mode)		
1. Scanning planes (Transtemporal window)	*Landmarks*	
1.1 Mesencephalic	Mesencephalon (Hypoechogenic "Butterfly") Basal cisterns (Hyperechogenic: Surrounded) Space-occuping lesions	
1.2 Diencephalic	Thalamus (Hypoechogenic) Third ventricle (Hyperechogenic)	
1.3 Ventricular	Frontal horns of the lateral ventricles (Hypoechogenic)	
2. Scanning (Transorbital window)	*Landmarks*	
2.1 ONSD	Optic nerve	
2.2 PLR	Pupil	
C. TCD/TCCS steps (Doppler/color-coded/spectral)		
1. Transtemporal acoustic window	Circle of Willis/carotid system (MCA(M1-M2)/ACA(A1)/PCA(P1-P2)/ICA-Siphon)	
2. Transforaminal acoustic window	BA/VA	
D. TCD/TCCS (Pulse Doppler/color Doppler/B-mode) – Fast track insonation protocol (1)		
1. Transtemporal acoustic window	MCA/ACA/PCA	
2. Transforaminal acoustic window	BA/VA	
3. Submandibular acoustic window	CCC/ICA/ECA	

MCA Middle cerebral artery, *M1* Segment of MCA, *M2* Segment of MCA, *ACA* Anterior cerebral artery, *A1* Segment of ACA, *PCA* Posterior cerebral artery, *P1* Segment of PCA, *P2* Segment of PCA, *ICA* Internal carotid artery, *BA* Basilar artery, *VA* Vertebral artery, *PLR* Pupillary light reflex, *ONSD* Optic nerve sheath diameter, *CCA* Common carotid artery, *ECA* External carotid artery

(1) Fast-track insonation protocol in acute ischemic stroke. Has been developed for rapid TCD/TCCS and carotid ultrasound in parallel with neurological examination in the emergency setting of acute ischemic stroke (AIS) [50].

68.6.1 TCD/TCCS: What We Should Monitor?

We must be careful and consider some important details in the patient with acute brain injury and AKI under RRT; nothing should be left to chance (Table 68.11).

Monitoring, in real time, the cerebral hemodynamic variables and brain parenchyma by TCCS during the RRT in the acute brain injury patient will help the ICU multidisciplinary team to take an individual clinical decision for each patient, diagnosing the complications bedside.

Patient with ABI represents a population which deserves special consideration when planning RRT. Treatment should be focused on preventing secondary brain injury by maintaining appropriate CBF, CPP, and controlling intracranial pressure, essential parameter when treating ABI [10].

Table 68.11 TCD/TCCS variable monitoring in the patient with acute neurologic injury and AKI [44, 45–49]

TCD/TCCS variable	Monitoring
1. Cerebral blood flow velocities (CBFV)	*Flow pattern*
1.1 Peak systolic velocity (PSV)	Low or high resistance?
1.2 Mean flow velocity (MFV)	
1.3 End diastolic velocity (EDV)	
2. Spectral Doppler waveform analysis	Changes and trends
MCA – ACA – PCA – BA – VA – ICA	
3. Hemodynamic indexes/ratios	
3.1 Pulsatility index (PI)	Non-invasive ICP estimation
3.2 Lindegaard ratio (LR)	Vasospasm/hyperemia
3.3 Mx (mean flow index)	>0.3: Increase ICP/vasospasm
4. Brain parenchyma	
4.1 Midline	Midline shift: Mass effect
4.2 Intra-extraaxial space-occupying lesions	Diagnosis/measurement/monitoring
4.3 Lateral ventricles/3rd ventricle	Hydrocephalus: Mass effect
4.4 ONSD	ICP estimation/therapeutic response
4.5 PRL	ICP estimation: Reactivity
5. Cerebral autoregulation (CA)	Preserved/impaired
5.1 Mx (mean flow index)	>0.3 (impaired)
6. Cerebral perfusión pressure (CPP)	Non-invasive estimation/optimize

ICP Intracranial pressure, *ONSD* Ocular nerve sheath diameter, *PRL* Pupillary light reflex

68.6.2 Neuroworsening: Clinical Situations

68.6.2.1 Cerebral Edema

Elevated ICP may be the final common pathway of acute brain injury. The Monro-Kellie Doctrine defines the relationship between the volumes of intracranial components. In this case, the increase in brain volume would be the cause. The osmolality gradient between serum and brain (uremia) results in the movement of water down the concentration gradient, leading to an increased risk for cerebral edema (increase in brain water).

- *TCD/TCCS*
  - *Noninvasive ICP estimation*

    Acoustic window: transtemporal

    - *Measurements*: MCA (bilateral)
      - PW Doppler/color Doppler

        Cerebral blood flow velocity (CBFV)

        - MFV
        - EDV
        - PSV

        Hemodynamic index

        - Pulsatility index (PI)**

    **Trends in pulsatility indices (right and left brain hemispheres) during hemodialysis may be a useful noninvasive bedside method to monitor for dialysis disequilibrium syndrome [27].

    - *Flow pattern*: hypoperfusion (high resistance pattern) (Fig. 68.8) [27]
      - PI >1.4
      - EDV < 20 cm/s
      - MFV < 30 cm/s

    Acoustic window: transorbital

    - *Measurements*: ONSD/papilledema

Consider, for the clinical interpretation of cerebral hemodynamics changes it is important to monitor the trends (real-time changes in the CBFV) and the analysis of spectral Doppler wave morphology.

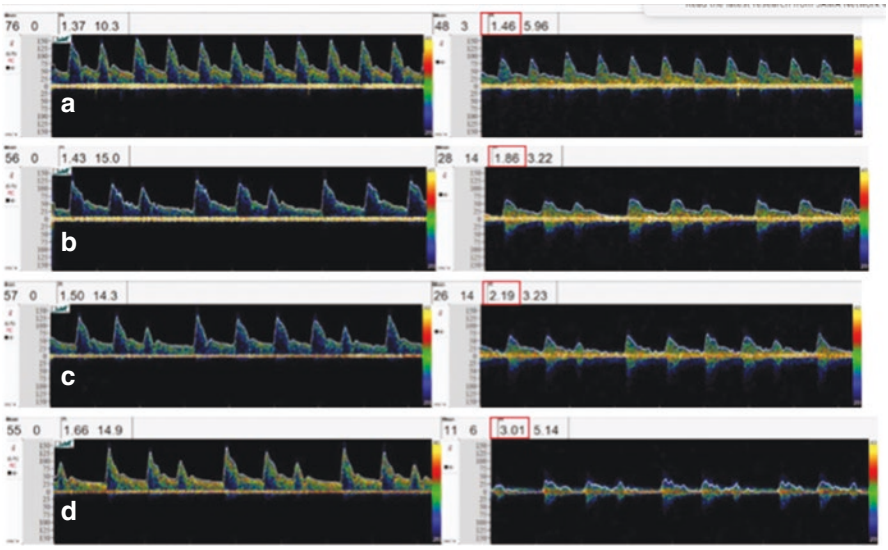

Fig. 68.8 Left and right MCA TCD waveforms during dialysis, shown on the left and right, respectively. (**a**) Baseline immediately prior to dialysis, (**b**) dialysis hour 1, (**c**) dialysis hour 2, and (**d**) dialysis hour 3. MFV is reported as the rst value on the left upper corner, PI is reported as the third value in the left upper corner. Through dialysis, velocities and waveforms on the left MCA stay relatively unchanged, with a slight increase in pulsatility index. On the right MCA, velocities are progressively reduced through dialysis, with markedly increased pulsatility index (marked by red rectangle) indicating increased distal resistance to flow. (Courtesy: Ghoshal et al. [27])

68.6.2.2 Noninvasive CPP Estimation

Cerebral perfusion pressure (CPP) is the driving pressure gradient for blood flow to the brain, which depends on the changes in the values of the ICP and the MAP.

$$\mathrm{CPP} = \mathrm{MAP} - \mathrm{ICP}$$

MAP: Mean arterial pressure

Both the decrease in MAP (ultrafiltration) and the increase in ICP (brain edema) can be influenced by the RRT technique chosen by the treating team. Therefore, much attention should be paid to the variability of CPP in the patient with ABI.

Focusing on noninvasive CPP monitoring via TCD/TCCS, there is a good correlation (r = 0.73) between CPP AND CPPE (NONINVASIVE) ESTIMATED from the MCA insonation (Eq. 68.2) [51].

$$\mathrm{eCPP} = \mathrm{MAP} \times \left(\mathrm{EDV} / \mathrm{MFV}\right) + 14 \tag{68.2}$$

- eCPP: Estimated CPP
- EDV: End-diastolic velocity
- MFV: Mean flow velocity

68.6.2.3 Cerebral Ischemia

Acute Ischemic Stroke (AIS)

In the context of the critical patient with ABI in RRT, the cause of acute ischemic stroke can be multifactorial. Sudden changes in CBF (possibly in the context of impaired CA) and/or the risk of cerebral microembolism must be considered.

- *TCD/TCCS*
  - Fast-track insonation protocol [50][(2)]
  - Detection of microembolic signals (MES) in the cerebral circulation

[(2)]For more details, see Chap. 51

Vasospasm: Delayed Cerebral Ischemia (DCI)

TCD/TCCS hemodynamic manifestation of vasospasm in the context of SAH: High MFV (cm/s) and high Lindegaard ratio (LR). Therefore, arterial vasospasm is considered the most common cause of ischemia and clinical deterioration; especially delayed cerebral ischemia (DCI). Alterations in CBF and potential electrolyte disturbance during RRT may predispose to this complication in patients with ABI, especially if it is an SAH and/or TBI.

- *TCD/TCCS*:
  - *Vasospasm*

    B-mode: color-coded duplex and PW Doppler
    Acoustic window: transtemporal, submandibular, and transforaminal
    Arterial CBFV: vasospasm [52]

    - MCA
    - ICA
    - *Measurements* (anterior circulation)
      - MFV_{MCA}

        Mild: 120–159 cm/s
        Moderate: 160–199 cm/s
        Severe: ≥ 200 cm/s

      - *Lindegaard ratio* (LR)

        LR: <3 (suggestive of hyperemia)
        LR: 3–6 (mild-to-moderate vasospasm)
        LR: > 6 (severe vasospasm)

68.6.2.4 Space-Occupying Lesion

Intracerebral Hemorrhage (ICH)

- *TCD/TCCS*
  - *Space-occupying lesion (mass effect)*

    Hemodynamic manifestations

    - *Acoustic window:* transtemporal (first step) and transforaminal
    - *Modes*
      - *TCD:* PW Doppler flow and power-motion mode Doppler (PMD)
      - *TCCS*: color Doppler flow imaging and PW Doppler
    - *Depth of insonation*
      - *TCCS:* 14–16 cm
      - (To recognize the hyperechoic contralateral skull)
      - *TCD:* according to the insonated vessel
    - *Spectral Doppler morphology analysis*
      - Middle cerebral artery (MCA)

        Bilateral insonation
        Consider trends of measurements
    - *Qualitative waveform changes*
      - Shape of wave (blood flow velocity pattern)
      - Differences in pulsatility amplitudes between PSV and EDV (characterized by a high diastolic component)
    - *Quantitative waveform* **changes**
      - EDV measurement
      - MFV measurement
      - Hemodynamic index

        Pulsatility index
      - Hemodynamic patterns

Parenchymal manifestations: mass effect and midline shift

- *Acoustic window*: transtemporal
  - Axial planes (supratentorial)
  - Axial plane (infratentorial): upper pons**
  - Coronal plane: (90° turn from mesencephalic plane with probe mark toward cephalic)

**Useful in cerebellar hematoma.
Using the same CT equation for estimation of intracranial hematoma volume, the formula (Eq. 68.3) [48]:

$$\mathrm{HV} = \left(A \times B \times C\right) / 2 \tag{68.3}$$

HV: Hematoma volume

- *Brain midline shift* (MLS): > 0.35–0.50 cm [53]
  - Transtemporal acoustic window through diencephalic plane to measure third ventricle
- *ONSD*
  - Transorbital acoustic window

68.7 Conclusion

In the critical patient with acute brain injury and AKI, the selection of the appropriate RRT strategy should be individualized for each patient's unique circumstances, focusing on how to best optimize all components of the dialysis prescription independently of the RRT technique chosen. The ICU multidisciplinary team must consider the "clinical moment" of the patient (e.g., plasmatic electrolytes status, serum urea concentration, urea kinetics, etc.) and acute brain injury evolution when prescribing the most appropriate RRT modality. The ICU team should consider TCCS neuroimaging as a very useful tool to monitor cerebral hemodynamic changes.

Algorithm

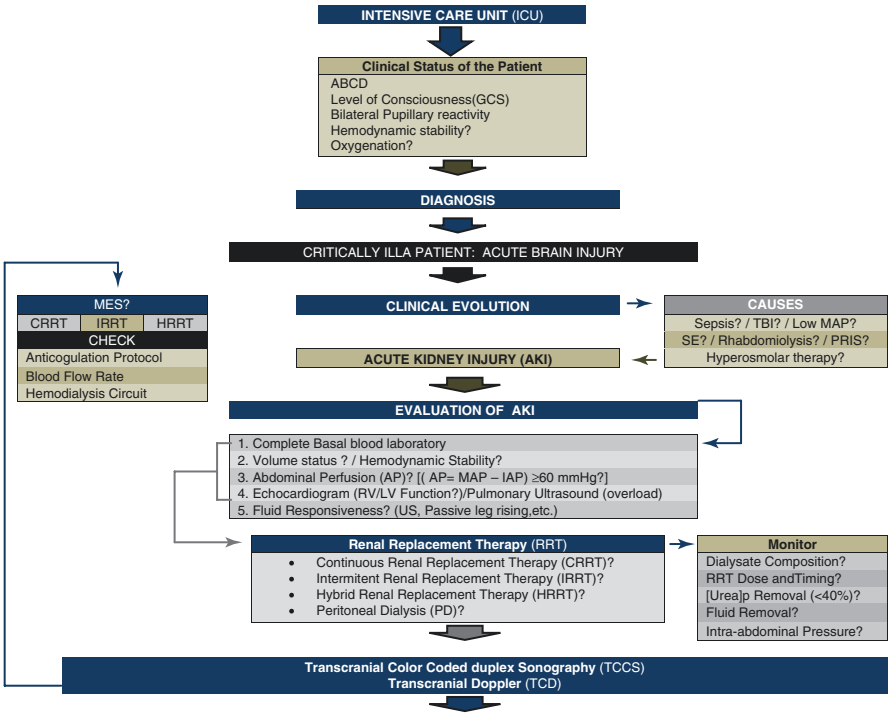

Cerebral Hemodynamic Monitoring / Brain Parenchima Monitoring (Clinical Trends)			
CRRT	**IRRT**	**HRRT**	**Peritoneal Dialysis (PD)**
Transtemporal Window	Transtemporal Window	Transtemporal Window	Transtemporal Window
Spectral Doppler Waveform Analysis and trends **(PSV- MFV- EDV)**	Spectral Doppler Waveform analysis and trends **(PSV – MFV – EDV)**	Spectral Doppler Waveform analysis and trends **(PSV – MFV – EDV)**	Spectral Doppler Waveform analysis and trends **(PSV – MFV – EDV)**
Pulsatility Index (PI)	Pulsatility Index (PI)	Pulsatility Index (PI)	Pulsatility Index (PI)
MLS?	MLS?	MLS?	MLS?
Space-occupying lesion? CA?	Space-occupying lesion? CA?	Space-occupying lesion? CA?	Space-occupying lesion? CA?
MES?	MES?	MES?	Intra-abdominal Pressure ?
Transorbital Window	Transorbital Window	Transorbital Window	Transorbital Window
ONSD? / PRL?	ONSD? / PRL?	ONSD? / PRL?	ONSD? / PRL?

ABCD Airway-breathing-circulation-disability, *TBI* Traumatic brain injury, *MAP* Mean arterial pressure, *[Urea]p* plasmatic urea, *PSV* Peak systolic velocity, *MFV* Mean velocity, *EDV* End-diastolic velocity, *ONSD* Optic nerve sheath diameter, *PRIS* Propofol infusion syndrome, *SE* Status epilepticus, *GCS* Glasgow coma scale, *MES* Microembolic signals, *US* Ultrasound, *RV* Right ventricle, *LV* Left ventricle, *MLS* Midline shift, *CA* Cerebral autoregulation

References

1. Osgood M, Muehlschlegel S. Should continuous venovenous hemofiltration always be the preferred mode of renal replacement therapy for the patient with acute brain injury? Yes. Chest. 2017;152(6):1109–11.
2. Moore PK, Hsu KR, Liu KD. Management of acute kidney injury: core curriculum 2018. Am J Kidney Dis. 2018;72(1):136–48.

3. Kellum JA, Lameire N, for the KDIGO AKI Guideline Work Group. Diagnosis, evaluation, and management of acute kidney injury: a KDIGO summary. Crit Care. 2013;17:204.
4. Kellum JA, Acute kidney injury. Crit Care Med. 2008;36(Suppl.):S141–5.
5. Uchino S, et al. Acute renal failure in critically ill patients**:** a multinational, multicenter study. JAMA. 2005;294:813–8.
6. Bellomo R, Kellum JA, Ronco C. Acute kidney injury. Lancet. 2012;380:756–66.
7. Freeman WD, Wadei HM. A brain – kidney connection: the delicate interplay of brain and kidney physiology. Neurocrit Care. 2015;22:173–5.
8. Kulkarni DK. Brain injury and the kidney. J Neuroanaesthesiol Crit Care. 2016;3:16–9.
9. Rabindranath K, Adams J, Macleod AM, Muirhead N. Intermittent versus continuous renal replacement therapy for acute renal failure in adults. Cochrane Database Sys Rev. 2007;(3):CD003773.
10. Davenport A. Renal replacement therapy in the patient with acute brain injury. Am J Kidney Dis. 2001;37(3):457–66.
11. Pickermann M, Oettl T, Mihatsch MJ. Osmotic nephrosis: acute kidney injury with accumulative of proximal lysosomes due to administration of exogenous solutes. Am J Kidney Dis. 2008;51:491–503.
12. Aiyagari V, Deibert E, Diringer MN. Hypertonic in the neurologic intensive care unit: how high is too high? J Crit Care. 2006;21:163–72.
13. Casserly B, et al. Propofol infusion syndrome: an unusual cause of renal failure. Am J Kidney Dis. 2004;44:98–101.
14. Gemmell L, Docking R, Black E. Renal replacement therapy in critical care. BJA Educ. 2017;17(3):88–93.
15. Zepeda-Orozco D, Quigley R. Dialysis disequilibrium syndrome. Pediatr Nephrol. 2012;27:2205–11.
16. Dalia T, Tuffaha AM. Dialysis disequilibrium syndrome leading to sudden brain death in a chronic hemodialysis patient. Hemodial Int. 2018;22:E39–44.
17. Lopez-Almaraz E, Correa-Rotter R. Dialysis disequilibrium syndrome and other treatment complications of extreme uremia: a rare occurrence yet not vanished. Hemodial Int. 2008;12:301–6.
18. Patel N, Dalal P, Panesar M. Dialysis disequilibrium syndrome: a narrative review. Semin Dial. 2008;21:493–8.
19. Arieff AI, Massry SG, Barrientos A, Kleeman CR. Brain water and electrolyte metabolism in uremia: effects of slow and rapid hemodialysis. Kidney Int. 1973;4:177–87.
20. Arieff AI. Dialysis disequilibrium syndrome: current concepts on pathogenesis and prevention. Kidney Int. 1996;45:629–35.
21. Daugirdas JT. Second generation logarithmic estimates of single-pool variable volume Kt/V: an analysis of error. J Am Soc Nephrol. 1993;4:1205–13.
22. Berger M, Faulstich M, Perl T, Zimmermann S. Continuous in-line monitoring of electrolyte concentrations in extracorporeal circuits for individualization of dialysis treatment. J Sens Sens Syst. 2018;7:559–67.
23. Lund A, Damholt MB, Wiis J, Kelsen J, Strange DG, Møller K. Intracranial pressure during hemodialysis in patients with acute brain injury. Acta Anaesthesiol Scand. 2019;63(4):493–9.
24. Davenport A. Renal replacement therapy for the patient with acute traumatic brain injury and severe acute kidney injury. Contrib Nephrol. 2007;156:333–9.
25. Hoste EAJ, Dhondt A. Clinical review: use of renal replacement therapies in special groups of ICU patients. Crit Care. 2012;16:201.
26. Shapiro JI, et al. Brain pH responses to sodium bicarbonate and carbicarb during systemic acidosis. Am J Phys. 1989;256:H1316–21.
27. Ghoshal S, Gomez J, Sarwal A. Transcranial Doppler monitoring of dialysis disequilibrium in an ESRD patient with traumatic brain injury. Neurocrit Care. 2020;32:353–6.
28. Stefanidis I, Bach R, Mertens PR, et al. Influence of hemodialysis on the mean blood flow velocity in the middle cerebral artery. Clin Nephrol. 2005;64:129–37.

29. Ronco C, Bellomo R, Brendolan A, Pinna V, La Greca G. Brain density changes during renal replacement in critically ill patients with acute renal failure. Continuous hemofiltration versus intermittent hemodialysis. J Nephrol. 1999;12(3):173–8.
30. Erdoes G, Uehlinger DE, Kobel B, Stucki MP, Wiest R, Stueber F, et al. Cerebral microembolism in the critically ill with acute kidney injury (COMET-AKI trial): study protocol for a randomized controlled clinical trial. Trials. 2018;19:189.
31. Gondo G, et al. Comparison of five modes of dialysis in neurosurgical patients with renal failure. Neurol Med Chir. 1989;29:1125–31.
32. Kellum JA, Bellomo R, Ronco C. Continuous renal replacement therapy: Chapter 11. Oxford: Oxford University Press; 2016.
33. John S, Eckardt KU. Renal replacement therapy in the treatment of acute renal failure-intermittent and continuous. Semin Dial. 2006;19(6):455–64.
34. Osgood M, et al. Rapid unexpected brain herniation in association with renal replacement therapy in acute brain injury: caution in the neurocritical cara unit. Neurocrit Care. 2015;22(2):176–83.
35. Kumar A, Cage A, Dhar R. Dialysis-induced worsening of cerebral edema in intracranial hemorrhage: a case series and clinical perspective. Neurocrit Care. 2015;22(2):283–7.
36. Davenport A. Practical guidance for dialyzing a hemodialysis patient following acute brain injury. Hemodial Int. 2008;12:307–12.
37. Tolwani A. Continuous renal-replacement therapy for acute kidney injury. N Engl J Med. 2012;367:2505–14.
38. Kidney Disease Improving Global Outcomes (KDIGO). Clinical practice guideline for acute kidney injury. Kidney Int Suppl. 2012;2(1):1–138.
39. Marshall MR, Golper TA, Shaver MJ, Alam MG, Chatoth DK. Sustained low-efficiency dialysis for critically ill patients requiring renal replacement therapy. Kidney Int. 2001;60:777–85.
40. Krane NK. Intracranial pressure measurement in a patient undergoing hemodialysis and peritoneal dialysis. Am J Kidney Dis. 1989;13:336–9.
41. Gondo G, et al. Comparison of five models of dialysis in neurosurgical patients with renal failure. Neurol Med Chir. 1989;29:1125–31.
42. Ivarsen P, Povlsen JV, Jensen JD. Increasing fill volume reduces cardiac performance in peritoneal dialysis. Nephrol Dial Transplant. 2007;22:2999–3004.
43. Bartels E. Transcranial color-coded duplex ulrasonography in routine cerebrovascular diagnostics. Pers Med. 2012;1:325–30.
44. Robba C, Cardim D, Sekhon M, Budohoski K, Czosnyka M. Transcranial Doppler: a stethoscope for the brain-neurocritical care use. J Neurosci Res. 2017:1–11.
45. Hakimi R, Alexandrov AV, Garami Z. Neuro-ultrasonography. Neurol Clin. 2020;38(1):215–29.
46. Lau VI, Jaidka A, Wiskar K, Packer N, Tang JE, Koenig S, Millington SJ, Arntfield RT. Better with ultrasound: transcranial Doppler. Chest. 2020;157(1):142–50.
47. Blanco P, Blaivas M. Applications of transcranial color-coded sonography in the emergency department. J Ultrasound Med. 2017;36(6):1251–66.
48. Seidel G, Kaps M, Dorndorf W. Transcranial color-coded duplex sonography of intracerebral hematomas in adults. Stroke. 1993;24(10):1519–27.
49. Robba C, Taccone FS. How I use transcranial Doppler. Crit Care. 2019;23(1):420.
50. Chernyshev OY, Garami Z, Calleja S, et al. Yield and accuracy of urgent combined carotid/transcranial ultrasound testing in acute cerebral ischemia. Stroke. 2005;36:32–7.
51. Czosnyka M, Matta BF, Smielewski P, Kirkpatrick PJ, Pickard JD. Cerebral perfusion pressure in head-injured patients: a noninvasive assessment using transcranial Doppler ultrasonography. J Neurosurg. 1998;88(5):802–8.
52. Bonow RH, Young CC, Bass DI, Moore A, Levitt MR. Transcranial Doppler ultrasonography in neurological surgery and neurocritical care. Neurosurg Focus. 2019;47(6):E2.
53. Motuel J, Biette I, Srairi M, Mrozek S, Kurrek MM, Chaynes P, et al. Assessment of brain midline shift using sonography in neurosurgical ICU patients. Crit Care. 2014;18(6):676.

Chapter 69
Central Nervous System Infection in ICU: Usefulness of Transcranial Doppler (TCD/TCCS) to Cerebral Hemodynamics Monitoring

Martin Müller, Mareike Österreich, Lehel Lakatos, and Manuel Bolognese

Key Points

1. Cerebrovascular complications are frequent in infectious meningitis.
2. Narrowing of the basal cerebral arteries is a marker of an increased stroke risk and a worse clinical outcome.
3. There is a distinct spectrum of causative pathogens which cause arterial narrowing.
4. The main purpose of TCD/TCCS monitoring is to alert physicians of potential complications.
5. The stage 1, from admission to day 3. In this period, raised intracranial pressure due to hydrocephalus, brain edema, and inflammatory mass effects is at the center to determine the cerebral hemodynamics.
6. The stage 2, from day 3 to day 8, and beyond. At this stage, a clear causative pathogen dependency of CBFV development exists.
7. The first sign of a disturbed cerebral blood flow is the disappearance of the systolic window as a result of the increasing number of low frequencies.

69.1 Introduction

Acute infectious meningitis involves not only the leptomeninges. A consequence of infected leptomeninges is a disturbed flow of the cerebrospinal fluid (CSF), which could be caused by a reduced rate of CSF adsorption. That can result in hydrocephalus, brain edema, and raised intracranial pressure. If the brain itself is infected, a diffuse encephalitis is present with brain edema and severe mass effect, again

M. Müller (✉) · M. Österreich · L. Lakatos · M. Bolognese
Department of Neurology, Luzerner Kantonsspitals, Lucerne, Switzerland
e-mail: martin.mueller@luks.ch; mareike.oesterreich@luks.ch; lehel-barna.lakatos@luks.ch; manuel.bolognese@luks.ch

C. N. Rodríguez et al. (eds.), *Neurosonology in Critical Care*,
https://doi.org/10.1007/978-3-030-81419-9_69

leading to raised intracranial pressure (ICP). If the encephalitis (or cerebritis) is encapsulated, a brain abscess has developed. Depending on the causative pathogen, arterial narrowing, or occlusion with consecutive strokes, sinus/venous thrombosis can occur [1]. Cerebral autoregulatory disturbances are frequent. When cerebral blood flow velocity (CBFV) is examined in these diseases, some systemic factors such as $PaCO_2$, pH, and hemoglobin concentration need to be considered in the analysis and interpretation of the data.

Most of the literature investigating CBFV dynamics in viral and bacterial meningoencephalitis arose from studies in the 1990s and early 2000s and demonstrated a cerebrovascular involvement in 20–50% of the patients [2–5]. These data were generated in the time period before corticosteroid therapy was established as a clinical relevant adjuvant therapy [6]. At least in the high-income countries, adjuvant steroid therapy reduces hearing loss and short-term neurological sequeale considering all bacterial pathogens [7] and mortality in meningitis due to *Streptococcus pneumoniae* [8]. It is, however, not proven that the corticosteroid therapy reduces the risk of vascular narrowing. In fact, in one recent study, patients with adjuvant steroid therapy had had a higher frequency of elevated CBFVs and strokes than the patients without steroid therapy [5]. Thus, increased CBFVs are still indicative for the risk of stroke occurring during the disease course which might deteriorate the clinical outcome.

69.2 TCD/TCCS: Monitoring and Interpretation

The main purpose of TCD/TCCS monitoring is to alert physicians of potential complications. Be always aware that the actual velocity and waveform depend on several factors. Use in each individual patient always the same ultrasound device (either TCD or TCCS, do not switch between them). According to our experience, monitoring should be performed until day 8 after admission because the most vascular complications with prognostic relevance occur within this time period [9].

69.3 Impact on Flow Velocities and Pulsatility Index

Three studies [2, 4, 5] demonstrated a relatively uniform CBFV pattern over time. Of note, the pathological CBFV findings are usually present across the whole arterial segment (e.g., the M1-segment; (Fig. 69.1)) and correspond more closely to the Doppler findings in subarachnoid hemorrhage (vasospasm) than to those in focal arteriosclerotic stenosis. We propose two stages of CBFV development:

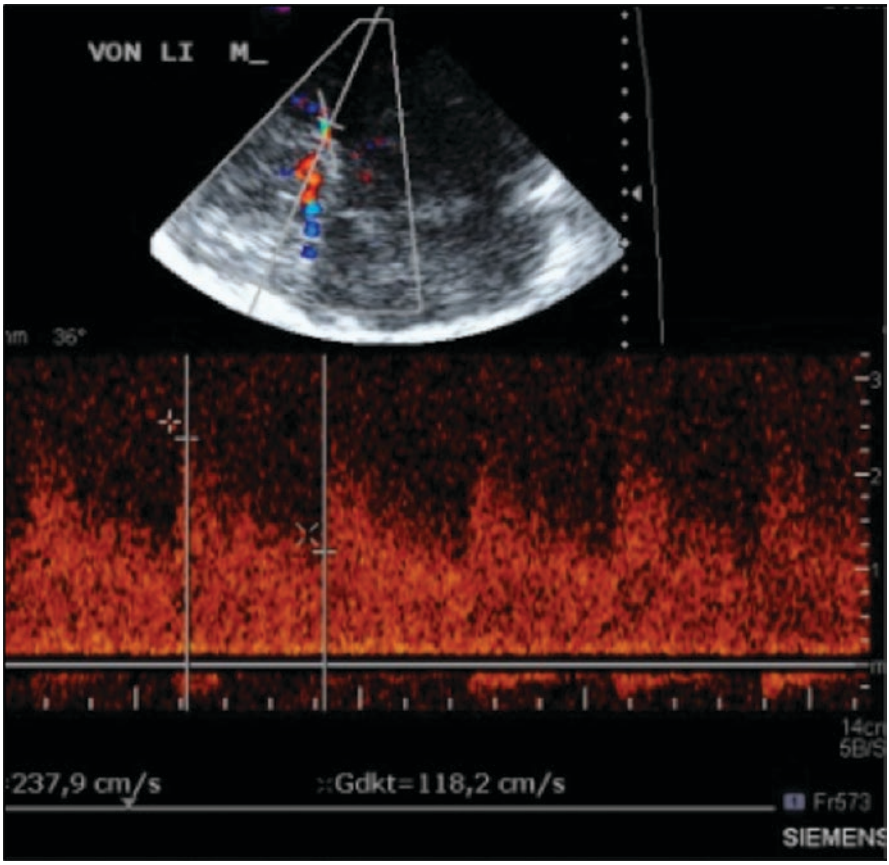

Fig. 69.1 A characteristic cerebral blood flow velocity finding across the whole M1-segment (MCA) in a patients with bacterial meningitis (von li indicates left side)

69.3.1 Stage 1

From admission to day 3. In this period, raised ICP due to hydrocephalus, brain edema, and inflammatory mass effects are at the center to determine the cerebral hemodynamics. At this stage, there is a high correlation between patient's clinical state [according to Glasgow Coma Scale (GCS)] with PI and mean CBFV (Table 69.1) [10]: At GCS 14–15, mean CBFV and Pulsatility index (PI) are increased; with decreasing GCS, mean CBFV decreases and PI increases. We consider the findings as hyperemic CBF when GCS is 14–15. Thereafter, ICP increases with the result that PI increases and mean CBFV decreases.

Table 69.1 MFV and pulsatility index (PI) in the middle cerebral artery in patients with bacterial and viral meningitis at different levels of Glasgow coma scale (GCS) at the early stage of the diseases

	Controls	GCS 14–15	GCS 10–13	GCS 3–9
MFV (cm/s)	57 ± 13	71 ± 18	55 ± 21	41 ± 41
PI	0.83 ± 0.15	0.93 ± 0.22	1.40 ± 0.58	2.81 ± 2.06

PI = (PSV – EDV)/MFV; *PSV* Peak-systolic velocity, *EDV* End-diastolic velocity
Courtesy: Adapted from Müller et al. [10]

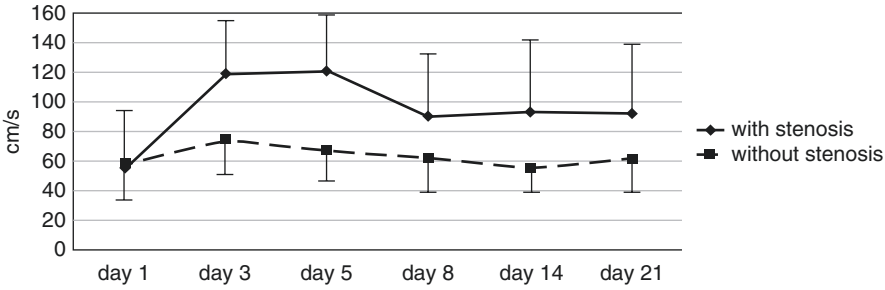

Fig. 69.2 Time course of mean middle cerebral artery blood flow velocity (MFV_{MCA}) (± SD) in patients with bacterial meningitis dichotomized in arteries with and without a stenosis during the first 8 days. (Courtesy: Adapted table 1 from Müller et al. [9])

69.3.2 Stage 2

From day 3 to day 8, and beyond. At this stage, a clear causative pathogen dependency of CBFV development exists. Causative pathogens which are frequently accompanied by vascular narrowing or strokes are Streptococcus pneumoniae, Neisseria meningitidis, Mycobacterium tuberculosis, Cryptococcus, Treponema pallidum and Borrelia burgdorferi, Varicella zoster virus, Herpes simplex virus and HIV, and Cysticercosis due to *Taenia solium* [2–5, 11, 12]. The formal pathogenesis of arterial narrowing is not clear yet because the causative pathogens are not regularly present in the vessel wall. In the group of pathogens causing arterial narrowing, a steep CBFV increases as correlate of vascular narrowing develops over time and is most frequently observed between days 3 and 8 with its maximum on days 5 or 6, thus demonstrating some similarities to the development of vasospasm due to subarachnoid hemorrhage (Fig. 69.2). Because raised ICP contradicts CBFV increase, the absolute CBFV might not reach the definition of a stenosis defined on CBFV solely. In our research, we defined a MCA stenosis as either a mean CBFV ≥120 cm/s (comparably to the diagnosis of vasospasm in subarachnoid hemorrhage) or by an MCA/ICA ratio of >3 (Lindegaard index >3) which is of help to correct for raised ICP [4]. Klein et al. [5] used a cutoff velocity of 150 cm/s peak systolic velocity. With CBFV increase, PI normalizes. Clinically, however, with the presence of arterial narrowing, patient's condition becomes worse or remains poor as indicated by either GCS or a stroke scale [13], and the frequency of strokes is

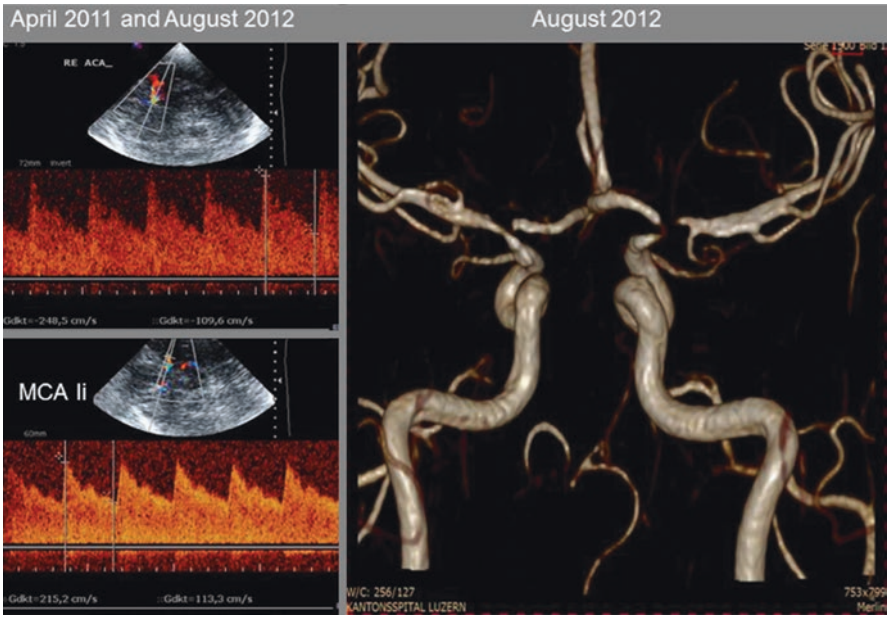

Fig. 69.3 The time course of an intracranial tuberculous ICA-stenosis from its initial diagnosis to its chronic phase. On the left, the Doppler findings in April 2011 and August 2012: at both time points the cerebral blood flow velocity elevations were nearly identical in the right (re) anterior cerebral artery (ACA) and the left (li) middle cerebral artery (MCA). On the right, the corresponding magnetic resonance imaging angiography after 1 year of adequate therapy

significantly increased [5]. Beyond day 8, most patients recover but those with stenosis remain more handicapped than those without [5, 13].

In all other causative pathogens, a CBFV increase of approximately 30% compared to the one on day 1 can be present which most likely reflects hyperemia [3, 4].

Beyond day 21 a persisting stenosis is rare in infections with *Streptococcus pneumoniae*, *Neisseria meningitides* but more frequently present in infections with tuberculosis, Cryptococcus, and Cysticercosis [11, 12]. An example is given in Fig. 69.3.

69.3.3 Pulsatility Index

The actual PI in the intracranial arteries is the product of mainly the following factors: cardiac stroke volume and intracranial vascular resistance, which by itself is determined by blood $PaCO_2$ concentration and ICP as long as no additional other vascular pathologies are present. In meningitis (mostly viral) which affects the meninges only and is not followed by CSF flow dynamic disturbances, the inflammatory process can cause a hyperemia and a reduced PI. With rising intracranial

pressure, the PI increases. If arterial narrowing of the basal cerebral arteries occurs, an intact cerebral autoregulation will lead to arteriolar vasodilation with PI becoming reduced again in the effort to compensate arterial narrowing. If cerebral autoregulation is exhausted, the PI is determined by intracerebral pressure again.

69.3.4 Changes in the Spectral Doppler Waveform

The spectral Doppler wave form changes to be observed in meningoencephalitis are quite similar to those observed in vasospasm of subarachnoid hemorrhage. The first sign of a disturbed flow is the disappearance of the systolic window as a result of the increasing number of low frequencies. The most frequent Doppler spectrum is the one shown in our figures with the presence of a frequency distribution over the whole frequency range. At very tight vessel narrowing, the bruits and aliasing phenomena are to hear/to observe.

69.3.5 Cerebral Autoregulation

Cerebral autoregulation in bacterial or viral meningitis has been rarely investigated by means of Doppler sonography in humans; in one study, 8 out of 9 patients demonstrated autoregulatory impairment [14]. There exist two lager studies which have used Single Photon Emission Computed Tomography (SPECT) to assess cerebral blood flow globally and regionally. In both studies, regional autoregulatory disturbances were frequent, and in one study, the findings corresponded to the actual disease severity [15, 16]. We did not find a study in humans on cerebral autoregulation in bacterial or viral meningitis in which the approach of dynamic cerebral autoregulation was used. This approach is noninvasive and more convenient than the approaches with manipulating blood pressure or $PaCO_2$ concentration, or with methods measuring directly cerebral blood flow.

69.4 Conclusion

The information derived from Doppler-Sonography in patients with bacterial, fungal, and viral meningoencephalitis correlates with the patient's actual clinical state and is relevant for patient's prognosis. Therefore, this information should be used to modify therapeutic strategies, for example, by lowering of ICP additionally to the therapy with antibiotics and corticosteroids. If the causative pathogen is not to identify, the knowledge of which pathogens cause arterial narrowing can help to guide the antibiotic chemotherapy.

Algorithm

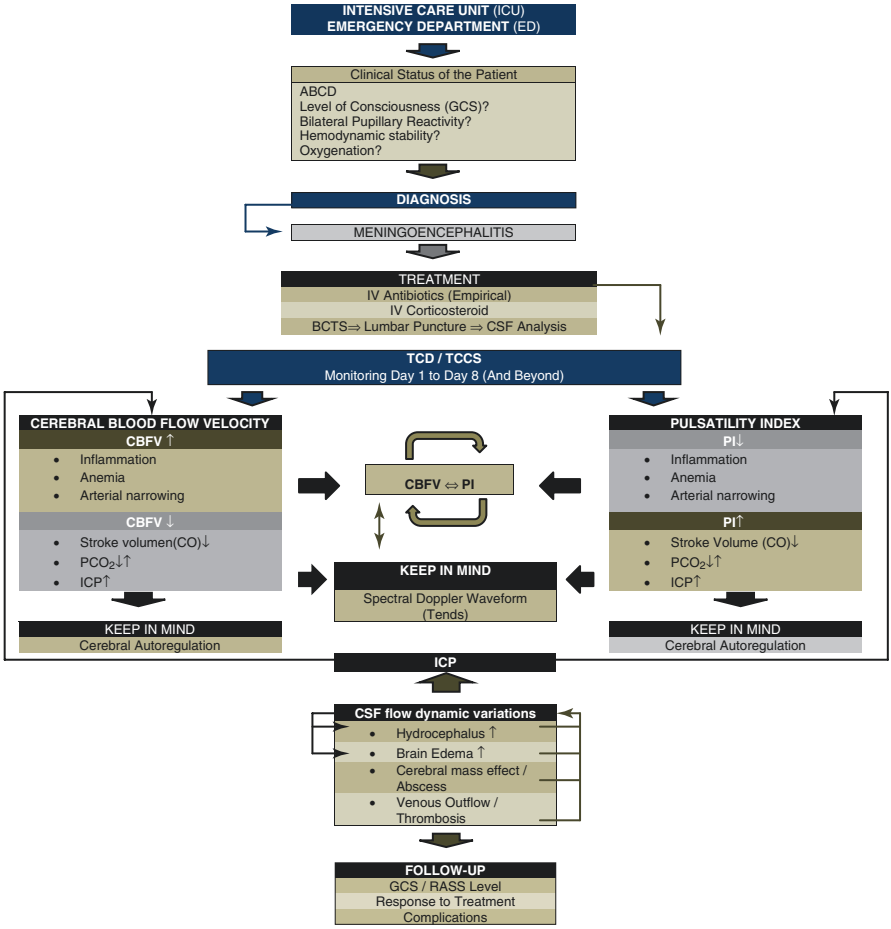

ABCD Airway-breathing-circulation-disability, *PI* Pulsatility index, *GCS* Glasgow coma scale, *RASS* Richmond agitation and sedation scale, *ICP* Intracranial pressure, *CO* Cardiac output, *IV* Intravenous, *BCTS* Brain computed tomography scan, *CSF* Cerebral spinal fluid, *ABC* Airway-breathing-circulation, *CBFV* Cerebral blood flow velocity

References

1. Pfister HW, Borasio GD, Dirnagl U, Bauer M, Einhäupl KM. Cerebrovascular complications of bacterial meningitis in adults. Neurology. 1992;42:1497–504.
2. Haring HP, Rötzer HK, Reindl H, Berek K, Kampfl A, Pfausler B, et al. Time course of cerebral blood flow velocity in central nervous system infections. A transcranial Doppler sonography study. Arch Neurol. 1993;50:98–101.

3. Müller M, Merkelbach S, Hasert K, Schimrigk K. Transkranielles Doppler-sonographisches Monito-ring von Patienten mit viralen Infektionen des zentralen Nervensystems. Nervenarzt. 1995;66:754–9.
4. Müller M, Merkelbach S, Huss GP, Schimrigk K. Clinical relevance and frequency of transient stenoses of the middle and anterior cerebral arteries in bacterial meningitis. Stroke. 1995;26:1399–403.
5. Klein M, Koedel U, Pfefferkorn T, Zeller G, Woehrl B, Pfister H-W. Arterial cerebrovascular complications in 94 adults with acute bacterial meningitis. Crit Care. 2011;15:R281.
6. Gans J, Beek D. Dexamethasone in adults with bacterial meningitis. N Engl J Med. 2002;347:1549–56.
7. Brouwer MC, McIntyre P, Prasad K, van de Beek D. Corticosteroids for acute bacterial meningitis. Cochrane Database Syst Rev. 2015;9:CD004405.
8. Buchholz G, Koedel W, Pfister H-W, Kastenbauer S, Klein M. Dramatic reduction of mortality in pneumococcal meningitis. Crit Care. 2016;20:312.
9. Müller M, Merkelbach S, Hermes M, König J, Schimrigk K. Relationship between short-term outcome and occurrence of basal cerebral artery stenosis in survivors of bacterial meningitis. J Neurol. 1998;245:87–92.
10. Müller M, Merkelbach S, Hermes M, Schimrigk K. Transcranial Doppler sonography at the early stage of acute central nervous systems infections in adults. Ultrasound Med Biol. 1996;22:173–8.
11. Chang WN, Lu CH, Chang HW, Lui CC, Tsai NW, Huang CR, et al. Time course of cerebral hemodynamics in cryptococcal meningitis in HIV-negative adults. Eur J Neurol. 2007;14:770–6.
12. Lu CH, Chang WN, Chang HW, Chung KJ, Tsai NW, Lui CC, et al. Clinical relevance of intracranial arterial stenoses in tuberculous and cryptococcal meningitis. Infection. 2007;35:359–63.
13. Merkelbach S, Röhn S, König J, Müller M. Usefulness of clinical scores to predict outcome in bacterial meningitis. Infection. 1999;27:239–43.
14. Møller K, Qvist T, Tofteng F, Sahl C, Sønderkaer S, Dethloff T, et al. Cerebral blood flow and metabolism during infusion of norepinephrine and propofol in patients with bacterial meningitis. Stroke. 2004;35:1333–9.
15. Haring H, Kampfl A, Grubwieser G, Donnemiller E, Pfausler B, Schmutzhard E. Cerebral blood flow velocity and perfusion in purulent meningitis: a comparative TCD and 99M-TC-HMPAO-SPECT study. Eur J Neurol. 1998;5:75–81.
16. Merkelbach S, Müller M, Huber G, Schimrigk K. Alterations of cerebral blood flow in the acute phase of bacterial and viral meningoencephalitis. AJNR Am J Neuroradiol. 1998;19:433–8.

Chapter 70
Pneumoperitoneum and Trendelenburg Position During Abdominal Surgery: Usefulness of Transcranial Doppler (TCD/TCCS) to Non-invasive Intracranial Pressure Monitoring

Karthikka Chandrapatham, Chiara Robba, and Danilo Cardim

Key Points

1. Comprehension of pathophysiological effects laparoscopy-induced pneumoperitoneum and the variations in brain homeostasis linked to Trendelenburg position.
2. Knowledge of the non-invasive techniques that can monitor changes in ICP in the perioperative setting.
3. Description of the measurements that can be used.
4. Proposal of an algorithm easily applicable in the operating room.

K. Chandrapatham
Department of Surgical Sciences and Integrated Diagnostics, Anaesthesia and Intensive Care, San Martino Policlinico Hospital, IRCCS for Oncology, University of Genoa, Genoa, Italy

C. Robba
Department of Anaesthesia and Intensive Care, Ospedale Policlinico San Martino IRCCS, IRCCS for Oncology, University of Genoa, Genoa, Italy

Deputy Neurointensive Care section - ESICM, Brussels, Belgium

D. Cardim (✉)
Brain Physics Laboratory, Division of Neurosurgery, Department of Clinical Neurosciences, Addenbrooke's Hospital, University of Cambridge, Cambridge, UK

Institute for Exercise and Environmental Medicine, Texas Health Presbyterian Hospital Dallas, Dallas, TX, USA

Department of Neurology and Neurotherapeutics, University of Texas Southwestern Medical Center, Dallas, TX, USA
e-mail: danilo.cardim@gmail.com

C. N. Rodríguez et al. (eds.), *Neurosonology in Critical Care*,
https://doi.org/10.1007/978-3-030-81419-9_70

70.1 Introduction

Laparoscopic surgery is becoming a common technique for different types of surgery, such as urologic, gynecologic, and general surgery, and this evolution implies that different categories of patients may be involved, including high risk and elderly patients potentially with many comorbidities. In addition to the growth in the number of surgery procedures, the progress in anesthetic management also has made the performance of prolonged laparoscopic interventions possible, carrying further risks for neurological complications.

Pneumoperitoneum consists in the insufflation of carbon dioxide gas (CO_2) inducing an iatrogenic increase of intra-abdominal pressure (IAP) that can lead to reduction of venous return and cardiac output, while there could be increased vascular resistances and both increase or decrease of heart rate. Elevated concentrations of CO_2 lead to hypercarbia and acidosis inducing cerebrovascular vasodilatation that could potentially lead to increases in intracranial pressure.

Several studies have reported the positive correlation between raised abdominal pressure and raised intracranial pressure with severe neurological complications during laparoscopic surgery. In this context, ancillary non-invasive techniques, like the TCD non-invasive assessment of intracranial pressure and the measurement of ONSD, could help clinicians to assess any changes of intracranial pressure due to variations of intra-abdominal pressure, especially in patients with history of cerebral disease.

70.2 Pneumoperitoneum and Trendelenburg: Inducing Cerebral Pathophysiological Changes

As described by Rosenthal et al. [1], the ICP increase in the framework of laparoscopic surgery is mediated by an early mechanical mechanism and a late chemical mechanism. In the early mechanical stage, IAP compresses the large abdomen vessels like the inferior vena cava, leading to a rise in central venous pressure (CVP) which impairs venous drainage from the intracranial cavity and the lumbar plexus [1]. The sudden impairment of venous return, according to Monroe-Kellie doctrine, cannot be buffered by the arterial and the parenchymal compartments, causing an elevation of intracranial pressure.

Pneumoperitoneum is induced by the insufflation of CO_2 in the abdominal cavity, which is hardly removed by ventilation considering the restrictive syndrome induced both by IAP and Trendelenburg position. The absorption of CO_2 results in an increase in arterial content of CO_2 and respiratory acidosis, which influences cerebrovascular autoregulation, causing vasodilatation, and an increase in cerebral blood flow potentially leading to ICP increase. The effect of CO_2 mediates the late chemical stage [1].

Moreover, the steep head-down position which is required for adequate surgical exposure increases central venous pressure. In supine patients, the cerebral perfusion pressure (CPP) is defined as the difference between mean arterial pressure (MAP) and the greater parameter between CVP and ICP, while in steep Trendelenburg position CPP is determined as the difference between MAP and the CVP, which is higher than ICP [2].

During head-down position, an increase in ABP and CVP can be observed. The latter impairs venous outflow from the brain, causing an increase in brain vessel's hydrostatic pressure which could lead to brain edema, impaired oxygen diffusion to the parenchyma, and increased cerebral resistances that can reduce cerebral blood flow (CBF). The increase of brain edema could change the critical closing pressure (or zero flow pressure) which is the arterial pressure at which blood flow ceases in the cerebral circulation and may represent the effective downstream pressure of the system [3]. Critical closing pressure is determined by two Starling resistors in series, one at the pre-capillary arteriolar level which is influenced by arteriolar smooth muscle tone and the other at the level of collapsible cerebral bridging veins influenced by ICP and CVP [4]. A Starling resistor is any collapsible tube surrounded in its middle section by an external pressure that is greater than the outflow pressure [5]. The pre-capillary Starling resistor ensures the effective downstream pressure as long as the ICP or CVP does not exceed the critical closing pressure of the arteriolar system and the collapsible veins in the context of prolonged steep Trendelenburg position [4].

Kalmar et al. observed that the cerebral microcirculation and cerebral autoregulation were preserved during prolonged steep Trendelenburg positioning in a study assessing zero flow pressure. They concluded that CBF increased with the increase of end-tidal CO_2, which guarantees cerebral perfusion in the context of steep Trendelenburg position and pneumoperitoneum [2].

70.3 TCD/TCCS: Perioperative Neurological Monitoring

All the variations in brain homeostasis described ahead suggest the need of monitoring cerebral blood flow and the incidence of increased intracranial pressure. During anesthesia, we should guarantee an adequate cerebral perfusion pressure and prevent ICP rises, especially in patients with higher risk of cerebrovascular conditions.

Invasive ICP monitoring using intraventricular catheters and microtransducer devices is the gold standard, but may lead to possible complications like infections, hemorrhages, and mispositioning. For routine surgeries, the risks of these invasive devices outweigh their clinical benefits, and the literature does not suggest any indications for invasive ICP monitoring in the context of abdominal surgery. In this context, non-invasive ICP monitoring could be useful in the perioperative setting.

As suggested by Robba et al., transcranial Doppler-derived formulas and optic nerve sheath ultrasound may be useful to detect variations in intracranial pressure [6].

TCD/TCCS should be performed using a 2 MHz probe in order to insonate middle cerebral artery via the trans-temporal window and the middle cerebral artery flow (MCA) velocities should be recorded: Peak systolic flow velocity (PSV), end-diastolic flow velocity (EDV), and mean flow velocity (MFV). For instance, a TCD-based non-invasive measurement of ICP (nICP) may be calculated according to Czosnyka's formula based on diastolic flow velocity [7, 8].

Firstly, non-invasive cerebral perfusion pressure (nCPP) should be calculated (Eq. 70.1):

$$\mathrm{nCPP} = \mathrm{MAP} \times \mathrm{EDV} / \mathrm{MFV} + 14 \left(\mathrm{mmHg}\right) \tag{70.1}$$

Then, nICP is calculated as the difference between MAP and nCPP (Eq. 70.2):

$$\mathrm{nICP} = \mathrm{MAP} - \mathrm{nCPP} \left(\mathrm{mmHg}\right) \tag{70.2}$$

Optic nerve sheath ultrasound should be performed using a linear probe on the closed upper eyelid. It should be measured 3 mm behind the globe using an electronic caliper. The sheath around the nerve is an extension of the dura mater and is filled with cerebrospinal fluid (CSF), so increases of intracranial pressure are detectable as rises of ONSD in the anterior, retrobulbar compartment, approximately 3 mm behind the globe.

This is the reason why ONSD has been shown to be an indirect marker of ICP [9]. The cut-off values of 5.7–5.8 mm are predictable of elevated ICP (≥20 mmHg) [10, 11] (Eq. 70.3).

$$\mathrm{ICP} \left(\text{derived from ONSD}\right) = 4.5 \times \mathrm{ONSD} - 11.3 \left(\mathrm{mmHg}\right) \left[1\right] \tag{70.3}$$

In order to detect any variations due to pneumoperitoneum and head-down positions, multiple measurements may be performed at different time points: for example, at baseline after induction of anesthesia; after pneumoperitoneum insufflation; nearly 10 minutes after Trendelenburg positioning with pneumoperitoneum insufflation; at the end of surgery, after pneumoperitoneum and in neutral position, still under general anesthesia [6].

Non-invasive methods to assess ICP, especially TCD-derived formulas, are very useful to point out relative variations of ICP, but they are less accurate in the absolute quantification of ICP values. Therefore, they are more helpful to distinguish the changes of nICP in the same individual at different time points, rather than assessing ICP as a single value [6].

70.4 Cerebral Blood Flow Velocities Changes

The insufflation of CO_2 into the abdominal cavity induces significant hemodynamic changes such as increased mean arterial pressure, central venous pressure, and systemic vascular resistance [12]. Pneumoperitoneum has the potential to increase cerebral blood flow (CBF), in addition to the rise of intracranial pressure and intraocular pressure, due to the elevated arterial CO_2 partial pressure ($PaCO_2$) that is caused by absorption of CO_2 from the peritoneal cavity.

Cerebral blood flow–carbon dioxide (CBF–CO_2) reactivity is one marker of the ability of the cerebral vasculature to react to cerebral metabolic demands. During pneumoperitoneum and Trendelenburg position CBF–CO_2 reactivity may change. Choi et al. demonstrated that there is no change in CBF–CO_2 reactivity between the supine position and the Trendelenburg position under pneumoperitoneum during sevoflurane anesthesia. They used Jugular venous oxygen saturation ($SjvO_2$) as marker of cerebrovascular reactivity. $SjvO_2$ is an indicator of global CBF, as long as the cerebral metabolic demand is constant [13]. They found that they needed higher respiratory rates to maintain the target $PaCO_2$ under Trendelenburg position and pneumoperitoneum. When $PaCO_2$ increased, $SjvO_2$ and CVP increased and arterial pH decreased significantly [14].

Another method for measuring the cerebrovascular reactivity may be transcranial Doppler ultrasonography or near-infrared spectroscopy [15]. One limitation is that they may not represent the changes of total CBF, but they are both non-invasive, safe, and repeatable techniques.

Huettemann et al. [16] showed in a TCD study on MCA CBFV data that the induction of pneumoperitoneum led to an increase in absolute CBF velocity but not in CBF–CO_2 reactivity in young children undergoing laparoscopic surgery. Cerebrovascular blood flow velocity increased, and PI decreased significantly compared with baseline values independent from $PetCO_2$. Although CBF cannot be absolutely quantified with this method, a comparison with PET measurements revealed a close correlation between changes in CBF and changes in cerebral blood flow velocities [17].

An increased cerebrovascular blood flow velocity during pneumoperitoneum indicates either an increase in CBF or a constriction of the insonated vessel. CBF remains constant if cerebral perfusion pressure is varied between 60 and 130 mmHg of MAP [18]. However, the increase in MAP occurring during pneumoperitoneum may be mediated by catecholamines and vasopressin [19, 20].

Differently from Huettemann et al. [16], Fujii et al. [21] reported that CBF velocity and CBF–CO_2 reactivity both increased with CO_2 insufflation during pneumoperitoneum in adult patients undergoing laparoscopic cholecystectomy. They kept ventilation constant and saw the increase of arterial CO_2 concentration ($PaCO_2$) from 36 to 39 mm Hg. However, this increase in $PaCO_2$ did not fully explain the

observed increase of cerebrovascular blood flow velocity. Despite a linear relationship between $PaCO_2$ and cerebrovascular blood flow velocity has been demonstrated [21–23], nearly 60–70% of the increase in CBFV was directly related to the pneumoperitoneum and not to hypercapnia [16].

70.5 ICP Changes

The effects of laparoscopy on intracranial pressure are well recorded [24, 25]. The precise mechanism by which intra-abdominal pressure influences ICP has not been clarified, but it seems to be multifactorial.

The ICP increase appears to be independent of arterial pH (and therefore carbon dioxide effects), oxygenation, or mean arterial pressure [24], and it is recorded even at low (8 mmHg) abdominal pressures, so it appears to be particularly significant when baseline ICP is increased for pre-existing neurological illnesses [26, 27].

Trendelenburg position worsens the increase in ICP during insufflation, but reverse Trendelenburg does not eliminate the observed increase. In a study of patients who underwent laparoscopy in Trendelenburg position, both the head-down and reverse Trendelenburg groups showed a statistically significant increase of ONSD, which did not return to baseline until 5 minutes after exsufflation [28].

As described by the Monroe–Kellie doctrine, the cranial cavity contains the parenchymal tissue, arterial and venous blood, and cerebrospinal fluid (CSF) in a dynamic equilibrium. When a rapid change in the volume of any of these components occurs, ICP rises. It has been proposed that increased intra-abdominal and intrathoracic pressure as well as impaired CSF absorption during insufflation hinders drainage of the lumbar venous plexus and leads to an increase in the vascular compartment of the sacral space provoking the rise in ICP [25].

Moreover, cerebral vasodilation induced by hypercapnia worsens the elevation of ICP. In most patients without pre-existing intracranial disease, the increase in ICP occurs often without clinical consequence, but adverse effects of raised ICP may arise in different ways. As demonstrated by Cooke et al., headache and nausea were significantly higher after laparoscopic abdominal surgery [29].

According to Robba et al. [27], all the nICP methods (measurement of ONSD, TCD Pulsatility Index (ICP_{PI}) and non-invasive measurement of ICP based on the diastolic component of TCD cerebral blood flow velocity (ICP_{EDV}) seem to have a good match in the detection of ICP variations during laparoscopic surgery. All of them highlighted a significant increase of estimated ICP after the institution of pneumoperitoneum and the Trendelenburg position. Only ICP_{EDV} increased significantly after pneumoperitoneum alone, maybe due to the increase of $PetCO_2$ promoting passive vasodilation and a subsequent increase of cerebral blood volume. The analysis of the ROC curve showed that ICP_{EDV} performed best to differentiate between different time points, compared with ICP_{PI} and ONSD. It seems that the concomitance of pneumoperitoneum and the head-down position causes an increase of ICP that can be detected with non-invasive methods.

Carbon dioxide increases due to gas insufflation in the abdomen, and the consequent cerebral vasodilation may act as the main mechanism involved in the observed ICP increase [27], but the threshold for risk of deranged cerebrovascular re-activity in patients during sevoflurane anesthesia is 6 kPa [30], so in patients at risk of developing intracranial hypertension (such as those with cerebral masses or any pre-existing neurological diseases) undergoing laparoscopic procedures, a non-invasive assessment of ICP would be useful to detect and eventually treat pathological increases of ICP (with the use of osmotic agents, hyperventilation, converting to an open procedure, or even abandoning the procedure) [27].

70.6 Conclusion

The main aim of medicine and the work of the anesthesiologist in the perioperative period is *"primum non nocere."* In order to avoid unexpected increases of intracranial pressure that could carry neurological scars or transitory illnesses, non-invasive monitoring such as transcranial Doppler and optic nerve sheath diameter could help the clinician to detect promptly variations to brain homeostasis in the developing setting of laparoscopy.

Algorithm

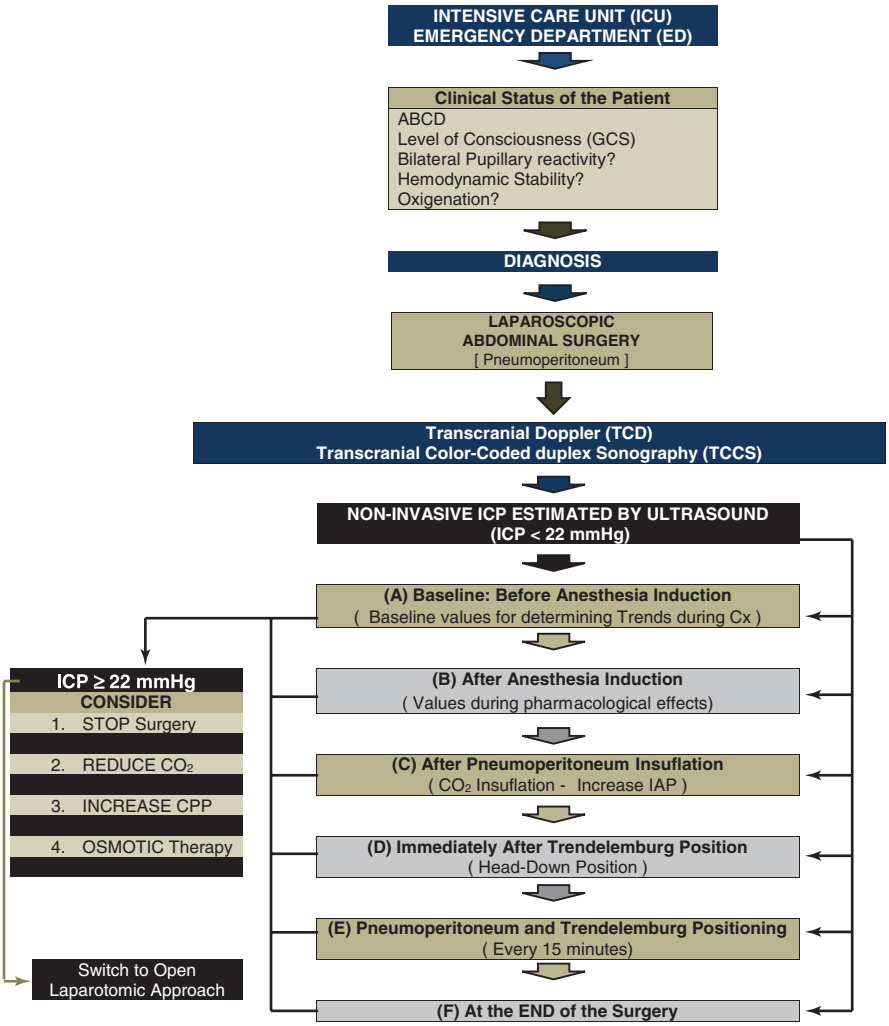

ABCD Airway-breathing-circulation-disability, *GCS* Glasgow coma scale, *CX* Surgery, *IAP* Intra-abdominal pressure, *CO_2* Carbon dioxide, *ICP* Intracranial pressure, *CPP* Cerebral perfusión pressure

References

1. Rosenthal RJ, Hiatt JR, Phillips EH, Hewitt W, Demetriou AA, Grode M. Intracranial pressure: effects of pneumoperitoneum in a large-animal model. Surg Endosc. 1997;11(4):376–80.

2. Kalmar AF, Foubert L, Hendrickx JFA, Mottrie A, Absalom A, Mortier EP, et al. Influence of steep Trendelenburg position and CO2 pneumoperitoneum on cardiovascular, cerebrovascular, and respiratory homeostasis during robotic prostatectomy. Br J Anaesth. 2010;104(4):433–9.
3. Athanassiou L, Hancock SM, Mahajan RP. Doppler estimation of zero flow pressure during changes in downstream pressure in a bench model of a circulation using pulsatile flow. Anaesthesia [Internet]. 2005 [cited 2019 Dec 7];60(2):133–8.
4. Kalmar AF, Dewaele F, Foubert L, Hendrickx JF, Heeremans EH, Struys MMRF, et al. Cerebral haemodynamic physiology during steep Trendelenburg position and CO2 pneumoperitoneum. Br J Anaesth. 2012;108(3):478–84.
5. Munis JR, Lozada LJ. Giraffes, siphons, and starling resistors: cerebral perfusion pressure revisited. J Neurosurg Anesthesiol. 2000;12:290–6.
6. Robba C, Cardim D, Donnelly J, Bertuccio A, Bacigaluppi S, Bragazzi N, et al. Effects of pneumoperitoneum and Trendelenburg position on intracranial pressure assessed using different non-invasive methods. Br J Anaesth [Internet]. 2016 [cited 2019 Mar 15];117(6):783–91.
7. Schmidt EA, Czosnyka M, Gooskens I, Piechnik SK, Matta BF, Whitfield PC, et al. Preliminary experience of the estimation of cerebral perfusion pressure using transcranial doppler ultrasonography. J Neurol Neurosurg Psychiatry. 2001;70(2):198–204.
8. Robba C, Cardim D, Sekhon M, Budohoski K, Czosnyka M. Transcranial Doppler: a stethoscope for the brain-neurocritical care use. J Neurosci Res [Internet]. 2018 [cited 2019 Mar 29];96(4):720–30.
9. Robba C, Cardim D, Tajsic T, Pietersen J, Bulman M, Donnelly J, et al. Ultrasound non-invasive measurement of intracranial pressure in neurointensive care: a prospective observational study. Schreiber M, editor. PLOS Med [Internet]. 2017 [cited 2018 Dec 19];14(7):e1002356.
10. Geeraerts T, Launey Y, Martin L, Pottecher J, Vigué B, Duranteau J, et al. Ultrasonography of the optic nerve sheath may be useful for detecting raised intracranial pressure after severe brain injury. Intensive Care Med [Internet]. 2007 [cited 2018 Nov 2];33(10):1704–11.
11. Moretti R, Pizzi B. Optic nerve ultrasound for detection of intracranial hypertension in intracranial hemorrhage patients. J Neurosurg Anesthesiol [Internet]. 2009 [cited 2018 Nov 2];21(1):16–20.
12. Joris JL, Noirot DP, Legrand MJ, Jacquet NJ, Lamy ML. Hemodynamic changes during laparoscopic cholecystectomy. Anesth Analg. 1993;76(5):1067–71.
13. Brown MM, Wade JPH, Bishop CCR, Ross Russell RW. Reactivity of the cerebral circulation in patients with carotid occlusion. J Neurol Neurosurg Psychiatry. 1986;49(8):899–904.
14. Choi SH, Lee SJ, Rha KH, Shin SK, Oh YJ. The effect of pneumoperitoneum and Trendelenburg position on acute cerebral blood flow-carbon dioxide reactivity under sevoflurane anaesthesia. Anaesthesia. 2008;63(12):1314–8.
15. Pollard V, Prough DS, Eric DeMelo A, Deyo DJ, Uchida T, Widman R. The influence of carbon dioxide and body position on near-infrared spectroscopic assessment of cerebral hemoglobin oxygen saturation. Anesth Analg. 1996;82(2):278–87.
16. Huettemann E, Terborg C, Sakka SG, Petrat G, Schier F, Reinhart K. Preserved CO2 reactivity and increase in middle cerebral arterial blood flow velocity during laparoscopic surgery in children. Anesth Analg [Internet]. 2002 [cited 2019 Dec 10];94(2):255–8.
17. Serrano-Villar S, Sainz T, Lee SA, Hunt PW, Sinclair E, Shacklett BL, et al. HIV-infected individuals with low CD4/CD8 ratio despite effective antiretroviral therapy exhibit altered T cell subsets, heightened CD8+ T cell activation, and increased risk of non-AIDS morbidity and mortality. PLoS Pathog [Internet]. 2014 [cited 2016 Jun 28];10(5):e1004078.
18. Hickey R, Albin MS, Bunegin L, Gelineau J. Autoregulation of spinal cord blood flow: is the cord a microcosm of the brain? [Internet]. Stroke. 1986 [cited 2019 Dec 10];17:1183–9.
19. Ishizuka B, Kudo Y, Amemiya A, Tanii M, Aoki T. Plasma catecholamine responses during laparoscopic gynecologic surgery with CO(2) insufflation. J Am Assoc Gynecol Laparosc [Internet]. 2000 [cited 2019 Dec 10];7(1):37–43.

20. Joris JL, Chiche JD, Canivet JLM, Jacquet NJ, Legros JJY, Lamy ML. Hemodynamic changes induced by laparoscopy and their endocrine correlates: effects of clonidine. J Am Coll Cardiol. 1998;32(5):1389–96.
21. Fujii Y, Tanaka H, Tsuruoka S, Toyooka H, Amaha K. Middle cerebral arterial blood flow velocity increases during laparoscopic cholecystectomy. Anesth Analg [Internet]. 1994 [cited 2019 Dec 10];78(1):80–3.
22. Eng C, Lam AM, Mayberg TS, Lee C, Mathisen T. The influence of propofol with and without nitrous oxide on cerebral blood flow velocity and CO2 reactivity in humans. Anesthesiology. 1992;77(5):872–9.
23. Widder B. The Doppler CO2 test to exclude patients not in need of extracranial/intracranial bypass surgery. J Neurol Neurosurg Psychiatry. 1989;52(1):38–42.
24. Grabowski JE, Talamini MA. Physiological effects of pneumoperitoneum. J Gastrointest Surg. 2009;13:1009–16.
25. Halverson A, Buchanan R, Jacobs L, Shayani V, Hunt T, Riedel C, et al. Evaluation of mechanism of increased intracranial pressure with insufflation. Surg Endosc. 1998;12(3):266–9.
26. Citerio G, Vascotto E, Villa F, Celotti S, Pesenti A. Induced abdominal compartment syndrome increases intracranial pressure in neurotrauma patients: a prospective study. Crit Care Med [Internet]. 2001 [cited 2019 Mar 15];29(7):1466–71.
27. Robba C, Bacigaluppi S, Cardim D, Donnelly J, Sekhon MS, Aries MJ, et al. Intraoperative non invasive intracranial pressure monitoring during pneumoperitoneum: a case report and a review of the published cases and case report series. J Clin Monit Comput. Springer Netherlands. 2016;30:527–538.
28. Sahay N, Sharma S, Bhadani UK, Singh A, Sinha C, Sahay A, et al. Effect of pneumoperitoneum and patient positioning on intracranial pressures during laparoscopy: a prospective comparative study. J Minim Invasive Gynecol [Internet]. 2017 [cited 2019 Dec 10];25:147–52.
29. Cooke SJ, Paterson-Brown S. Association between laparoscopic abdominal surgery and postoperative symptoms of raised intracranial pressure. Surg Endosc. 2001;15(7):723–5.
30. Wilson-Smith E, Karsli C, Luginbuehl I, Bissonnette B. Effect of nitrous oxide on cerebrovascular reactivity to carbon dioxide in children during sevoflurane anaesthesia. Br J Anaesth. 2003;91(2):190–5.

Chapter 71
Transcranial Doppler (TCD): Role for Patients After Concussion

Alexander Razumovsky

Key Points

1. Reproducibility and non-invasive testing capabilities of TCD support studies for its use as a diagnostic tool for mild TBI and marker for recovery.
2. TCD criteria for cerebral blood flow velocity and pulsatility index might allow for the differentiation of patients who may undergo secondary neurologic deterioration after acute mTBI and allow physicians better define management strategies.
3. Current results support the use of TCD measured cerebrovascular reactivity as a non-expensive and easy implemented research tool for identifying altered neurophysiology and monitoring recovery in long-term effects of mTBI.
4. In patients after mTBI TCD testing of cerebral hemodynamics may reveal earlier signs of intracranial stenosis that could lead to treatment of post-concussive symptoms.
5. TCD as a non-invasive and simple procedure must be engaged in the management of mTBI patients and must be utilized as a quantitative screening test to detect cerebrovascular disease presence.

71.1 Introduction

Traumatic brain injury (TBI) is a serious public health and medicine problem in the United States and around world because of its magnitude, cost, and consequences (e.g., death and disability), and because it is often avoidable. Each year, in the USA

A. Razumovsky (✉)
TCD Global Inc., York, PA, USA

Specialty Care, Inc., York, PA, USA
e-mail: arazumovsky@sentientmedical.com

C. N. Rodríguez et al. (eds.), *Neurosonology in Critical Care*,
https://doi.org/10.1007/978-3-030-81419-9_71

TBI contribute to a substantial number of deaths and cases of permanent disability. In 2014, there were approximately 2.87 million TBI-related emergency department (ED) visits, hospitalizations, and deaths in the USA [1]. An estimated 812,000 children (age 17 or younger) after mTBI were treated in the USA for concussion, alone or in combination with other injuries [1]. Of them, as many as 75 percent sustain a mild traumatic brain injury (mTBI) [2]. Concussions are classified as mTBI and according to USA Center for Disease Control (CDC) are the most common type of TBIs [3]. A concussion can happen when the head or body is moved back and forth quickly with an "impulsive" force transmitted to the brain, such as during a motor vehicle accident or sports injury. Concussions are often called "mild TBI" because they are usually not life-threatening. However, they still can cause serious complications, and studies suggest that recurrent concussions can be particularly dangerous [4, 5]. Worldwide, concussions are estimated to affect more than 3.5 per 1000 people a year [6]. The rate per 100,000 population of mTBI ED visits in the United States increased significantly from 569.4 (in 2006) to 807.9 (in 2012) [7]. According to CDC, there are up to 3.8 million sport-related concussions every year and up to 50% playing collision sports have concussion symptoms but only 10% report them [8]. mTBI also represents a serious concern for concussions taking place in military personnel. Information from US Department of Defense between 2000 and 2018 Q1 revealed that there were worldwide 383,947 all severities of TBI (penetrating, severe, moderate, mild, and not classifiable) and among them there were 315,897 mTBI or 82.3% [9]. At the same time, all these numbers in civilian or military health systems might not reflect the true incidence of mTBI because they do not include people who are treated in physicians' offices or outpatient facilities or those who are not seeking medical care at all. The actual number of people who sustain an mTBI is unknown; however, it is likely much higher than these estimates; individuals having less evident symptoms may not seek medical attention for their injuries or be diagnosed with mTBI at the hospital [10].

However, mTBI may cause long-term or permanent impairments and disabilities. Many people with mTBI have difficulty returning to routine, daily activities and may be unable to return to work for many weeks or months. The impact of mTBI is still mostly unknown, plus it is a well-known fact of underreporting injuries in sport and military concussions. Current methods and approaches can only describe or detect the visible brain injury and there is no correlation between imaging and physical or permanent cognitive deficits in mTBI patients [11]. Neuropsychology can detect functional impairment but may not be repeatable at frequency to monitor recovery and could be susceptible due to its subjectivity. Therefore, we still lack detailed understanding the pathophysiology following mTBI and its relation to symptoms and recovery in acute and late effects of mTBI. Further, there is lack of data on cerebral blood flow investigation in mTBI patients and the extent of neurovascular compromise in mTBI, particularly of late hemodynamic response is still largely unknown.

71.2 mTBI: Pathophysiology

The brain's response to the long-term effect of mTBI is only partially understood. Advances in brain imaging offer important tools of structural, functional, and metabolic information concerning the brain. However, significant challenges exist in terms of summarizing existing findings and translating data to improve clinical practice. Studies often involve diverse cohorts (e.g., mTBI, moderate and severe TBI, combat veterans) and employ different paradigms (symptom provocation, cognitive activation) and modalities (e.g., diffusion tensor imaging [DTI], functional magnetic resonance imaging [fMRI], single photon emission computed tomography [SPECT]) [12–14]. Current mTBI pathophysiology theory starts with rotational and/or acceleration/deceleration forces differentially affect brain tissues, that is, shearing, following by complex cascade of neurochemical/metabolic events, disruption of neuronal cell membranes and axonal stretching with indiscriminate ion flux, changes in cerebral blood flow (CBF) causing neuronal dysfunction with post-concussive metabolic vulnerability without significant acute cell death. All mentioned factors could lead to so-called neurovascular deficiency or neurovascular coupling deregulation [15–18]. In acute to sub-acute period (3 hours to 10 days) after mTBI, the increased CBF combined with increased venous oxygenation suggests an increase in CBF that exceeds the oxygen demand of the tissue, in contrast to the regional hypoxia seen in more severe TBI [19]. Though, other group of researchers also with MRI utilization showed contrary results that concussed athletes demonstrated a significant decrease in CBF at 8 days relative to within 24 hours [20] up to 1 month after concussion [21]. Reduced CBF during the acute and sub-acute phases of mTBI has been detected using imaging methods such as SPECT [22, 23] and perfusion computed tomography [24] which have several disadvantages, including financial cost, ionizing radiation, limited repetition of testing, and availability. Tagge et al. suggest that TBI, concussion, and chronic traumatic encephalopathy (CTE) represent separate nosological entities induced by different pathological mechanisms and these authors' neuropathological and ultrastructural findings are consistent with impact-induced microvascular dysfunction [25]. Tagge and co-authors also speculate that their results indicate that closed-head impact TBI represents a potent insult with potential to prompt lasting neurophysiological dysfunction and persistent (and possibly progressive) sequelae, including CTE [25]. Based on existing but still spare data, it is possible to conclude that mTBI has significant impact on the control and regulation of CBF [20–24], cerebrovascular reactivity [26], cerebral oxygenation [27], neuroinflammation [28], cardiovascular regulation [29], all of which may be compromised with mTBI [30].

71.3 mTBI: Cerebral Vasomotor Reactivity

Traditionally, research on the impact of concussions or mTBI has focused on its detrimental effect on neuropsychological function. In the sports arena, the majority of decisions regarding an athlete's recovery from such an episode and subsequent return to play and thus exposure to additional impact forces centered around performance on neuropsychological tests. However, it is well known that administration and evaluation of these tests is subjective and may not be very accurate. There is still no quantitative "biomarker" to evaluate patients with mTBI. It has been demonstrated that concussions/mTBI and sub-"event" impact forces could affect cerebral blood flow autoregulation and cerebral vasomotor reactivity (VMR). TBI has been inducing cerebral vascular dysfunction that will be reflected in altered responses to various vasodilators. VMR is a key factor in regulating CBF and represents a marker for the status of autonomic nervous system. If the brain's autoregulation is not working or impaired, testing of VMR is one method of assessing the brain's controlling capabilities or CBF autoregulation. Transcranial Doppler (TCD) methodology is a very convenient and non-expensive tool to measure VMR [31, 32]. In this method, carbon dioxide in the blood is transiently increased (i.e., as with the holding of breath), and the breath-holding index (BHI) that reflects status of VMR can be easily calculated [33, 34]. The breath-holding maneuver is a useful and well-tolerated screening method for VMR evaluation and was validated in numerous per reviewed publications [35–37].

Although assessment of cerebrovascular responses to changes in carbon dioxide pressure (i.e., VMR) after TBI, including mTBI, is not a new concept, this concept has been underexplored in long-term consequence of mTBI. While numerous studies have focused on the acute and sub-acute brain parenchymal, behavioral, and vascular changes associated with acute mTBI [35–40], few have followed these changes over a more prolonged, chronic course of injury or have attempted to correlate these changes with any enduring morbidity, like post-concussion symptoms (PCS). These PCS include headache, dizziness, fatigue, concentration problems, sadness, and irritability. Previous reports have focused primarily on the short-term vascular alterations; nobody yet attempted to correlate these alterations with any persisting behavioral changes or potential therapeutic modulation. On the vascular front, there were significant contributions to the understanding of the brain's microvascular response to injury, illustrating that in the early hours post-injury the cerebral microcirculation shows impaired vascular reactivity to known vasodilator challenges [41]. Further, research suggested that this impaired VMR may persist for at least 1 week post-injury [36, 38–40, 42]; however, beyond this period nobody till recently followed the persistence of these VMR abnormalities. Lately it was shown with MRI that there is a correlation between lower grey matter (GM) VMR indexes and lower performance on Sport Concussion Assessment Tool 2 in patients with mTBI, which seems to be associated with more symptoms. This correlation seems

to persist well beyond 120 days. mTBI may lead to a decrease in GM volume in these patients [43]. Another study also with MRI showed that individual sport-related concussion patients demonstrated both quantitative and qualitative patient-specific alterations in VMR ($p < 0.005$) that correlated strongly with clinical findings and that persisted beyond clinical recovery up to 376 days [44]. Other authors demonstrated that a panel of plasma biomarkers (Ang-1/Ang-2, SAA, VEGF, P-selectin, and vWF) and assessment of VMR might be useful combination as predictive biomarkers for therapies designed to improve cerebrovascular function in patients after TBI with persistent PCS [45].

In spite of the fact that there is a limited information available on the VMR impairment in mTBI patients with chronic symptoms, recent theories postulate that generalized autonomic dysfunction, includes abnormal VMR. Impaired axonal function/diffuse axonal injury, neuronal metabolism, perfusion, and inflammation, suggesting involvement of the neurovascular unit in the presence of persistent PCS in mTBI patients [46]. First longitudinal study to focus on PCS defined specifically as a minimum of 3 months of symptoms, negative CT and/or MRI, negative TOMM test, and no litigation. This study established that PCS may be permanent if recovery has not occurred by 3 years [47]. Another clinical longitudinal study revealed that most neuropsychological and functional differences abate by 1 year, reporting three or more post-traumatic symptoms remain for about half of individuals [48]. To address potential autonomic disturbance, some researches integrated mind-body techniques, known to affect parasympathetic tone and autonomic balance, into a four-week intensive interdisciplinary outpatient treatment program for service members with combat-related TBI and post-traumatic stress (PTS) [49]. TCD BHI testing performed in patients with chronic mTBI revealed a high prevalence of cerebral autonomic disturbance. A retrospective review of TCD studies and subjective questionnaires (Neurobehavioral Symptom Index, NSI; PTSD Symptom Checklist-Military Version, PCL-M; and Patient Health Questionnaire-9, PHQ-9) was performed on active duty service members with post-concussive headaches and mTBI. Forty-four percent had abnormal BHI's indicating impaired VMR. Abnormal BHI group had significantly higher scores on the PCL-M than the normal BHI group suggesting higher levels of PTSD in those with abnormal BHIs. The authors concluded that these autonomic disturbances may be associated with post-traumatic stress or may be an independent entity of PCS that overlaps with PTSD [49]. Exposure to mind-body training was associated with improved cerebral autoregulation as measured by changes in BHI, suggesting that this TCD BHI test might have utility as a quantitative biomarker of treatment response in patients with mTBI and PTS [49]. However, we need better understanding the sensitivity and prognostic value of CVR in chronic mTBI. It is also clear that it is a myth that all mTBI typically associated with short-term difficulties that resolve in 3 months to 1 year following injury. Larger cross-sectional, prospective, and longitudinal studies needed to examine the utility of TCD BHI testing as a clinical tool to help guide the evaluation, classification, and longitudinal management of mTBI patients.

71.4 mTBI: Cerebral Hemodynamics

Research in cerebral hemodynamics with utilization of neuroimaging modalities primarily focused on mTBI because it is the most common, the most difficult to diagnose, and the least associated with radiologic diagnosis. Currently, there are no routine imaging protocols used to evaluate concussion besides traditional clinical MR imaging (T1-weighted), or CT scans, neither of which can detect subtle structural changes, and thus are inadequate for use in the assessment and management of mTBI. Pilot study by Cubon VA et al. provided evidence of structural changes in the white matter of the brain, creating a link between concussive injury with persistent symptoms and changes on diffusion-tension imaging [50]. However, there are conflicting data on the significance of intracranial lesions on conventional brain MRI scans for mTBI, where some analyses have shown no correlation with neurocognitive symptoms or outcomes [51–53], while a multicenter study has demonstrated strong correlation and prognostic value in predicting Extended Glasgow Outcome Scale at 3-month follow-up [54]. PET represent a powerful tool for clinical research in TBI. PET measurements of CBF, oxygen metabolism, and glucose metabolism have been used to study the pathophysiology and effect of treatment in acute TBI and the relationship between clinical deficits and brain abnormalities in chronic TBI [55]. However, the clinical utility of PET in the management of individual patients with TBI, however, has not yet been demonstrated. SPECT is another promising capability to evaluate mTBI. It has an advantage over anatomic imaging in assessing brain parenchymal activity and physiologic changes. The quality of evidence for mTBI patients is strong for determining a positive prognosis in patients with normal SPECT perfusion imaging. SPECT can identify perfusion/blood deficits in mTBI that anatomic imaging inaccurately identifies or misses altogether. SPECT study showed high accuracy for negative predictive value: a negative examination usually indicates a good prognosis for mTBI and recovery from post-concussive symptoms [56]. However, detecting patients at risk for secondary neurological deterioration (SND) after mTBI in acute phase is still challenging. One of the most important challenges for the treating physician in the ED is deciding whether neuroimaging needed in patients presenting with mTBI. A non-contrast CT scan is usually the test of choice, but fewer than 10% of patients with mTBI have abnormalities detected on an acute CT scan [55] and most of those abnormalities are of little neurosurgical consequence. The need for neurosurgical intervention is extremely uncommon in patients presenting to the ED with mTBI, and CT scanning is not without disadvantages. Studies by Bouzat et al. showed that in patients with no severe brain lesions on CT after mild to moderate TBI, TCD on admission, in complement with brain CT scan, could accurately screen patients at risk for SND [57]. They showed that in patients with SND after mild to moderate TBI and no evidence of severe injury on initial CT scan presented to the ED with abnormally altered cerebral blood flow velocities (CBFVs) and Pulsatility Index (PI) measured by TCD. PI >1.25 and/or diastolic CBFV <25 cm/s on admission were significantly associated with the occurrence of SND [57, 58]. Study by Vavilala et al. demonstrated that in 1 week

after sports-related mTBI impaired cerebral autoregulation (CA) measured by TCD was common and impaired CA occurs even when GCS is 15 [59]. Recent longitudinal study in pediatric population using TCD and measurement of VMR with BHI between day 2 and 8 after concussion revealed multiple hemodynamic changes that could ultimately lead to a better understanding of the underlying pathophysiology [60].

It is well known and described that mTBI has been inducing cerebral vascular dysfunction that is reflected in altered responses to various vasodilators [41]. Extensive cerebral microvascular injury in humans and experimental animals is seen in acute and chronic TBI and in CTE [41]. While numerous studies have focused on the acute brain behavioral and vascular changes associated with mTBI, few have followed these changes over a more prolonged, chronic course of injury, or have attempted to correlate these changes with any enduring morbidity, like PCS. On the vascular front, there were significant contributions to the understanding of the brain's microvascular response to acute injury, illustrating that in the early hours or days post-concussion the cerebral microcirculation shows impaired VMR to known vasodilator challenges or other provocative maneuvers [25, 26, 30, 35–40, 60]. It is also becoming increasingly evident that changes in CBF and metabolism play a significant role in the evolution of injury, as well as in the process of post-traumatic brain repair. However, beyond acute or sub-acute period not much known. While previous reports have focused primarily on the short-term vascular changes and cerebral hemodynamics [61, 62], during last decade more and more publications linking single mTBI and repetitive mTBI with persisting behavioral changes or potential therapeutic modulation in subjects with PCS [62–64]. Recently published study showed persistent MRI changes 1 year after concussion, specifically grey matter CBF and mean diffusivity exhibited persistent long-term effects [65]. Another new study with MRI also showed that regional CBF analyses suggested that youth with a history of concussion had hypoperfusion in posterior and inferior regions and hyperperfusion in anterior/frontal/temporal regions [66]. Chronic mTBI patients have a brain regions with abnormal perfusion compared to controls [67]. Relationships between peripheral blood biomarkers and MRI measures were demonstrated in both recently concussed athletes and healthy athletes with a history of concussion and authors concluded that concussion is associated with inflammation, oxidative stress, and cellular damage and that physiological perturbations may extend chronically beyond recovery [68].

Advanced imaging methods detected a spectrum of injury including impaired axonal function, neuronal metabolism, and perfusion, suggesting involvement of the neurovascular unit in the presence of persistent symptoms in pediatric sport-related concussion patients 3–12 months after injury [69, 70]. mTBI has been proposed as a risk factor for the development of Alzheimer's disease, Parkinson's disease, depression, and other illnesses. Meta-analysis, 27 studies, mTBI is a risk factor for heterogeneous pathological processes or may contribute to common pathological processes [71]. More and more publications in the last decade forming and supporting opinion that cerebrovascular pathology could represent a mechanistic link between Aβ/tau deposition after TBI and the development of PCS, dementia,

and CTE [72, 73]. Vascular amyloid deposits render blood vessels rigid and reduce the dynamic range of affected vessel segments: potential mechanism that could account in part for the reduction in CBF in patients with Alzheimer's disease [74]. Military personnel with PCS also showed findings suggested that chronic post-concussive symptoms following an mTBI relate to altered exosomal activity and that greater tau pathology may underlie chronic post-concussive symptoms that develop following TBIs [75, 76].

Today it is documented that athletes playing contact sports and military personnel, who may suffer from repeated exposure to mild TBI, will have CBF abnormalities. This effect presents in the acute phase of mTBI [57–60] and now we have data showing that it also happens in subjects with PCS months and years after last concussion [66–68]. However, the development of vascular wall abnormalities, which can lead to luminal narrowing and consequently abnormally elevated CBFV, has not been studied in the long-term effects of mTBI. Preliminary pilot studies in active duty service members (SM) in many years (range between 1 and 27 years), after last mTBI, indicate that concussions leads to the vascular injury that is reflected in abnormally elevated CBFVs measured by TCD due to the enduring stenotic process and potentially most likely represent early signs of atherosclerosis [77]. TCD recordings of mean CBFV were recorded from 431 SMs (mean age 39.2 ± 6.4 years and average time since last TBI was 4.9 ± 3.8 years). TCD data analyzed to determine whether SMs exhibited abnormal CBFVs in the middle cerebral artery (MCA), internal carotid artery, and/or basilar artery. Abnormally elevated CBFV values in 218 (34%) of SMs, 63 (10%), and 155 (24%) demonstrated uncharacteristically (for patient age) high CBFV in one or more vessels. This data reveals that a large proportion of SMs have elevated CBFVs following mTBI exposure in many years after last mTBI. The authors suggested that head injuries due to combat and training blast and blunt force trauma exposure cause early atherosclerotic or fibrotic changes in the large vessel walls of the circle of Willis, which results in vascular lumen narrowing and increased CBFVs.

71.5 Conclusion

Associated long-term personal and societal costs are high, and therefore, improved diagnosis and treatment of mTBI are needed for patients after mTBI and society. TCD evaluation of VMR and cerebral hemodynamics seems like an important adjunct or primary diagnostic tool capable of quantifying and following mTBI patients, as well as providing useful prognostic information to better direct the care and management of these individuals. Considering the available information, it is possible that mTBI leads to the impairment of NVU function that is reflected in abnormally elevated CBFVs due to the enduring stenotic process. It seems that it is possible to suggest some pathway for pathological processes that are followed after single or multiple mTBIs (Fig. 71.1).

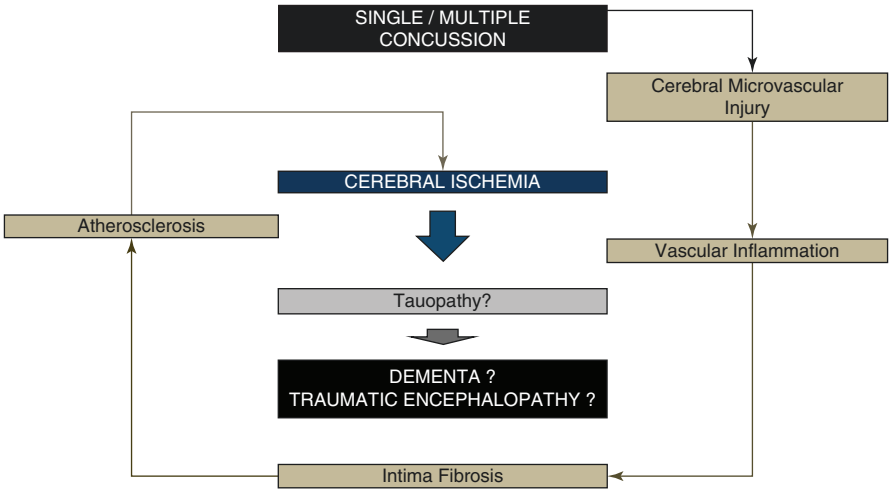

Fig. 71.1 Hypothesis for post-concussive pathways of pathological processes

Post-mTBI disruption of ANS and CBF autoregulation continue to adversely affect a significant proportion of the mTBI population and remain a challenge for all clinicians. At the present time, no proven treatment regimen aimed specifically at decreasing the potential detrimental effects of long-term effects of mTBI exists. Therefore, by our opinion, vigilant diagnostic surveillance, including serial TCD studies and the prevention or treatment of potential CVD, is crucial. TCD illuminates status of cerebral hemodynamics and could be offered as a good screening test to detect abnormal changes in patients after mTBI but the quest for "fine-tuning" of TCD application for mTBI continues.

Based on available data, we can conclude that there is a potential for much broader utilization of TCD for patients after mTBI. TCD makes good clinical and economic sense as it is a reliable, quantitative, and non-expensive "biomarker" to the acute clinical manifestations of mTBI and long-term effects of concussion or mTBI. TCD clinical utilization holds promise for better detection, characterization, and monitoring of objective cerebral hemodynamics changes in symptomatic patients with mTBI not readily apparent by standard CT or conventional MRI techniques. TCD utilization will improve the sensitivity of neuroimaging to subtle brain perturbations and combining these objective measures with careful clinical characterization of patients may facilitate better understanding of the neural bases and treatment of the signs and symptoms of mTBI. A paradigm shift in the importance of the vascular response to injury opens new avenues of drug-treatment strategies for mTBI.

TCD makes good clinical and economic sense, as it is a reliable, quantitative, and non-expensive "biomarker" to the acute clinical manifestations and long-term effects of mTBI. TCD utilization will improve the sensitivity of neuroimaging to subtle brain perturbations, and combining these objective measures with careful

clinical characterization of patients may facilitate better understanding of the neural bases and treatment of the signs and symptoms of mTBI. TCD is a fast and reliable efficient ultrasound technology and has greater value to improve the management of patients with acute and long-term mTBI.

References

1. Centers for Disease Control and Prevention. Surveillance report of traumatic brain injury-related emergency department visits, hospitalizations, and deaths—United States, 2014. Centers for Disease Control and Prevention, U.S. Department of Health and Human Services; 2019.
2. Coronado VG, Thurman DJ, Greenspan AI, Weissman BM. Epidemiology. In: Jallo J, Loftus CM, editors. Neurotrauma and critical care of the brain. New York: Thieme; 2009.
3. Centers for Disease Control and Prevention. How many people have TBI? 2012.
4. Centers for Disease Control and Prevention. Concussion and mild TBI. 2011.
5. Centers for Disease Control and Prevention. Concussion: feeling better. 2010.
6. Nguyen R, Fiest KM, McChesney J, Kwon CS, Jette N, Frolkis AD, et al. The international incidence of traumatic brain injury: a systematic review and meta-analysis. Can J Neurol Sci. 2016;43(6):774–85.
7. Cancelliere C, Coronado VG, Taylor CA, Xu L. Epidemiology of isolated versus nonisolated mild traumatic brain injury treated in emergency departments in the United States, 2006–2012: sociodemographic characteristics. J Head Trauma Rehabil. 2017;32:E37–46.
8. Report to congress on mild traumatic brain injury in the United States: steps to prevent a serious public health problem.
9. Source: Defense Medical Surveillance System (DMSS), Theater Medical Data Store (TMDS) provided by Armed Forces Health Surveillance Center (AFHSC) prepared by DVBIC.
10. Cassidy JD, Carroll LJ, Peloso PM, Borg J, von Holst H, Holm L, et al. Incidence, risk factors and prevention of mild traumatic brain injury: results of the WHO collaborating centre task force on mild traumatic brain injury. J Rehabil Med. 2004;43:28–60.
11. Bonow RH, Friedman SD, Perez FA, Ellenbogen RG, Browd SR, et al. Prevalence of abnormal magnetic resonance imaging findings in children with persistent symptoms after pediatric sports-related concussion. J Neurotrauma. 2017;34:1–7.
12. Kennedy JE, Jaffee MS, Leskin GA, Stokes JW, Leal FO, Fitzpatrick PJ. Posttraumatic stress disorder and posttraumatic stress disorder-like symptoms and mild traumatic brain injury. J Rehabil Res Dev. 2007;44(7):895–920.
13. Terrio H, et al. Traumatic brain injury screening: preliminary findings in a US Army Brigade Combat Team. J Head Trauma Rehabil. 2009;24(1):14–23.
14. Garfinkel SN, Liverzon I. Neurobiology of PTSD: a review of neuroimaging findings. Psychiatr Ann. 2009;39:370–81.
15. Liu N, Jiang Y, Chung JY, Li Y, Yu Z, Kim JW, et al. Annexin A2 deficiency exacerbates neuroinflammation and long-term neurological deficits after traumatic brain injury in mice. Int J Mol Sci. 2019;20:6125.
16. Tan CO, Meehan WP 3rd, Iverson GL, Taylor JA. Cerebrovascular regulation, exercise, and mild traumatic brain injury. Neurology. 2014;83:1665–72.
17. Enzmann G, Mysiorek C, Gorina R, Cheng YJ, Ghavampour S, Hannocks MJ, Prinz V, et al. The neurovascular unit as a selective barrier to polymorphonuclear granulocyte (PMN) infiltration into the brain after ischemic injury. Acta Neuropathol. 2013;125:395–412.
18. Daglas M, Adlard PA. The involvement of iron in traumatic brain injury and neurodegenerative disease. Front Neurosci. 2018;12:981.
19. Doshi H, Wiseman N, Liu J, Wang W, Welch RD, O'Neil BJ et al. Cerebral hemodynamic changes of mild traumatic brain injury at the acute stage. PLoS One. 2015;10(2):e0118061.

20. Wang Y, Nelson LD, LaRoche AA, et al. Cerebral blood flow alterations in acute sport-related concussion. J Neurotrauma. 2016;33:1227–36.
21. Meier TB, Bellgowan PS, Singh R, et al. Recovery of cerebral blood flow following sports-related concussion. JAMA Neurol. 2015;72:530–8.
22. Audenaert K, Jansen HM, Otte A, Peremans K, Vervaet M, Crombez R, et al. Imaging of mild traumatic brain injury using 57Co and 99mTc HMPAO SPECT as compared to other diagnostic procedures. Med Sci Monit. 2003;9:MT112–7.
23. Gowda NK, Agrawal D, Bal C, Chandrashekar N, Tripati M, Bandopadhyaya GP, et al. Technetium Tc-99m ethyl cysteinate dimer brain single-photon emission CT in mild traumatic brain injury: a prospective study. AJNR: Am J Neuroradiol. 2006;27:447–51.
24. Metting Z, Spikman JM, Rödiger LA, van der Naalt J. Cerebral perfusion and neuropsychological follow up in mild traumatic brain injury: acute versus chronic disturbances? Brain Cogn. 2014;86:24–31.
25. Tagge CA, Fisher AM, Minaeva OV, Gaudreau-Balderrama A, Moncaster JA, Zhang XL, et al. Concussion, microvascular injury, and early tauopathy in young athletes after impact head injury and an impact concussion mouse model. Brain. 2018;1(141):422–58.
26. Len TK, Neary JP, Asmundson GJ, Goodman DG, Bjornson B, Bhambhani YN. Cerebrovascular reactivity impairment after sport-induced concussion. Med Sci Sports Exerc. 2011;43:2241–8.
27. Hocke LM, Duszynski CC, Debert CT, Dleikan D, Dunn JF. Reduced functional connectivity in adults with persistent post-concussion symptoms: a functional near-infrared spectroscopy study. J Neurotrauma. 2018;35:1224–32.
28. Szmydynger-Chodobska J, Shan R, Thomasian N, Chodobski A. The involvement of pial microvessels in leukocyte invasion after mild traumatic brain injury. PLoS One. 2016;11(12):e0167677.
29. Wright AD, Smirl JD, Bryk K, van Donkelaar P. Systolic and diastolic regulation of the cerebral pressure-flow relationship differentially affected by acute sport-related concussion. Acta Neurochir Suppl. 2018;126:303–8.
30. Len TK, Neary JP. Cerebrovascular pathophysiology following mild traumatic brain injury. Clin Physiol Funct Imaging. 2011;31:85–93.
31. Markwalder TM, Grolimund P, Seiler RW, Roth F, Aaslid R. Dependency of blood flow velocity in the middle cerebral artery on end-tidal carbon-dioxide partial pressure: a transcranial ultrasound Doppler study. J Cereb Blood Flow Metab. 1984;4:368–72.
32. Aaslid R. Cerebral autoregulation and vasomotor reactivity. Front Neurol Neurosci. 2006;21:216–28.
33. Markus HS, Harrison MJ. Estimation of cerebrovascular reactivity using transcranial Doppler, including the use of breath-holding as the vasodilatory stimulus. Stroke. 1992;23:668–73.
34. Settakis G, Lengyel A, Molnár C, Bereczki D, Csiba L, Fülesdi B. Transcranial Doppler study of cerebral hemodynamic changes during breath-holding and hyperventilation tests. J Neuroimaging. 2002;12:252–8.
35. Gardner AJ, Tan CO, Ainslie PN, van Donkelaar P, Stanwell P, Levi CR, et al. Cerebrovascular reactivity assessed by transcranial Doppler ultrasound in sport-related concussion: a systematic review. Br J Sports Med. 2015;49:1050–5.
36. Len TK, Neary JP, Asmundson GJ, Goodman DG, Bjornson B, Bhambhani YN. Cerebrovascular reactivity impairment following sport-induced concussion. Med Sci Sports Exerc. 2011;43:2241–8.
37. Ellis MJ, Ryner LN, Sobczyk O, Fierstra J, Mikulis DJ, Fisher JA, et al. Neuroimaging assessment of cerebrovascular reactivity in concussion: current concepts, methodological considerations, and review of the literature. Front Neurol. 2016;7:61.
38. Len TK, Neary JP, Asmundson GJ, Candow DG, Goodman DG, Bjornson B, et al. Serial monitoring of CO2 reactivity following sport concussion using hypocapnia and hypercapnia. Brain Inj. 2013;27:346–53.
39. Churchill NW, Hutchison MG, Graham SJ, Schweizer TA. Evaluating cerebrovascular reactivity during the early symptomatic phase of sport concussion. J Neurotrauma. 2019;36:1518–25.

40. Mutch WAC, Ellis MJ, Ryner LN, McDonald PJ, Morissette MP, Pries P, et al. Patient-specific alterations in CO2 cerebrovascular responsiveness in acute and sub-acute sports-related concussion. Front Neurol. 2018;9:23.
41. Kenney K, Amyot F, Haber M, Pronger A, Bogoslovsky T, Moore C, et al. Cerebral vascular injury in traumatic brain injury. Exp Neurol. 2016;275(Pt 3):353–66.
42. Dobson JL, Yarbrough MB, Perez J, Evans K, Buckley T. Sport-related concussion induces transient cardiovascular autonomic dysfunction. Am J Physiol Regul Integr Comp Physiol. 2017;1(312):R575–84.
43. da Costa L, van Niftrink CB, Crane D, Fierstra J, Bethine A. Temporal profile of cerebrovascular reactivity impairment, gray matter volumes, and persistent symptoms after mild traumatic head injury. Front Neurol. 2016;7:70.
44. Mutch WAC, Ellis MJ, Ryner LN, Morissette MP, Pries PJ, Dufault B, et al. Longitudinal brain magnetic resonance imaging CO2 stress testing in individual adolescent sport-related concussion patients: a pilot study. Front Neurol. 2016;7:107.
45. Gong Y, Amyot F, Qu B, Kenney K, Moore C, Bogoslovsky T, et al. Biomarkers of vascular integrity in traumatic brain injury and correlation with cerebrovascular reactivity. Biom J. 2017;3:1–5.
46. Levin HS, Diaz-Arrastia RR. Diagnosis, prognosis, and clinical management of mild traumatic brain injury. Lancet Neurol. 2015;14:506–17.
47. Hiploylee C, Dufort PA, Davis HS, Wennberg RA, Tartaglia MC, Mikulis D, et al. Longitudinal study of postconcussion syndrome: not everyone recovers. J Neurotrauma. 2017;34:1511–23.
48. Dikmen S, Machamer J, Temkin N. Mild traumatic brain injury: longitudinal study of cognition, functional status, and post-traumatic symptoms. J Neurotrauma. 2017;34:1524–30.
49. Neuges D, Grammer G, Yam P, Williams K, Dretsch M, Razumovsky A, et al. Transcranial Doppler measure of persistent cerebral vasomotor reactivity abnormality in service members with chronic mTBI. Poster presentation during 2014 Military Health System Research Symposium, August 18–21, 2014.
50. Cubon VA, Putukian M, Boyer C, Dettwiler A. A diffusion tensor imaging study on white matter skeleton in individuals with sport concussion. J Neurotrauma. 2011;28(2):189–201.
51. Smits M, Hunink MG, van Rijssel DA, Dekker HM, Vos PE, Kool DR, et al. Outcome after complicated minor head injury. AINR Am J Neuroradiol. 2008;29:506–13.
52. Hughes DG, Jackson A, Mason DL, Berry E, Hollis S, Yates DW. Abnormalities on magnetic resonance imaging seen acutely following mild traumatic brain injury: correlation with neuropsychological tests and delayed recovery. Neuroradiology. 2004;46:550–8.
53. Hofman PA, Stapert SZ, van Kroonenburgh MJ, Jolles J, de Kruijk J, Wilmink JT. MR imaging, single-photon emission CT, and neurocognitive performance after mild traumatic brain injury. AJNR Am J Neuroradiol. 2001;22:441–9.
54. Yuh EL, Mukherjee P, Lingsma HF, TRACK-TBI Investigators. Magnetic resonance imaging improves 3-month outcome prediction in mild traumatic brain injury. Ann Neurol. 2013;73:224–35.
55. Amyot F, Arciniegas DB, Brazaitis MP, Curley KC, Diaz-Arrastia R, Gandjbakhche A, et al. A review of the effectiveness of neuroimaging modalities for the detection of traumatic brain injury. J Neurotrauma. 2015;32(22):1693–72.
56. Davalos DB, Bennett TL. A review of the use of single-photon emission computerized tomography as a diagnostic tool in mild traumatic brain injury. Appl Neuropsychol. 2002;9:92–105.
57. Bouzat P, Francony G, Declety P, Genty C, Kaddour A, Bessou P, et al. Transcranial Doppler to screen on admission patients with mild to moderate traumatic brain injury. Neurosurgery. 2011;68:1603–9.
58. Bouzat P, Almeras L, Manhes P, Sanders L, Levrat A, David JS, et al. Transcranial Doppler to predict neurologic outcome after mild to moderate traumatic brain injury. Anesthesiology. 2016;125:346–54.

59. Vavilala MS, Farr CK, Watanitanon A, Clark-Bell BC, Chandee T, Moore A, et al. Early changes in cerebral autoregulation among youth hospitalized after sports-related traumatic brain injury. Brain Inj. 2018;32(2):269–75.
60. Thibeault CM, Thorpe S, O'Brien MJ, Canac N, Ranjbaran M, Patanam I, et al. A cross-sectional study on cerebral hemodynamics after mild traumatic brain injury in a pediatric population. Front Neurol. 2018;9:200.
61. Wang Y, Nelson LD, LaRoche AA, Pfaller AY, Nencka AS, Koch KM, et al. Cerebral blood flow alterations in acute sport-related concussion. J Neurotrauma. 2016;33(13):1227–36.
62. Stephens JA, Liu P, Lu H, Suskauer SJ. Cerebral blood flow after mild traumatic brain injury: associations between symptoms and post-injury perfusion. J Neurotrauma. 2018;35(2):241–8.
63. Giza CC, Hovda DA. The new neurometabolic cascade of concussion. Neurosurgery. 2014;75(Suppl 4):S24–33.
64. Solomon GS, Ott SD, Lovell MR. Long-term neurocognitive dysfunction in sports: what is the evidence? Clin Sports Med. 2011;30(1):165–77.
65. Reid MW, Miller KJ, Lange RT, et al. A multisite study of the relationships between blast exposures and symptom reporting in a post-deployment active duty military population with mild traumatic brain injury. J Neurotrauma. 2014;31:1899–906.
66. Churchill NW, Hutchison MG, Graham SJ, Schweizer TA. Baseline vs. cross-sectional MRI of concussion: distinct brain patterns in white matter and cerebral blood flow. Sci Rep. 2020;10(1):1643.
67. Brooks BL, Low TA, Plourde V, Virani S, Jadavji Z, MacMaster FP, et al. Cerebral blood flow in children and adolescents several years after concussion. Brain Inj. 2019;33(2):233–41.
68. Newberg AB, Serruya M, Gepty A, Intenzo C, Lewis T, Amen D, et al. Clinical comparison of 99mTc exametazime and 123I Ioflupane SPECT in patients with chronic mild traumatic brain injury. PLoS One. 2014;9(1):e87009.
69. Di Battista AP, Churchill N, Schweizer TA, Rhind SG, Richards D, Baker AJ, et al. Blood biomarkers are associated with brain function and blood flow following sport concussion. J Neuroimmunol. 2018;15(319):1–8.
70. Bartnik-Olson BL, Holshouser B, Wang H, Grube M, Tong K, Wong V, et al. Impaired neurovascular unit function contributes to persistent symptoms after concussion: a pilot study. J Neurotrauma. 2014;31(17):1497–506.
71. Perry DC, Sturm VE, Peterson MJ, Pieper CF, Bullock T, Boeve BF, et al. Association of traumatic brain injury with subsequent neurological and psychiatric disease: a meta-analysis. J Neurosurg. 2016;124(2):511–26.
72. Tarantini S, Tran CHT, Gordon GR, Ungvari Z, Csiszar A. Impaired neurovascular coupling in aging and Alzheimer's disease: contribution of astrocyte dysfunction and endothelial impairment to cognitive decline. Exp Gerontol. 2017;94:52–8.
73. Ramos-Cejudo J, Wisniewski T, Marmar C, Zetterberg H, Blennow K, de Leon MJ, et al. Traumatic brain injury and Alzheimer's disease: the cerebrovascular link. EBioMedicine. 2018;28:21–30.
74. Kimbrough IF, Robel S, Roberson ED, Sonheimer H. Vascular amyloidosis impairs the gliovascular unit in a mouse model of Alzheimer's disease. Brain. 2015;138(Pt 12):3716–33.
75. Gill J, Mustapic M, Diaz-Arrastia R, Lange R, Gulyani S, Diehl T, et al. Higher exosomal tau, amyloid-beta 42 and IL-10 are associated with mild TBIs and chronic symptoms in military personnel. Brain Inj. 2018;32(10):1277–84.
76. Kenney K, Qu BX, Lai C, Devoto C, Motamedi V, Walker WC, et al. Higher exosomal phosphorylated tau and total tau among veterans with combat-related repetitive chronic mild traumatic brain injury. Brain Inj. 2018;32(10):1276–84.
77. Razumovsky A, Rampino M, Kouperberg E, Neuges D, DeGraba TJ. Long-term changes in cerebral hemodynamics in service members with mTBI exposure. Poster presentation during 2014 Military Health System Research Symposium, August 15–18, 2016.

Index

C. N. Rodríguez et al. (eds.), *Neurosonology in Critical Care*,
https://doi.org/10.1007/978-3-030-81419-9